G.L.Grodzovskii, Yu.N.Ivanov and V.V.Tokarev

MECHANICS OF LOW-THRUST SPACEFLIGHT

CASE FILE COPY

TRANSLATED FROM RUSSIAN

Published for the National Aeronautics and Space Administration
and the National Science Foundation, Washington, D.C.
by the Israel Program for Scientific Translations

G.L. Grodzovskii, Yu.N. Ivanov,
and V.V. Tokarev

MECHANICS OF SPACEFLIGHT LOW-THRUST

(Mekhanika kosmicheskogo poleta s maloi tyagoi)

Izdatel'stvo "Nauka"
Glavnaya Redaktsiya
Fiziko-Matematicheskoi Literatury
Moskva 1966

Translated from Russian

Israel Program for Scientific Translations
Jerusalem 1969

NASA TTF-507
TT 68-50301

Published Pursuant to an Agreement with
THE NATIONAL AERONAUTICS AND SPACE ADMINISTRATION
and
THE NATIONAL SCIENCE FOUNDATION, WASHINGTON, D.C.

Copyright © 1969
Israel Program for Scientific Translations Ltd.
IPST Cat. No. 5140

UDC 629.195

Translated by A. Baruch, M.Sc.
Edited by Dr. Y. M. Timnat
and IPST Staff

Printed in Jerusalem by IPST Press
Binding: Wiener Bindery Ltd., Jerusalem

Available from the
U.S. DEPARTMENT OF COMMERCE
Clearinghouse for Federal Scientific and Technical Information
Springfield, Va. 22151

XI/16/5

Table of Contents

Page

Preface xi
Introduction xiii

Part I

PHYSICAL PRINCIPLES AND GENERALIZED PARAMETERS OF SPACE PROPULSION SYSTEMS 1

Chapter One. BASIC PARAMETERS AND LAYOUT OF SPACE PROPULSION SYSTEMS 1

§1. Basic parameters of space propulsion systems 1
§2. Layout of space propulsion systems 2
§3. Conditions of spaceflight 4

1. Gravitational fields (4). 2. Environmental parameters (9). 3. Meteors (12).

Chapter Two. PHYSICAL PRINCIPLES OF THE ELEMENTS OF SPACE PROPULSION SYSTEMS 14

§1. Rocket engines 14

1. Rocket thrust and drag (14). 2. Nozzles (15). 3. High-temperature thermal rocket engines (24). 4. Electrodynamic and electrostatic engines (27). 5. Solar sail (40). 6. Isotope sail (43).

§2. Power plants of spacecraft 45

1. Energy sources (45). 2. Systems of energy conversion (51). 3. Energy accumulators (56). 4. Working-fluid supply and storage systems (58). 5. Power plants using up working fluid from the environment (58). 6. Drag acting on the spacecraft during flight in the atmosphere (63).

§3. Cooling systems for spacecraft power plants 68

1. Radiation cooling systems (68). 2. System of energy removal from a flat tube radiator with fins (70). 3. Energy removal from a star-shaped tube radiator with fins (75). 4. Energy removal from a belt radiator (77). 5. Weight characteristics of spacecraft power plants (79).

Chapter Three. GENERALIZED PARAMETERS OF SPACE PROPULSION SYSTEMS 82

§1. Propulsion systems with limited exhaust velocity 82
§2. Power-limited propulsion systems 84
§3. Thrust-limited propulsion systems (sail systems) 85

Part II

PROBLEMS OF OPTIMIZATION 86

Chapter Four. IDEAL POWER-LIMITED ENGINE. SEPARATION OF THE VARIATIONAL PROBLEM. OPTIMUM WEIGHT RATIOS . . . 89

§1. Optimum weight ratios when engine weight is constant or varies stepwise 90

1. Separation of problem, power control (90). 2. Optimum weight ratios (92). 3. Stepwise variation of the engine weight (94).

§2. Optimum program of engine-weight variation 96

1. Formulation of the problem (96). 2. Separating the variational problem (98). 3. Solution of the weight part of the variational problem (99). 4. Stepwise approximation of optimum variation of engine weight (102).

§3. Utilization of jettisoned engine parts as working fluid 103

1. Statement of the problem (103). 2. Optimization of control functions (104). 3. Alternation of optimum flow-rate programs (106). 4. Separating the problem into weight and dynamic parts (110). 5. Solution of the weight part of the problem (112). 6. Discrete reduction of the engine weight (115).

Chapter Five. IDEAL POWER-LIMITED ENGINE. OPTIMUM PROGRAMS OF THRUST ACCELERATION 118

§1. Equations of the extremals and their properties 118

1. Equations of the extremals for the general case (118). 2. First integrals of the equations of the extremals for three-dimensional motion in a central field (119). 3. Equations of the extremals for plane motion in a central field (119). 4. Properties of equations (5.13) (121). 5. Singular point of equation (5.13) (121). 6. Integration in the neighborhood of the singular point (122). 7. Relationship between parameters at the beginning and end of a trajectory (123). 8. Equations of the extremals for plane motion in a bicentric field (123). 9. Analytic solutions for a plane-parallel field (124). 10. Analytic solutions for a homogeneous central field (125). 11. Analytic solution for a central field (126).

§2. Optimum interplanetary trajectory with ideal power-limited engine 126

1. Zero energy build-up (127). 2. Numerical results for zero energy build-up (129). 3. Analytic solution for zero energy build-up (131). 4. Orbital transfer (132). 5. Solution of the boundary-value problem (5.48) by the method of the "transport" trajectory (134). 6. Numerical results of the boundary-value problem (5.48) (137). 7. Round-trip interplanetary trajectory (144).

§3. Optimum maneuvers of guided satellites with ideal power-limited engine 151

1. Rotation of the plane of a circular orbit (151). 2. Transfer between coplanar circular orbits (153). 3. Transfer between noncoplanar circular orbits of different radii (156).

§4. Parameters of a vehicle with ideal power-limited engine . . . 159

1. Formulas for calculations (159). 2. Optimum parameters of interplanetary vehicles (160). 3. Optimum parameters of guided satellites (165).

Chapter Six. UNTHROTTLED ENGINES. SEPARATION OF THE VARIATIONAL PROBLEM. OPTIMUM PROGRAMS OF THE THRUST VECTOR 167

§1. Separating the variational problem into weight and dynamic parts 167
1. Statement of the problem (167). 2. Separation of the dynamic part of the problem (168).

§2. Equations for the optimum thrust vector program. Similarity problems 170
1. Arbitrary gravitational field (170). 2. Central field (171). 3. Plane-parallel field (172). 4. Velocity build-up in a gravitation-free field (172). 5. Displacement between points of rest in a gravitation-free field (173).

§3. Optimum interplanetary flight with unthrottled engines 176
1. Zero energy build-up (177). 2. Orbital transfer (179). 3. Interplanetary round-trip flight (184).

§4. Optimum maneuvers of guided satellites with unthrottled engines 187
1. Holding the satellite within a given spherical layer (187). 2. Rotation of the plane of a circular orbit (191).

§5. Parameters of a vehicle with power-limited unthrottled engine 194
1. Formulas for calculations (194). 2. Build-up of a velocity magnitude (197). 3. Displacement between points of rest (197). 4. Interplanetary Earth-Mars flight (199). 5. Holding the satellite in a specified spherical layer (200). 6. Rotating the plane of a circular orbit (201).

Chapter Seven. REAL POWER-LIMITED ENGINES 202

§1. Additional weight components 203
1. Allowing for the weight of the tanks (203). 2. Allowing for the nozzle weight (205).

§2. Specified operating time of the engine 209
1. General method (209). 2. Application of the general method to the problem studied (211). 3. Maneuvers in a gravity-free field (212). 4. Rotating the plane of a circular orbit (213). 5. Orbital transfer (215).

§3. Optimum staged thrust program 217
1. General method (218). 2. Examples of a step approximation to the thrust-acceleration program (221). 3. The problem of approximating the thrust program while allowing for the engine weight (226). 4. Staged thrust program with an optimum number of levels for an orbital transfer (228).

§4. Real control and weight characteristics 232
1. Characteristics of an electrostatic engine (232). 2. Optimum control programs of real engines (233). 3. Optimum parameters of unthrottlable real engines (236).

Chapter Eight. ENGINES WITH LIMITED EXHAUST VELOCITY. OPTIMUM COMBINATION OF ENGINES WITH LIMITED EXHAUST VELOCITY AND LIMITED POWER 239

§1. Characteristics and optimum operating regimes for engines with limited exhaust velocities 240
1. Characteristics of engines with limited exhaust velocities (240). 2. Characteristic features of the optimum operating regimes for an ideal engine with limited exhaust velocity (240). 3. Allowing for the engine weight (242).

§2. Optimum conditions for combining engines of limited exhaust velocities and limited power 248
1. General conditions for optimum combination (248). 2. Optimum conditions for combining unthrottled engines (250). 3. Optimum conditions for combining ideal engines (254).

§3. Regions of application of power-limited engines 260
1. Build-up of parabolic velocity (260). 2. Transfer between circular orbits (262). 3. Round-trip interplanetary flight (263). 4. Notes (264).

Chapter Nine. PROPULSION SYSTEMS WITH ENERGY AND MASS ACCUMULATION. ENGINES WHOSE THRUST AND POWER ARE FUNCTIONS OF THE COORDINATES AND TIME 265

§1. Power-limited engines with energy accumulation: the ideal case 265
1. Control and weight characteristics (266). 2. Formulation of the variational problem; structure of the optimum control function (267). 3. Ideally throttlable propulsion system (270). 4. Maneuvers of displacement between points of rest and rotating the plane of a circular orbit (274).

§2. Power-limited engines with energy accumulation: additional restrictions on the control characteristics of the engine 277
1. Unthrottled engine (278). 2. Power-limited engine (281). 3. Constant-power engine (283). 4. Engine with limited thrust (290). 5. Engine with limited exhaust velocity (292). 6. Engine with limited operating time (293).

§3. Propulsion systems which accumulate air 294
1. Characteristics of the propulsion system with working-fluid accumulation (295). 2. Accumulation in a stationary regime (297). 3. Air intake in a nonstationary regime (298). 4. Outer-space maneuver of an air-breathing vehicle with a power-limited engine (306). 5. Outer-space maneuver of an air-breathing vehicle with limited exhaust velocity engine (312).

§4. Solar sail 315
1. Statement of the optimization problem for flight with solar sail (315). 2. Interorbital transfer of a spacecraft with solar sail (317). 3. Escape of a spacecraft with solar sail from the field of planetary attraction (320).

§5. Isotopic sail 323
1. Basic characteristics of the isotopic sail and formulation of the variational problem (323). 2. Determination of the optimum control (324). 3. Model problem (324).

§6. Engine with solar power source 325
1. Formulation of the optimization problem (325). 2. Optimum weight ratios and design distance to the Sun (326). 3. Equations of the optimum trajectory (328). 4. Approximate method for determining the optimum trajectory (329). 5. Calculation of the orbital transfer by means of the transport trajectory (330).

§7. Engine with isotopic energy source 332
1. Engine characteristics and formulation of the variational problem (332). 2. Build-up of a velocity (333). 3. Displacement between points of rest (334).

Chapter Ten. MODIFICATIONS OF THE OPTIMUM CRITERION . . . 337

§1. Minimizing the cost of a maneuver 337
1. Cost formula (337). 2. Optimum criterion (338). 3. Formulation of the variation problem (338). 4. Ideal power-limited engine (339).

§2. Universal propulsion system for a given class of maneuvers . . . 341
1. General formulation of the problem (341). 2. Optimum criterion (342). 3. Formulation of the problem for a given number of types of systems (343). 4. Formulating the problem for the universal section (344). 5. Ideal power-limited engine (344).

§3. The game approach to the problem of selecting the optimum parameters of the propulsion system 350
1. Statement of the problem (350). 2. Payoff function (352). 3. Value of the game. Optimum strategies of the Designer and Nature (355).

§4. Optimum working-fluid reserve for a given maneuver with fixed engine parameters 359
1. Formulation of the variational problem (359). 2. Ideal engines with limited power and limited exhaust velocity (360). 3. Unthrottled engines (361).

Chapter Eleven. RELIABILITY CONSIDERATIONS IN OPTIMIZATION PROBLEMS 365

§1. Optimum control for a specified probability of successfully executing the maneuver 365
1. Formulation of the variational problem (365). 2. Power-limited engines (367). 3. Engine with limited exhaust velocity (376).

§2. Formulation and equations of the variational problem for a composite power-limited engine 379
1. Expected failure times (379). 2. Probability of the failures occurring (380). 3. Weight relations (383). 4. Formulation of the problem (384). 5. Equations of the variational problem (384). 6. Continuous approximation to the step function governing failures (385).

§3. Some solutions for maneuvers with a composite power-limited engine 386
1. Step function governing failures (387). 2. Continuous function governing failures (390). 3. Round-trip flight (391). 4. Motion with a specified time of powered flight (392). 5. Nonlinear dependence of the power on the number of operating sections (394).

§4. Optimum probability of executing a maneuver 396
1. Formulation of the transportation problem (397). 2. Maximum mathematical expectation of the total load (398). 3. Maximum total load for specified probability of achieving the solution (401).

Chapter Twelve. EXTRA WEIGHT REQUIRED FOR TRAJECTORY CORRECTION 403

§1. Errors when implementing the thrust-acceleration program, and deviations from the required trajectory 403
1. Errors in the thrust acceleration (403). 2. Mean square deviations from the required trajectory (404).

§2. Optimum correction program 405
1. Measurement of the coordinates and velocities (405). 2. Optimum corrections of the thrust-acceleration program (406). 3. Increment of the functional (407). 4. Optimum distribution of the correction points (409).

Part III

ESTABLISHING OPTIMUM SOLUTIONS 411

Chapter Thirteen. ANALYTIC SOLUTIONS OF THE EQUATIONS OF DYNAMICS 411

§1. Radial acceleration ($a_\varphi = 0$ in (A.9)) 412

1. Equations and integrals of motion (412). 2. Build-up of a parabolic velocity (414). 3. Orbital transfer (416). 4. Variation of the orbital elements (417).

§2. Transverse acceleration ($a_r = 0$ in (A.7)) 418

1. Equations of motion (418). 2. Parabolic velocity build-up (418). 3. Representing the solution in series form (419). 4. Variation of the orbital elements (419).

§3. Tangential acceleration ($\gamma = 0$ in (A.16)) 420

1. Equations and integral of motion (420). 2. Approximate solutions of (13.48) (421). 3. Asymptotic solutions of the acceleration problem (421). 4. Motion along a logarithmic spiral (427).

§4. Normal acceleration ($\gamma = \frac{1}{2}\pi$ in (A.14)). Binormal acceleration ($a_B = 0$, $a_\Phi = 0$ in A.37)) 428

1. Equations and integrals of motion with normal acceleration (428). 2. Properties of the trajectories of motion with normal acceleration (429). 3. Equations and integrals of motion with binormal acceleration (429). 4. Properties of the trajectories of motion with binormal acceleration (431).

§5. Constant acceleration vector ($a_y = a_z = 0$, $a_x = a = \text{const}$ in (A.3)). 431

1. Equations and integrals of motion (431). 2. Classification of plane trajectories (432).

Chapter Fourteen. FUNCTIONAL NUMERICAL METHODS FOR ESTABLISHING OPTIMUM SOLUTIONS 434

§1. Steepest descent in phase space 435

1. Algorithm of the method (436). 2. Computational procedure (439). 3. Generalization of the algorithm (439). 4. Example (440).

§2. Steepest descent in the space of control variables 443

1. Algorithm of the method for problems with a free trajectory terminal point (444). 2. Control function with constraints (446). 3. Algorithm of the method for problems with fixed initial and terminal points of the trajectory (446). 4. Generalization of the procedure for arbitrary boundary conditions (449). 5. Algorithm of the method for problems with free terminal point and free time of motion (449). 6. Examples (450). 7. Constraints on the phase coordinates (452). 8. Numerical methods based on Pontryagin's maximum principle (455).

§3. Newton's functional method 457

1. Algorithm of the method (458). 2. Example (460).

Chapter Fifteen. FINITE-DIMENSIONAL NUMERICAL METHODS OF ESTABLISHING OPTIMUM SOLUTIONS 463

§1. Minimizing a function subject to additional constraints 463

1. The gradient method (464). 2. Newton's method (466).

§2. Reduction of variational problems to finite-dimensional problems 468

1. The Ritz method with the coefficient determined by the steepest descent method (468). 2. Method of polygonal lines for the Lagrange problem (470). 3. Method of polygonal lines for the Mayer problem (472). 4. Selecting the missing initial values in the boundary-value problem (473).

Appendix. DESCRIPTION OF THE DYNAMIC MANEUVERS . . . 476

§1. Forms of the equations of motion 476

1. Equations of motion in a central field (476). 2. Equations of motion in a field with two gravitational centers (485). 3. Equations of motion for model fields (486).

§2. Interplanetary flight 487

1. Dividing the interplanetary flight into elementary maneuvers (487). 2. Round-trip interplanetary flight (488). 3. Models of maneuvers (490).

§3. Satellite maneuvers 490

1. Holding a satellite within a given spherical layer (490). 2. Rotating the plane of the circular orbit of a satellite by a lateral thrust (495).

Nomenclature 497
Bibliography 504
Author index 553

PREFACE

This book presents a theoretical background to the new discipline of spaceflight mechanics. This discipline aims at simultaneously solving the problems of selecting the optimum weight parameters of a spacecraft, the optimum control functions of its propulsion system, and the optimum flight trajectories which ensure delivery of a maximum payload. The necessity for a simultaneous treatment of these three problems stems from the high relative weight and the wide possibilities of adjusting parameters for conceivable types of space propulsion systems including chemical (at high thrust-to-weight ratios), thermonuclear, and electric propulsion engines.

Theoretical studies of low-thrust spaceflight mechanics have nowadays reached the stage at which the results attained can be presented systematically. This, however, has not been done thus far, and data on the subject are scattered over hundreds of publications. This book represents the first attempt at a systematic exposition of the basic problems of spaceflight mechanics. The authors' object is not an exhaustive treatment of all the papers published on the subject, although a very detailed bibliography is included.

The first part of the book investigates the physical principles of space propulsion systems, and gives generalized characteristics of the basic types of propulsion systems necessary for the ensuing analysis.

Problems of optimizing spacecraft parameters for various types of propulsion systems are considered in the second part of the book, which treats the mechanics of flight for propulsion systems with limited power, limited exhaust velocity and thrust, and for throttled and unthrottled power plants with energy and mass storage. Particular attention is paid to the following problems: optimum combination of different types of propulsion systems in one spacecraft; optimum correction of a space trajectory; influence of propulsion-system reliability on spacecraft parameter optimization.

The third part of the book examines the question of optimum trajectories from the viewpoint of spaceflight mechanics, giving both analytic solutions and numerical methods for obtaining the trajectories.

The main sections are illustrated with examples of the characteristics for flight to the solar-system planets, maneuvers of guided satellites, and flight in homogeneous gravitational fields; these examples elucidate the requirements which the propulsion systems must meet, and the possibilities of achieving spaceflight.

The book is intended for scientists, engineers, and graduate students. It is assumed that the reader is familiar with the fundamentals of variational calculus; however, one may use the basic results given in the book even if the sections devoted to variational calculus are omitted.

In view of the book's size, the work was divided among the authors as follows: the first three chapters and Chapter Nine were prepared by G. L. Grodzovskii, Chapters Seven, Eight and Thirteen to Fifteen, and the Appendix by Yu. N. Ivanov, and the fourth, fifth and sixth chapters together with Chapters Ten to Twelve by V. V. Tokarev.

The authors consider it a pleasant duty to express their gratitude to V. V. Beletskii, Yu. Kuznetsov, and F. L. Chernous'ko who read the manuscript and made many helpful suggestions. The authors also wish to acknowledge the help of L. A. Artsimovich, V. A. Egorov, V. K. Isaev, G. E. Kuzmak, A. I. Kur'yanov, A. I. Lur'e, N. N. Moiseev, G. P. Svishchev, L. A. Simonov, V. V. Sonin, G. G. Chernom, L. M. Shkadov, and T. M. Eneev in discussing the problems treated in the book. The authors are particularly indebted to L. I. Sedov and D. E. Okhotsimskii, whose attention to the work of the authors contributed considerably to the appearance of this book.

All readers' suggestions will be welcome.

G. Grodzovskii
Yu. Ivanov
V. Tokarev

Moscow, 1966

INTRODUCTION

13 The progress of spacecraft engineering has led to the creation of new branches of mechanics. The idea of using rocket propulsion for spaceflight, first formulated at the end of the nineteenth century, has stimulated the development of spaceflight mechanics (I.V. Meshcherskii, K.E. Tsiolkovskii, R.H. Goddard, F.A. Tsander, H. Oberth, W. Hohmann, R. Esnault-Pelterie, S.P. Korolev, and others /1.1—1.9/). This discipline treats the motion of a spacecraft, considered as a body of varying mass, with the aim of establishing the conditions for the delivery of a maximum payload.

The decisive factor here is the type of propulsion system. During the first stage of its development, spaceflight mechanics was primarily concerned with the flight of spacecraft using chemical engines, and characterized by a propulsion system of low specific weight (this is defined as the ratio between the propulsion-system weight and the maximum thrust it develops) of the order of several per cent. For moderate thrust-to-weight ratios it was possible to neglect the weight of the propulsion system in a first approximation, and the optimization problem was thus reduced to finding the conditions of minimum fuel expenditure for executing a given space maneuver.* On the basis of Tsiolkovskii's formula the latter condition is reduced to minimizing a simple kinematic parameter, the so-called characteristic velocity; this only necessitates the determination of optimum trajectories for which the times and directions of application of the thrust impulses must be indicated. These problems are exhaustively treated in well-known papers and books on rocket dynamics /1.10—1.59/.

The promising types of space propulsion systems now being developed (the solar sail, the electric rocket engines, the thermonuclear rocket engines, etc.) are characterized by a high specific weight and wide possi-
14 bilities for controlling the parameters (such as exhaust velocity and mass flow). The advantage of such propulsion systems derives from the low mass discharge per unit thrust for the electric and thermonuclear rocket engines (due to the high exhaust velocity), and from the absence of mass discharge for the solar sail. The technical progress achieved in recent years in the realm of nuclear power engineering, electric accelerators, thin-film technology, etc., has made the problem of the scientific and technical development of these propulsion systems very topical. With an increase in the thrust-to-weight ratio, it is inadmissible to neglect the propulsion-system weight, even for chemical rocket engines.

This development led in turn to the appearance of a new branch of spaceflight mechanics, treating simultaneously the optimum ratios between

* The use of a number of rocket stages, i.e., allowing for the successive discarding of containers whose weight is proportional to the fuel reserve, does not basically alter this formulation.

the weight components of the rocket, whilst allowing for the weight of the basic elements of the propulsion system, the optimum control and throttling of the propulsion system, and the optimum trajectories of spaceflight /1.60/.

The problem of determining the conditions for maximum payload delivery occupies a prominent place in spaceflight mechanics in view of its decisive influence on the arrangement and control of the spacecraft. The formulation of problems concerning the optimization of flight trajectories, control parameters, and weight components of the propulsion system is invariably linked with this factor. This formulation of the basic problem of spaceflight mechanics is organically connected to the characteristics of any propulsion system.

Many types of spacecraft propulsion systems are discussed in contemporary literature. The most promising systems are shown in Table 1.1 (/1.61—1.67/ and others) together with some of their parameters, e.g., the characteristic values of the exhaust velocity V, the specific weight of the propulsion system γ_Σ (the weight of the propulsion system per unit thrust generated), and the spacecraft acceleration a caused by the thrust; the characteristics of the propulsion systems in the table are arranged in order of increasing exhaust velocity.

15 TABLE 1.1. Characteristic parameters of space propulsion systems

Type of propulsion system	Basic scheme	Jet composition	Exhaust velocity, m/sec	Specific weight of the propulsion system, γ_Σ	Thrust acceleration, a/g
Thermal rocket engines	Chemical burning chamber	Gaseous burning products	up to $4.5 \cdot 10^3$	0.01	1—100
	Reactor with solid nuclear fuel	Dissociated gas	$8.1 \cdot 10^3 - 1.2 \cdot 10^4$	0.1	1—10
	Solar heater	Ditto	$8.0 \cdot 10^3 - 1.2 \cdot 10^4$	10^2	10^{-2}
	Isotopic heater	"	$8.0 \cdot 10^3 - 1.2 \cdot 10^4$	10^3	10^{-3}
	Reactor with liquid nuclear fuel	"	$1.2 \cdot 10^4 - 2.0 \cdot 10^4$	0.1	1—10
	Reactor with gaseous nuclear fuel	"	$2.0 \cdot 10^4 - 7.0 \cdot 10^4$	0.1	1—10
	Nuclear fuel combined with a chemical burning chamber	Nuclear fragments with gaseous burning products	$5.0 \cdot 10^4$	0.1	1—10
Electric rocket engines	Electric arc heater	Plasma	up to $2.5 \cdot 10^4$	$2.5 \cdot 10^2 - 2.5 \cdot 10^3$	$4.0 \cdot 10^{-3} - 4.0 \cdot 10^{-4}$
	Electrodynamic accelerator	"	$5.0 \cdot 10^4 - 10^5$	$5.0 \cdot 10^2 - 10^4$	$2.0 \cdot 10^{-3} - 10^{-4}$
	Electrostatic accelerator	"	$5.0 \cdot 10^4 - 10^6$	$5.0 \cdot 10^2 - 10^5$	$2.0 \cdot 10^{-3} - 10^{-5}$
Sail systems	Isotopic sail	Alpha-particles	$8.0 \cdot 10^6$	$2.5 \cdot 10^4$	$4 \cdot 10^{-5}$
	Solar sail	Solar radiation photons	$3.0 \cdot 10^8$	$5 \cdot 10^3$	$2 \cdot 10^{-4}$

The characteristic values given in Table 1.1 of the specific weight of the propulsion system γ_Σ explain the recently-adopted classification of engines into high-thrust and low-thrust types. The upper limit of the thrust acceleration a_{max} is attained when the weight of the propulsion system predominates over that of all the other spacecraft components: then $a_{max} \to g/\gamma_\Sigma$ (g is the acceleration of gravity on the Earth's surface). If $\gamma_\Sigma < 1$, then $a_{max} > g$; if $\gamma_\Sigma > 1$, then $a_{max} < g$. Engines of the first type are called high-thrust engines, and those of the second type low-thrust engines (it would have been more correct to call them high-acceleration and low-acceleration engines (Figure 1.1)). It should be noted that the high values of the specific weight for low-thrust engines are not a distinctive physical feature, but only characterize the contemporary assessment of the development level of such propulsion systems. Therefore the term "low thrust" has become widely used. The authors have, however, found it advisable to preserve this term even in the book title, since spaceflight mechanics has been developed mainly to fit "low-thrust" propulsion systems, in which the weight of the power plant plays an essential part.

16

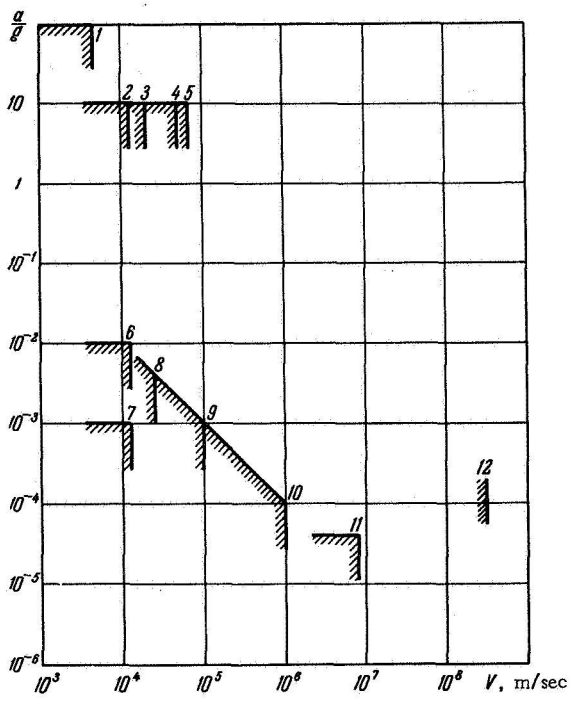

FIGURE 1.1. Space propulsion systems: 1—5 represent high-thrust engines, 6—12 represent low-thrust engines. 1) Chemical burning chamber; 2) heating in reactor with solid nuclear fuel; 3) heating in reactor with liquid nuclear fuel; 4) heating in reactor in combination with chemical burning chamber; 5) heating in reactor with gaseous nuclear fuel; 6) solar heater; 7) isotopic heater; 8) electric-arc; 9) electrodynamic; 10) electrostatic; 11) isotopic sail; 12) solar sail.

17 From the viewpoint of spaceflight mechanics, two characteristics of the power plant are of decisive importance: the possibility of throttling, and the weight required to obtain a given thrust (this includes the necessary working-fluid reserve and the weight of the propulsion system).

The first part of the book is devoted to elucidating these problems by considering the physical principles and basic characteristics of space propulsion systems, a knowledge of which is necessary for the subsequent treatment of the problems of spaceflight mechanics.

The spacecraft is treated as a material point. Questions concerning the spacecraft motion about the center of gravity are not discussed in this book; for an examination of these questions, see /1.68/.

The requirement usually imposed on the spacecraft trajectory is that it should start at a specified point of the phase space (i.e., at specified coordinates and velocity components), and that it should reach another specified point in the phase space during a given time interval. This requirement can be satisfied in different ways. From the multitude of trajectories which link two given points in a phase space over a fixed time interval we select that trajectory which corresponds to the motion of a spacecraft with maximum payload at a fixed take-off weight. This is the formulation of the basic variational problem of spaceflight mechanics for finding the optimum control functions of the propulsion system and the optimum relations between the weight components of the spacecraft, so that motion along the optimum trajectory is ensured.

There is an equivalent alternative formulation of the variational problem which is stated thus: we must determine the optimum control functions and plot the trajectory connecting two given points of the phase space for a minimum flight time, to ensure the motion of a spacecraft with given take-off weight and payload. This second formulation is more convenient when there is no certainty with respect to the energy feasibility of the maneuver over the range of flight times considered.

18 In addition to these two basic variational formulations, particular formulations are also used, corresponding to different types of space maneuvers: orbital transfer maneuvers, escape from the gravitational field of a planet, maneuvers in the vicinity of a planet, etc. The variational formulations of these problems do not necessitate that we satisfy all the boundary conditions relative to the coordinates and velocities; instead, only some of them or their combinations are specified. The free boundary conditions are determined in this case from considerations of an optimum trajectory.

The formulations of the variational problems and their links with the two basic formulations given above will be emphasized in the course of the treatment.

Part I

PHYSICAL PRINCIPLES AND GENERALIZED PARAMETERS OF SPACE PROPULSION SYSTEMS

Chapter One

BASIC PARAMETERS AND LAYOUT OF SPACE PROPULSION SYSTEMS

21 §1. BASIC PARAMETERS OF SPACE PROPULSION SYSTEMS

The working principles and characteristics of space propulsion systems are described in detail in standard treatises, reviews, and textbooks (/1.61—1.67/ etc.). The basic physical principles and generalized parameters of space propulsion systems are described below as far as necessary for a discussion of the mechanics of spaceflight. As mentioned in the introduction, the weight problem (for instance, the problem of finding the conditions for delivery of a maximum payload) is of outstanding importance in spaceflight mechanics, because of its determining influence on the spacecraft parameters. The weight of a spacecraft is determined to a considerable extent by its propulsion system. The motion of the center of mass of the spacecraft is actively controlled by the thrust P created by its propulsion system.

The motion, due to the thrust, of the center of mass of the spacecraft in a gravitational field can be described by the vectorial differential equation (cf. for instance /1.60/):

$$\frac{1}{g}G(t)\ddot{\mathbf{r}} = \mathbf{P} + \frac{1}{g}G(t)\mathfrak{R} + \mathbf{F}, \tag{1.1}$$

where $G(t)$ is the weight of the spacecraft, $\mathbf{r}(t)$ is the radius vector in an inertial frame, $\mathbf{P} = P\mathbf{e}$ is the thrust vector, $\mathbf{e}$ is the unit vector in the direction of thrust, $\mathfrak{R}(\mathbf{r}, t)$ is the vector of the acceleration due to gravitational forces, t is the time, $\mathbf{F}$ is the vector of the external forces acting on the spacecraft (drag, etc.), determined by the external flight conditions.

The complete system of equations describing the behavior of the spacecraft consists of the vectorial equation of motion (1.1) and the relationships between the weight characteristics and the propulsion-system parameters. The determining functions for the optimization of the spacecraft parameters are the unit vector $\mathbf{e}$ in the direction of thrust and the parameters of the nozzle propulsion system, which determine the thrust P and the weight G.

22 Creation of a thrust P requires a flow rate of mass q through the engine (for instance, the mass of the discharged working fluid). The total mass decrease per unit time is

$$q_0 = -\frac{dm}{dt} = q + q_s - q_v, \tag{1.2}$$

where $m = G/g$, q_t is the mass expended per unit time during power generation, q_v is the mass per unit time taken in from the environment.

The weight $G_p(t)$ of the propulsion system proper, the thrust $P(t)$, and the mass flow rate $q(t)$ for the engine thrust are the basic parameters of the space propulsion system.

The variable weight $G(t)$ of the spacecraft can be presented in the form

$$G(t) = G_a(t) + G_p(t), \tag{1.3}$$

where $G_a(t) = G_0 - G_p(t) - g\int_0^t q_a(t)\,dt$, and G_0 is the initial weight of the spacecraft.

The final weight G_a (at the flightpath end $t = T$) may be considered as equal to the payload G_n. It is clear from (1.1), (1.2), and (1.3) that the basic parameters of the propulsion system determine the motion of the spacecraft; $G_p(t)$, $P(t)$, $q(t)$ and the unit vector $\mathbf{e}$ in the direction of thrust are decisive for spaceflight optimization.

The parameters $P(t)$ and $q(t)$ determine the mean effective exhaust velocity and the effective jet power. The quotient P/q, which has the dimensions of a velocity, can be considered as a mean effective jet velocity V (for flights without intake of working fluid from the environment at subrelativistic velocities), so that

$$V = P/q. \tag{1.4}$$

The ratio $I^\circ = V/g$, which has the dimension of time (for instance, sec), characterizes the thrust per unit weight discharge; it is accordingly called the specific impulse of the propulsion system.

The effective jet power is by (1.2) and (1.4)

$$N = \tfrac{1}{2} qV^2. \tag{1.5}$$

23 The propulsive efficiency is

$$\eta = \frac{N}{N_n}, \tag{1.6}$$

where N_n is the power produced by the propulsion system.

The control characteristics of the basic parameters $G_p(t)$, $P(t)$, $q(t)$, and the relationships between them depend on the type of propulsion system and its operating principles. We shall determine the generalized parameters by considering the layout of space propulsion systems.

§ 2. LAYOUT OF SPACE PROPULSION SYSTEMS

The general layout of a space propulsion system is shown in Figure 1.2. The first element of the propulsion system is the power generator; the final element is the nozzle, where part of the energy produced by the power generator is transformed into kinetic energy of the directed motion of the jet. If the type of energy required by the nozzle is different from that

produced by the power generator, an energy converter is installed between the two. Part of the energy produced during interruptions in the operation of the propulsion system can be stored in an energy accumulator. The mass of the working fluid needed to create the thrust is supplied from tanks through a feed system to the nozzle. During flight in a medium of finite density the working fluid can be replenished from outside. A suitable storage system adjusts the conditions of the entering working fluid into those in the tanks.

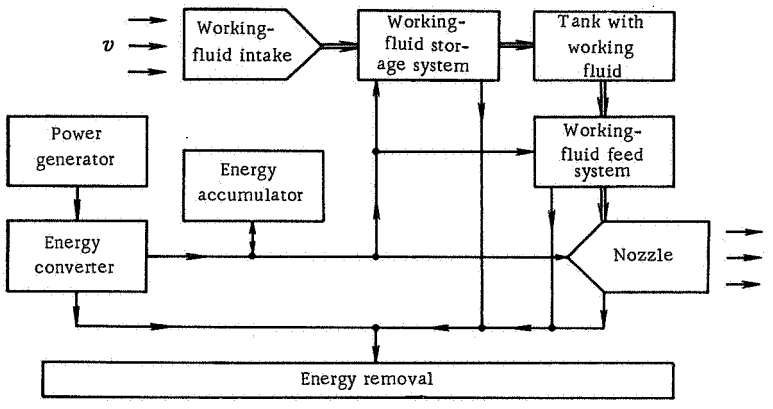

FIGURE 1.2. Layout of space propulsion system.

24 Since the energetic efficiency differs from unity, a considerable part of the power produced by the power generator must be removed from the propulsion system.

The elements described are, of course, not found in all types of space propulsion systems; various combinations are possible within the general layout considered.

From the viewpoint of spaceflight mechanics, the characteristic parameters of the power generator are the power $N_n(t)$ produced by it (the possibility of regulating this power is essential), its weight $G_n(N_n, t)$, and the mass q_e expended per unit time during power generation. The characteristic parameters of the energy converter are the ratio of the useful power $N_v(t)$ delivered by it to the power $N_n(t)$ taken up, this being the converter efficiency $\eta_\tau(N_n)$, and the weight $G_\tau(N_{v\,max})$ of the converter. The characteristic parameters of the accumulator are the amount E of the energy stored in it, the maximum required power $\dot{E}_{max}$ and the useful power $\dot{E}_{min}$ (the dot denotes time differentiation), and the weight $G_e(E_{max})$ of the accumulator. The characteristic parameters of the working fluid taken into the storage system are the mass flow rate q_v, the power N_{qv} contributed by this working fluid, the power $N_v(q_v)$ used by the storage system, and the weight $G_v(q_{v\,max})$ of the latter with intake. The characteristic parameter of the tanks for the working fluid is their weight $G_\beta(t)$, which depends on the working-fluid reserve $G_\mu(t) = G_\sigma(t) - G_\pi$ (cf. (1.3)).

The characteristic parameters of the working-fluid feed system are the mass flow rate q, the power $N_q(q)$, used up by this system and its weight $G_q(q_{max})$.

The characteristic parameters of the nozzle are the thrust $P(t)$ created by it, the power $N(P)$ used by it, the mass flow rate $q(P)$, and the nozzle weight $G_\gamma(P_{max}, N_{\gamma max})$.

The difference between the power N_n produced by the power generator together with the power N_{qv} contributed by the working fluid taken in from outside, and the total power N_λ of the jet discharged through the nozzle must be removed by a suitable system.

The characteristic parameter of the latter is its weight $G_\zeta(N_\zeta)$, where

$$N_\zeta = N_n + N_{qv} - N_\lambda.$$

25 These characteristic elements of the space propulsion system define its basic parameters:

$$\left.\begin{aligned} &P(t),\ q_\sigma(t) = q + q_\varepsilon - q_v, \\ &G_p(t) = G_n + G_\tau + G_\varepsilon + G_v + G_\beta + G_q + G_\gamma + G_\zeta. \end{aligned}\right\} \tag{1.7}$$

These parameters depend, of course, on the operating principles of the space propulsion systems, which will be discussed in detail in the following chapters. The external conditions of the spaceflight, which will now be briefly described considerably affect the parameters of the space propulsion system.

§ 3. CONDITIONS OF SPACEFLIGHT

1. Gravitational fields. Gravity represents the principal external influence in spaceflight. In a typical spaceflight, when the masses can be considered as spherical, the acceleration due to the gravitational forces (cf. (1.1)) is /1.69/:

$$\mathbf{R} = \sum f\mathfrak{M}_i \frac{\mathbf{R}_i}{R_i^3} = -\operatorname{grad} U, \tag{1.8}$$

where U is the gravitational potential, f is the universal gravitational constant, $\mathfrak{M}_i$ is the mass of the i-th gravitational center, $\mathbf{R}_i$ is the position vector referred to the center of mass of the spacecraft.

Tables 1.2 and 1.3 contain the values of $\mathfrak{M}_i$ for the celestial bodies of the solar system, together with their basic orbital and physical data /1.70/. In flights near planets the nonsphericity of their surfaces and their gravitational fields must be taken into account. Thus, the gravitational potential, due to the Earth at a point of geocentric latitude φ is

$$U = \frac{f\mathfrak{M}}{R}\left[1 + \frac{j}{3}\left(\frac{R_s}{R}\right)^2(1 - 3\sin^2\varphi) + \frac{h}{5}\left(\frac{R_s}{R}\right)^3(3\sin\varphi - 5\sin^3\varphi) + \right.$$
$$\left. + \frac{k_1}{30}\left(\frac{R_s}{R}\right)^4(3 - 30\sin^2\varphi + 35\sin^4\varphi) + \ldots\right], \tag{1.9}$$

where $R_s = 6.37815 \cdot 10^6$ m is the equatorial radius; j, h, k_1 are coefficients of the second, third, and fourth zonal harmonics; $j = 1623 \cdot 10^{-6}$, $h = 6.0 \cdot 10^{-6}$, $k_1 = 6.4 \cdot 10^{-6}$.

Motion of a spacecraft in a gravitational field is conservative in the absence of other forces ($P = 0$, $\mathbf{F} = 0$ in (1.1)) (cf. for instance, /1.71 — 1.72/), the total energy remaining a constant.

29 During flight in a gravitational field, the total energy of motion in the absence of other forces is, according to (1.1), (1.8) ($\ddot{\mathbf{r}} = \mathfrak{R}$):

$$\mathcal{E} = \frac{G}{g}\left(\frac{v^2}{2} - \sum f\frac{\mathfrak{M}_i}{R_i}\right) = \text{const}, \tag{1.10}$$

where $\mathbf{v} = \dot{\mathbf{r}}$ is the flight velocity.

During flight in the gravitational field of a celestial body, (1.10) becomes

$$\frac{v^2}{2} - f\frac{\mathfrak{M}_i}{R_i} = \text{const}. \tag{1.11}$$

The specific potential energy $\mathfrak{b} = f\frac{\mathfrak{M}_i}{R_i}$ on the surface of the celestial body $R_i = R_s$ defines the energy necessary for escaping from it. This energy may also be characterized by the minimum initial velocity necessary for escape: $v_e = \sqrt{2f\mathfrak{M}_i/R_s}$. Values of $\mathfrak{b}$ and v_e for the celestial bodies of the solar system are given in Tables 1.2 and 1.3. Figure 1.3 shows the total energy levels $\mathcal{E}g/G$ on the surfaces of the planets (lower points) and in their orbits (upper points), assuming that $\mathcal{E}_\infty = 0$ beyond the solar system. Figure 1.3 thus shows the energy necessary for spaceflights.

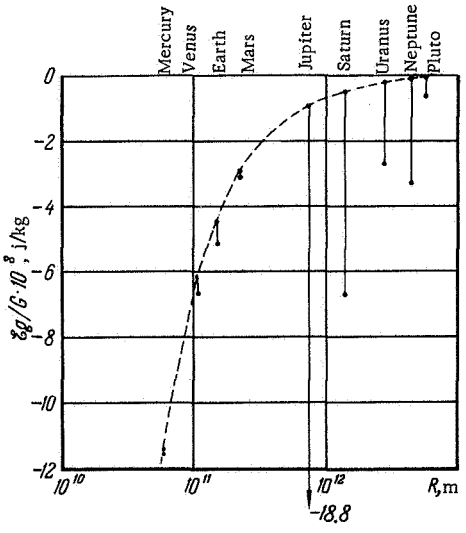

FIGURE 1.3. Levels of specific total energy in orbits and on surfaces of planets of solar system.

The variation of the total energy of motion of the spacecraft, necessary for the spaceflight, does not correspond directly to the energy developed in

TABLE 1.2. Principal orbital and physical data of Sun and planets

Celestial body	Sun	Mercury	Venus	Earth	Mars	Ceres
Mass $\mathfrak{M}$, kg	$1.99 \cdot 10^{30}$	$3.17 \cdot 10^{23}$	$4.87 \cdot 10^{24}$	$5.98 \cdot 10^{24}$	$6.40 \cdot 10^{23}$	$8 \cdot 10^{20}$
Radius R_s, m	$6.96 \cdot 10^{8}$	$2.42 \cdot 10^{6}$	$6.20 \cdot 10^{6}$	$6.38 \cdot 10^{6}$	$3.40 \cdot 10^{6}$	$3.7 \cdot 10^{5}$
Relative gravitational acceleration g_i/g	28.039	0.386	0.895	1.000	0.381	0.040
Period of revolution, days-hours-min-sec	25 9 7 12	87 23 15 —	—	— 23 56 4	— 24 37 23	—
Inclination of equator to orbit	—	7°	—	23°30'	24°	—
Specific potential energy on surface $\mathfrak{b}$, j/kg	$1.91 \cdot 10^{11}$	$8.74 \cdot 10^{6}$	$5.24 \cdot 10^{7}$	$6.25 \cdot 10^{7}$	$1.25 \cdot 10^{7}$	$1.4 \cdot 10^{5}$
Escape velocity v_e, m/sec	$6.18 \cdot 10^{5}$	$4.18 \cdot 10^{3}$	$1.02 \cdot 10^{4}$	$1.12 \cdot 10^{4}$	$5.00 \cdot 10^{3}$	$5 \cdot 10^{2}$
Mean distance from Sun R, m	—	$5.79 \cdot 10^{10}$	$1.081 \cdot 10^{11}$	$1.495 \cdot 10^{11}$	$2.278 \cdot 10^{11}$	$4.137 \cdot 10^{11}$
Minimum radius of orbit R_{min}, m	—	$4.59 \cdot 10^{10}$	$1.071 \cdot 10^{11}$	$1.467 \cdot 10^{11}$	$2.060 \cdot 10^{11}$	$3.823 \cdot 10^{11}$
Maximum radius of orbit R_{max}, m	—	$6.97 \cdot 10^{10}$	$1.088 \cdot 10^{11}$	$1.520 \cdot 10^{11}$	$2.488 \cdot 10^{11}$	$4.451 \cdot 10^{11}$
Sidereal period (Earth year = 1)	—	0.241	0.615	1.000	1.881	4.48
Inclination of orbit to ecliptic	—	7°0'14.3"	3°23'39.2"	0°0'0"	1°50'59.8"	10°36'25"
Mean velocity along orbit, m/sec	—	$4.785 \cdot 10^{4}$	$3.501 \cdot 10^{4}$	$2.976 \cdot 10^{4}$	$2.411 \cdot 10^{4}$	$1.84 \cdot 10^{4}$
Temperature of surface or cloud layer T_s, °K	5800	610	234	287	253	—
Albedo A	—	0.069	0.59	0.39	0.15	0.055

TABLE 1.2 (continued)

Celestial body	Pallas	Jupiter	Saturn	Uranus	Neptune	Pluto
Mass $\mathfrak{M}$, kg	$2 \cdot 10^{20}$	$1.90 \cdot 10^{27}$	$5.69 \cdot 10^{26}$	$8.70 \cdot 10^{25}$	$1.03 \cdot 10^{26}$	$5.40 \cdot 10^{24}$
Radius R_s, m	$2.4 \cdot 10^{5}$	$7.14 \cdot 10^{7}$	$6.04 \cdot 10^{7}$	$2.38 \cdot 10^{7}$	$2.23 \cdot 10^{7}$	$7.20 \cdot 10^{6}$
Relative gravitational acceleration g_i/g	0.024	2.918	1.326	0.961	1.000	0.492
Period of revolution, days-hours-min-sec	—	— 9 55 41	— 10 14 24	— 10 8 —	— 15 40 —	—
Inclination of equator to orbit	—	3°	26°45'	98°	151°	—
Specific potential energy on surface $\mathfrak{b}$, j/kg	$5.5 \cdot 10^{4}$	$1.77 \cdot 10^{9}$	$6.28 \cdot 10^{8}$	$2.44 \cdot 10^{8}$	$3.08 \cdot 10^{8}$	$5.00 \cdot 10^{7}$
Escape velocity v_e, m/sec	$3 \cdot 10^{2}$	$5.97 \cdot 10^{4}$	$3.54 \cdot 10^{4}$	$2.20 \cdot 10^{4}$	$2.48 \cdot 10^{4}$	$1.00 \cdot 10^{4}$
Mean distance from Sun R, m	$4.144 \cdot 10^{11}$	$7.778 \cdot 10^{11}$	$1.426 \cdot 10^{12}$	$2.869 \cdot 10^{12}$	$4.495 \cdot 10^{12}$	$5.899 \cdot 10^{12}$
Minimum radius of orbit R_{min}, m	$3.174 \cdot 10^{11}$	$7.400 \cdot 10^{11}$	$1.344 \cdot 10^{12}$	$2.728 \cdot 10^{12}$	$4.430 \cdot 10^{12}$	$4.430 \cdot 10^{12}$
Maximum radius of orbit R_{max}, m	$5.114 \cdot 10^{11}$	$8.150 \cdot 10^{11}$	$1.503 \cdot 10^{12}$	$3.000 \cdot 10^{12}$	$4.530 \cdot 10^{12}$	$7.410 \cdot 10^{12}$
Sidereal period (Earth year = 1)	4.50	11.862	29.458	84.015	164.788	247.697
Inclination of orbit to ecliptic	34°47'53"	1°18'19.5"	2°29'23.9"	0°46'23"	1°46'25.8"	17°8'38.4"
Mean velocity along orbit, m/sec	$1.84 \cdot 10^{4}$	$1.305 \cdot 10^{4}$	$0.964 \cdot 10^{4}$	$0.678 \cdot 10^{4}$	$0.547 \cdot 10^{4}$	$0.484 \cdot 10^{4}$
Temperature of surface or cloud layer T_s, °K	—	130	128	103	63	53
Albedo A	0.072	0.44	0.42	0.45	0.52	0.16

TABLE 1.3 Principal orbital and physical data of the largest satellites

Planet	Earth	Mars		Jupiter		
Satellite	Moon	Phobos	Deimos	Io	Europa	Ganymede
Mass $\mathfrak{M}$, kg	$7.34 \cdot 10^{22}$	$\sim 6.4 \cdot 10^{15}$	$\sim 6.4 \cdot 10^{14}$	$8.54 \cdot 10^{22}$	$4.82 \cdot 10^{22}$	$1.52 \cdot 10^{23}$
Radius R_s, m	$1.738 \cdot 10^{6}$	$8 \cdot 10^{3}$	$4 \cdot 10^{3}$	$1.775 \cdot 10^{6}$	$1.550 \cdot 10^{6}$	$1.800 \cdot 10^{6}$
Relative gravitational acceleration g_i/g	0.165	0.0007	0.0003	0.185	0.137	0.132
Specific potential energy on the surface $\mathfrak{b}$, j/kg	$2.81 \cdot 10^{6}$	53.4	10.7	$3.21 \cdot 10^{6}$	$2.07 \cdot 10^{6}$	$3.62 \cdot 10^{6}$
Escape velocity v_e, m/sec	$2.37 \cdot 10^{3}$	10.3	4.6	$2.53 \cdot 10^{3}$	$2.04 \cdot 10^{3}$	$2.69 \cdot 10^{3}$
Mean distance from planet, m	$3.844 \cdot 10^{8}$	$9.4 \cdot 10^{6}$	$2.35 \cdot 10^{7}$	$4.28 \cdot 10^{8}$	$6.714 \cdot 10^{8}$	$1.071 \cdot 10^{9}$
Eccentricity	0.0549	0.0190	0.0031	0	0.0003	0.0015
Sidereal period (Earth day = 1)	27.322	0.319	1.262	1.769	3.551	7.154

Planet	Jupiter	Saturn			Uranus	Neptune
Satellite	Callisto	Dione	Rhea	Titan	Titania	Triton
Mass $\mathfrak{M}$, kg	$8.55 \cdot 10^{22}$	$1.08 \cdot 10^{21}$	$2.28 \cdot 10^{21}$	$1.21 \cdot 10^{23}$	—	$1.86 \cdot 10^{22}$
Radius R_s, m	$2.525 \cdot 10^{6}$	$7.00 \cdot 10^{5}$	$9.25 \cdot 10^{5}$	$2.475 \cdot 10^{6}$	$\sim 8.00 \cdot 10^{5}$	$2.40 \cdot 10^{6}$
Relative gravitational acceleration g_i/g	0.091	0.015	0.018	0.134	—	0.022
Specific potential energy on the surface $\mathfrak{b}$, j/kg	$2.26 \cdot 10^{6}$	$1.03 \cdot 10^{5}$	$1.64 \cdot 10^{5}$	$3.26 \cdot 10^{6}$	—	$5.17 \cdot 10^{5}$
Escape velocity v_e, m/sec	$2.12 \cdot 10^{3}$	$4.5 \cdot 10^{2}$	$5.7 \cdot 10^{2}$	$2.55 \cdot 10^{3}$	—	$1.02 \cdot 10^{3}$
Mean distance from planet, m	$1.884 \cdot 10^{9}$	$3.775 \cdot 10^{8}$	$5.272 \cdot 10^{8}$	$1.222 \cdot 10^{9}$	$4.392 \cdot 10^{8}$	$3.537 \cdot 10^{8}$
Eccentricity	0.0075	0.0020	0.0009	0.0289	0.0023	0
Sidereal period (Earth day = 1)	16.689	2.737	4.518	15.945	8.706	5.877

30 the propulsion system of the spacecraft. The work done by the force P is

$$\Delta\mathcal{E} = \int_{r_1}^{r_2} \mathbf{P}\cdot d\mathbf{r} = \frac{\mathbf{v}_1 + \mathbf{v}_2}{2}\int_{t_1}^{t_2} \mathbf{P}\,dt. \qquad (1.12)$$

Hence, the work done by the thrust during a certain time (related to the given amount of energy developed in the propulsion system) depends mainly on the velocity of the spacecraft during this time. It is therefore desirable to operate the propulsion system in the regions of the gravitational field, where the spacecraft velocity is maximum (this is discussed in greater detail in /1.4/).

2. Environmental parameters. The density, pressure, and temperature of the external medium vary greatly along the flight path from the surface of the take-off planet through outer space to the surface of the planet of destination. These three parameters determine the vector of external forces **F** acting on the spacecraft (cf. (1.1)) and the possibility of replenishing the working fluid from outside and are of particular importance for the mechanics of flight near the surface of the planet, i.e., in its atmosphere. The density and pressure of the atmospheres of planets decrease sharply with increasing altitude. Figure 1.4 /1.73/ shows the variation of the density ρ, pressure p_h, and temperature T_h of the Earth's atmosphere with altitude h; the local velocity of sound a and the kinematic viscosity ν, which depend on the altitude, are also given.

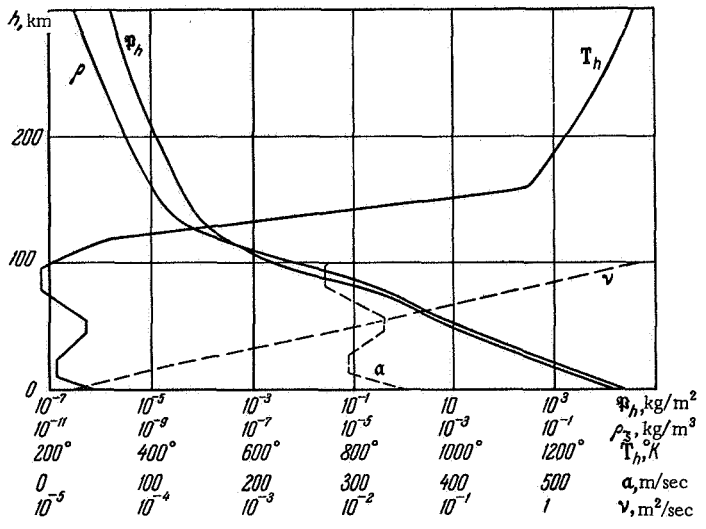

FIGURE 1.4. Variation of pressure, density, and temperature of Earth's atmosphere with altitude; dashed lines represent velocity of sound and kinematic viscosity.

The density of the gaseous medium in interplanetary space depends mainly on the corpuscular radiation of the Sun, which consists of a stream of protons (ionized hydrogen atoms) whose energy is of the order of 1 kev

(velocity $w = 4.5 \times 10^5$ m/sec); its intensity during periods of quiet Sun is (cf. /1.75/):

$$\mathfrak{I} \approx 3 \cdot 10^{14} \left(\frac{R_\delta}{R}\right)^2 1/\mathrm{m}^2 \times \mathrm{sec}, \tag{1.13}$$

where R is the distance to the Sun; $R_\delta = 1.495 \times 10^{11}$ m is the mean radius of the Earth's orbit.

The distribution density of the protons is in accordance with (1.13)

$$\rho_\mathfrak{I} \approx 10^{-18} \left(\frac{R_\delta}{R}\right)^2 \mathrm{kg/m}^3. \tag{1.14}$$

31 The corpuscular radiation of the Sun exerts on the spacecraft a pressure which by (1.13) is

$$p_\mathfrak{I} \approx \rho_\mathfrak{I} w^2 \approx 2 \cdot 10^{-8} \left(\frac{R_\delta}{R}\right)^2 \mathrm{kg/m}^2 \tag{1.15}$$

and supplies power

$$\mathfrak{N}_\mathfrak{I} \approx 5 \cdot 10^{-2} \left(\frac{R_\delta}{R}\right)^2 \mathrm{w/m}^2. \tag{1.16}$$

The intensity of the corpuscular radiation may increase by two to three orders of magnitude during periods of solar activity /1.74/.

The principal energy flux in interplanetary space consists of the electromagnetic radiation of the Sun, which has a maximum in the optical range at a wavelength ~ 5500 Å /1.75/.

The solar spectrum is continuous (Figure 1.5); a large part of it corresponds to blackbody radiation at a temperature $T_\odot \approx 5800$°K. The power of the solar light flux is

$$\mathfrak{N}_\mathrm{A} \approx 1400 \left(\frac{R_\delta}{R}\right)^2 \mathrm{w/m}^2. \tag{1.17}$$

32 The ponderomotive interaction between the radiation and the body reflecting (or absorbing) light produces a pressure on the body. The force of the light pressure depends on the power of the radiation and is, according to Maxwell, at normal incidence of the light on the body,

$$p_\mathrm{A} = \frac{\mathfrak{N}_\mathrm{A}}{c}(1 + \varepsilon) \approx 0.464 \cdot 10^{-6} \left(\frac{R_\delta}{R}\right)^2 (1 + \varepsilon) \mathrm{kg/m}^2, \tag{1.18}$$

where c is the velocity of light, ε is the reflection coefficient of the body ($\varepsilon = 0$ for a perfect blackbody, $\varepsilon = 1$ for an ideal mirror). In the orbit of the Earth the maximum pressure of solar light is $p \approx 0.928 \times 10^{-6}$ kg/m^2 (for $\varepsilon = 1$) /1.76/.

During flight near a celestial body, the heat flux radiated by it (cf. surface temperatures of celestial bodies in Table 1.2) and the solar radiation reflected from its surface are important. The latter is

determined by the albedo A of the celestial body, defined as the ratio of the reflected to the incident light flux (cf. Table 1.2).

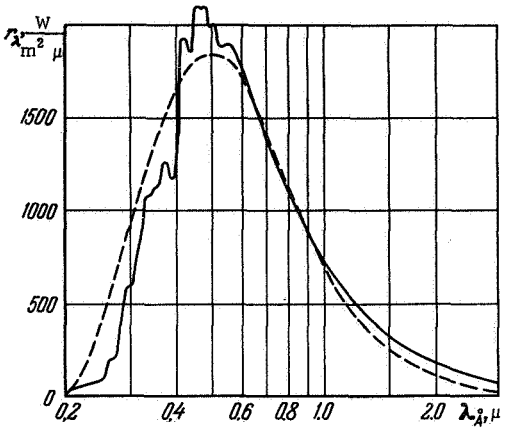

FIGURE 1.5. Solar spectrum (solid line); r_λ — intensity of radiation in orbit of Earth; dashed line — blackbody radiation at $T_\odot = 5800°K$.

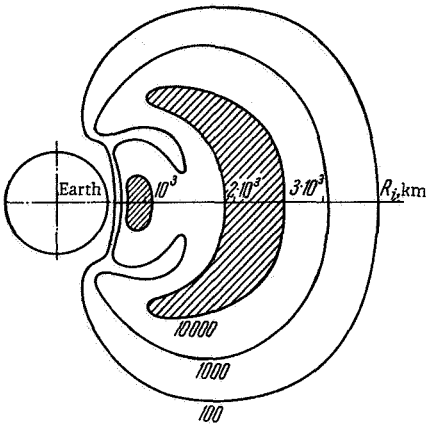

FIGURE 1.6. Radiation (Van Allen) belts of the Earth; the contours correspond to a constant intensity of recorded particles.

Compared with these principal energy fluxes in interplanetary space, the heat radiation in outer space, corresponding to a temperature $T_k \approx 4°K$, is negligibly small:

$$\mathfrak{N}_k \approx 1.5 \cdot 10^{-5} \text{ w/m}^2. \tag{1.19}$$

33 The balance of these energy fluxes and of the energy dissipated by the spacecraft determines the temperature conditions of the latter during flight. Thus, the maximum effective temperature T_τ of a perfect black heat-conducting sphere moving near the surface of a celestial body and possessing no energy sources is

$$T_\tau = \left[\frac{\omega_\odot}{4\pi} (1 + A) T_\odot^4 + \frac{\omega_s}{4\pi} T_s^4 \right], \tag{1.20}$$

where $\omega_\odot$ is the angle at which the Sun is seen, ω_s is the angle at which the celestial body is seen [$T_\odot$ is the surface temperature of the Sun; T_s is the surface temperature of the celestial body].

In addition to the energy fluxes, we must also consider, in problems of spaceflight mechanics, the radiation in outer space, which represents a biological hazard and necessitates weight to be expended for protection. Besides the corpuscular radiation of the Sun already mentioned, cosmic rays must be taken into account. These consist of atomic nuclei with energies up to 10^{17} ev; the specific power of cosmic radiation is $\sim 7 \times 10^{-6}$ w/m^2, the intensity being $\sim 6 \times 10^3$ m^{-2}sec^{-1}.

The magnetic field of a celestial body leads to the formation of magnetic "traps" in which the radiation flux is considerably intensified. Near the Earth such "traps" are formed by a magnetic field of comparatively low intensity, which has a small dynamic effect on the spacecraft. Thus, the

horizontal component of the magnetic field of the Earth is $\sim 3.1 \times 10^{-5}$ weber/m^2 on the geomagnetic equator, while the vertical component is $\sim 6.3 \times 10^{-5}$ weber/m^2 at the geomagnetic poles. Nevertheless, this field causes radiation (Van Allen) belts, with a high intensity of charged particles (Figure 1.6), to be formed near the Earth. These represent a considerable biological hazard /1.62/.

3. **Meteors.** Meteors moving in the solar system may cause considerable weight to be expended on protecting the spacecraft; the distribution of
34 meteors in the solar system may influence the selection of the flight path.

Meteors near the Earth are at present being studied with the aid of photographic and radar techniques, and direct measurements from artificial satellites (/1.77—1.78/ and others). The measured velocities of the meteors are between 11 and 72 km/sec. The lower limit is equal to the escape velocity from the Earth; this is the velocity of meteors approaching the surface of the Earth from a state of rest relative to the Earth. The upper limit is the maximum velocity, relative to the Earth, which a meteor moving in a closed orbit around the Sun can have. The mean velocity of meteors near the Earth varies between ~ 15 and 28 km/sec /1.79/, increasing with their mass m (Figure 1.7).

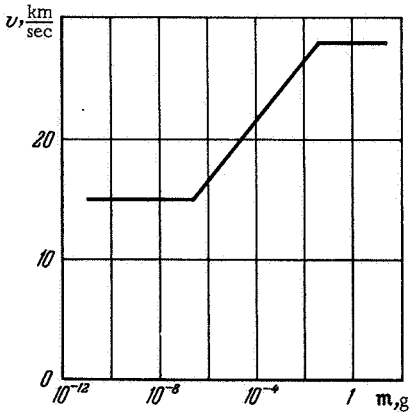

FIGURE 1.7. Velocity of meteors as function of their mass (near Earth).

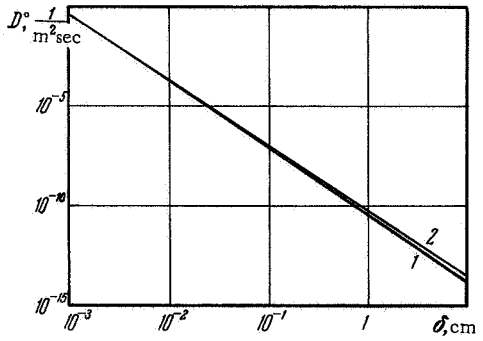

FIGURE 1.8. Required thickness of protective steel wall as function of permissible intensity of punctures by meteors (near Earth).

The intensity D° of a meteoric stream depends mainly on the mass of the particles; according to /1.77—1.79/, it can be represented near the Earth by

$$D^\circ = 10^{-12} m^{-\frac{10}{9}} \ 1/m^2 \cdot sec, \qquad (1.21)$$

where m is given in grams, D° is the intensity of the stream of all meteors whose mass is larger than m.

Opinions differ on the effects of meteors on obstacles. Various relationships are given between the thickness δ of the pierced material and the momentum mv or the energy $\frac{1}{2}mv^2$ of the meteor (/1.77—1.86/ and others).

The results of computations by these methods are in satisfactory agreement with the results obtained by laboratory studies of the process of collision of high-speed particles with targets, as regards the required thickness δ of the protective wall as a function of the permissible intensity $D^\circ(\delta)$ of the punctures. The relationship $D^\circ(\delta)$ for a protective steel wall is given in Figure 1.8, where curve 1 corresponds to $\delta(mv)$, and curve 2 to $\delta\left(\frac{1}{2}mv^2\right)$.

The relationships represented in Figure 1.8 were obtained from (1.21) for flights near the Earth, where the spacecraft is protected from the meteors on one side by the Earth. It may therefore be expected that at a distance from the Earth of the order of several Earth radii, the intensity $D^\circ(\delta)$ of the punctures is doubled.

In order to determine the expected meteoric hazard we may assume /1.79/ that piercing of the wall by meteors is subject to the Poisson distribution

$$\mathfrak{P}(n) = \frac{(D^\circ ST)^n \exp(-D^\circ ST)}{n!}, \tag{1.22}$$

where $\mathfrak{P}$ is the probability that a wall of surface area S is pierced by meteors n times during time T. Thus, for $D^\circ ST = 1$ the probability that the wall is pierced one to four times by meteors is

n	$\mathfrak{P}(n)$
0	0.3679
1	0.3679
2	0.1840
3	0.0613
4	0.0153
	0.9964

Relationship (1.22) and data such as those given in Figure 1.8 allow the weight necessary for protecting the spacecraft from meteors to be estimated with the required accuracy.

Chapter Two

PHYSICAL PRINCIPLES OF THE ELEMENTS OF SPACE PROPULSION SYSTEMS

36 § 1. ROCKET ENGINES

1. Rocket thrust and drag. The rocket nozzle is the final element of the propulsion system, in which the useful part of the energy produced by the power generator is transformed into kinetic energy of the directed motion of the jet and creates the thrust P. The sum of the rocket thrust and the external forces acting on the flying vehicle as a result of drag is equal to the integral, over a closed contour (for instance, that of the vehicle), of the components of the pressure $\mathfrak{p}$, the frictional stresses τ°, and the change of momentum:

$$P + F_x = \oint \{V_i \cos(V_i, x)\, dq_i + [\mathfrak{p} \cos(n, x) + \tau^\circ \sin(n, x)]\, dS\}, \qquad (2.1)$$

where n is the direction of the normal to the contour, and the thrust is directed along the x-axis. For flight in the atmosphere (cf. /2.1/) the drag F_x is considered to be the integral of the frictional stresses and the pressure in excess of the atmospheric pressure $\mathfrak{p}_h$, over the external contour of the vehicle AA_1B_1B outside the jet and the working fluid intake q_v (Figure 2.1, a and b):

$$F_x = \int_A^B [(\mathfrak{p} - \mathfrak{p}_h) \cos(n, x) + \tau^\circ \sin(n, x)]\, dS. \qquad (2.2)$$

Substituting (2.2) in (2.1), and noting that there is no mass flow ($q_i = 0$) across the contours AA_1 and B_1B we obtain the rocket thrust during flight in the atmosphere (cf. /2.2/ etc.)

$$P = \int_B^A [V_i \cos(V_i, x)\, dq_i + (\mathfrak{p} - \mathfrak{p}_h) \cos(n, x)\, dS] = qV_c + (\mathfrak{p}_c - \mathfrak{p}_h)\mathcal{F}_c - q_v v, \qquad (2.3)$$

where $\mathfrak{p}_c$, V_c are respectively the mean pressure and velocity in the jet in section BA, $\mathcal{F}_c$ is the area of this section.

37 This widely-accepted grouping into thrust and drag of the forces acting on the rocket-propelled vehicle is, of course, arbitrary. Thus, the forces on the parts aA and bB (Figure 2.1) of the vehicle depend largely on the jet (/2.1/), i.e., on the thrust, although here it is included in the drag. This classification has, however, a definite physical meaning, with sharp

transitions in the limiting cases (absence of drag or thrust); in detailed analyses it is, nevertheless, necessary to allow for a possible interaction between thrust and drag.

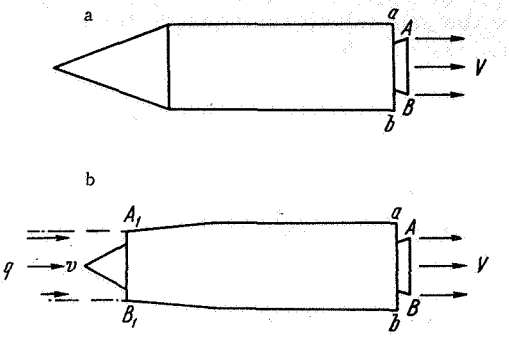

FIGURE 2.1. Reaction-propelled vehicles:

a) *without intake;* b) *with intake from outside at mass flow rate* q_v.

A simpler expression is obtained for the thrust during flight in outer space, where the drag practically vanishes ($F = 0$); with $p_h = 0$ and $q_v = 0$

$$P_k = qV_c + p_c\mathcal{F}_c. \tag{2.4}$$

2. **Nozzles.** In thermal jet engines the thrust is created by the nozzle, which transforms the heat energy of the gas into kinetic energy of the directed jet. The physical principles of nozzle operations are explained by the theory of gas dynamics (/2.2—2.12/).

The measure of the heat energy of the gas is the stagnation temperature T_0, which is the gas temperature at zero flow velocity ($V_i = 0$). The maximum possible velocity of the directed motion of the gas $V_{\max\max}$ is equal to the average velocity of the molecular motion in the gas at rest; for a perfect gas this is $V_{\max\max}$ given by

$$V_{\max\max} = \sqrt{\frac{2\varkappa}{\varkappa-1}\mathcal{R}T_0}, \tag{2.5}$$

where $\varkappa$ is the ratio of specific heats, equal to 1.66, 1.40, and 1.33 respectively for monatomic, diatomic and multiatomic gases, $\mathcal{R}$ is the gas constant. This maximum velocity is $\sqrt{\frac{\varkappa+1}{\varkappa-1}}$ times higher than the critical velocity of sound in the gas: $a_* = \sqrt{\frac{2\varkappa}{\varkappa+1}\mathcal{R}T_0}$; supersonic nozzles are therefore required for high exhaust velocities. A supersonic axisymmetrical nozzle is shown in Figure 2.2.

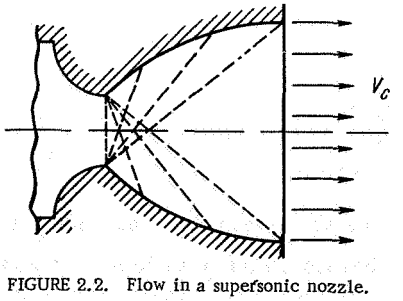

FIGURE 2.2. Flow in a supersonic nozzle.

In accordance with the theory of one-dimensional gas flow (/2.4, 2.6/), the relative gas velocity $\lambda_c = \frac{V_c}{a_*}$ in the exit section of an ideal supersonic nozzle, in which there are no losses and where the axial flow velocity is uniform, is determined by the ratio of the area of the critical (throat) section $\mathcal{F}_*$ (where the gas velocity is equal to the local sound velocity a_*) to the area of the exit section $\mathcal{F}_c$:

$$q(\lambda_c) = \lambda_c\left(1 - \frac{\varkappa - 1}{\varkappa + 1}\lambda_c^2\right)^{\frac{1}{\varkappa-1}}\left(\frac{\varkappa+1}{2}\right)^{\frac{1}{\varkappa-1}} = \frac{\mathcal{F}_*}{\mathcal{F}_c}. \tag{2.6}$$

At a mass flow rate q the total thrust is

$$\Upsilon = qV + p\mathcal{F} = \frac{\varkappa+1}{2\varkappa} q a_* z(\lambda), \tag{2.7}$$

where $z(\lambda) = \lambda + \frac{1}{\lambda}$. The equation of continuity for one-dimensional gas flow yields the mass flow rate through an ideal nozzle

$$q = \left(\frac{2}{\varkappa+1}\right)^{\frac{1}{\varkappa-1}} \frac{p_0}{\mathcal{R}T_0} a_* q(\lambda)\mathcal{F} = \frac{p_0\mathcal{F}_*}{\mathcal{R}T_0} a_* \left(\frac{2}{\varkappa+1}\right)^{\frac{1}{\varkappa-1}}, \tag{2.8}$$

where $q(\lambda_c)$ is given by (2.6), p_0 is the total stagnation pressure of the gas at the nozzle inlet.

The thrust developed by an ideal nozzle during spaceflight, which equals
39 the total impulse of the gas stream at the nozzle exit (compare (2.4) and (2.7)) is by (2.7) and (2.8):

$$P_k = \Upsilon_c = p_0\mathcal{F}_*\left(\frac{2}{\varkappa+1}\right)^{\frac{1}{\varkappa-1}} z(\lambda_c). \tag{2.9}$$

The thrust developed by a nozzle during flight in vacuum is thus independent of the total gas temperature T_0 and depends only on the total gas pressure p_0, the throat area $\mathcal{F}_*$, and the expansion ratio $\mathcal{F}_c/\mathcal{F}_*$ (which determines λ_c and $z(\lambda_c)$). At given p_0 and $\mathcal{F}_*$, the thrust developed by an ideal nozzle in vacuum increases continuously with the expansion ratio, reaching a theoretical maximum when $\mathcal{F}_c/\mathcal{F}_* \to \infty$, when the exhaust velocity of the gases becomes the maximum possible:

$$P_{k\max} = p_0\mathcal{F}_*\left(\frac{2}{\varkappa+1}\right)^{\frac{1}{\varkappa-1}}\left(\sqrt{\frac{\varkappa+1}{\varkappa-1}} + \sqrt{\frac{\varkappa-1}{\varkappa+1}}\right) \tag{2.10}$$

with $V_c = V_{\max}$, $\lambda_{c\max} = \sqrt{\frac{\varkappa+1}{\varkappa-1}}$. In real nozzles the expansion ratio should not exceed a certain limit beyond which the additional frictional losses at the

nozzle walls, caused by their increase in surface, cancel out the increment in thrust due to the increase in expansion ratio. Allowing for inertia forces during acceleration of the vehicle has a similar effect. The frictional losses in the nozzle determine the optimum expansion ratio (and thus $\lambda_{c\,opt}$): at this optimum ratio the thrust may be $\sim 95\%$ $P_{k\,max}$ (cf., for instance, /2.7—2.11/). The gas-dynamic principles and variational problems of optimizing the contours of supersonic nozzles are considered in /2.13—2.21/. Introducing the impulse loss factor $\overline{\Gamma}_c$, the maximum thrust developed by a real nozzle during flight in vacuum is

$$P_{max} = \overline{\Gamma}_c p_0 \mathcal{F}_* \left(\frac{2}{\varkappa+1}\right)^{\frac{1}{\varkappa-1}} z(\lambda_{c\,opt}). \tag{2.11}$$

Hence, when p_0 and $\mathcal{F}_*$ are given, the maximum thrust developed by the nozzle during flight in vacuum is constant. The gas temperature T_0 at the nozzle inlet determines the mass flow rate through the nozzle when p_0 and
40 $\mathcal{F}_*$ are given (cf. (2.8)). When the thrust is given the mass flow rate q decreases with increasing gas temperature T_0; the specific impulse of the propulsion system increases accordingly.

We obtain the thrust developed by the nozzle during flight in the atmosphere (assuming $q_\tau = 0$ for simplicity) by subtracting from the value (2.11) of the thrust in vacuum a term allowing for the atmospheric pressure p_h (cf. (2.3)); hence

$$P = p_0 \mathcal{F}_* \left(\frac{2}{\varkappa+1}\right)^{\frac{1}{\varkappa-1}} \left[\overline{\Gamma}_c z(\lambda_c) - \frac{p_h \left(\frac{\varkappa+1}{2}\right)^{\frac{1}{\varkappa-1}}}{p_0 q(\lambda_c)}\right]. \tag{2.12}$$

When p_0, $\mathcal{F}_*$ and λ_c are given the thrust developed by the nozzle increases with altitude by ~ 10 to 30%, attaining a maximum P_{max} in outer space.

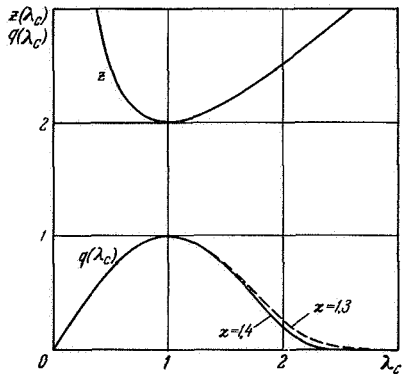

FIGURE 2.3. Variation of $z(\lambda)$ and $q(\lambda)$ with relative flow velocity.

The functions $z(\lambda_c)$ and $q(\lambda_c)$ are shown in Figure 2.3. They vary with λ_c in such a way that when p_0, p_h, $\mathcal{F}_*$ are given, the thrust P becomes maximum

at the expansion ratio $\mathcal{F}_c/\mathcal{F}_*$ and the corresponding exhaust velocity $V_c(\lambda_c) = V_p(\lambda_p)$, for which the static pressure in the jet at the nozzle exit is atmospheric: for $p_c = p_h$,

$$P_{h\max} = \bar{\Gamma}_c p_0 \mathcal{F}_* \lambda_p \frac{2\varkappa}{\varkappa+1}\left(\frac{2}{\varkappa+1}\right)^{\frac{1}{\varkappa-1}}, \qquad (2.13)$$

where

$$\left(1-\frac{\varkappa-1}{\varkappa+1}\lambda_p^2\right)^{\frac{\varkappa}{\varkappa-1}} = \frac{p_h}{p_0}.$$

These are the design conditions for the nozzle. For a fixed nozzle ($\mathcal{F}_*/\mathcal{F}_c$ = = const) and variable pressure drop p_0/p_h (for instance, p_0 = const, p_h varying with altitude), the nozzle will develop the maximum possible thrust $\frac{P}{P_{h\max}} = 1$ only at the design conditions $p_h = p_p$. When $\frac{p_0}{p_h} < \frac{p_0}{p_p}$ or $\frac{p_0}{p_h} > \frac{p_0}{p_p}$
41 the thrust will be less than the maximum possible $\left(\frac{P}{P_{h\max}} < 1\right)$, obtainable at the optimum expansion ratio.

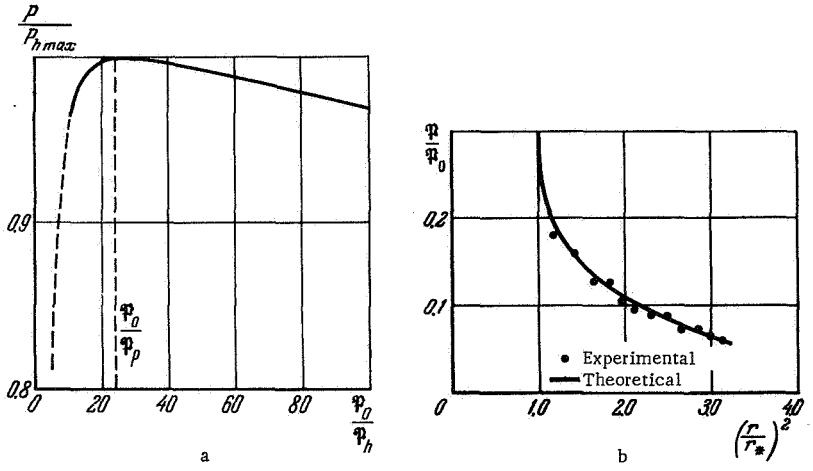

FIGURE 2.4. Relative thrust developed by nozzle at $\lambda_c = 1.89$, as function of pressure drop.

From (2.12) and (2.13), we have plotted on Figure 2.4,a the relative thrust

$$\frac{P}{P_{h\max}} = \frac{\varkappa+1}{2\varkappa\lambda_p\bar{\Gamma}_c}\left[\bar{\Gamma}_c z(\lambda_c) - \frac{p_h\left(\frac{\varkappa+1}{2}\right)^{\frac{1}{\varkappa-1}}}{p_0 q(\lambda_c)}\right] \qquad (2.14)$$

as a function of the pressure drop p_0/p_h for $\lambda_c = 1.89$ and $\bar{\Gamma}_c \approx 0.99$ /2.20/. The considerable losses in thrust during under- and overexpansion do not depend on the flow inside the nozzle, where the velocity and pressure distributions are fixed (Figure 2.4, b) but are due to the shocks formed in the jet behind the nozzle when nonoptimum flow conditions apply (cf. Figure 2.5 /2.22/).

a

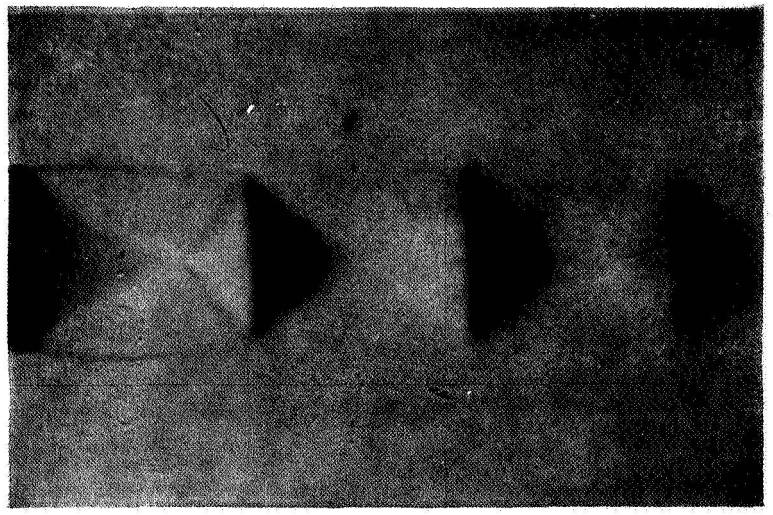

b

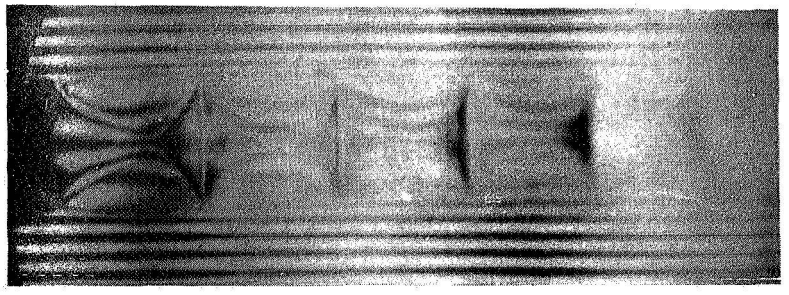

c

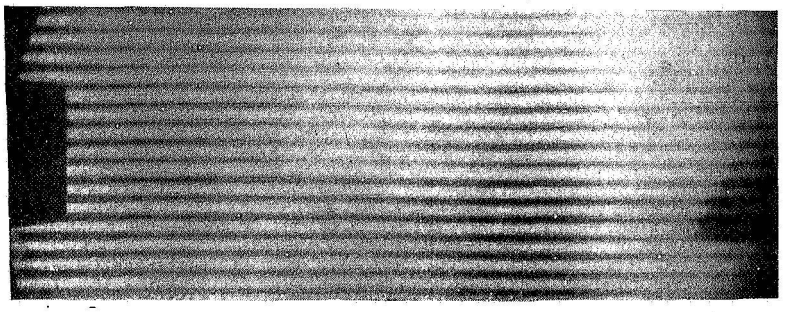

FIGURE 2.5. Flow pattern behind nozzle in case of underexpansion $\left(\frac{p_0'}{p_h} > \frac{p_0'}{p_p}\right)$:

a) colored schlieren photograph; b) interferogram; c) ditto without flow.

42 In reality, the constancy of supersonic conditions inside the nozzle, implied in determining the relative thrust by (2.14) (cf. Figure 2.4), is observed throughout the region of underexpansion and in a considerable part of the region of overexpansion close to the optimum expansion ratio.

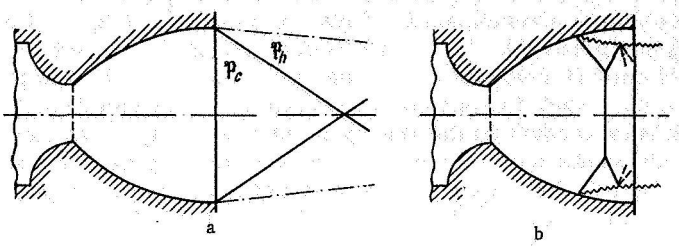

FIGURE 2.6. Flow from a supersonic nozzle with overexpansion:
a) without separation; b) with separation from nozzle walls.

In the case of overexpansion, the pressure rise p_0/p_h in the shock at the nozzle exit varies inversely with the ratio p_h/p_c (since $p_c/p_0 = \text{const}$); after a critical value $(p_h/p_c)_{cr}$ has been attained the strong shock causes separation of the boundary layer from the nozzle walls and a change in the flow pattern inside the nozzle (Figure 2.6 /2.23/). The values of the critical pressure rise in the shock, given in Figure 2.7 (/2.23, 2.24/), indicate the region in which no separation occurs during overexpansion, with constant supersonic flow being maintained in the nozzle; for this region the thrust losses are determined from (2.14).

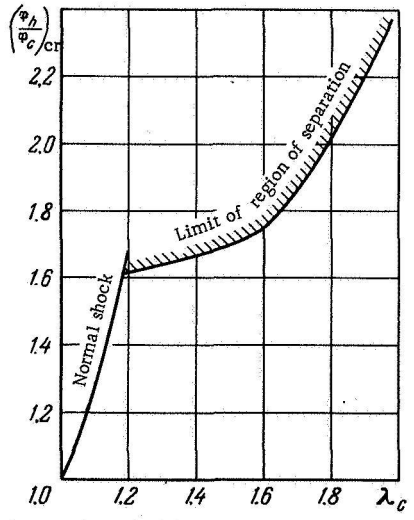

FIGURE 2.7. Critical pressure rise in shock, causing separation of turbulent boundary layer at nozzle exit, as function of relative exhaust velocity.

43 When flow separation occurs in the nozzle, the pressure acting on the nozzle walls in the separation zone is higher than the computed pressure, and the thrust losses are correspondingly reduced. This phenomenon is most pronounced in annular supersonic nozzles. With underexpansion or optimum expansion ratio the flow in an annular supersonic nozzle (Figure 2.8, a /2.20/) does not differ in principle from the flow in an ordinary supersonic nozzle. With overexpansion, however, reflection of shocks, coming from the nozzle edge at the core, causes a considerable increase in the pressure acting on the latter (Figure 2.8, b). This intensifies flow separation because of interaction between the shocks and the boundary layer. Such nozzles have small thrust losses with

overexpansion. Figure 2.9 shows the characteristics of an annular nozzle with $\frac{p_0}{p_c}=165$ /2.25/; an example of a rocket with such a nozzle is given in /2.26/.

Within the scope of the theory of gas dynamics the thrust developed by the nozzle is determined by (2.12), with suitable corrections for flow separation due to overexpansion (these corrections may be included in the impulse loss factor $\bar{\Upsilon}_r$). The results obtained in the theory of gas dynamics apply to chemical-reaction rocket engines, provided the temperature levels are such that dissociation, ionization, and recombination of the gas (not taken into account in the theory mentioned) may be neglected. A typical representative of such space propulsion engines is the liquid-fuel rocket, in which the nozzle acts as a structural element (Figure 2.10) /2.27/. Because the structural and gas-dynamic functions of the parts of liquid-fuel rockets are interrelated, separate weight analyses for nozzle, combustion chamber, and working-fluid supply systems should not be carried out.

The maximum thrust of a liquid-fuel rocket is by (2.11) and (2.12) proportional to the total pressure p_0 of the gas in the combustion chamber and to the nozzle throat area $\mathcal{F}_*$:

$$P_{\max} \sim p_0 \mathcal{F}_*. \tag{2.11'}$$

The weight of the nozzle (which acts simultaneously as an energy-removal system, cf. Figure 2.10) must, for reasons of static strength, be proportional to $p_0 \mathcal{F}_*^{1/2}$; due, however, to the improvement in construction, possible with larger engines, the weight increases more slowly than the cube of the characteristic dimension, being approximately proportional to $p_0 \mathcal{F}_*$. The weight of the combustion chamber, which acts both as a power generator and a power converter, varies similarly (cf. § 2 of Chapter Two).
45 The weight of the working-fluid supply system must be proportional to the mass flow rate q, which, by (2.8), is also proportional to $p_0 \mathcal{F}_*$. For a liquid-propellant rocket we have, therefore,

$$(G_\gamma + G_\zeta + G_n + G_\tau + G_q) \sim p_0 \mathcal{F}_*, \tag{2.15}$$

or by (2.11')

$$G_\gamma + G_\zeta + G_n + G_\tau + G_q \approx \gamma_\xi P_{\max}, \tag{2.16}$$

where $\gamma_\xi = \frac{G_p - G_\delta}{P_{\max}}$ is the specific weight of the engine (for a liquid-fuel rocket $G_e = 0$ and $G_v = 0$).

46 Figure 2.11 gives the specific weight of the engines of the "Saturn" rocket (/2.11, 2.27/); the data for the engine of the V-2 rocket, which are also given, show the progress made in the last 20 years in improving the weight characteristics of liquid-fuel engines. It is seen that the specific weight of liquid-fuel rocket engines is quite low.

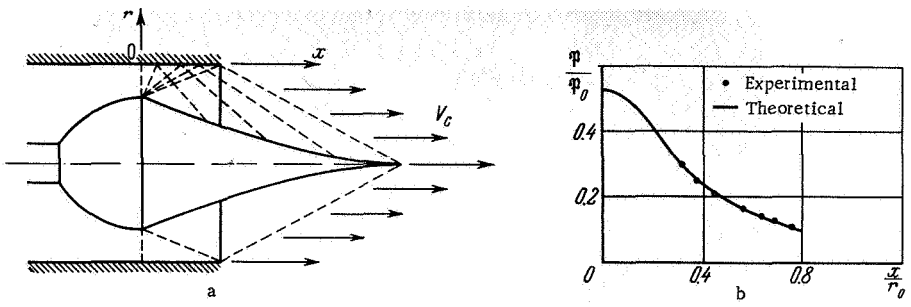

FIGURE 2.8. Flow pattern in an annular supersonic nozzle ($\lambda_c = 1.68$).

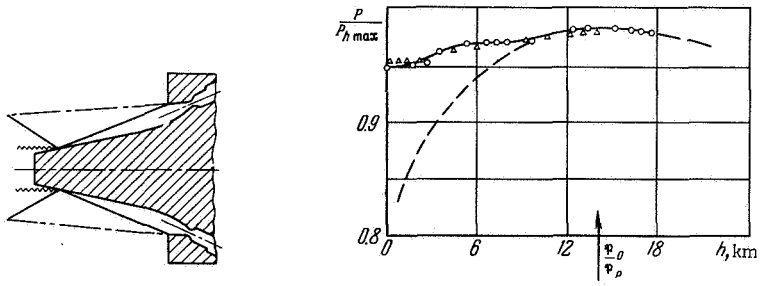

FIGURE 2.9. Relative thrust developed by annular nozzle as function of flight altitude; $\frac{p_0}{p_c} = 165$, $p_0 = 3.5 \times 10^5$ kg/m^2; solid curve shows experimental results; dashed curve shows theoretical results for ordinary nozzle.

The mean effective exhaust velocity V of the gases, and the corresponding specific impulse I° of the propulsion system are important nozzle parameters. We obtain from (2.8), (2.12), and (1.4)

$$V = \frac{P}{q} = \sqrt{\frac{\varkappa+1}{2\varkappa}\mathcal{R}T_0}\left[\overline{\Gamma}_c z(\lambda_c) - \frac{p_h\left(\frac{\varkappa+1}{2}\right)^{\frac{1}{\varkappa-1}}}{p_0 q(\lambda_c)}\right], \quad I^\circ = \frac{V}{g}. \qquad (2.17)$$

When the nozzle parameters and the flight altitude are given, the nozzle exhaust (and hence the specific impulse) depend on the composition ($\mathcal{R}$, $\varkappa$) and on the stagnation temperature T_0 of the gases. The maximum exhaust velocity in chemical engines is limited by the maximum temperature attainable from chemical reactions (cf. below § 2), the possibility of selecting fuels and oxidizer whose combustion products have low molecular weights (i.e., for which the value of $\mathcal{R}$ is higher) and the permissible $T_{0\,max}$ temperature level for the structure. Chemical rocket engines can accordingly
47 be considered as propulsion systems with limited gas exhaust velocities:

$$V \leqslant V_{max} = \sqrt{\frac{\varkappa+1}{2\varkappa}\mathcal{R}_{max}T_{0\,max}}\left[\overline{\Gamma}_c z(\lambda_c) - \frac{p_h\left(\frac{\varkappa+1}{2}\right)^{\frac{1}{\varkappa-1}}}{p_0 q(\lambda_c)}\right]. \qquad (2.18)$$

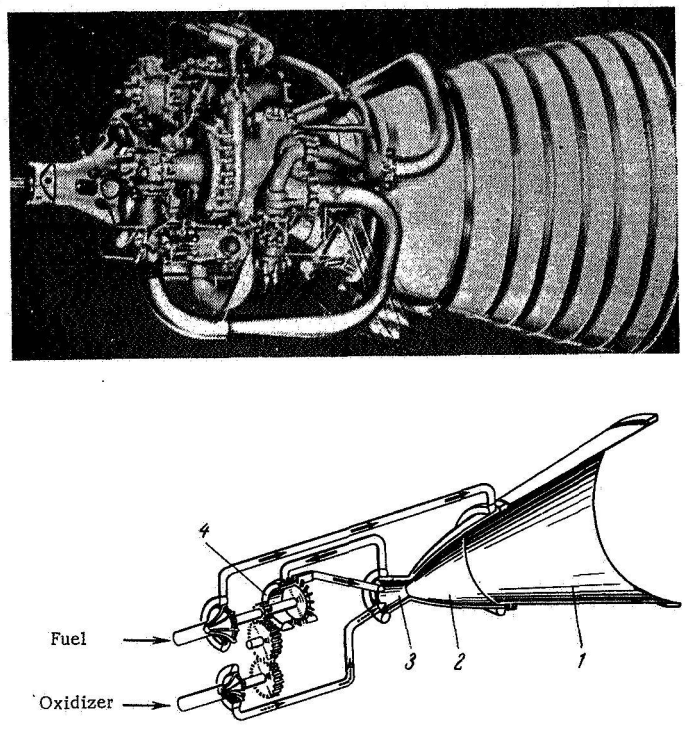

FIGURE 2.10. RL10A-3 liquid-fuel engine of second stage of Saturn 1 rocket; fuel — liquid hydrogen, oxidizer — liquid oxygen:

1) radiation-cooled part of nozzle; 2) fuel-cooled part of nozzle; 3) combustion chamber; 4) fuel and oxidizer supply lines.

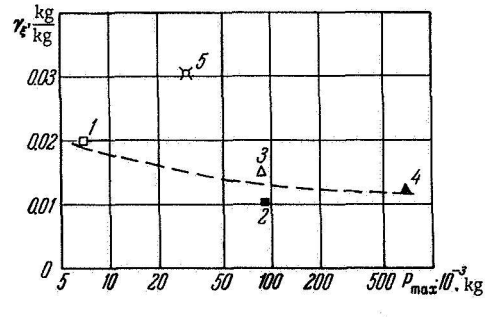

FIGURE 2.11. Specific weight of liquid-fuel engine as function of maximum thrust developed (dashed curve refers to engines 1 to 4 of Saturn rocket):

1) RL10A-3 (H_2+O_2); 2) J-2 (H_2+O_2); 3) H-1 (kerosene + O_2); 4) F-1 (kerosene + O_2); 5) engine of V-2 rocket (ethyl alcohol 75% + O_2).

It follows from (2.18) that the maximum effective exhaust velocity increases with altitude (corresponding to the increase in thrust, cf. (2.12)) by about 10 to 30% /2.27/. The critical conditions are the take-off from the Earth's surface and the flight in outer space. Thus, for the engines of the "Saturn" rocket (Figure 2.11) the maximum exhaust velocity and the specific impulse are respectively /2.27/:

for the liquid-fuel engines of the first stage, which use kerosene $+O_2$: at $h = 0$, $V_{\max 0} = 2550\,\text{m/sec}$, $I_0^\circ \approx 255$ sec; in vacuum, $V_{\max} = 2800\,\text{m/sec}$, $I^\circ \approx 280$ sec;

for the liquid-fuel engines of the other stages, which use $H_2 + O_2$: at $h = 0$, $V_{\max 0} = 3200\,\text{m/sec}$, $I_0^\circ \approx 320$ sec; in vacuum, $V_{\max} = 4200\,\text{m/sec}$, $I^\circ \approx 420$ sec.

The variation with altitude of thrust, effective exhaust velocity, and specific impulse of a high-altitude liquid-fuel engine is represented in Figure 2.12; the curve is based on the data given above (2.12), (2.18), and the data in Figure 1.4.

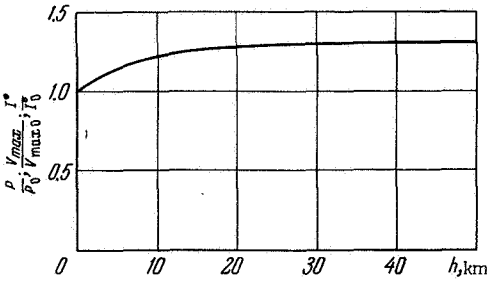

FIGURE 2.12. Variation with altitude of thrust, effective exhaust velocity, and specific impulse of high-altitude liquid-fuel engine.

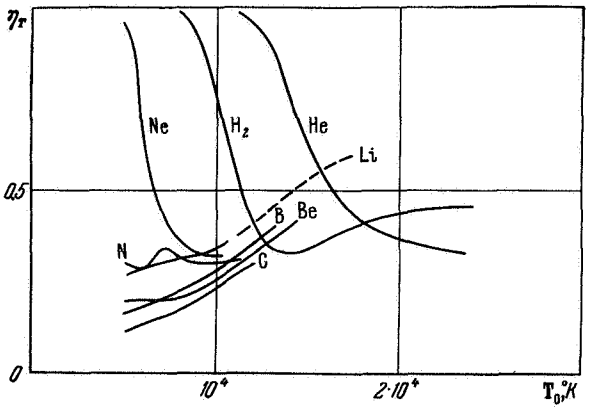

FIGURE 2.13. Thermal-energy fraction of gases as function of stagnation temperature ($p_0 = 10^4\,\text{kg/m}^2$).

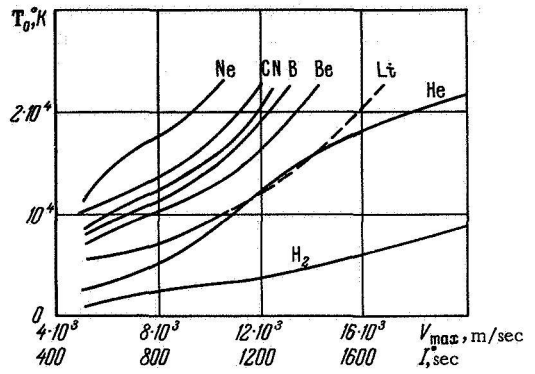

FIGURE 2.14. Maximum effective exhaust velocity and specific impulse in vacuum as functions of stagnation temperature.

3. **High-temperature thermal rocket engines.** Various proposals for increasing the effective exhaust velocity and the specific impulse have been discussed in the literature; these include replacing the combustion engines by thermal propulsion systems in which the working fluid is brought to a high temperature by an electrical discharge, using either a heat exchanger
48 heated by a nuclear or isotope reactor, or by solar energy (/2.28 –2.41/ etc.). A characteristic feature of such propulsion systems is the very high temperature T_0 of the gas at the nozzle inlet. When the gas temperature in front of the nozzle is high, a large part $(1 - \eta_T) N_\lambda$ of the energy supplied is spent on dissociation and ionization of the gas. The thermal-energy fraction of the gas defines the efficiency η_T whose temperature dependence
49 is given in Figure 2.13 for different working fluids /2.39/. A conservative estimate of the effective exhaust velocity and the specific impulse in high-temperature nozzles is obtained by assuming (cf. for instance /2.33, 2.39/) that during the short duration of expansion in the nozzle the dissociation and ionization energy of the gas is not liberated (so-called "frozen flow"). The effective exhaust velocity and the specific impulse can then be determined by a formula similar to (2.17), in which the efficiency η_T is taken into account if T_0 defines the total energy of the gas, namely,

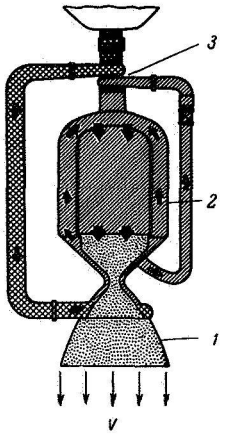

FIGURE 2.15. Thermal-propulsion engine with nuclear reactor:

1) nozzle; 2) nuclear reactor and heat exchanger; 3) working-fluid supply system.

$$V = \sqrt{\frac{\varkappa+1}{2\varkappa}\mathcal{R}T_0\eta_T}\left[\overline{\Gamma}_c z(\lambda_c)\frac{p_h\left(\frac{\varkappa+1}{2}\right)^{\frac{1}{\varkappa-1}}}{p_0 q(\lambda_c)}\right],$$

$$I^\circ = \frac{V}{g}. \qquad (2.19)$$

Using the data of /2.39/, we have plotted in Figure 2.14 the maximum effective exhaust velocity and the specific impulse in vacuum for high-temperature nozzles as functions of the stagnation temperature for different working fluids. The advantages of hydrogen as a working fluid are clearly seen, as it ensures high exhaust velocities at a minimum gas temperature. The thrust of such propulsion systems, which does not depend on the gas temperature, is determined from (2.12).

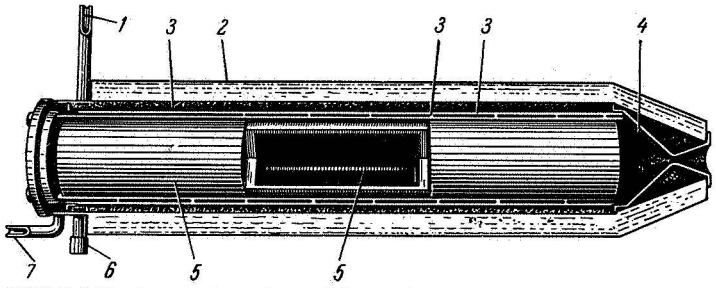

FIGURE 2.16. Isotope thermal-propulsion engine:

1) coolant pipe; 2) thermal insulation; 3) heat-exchanger duct for working fluid; 4) nozzle; 5) capsule with radioactive isotope; 6) supply-system valve; 7) working-fluid supply.

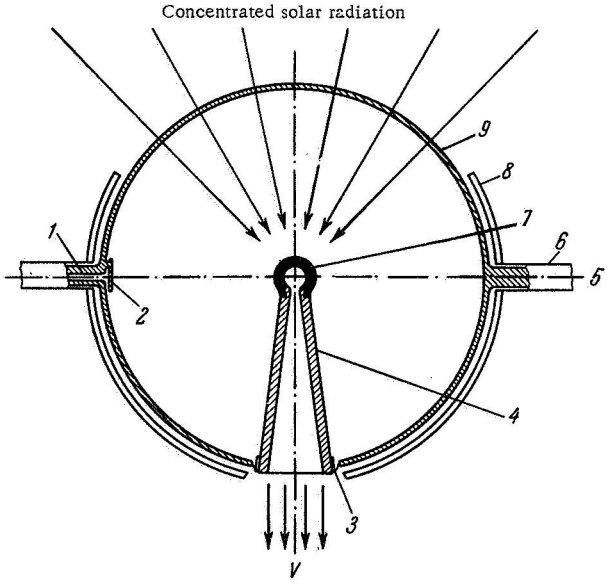

FIGURE 2.17. Thermal-propulsion engine with solar heating:

1) working-fluid (hydrogen) supply; 2) gas deflector; 3) joint between transparent quartz sphere and nozzle; 4) nozzle; 5) and 6) axis of rotation and bearings of orientation system; 7) porous heat exchanger and radiation collector; 8) multilayer screen; 9) transparent quartz sphere.

High-temperature thermal-propulsion engines with heat exchangers and a nuclear reactor /2.41/, an isotope reactor /2.40/, or a solar-radiation collector /2.39/, are shown in Figures 2.15 to 2.17.

In these engines a high-temperature gas stream is formed in the heat exchanger and accelerated to high exhaust velocities in the nozzle. The weights of the heat exchanger and nozzle should be analyzed together. The generalized layout of thermal-propulsion engines with heat exchangers is given in Figure 2.18. The heat-exchanger duct, in which the gas is heated to the stagnation temperature T_0 at the nozzle inlet, is represented by an equivalent

tube of diameter D and length L. As will be shown below (§ 2 of Chapter Two) the required heating of the gas determines the ratio $L/D = k_T$. Allowing
51 for erosion, we take the thickness of the duct wall as approximately proportional to the total pressure: $\delta \sim p_0$. The weight of the heat exchanger is then

$$G_т \sim \mathcal{F}_T LD\delta n_T \sim p_{0T}\mathcal{F}_T, \tag{2.20}$$

where $\mathcal{F}_T$ is the frontal area of the heat exchanger, $n_T \sim \frac{1}{D^2}$ is the number of heat-exchanger tubes per unit frontal area.

From $p_{0T}\mathcal{F}_T \sim p_0\mathcal{F}_*$ and (2.13) we find that the weight of the heat exchanger is proportional to the maximum thrust

$$G_т \sim p_0\mathcal{F}_* \sim P_{max}, \tag{2.21}$$

and, by analogy with (2.16), we obtain for high-temperature thermal-propulsion engines with heat exchangers

$$G_{\gamma T} = G_\gamma + G_т + G_\zeta + G_q \approx \gamma_T P_{max}, \tag{2.22}$$

where γ_T is the generalized unit weight of the engine (weight per unit thrust).

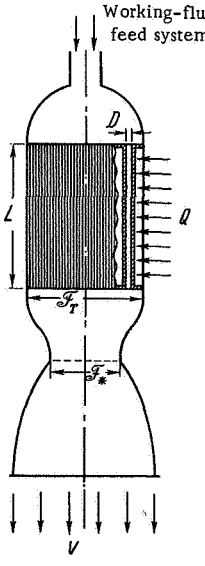

FIGURE 2.18. Thermal-propulsion engine with heat exchanger; Q is the thermal flux from energy source (nuclear reactor, isotope reactor, solar-radiation collector).

In nuclear thermal-propulsion engines, power increase causes a negligible increase in the weight G_n of the fissionable material representing the power source, since the latter accounts only for a small part of the engine weight. Therefore, for nuclear engines, $G_{\gamma T} \approx G_\xi$ ($G_\theta \approx 0$, $G_v = 0$). In isotope and solar-heat engines, on the other hand, the weight of the power source represents a substantial part of the total weight, and is determined in accordance with § 2 of this chapter. Tentative values of the generalized unit weight γ_T of thermal-propulsion engines with heat exchangers are given in Table 2.1 (/2.32, 2.39, 2.40/).

The maximum effective exhaust velocity and specific impulse in thermal-propulsion engines with heat exchangers depend on the maximum permissible gas temperature $T_{0\,max}$ (cf. (2.19) and Figure 2.14), which is determined by the temperature limitations of the engine materials. The properties of some high-melting materials for thermal-propulsion engines with heat exchangers are given in Table 2.2 /2.29/.

It is seen from this table that there are limitations to the thrust developable by engines with heat exchangers; thus, if the maximum permissible temperature for the heat exchanger is 2,800°K, the maximum exhaust velocity in vacuum of hydrogen (which is the optimum working fluid, cf. Figure 2.14) is $V_{max} \approx 8{,}000$ m/sec, $I^\circ \approx 800$ sec.

52 TABLE 2.1. Generalized unit weight of high-temperature thermal-propulsion engines with heat exchangers

Type of engine	$\gamma_T = \frac{G_{\gamma T}}{P_{max}}, \frac{kg}{kg}$
With heat exchanger and nuclear reactor	$\sim 5 \cdot 10^{-2}$
With heat exchanger and isotope reactor	~ 100
With heat exchanger and concentrated solar-radiation collector	$\sim 150^*$

* Including weight of solar-radiation collector

TABLE 2.2. Properties of some high-melting materials for thermal-propulsion engines with heat exchangers

Material	BeO	Graphite	W
Melting point, °K	2800	3900 (sublimates)	3650
Density at 20°C, kg/m^3	$2.7 \cdot 10^3$	$1.7 \cdot 10^3$	$19.1 \cdot 10^3$
Short-time tensile strength, kg/cm^2 . . .	70—280 at 1500°K	210—420 at 2780°K	350—630 at 2780°K

Considerably higher temperatures and exhaust velocities are possible in electric-arc propulsion engines, in which the working fluid is heated by an electric discharge (Figure 2.19). The arc is stabilized either magnetically or by causing the working fluid to flow around it. A large radial temperature gradient is created, which makes possible working-fluid temperatures of tens of thousands °K while the wall temperatures remain within permissible limits (cf. /2.42—2.45/); as a result, exhaust velocities $V_{max} \approx 25{,}000$ m/sec and specific impulses $I^\circ \approx 2{,}500$ sec can be attained.
53 The unit weight of an electric-arc engine is according to /2.33/ $\gamma = G_\gamma / P_{max} \approx 10$. The maximum gas temperature is limited by the temperatures permissible for the wall materials. Nevertheless, the maximum temperatures of the working fluid are considerably higher than in chemical or thermal-propulsion engines with heat exchangers. An important parameter is the engine efficiency $\eta_\gamma = N/N_\gamma$ defined as the ratio of the power N of the jet to the power N_γ consumed by the engine. According to /2.46/, the efficiency of an electro-arc propulsion engine remains almost constant when the exhaust velocity V and the mass flow rate q are varied, decreasing slightly with increasing V (Figure 2.20). Efficient regulation of the exhaust velocity V at a nearly constant useful power N is therefore possible when N_γ is limited; this is often advantageous from the viewpoint of flight mechanics (see below).

4. Electrodynamic and electrostatic engines These allow variations of the exhaust velocities V over a practically unlimited range up to relativistic values. The thrust developed by the heat engines considered so far is produced by the dynamic pressure of the gas on the nozzle walls. A by-product of this pressure is the heat energy transmitted to these walls, which limits the effective exhaust velocity and specific impulse of such engines. Electrodynamic and electrostatic propulsion engines, on the other hand, utilize the magnetic or electrostatic pressure on the nozzle walls; this practically removes the temperature-induced limitations on the effective exhaust velocity.

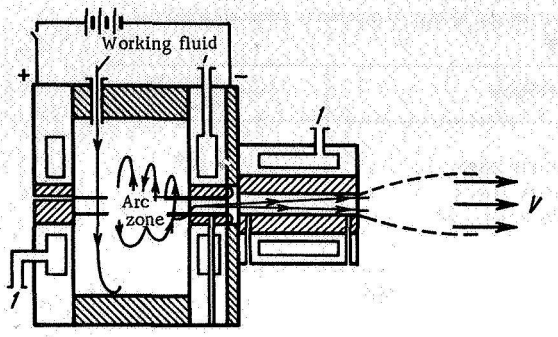

FIGURE 2.19. Electric-arc propulsion engine:
1) coolant inlet.

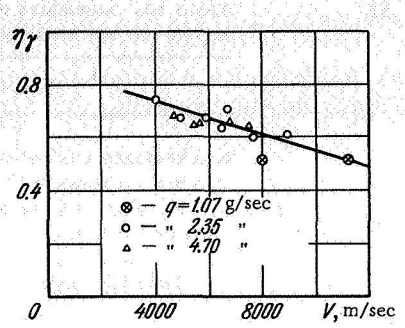

FIGURE 2.20. Experimental characteristic of electric-arc propulsion engine using helium as working fluid.

54 The operating principles of electrodynamic and electrostatic propulsion engines are discussed in detail in /2.32, 2.36, 2.38, 2.47—2.62/. We shall examine the properties of such propulsion engines. The magnetic pressure p_H and the electrostatic pressure p_E are respectively /2.63/

$$p_H = \frac{H^2}{8\pi}, \quad p_E = \frac{E^2}{8\pi}, \tag{2.23}$$

where H is the magnetic field strength, E is the electric field strength. The value of H is limited by the intensity of the current used to create the magnetic field. The commonly applied magnetic field strength $H \approx 1$ megaline $= 10{,}000$ gauss, corresponds to a magnetic pressure $p_H \approx \approx 4 \cdot 10^4$ kg/m^2. The value of E is limited by the dielectric strength of the insulation (including vacuum) between the conductors; the commonly applied electric field strength $E \approx 10^6$ v/m ≈ 30 CGSE units corresponds to an electrostatic pressure $p_E \approx 0.4$ kg/m^2.

It is thus seen that electrodynamic propulsion engines can develop much higher thrusts per unit midship section than electrostatic propulsion engines. Both pulsating and constant-action electrodynamic propulsion engines have been studied (cf. for instance /2.32, 2.36, 2.38, 2.57/). Figure 2.21 shows schematically the simplest pulsed rail accelerator, which was tested at the Atomic Energy Institute of AN SSSR in 1953 as a plasma injector to be used for studying thermonuclear processes /2.64/. In this accelerator the capacitor C_0 is discharged across a thin metallic wire ab stretched between two parallel rigid conductors ("rails"). When the spark gap P is closed the thin wire evaporates almost instantaneously; the vapor
55 is ionized and transformed into a plasma filament. The interaction between the electric current flowing along the plasma and the magnetic field of the conductors creates an electrodynamic force which accelerates the plasmoid along the "rails"; the magnetic pressure acting on the conductors determines the thrust. The main properties of the pulsed rail accelerator can be described with the aid of the following theoretical model /2.64—2.66/. If the mass m of the plasmoid is assumed to be constant during the acceleration period, the equation of motion becomes

$$m\frac{d^2x}{dt^2} = \frac{1}{2}\mathcal{J}^2\frac{d\mathcal{L}}{dx}, \tag{2.24}$$

where $\mathcal{J}$ is the current intensity in the circuit, $\mathcal{L}$ is the self-inductance of the circuit, the x-axis is directed along the rails; it is further assumed that the ohmic resistance of the circuit (including the plasma filament) may be neglected. The voltage across the rails is then

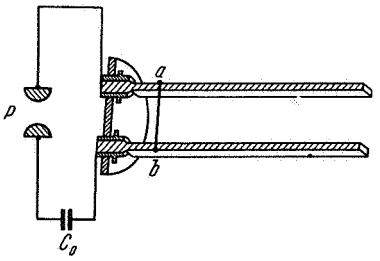

FIGURE 2.21. Pulsed rail accelerator: C_0 – capacitor; P – spark gap.

$$\mathcal{U} = \frac{d(\mathcal{L}\mathcal{J})}{dt}. \qquad (2.25)$$

The energy equation for the discharge of a capacitor of capacitance C_0 is

$$\mathcal{J} = -C_0 \frac{d\mathcal{U}}{dt}. \qquad (2.26)$$

When the plasmoid is accelerated along the "rails", the self-inductance of the circuit increases linearly with x:

$$\mathcal{L} = \mathcal{L}_0 + b_1 x, \qquad (2.27)$$

where $\mathcal{L}_0$ is the initial self-inductance of the circuit for $t=0, x=0$; $b_1 = \frac{d\mathcal{L}}{dx} =$ $=$ const. Substituting (2.27) in (2.24) we obtain the following system of equations:

$$\left.\begin{aligned} m\frac{d^2x}{dt^2} &= \frac{1}{2}\mathcal{J}^2 b_1, \\ \mathcal{U} &= \frac{d(\mathcal{L}\mathcal{J})}{dt}, \quad \mathcal{J} = -C_0\frac{d\mathcal{U}}{dt} \end{aligned}\right\} \qquad (2.28)$$

with initial conditions at $t=0$: $x=0$, $V=\frac{dx}{dt}=0$, $\mathcal{U}=\mathcal{U}_0$, $\mathcal{J}=0$.

56 An important parameter of this accelerator, considered as a propulsion engine, is the efficiency at which the energy stored in the capacitor $E=\frac{1}{2}C_0\mathcal{U}_0^2$ is converted into kinetic energy of the directed motion of the plasmoid:

$$\eta_\gamma = \frac{N}{N_\gamma} = \frac{mV^2}{C_0\mathcal{U}_0^2}. \qquad (2.29)$$

Introducing the dimensionless variables

$$\bar{x} = \frac{b_1}{\mathcal{L}_0}x, \quad \bar{t} = \frac{t}{\sqrt{\mathcal{L}_0 C_0}}, \quad \bar{\mathcal{U}} = \frac{\mathcal{U}}{\mathcal{U}_0}, \quad \bar{\mathcal{J}} = -\frac{d\bar{\mathcal{U}}}{d\bar{t}} = \frac{\mathcal{J}}{\mathcal{U}_0\sqrt{C_0/\mathcal{L}_0}}, \qquad (2.30)$$

the system of equations (2.28) becomes

$$\left.\begin{aligned} &\frac{d^2\bar{x}}{d\bar{t}^2} = \theta\left(\frac{d\bar{\mathcal{U}}}{d\bar{t}}\right)^2, \qquad \bar{\mathcal{U}} = \frac{d}{d\bar{t}}\left[(1+\bar{x})\frac{d\bar{\mathcal{U}}}{d\bar{t}}\right], \\ &\bar{x}(0)=0, \quad \frac{d\bar{x}}{d\bar{t}}(0)=0, \quad \bar{\mathcal{U}}(0)=1, \quad \frac{d\bar{\mathcal{U}}}{d\bar{t}}=0, \end{aligned}\right\} \qquad (2.28')$$

which depends only on the parameter

$$\theta = \frac{b_1^2 C_0^2 \mathcal{U}_0^2}{2m\mathcal{L}_0}, \qquad (2.31)$$

through which the energy-conversion efficiency is expressed in the form

$$\eta_\gamma = \frac{1}{20}\left(\frac{d\bar{x}}{d\bar{t}}\right)^2. \qquad (2.29')$$

Solutions of system (2.28') are given in /2.65/ and /2.66/. Comparison with experimental data shows that the theory satisfactorily describes the basic properties of pulsed rail accelerators. It follows from (2.30), (2.28'), (2.31), (2.29') that this propulsion engine can be controlled within wide limits. Thus, if at the end of the acceleration process of the plasmoid $(d\bar{x}/d\bar{t})_\gamma = \text{const}$ and $\theta = \text{const}$, then the efficiency remains constant throughout the control process $\eta_\gamma = \text{const}$. Considering the number of pulses per second k as the controlled variable, we obtain the following expressions for the mass flow rate q of the working fluid and the jet power N:

$$q = km, \quad N = \eta_\gamma k \frac{C_0 \mathscr{U}_0^2}{2}, \qquad (2.32)$$

57 so that

$$\theta = \frac{b_1^2 N C_0}{\mathscr{L}_0 \eta_\gamma q} = \text{const}. \qquad (2.33)$$

When the gap between the electrodes ("rails") is constant $b_1 = \text{const}$. Furthermore, for $\mathscr{L}_0 = \text{const}$, $\mathscr{U}_0 = \text{const}$, the capacitance C_0 of the capacitor and the number of pulses per second vary according to the law

$$C_0 \sim q, \quad k \sim \frac{1}{q}, \qquad (2.34)$$

and jet power and the power consumed by the engine remain constant ($N = \text{const}$, $N_\gamma = \text{const}$) when the exhaust velocity is varied; hence,

$$V = \sqrt{\frac{2N}{q}} \sim \sqrt{k}, \quad P = qV \sim \frac{1}{\sqrt{k}}. \qquad (2.35)$$

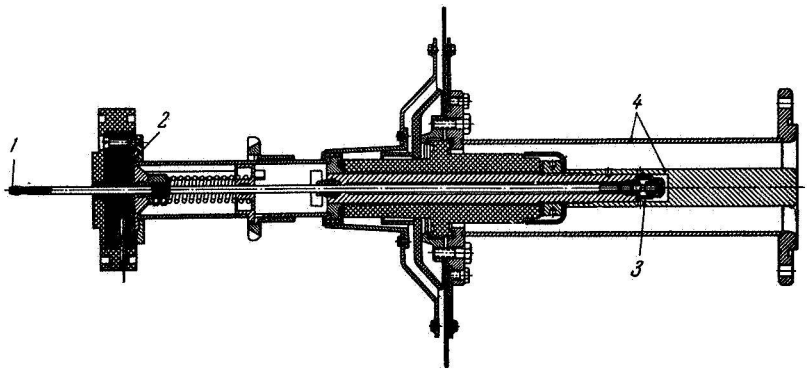

FIGURE 2.22. Coaxial pulsed plasma rail accelerator:

1) working-fluid supply; 2) solenoid actuating feed valve; 3) working-fluid feed valve; 4) coaxial electrodes (rails).

The maximum capacitance C_0 necessary is determined by the minimum exhaust velocity V. The pulse frequency k can be adjusted by means of a feed valve for the working fluid (gas) (Figure 2.22, /2.64/). When the rails, of
58 radii r_1 and r_2, are concentric, the inductance per unit length is

$$b_1 = \ln \frac{r_2}{r_1}.$$

Exhaust velocities up to 2×10^5 m/sec were attained in pulsating electrodynamic propulsion engines (cf. /2.33, 2.38/) at unit weights of the order of $\gamma = \frac{G_\gamma}{P_{max}} \approx 10-100$ kg/kg /2.36/. This does not include the weight of the capacitor which, although it represents the storage element of the system (cf. § 2 below), is an integral part of the engine.

A continuous-action electrodynamic propulsion engine /2.33/ is shown in Figure 2.23. The first stage is the electric arc heater, in which the working fluid is ionized to become plasma before entering the accelerator. The accelerator is of the crossed-fields type. The working fluid in it is a neutral plasma of conductivity σ_*. The voltage between the electrodes (Figure 2.23) creates in the accelerator channel an electric field of strength E, which causes a current of density i to flow through the plasma. The interaction between the magnetic field H (perpendicular to the electric field) and the electric current induces a force F_x, perpendicular to i and H, which accelerates the plasma, so that

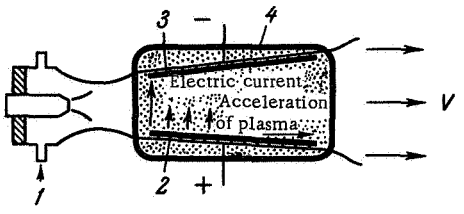

FIGURE 2.23. Electrodynamic propulsion engine with continuous plasma-jet discharge:

1) inlet of working fluid into arc ionizer; 2) anode; 3) cathode; 4) solenoid.

$$\bar{F}_x = \frac{iH}{\rho}, \qquad (2.36)$$

where $\bar{F}_x$ is the force acting on unit mass of the plasma, ρ is the density of the plasma.

Such a propulsion engine has, according to /2.33/, an efficiency $\eta_T \approx 0.8$ and a unit weight $\gamma = \frac{G_\gamma}{P_{max}} \approx$ of the order of 10 kg/kg at $V = 2\times10^4$ m/sec and
59 $N_T = 4800$ kw. This engine is regulated by varying the magnetic and electric fields; in accordance with (2.36), this changes the force accelerating the plasma.

Various electrodynamic propulsion engines with pulsating or continuous thrust have been described (/2.30−2.33, 2.36, 2.45, 2.57/); in principle they do not differ from those mentioned above. From the viewpoint of flight mechanics the main property common to electrodynamic propulsion engines is the possibility of varying the exhaust velocity within wide limits. This property is also shared by the electrostatic (ionic) propulsion engines.

While a quasineutral plasma is accelerated in electrodynamic propulsion engines, electrostatic propulsion engines accelerate charged particles, i.e.,

ions and electrons, which mix after acceleration to become a quasineutral jet (/2.31, 2.32, 2.36, 2.38, 2.47—2.56, 2.58—2.62/). Figure 2.24 shows schematically an electrostatic propulsion engine consisting of an ion source, an electrostatic accelerating system, and an electron emitter; $\mathcal{U}$ is the voltage giving rise to the electric field accelerating the ions, and $\Delta\mathcal{U}$ is a voltage applied to prevent inverse flow of electrons.

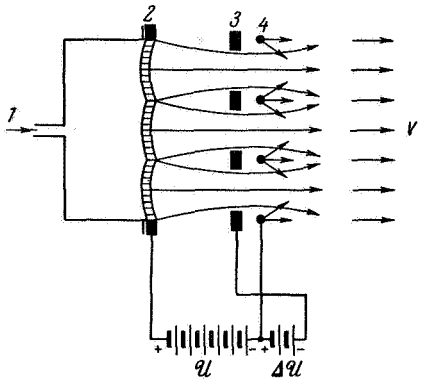

FIGURE 2.24. Electrostatic propulsion engine: 1) working-fluid supply; 2) ionizer; 3) electrostatic accelerating system; 4) electron emitter.

When charged particles of zero initial velocity are electrostatically accelerated, the final velocity V_i depends on the potential difference $\mathcal{U}$ of the accelerating field through which the particle has passed:

$$V_i = \sqrt{2\mathcal{U}\frac{e}{\mu}}, \qquad (2.37)$$

where e is the charge, and μ the mass of the particle.

The flow of charged particles constitutes an electric current $\mathcal{J}$, related to the mass flow rate as follows:

$$q_i = \frac{\mu}{e}\mathcal{J}. \qquad (2.38)$$

60 The thrust and jet power developed by the ion beam are respectively

$$P_i = q_i V_i = \mathcal{J}\sqrt{2\mathcal{U}\frac{\mu}{e}}, \quad N_i = \frac{q_i V_i^2}{2} = \mathcal{J}\mathcal{U}. \qquad (2.39)$$

The condition of quasineutrality of the jet requires that ion and electron beams represent equal currents ($\mathcal{J}_i = \mathcal{J}_e$) and have the same particle velocities ($V_i = V_e$); hence,

$$\frac{P_e}{P_i} = \frac{N_e}{N_i} = \frac{\mu_e}{\mu_i}. \qquad (2.40)$$

For singly charged ions the ratio of an electron to an ion mass, $\mu_e/\mu_i \approx 10^{-5}$; it follows therefore from (2.40) that the contribution of the electrons to the thrust and power of the electrostatic propulsion engine may be neglected. For this reason the name ion propulsion engine has been adopted. In accordance with the Child-Langmuir law (cf. for instance /2.67/), the maximum thrust of the ion propulsion engine is determined by the maximum current density $i = \mathcal{J}/\mathcal{F}$ of the ion beam created by the electrostatic accelerating system ($\mathcal{F}$ is the cross-sectional area of the ion beam); this current density is limited due to the space charge created by the ions, which counteracts the accelerating effect of the electric field. The potential $\mathcal{U}$ at every point of the electric field is related to the density ρ_i of the space

charge by Poisson's equation

$$\nabla^2 \mathcal{U} = -4\pi\rho_i. \tag{2.41}$$

Using (2.37), the parameters of the ion beam are found in the two-dimensional case by integrating the following differential equation:

$$\frac{d^2\mathcal{U}}{dx^2} = 2\sqrt{2}\pi \sqrt{\frac{\mu}{e}} \frac{i}{\sqrt{\mathcal{U}}}, \tag{2.42}$$

where $i = \frac{\mathcal{J}}{\mathcal{F}} = -\rho_i V_i$. The boundary conditions are: at $x = 0$, $\mathcal{U} = 0$, $d\mathcal{U}/dx = 0$.

Integrating, we obtain the maximum possible ion-current density i_{max} created by the electrostatic accelerating system (potential = $\mathcal{U}$, distance between electrodes = d):

$$i_{\max} = \frac{\sqrt{2}}{9\pi} \sqrt{\frac{e}{\mu}} \frac{\mathcal{U}^{3/2}}{d^2}, \quad q_{i\max} = \frac{\sqrt{2}}{9\pi} \sqrt{\frac{\mu}{e}} \frac{\mathcal{U}^{3/2}}{d^2} \mathcal{F}, \tag{2.43}$$

61 and from (2.39) the maximum thrust developed:

$$P_{\max} = \frac{2}{9\pi} \frac{\mathcal{U}^2}{d^2} \mathcal{F}. \tag{2.44}$$

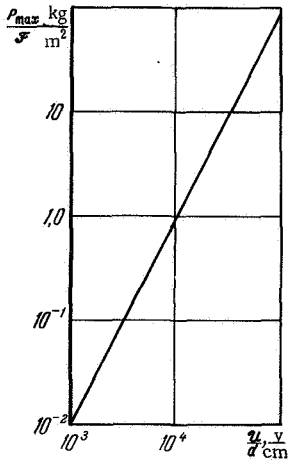

FIGURE 2.25. Unit thrust of ion propulsion engine as function of accelerating voltage and gap between electrodes.

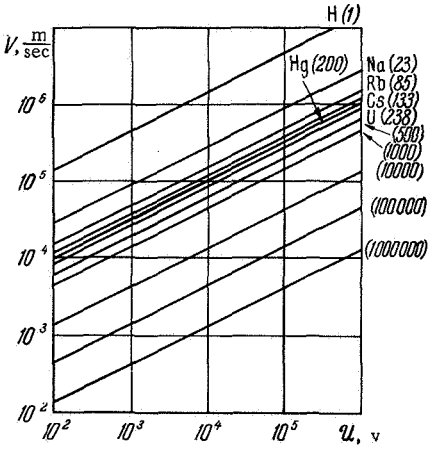

FIGURE 2.26. Exhaust velocity of ion beam as function of accelerating voltage; atomic weights of atoms or colloidal particles are given in parentheses.

The maximum thrust developed is thus independent of the properties of the working fluid (ion mass μ and charge e), depending only on the electrostatic pressure, which is proportional to the square of the electric field strength; $P \sim \mathcal{U}^2/d^2$ (cf. (2.23)). The thrust per unit area (unit thrust) $P_{max}/\mathcal{F}$ has been plotted in Figure 2.25 as a function of the accelerating voltage $\mathcal{U}$

and the gap d between the electrodes. The maximum unit thrust is limited, since arcing between the electrodes takes place at electric field strengths exceeding $\sim 10^8$ v/m (/2.53, 2.67/).

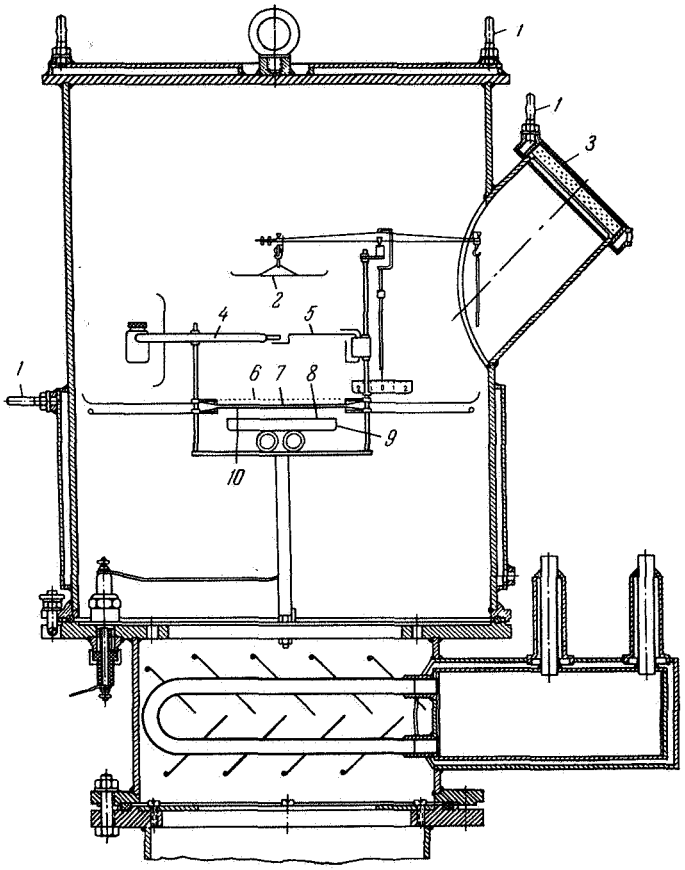

FIGURE 2.27. Laboratory model of ion propulsion engine with contact-surface ionization:

1) cooling of vacuum-chamber housing; 2) scales for measuring thrust; 3) observation window; 4) – 5) working-fluid (cesium) supply system; 6) screening grid; 7) accelerating grid-electron emitter; 8) tungsten ionizer; 9) ionizer heater; 10) blocking grid.

The exhaust velocity V_i, on the other hand, depends largely on the properties of the working fluid (cf. (2.37)). Figure 2.26 shows the exhaust velocity as a function of the accelerating voltage $\mathcal{U}$ for the ions of several working fluids and for heavy colloidal particles /2.53/.

62 It is seen from Figures 2.25 and 2.26 that the ion propulsion engine can be regulated within very wide limits. However, (2.44) defines the maximum thrust attained at the maximum possible ion-current density i_{max} (2.43) and the maximum working-fluid mass flow rate $q_{i\,max}$. The properties of ion propulsion engines are thus largely determined by the characteristics of the ion sources.

63 In addition to electric-arc ion sources (similar to the electric-arc propulsion engines considered above), two other types of ion sources based on contact ionization (cf. Figure 2.27 /2.50/ showing a laboratory model), and on bombardment volume ionization (cf. below) have been thoroughly discussed (/2.31, 2.32, 2.36, 2.38, 2.47—2.56, 2.58—2.62, 2.67—2.69/).

In ion sources with contact ionization (Figure 2.27) atoms of low ionization potential, constituting working fluid, are ionized when they come into contact with the heated surface of a material having a high work function (the ion source).

The ionization potential of the working fluid is the energy necessary for removing an outer electron from the atom. The work function of the ionizer material corresponds to the energy of the captured electron. The probability of ionizing events (capture of outer electrons of working-fluid atoms by the ionizer surface) increases with increasing difference between the work function and the ionization potential. This difference is maximum in the pair Cs—W (/2.53, 2.68/) (cf. 2.3 and 2.4, where the work function and the ionization potential are given in electron-volts).

TABLE 2.3. Ionization potential of some elements

Element	Atomic weight	Ionization potential, ev	Element	Atomic weight	Ionization potential, ev
He	4.003	24.50	Li	6.940	5.36
Kr	83.800	13.90	Na	22.991	5.12
H	1.008	13.50	K	39.100	4.32
C	12.011	11.20	Rb	85.480	4.16
Hg	200.610	10.39	Cs	132.910	3.87

TABLE 2.4. Work function and melting point of some metals

Metal	Work function, ev	Melting point, T°C	Metal	Work function, ev	Melting point, T°C
Ta	4.10	3027	C	4.81	3550
Mo	4.30	2620	Ir	4.90	2454
Cr	4.37	1890	Re	5.10	3167
Os	4.50	2700	Pt	5.20	1773
Ag	4.70	960	W	5.50	3370

The ions formed when the working fluid comes into contact with the ionizer surface must have sufficient thermal energy to move away, since otherwise the layer of atoms adsorbed on the surface would reduce the work function and thus the ionization. Figure 2.28 shows the degree of ionization K of cesium as a function of the temperature T of the tungsten ionizer surface, where K is the ratio of the number of ions formed to the
64 number of cesium atoms in contact with the ionizer surface. It is seen that above a minimum temperature T_i (which depends on the ion-current density i), at which the cesium layer adsorbed on the ionizer surface disappears, the degree of ionization approaches unity. Figure 2.28 shows that the

ion-current density $i \leqslant i_{max}$ (and thus the working-fluid mass flow rate $q_i \leqslant q_{i\,max}$, cf. (2.43)) depends on the temperature of the ionizer surface and can be varied by adjusting the supply of working fluid and the ionizer temperature. From the viewpoint of spaceflight applications it is important that the mass-flow regulation in the ion accelerator is not linked with the exhaust velocity V_i, which depends only on the accelerating voltage $\mathcal{U}$. This is very important in spaceflight. When the temperature T_i (Figure 2.28) is exceeded, the ion-current density i and the working-fluid mass flow rate q_i are limited in accordance with the Child-Langmuir law (cf. (2.43)). The maximum possible thrust depends only on the accelerating electric field strength $\mathcal{U}/d$ (cf. (2.44) and Figure 2.25). Thus, at an ionizer temperature $T \approx T_i = 1173\,°K$ ($\mathcal{J} \approx 70$ ma, $\mathcal{F} = 70$ cm, $i \approx 1$ ma/cm^2) the laboratory model of an ion propulsion engine /2.50/ developed a maximum thrust $P_{max} \approx 5 \times 10^{-4}$ kg, corresponding to accelerating electric field strength $\mathcal{U}/d \approx$ $\approx$ 3000 v/cm. The exhaust velocity of the ion beam was $V_i \approx 70{,}000$ m/sec in these experiments (specific impulse $I° \approx 7000$ sec).

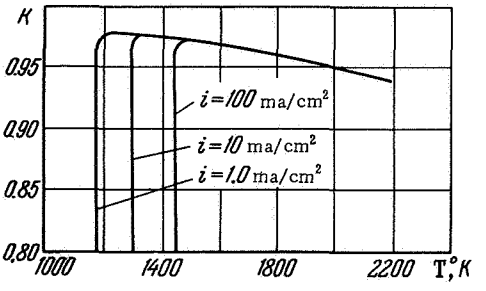

FIGURE 2.28. Degree of cesium ionization as function of tungsten-ionizer surface temperature.

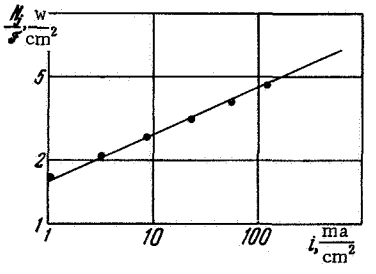

FIGURE 2.29. Radiation losses from incandescent tungsten-ionizer surface for contact-surface ionization of cesium.

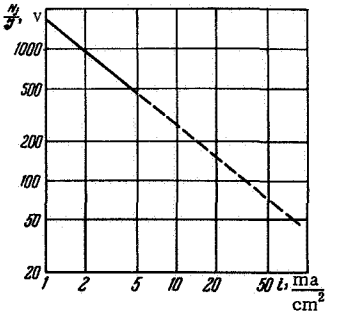

FIGURE 2.30. Specific power losses in ion propulsion engine with contact ionization of cesium on tungsten, as function of maximum ion-current density (i_{max} corresponds to a breakdown voltage $\mathcal{U}_{max} \approx 10{,}000$ v for $d = 1$ cm).

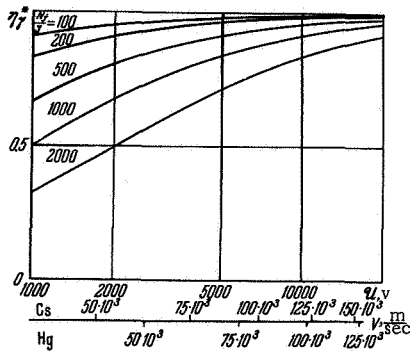

FIGURE 2.31. Efficiency of ion propulsion engine using cesium or mercury vapors as working fluid, as function of exhaust velocity.

The power N_j lost by radiation from the incandescent ionizer surface /2.53/ represents the principal power loss in ion propulsion engines with contact ionization. These losses

$$N_T - N_i \approx N_j = \sigma\omega T_i^4 \mathcal{F} \tag{2.45}$$

are related to the ion-current density i ($T_i = f(i)$) and to the cross-sectional area of the ion beam, but do not depend on the exhaust velocity V_i (i.e., on the accelerating voltage $\mathcal{U}$). According to /2.53/, in the case of ionization of cesium by tungsten the specific loss $N_j/\mathcal{F}$ (w/cm²) is related to the ion-current density i (ma/cm²) as follows (Figure 2.29):

$$\lg \frac{N_j}{\mathcal{F}} = 0.20 + 0.22 \lg i. \tag{2.46}$$

It is convenient to refer the power loss in the ion propulsion engine to the total current $\mathcal{J}$ of the ion beam; measured in ev/ion (in electron-volts per ion, i.e., in volts), the ratio $N_j/\mathcal{J}$ represents the potential difference for each ion, equivalent to the power loss (Figure 2.30). The energy efficiency of the ion propulsion engine can be expressed through the useful
66 potential difference $\mathcal{U}$ accelerating the ion beam (cf. (2.37));

$$\eta_T^* = \frac{N_i}{N_T} = \frac{\mathcal{U}}{\mathcal{U} + \frac{N_j}{\mathcal{J}}} = \frac{V_i^2}{V_i^2 + 2\frac{e}{\mu}\frac{N_j}{\mathcal{J}}}. \tag{2.47}$$

Figure 2.31 shows the energy efficiency of an ion propulsion engine as a function of the exhaust velocity when cesium or mercury is used as a working fluid. It is seen from a comparison of Figures 2.31 and 2.30 that ion propulsion engines with contact ionization of cesium by tungsten have high energy efficiencies, approaching unity when the exhaust velocity is large; this was confirmed by experiments /2.54/. The unit weight of an ion propulsion engine with contact ionization is $\gamma = G_T/P_{max} \approx 750 - 1750$, according to /2.54/.

Also well known is the electron-bombardment ion source (/2.52, 2.54, 2.56, 2.59, 2.61, 2.62, 2.67—2.69/), in which atoms of gas are ionized through inelastic collisions with electrons having energies of tens of electron volts, as in discharges in gas (/2.67—2.69/). Ionization of

the atoms of a gas or vapor by electron impact is characterized by the ionization probability p_i, which represents the average number of ionizing events in which an electron of energy is involved over a path of 1 cm at a pressure of 1 mm Hg at 0°C. Figure 2.32 shows the ionization probability as a function of the electron energy for four elements.

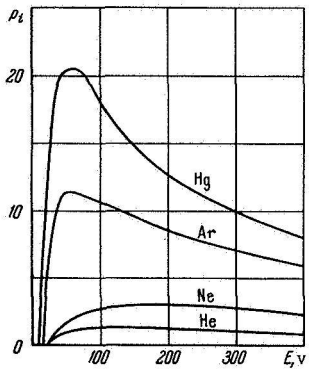

FIGURE 2.32. Probability of ionization, through collision with electrons, of mercury, argon, neon, and helium.

The high ionization probability of mercury vapor at low electron energies led to their selection as a working fluid in ion propulsion engines with electron-bombardment ionization (cf. /2.52, 2.56/).

Irrespective of the type of ion source, the ion-current density is relatively small because of the limitations in the electrostatic accelerating system. Hence, the pressure in the ionization chamber must be low ($\sim 10^{-4}$ mm Hg) to ensure a relatively small parasitic discharge of neutral atoms of the working fluid. At an ionization-chamber pressure $p_i \sim 10^{-4}$ mm Hg and an ionization probability $p_i \approx 20$ (Figure 2.32), the free path l_i of an electron up to an ionizing event is

$$l_i = \frac{1}{p_i p_i} \approx 5 \cdot 10^2 \text{cm}$$

Efficient ionization by electron impact is obtained at a relatively small characteristic dimension of the ionization chamber $D_i \ll l_i$ with the aid of electromagnetic traps similar to those used in thermonuclear research /2.64/.

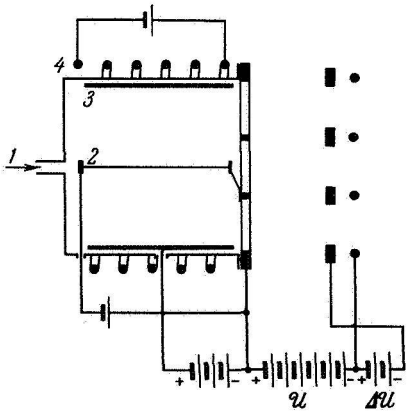

FIGURE 2.33. Schematic layout of ion propulsion engine with ionization of mercury vapors by electron bombardment:

1) working-fluid supply; 2) cathode; 3) anode; 4) solenoid.

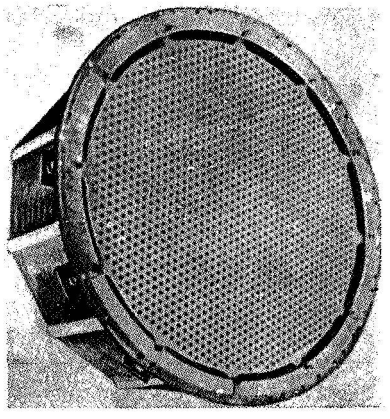

FIGURE 2.34. Ion propulsion engine with electron-bombardment ionization, using mercury as working fluid.

Figure 2.33 and 2.34 show an ion propulsion engine with ionization of mercury vapor by electron bombardment (P_{max} = 0.06 kg, G_Y = 19.5 kg, $V = 91 \cdot 10^3$ m/sec). The revolving toroidal ionizing electron cloud is
68 formed by an electromagnetic trap created by a radial electric field (central cathode and cylindrical anode in the chamber) and a longitudinal magnetic field created by an external solenoid. The electrons are emitted by the incandescent cathode; a potential of several tens of volts applied to the anode provides the energy necessary for ionization, while the weak longitudinal magnetic field created by the solenoid prevents direct impingement of the electrons on the anode. The mercury vapor is ionized by collisions with electrons during its passage through the revolving electron cloud. The ion beam is then accelerated as shown in Figure 2.24. Ion propulsion engines with electron-bombardment ionization can be regulated in the same way as ion propulsion engines with contact ionization.

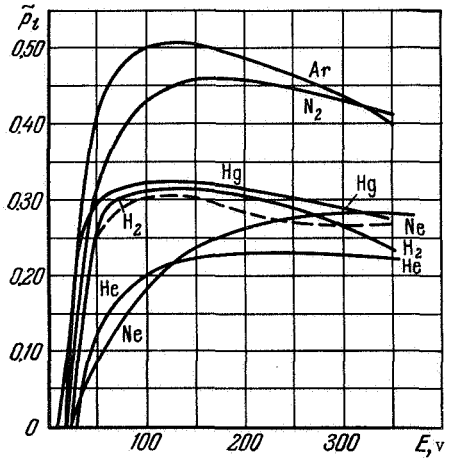

FIGURE 2.35. Probability $\tilde{p}_i$ of ionization at each collision as function of electron energy.

Table 2.3 shows that the ionization potential of mercury is 10.39 v. During electron-bombardment ionization, however, only some of the collisions lead to the formation of ions /2.67/ (Figure 2.35). In addition, ions are lost on the ionization-chamber walls and on the anode, and energy is used to heat the cathode and feed the solenoid. According to /2.52/, /2.56/, the specific power losses in ion propulsion engines with electron-bombardment ionization of mercury vapor considerably exceed the ionization potential; $N_j/\mathcal{J} \approx 500$ v, nevertheless, this ensures a high energy efficiency η_Y^* (cf. Figure 2.31).

The propulsive-mass efficiency of ion propulsion engines with electron-bombardment ionization is

$$\eta_\mu = \frac{q_i}{q}, \qquad (2.48)$$

69 and represents the ratio of the mass flow rate q_i of the ion beam to the total mass flow rate q of the working fluid. The maximum values of η_μ in ion propulsion engines with contact ionization are determined by the degree of ionization, and are close to unity according to Figure 2.28. In ion propulsion engines with electron-bombardment ionization, some neutral atoms escape from the ionization chamber through the nozzle (cf. Figures 2.33 and 2.34). The propulsive-mass efficiency of such engines is $\eta_\mu \approx 0.8 - 0.9$ according to /2.61/. Since the neutral atoms move at thermal velocities which are much lower than the velocities of the ions in the beam, the contribution of these atoms to the thrust and useful power may be neglected.

We thus obtain from (1.4), (1.5) [and (2.47)]:

$$\left.\begin{aligned} P = q_i V_i = qV, \quad V = \eta_\mu V_i, \\ \eta_\gamma = \frac{N}{N_\gamma} = \frac{\frac{1}{2} qV^2}{N_\gamma} = \eta_\mu \eta_\gamma^*. \end{aligned}\right\} \tag{2.49}$$

The unit weight of ion propulsion engines with electron-bombardment ionization is according to /2.64/ $\gamma = G_\gamma / P_{max} \approx 250-500$; it decreases slightly with increasing maximum exhaust velocity (Figure 2.36).

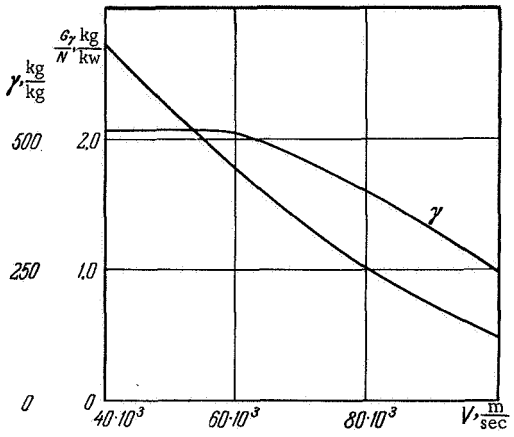

FIGURE 2.36. Unit weight of ion propulsion engines with electron-bombardment ionization, using mercury as working fluid.

70 It is thus seen that in electrostatic propulsion engines the exhaust velocity V and the thrust P can be regulated within wide limits without loss of efficiency.

5. Solar sail. The thrust in a propulsion system with solar sail is developed by a mirror surface which reflects the sunlight (Figure 2.37). The idea of using the pressure of sunlight for spaceflights appeals by its simplicity. It was first seriously considered in 1924 and 1925 by F. A. Tsander, who suggested the use of mirrors made of thin aluminum sheets. Tsander shows that interplanetary flight is theoretically possible with the aid of sunlight pressure. Thus, when the aluminum mirror is one thousandth of a millimeter thick a spacecraft weighing one ton can be transferred from the orbit of the Earth to the orbit of Mars in about 300 days; the sail of this spacecraft would weigh about 400 kg and have an area of $\sim 0.15 \cdot 10^6$ m^2, equivalent to that of a circular sail of $\sim$ 450 m diameter.

The solar-sail engine develops a thrust by using the energy and mass flux of the electromagnetic radiation of the Sun (cf. (1.17), (1.18)). Interaction between the solar radiation flux and the sail surface changes the momentum of the photon stream.

The thrust developed by a flat sail of area S, illuminated by the Sun, is by (1.18) /2.72/

$$\mathbf{P} = \tfrac{1}{2} p_A \left(\frac{R_\odot}{R}\right)^2 S \sqrt{1 + \varepsilon^2 + 2\varepsilon \cos 2(\widehat{\mathbf{ni}})}\, (\mathbf{n} \cdot \mathbf{i})\, \mathbf{e}; \tag{2.50}$$

71 the direction of thrust lies between the normal **n** to the shady side of the sail and the direction of the sunrays (**i**) (Figure 2.38):

$$\widehat{\mathbf{nP}} = \arcsin \frac{(1-\varepsilon)\sin(\widehat{\mathbf{ni}})}{\sqrt{1+\varepsilon^2+2\varepsilon\cos 2(\widehat{\mathbf{ni}})}}, \qquad (2.51)$$

where **n** is the unit vector normal to the surface, **i** is the unit vector in the direction of the sunrays, $\widehat{\mathbf{ni}}$, $\widehat{\mathbf{nP}}$ are respectively the angles between the vectors **n** and **P**, **n** and **i**, $(\mathbf{n}\cdot\mathbf{i})$ is the scalar product of the unit vectors **n** and **i** (i.e. $(\mathbf{n}\cdot\mathbf{i}) = \cos\vartheta$).

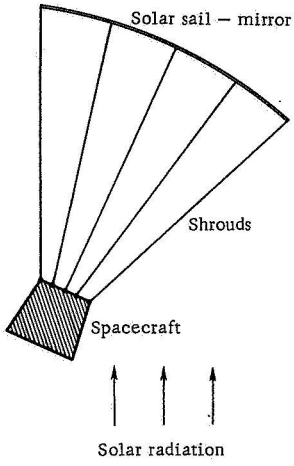

FIGURE 2.37. Spacecraft with solar sail.

The parameter of the solar sail as a propulsion system, on which direction and magnitude of the thrust depend, is the angle ϑ at which the sail is set.

When the sunlight is completely absorbed by the surface of the sail ($\varepsilon = 0$), we have, according to (2.50), (2.51):

$$\mathbf{P}_{\varepsilon=0} = \frac{1}{2} p_{\text{Å}} \left(\frac{R_\odot}{R}\right)^2 S\cos\vartheta\,\mathbf{i}, \qquad (2.52)$$

i.e., in the limiting case of a completely absorbing sail the thrust is in the direction of the sunrays, irrespectively of the angle at which the sail is set.

When the mirror surface is perfectly reflecting ($\varepsilon = 1$), the direction of thrust coincides with the normal to the shady side of the sail, and can be regulated by varying the orientation of the sail relative to the direction of the sunrays (Figure 2.39):

$$\mathbf{P}_{\varepsilon=1} = p_{\text{Å}} \left(\frac{R_\odot}{R}\right)^2 S\cos\vartheta\,\mathbf{n}. \qquad (2.53)$$

All contemporary studies of solar sails (cf. Chapter Nine) are limited to this simple case. Additional possibilities of thrust control are obtained in a system of mirrors set at different angles to the sunrays (/2.71/).

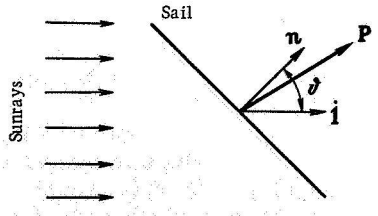

Figure 2.38 Direction of thrust of solar sail.

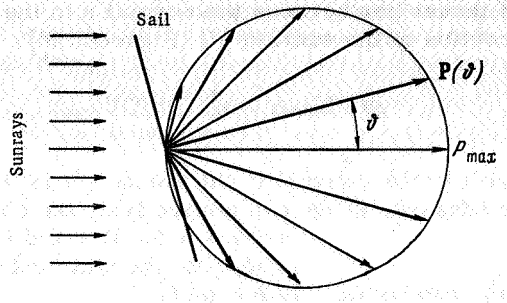

FIGURE 2.39. Thrust of solar sail with perfectly reflecting mirror surface as function of angle at which sail is set.

Aluminum and silver (used as materials or coatings for the solar sail) possess reflection coefficients close to unity (Figure 2.40); we may, therefore, assume that $\varepsilon = 1$ in a tentative analysis of the characteristics of the solar-power spacecraft /2.32/.

72 Consider the weight necessary for developing a given thrust by means of a flat solar sail. The only weight to be taken into account is that of the sail proper:

$$G_\gamma = kgS\sum\rho\delta, \qquad (2.54)$$

where ρ is the density of the material of the sail layers, δ is the thickness of each layer, k is a coefficient by which the weight of ancillary elements of the sail structure is taken into account; according to /2.73/ $k \approx 1$.

The maximum thrust P_{max} developed by a sail set perpendicular to the sunrays ($\vartheta = 0$), is, according to (2.53) for $\varepsilon = 1$

$$P_{max} = p_A\left(\frac{R_\delta}{R}\right)^2 S. \qquad (2.55)$$

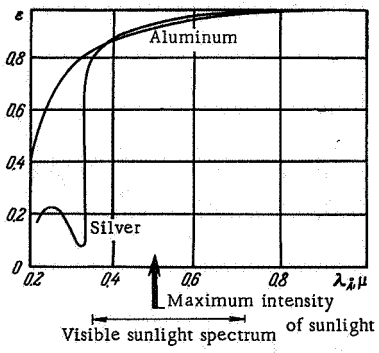

FIGURE 2.40. Reflection coefficient of metallic surfaces as function of wavelength of incident sunrays.

The unit weight of the sail as a propulsion engine is

$$\gamma = \frac{G_\gamma}{P_{max}} = \frac{kg\Sigma\rho\delta}{p_A\left(\frac{R_\delta}{R}\right)^2}, \qquad (2.56)$$

and the expression

$$a_{max} = \frac{g}{\gamma} \qquad (2.57)$$

is the maximum acceleration which can be given to the spacecraft by the solar sail (for $G = G_\gamma$).

73 Figure 2.41 gives tentative values of the unit weight of a solar sail and of the maximum acceleration developed by it (in Earth's orbit, $R_\delta/R = 1$, and for $k = 1$) as functions of the thickness of its material, which is either aluminum ($\rho g \approx 2.7 \cdot 10^3$ kg/m^3) or aluminized plastic film ($\rho g \approx 1.2 \cdot 10^3$ kg/m^3). With the sail thicknesses discussed in the books mentioned ($\delta \sim 10^{-6}$ m for aluminum foil and $\delta \sim 2.5 \cdot 10^{-6}$ m for aluminized plastic film) the unit weight of the solar

sail in the Earth's orbit is $\gamma \approx 3{,}000$ kg/kg, and the maximum acceleration imparted to the spacecraft by the sail $a_{max} \approx 3 \cdot 10^{-3}$ m/sec^2. The unit weight cannot be reduced much further by the use of thinner films, since the mirror properties of the surface are lost at thicknesses of the order of the wavelength of visible light and because thin films are subject to sublimation in vacuum and to micrometeoric erosion.

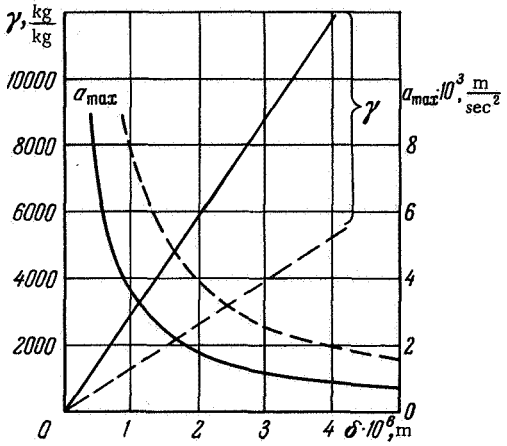

FIGURE 2.41. Unit weight of solar sail and maximum acceleration developed by it (in Earth's orbit) as functions of its thickness; solid curves refer to aluminum foil, dashed curves to aluminized plastic film.

However, even with the sail characteristics shown in Figure 2.41, corresponding to a thickness of between $1 \cdot 10^{-6}$ to $2.5 \cdot 10^{-6}$ m, a solar sail can transfer the spacecraft from the Earth's orbit to that of a near planet in 100 to 200 days (cf. Chapter Nine).

74 **6. Isotope sail.** Another type of propulsion device discussed in the literature is the isotope sail, which develops thrust through the discharge of α-particles on one side (/2.32, 2.38/). Although radioactive isotopes (cf. Table 2.8 and § 2) can release both α-particles (helium ions) and β-particles (electrons) of high energy, α-particles are to be preferred because of their considerably higher mass and lower penetrating power. The latter property is particularly important, since the main problem which has to be solved with regard to the isotope sail functioning as a propulsion device is the release of α-particles on one side only [the α-particles released in the opposite direction must be absorbed]. Figure 2.42 shows schematically an isotope sail /2.32/ using as α-particle source radioactive Po^{210} applied in a thin layer of thickness δ^* on a plastic film of thickness δ^{**} which acts as a particle absorber. A beam of positively charged α-particles is emitted which must be neutralized by a supply of electrons. The main parameters of an isotope sail are given in Table 2.5.

Table 2.5 shows that the thickness δ^{**} of the plastic film is selected so as to be equal to the range of the α-particle in the plastic; this reduces substantially the flow of α-particles beyond the plastic film. The thickness δ^* of the Po^{210} layer is selected so as to be one tenth of the range of
75 α-particles in Po^{210} so that about half the α-particles formed escape from the

sail on the side of the isotope layer /2.32/. The mass flow rate is determined by the number of α-particles formed during radioactive decay:

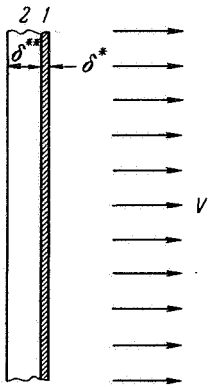

FIGURE 2.42. Isotope sail:

1) layer of Po^{210} – (α-source);
2) plastic film – (absorber of α-particles).

$$q = \frac{1}{2}\lambda_\tau \frac{A^* \rho^*}{A} S\delta^* m_\alpha e^{-\lambda_\tau t}, \qquad (2.58)$$

where A is the atomic weight of the isotope, A^* is Avogadro's number, S is the surface area of the sail; the other symbols are indicated in Table 2.5.

The exhaust velocity V is determined by the energy E_α of the α-particles; the effective value of V, averaged over a hemisphere, is equal to half the true velocity of the α-particles:

$$V = \frac{1}{2}\sqrt{2E_\alpha/m_\alpha}. \qquad (2.59)$$

By (2.58) and (2.59) the thrust developed by the isotope sail is

$$P = qV = \frac{1}{2\sqrt{2}}\lambda_\tau \frac{A^* \rho^*}{A} S\delta^* m_\alpha^{3/2} E_\alpha^{1/2} e^{-\lambda_\tau t}. \qquad (2.60)$$

For the values given in Table 2.5, the unit thrust, the unit weight, and the exhaust velocity are respectively

$$\left.\begin{aligned} &\frac{P_{\max}}{S} \approx 2.6\cdot 10^{-6} e^{-\lambda_\tau t}\,\mathrm{kg/m^2}, \gamma = \frac{G_\gamma}{P_{\max}} \approx 25\,000, \\ &V \approx 8\cdot 10^6\,\mathrm{m/sec}, \frac{gq_0}{G_\gamma} = \frac{gP_{\max}}{VG_\gamma} \approx 5\cdot 10^{-11} \ll \lambda_\tau. \end{aligned}\right\} \qquad (2.61)$$

From the viewpoint of flight mechanics the isotope sail is a propulsion device developing a thrust varying slowly with time, and having a mass flow rate of practically zero.

TABLE 2.5. Parameters of isotope sail

ρ^* – density of Po^{210}, g/cm³	9.2
m_α – mass of α-particle, g	$6.7\cdot 10^{-24}$
$\frac{1}{\lambda_\tau}$ – half-life of Po^{210}, days	138
λ_τ – decay constant of Po^{210}, 1/sec	$5.8\cdot 10^{-8}$
E_α – energy of α-particle of Po^{210}, j	$8.5\cdot 10^{-13}$
Range of α-particle in Po^{210}, m	$6.5\cdot 10^{-6}$
δ^* – thickness of Po^{210} layer, m	$6.5\cdot 10^{-7}$
ρ^{**} – density of plastic, g/cm³	2.0
Range of α-particle in plastic, m	$3\cdot 10^{-5}$
δ^{**} – thickness of plastic layer, m	$3\cdot 10^{-5}$

More far-fetched (photon, thermonuclear, etc.) propulsion devices are also discussed in the literature; basic information on their operating principles is given, e.g., in /2.32/.

1. Energy sources. The power requirements of spacecraft can be supplied by chemical, nuclear, radioisotope and solar energy (2.2, 2.7—2.11, 2.27—2.33, 2.38/ and others).

Sources of chemical energy are substances capable of participating in exothermal reactions. The most common of the latter is oxidation (burning) in which a fuel and an oxidizer participate. Another exothermal reaction is the disintegration of some substances, utilized in engines with a single working fluid. From the viewpoint of flight mechanics, the main parameters of chemical-energy sources are the composition and temperature of the reaction products, which determine the maximum exhaust velocity of the jet (cf. § 1). The initial parameters of the propellant (state of aggregation, density, etc.) are also of importance. These affect the weight of the supply and storage systems for the working fluid. Table 2.6 based on /2.11, 2.30/, and /2.74/ gives the main characteristics of some rocket propellants.

TABLE 2.6. Main characteristics of some rocket propellants

Propellant	Maximum specific impulse at $p_0 = 35\times10^4$ kg/m^2, I° sec		Density ρ, kg/m^3	Optimum mixture ratio α^*_{opt}	Combustion temperature T_0, °C
	at sea level for $\mathcal{F}_c/\mathcal{F}_* = 8$	in space for $\mathcal{F}_c/\mathcal{F}_* = 2.5$			
Liquid oxygen + kerosene	261	324	1,010	2.25	3,200
Liquid $O_2 + H_2$	357	441	256	3.5	2,480
Liquid $F_2 + H_2$	364	447	304	4.0	2,600
Nitric acid + unsymmetrical dimethylhydrazine	246	304	1,210	2.4	2,820
Mono-propellant H_2O_2 90%	137	167	1,390	–	740
Solid-propellant ballistite JPN	200 – 230	–	1,610	–	2,900

77 When chemical energy is used, the temperature T_0 of the combustion products (and the exhaust velocity V, cf. § 1) can be regulated by using a propellent mixture ratio differing from the optimum ratio α^*_{opt}. Figure 2.43 shows the combustion temperature of kerosene in oxygen as function of the relative oxidizer excess α^*/α^*_{opt} /2.10/. Obviously this regulation allows only to decrease the combustion temperature, $T_0 \leqslant T_{0\,max}$, and hence the exhaust velocity $V \leqslant V_{max}$.

The chemical energy is released in the combustion chamber. The mass flow rate q of the products of combustion in the jet depends on the supply of components to the combustion chamber (in the case of liquid propellants) or on the burning rate of the propellant (in the case of solid propellants). From (2.8), the maximum mass flow rate q_{max} discharged from the combustion chamber through the nozzle is proportional to the maximum total pressure $p_{0\,max}$ in the combustion chamber which is limited by the strength of the latter. By reducing the propellant supply to the combustion chamber, it is possible to lower the pressure in the chamber and thus vary the mass flow rate $q \leqslant q_{max}$. When the maximum temperature $T_{0\,max}$ (and thus also the maximum exhaust velocity V_{max}) is maintained in the chamber, a variation of

the mass flow rate q produces an almost proportional change in thrust: $\frac{P}{P_{max}} \approx \frac{q}{q_{max}}$ (Figure 2.44) /2.2/. More accurate relationships are given in /2.75–2.77/.

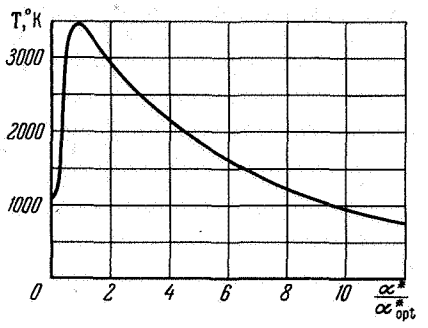

FIGURE 2.43. Combustion temperature of kerosene in oxygen as function of relative oxidizer excess.

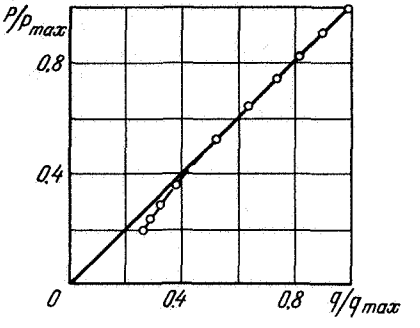

FIGURE 2.44. Regulation characteristic of a liquid-propellant engine (thrust as function of propellent mass flow rate at $T_0 = T_{0max}$). Solid line represents theoretical curve, circles being experimental points.

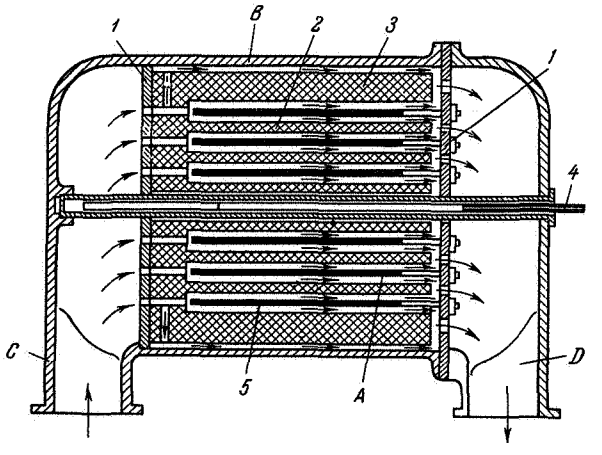

FIGURE 2.45. Nuclear reactor:

A) reactor core; B) reactor vessel; C) and D) inlet and outlet coolant headers; 1) mounting plate; 2) neutron moderator; 3) neutron reflector; 4) control rod; 5) fuel element.

Fission of heavy nuclei is utilized in nuclear-energy sources. At the present stage of development of nuclear physics (cf. /2.2, 2.28, 2.29/), the fission materials used are the uranium isotope U-235 and plutonium Pu-239, obtained in special reactors. Fission occurs when a free neutron penetrates a fissionable nucleus. An excited compound nucleus is formed which subsequently decays with the release of two or three secondary neutrons; the latter sustain the chain reaction. The main part of the nuclear-fission energy (more than 80%) consists of the kinetic energy of the scattered "fragments", which is transformed into thermal energy when the

78

fragments are braked by the fuel elements (Figure 2.18). The power N_n released by the reactor can be regulated by varying the parameters of the chain reaction, e. g., slowing down the latter by the introduction of control rods made from neutron-absorbing substances (cadmium, boron steel) into the reactor. A solid-core reactor is shown schematically in Figure 2.45 /2.2/. Liquid- and gaseous-phase reactors are also discussed in the literature (/2.32, 2.37, 2.38/).

The critical mass of the fission material necessary for sustaining the chain reaction is $G_n' \approx 5.0$ to 200 kg /2.32/, irrespective of the reactor capacity. Hence, the weight of a high-power reactor is mainly determined
79 by the weight of the heat-transfer system. Typical elements of such a system are the ducts of the heat exchanger, formed by fuel elements, which heat the coolant to the specified temperature (cf. Figures 2.18, 2.45). The motion of a gaseous coolant in a duct of uniform cross section is satisfactorily described by the theory of one-dimensional steady flow of a viscous gas, applying the hydrodynamic theory of heat exchange (/2.4, 2.78 — 2.83/). Using the relationship between the heat-transfer coefficient k_1 and the hydraulic-resistance coefficient ζ,

$$k_1 = \frac{1}{8}\zeta\rho c_p W\psi_1,$$

the differential equations of gas flow in a pipe become, when friction and convective heat exchange are taken into account,

$$\left.\begin{aligned} \zeta\frac{dx}{D} &= -\frac{\frac{\varkappa+1}{\varkappa}(\lambda^2-1)\lambda\,d\lambda}{\lambda^2\left[\lambda^2+\psi_1\frac{\varkappa+1}{2\varkappa}\left(\frac{T_w}{T_0}-1\right)(\lambda^2+1)\right]},\\ \frac{dT_0}{T_0} &= \psi_1\frac{\zeta}{2}\left(\frac{T_w}{T_0}-1\right)\frac{dx}{D} = -\frac{\psi_1}{2}\left(\frac{T_w}{T_0}-1\right)\times\\ &\quad\times\frac{\frac{\varkappa+1}{\varkappa}(\lambda^2-1)\lambda\,d\lambda}{\lambda^2\left[\lambda^2+\psi_1\frac{\varkappa+1}{2\varkappa}\left(\frac{T_w}{T_0}-1\right)(\lambda^2+1)\right]}, \end{aligned}\right\} \qquad (2.62)$$

where ρ is the density, c_p is the specific heat at constant pressure, λ is the flow velocity of the gas, D is the reduced velocity, W is the pipe diameter, T_w is the temperature of the pipe wall, T_0 is the stagnation temperature of the gas, $\psi_1 = [1 - 1.74\,\mathrm{Re}^{-1/5}\times(\mathrm{Pr}-1)]$ is a coefficient allowing for the difference of the Prandtl number Pr from unity, Re is the Reynolds number.

The solutions of system (2.62) agree satisfactorily with experimental results.

Theoretical /2.80/ and experimental /2.82/ data on gas flow in a heated pipe are compared in Figure 2.46. Equations (2.62) yields a linear relationship between the specified temperature rise $\Delta T_0/T_0$ of the gas and the necessary heat-exchanger length L/D expressed in pipe diameters. The maximum
80 temperature rise is obtained when the flow velocity at the end of the heat-exchanger pipe is sonic (Figure 2.46). Hence, taking (2.20) and the temperature limitation of the reactor material ($T_0 \leqslant T_{w\max}$) into account the weight of a high-power reactor with gaseous coolant is N_n, since

$$G_n \sim p_{0T}\mathcal{F}_T\Delta T_0 \sim N_n. \qquad (2.63)$$

A similar relationship must be satisfied by a reactor with liquid coolant (limiting case $\lambda \to 0$ in (2.62)), and also in the case of a change of state of the coolant, since the laws of flow of two-phase media and gases are similar /2.84/. The unit weight G_n/N_n of the reactor has been plotted in Figure 2.47 as a function of the total power N_n of the reactor /2.32/. It is seen that for $N_n \geqslant 10^4$ kw the unit weight of the reactor becomes constant.

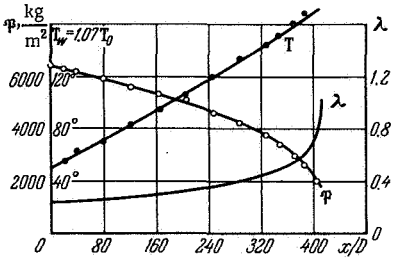

FIGURE 2.46. Variation of pressure, temperature, and reduced velocity of gas flowing in a heated pipe. Curves give theoretical solution, circles represent experimental values.

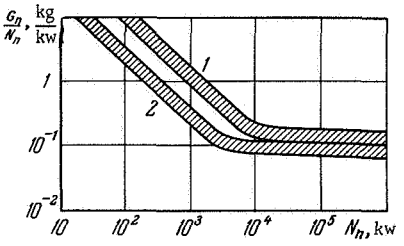

FIGURE 2.47. Unit reactor weight G_n/N_n as function of total released power N_n:

1) gaseous coolant; 2) liquid-metal coolant.

In a high-temperature thermal propulsion engine with reactor and heat exchanger, the weight of the latter is approximately proportional to the engine thrust (2.21), so that (§ 1) its parameters can be included in the generalized unit weight of the propulsion system (Table 2.1).

The mass loss q_ε of the fission material during the release of energy in the reactor can be estimated from the relationship linking mass with energy. Let $\varkappa_0$ be the coefficient of conversion of the mass q_ε into kinetic energy of the jet. The mass flow rate of the working fluid is then given by the following relationship:

$$\frac{1}{2} qV^2 = \varkappa_0 q_\varepsilon c^2, \tag{2.64}$$

where c is the velocity of light. Table 2.7 gives values of q_ε/q at different exhaust velocities V for $\varkappa_0 \approx 5 \cdot 10^{-2}$ /2.28/. It is seen that at exhaust velocities $V \approx 10^4$ to 10^6 m/sec, which are usually considered /2.32, 2.38/, the mass loss q_ε of fission material is negligibly small compared with the mass flow rate q of the working fluid.

81

TABLE 2.7. Ratio of mass loss q_ε of fission material in reactor to mass flow rate q of working fluid in a nuclear-propulsion system, as function of exhaust velocity V

V m/sec	10^4	10^5	10^6
q_ε/q	10^{-8}	10^{-6}	10^{-4}

An important weight component in propulsion systems with nuclear reactors is the weight G_n^* of the neutron and γ-radiation shielding. Since the radiation intensity is inversely proportional to the square of the distance from the reactor, it has been suggested that G_n^* be reduced by means of shadow shielding, the payload being carried at a distance l^* from the reactor (Figure 2.48 /2.32/). The variational problem for the optimum design of the shielding layer (x^*) was considered in /2.85/ and /2.86/.

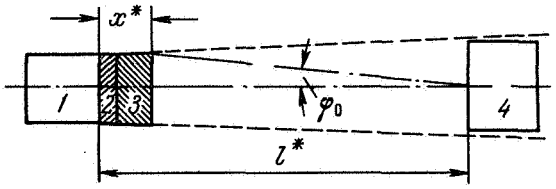

FIGURE 2.48. Shadow shielding of a nuclear reactor for spacecraft:

1) reactor: 2) shielding against γ-radiation; 3) shielding against neutron beam; 4) payload.

From the data in /2.86/ we have plotted in Figure 2.49 the optimum dimensionless weight $\bar{G}_n^*$ of the shielding against γ-radiation from a disk source, as a function of the dimensionless permissible radiation dose $\bar{\sigma}^*$:

$$\bar{G}_n^* = \frac{G_n^* \mu^*}{2\pi l^{*2} \rho g}, \qquad \bar{\sigma}^* = \frac{\sigma^*}{2k\pi\Gamma}, \tag{2.65}$$

82 where μ^* is the coefficient of attenuation in the shielding, ρ is the density of the shielding material, σ^* is the permissible radiation dose, Γ is the surface intensity of the radiation source, k is a conversion coefficient for the radiation intensity; the angle φ_0 is shown in Figure 2.48.

The shield weight G_n^* depends on the total reactor power N_n. According to /2.32/, the unit weight of the shielding becomes almost constant for $N_n \geqslant 10^4$ kw (Figure 2.50).

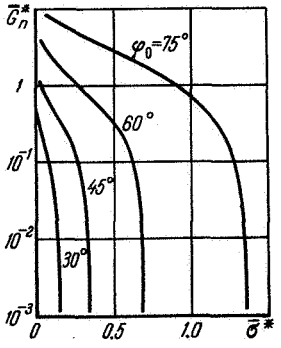

Figure 2.49. Optimum dimensionless weight of shielding as function of dimensionless permissible radiation dose $\bar{\sigma}^*$ for disk source of γ-radiation.

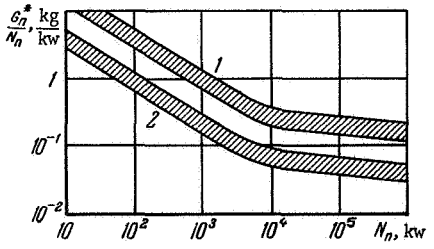

FIGURE 2.50. Unit weight of shielding as function of total reactor power when payload is carried at distance $l^* = 25$ m and dose = 100 mrem/day:

1) reactor with gaseous coolant; 2) reactor with liquid-metal coolant.

Another source of nuclear energy is the disintegration of radioactive isotopes (/2.32, 2.38, 2.87/, etc.). This energy may be utilized in thermal rocket engines, directly by means of sails (§ 1), or in thermal-energy sources of power plants.

Some hundreds of radioactive isotopes are known, but only a few of them are suitable as energy sources of spacecraft.

The first criterion of suitability is the half-life $1/\lambda_\tau$ (λ_τ is the decay constant). Only isotopes with half-lives exceeding 100 days are efficient, since isotopes having shorter half-lives cannot be stored economically or used in long flights. A second important criterion is the maximum unit power and the type of emitted radiation. The characteristic parameters of some radioactive isotopes suitable for space propulsion systems are given in Table 2.8 /2.87/. The unit power of a radioisotopic
83 energy source decreases with time:

$$\frac{N_n}{G_n} = \left(\frac{N_n}{G_n}\right)_{\max} e^{-\lambda_\tau t}. \tag{2.66}$$

The external energy flux of highest intensity in interplanetary space is that of the sunlight, whose power in the Earth's orbit is $\mathfrak{N}_{\text{Å}\odot} \approx 1400\,\text{w/m}^2$ (1.17).

TABLE 2.8. Parameters of radioactive isotopes considered as energy sources for spacecraft power plants

Isotope	Type of radiation	Half-life $1/\lambda_\tau$	Fuel compound	Density ρ, kg/m$^3 \cdot 10^{-3}$	Maximum unit power $\left(\frac{N_n}{G_n}\right)_{\max}$, kw/kg
Po^{210}	Alpha	138 days	Po	9.3	141
Cm^{242}	"	162 "	Cm_2O_3	11.8	100
Pu^{238}	"	86.4 years	PuC	12.5	0.55
Ce^{144}	Beta-gamma	285 days	CeO_2	6.4	1.95
Pm^{147}	"	2.6 years	Pm_2O_3	6.6	0.12
Cs^{137}	"	33 "	CsCl	3.9	0.33
Sr^{90}	"	28 "	$SrTiO_3$	4.8	0.11
Co^{60}	"	5.3 "	Co	9.0	0.30

Solar-energy collectors in the form of parabolic mirrors, Fresnel reflectors, etc., have been thoroughly discussed in /2,39, 2.87, 2.88/, etc. According to /2.87/, the unit weight of a solar-energy collector in the Earth's orbit is

$$\beta_* = \frac{G_n}{S_\odot} \approx 1.5 - 3.0\,\text{kg/m}^2; \left(\frac{G_n}{N_n}\right)_\odot \approx 1\text{—}2\,\text{kg/kw},$$

and varies with the square of the distance R to the Sun:

$$\frac{G_n}{N_n} = \left(\frac{G_n}{N_n}\right)_\odot \left(\frac{R_\odot}{R}\right)^2. \tag{2.67}$$

Examples of such collectors are shown in Figure 2.51 /2.87/.

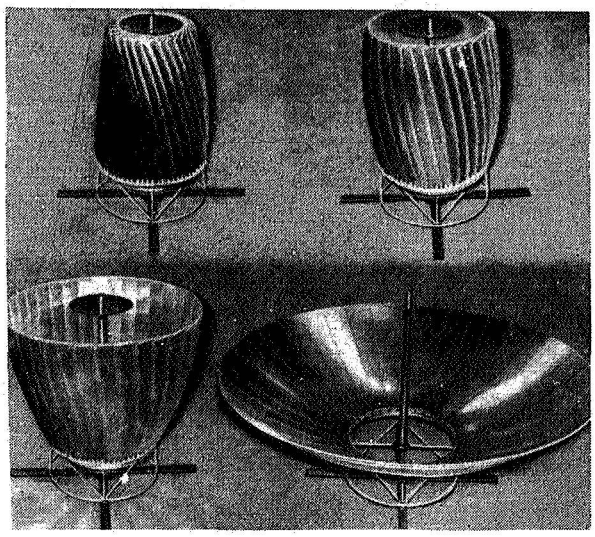

FIGURE 2.51. "Sunflower" solar-energy collectors (model scale 1:3); total area $S_{\odot} = 68\ m^2$, weight of collector and structure, $G_n = 115$ kg.

2. Systems of energy conversion. In thermal-propulsion engines the energy converter is the nozzle (§ 1), which transforms the thermal energy of the hot gas into kinetic energy of the jet. In a propulsion system using a solar or isotopic sail these latter represent the energy converter.
84 The electric propulsion systems (§ 1) require conversion of the mainly thermal energy of the sources into electrical energy. Various types of energy converters and their elements have been considered in /2.32, 2.36, 2.38, 2.87—2.115/. Figure 2.52 shows the basic layout of energy converters for electric propulsion systems using solar energy, radioactive isotopes, or nuclear reactors /2.47/.

Energy conversion is possible by mechanical means or directly. The former (/2.32, 2.36, 2.87, 2.92—2.94/) employ the Brayton gas-turbine cycle or the Rankine steam-turbine cycle. In the Brayton cycle (Figure 2.53), the gas is heated by the energy source and drives a gas turbine, whose shaft carries a compressor (compensating for the pressure drop in the cycle) and an electric generator; the unused thermal energy is removed by the radiator. In the steam-turbine cycle (Figure 2.54), the working fluid evaporated by the energy source drives a steam turbine and an electric
87 generator; in the radiator the steam is condensed into a liquid whose pressure is raised by a pump. Temperature—entropy diagrams for these thermodynamic cycles are given in Figure 2.55. It is seen that at the same maximum temperatures T_3 (determined by the permissible temperatures of the materials) and temperature drops $T_3 - T_4$ across the turbine, the mean temperature of the radiator in the gas-turbine cycle is considerably

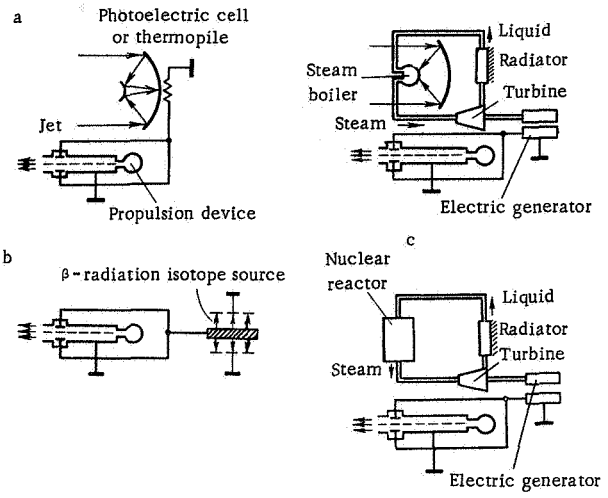

FIGURE 2.52. Basic layouts of energy converters for spacecraft power plants: a) using solar energy, b) for β-radiation from isotopic source, c) for nuclear reactor.

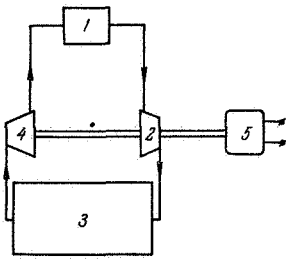

FIGURE 2.53 Mechanical conversion of thermal into electric energy according to Brayton cycle:

1) thermal-energy source, 2) turbine, 3) radiator, 4) compressor, 5) electric generator.

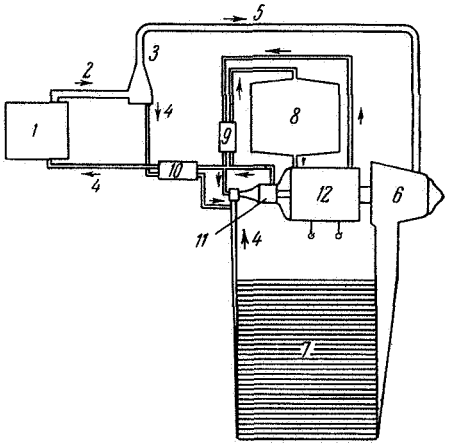

FIGURE 2.54. Energy conversion according to the Rankine cycle:

1) thermal-energy source, 2) wet steam, 3) separator, 4) liquid working fluid, 5) saturated steam, 6) turbine, 7 and 8) radiators, 9 and 10) additional heat exchangers, 11) pump with ejector, 12) electric generator.

lower than that of the radiator (condenser) in the steam-turbine cycle. Since in spacecraft power plants heat is removed by radiation (this is discussed in more detail in § 3), the required surface area and weight of the radiator are considerably larger in the gas-turbine cycle than in the steam-turbine cycle. Figure 2.56 shows the radiator surface area S_r, as a function of the temperature T_3 in front of the turbine for the gas- and steam-turbine cycles for a useful power $N_v = 1000$ kw of the energy converter /2.35/.

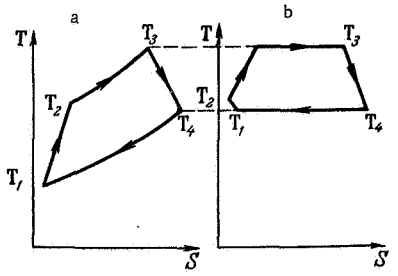

FIGURE 2.55. Thermodynamic cycles of mechanical energy converters in temperature-entropy diagrams: a) Brayton gas-turbine cycle, T_1-T_2-compression, T_2-T_3-heat supply, T_3-T_4-expansion in turbine, T_4-T_1-heat removal in radiator; b) Rankine steam-turbine cycle, T_1-T_2-pressure increase of liquid working fluid pump, T_2-T_3-heating to boiling point and evaporation, T_3-T_4-expansion of steam in turbine, T_4-T_1-condensation in radiator.

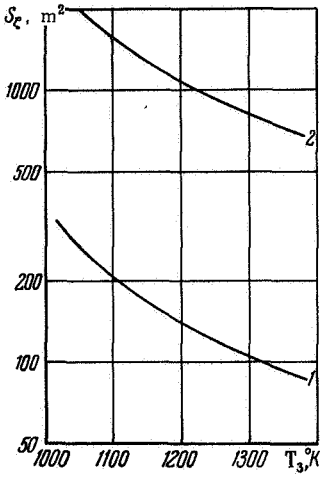

FIGURE 2.56. Radiator surface area as function of temperature in front of turbine for mechanical energy converter of useful power $N_v = 1000$ kw:

1) Rankine steam-turbine cycle,
2) Brayton gas-turbine cycle.

The steam turbine cycle is more often considered in the literature (/2.32, 2.36, 2.87, 2.93—2.94/) because of the smaller radiator surface area required. Its performance depends largely on improvements of the turbounit /2.95—2.98/, taking into account erosion of the components in the two-phase stream /2.99/. The weight of the components of mechanical energy converters is approximately proportional to the useful power N_v. Tentative values of the unit weight of turbounits are given in Figure 2.57 /2.32/. The unit weight of the electric generator $G''_r/N_v \approx 0.4$ kg/kw according to /2.36/.

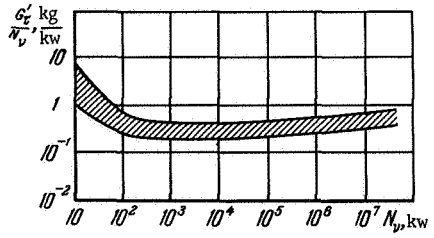

FIGURE 2.57. Unit weight G_r/Nv of turbine unit as function of useful power.

Nonmechanical converters of thermal energy into electric energy

88 with two-phase flow include those based on a liquid-metal cycle with a MHD generator (/2.100, 2.101/). Such a converter (Figure 2.58) contains two cycles, e.g., a liquid-lithium and a potassium-vapor cycle. The liquid lithium is heated by the energy source and introduced into the mixer so that the liquid potassium evaporates. The potassium vapors expand in the nozzle and accelerate the lithium which is then removed in the separator. The accelerated liquid lithium produces electrical energy in the MHD generator. It is stated in /2.100/ and /2.101/ that for $N_v \geqslant 500$ kw such energy converters compare favorably, as regards weight, with the turbogenerator converters.

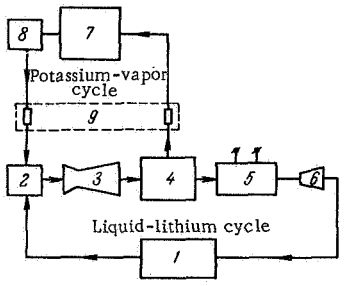

FIGURE 2.58. Energy converter based on liquid-metal cycle with MHD generator:

1) thermal-energy source; 2) mixer, 3) nozzle, 4) separator, 5) MHD-generator, 6) diffuser, 7) radiator, 8) pump, 9) heat exchanger.

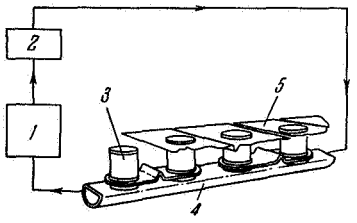

FIGURE 2.59. Thermoelectric energy converter:

1) thermal-energy source, 2) liquid-metal circulation, 3) thermopiles, 4) working-fluid duct, 5) radiator (cold junction).

Direct-conversion units employ thermoelectric, solar, or thermionic cells (/2.32, 2.36, 2.87, 2.102—2.115/). Thermoelectric converters use the Seebeck effect, in which thermal energy is directly converted into electrical energy when a temperature difference exists between two junctions of dissimilar materials (Figure 2.59). The efficiency of the thermoelectric converter is /2.87, 2.102—2.104/

$$\eta_\tau = \frac{T_1 - T_2}{\frac{4}{z} + 2T_1 - \frac{T_1 - T_2}{2}}, \quad z = \frac{s^2\sigma_*}{\lambda_*}, \tag{2.68}$$

where T_1 is the temperature of the hot junction, T_2 is the temperature of the cold junction, z is the thermoelectric Q-factor of the material, s is the Seebeck coefficient, σ_* is the [electric] conductivity, λ_* is the thermal conductivity.

Semiconducting thermopiles with z of the order of $2 \cdot 10^{-3}$ 1/°K have efficiencies of ~10% when $T_1 - T_2 \sim 200$ °K /2.103/. The unit weight of the SNAP-10A thermoelectric converter together with the radiator (SiGe thermopiles, $z \approx 0.6 \cdot 10^{-3}$ 1/°K) is tentatively given by /2.103/ as

$$\frac{G_\tau + G_\zeta}{N_v} \approx 125 \text{ kg/kw}. \tag{2.69}$$

Another type of semiconducting thermopile which converts sunlight directly into electrical energy is the silicon photovoltaic solar cell /2.32, 2.36, 2.87, 2.105—2.107/, consisting of a thin p-layer of silicon, about 2.5μ thick, applied on a n-layer of silicon (Figure 2.60). Photons falling on the cell cause the formation of electron-"hole" pairs, which diffuse through the contact surface under the action of the electric field between the n- and p-layers, creating a potential difference of 0.3 to 0.5 v.
89 The cells are grouped on panels as batteries. The unit weight of such an energy converter increases with the square of the distance to the Sun:

$$\frac{G_\tau}{N_\nu} = \frac{G_\tau}{N_{\nu\delta}}\left(\frac{R}{R_\delta}\right)^2. \tag{2.70}$$

The unit weight of an energy converter with solar cells $G_\tau/N_{\nu\delta} \approx 50$ kg/kw in the Earth's orbit the efficiency being 10 to 14% /2.32, 2.105/. In addition, the weight of the system turning the batteries toward the Sun must be taken into account /2.107/.

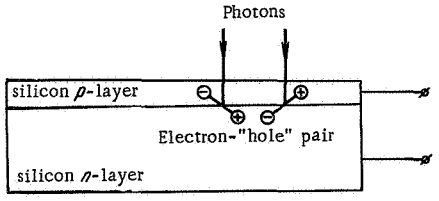

FIGURE 2.60. Silicon photovoltaic cell converting sunlight into electrical energy.

In thermionic converters of heat into electrical energy electrons are emitted from the hot cathode and collected by the colder anode /2.32, 2.36, 2.87, 2.108 — 2.115/. In flowing back to the cathode the electron current produces useful work. To make this process possible, the work function φ_k of the cathode material must be higher than the work function φ_a of the anode material. Values of the work function of different materials are given in Table 2.4. The electron thermionic current density depends strongly on temperature, in accordance with Richardson's formula:

$$i = AT^2 \exp\left[-\frac{e\varphi}{kT}\right], \tag{2.71}$$

where A is a universal constant, which, for pure metals, is 120 $a/cm^2 \cdot deg^2$, and k is the Boltzmann constant.

To make possible a flow of electrons from the cathode to the anode when $\varphi_k > \varphi_a$, the anode temperature must be considerably lower than the temperature of the cathode. The distribution of the potential energy in the interelectrode gap of the thermionic converter is shown in Figure 2.61. The output voltage created by the thermionic converter is

$$\mathcal{U} = \varphi_k + \varphi_c - \varphi_a - \varphi_p, \tag{2.72}$$

where φ_c is the kinetic energy of the electrons, φ_p is the potential drop in the discharge plasma. For the typical materials listed in Table 2.4 the voltage $\mathcal{U}$ is of the order of 1 volt. A large unit power of the thermionic
90 converter thus necessitates a high current density i. On the other hand, the value of i is limited by the space charge (cf. (2.41) to (2.43). A high

current density necessitates, according to (2.43), very small gaps d between the electrodes of the thermionic converter; thus if i is ~ 1 a/cm^2 (a power of ~ 1 w/cm^2), the gap must be less than 10μ. These severe requirements are considerably relaxed if the thermionic converter is filled with vapors of alkali metals (Cs, Ba), which are easily ionized and form plasma layers in the interelectrode space. The effective gap then becomes practically equal to the length of the free path of the electron up to the plasma layer, which is much smaller than the geometric gap. In addition, filling the thermionic converter with Cs vapors increases the emissive properties of the cathode. The characteristics of a thermionic converter filled with the alkali metal vapors are given in Figure 2.62 /2.115/.

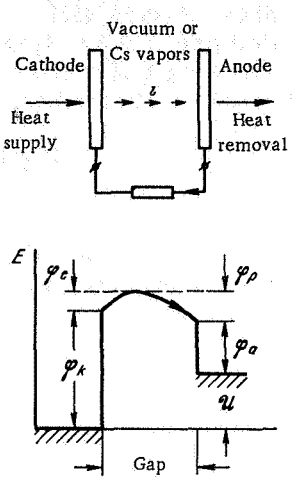

FIGURE 2.61. Scheme of thermionic energy converter and distribution of potential energy E in its interelectrode gap.

Structurally, thermionic cells are considered (cf. /2.36, 2.87 – 2.114/) to be built into liquid-metal cooled nuclear reactors. Figure 2.63 gives tentative values of the unit weight of reactors with thermionic converters as a function of the useful power N_v for the design shown in Figure 2.64 /2.87/.

Another important item in the weight balance of the spacecraft power plant is the system for removing the thermal energy not used in the cycle /2.32/. The complete weight analysis of power plants is given in § 3, after the characteristics of the heat-removal system have been considered.

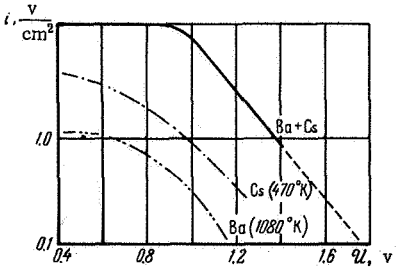

FIGURE 2.62. Characteristics of thermionic energy converter filled with Cs or Ba vapor; anode W, $T_1 = 2000$ °K, cathode Mo, 0.25 mm gap, vapor pressure corresponds to boiling at temperatures indicated.

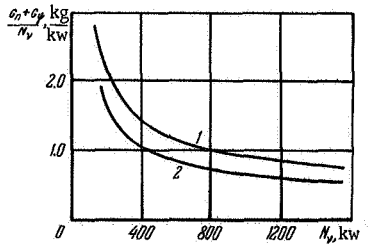

FIGURE 2.63. Unit weight of reactor with thermionic converter as function of useful power N_v:

1) unit converter power = 10 w/cm^2;
2) unit converter power = 20 w/cm^2.

3. Energy accumulators. Spacecraft power plants utilize mainly thermal and electrical energy. Accumulators for these types of energy are considered in /2.32/ and /2.87/.

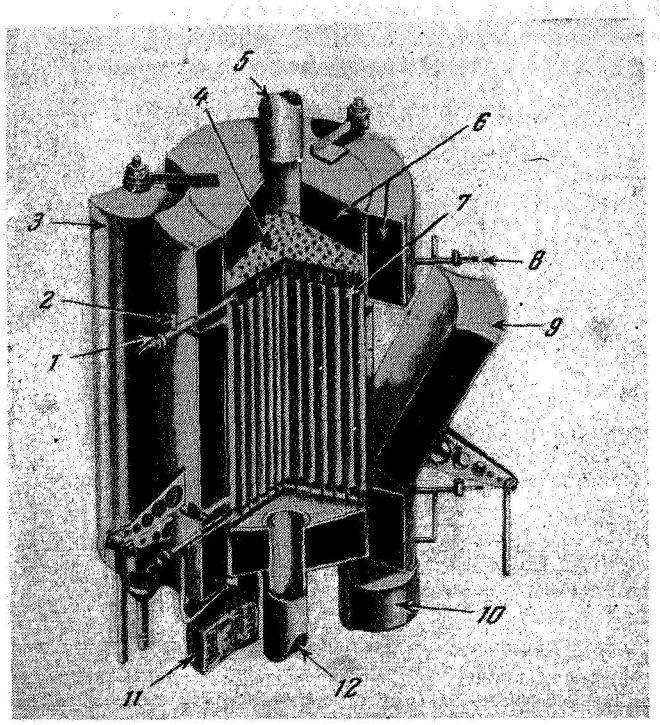

FIGURE 2.64. Nuclear reactor with thermionic converters:

1) power supply terminal, 2) removal of fission products, 3) regulator, 4) supporting grid, 5) coolant inlet, 6) reflector, 7) thermionic cells, 8) power supply terminal for pump, 9) damage protection, 10 and 11) Cs tanks, 12) coolant outlet.

92 Storage of thermal energy is possible by utilizing the heat capacity of the accumulator substance or the heat of phase transformation; the second method is preferable, since it permits energy storage at a nearly constant temperature T_n. The phase transformation usually considered is the fusion of a heat-storing substance, since evaporation would cause a pressure increase in the storage container. Thermal-energy accumulators will have a minimum unit weight $\beta = G_e/E_0$ when chlorides and hydrides of metals are used /2.32, 2.87/ (Table 2.9). Use of pure metals (e.g., Pt /2.116/), leads to higher values of the unit weight β.

TABLE 2.9. Unit weight of thermal-energy accumulator (excluding container weight)

Heat-storing substance	Temperature T_n, °K	Unit weight $\beta = \frac{G_e}{E_0}, \frac{\text{kg}}{\text{J}}$
LiH	950	$0.36 \cdot 10^{-6}$
NaCl	1077	$1.95 \cdot 10^{-6}$
Pt	2042	$8.8 \cdot 10^{-6}$

The electrical energy accumulators having the least unit weight are silver-zinc accumulators /2.32, 2.117/ whose unit weights are given in Figure 2.65 /2.117/. The unit weight of the capacitors is $\beta \approx 0.015$ kg/j /2.36/.

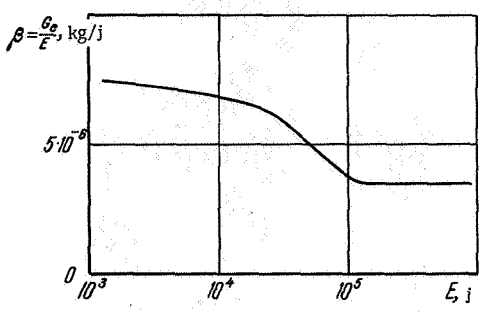

FIGURE 2.65. Unit weight of silver-zinc accumulator as function of energy stored in one cell (voltage $u \approx 1.5$ v).

Table 2.9 and Figure 2.65 show that the unit weights of the thermal and electrical-energy accumulators are of the same order: $\beta \approx 1$ to $5 \cdot 10^{-6}$ kg/j.

4. **Working-fluid supply and storage systems.** Liquid working fluids are supplied by centrifugal or positive-displacement pumps /2.2, 2.30, 2.36, 2.118, 2.119/. The weight G_q of the supply system in thermal propulsion engines with liquid working fluid (cf. § 1 of this chapter), is approximately proportional to the maximum thrust P_{max}. The unit weight of centrifugal-pump units is, according to /2.2/ and /2.119/, $G_q/P_{max} \approx 0.005$; in an analysis of thermal propulsion engines from the viewpoint of flight mechanics it is advisable to include the unit weight of the supply system in the total unit weight of the engine (cf. (2.16)).

The weight of circulating systems must also be taken into account in power plants in which thermal energy is converted into electric energy
93 (Figures 2.54, 2.58, and 2.59). According to /2.94/, the unit weight of the supply and pumping systems is $G_q/N_v \approx 0.35$ kg/kw for $N_v = 415$ kw.

The parameters of working-fluid tanks have been analyzed in detail in /2.30/. The weight of the tanks G_β is proportional to the weight G_μ of the stored working fluid. The unit weight of the tanks is: for liquid oxygen + kerosene, $G_\beta/G_\mu \approx 0.004$ /2.120/; for Cs $G_\beta/G_\mu \approx 0.006$ /2.94/.

In solid-propellant rocket engines (/2.11, 2.30/), the weight of the propellant container is of the same order as that of the engine, being proportional to the total impulse Pt; the unit weight of a solid-propellant container is, according to /2.11/, $G_\beta/Pt \approx G_\xi/Pt \approx 0.8 \cdot 10^{-3}$ 1/sec.

5. **Power plants using up working fluid from the environment.** Working fluid from the atmosphere enters the engine in air-breathing propulsion engines /2.2, 2.121—2.131/, and in propulsion engines with working-fluid accumulators, during orbital flights in the upper layers of the atmosphere /2.134—2.137/.

An element common to all such propulsion systems is the air inlet, which must be designed so as to take in the working fluid with minimum

loss of total pressure and minimum drag. Braking of the impinging stream
94 by the inlet at supersonic flight velocities may cause a considerable loss in the total pressure p_0 of the air, where

$$p_0 = p_h\left(1 + \frac{\varkappa - 1}{2} M_0^2\right)^{\frac{\varkappa}{\varkappa - 1}}, \tag{2.73}$$

and $M_0 = v/a$ is the Mach number of the flight, a is the speed of sound (cf. Figure 1.4).

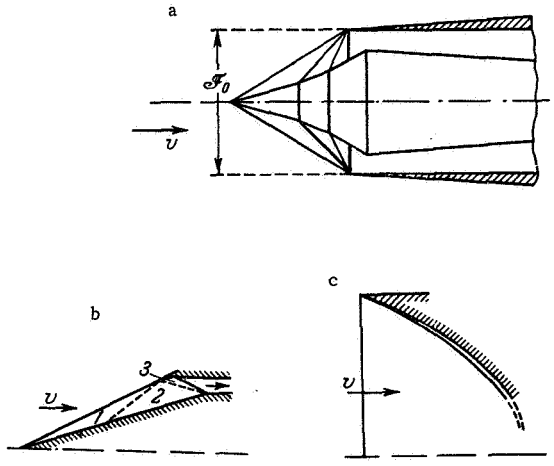

FIGURE 2.66. Supersonic diffusers:

a) multiple-shock diffuser with external compression; b) diffuser with conical flows; 1) zone of flow past central cone, 2) isentropic flow, 3) diverging conical flow in front of conical shock /2.132/; c) hypersonic flow with parabolic shock in duct.

This total-pressure loss, which causes a corresponding loss in thrust (cf. § 1 of this chapter), may be reduced by using a supersonic diffuser as an inlet (Figure 2.66) /2.2, 2.132, 2.133/. Figure 2.67 gives the relative total pressure p_0'/p_0 at the exit from an ideal inlet as a function of the number of shocks and the flight Mach number M_0 of the flight. Such a supersonic diffuser causes no additional drag for an incoming flow whose cross-sectional area is equal to the inlet area $\mathcal{F}_0$ (Figure 2.66) at a mass flow rate

$$q_v = -\rho v \mathcal{F}_0. \tag{2.74}$$

95 The ramjet (Figure 2.68) has a combustion chamber or another heat source between the inlet and the nozzle; in a turbojet or turborocket engine the air is compressed by a turbocompressor before entering the combustion chamber, in order to provide thrust at low flight velocities (/2.2, 2.121—2.131/). The characteristics of air-breathing engines are determined on the basis of the theory of gas dynamics /2.2, 2.4, 2.6/.

The thrust P of an air-breathing engine is approximately proportional to the inlet area $\mathcal{F}_0$ and to the atmospheric pressure p_h which depends on the flight altitude, so that

$$P \approx k\mathcal{F}_0 p_h. \tag{2.75}$$

The thrust coefficient $P/\mathcal{F}_0 p_h$ depends on the Mach number M_0 and at first increases with the flight velocity in accordance with the increase in the compression ratio p_0'/p_h of the air flowing into the inlet duct. At the same time, however, the stagnation temperature T_0' of the impinging air also increases:

$$T_0' = T_h\left(1 + \frac{\varkappa - 1}{2} M_0\right). \tag{2.76}$$

When the maximum permissible temperature T_0 in the combustion chamber (heat source) is given, this reduces the possible temperature $\Delta T_0 = T_0 - T_0'$ of the air in the engine and the thrust coefficient at high Mach numbers M_0.

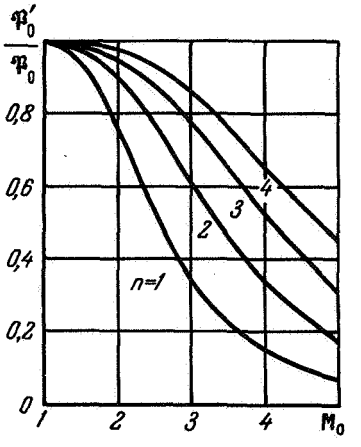

FIGURE 2.67. Variation of relative total pressure at exit from ideal inlet, as function of number of shocks n and flight Mach number.

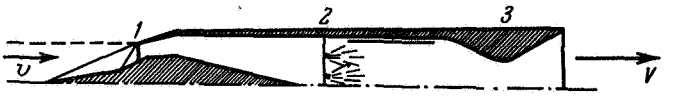

FIGURE 2.68. Ramjet:

1) inlet, 2) combustion chamber (heat source), 3) nozzle.

Figure 2.69, based on /2.127/, shows the thrust coefficient of air-breathing engines as a function of the flight Mach number. The effective specific impulse $I^\circ = P/gq_a$ of air-breathing engines also depends on the Mach number (Figure 2.70) /2.127/. The weight of air-breathing engines is approximately

96

proportional to the inlet area: $G_p \sim \mathcal{F}_0$; unit weights of various air-breathing engines are given in Table 2.10 /2.127/.

TABLE 2.10. Unit weights of air-breathing propulsion engines

Type of engine	Ramjet	Turborocket	Turbojet
Unit weight $\frac{G_p}{\mathcal{F}_0}$, kg/m^2	1050	1350	2600

The characteristics of air-breathing engines using liquid hydrogen as fuel are improved by utilizing the heat capacity of liquid hydrogen to liquefy part of the air (oxygen) entering through the inlet (for a more detailed discussion cf. /2.127/).

Another type of propulsion system is that in which working fluid is accumulated during orbital flight in the upper layers of the atmosphere (/2.134 — 2.137/). The basic layout of such a propulsion system is shown in Figure 2.71 /2.136/. Air enters the propulsion system at a mass flow rate q_v through the inlet, is first cooled by a system of heat exchangers with radiators, then liquefied in an expansion machine /2.138/ and finally led into tanks with possible separation of the components. The drag $q_v v$, like the entire aerodynamic resistance of the spacecraft, is compensated for by the thrust, developed by part of the air entering through the inlet: $q < |q_v|$. The difference $q_a = q - q_v$ is stored in the tanks. Since $q < |q_v|$, the exhaust velocity V must be considerably higher than the orbital flight velocity v:

$$V \geqslant \frac{|q_v|}{q} v. \tag{2.77}$$

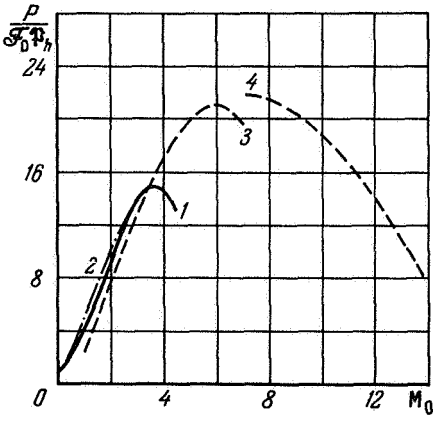

FIGURE 2.69. Thrust coefficients of air-breathing engines as function of Mach number:

1) turbojet; 2) turborocket; 3) ramjet with subsonic combustion, 4) ramjet with supersonic combustion.

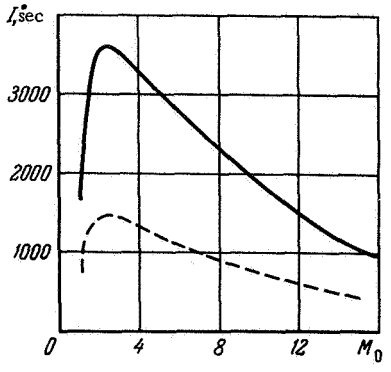

FIGURE 2.70. Effective specific impulse of air-breathing engines as function of Mach number. Solid curve refers to hydrogen as fuel, the dashed curve to kerosene as fuel.

98 Since for flights in the upper layers of the atmosphere $v \approx 8$ km/sec, the necessary exhaust velocity V can be attained only in electrical propulsion engines (cf. § 1 of this chapter).

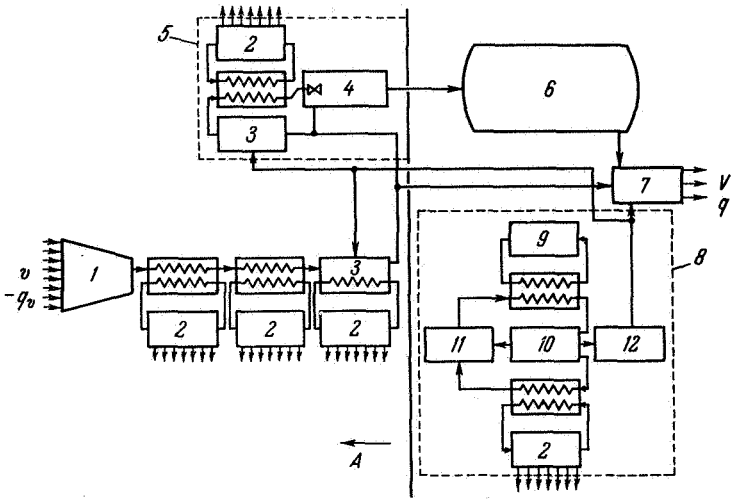

FIGURE 2.71. Basic layout of propulsion system in which working fluid is accumulated during orbital flight in upper layers of atmosphere:

1) inlet, 2) radiators, 3) compressors, 4) expansion machine, 5) liquefying installation, 6) working-fluid tank, 7) nozzle, 8) power plant, 9) nuclear reactor, 10) turbine, 11) pump, 12) electric generator; A) all components to the left of line operate only during accumulation period.

The power N_γ consumed by the propulsion engine and the power N_v consumed by the liquefying installation are supplied by the power plant (Figure 2.71). The power N_{v0}, ideally consumed for liquefaction at 100%

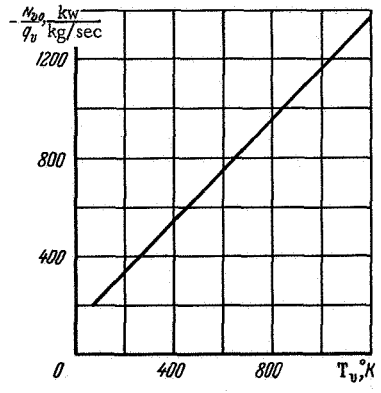

FIGURE 2.72. Specific power consumed ideally for liquefaction of air, as function of air temperature T_v at inlet to liquefying installation.

efficiency is shown in Figure 2.72 as a function of the air temperature at the inlet to the liquefying installation /2.139/. The specific power N_{v0}/q_v is less than 1/100th of the specific power of the jet:

$$\frac{N_\gamma}{q} \approx 2 \cdot 10^5 \text{ kw/kg/sec at } V \approx 2 \cdot 10^4 \text{ m/sec.} \qquad (2.78)$$

It is accordingly assumed in /2.134 — 2.136/ that the unit weight of a propulsion system, in which working fluid accumulates during orbital flight, is mainly determined by the weight of its electrical propulsion system, whose elements were considered above.

6. Drag acting on the spacecraft during flight in the atmosphere. During flight in the atmosphere the drag may considerably influence the mechanics of flight, in particular when working fluid enters the engine from the environment. Since spacecrafts are usually bodies of revolution, we shall consider the basic laws of drag of such bodies. The aerodynamic resistance F_x of a body (cf. (2.2)) is characterized by the drag coefficient

$$c_x = \frac{F_x}{\frac{\rho v^2}{2} \mathcal{F}_m}, \qquad (2.79)$$

99 where $\rho v^2/2$ is the velocity head of the impinging air flow, $\mathcal{F}_m$ is a characteristic area, e.g., that of the midship section of the body. For a given body geometry the drag depends mainly on two dimensionless parameters /2.140/, viz., the Mach number of the flight $M_0 = v/a$ and the Reynolds number $\mathrm{Re} = vL/\nu$ (L is a characteristic linear dimension, e.g., the length of the body, ν is the kinematic viscosity of the impinging air), or, on the velocity v and flight altitude h, since the speed of sound $a = \sqrt{\varkappa \frac{p_h}{\rho}}$ and the kinematic viscosity $\nu = f(T)$ depend on the flight altitude (Figure 1.4). Figure 2.73 shows the drag coefficient c_x as a function of flight velocity and altitude for a typical rocket engine /2.141/.

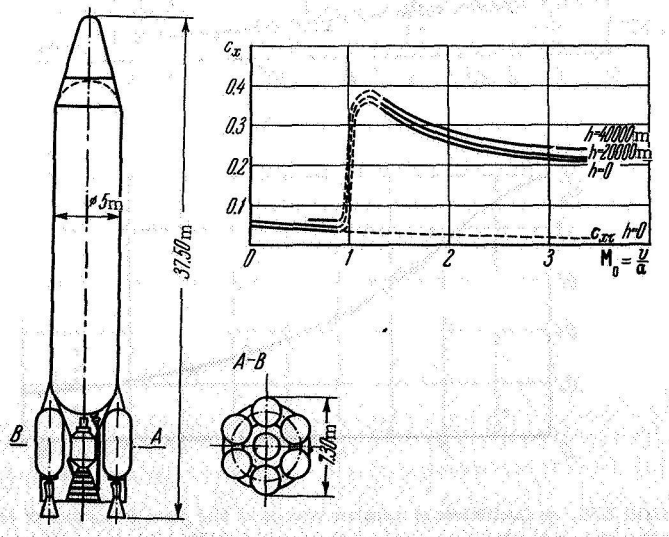

FIGURE 2.73. Drag coefficient as function of flight velocity and altitude for typical rocket engine; dashed line at bottom represents friction drag at $h = 0$.

The drag consists of two components, representing respectively the friction forces [skin friction] and the pressure forces [form drag] acting on the body (cf. (2.2)):

$$c_x = c_{x\tau} + c_{xp}. \tag{2.80}$$

At subsonic velocities ($M_0 < 1$) the drag of a streamlined body is mainly determined by friction (cf. dashed line at bottom of Figure 2.73). The friction drag can be estimated from the friction coefficient of a flat
100 plate of surface areas S,

$$c_F = \frac{F_{x\tau}}{\frac{\rho v^2}{2} S}, \tag{2.81}$$

which for a turbulent boundary layer on a heat-insulated surface (/2.1, 2.142 — 2.145/) is

$$c_F = \frac{0.0905}{(\lg 0.0355\,\mathrm{Re})^2}(1 + 0.144\,M_0^2)^{-0.65}. \tag{2.82}$$

The first factor in this formula represents the dependence of the friction coefficient on the Reynolds number at $M_0 = 0$ (Figure 2.74, a) /2.143/, while the second represents the influence of the Mach number (Figure 2.74, b) /2.145/. Equation (2.82) gives the friction coefficient as referred to the "wetted"

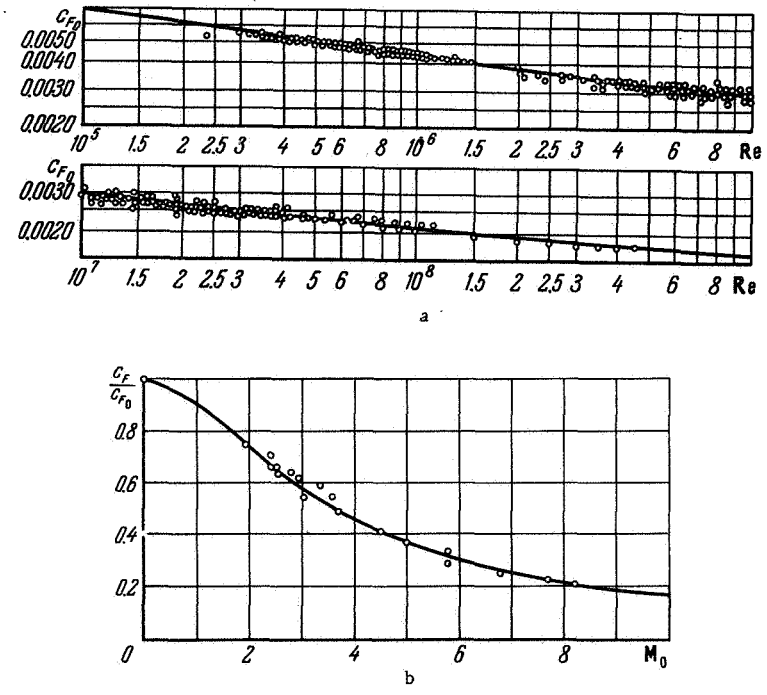

FIGURE 2.74. a) Coefficient of turbulent friction of flat plate as function of Reynolds number at $M_0 = 0$: solid curve represents first factor in (2.82), circles represent experimental values; b) influence of Mach number on friction coefficient: solid curve represents second factor in (2.82).

101 surface S. The friction drag coefficient $c_{x\tau}$, referred to the midship-section area $\mathcal{F}_m$, is

$$c_{x\tau} = c_F \frac{S}{\mathcal{F}_m}. \tag{2.83}$$

At supersonic velocities (Figure 2.73) the drag coefficient increases sharply and is mainly determined by the pressure forces caused by the wave flow past the body /2.1, 2.146, 2.147/. The wave drag coefficient c_{xp} at supersonic velocities can be determined by applying the general theory of supersonic flow /2.1, 2.5, 2.12, 2.14, 2.146 — 2.153/. The peculiar features of hypersonic flow past thin bodies can be studied by considering a gas displaced by a piston (/2.140, 2.145, 2.154 — 2.162/ etc.; in fact, in accordance with the law of plane sections /2.163/, the problem of hypersonic flow past thin bodies (Figure 2.75, a) is the same as that of the two-dimensional unsteady motion of a gas displaced by a piston expanding according to this law (Figure 2.75, b).

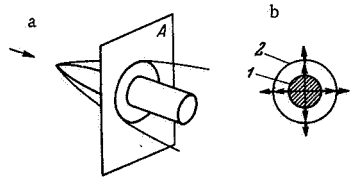

FIGURE 2.75. Law of plane sections: gas moves in plane A as if displaced by equivalent piston:

1) piston, 2) shock.

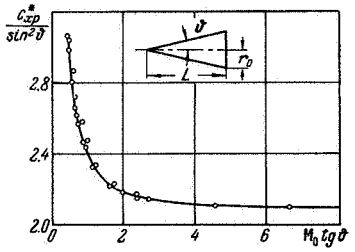

FIGURE 2.76. Wave drag coefficient c^*_{xp} of conical bodies as function of cone angle ϑ and Mach number; curve is plotted according to law of plane sections applied to uniformly expanding cylindrical piston; circles represent computed results for conical flow with $\vartheta = 5°$, 10°, and 15°.

Figure 2.76 shows the wave drag coefficient c^*_{xp} of a conical body as a function of the cone angle ϑ and the Mach number, obtained on the basis of the law of plane sections /2.162, 2.164/; the results of the exact calculation for conical flow are shown for comparison. These data indicate the
102 influence of the velocity (Mach number) and the nose elongation $\bar{L} = L/r_0 = \operatorname{ctg}\vartheta$ on the drag coefficient.

A study of gas flow with shocks propagating according to the power law $r = ct^m$ (/2.165 — 2.167/) permitted a determination, for large values of M_0, of the effect on c_{xp} of transition from the conical shape to that defined by $r = cx^m$, which has a larger volume v (Figure 2.77). Figure 2.77 shows that when the nose elongation of a body defined by a power law is given, the wave drag is minimum for $m \approx 0.70$; the wave drag of a body of this shape is approximately 25% less than that of a conical body, while the volume is about 25% larger. Bodies of this shape become more blunt-nosed with decreasing $m < 1$; $m \to 0.5$ corresponds to a strong cylindrical detonation. It has to be taken into account that the increasing bluntness is accompanied by increasing effects of the high-entropy skin flow, which,

according to /2.168/, is, however, negligible for $1 \geqslant m \geqslant 0.65$ (Figure 2.78).

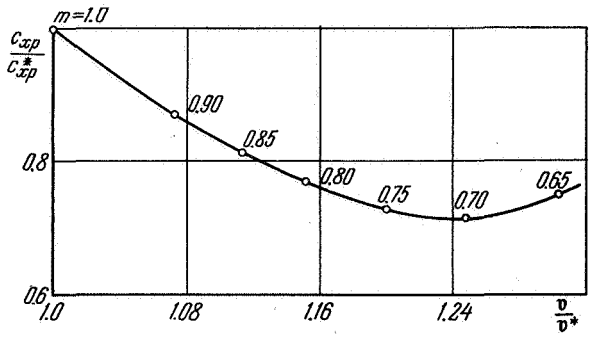

FIGURE 2.77. Wave drag coefficient of bodies of revolution whose shapes are defined by $r = cx^m$, as function of relative volume $\mathfrak{v}/\mathfrak{v}^*$; $\mathfrak{v}^*$ and c_{xp} refer to conical bodies ($m = 1$) of equal elongation.

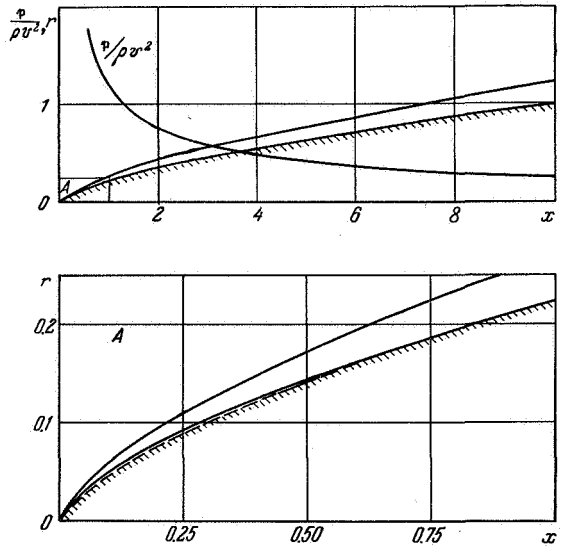

FIGURE 2.78. Influence of high-entropy skin flow on parameters of hypersonic flow with shock past body of revolution $r = cx^{0.65}$. Solid curve represents exact contour of body, dashed curve represents contour when high-entropy skin flow is neglected.

A body of revolution whose shape is defined by $r = cx^m$ is found to have minimum wave drag when $m \approx 0.75$ also on the basis of the approximate relationship for the relative pressure $\bar{p}$ acting on the body (cf. /2.165/ for more details):

$$\bar{p} = \bar{p}_n \frac{\sin^2 \vartheta_i}{\sin^2 \vartheta_n}, \tag{2.84}$$

where $\bar{p} = \frac{p - p_h}{\rho v^2/2}$ (c_{xp} is equal to the mean value of $\bar{p}$ acting on the midship section), ϑ_i is the local inclination of the body surface [to the direction of flight], $\bar{p}_n$ and ϑ_n are respectively the relative pressure and inclination at a fixed point, e.g., at the nose.

Using (2.84) it can be shown that if friction is taken into account /2.165/ the optimum shape of the nose is negligibly altered (Figure 2.79) /2.210/. When the local friction coefficient $c_F = \text{const}$, the optimum shape of a thin body of revolution is defined by /2.165/

$$\frac{\bar{x}}{c_1} + c_2 = \frac{z^2}{\frac{c_F}{2k}\left(z^3 - \frac{c_F}{2k}\right)} \frac{1}{6\left(\frac{c_F}{2k}\right)^{4/3}} \ln \frac{z^2 + z\left(\frac{c_F}{2k}\right)^{1/3} + \left(\frac{c_F}{2k}\right)^{2/3}}{\left[z - \left(\frac{c_F}{2k}\right)^{1/3}\right]^2} + \\ + \frac{1}{\sqrt{3}\left(\frac{c_F}{2k}\right)^{4/3}} \operatorname{arctg} \frac{2z + \left(\frac{c_F}{2k}\right)^{1/3}}{\sqrt{3}\left(\frac{c_F}{2k}\right)^{1/3}} \left(z = \sqrt[3]{\frac{c_1}{\bar{r}} + \frac{c_F}{2k}}\right).$$

104 Using (2.84), we can also determine the optimum shapes of noses of bodies of revolution when their volumes are given /2.165/; these are close to power-function profiles, determined by

$$\bar{x} = \int_0^1 \frac{c\sqrt[3]{\bar{r}}\, d\bar{r}}{\sqrt[3]{1 + A\bar{r}^2}},$$

$$\bar{r} = \frac{r}{r_0},$$

$$\bar{x} = \frac{x}{L}. \qquad (2.85)$$

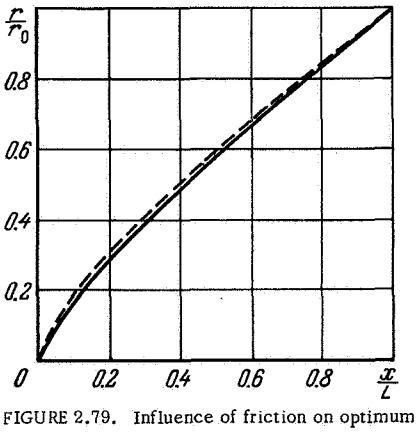

FIGURE 2.79. Influence of friction on optimum shape of nose of body of revolution at hypersonic flight velocities. Solid curve represents optimum shape when friction is taken into account; dashed curve represents optimum shape when friction is neglected /2.165/.

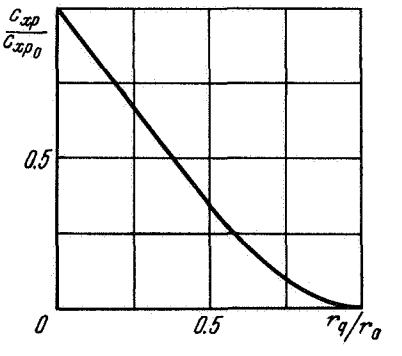

FIGURE 2.80. Wave drag coefficient of body with open nose as function of relative inlet radius r_q/r_0; c_{xp} is referred to area of annular midship section.

The wave drag of bodies of revolution having open noses depends on the relative inlet radius $\bar{r}_q = r_q/r_0$; the variation c_{xp} of the drag coefficient with $\bar{r}_q$ is shown in Figure 2.80 /2.165/.

105 § 3. COOLING SYSTEMS FOR SPACECRAFT POWER PLANTS

1. Radiation cooling systems. Thermal open-cycle jet engines (Figure 2.10) are mainly cooled by preheating the working fluid. Thus, the OP-1 jet engine designed by Tsander in 1930 (Figure 2.81) was cooled by the oxidizer (compressed air) flowing through a jacket surrounding the combustion chamber before entering the latter /2.71/.

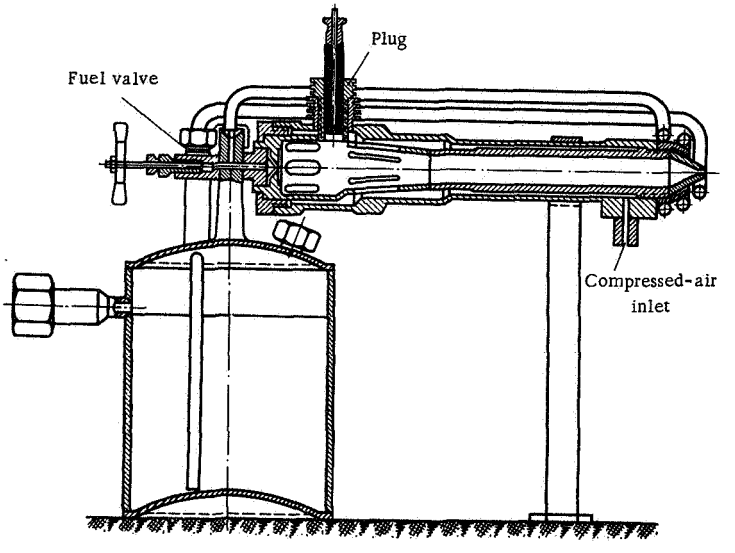

FIGURE 2.81. OR-1 jet engine using benzine as fuel and compressed air as oxidizer; $P = 0.5$ kg.

The energy efficiency of a space propulsion system having a closed-cycle power plant (Figure 2.52) is $\eta_\theta = N_\lambda/N_n$, i.e., the ratio of the total jet power $N_\lambda \approx N_v$ to the power N_n of the energy source; in power plants it is usually of the order of 10%. Hence, in closed-cycle power plants a large
106 part of the power produced by the energy source, namely

$$N_\zeta = N_n - N_\lambda = N_\lambda \frac{1-\eta_\theta}{\eta_\theta}, \qquad (2.86)$$

must be removed at about the minimum temperature T_{min} of the working cycle*.

* Taking into account power N_{qv} contributed by the scooped-up working fluid (cf. Chapter One, § 2) does not basically affect the analysis. We assume $N_{qv}=0$ for simplicity.

The principal cooling method discussed in the literature (/2.32, 2.87/) is radiation cooling by various types of radiators. The required surface area S_ζ of the radiator is related to the power N_λ by the Stephan — Boltzman law

$$S_\zeta = \frac{N_\zeta}{\sigma\omega T_{min}^4} = \frac{N_\lambda}{\sigma\omega T_{min}^4}\frac{1-\eta_\theta}{\eta_\theta}. \qquad (2.87)$$

Equation (2.87) is true in the absence of heat flux from outside and for radiators without self-irradiating surfaces; an example of such a system is a flat radiating surface in space, located parallel to the solar-radiation flux.

Typical space power plants operate according to a thermal working cycle. The energy efficiency η_θ depends on the maximum and minimum temperatures of the cycle:

$$\eta_\theta = \eta_* \frac{T_{max} - T_{min}}{T_{max}} = \eta_*(1-\overline{T}), \qquad (2.88)$$

where $\overline{T} = \frac{T_{min}}{T_{max}}$ and the coefficient η_* takes into account the deviation from the ideal cycle.

The required radiator surface area is, by (2.87) and (2.88), given by

$$S_\zeta = \frac{N_\lambda[1-\eta_*(1-\overline{T})]}{\sigma\omega T_{max}^4 \eta_*(1-\overline{T})\overline{T}^4}. \qquad (2.89)$$

When the jet power N_λ and the maximum permissible cycle temperature T_{max} (ω and η_*) are given, the radiator surface area is minimum for

$$\min S_\zeta \quad \text{at} \quad \overline{T}_{opt} = 1 - \frac{5}{8\eta_*} + \sqrt{\left(1-\frac{5}{8\eta_*}\right)^2 + \frac{1}{\eta_*} - 1}. \qquad (2.90)$$

107 The functional relationship $\overline{T}_{opt}(\eta_*)$ has been plotted in Figure 2.82; it is seen that for $\eta_* = 1.0$, $\overline{T}_{opt} = 3/4$, increasing slightly with decreasing η_*. The corresponding minimum specific surface areas $S_\zeta\omega/N_\lambda$ are shown in Figure 2.83. It is seen that for $T_{max} \approx 1000$ to 2500 °K /2.32, 2.87/ the specific surface area of the radiator is $\sim 10^{-1}$ to 10^{-2} m²/kw, so that even

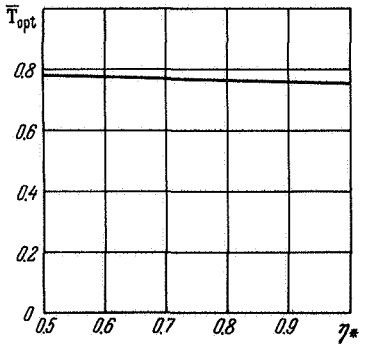

FIGURE 2.82. Optimum temperature ratio $\overline{T}_{opt} = T_{min}/T_{max}$ of spacecraft power plant, corresponding to minimum required radiator surface area.

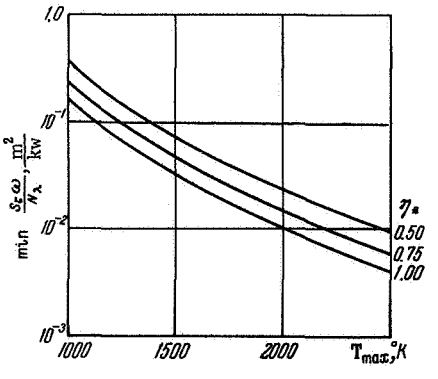

FIGURE 2.83. Specific radiator surface area as function of maximum cycle temperature.

for a power $N_v \approx N_\lambda \approx 20{,}000$ kw (i.e., for a thrust of the order of 10.0 kg at a specific impulse $I^\circ \approx 10{,}000$ sec) a radiator surface area of hundreds of m^2 is required. This makes it necessary to consider ways to minimize the radiator weight. This will be done for the typical cases of a radiator with fins and of a strip radiator.

2. System of energy removal from a flat-tube radiator with fins.

A flat tube radiator with fins is shown in Figure 2.84 /2.32/. The
108 thermal energy of the coolant flowing inside the tubes is removed by radiation from the surface of the fins.

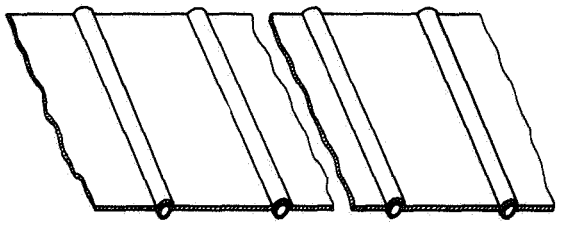

FIGURE 2.84. Flat tube radiator with fins.

We shall first consider the problem of weight minimization of systems with tubes of very small diameter. This is equivalent to the two-dimensional problem of minimizing the weight of a system of fins cooled by radiation linear heat sources arranged in parallel with a spacing $2L$ (Figure 2.85, a). Because of symmetry it suffices to consider the fin part of length L cooled by radiation from AB. Heat is supplied to the fin on one side along its base OA (Figure 2.85, b), the minimum fin thickness $O'B$ being given /2.169/. We shall consider a thin fin of smooth contour, for which the equations of heat conduction and heat radiation are respectively

$$Q = 2\lambda_* y \frac{dT}{dy}, \qquad \frac{dQ}{dx} = 2\sigma\omega T^4, \tag{2.91}$$

where y is the thickness of the fin, the x-axis is directed along the fin width, Q is the heat flux in the x-direction per unit fin length, λ_* is the coefficient of thermal conductivity, T is the temperature of the fin.

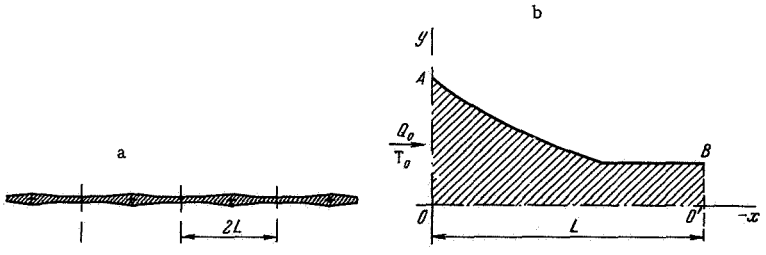

FIGURE 2.85. Heat flow in flat tube radiator with fins.

The optimum contour (fin of minimum weight) corresponds to the minimum cross-sectional area $\mathcal{F} = -2\int_0^L y dx$ of the fin when the initial heat flux Q_0, initial temperature T_*, and minimum fin thickness y_{min} ($y \geqslant y_{min}$) are given.

We introduce the dimensionless variables:

$$\left.\begin{aligned} \bar{Q} &= \frac{Q}{Q_0}, \quad \bar{T} = \frac{T}{T_*}, \\ \bar{x} &= \frac{x}{\frac{Q_0}{2\sigma\omega T_*^4}}, \quad \bar{y} = \frac{y}{\frac{Q_0^2}{4\lambda_* \sigma\omega T_*^5}}, \quad \bar{\mathcal{F}} = \frac{\mathcal{F}}{\frac{Q_0^3}{8\lambda_*^2 \sigma^2\omega^2 T_*^9}}. \end{aligned}\right\} \tag{2.92}$$

Then

$$\left.\begin{aligned} \bar{Q} &= \bar{y}\frac{d\bar{T}}{d\bar{x}}, \quad \frac{d\bar{Q}}{d\bar{x}} = \bar{T}^4, \quad \bar{\mathcal{F}} = -2\int_0^{\bar{L}} \bar{y} d\bar{x}. \end{aligned}\right\} \tag{2.93}$$

109 At the fin edge $\bar{x} = \bar{L}$ we have $\bar{Q} = \bar{Q}_L = 0$. It is therefore advisable to determine the other variables as functions of $\bar{Q}$: $\bar{T}(\bar{Q})$, $\bar{x}(\bar{Q})$, $\bar{y}(\bar{Q})$. Equations (2.93) can then be rewritten as follows:

$$\frac{d\bar{T}}{d\bar{Q}} = \frac{\bar{Q}}{\bar{y}\bar{T}^4}, \quad \bar{\mathcal{F}} = -2\int_1^0 \frac{\bar{y}}{\bar{T}^4} d\bar{Q}, \tag{2.94}$$

where for $\bar{Q} = 1$, $\bar{T} = 1$, $\bar{y} = \bar{y}_0$; for $\bar{Q} = 0$, $\bar{T} = \bar{T}_L$, $\bar{y} = \bar{y}_{min}$.

In this formulation the problem can be solved by maximization /2.170/.

We introduce a new variable $\bar{\mathcal{F}}_i = -2\int_1^{\bar{Q}} \frac{\bar{y}}{\bar{T}^4} d\bar{Q}$ and consider the problem of optimizing the boundary value of this variable for $\bar{Q} = 0$. The Hamiltonian /2.170/ is

$$H = p_1 \frac{\bar{Q}}{\bar{y}\bar{T}^4} - p_2 \frac{2\bar{y}}{\bar{T}^4}, \tag{2.95}$$

where

$$p_1' = -\frac{\partial H}{\partial \bar{T}} = \frac{4}{\bar{T}^5}\left(\frac{p_1\bar{Q}}{\bar{y}} - 2p_2\bar{y}\right), \quad p_2' = -\frac{\partial H}{\partial \bar{\mathcal{F}}_i} = 0, \tag{2.96}$$

with the boundary conditions: for $\bar{Q} = 0$, $p_1 = 0$, $p_2 = 1.0$. The momentum p_2 is constant: $p_2 = 1.0$ (cf. (2.96)). According to /2.170/, H must be maximum at $\bar{y}$ for any values of $\bar{T}$ and p_1. At the rib edge, where $\bar{Q} = 0$ and $p_1 = 0$, the maximum H is attained for $\bar{y}_L = \bar{y}_{min}$, so that $H_L = -\frac{2\bar{y}_{min}}{\bar{T}_L^4}$, $(p_1')_L = -\frac{8\bar{y}_{min}}{\bar{T}^5}$.

Moving away from the fin edge, we see that as long as $\sqrt{-\frac{p_1\bar{Q}}{2}} < \bar{y}$, the maximum of H occurs at $\bar{y} = \bar{y}_{min}$. Hence, for this part of the fin the optimum profile is $\bar{y} = \bar{y}_{min} = \text{const}$.

At some point $\bar{Q} = \bar{Q}_{**}$ the magnitude $\sqrt{-\frac{p_1\bar{Q}}{2}}$ becomes equal to $\bar{y}_{min}$; hence, for $\bar{Q} > \bar{Q}_{**}$ the function H has a maximum at $\bar{y} \geqslant \bar{y}_{min}$ and $p_1 = -\frac{2\bar{y}^2}{\bar{Q}}$,

which leads to the following differential equation:

$$2\overline{Q}\overline{T}\frac{d^2\overline{T}}{d\overline{Q}^2}+16\overline{Q}\left(\frac{d\overline{T}}{d\overline{Q}}\right)^2-\overline{T}\frac{d\overline{T}}{d\overline{Q}}=0. \tag{2.97}$$

110 Integration of this equation yields

$$\overline{T}=[(1-\overline{T}_L^9)\,\overline{Q}^{3/2}+\overline{T}_L^9]^{1/9}, \tag{2.98}$$

the contour being determined by integrating the following system:

$$d\bar{x}=\frac{d\overline{Q}}{[(1-\overline{T}_L^9)\,\overline{Q}^{3/2}+\overline{T}_L^9]^{1/6}}, \qquad \bar{y}=\frac{6\overline{Q}^{1/2}}{1-\overline{T}_L^9}\frac{d\overline{Q}}{d\bar{x}}, \tag{2.99}$$

where $\overline{T}_L$ corresponds to the temperature at the fin edge, if the contour given by (2.99) is continued in the region $\bar{y}<\bar{y}_{min}$. Figure 2.86 shows the optimum contours ((2.99)) for some values of $\overline{T}_L$ /2.169/ (the calculations were performed by Yu. V. Shalaev).

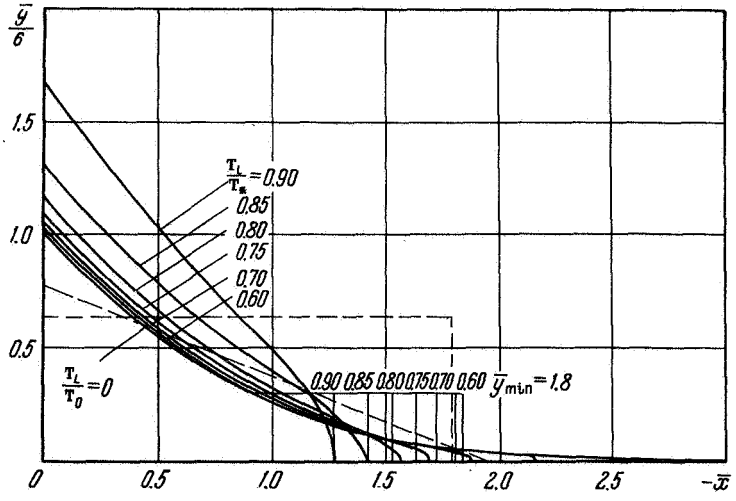

FIGURE 2.86. Optimum contours of a flat fin cooled by radiation.

For $\overline{T}_L=0$, we obtain the absolute-minimum fin area $\overline{\mathcal{F}}_{opt}$, which corresponds to the particular case considered in /2.171 — 2.174/ of a
111 fin with $\bar{y}_{min}=0$ (cf. /2.169/ for more details). For this fin

$$\left.\begin{aligned}
&\overline{T}=\overline{Q}^{1/6}, \quad \overline{Q}=\left(1+\frac{\bar{x}}{3}\right)^3, \quad \overline{T}=\left(1+\frac{\bar{x}}{3}\right)^{1/2},\\
&\bar{y}=6\left(1+\frac{\bar{x}}{3}\right)^{3.5},\\
&\bar{y}_0=6., \qquad \overline{L}_{opt}=-3., \qquad \overline{\mathcal{F}}_{opt}=8.,\\
&L_{opt}=-\frac{3}{2}\frac{Q_0}{\sigma\omega T_*^4}, \quad y_{0\,opt}=\frac{3}{2}\frac{Q_0^2}{\lambda_*\sigma\omega T_*^5}, \quad \mathcal{F}_{opt}=\frac{Q_0^3}{\lambda_*^2\sigma\omega T_*^9}.
\end{aligned}\right\} \tag{2.100}$$

It is convenient to refer to the values of $\mathcal{F}$ for all analyzed contours to this value $\mathcal{F}_{opt}$.

When $\bar{y}_{min}$ is given the optimum contour from the fin center line to $\bar{y} = \bar{y}_{min}$ ($\bar{x}_{**}$, $\bar{Q}_{**}$, $\bar{T}_{**}$) is plotted in Figure 2.86, with $\bar{T}_L$ as parameter; the parameters of the part of constant thickness $\bar{y} = \bar{y}_{min}$ adjoining the fin edge are determined by the following formulas (at $Q_{**} \geqslant \bar{Q} \geqslant 0$):

$$\bar{T}^5 - \bar{T}_{**}^5 = \frac{5}{2\bar{y}_{min}}(\bar{Q}^2 - \bar{Q}_{**}^2),$$

$$\bar{x} - \bar{x}_{**} = \int_{\bar{Q}_{**}}^{\bar{Q}} \frac{d\bar{Q}}{\left[\frac{5}{2\bar{y}_{min}}(\bar{Q}^2 - \bar{Q}_{**}^2) + \bar{T}_{**}^5\right]^{4/5}}. \qquad (2.101)$$

Figure 2.86 shows the optimum contours for $\bar{y}_{min} = 1.8$. The relative cross-sectional areas $\bar{\mathcal{F}}/\bar{\mathcal{F}}_{opt}$ of these fins in Figure 2.87 are shown as a function of $\bar{T}_L$; the dashed curve $\bar{\mathcal{F}}/\bar{\mathcal{F}}_{opt}$ for $\bar{y}_{min} = 0$. For $\bar{y}_{min} = 1.8$, $\bar{y}_{min}/\bar{y}_0 = 0.31$; the area for a gently sloping optimum contour is minimum at $\bar{T}_L \approx 0.70$, being $\bar{\mathcal{F}}/\bar{\mathcal{F}}_{opt} = 1.205$, which is considerably less than for the optimum rectangular rib, where $\bar{\mathcal{F}}/\bar{\mathcal{F}}_{opt} = 1.635$ (cf. dashed line in Figure 2.86 /2.175, 2.176/). The contour of an optimum triangular fin /2.177/ for which $\bar{\mathcal{F}}/\bar{\mathcal{F}}_{opt} = 1.103$ (with $\bar{y}_{min} = 0$) is also shown dashed in Figure 2.86.

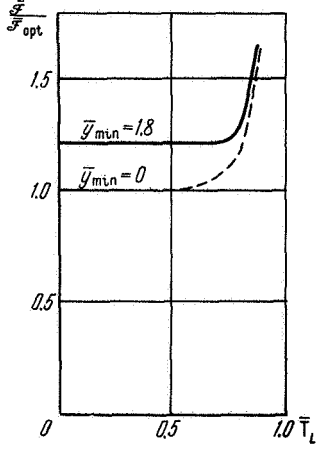

FIGURE 2.87. Influence of relative temperature of fin edge on cross-sectional area of cooling fin.

In real flat tube radiators with fins having tubes of finite diameter (Figure 2.84), radiation from the surface of the tubes and mutual irradiation of tubes and fins must be taken into account. The latter is, according to /2.175/, relatively unimportant in radiators with sufficiently long fins, and will therefore be neglected in a first approximation. We shall consider an optimum combination, of minimum weight, of fins and tubes /2.169/ heated on the inside by the coolant, the tube-wall temperature $T_w = T_*$ and the tube geometry (diameter D, wall thickness δ) being given. As before, Q_0 is the initial heat flux along one fin; the total heat removed in unit time per unit tube length z is given by

$$\frac{dN_\zeta}{dz} = 2Q_0 + \pi(D+\delta)\sigma\omega T_*^4. \qquad (2.102)$$

The weights of unit length of tube and fin are determined from

$$\frac{dG_\zeta}{dz} = \frac{\pi(D+\delta) - \pi D^2}{4}\gamma_1 + \frac{2\frac{\bar{\mathcal{F}}}{\bar{\mathcal{F}}_{opt}}Q_0^3}{\lambda_* \sigma^2 \omega^3 T_*^9}\gamma_2, \qquad (2.103$$

where γ_1 is the specific weight of the material of the tube, γ_2 is the specific weight of the material of the fin.

The weight of the radiator per unit of heat removed in unit time [relative weight] is by (2.102) and (2.103):

$$\frac{dG_\zeta}{dN_\zeta} = \frac{\mathcal{A} + \mathcal{B}Q_0^3}{Q_0 + \mathcal{C}}, \tag{2.104}$$

where

$$\mathcal{A} = \pi \frac{(D+\delta)^2 - D^2}{8} \gamma_1, \quad \mathcal{B} = \frac{\overline{\mathcal{F}}/\overline{\mathcal{F}}_{opt}}{\lambda_* \sigma^2 \omega^2 T_*^3} \gamma_2, \quad \mathcal{C} = \frac{\pi (D+\delta)}{2} \sigma \omega T_*^4.$$

The relative weight of the radiator is minimum for

$$Q_0^2 = \frac{\mathcal{A}}{\mathcal{B}(2Q_0 + 3\mathcal{C})},$$

or

$$(1+\chi)\chi^2 = \frac{4}{27} \frac{\mathcal{A}}{\mathcal{B}\mathcal{C}^3}, \tag{2.105}$$

where

$$\chi = \frac{2}{3} \frac{Q_0}{\mathcal{C}}.$$

113 The minimum relative weight is

$$\left(\frac{dG_\zeta}{dN_\zeta}\right)_{min} = \frac{\mathcal{A}/\mathcal{C}}{1+\chi}, \tag{2.106}$$

i.e., is a $(1+\chi)$-th part of that of a finless tube radiator.

Figure 2.88 shows $\frac{1}{1+\chi}$ for $D = 10$ mm, $\delta = 0.25$ to 0.75 mm, $T_* = 1100$ °K, $\omega = 0.9$; the tube is made of steel, the fins are of steel, copper, or beryllium with $\overline{\mathcal{F}}/\overline{\mathcal{F}}_{opt} = 1.205$ and have the above-considered optimum contour with $\bar{y}_{min}/\bar{y}_0 = 0.31$. The optimum flat tube radiator with fins has a relative weight approximately one half that of a finless tube radiator.

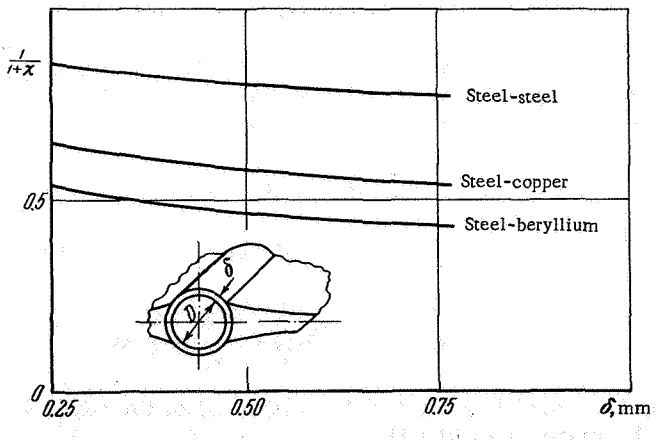

FIGURE 2.88. Influence of fins on relative weight of flat tube radiator.

The relative weight of a tube radiator is a function of the minimum thickness δ of the tube wall, which depends on the meteoric hazard (cf. § 3 of Chapter One). The relative weight of a tube radiator has been plotted in Figure 2.89 as a function of its temperature T_* for different permissible numbers of penetrations of the radiator by meteors, per unit radiated energy /2.32/, using Figure 1.8 and equation (2.104) for a finless tube radiator ($Q_0 = 0$). The useful power of the propulsion system (e.g., the total jet power N_λ) is, of course, much less than the power N_ζ removed by the radiator; even in an ideal cycle ($\eta = 1.0$) the useful power is a third of the radiated power. The unit weight of the tube radiator (weight per unit useful power of the propulsion system) thus is several times larger than the relative weight given in Figure 2.89 (the number scale of penetrations per kw-hr of useful energy is altered accordingly). It is seen that the unit weight of a tube radiator is considerable compared with the unit weights of power sources, power converters, and nozzles; cf. §§ 1 and 2 of this chapter. A flat optimum tube radiator with fins has about half the unit weight of a finless tube radiator (cf. Figure 2.88). An even larger weight reduction can be achieved by the use of star-shaped radiators.

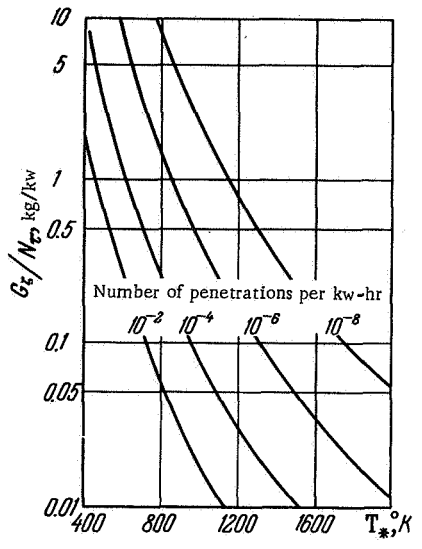

FIGURE 2.89. Relative weight of tube radiator (per unit radiated power), taking into account meteoric hazard during flights near Earth, as function of the radiator temperature T_*.

3. Energy removal from a star-shaped tube radiator with fins. We have just discussed the two-dimensional problem of the optimum contour of a heat-radiating fin to which heat is supplied from one side. It was shown that the cross-sectional area of the optimum (minimum-mass) fin is

$$\mathcal{F} = \frac{\overline{\mathcal{F}}}{\overline{\mathcal{F}}_{\text{opt}}} \frac{Q_0^3}{\lambda_* \sigma^2 \omega^2 T_*^9}, \qquad (2.107)$$

i.e., the cross-sectional area (weight) of the optimum fin is proportional to the third power of the heat flux Q_0 radiated by it. Hence, if a specified quantity of heat Q_Σ is to be radiated in unit time by n fins ($Q_\Sigma = nQ_0$) the total cross-sectional area of the fins (i.e., their weight) will be inversely proportional to n^2 (neglecting the mutual irradiation of the fins):

$$\mathcal{F}_\Sigma = n\mathcal{F} \sim \frac{1}{n^2} \text{ when } Q_\Sigma = nQ_0 = \text{const}. \qquad (2.108)$$

115 The heat-radiating fins may be arranged like a star at the apexes of the polyhedron (tube) being cooled (Figure 2.90). When $n > 2$ the mutual irradiation of the fins becomes important, and determines the optimum

number of fins (n_{opt}) and the corresponding optimum shape of their cross section /2.178/.

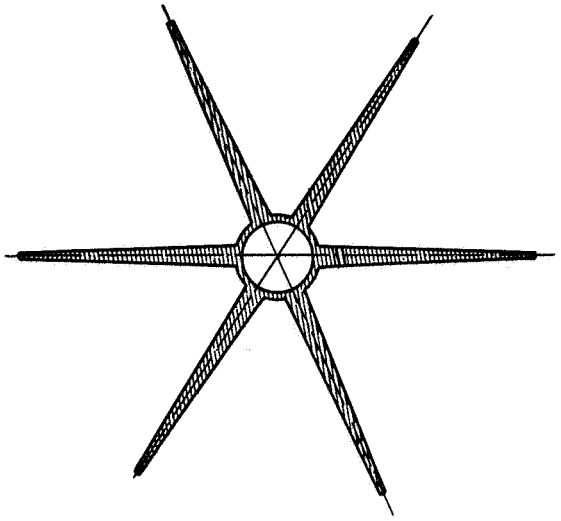

FIGURE 2.90. Star-shaped tube radiator with fins.

The problem of the optimum star-shaped fin arrangement was solved in this formulation in /2.178/ and /2.179/. Figure 2.91 shows the optimum shapes of star-shaped fins for $\omega = 1.0$ when the central tube is small.

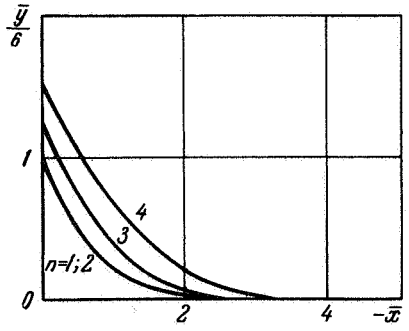

FIGURE 2.91. Influence of number of fins (n) on optimum shape of fins in star-shaped radiator.

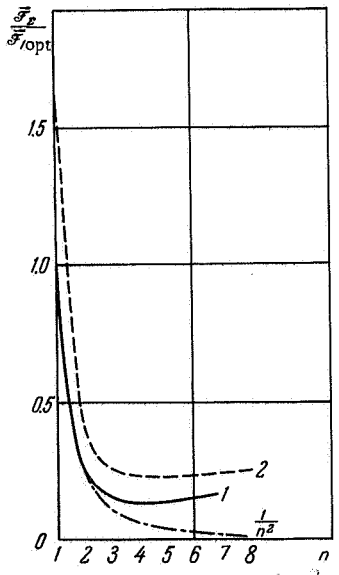

FIGURE 2.92. Influence of number of fins (n) on cross-sectional area of star-shaped radiator:

1) fins of optimum shape, 2) rectangular fins.

The influence of mutual irradiation is for $n > 2$ clearly expressed by the increase of the relative fin dimensions with increasing number of fins. However, taking (2.108) into account, we find that the absolute cross-sectional area $\mathcal{F}_\Sigma$ of the fins (and hence the radiator weight) has a minimum for a star-shaped arrangement of 4 or 5 fins when the total heat flux Q_Σ is given (cf. solid curve in Figure 2.92, where $\mathcal{F}_\Sigma$ is referred to the area $\mathcal{F}_{1\,opt}$
116 of a single optimum fin radiating the same quantity of heat Q_Σ in unit time). The dashed curve in Figure 2.92 has been plotted from the computed values, given in /2.80/ and /2.81/, for the best rectangular fins in a star-shaped arrangement, whose cross-sectional area is ~ 1.5 times larger than that of the optimum fins. The dot-dash curve corresponds to (2.108), the mutual irradiation of the fins being neglected. More detailed information on flat and star-shaped fin arrangements of radiators can be found in /2.178 — 2.195/.

When comparing a star-shaped radiator with a flat tube radiator with fins it should be remembered that for the latter $n = 2$. The weight of the fins is, according to Figure 2.92, approximately 40% less in the optimum star-shaped radiator than in a flat radiator.

4. Energy removal from a belt radiator. Since the high unit weight of a tube radiator is largely due to the requirements of shielding against meteors, a belt radiator was proposed in /2.196/, the weight of whose main element — the belt — does not depend on the meteoric hazard. In this radiator a flexible belt is pressed against the cylinder containing the coolant by means of rollers /2.196/ (Figure 2.93, a), or by the centrifugal forces (/2.197/ and /2.198/) in the case of a revolving belt.

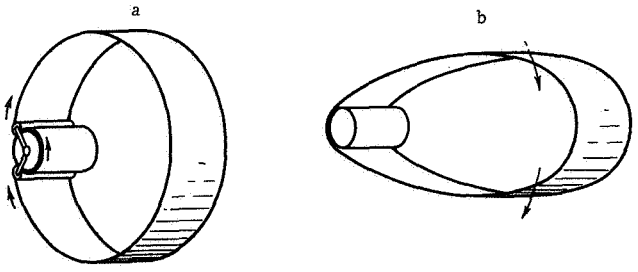

FIGURE 2.93. Energy removal by means of belt radiator.

The belt removes the heat from the cylinder and radiates it from its surface. Penetration of the belt by micrometeorites does not affect the operation of such a radiator. Details on the belt shape and its stability in space, on the effects of mutual irradiation of the belt elements, etc., can be found in /2.197 — 2.205/. We shall now consider the main parameters of a belt radiator /2.196/.

117 Let $G_{\zeta 1}$ be the belt weight, c_* the specific heat of its material, L its length, W the tangential speed of the drum, T_* the maximum temperature at the point where the belt leaves the drum, T_2 the temperature at the point where the belt comes into contact with the drum; the power removed by the belt (neglecting the part in contact with the drum) is then

$$N_\zeta = G_{\zeta 1} c_* (T_* - T_2) \frac{W}{L}. \qquad (2.109)$$

This power must be radiated by the belt. Neglecting the mutual irradiation of the belt elements, we can write in a first approximation /2.196/

$$N_\zeta = 2b_* L\sigma\omega T_\sigma^4, \tag{2.110}$$

where b_* is the width of the belt, $T_\sigma = \left(\frac{1}{L}\int_0^L T^4 dx\right)^{1/4}$.

The average temperature T_σ of the belt is determined by the temperature drop along the belt:

$$\frac{dT}{dx} = c_1 T^4. \tag{2.111}$$

Integrating (2.111) with the boundary conditions $T = T_*$ at $x = 0$, $T = T_2$ at $x = L$, we obtain

$$c_1 = \frac{T_*^{-3} - T_2^{-3}}{3L},$$

whence

$$T_\sigma = \left(\frac{1}{L}\int_{T_*}^{T_2} \frac{dT}{c_1}\right)^{1/4} = T_* \left[\frac{3\left(1 - \frac{T_2}{T_*}\right)}{\left(\frac{T_2}{T_*}\right)^{-3} - 1}\right]^{1/4}. \tag{2.112}$$

The weight of the belt is by (2.109), (2.110), and (2.112)

$$G_{\zeta 1} = \frac{N_\zeta^2\left[\left(\frac{T_2}{T_*}\right)^{-3} - 1\right]}{6c_* b_* W\sigma\omega T_*^5\left(1 - \frac{T_2}{T_*}\right)^2}. \tag{2.113}$$

The belt weight has a minimum for $(T_2/T_*)_{opt} = 0.69$. Thus,

$$\min G_{\zeta 1} = 3.55\,\frac{N_\zeta^2}{c_* b_* W\sigma\omega T_*^5}, \qquad L_{opt} = 0.31\,\frac{G_{\zeta 1\,\min} c_* T_* W}{N_\zeta}. \tag{2.114}$$

The temperature T_* is approximately equal to the minimum cycle temperature T_{min} (the thermal contact resistance is very small /2.206—2.208/). The belt speed W is limited by its mechanical properties; if we assume that the belt width b_* (and the width of the cylinder containing the coolant) is proportional to the power removed, i.e., $b_* = kN_\zeta$, then the first equation (2.114) determines the relative belt weight $G_{\zeta 1}/N_\zeta$.

According to /2.196/, for $N_\lambda = 20{,}000$ kw, $N_\zeta = 68{,}000$ kw, a steel belt with graphite coating, $W = 15.2$ to 30.5 m/sec, $b_* = 11.6$ m, $T_{min} = 1000$ °K the total weight of the belt radiator with the cylinder containing the coolant and the drive is $\sim G_\zeta = 3850$ to 7250 kg ($G_\zeta/N_\zeta \approx 0.057$ to 0.107 kg/kw, $G_\zeta/N_\lambda \approx \approx 0.19$ to 0.36 kg/kw); this is considerably less than the weight of a tube radiator with fins for the same power and temperature, which, according to /2.209/, is $\sim G_\zeta = 19{,}400$ kg ($G_\zeta/N_\zeta \approx 0.285$ kg/kw, $G_\zeta/N_\lambda \approx 0.97$ kg/kw).

Figure 2.94 gives the relative weights $\frac{G_\zeta}{N_\lambda} \approx \frac{G_\zeta}{N_\nu}$ of flat tube radiators with fins (solid curves) and belt radiators (shaded region between dashed curves) as a function of the maximum cycle temperature T_{max}. The curves for

119 tube radiators with fins show the number of [meteor] penetrations per kw.hr useful energy; these curves were plotted from the data in Figure 2.89 under the assumption that the weight advantage due to the fins approximately compensates for the replacement of N_ζ by $N_\lambda \approx N_v$. The parameters of the heat-removal system with belt radiator were extrapolated from those of the example considered above /2.196/, with the aid of (2.114).

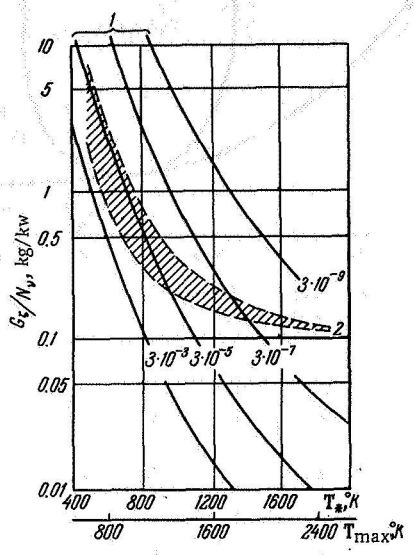

FIGURE 2.94. Unit weights of radiative heat-removal systems of spacecraft power plants (per unit useful power):

1) flat tube radiator with fins; curves show number of meteor penetrations per kw.hr.; 2) belt radiator.

Figure 2.94 shows that even with the possibility of minimization, the unit weights of radioactive heat-removal systems in spacecraft power plants are large. The weight of the heat-removal system is thus a considerable part of the total weight of spacecraft power plants.

5. **Weight characteristics of spacecraft power plants.** Figure 2.95, based on /2.89/, shows the optimum zone for each of the power sources and energy converters discussed in § 2 depending on the operating period T and the useful power N_v. The unit weights of elements of spacecraft power plants given in §§ 2 and 3 determine their overall weight characteristics.

120 The total weight G_v of the power source depends on the maximum generated power N_v. Table 2.11 gives the parameters of some of the power sources considered /2.90, 2.91, 2.104/. It is seen from this table and from Figure 2.96 which is based on it and on /2.38/ that the unit weight of the power source $\alpha = G_v/N_v$ is nearly constant, for $N_v \gtrsim 10^2$ to 10^3; it decreases slightly with increasing useful power N_v.

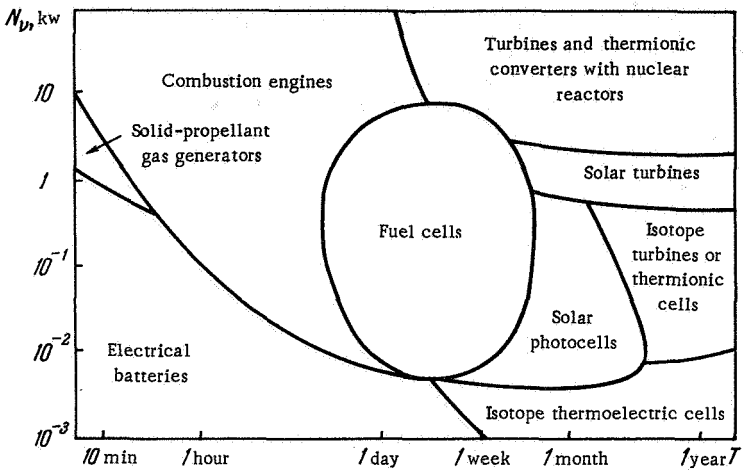

FIGURE 2.95. Optimum zones for different types of spacecraft power plants, depending on operating period T and useful power N_v.

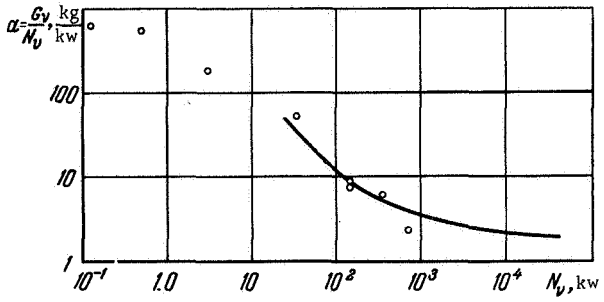

FIGURE 2.96. Unit weights of spacecraft power plants; curve is plotted from data in /2.38/, circles represent data in Table 2.11.

TABLE 2.11. Parameters of spacecraft power plants

Power plant	Snap 1A	Snap 10A	Snap 2	Snap 8	Snap 50	BBC-Krupp	BBC-I	BBC-II
Useful power N_v, kw . . .	0.125	0.5	3.0	35	350	150	150	700
Maximum temperature. . T_{max}, °K	—	810	925	980	1370	1180	—	—
Heat source and cycle . .	Radio-isotope, thermo-electric cell	Reactor, thermo-electric cell	Reactor, Rankine cycle	Reactor, Rankine cycle	Reactor, Rankine cycle	Reactor, Rankine cycle	Reactor, therm-ionic cell	Reactor, therm-ionic cell
Radiator area S, m^2 . . .	—	5.8	11.15	130	—	320	—	—
Weight G_v, kg.	79.3	295	544	1905	2270	1350	1200	1660
Unit weight $\alpha = \frac{G_v}{N_v}$, kg/kw	635	590	181	55	6.5	9.0	8.0	2.4

121 Comparison of these values of α (≈ 1 to 10 kg/kw for $N_e \geqslant 10^2$ kw) with the unit weights of electric propulsion engines and other elements shows that the weight of such a propulsion system is mainly determined by the unit weight α of the power source /2.48/. Thus, from the viewpoint of spaceflight mechanics, the power of such a propulsion system is limited and is the principal factor determining the weight of the propulsion system.

Chapter Three

GENERALIZED PARAMETERS OF SPACE PROPULSION SYSTEMS

122 The generalized characteristics of the main types of space propulsion systems discussed in the literature are considered below from the viewpoint of spaceflight mechanics /3.1—3.3/. This chapter is based on Chapter Two, dealing with the physical principles of the elements of space propulsion systems.

The introduction of generalized parameters schematizes the problem while preserving its principal traits. A more detailed study may be based on the principles described.

The propulsion systems are grouped into three classes (cf. §§ 1, 2, and 3 of this chapter), depending on the basic limitations imposed by the physical principles. A limitation is basic if the flight conditions are optimum when the limit considered is reached; such limitations may be imposed on the exhaust velocity of the gases in the jet, the power, or the thrust.

The propulsion systems considered exclude those taking up working fluid from the environment, which were discussed in Chapter Two.

§ 1. PROPULSION SYSTEMS WITH LIMITED EXHAUST VELOCITY

This class includes thermal propulsion systems whose schematic layout is shown in Figure 3.1. The thrust in such propulsion systems is developed by a nozzle, which converts the thermal energy of the working fluid into kinetic energy of the directed motion of the jet.

During space flight the main parameters of thermal propulsion engines are determined by the nozzle throat area $\mathcal{F}_*$, the total pressure p_0, and
123 the gas temperature T_0 at the nozzle inlet:

$$\left.\begin{aligned} P &= k_1 \mathcal{F}_* p_0, & q &= k_2 \frac{\mathcal{F}_* p_0}{\sqrt{T_0}}, \\ V &= \frac{P}{q} = k_3 \sqrt{T_0}, & N &= \frac{qV^2}{2} = k_4 \mathcal{F}_* p_0 \sqrt{T_0}. \end{aligned}\right\} \qquad (3.1)$$

When the engine geometry is given ($\mathcal{F}_* = \text{const}$), the main parameters P and q of the propulsion system can be varied if independent adjustment of the total pressure p_0 and the temperature T_0 is possible. The basic

limitation of heat engines is the maximum temperature T_{0max} permissible for the structure; this limits the possible exhaust velocity (cf. (3.1)) to

$$V \leqslant V_{max} = k_3 \sqrt{T_{0max}}. \tag{3.2}$$

When the strength of the structure is given, the second limitation is imposed by the maximum permissible total pressure p_{0max} which determines the maximum thrust and power per unit cross-sectional area of the nozzle:

$$\frac{P_{max}}{\mathcal{F}_*} = k_1 p_{0max}, \quad \frac{N_{max}}{\mathcal{F}_*} = k_4 p_{0max} \sqrt{T_{0max}}. \tag{3.3}$$

The control characteristics of a thermal propulsion system during spaceflight are shown schematically in Figure 3.2. The thrust decreases during flight in the atmosphere (cf. Figure 2.12).

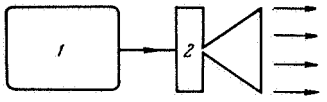

FIGURE 3.1. Schematic layout of thermal propulsion system:

1) container with working fluid, 2) nozzle with power source, energy converter, working-fluid supply system, and cooling system.

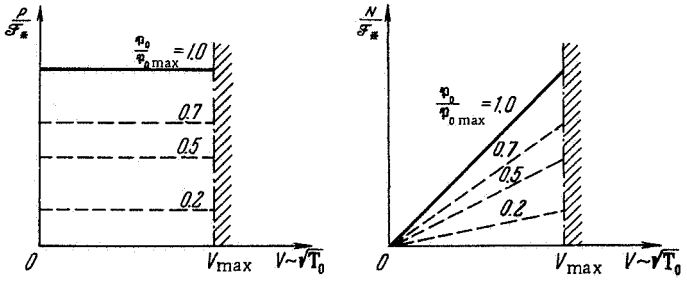

FIGURE 3.2. Control characteristics of thermal propulsion system.

124 The weight of a propulsion system of limited exhaust velocity is mainly determined by the weight G_μ of the container in which the working fluid is stored and by the maximum thrust P_{max}:

$$G_p = \beta_\mu G_\mu + \gamma_\Sigma P_{max}. \tag{3.4}$$

Values of the weight coefficients were given in Chapter Two.

§ 2. POWER-LIMITED PROPULSION SYSTEMS

Power-limited propulsion systems consist of a power plant (energy source, energy converter, cooling system), a nozzle with working-fluid supply system, and a container with the working fluid (Figure 3.3). The energy developed by the power plant is converted in the nozzle into kinetic energy of the directed motion of the jet. The existence of a separate plant of limited power $N_v \leqslant N_{v\max}$ determines the main properties of this group of propulsion systems.

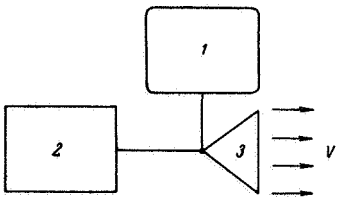

FIGURE 3.3. Schematic layout of power-limited propulsion system:

1) container with working fluid, 2) power source, 3) nozzle.

A characteristic property of power-limited propulsion systems is the possibility of varying the parameters q and V within wide limits. In addition, the power N_v delivered to the nozzle may be varied.

In an ideal nozzle all the power delivered to it is transformed into jet power. Hence,

$$\frac{qV^2}{2} = N_v \leqslant N_{v\max}, \quad P = qV, \tag{3.5}$$

where $N_{v\max}$ may be a function of the position and of time.

The characteristics of real nozzles were examined in detail in Chapter Two. Taking the actual properties into account, the jet power $^1/_2qV^2$ depends on the nozzle parameters, such as the exhaust velocity V.

The maximum power $N_{v\max}$ determines the maximum thrust, which for an ideal nozzle is by (3.5):

$$P_{\max} = \frac{2N_{v\max}}{V}. \tag{3.6}$$

125 The control characteristics of power-limited propulsion systems (with ideal nozzle) are shown in Figure 3.4.

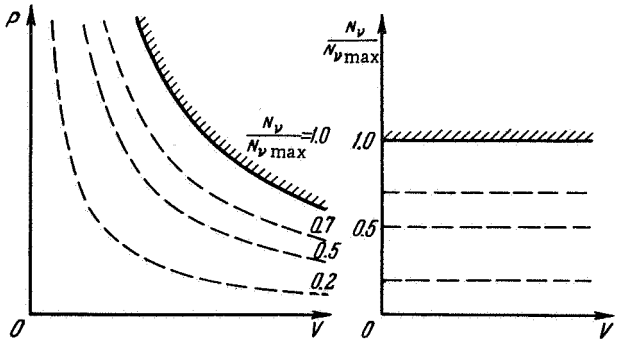

FIGURE 3.4. Control characteristic of power-limited propulsion system with ideal nozzle.

The weight of a power-limited propulsion system consists mainly of three components: the weight G_μ of the container in which the working fluid is stored, the weight G_ν of the power plant, and the nozzle weight G_γ:

$$G_p = \beta_\mu G_\mu + \alpha N_{\nu\max} + \gamma P_{\max}. \tag{3.7}$$

It is also possible to use an energy accumulator, whose weight is proportional to the maximum stored energy: $G_e = \beta E_0$. Values of the weight coefficients were given in Chapter Two.

§ 3. THRUST-LIMITED PROPULSION SYSTEMS (SAIL SYSTEMS)

This class of propulsion systems includes solar and isotope sails, whose thrust is limited by the maximum sail area $S_{\max}$:

$$P \leqslant P_{\max} = kS_{\max}. \tag{3.8}$$

No mass is discharged in sail systems; the thrust depends on the position or on the time. In an ideal solar sail with mirror reflecting properties the thrust is directed along the normal to the sail surface; its magnitude depends on the angle ϑ at which the sail is set, and on the distance R to the Sun:

$$\frac{P}{S} = k_\delta \frac{\cos\vartheta}{R^2}. \tag{3.9}$$

126 In an isotope sail the thrust depends on the ratio of the operating period t to the half-life $1/\lambda_\tau$ [of the isotope]:

$$\frac{P}{S} = k_\theta e^{-\lambda_\tau t}. \tag{3.10}$$

The weight of a thrust-limited propulsion system is determined by the maximum thrust:

$$G_p = \gamma P_{\max}. \tag{3.11}$$

The weight coefficients and their dependence on the basic parameters were discussed in detail in Chapter Two.

Part II

PROBLEMS OF OPTIMIZATION

129 After the purpose of the space flight has been determined, there arises the problem of attaining it most economically by selecting the optimum spacecraft with the most suitable propulsion system, determining the optimum control parameters, and working out the best program for the control functions.

The economy in carrying out the spaceflight is characterized by some optimality criterion: maximum payload, minimum cost, etc. We shall consider mainly the criterion of maximum payload; the optimization problem will be formulated for this case.

We shall call dynamic maneuver the flight from a fixed point 0 $\{\mathbf{r}_0, \mathbf{v}_0\}$ of the position-velocity phase space to another fixed point 1 $\{\mathbf{r}_1, \mathbf{v}_1\}$ during a given time T.

The variational problem is as follows: the given dynamic maneuver has to be carried out with maximum payload G_π at given take-off weight G_0.

The differential equations of the variational problem with the corresponding boundary conditions include the mass-flow equation and the equations describing the motion of the center of mass of the spacecraft:

$$\left.\begin{array}{lll} \dot{G} = -gq, & G(0) = G_0, & G(T) = G_\pi + G_\varkappa, \\ \dot{\mathbf{r}} = \mathbf{v}, & \mathbf{r}(0) = \mathbf{r}_0, & \mathbf{r}(T) = \mathbf{r}_1, \\ \dot{\mathbf{v}} = g\dfrac{P\mathbf{e}}{G} + \mathbf{R}, & \mathbf{v}(0) = \mathbf{v}_0, & \mathbf{v}(T) = \mathbf{v}_1. \end{array}\right\} \qquad \text{(II.1)}$$

Here $\mathbf{r}$ and $\mathbf{v}$ are respectively the radius vector and the velocity of the center of mass of the spacecraft, G is the variable weight of the spacecraft (q is the mass flow rate of the working fluid, P and $|\mathbf{e}| \equiv 1$ are respectively the magnitude and the direction of the thrust vector), $\mathbf{R} = \mathbf{R}(\mathbf{r}, t)$ is the vector of the acceleration due to the gravitational forces, g is the ratio of the weight to the mass, $G_\varkappa$ is the weight of the propulsion system.

The following points should be noted:

130 1. System (II.1) has the form of ordinary differential equations of the first order, solved for derivatives. This makes it possible to formulate Mayer's problem and to reduce the variational problem to a boundary-value problem for a system of ordinary differential equations with finite expressions for the control functions q, P, and $\vec{\mathbf{e}}$.

2. The right-hand side of the third equation (II.1) represents the accelerations due to the propulsive and gravitational forces. Other forces, such as drag, may also be taken into account.

3. In (II.1) the spacecraft is assumed to consist of a payload G_π, a weight $G_\varkappa$ of working fluid, and a propulsion engine of weight G_μ:

$$G = G_\pi + G_\mu + G_\varkappa. \qquad \text{(II.2)}$$

The remaining weight components (the weight of the structural elements and of the working-fluid tanks) are arbitrarily included in the payload. If necessary, it is possible to allow for these components in the variational formulation.

4. When the problem becomes more complex it is possible to increase the number of dimensions of the phase space, by adding, e.g., the coordinate t_μ, defining the time of engine operation (for flights with limited working-fluid reserves), or $G_\varkappa$ and G_β, being respectively the weight of the propulsion system and of the tanks (for problems concerning the jettisoning of parts of the engine and of the tanks). Differential equations describing the variation of these coordinates have then to be added to (II.1); in the examples given these equations have the following form:

in the first case

$$\dot{t}_\mu = \delta, \tag{II.3}$$

in the second case

$$\dot{G}_\varkappa = -gq_\varkappa, \quad \dot{G}_\beta = -gq_\beta. \tag{II.4}$$

We then obtain new control functions: $\delta(t) = 1$ or 0 according to whether the engine is fired or cut off; $q_\varkappa(t) \geqslant 0$, $q_\beta(t) \geqslant 0$ are functions determining the jettisoning of parts of the engine and of the tanks.

We shall now rewrite the initial system (II.1) in a form convenient for formulating Mayer's variational problem, adding the formal equation of payload constancy $\dot{G}_\pi = 0$, and substituting (II.2) for the total weight of the
131 spacecraft. The complete system of equations and boundary conditions then becomes:

$$\left.\begin{array}{lll} \dot{G}_\pi = 0, & G_\pi(0) + G_\varkappa + & G_\pi(T) = \max, \\ \dot{G}_\mu = -gq, & + G_\mu(0) = G_0, & G_\mu(T) = 0, \\ \dot{\mathbf{r}} = \mathbf{v}, & \mathbf{r}(0) = \mathbf{r}_0, & \mathbf{r}(T) = \mathbf{r}_1, \\ \dot{\mathbf{v}} = g\dfrac{Pe}{G_\pi + G_\mu + G_\varkappa} + \mathfrak{R}, & \mathbf{v}(0) = \mathbf{v}_0, & \mathbf{v}(T) = \mathbf{v}_1. \end{array}\right\} \tag{II.5}$$

Mayer's problem is now formulated as follows:

The system (II.5) must be solved for the control functions and control parameters (e, q, P, $G_\varkappa$, or others through which these are expressed) such that G_π is maximized for the given boundary conditions.

The variational formulation (II.5) can be simplified in many cases. We shall describe one transformation possible if the weight of the spacecraft has no components depending on the weight of the working fluid.

The sum of the payload G_π and the weight G_μ of the working fluid is

$$G_\sigma = G_\pi + G_\mu. \tag{II.6}$$

At the start G_σ is the difference between the take-off weight and the engine weight, while at the end of the flight it coincides with the payload:

$$G_\sigma(0) = G_0 - G_\varkappa, \quad G_\sigma(T) = G_\pi. \tag{II.7}$$

Introducing the new coordinate $G_\sigma(t)$, system (II.5) becomes:

$$\left.\begin{array}{lll} \dot{G}_\sigma = -gq, & G_\sigma(0) + G_\varkappa = G_0, & G_\sigma(T) = \max, \\ \dot{\mathbf{r}} = \mathbf{v}, & \mathbf{r}(0) = \mathbf{r}_0, & \mathbf{r}(T) = \mathbf{r}_1, \\ \dot{\mathbf{v}} = g\dfrac{P\mathbf{e}}{G_\sigma + G_\varkappa} + \mathbf{R}, & \mathbf{v}(0) = \mathbf{v}_0, & \mathbf{v}(T) = \mathbf{v}_1; \end{array}\right\} \qquad \text{(II.8)}$$

Mayer's problem is formulated in the same way as for the initial system, the only difference being that the final value of the weight G_σ is the control function.

In these formulations the dynamic maneuver and the initial weight are given, and the maximum payload is sought. The following formulations are also possible: the dynamic maneuver and the payload are specified and the minimum take-off weight has to be determined; the payload and the take-off weight are given, and the minimum flight time or the extremum of some coordinate has to be found.

132 The latter formulation may be advantageous when the weight distribution is known beforehand. On the other hand, this formulation is not universal, since in many problems the flight duration and some coordinates are unknown and must be found by optimization. We shall henceforth consider the problem of maximizing the payload when the take-off weight and the dynamic maneuver are specified.

This variational formulation must be adapted to each type of propulsion system.

1. The thrust P and the mass flow rate q have to be expressed through the independent control functions $\mathbf{u} = (u_1, \ldots, u_n)$ and the parameters $\mathbf{w} = (w_1, \ldots, w_m)$ of the propulsion system (the control characteristic of the engine):

$$P = P(\mathbf{u}, \mathbf{w}),\ q = q(\mathbf{u}, \mathbf{w}), \mathbf{u}_{\min} \leqslant \mathbf{u}(t) \leqslant \mathbf{u}_{\max}, \mathbf{w} = \text{const}. \qquad \text{(II.9)}$$

2. The weight $G_\varkappa$ of the propulsion system has to be determined as a function of the parameters $\mathbf{w}$ and the limiting values of the control functions $\mathbf{u}$ (the weight formula for the engine):

$$G_\varkappa = G_\varkappa(\mathbf{u}_{\min}, \mathbf{u}_{\max}, \mathbf{w}). \qquad \text{(II.10)}$$

These are the basic characteristics of the propulsion system. They are not exhaustive; with increasing complexity of the problem it may become necessary to add further information on the properties of the propulsion system. This will be done as required.

Chapter Four

IDEAL POWER-LIMITED ENGINE. SEPARATION OF THE VARIATIONAL PROBLEM. OPTIMUM WEIGHT RATIOS

133 We shall consider the problem of delivering a maximum payload with an ideal propulsion system of limited power. Study of the ideal case is interesting because it reveals the limitations of such engines.

The control characteristic (II.9) and the weight formula (II.10) for an ideal engine of limited power are ($u_1 = N$, $u_2 = q$):

$$P = \sqrt{2Nq}, \quad q = q, \quad G_\varkappa = \alpha N_{\max} \qquad (0 \leqslant N(t) \leqslant N_{\max}, \quad 0 \leqslant q(t) < \infty). \tag{4.1}$$

These equations describe the following properties of the ideal engine: a) there are no losses of working fluid or power*; b) the control is subjected only to a power limitation (the requirement that the mass flow rate q be nonnegative is not taken into account); c) the weight of the engine depends linearly on the maximum power.

In (4.1) the characteristics are expressed through the power N and the mass flow rate q. We may also select other systems of independent control functions. The power N must appear in all cases, since it is directly subjected to limitations. The mass flow rate q may be replaced by the exhaust velocity V or the thrust P, since neither of these magnitudes is limited in the ideal case (the requirement that the thrust P and the exhaust velocity V be nonnegative are again not taken into account). Thus ($u_1 = N$, $u_2 = V$)

$$P = 2N/V, \quad q = 2N/V^2, \quad G_\varkappa = \alpha N_{\max} \qquad (0 \leqslant N(t) \leqslant N_{\max}, \quad 0 \leqslant V(t) \leqslant \infty), \tag{4.2}$$

134 or ($u_1 = N$, $u_2 = P$)

$$P = P, \quad q = P^2/2N, \quad G_\varkappa = \alpha N_{\max} \qquad (0 \leqslant N(t) \leqslant N_{\max}, \quad 0 \leqslant P(t) < \infty). \tag{4.3}$$

* The subsequent procedure remains the same if we assume the losses to differ from zero but take the engine efficiency η_γ as constant: $\eta_\gamma = \text{const} < 1$ (irrespective of the mass flow rate and the power supplied to the nozzle). In this case α is the weight of the engine per unit maximum jet power $N_{\max}$; if the weight $G_\varkappa$ is referred to the maximum power $N_{\nu 0} = N_{\max}/\eta_\gamma$ of the energy souce, we have to write everywhere α/η_γ instead of α. This applies to all sections dealing with ideal engines of limited power.

It will be seen that in the ideal case it is advisable to express the thrust and the mass flow rate through the variable weight G of the spacecraft and through the acceleration a due to the thrust ($u_1 = N$, $u_2 = a$)

$$P = aG/g, \quad q = a^2G^2/2Ng^2, \quad G_\varkappa = \alpha N_{\max} \qquad (4.4)$$
$$(0 \leqslant N(t) \leqslant N_{\max}, \quad 0 \leqslant a(t) < \infty).$$

It then becomes possible to divide the optimization problem into two:

1) a weight problem — finding the optimum weight ratios and the optimum power control;

2) a dynamic problem — finding the optimum program of acceleration by means of the thrust.

Dividing the problem greatly simplifies the investigation and thus justifies the idealization.

§ 1. OPTIMUM WEIGHT RATIOS WHEN ENGINE WEIGHT IS CONSTANT OR VARIES STEPWISE

1. Separation of problem, power control. When the engine characteristic is given in the form (4.4) and the engine weight is constant during flight, (II.1) becomes

$$\left.\begin{aligned} &\dot G = -G^2a^2/2Ng, \quad G(0) = G_0, \quad G(T) = G_\pi + G_\varkappa, \\ &\mathbf{r} = \mathbf{v}, \qquad\qquad \mathbf{r}(0) = \mathbf{r}_0, \quad \mathbf{r}(T) = \mathbf{r}_1, \\ &\mathbf{v} = a\mathbf{e} + \mathfrak{R}, \qquad \mathbf{v}(0) = \mathbf{v}_0, \quad \mathbf{v}(T) = \mathbf{v}_1 \\ &(0 \leqslant N(t) \leqslant G_\varkappa/\alpha, \ 0 \leqslant a(t) < \infty, \ |\mathbf{e}(t)| = 1, \ G_\varkappa = \text{const}). \end{aligned}\right\} \qquad (4.5)$$

The problem consists of establishing the optimum programs for $N(t)$, $a(t)$, $\mathbf{e}(t)$ and selecting the optimum value of $G_\varkappa$, so that the boundary conditions for system (4.5) are satisfied and the maximum payload $G_\pi = G(T) - G_\varkappa$ is delivered, the take-off weight G_0 being specified (the unit weight α of the nozzle is given).

The power should be maintained at the maximum level during flight, since at a high power less working fluid has to be discharged in order to create the same thrust (cf. (4.1)). If we select a high maximum power,
135 the mass flow rate of working fluid will decrease, but the weight of the propulsion system will increase. Beyond some value of the maximum power, the increase of the engine weight will exceed the gain due to the reduced consumption of working fluid. For each flight program there exists an optimum ratio between the weight of the working fluid and the weight of the engine, for which the payload is maximum.

The existence of optimum weight ratios for spacecraft with engines of limited power was first established by means of models (/4.1 — 4.20/). The main simplification consisted in replacing the true gravitational field by a gravity-free field and in assuming one-dimensional motion. A simplification was also introduced in the control functions: the power and weight of the engine were assumed to be constant, and the thrust control corresponded either to the case of constant acceleration or to the case of constant thrust. These problems are used by us to illustrate the general procedure.

We shall now analyze system (4.5). The first equation in (4.5) can be integrated /4.15, 4.21/

$$G(t) = G_0\left(1 + \frac{G_0}{2g}\int_0^t \frac{a^2}{N}\,dt\right)^{-1}. \tag{4.6}$$

This relationship yields the law of variation of the total weight during flight. From this we obtain the final weight $G_1 = G(T)$, and also the payload $G_\pi = G_1 - G_\varkappa$:

$$G_\pi = G_0\left(1 + \frac{G_0}{2g}\int_0^T \frac{a^2}{N}\,dt\right)^{-1} - G_\varkappa. \tag{4.7}$$

Hence, when $G_\varkappa$ and G_0 are given, the payload varies inversely with the value of the integral

$$\int_0^T \frac{a^2}{N}\,dt. \tag{4.8}$$

The control function $N(t)$ enters only in (4.8) but not in the equation of motion (cf. the second and third equations (4.5)). For $N_{\max} = \text{const}$, as in the example considered, the optimum law of variation of $N(t)$, which
136 makes (4.8) a minimum, is independent of the other control function /4.15/:

$$N(t) = N_{\max} \text{ for } 0 \leqslant t \leqslant T. \tag{4.9}$$

We then obtain from (4.7):

$$G_\pi = G_0\left(1 + \frac{G_0}{2gN_{\max}}J\right)^{-1} - G_\varkappa \qquad \left(J = \int_0^T a^2 dt\right). \tag{4.10}$$

The integral J in (4.10) is independent of the power $N_{\max}$ and the weights $G_\varkappa$ and G_0, and can be evaluated if the flight path $\mathbf{r}(t)$ is known. This integral represents the dynamic part of the problem in the formula for the payload. The smaller its value, the larger is the payload when G_0, $N_{\max}$, and $G_\varkappa$ are given.

The original problem has thus been divided into two independent parts, a dynamic problem and a weight problem.

The dynamic part consists in establishing the optimum laws of variation of the magnitude $a(t)$ and the direction $\mathbf{e}(t)$ of the acceleration vector, which minimize the integral J for the given flight program:

$$\left.\begin{aligned} &J = \int_0^T a^2 dt = \min, \\ &\dot{\mathbf{r}} = \mathbf{v}, \qquad \mathbf{r}(0) = \mathbf{r}_0, \quad \mathbf{r}(T) = \mathbf{r}_1, \\ &\dot{\mathbf{v}} = a\mathbf{e} + \mathbf{R}, \quad \mathbf{v}(0) = \mathbf{v}_0, \quad \mathbf{v}(T) = \mathbf{v}_1 \\ &(0 \leqslant a(t) < \infty, \quad |\mathbf{e}(t)| = 1). \end{aligned}\right\} \tag{4.11}$$

The weight part of the problem consists in determining the optimum weight G_x of the propulsion system or the optimum value of N_{max} from the condition of payload maximum (4.10):

$$\max G_\pi = \max_{N_{max}>0} \left[G_0 \left(1 + \frac{G_0}{2gN_{max}} J \right)^{-1} - G_x (N_{max}) \right], \tag{4.12}$$

when the value of the integral J and the take-off weight G_0 are given, and the relationship $G_x (N_{max})$ is specified.

2. **Optimum weight ratios.** If the engine weight G_x is a linear function of the power N_{max},

$$G_x = \alpha N_{max} \quad (\alpha = \text{const}), \tag{4.13}$$

137 the relative payload can, in accordance with (4.10), be written as follows:

$$\frac{G_\pi}{G_0} = \frac{1}{1 + (G_0/G_x)\Phi} - \frac{G_x}{G_0} \qquad \left(\Phi = \frac{\alpha}{2g} \int_0^T a^2 dt \right). \tag{4.14}$$

The right-hand side of (4.14) has a maximum as a function of (G_x/G_0) (Figure 4.1). When Φ is given, we obtain the following solution of (4.12):

$$G_x/G_0 = \sqrt{\Phi} - \Phi. \tag{4.15}$$

The maximum relative payload (4.14), corresponding to (4.15), is

$$G_\pi/G_0 = (1 - \sqrt{\Phi})^2. \tag{4.16}$$

The optimum value of the working-fluid reserve $G_{\mu 0} = G_0 - G_x - G_\pi$ is given by

$$G_{\mu 0}/G_0 = \sqrt{\Phi}. \tag{4.17}$$

The optimum weight ratios (4.15) to (4.17) /4.15, 4.21/ are shown in Figure 4.2. The functions (4.15) and (4.16) exist only in the interval $0 \leqslant \Phi \leqslant 1$; hence, when the engine weight is given, a flight for which $J > 2g/\alpha$ is impossible (the payload, given by (4.16), becomes zero for $\Phi = 1$). The optimum engine weight does not exceed $^1/_4$ of the take-off weight.

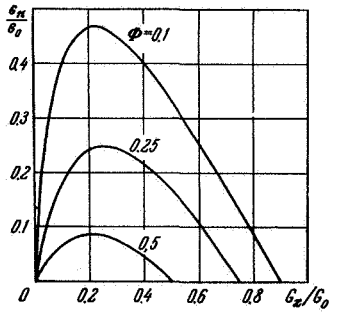

FIGURE 4.1. Payload G_π as function of engine weight G_x for given values of Φ (dynamic problem).

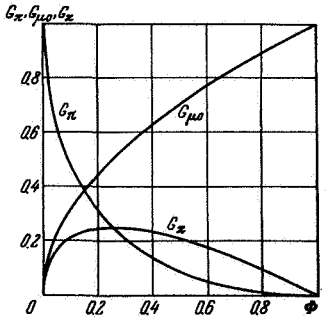

FIGURE 4.2. Optimum relative values of G_π, G_x, $G_{\mu 0}$ as functions of Φ (dynamic problem).

138 If the relationship between the engine weight and the maximum power is nonlinear:

$$G_\varkappa = G_\varkappa(N_{\max}), \tag{4.18}$$

the optimum weight ratios cannot be found explicitly in the general case. We shall obtain an equation for determining the optimum value of $N_{\max}$ /4.22/.

If (4.18) is nonlinear, the unit engine weight $\alpha = G_\varkappa/N_{\max}$ is a function of $N_{\max}$. We select an average value α_*, which is independent of $N_{\max}$, and express the payload (4.10) through two dimensionless magnitudes

$$\tilde{N} = \frac{N_{\max}}{G_0/\alpha_*}, \quad \Phi = \frac{\alpha_*}{2g}\int_0^T a^2 dt \qquad (\alpha_* = \text{const}). \tag{4.19}$$

The first of these is unknown, while the second is given (cf. (4.14)); the weight $G_\varkappa$ in (4.10) can be considered as a function of $\tilde{N}$, since the relationship $G_\varkappa(N_{\max})$ is given, and G_0 and α_* are specified.

Substituting (4.19) in (4.12) and setting $\partial G_\pi/\partial\tilde{N} = 0$, we obtain

$$\frac{d(G_\varkappa/G_0)}{d\tilde{N}}\left(\frac{\tilde{N}}{\sqrt{\Phi}} + \sqrt{\Phi}\right)^2 = 1. \tag{4.20}$$

Solving (4.20) for the dimensionless power $\tilde{N}$, we can obtain $N_{\max}$, $G_\varkappa$ and G_π by means of (4.18), (4.18) and (4.10) respectively. If the solution of (4.20) is not unique (this depends on the form of (4.18)), we select the solution which gives an absolute maximum of (4.10).

If (4.13) is linear, we write $\alpha_* = \alpha = \text{const}$, whence $\tilde{N} = G_\varkappa / G_0$ and (4.20) yields again (4.15). It is easily seen that (4.15) to (4.17) remain true also for a general linear relationship*

$$G_\varkappa = G_\varkappa(0) + \alpha_* N_{\max}, \tag{4.21}$$

if $G_\varkappa$ and G_π are replaced by $G_\varkappa - G_\varkappa(0)$ and $G_\pi - G_\varkappa(0)$ respectively. The permissible range of variation of Φ is then

$$0 \leqslant \Phi \leqslant 1 - \sqrt{G_\varkappa(0)/G_0}. \tag{4.22}$$

139 Consider the left-hand side of (4.20). The expression in parentheses is a monotonically increasing function of $\tilde{N}$. At the point $\tilde{N}_1 = \sqrt{\Phi} - \Phi$, i.e., for the optimum value of (4.13), it is equal to unity. The optimum will therefore move from the point $\tilde{N}_1 = \sqrt{\Phi} - \Phi$ to the right when $d(G_\varkappa/G_0)/d\tilde{N}_1 < 1$ (larger power) and to the left when $d(G_\varkappa/G_0)/d\tilde{N} > 1$ (smaller power).

We can interchange the roles of Φ and $\tilde{N}$ in (4.20), i.e., consider $\tilde{N}$ as the independent variable and Φ as the unknown. In this case the solution of (4.20) is

$$\sqrt{\Phi} = \frac{1}{2\sqrt{\dfrac{d(G_\varkappa/G_0)}{d\tilde{N}}}} \mp \sqrt{\frac{1}{4\dfrac{d(G_\varkappa/G_0)}{d\tilde{N}}} - \tilde{N}}$$
$$\left(\frac{d(G_\varkappa/G_0)}{d\tilde{N}} > 0, \quad 0 \leqslant \tilde{N} \leqslant \frac{1}{4\dfrac{d(G_\varkappa/G_0)}{d\tilde{N}}}\right). \tag{4.23}$$

* This applies also to the following two sections of this chapter.

The sign in (4.23) determines the two ranges of values of Φ, which are separated by

$$\Phi_* = \left[4\frac{d(G_\varkappa/G_0)}{d\bar{N}}\right]^{-1}; \tag{4.24}$$

the negative sign yields $0 \leqslant \Phi \leqslant \Phi_*$ (the ascending branch of the optimum relationship $G_\varkappa(\Phi)$ (cf. Figure 4.2)), while the positive sign corresponds to $\Phi \geqslant \Phi_*$ (the descending branch of $G_\varkappa(\Phi)$).

We can determine quantitatively the influence of the nonlinearity of (4.18) on the optimum weight ratios (4.15) to (4.17) by considering the relationship $G_\varkappa(N_{max})$ corresponding to the curve $\alpha(N_{max})$ in Figure 2.96. This relationship is shown in Figure 4.3 (curve 1), where the linear relationship (4.13) $G_\varkappa$ (kg) = 4 kg/kw N_{max} (kw) (curve 2), and the general linear relationship (4.21) $G_\varkappa$ (kg) = $1.5 \cdot 10^3$ kg + 2.2 kg/kw N_{max} (kw) (curve 3) have also been plotted. Optimum values of $G_\varkappa(\Phi)$ and $G_\pi(\Phi)$ corresponding to these three curves are given in Figure 4.4 for $G_0 = 10^5$ kg, $\alpha_* = 4$ kg/kw.

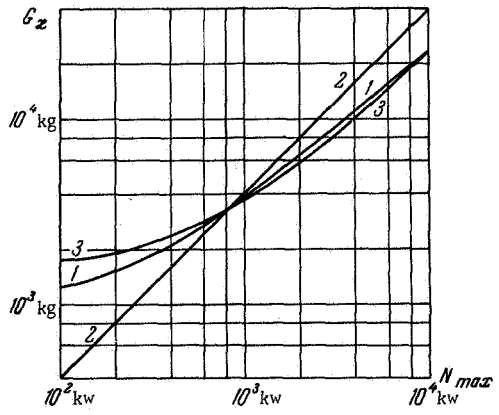

FIGURE 4.3. Dependence of engine weight $G_\varkappa$ on maximum power N_{max}:

1) Actual relationship according to Figure 2.96; 2) linear relationship (4.13); 3) general linear relationship (4.21).

3. Stepwise variation of the engine weight. As was shown in the preceding subsection, a flight is impossible when $J > 2g/\alpha$ if the engine weight is constant. This limitation is eliminated if parts of the propulsion system are jettisoned during the flight /4.23/.

140 A reduction in engine weight is accompanied by a proportional decrease in the maximum power, since $N_{max} = G_\varkappa/\alpha$ (we consider the case $\alpha = \text{const}$; all nonjettisoned parts of the engine operate in parallel). It can again be 141 shown that the maximum power should always be used: $N(t) = N_{max}(t)$.

The payload $G_\pi^{(i)}$ $(i = 1, \ldots, n)$ at the i-th stage is equal to the sum of the actual payload G_π and the weight of the working fluid remaining at the instant at which the i-th part of the engine is jettisoned. We obtain the recurrence relationship

$$G_\pi^{(i-1)} = G_\pi^{(i)} + \Delta G_\mu^{(i)}, \tag{4.25}$$

where $\Delta G_{\mu}^{(i)}$ is the weight of the working fluid used up in the i-th stage $(t_{i-1} < t < t_i)$.

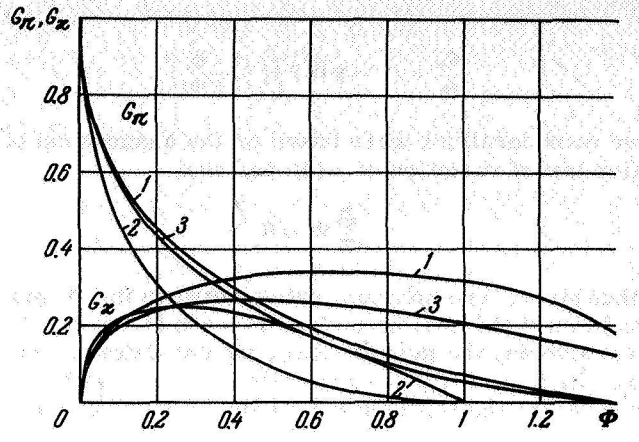

FIGURE 4.4. Optimum relative weights for linear and nonlinear relationships between engine weight and maximum power (numbers of curves correspond to Figure 4.3).

We shall determine $\Delta G_{\mu}^{(i)}$ with the aid of (4.6), applied to the interval $t_{i-1} < t < t_i$:

$$G_i^- = \frac{G_{i-1}^+}{1 + \Phi_i G_{i-1}^+ / G_x^{(i)}} \quad \left(\Phi_i = \frac{\alpha}{2g} \int_{t_{i-1}}^{t_i} a^2 dt\right), \tag{4.26}$$

where G_i^- is the weight of the spacecraft before the i-th engine part is jettisoned, G_{i-1}^+ is the weight of the spacecraft after the $(i-1)$-th engine part has been jettisoned, $G_x^{(i)}$ is the weight of the engine at the i-th stage. By definition $\Delta G_{\mu}^{(i)} = G_{i-1}^+ - G_i^-$. Substituting this expression in (4.25) and writing $G_{i-1}^+ = G_{\pi}^{(i-1)} + G_x^{(i)}$ we obtain

$$\frac{G_{\pi}^{(i)}}{G_{\pi}^{(i-1)}} = \frac{1 - (1 + G_x^{(i)}/G_{\pi}^{(i-1)})\,\Phi_i}{1 + (1 + G_{\pi}^{(i-1)}/G_x^{(i)})\,\Phi_i}. \tag{4.27}$$

We write

$$\frac{G_{\pi}}{G_0} = \frac{G_{\pi}^{(n)}}{G_{\pi}^{(n-1)}} \cdot \frac{G_{\pi}^{(n-1)}}{G_{\pi}^{(n-2)}} \cdots \frac{G_{\pi}^{(2)}}{G_{\pi}^{(1)}} \cdot \frac{G_{\pi}^{(1)}}{G_0} \quad (G_{\pi}^{(n)} = G_{\pi}), \tag{4.28}$$

where the last factor is by (4.14):

$$\frac{G_{\pi}^{(1)}}{G_0} = \frac{1}{1 + (G_0/G_x^{(1)})\,\Phi_1} - \frac{G_x^{(1)}}{G_0}, \tag{4.29}$$

while the other factors are determined by (4.27). Each factor depends only on $G_x^{(i)}/G_{\pi}^{(i-1)}$ (for $i = 2, \ldots, n$) or $G_x^{(1)}/G_0$ (for $i = 1$) when Φ_i is given. These factors are independent; the maximum of G_{π}/G_0 is therefore attained when each factor considered as a function of $G_x^{(i)}/G_{\pi}^{(i-1)}$ is maximal. When Φ_i is

142 given this maximum occurs when

$$\frac{G_x^{(i)}}{G_\pi^{(i-1)}} = \frac{1-\Phi_i}{1+\Phi_i} \qquad (i = 2, \ldots, n), \quad \frac{G_x^{(1)}}{G_0} = \sqrt{\Phi_1} - \Phi_1. \tag{4.30}$$

Hence,

$$\frac{G_\pi}{G_0} = (1-\sqrt{\Phi_1})^2 \prod_{i=2}^{n} \left(\frac{1-\Phi_i}{1+\Phi_i}\right)^2. \tag{4.31}$$

The above considerations were based on the assumption of a fixed flight path (specified law of variation of $a(t)$); the sum

$$\sum_{i=1}^{n} \Phi_i = \Phi \tag{4.32}$$

in (4.31) is thus given. The optimum ratios between the Φ_i must be determined from the condition that (4.31) be maximum when (4.32) is fulfilled.

Without considering the general case, we can determine the limiting value of Φ at which the flight program becomes impossible ($G_\pi = 0$). Substituting in (4.31) and (4.32) $\Phi_i = 1 - \varepsilon_i (0 < \varepsilon_i \ll 1)$, we obtain

$$\frac{G_\pi}{G_0} \approx \frac{1}{4^n} \prod_{i=1}^{n} \varepsilon_i^2, \quad \Phi = n - \sum_{i=1}^{n} \varepsilon_i. \tag{4.33}$$

When $\varepsilon_i \to 0$, we obtain $G_\pi = 0$ for $\Phi = n$. Thus, when the engine weight is decreased in n steps, flights become possible for which

$$0 \leqslant J \leqslant 2ng/\alpha; \tag{4.34}$$

this is a n-fold increase in the range, over that possible with an engine of constant weight.

§ 2. OPTIMUM PROGRAM OF ENGINE-WEIGHT VARIATION

1. Formulation of the problem. The weight of a propulsion system of limited power may represent up to one fourth of the take-off weight of the spacecraft in the optimum case. At the end of the flight, when most of the working fluid has already been used, the engine weight becomes predominant if the payload is small. It may then become advantageous to jettison part of the engine; this will reduce both the weight of the space-
143 craft and the power available to accelerate the working fluid. The thrust will thus be less. If the jettisoned engine part is of the correct size, less working fluid will then be discharged.

We may consider the problem of determining a law of continuous variation of the engine weight; this is the limiting case of a stepwise weight decrease /4.24, 4.25/. A second method of solving the problem of stepwise engine jettisoning is also described in this section.

The characteristic of the ideal engine is again given in the form (4.4). The variational problem is formulated as Mayer's problem (II.8). The controls are: the unit vector $\mathbf{e}(t)$ in the thrust direction, the magnitude of the acceleration $a(t)$ due to the thrust, the power $N(t)$, and the engine weight $G_\varkappa(t)$. The optimum laws of variation of $\mathbf{e}(t)$ and $a(t)$ can be found by the standard rules of variational analysis; this becomes difficult for $N(t)$ and $G_\varkappa(t)$ since these controls are not independent. The upper limit of $N(t)$ depends on $G_\varkappa(t)$:

$$N_{\max}(t) = G_\varkappa(t)/\alpha, \tag{4.35}$$

and $G_\varkappa$ enters in the initial conditions (II.7):

$$G_\sigma(0) + G_\varkappa(0) = G_0. \tag{4.36}$$

We shall now show how two independent controls may be substituted for $N(t)$ and $G_\varkappa(t)$, so that L. S. Pontryagin's method may be used.

Instead of the control function $N(t)$, which varies in the range

$$0 \leqslant N(t) \leqslant N_{\max}(t) = G_\varkappa(t)/\alpha, \tag{4.37}$$

we introduce the dimensionless function $\overline{N}(t)$:

$$\overline{N}(t) = N(t)/N_{\max}(t) = \alpha N(t)/G_\varkappa(t), \tag{4.38}$$

whose limits are

$$0 \leqslant \overline{N}(t) \leqslant 1, \tag{4.39}$$

and which is independent.

We add to system (II.8) a differential relationship which expresses the variation of the engine weight (cf. (II.4)):

$$\dot{G}_\varkappa = -gq_\varkappa \tag{4.40}$$

($q_\varkappa$ is the rate at which the engine mass decreases, $0 \leqslant q_\varkappa(t) \leqslant \infty$); we shall consider $q_\varkappa$ as an independent new control function, and the weight $G_\varkappa$ as a new coordinate.

144 The laws of variation of the engine weight $q_\varkappa(t)$ and power $\overline{N}(t)$ are:

$$G_\varkappa(t) = G_\varkappa(0) - g\int_0^t q_\varkappa(t)\,dt, \quad N(t) = G_\varkappa(t)\,\overline{N}(t)/\alpha. \tag{4.41}$$

This method is of a general character and will be used when applicable (e.g., in § 3 of this chapter). The optimum law of variation of $G_\varkappa(t)$ may be found without using (4.40), in view of the properties of the variational problem.

We now express the weights G_σ, $G_\varkappa$, G_π in fractions of the take-off weight G_0, and substitute (4.38); the symbols used for the weight ratios are those of the corresponding dimensional magnitudes.

System (II.8) then becomes

$$\left.\begin{aligned} &\dot{G}_\sigma = -\frac{(G_\sigma + G_\varkappa)^2}{NG_\varkappa}\frac{\alpha}{2g}a^2,\ G_\sigma(0) + G_\varkappa(0) = 1, && G_\sigma(T) = \max,\\ &\dot{\mathbf{r}} = \mathbf{v}, && \mathbf{r}(0) = \mathbf{r}_0, \quad \mathbf{r}(T) = \mathbf{r}_1,\\ &\dot{\mathbf{v}} = a\mathbf{e} + \mathfrak{R}, && \mathbf{v}(0) = \mathbf{v}_0, \quad \mathbf{v}(T) = \mathbf{v}_1\\ &(|\mathbf{e}(t)| = 1, \quad 0 \leqslant N(t) \leqslant 1, && a(t) \geqslant 0, \quad \dot{G}_\varkappa(t) \leqslant 0). \end{aligned}\right\} \tag{4.42}$$

2. Separating the variational problem. We shall now investigate the optimum variation of $N(t)$, $\mathbf{e}(t)$, $a(t)$, $G_\varkappa(t)$. Following L. S. Pontryagin, we introduce the Hamiltonian H and the momenta p:

$$\left.\begin{aligned} &H = -p_\sigma\frac{(G_\sigma + G_\varkappa)^2}{NG_\varkappa}\frac{\alpha}{2g}a^2 + \mathbf{p}_r\cdot\mathbf{v} + \mathbf{p}_v\cdot(a\mathbf{e} + \mathfrak{R}),\\ &\dot{p}_\sigma = -\frac{\partial H}{\partial G_\sigma} = p_\sigma\frac{G_\sigma + G_\varkappa}{NG_\varkappa}\frac{\alpha}{g}a^2,\\ &\dot{\mathbf{p}}_r = -\frac{\partial H}{\partial \mathbf{r}} = -\frac{\partial}{\partial \mathbf{r}}(\mathbf{p}_v\cdot\mathfrak{R}), \quad \dot{\mathbf{p}}_v = -\frac{\partial H}{\partial \mathbf{v}} = -\mathbf{p}_r. \end{aligned}\right\} \tag{4.43}$$

The momenta $\mathbf{p}_\sigma$, $\mathbf{p}_r$, $\mathbf{p}_v$ are normalized so that

$$p_\sigma(T) = -1. \tag{4.44}$$

The function $p_\sigma(t)$ is negative in the interval $0 \leqslant t \leqslant T$, since the differential equation (4.43) for p_σ is linear and homogeneous, while p_σ is negative
145 at time T:

$$p_\sigma(t) < 0 \text{ for } 0 \leqslant t \leqslant T. \tag{4.45}$$

The optimum variations of $N(t)$, $\mathbf{e}(t)$, $a(t)$, $G_\varkappa(t)$ must give an absolute minimum of the Hamiltonian (4.43).

The coefficient of $1/N$ in the first term of the Hamiltonian is positive by (4.45); the optimum variation of $N(t)$ is therefore by (4.9)

$$N(t) = 1 \text{ for } 0 \leqslant t \leqslant T. \tag{4.46}$$

Physically this means that all the power available must be used to develop thrust.

The optimum vector control $\mathbf{e}(t)$ is selected so as to minimize the scalar product $\mathbf{p}_v\cdot\mathbf{e}$, where

$$\mathbf{e} = -\mathbf{p}_v/p_v \qquad (p_v = |\mathbf{p}_v|), \tag{4.47}$$

i.e., the thrust vector must be opposed to the vector $\mathbf{p}_v$.

From the condition $\partial H/\partial a = 0$, since a is not limited, we obtain the optimum law of variation of $a(t)$:

$$a = -\frac{p_v}{p_\sigma}\frac{G_\varkappa}{(G_\sigma + G_\varkappa)^2}\frac{g}{\alpha}. \tag{4.48}$$

The optimum acceleration due to the thrust thus differs from zero everywhere except at isolated points where $p_v = 0$; in other words, an ideal engine of limited power is switched on during the entire flight.

We shall now consider the optimum law of continuous variation of the engine weight.* The Hamiltonian (4.43), considered as a function of $G_\varkappa$, has a relative minimum at

$$G_\varkappa = G_0. \tag{4.49}$$

We add to (4.49) the limiting condition for $G_\varkappa$, corresponding to the equality sign in the condition $G_\varkappa \leqslant 0$ in (4.42):

$$G_\varkappa = \text{const}; \tag{4.50}$$

it will be shown later that (4.50) is included in the optimum law of variation of $G_\varkappa(t)$.

When (4.49) and (4.50) are satisfied, the coefficient of $(\alpha/2g)\,a^2$ in the Hamiltonian (4.43) is independent of time and is negative in the entire
146 interval $[0, T]$:

$$p_0 \frac{(G_0 + G_\varkappa)^2}{G_\varkappa} = \text{const} < 0; \tag{4.51}$$

this can be shown by differentiating this expression and substituting for $\dot{p}_0$ from (4.43) and for $\dot{G}_0$ from (4.42). The sign of the constant follows from (4.45).

We shall now consider the combination (4.51) as a new momentum; the function H will then correspond to the variational problem of maximizing the integral

$$-J = -\int_0^T a^2 dt, \tag{4.52}$$

formulated in (4.42). The control functions are $a(t)$ and $\mathbf{e}(t)$. Changing the sign in (4.52), we transform the problem of maximizing J into the problem of minimizing J, i.e., the variational problem (4.11).

After the variational problem (4.11) has been solved we must determine the optimum law of variation of $G_\varkappa(t)$, which maximizes $G_0(T) = G_\pi$ when the laws of variation of $a(t)$ and $\mathbf{e}(t)$ are known, and J is given.

From the mass-flow equation and the boundary conditions (4.42) for the weights we obtain the integral relationship

$$-\int_{1-G_\varkappa(0)}^{G_\pi} \frac{G_\varkappa dG_0}{(G_\varkappa + G_0)^2} = \frac{\alpha}{2g} J. \tag{4.53}$$

The law of variation of $G_\varkappa(t)$ must be combined from (4.49) and (4.50) in such a way that G_π becomes maximal while condition (4.53) is satisfied.

Thus, as in the case of constant engine weight (§ 1), the variational problem (4.42) is divided into a dynamic part (4.11) and a weight part (4.53).

3. Solution of the weight part of the variational problem. It is required to determine the piecewise continuous function $G_\varkappa(G_0)$, consisting of the sections $G_\varkappa = G_0$ and $G_\varkappa = \text{const}$, for which G_π is maximum when J is given (cf. (4.53)). This formulation is equivalent to the following one: it is

* A continuous function $G_\varkappa(t)$ corresponds to a continuous jettisoning of infinitesimal engine elements; this is the limiting case of a stepwise variation of $G_\varkappa$.

147 required to determine the function G_x (G_σ), which maximizes J when G_π is given:

$$\max_{G_x} \frac{\alpha}{2g} J = \max_{G_x} \left[-\int_{1-G_{x(0)}}^{G_\pi} \frac{G_x dG_\sigma}{(G_\sigma + G_x)^2} \right] \tag{4.54}$$

[in other words, J (or Φ) and G_π are interchanged].

This formulation will be considered henceforth since it is the most convenient.

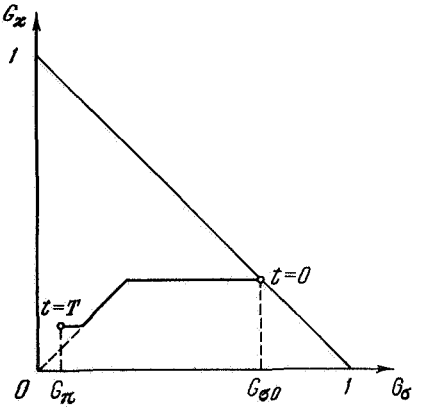

FIGURE 4.5. Optimum law of variation of engine weight G_x as a function of total weight G_σ $(t) = G_\pi + G_\mu(t)$; (G_π = payload, weight of working fluid = G_μ (t)).

We note first that when $G_\pi > 0.5$ the optimum variation of G_x (G_σ) cannot include the straight line (4.49), since in this case the initial condition $G_x(0) + G_\sigma(0) = 1$ would not be fulfilled. Hence, for $G_\pi > 0.5$ the optimum law is

$$G_x(G_\sigma) = G_{x0} = \text{const}, \tag{4.55}$$

and

$$\frac{\alpha}{2g} J = \frac{G_{x0}}{G_\pi + G_{x0}} - G_{x0}. \tag{4.56}$$

From the condition that J be maximum we obtain

$$G_{x0} = \sqrt{G_\pi} - G_\pi, \tag{4.57}$$

whence

$$\Phi = (1 - \sqrt{G_\pi})^2 \left(\Phi = \frac{\alpha}{2g} J\right); \tag{4.58}$$

this is equivalent to (4.15) and (4.16).

If $G_\pi < 0.5$, the optimum variation of G_x (G_σ) can consist of no more than three straight lines (Figure 4.5):

$$\left.\begin{array}{lll} G_x = G_{x0} & \text{for} & 1 - G_{x0} \geqslant G_\sigma \geqslant G_{x0}, \\ G_x = G_\sigma & \text{for} & G_{x0} \geqslant G_\sigma \geqslant G_{x1}, \\ G_x = G_{x1} & \text{for} & G_{x1} \geqslant G_\sigma \geqslant G_\pi. \end{array}\right\} \tag{4.59}$$

Evaluating the integral (4.54) over the sections (4.59), we obtain

$$\Phi = \frac{G_{x1}}{G_{x1} + G_\pi} - \frac{1}{4} \ln G_{x1} + \frac{1}{4} \ln G_{x0} - G_{x0}, \tag{4.60}$$

where G_{x0} and G_{x1} must satisfy the inequalities (cf. (4.59))

$$1 - G_{x0} \geqslant G_{x0} \geqslant G_{x1} \geqslant G_\pi. \tag{4.61}$$

148 From the condition that Φ, considered as a function of G_{x0} and G_{x1}, be maximum, we find

$$G_{x0} = 0.25, \quad G_{x1} = G_\pi. \tag{4.62}$$

The maximum value of Φ is

$$\Phi = 0.25\,(1 - \ln 4G_\pi). \tag{4.63}$$

Returning to (4.59), we find that the piecewise extremum consists only of the two straight lines

$$\left.\begin{array}{lll} G_x = 0.25 & \text{for} & 0.75 \geqslant G_\sigma \geqslant 0.25, \\ G_x = G_\sigma & \text{for} & 0.25 \geqslant G_\sigma \geqslant G_\pi. \end{array}\right\} \tag{4.64}$$

This solution is true for $0.25 \geqslant G_\pi \geqslant 0$, since (4.61) is not satisfied when $G_\pi > 0.25$ and G_{x0}, G_{x1} are given by (4.62). If $1 \geqslant G_\pi \geqslant 0.25$, the optimum function G_x (G_σ) is the straight line (4.55), the optimum value of G_{x0} and the maximum value of Φ being given by (4.57) and (4.58) respectively.

The solution of the weight part of the variational problem is therefore:

$$\left.\begin{array}{l} \text{for } 0 \leqslant \Phi \leqslant 0.25 \\ G_\pi = (1 - \sqrt{\Phi})^2, \quad G_x \equiv \sqrt{\Phi} - \Phi, \\ \text{for } 0.25 \leqslant \Phi \leqslant \infty \\ G_\pi = \frac{1}{4} e^{1-4\Phi}, \quad G_x = \begin{cases} 0.25 & \text{for } 0.75 \geqslant G_\sigma \geqslant 0.25, \\ G_\sigma & \text{for } 0.25 \geqslant G_\sigma \geqslant G_\pi. \end{cases} \end{array}\right\} \tag{4.65}$$

The curve $G_\pi(\Phi)$ in Figure 4.6 represents the variation of $n = \infty$ according to (4.65). A gain in relative payload of 0.01 to 0.015 ($0 \leqslant G_\pi(\infty) - G_\pi(1) \leqslant 0.017$) over that possible with an engine of constant weight (curve $n = 1$) is obtained at small payloads. This gain is very important. At $\Phi = 0.7$ the payload is increased by 50%, at $\Phi = 0.8$ by 150%, and at $\Phi = 0.9$ by 500%; at $\Phi = 1$ the relative increase is infinite. The possible range of values of J, which characterizes the flight, is extended to infinity ($0 \leqslant J \leqslant \infty$).

Consideration of the problem of optimizing the variation of the engine weight when the law of variation of the acceleration due to the thrust is given (e.g., $a(t) = \text{const}$) /4.26/, leads to similar results on the strength of what was said in subsection 2.

149

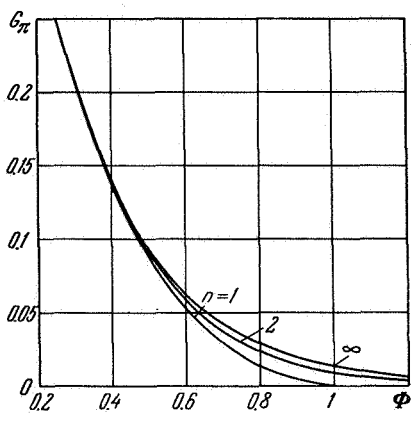

FIGURE 4.6. Payload G_π in case of continuous variation of engine weight ($n=\infty$), stepwise variation of engine weight ($n=2$), and constant engine weight ($n=1$).

4. Stepwise approximation of optimum variation of engine weight. Let G_x be a piecewise-constant (step) function of the time t (or of the weight G_σ of the working fluid). It is required to determine the optimum levels of the steps and the optimum instants of transition from one step to the next, if the number of steps is given. Here G_x is a nonincreasing function of the time t (or a nondecreasing function of the weight G_σ), so that the levels of the steps must decrease with time t (or increase with the weight G_σ).

The integral (4.54) is in this case replaced by the sum of n integrals over intervals in which the function G_x is constant; integrating and substituting the respective limits, we obtain

$$\Phi = G_x^{(1)}\left(\frac{1}{G_\sigma^{(1)}+G_x^{(1)}}-1\right)+\sum_{i=2}^{n-1}G_x^{(i)}\left(\frac{1}{G_\sigma^{(i)}+G_x^{(i)}}-\frac{1}{G_\sigma^{(i-1)}+G_x^{(i)}}\right)+ \\ +G_x^{(n)}\left(\frac{1}{G_\pi+G_x^{(n)}}-\frac{1}{G_\sigma^{(n-1)}+G_x^{(n)}}\right). \qquad (4.66)$$

Here n is the given number of steps; $G_x^{(1)}, \ldots, G_x^{(n)}$ are the levels of the steps; $G_\sigma^{(1)}, \ldots, G_\sigma^{(n-1)}$ correspond to the instants of transition from one step to the next.

We find the $(2n-1)$ unknowns: $G_x^{(1)}, \ldots, G_x^{(n)}$; $G_\sigma^{(1)}, \ldots, G_\sigma^{(n-1)}$ from the condition that the function Φ be maximum. Differentiating (4.66) we obtain

$$\left.\begin{aligned} &G_\sigma^{(i)} = \sqrt{G_x^{(i+1)}G_x^{(i)}} \quad \text{or} \quad G_x^{(i+1)} = G_x^{(i)} \quad (i=1,\ldots,n-1), \\ &G_x^{(i+1)} = \sqrt{G_\sigma^{(i+1)}G_\sigma^{(i)}} \quad (i=1,\ldots,n-1), \\ &G_x^{(1)} = \sqrt{G_\sigma^{(1)}} - G_\sigma^{(1)}. \end{aligned}\right\} \qquad (4.67)$$

150 The top line of (4.67) contains two groups of equations, obtained by maximizing Φ as a function of $G_\sigma^{(i)}$. In the second case ($G_x^{(i+1)} = G_x^{(i)}$) all the n steps of G_x are at the same level; this corresponds to (4.55).

We shall now show how to solve the system of algebraic equations obtained. The magnitudes $G_\sigma^{(i)}$ and $G_\sigma^{(i+1)}$ satisfy the following recurrence relationship:

$$(G_\sigma^{(i)})^{(i+1)} = (G_\sigma^{(i+1)})^i G_\pi \qquad (i=2,\ldots,n-1), \qquad (4.68)$$

as is easily shown by the method of complete induction (cf. (4.67)). The magnitude $G_0^{(n)}$ is determined from the equation

$$(G_0^{(n)})^{n+1} = (1 - \sqrt{G_0^{(n)}})^n G_n. \tag{4.69}$$

We obtain $G_0^{(n)}$ from (4.69) for the given value of G_n, find successively all $G_0^{(n-1)}, \ldots, G_0^{(2)}$ and from them also $G_x^{(i)}$ by (4.67), and then determine Φ by (4.66). The result is shown in Figure 4.6 for $n = 2$. Comparison with the curve corresponding to a continuous variation of the engine weight ($n = \infty$) shows that even if only a single part of the engine is jettisoned ($n = 2$) it is possible to realize most of the gain achieved through the optimum variation of the engine weight.

The problem may be solved in the same way when it is required that the engine consists of equal parts. In this case it is necessary to select in (4.66) only one level $G_x^{(1)}$ as optimum; the other levels are determined by the formula

$$G_x^{(i)} = G_x^{(1)}\left(1 - \frac{i-1}{n}\right) \quad \text{or} \quad G_x^{(i)} = G_x^{(1)}. \tag{4.70}$$

In conclusion we note that the limiting optimum variation (4.64), and also the stepwise optimum variation corresponding to it, plotted as functions of G_0, may also be written as functions of t, if the law of variation of the acceleration $a(t)$, due to the thrust, is known. The variables G_0 and t are related by the equation

$$-\int_{1-G_{x0}}^{G_0} \frac{G_x dG_0}{(G_0 + G_x)^2} = \frac{\alpha}{2g}\int_0^t a^2 dt \tag{4.71}$$

where the optimum variation of G_x (G_0) is substituted in the integral on the left.

151 § 3. UTILIZATION OF JETTISONED ENGINE PARTS AS WORKING FLUID

1. **Statement of the problem.** In discussing in the preceding two sections the optimum laws of variation of the engine weight it was assumed that the jettisoned parts leave the spacecraft at zero velocity and do not impart any additional impulse to it (passive jettisoning). If the engine parts to be jettisoned are transformed into working fluid and leave at the velocity of the jet (active jettisoning), an additional advantage is gained. This method of using superfluous structural elements was suggested by Tsander /4.27/.

We shall now formulate the problem of the optimum utilization of the jettisoned engine parts /4.22, 4.28/. It will be assumed that only part of the jettisoned mass can be transformed into working fluid:

$$0 \leqslant \varkappa(t) \leqslant \varkappa_{\max} \qquad (0 \leqslant \varkappa_{\max} = \text{const} \leqslant 1), \tag{4.72}$$

where $\varkappa_{max}$ is considered as given. Thus, the part $(1-\varkappa)\,q_\varkappa$ of the mass $q_\varkappa \geqslant 0$ discharged per unit time (cf. (4.40)) is not utilized and leaves the spacecraft at zero velocity. The remaining part $\varkappa q_\varkappa$, which is converted into working fluid, enters the nozzle. The total mass flow rate through the nozzle is thus

$$q = q_\mu + \varkappa q_\varkappa, \tag{4.73}$$

where q_μ is the mass flow rate of the proper working fluid.

We shall first consider the limiting case of continuous jettisoning. Stepwise jettisoning will be discussed in the last subsection.

We select as independent control functions the dimensionless power (4.38), the mass flow rates q_μ and $q_\varkappa$, and the coefficient $\varkappa$ defined by (4.72). The propulsion system is again considered as ideal, its characteristics being given in the form (4.1). The variational problem will be formulated as Mayer's problem (II.8). We add (4.40) to system (II.8), and rewrite it in terms of the above-listed control functions:

$$\left.\begin{aligned}
&\dot G_0 = -q_\mu, && G_0(0) + && G_0(T) = \max,\\
&\dot G_\varkappa = -q_\varkappa, && +G_\varkappa(0) = 1, && G_\varkappa(T) \geqslant 0,\\
&\dot{\mathbf{r}} = \mathbf{v}, && \mathbf{r}(0) = \mathbf{r}_0, && \mathbf{r}(T) = \mathbf{r}_1,\\
&\dot{\mathbf{v}} = \frac{\sqrt{(2g/\alpha)\,G_\varkappa N (q_\mu + \varkappa q_\varkappa)}}{G_0 + G_\varkappa}\,\mathbf{e} + \mathbf{R}, && \mathbf{v}(0) = \mathbf{v}_0, && \mathbf{v}(T) = \mathbf{v}_1\\
&(|\mathbf{e}(t)| = 1, && 0 \leqslant N(t) \leqslant 1, && 0 \leqslant \varkappa(t) \leqslant \varkappa_{max},\\
& && && q_\mu(t) \geqslant 0, \quad q_\varkappa(t) \geqslant 0).
\end{aligned}\right\} \tag{4.74}$$

152 Here the weights are referred to the take-off weight, the mass flow rates to the take-off mass, and the power to the maximum possible power at the given instant; these dimensionless magnitudes are represented by the same symbols as the dimensional ones.

It is required to select the optimum take-off weight $G_\varkappa$ and to determine the optimum laws of variation of $\mathbf{e}(t)$, $N(t)$, $\varkappa(t)$, $q_\mu(t)$, $q_\varkappa(t)$ (the structural parameters α, $\varkappa_{max}$ and the dynamic maneuver $\{\mathbf{r}_0, \mathbf{v}_0, \mathbf{r}_1, \mathbf{v}_1, T\}$ are specified). The final value of G_0, which by definition (cf. (II.6), (II.7)) is the payload, has to be maximized.

2. Optimization of control functions. The optimum control functions will be determined by Pontryagin's method. The Hamiltonian

$$\left.\begin{aligned}
&H = -p_0 q_\mu - p_\varkappa q_\varkappa + \mathbf{p}_r\cdot\mathbf{v} + \mathbf{p}_v\cdot\mathbf{R} +\\
&\qquad + \mathbf{p}_v\cdot\mathbf{e}\sqrt{(2g/\alpha)\,G_\varkappa N (q_\mu + \varkappa q_\varkappa)}\,(G_0 + G_\varkappa)^{-1},\\
&\dot p_0 = -\frac{\partial H}{\partial G_0}, \quad \dot p_\varkappa = -\frac{\partial H}{\partial G_\varkappa}, \quad \dot{\mathbf{p}}_r = -\frac{\partial H}{\partial \mathbf{r}}, \quad \dot{\mathbf{p}}_v = -\frac{\partial H}{\partial \mathbf{v}}
\end{aligned}\right\} \tag{4.75}$$

considered as a function of the variables $\mathbf{e}$, N, $\varkappa$, q_μ, and $q_\varkappa$ limited according to (4.74) must have an absolute minimum on the optimum flight path.

The direction of the thrust vector is again given by (4.47), since the coefficient of the scalar product $\mathbf{p}_v\cdot\mathbf{e}$ in the expression for H is non-negative.

Analyzing this term and noting (4.47), we find that the optimum corresponds to full power ((4.46)).

We confirm similarly the physically obvious conclusion that the part of $q_\varkappa$ which is transformed into working fluid must be the maximum possible

$$\varkappa(t) = \varkappa_{\max} \text{ for } 0 \leqslant t \leqslant T. \tag{4.76}$$

We determine the laws of variation of q_μ and $q_\varkappa$ by substituting (4.46), (4.47), (4.76) in the part of the Hamiltonian which depends on these variables:*

$$\mathcal{H} = -p_\sigma q_\mu - p_\varkappa q_\varkappa - p_v \sqrt{(2g/\alpha) G_\varkappa (q_\mu + \varkappa q_\varkappa)}\,(G_\sigma + G_\varkappa)^{-1} \tag{4.77}$$

and so obtain

$$\left.\begin{aligned} \dot{p}_\sigma &= -p_v \sqrt{(2g/\alpha) G_\varkappa (q_\mu + \varkappa q_\varkappa)}\,(G_\sigma + G_\varkappa)^{-2}, \\ \dot{p}_\varkappa &= \tfrac{1}{2}\dot{p}_\sigma (1 - G_\sigma/G_\varkappa). \end{aligned}\right\} \tag{4.78}$$

153 It follows from the condition that (4.77) be minimum that if p_σ and/or $p_\varkappa$ are greater than or equal to zero, the optimum value of q_μ and/or $q_\varkappa$ becomes infinitely large.

Consider now the case

$$p_\sigma < 0, \quad p_\varkappa < 0. \tag{4.79}$$

We express (4.77) in terms of the total mass flow rate (4.73) and $q_\varkappa$:

$$\mathcal{H} = -p_\sigma q - p_v \sqrt{(2g/\alpha) G_\varkappa q}\,(G_\sigma + G_\varkappa)^{-1} - (p_\varkappa - \varkappa p_\sigma) q_\varkappa \tag{4.80}$$
$$(q \geqslant 0,\ 0 \leqslant q_\varkappa \leqslant q/\varkappa).$$

The optimum distribution of the total mass flow rate $q_\varkappa$ between q and $q_\mu = q - \varkappa q_\varkappa$ is determined by the sign of

$$\Delta = p_\varkappa - \varkappa p_\sigma. \tag{4.81}$$

In fact, if $\Delta < 0$, the minimum of $\mathcal{H}$ as a function of $q_\varkappa$ is attained when $q_\varkappa = 0$, i.e., for $q_\mu = q$, while if $\Delta > 0$, it is attained when $q_\varkappa = q/\varkappa$, i.e., for $q_\mu = 0$. When $\Delta = 0$ the function $\mathcal{H}$ is independent of q_μ and $q_\varkappa$ taken separately, and is determined by the total mass flow rate q.

Thus, in each of the three possible cases the function $\mathcal{H}$ depends only on one of the magnitudes q_μ, $q_\varkappa$, or q, which must be nonnegative:

$$\left.\begin{aligned} \mathcal{H}_1 &= -p_\sigma q_\mu - p_v \sqrt{(2g/\alpha) G_\varkappa q_\mu}\,(G_\sigma + G_\varkappa)^{-1} \\ &\qquad \text{when } \Delta < 0 \ (q_\varkappa = 0), \\ \mathcal{H}_2 &= -p_\varkappa q_\varkappa - p_v \sqrt{(2g/\alpha) G_\varkappa \varkappa q_\varkappa}\,(G_\sigma + G_\varkappa)^{-1} \\ &\qquad \text{when } \Delta > 0 \ (q_\mu = 0), \\ \mathcal{H}_3 &= -p_\sigma q - p_v \sqrt{(2g/\alpha) G_\varkappa q}\,(G_\sigma + G_\varkappa)^{-1} \quad \text{when } \Delta = 0. \end{aligned}\right\} \tag{4.82}$$

The conditions of absolute minimum $\partial\mathcal{H}_1/\partial q_\mu = 0$ and $\partial\mathcal{H}_2/\partial q_\varkappa = 0$, yield the optimum laws of variations of q_μ and $q_\varkappa$ when $\Delta \neq 0$:

$$q_\mu = \frac{(g/\alpha) G_\varkappa p_v^2}{2p_\sigma^2 (G_\sigma + G_\varkappa)^2}, \quad q_\varkappa = 0 \qquad (\Delta < 0). \tag{4.83}$$

* Here and henceforth the symbol $\varkappa$ without subscript means $\varkappa_{\max}$.

$$q_\mu = 0, \quad q_\varkappa = \frac{\varkappa (g/\alpha) G_\varkappa p_v^2}{2p_\varkappa^2 (G_\sigma + G_\varkappa)^2} \qquad (\Delta > 0). \tag{4.84}$$

154 If $\Delta = 0$, the condition $\partial \mathcal{H}_3/\partial q = 0$ yields

$$q_\mu + \varkappa q_\varkappa = \frac{(g/\alpha) G_\varkappa p_v^2}{2p_\sigma^2 (G_\sigma + G_\varkappa)^2} \qquad (\Delta = 0). \tag{4.85}$$

For the singular case in which Δ is zero over a finite time interval, the derivative of Δ also vanishes in this interval, so that

$$\dot{\Delta} = \frac{1}{2} \dot{p}_\sigma \left(1 - 2\varkappa - \frac{G_\sigma}{G_\varkappa}\right) = 0. \tag{4.86}$$

(This equation is obtained from (4.81) and (4.78).)

It follows from (4.86) that either $\dot{p}_\sigma = 0$ or $(1 - 2\varkappa - G_\sigma/G_\varkappa) = 0$. Let us consider the first possibility. We eliminate $(q_\mu + \varkappa q_\varkappa)$ from (4.78) with the aid of (4.85) to obtain

$$\dot{p}_\sigma = \frac{(g/\alpha) G_\varkappa}{(G_\sigma + G_\varkappa)^2} \frac{p_v^2}{p_\sigma^2}. \tag{4.87}$$

The right-hand side of (4.87) is positive, except at isolated points. In fact, the engine weight $G_\varkappa$ can vanish only at $t = T$, since by (4.75)

$$\dot{\mathbf{p}}_v = -\mathbf{p}_r, \quad \dot{\mathbf{p}}_r = -\frac{\partial}{\partial \mathbf{r}} (\mathbf{p}_v \cdot \mathbf{R}). \tag{4.88}$$

The momentum $\mathbf{p}_v$ may vanish either at isolated points or identically over the entire flight path. The latter case is degenerate, since it corresponds to $q_\mu = q_\varkappa = 0$ (cf. (4.83) to (4.85) for $p_v = 0$).

The first possibility $\dot{p}_\sigma = 0$ is thus eliminated, and there remains only

$$1 - 2\varkappa - G_\sigma/G_\varkappa = 0. \tag{4.89}$$

This means that the weights of the engine and of the working-fluid reserve vary proportionally (cf. (4.49)). Together with (4.85) this yields the optimum control functions of q_μ and $q_\varkappa$ in the singular case so that

$$q_\mu = (1 - 2\varkappa) q_\varkappa = \frac{(1 - 2\varkappa)(g/\alpha) G_\varkappa p_v^2}{2(1 - \varkappa) p_\sigma^2 (G_\sigma + G_\varkappa)^2} \qquad (\Delta = 0). \tag{4.90}$$

It is easily seen that (4.89) and (4.90) are meaningful only when $\varkappa < 0.5$ and $G_\varkappa < 0.5$ (otherwise $1 - 2\varkappa < 0$ and $G_\sigma/G_\varkappa > 1$).

155 **3. Alternation of optimum flow-rate programs.** It was established above that the form of the optimum control functions of the flow rates q_μ and $q_\varkappa$ depends on the signs of the momenta p_σ and $p_\varkappa$, and of the function Δ.

According to the transversality condition at time $t = 0$, the momentum vector $(p_\sigma, p_\varkappa)$ must be directed along the normal to the straight line $G_\sigma(0) + G_\varkappa(0) = 1$ (cf. (4.74)), i.e.,

$$p_\sigma(0) = p_\varkappa(0). \tag{4.91}$$

By normalization, we have that at the final time $t = T$

$$p_\sigma(T) = -1 \tag{4.92}$$

(since the momentum p_σ corresponds to the coordinate G_σ, whose final value is maximized).

There are two alternatives for the final value of the momentum $p_\varkappa$, namely, either the final value of $G_\varkappa$ in the optimum case reaches the limit $G_\varkappa(T) = 0$ (cf. (4.74)), and thus the value of $p_\varkappa(T)$ is indeterminate, or the optimum value $G_\varkappa(T) > 0$, and thus $G_\varkappa(T)$ can be considered as unspecified, and from the transversality condition $p_\varkappa(T) = 0$. Hence we obtain

$$G_\varkappa(T) = 0 \quad \text{or} \quad p_\varkappa(T) = 0. \tag{4.93}$$

(These two conditions can be fulfilled simultaneously, if $\partial G_\sigma(T)/\partial G_\varkappa(T) = 0$ for $G_\varkappa(T) = 0$).

The initial value (4.91) of the momenta p_σ, $p_\varkappa$ must be negative. Otherwise it follows from the condition for (4.77) to be minimum that $q_\mu = \infty$ and $q_\varkappa = \infty$, i.e., the final portion of the working-fluid reserve and the propulsion system are jettisoned at an infinitesimal velocity ($V = \sqrt{2N/(q_\mu + \varkappa q_\varkappa)}$), a case in which the initial weight ratios are not optima. It is also possible to obtain a lower bound for (4.91). The derivative (4.78) of p_σ is everywhere negative, and its final value is -1 (4.92); therefore

$$-1 < p_\sigma(0) = p_\varkappa(0) < 0. \tag{4.94}$$

Thus, p_σ is negative throughout the flight ($p_\sigma(0) < 0$, $\dot{p}_\sigma(t) < 0$). This is also true for the momentum $p_\varkappa$ (except for the final instant, when $p_\varkappa$ may be zero (4.93)). In the neighborhood of the initial point, $t = 0$, $p_\varkappa$ is negative (4.94). If it becomes zero after a certain time ($0 < t_* < T$), the derivative
156 $\dot{p}_\varkappa(t_* - 0) \geqslant 0$, and by (4.78) $G_\sigma(t_* - 0) \geqslant G_\varkappa(t_* - 0)$. This inequality becomes stronger to the right of the point $t = t_*$, since $q_\mu = 0$, $q_\varkappa = \infty$ for $p_\sigma < 0$, $p_\varkappa = 0$. It follows that the derivative $\dot{p}_\varkappa$ will remain positive whilst passing through the point $t = t_*$, and $p_\varkappa(t) > 0$ for $t > t_*$. If the last inequality holds over the final time interval, the engine weight vanishes ($q_\varkappa = \infty$ for $p_\varkappa > 0$), which is possible only at $t = T$.

It has thus been shown that inequalities (4.79) hold over the entire time interval $0 \leqslant t < T$. It remains to analyze the behavior of expression (4.81), whose sign will determine which of th optimum flow-rate control functions (4.83), (4.84), (4.90) will be valid in a given case.

We first consider the case $0 < \varkappa < 1$. From the optimum boundary condition for the momenta (4.94) it follows that the initial value of the function Δ is negative,

$$\Delta(0) = (1 - \varkappa)\, p_\sigma(0) < 0. \tag{4.95}$$

The final value of the function Δ must be positive,

$$\Delta(T) = p_\varkappa(T) - \varkappa p_\sigma(T) > 0, \tag{4.96}$$

since, according to condition (4.93), either $p_\varkappa(T) = 0$ or $G_\varkappa(T) = 0$. In the first case the validity of inequality (4.96) follows directly from (4.92), since $\Delta(T) = -\varkappa p_\sigma(T) = \varkappa$. In the second case it follows from (4.84), since near the final instant the weight $G_\varkappa$ must decrease to zero. This is possible only with the optimum control function (4.84), which is applicable for $\Delta > 0$ ($G_\varkappa(t) =$ const in (4.83) and $G_\varkappa(t) = G_\sigma(t)/(1 - 2\varkappa)$ in (4.89), (4.90)).

We shall study the function Δ within the interval $[0, T]$. Its derivative is defined by (4.86). The first factor of this expression $^1/_2\dot{p}_\sigma$ is everywhere negative. It follows that the character of the function Δ will be determined by the second factor

$$\chi = 1 - 2\varkappa - G_\sigma/G_\varkappa. \tag{4.97}$$

At the beginning of the flight, the function Δ is negative (cf. (4.95)). Therefore, the weight varies according to (4.83), which states that the weight $G_\varkappa$ remains constant, and G_σ decreases, i.e., χ increases by (4.83). If we assume that $\dot{\Delta}(0) \leqslant 0$, the final value of $\Delta(T)$ will be negative, since $\Delta(0) < 0$ and $\dot{\Delta}(t) \leqslant 0$ (as a result of the increase in χ). The negativity of $\Delta(T)$ contradicts condition (4.96).

Thus, the derivative of Δ is positive at the beginning of the flight. We shall consider all the possible combinations which can exist within the interval $[0, T]$.

1. The derivative $\dot{\Delta}(t)$ is everywhere positive. Thus $\Delta(t)$ must intersect the t-axis at some time $t = t_*$ (since $\Delta(0) < 0$ and $\Delta(T) > 0$). In the
157 first interval $0 \leqslant t \leqslant t_*$ the control functions (4.83) hold, according to which $G_\varkappa(t) = G_{\varkappa 0}$, and in the second one $t_* \leqslant t \leqslant T$ the control functions hold (4.84), by which $G_\sigma(t) = G_\sigma(t_*)$ (Figure 4.7), where $G_\sigma(t_*) = G_\pi$, since $G_\sigma(T) = G_\pi$ by condition (II.7).

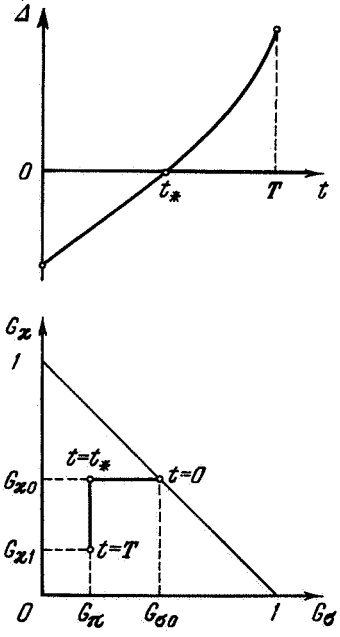

FIGURE 4.7. The function $\Delta(t)$ (first alternative) and corresponding optimum engine-weight control function ($0 < \varkappa < 1$).

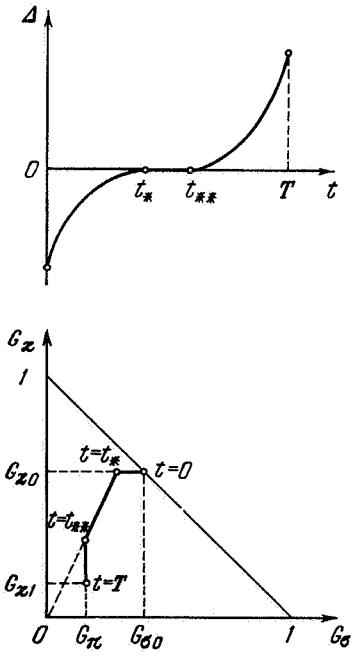

FIGURE 4.8. The function $\Delta(t)$ (second alternative) and corresponding optimum engine-weight control function ($0 < \varkappa < 0.5$, $0 \leqslant G_\pi < 0.5$).

2. The derivative $\dot{\Delta}(t)$ is positive at first, and then vanishes together with the function itself ($\dot{\Delta}(t_*) = \Delta(t_*) = 0$). In the interval $0 \leqslant t \leqslant t_*$ the weight variation follows law (4.83), while at $t = t_*$ this law is replaced by (4.89), according to which the weights G_σ and $G_\varkappa$ vary proportionally, so that χ and $\dot{\Delta}$ remain equal to zero. At some time $t = t_{**}$ the working-fluid reserve will be exhausted, $G_\sigma(t_{**}) = G_\pi$. After this only the weight $G_\varkappa$ can vary. The
159 expression χ again becomes negative as $\dot{\Delta}$ decreases, and the derivative $G_\varkappa$ becomes positive. The function Δ passes into the positive region, and the weight will be controlled by (4.84) (Figure 4.8).

3. The derivative $\dot{\Delta}(t)$ vanishes for $\Delta(t) < 0$. For $\Delta < 0$ the weights G_σ, $G_\varkappa$ vary according to (4.83), by which χ increases. Therefore, after it vanishes, the derivative of $\dot{\Delta}$ becomes negative and the function Δ will never enter region $\Delta > 0$, which contradicts condition (4.96).

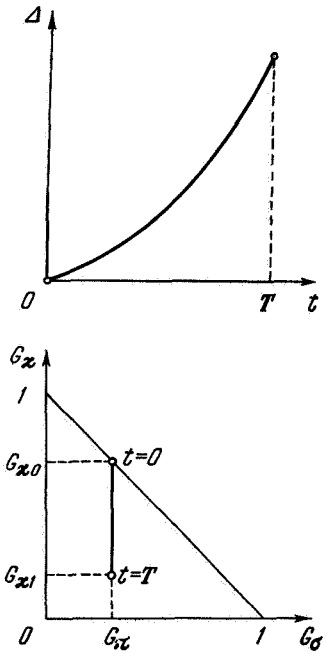

FIGURE 4.9. The function $\Delta(t)$ at $\varkappa = 1$ and corresponding optimum engine-weight control function.

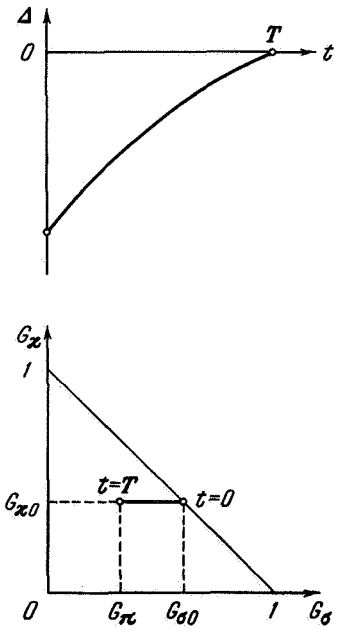

FIGURE 4.10. The function $\Delta(t)$(first alternative) at $\varkappa = 0$ and corresponding optimum engine-weight control function.

4. The derivative $\dot{\Delta}(t)$ vanishes for $\Delta(t) > 0$. This possibility is likewise eliminated, since for $\Delta > 0$ the function χ must decrease according to (4.84) and (4.97), while in order to have a positive value of the function Δ at some time $t = t_*$ we must have $\dot{\Delta}(t_*) > 0$. Therefore for $\Delta > 0$ the derivative $\dot{\Delta}$ remains positive, thus contradicting our original assumption. Hence, the last two alternatives 3 and 4 are eliminated.

We shall now study the behavior of the function Δ for the extreme values of the parameter $\varkappa$, namely $\varkappa = 1$ and $\varkappa = 0$. At $\varkappa = 1$ the initial value of the function Δ is zero (cf. (4.95)), and its derivative is everywhere positive (cf. (4.86)). Therefore all the subsequent values of Δ lie

in the positive region, and only the weight of the engine $G_\varkappa$ varies in the course of the motion, according to (4.84). Here $G_\sigma(t) = G_\sigma(T) = G_\pi$, i.e., there is no working-fluid reserve (Figure 4.9).

In the case $\varkappa = 0$, considered in the preceding section, the function Δ cannot enter the positive region, since at $\varkappa = 0$ the control function (4.84) is meaningless. Therefore the function Δ is either everywhere negative (with the possible exception of the point $t = T$), and then $G_\varkappa(t) = G_{\varkappa 0}$ (Figure 4.10), or it is negative at the beginning and then vanishes at $t = t_* < T$. Thus the derivative $\dot{\Delta}(t_*)$ also vanishes, and remains equal to zero until the end of the flight. In the first interval $0 \leqslant t \leqslant t_*$ the weight varies according to (4.83), and in the second interval $t_* \leqslant t \leqslant T$ according to (4.89) (Figure 4.11). The other possibilities are eliminated in the same way as was carried out for $0 < \varkappa < 1$.

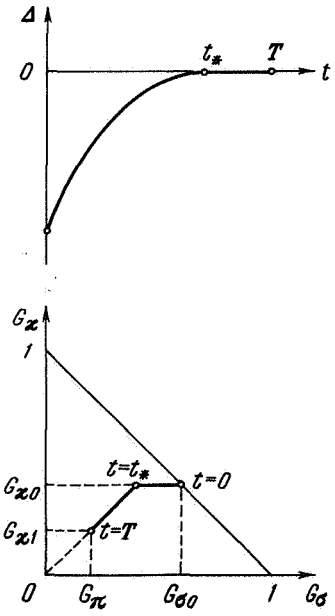

FIGURE 4.11. The function $\Delta(t)$ (second alternative) at $\varkappa = 0$ and corresponding optimum engine-weight control function ($0 \leqslant G_\pi < 0.5$).

4. Separating the problem into weight and dynamic parts. We pass from the flow rates q_μ and $q_\varkappa$ to a new control function a, the thrust acceleration (cf. (4.74)), given by

$$a = \sqrt{(2g/\alpha) G_\varkappa N (q_\mu + \varkappa q_\varkappa)} (G_\sigma + G_\varkappa)^{-1}. \tag{4.98}$$

Thus the two vector equations (4.74) defining the flight trajectory will contain no weight parameters; so $\dot{\mathbf{r}} = \mathbf{v}$, $\dot{\mathbf{v}} = a\mathbf{e} + \mathfrak{R}$, and equations (4.74), which describe the variations of the weights $G_\varkappa$ and G_σ, will be expressed for each of the optimum equations (4.83), (4.90), and (4.84) through the

160 weight parameters and the square of the thrust acceleration (the dimensionless power N is equal to unity on the optimum trajectory) in the forms:

for $\Delta(t) < 0$

$$\dot{G}_\sigma = -\frac{(G_\sigma + G_\varkappa)^2}{G_\varkappa}\frac{\alpha}{2g}a^2, \quad G_\varkappa(t) = \text{const}; \tag{4.99}$$

for $\Delta(t) < 0$

$$\dot{G}_\sigma = -4(1-\varkappa)G_\sigma\frac{\alpha}{2g}a^2, \quad G_\varkappa(t) = \frac{G_\sigma(t)}{1-2\varkappa} \quad (\varkappa < 0.5;\ G_\pi < 0.5); \tag{4.100}$$

for $\Delta(t) > 0$

$$G_\sigma(t) = \text{const}, \quad G_\varkappa = -\frac{(G_\sigma + G_\varkappa)^2}{\varkappa G_\varkappa}\frac{\alpha}{2g}a^2 \qquad (\varkappa > 0). \tag{4.101}$$

It was shown in the preceding paragraph that at $0 < \varkappa < 1$ two solutions are possible; the first consists of (4.99) and (4.101) joined one after the other, and the second of (4.99), (4.100), and (4.101). The variables in each of the differential equations (4.99) and (4.101) are separated. According to the continuity requirement of the coordinates G_σ and $G_\varkappa$, the initial condition $G_{\sigma 0} + G_{\varkappa 0} = 1$, and the final condition $G_{\sigma 1} = G_\pi$, the following integrals are obtained:

for the case (4.99) + (4.101)

$$-G_{\varkappa 0}\int_{1-G_{\varkappa 0}}^{G_\pi}\frac{dG_\sigma}{(G_\sigma + G_{\varkappa 0})^2} - \varkappa\int_{G_{\varkappa 0}}^{G_{\varkappa 1}}\frac{G_\varkappa dG_\varkappa}{(G_\pi + G_\varkappa)^2} = \Phi; \tag{4.102}$$

for the case (4.99) + (4.100) + (4.101)

$$-G_{\varkappa 0}\int_{1-G_{\varkappa 0}}^{(1-2\varkappa)G_{\varkappa 0}}\frac{dG_\sigma}{(G_\sigma + G_{\varkappa 0})^2} - \frac{1}{4(1-\varkappa)}\int_{(1-2\varkappa)G_{\varkappa 0}}^{G_\pi}\frac{dG_\sigma}{G_\sigma} - \varkappa\int_{G_\pi/(1-2\varkappa)}^{G_{\varkappa 1}}\frac{G_\varkappa dG_\varkappa}{(G_\pi + G_\varkappa)^2} = \Phi. \tag{4.103}$$

Here, as in the two preceding sections,

$$\Phi = \frac{\alpha}{2g}\int_0^T a^2 dt. \tag{4.104}$$

After calculating the integrals appearing on the left-hand side of equations (4.102) and (4.103), a finite relationship between the payload G_π, the initial and final weights of the engine $G_\varkappa$, the parameter $\varkappa$, and the functional Φ is established as follows:

161 for case (4.99) + (4.101)

$$1 - G_{\varkappa 0} - \frac{(1-\varkappa)G_\pi}{G_{\varkappa 0} + G_\pi} + \varkappa\ln\frac{G_{\varkappa 0} + G_\pi}{G_{\varkappa 1} + G_\pi} - \frac{\varkappa G_\pi}{G_{\varkappa 1} + G_\pi} = \Phi; \tag{4.105}$$

for case (4.99) + (4.100) + (4.101)

$$\frac{1+2\varkappa}{2} - G_{\varkappa 0} + \frac{1}{4(1-\varkappa)}\ln\frac{(1-2\varkappa)G_{\varkappa 0}}{G_\pi} - \varkappa\ln\frac{(1-2\varkappa)(G_{\varkappa 1} + G_\pi)}{2(1-\varkappa)G_\pi} - \frac{\varkappa G_\pi}{G_{\varkappa 1} + G_\pi} = \Phi. \tag{4.106}$$

In view of (4.105) and (4.106), the functions $\Phi(G_\pi)$ are monotonic decreasing ($\partial\Phi/\partial G_\pi < 0$). This enables us, as in §§ 1 and 2, to separate the problem into independent weight and dynamic parts. The dynamic part of the problem consists as before in determining the optimum program of the thrust-acceleration vector, and is formulated in the form (4.11). The weight part of the problem consists in determining the initial value $G_{\varkappa 0}$ and the final value $G_{\varkappa 1}$ of the engine weight, and ensuring the maximum of the function Φ in (4.105) and (4.106) at fixed values of the payload,* and also in establishing the limits of applicability of solutions (4.105), (4.106).

It is possible to use a similar approach to determine the limiting values of the parameter $\varkappa$; for $\varkappa = 1$ it is necessary to take the single solution (4.101), and for $\varkappa = 0$ either the single solution (4.99) or the two solutions (4.99) and (4.100).

5. Solution of the weight part of the problem. Examining the partial derivatives $\partial\Phi/\partial G_{\varkappa 0}$, $\partial\Phi/\partial G_{\varkappa 1}$ we find the optimum values of $G_{\varkappa 0}$ and $G_{\varkappa 1}$ to be:

for the case (4.99) + (4.101)

$$G_{\varkappa 0} = {}^1/_2\varkappa - G_\pi + \sqrt{{}^1/_4\varkappa^2 + (1-\varkappa)G_\pi}, \qquad G_{\varkappa 1} = 0; \tag{4.107}$$

for the case (4.99) + (4.100) + (4.101)

$$G_{\varkappa 0} = \frac{1}{4(1-\varkappa)}, \quad G_{\varkappa 1} = 0. \tag{4.108}$$

By comparing (4.105) and (4.106) after the optimum values (4.107) and (4.108) of the weights $G_{\varkappa 0}$, $G_{\varkappa 1}$ have been substituted in them, one may establish the exact limits of applicability for each type of solution. Solution (4.99) + (4.101) is valid in the region

$$\begin{gathered}(1-2\varkappa)/4(1-\varkappa) \leqslant G_\pi \leqslant 1, \quad 0 < \varkappa \leqslant 0.5 \\ \text{and} \quad 0 \leqslant G_\pi \leqslant 1, \quad 0.5 \leqslant \varkappa < 1,\end{gathered} \tag{4.109}$$

162 and solution (4.99) + (4.100) + (4.101) in the region

$$0 \leqslant G_\pi \leqslant (1-2\varkappa)/4(1-\varkappa), \quad 0 < \varkappa < 0.5. \tag{4.110}$$

Regions (4.109) and (4.110) are shown in Figure 4.12; region (4.110) is shaded. At $\varkappa = 1$ the weight varies according to (4.101) over the entire interval $0 \leqslant G_\pi \leqslant 1$, and $G_{\varkappa 0}$ and $G_{\varkappa 1}$ are determined by (4.107). At $\varkappa = 0$ the solution (4.99) is valid over the interval $0.25 \leqslant G_\pi \leqslant 1$, where

$$G_\varkappa(t) = \sqrt{G_\pi} - G_\pi,$$

and the solution (4.99) + (4.100) over the interval $0 \leqslant G_\pi \leqslant 0.25$; here $G_{\varkappa 0} = 0.25$, $G_{\varkappa 1} = G_\pi$.

Figure 4.13 represents curves of the optimum take-off engine weight $G_{\varkappa 0}$ as a function of the payload G_π for different values of parameter $\varkappa$. The curves are plotted according to (4.107) and (4.108), and the limits of applicability (4.109) and (4.110). The lower solid curve corresponds to the passive jettisoning of the engine ($\varkappa = 0$, cf. § 2). The dashed continuation of the lower curve and the right-hand branch of this curve correspond

* Relations (4.105) and (4.106) are solved for Φ, and therefore it is expedient here to replace the problem of maximum payload G_π for fixed Φ by the equivalent problem of maximum Φ for fixed G_π.

to the case of fixed engine weight, treated in §1. It is seen that the optimum take-off engine weight increases as a result of using the jettisoned sections of the engine as working mass ($\varkappa > 0$, active jettisoning) at the expense of the working fluid.

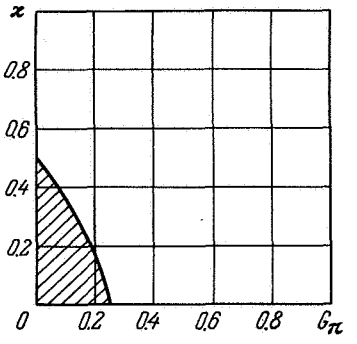

FIGURE 4.12. Regions of applicability of different types of solutions (unshaded region corresponds to the first type — Figure 4.7, and shaded region to the second type — Figure 4.8).

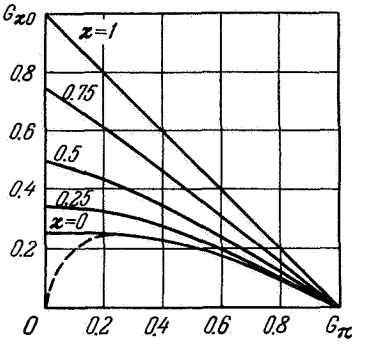

FIGURE 4.13. Optimum take-off engine weight $G_{\varkappa 0}$ as a function of payload G_π for fixed values of the conversion coefficient $\varkappa$.

From the results obtained we derive the following optimum control functions for the engine weight and the working fluid:

for the cases $0 < \varkappa \leqslant 0.5$, $(1-2\varkappa)/4\,(1-\varkappa) \leqslant G_\pi \leqslant 1$ and $0.5 \leqslant \varkappa < 1$, $0 \leqslant G_\pi \leqslant 1$ (Figure 4.7)

163
$$\left.\begin{aligned} G_\varkappa(t) = G_{\varkappa 0} &= \frac{\varkappa}{2} - G_\pi + \sqrt{\frac{\varkappa^2}{4} + (1-\varkappa)G_\pi}, \\ \dot G_\sigma &= -\frac{(G_\sigma + G_{\varkappa 0})^2}{G_{\varkappa 0}}\frac{\alpha}{2g}a^2 \\ &\text{(for } 1 - G_{\varkappa 0} \geqslant G_\sigma(t) \geqslant G_\pi\text{)}, \\ \dot G_\varkappa = -\frac{(G_\varkappa + G_\pi)^2}{\varkappa G_\varkappa}\frac{\alpha}{2g}a^2, &\quad G_\sigma(t) = G_\pi \\ &\text{(for } G_{\varkappa 0} \geqslant G_\varkappa(t) \geqslant 0\text{)}; \end{aligned}\right\} \qquad (4.111)$$

for the case $0 < \varkappa < 0.5$, $0 \leqslant G_\pi \leqslant (1-2\varkappa)/4\,(1-\varkappa)$ (Figure 4.8)

$$\left.\begin{aligned} G_\varkappa(t) = G_{\varkappa 0} = \frac{1}{4(1-\varkappa)}, &\quad \dot G_\sigma = -\frac{(G_\sigma + G_{\varkappa 0})^2}{G_{\varkappa 0}}\frac{\alpha}{2g}a^2 \\ &\text{(for } 1 - G_{\varkappa 0} \geqslant G_\sigma(t) \geqslant (1-2\varkappa)G_{\varkappa 0}\text{)}, \\ G_\varkappa(t) = \frac{G_\sigma(t)}{1-2\varkappa}, &\quad \dot G_\sigma = -4(1-\varkappa)G_\sigma\frac{\alpha}{2g}a^2 \\ &\text{(for } (1-2\varkappa)G_{\varkappa 0} \geqslant G_\sigma(t) \geqslant G_\pi\text{)}, \\ \dot G_\varkappa = -\frac{(G_\pi + G_\varkappa)^2}{\varkappa G_\varkappa}\frac{\alpha}{2g}a^2, &\quad G_\sigma(t) = G_\pi \\ &\left(\text{for } \frac{G_\pi}{1-2\varkappa} \geqslant G_\varkappa(t) \geqslant 0\right); \end{aligned}\right\} \qquad (4.112)$$

for the case $\varkappa = 1$, $0 \leqslant G_\pi \leqslant 1$ (Figure 4.9)

$$\dot G_\varkappa = -\frac{(G_\pi + G_\varkappa)^2}{\varkappa G_\varkappa}\frac{\alpha}{2g}a^2, \quad G_\sigma(t) = G_\pi \quad (\text{for } 1 - G_\pi \geqslant G_\varkappa(t) \geqslant 0); \qquad (4.113)$$

for the case $\varkappa = 0$, $0.25 \leqslant G_\pi \leqslant 1$ (Figure 4.10)

$$G_\varkappa(t) = G_{\varkappa 0} = \sqrt{G_\pi} - G_\pi, \quad \dot{G}_\sigma = -\frac{(G_\sigma + G_{\varkappa 0})^2}{G_{\varkappa 0}} \frac{\alpha}{2g} a^2$$
$$(\text{for } 1 - G_{\varkappa 0} \geqslant G_\sigma(t) \geqslant G_\pi); \tag{4.114}$$

for the case $\varkappa = 0$, $0 \leqslant G_\pi \leqslant 0.25$ (Figure 4.11)

$$\left.\begin{aligned} G_\varkappa(t) = G_{\varkappa 0} = 0.25, \quad \dot{G}_\sigma = -\frac{(G_\sigma + G_{\varkappa 0})^2}{G_{\varkappa 0}} \frac{\alpha}{2g} a^2 \\ (\text{for } 1 - G_{\varkappa 0} \geqslant G_\sigma(t) \geqslant G_{\varkappa 0}), \\ G_\varkappa(t) = G_\sigma(t), \quad \dot{G}_\sigma = -4G_\sigma \frac{\alpha}{2g} a^2 \\ (\text{for } G_{\varkappa 0} \geqslant G_\sigma(t) \geqslant G_\pi). \end{aligned}\right\} \tag{4.115}$$

164 Finally, the functional Φ is expressed as follows in terms of G_π: for $0 \leqslant \varkappa \leqslant 0.5$, $(1-2\varkappa)/4(1-\varkappa) \leqslant G_\pi \leqslant 1$ and for $0.5 \leqslant \varkappa \leqslant 1$, $0 \leqslant G_\pi \leqslant 1$

$$\Phi = (1-\varkappa)\left(1 - \frac{G_\pi}{K}\right) - \varkappa \ln \frac{G_\pi}{K} + G_\pi - K$$
$$\left(K = \frac{\varkappa}{2} + \sqrt{\frac{\varkappa^2}{4} + (1-\varkappa)\, G_\pi}\right); \tag{4.116}$$

for $0 \leqslant \varkappa \leqslant 0.5$, $0 \leqslant G_\pi \leqslant (1-2\varkappa)/4(1-\varkappa)$

$$\Phi = \frac{1-2\varkappa}{4(1-\varkappa)} - \varkappa \ln \frac{1-2\varkappa}{2(1-\varkappa)} - \frac{1}{4(1-\varkappa)} \ln \frac{4(1-\varkappa) G_\pi}{1-2\varkappa}.$$

The maximum payload G_π has been plotted in Figure 4.14 as a function of the functional Φ for different fixed values of the parameter $\varkappa$, according to (4.16). The lowest solid curve corresponds, in Figure 4.13, to the case $\varkappa = 0$ which was treated in § 2. This same curve (in the range $0 \leqslant \Phi \leqslant 0.25$) and its dashed curve continuation (in the range $0.25 \leqslant \Phi \leqslant 1$) correspond to the case of a constant weight $G_\varkappa$, which was treated in § 1.

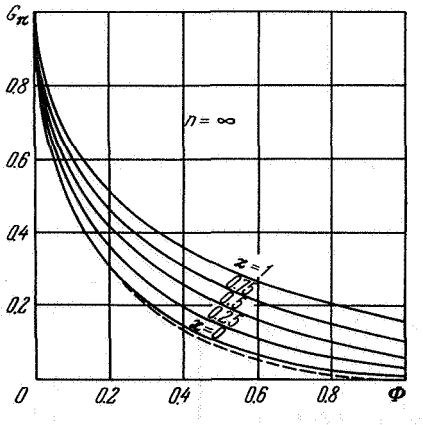

FIGURE 4.14. Maximum payload G_π as a function of the functional Φ of the dynamic part of the problem for fixed values of the conversion coefficient $\varkappa$.

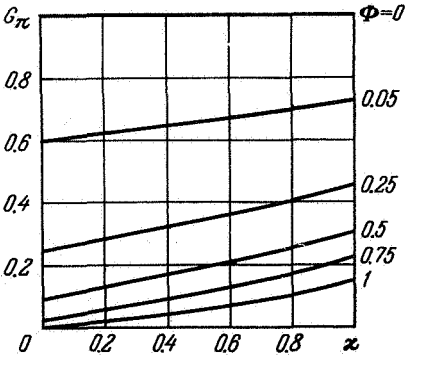

FIGURE 4.15. Payload G_π as a function of the conversion coefficient $\varkappa$ for fixed values of the functional Φ.

All the curves are represented in the interval $0 \leqslant \Phi \leqslant 1$. Whereas in the case of constant engine weight the function $G_\pi(\Phi)$ becomes physically meaningless outside this interval (cf. § 1), here the function $G_\pi(\Phi)$ has a meaning along the entire semiaxis $0 \leqslant \Phi < \infty$. The behavior of $G_\pi(\Phi)$ outside the range $0 \leqslant \Phi \leqslant 1$ is approximately (for $G_\pi \ll 1$) described by the following formulas:

$$\left.\begin{aligned} G_\pi &\approx \frac{1-2\varkappa}{4(1-\varkappa)} \exp[-4(1-\varkappa)\Phi] \quad \text{for } 0 \leqslant \varkappa < 0.5, \\ G_\pi &\approx \exp(-\Phi/\varkappa) \qquad\qquad\qquad\quad \text{for } 0.5 \leqslant \varkappa \leqslant 1. \end{aligned}\right\} \tag{4.117}$$

The dependence of the payload on the parameter $\varkappa$ is nearly linear for low values of the functional $0 \leqslant \Phi \leqslant 0.5$ (Figure 4.15), and becomes exponential for large values (4.117).

165 The gain in payload achieved by utilizing the jettisoned engine sections as working mass ($\varkappa > 0$) can be considerable. Thus, at the limit $\varkappa = 1$ (full conversion) the payload is increased (compared with simple jettisoning, $\varkappa = 0$) by a factor of 1.2 for $\Phi = 0.05$, 1.8 for $\Phi = 0.25$, more than 3 for $\Phi = 0.5$, 7 for $\Phi = 0.75$, and 15 for $\Phi = 1$.

A comparison of payloads for the same values of the functional $\Phi = (\alpha/2g)J$, however, yields results which are too high. The conversion of the engine material into working mass obviously necessitates some additional devices, which increase the engine weight per unit power, and hence the value of Φ (for a fixed value of the integral J). The full conversion of the engine material into working mass ($\varkappa = 1$) becomes inefficient when the unit weight α increases by a factor of 2 for $\Phi = 0.05$, 2.5 for $\Phi = 0.25$, 3 for $\Phi = 0.5$, etc., (where $\Phi = (\alpha_{\varkappa=0}/2g)J$). The problem of selecting the optimum value of $\varkappa$ (the value which yields a maximum payload for a given value of the integral J) can be solved if there is a functional relationship $\alpha(\varkappa)$.

6. Discrete reduction of the engine weight. The previous case of continuous reduction of the engine weight corresponds to an infinitely large number of infinitesimal engine sections ($n = \infty$ in Figure 4.14). We shall now compare this limiting case with that of a finite number of finite-size sections, as in § 2 for $\varkappa = 0$.

Let the j-th section of the engine be jettisoned at time t_j, and let some of this section, defined by the coefficient $\varkappa$, be added to the working-fluid reserve, i.e.,

$$G_0^{(j)+} = G_0^{(j)-} + \varkappa(G_\varkappa^{(j)-} - G_\varkappa^{(j)+}) \quad (j = 1, \ldots, n-1), \tag{4.118}$$

where the subscript j indicates time t_j, and the plus or minus superscripts correspond to the values of the function to the right or left of this time t_j.

166 The engine weight remains constant during the time interval $t_j < t < t_{j+1}$, so

$$G_\varkappa^{(j)-} = G_\varkappa^{(j-1)+} \quad (j = 1, \ldots, n). \tag{4.119}$$

The power N and the parameter $\varkappa$ should be maximized, as in the case of a continuous decrease of the engine weight. The variation of the vehicle

weight between jettisons is described by equation (4.99). Integrating this equation by parts from t_j to t_{j+1} ($j = 0, 1, \ldots n-1$; $t_n = T$) and summing, we obtain

$$\Phi = \sum_{j=0}^{n-1} G_{\varkappa}^{(j)+} \frac{1}{G_{\sigma}^{(j+1)-} + G_{\varkappa}^{(j)+}} - \frac{1}{G_{\sigma}^{(j)+} + G_{\varkappa}^{(j)+}} \Bigg). \tag{4.120}$$

Using (4.118) for the working fluid at the points of discontinuity, and the condition that the engine weight be constant between times of jettisoning (4.119), we can rewrite (4.120) in the form

$$\Phi = \sum_{j=0}^{n-1} G_{\varkappa}^{(j)+} \left(\frac{1}{G_{\sigma}^{(j+1)-} + G_{\varkappa}^{(j)+}} - \frac{1}{G_{\sigma}^{(j)-} + \varkappa G_{\varkappa}^{(j-1)+} + (1-\varkappa)\, G_{\varkappa}^{(j)+}} \right) \tag{4.121}$$

$$(G_{\varkappa}^{(-1)+} = G_{\varkappa}^{(0)+} = G_{\varkappa 0}, \quad G_{\sigma}^{(0)-} = G_{\sigma 0}, \quad G_{\sigma}^{(n)-} = G_{\sigma 1} = G_{\pi}).$$

By calculating the partial derivative $\partial\Phi/\partial G_{\pi}$ we can see that the function $\Phi(G_{\pi})$ is monotonic decreasing. The problem is again separated, and the weight part reduces to finding the values of

$$G_{\varkappa}^{(j)+}, \quad G_{\sigma}^{(j)-} \qquad (j = 0, 1, \ldots, n-1), \tag{4.122}$$

which maximize the function (4.121) for a fixed value of G_{π}, and satisfy the conditions

$$G_{\sigma 0} + G_{\varkappa 0} = 1, \quad G_{\varkappa}^{(j)+} \leqslant G_{\varkappa}^{(j-1)+}. \tag{4.123}$$

(In the following, the superscripts + and − will be dropped for simplicity.)

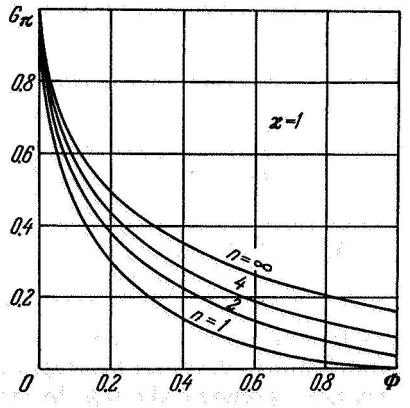

FIGURE 4.16. Comparison of the payload G_{π} for continuous ($n = \infty$) and discrete ($n = 2, 4$) decrease of engine weight; $n = 1$ gives payload for fixed engine weight with full conversion of engine material into working mass ($\varkappa = 1$).

167 We thus obtain a system of $2n$ algebraic equations (at $0 \leqslant \varkappa < 1$) for determining the $2n$ unknowns (4.122):

$$\left.\begin{aligned}
&(G_\sigma^{(j)} + G_\varkappa^{(j-1)})\sqrt{G_\varkappa^{(j)}} = (G_\sigma^{(j)} + \varkappa G_\varkappa^{(j-1)} + (1-\varkappa)G_\varkappa^{(j)})\sqrt{G_\varkappa^{(j-1)}} \\
&\qquad\qquad \left(\frac{\partial\Phi}{\partial G_\sigma^{(j)}} = 0\right), \\
&\frac{G_\sigma^{(j+1)}}{(G_\sigma^{(j+1)} + G_\varkappa^{(j)})^2} + \frac{\varkappa G_\varkappa^{(j+1)}}{(G_\sigma^{(j+1)} + \varkappa G_\varkappa^{(j)} + (1-\varkappa)G_\varkappa^{(j+1)})^2} = \\
&\qquad\qquad = \frac{G_\sigma^{(j)} + \varkappa G_\varkappa^{(j-1)}}{(G_\sigma^{(j)} + \varkappa G_\varkappa^{(j-1)} + (1-\varkappa)G_\varkappa^{(j)})^2}, \\
&\left(\frac{\partial\Phi}{\partial G_\varkappa^{(j)}} = 0\right) \text{ or } G_\varkappa^{(j)} = G_\varkappa^{(j+1)}, \\
&\frac{G_\sigma^{(1)}}{(G_\sigma^{(1)} + G_\varkappa^{(0)})^2} + \frac{\varkappa G_\varkappa^{(1)}}{(G_\sigma^{(1)} + \varkappa G_\varkappa^{(0)} + (1-\varkappa)G_\varkappa^{(1)})^2} = 0 \\
&\qquad\qquad \left(\frac{\partial\Phi}{\partial G_\varkappa^{(0)}} = 0\right), \\
&\qquad\qquad G_\sigma^{(0)} + G_\varkappa^{(0)} = 1 \qquad (j = 1, \ldots, n-1).
\end{aligned}\right\} \tag{4.124}$$

At the limit $\varkappa = 1$ the corresponding system of equations has the simple solution

$$\left.\begin{aligned}
&G_{\sigma 0} = 1 - (G_\pi^{-n/(n+1)} - 1)G_\pi, \quad G_\sigma^{(j)} = G_\pi \quad (j = 1, \ldots, n-1), \\
&G_\varkappa^{(j)} = (G_\pi^{-(n-j)/(n+1)} - 1)G_\pi \qquad (j = 0, 1, \ldots, n-1;\ \varkappa = 1).
\end{aligned}\right\} \tag{4.125}$$

Substituting (4.125) in (4.121), we obtain the relationship between the maximum payload G_π and the functional Φ in the form

$$\Phi = (n+1)(1 - G_\pi^{1/(n+1)}) + G_\pi - 1 \text{ for } \varkappa = 1. \tag{4.126}$$

As $n \to \infty$ this formula reduces to the first relationship of (4.116). In Figure 4.16, equation (4.126) has been plotted in the form of curves $G_\pi(\Phi)$ corresponding to fixed values of n. It is seen from the figure that in passing from $n = 1$ (constant engine weight) to $n = 2$, roughly one-third of the maximum possible gain in payload is obtained, while $n = 4$ gives about two-thirds of the maximum gain. In the transition from $n = 4$ to $n = \infty$ the full maximum gain is attained. For $\varkappa = 0$ (cf. § 2) most of the gain is already obtained at $n = 2$. It is thus possible to conclude that the payload limit can be approached by means of a relatively small finite number of engine sections; this number decreases with the coefficient $\varkappa$. Note that the maximum permissible value of the functional Φ is equal to n, as in the case $\varkappa = 0$.

Chapter Five

IDEAL POWER-LIMITED ENGINE. OPTIMUM PROGRAMS OF THRUST ACCELERATION

168 It was established in the preceding chapter that for an ideal power-limited engine, the variational problem (4.11) of the optimum law of thrust acceleration (the dynamic problem) can be solved independently of the general optimization problem. After it has been solved for each specific maneuver, the optimum parameters of both the propulsion system and the vehicle may be calculated by the formulas of Chapter Four.

The dynamic problem (4.11) was formulated as a Lagrange problem with differential constraints and boundary conditions. The thrust acceleration $a(t)$ in the optimum regime differs from zero throughout the flight, except at isolated points, as follows from §§ 2 and 3 of Chapter Four. The absence of boundary controls makes it possible to solve (4.11) by the classical methods of variational calculus.

In some cases it is convenient to alter the formulation of (4.11) so as to eliminate the differential constraints. To that end it is necessary to eliminate the acceleration a from the functional integrand using the equations of motion (cf. Appendix (A.47)) so that

$$J = \int_0^T [\ddot{\mathbf{r}} - \mathfrak{R}(\mathbf{r}, t)]^2 \, dt \tag{5.1}$$
$$(\mathbf{r}(0) = \mathbf{r}_0, \ \dot{\mathbf{r}}(0) = \mathbf{v}_0, \ \mathbf{r}(T) = \mathbf{r}_1, \ \dot{\mathbf{r}}(T) = \mathbf{v}_1).$$

The problem reduces to the determination of extremals, paths in position-velocity space (between given points $(\mathbf{r}_0, \mathbf{v}_0)$ and $(\mathbf{r}_1, \mathbf{v}_1)$) along which the functional (5.1) is a minimum for some given time interval.

Alternately, we can formulate the variational problem (4.11) as Mayer's problem in the form

$$\left.\begin{array}{lll} \dot{J} = a^2 = (a\mathbf{e})^2, & J(0) = 0, & J(T) = \min, \\ \dot{\mathbf{r}} = \mathbf{v}, & \mathbf{r}(0) = \mathbf{r}_0, & \mathbf{r}(T) = \mathbf{r}_1, \\ \dot{\mathbf{v}} = a\mathbf{e} + \mathfrak{R}, & \mathbf{v}(0) = \mathbf{v}_0, & \mathbf{v}(T) = \mathbf{v}_1 \\ \multicolumn{3}{c}{(a(t) \geqslant 0, \quad |\mathbf{e}(t)| = 1).} \end{array}\right\} \tag{5.2}$$

169 ### § 1. EQUATIONS OF THE EXTREMALS AND THEIR PROPERTIES

1. Equations of the extremals for the general case. We represent the functional (5.1) in a rectangular inertial frame so that

$$J = \int_0^T [(\ddot{x} - X)^2 + (\ddot{y} - Y)^2 + (\ddot{z} - Z)^2] dt = \int_0^T F(t, x, \dot{x}, y, \dot{y}, z, \dot{z}) \, dt \tag{5.3}$$

with boundary conditions

$$x(0)=x_0,\ y(0)=y_0,\ z(0)=z_0,\ \dot{x}(0)=u_0,\ \dot{y}(0)=v_0,\ \dot{z}(0)=w_0,$$
$$x(T)=x_1,\ y(T)=y_1,\ z(T)=z_1,\ \dot{x}(T)=u_1,\ \dot{y}(T)=v_1,\ \dot{z}(T)=w_1,$$

where $X=X(t, x, y, z)$, $Y=Y(t, x, y, z)$, $Z=Z(t, x, y, z)$ are the components of the vector of gravitational acceleration $\mathbf{R}(\mathbf{r}, t)$.

The first variation of the functional (5.3) is

$$\begin{aligned}\delta J=&\left(2F-\frac{\partial F}{\partial\dot{x}}\dot{x}-\frac{\partial F}{\partial\dot{y}}\dot{y}-\frac{\partial F}{\partial\dot{z}}\ddot{z}+\frac{d}{dt}\frac{\partial F}{\partial\dot{x}}\dot{x}+\frac{d}{dt}\frac{\partial F}{\partial\dot{y}}\dot{y}+\frac{d}{dt}\frac{\partial F}{\partial\dot{z}}\dot{z}\right)\delta t\Big|_0^1+\\&+\left(\frac{\partial F}{\partial\dot{x}}\delta\dot{x}+\frac{\partial F}{\partial\dot{y}}\delta\dot{y}+\frac{\partial F}{\partial\dot{z}}\delta\dot{z}\right)\Big|_0^1-\\&-\left(\frac{d}{dt}\frac{\partial F}{\partial\dot{x}}\delta x+\frac{d}{dt}\frac{\partial F}{\partial\dot{y}}\delta y+\frac{d}{dt}\frac{\partial F}{\partial\dot{z}}\delta z\right)\Big|_0^1+\\&+\int_0^T\left[\left(\frac{d^2}{dt^2}\frac{\partial F}{\partial\ddot{x}}+\frac{\partial F}{\partial x}\right)\delta x+\left(\frac{d^2}{dt^2}\frac{\partial F}{\partial\ddot{y}}+\frac{\partial F}{\partial y}\right)\delta y+\left(\frac{d^2}{dt^2}\frac{\partial F}{\partial\ddot{z}}+\frac{\partial F}{\partial z}\right)\delta z\right]dt.\end{aligned}\tag{5.4}$$

Since the initial data $(x_0, y_0, z_0, u_0, v_0, w_0)$ and final data $(x_1, y_1, z_1, u_1, v_1, w_1)$ of the trajectory are fixed, their variations in (5.4) vanish. If the expressions multiplying the variations δx, δy, δz in the integrand are set equal to zero, we obtain the Euler equation of the variational problem considered, namely,

$$\left.\begin{aligned}\ddot{a}_x&=\frac{\partial X}{\partial x}a_x+\frac{\partial Y}{\partial x}a_y+\frac{\partial Z}{\partial x}a_z,\\ \ddot{a}_y&=\frac{\partial X}{\partial y}a_x+\frac{\partial Y}{\partial y}a_y+\frac{\partial Z}{\partial y}a_z\\ \ddot{a}_z&=\frac{\partial X}{\partial z}a_x+\frac{\partial Y}{\partial z}a_y+\frac{\partial Z}{\partial z}a_z\\ (a_x&=\ddot{x}-X,\quad a_y=\ddot{y}-Y,\ a_z=\ddot{z}-Z),\end{aligned}\right\}\tag{5.5}$$

or, in vector form,

$$\ddot{\mathbf{a}}=\frac{\partial}{\partial\mathbf{r}}(\mathbf{a}\cdot\mathbf{R}),\quad \mathbf{a}=\ddot{\mathbf{r}}-\mathbf{R}.\tag{5.6}$$

2. First integrals of the equations of the extremals for three-dimensional motion in a central field. In the case considered ($\mathbf{R}=-k\mathbf{r}/r^3$) the equations
170 of the extremals (5.5) or (5.6) possess four first integrals expressed as one scalar and one vector integral /5.1/ and written

$$\left.\begin{aligned}{}^1/_2(\mathbf{a}\cdot\mathbf{a})-(\dot{\mathbf{a}}\cdot\mathbf{v})-(\mathbf{a}\cdot k\mathbf{r}/r^3)&=H=\text{const},\\ (\mathbf{a}\times\mathbf{v})-(\dot{\mathbf{a}}\times\mathbf{r})&=\mathbf{M}=\text{const}.\end{aligned}\right\}\tag{5.7}$$

(The scalar integral is due to the absence of time in the integrand ($\partial F/\partial t=0$) of (5.3), and exists for any stationary field $\partial\mathbf{R}/\partial t=0$; if the full time of motion is unspecified, then $H=0$.)

In the two-dimensional case there are only two integrals /5.2/

$$\left.\begin{aligned}{}^1/_2(a_x^2+a_y^2)-(\dot{a}_xu+\dot{a}_yv)-k(a_xx+a_yy)(x^2+y^2)^{-3/2}&=\text{const},\\ (a_xv-a_yu)-(\dot{a}_xy-\dot{a}_yx)&=\text{const}.\end{aligned}\right\}\tag{5.8}$$

3. Equations of the extremals for plane motion in central field. We shall study in detail the important particular case of optimum motion described by

system (5.5), that of plane motion ($z \equiv a_z \equiv 0$) in a central gravitational field ($X = -kxr^{-3}$, $Y = -kyr^{-3}$, $r = \sqrt{x^2 + y^2}$) /5.3, 5.4/.

Dimensionless variables will be used in what follows. The values (A.2) will be taken as characteristic values. For the functional J we thus obtain the characteristic value $k^{2/5} r_*^{-1/5}$. The same symbols as before will be used for the dimensionless variables.

After transforming (5.3) to polar coordinates (r, φ), which are related to rectangular coordinates (x, y) by formulas (A.4), write $\theta = 0$, and obtain

$$J = \int_0^T [(\ddot{r} - r\dot{\varphi}^2 + 1/r^2)^2 + (\ddot{\varphi}r + 2\dot{\varphi}\dot{r})^2]\, dt \tag{5.9}$$

$$(r(0) = r_0,\ \varphi(0) = \varphi_0,\ \dot{r}(0) = \dot{r}_0,\ \dot{\varphi}(0) = \dot{\varphi}_0,$$

$$r(T) = r_1,\ \varphi(T) = \varphi_1,\ \dot{r}(T) = \dot{r}_1,\ \dot{\varphi}(T) = \dot{\varphi}_1).$$

Since the integrand in (5.9) does not contain the argument t or the function $\varphi(t)$, the order of the differential expression in the integrand can be reduced. We shall use the notation (A.8) for the first derivatives $\dot{r}$, $\dot{\varphi}$ given by $\dot{r} = v_r$, $\dot{\varphi} = v_\varphi / r$ and replace argument t with argument r to yield $dt = dr/v_r$.

171 By these substitutions the integral in (5.9) is reduced to

$$J = \int_{r_0}^{r_1} \left[\left(v_r v_r' - \frac{v_\varphi^2}{r} + \frac{1}{r^2}\right)^2 + \left(v_r v_\varphi' + \frac{v_r v_\varphi}{r}\right)^2\right] \frac{dr}{v_r}, \tag{5.10}$$

where the primes indicate differentiation with respect to r. The extremals of this functional satisfy the initial and final conditions relative to v_φ, v_r and r. Using the known relationships $v_r(r)$, $v_\varphi(r)$ it is possible to calculate the time T and the angular displacement $\varphi_1 - \varphi_0$ in the forms

$$T = \int_{r_0}^{r_1} \frac{dr}{v_r(r)}, \quad \varphi_1 - \varphi_0 = \int_{r_0}^{r_1} \frac{v_\varphi(r)\, dr}{r v_r(r)}. \tag{5.11}$$

If the magnitudes T and $\varphi_1 - \varphi_0$ are specified, expressions (5.11) must appear as conditions of isoperimetry. The variational problem equivalent to (5.9) is written in the new variables as

$$\left.\begin{aligned} J &= \int_{r_0}^{r_1} \left[\left(v_r v_r' - \frac{v_\varphi^2}{r} + \frac{1}{r^2}\right)^2 + \left(v_r v_\varphi' + \frac{v_r v_\varphi}{r}\right)^2 + 2\lambda + 2\nu \frac{v_\varphi}{r}\right] \frac{dr}{v_r}, \\ v_r(r_0) &= v_{r0},\quad v_\varphi(r_0) = v_{\varphi 0},\quad v_r(r_1) = v_{r1},\quad v_\varphi(r_1) = v_{\varphi 1}. \end{aligned}\right\} \tag{5.12}$$

(The parameters 2λ, 2ν are constant Lagrange multipliers, ensuring the fulfillment of conditions (5.11); the coefficient 2 is introduced for convenience.)

If the first variation of the functional (5.12) is equated to zero, we find two differential equations of the second order for v_r and v_φ. Returning to the argument t, and using the equations of motion (A.8), we obtain a system of equations of the first order describing the optimum regions of plane motion in a central field /5.3, 5.5/; this is

$$\left.\begin{aligned} \dot{r} &= v_r,\quad \dot{\varphi} = v_\varphi / r,\quad \dot{v}_r = a_r + v_\varphi^2/r - 1/r^2,\quad \dot{v}_\varphi = a_\varphi - v_r v_\varphi / r, \\ \dot{a}_r &= \frac{1}{v_r}\left[{}^1\!/_2 (a_r^2 + a_\varphi^2) + a_r\left(\frac{v_\varphi^2}{r} - \frac{1}{r^2}\right) - \lambda - \nu \frac{v_\varphi}{r}\right], \\ \dot{a}_\varphi &= \frac{1}{r}(a_\varphi v_r - 2 a_r v_\varphi + \nu). \end{aligned}\right\} \tag{5.13}$$

The last two equations of the system define the optimum program for the components of the thrust-acceleration vector.

4. Properties of equations (5.13). The system of differential equations (5.13) is of the sixth order and contains two constants λ and ν (the first
172 integrals of the system, cf. (5.8)), and therefore its solution requires eight boundary conditions such as (5.9). If some of the boundary values are unspecified, it is necessary to calculate instead the corresponding optimum values. These are obtained by equating to zero the differential part of the first variation of the functional (5.12), namely,

$$\delta J = 2\left[a_r \delta v_r + a_\varphi \delta v_\varphi + (2a_\varphi v_\varphi / r - \dot{a}_r)\ \delta r - \nu \delta \varphi - \lambda \delta t\right]_0^1. \tag{5.14}$$

When the angular displacement and the time of motion are unspecified, the multipliers of the corresponding variations, ν and λ, must be equated to zero.

Equations (5.13) are invariant under the linear transformation /5.4/

$$\left.\begin{aligned} &r \to lr,\ t \to l^{3/2}t,\ \varphi \to \varphi,\ v_r \to l^{-1/2}v_r,\ v_\varphi \to l^{-1/2}v_\varphi, \\ &a_r \to l^{-2}a_r,\ a_\varphi \to l^{-2}a_\varphi,\ \lambda \to l^{-4}\lambda,\ \nu \to l^{-5/2}\nu,\ J \to l^{-5/2}J, \end{aligned}\right\} \tag{5.15}$$

and under the sign-inversion transformation

$$\left.\begin{aligned} &t \to -t,\quad r \to r,\quad \varphi \to -\varphi,\quad v_r \to -v_r,\quad v_\varphi \to v_\varphi, \\ &a_r \to a_r,\quad a_\varphi \to -a_\varphi,\quad \lambda \to \lambda,\quad \nu \to \nu,\quad J \to J. \end{aligned}\right\} \tag{5.16}$$

Invariance under the linear transformation (5.15) can be used to obtain the optimum trajectories of zero energy build-up starting from a circular orbit of radius $r(0) = l$ (if the optimum trajectories starting from the circular orbit of radius $r(0) = 1$ are known), or for passing from the optimum transfer trajectories between the circular orbits $r(0) = 1$, $r(T) = r_1$ to the transfer trajectories between the orbits $r(0) = l$, $r(T) = lr_1$.

Invariance under the sign-inversion transformation (5.16) can be used for passing from a given transfer trajectory to the inverse symmetrical transfer trajectory, and from the energy build-up trajectory to the deceleration trajectory.

5. Singular point of equation (5.13). The expression for $\dot{a}_r$ has v_r in the denominator, so that $\dot{a}_r \to \infty$ as $v_r \to 0$, provided the numerator does not approach zero simultaneously. In the latter case the point $v_r = 0$ is singular; its type can be determined as follows /5.3/.

We examine the third and fifth equations of system (5.13) near the point $v_r = 0$; the functions $r(t)$, $v_\varphi(t)$, $a_\varphi(t)$ on the right-hand sides will be considered as known in the neighborhood of this point. We write these equations in the
173 form

$$\dot{v}_r = a_r + h_1,\ \dot{a}_r = \frac{1}{v_r}\left(\tfrac{1}{2}a_r^2 + a_r h_1 + h_2\right) \tag{5.17}$$
$$\left(h_1 = v_\varphi^2/r - 1/r^2,\ h_2 = \tfrac{1}{2}a_\varphi^2 - \lambda - \nu v_\varphi / r\right).$$

Eliminating a_r from system (5.17), we obtain a linear equation for $\frac{1}{2}\dot{v}_r^2$, in which the argument is v_r instead of t; the solution of this equation is

$$\tfrac{1}{2}\dot{v}_r^2 = v_r\left[c + \int (\dot{h}_1 v_r - \tfrac{1}{2}h_1^2 + h_2)\, v_r^{-2} dv_r\right], \tag{5.18}$$

where c is an integration constant. We expand the integrand about the point $v_r = 0$ as a power series in v_r, and calculate the integral

$$^1/_2\dot{v}_r^2 = {}^1/_2h_{10}^2 - h_{20} + cv_r + \ldots . \tag{5.19}$$

The subscript 0 indicates that the value corresponds to the point $v_r = 0$, and the terms of the expansion which we neglected contain powers of v_r higher than the first whose coefficients are independent of c.

Thus, in the $(v_r, {}^1/_2\dot{v}_r^2)$ plane the integral curves (5.19) intersect the axis $v_r = 0$ at the same point, independently of the value of the constant c. This point has coordinates

$$v_r = 0, \quad {}^1/_2\dot{v}_r^2 = {}^1/_2h_{10}^2 - h_{20}. \tag{5.20}$$

This is a singular point of the node type. When $\dot{v}_r$, h_1 and h_2 from (5.17) are substituted in (5.20), the numerator in the expression for $\dot{a}_r$ vanishes, i.e.,

$$^1/_2(a_r^2 + a_\varphi^2) + a_r(v_\varphi^2/r - 1/r^2) - \lambda - \nu v_\varphi/r = 0 \quad \text{for} \quad v_r = 0. \tag{5.21}$$

6. Integration in the neighborhood of the singular point. We note a property of the differential system (5.13) pertaining to the singular point. Taking the time derivative of the fifth equation of (5.13), and introducing the resulting equation in place of the original one, we get

$$\left.\begin{aligned} &\dot{r} = v_r, \quad \dot{\varphi} = v_\varphi/r, \quad \dot{v}_r = a_r + v_\varphi^2/r - 1/r^2, \quad \dot{v}_\varphi = a_\varphi - v_r v_\varphi/r, \\ &\dot{a}_r = \frac{1}{r}\left(a_\varphi - 3\frac{a_r v_\varphi^2}{r} + 2\frac{a_r}{r^2} + \nu\frac{v_\varphi}{r}\right), \quad \dot{a}_\varphi = \frac{1}{r}(a_\varphi v_r - 2a_r v_\varphi + \nu). \end{aligned}\right\} \tag{5.22}$$

In the new system there is no indeterminacy at the point $v_r = 0$ to complicate the numerical integration; moreover, we have eliminated an integral of the system containing the parameter λ, and the order of
174 the system has increased without changing the number of degrees of freedom. Therefore system (5.13) is preferable to (5.22) everywhere except at the singular points (which can exist at the beginning, at the end, or in the middle of the integration interval).

Let the coordinates, the velocity components, the parameter ν, and the acceleration components be specified at the initial instant of time by

$$\begin{aligned} r(0) = r_0, \varphi(0) = \varphi_0, v_r(0) = v_{r0}, v_\varphi(0) = v_{\varphi 0}, \nu = \nu, \\ a_r(0) = a_{r0}, \quad a_\varphi(0) = a_{\varphi 0}. \end{aligned} \tag{5.23}$$

If $v_{r0} \neq 0$, the parameter λ appears in the system of initial conditions together with (5.23). This set of initial values defines the Cauchy problem for equations (5.13).

If $v_{r0} = 0$, the initial point is singular, and relation (5.21) applies; from this relation we find the value of the parameter λ. In this case the Cauchy problem is formulated for equations (5.23), and it will be defined if, in addition to (5.23), we require that $\dot{a}_r(0) = \dot{a}_{r0}$.

The procedure described for integrating the Cauchy problem set out in (5.13) and (5.23) can be used at each step of the solution of any boundary-value problem for equations (5.13), if the latter system is solved by successive selection of the missing initial conditions.

7. Relationship between parameters at the beginning and end of a trajectory. If the dynamic maneuver consists in the transfer between two circular orbits, the extreme points of the trajectory are singular. In this case the initial and final values of the radius r and of the velocities v_r, v_φ are given by

$$r(0) = 1, \quad v_r(0) = 0, \quad v_\varphi(0) = 1, \quad r(T) = r_1, \quad v_r(T) = 0, \quad v_\varphi(T) = r_1^{-1/2}. \tag{5.24}$$

Applying the condition at the singular point (5.21) to the beginning and end of the trajectory, we obtain the two relations

$$^1/_2 a_0^2 - \lambda - \nu = 0, \quad ^1/_2 a_1^2 - \lambda - \nu r_1^{-3/2} = 0, \tag{5.25}$$

where a_0 and a_1 are the initial and final values of the thrust acceleration. Eliminating λ from (5.25), we obtain

$$a_1^2 = a_0^2 - 2\nu(1 - r_1^{-3/2}). \tag{5.26}$$

It follows that for $r_1 > 1$

$$a_1 = a_0 \quad \text{if} \quad \nu = 0, \quad a_1 > a_0 \quad \text{if} \quad \nu < 0, \quad a_1 < a_0 \quad \text{if} \quad \nu > 0. \tag{5.27}$$

For the condition $a_1^2 \geqslant 0$ to hold, the parameter ν must satisfy the inequality

$$\nu \leqslant {}^1/_2 a_0^2 (1 - r_1^{-3/2})^{-1}. \tag{5.28}$$

175 For $r_1 < 1$, inequalities (5.27) and (5.28) are replaced by the reverse inequalities.

8. Equations of the extremals for plane motion in a bicentric field. The equations of the optimum thrust-acceleration program for plane motion in a bicentric field can be written in the following form similar to (5.13), with the Sun ($i=1$) and a planet ($i=2$) representing the two centers (cf. (A.49), (A.50), and Figure A.6) /5.3/:

$$\left.\begin{aligned}
&\dot{a}_r^{(i)} = \frac{1}{v_r^{(i)}}\left[\frac{1}{2}(a_r^{(i)})^2 + \frac{1}{2}(a_\varphi^{(i)})^2 + a_r^{(i)}\frac{(v_\varphi^{(i)})^2}{r^{(i)}} - \right.\\
&\qquad\qquad \left. - \frac{k^{(i)}}{(r^{(i)})^2} - \lambda^{(i)} - \nu^{(i)}\frac{v_\varphi^{(i)}}{r^{(i)}}\right],\\
&\dot{a}_\varphi^{(i)} = \frac{1}{r^{(i)}}(a_\varphi^{(i)} v_r^{(i)} - 2a_r^{(i)} v_\varphi^{(i)} + \nu^{(i)}),\\
&\dot{\nu}^{(i)} = a_\varphi^{(i)}\partial\Psi^{(i)}/\partial\psi^{(i)} + a_r^{(i)}\partial\mathfrak{R}^{(i)}/\partial\psi^{(i)},\\
&\dot{\lambda}^{(i)} = -v_r^{(i)}(a_\varphi^{(i)}\partial\Psi^{(i)}/\partial r^{(i)} + a_r^{(i)}\partial\mathfrak{R}^{(i)}/\partial r^{(i)} + a_\varphi^{(i)}\Psi^{(i)}/r^{(i)}) -\\
&\qquad - \nu^{(i)}\Psi^{(i)}/r^{(i)} - \mathfrak{R}^{(i)}\dot{a}_r^{(i)} - (v_\varphi^{(i)}/r^{(i)})(\nu^{(i)} - 2a_r^{(i)}\Psi^{(i)})\\
&(v_r^{(i)} = \dot{r}^{(i)}, \quad v_\varphi^{(i)} = (\dot{\psi}^{(i)} + \omega) r^{(i)}, \quad i = 1, 2).
\end{aligned}\right\} \tag{5.29}$$

Here ν and λ are no longer constant, since the variables φ and t appear explicitly in system (A.49), (A.50). (The variables in (5.29) are dimensional.)

If the motion occurs in the immediate neighborhood of one of the centers, i.e., in a quasi-central field, the derivatives $\dot{\nu}$ and $\dot{\lambda}$ will be small in absolute value; at the limit, equations (5.29) reduce to the last two equations of (5.13).

A different form of the extremum equations is given in /5.6/, where the fulfillment of the second and third necessary conditions for a minimum of the functional is also checked.

9. **Analytic solutions for a plane-parallel field.*** The problem of determining the extremals of the functional J in the general case requires numerical integration, but for model gravitational fields simple analytic solutions can be found. The most important of these fields is the plane-parallel field ($\mathbf{R}(\mathbf{r}, t) \equiv \mathbf{g} = (0, -g, 0)$ which is a constant vector, cf. § 1 of the Appendix), and the particular case of the gravitation-free field ($\mathbf{g} = 0$). By integrating (5.5) we determine the optimum program of the thrust-acceleration vector, and from it the trajectory, with the aid of the equations of motion (A.53) and the functional, so that

$$\left.\begin{aligned} \mathbf{a}(t) = \mathbf{b}_1 t + \mathbf{b}_2, \quad \mathbf{r}(t) = {}^1/_6\mathbf{b}_1 t^3 + {}^1/_2(\mathbf{b}_2 + \mathbf{g})t^2 + \mathbf{b}_3 t + \mathbf{b}_4, \\ J = {}^1/_3 b_1^2 T^3 + (\mathbf{b}_1 \cdot \mathbf{b}_2) T^2 + b_2^2 T. \end{aligned}\right\} \tag{5.30}$$

176 The constant vectors $\mathbf{b}_1, \ldots, \mathbf{b}_4$ are found from the boundary conditions; thus, when the coordinates and the velocity at the beginning ($\mathbf{r}_0$, $\mathbf{v}_0$) and at the end ($\mathbf{r}_1$, $\mathbf{v}_1$) of the trajectory are given, we have

$$\mathbf{b}_1 = \frac{6}{T^2}\left(\mathbf{v}_1 + \mathbf{v}_0 - 2\frac{\mathbf{r}_1 - \mathbf{r}_0}{T}\right), \quad \mathbf{b}_2 = -\frac{2}{T}\left(\mathbf{v}_1 + 2\mathbf{v}_0 - 3\frac{\mathbf{r}_1 - \mathbf{r}_0}{T}\right),$$
$$\mathbf{b}_3 = \mathbf{v}_0, \quad \mathbf{b}_4 = \mathbf{r}_0. \tag{5.31}$$

Something of the character of the optimum thrust-acceleration programs may be learned by considering the two simplest maneuvers for one-dimensional motions in a gravitation-free field (/5.1, 5.3, 5.5, 5.7/, etc.).

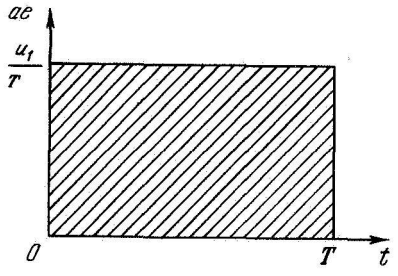

FIGURE 5.1. Optimum program of thrust acceleration for the problem of velocity magnitude build-up in a gravitation-free field (a is the magnitude of the acceleration, $e = \pm 1$ is the direction).

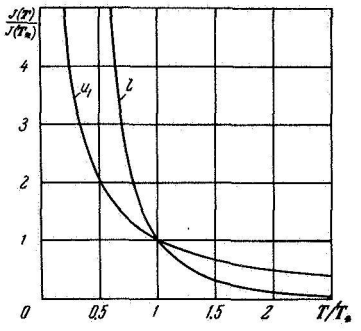

FIGURE 5.2. Functional of the dynamic problem $J(T)/J(T_*)$ as a function of the total time of motion T/T_* for maneuvers in a gravitation-free field (curve u_1 is the velocity build-up, $J(T_*) = u_1^2/T_*$, curve l is the displacement between points of rest, $l/T = 2l^2/T_*^2$).

1) Build-up of a given velocity magnitude u_1 during a given time T. The initial position and velocity are given; the final position is not fixed (cf. (A.64)).

* Dimensional variables are used in this section.

The boundary conditions (A.64), together with the transversality conditions, yield the following expressions for b_1 and b_2: $b_1 = 0$, $b_2 = u_1/T$, whence

$$a(t) = u_1/T, \quad e(t) = +1, \quad J = u_1^2/T. \tag{5.32}$$

Note that in this case the thrust acceleration is constant and is in the direction of the velocity (Figure 5.1); the value of the functional is inversely proportional to the time necessary for executing the maneuver (Figure 5.2, curve u_1). A relationship $J(T)$ of the same form is obtained for maneuvers in a central field when the thrust acceleration is much smaller than the gravitational acceleration.

2) Displacement between two points of rest situated at a distance l apart during a specified time T (cf. (A.65)).

177 Substituting the boundary conditions (A.65) of this maneuver in (5.31), we find

$$\left.\begin{aligned} a(t) &= \tfrac{6l}{T^2}\left(1 - 2\tfrac{t}{T}\right), \quad e(t) = +1 \quad \text{for } 0 \leqslant t \leqslant {}^1/_2 T, \\ a(t) &= \tfrac{6l}{T^2}\left(2\tfrac{t}{T} - 1\right), \quad e(t) = -1 \quad \text{for } {}^1/_2 T \leqslant t \leqslant T, \\ J &= 12l^2/T^3. \end{aligned}\right\} \tag{5.33}$$

Here the thrust-acceleration vector is a linear function of time (Figure 5.3), and the functional is inversely proportional to the cube of the maneuver time (cf. curve l in Figure 5.2). This maneuver represents a rapid orbital transfer in a central field (the thrust acceleration is much larger than the gravitational acceleration).

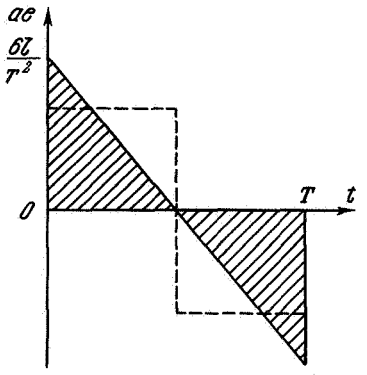

FIGURE 5.3. Optimum thrust-acceleration program for the problem of displacement between points of rest in a gravitation-free field (a is the magnitude of the acceleration, $e = \pm 1$ is the direction, the dashed line is the acceleration program, given for comparison).

We shall determine the gain in the functional produced by replacing one of the nonoptimum programs of the thrust-acceleration vector (/5.8, 5.9/) by the optimum program. Consider a thrust-acceleration vector (dashed line in Figure 5.3) of constant magnitude ($a(t) = 4l/T^2$ whose direction changes only once during the flight (at $t = {}^1/_2 T$). Such an acceleration program corresponds to the functional $J = 16l^2/T^3$, so that in this case a gain of 25% in the functional is achieved by the optimum program (5.33).

10. Analytic solutions for a homogeneous central field. Next we consider the so-called homogeneous central field /5.10/. Here the vector of gravitational acceleration is given by $\mathbf{R} = -k\mathbf{r}/r_*^3$, $r_* = \text{const}$ (cf. (A.54)). A transformation is made to dimensionless variables, taking r_* as the characteristic distance, and (A.2) as the other characteristic quantities. Then $\mathbf{R} = -\mathbf{r}$, and system (5.6) reduces to a linear homogeneous vector equation with constant coefficients

$$\frac{d^4\mathbf{r}}{dt^4} + 2\frac{d^2\mathbf{r}}{dt^2} + \mathbf{r} = 0. \tag{5.34}$$

The general solution of (5.34) is of the form

$$\mathbf{r} = (\mathbf{c}_1 + \mathbf{c}_2 t)\cos t + (\mathbf{c}_3 + \mathbf{c}_4 t)\sin t, \tag{5.35}$$

178 where the constant vectors $\mathbf{c}_1, \ldots, \mathbf{c}_4$ are determined from the boundary conditions; for instance, if $\mathbf{r}(0) = \mathbf{r}_0$, $\dot{\mathbf{r}}(0) = \mathbf{v}_0$, $\mathbf{r}(T) = \mathbf{r}_1$, $\dot{\mathbf{r}}(T) = \mathbf{v}_1$, then

$$\left.\begin{aligned}
&\mathbf{c}_1 = \mathbf{r}_0,\\
&\mathbf{c}_2 = \frac{1}{\sin^2 T - T^2}[(\sin T\cos T + T)\mathbf{r}_0 +\\
&\qquad + \mathbf{v}_0 \sin^2 T - (\sin T + T\cos T)\mathbf{r}_1 + T\mathbf{v}_1 \sin T],\\
&\mathbf{c}_3 = \frac{1}{\sin^2 T - T^2}[-(\sin T\cos T + T)\mathbf{r}_0 - T^2\mathbf{v}_0 +\\
&\qquad + (\sin T + T\cos T)\mathbf{r}_1 - T\mathbf{v}_1 \sin T],\\
&\mathbf{c}_4 = \frac{1}{\sin^2 T - T^2}[\mathbf{r}_0 \sin^2 T + (T - \sin T\cos T)\mathbf{v}_0 -\\
&\qquad - T\mathbf{r}_1 \sin T + (\sin T - T\cos T)\mathbf{v}_1];\\
&\text{for } T = 2\pi s\ (s = 1, 2, \ldots)^*\\
&\mathbf{c}_1 = \mathbf{r}_0,\quad \mathbf{c}_2 = \frac{\mathbf{r}_1 - \mathbf{r}_0}{T},\quad \mathbf{c}_3 = \mathbf{v}_0 - \frac{\mathbf{r}_1 - \mathbf{r}_0}{T},\ \mathbf{c}_4 = \frac{\mathbf{v}_1 - \mathbf{v}_0}{T}.
\end{aligned}\right\} \tag{5.36}$$

The optimum thrust-acceleration program and the integral J are, in accordance with (5.35), given by

$$\left.\begin{aligned}
&\mathbf{a}(t) = 2(\mathbf{c}_4\cos t - \mathbf{c}_2 \sin t),\\
&J = 2(c_4^2 + c_2^2)T + (c_4^2 - c_2^2)\sin 2T - 4(\mathbf{c}_2 \cdot \mathbf{c}_4)\sin^2 T;\\
&\text{for } T = 2\pi s\ (s = 1, 2, \ldots)^*\\
&\mathbf{a}(t) = 2\left(\frac{\mathbf{v}_1 - \mathbf{v}_0}{T}\cos t - \frac{\mathbf{r}_1 - \mathbf{r}_0}{T}\sin t\right),\\
&J = \frac{2}{T}[(\mathbf{r}_1 - \mathbf{r}_0)^2 + (\mathbf{v}_1 - \mathbf{v}_0)^2].
\end{aligned}\right\} \tag{5.37}$$

11. Analytic solution for a central field. A particular solution of system (5.6) for the case of an arbitrary potential field ($\mathfrak{R} = -\text{grad } U$) is given in /5.11/ by

$$\mathbf{a}(t) = \frac{b}{1 + \frac{1}{2}bt}\mathbf{v} \qquad (b = \text{const}). \tag{5.38}$$

This law of thrust acceleration satisfies the Euler equations exactly, as is easily seen by direct substitution. It can be used for determining the trajectory during the acceleration period, but then the transversality conditions will not be completely fulfilled. The relative error in the functional for values of the thrust acceleration which are small compared with the gravitational acceleration is, however, also small and of the order of a (where a is the relative acceleration).

179 § 2. OPTIMUM INTERPLANETARY TRAJECTORY WITH IDEAL POWER-LIMITED ENGINE

We present here a numerical solution of the variational problem (5.1) for interplanetary flights. The extreme values and the extremals of the

* The time T is a multiple of the period of motion along a circular orbit of radius r_0.

functional studied were determined by solving the corresponding boundary-value problems for system (5.13) using either the method of systematically selecting the missing initial values in the equivalent Cauchy problem /5.4, 5.5, 5.12—5.21/, or by direct methods applied to the functional (5.1) /5.18—5.21/. Two approximate solutions were also obtained. The first corresponds to the sections of flight in the neighborhood of the planets /5.3, 5.11, 5.22—5.24, 5.37/, and the second to the mid-course sections of flight /5.1, 5.25/.

The scheme of interplanetary trajectory with a low-thrust engine is described in § 2 of the Appendix. Two qualitatively different sections of the trajectory of such a flight are indicated there: the section in which the gravitational field of the planet is predominant and the Sun has only a perturbing effect, and the section in which the gravitational field of the Sun is predominant and the planets have only a perturbing effect. In these sections the deviations of the gravitational field from a central field have little influence on the integral characteristics of the trajectory /5.4/. The use of the approximate boundary conditions (A.55), (A.56) or (A.57), (A.58) for each section also has only a minor effect. In view of this the problem is solved independently for the following two elementary maneuvers: zero energy build-up in the central field of the planet (or deceleration after orbital transfer), and orbital transfer in the central field of the Sun.

1. **Zero energy build-up.** The maneuver starts at a given point of the initial orbit; during the given time T it is required to build up the full zero energy $E(T) = 0$.

The angular displacement is not fixed; the final values of the radius r_1, together with the radial and transverse projections of the velocity v_{r1}, and $v_{\varphi 1}$, respectively, are related by $E(T) = {}^1/_2(v_{r1}^2 + v_{\varphi 1}^2) - 1/r_1 = 0$ (cf. (A.55)). Since the first variation of the functional (5.14) must vanish, we obtain the optimum relations

$$\nu = 0, \quad a_{r1}/a_{\varphi 1} = v_{r1}/v_{\varphi 1}, \quad a_{r1} - 2a_{\varphi 1}v_{r1}r_1 - a_{r1}v_{r1}r_1^2 = 0. \tag{5.39}$$

Note that according to the last two relations of (5.39), the angle γ between the thrust and velocity vectors, and the derivative $\dot{\gamma}$ must vanish at the end of the flight /5.11/.

The complete system of differential equations and boundary conditions which defines the optimum zero energy build-up maneuver consists of (5.13), (A.55), and (5.39). We shall study below the case of a circular
180 initial orbit, for which the entire system can be written in the form (cf. (5.22))

$$\left.\begin{aligned}
&\dot{r} = v_r, && r(0) = 1, \quad {}^1/_2[v_r^2(T) + v_\varphi^2(T)] - 1/r(T) = 0,\\
&\dot{v}_r = a_r\frac{v_\varphi^2}{r} - \frac{1}{r^2}, && v_r(0) = 0, \quad \frac{a_r(T)}{a_\varphi(T)} - \frac{v_r(T)}{v_\varphi(T)} = 0,\\
&\dot{v}_\varphi = a_\varphi - \frac{v_r v_\varphi}{r}, && v_\varphi(0) = 1,\\
& && a_r(T) - 2a_\varphi(T)v_r(T)r(T) - \dot{a}_r(T)v_r(T)r^2(T) = 0,\\
&\ddot{a}_r = \frac{a_\varphi}{r} - 3\frac{a_r v_\varphi^2}{r^2} + 2\frac{a_r}{r^3},\\
&\dot{a}_\varphi = \frac{1}{r}(a_\varphi v_r - 2a_r v_\varphi).
\end{aligned}\right\} \tag{5.40}$$

The other characteristics of the motion, such as the angular displacement φ and the value of the control functional J, are determined after the boundary-value problem (5.40) has been solved, by integrating the corresponding differential equations

$$\dot{\varphi} = v_\varphi(t)/r(t),\ \varphi(0) = 0;\ J = a_r^2(t) + a_\varphi^2(t),\ J(0) = 0. \tag{5.41}$$

The optimum acceleration equations are represented in the form (5.22), since the initial point of the trajectory is singular, $v_r(0) = 0$. Away from the singular point it is possible to replace the equation for $\ddot{a}_r$ in (5.40) with a first-order equation having a first integral λ (cf. (5.14)). The latter is determined from the condition

$$\lambda = {}^1/_2\,[a_r^2(0) + a_\varphi^2(0)]. \tag{5.42}$$

Note that the trajectory of the acceleration period may have more than one singular point, since the motion at low accelerations a is quasi-periodical, and the singular point may appear during each circuit.

The boundary-value (5.40) can be solved by reducing it to the Cauchy problem with the selection of the three missing initial values a_{r0}, $a_{\varphi 0}$, $\dot{a}_{r0}$ /5.4, 5.5, 5.11, 5.12/. Another procedure consists in applying direct methods to the minimization of the functional (5.9) with the boundary conditions (A.55), (5.39), /5.19/.

Problem (5.40) contains the single parameter T. The trajectories and the control functions of problem (5.40) are recalculated for initial circular orbits of arbitrary radius and different planets by the criteria of similitude (5.15). The required characteristic values for Venus, Earth, Mars, and
181 the Moon are given in Table 5.1. Four values are given for each parameter, corresponding to circular orbits at altitudes of 200, 250, 300, and 350 km.

TABLE 5.1. Characteristic values of parameters in planetocentric (Venus, Earth, Mars) and selenocentric reference frames for circular orbits at altitudes of 200, 250, 300, and 350 km

Planet	r_*, km	t_*, sec	v_*, m/sec	g_*, m/sec^2	J_*, v_*, m^2/sec^3	λ_*, m^2/sec^4
Venus	$6.361\cdot10^3$	879	$7.238\cdot10^3$	8.236	$5.962\cdot10^4$	67.84
	$6.411\cdot10^3$	889	$7.210\cdot10^3$	8.108	$5.846\cdot10^4$	65.75
	$6.461\cdot10^3$	900	$7.182\cdot10^3$	7.983	$5.734\cdot10^4$	63.74
	$6.511\cdot10^3$	910	$7.154\cdot10^3$	7.861	$5.624\cdot10^4$	61.80
Earth	$6.571\cdot10^3$	844	$7.783\cdot10^3$	9.219	$7.175\cdot10^4$	84.99
	$6.621\cdot10^3$	854	$7.754\cdot10^3$	9.080	$7.040\cdot10^4$	82.45
	$6.671\cdot10^3$	864	$7.725\cdot10^3$	8.944	$6.909\cdot10^4$	80.00
	$6.721\cdot10^3$	873	$7.696\cdot10^3$	8.812	$6.781\cdot10^4$	77.65
Mars	$3.532\cdot10^3$	1030	$3.427\cdot10^3$	3.326	$1.140\cdot10^4$	11.06
	$3.582\cdot10^3$	1052	$3.403\cdot10^3$	3.234	$1.101\cdot10^4$	10.46
	$3.632\cdot10^3$	1075	$3.380\cdot10^3$	3.145	$1.063\cdot10^4$	9.89
	$3.682\cdot10^3$	1097	$3.357\cdot10^3$	3.061	$1.027\cdot10^4$	9.37
Moon	$1.938\cdot10^3$	1239	$1.564\cdot10^3$	1.262	$0.197\cdot10^4$	1.59
	$1.988\cdot10^3$	1288	$1.544\cdot10^3$	1.199	$0.185\cdot10^4$	1.44
	$2.038\cdot10^3$	1336	$1.525\cdot10^3$	1.141	$0.174\cdot10^4$	1.30
	$2.088\cdot10^3$	1386	$1.507\cdot10^3$	1.087	$0.164\cdot10^4$	1.18

In view of the reversibility property of the optimum trajectories (5.16), all the results obtained in the problem of zero energy build-up can also be used in the deceleration problem. In accordance with the boundary conditions of the zero energy build-up maneuver, it is necessary to note here that at the beginning only the condition of zero energy is specified (the radius and velocity are not fixed separately), while at the end only the condition of transfer to a circular orbit of specified radius is given (the angular displacement is not fixed).

2. **Numerical results for zero energy build-up.** The numerical solution of problem (5.40) shows that for large values of the time, $T \geqslant 10^2$, (small acceleration values, $a \leqslant 10^{-2}$) the escape trajectory from a circular orbit represents a shallow unwinding spiral (Figure 5.4).

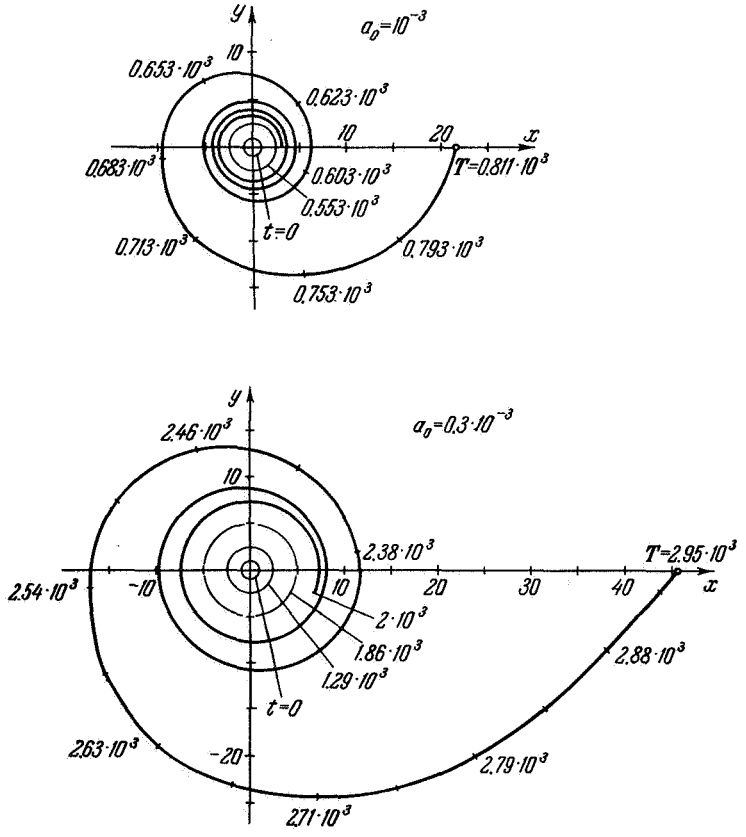

FIGURE 5.4. Examples of optimum trajectories of zero energy build-up at takeoff from a circular orbit (the first circuits of the spiral are not drawn to scale; the markings along the trajectory are in time units; all parameters are dimensionless).

The direction of the acceleration forms a small angle with the direction of the velocity (included between the tangent and the transversal), coinciding with the latter at the final stage of the motion (cf. the second condition

of (5.39)). The modulus of the thrust acceleration varies slightly along
182 the trajectory, increasing in the final section by 10 to 20%. The variation of the thrust-acceleration components with time is illustrated by Figure 5.5 from /5.19/, together with the corresponding functions $r(t)$ and $v_\varphi(t)\, r(t)$. Table 5.2 compares the parameters of three trajectories of zero energy build-up /5.19/ (all parameters are dimensionless). The time of motion, $T = 100$, is the same for all trajectories. The first column of the table shows results of the calculation for the optimum escape trajectory from
183 an initial circular orbit, and the second is for escape from an elliptic orbit with eccentricity $\varepsilon_0 = 0.1$. The third column gives parameters of a trajectory with constant transverse acceleration at takeoff from a circular orbit.

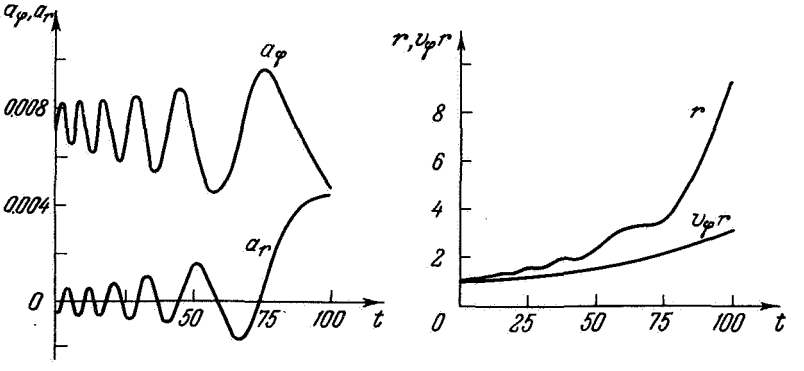

FIGURE 5.5. Optimum control function of the transverse, a_φ, and radial, a_r, components of thrust acceleration, radius r, and momentum $v_\varphi r$ for the zero energy build-up maneuver (circular initial orbit, time of maneuver $T = 100$, dimensionless parameters).

TABLE 5.2. Comparison of trajectories of zero energy build-up from circular and elliptic orbits for optimum program of thrust acceleration and for a constant transverse acceleration

Trajectory parameters	$\varepsilon_0 = 0$, $a_r(t) = \text{opt}$, $a_\varphi(t) = \text{opt}$	$\varepsilon_0 = 0.1$, $a_r(t) = \text{opt}$, $a_\varphi(t) = \text{opt}$	$\varepsilon_0 = 0$, $a_r(t) \equiv 0$, $a_\varphi(t) \equiv \text{const}$
a_{r0}	$-0.2257 \cdot 10^{-3}$	$-0.3068 \cdot 10^{-3}$	0
$a_{\varphi 0}$	$0.6465 \cdot 10^{-2}$	$0.6891 \cdot 10^{-2}$	$0.7755 \cdot 10^{-2}$
a_{r1}	$0.4627 \cdot 10^{-2}$	$0.4481 \cdot 10^{-2}$	0
$a_{\varphi 1}$	$0.4521 \cdot 10^{-2}$	$0.4576 \cdot 10^{-2}$	$0.7755 \cdot 10^{-2}$
r_1	9.139	9.489	9.660
J	$0.5531 \cdot 10^{-2}$	$0.5620 \cdot 10^{-2}$	$0.6014 \cdot 10^{-2}$

The dependence of the functional J on time T of zero energy build-up from a circular initial orbit is shown in Figure 5.6 /5.4/. Figure 5.7 depicts the gain in the functional resulting from the programing of the thrust-acceleration vector /5.4, 5.5, 5.11, 5.12, 5.26/. It is seen that
184 the difference between the optimum program of thrust acceleration and a tangential acceleration of constant magnitude is small and decreases with an increase in maneuvering time.

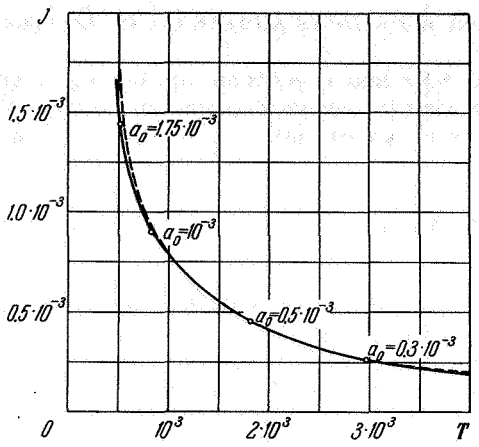

FIGURE 5.6. Functional J of the dynamic problem for zero energy build-up maneuver (solid curve) as a function of the time of motion T (circular initial orbit, dashed curve corresponds to build-up maneuver of velocity $u_1 = 0.895$ in gravitation-free field, dimensionless parameters).

The optimum law $a(t)$, as well as the relationship $J(T)$ for the zero energy build-up maneuver in a central field, resemble those for the velocity build-up maneuver in a gravitation-free field (cf. (5.32) and Figure 5.6). Thus, the latter is considered as a maneuver representing the zero energy build-up in a central field.

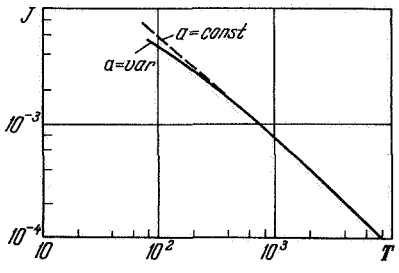

FIGURE 5.7. Comparison, using the functional J, of the optimum program of thrust acceleration (solid curve) and of a tangential acceleration of constant magnitude (dashed line) for zero energy build-up maneuver from a circular orbit (dimensionless parameters).

Neglecting the influence of the third body — the Sun — on the functional J leads, in the case considered (near the Earth), to a relative error smaller than 10^{-3}, as shown by calculations performed in /5.4/.

3. **Analytic solution for zero energy build-up.** We turn to the analytic representation of the results obtained. When the thrust acceleration is much smaller than the gravitational acceleration ($a \lesssim 10^{-2}$), the trajectory during the acceleration period is initially a shallow spiral, on which the gravitational and centrifugal accelerations are approximately equal: $1/r^2 \approx v_\varphi^2/r$. We shall find the optimum formula $a(t)$ for the initial section of the escape trajectory under the assumption that the latter condition is fulfilled exactly.

The equations of motion and the initial conditions at takeoff from a circular orbit are

$$\left.\begin{aligned} \dot r &= v_r, & r(0) &= 1, \\ \dot v_r &= a_r, & v_r(0) &= 0, \\ \dot v_\varphi &= a_\varphi - v_r v_\varphi / r, & v_\varphi(0) &= 1 \end{aligned}\right\} \qquad (5.43)$$

(where the condition $v_\varphi^2/r = 1/r^2$ is allowed for in the equations of motion (A.8)).

Eliminating $v_\varphi = 1/\sqrt{r}$ and $v_r = \dot{r}$ from the last equation of (5.43), we obtain $^1/_2 \dot{r} r^{-3/2} = a_\varphi$. Integrating this equation, we can express the radius r and the velocity components v_φ, v_r with the aid of (5.43) as a function of the time integral of a_φ:

$$r = \left(1 - \int_0^t a_\varphi\, dt\right)^{-2}, \quad v_r = 2a_\varphi \left(1 - \int_0^t a_\varphi dt\right)^{-3}, \quad v_\varphi = 1 - \int_0^t a_\varphi\, dt. \tag{5.44}$$

The initial conditions (5.43) are satisfied for r and v_φ from (5.44), but not for v_r. For low values of the transverse acceleration $a_{\varphi 0} \ll 1$, however, the radial velocity is likewise small at the beginning $v_{r0} = 2a_{\varphi 0} \ll 1$, so that finally this disturbance of the initial conditions has only a small effect on the result.

The characteristic time of the problem, according to (5.44), is of the order of $1/a_\varphi$. Therefore when the time derivative is taken, the order of smallness relative to a_φ increases by about one. Thus, at the beginning of the motion, v_r is of the order of a_φ, and $a_r = \dot{v}_r$ is of the order of a_φ^2.

The kinematic characteristics r, v_r, v_φ are determined by the magnitude of the integral in (5.44). Therefore the problem of optimum transition from a fixed initial position to a fixed final position (for instance, $E(T) = {}^1/_2 (v_{r1}^2 + v_{\varphi 1}^2) - 1/r_1 = E_1$) during a specified time is formulated as the problem of minimizing

$$J = \int_0^T a^2\, dt \approx \int_0^T a_\varphi^2\, dt \tag{5.45}$$

for a given $\int_0^T a_\varphi dt$.

186 Performing the usual procedure of variational analysis, we may obtain the optimum program for the projection of the acceleration a_φ. This is

$$a_\varphi(t) \equiv \text{const}, \tag{5.46}$$

where

$$a_r(t) = 6a_\varphi^2 (1 - a_\varphi t)^{-4}. \tag{5.47}$$

This result was obtained for the case $a_r \ll a_\varphi$. In the neighborhood of the escape point ($E_1 = 0$) this inequality does not hold, since a_r reaches the order of a_φ (as can be seen by substituting in (5.47) the value of the escape time, found from the condition $E(T) = 0$, using (5.44)). Therefore, the optimum law (5.46) is correct only on the initial section of the trajectory of zero energy build-up. Methods of solving the problem, which are different from the one described here, have been obtained in /5.11, 5.22 – 5.24, 5.37/.

4. Orbital transfer. The maneuver begins at a fixed point on the orbit of one planet and ends at a fixed point on the orbit of the second. The velocity vectors at the beginning and end of the motion coincide with the corresponding orbital velocities; the time of motion is specified (cf. (A.56)).

The optimum transfer between coplanar orbits (we are mainly concerned here with this type of orbit) is described by the differential equations (5.13) with the boundary conditions (A. 56)

$$\left.\begin{aligned}
&\dot{r} = v_r, && r(0) = 1, && r(T) = r_1,\\
&\dot{\varphi} = \frac{v_\varphi}{r}, && \varphi(0) = \varphi_0, && \varphi(T) = \varphi_1,\\
&\dot{v}_r = a_r + \frac{v_\varphi^2}{r} - \frac{1}{r^2}, && v_r(0) = v_{r0}, && v_r(T) = v_{r1},\\
&\dot{v}_\varphi = a_\varphi - \frac{v_r v_\varphi}{r}, && v_\varphi(0) = v_{\varphi 0}, && v_\varphi(T) = v_{\varphi 1},\\
&\dot{a}_r = \frac{1}{v_r}\left[\frac{1}{2}(a_r^2 + a_\varphi^2) + a_r\left(\frac{v_\varphi^2}{r} - \frac{1}{r^2}\right) - \lambda - \nu\frac{v_\varphi}{r}\right],\\
&\dot{a}_\varphi = \frac{1}{r}(a_\varphi v_r - 2a_r v_\varphi + \nu).
\end{aligned}\right\} \qquad (5.48)$$

The system of differential equations (5.48) is of the sixth order and contains two arbitrary constants λ and ν, i.e., the number of degrees of freedom in the equations is equal to the number of boundary conditions.

For singular points, $v_r = 0$, on the transfer trajectory (such as the initial and final points of a trajectory connecting circular orbits, cf. (A. 58)), the equation for $\dot{a}_r$ in (5.48) is replaced by a second-order equation from (5.22). The procedure of mutual transformations (5.48) $\leftrightarrow$ (5.22) is similar to the one described in § 2.1.

187 In the case of circular orbits, the parameters of the problem are r_1, a_0, and ν. For a fixed r_1, there corresponds, to each pair (a_0, ν) a pair (T, φ_1) (or several pairs (T, φ_1), if the problem has more than one solution). Orbital transfers can be classified either according to the parameters a_0, ν, or the parameters T, φ_1. The first method of classification is convenient when the boundary-value problem is solved by reducing it to the Cauchy problem, and the second is used when the functional extrema are found by direct methods /5.18, 5.20, 5.21/.

If the actual motion of the planets is taken into account in the calculations, one uses as parameters either the date of departure t_0 and the flight duration time T, or the departure date t_0 and the arrival date t_1. The transformation $t_0, t_1 \leftrightarrow t_0, T$ is the very simple one $T = t_1 - t_0$, $t_0 = t_0$. The relationship between the parameters t_0, t_1 and T, φ_1 is determined from tables in the ephemerides of the planets, assuming the angular displacements of the vehicle and the destination planet at arrival time are equal. If the planets are assumed to move uniformly along average circular orbits, and the departure and arrival dates t_0 and t_1 are reckoned from the time of opposition of the planets, we can write the formulas for the transformation $t_0, t_1 \leftrightarrow T, \varphi_1$ in the form

$$\begin{aligned}
T &= t_1 - t_0,\\
\varphi_1 &= \omega_1 t_1 - \omega_2 t_0 \pm 2\pi s \quad (s = 0, 1, 2, \ldots),
\end{aligned} \qquad (5.49)$$

where ω_1 and ω_2 are the average angular velocities of motion of the departure and destination planets; s is a positive integer (the number of additional revolutions of the planet of larger angular velocity), the positive sign representing transfer to an external orbit, and the negative sign transfer to an inner one.

Note that the transfer from orbit 1 to orbit 2 can be converted to the inverse transfer (the mirror image) by formulas (5.16). The transformation from the dimensionless variables used in the text is performed as usual. The characteristic magnitudes used for the average circular orbits of Venus, Earth, and Mars are given in Table 5.3.

TABLE 5.3. Characteristic magnitudes in the heliocentric coordinate system for average circular orbits of Venus, Earth, and Mars

Planet	r_*, km	t_*, days	v_*, km/sec	g_*, m/sec^2	J_*, v_*, m^2/sec^3	λ_*, m^2/sec^4
Venus	$108.1 \cdot 10^6$	35.7	35.01	$1.141 \cdot 10^{-2}$	399.6	$1.303 \cdot 10^{-4}$
Earth	$149.5 \cdot 10^6$	58.1	29.76	$0.597 \cdot 10^{-2}$	177.6	$0.356 \cdot 10^{-4}$
Mars	$227.8 \cdot 10^6$	109.3	24.11	$0.257 \cdot 10^{-2}$	61.9	$0.066 \cdot 10^{-4}$

188 **5. Solution of the boundary-value problem (5.48) by the method of the "transport" trajectory.** The boundary-value problem (5.48) for optimum orbital transfer was solved either by selecting the missing initial conditions in the equivalent Cauchy problem /5.4, 5.5, 5.12—5.17/, or by the method of the "transport" trajectory /5.1, 5.25/.

In the second method, a Keplerian trajectory passing through specified points of orbits 1 and 2 is selected. It is assumed that the motion to be determined differs only slightly from the Keplerian motion, so that the equations of the variational problem can be linearized in this neighborhood. A boundary-value problem is set up for the system of linear differential equations.

Let $x^{(0)}(t)$, $y^{(0)}(t)$ be a plane Keplerian trajectory (called transport trajectory) which passes through the specified coordinates $\mathbf{r}_0$ and $\mathbf{r}_1$ at the beginning and end of the motion. We choose the z-axis normal to the plane of the transport trajectory, and represent the true trajectory in the form

$$x = x^{(0)} + \xi, \quad y = y^{(0)} + \eta, \quad z = \zeta. \tag{5.50}$$

Assuming the functions ξ, η, ζ to be small, we linearize equations (A.1)

$$\left.\begin{aligned} \ddot{\xi} &= \left(\frac{\partial^2 U}{\partial x^2}\right)^{(0)} \xi + \left(\frac{\partial^2 U}{\partial x \partial y}\right)^{(0)} \eta + a_x, \\ \ddot{\eta} &= \left(\frac{\partial^2 U}{\partial x \partial y}\right)^{(0)} \xi + \left(\frac{\partial^2 U}{\partial y^2}\right)^{(0)} \eta + a_y, \\ \ddot{\zeta} &= -\left[(x^{(0)})^2 + (y^{(0)})^2\right]^{-3/2} \zeta + a_z, \end{aligned}\right\} \tag{5.51}$$

where $U = -1/r$ is the field potential $X = \partial U/\partial x$, $Y = \partial U/\partial y$, $Z = \partial U/\partial z$ ($r = \sqrt{x^2 + y^2 + z^2}$).

The second derivatives $(\partial^2 U/\partial x^2)^{(0)}$, $(\partial^2 U/\partial x\, \partial y)^{(0)}$, $(\partial^2 U/\partial y^2)^{(0)}$ are functions of time calculated along the known transport trajectory $x^{(0)}(t)$, $y^{(0)}(t)$. We represent the Keplerian trajectory in terms of the osculating element, where p is the focal parameter, ε the eccentricity, ω the longitude of perigee,

and ϑ the true anomaly (cf. Appendix); the coefficients in the linear equations (5.51) will then have the form

$$\left.\begin{aligned}(\partial^2 U/\partial x^2)^{(0)} &= -(r^{(0)})^{-3}(1-3\cos^2 u),\\ (\partial^2 U/\partial x\,\partial y)^{(0)} &= (r^{(0)})^{-3}\,3\sin u\cos u,\\ (\partial^2 U/\partial y^2)^{(0)} &= -(r^{(0)})^{-3}(1-3\sin^2 u),\\ (r^{(0)} = p^{(0)}/(1+\varepsilon^{(0)}\cos\vartheta),\ u &= \vartheta+\omega^{(0)}).\end{aligned}\right\} \tag{5.52}$$

The formulation of the variational problem is preserved under the transformation to the transport coordinate system; as before, it is necessary to
189 find the minimum of the initial functional

$$J=\int_0^T (a_x^2+a_y^2+a_z^2)\,dt. \tag{5.53}$$

This is due to the fact that we selected as transport trajectory the Keplerian trajectory, i.e., the trajectory of passive motion. Therefore in equations (5.51) we have the total value of the acceleration, rather than contributions to the thrust acceleration.

The boundary conditions for equations (5.51) are

$$\left.\begin{aligned}&\xi(0)=\eta(0)=\zeta(0)=\xi(T)=\eta(T)=\zeta(T)=0,\\ &\dot\xi(0)=u_0-\dot x_0^{(0)},\quad \dot\eta(0)=v_0-\dot y_0^{(0)},\quad \dot\zeta(0)=w_0,\\ &\dot\xi(T)=u_1-\dot x_1^{(0)},\quad \dot\eta(T)=v_1-\dot y_1^{(0)},\quad \dot\zeta(T)=w_1,\end{aligned}\right\} \tag{5.54}$$

where u_0, v_0, w_0, u_1, v_1, w_1 are given (components of the orbital velocities of the planets), and $\dot x_0^{(0)}$, $\dot y_0^{(0)}$, $\dot x_1^{(0)}$, $\dot y_1^{(0)}$ are calculated at the beginning and end of the transport trajectory.

Thus, in the transport coordinate system the motion starts from the zero point with a given velocity vector, and after a fixed time interval it ends at the same point with a different given velocity vector. The initial and final velocity vectors are equal to the differences between the orbital velocities of the departure and destination planets and the velocities at the beginning and end of the transport ellipse.

If the thrust acceleration is much higher than the gravitational acceleration, equations (5.51) can be simplified (first approximation) to

$$\ddot\xi=a_x,\quad \ddot\eta=a_y,\quad \ddot\zeta=a_z. \tag{5.55}$$

These equations coincide with the equations of motion in a gravitation-free field (A.53). The general solution of the equations of the variational problem (5.53), (5.55) is given by (5.30). The integration constants are determined from (5.31), in which, according to the boundary conditions (5.54), it is necessary to write $\mathbf{r}_0=\mathbf{r}_1=0$, $\mathbf{v}_0=(\dot\xi(0),\ \dot\eta(0),\ \dot\zeta(0))$, $\mathbf{v}_1=(\dot\xi(T),\ \dot\eta(T),\ \dot\zeta(T))$. In vector form, where $\rho=(\xi,\eta,\zeta)$, this solution is written as

$$\left.\begin{aligned}\mathbf{a}(t) &= 6(\dot\rho_0+\dot\rho_1)\frac{t}{T^2}-(2\dot\rho_0+\dot\rho_1)\frac{2}{T},\\ \rho(t) &= (\dot\rho_0+\dot\rho_1)\frac{t^3}{T^2}-(2\dot\rho_0+\dot\rho_1)\frac{t^2}{T}+\dot\rho_0 t,\\ J &= \frac{4}{T}\,[\dot\rho_0^2-(\dot\rho_0\cdot\dot\rho_1)+\dot\rho_1^2].\end{aligned}\right\} \tag{5.56}$$

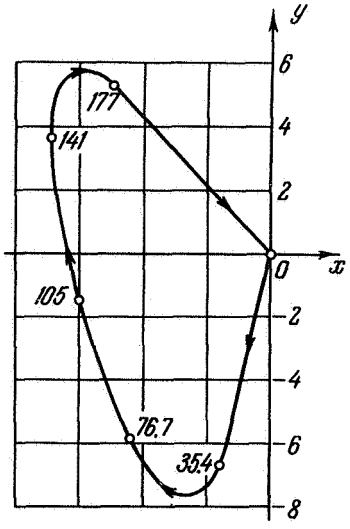

FIGURE 5.8. Shape of optimum trajectory of Earth—Mars orbital transfer in transport coordinate system (arrows show direction of motion, dots give time spread in days, total time $T = 212$ days).

Figure 5.8 shows an ideal orbital transfer trajectory in the transport coordinate system /5.1/. The calculation was performed using (5.56) for the Earth—Mars orbital transfer. The departure date was 27 September 1960 and the time of flight 212 days. The orbits of Earth and Mars were assumed to be coplanar ($\zeta \equiv 0$). The boundary conditions (5.54) are in this case $\xi(0) = \eta(0) = \xi(T) = \eta(T) = 0$, $\dot{\xi}(0) = -0.0145$, $\dot{\eta}(0) = -0.1283$, $\dot{\xi}(T) = 0.0769$, $\dot{\eta}(T) = -0.1099$. (The velocities are expressed as fractions of the orbital velocity of Earth at departure time.) It is seen from the figure that the maximum deviation of the trajectory from the beginning of the transport coordinate system (~8 million km) is small compared with the radius of the Earth's orbit (150 million km).

In more accurate calculations one must take into account, in addition to the thrust acceleration, the linear terms of the gravitational acceleration of the Sun (second approximation), caused by the displacement of the moving point away from the origin of the transport coordinate system (5.51).

The Euler equations for the extrema of functional (5.53), written in accordance with the general formulas (5.5), are, in this case, given by

$$\left.\begin{aligned} \ddot{a}_x &= \left(\frac{\partial^2 U}{\partial x^2}\right)^{(0)} a_x + \left(\frac{\partial^2 U}{\partial x \partial y}\right)^{(0)} a_y, \quad \ddot{a}_y = \left(\frac{\partial^2 U}{\partial x \partial y}\right)^{(0)} a_x + \left(\frac{\partial^2 U}{\partial y^2}\right) a_y, \\ \ddot{a}_z &= -\left[(x^{(0)})^2 + (y^{(0)})^2\right]^{-3/2} a_z. \end{aligned}\right\} \qquad (5.57)$$

The derived system of linear differential equations, (5.51) and (5.57) with coefficients given by (5.52), is integrated by quadratures (cf /5.1/).

The accuracy of the first and second approximations is illustrated by Table 5.4, in which some parameters of the optimum trajectories of Earth—Mars and Earth—Venus orbital transfers are given (taken from /5.1/). The first and second columns show the duration and angular range of the flight; these are followed by the values of the functional of the dynamic problem, J, and the initial, a_0, and final, a_1, values of the thrust acceleration. Three values are given for each of the last three parameters listed. These are obtained from the first and second approximation and by numerical integration of the exact equations respectively.

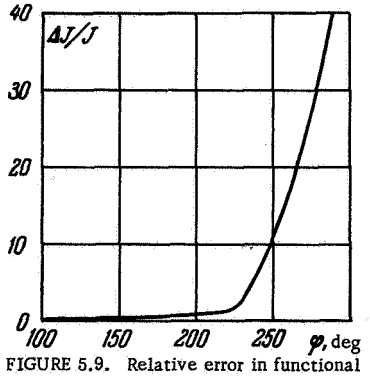

FIGURE 5.9. Relative error in functional for second approximation of the transport trajectory method, vs. angular range of flight (Earth—Mars and Earth—Venus orbital transfers).

It is seen from the table that the method proposed is highly accurate. Its accuracy

TABLE 5.4. Accuracy of the transport trajectory method when calculating optimum transfers between orbits of planets (error relative to exact solution given in parentheses)

Flight	T, days	φ_1, deg	J, m^2/sec^3			a_0, mm/sec^2			a_1, mm/sec^2		
			first approximation	second approximation	third approximation	first approximation	second approximation	third approximation	first approximation	second approximation	third approximation
Earth—Mars	130	89.06	60.88 (14.5 %)	71.29 (0.13 %)	71.20	3.80 (19.3 %)	4.64 (1.5 %)	4.71	4.08 (8.9 %)	4.54 (1.3 %)	4.48
	212	147.38	9.33 (19.2 %)	11.53 (0.09 %)	11.54	1.21 (20.4 %)	1.51 (0.66 %)	1.52	1.22 (14.7 %)	1.44 (0.7 %)	1.43
	330	222.65	3.60 (12.5 %)	3.23 (0.94 %)	3.20	0.61 (30.4 %)	0.89 (1.1 %)	0.88	0.62 (47.6 %)	0.40 (4.8 %)	0.42
Earth—Venus	121	136.35	19.03 (27.8 %)	26.44 (0.04 %)	26.43	2.09 (13.6 %)	1.85 (0.54 %)	1.84	2.51 (38.5 %)	4.02 (1.5 %)	4.08
	220	234.79	12.65 (11.2 %)	11.98 (5.3 %)	11.38	1.5 (30.4 %)	1.26 (9.6 %)	1.15	1.29 (42.4 %)	2.25 (0.45 %)	2.24
	240	255.05	15.45 (65.8 %)	10.39 (11.5 %)	9.32	1.58 (51,9 %)	1.19 (14.4 %)	1.04	1.37 (29.7 %)	2.01 (3.1 %)	1.95

increases with a decrease in flight time, since this leads to an increase in the thrust-acceleration level, and the optimum trajectory approaches the momentum transfer trajectory (which is taken as the transport trajectory). With increasing angular range the accuracy of the method drops (cf. Figure 5.9 from /5.1/); an increase in the radial displacements has the same effect. It is suggested in /5.1/ that in the case of large angular ranges the accuracy of the method can be improved by constructing the transport trajectory from several ellipses instead of only one.

6. Numerical results of the boundary-value problem (5.48). Figures 5.10 to 5.13 give examples of transfers between the coplanar circular orbits $r_0 = 1$ and $r_1 = 1.52$ (Earth orbit — average Mars orbit, Figures 5.10 to 5.12), and $r_0 = 1$ and $r_1 = 1.38$ (average Venus orbit — Earth orbit, Figure 5.13) /5.4/. Each of the figures shows the trajectory $y(x)$, the control function of the thrust-acceleration magnitude $a(t)$, and the hodograph $a_y(a_x)$. On both the trajectory and the hodograph the time is marked in increments of $\Delta t = 0.2$. The captions of the figures give the integral characteristics of the flight, as well as the initial values a_{r0}, arctg $(a_{r0}/a_{\varphi 0})$ necessary for solving the Cauchy problem. All parameters are dimensionless.

For large values of the parameter a_0 (Figure 5.10) the function $a(t)$ and the hodograph $a_y(a_x)$ resemble the corresponding relationships for two-dimensional motion in a gravitation-free field (cf. (5.30)), namely,

$$a_x = b_{1x}t + b_{2x}, \quad a_y = b_{1y}t + b_{2y}. \tag{5.58}$$

In fact, the larger the thrust acceleration, the smaller the effect of the gravitational terms in the equations of motion, and the better the

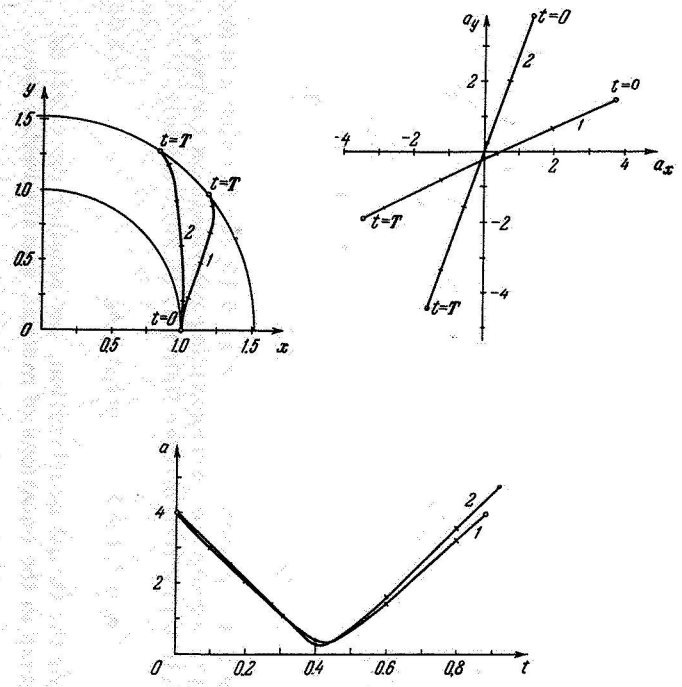

FIGURE 5.10. Optimum Earth—Mars flights with thrust acceleration higher than gravitational acceleration (dimensionless parameters).

Curves 1

$r_1 = 1.52,\ a_0 = 4,\ v = 0,$
$T = 0.880,\ \varphi_1 = 0.664,\ J = 4.561,$
$a_{r0} = -7.950,\ \text{arctg}\ (a_{r0}/a_{\varphi 0}) = 1.205.$

Curves 2

$r_1 = 1.52,\quad a_0 = 4,\ v = -7,$
$T = 0.920,\ \varphi_1 = 0.988,\ J = 5.920,$
$a_{r0} = -0.100,\ \text{arctg}\ (a_{r0}/a_{\varphi 0}) = 0.350.$

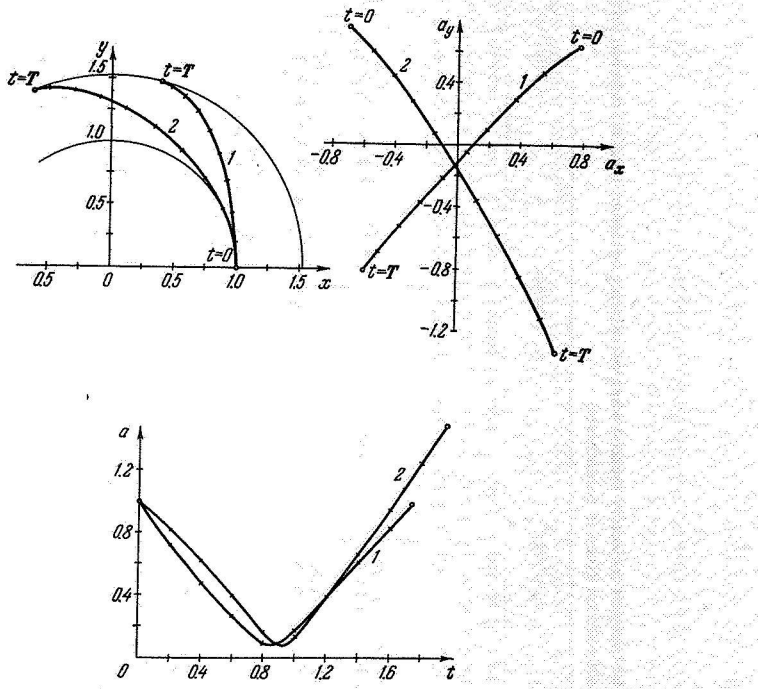

FIGURE 5.11. Optimum Earth—Mars flights with thrust acceleration of the same order as gravitational acceleration (dimensionless parameters).

Curves 1

$r_1 = 1.52,\ a_0 = 1,\ v = 0,$
$T = 1.741,\ \varphi_1 = 1.312,\ J = 0.538,$
$a_{r0} = -0.670,\ \text{arctg}\ (a_{r0}/a_{\varphi 0}) = 0.898.$

Curves 2

$r_1 = 1.52,\ a_0 = 1,\ v = -1.3,$
$T = 1.947,\ \varphi_1 = 1.973,\ J = 1.053,$
$a_{r0} = 1.326,\ \text{arctg}\ (a_{r0}/a_{\varphi 0}) = -0.604$

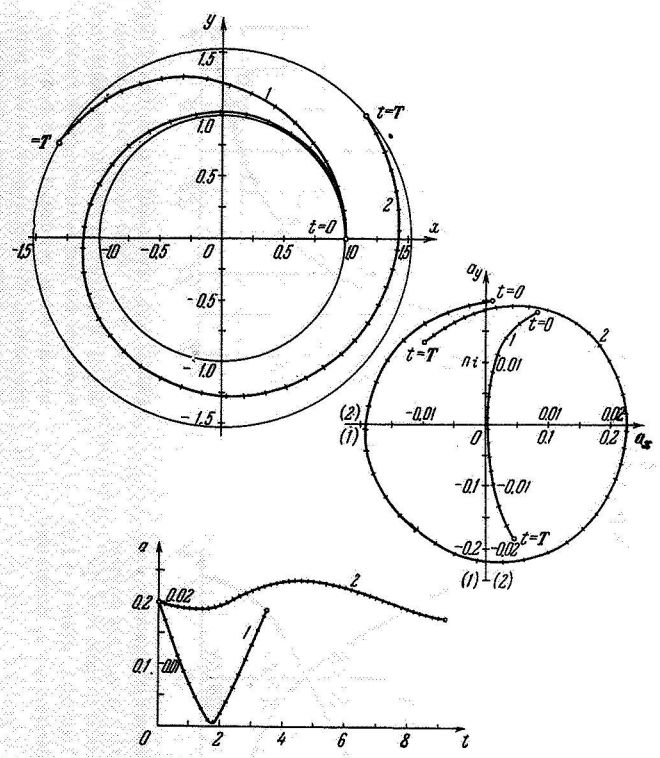

FIGURE 5.12. Optimum Earth—Mars flights with thrust acceleration lower than gravitational acceleration (dimensionless parameters).

Curves 1: $r_1 = 1.52$, $a_0 = 0.2$, $v = 0$, $T = 3.478$, $\varphi_1 = 2.636$, $J = 0.037$, $\dot{a}_r = 0.015$, arctg $(a_{r0}/a_{\varphi 0}) = 0.420$.
Curves 2: $r_1 = 1.52$, $a_0 = 0.02$, $v = 0$, $T = 9.183$, $\varphi_1 = 6.987$, $J = 0.004$, $\dot{a}_{r0} = 0.001$, arctg $(a_{r0}/a_{\varphi 0}) = 0.044$.

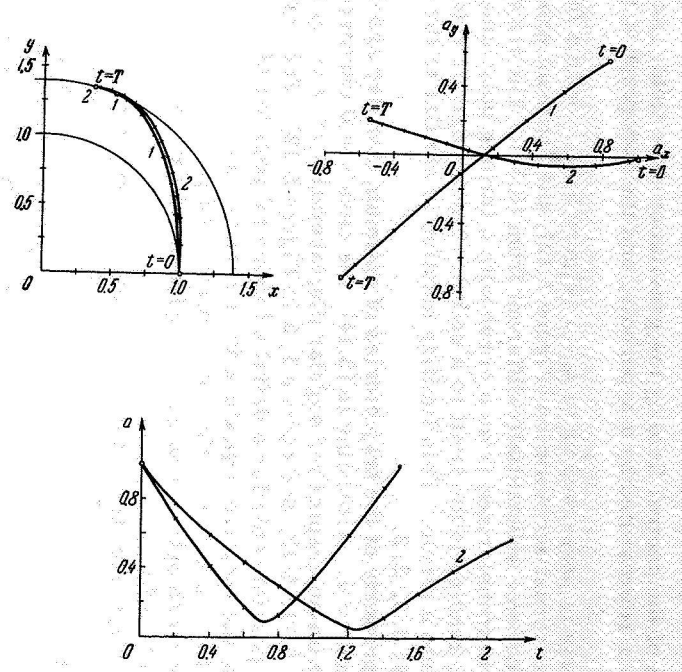

FIGURE 5.13. Examples of optimum Venus—Earth flights (dimensionless parameters).

Curves 1: $r_1 = 1.38$, $a_0 = 1$, $v = 0$, $T = 1.492$, $\varphi_1 = 1.196$, $J = 0.465$, $\dot{a}_{r0} = -0.908$, arctg $(a_{r0}/a_{\varphi 0}) = 0.980$.
Curves 2: $r_1 = 1.38$, $a_0 = 1$, $v = 0.82$, $T = 2.140$, $\varphi_1 = 1.298$, $J = 0.446$, $\dot{a}r0 = -1.372$, arctg $(a_{r0}/a_{\varphi 0}) = 1.588$.

197 approximation of the central field by the gravitation-free field. According to (5.58), $a(t)$ is represented by a hyperbola, and the hodograph $a_y(a_x)$ by a straight line.

This property is preserved up to $a_0 \sim 1$ (Figure 5.11). With a further decrease of the thrust acceleration (Figure 5.12), the optimum programs $a(t)$ and $a_y(a_x)$ become substantially different from (5.58). The trajectory of the motion is transformed from a curve with a turning point into a smooth curve, tending in the limit to a spiral. The hodograph $a_y(a_x)$ is transformed into a circle. This limiting solution is similar to the one described in §§ 2.2, 2.3.

We note a property of the trajectories of optimum transfer associated with the parameter ν. According to (5.14), the case $\nu = 0$ corresponds to a transfer with an unspecified angular displacement (cf. curves 1 in Figures 5.10, 5.11, 5.13, and curves 1, 2 in Figure 5.12). Such orbital transfers are possible only for a definite (optimum) position of the planets in their orbits; the optimum departure dates recur at intervals equal to the synodic period. In addition to the above-mentioned paper /5.4/, data on orbital transfer with optimum angular displacement can be found in /5.1, 5.5, 5.12—5.17, 5.25/.

At $\nu = 0$ and $r_1 = 1.52$ the ratio φ_1/T (the average angular velocity) is approximately equal to 0.75—0.76 for all a_0 in the range studied ($0.02 \leqslant a_0 \leqslant 4$). With a decrease of the parameter ν the average angular velocity increases (Figure 5.14), and the trajectory enters the orbit closer to the center (cf. trajectories 2 in Figures 5.10, 5.11); with an increase of ν the average angular velocity decreases and the trajectory escapes beyond the external orbit (cf. trajectory 2 in Figure 5.13).

Let us now examine the dependence of the functional J on the flight parameters. For flights with an optimum angular displacement ($\nu = 0$) the dependence of the functional J on the time T in the range of practical interest is similar to relationship (5.33) for the displacement maneuver

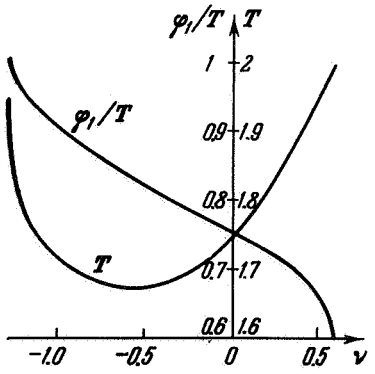

FIGURE 5.14. Influence of parameter ν on average angular velocity φ_1/T and duration T of an orbital transfer (transfer from the Earth orbit to the Mars orbit, where $r_1 = 1.52$, initial thrust acceleration $a_0 = 1$, dimensionless parameters).

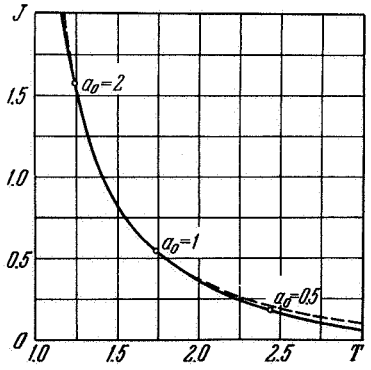

FIGURE 5.15. Functional J as function of flight duration T for orbital transfers with optimum angular displacement ($\nu = 0$). The solid curve represents the Earth—Mars flight for circular coplanar orbits; the dashed curve shows, for comparison, the displacement between points of rest $t = 0.487$ in a gravitation-free field; dimensionless parameters.

between points of rest in a gravitation-free field (cf. Figure 5.15, based on the data of /5.4, 5.5, 5.12/). This further substantiates the fact that for sufficiently short flight duration (at high thrust accelerations) the gravitation-free field closely approximates the central field. Figure 5.16, taken from /5.20/, shows the dependence of the functional J on the parameters T, φ_1, as obtained by the method of steepest descent (cf. Part III).

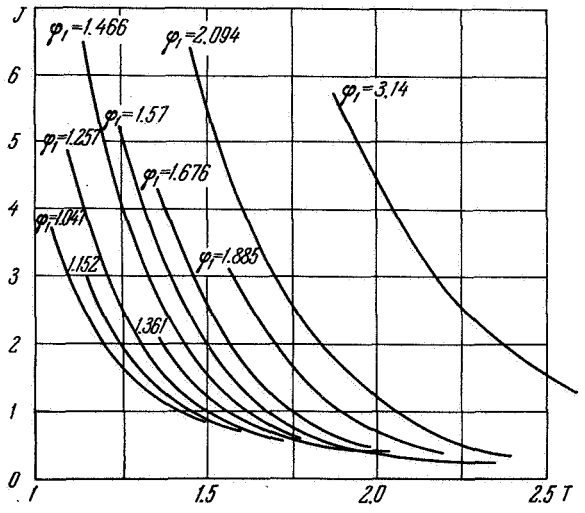

FIGURE 5.16. Functional J as function of flight duration with different angular displacements T for orbital transfers (Earth—Mars flight for circular and coplanar orbits, dimensionless parameters).

The parametric calculations conducted in /5.16/ by Newton's method (cf. Part III) revealed an interesting type of nonuniqueness in the solution of the boundary-value problem. Figure 5.17 shows the functional for Earth—Mars flights (allowing for the real motion of the planets) as a function of the departure date and the flight duration. Two families of curves, I and II, corresponding to two optimum departure periods
198 (family I: January—April 1969, family II: March—July 1971) are presented. The points of intersection of the curves of the two families having equal flight durations (September—October 1970) represent the points of nonuniqueness in the solution of the boundary-value problem for system (5.5). In fact, at these points the time T, the initial and final values of the coordinates and velocities, and the value of the functional coincide. An example of two flights identical in these integral characteristics but differing in their trajectories and thrust accelerations is given in Figure 5.18. Another type of nonuniqueness in the solution of the boundary-value problem for optimum flights will be noted in § 2.7.

All results given above were obtained assuming a central field. The relative error caused by neglecting planetary attraction forces is of the order of 10^{-3} to 10^{-4} (cf. /5.4/).

A larger error is caused by neglecting the ellipticity of the planetary orbits. This is illustrated by Figure 5.19 from /5.15, 5.16/, which gives

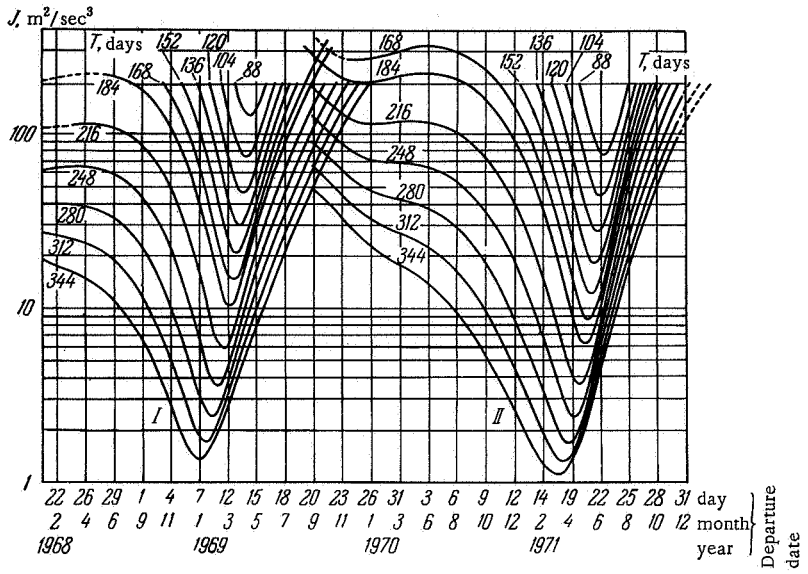

FIGURE 5.17. Functional J as function of departure date for different flight durations of Earth—Mars flights (actual orbits of planets).

data about the transfer from the circular orbit of the Earth to the coplanar elliptic orbit of Mars (solid curves 1 and 2). The lower curve 1 corresponds to the attainment of the best point of the elliptic orbit of Mars, and the upper curve 2 to the attainment of the least favorable point. The difference obtained between the corresponding values of the functional is considerable. Calculations conducted for the average circular orbits give a value of the functional lying between these two extremes (cf. the dashed curve 3 on Figure 5.19).

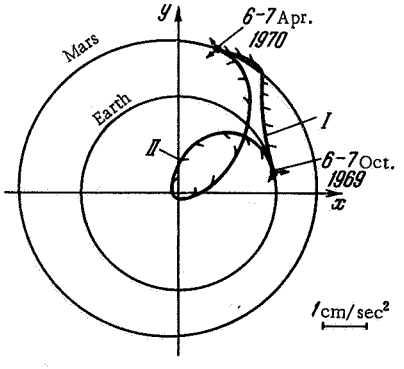

FIGURE 5.18. Example of two optimum Earth—Mars trajectories belonging to different families (I and II, cf. Figure 5.17), with coincident departure and arrival dates, initial and final points, and functional. Arrows indicate optimum program of thrust-acceleration vector; acceleration scale given in lower right-hand corner.

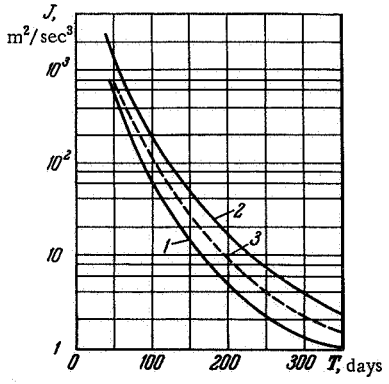

FIGURE 5.19. Influence of ellipticity of planetary orbits on functional for Earth—Mars orbital transfer:

1) transfer at "best" point of elliptic orbit of Mars; 2) transfer at "worst" point of Mars orbit; 3) transfer between average circular orbits.

201 The allowance for the noncoplanarity of the orbits has a weak effect on the integral characteristics of the flights (cf. Table 5.5 from /5.16/, and also data in /5.14, 5.25/).

TABLE 5.5. Influence of noncoplanarity of Earth and Mars orbits on functional of orbital transfer problem (T = 184 days)

Departure date (1971)	J, m²/sec³ three-dimensional trajectory J_1	J, m²/sec³ two-dimensional trajectory J_2	Error $\frac{J_1-J_2}{J_1}\cdot 100\%$	Departure date (1971)	J, m²/sec³ three-dimensional trajectory J_1	J, m²/sec³ two-dimensional trajectory J_2	Error $\frac{J_1-J_2}{J_1}\cdot 100\%$
14 February	37.373	37.230	0.38	21 May	6.406	6.247	2.5
2 March	27.733	27.597	0.49	6 June	7.459	7.303	2.1
18 March	19.931	19.796	0.68	22 June	10.558	10.413	1.4
3 April	13.938	13.798	1.00	8 July	16.046	15.918	0.80
19 April	9.703	9.555	1.5	24 July	24.395	24.292	0.42
5 May	7.187	7.032	2.2	9 August	36.217	36.139	0.22
13 May	6.576	6.418	2.4	17 August	43.648	43.584	0.15

The results of systematic calculations of the optimum trajectories of orbital transfers for different planets of the solar system (Earth—Mercury, Earth—Venus, Earth—Mars, Earth—Jupiter, Earth—Saturn) can be found in /5.13—5.18, and 5.25/.

The data given in § 2.2 and here make it possible to determine the parameters of the optimum one-way trajectory "Earth satellite—Mars satellite". To that end we use the following approximations: for zero energy build-up from a circular orbit $r_0 = 1$ (Figure 5.6), $J(T) \approx (0.895)^2/T$, and for transfer between circular coplanar orbits $r_0 = 1$ and $r_1 = 1.52$ with unspecified angular displacement (Figure 5.15) $J(T) \approx 12\,(0.487)^2/T^3$ (dimensionless variables). We assume circular orbits at an altitude of 300 km for the satellites, and consider the transfer trajectory to be two-dimensional.

Substituting the corresponding characteristic values of the functional J_* and the time t_* from Tables 5.1 and 5.3 in the approximate formulas, we obtain:

for the acceleration in the Earth's field

$$J_{+1}\ [\text{m}^2/\text{sec}^3] \approx 5\cdot 10^2/T_{+1}\ [\text{days}],$$

for the orbital transfer Earth—Mars

$$J_1\ [\text{m}^2/\text{sec}^3] \approx 10^2/T_1\ [\text{days}],$$

for the deceleration in the Mars field

$$J_{-2}\ [\text{m}^2/\text{sec}^3] \approx 10^2/T_{-2}\ [\text{days}].$$

The total flight time $T_\Sigma = T_{+1} + T_1 + T_{-2}$ is given, but the departure date is not fixed; it is required to find the distribution of this time among the three sections of the flight which minimizes the total functional $J_\Sigma = J_{+1} + J_1 + J_{-2}$.

Performing this calculation, we obtain the following expressions for the optimum times T_{+1}, T_1, T_{-2} and the minimum value of the functional J_σ:

$$T_{+1}\ [\text{days}] = 10^2\tau^2,\quad T_1\ [\text{days}] = 2.783\cdot 10^2\tau,\quad T_{-2}\ [\text{days}] = T_\sigma\ [\text{days}] - \\ - 10^2\ (\tau^2 + 2.783\tau)\ \ (\tau = \sqrt{0.922 + 0.691\cdot 10^{-2} T_\sigma\ [\text{days}]} - 0.96),$$

$$J_\sigma\ [\text{m}^2/\text{sec}^3] = \frac{5}{\tau^2} + \frac{4.63}{\tau^3} + \frac{1}{10^{-2}T_\sigma[\text{days}] - (\tau^2 + 2.783\tau)};$$

the optimum angular displacement of the orbital transfer is then equal to φ_1 [rad] $\approx 3.62\,\tau$. In view of the reversibility properties (5.16), the formulas obtained also apply to the flight "Mars satellite — Earth satellite" (it is only necessary to replace T_{+1} by T_{-1} and T_{-2} by T_{+2}).

202 **7. Round-trip interplanetary trajectory.** In the problem of the round-trip interplanetary trajectory the total flight time T_σ and the time of sojourn on the destination planet T_ω are specified; the departure time from the initial orbit is unspecified (cf. § 2 of the Appendix). The kinematic parameters of the elementary maneuvers forming the interplanetary trajectory are not defined separately. Here it is necessary to find the optimum flight-time values for the maneuvers of both zero energy build-up and deceleration in the field of the planets as well as the flight time and the angular displacement for the outbound and return trips between the orbits of the planets. The selection of the optimum values for deceleration and zero energy build-up in the field of the destination planet are not examined here (these times are included in the fixed time T_ω). The energy expended in performing these maneuvers is similarly neglected. The orbits of the planets are assumed to be circular and coplanar.

Let the time for zero energy build-up and that for deceleration near the departure planet be specified; the problem then reduces to determining the optimum kinematic parameters of the round-trip orbital transfer. The values specified here are the initial and final radii, the velocity projections for outbound and return transfer, and the sums of the angular displacements and of the flight times* (cf. (A.61), (A.62)). In order to determine the optimum distribution of the total angular displacement $\varphi_1 + \varphi_2$ and the total time $T_1 + T_2$ between (1) the outbound, and (2) the return transfers, we make use of the condition that the part of the first variation of the functional outside the integral must vanish. In our case the functional is the sum of the two integrals (5.9) corresponding to the outbound and return flights

$$\left.\begin{aligned} J_1 + J_2 = &\int_0^{T_1} [(\ddot{r} - r\dot{\varphi}^2 + 1/r^2)^2 + \\ &+ (\ddot{\varphi}r + 2\dot{\varphi}\dot{r})^2]\,dt \Big|_{\substack{r(0)=1,\ \varphi(0)=0,\ \dot{r}(0)=0,\ \dot{\varphi}(0)=1,\\ r(T_1)=r_1,\ \varphi(T_1)=\varphi_1,\ \dot{r}(T_1)=0,\ \dot{\varphi}(T_1)=-r_1^{-3/2}}} + \\ &+ \int_0^{T_2} [(\ddot{r} - r\dot{\varphi}^2 + 1/r^2)^2 + \\ &+ (\ddot{\varphi}r + 2\dot{\varphi}\dot{r})^2]\,dt \Big|_{\substack{r(0)=r_1,\ \varphi(0)=0,\ \dot{r}(0)=0,\ \dot{\varphi}(0)=r_1^{-3/2},\\ r(T_2)=1,\ \varphi(T_2)=\varphi_2,\ \dot{r}(T_2)=0,\ \dot{\varphi}(T_2)=1}}. \end{aligned}\right\} \qquad (5.59)$$

* If, in addition, the departure date is specified $T_1 + T_2$, $\varphi_1 - \omega_3 T_1$ and $\varphi_2 - \omega_3 T_2$ will also be determined.

In accordance with (5.14), the required terms of the first variation of (5.59) are written in the form /5.4/

$$\delta J_1 + \delta J_2 = -2(\nu_1 \delta\varphi_1 + \lambda_1 \delta T_1 + \nu_2 \delta\varphi_2 + \lambda_2 \delta T_2). \tag{5.60}$$

203 If the sums $(\varphi_1 + \varphi_2)$, $(T_1 + T_2)$ are given, the conditions for (5.60) to vanish will be*

$$\nu_1 = \nu_2, \ \lambda_1 = \lambda_2. \tag{5.61}$$

Equalities (5.61) are satisfied if we consider a symmetrical return flight (cf. (5.16)); then $\varphi_1 = \varphi_2$, $T_1 = T_2$, $J_1 = J_2$. However, it has been shown by a number of authors (/5.2, 5.13, 5.15, 5.20, 5.21, 5.36/) that this does not always lead to an absolute minimum for the sum of the functionals $J_1 + J_2$.

Conditions (5.61) can also be satisfied for symmetrical outbound and return flights. The solution of the boundary-value problem (cf. (5.13))

$$\left.\begin{aligned}
&\dot{r} = v_r, \\
&\dot{v}_r = a_r + \frac{v_\varphi^2}{r} - \frac{1}{r^2}, \quad v_r(r_0) = v_{r0}, \quad v_r(r_1) = v_{r1}, \\
&\dot{v}_\varphi = a_\varphi - \frac{v_r v_\varphi}{r}, \qquad v_\varphi(r_0) = v_{\varphi 0}, \quad v_\varphi(r_1) = v_{\varphi 1}, \\
&\dot{a}_r = \frac{1}{v_r}\left[\frac{1}{2}(a_r^2 + a_\varphi^2) + a_r\left(\frac{v_\varphi^2}{r} - \frac{1}{r^2}\right) - \lambda - \nu\frac{v_\varphi}{r}\right], \\
&\dot{a}_\varphi = \frac{1}{r}(a_\varphi v_r - 2a_r v_\varphi + \nu)
\end{aligned}\right\} \tag{5.62}$$

with fixed parameters λ and ν yields two families of integral curves $v_r(r)$, $v_\varphi(r)$, $a_r(r)$, $a_\varphi(r)$ and therefore two pairs of values for φ_1 and T, i.e., the boundary-value problem (5.62) does not have a unique solution. In order to illustrate this fact, consider the curve $\nu(\lambda)$. In Figure 5.20 we have plotted, in (ν, λ) coordinates, the lines of equal angular displacement φ_1 for transfers between the orbits of Earth and Mars /5.20/. (The relationship $J(T)$ for the same values of φ_1 was shown in Figure 5.16.) The intersection of the curves in Figure 5.20 indicates the nonuniqueness of the solution of (5.62), i.e., the conditions of optimum conjugation (5.61) can also be fulfilled for nonsymmetrical trajectories.

We shall give an example of an asymmetrical round-trip flight for which the functional value is 16% lower than for the corresponding symmetrical flight; the parameters of the symmetrical flight are $T_1 = T_2 = 1.88$, $\varphi_1 = \varphi_2 = 2.14$, $J_1 + J_2 = 3.80$; the parameters of the asymmetrical flight are $T_1 = 2.41$, $T_2 = 1.35$, $\varphi_1 = 3.14$, $\varphi_2 = 1.14$, $J_1 + J_2 = 3.20$. The total time and the total angular displacement are the same for the two flights, and are given by $T_1 + T_2 = 3.76$, $\varphi_1 + \varphi_2 = 4.28$.

204 The optimum distribution of the given total time and angular displacement between the outbound and return flights is found after solving the problem of minimizing the sum $J_1 + J_2$ with respect to the arguments φ_1, T_1 for $\varphi_1 + \varphi_2 = \text{const}$, $T_1 + T_2 = \text{const}$. This is done in /5.17/ for the flight Earth—Mars—Earth employing a wide range of parameters. The results obtained there will be used below.

* For a given departure date, conditions (5.61) are replaced by $(\nu_1 - \nu_2)\omega_2 + (\lambda_1 - \lambda_2) = 0$ (cf. note on p. 144).

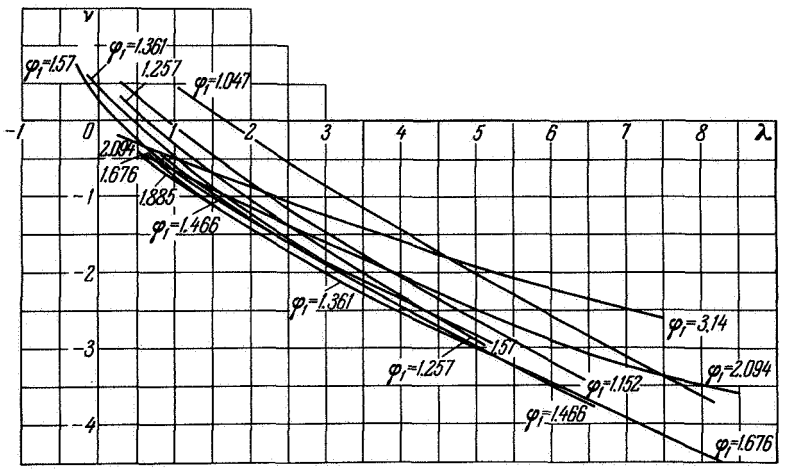

FIGURE 5.20. Lines of equal angular displacement φ_1 in (ν, λ) coordinates for Earth—Mars orbital transfers.

The minimum of $J_1 + J_2$ is calculated in terms of the departure date from the Earth orbit t_0 (reckoned from the date of opposition between Earth and Mars) and the time of outbound flight T_1 (t_0 and φ_1 are related by (5.49), where we must assume that $T = T_1$). Figure 5.21 shows a typical example of the dependence of the total functional $J_1 + J_2$ on t_0 and T_1 for a given total time $T_1 + T_2 = 496$ days and a time of sojourn in the field of the destination planet given by $T_\omega = 0$. The minimum of $J_1 + J_2$ in this example occurs at $t_0 = -85$ days, $T_1 = 184$ days (cf. curve 3), i.e., here too the optimum flight is asymmetrical. The influence of how the time $T_1 + T_2$ is distributed between the outbound, T_1, and return, T_2, flights on the functional $J_1 + J_2$ is illustrated in Figure 5.22 (the time of sojourn near Mars is fixed, $T_\omega = 0$, and the departure date at each point is an optimum). It is seen that the symmetrical flights ($T_1 = T_2$ represented by the dashed line on Figure 5.22) become optimum when the total time $T_1 + T_2$ is reduced.

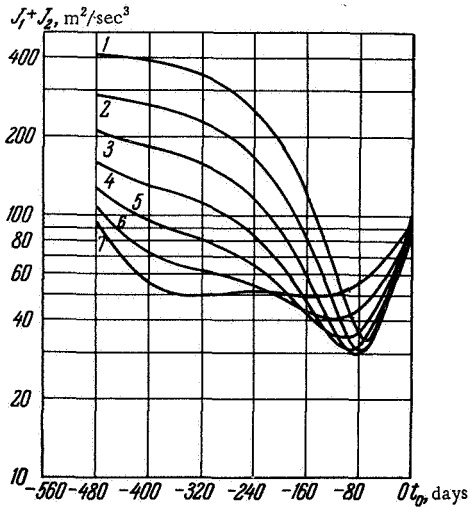

FIGURE 5.21. Total functional $J_1 + J_2$ for a round-trip flight between the orbits of Earth and Mars, as a function of the departure date t_0 (date of opposition) for different distributions of the specified total time $T_1 + T_2 = 496$ days between outbound, T_1, and return, T_2, flights:

1) $T_1 = 152$ days, $T_2 = 344$ days; 2) $T_1 = 168$ days, $T_2 = 328$ days; 3) $T_1 = 184$ days, $T_2 = 312$ days; 4) $T_1 = 200$ days, $T_2 = 296$ days; 5) $T_1 = 216$ days; $T_2 = 280$ days; 6) $T_1 = 232$ days, $T_2 = 264$ days; 7) $T_1 = 248$ days, $T_2 = 248$ days (fixed time of sojourn in the vicinity of Mars $T_\omega = 0$).

Figure 5.23 gives the optimum time T_1 of the outbound flight as a function of $T_1 + T_2$ for fixed values of T_ω. The negative values of T_ω are introduced formally so that the

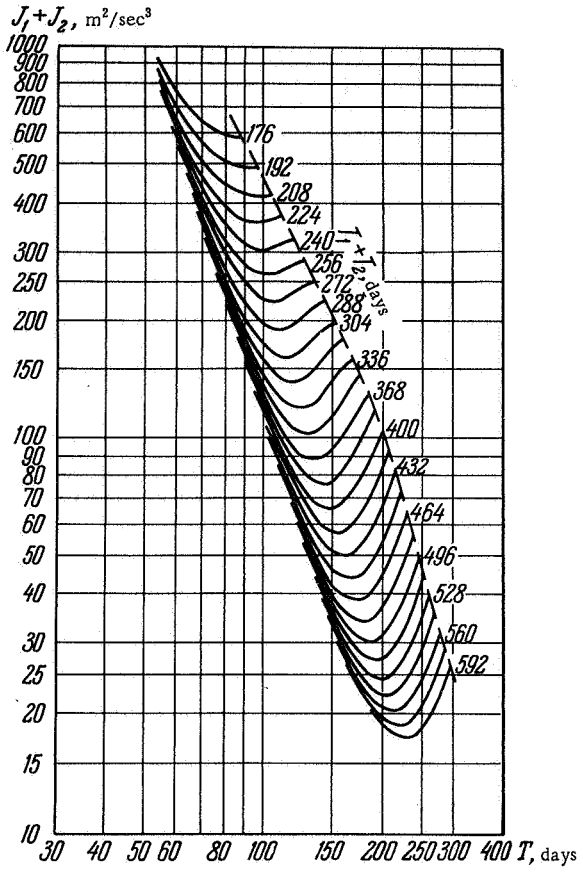

FIGURE 5.22. Values of the total functional J_1+J_2, minimized relative to the departure date, for an Earth—Mars—Earth orbital transfer as a function of the duration of an outbound flight T_1 for fixed values of the total time T_1+T_2. $T_1+T_2=16$ days; time of sojourn in vicinity of Mars $T_\omega=0$; dashed line corresponds to a symmetrical flight $T_1=T_2$.

205 corresponding relationships are monotonic. In order to obtain the true values of T_ω it is necessary to add to the synodic period (which, for the Earth and Mars, is about 780 days) these negative values.

The functional J_1+J_2, minimized with respect to T_1 and t_0, is given in Figure 5.24 in the form $f(T_1+T_2, T_\omega)$. This relationship, together with Figure 5.23, represents the entire problem of the optimization of the round-trip interorbital flight. The envelope of the lower curve, represented by a dashed line on Figure 5.24, corresponds to a flight with unspecified (optimum) time of sojourn in the neighborhood of the destination planet ($v_1=v_2=0$).

We now proceed to the problem of determining the optimum times of zero energy build-up T_{+1} and deceleration T_{-1} in the field of the Earth. In the first place, these times must be equal to each other. In fact, the initial and final orbits of the Earth satellites are assumed to be identical,

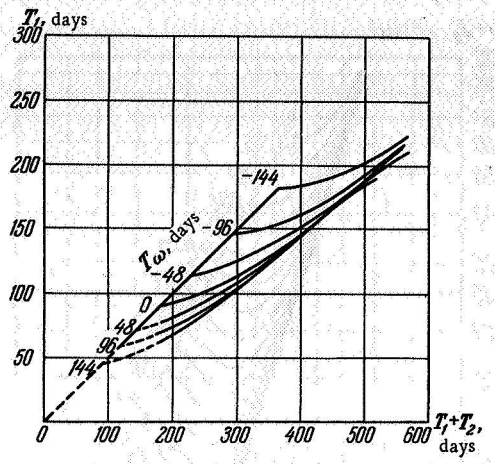

FIGURE 5.23. Optimum time T_1 of transfer from Earth orbit to Mars orbit as function of the total time $T_1 + T_2$ of the outbound and return orbital transfers for fixed values of a sojourn time near Mars T_ω (for $T_\omega < 0$, add 780 days).

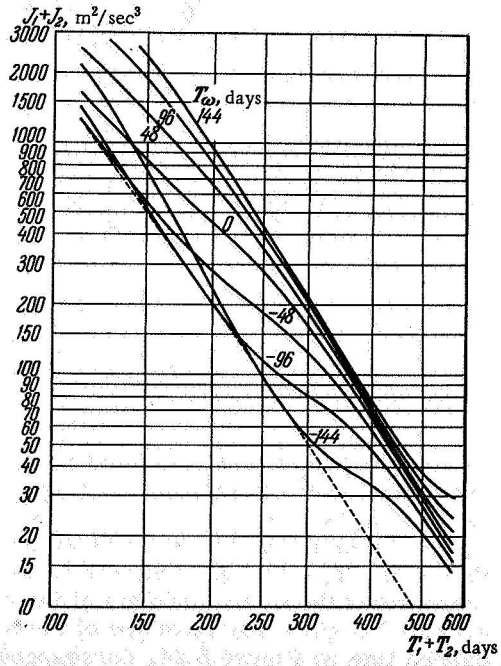

FIGURE 5.24. Minimum value of the total functional J_1+J_2 (minimum for t_0 and T_1) for an Earth—Mars—Earth orbital transfer as a function of the total time T_1+T_2 of the outbound and return flights for fixed values of the sojourn time near Mars T_ω (dashed line corresponds to flights with T_ω unspecified; for $T_\omega < 0$, add 780 days).

and therefore the energy expenditures for the maneuvers of zero energy
208 build-up J_{+1} and of deceleration J_{-1} are expressed by the same function $J(T)$ in view of (5.16). This function, calculated in § 2.2 (cf. Figure 5.6), is monotonic and has a positive second derivative. It can be shown that for such functions the minimum of the sum of two values of the function for a given sum of the arguments (i.e., the minimum of $J(T_{+1}) + J(T - T_{+1})$ with respect to T_{+1}) is achieved when the arguments are equal ($T_{+1} = T_{-1} = {}^1/_2 T$).

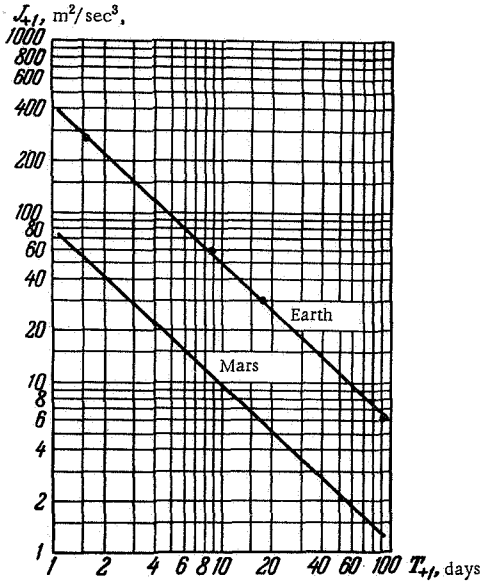

FIGURE 5.25. Functional J_{+1} for maneuvers of zero energy build-up and deceleration in gravitational fields of Earth and Mars as a function of the maneuver time T_{+1}, calculated by the approximate formula (5.65) (dots represent exact values taken from Figure 5.6, 300-km high circular orbit).

Thus, the total time spent on the maneuvers of zero energy build-up and of deceleration in the field of the Earth is equal to $2T_{+1}$, and the total functional to $2J_{+1}$. It is now necessary to find the minimum with respect to T_{+1} of the total functional

$$J_\Sigma = 2J_{+1} + (J_1 + J_2) \tag{5.63}$$

for a given total time of flight

$$T_\Sigma = 2T_{+1} + (T_1 + T_2) + T_\omega \tag{5.64}$$

(the time of sojourn in the vicinity of Mars T_ω is also specified).

The dependence of $J_1 + J_2$ on $T_1 + T_2$ and T_ω is shown in Figure 5.24; the relationship $J_{+1}(T_{+1})$ is represented by the approximate formula

(given in dimensionless variables, where the transition to dimensional variables is performed by Table 5.1)

$$J_{+1} = 0.3934 T_{+1}^{-0.9137}, \tag{5.65}$$

derived under the assumption of a constant tangential acceleration (cf. (6.48)). The results of calculations which employ (5.65) are very close to the exact results, and therefore also to the optimum ones (cf. Figure 5.6). In Figure 5.25 the results of the approximate and exact formulas are compared for a 300-km high circular orbit of an Earth satellite. (This orbit is used in the following calculations.) In the same figure a line corresponding to the circular orbit of a Mars satellite at the same altitude has also been drawn (we recall that the energy expended on the deceleration and acceleration maneuvers on Mars is neglected).

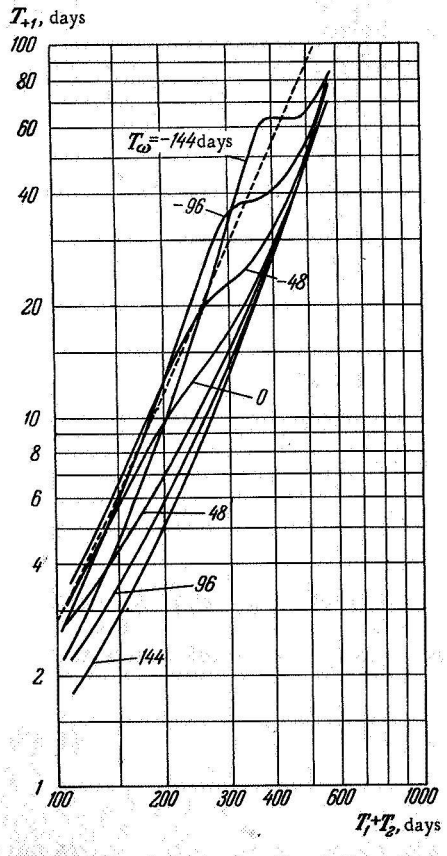

FIGURE 5.26. Optimum time T_{+1} of zero energy build-up in gravitational field of the Earth (equal to the deceleration time) as a function of the total time $T_1 + T_2$ of outbound and return flights between orbits of the Earth and Mars at fixed values of the sojourn time T_ω in the vicinity of Mars (300-km high circular orbit; add 780 days when $T_\omega < 0$; dashed line corresponds to an unspecified T_ω).

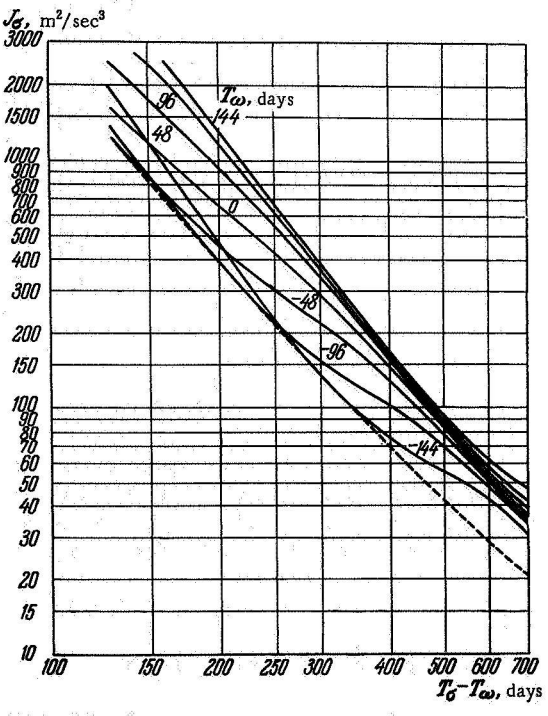

FIGURE 5.27. Full functional $J_\sigma = 2J_{+1} + J_1 + J_2$ of the interplanetary Earth—Mars—Earth flight as a function of the total flight time $T_\sigma - T_\omega = 2T_{+1} + T_1 + T_2$ (total travel time T_σ minus the fixed time of sojourn T_ω in the field of Mars; add 780 days when $T_\omega < 0$; dashed line corresponds to an unspecified T_ω).

211 The equality

$$\frac{dJ_{+1}}{dT_{+1}} - \frac{d(J_1 + J_2)}{d(T_1 + T_2)} = 0 \qquad (5.66)$$

must be fulfilled at the point where (5.63) has a minimum. We have obtained (5.66) by differentiating (5.63), and using (5.64) in the form $2dT_{+1} = -d(T_1 + T_2)$, $T_\sigma = \text{const}$, $T_\omega = \text{const}$.

The first term of (5.66) was found by differentiating (5.65) to obtain

$$\frac{dJ_{+1}}{dT_{+1}} = -370.8T_{+1}^{-1.9127} \qquad (5.67)$$

($[J_{+1}] = \text{m}^2/\text{sec}^3$, $[T_{+1}] = \text{days}$, 300-km high orbit of an Earth satellite). The optimum time T_{+1} was found by (5.66) for each pair of values $T_1 + T_2$ and T_ω, given by

$$T_{+1} = \left[-0.2697 \cdot 10^{-4} \frac{d(J_1 + J_2)}{d(T_1 + T_2)}\right]^{-0.5228}. \qquad (5.68)$$

The derivative is calculated on the basis of the data used in Figure 5.24. The results of the corresponding calculations are given in Figure 5.26. The full functional $J_\sigma = 2J_{+1} + J_1 + J_2$ of the round-trip interplanetary flight Earth—Mars is shown in Figure 5.27 as a function of the time $T_\sigma - T_\omega = 2T_{+1} + T_1 + T_2$ (the total travel time T_σ minus the time of sojourn T_ω in the field of Mars) for fixed values of T_ω.

§ 3. OPTIMUM MANEUVERS OF GUIDED SATELLITES WITH IDEAL POWER-LIMITED ENGINE

This section presents the solution of the variational problem (5.2) for the following maneuvers in the vicinity of a planet: (1) rotation of the plane of a circular orbit; (2) variation of the radius of a circular orbit; (3) simultaneous variation of the radius and angle of inclination of a circular orbit.

A common feature of all the maneuvers of guided satellites with power-limited engines is the small ratio between the thrust acceleration and the gravitational acceleration. This enables us to obtain an analytic solution by means of various approximation methods. The problems in this section have been selected in order to include the most useful of these methods.

1. Rotation of the plane of a circular orbit. We shall determine the optimum thrust-acceleration program for the maneuver of varying the angle of inclination of the plane of the satellite's circular orbit (cf. § 3 of the Appendix) /5.27/. The thrust is perpendicular to the instantaneous plane
212 of the orbit (along the normal, $e = +1$, or in the opposite direction, $e = -1$); the angle i between the initial and final planes (the angle of rotation), the final position of the nodal line Ω_1, and the time of motion T are considered as given. To simplify calculations, the time T is taken as a multiple of the number of revolutions: $T = 2\pi s$, for $s = 1, 2, 3, \ldots$ (all parameters are dimensionless, cf. (A.2), where $r_* = r_0$). The initial orbit lies in the equatorial plane (Figure 5.28).

The variational problem considered is written in the form of Mayer's problem

$$\left.\begin{array}{lll} \dot{J} = (ae)^2, & J(0) = 0, & J(2\pi s) = \min, \\ \dot{\chi} = ae\sin(t-\Omega_1), & \chi(0) = 0, & \chi(2\pi s) = 0, \\ \dot{\omega} = ae\cos(t-\Omega_1), & \omega(0) = 0, & \omega(2\pi s) = i \\ (a(t) \geqslant 0, & e(t) = \pm 1). & \end{array}\right\} \tag{5.69}$$

The derivation of the dynamic equations (5.69) is given in the Appendix (cf. (A. 94)); the latter are obtained from a system in osculating variables assuming that the angle of rotation i is small.

Problem (5.69) will be solved by Pontryagin's method. Thus, we write the Hamiltonian and the differential equations governing the momenta

$$\left.\begin{array}{l} H = -(ae)^2 + p_\chi ae\sin(t-\Omega_1) + p_\omega ae\cos(t-\Omega_1), \\ \dot{p}_\chi = -\partial H/\partial\chi = 0, \quad \dot{p}_\omega = -\partial H/\partial\omega = 0. \end{array}\right\} \tag{5.70}$$

Here it has been assumed that the momentum corresponding to the minimized phase coordinate J is constant. This is in accordance with the generally accepted normalization procedure and its value has been taken as -1.

The control variables a and e appear in the differential equations (5.69) and the Hamiltonian (5.70) in the form of the product ae. The optimum program for this combination is given by the expression (from the condition for H to be maximum)

$$ae = {}^1/_2\,[p_\chi\sin(t-\Omega_1) + p_\omega\cos(t-\Omega_1)]. \tag{5.71}$$

The optimum control variables a and e are given by the expressions*

$$\left.\begin{array}{l} e = \operatorname{sgn}[p_\chi\sin(t-\Omega_1) + p_\omega\cos(t-\Omega_1)], \\ a = {}^1/_2\,|p_\chi\sin(t-\Omega_1) + p_\omega\cos(t-\Omega_1)|. \end{array}\right\} \tag{5.72}$$

Substituting the optimum law (5.71) in the equations of motion (5.69), and integrating to the final time $T = 2\pi s$, we obtain values of the constants p_χ and p_ω which satisfy the given boundary values in (5.69). These are

$$p_\chi = 0, \; p_\omega = 2i/s\pi. \tag{5.73}$$

213 Then

$$ae = (i/s\pi)\cos(t-\Omega_1), \tag{5.74}$$

and the value of the control functional J will be

$$J(T) = i^2/s\pi = 2i^2/T \qquad (T = 2\pi s). \tag{5.75}$$

The optimum control function of the thrust acceleration (5.74) in the course of one revolution is shown in Figures 5.28 and 5.29. According to

* The function sgn x (the sign of x) is defined as sgn $x = +1$ for $x > 0$, sgn $x = 0$ for $x = 0$, sgn $x = -1$ for $x < 0$.

(5.74), the magnitude of the acceleration has a maximum when passing the final position of the nodal line. The thrust-acceleration vector changes direction twice per revolution, namely when $a(t)$ vanishes. These points are shifted through $\pi/2$ from the maxima.

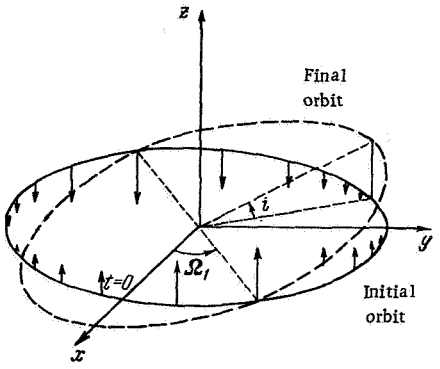

FIGURE 5.28. Scheme of the rotation maneuver of the plane of circular orbit; arrows indicate the optimum program of the thrust-acceleration vector.

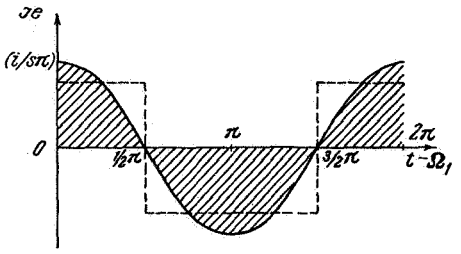

FIGURE 5.29. Optimum thrust-acceleration program for rotation of plane of a circular orbit in a central field (acceleration normal to the instantaneous plane of the orbit, $e = \pm 1$, a = magnitude of the acceleration, dashed line represents program shown for comparison).

The value of the control functional J is independent of the position of the nodal line of the final orbit (i.e., of the angle Ω_1). The dependence of the functional on the time of execution of the maneuver is the same as for the problem of velocity build-up in a gravitation-free field (cf. (5.30) and curve u in Figure 5.2). If, instead of the optimum thrust-acceleration program (5.74), we consider an acceleration of constant magnitude with simultaneous changes of direction $ae = (i/4s)\,\mathrm{sgn}\cos(t - \Omega_1)$ (dashed line on Figure 5.29, cf. § 4 of Chapter Thirteen), the value of the functional will increase by a factor of 1.23 to become $J = i^2\pi/8s$. We recall that the results of this section were obtained under the assumption that the maneuvering time is an integral multiple of the number of revolutions, namely, $T = 2\pi s$.

214 **2. Transfer between coplanar circular orbits.** The problem considered is a particular case of the problem of orbital transfer (§ 2.2). The parameters specified are the time of motion and the radii of the initial and final orbits. The initial and final velocities are circular (cf. (A.58)); no angular displacement is specified ($\nu = 0$). The final orbit is considered as external relative to the initial one, and by means of the transformations (5.16) all the results can be converted to the inverse cases.

If the thrust acceleration is small compared with the gravitational acceleration, it is possible to use the approximate solution (5.44), (5.46), (5.47) in § 2.3. According to this solution, the optimum program of the thrust-acceleration vector (5.46), (5.47) (for $a_\varphi t \ll 1$) is such that the acceleration magnitude is almost constant, and its direction is close to that of the velocity (whose vector here is almost directed along the

transversal). The magnitude of the acceleration a_φ is determined using the first relation of (5.44) with the final condition $r(T) = r_1$, and is found to be given by

$$a_\varphi \equiv \frac{1}{T}\left(1-\frac{1}{\sqrt{r_1}}\right); \tag{5.76}$$

here and below all parameters are dimensionless (cf. (A.2) for $r_* = r_0$).

The optimum trajectory is described by (5.44) with a_φ given in (5.76). The functional J is approximately

$$J \approx \left(1-\frac{1}{\sqrt{r_1}}\right)^2 \frac{1}{T} \tag{5.77}$$

(cf. (5.45)).

The expressions obtained here for $J(T)$ and the optimum thrust-acceleration program are similar to those derived for the maneuver of velocity build-up in a gravitation-free field (5.32). The function $J(T)$ has the same form for the maneuver of rotating the orbit plane as well (5.75), although the acceleration program there (5.74) is substantially different.

We shall consider briefly the accuracy of the solution. The part of the functional J not allowed for in (5.77) has the value (cf. (5.45), (5.47), (5.76))

$$\int_0^T a_r^2 dt = \frac{36}{7}\frac{(\sqrt{r_1}-1)^3 (r_1^{7/6}-1)}{r_1^{3/2}T^3}; \tag{5.78}$$

the maximum value of the neglected thrust-acceleration component a_r is (cf. (5.47), (5.76))

$$\max_{0\leqslant t\leqslant T} a_r(t) = a_r(T) = \frac{6r_1(\sqrt{r_1}-1)^2}{T^2}. \tag{5.79}$$

The discrepancies in the radial-velocity boundary conditions ($v_{r0} = v_{r1} = 0$) are (cf. (5.44), (5.76))

$$v_r(0) - v_{r0} = \frac{2(\sqrt{r_1}-1)}{T\sqrt{r_1}}, \quad v_r(T) - v_{r1} = \frac{2r_1(\sqrt{r_1}-1)}{T}. \tag{5.80}$$

215 With the aid of (5.78) to (5.80) it is possible to determine the range within which the solution (5.44), (5.76) provides the required accuracy.

We shall examine an approximate solution of the problem in which the model of a homogeneous central field was used (cf. § 1 of the Appendix and (5.34) to (5.37)). In this case there is no need to assume a small thrust acceleration; instead, we must assume that the radial displacement is small. The general solution of the equations of the variational problem in a homogeneous central field was given in § 1 (cf. (5.35) to (5.37)). It remains only to substitute the corresponding boundary conditions.

Before the maneuver starts and after it ends the motion must follow circular equilibrium orbits of specified radii. In a central field the equations of this motion in the (x, y) plane will be $x(t) = r\cos(r^{-3/2}t)$, $y(t) = r\sin(r^{-3/2}t)$, $r = \text{const}$ (cf. (A.3) for $a_x = a_y = 0$). In a homogeneous central field this is replaced by $x(t) = r\cos t$, $y(t) = r\sin t$, $r = \text{const}$ (cf. (A.54) for $a_x = a_y = 0$). Thus, the equilibrium velocity along a circular trajectory

of radius r is equal in the first case to $r^{-1/2}$, and in the second to r (dimensionless variables).

In accordance with what was said above, the vectors $\mathbf{r}_0$, $\mathbf{v}_0$, $\mathbf{r}_1$, $\mathbf{v}_1$ in (5.36) will have the following components in an (x, y) rectangular coordinate system (Figure A.4):

$$\left.\begin{aligned} &\mathbf{r}_0 = (r_0, 0),\ \mathbf{v}_0 = (0, r_0),\\ &\mathbf{r}_1 = (r_1 \cos\varphi_1,\ r_1 \sin\varphi_1),\\ &\mathbf{v}_1 = (-r_1 \sin\varphi_1,\ r_1 \cos\varphi_1). \end{aligned}\right\} \tag{5.81}$$

It is assumed here that the initial point lies on the x-axis. By the formulation of the problem the polar angle φ_1 is not fixed, and therefore it is necessary to select its optimum value so that the functional J will be minimum.

All variables are expressed as fractions of their value on a circular orbit of radius r_* (cf. (A.2)), on which the approximate value of the gravitational acceleration is assumed to be equal to the actual value. In the field model used, the gravitational acceleration increases linearly with increasing radius, while in a central field it decreases with the square of the radius. A certain compensation for the errors resulting from this is possible by a suitable choice of r_*.*

216 We shall assume for simplicity that the maneuvering time is a multiple of the period of revolution along the circular orbit of radius r_*. Substituting (5.81) in the last formula of (5.37), we obtain

$$J = \frac{4}{T}(r_1^2 - 2r_0 r_1 \cos\varphi_1 + r_0^2) \qquad (T = 2\pi s,\ s = 1, 2, \ldots). \tag{5.82}$$

This shows that the minimum of J with respect to φ_1 is attained when $\cos\varphi_1 = 1$. Using this relation, we write the expressions for the optimum program of thrust acceleration, the optimum trajectory, and the functional $J(t)$, in the form (cf. (5.35) to (5.37), (5.81))

$$\left.\begin{aligned} &a_x(t) = -\frac{2}{T}(r_1 - r_0)\sin t, \quad a_y(t) = \frac{2}{T}(r_1 - r_0)\cos t,\\ &x(t) = \left[r_0 + (r_1 - r_0)\frac{t}{T}\right]\cos t - \frac{r_1 - r_0}{T}\sin t,\\ &y(t) = \left[r_0 + (r_1 - r_0)\frac{t}{T}\right]\sin t\\ &\qquad\qquad (0 \leqslant t \leqslant T = 2\pi s,\ s = 1, 2, \ldots),\\ &J(T) = \frac{4}{T}(r_1 - r_0)^2. \end{aligned}\right\} \tag{5.83}$$

The resulting optimum thrust-acceleration program is identical with the solution of the problem previously considered. The constant acceleration magnitude is given by $a = \sqrt{a_x^2 + a_y^2} = 2(r_1 - r_0)/T$ and the direction coincides with the transversal $a_x/a_y = -\operatorname{tg} t = -\operatorname{tg}\varphi$. If, instead of boundary conditions (5.81), we take here the ordinary boundary conditions for circular orbits

* In the substitution $r_* \to l^{-1}r_*$ it is necessary to alter all the dimensionless magnitudes in accordance with (5.15); the corresponding dimensional magnitudes will remain unchanged. A different method for refining the solution, based on numerical integration, is suggested in /5.10/; the thrust-acceleration program (5.37) is substituted in the exact equations of motion, and the constant vectors $\mathbf{c}_2$ and $\mathbf{c}_4$ are selected according to the exact boundary conditions.

in a central field, there results a thrust-acceleration program greatly differing from the optimum one given by

$$a_x = -\frac{2}{T}(r_1 - r_0)\sin t, \quad a_y(t) = -\frac{2}{T}\left(\frac{1}{\sqrt{r_1}} - \frac{1}{\sqrt{r_0}}\right)\cos t. \tag{5.84}$$

Compare the functionals (5.77) and (5.83); we shall designate the first by $J^{(1)}$, and the second by $J^{(2)}$. We rewrite $J^{(2)}$ in the same dimensionless variables as $J^{(1)}$ (i.e., we take the characteristic values of the variables on the initial orbit, and not on the orbit of radius r_*) so that

$$J^{(2)} = \frac{4}{T}\frac{(r_1 - 1)^2}{r_*^3}. \tag{5.85}$$

Assuming that $r_1 - 1 = \Delta r \ll 1$ we obtain

$$J^{(1)} = \frac{(r_1 - 1)^2}{4T}, \quad J^{(2)} = \frac{4(r_1 - 1)^2}{r_*^3 T} \tag{5.86}$$

to an accuracy of the order of $o(\Delta r^2)$.

217 For equal r_1 and T the functionals will coincide if we take $r_* = 2.52$. For this value of r_* the values of the thrust acceleration also coincide (since $a^{(1)}(t) \approx$ const and $a^{(2)}(t) =$ const, cf. (5.76) and (5.83)). Formula (5.77) for the functional is corroborated in § 3.3, where it is obtained by a different method, namely, the traditional one of linearizing the equations of motion.

3. Transfer between noncoplanar circular orbits of different radii.

The radii of the initial and final orbits, $r(0) = 1$ and $r(T) = r_1$ respectively, as well as the angle i between their planes, are given. The time of motion is fixed, but the position of the nodal line and the escape point on the final orbit are unspecified. It is assumed that the initial and final orbits are close to each other, where $|i| \ll 1, |r_1 - 1| \ll 1$. (The variables are dimensionless, and the values of the corresponding parameters on the initial orbit are taken as characteristic values, $r_* = r_0$ in (A.2).)

To solve the problem, we use the linearization method in the neighborhood of the initial motion /5.28, 5.29/. We select a reference frame ξ, η, ζ moving at equilibrium velocity along the initial circular orbit. The coordinates (ξ, η, ζ) are related to the spherical coordinates (r, φ, θ) (cf. Figure A.4) by the relationships

$$\xi = t - \varphi, \ \eta = r - 1, \ \zeta = \theta. \tag{5.87}$$

Using formulas (A.4), (A.6) for the transition to Cartesian coordinates, we can write the equations of motion in (ξ, η, ζ) coordinates and formulate the corresponding boundary conditions. The deviations from the initial motion and their derivatives are considered to be small during the entire time of motion. The equations of motion are linearized, and likewise only the main terms are preserved in the boundary conditions.

Finally, the variational problem is written in the following form (see 5.2)):

$$\begin{aligned}
&\dot J = a_\xi^2 + a_\eta^2 + a_\zeta^2, && J(0) = 0, \quad J(T) = \min,\\
&\dot\xi = u, && \xi(0) = 0, \quad \xi(T) = \text{opt},\\
&\dot\eta = v, && \eta(0) = 0, \quad \eta(T) = r_1 - 1,\\
&\dot\zeta = w, && \zeta(0) = 0, \quad \zeta^2(T) + w^2(T) = i^2,
\end{aligned} \tag{5.88}$$

$$\begin{aligned} &\dot{u} = a_\xi + 2v, && u(0) = 0, \quad u(T) = {}^3/_2(r_1 - 1), \\ &\dot{v} = a_\eta + 3\eta - 2u, && v(0) = 0, \quad v(T) = 0, \\ &\dot{w} = a_\zeta - \zeta, && w(0) = 0. \end{aligned} \tag{5.88}$$

The control functions $a_\xi(t)$, $a_\eta(t)$, $a_\zeta(t)$ (the thrust-acceleration components) are not limited. The final value of the phase coordinate ξ is unspecified. The final values of the phase coordinates ζ and w are also not
218 specified separately, but are related by the condition $\zeta^2(T) + w^2(T) = i^2$.

Note that the fourth and seventh equations of (5.88), which describe motion in a plane perpendicular to the initial orbit, are independent of the remaining equations of motion (for the given approximation). In view of this, we can use the results of the two preceding parts of this section to form the required solution as a superposition of those already found. Here, however, we shall treat the problem independently, in order to corroborate the results of § 3.2 and demonstrate how the method is applied.

Let us write the Hamiltonian

$$\begin{aligned} H = -(a_\xi^2 + a_\eta^2 + a_\zeta^2) + p_\xi u + p_\eta v + p_\zeta w + p_u(a_\xi + 2v) + \\ + p_v(a_\eta + 3\eta - 2u) + p_w(a_\zeta - \zeta) \end{aligned} \tag{5.89}$$

together with the differential equations for the momenta ($\dot{p}_i = -\partial H/\partial x_i$) in the form

$$\left.\begin{aligned} &\dot{p}_\xi = 0, && \dot{p}_\eta = -3p_v, && \dot{p}_\zeta = p_w, \\ &\dot{p}_u = -p_\xi + 2p_v, && \dot{p}_v = -p_\eta - 2p_u, && \dot{p}_w = -p_\zeta. \end{aligned}\right\} \tag{5.90}$$

The optimum thrust-acceleration program is given by the relationships ($\partial H/\partial a_i = 0$)

$$a_\xi = {}^1/_2 p_u, \quad a_\eta = {}^1/_2 p_v, \quad a_\zeta = {}^1/_2 p_w. \tag{5.91}$$

The equations for the momenta (5.90) are integrated independently of the main system (5.88), since the problem is linear, to yield

$$\left.\begin{aligned} &p_\xi = c_1, && p_u = 3c_1 t - 4c_2 \cos t + \\ &&& \quad + 4c_3 \sin t + 3c_5, \\ &p_\eta = -6(c_1 t - c_2 \cos t + && p_v = 2(c_1 + c_2 \sin t + c_3 \cos t), \\ &\quad + c_3 \sin t + c_5), \\ &p_\zeta = 2(c_4 \cos t + c_6 \sin t), && p_w = -2(c_4 \sin t - c_6 \cos t), \end{aligned}\right\} \tag{5.92}$$

where $c_1, \ldots, c_6$ are six unknown integration constants. These will be determined from the final conditions of (5.88) after the main system (5.88) and the optimum thrust-acceleration program (5.91) have been solved.

In (5.88), some of the phase coordinates at the end of the motion are unspecified. We shall write the corresponding transversality conditions for them. The final value of the coordinate ξ is unspecified too, and therefore the momentum p_ξ corresponding to it must vanish at $t = T$. We thus obtain, in accordance with the first equation of (5.92),

$$c_1 = 0. \tag{5.93}$$

219 The final values of ζ and w lie on the circle $\zeta^2(T) + w^2(T) = i^2$ and from the condition for an optimum it follows that the momentum vector (p_ζ, p_w) must

be directed along the radius (normal to the circle), i.e.,*

$$p_\zeta(T)/\zeta(T) = p_w(T)/w(T). \tag{5.94}$$

We now write the optimum control function of the thrust-acceleration components with respect to time, substituting (5.92) in (5.91), and taking (5.93) into account; this is expressed as

$$\left.\begin{aligned} a_\xi(t) &= -2c_2\cos t + 2c_3\sin t + {}^3/_2\,c_5,\\ a_\eta(t) &= c_2\sin t + c_3\cos t,\\ a_\zeta(t) &= -c_4\sin t + c_6\cos t. \end{aligned}\right\} \tag{5.95}$$

After functions (5.95 have been substituted in the right-hand side of equations (5.88), this system of nonhomogeneous linear equations with constant coefficients is integrated to give the results

$$\left.\begin{aligned} J(t) &= {}^1/_2\,(5c_2^2 + 5c_3^2 + {}^9/_2c_5^2 + c_4^2 + c_6^2)\,t - 6c_2c_5\sin t + \\ &\quad + 6c_3c_5(1-\cos t) + {}^1/_2\,(3c_2^2 - 3c_3^2 - c_4^2 + c_6^2)\sin t\cos t - \\ &\quad - (3c_2c_3 + c_4c_6)\sin^2 t,\\ \xi(t) &= c_2\,[8(1-\cos t) - 5t\sin t] + c_3(11\sin t - 5t\cos t - 6t) - \\ &\quad - c_5\,[{}^9/_4t^2 - 6(1-\cos t)],\\ \eta(t) &= {}^5/_2c_2(\sin t - t\cos t) + c_3\,[{}^5/_2t\sin t - 4(1-\cos t)] + \\ &\quad + 3c_5(\sin t - t),\\ \zeta(t) &= {}^1/_2c_4(t\cos t - \sin t) + {}^1/_2c_6t\sin t,\\ u(t) &= c_2(3\sin t - 5t\cos t) + c_3\,[5t\sin t - 6(1-\cos t)] - \\ &\quad - c_5\,({}^9/_2t - 6\sin t),\\ v(t) &= {}^5/_2\,c_2t\sin t + {}^1/_2c_3(5t\cos t - 3\sin t) - 3c_5(1-\cos t),\\ w(t) &= -{}^1/_2c_4t\sin t + {}^1/_2c_6(\sin t + t\cos t). \end{aligned}\right\} \tag{5.96}$$

Here we have taken into account the zero initial conditions (5.88) for all phase coordinates. The third, fifth, and sixth final conditions in (5.88) define the constants c_2, c_3, c_5 (motion in the plane of the initial orbit); we obtain a system of linear algebraic equations for them. The fourth final condition of (5.88) and the transversality condition (5.94) yield a system of two quadratic equations for the constants c_4 and c_6 (motion in a plane perpendicular to the plane of the initial orbit). We select the roots of this system which ensure that $J(T)$ is a minimum.

220 The final expressions for the constants $c_2, \ldots, c_6$ as functions of the parameters of the dynamic maneuver considered are

$$\left.\begin{aligned} &c_2 = \frac{2(r_1-1)\sin T}{16(1-\cos T) - T(5T+3\sin T)},\quad c_3 = \frac{-2(r_1-1)(1-\cos T)}{16(1-\cos T) - T(5T+3\sin T)},\\ &c_4 = \frac{\sqrt{2}\,i(1-\cos T)}{T+|\sin T|},\qquad c_5 = \frac{{}^1/_3(r_1-1)(5T+3\sin T)}{16(1-\cos T) - T(5T+3\sin T)},\\ &c_6 = \frac{\sqrt{2}\,i\sin T}{(1-\cos T)(T+|\sin T|)}\\ &(\text{for } T = 2\pi s,\ s = 1,2,\ldots:\ c_2 = c_3 = c_4 = 0,\ c_5 = (1-r_1)/3T,\\ &\qquad c_6 = 2i/T). \end{aligned}\right\} \tag{5.97}$$

* In /5.28/, the erroneous formula $p_\zeta(T) = 0$ was used instead of condition (5.94); the correct formulas were derived in /5.29/.

Substituting (5.97) in the first equation of (5.96), the functional of the problem is given by

$$J(T)=\frac{(r_1-1)^2(5T+3\sin T)}{4[T(5T+3\sin T)-16(1-\cos T)]}+\frac{2i^2}{T+|\sin T|}$$

$$\left(J(2\pi s)=\frac{(r_1-1)^2}{4T}+\frac{2i^2}{T}\right). \tag{5.98}$$

The expression obtained for the functional consists of two independent terms, the first of which is determined by the radius of the final orbit r_1, and the second by the angle of inclination of its plane i. This sum is associated with the fact that in a linear approximation the equations of motion in the plane of the initial orbit are unrelated to the equations of motion in the perpendicular plane.

We compare the functionals and the optimum thrust-acceleration programs obtained here and in §§ 3.1, 3.2. It will be assumed that the maneuvering time is a multiple of the period of motion along the initial orbit ($T = 2\pi s$, for $s = 1, 2, \ldots$). The first term of the functional (5.98) coincides with $J^{(1)}$ in (5.86), and the second one with (5.75). With the aid of (5.97), the optimum acceleration program (5.95) becomes

$$a_\xi(t)=\frac{1-r_1}{2T},\quad a_\eta(t)=0,\quad a_\zeta(t)=\frac{2i}{T}\cos t \tag{5.99}$$
$$(T=2\pi s,\ s=1,2,\ldots).$$

Since $a_\xi = -a_\varphi$, $a_\eta = a_r$, the first two relations of (5.99) give the optimum program (5.76) for the maneuver of changing the radius (with an accuracy of up to $o(r_1 - 1)$), and the last relation gives program (5.74) for the maneuver of changing the angle of inclination of the orbit plane (for $\Omega_1 = 0$). Thus, the complex maneuver of altering both the radius and angle of inclination
221 of a circular orbit is formulated linearly as a superposition of two simple maneuvers, namely, changing the radius and then rotating the plane of a circular orbit.

In addition to the solutions described above, many other solutions for the optimum maneuvers of guided satellites with ideal power-limited engines can be found in the literature. The differential equations are given in /5.30/, in which the final relations of the zero approximation for the optimum thrust-acceleration program are obtained when all the elements of the orbit change. The maneuvers of transfer between circular and elliptical coplanar orbits of different radii, and of build-up of a specified energy, etc., are treated in /5.31—5.33/ on the basis of Krylov—Bogolyubov's averaging method. The solution (5.95), (5.96) is used when studying the problems of optimum rendezvous of satellites /5.34/ and optimum interplanetary transfers /5.35/.

§ 4. PARAMETERS OF A VEHICLE WITH IDEAL POWER-LIMITED ENGINE

1. Formulas for calculations. In order to calculate the optimum working regime of an ideal power-limited engine, and the optimum parameters of

the engine and the vehicle as a whole, it is only necessary to know the functions

$$a(t), \quad J(t)=\int_0^t a^2 dt \tag{5.100}$$

representing respectively the control function of the thrust acceleration and the time integral of the square of the acceleration (cf. Chapter Four).

To understand this approach, we summarize here the necessary formulas for the case of a single-stage vehicle (without jettisoning sections of the propulsion system).

The weight parameters of the vehicle (G_π = payload, $G_{\mu 0}$ = weight of the working fluid, $G_\varkappa$ = weight of the propulsion system, $G(t)$ = variable engine weight) are determined by the following relationships (cf. (4.6), (4.15) to (4.17)):

$$\left.\begin{aligned} &\frac{G_\pi\,[\mathrm{kg}]}{G_0\,[\mathrm{kg}]}=(1-\sqrt{\Phi_1})^2, \quad \frac{G_{\mu 0}\,[\mathrm{kg}]}{G_0\,[\mathrm{kg}]}=\sqrt{\Phi_1}, \quad \frac{G_\varkappa\,[\mathrm{kg}]}{G_0\,[\mathrm{kg}]}=\sqrt{\Phi_1}-\Phi_1, \\ &\frac{G(t)\,[\mathrm{kg}]}{G_0\,[\mathrm{kg}]}=\left[1+\frac{G_0\,[\mathrm{kg}]}{G_\varkappa\,[\mathrm{kg}]}\,\Phi(t)\right]^{-1} \\ &\qquad (\Phi_1=\Phi(T),\ \Phi(t)=0.5\cdot 10^{-3}\alpha\,[\mathrm{kg/kw}]\,J(t)\,[\mathrm{m^2/sec^3}]), \end{aligned}\right\} \tag{5.101}$$

where G_0 is the take-off weight of the vehicle and α the weight of the propulsion system per unit jet power.

222 The maximum engine power $N_{\max}$, the thrust program $P(t)$, the exhaust velocity $V(t)$, and the propellant flow rate $q(t)$ are calculated by the formulas (cf. (4.2), (4.4))

$$\left.\begin{aligned} N_{\max}\,[\mathrm{kw}] &= \frac{G_\varkappa\,[\mathrm{kg}]}{\alpha\,[\mathrm{kg/kw}]}, \ \frac{P(t)\,[\mathrm{kg}]}{G_0\,[\mathrm{kg}]}=\frac{a(t)\,[\mathrm{m/sec^2}]}{9.81}\,\frac{G(t)\,[\mathrm{kg}]}{G_0\,[\mathrm{kg}]}, \\ V(t)\,[\mathrm{m/sec}] &= \frac{204\,G_\varkappa\,[\mathrm{kg}]/G_0\,[\mathrm{kg}]}{\alpha\,[\mathrm{kg/kw}]\ P(t)\,[\mathrm{kg}]/G_0\,[\mathrm{kg}]}, \\ q(t)\ [\mathrm{g/sec}] &= \frac{9.81\cdot 10^3\,P(t)\,[\mathrm{kg}]}{V(t)\,[\mathrm{m/sec}]}. \end{aligned}\right\} \tag{5.102}$$

We note that in order to calculate G_π, $G_{\mu 0}$, $G_\varkappa$, it suffices to know the final value of the functional $J(T)$, whereas when calculating $G(t)$, $P(t)$, $V(t)$, $q(t)$ we need both functions in (5.100).

If the maneuver is split into n consecutive stages, and the functions (5.100) are known at each stage, namely $a^{(i)}(\tau), J^{(i)}(\tau)$ $(0 \leqslant \tau \leqslant T^{(i)}, \ J^{(i)}(0)=0$, and the time τ and the functional J are measured at each stage from zero), the following expressions can be substituted in (5.101) and (5.102) for the functions $a(t)$ and $J(t)$ so that

$$\left.\begin{aligned} &a(t)=a^{(i)}\Big(t-\sum_{j=1}^{i-1}T^{(j)}\Big), \ J(t)=\sum_{j=1}^{i-1}J^{(j)}(T^{(j)})+J^{(i)}\Big(t-\sum_{j=1}^{i-1}T^{(j)}\Big) \\ &\text{for } \sum_{j=1}^{i-1}T^{(j)}<t<\sum_{j=1}^{i}T^{(j)} \ \Big(i=1,\ldots,n, \ \sum_{j=1}^{0}=0, \ \sum_{j=1}^{n}T^{(j)}=T\Big). \end{aligned}\right\} \tag{5.103}$$

2. Optimum parameters of interplanetary vehicles. The solution of the variational problem of the Earth—Mars—Earth flight (§ 2.7) will tell us something about the parameters of interplanetary vehicles with ideal power-limited engines.

For each pair of values of the total travel time T_σ and the time of sojourn in the vicinity of Mars T_ω, we may find the final value of the functional J from Figure 5.27. We then calculate G_π/G_0, $G_{\mu 0}/G_0$, $G_\varkappa/G_0$ by means of (5.101) (where the unit weight α of the engine is specified). Figure 5.30, taken from /5.17/, shows the dependence of the maximum payload G_π/G_0 on the time $T_\sigma - T_\omega$ for different values of the unit weight α and the time T_ω. The values of $G_{\mu 0}/G_0$ and $G_\varkappa/G_0$ can be found from Figure 4.2 using the known value of G_π/G_0.

If a payload level is specified, it is possible to find the corresponding minimum travel times from Figure 5.30. Such values are given in Table 5.6 for $G_\pi/G_0 = 0.3$.

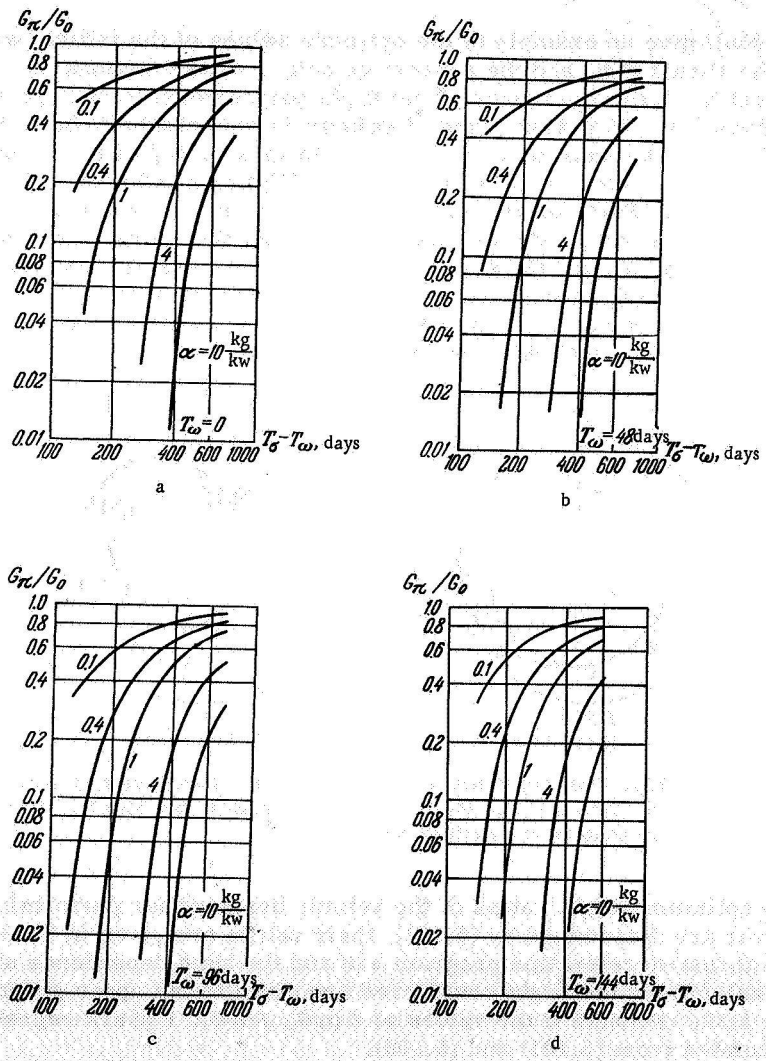

FIGURE 5.30. Maximum payload G_π/G_0 of Earth—Mars—Earth vehicle with ideal power-limited engine as function of the total travel time $T_\sigma - T_\omega$ for fixed values of unit engine weight α and sojourn time T_ω in the field of Mars.

TABLE 5.6. Minimum times T_σ of Earth—Mars—Earth expedition at 30% payload level for different values of α (unit engine weight) and T_ω (sojourn time in the field of Mars).

T_ω, days	T_σ, days				
	$\alpha = 0.1$ kg/kw	$\alpha = 0.4$ kg/kw	$\alpha = 1$ kg/kw	$\alpha = 4$ kg/kw	$\alpha = 10$ kg/kw
0	90	160	255	460	680
48	157	238	326	514	738
96	223	304	386	566	806
144	282	358	440	624	884

We shall give an example of the optimum values of the vehicle weight $G(t)$, the thrust $P(t)$, and the exhaust velocity $V(t)$ as functions of the time t. We select the following values of the flight parameters: total flight time T_σ = = 644 days ($\approx$ 1.76 years), time of sojourn in the neighborhood of Mars T_ω = 48 days. We shall make use of calculations /5.14/ of the optimum heliocentric trajectories, allowing for the ellipticity and noncoplanarity of the Mars and Earth orbits for specific departure dates (Figure 5.31). For greater accuracy, we also take into account the energy expended for the deceleration J_{-2} and the acceleration J_{+2} in the neighborhood of Mars. These are determined from Figure 5.25, assuming that $T_{-2} = T_{+2} = {}^1/_2 T_\omega$.

225 A summary of the parameters of the elementary maneuvers forming the Earth—Mars—Earth flight is given in Table 5.7.

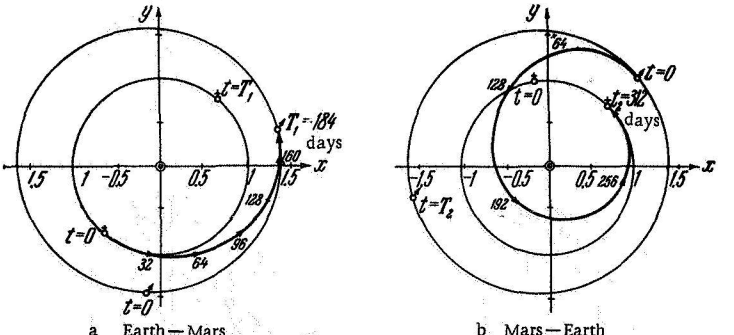

a Earth—Mars b Mars—Earth

FIGURE 5.31. Trajectory of heliocentric sections of Earth—Mars—Earth flight with parameters. Total time T_σ = 644 days, sojourn time in the field of Mars T_ω = 48 days (trajectories projected on the ecliptic plane).

The optimum weight ratios of the vehicle designed for performing this maneuver are determined by (5.101); their values are given in Table 5.8.

The thrust-acceleration program $a(t)$ and the time dependence of the functional $J(t)$ for the flight considered are given in the upper graph of Figure 5.32. Beneath it the values of $G(t)/G_0$, $P(t)/G_0$, $V(t)$ are represented, as calculated from (5.101) and (5.102).

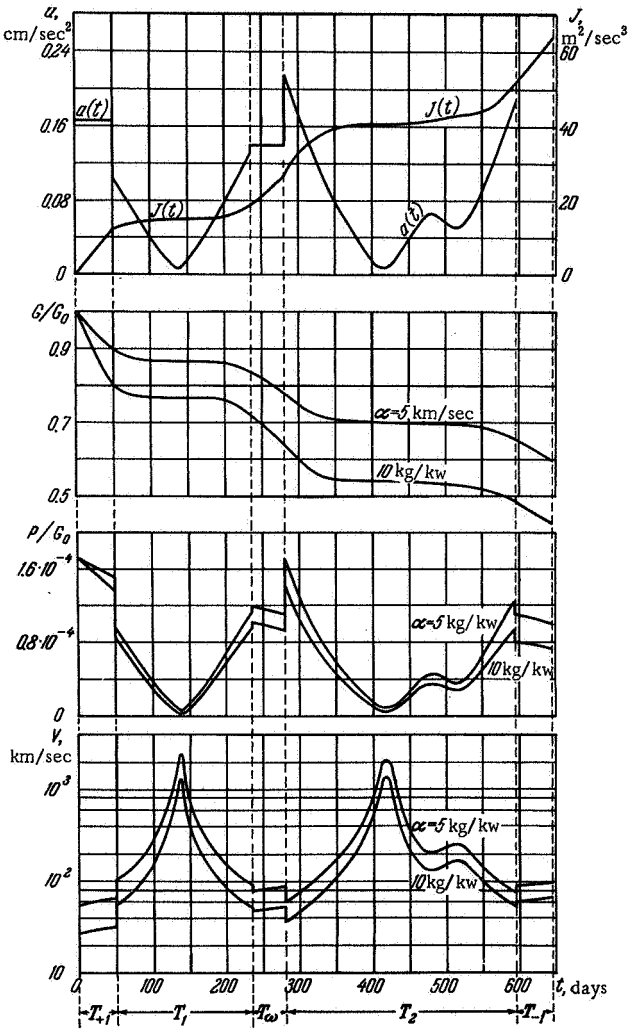

FIGURE 5.32. Example of optimum relationships, where $a(t)$ is the thrust acceleration, $J(t)$ the functional, $G(t)$ the total weight, $P(t)$ the thrust, and $V(t)$ is the exhaust velocity, for the Earth—Mars—Earth flight (T_σ = = 644 days = total time); T_ω = 48 days = $T_{-2} + T_{+2}$ is the sojourn time on Mars, T_{+1} is time spent on the Earth, T_1 is Earth—Mars flight time, T_2 is Mars—Earth flight time, T_{-1} is deceleration time in Earth's field.

TABLE 5.7. Parameters of optimum Earth—Mars—Earth flight (T_σ = 644 days, T_ω = 48 days)

Maneuver	Starting date of maneuver	Date at end of maneuver	Maneuver time, days	Energy expended J, m^2/sec^3
Acceleration in Earth's field	24 March 1971	12 May 1971	50	12
Orbital transfer Earth—Mars	13 May 1971	12 November 1971	184	6.6
Deceleration and acceleration in Mars' field	13 November 1971	30 December 1971	48	8
Orbital transfer Mars—Earth	31 December 1971	7 November 1972	312	25
Deceleration in Earth's field	8 November 1972	27 December 1972	50	12
Total flight Earth—Mars—Earth	24 March 1971	27 December 1972	644	63.6

TABLE 5.8. Optimum distribution of vehicle weight for Earth—Mars—Earth flight (T_σ = 644 days, T_ω = 48 days) for two values of the unit weight of the propulsion system

Unit weight of engine α, kg/kw	Payload G_π/G_0	Engine weight $G_\varkappa/G_0$	Working-fluid weight G_{μ_0}/G_0
5	0.36	0.24	0.4
10	0.19	0.24	0.57

We shall point out two characteristic features of the optimum working regimes of ideal engines in interplanetary flights. These are important
227 in what follows. In the first place, the ideal engine operates throughout the entire flight, and therefore a working-fluid reserve sufficient to burn for 10^4 hours is required. Secondly, according to the optimum program it is necessary to vary the thrust, exhaust velocity, and propellant flow rate through a very large range. Thus, in Figure 5.32 P and V vary by an order of magnitude.

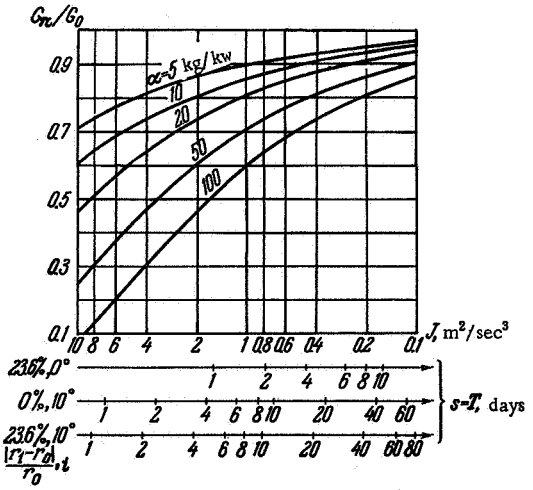

FIGURE 5.33. Maximum payload G_π/G_0 of guided satellites with ideal power-limited engine for maneuvers involving change of angle of inclination i and radius $r_0 \to r_1$ for a circular orbit (axes marked according to maneuvering time T for a 24-hour Earth satellite, $r_0 = 42.3 \cdot 10^3$ km, $s = T$ = number of revolutions).

3. Optimum parameters of guided satellites. We shall write the optimum functions (5.100) in dimensional form for the following maneuvers in the neighborhood of a planet (cf. § 3).

1) For a rotation of the plane of a circular orbit of radius r_0 through an angle i with given angular position of the nodal line Ω_1, the optimum functions are (cf. (5.74), (5.75))

$$a(t) = kr_0^{-2}\frac{i}{\pi s}\cos(\tau - \Omega_1),$$
$$J(t) = k^{3/2}r_0^{-5/2}\frac{i^2}{2\pi^2 s^2}[\tau + \sin\tau\cos(\tau - 2\Omega_1)]. \qquad (5.104)$$

2) For the transfer between circular coplanar orbits of radii r_0 and r_1 the optimum functions are (cf. (5.76), (5.77))

$$a(t) = kr_0^{-2}\frac{1}{2\pi s}\left|1 - \sqrt{\frac{r_0}{r_1}}\right|, \quad J(t) = k^{3/2}r_0^{-5/2}\frac{1}{4\pi^2 s^2}\left(1 - \sqrt{\frac{r_0}{r_1}}\right)^2\tau. \qquad (5.105)$$

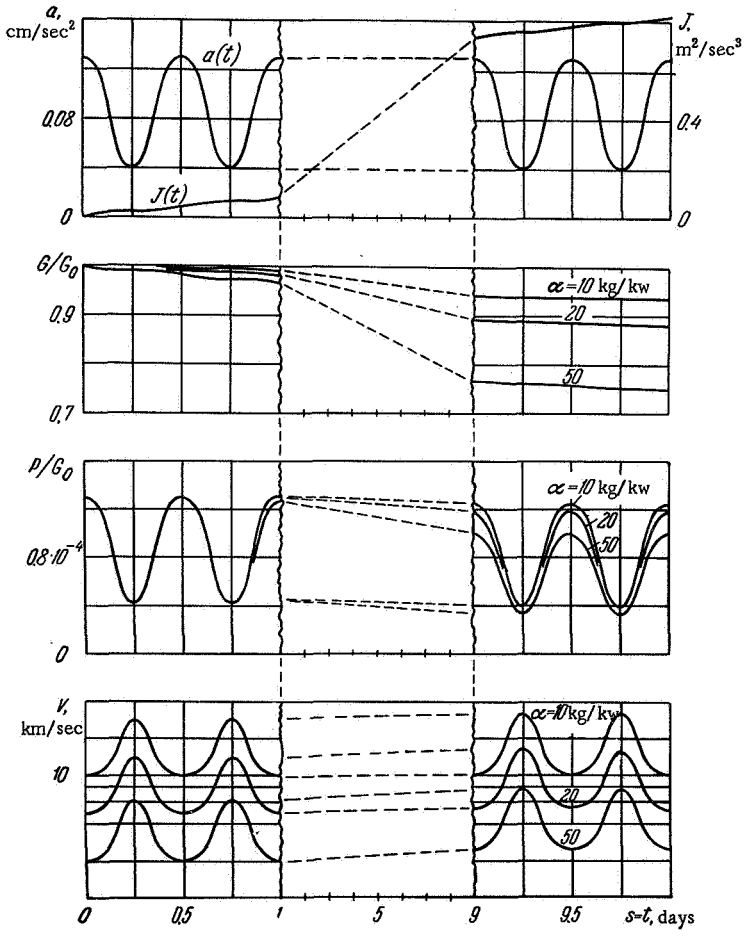

FIGURE 5.34. Example of optimum relations $a(t)$, $J(t)$, $G(t)$, $P(t)$, $V(t)$ for the maneuver of rotating the plane of a circular orbit through an angle $i = 10°$ whilst simultaneously varying the radius so that $|(r_1/r_0) - 1| = 23.6\%$ (24-hour Earth satellite, with $r_0 = 42.3 \cdot 10^2$ km, $s = 10$, $T = 10$ days, where the intermediate revolutions $1 < S < 9$ only are indicated).

229 3) For the transfer between circular orbits of radii r_0 and r_1, whose planes form an angle i, the optimum functions are (cf. (5.96) to (5.99))

$$a(t) = kr_0^{-2}\frac{1}{\pi s}\left[\left(\frac{r_1 - r_0}{4r_0}\right)^2 + i^2\cos^2\tau\right]^{1/2},$$
$$J(t) = k^{3/2}r_0^{-3/2}\frac{1}{2\pi^2 s^2}\left[2\left(\frac{r_1 - r_0}{4r_0}\right)^2\tau + i^2(\tau + \sin\tau\cos\tau)\right]. \qquad (5.106)$$

In formulas (5.104) to (5.106) the maneuvering time T is taken as a multiple of the period of revolution ($s = 1, 2, \ldots$) along the initial orbit, given by $2\pi k^{-1/2}r_0^{3/2}$. The time τ is dimensionless ($0 \leqslant \tau \leqslant 2\pi s$) and is related to the dimensional time by $t = k^{-1/2}r_0^{3/2}\tau$. The other quantities are given in the following units: $[a] = \mathrm{m/sec^2}$, $[J] = \mathrm{m^2/sec^3}$, $[k] = \mathrm{m^3/sec^2}$ (for the Earth $k = 0.3986 \cdot 10^{15}\ \mathrm{m^3/sec^2}$), $[r_0] = [r_1] = \mathrm{m}$, and i and Ω_1 are angles expressed in radians.

The relative payload G_π/G_0 is again calculated by (5.101) and shown in Figure 5.33 as a function of J and the time T for maneuvers 1 to 3. The curves were calculated for fixed values of the unit engine weight α. Several time scales for different sets of maneuver parameters (r_0, i, r_1) of a 24-hour Earth satellite are given on the graph. Examples of the functions $G(t)$, $P(t)$, $V(t)$, corresponding to (5.104) to (5.106) are shown in Figure 5.34.

Compared with the case of interplanetary flight considered above, the working conditions of an ideal engine for guided satellites are somewhat more lenient; the necessary range of variation of the controlled parameters is fairly narrow for many of the maneuvers.

Chapter Six

UNTHROTTLED ENGINES. SEPARATION OF THE VARIATIONAL PROBLEM. OPTIMUM PROGRAMS OF THE THRUST VECTOR

230 Ideal engines must be ideally throttled, i.e., the only limitations imposed on their control must be those inherent in the type of engine studied (such as the limitations imposed on the power (Chapters Four and Five) or the exhaust velocity (Chapter Eight)).

The solution of the optimization problem with this formulation usually leads to impracticable control functions for some of the engine parameters.

This chapter treats the other extreme of the control possibilities, namely, the unthrottled engine.

An engine is u n t h r o t t l e d if it can either be fired so that the thrust P and the propellant flow rate q are constant, or cut off so that the thrust P and the propellant flow rate vanish. No restrictions are imposed on the change in thrust direction.

As with ideal engines, the variational problem is separated into weight and dynamic parts. It differs from the ideal case in that the dynamic part contains two engine parameters P and q; it is, however, applicable to all types of unthrottled engines (a knowledge of the characteristics (A.9) and (A.10) is unnecessary for its solution). After establishing this fact we proceed to calculate the functional of the dynamic part for a number of maneuvers; examples of the solution of the weight part of the problem are given for power-limited unthrottled engines.

§ 1. SEPARATING THE VARIATIONAL PROBLEM INTO WEIGHT AND DYNAMIC PARTS

1. Statement of the problem. We introduce the Dirac function $\delta(t)$, whose value is 1 when the engine is fired, and 0 when it is cut off. The thrust $P(t)$ and the propellant flow rate $q(t)$ of the unthrottled engine can be written in the form $P\delta(t)$ and $q\delta(t)$. In this notation P and q are constant control parameters, and the function $\delta(t)$ defines engine firings and cutoffs.

231 The variational problem for the delivery of maximum payload is written in the form (A.8)

$$\begin{aligned} &\dot{G}_\sigma = -gq\delta, && G_\sigma(0) = G_0 - G_\varkappa, && G_\sigma(T) = \max, \\ &\dot{\mathbf{r}} = \mathbf{v}, && \mathbf{r}(0) = \mathbf{r}_0, && \mathbf{r}(T) = \mathbf{r}_1, \\ &\dot{\mathbf{v}} = \frac{gP\delta}{G_\sigma + G_\varkappa}\mathbf{e} + \mathfrak{R}, && \mathbf{v}(0) = \mathbf{v}_0, && \mathbf{v}(T) = \mathbf{v}_1 \\ &(P, q = \text{const}, && \delta(t) = 1 \text{ or } 0, && |\mathbf{e}(t)| \equiv 1). \end{aligned} \tag{6.1}$$

Here the engine weight must be expressed via the parameters P and q in the form $G_\varkappa(P, q)$. In the variational problem (6.1) the optimum programs $\mathbf{e}(t)$ and $\delta(t)$ must be found together with the optimum values of the parameters P and q. Instead of directly using P and q, one may employ other parameters of the engine.

2. **Separation of the dynamic part of the problem.** The various features of the engine when functioning in an unthrottled regime are determined only by the functional relationship $G_\varkappa(P, q)$. The optimum unthrottled engine can be found by separating the variational problem into two parts: a dynamic part, for which one does not need to know the function $G_\varkappa(P, q)$ (and which is thus general), and a weight part, for which the function $G_\varkappa(P, q)$ must be known.

We introduce a new phase coordinate $t_\mu(t)$, which is the instantaneous operating time of the engine, and defined by the following differential equation and initial value /6.1, 6.2/

$$\dot{t}_\mu = \delta, \quad t_\mu(0) = 0. \tag{6.2}$$

The third equation of (6.1) is integrated to give

$$G(t) = G_0 - G_\varkappa(P, q) - gqt_\mu(t), \tag{6.3}$$

and the payload G_π is expressed in terms of the parameters P and q and the final operating time of the engine $t_\mu(T) = T_\mu$ in the form

$$G_\pi = G_0 - G_\varkappa(P, q) - gqT_\mu. \tag{6.4}$$

If P and q are fixed, the maximum payload G_π will correspond to the minimum time T_μ.

We now replace the functional in the variational problem. Instead of looking for the maximum G_π, we shall look for the minimum T_μ for fixed P and q. The variational problem obtained takes the form (cf. (6.3))

$$\left.\begin{array}{llll} \dot{t}_\mu = \delta, & t_\mu(0) = 0, & t_\mu(T) = \min, \\ \dot{\mathbf{r}} = \mathbf{v}, & \mathbf{r}(0) = \mathbf{r}_0, & \mathbf{r}(T) = \mathbf{r}_1, \\ \dot{\mathbf{v}} = \frac{a_0\delta}{1-\mu t_\mu}\mathbf{e} + \mathbf{R}, & \mathbf{v}(0) = \mathbf{v}_0, & \mathbf{v}(T) = \mathbf{v}_1 \\ (a_0, \mu = \text{const}, \ \delta(t) = 1 \text{ or } 0, \ |\mathbf{e}(t)| \equiv 1). & & \end{array}\right\} \tag{6.5}$$

232 In this notation $a_0 = gP/G_0$, $\mu = gq/G_0$ are the parameters of the problem (representing the initial thrust acceleration and the unit propellant flow rate). Instead of μ one frequently uses the exhaust velocity $V = a_0/\mu$. In the limit $\mu \to 0$ or $V \to \infty$ we obtain the case of constant thrust acceleration $a(t) \equiv a_0$.

The variational problem (6.5) represents the dynamic part of the general problem; its solution takes the form $T_\mu(gP/G_0, gq/G_0)$.

If the functions $T_\mu(gP/G_0, gq/G_0)$ and $G_\varkappa(P, q)$ are known, it is possible to solve the remaining (weight) part of the variational problem, i.e., to find the maximum payload with respect to the parameters P and q, where

$$\max G_\pi = \max_{P,q}\left[G_0 - G_\varkappa(P, q) - gqT_\mu\left(\frac{gP}{G_0}, \frac{gq}{G_0}\right)\right]. \tag{6.6}$$

We note the following points:

1) We can use a different procedure to separate that part which does not depend on the form of $G_x(P, q)$, from the general variational problem. If, in place of $t_\mu(t)$, we introduce the phase coordinate

$$G(t) = G_x + G_\sigma(t), \tag{6.7}$$

representing the instantaneous total weight, we obtain the same result. The following relationship obviously exists between the functionals $G(T) = G_1$ and $t_\mu(T) = T_\mu$:

$$G_1 = G_0 - gqT_\mu \quad \text{or} \quad G_1/G_0 = 1 - \mu T_\mu. \tag{6.8}$$

2) If the solution of the variational problem (6.5) indicates that $\delta(t) \equiv 1$ at $0 \leqslant t \leqslant T$, i.e., that the minimum engine operating time T_μ is equal to the specified maneuvering time T, formulation (6.5) becomes meaningless. In this case it is necessary either to reject the separation of the dynamic part of the problem and return to formulation (6.1), or to reformulate the problem so that the time T_μ is specified, and we need to find the minimum of T.

The new variational problem is the minimum-time problem:

$$\left.\begin{array}{llll} \dot{t}_\mu = \delta, & t_\mu(0) = 0, & t_\mu(T) = T_\mu, & \\ \dot{\mathbf{r}} = \mathbf{v}, & \mathbf{r}(0) = \mathbf{r}_0, & \mathbf{r}(T) = \mathbf{r}_1, & T = \min, \\ \dot{\mathbf{v}} = \frac{a_0\delta}{1-\mu t_\mu}\mathbf{e} + \mathbf{R}, & \mathbf{v}(0) = \mathbf{v}_0, & \mathbf{v}(T) = \mathbf{v}_1 & \\ (a_0, \mu = \text{const}, & \delta(t) = 1 \text{ or } 0, & |\mathbf{e}(t)| \equiv 1). & \end{array}\right\} \tag{6.9}$$

In this case $\delta(t) \equiv 1$ is obtained when the time T_μ is unspecified, i.e., $t_\mu(T) = \text{opt}$ (cf. § 2.1).

3) If the engine-operating time is limited (the total resources of the propulsion system are specified (cf. § 2 of Chapter Seven)), the formulation of the variational problem (6.5) can be preserved. Its solution yields a
233 function of the form $T_\mu(gP/G_0, gq/G_0)$, and an additional condition gives the relation between gP/G_0 and gq/G_0, where

$$T_\mu(gP/G_0, gq/G_0) \leqslant \tau. \tag{6.10}$$

The quantity τ is the given value of the engine-operating time. The solution of the weight part of the problem now reduces to finding the maximum of (6.6) under condition (6.10).

4) Allowance for the weight component G_β, i.e., for the weight of the working-fluid tanks (cf. § 1 of Chapter Seven), can be made in the weight part of the variational problem by replacing (6.6) by

$$\max G_\pi = \max_{P,q}\left[G_0 - G_x(P, q) - (1+\beta)\, gqT_\mu\left(\frac{gP}{G_0}, \frac{gq}{G_0}\right)\right]. \tag{6.11}$$

§ 2. EQUATIONS FOR THE OPTIMUM THRUST VECTOR PROGRAM. SIMILARITY PROBLEMS

1. Arbitrary gravitational field. The relationships determining the optimum thrust program are based on the maximum principle. The two formulations examined, (6.5) and (6.9), are identical except for one boundary condition. For specific maneuvers, the choice of this boundary condition will depend on the primary source.

The Hamiltonian of the dynamic part of the problem, and the equations of the momenta, take the forms

$$H = p_\mu \delta + (\mathbf{p}_v \cdot \mathbf{e}) \frac{a_0 \delta}{1 - \mu t_\mu} + (\mathbf{p}_v \cdot \mathbf{R}) + (\mathbf{p}_r \cdot \mathbf{v}), \tag{6.12}$$

and

$$\dot{p}_\mu = -\frac{\partial H}{\partial t_\mu} = -(\mathbf{p}_v \cdot \mathbf{e}) \frac{a_0 \mu \delta}{(1 - \mu t_\mu)^2},$$
$$\dot{\mathbf{p}}_r = -\frac{\partial}{\partial \mathbf{r}} (\mathbf{p}_v \cdot \mathbf{R}), \quad \dot{\mathbf{p}}_v = -\mathbf{p}_r. \tag{6.13}$$

The optimum relations for the control functions $\mathbf{e}(t)$ and $\delta(t)$ are found from the condition that (6.12) be an absolute maximum for the corresponding variable (since in both problems we seek the minimum of the functionals T_μ and T in (6.5) and (6.9) respectively).

The optimum program obtained for the thrust direction is (max H with respect to $\mathbf{e}$, where $|\mathbf{e}(t)| \equiv 1$):

$$\mathbf{e} = \mathbf{p}_v / p_v \qquad (p_v = |\mathbf{p}_v|). \tag{6.14}$$

Allowing for (6.14), we obtain the following definition of the function $\delta(t)$,
234 expressing engine firings ($\delta = 1$) and cutoffs ($\delta = 0$) (max H with respect to δ):

$$\delta = \begin{cases} 1 & \text{for } \Delta > 0, \\ 0 & \text{for } \Delta < 0, \end{cases} \qquad \Delta = p_\mu + p_v \frac{a_0}{1 - \mu t_\mu}; \tag{6.15}$$

the singular case $\Delta = 0$, $\dot{\Delta} = 0$ can happen only for $\dot{p}_v = 0$ (§ 2.3, cf. /6.3/ for more detail).

We now write the boundary condition corresponding to the functional of the problem. In formulation (6.5) the functional is the final value of the phase coordinate $t_\mu(T)$; the corresponding boundary condition here is $p_\mu(T) < 0$, or, after normalization,

$$p_\mu(T) = -1. \tag{6.16}$$

In formulation (6.9) the functional is the time T, and therefore the boundary condition will be $H(T) > 0$, or, after normalization

$$H(T) = \left(p_\mu(T) + p_v(T) \frac{a_0}{1 - \mu T_\mu}\right) \delta(T) + \mathbf{p}_v(T) \cdot \mathbf{R}(\mathbf{r}(T), T) + \mathbf{p}_r(T) \cdot \mathbf{v}(T) = 1. \tag{6.17}$$

Thus, the complete system of equations of the optimum motion consists of (6.5) and (6.13) to (6.16) in case (6.5), and of (6.9), (6.13) to (6.15), and (6.17) in case (6.9).

We shall now consider how to obtain the optimum region $\delta(t) \equiv 1$ for (6.9) (cf. note § 1.2). Let $t_\mu(T)$ be unspecified. Then, according to the optimality condition $p_\mu(T) = 0$. The derivative of the momentum p_μ, according to (6.13), (6.14), is always nonpositive, so that

$$\dot{p}_\mu = -p_v \frac{a_0 \mu \delta}{(1-\mu t_\mu)^2} \leqslant 0 \quad \text{for} \quad 0 \leqslant t \leqslant T, \tag{6.18}$$

and therefore in the given case $p_\mu(t) \geqslant 0$ for $0 \leqslant t \leqslant T$ and from (6.15), $\delta(t) \equiv 1$. The latter condition means that the engine is never cut off ($T_\mu = T$).

If $T_\mu < T$, it follows from (6.15) that $p_\mu(T) < 0$, while in the opposite case $\delta(t) \equiv 1$ and $T_\mu = T$.

2. Central field. The equations of optimum motion in a central gravitational field are obtained as a particular case of (6.5) and (6.13) to (6.16), or (6.9), (6.13) to (6.15), and (6.17) for

$$\mathbf{R}(\mathbf{r}, t) = -k\mathbf{r}/r^3.$$

235 For plane motion in polar coordinates (A.8) they take the form (without the boundary conditions)

$$\left.\begin{aligned}
&\dot{t}_\mu = \delta, && \dot{p}_\mu = -\sqrt{p_{v_r}^2 + p_{v_\varphi}^2}\,\frac{a_0\mu\delta}{(1-\mu t_\mu)^2},\\
&\dot{r} = v_r, && \dot{p}_r = p_\varphi \frac{v_\varphi}{r^2} + p_{v_r}\left(\frac{v_\varphi^2}{r^3} - \frac{2}{r^3}\right) - \\
& && \qquad - p_{v_\varphi}\frac{v_r v_\varphi}{r^2},\\
&\dot{\varphi} = v_\varphi/r, && \dot{p}_\varphi = 0,\\
&\dot{v}_r = \frac{a_0\delta}{1-\mu t_\mu}\frac{p_{v_r}}{\sqrt{p_{v_r}^2 + p_{v_\varphi}^2}} + && \dot{p}_{v_r} = -p_r + p_{v_\varphi}\frac{v_\varphi}{r},\\
&\qquad + \frac{v_\varphi^2}{r} - \frac{1}{r^2}, && \\
&\dot{v}_\varphi = \frac{a_0\delta}{1-\mu t_\mu}\frac{p_{v_\varphi}}{\sqrt{p_{v_r}^2 + p_{v_\varphi}^2}} - && \dot{p}_{v_\varphi} = \frac{1}{r}(p_{v_\varphi} v_r - 2p_{v_r} v_\varphi - p_\varphi)\\
&\qquad - \frac{v_r v_\varphi}{r}, && \\
&\qquad (\delta = 1 \text{ for } \Delta > 0,\ \delta = 0 \text{ for } \Delta < 0, && \\
&\qquad \Delta = p_\mu + a_0\sqrt{p_{v_r}^2 + p_{v_\varphi}^2}(1-\mu t_\mu)^{-1}). &&
\end{aligned}\right\} \tag{6.19}$$

Here, all magnitudes are dimensionless and we choose the same characteristic values as in the corresponding sections of Chapter Five. The characteristic value for the parameter μ is inversely proportional to the characteristic time t_*. The boundary values for r, φ, v_r, and v_φ are written according to the dynamic maneuver considered, and we impose the conditions $t_\mu(0) = 0$ and (6.16) in formulation (6.5), or $t_\mu(0) = 0$ and (6.17) in formulation (6.9).

System (6.19) has two first integrals, namely, $p_\varphi(t) = \text{const}$ and $H(t) = \text{const}$, since the angle φ and the time t do not appear explicitly on the right-hand sides of the equations.

Equations (6.19) are invariant relative to the following two transformations, analogous to (5.15) and (5.16):

the linear transformation

$$\left.\begin{array}{llllll} t_\mu \to l^{3/2}t_\mu, & r \to lr, & \varphi \to \varphi, & v_r \to l^{-1/2}v_r, & v_\varphi \to l^{-1/2}v_\varphi, \\ p_\mu \to l^{-2}p_\mu, & p_r \to l^{-3/2}p_r, & p_\varphi \to l^{-1/2}p_\varphi, & p_{v_r} \to p_{v_r}, & p_{v_\varphi} \to p_{v_\varphi}, \\ & t \to l^{3/2}t, & a_0 \to l^{-2}a_0, & \mu \to l^{-3/2}\mu; & \end{array}\right\} \quad (6.20)$$

236 and the sign-inversion transformation

$$\left.\begin{array}{llllll} t_\mu \to -t_\mu, & r \to r, & \varphi \to -\varphi, & v_r \to -v_r, & v_\varphi \to v_\varphi, \\ p_\mu \to p_\mu, & p_r \to -p_r, & p_\varphi \to p_\varphi, & p_{v_r} \to p_{v_r}, & p_{v_\varphi} \to -p_{v_\varphi}, \\ & t \to -t, & a_0 \to a_0, & \mu \to -\mu. & \end{array}\right\} \quad (6.21)$$

Unlike the case in § 1 of Chapter Five, the use here of transformation (6.21) for passing from the outbound trajectory to the return trajectory is difficult, since it is necessary to have outbound trajectories with negative values of the propellant flow rate ($\mu \to -\mu$).

3. Plane-parallel field. If the gravitational acceleration is taken as constant ($\mathfrak{R}(r, t) \equiv$ const, cf. (A.52)), the system of equations for optimum motion is simplified. The momenta $\mathbf{p}_r$ and $\mathbf{p}_v$ are expressed in a finite form

$$\mathbf{p}_r = \mathbf{b}_1, \quad \mathbf{p}_v = \mathbf{b}_2 - \mathbf{b}_1 t, \quad (6.22)$$

where $\mathbf{b}_1$ and $\mathbf{b}_2$ are constant vectors, determined from the boundary conditions.

We may determine the thrust direction according to (6.14) so that

$$\mathbf{e}(t) = \frac{\mathbf{b}_2 - \mathbf{b}_1 t}{\sqrt{b_2^2 - 2\mathbf{b}_2 \cdot \mathbf{b}_1 t + b_1^2 t^2}}. \quad (6.23)$$

For one-dimensional motions (§§ 2.4, 2.5), when the thrust can be directed either along or in the opposite direction to the velocity, this relationship reduces to

$$e(t) = \operatorname{sgn}(b_2 - b_1 t). \quad (6.24)$$

The firing and cutoff condition (6.15), together with equation (6.22) for the momentum $\mathbf{p}_v$, make it possible to draw the following conclusion regarding the number of coasting periods. During a coasting period the relations $\delta(t) = 0$, $p_\mu = \text{const}$, $t_\mu = \text{const}$ are satisfied (cf. (6.13)), and therefore at the beginning ($t = t_1$) and ($t = t_2$) we must have $p_v(t_1) = p_v(t_2)$ from the condition $\Delta(t_1) = \Delta(t_2) = 0$. Since for a plane-parallel field the inverse function of $p_v(t)$ is double-valued in the general case, no more than one coasting period can exist in the optimum trajectory /6.1, 6.3/.

4. Velocity build-up in a gravitation-free field. The differential equations and boundary conditions (6.5) reduce to the following for the build-up maneuver of a specified velocity magnitude (cf. (A.64)):

$$\left.\begin{array}{llll} \dot{t}_\mu = \delta, & t_\mu(0) = 0, & t_\mu(T) = \min, & \\ \dot{u} = \frac{a_0\delta}{1 - \mu t_\mu} e, & u(0) = 0, & u(T) = u_1 & \\ (a_0, \mu = \text{const}, \ \delta(t) = 1 \text{ for } 0, \ e(t) = \pm 1). & & & \end{array}\right\} \quad (6.25)$$

237 The Hamiltonian and the momenta are represented here by the expressions

$$H = \left(p_\mu + p_u \frac{a_0 e}{1-\mu t_\mu}\right)\delta, \qquad \dot{p}_\mu = -\, p_u \frac{a_0 e \mu \delta}{(1-\mu t_\mu)^2}, \qquad (6.26)$$
$$p_\mu(T) = -1, \quad \dot{p}_u = 0.$$

The maximum of H with respect to e is attained when $e(t) = \operatorname{sgn} p_u = \text{const}$, and assuming $u_1 > 0$ we obtain

$$e(t) \equiv 1 \qquad (p_u > 0). \qquad (6.27)$$

The expression Δ (cf. (6.15)), which occurs in (6.26), is constant in view of differential equations (6.25) and (6.26); therefore

$$\delta(t) \equiv \begin{cases} 1 & \text{for } \Delta(0) > 0, \\ 0 & \text{for } \Delta(0) < 0, \end{cases} \qquad \Delta = p_\mu + p_u \frac{a_0}{1-\mu t_\mu}. \qquad (6.28)$$

The second case in (6.28) reduces to the trivial case $u_1 = 0$. One still needs to consider $\Delta(0) = 0$, for which the function H will be independent of δ (since $\Delta(t) \equiv 0$); the distribution of engine firing and cutoff times can be arbitrary, and only the total duration of the powered flight periods is determined (from the condition $u(T) = u_1$).

If the equation for u in (6.25) is integrated using condition (6.27), we obtain the finite relationship (the Tsiolkovskii formula)

$$u_1 = -\frac{a_0}{\mu} \ln(1 - \mu T_\mu), \qquad (6.29)$$

whereby we may express the total engine operating time T_μ in terms of the maneuver parameter u_1 and the engine parameters a_0 and μ. The total time of motion T does not affect the functional T_μ; it coincides with T_μ when $\Delta(0) > 0$, and is larger than T_μ when $\Delta(0) = 0$. The final expression for the functional T_μ is

$$T_\mu = \frac{1}{\mu}\left(1 - e^{-\frac{\mu}{a_0} u_1}\right) = \frac{V}{a_0}\left(1 - e^{-u_1/V}\right) \leqslant T. \qquad (6.30)$$

When finding the maximum payload for the parameters a_0 and μ (which will be carried out in § 5), we see that in the optimum case $T_\mu = T$.

5. Displacement between points of rest in a gravitation-free field.

238 For flight between two positions of rest, the differential equations and boundary conditions (6.5) reduce to the following (cf. (A.65)):

$$\left.\begin{aligned} &\dot{t}_\mu = \delta, && t_\mu(0) = 0, && t_\mu(T) = \min, \\ &\dot{x} = u, && x(0) = 0, && x(T) = l, \\ &\dot{u} = \frac{a_0 \delta}{1-\mu t_\mu} e, && u(0) = 0, && u(T) = 0 \\ &(a_0, \mu = \text{const}, \ \delta(t) = 1 \text{ or } 0, \ e(t) = \pm 1). \end{aligned}\right\} \qquad (6.31)$$

The equations for the momenta p_x and p_u are integrable (cf. (6.22) for the x component). The optimum thrust direction (parallel or in the opposite direction to the velocity vector) is determined by (6.24), from which the

sign of the constants b_1 and b_2 may be found. According to (6.24), the thrust direction cannot be reversed more than once. The boundary conditions (6.31) for x and u are such that at the beginning of the motion the thrust is directed along the velocity, and at the end it points in the opposite direction. It follows that $b_1 > 0$, $b_2 < 0$ and that the time t_* at which p_u vanishes ($b_2 - b_1 t_* = 0$) lies within the interval $[0, T]$. Therefore, (6.22) and (6.24) can be rewritten as

$$p_x = b_1,\ p_u = b_1(t_* - t),\ e = \operatorname{sgn}(t_* - t) \quad (b_1 > 0,\ 0 < t_* < T), \tag{6.32}$$

i.e., in the interval $0 \leqslant t < t_*$ the thrust is directed along the velocity, and in the interval $t_* < t \leqslant T$ in the opposite direction (Figure 6.1). The function Δ, which determines the engine firing and cutoff times (cf. (6.15)), is given here by

$$\Delta = p_\mu + b_1 |t_* - t| \frac{a_0}{1 - \mu t_\mu}. \tag{6.33}$$

In order to determine the behavior of the function Δ, we write its derivative as

$$\dot{\Delta} = -b_1 \frac{a_0}{(1 - \mu t_\mu)^2} \operatorname{sgn}(t_* - t) \qquad (t \neq t_*) \tag{6.34}$$

(the expressions for $\dot{p}_\mu$ and $\dot{t}_\mu$ are taken from the corresponding differential equations (6.18) and (6.31)). We thus obtain the inequalities

$$\dot{\Delta}(t) < 0 \text{ for } 0 \leqslant t < t_*,\ \dot{\Delta}(t) > 0 \text{ for } t_* < t \leqslant T \tag{6.35}$$

239 (where the point $t = t_*$ is a turning point). The initial value $\Delta(0)$ must be strictly positive; otherwise, according to (6.35), we shall have either $\Delta(t) < 0$ for $0 < t \leqslant T$ (strictly coasting flight), or $\Delta(t) < 0$ for $0 < t < t_{**}$ and $\Delta(t) > 0$ for $t_{**} < t \leqslant T$ (one powered flight period with $e(t) = -1$, since $t_{**} > t_*$). Neither of these cases satisfies the boundary conditions (6.31), and therefore

$$\Delta(0) > 0. \tag{6.36}$$

We may conclude from (6.35) and (6.36) that two cases are possible: the first is

$$\Delta(t) \geqslant 0 \text{ for } 0 \leqslant t \leqslant T \tag{6.37}$$

(there is no coasting period), and the second one

$$\Delta(t) > 0 \text{ for } 0 \leqslant t < t_1 \text{ and } t_2 < t \leqslant T,\quad \Delta(t) < 0 \text{ for } t_1 < t < t_2 \quad (0 < t_1 \leqslant t_* \leqslant t_2 < T) \tag{6.38}$$

(there is a coasting period in the middle of the trajectory, when $t_1 < t < t_2$ (Figure 6.2)).

In the following, we shall consider the second case, since it is more general. The inequality (6.37) is obtained from (6.38) for $t_1 = t_* = t_2$.

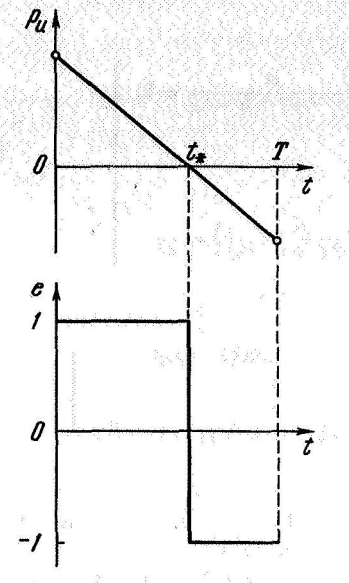

FIGURE 6.1. Time dependence of momentum p_u and the corresponding optimum thrust direction law $e(t)$ ($e = 1$ parallel to the velocity, $e = -1$ in the opposite direction), for the problem of the displacement between points of rest.

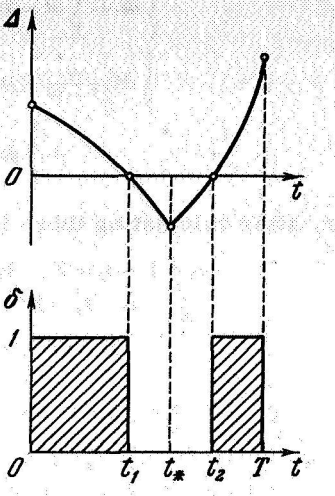

FIGURE 6.2. Behavior of the function $\Delta(t)$, and corresponding optimum firing and cutoff program $\delta(t)$ ($\delta = 1$ if engine is fired, $\delta = 0$ if engine is cut off), for the problem of the displacement between points of rest.

Note that the times t_1 and t_2 of engine firings and cutoffs are symmetric with respect to $t = t_*$ /6.3/. In fact, p_μ and t_μ are constant during the coasting period (cf. (6.18), (6.31) for $\delta = 0$), and

$$\Delta(t) = p_\mu(t_1) + b_1 |t_* - t| \frac{a_0}{1 - \mu t_\mu(t_1)} \quad \text{for } t_1 \leqslant t \leqslant t_2. \tag{6.39}$$

It is thus seen that the roots of the equation $\Delta(t) = 0$ are equidistant from t_*.

This analysis suffices for solving the problem without integrating the complete system of equations (together with the equations for the momenta). We take as unknowns the constant times t_1 and t_2 instead of b_1 and t_*. The optimum control function $e(t)$ and $\delta(t)$ are written as follows /6.1, 6.3/:

$$\left.\begin{aligned} e = +1,\ \delta = 1 \quad & \text{for } 0 \leqslant t < t_1 \text{ (boosting period)} \\ \delta = 0 \quad & \text{for } t_1 < t < t_2 \text{ (coasting period)} \\ e = -1,\ \delta = 1 \quad & \text{for } t_2 < t \leqslant T \text{ (deceleration period).} \end{aligned}\right\} \tag{6.40}$$

240 Relations (6.40) are substituted in the right-hand sides of the differential equations (6.31), which are then integrated by parts allowing for the

corresponding boundary conditions

$$\left.\begin{aligned}&\int_0^{t_1} dt + \int_{t_2}^{T} dt = T_\mu, \quad \int_0^{t_1} \frac{dt}{1-\mu t} - \int_{t_2}^{T} \frac{dt}{1-\mu(t+t_1-t_2)} = 0,\\ &\int_0^{t_1} dt \int_0^{t} \frac{dt}{1-\mu t} + (t_2-t_1)\int_0^{t_1} \frac{dt}{1-\mu t} + \\ &\qquad + \int_{t_2}^{T} dt \left(\int_0^{t_1} \frac{dt}{1-\mu t} - \int_{t_2}^{t} \frac{dt}{1-\mu(t+t_1-t_2)} \right) = \frac{l}{a_0},\end{aligned}\right\} \tag{6.41}$$

or, after calculating these integrals,

$$\left.\begin{aligned}&t_1 + T - t_2 = T_\mu, \quad \ln[1-\mu(t_1+T-t_2)] - 2\ln(1-\mu t_1) = 0,\\ &\left(\frac{2}{\mu} - t_1 + t_2 - 2T\right)\ln(1-\mu t_1) - \\ &-\left(\frac{1}{\mu} - t_1 + t_2 - T\right)\ln[1-\mu(t_1+T-t_2)] + t_1 + t_2 - T = \frac{\mu}{a_0} l.\end{aligned}\right\} \tag{6.42}$$

The first two relationships of (6.42) enable t_1 and t_2 to be expressed in terms of T_μ, T, μ: $t_1 = \mu^{-1}(1 - \sqrt{1-\mu T_\mu})$, $t_2 = T - T_\mu + t_1$. It is seen from here that the boosting period is longer than the deceleration period. As the propellant flow rate decreases, their difference tends to zero (cf. Figure 6.3 for the dependence of t_1/T_μ on μT_μ).

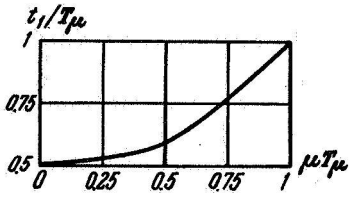

FIGURE 6.3. Fraction t_1/T_μ of the total engine-operating time corresponding to the boosting period, in the problem of the displacement between points of rest.

Eliminating t_1 and t_2 from the third relation of (6.42), we obtain the required expression $T_\mu(a_0, \mu)$ for the functional of the dynamic part of the problem in the implicit form

$$\frac{\mu}{a_0} l = \frac{2}{\mu}(1 - \sqrt{1-\mu T_\mu}) - T_\mu - (T - T_\mu)\ln\sqrt{1-\mu T_\mu}. \tag{6.43}$$

§ 3. OPTIMUM INTERPLANETARY FLIGHT WITH UNTHROTTLED ENGINES

Consider the variational problem (6.5) for interplanetary flights. Although (6.5) or (6.9) applies to all types of unthrottled engines, the range
241 of variation of the parameters a_0 and μ, and the flight adopted here correspond to the group of low thrust engines. First, we present a solution for

each of the elementary maneuvers forming the interplanetary flight (cf. § 2 of the Appendix and § 2 of Chapter Five), and then one for the entire maneuver.

1. Zero energy build-up. Just as in the similar problem of § 2.4, it is assumed that the engine is turned on throughout the entire trajectory (problem (6.9) where $t_\mu(T)$ = opt for minimum time). For this case the equations of optimum motion (6.19) become ($\delta \equiv 1$, $t_\mu \equiv t$)

$$\left.\begin{aligned} &\dot r = v_r, && \dot p_r = p_{v_r}\left(\frac{v_\varphi^2}{r^2} - \frac{2}{r^3}\right) - p_{v_\varphi}\frac{v_r v_\varphi}{r^2},\\ &\dot v_r = \frac{a_0}{1-\mu t}\frac{p_{v_r}}{\sqrt{p_{v_r}^2 + p_{v_\varphi}^2}} + \frac{v_\varphi^2}{r} - \frac{1}{r^2}, && \dot p_{v_r} = -p_r + p_{v_\varphi}\frac{v_\varphi}{r},\\ &\dot v_\varphi = \frac{a_0}{1-\mu t}\frac{p_{v_\varphi}}{\sqrt{p_{v_r}^2 + p_{v_\varphi}^2}} - \frac{v_r v_\varphi}{r}, && \dot p_{v_\varphi} = \frac{1}{r}(p_{v_\varphi} v_r - 2p_{v_r} v_\varphi). \end{aligned}\right\} \qquad (6.44)$$

The equation for the polar angle φ in (6.44) has been omitted, since φ does not appear on the right-hand sides of the equations of motion, and the final value of $\varphi(T)$ for the maneuver considered is not fixed. This equation can be integrated separately after the problem has been solved.

We shall recalculate the boundary conditions for (6.44). Assuming an initial circular orbit, we adopt boundary conditions (A. 57) for the kinematic parameters. The optimality condition for the final point of the trajectory requires the momentum vector $(p_r, p_{v_r}, p_{v_\varphi})$ to be collinear with the normal to the surface $E(T) = 0$, so that

$$p_{v_r}(T)/p_{v_\varphi}(T) = v_r(T)/v_\varphi(T),\ p_{v_r}(T)/p_r(T) = v_r(T)\, r^2(T). \qquad (6.45)$$

According to (6.14), the first relation of (6.45) indicates that the thrust vector at the end of the motion is parallel to the velocity vector, and the second one corresponds to the vanishing of the derivative of the angle γ between these vectors (cf. (5.39)).

The last boundary condition of the problem studied, (6.17), can be written in the form (using (6.45) and $E(T) = 0$)

$$\frac{a_0}{1-\mu T}\sqrt{\frac{2p_{v_r}^2(T)}{v_r^2(T)\, r(T)}} = 1. \qquad (6.46)$$

The problem reduces to integrating the system of sixth-order differential equations (6.44) with three initial and four final conditions (A. 57), (6.45), (6.46); the redundant boundary condition serves to determine the time T. The boundary-value problem obtained is solved numerically by Newton's method /6.4, 6.5/ (cf. Chapter Fifteen). The calculations were performed for a wide range of the parameters a_0 and μ.

242

In the region of high accelerations $a_0 \sim 1$ the numerical solution is close to the approximate solution for $a_0 \gg 1$ given in /6.6/. An example of the optimum control function of the angle γ between the thrust vector and the velocity vector at $a_0 = 0.8$, $\mu = 0$ is given in Figure 6.4; the solid curve corresponds to the numerical solution /6.4/, and the dashed curve to the approximate solution /6.6/. The thrust direction monotonically approaches the velocity direction.

For low accelerations a_0 the character of the optimum thrust direction program changes in that the thrust vector oscillates slightly about the

velocity vector with a period approximately equal to one revolution (Figure 6.5); at the final instant the angle γ and its derivative $\dot{\gamma}$ vanish (cf. (6.45)).

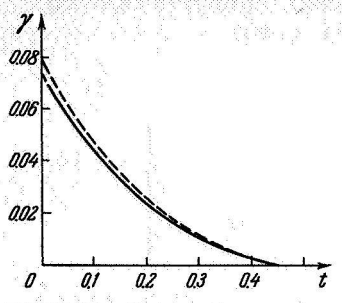

FIGURE 6.4. Optimum program of variation of angle $\gamma(t)$ between thrust and velocity for zero energy build-up maneuver with high thrust ($a_0 = 0.8$, $\mu = 0$). Solid curve represents the numerical solution, and dashed curve, the approximate one.

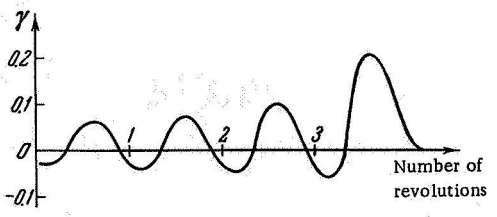

FIGURE 6.5. Optimum program $\gamma(t)$ of thrust direction for the zero energy build-up maneuver with low thrust ($a_0 = 10^{-2}$, $\mu = 0$).

Figure 6.6 represents the minimum time of zero energy build-up as a function of the acceleration a_0, for the case of constant thrust acceleration $a(t) \equiv a_0$ and is obtained by taking the limit $\mu = 0$ in the formulas for a constant-thrust motion. Drawn in logarithmic coordinates, this curve consists of two linear segments corresponding to low and high values of the acceleration respectively, and of a transition section connecting them.

243 The following approximate analytic expression for the functional was found /6.5/ by processing the numerical results:

$$T = T_\mu \approx \frac{1}{a_0}(1 - 0.8209\sqrt[4]{a_0})\left[1 - \frac{\mu}{2a_0}(1 - 0.8209\sqrt[4]{a_0})\right] = \\ = \frac{1}{a_0}(1 - 0.8209\sqrt[4]{a_0}\left[1 - \frac{1}{2V}(1 - 0.8209\sqrt[4]{a_0})\right]; \qquad (6.47)$$

this was begun with a formula similar to (13.37).

Similar expressions were obtained for tangential and transverse* thrust directions:

for tangential thrust

$$T = T_\mu \approx \frac{1}{a_0}(1 - 0.8082\sqrt[4]{a_0})\left[1 - \frac{\mu}{2a_0}(1 - 0.8082\sqrt[4]{a_0})\right], \qquad (6.48)$$

for transverse thrust

$$T = T_\mu \approx \frac{1}{a_0}(1 - 0.7555\sqrt[4]{a_0})\left[1 - \frac{\mu}{2a_0}(1 - 0.7555\sqrt[4]{a_0})\right]. \qquad (6.49)$$

Equations (6.47) to (6.49) are correct for low values of a_0 and μ (low thrust); for $a_0 < 10^{-2}$, $\mu < 0.25 \cdot 10^{-2}$ the relative error does not exceed 1%,

* The complete results of the build-up maneuver of a hyperbolic velocity with constant tangential thrust are given in /6.7—6.9/.

while for $a_0 < 10^{-2}$, $\mu < 0.17 \cdot 10^{-2}$ it is smaller than 0.5%; the error decreases monotonically with decreasing a_0 and μ.

It is seen from a comparison of the functionals (6.47) to (6.49) that for zero energy build-up in a central field the tangential and transverse thrust directions yield results close to the optimum. The relative gain in time for $a_0 = 10^{-2}$, $\mu = 0$ is 0.5% in the first case, and approximately 2.5% in the second case (cf. also /6.10/); the time gain decreases with decreasing a_0 and μ.

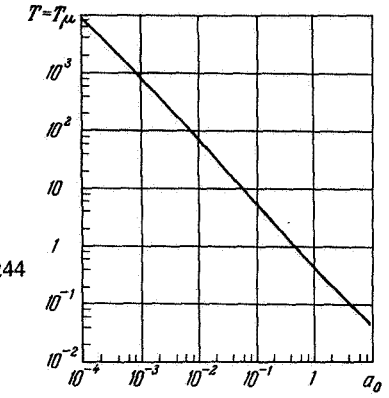

FIGURE 6.6. Minimum time of zero energy build-up $T = T_\mu$ at constant thrust acceleration a_0 ($\mu = 0$, and T and a_0 are dimensionless).

Relations (6.47) to (6.49) can also be used for deceleration in a central field, starting at the point of zero energy $E = 0$ and ending on a circular orbit of specified radius r_0 (the initial values of the coordinates and velocity components, as well as the angular displacement, are not specified separately). The parameters a_0 and μ are then calculated from the vehicle weight $G(E_0)$ at $E = 0$, to yield $a_0 = gk^{-1}r_0^2 P/G(E_0)$, $\mu = gk^{-1/2}r_0^{3/2} q/G(E_0)$.

This calculation for the duration of the inverse maneuver using the formulas obtained for the direct one differs in two aspects from the exact calculation (which uses transformation (6.21)). Firstly, the values a_0 and μ in (6.21) must be calculated using the vehicle weight $G(r_0)$ on the final orbit, where $a_0' = gk^{-1}r_0^2 P/G(r_0)$, $|\mu'| = gk^{-1/2}r_0^{3/2} q/G(r_0)$; and secondly, the inverse maneuver must be calculated by (6.21) with negative values of the parameter $\mu' = -|\mu'|$ (increasing vehicle weight).

However, these two errors compensate each other. In an approximate calculation the thrust-acceleration program $a(t) = a_0(1 - \mu t)^{-1}$ and the exact program $a'(t) = a_0[1 - \mu(T - t)]^{-1}$ are symmetrical with respect to the midpoint of the interval $[0, T]$, and therefore the overall effect produced by the two programs must be roughly the same (with an accuracy of the order of the gravitational losses). These qualitative considerations are corroborated by the quantitative comparison made in /6.11/. The accuracy of the calculation to find the time of the inverse maneuver using formulas (6.47) to (6.49) is of the same order as that for the direct maneuver; the accuracy increases with decreasing a_0 and μ.

2. Orbital transfer. The optimum trajectories for transfer between the orbits of planets in the central field of the Sun will be calculated using the variational formulation (6.9). Equations (6.9) and (6.13) to (6.15) are written in polar coordinates; the angle φ replaces the time t as independent variable so that $d/dt = (v_\varphi/r)\, d/d\varphi$. The complete system of equations of the optimum motion is thus

$$\begin{aligned}
&dt/d\varphi = r/v_\varphi, && t(0) = 0, \quad t(\varphi_1) = \min,\\
&dt_\mu/d\varphi = (r/v_\varphi)\,\delta, && t_\mu(0) = 0, \quad t_\mu(\varphi_1) = T_\mu,\\
&dr/d\varphi = rv_r/v_\varphi, && r(0) = 1, \quad r(\varphi_1) = r_1,\\
&\frac{dv_r}{d\varphi} = \frac{r}{v_\varphi}\frac{a_0\delta}{1-\mu t_\mu}\frac{p_{v_r}}{\sqrt{p_{v_r}^2 + p_{v_\varphi}^2}} + v_\varphi - \frac{1}{rv_\varphi}, && v_r(0) = 0, \quad v_r(\varphi_1) = 0,
\end{aligned} \tag{6.50}$$

$$\frac{dv_\varphi}{d\varphi} = \frac{r}{v_\varphi}\frac{a_0\delta}{1-\mu t_\mu}\frac{p_{v_\varphi}}{\sqrt{p_{v_r}^2+p_{v_\varphi}^2}} - v_r, \qquad v_\varphi(0)=1, \quad v_\varphi(\varphi_1) = r_1^{-1/2}$$

$$(\delta = 1 \text{ for } \Delta > 0,\ \delta = 0 \text{ for } \Delta < 0,$$
$$\Delta = p_\mu + a_0(1-\mu t_\mu)^{-1}\sqrt{p_{v_r}^2+p_{v_\varphi}^2}),$$

$$\frac{dp_\mu}{d\varphi} = -\frac{r}{v_\varphi}\frac{a_0\mu\delta}{(1-\mu t_\mu)^2}\sqrt{p_{v_r}^2+p_{v_\varphi}^2}, \quad \frac{dp_r}{d\varphi} = -\frac{\Delta}{v_\varphi}\delta + \frac{1}{v_\varphi} - \tag{6.50}$$
$$- p_r\frac{v_r}{v_\varphi} - p_{v_r}\frac{1}{v_\varphi r^2},$$

$$\frac{dp_{v_r}}{d\varphi} = -p_r\frac{r}{v_\varphi} + p_{v_\varphi}, \qquad \frac{dp_{v_\varphi}}{d\varphi} = \frac{r\Delta}{v_\varphi^2}\delta - \frac{r}{v_\varphi^2} + p_r\frac{rv_r}{v_\varphi^2} -$$
$$- p_{v_r}\left(1+\frac{1}{rv_\varphi^2}\right)$$

245 (the momentum $p_t \equiv -1$, since t does not appear on the right-hand sides of the equations and we look for the minimum $t(\varphi_1)$; here the condition $p_t \equiv -1$ replaces (6.17)).

System 6.50 has a first integral

$$H(\varphi) = (r\Delta/v_\varphi)\,\delta - r/v_\varphi + p_r r v_r/v_\varphi + p_{v_r}(v_\varphi - 1/rv_\varphi) - p_{v_\varphi}v_r =$$
$$= \Delta(0)\,\delta(0) - 1 = r_1^{3/2}\Delta(\varphi_1)\,\delta(\varphi_1) - r_1^{3/2} = \text{const}. \tag{6.51}$$

The limiting case $T_\mu = T$ (the engine is not cut off) occurs at $p_\mu(\varphi_1) = 0$ as was established in § 2.1; in the ordinary situation ($T_\mu < T$), $-p_\mu(\varphi_1) < 0$.

The results of the numerical solution of the boundary-value problem (6.50) for Earth—Mars and Mars—Earth orbital transfers are shown in Figures 6.7 to 6.9. These results were obtained in /6.12/ by Newton's method (optimum angular displacement $H(\varphi_1) = 0$, Figure 6.7).

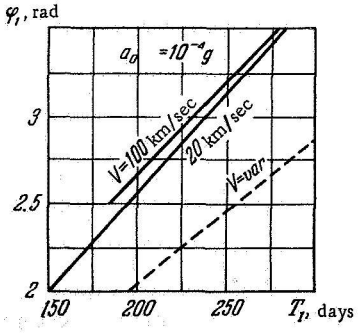

FIGURE 6.7. Optimum angular displacement φ_1 for Earth—Mars orbital
246 transfer with unthrottled engine (solid lines: $a_0 = 10^{-4}$ g, $V = 100$ km/sec, 20 km/sec) and with ideal power-limited engine (dashed line).

For the range of parameters considered, the optimum trajectory consists of an initial powered-flight period (of duration t_1), an intermediate coasting period (of duration $T - T_\mu$), and a final powered period (of duration $T_\mu - t_1$), just as in the problem of the displacement between points of rest, (6.40). The optimum time distribution is shown in Figure 6.8, where the regions enclosed by the lower and upper branches of the curves correspond to the coasting time. The figure shows that when the flight time T is shortened for fixed values of the parameters a_0 and V, the coasting time $T - T_\mu$ decreases, and vanishes at the extreme left-hand point of each curve. It is impossible to further shorten the flight time for these values of a_0 and V.

The resulting relationship $T_\mu(a_0, V, T)$ for the dynamic part of the problem is shown in Figure 6.9. Similar results were obtained in /6.13/. The
247 optimum trajectories of orbital transfers with unthrottled engines may also be determined by direct methods /6.14/. Data on the optimum trajectories with constant thrust acceleration are given in /6.15—6.20/. In some of the papers (/6.18—6.20/) the integral (4.11) is taken as the functional of the problem when the calculations for constant thrust are being made. This substitution yields substantial errors when the weight part of the problem is being solved.

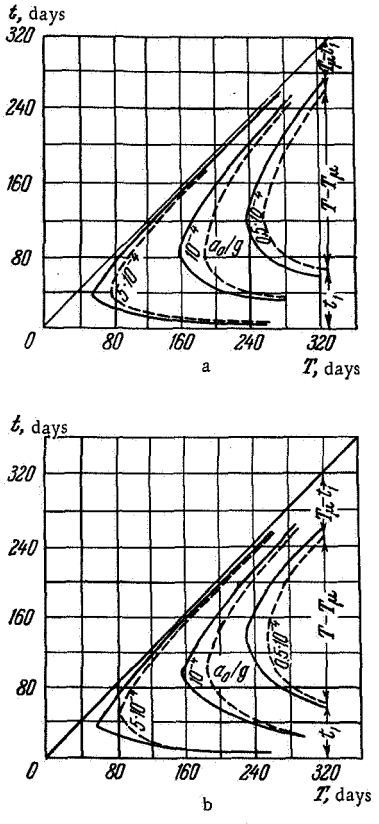

FIGURE 6.8. Distribution of total time T between powered and coasting periods for orbital transfers: t_1, $T_\mu - t_1$ are first and second powered flight periods, $T - T_\mu$ is coasting period. Solid curves represent $V = 20$ km/sec, dashed curves represent $V = 100$ km/sec, $\varphi_1 =$ opt. a) Earth—Mars, b) Mars—Earth.

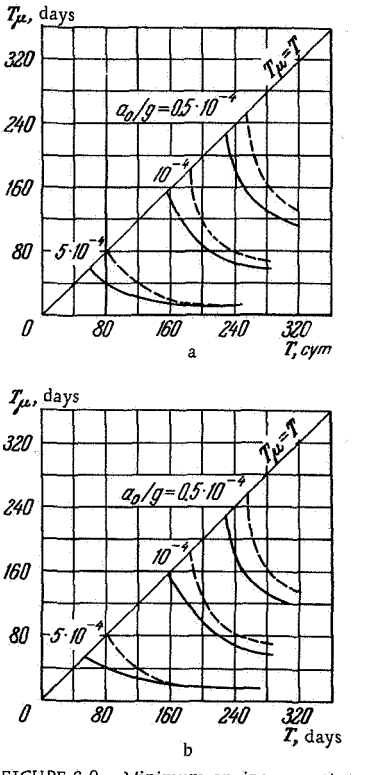

FIGURE 6.9. Minimum engine operating time T_μ as a function of the initial acceleration a_0, exhaust velocity V, and total time T of orbital transfer, where $\varphi_1 =$ opt. Solid curves represent $V = 20$ km/sec, dashed curves represent $V = 100$ km/sec. a) Earth—Mars, b) Mars—Earth.

Using the results of §§ 3.1, 3.2 we may calculate the optimum parameters of the one-way flight, Earth satellite—Mars satellite (or Mars satellite—Earth satellite). This calculation will now be made for the transfer from a 300-km high circular Earth-satellite orbit to a 300-km

high circular Mars-satellite orbit. The orbits of the planets will be considered circular and coplanar, and the transfer trajectory will be taken as planar.

The solution of the dynamic part of the problem for the acceleration period in the Earth's field $T_{\mu,+1} = f(a_0^{(1)}, V, T_{+1})$, and the deceleration period near Mars $T_{\mu,-2} = f(a_0^{(3)}, V, T_{-2})$ is given by (6.47), or, in dimensional form by (Figure 6.10)

$$T_{\mu,+1}\,[\text{days}] = T_{+1}\,[\text{days}] \approx \frac{91}{a_0^{(1)}\,[10^{-4}g]}\left(1 - 0.084\sqrt[4]{a_0^{(1)}\,[10^{-4}g]}\right) \times$$
$$\times \left[1 - \frac{3.86}{V\,[\text{km/sec}]}\left(1 - 0.084\sqrt[4]{a_0^{(1)}\,[10^{-4}g]}\right)\right],$$
$$T_{\mu,-2}\,[\text{days}] = T_{-2}\,[\text{days}] \approx \frac{39.8}{a_0^{(3)}\,[10^{-4}g]}\left(1 - 0.109\sqrt[4]{a_0^{(3)}\,[10^{-4}g]}\right) \times$$
$$\times \left[1 - \frac{1.688}{V\,[\text{km/sec}]}\left(1 - 0.109\sqrt[4]{a_0^{(3)}\,[10^{-4}g]}\right)\right].$$

The function $T_{\mu 1} = f(a_0^{(2)}, V, T_1)$ for the interorbital section of the Earth—Mars flight has been plotted in Figure 6.9a.

The sections of initial thrust acceleration $a_0^{(1)}$, $a_0^{(2)}$, $a_0^{(3)}$ are joined according to the conditions of constant thrust, P, and exhaust velocity, V, making use of the equatorial continuity

$$a_0^{(i)}\,[10^{-4}g] = \frac{a_0^{(i-1)}\,[10^{-4}g]}{1 - 8.48\cdot 10^{-2} a_0^{(i-1)}\,[10^{-4}g]\,T_\mu^{(i-1)}[\text{days}]/V\,[\text{km/sec}]}$$
$$(a_0^{(1)} = a_0,\ T_\mu^{(1)} = T_{\mu,+1} = T_{+1},\ T_\mu^{(2)} = T_{\mu 1},\ T_\mu^{(3)} = T_{\mu,-2} = T_{-2}).$$

The results of the corresponding calculations are shown in Figures 6.11 and 6.12.

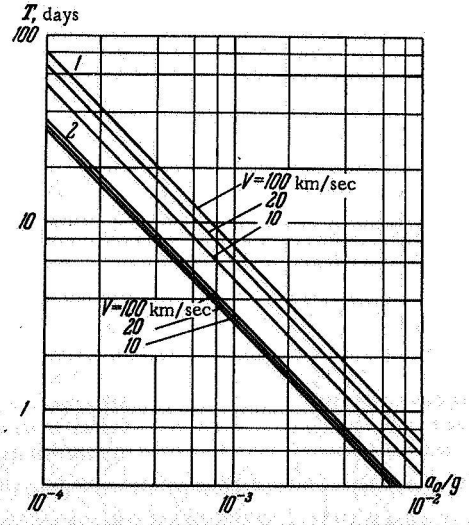

FIGURE 6.10. Minimum acceleration and deceleration times in fields of Earth (curves 1) and Mars (curves 2) for a 300-km high circular orbit.

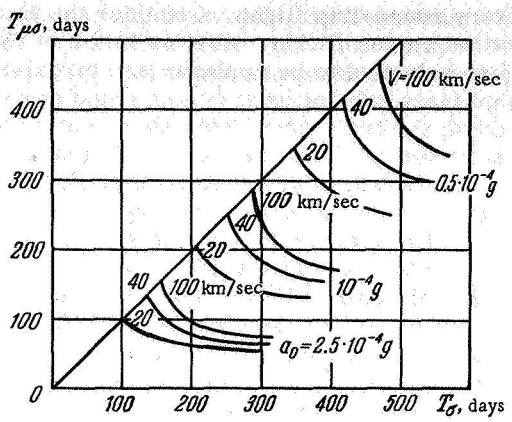

FIGURE 6.11. Minimum engine-operating time $T_{\mu\sigma}$ for the transfer from the 300-km high Earth-satellite orbit to the 300-km high Mars-satellite orbit as a function of the time of motion T_σ for different values of initial thrust acceleration a_0 and exhaust velocity V.

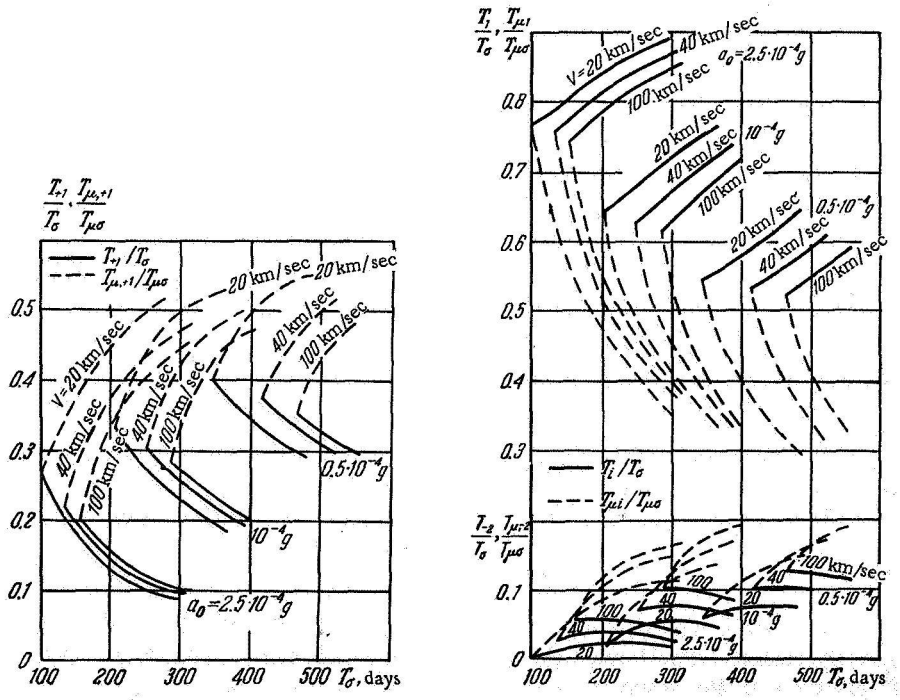

FIGURE 6.12. Optimum distribution of total time of motion T_σ (solid curves) and total energy-operating time $T_{\mu\sigma}$ (dashed curves) between acceleration periods in the Earth's field ($T_{+1} = T_{\mu,+1}$), the Earth—Mars orbital transfer (T_1, $T_{\mu 1}$), and the deceleration in the field of Mars ($T_{-2} = T_{\mu,-2}$).

3. Interplanetary round-trip flight. Consider the Earth—Mars—Earth flight with unthrottled engine /6.11/. Just as in § 2 of Chapter Five, the planetary orbits are assumed to be coplanar and circular with only the influence of the dominant gravitational center being allowed for in each characteristic period; the trajectory sections cannot be joined according
248 to the kinematic parameters. It is also assumed that the deceleration in the neighborhood of the Earth is achieved by aerodynamic forces, the time required for this maneuver as well as the weight expended being neglected in the calculations.* The fuel and the time required for deceleration (T_{-2}) and acceleration (T_{+2}) in the field of Mars are taken into account, unlike the procedure used in § 2 of Chapter Five. The orbits of the Earth and Mars satellites are assumed to be circular, and at an altitude of 300 km.

The minimum total flight time has to be determined for specified thrust, propellant flow rate, and total engine-operating time. Optimum coasting time along the Mars-satellite orbit (the parking time T_0) is chosen, and the departure date is unspecified.

The acceleration and deceleration sections of the trajectory in the neighborhood of the planets were calculated by (6.47). In these sections the engine operates without being cut off. The corresponding dimensional values of the time T as a function of a_0 and V are given in Figure 6.10.

In the interorbital trajectory sections the boundary-value problem (6.50) was solved by the modified Newton method (cf. Chapter Fifteen).

The dimensionless parameters $\mu^{(i)}$ and $a_0^{(i)}$ for the i-th elementary
250 maneuver are determined from mass conservation and the conditions of constant thrust P, and propellant flow rate q, as follows:

$$\left.\begin{aligned} \mu^{(i)} &= \frac{\mu^{(1)} t_*^{(i)}/t_*^{(1)}}{1-\mu^{(1)}\sum_{j=1}^{i-1} T_\mu^{(j)} t_*^{(j)}/t_*^{(1)}}, & a_0^{(i)} &= a_0^{(1)} \frac{\mu^{(i)} v_*^{(i)}}{\mu^{(1)} v_*^{(i)}}, \\ \mu^{(1)} &= gqt_*^{(1)}/G_0, & a_0^{(1)} &= gP/G_0 g_*^{(1)}. \end{aligned}\right\} \qquad (6.52)$$

To simplify the notation, the elementary maneuvers are numbered by superscripts in consecutive order (the correspondence between the old and the new superscripts is: $+1 \leftrightarrow i = 1$, $1 \leftrightarrow i = 2$, $-2 \leftrightarrow i = 3$, $+2 \leftrightarrow i = 4$, $2 \leftrightarrow i = 5$). The characteristic values of the time $t_*^{(i)}$, the velocity $v_*^{(i)}$, and the acceleration $g_*^{(1)}$ (dimensional quantities) are taken from Tables 5.1 and 5.3 (with $t_*^{(3)} = t_*^{(4)}$, $v_*^{(3)} = v_*^{(4)}$). The time is measured from zero in each section.

The complete flight calculation was performed as follows. The parameters $a_0^{(1)}$ and $\mu^{(1)}$, and the total flight time $T_{\mu\sigma}$ are specified. The time of zero energy build-up in the Earth's field is calculated by (6.47), so that

$$T_{+1} = T_{\mu,+1} = f_+ (a_0^{(1)}, \mu^{(1)}). \qquad (6.53)$$

The angle φ_1 and the engine-operating time $T_{\mu 1}$ for the Earth—Mars flight are specified. The boundary-value problem (6.50) is thus solved for the flight time in the form

$$T_1 = f_1 (a_0^{(2)}, \mu^{(2)}, \varphi_1, T_{\mu 1}). \qquad (6.54)$$

* In the conclusion this is compared with the deceleration in the Earth's field by means of a retroengine.

The deceleration and acceleration times T_{-2} and T_{+2} near Mars are calculated by (6.47) to give

$$T_{-2} = T_{\mu,-2} = f_+ (a_0^{(3)}, \mu^{(3)}), \quad T_{+2} = T_{\mu,+2} = f_+ (a_0^{(4)}, \mu^{(4)}). \tag{6.55}$$

The angle φ_2 of the Mars—Earth flight is specified. The engine-operating time $T_{\mu 2}$ is calculated as the difference

$$T_{\mu 2} = T_{\mu\sigma} - (T_{\mu,+1} + T_{\mu 1} + T_{\mu,-2} + T_{\mu,+2}), \tag{6.56}$$

and by solving the boundary-value problem (6.50) we find the time

$$T_2 = f_2 (a_0^{(5)}, \mu^{(5)}, \varphi_2, T_{\mu 2}). \tag{6.57}$$

The parking time on the Mars-satellite orbit is found from the condition (A.60) for the angular displacements of both the Earth and the vehicle at the end of the Mars—Earth flight to be equal,

$$T_0 = \frac{1}{\omega_1 - \omega_2} [\varphi_1 + \varphi_2 - \omega_1 (T_1 + T_2) - (\omega_1 - \omega_2)(T_{-2} + T_{+2}) + 2\pi s] \geqslant 0 \tag{6.58}$$

251 ($\omega_1 = 0.19968 \cdot 10^{-6}$ sec^{-1}, $\omega_2 = 0.10615 \cdot 10^{-6}$ sec^{-1} are the average angular velocities of motion of Earth and Mars, dimensional time [T] is in seconds, the angles φ_1, φ_2 are in radians, and $s = 0, 1, 2, \ldots$ is selected so as to make T_0 the smallest nonnegative number).

Finally, we determine the optimum values of the angles φ_1, φ_2, and the time $T_{\mu 1}$ which ensure an absolute minimum of the sum $T_1 + T_{-2} + T_{+2} + T_2 + T_0$.

For each pair of values of $a_0^{(1)}$ and $\mu^{(1)}$ the calculation begins with an unspecified engine-operating time ($\delta \equiv 1$). In problem (6.50), the condition $t_\mu (\varphi_1) = T_\mu$ is replaced by $p_\mu (\varphi_1) = 0$, and the minimum of the total flight time is only sought for φ_1 and φ_2. This yields the smallest time of motion $T'_\sigma (a_0^{(1)}, \mu^{(1)})$ for the given $a_0^{(1)}$ and $\mu^{(1)}$. The calculation is then made for a given engine-operating time $T_{\mu\sigma} < T'_\sigma$.

The results of the calculations are shown in Figures 6.13 to 6.16. Examples of the optimum trajectories for orbital transfers are given in Figure 6.13. The arrows indicate the direction of the thrust vector, and the dashed curves represent the coasting sections of the trajectory. Examples a) to c) correspond to the minimum flight-trajectory times without coasting periods for the given values of a_0 and V. For longer flight times, and the same values of the initial acceleration a_0 and exhaust velocity V, there are coasting periods (see example d)).

The Earth—Mars and Mars—Earth transfer trajectories are asymmetrical. This is illustrated in Figure 6.14, which represents the optimum angular displacements $\varphi_1 (a_0, T_\sigma)$ and $\varphi_2 (a_0, T_\sigma)$ for transfer in both directions without cutting off the engine. The optimum parking time was found to be $T_0 = 0$.

The distribution of the total time T_σ for motion without cutting off the engine is shown in Figure 6.15 (acceleration in the Earth's field T_{+1}, Earth—Mars orbital transfer T_1, deceleration and acceleration near Mars $T_{-2} + T_{+2}$, Mars—Earth orbital transfer T_2).

The dependence of the minimum total flight time T_σ on the parameters a_0 and V is shown in Figure 6.16. The solid curves correspond to the case

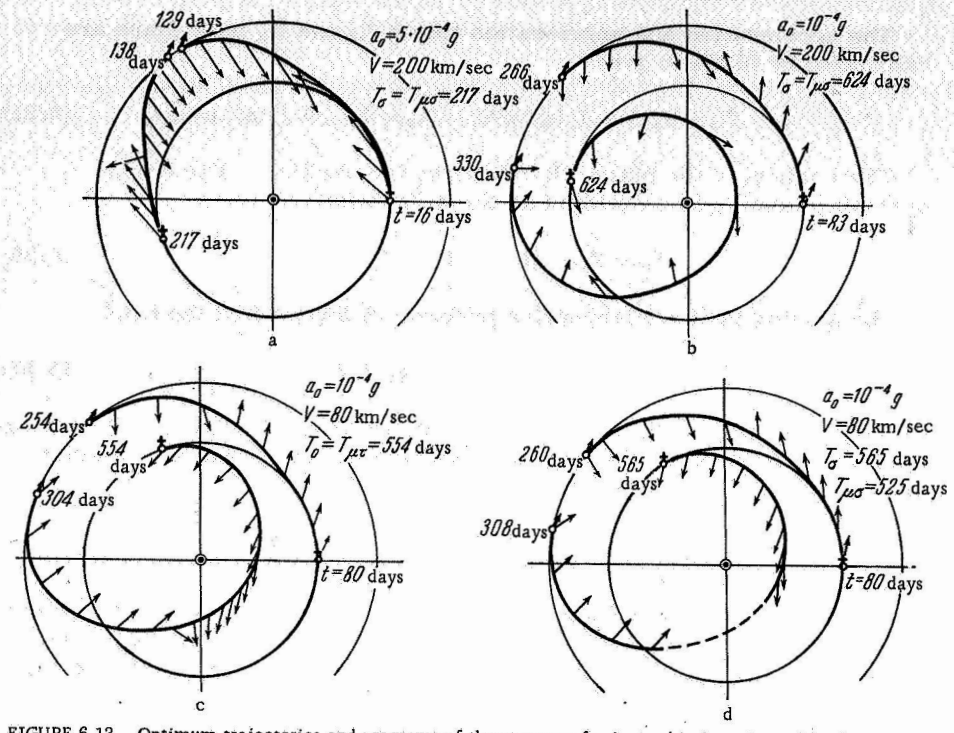

FIGURE 6.13. Optimum trajectories and programs of thrust vector for interorbital sections of Earth—Mars—Earth flight (aerodynamic deceleration near the Earth):

a) $a_0 = 5\cdot10^{-4}$ g, $V = 200$ km/sec, $T_\sigma = T_{\mu\sigma} = 217$ days, b) $a_0 = 10^{-4}$ g, $V = 200$ km/sec, $T\sigma = T_{\mu\sigma} =$ $= 624$ days, c) $a_0 = 10^{-4}$ g, $V = 80$ km/sec, $T\sigma = T_{\mu\sigma} = 554$ days, d) $a_0 = 10^{-4}$ g, $V = 80$ km/sec, $T\sigma =$ $= 565$ days, $T_{\mu\sigma} = 525$ days.

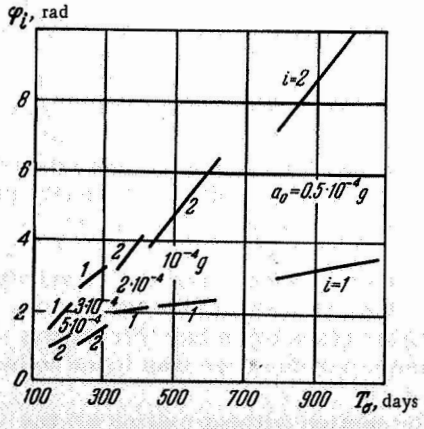

FIGURE 6.14. Angular displacements of outbound, φ_1, and return, φ_2, flights between Earth and Mars orbits as a function of the total time of motion, T_σ, for fixed values of the initial acceleration a_0 (engine never cut off, $T_{\mu\sigma} = T_\sigma$, aerodynamic deceleration near the Earth).

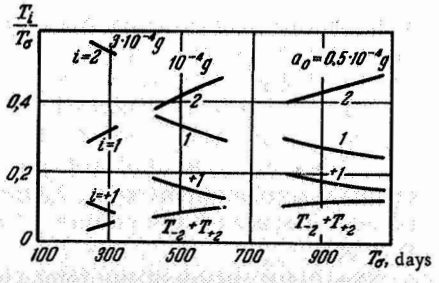

FIGURE 6.15. Optimum distribution of total time T_σ of Earth—Mars—Earth flight between trajectory sections: T_{+1} is acceleration near the Earth, T_1 is Earth—Mars orbital transfer, $T_{-2} + T_{+2}$ deceleration and acceleration near Mars, T_2 is Mars—Earth orbital transfer (engine never cut off, $T_{\mu i} = T_i$, aerodynamic deceleration near the Earth).

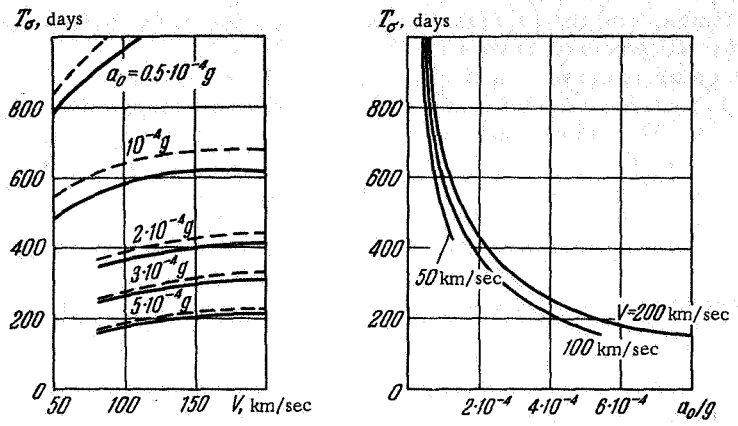

FIGURE 6.16. Minimum possible time T_σ of Earth—Mars—Earth flight as function of initial thrust acceleration a_0 and exhaust velocity V. Solid curves correspond to aerodynamic deceleration near the Earth, dashed curves to powered deceleration (engine never cut off, $T_{\mu\sigma} = T_\sigma$).

of aerodynamic deceleration during return to Earth, and the dashed curves to the case of powered deceleration. The latter were obtained as follows. After the optimum trajectory with aerodynamic deceleration had been calculated, the additional time $T_{-1} = f_+ (a_0^{(6)}, \mu^{(6)})$ necessary for powered deceleration was calculated by (6.47). The distribution of the time between the other trajectory sections was unaltered and the time found, T_{-1}, was added to the total time of motion and the total engine-operating time.

§ 4. OPTIMUM MANEUVERS OF GUIDED SATELLITES WITH UNTHROTTLED ENGINES

254

The dynamic problem is solved in this section for two maneuvers in the neighborhood of a planet, namely, holding the satellite within a given spherical layer (§ 3.1), and rotating the plane of a circular orbit (§ 3.2). The second maneuver has already been considered for a power-limited ideal engine (§ 3 of Chapter Five).

1. **Holding the satellite within a given spherical layer.** The satellite must remain within a spherical layer of given maximum and minimum radii r_{max} and r_{min} over a period of s revolutions. We assume that at $t = 0$ the satellite is projected into a circular orbit within this layer (cf. § 3 of the Appendix): $1 + \max \xi^{(1)}(t) < r_{max}$, $1 + \min \xi^{(1)}(t) > r_{min}$, where $\max \xi^{(1)}(t)$, $\min \xi^{(1)}(t)$ give the amplitudes of the radial oscillations during the first revolution. Under the action of atmospheric drag, the satellite will gradually lose height, and will fall below the lower boundary of the layer after n revolutions. The engine must, therefore, be fired before the n-th revolution.

We require a periodic engine operating rule, so that during $(m-1)$ revolutions we have coasting motion, and at the m-th revolution (the last revolution of the period, $1 \leqslant m \leqslant n$) the engine is fired. The firing and

cutoff times, and the formula for the orientation of the thrust vector are the same for all powered revolutions.

The establishment of a periodic control function for the engine is hindered by the monotonic time function $G(t)$ appearing in the equations of motion (A.83), and by long-period oscillating terms appearing in the formula for the density ρ.

It is possible to establish the required periodic control program G by taking the weight as constant, namely, $G(t) = \text{const}$, neglecting the long-period terms in the expression for $\rho(t)$, and then checking the condition for keeping the orbit within the specified layer during some given time. If the conditions of orbit conservation are not satisfied, an additional powered revolution must be introduced for correction. Another factor favoring such an approach is that since the density law assumed in the calculations is not exact, the motion in a real atmosphere can be so different from the idealized motion that an orbit correction becomes necessary; this will also take care of the above-mentioned inaccuracies, which are in any case negligible.

The periodic region of engine operation is possible only if the values of the parameters $\xi, \dot{\xi}, \eta$ recur in every m-th revolution, i.e.,

$$\xi_m = 0, \quad \dot{\xi}_m = 0, \quad \eta_m = 0. \tag{6.59}$$

255 These parameters are responsible for keeping the orbit within the specified layer; in particular, they determine the amplitude of the radial oscillations of the orbit, $\max \xi^{(m)}(t) - \min \xi^{(m)}(t)$. The sojourn in the specified layer imposes no restrictions on the remaining parameters of motion $(\eta, \theta, \dot{\theta})$ and therefore there are no recurring conditions for them.

The variational problem for the maneuver considered, performed by a vehicle with an unthrottled engine, is formulated using integral expressions. It is required to establish the optimum laws $e_\varphi(t)$, $e_r(t)$, $\delta(t)$ $(e_\theta = \pm\sqrt{1 - e_\varphi^2 - e_r^2})$ which minimize the integral functional

$$t_\mu^{(m)} = \int_0^{2\pi m} \delta(t)\, dt, \tag{6.60}$$

where the engine operates during a period of m revolutions (the first $m-1$ are coasting revolutions, whereas the m-th is powered), while preserving the periodic conditions (cf. (A.74), (6.59))

$$\left.\begin{aligned} 2\varkappa(1 - 2j_z\cos i)\int_0^{2\pi m} \rho\cos t\, dt - a_0\Big(2\int_0^{2\pi m} e_\varphi\delta\cos t + \\ + \int_0^{2\pi m} e_r\delta\sin t\, dt\Big) = 0, \\ 2\varkappa(1 - 2j_z\cos i)\int_0^{2\pi m} \rho\sin t\, dt - a_0\Big(2\int_0^{2\pi m} e_\varphi\delta\sin t\, dt - \\ - \int_0^{2\pi m} e_r\delta\cos t\, dt\Big) = 0, \\ \varkappa(1 - 2j_z\cos i)\int_0^{2\pi m} \rho\, dt - a_0\int_0^{2\pi m} e_\varphi\delta\, dt = 0. \end{aligned}\right\} \tag{6.61}$$

Here the parameters $\varkappa$, j_z, a_0, and the density ρ are dimensionless (cf. § 3 of the Appendix).

The density ρ is a known function of the time t, the radius r_0, and certain angles. It follows that the integrals

$$\int_0^{2\pi m} \rho\, dt = 2\pi m\lambda_0, \quad \int_0^{2\pi m} \rho \cos t\, dt = \pi m\lambda_1, \quad \int_0^{2\pi m} \rho \sin t\, dt = \pi m\nu_1 \tag{6.62}$$

are known if the radius r_0, these angles, and the number of revolutions m are specified.

256 On the basis of the differential relation $\dot{t}_\mu = \delta$ it is possible to write the last equality of (6.61) as follows:

$$\int_0^{t_\mu^{(m)}} e_\varphi\, dt_\mu = \varkappa (1 - 2j_z \cos i)\, 2\pi m\lambda_0/a_0. \tag{6.63}$$

The right-hand side of (6.63) is known, while in the left-hand side are the control functional $t_\mu^{(m)}$ (in the upper limit of the integral) and the control function $e_\varphi(t)$. This control function $e_\varphi(t)$ must be selected so as to make the upper limit $t_\mu^{(m)}$ a minimum. Thus, the problem of finding the optimum control function $e_\varphi(t)$ is separated from the variational problem (6.60), (6.61). If the natural limitation $|e_\varphi(t)| \leqslant 1$, is taken into account, we obtain the optimum control function

$$e_\varphi(t) \equiv 1 \tag{6.64}$$

and therefore

$$e_r(t) \equiv 0, \quad e_\theta(t) \equiv 0. \tag{6.65}$$

The minimum value of the functional $t_\mu^{(m)}$ is found from (6.63); it is independent of the control function $\delta(t)$, and given by

$$t_\mu^{(m)} = \varkappa (1 - 2j_z \cos i)\, 2\pi m\lambda_0/a_0. \tag{6.66}$$

Note the restriction on the time $t_\mu^{(m)}$, where

$$t_\mu^{(m)} \leqslant 2\pi \tag{6.67}$$

(the engine operating time cannot exceed the time of motion). We thus obtain a lower bound for the acceleration a_0, so that

$$a_0 \geqslant \varkappa (1 - 2j_z \cos i)\, m\lambda_0. \tag{6.68}$$

As already indicated, the control function $\delta(t)$ does not influence the functional $t_\mu^{(m)}$ (cf. (6.66)). The number of powered periods per revolution, and their firing and cutoff times must be selected so as to satisfy the three integral conditions (6.61) (the last of which coincides with (6.66)).

Allowing for (6.64) and (6.65), and using (6.62) and (6.66), we reduce the first two equalities of (6.61) to the form

$$\int_0^{2\pi} \delta \cos t\, dt = t_\mu^{(m)} \lambda_1/\lambda_0, \quad \int_0^{2\pi} \delta \sin t\, dt = t_\mu^{(m)} \nu_1/\lambda_0. \tag{6.69}$$

257 (The integration is performed along the powered revolution, where $2\pi(m-1) \leqslant t \leqslant 2\pi m$; since the integrand is independent of m, it is integrable over the interval $0 \leqslant t \leqslant 2\pi$.)

We assume for simplicity that there are only two powered periods in each revolution. Therefore,

$$\delta = 1 \text{ for } t_1 < t < t_2 \text{ and for } t_3 < t < t_4. \tag{6.70}$$

In order to satisfy conditions (6.69), we must have

$$\left.\begin{aligned} \cos\frac{t_2+t_1}{2}\sin\frac{t_2-t_1}{2} + \cos\frac{t_4+t_3}{2}\sin\frac{t_4-t_3}{2} &= \frac{1}{2}\, t_\mu^{(m)}\frac{\lambda_1}{\lambda_0}, \\ \sin\frac{t_2+t_1}{2}\sin\frac{t_2-t_1}{2} + \sin\frac{t_4+t_3}{2}\sin\frac{t_4-t_3}{2} &= \frac{1}{2}\, t_\mu^{(m)}\frac{\nu_1}{\lambda_0}, \end{aligned}\right\} \tag{6.71}$$

and furthermore, the total of the duration of the powered periods during each revolution is equal to $t_\mu^{(m)}$, so

$$t_2 - t_1 + t_4 - t_3 = t_\mu^{(m)}. \tag{6.72}$$

Since we have three equations for the four unknowns t_1, t_2, t_3, t_4, namely, (6.71) and (6.72), one of the unknowns is undetermined.

If $\rho(t) \equiv 1$ then $\lambda_0 = 1$, and equations (6.71) and (6.72) have the following simple solution: both powered sections have equal cutoff times, and their corresponding points are shifted through half a revolution; the starting point of the first powered section is arbitrary within certain limits (Figure 6.17).

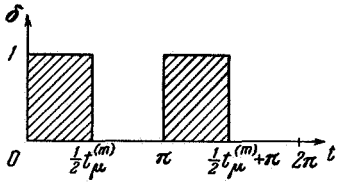

FIGURE 6.17. Possible optimum program of engine firing during a powered revolution for an orbit-holding maneuver.

The solution obtained for one operating period of the engine is easily generalized to $[s/m]$ periods,* i.e., to a satellite life not shorter than s revolutions in the specified layer, where

$$T_\mu = [s/m]\, t_\mu^{(m)} = [s/m]\, \varkappa (1 - 2j_z \cos i)\, 2\pi m \lambda_0/a_0. \tag{6.73}$$

The optimum functions e_φ, e_r, e_θ, δ are conserved in the form (6.64), (6.65), and (6.70) to (6.72).

In formulating the problem it was assumed that the engine operates during the m-th revolution only after $m-1$ coasting revolutions of the satellite. In the same way one can study the problem of an engine operating throughout several revolutions instead of during only one at the end of the period.

* The symbol $[s/m]$ denotes the integral part of the number s/m.

258 **2. Rotation of the plane of a circular orbit** (cf. § 3 of the Appendix and § 3 of Chapter Five). Problem (6.5) for the given maneuver is written as follows (/6.2/, cf. (A.94) and (5.69)):

$$\left.\begin{aligned} &\dot{t}_\mu = \delta, && t_\mu(0) = 0, \quad t_\mu(T) = \min, \\ &\dot{\chi} = \frac{a_0\delta}{1-\mu t_\mu} e \sin(t-\Omega_1), && \chi(0) = 0, \quad \chi(T) = 0, \\ &\dot{\omega} = \frac{a_0\delta}{1-\mu t_\mu} e \cos(t-\Omega_1), && \omega(0) = 0, \quad \omega(T) = i \\ &(a_0, \mu = \text{const}, \ \delta(t) = 1 \text{ for } 0, \ e(t) = \pm 1). \end{aligned}\right\} \tag{6.74}$$

We shall assume that the change in the vehicle weight due to the consumption of working fluid is much smaller than the take-off weight of the vehicle ($\mu T_\mu \ll 1$, $T_\mu = t_\mu(T)$). The thrust-acceleration magnitude $a(t) = a_0\delta(t)(1-\mu t_\mu)^{-1}$ in the right-hand side of (6.74) can then be replaced by

$$a(t) = a_0\delta(t). \tag{6.75}$$

To simplify the formulas we assume that $T = 2\pi s$, $s = 1, 2, \ldots$ (the maneuvering time is a multiple of the period of revolution along the given orbit). The variational problem is thus finally written as

$$\left.\begin{aligned} &\dot{t}_\mu = \delta, && t_\mu(0) = 0, \quad t_\mu(2\pi s) = \min, \\ &\dot{\chi} = a_0\delta e \sin(t-\Omega_1), && \chi(0) = 0, \quad \chi(2\pi s) = 0, \\ &\dot{\omega} = a_0\delta e \cos(t-\Omega_1), && \omega(0) = 0, \quad \omega(2\pi s) = i \\ &(a_0 = \text{const}, \quad \delta(t) = 1 \text{ or } 0, \quad e(t) = \pm 1). \end{aligned}\right\} \tag{6.76}$$

We now form the Hamiltonian and write the momentum equations

$$\left.\begin{aligned} &H = -\delta + p_\chi a_0 \delta e \sin(t-\Omega_1) + p_\omega a_0 \delta e \cos(t-\Omega_1), \\ &p_\chi = \text{const}, \quad p_\omega = \text{const}. \end{aligned}\right\} \tag{6.77}$$

The optimum functions $e(t)$ and $\delta(t)$ are represented by the expressions

$$\left.\begin{aligned} &e(t) = \operatorname{sgn}[p_\chi \sin(t-\Omega_1) + p_\omega \cos(t-\Omega_1)], \\ &\delta(t) = 1 \text{ for } \Delta > 0, \quad \delta(t) = 0 \text{ for } \Delta < 0 \\ &(\Delta = -1 + a_0 |p_\chi \sin(t-\Omega_1) + p_\omega \cos(t-\Omega_1)|). \end{aligned}\right\} \tag{6.78}$$

The parameters p_χ and p_ω are calculated from the boundary conditions for χ and ω.

If the time of motion is a multiple of the revolution period (as in the example considered), the optimum programs (6.78) are periodic with a
259 period of 2π. The powered trajectory sections are of equal duration; the time between the beginning and end of two adjacent sections differs by π (with the possible exception of the first and last sections), and the positive and negative directions of the thrust vector alternate. It is thus possible to establish an explicit relationship between e and δ and the angle Ω_1.

Assume that we know the optimum control variables e and δ for rotating the orbit plane through an angle i during a time $2\pi s$ at a position of the nodal line characterized by the angle Ω_1.

The variables e' and δ', rotating the orbit plane through the same angle i during the same time $2\pi s$, but at an angle Ω_1' different from Ω_1, are expressed as follows in terms of e and δ:

$$e'(t) = e(t + \Omega_1 - \Omega_1'), \quad \delta'(t) = \delta(t + \Omega_1 - \Omega_1'). \tag{6.79}$$

This is proved as follows. The control variables e, δ, and e', δ' are characterized by the parameters p_χ, p_ω and p_χ', p_ω', and are determined from the conditions

$$\left.\begin{aligned} &\int_0^{2\pi s} e\delta \sin(t - \Omega_1)\,dt = 0, \quad \int_0^{2\pi s} e\delta \cos(t - \Omega_1)\,dt = i/a, \\ &\int_0^{2\pi s} e'\delta' \sin(t - \Omega_1')\,dt = 0, \quad \int_0^{2\pi s} e'\delta' \cos(t - \Omega_1')\,dt = i/a_0 \end{aligned}\right\} \tag{6.80}$$

(where e, e', δ, δ' are given in (6.78)).

The two upper relationships in (6.80) are satisfied; it remains to show that in this case the two lower equalities hold when equations (6.79) are fulfilled. We make the substitution

$$t' = t + \Omega_1 - \Omega_1', \tag{6.81}$$

as a result of which the integration interval is shifted by $\Omega_1 - \Omega_1'$ and moves beyond the limits of the interval $[0, 2\pi s]$. The required equalities are obtained by determining the periodic integrand functions in the interval $[2\pi s, 2\pi s + |\Omega_1 - \Omega_1'|]$ (or $[-|\Omega_1 - \Omega_1'|, 0]$ according to the sign of the difference $\Omega_1 - \Omega_1'$).

We shall now determine the optimum control variables e and δ for one selected value of the angle Ω_1^*; let this be the value for which

$$\delta(+0) = 1, \quad \delta(-0) = 0. \tag{6.82}$$

All the powered periods without exception have equal duration, the beginning and end of adjacent sections are shifted by π, and the function $e(t)$ has different signs for them. We find the following laws for $\delta(t)$ and $e(t)$
260 (Figure 6.18):

$$\left.\begin{aligned} &e = +1, \quad \delta = 1 \quad \text{for} \quad 0 < t < T_\mu/2s, \\ &e = -1, \quad \delta = 1 \quad \text{for} \quad \pi < t < \pi + T_\mu/2s, \\ &e = +1, \quad \delta = 1 \quad \text{for} \quad 2\pi < t < 2\pi + T_\mu/2s, \\ &\vdots \qquad\quad \vdots \qquad\quad \vdots \\ &e = -1, \quad \delta = 1 \quad \text{for} \quad (s-1)\pi < t < (s-1)\pi + T_\mu/2s, \end{aligned}\right\} \tag{6.83}$$

where $T_\mu/2s$ is the engine operating time for one section.

After calculating the integrals (6.80) we determine the relations

$$\Omega_1^* = T_\mu/4s, \quad i/a_0 = 4s \sin(T_\mu/4s). \tag{6.84}$$

In accordance with (6.79), the following functions for $e(t)$ and $\delta(t)$ are obtained for an arbitrary angle Ω_1 different from Ω_1^*:

for $T_\mu/4s < \Omega_1 < T_\mu/4s$

$$\left.\begin{array}{llll} e=+1, & \delta=1 & \text{for} & 0<t<t_1, \\ e=-1, & \delta=1 & \text{for} & t_2<t<t_1+\pi, \\ e=+1, & \delta=1 & \text{for} & t_2+\pi<t<t_1+2\pi, \\ \vdots & \vdots & \vdots & \vdots \\ e=(-1)^{m-1}, & \delta=1 & \text{for} & t_2+(m-2)\pi<t<t_1+(m-1)\pi \\ \vdots & \vdots & \vdots & \vdots \end{array}\right\} \quad (6.85)$$

$$(t_1 = \Omega_1 + T_\mu/4s, \quad t_2 = \Omega_1 - T_\mu/4s + \pi);$$

for $T_\mu/4s < \Omega_1 < \pi - T_\mu/4s$

$$\left.\begin{array}{llll} e=+1, & \delta=1 & \text{for} & t_1<t<t_2, \\ e=-1, & \delta=1 & \text{for} & t_1+\pi<t<t_2+\pi, \\ e=+1, & \delta=1 & \text{for} & t_1+2\pi<t<t_2+2\pi, \\ \vdots & \vdots & \vdots & \vdots \\ e=(-1)^{m-1}, & \delta=1 & \text{for} & t_1+(m-1)\pi<t<t_2+(m-1)\pi \\ \vdots & \vdots & \vdots & \vdots \end{array}\right\} \quad (6.86)$$

$$(t_1 = \Omega_1 - T_\mu/4s, \quad t_2 = \Omega_1 + T_\mu/4s).$$

Taken together, the two cases (6.85) and (6.86) comprise an interval over which Ω_1 varies through an angle π given by

$$-T_\mu/4s < \Omega_1 < \pi - T_\mu/4s. \quad (6.87)$$

The extension of this interval (6.87) to 2π is obtained by changing the sign of the control function $e(t)$.

261 After substituting (6.85) and (6.86) in the second integral of (6.80) we obtain the following relation between i, T_μ, s, and a_0:

$$T_\mu = 4s \arcsin(i/4sa_0) \qquad (T = 2\pi s,\ s = 1, 2, \ldots). \quad (6.88)$$

This is the required expression for the problem functional in terms of the maneuver parameters i, s, and the engine parameter a_0. Note that, just as for the ideal power-limited engine, the control functional is independent of the final position of the nodal line, i.e., of the angle Ω_1, on which the middle points of the powered sections are situated (cf. (6.88) and (5.75), (6.83) and (5.74), Figure 6.18 and Figure 5.29). The maneuver of rotating the orbit plane is also considered in /6.21/.

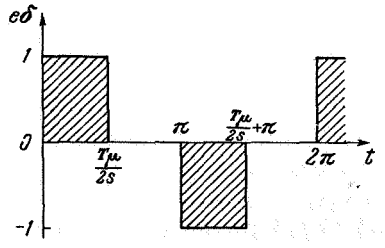

FIGURE 6.18. Optimum program of thrust orientation and of engine ignition during one revolution for the maneuver of rotating the plane of a circular orbit.

In concluding this section, we give an approximation formula for the time required to rotate the plane of a circular orbit (through the angle i) with a simultaneous change of radius (from 1 to r_1)

/6.5/, in the form

$$T = T_\mu = \frac{1}{\mu}\left[1 - \exp\left(-\frac{\mu}{a_0}\sqrt{1 - \frac{2}{\sqrt{r_1}}\cos\frac{\pi i}{2} + \frac{1}{r_1}}\right)\right] =$$
$$= \frac{V}{a_0}\left[1 - \exp\left(-\frac{1}{V}\sqrt{1 - \frac{2}{\sqrt{r_1}}\cos\frac{\pi i}{2} + \frac{1}{r_1}}\right)\right]. \qquad (6.89)$$

It has been assumed here that the engine operates along the entire trajectory, and that the radial component of the thrust vector vanishes; the two components considered were those parallel to the velocity vector and normal to the instantaneous orbit plane (the normal component changes sign on the diameter perpendicular to the nodal line). The absolute values of these two components of the thrust vector are considered as slowly varying functions of time.

By this assumption it becomes possible to average the equations of motion along the revolution. The optimum program of thrust orientation (from revolution to revolution), ensuring the minimum maneuvering time, was found for the averaged equations. It was not assumed that the angle of inclination i and the radial displacement $|r_1 - 1|$ are small. The relation obtained, (6.89), is sufficiently accurate for a wide range of the parameters i and r_1.

262 § 5. PARAMETERS OF A VEHICLE WITH POWER-LIMITED UNTHROTTLED ENGINE

Here we present examples of the solution for the weight part of the optimization problem (the problem of maximizing (6.6)) for power-limited unthrottled engines; use is made of the expressions for the functional $T_\mu(a_0, \mu)$ found in the preceding sections. The values of the payload corresponding to an ideal power-limited engine (from § 4 of Chapter Five) are compared with those obtained here, in order to assess the gain attained by thrust control.

1. **Formulas for calculations.** If the acceleration process in a power-limited engine takes place without losses, the power N is linked with the thrust P and the propellant flow rate q (or the exhaust velocity $V = P/q$) by the ideal relation (cf. (4.1) to (4.3))

$$N = P^2/2q = {}^1/_2 PV \qquad (6.90)$$
$$(N\ [\text{kw}] = 0.481\cdot 10^{-1} P^2[\text{kg}]/q\ [\text{kg/sec}] = 0.49\cdot 10^{-2} P\,[\text{kg}]\,V[\text{m/sec}]).$$

The weight of the propulsion system (4.13) can be represented in the following form*

$$G_\varkappa = \alpha P^2/2q = {}^1/_2\alpha PV, \quad G_\varkappa/G_0 = (\alpha/2g)\, a_0^2/\mu = (\alpha/2g)\, a_0 V$$
$$(G_\varkappa\ [\text{kg}] = 0.481\cdot 10^{-1}\alpha\ [\text{kg/kw}]\, P^2\,[\text{kg}]/q\ [\text{kg/sec}] =$$
$$= 0.49\cdot 10^{-2}\alpha\,[\text{kg/kw}]\, P\,[\text{kg}]\, V\ [\text{m/sec}]). \qquad (6.91)$$

* Relationships for N and $G_\varkappa$ for real power-limited engines, and corresponding examples of the solution for the weight part of the variational problem, are given in Chapter Seven.

Criterion (6.6) for selecting the optimum values of P, q, and V (or a_0, μ, and V) is, in the case considered,

$$\left.\begin{aligned}
&\max G_\pi = \max_{P,\,q}\left(G_0 - \frac{\alpha P^2}{2q} - gqT_\mu\right) = \max_{P,\,V}\left(G_0 - \frac{1}{2}\alpha PV - g\frac{P}{V}T_\mu\right),\\
&\max\frac{G_\pi}{G_0} = \max_{a_0,\,\mu}\left(1 - \frac{\alpha}{2g}\frac{a_0^2}{\mu} - \mu T_\mu\right) = \max_{a_0,\,V}\left(1 - \frac{\alpha}{2g}a_0V - \frac{a_0}{V}T_\mu\right)\\
&\{\max G_\pi\,[\mathrm{kg}] =\\
&\quad = \max_{P,\,q}(G_0\,[\mathrm{kg}] - 0.481\cdot 10^{-1}\alpha\ [\mathrm{kg/kw}]\ P^2\,[\mathrm{kg}]/\,q\,[\mathrm{kg/sec}] -\\
&\qquad - q\,[\mathrm{kg/sec}]\ T_\mu\,[\mathrm{sec}] = \max_{P,\,V}(G_0\,[\mathrm{kg}] -\\
&\qquad - 0.49\cdot 10^{-2}\alpha\,[\mathrm{kg/kw}]\,P\,[\mathrm{kg}]\,V\,[\mathrm{m/sec}] -\\
&\qquad\qquad - 9.81\,P[\mathrm{kg}]\,T_\mu[\mathrm{sec}]/V[\mathrm{m/sec}])\},
\end{aligned}\right\} \tag{6.92}$$

263 where $T_\mu = T_\mu(gP/G_0,\ gq/G_0)$ or $T_\mu = T_\mu(a_0, \mu)$ is the solution of the dynamic part of the problem; the last term in (6.92) represents the initial weight of the working fluid

$$\begin{gathered}
G_{\mu 0} = gqT_\mu = gPT_\mu/V,\ G_{\mu 0}/G_0 = \mu T_\mu = a_0T_\mu/V\\
(G_{\mu 0}\,[\mathrm{kg}] = q[\mathrm{kg/sec}]\,T_\mu\ [\mathrm{sec}] = 9.81\,P\,[\mathrm{kg}]\,T_\mu\ [\mathrm{sec}]/V\,[\mathrm{m/sec}]).
\end{gathered} \tag{6.93}$$

If the parameter μ (or V) does not appear in the expression for the functional T_μ, as in the problems of §§ 4.1, 4.2 (cf. (6.73) and (6.88)), the maximum of G_π/G_0 for μ (or V) is attained when

$$\begin{gathered}
\mu = a_0\Big/\sqrt{\frac{2g}{\alpha}T_\mu}\quad \text{or}\quad V = \sqrt{\frac{2g}{\alpha}T_\mu}\\
(q = 0.219P\sqrt{\alpha/T_\mu}\quad \text{or}\quad V = 0.447\cdot 10^2\sqrt{T_\mu/\alpha}).
\end{gathered} \tag{6.94}$$

(The dimensions of the magnitudes between parentheses here and below are the same as in formulas (6.90) to (6.93).)

With the aid of (6.94) the criterion (6.92) can be represented in the form

$$\begin{gathered}
\max\frac{G_\pi}{G_0} = \max_{a_0}\left(1 - 2a_0\sqrt{\frac{\alpha}{2g}T_\mu}\right)\\
(\max G_\pi = \max_P(G_0 - 0.439P\sqrt{\alpha T_\mu})).
\end{gathered} \tag{6.95}$$

Note that the value of μ (or V) determined by (6.94) corresponds to the case in which the initial weight of the working fluid is equal to the weight of the engine*

$$\frac{G_{\mu 0}}{G_0} = \frac{G_\varkappa}{G_0} = a_0\sqrt{\frac{\alpha}{2g}T_\mu}\quad (G_{\mu 0} = G_\varkappa = 0.219P\sqrt{\alpha T_\mu}). \tag{6.96}$$

Taking the payload as the independent variable in (6.96), we obtain the optimum ratios between the weight components (curve 3 in Figure 6.19)

$$G_{\mu 0}/G_0 = G_\varkappa/G_0 = {}^1/_2\,(1 - G_\pi/G_0), \tag{6.97}$$

* This result for the case of a specified engine operating time for fixed thrust magnitude was obtained by Stuhlinger /6.22/, Moeckel /6.23/, and Preston-Thomas /6.24/. In /6.25/ the corresponding expression was found for optimum weight ratios allowing for relativistic effects caused by high exhaust velocities. It is shown there that for values of the parameter $(T/\alpha) \sim 1$ year · kw/kg the relativistic corrections to terms of the order of unity in the formulas for the weight ratios are of the order of $\sim 10^{-6}$.

whereas for an ideal power-limited engine we obtained

$$G_{\mu 0}/G_0 = 1 - \sqrt{G_\pi/G_0}, \quad G_\varkappa/G_0 = \sqrt{G_\pi/G_0} - G_\pi/G_0 \tag{6.98}$$

(cf. (4.15) to (4.17) and the dashed curves in Figure 6.19).

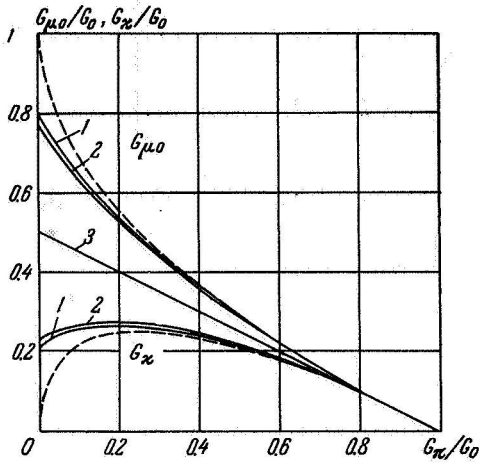

FIGURE 6.19. Comparison of optimum weight ratios for ideally throttled and unthrottled power-limited engines. Dashed curves represent an ideal engine (applicable to all maneuvers); solid curves represent an unthrottled engine (curve 1 is the velocity build-up, curve 2 is displacement between points of rest, curve 3 is rotation of plane of circular orbit, holding the satellite orbit and other maneuvers, where the engine operating time is independent of the propellant flow rate).

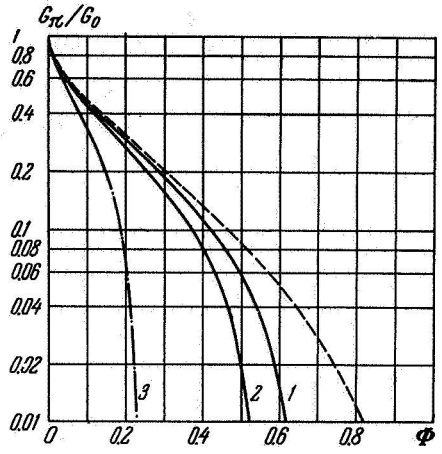

FIGURE 6.20. Payload comparison for vehicles with ideally throttled and unthrottled power-limited engines (symbols as in 6.19, except curve 3, which correspond here to rotation of plane of circular orbit).

264 The ratios (6.98) for an ideal engine are independent of the type of the dynamic maneuver. Such an invariance does not exist for an unthrottled engine, as can be seen in the example of the maneuvers studied in §§ 2 to 4 (Figure 6.19).

The dynamic maneuver in the case of an ideal power-limited engine determines the value of the payload by means of the functional J. The values of J depend on definite combinations of the maneuver parameters:

for the velocity build-up maneuver (cf. (5.32))

$$J_u = u_1^2 T^{-1}, \tag{6.99}$$

for the maneuver of displacement between points of rest (cf. (5.33))

$$J_l = 12 l^2 T^{-3}, \tag{6.100}$$

for the maneuver of rotating the plane of a circular orbit (cf. (5.75) in dimensional form)

$$J_i = 2k r_0^{-1} i^2 T^{-1} \quad (T = 2\pi s k^{-1/2} r_0^{3/2},\ s = 1, 2, \ldots). \tag{6.101}$$

It is interesting to note that the payload of vehicles with unthrottled power-limited engines for the maneuvers listed are determined by the
265 same expressions (6.99) to (6.101), where $\Phi = (\alpha/2g)\,J$ (Figure 6.20). This will be established below whilst solving the weight part of the problem.

2. **Build-up of a velocity magnitude.** The solution of the dynamic problem for this maneuver, performed by an unthrottled engine, is given by (6.30). We select a_0 and V as engine parameters which will be optimized. The criterion (6.92) is then written in the form

$$\max G_\pi/G_0 = \max_{a_0,\,V}\left(e^{-u_1/V} - \frac{\alpha}{2g}\,a_0 V\right), \qquad a_0 \geqslant \frac{V}{T}\,(1 - e^{-u_1/V}). \tag{6.102}$$

The lower bound of a_0 follows from (6.30). Since $-a_0$ appears linearly in (6.102), the maximum of G_π occurs when

$$a_0 = \frac{V}{T}\,(1 - e^{-u_1/V}), \tag{6.103}$$

i.e., in the optimum case the engine should not be cut off during the velocity build-up (cf. (6.30)).

After optimizing the payload G_π/G_0 with respect to the exhaust velocity V
266 we obtain the solution of the weight part of the problem in parametric form (cf. /6.26, 6.27/, etc.), where

$$\left.\begin{aligned} &\frac{G_\pi}{G_0} = \frac{2\,(1 - e^{-\xi}) - \xi}{2\,(e^{\xi} - 1) - \xi}, \quad \frac{G_{\mu 0}}{G_0} = 1 - e^{-\xi}, \quad \frac{G_\varkappa}{G_0} = e^{-\xi} - \frac{G_\pi}{G_0}, \\ &\Phi_u = \frac{\alpha}{2g}\,u_1^2 T^{-1} = \frac{\xi^3}{2\,(e^{\xi} - 1) - \xi}, \quad \frac{u_1}{V} = \xi. \end{aligned}\right\} \tag{6.104}$$

The optimum weight ratios $G_\varkappa\,(G_\pi)$ and $G_{\mu 0}\,(G_\pi)$ are shown in Figure 6.19 (curves 1), the dependence of the maximum payload G_π on Φ_u in Figure 6.20 (curve 1), and the optimum exhaust velocity in Figure 6.21 as the relationship $\xi\,(\Phi_u)$. The limit of the functional Φ here is ~ 0.65 ($G_\pi = 0$ for $\Phi_u \approx \approx 0.65$) instead of $\Phi = 1$, as for the ideal engine. Nowhere does the optimum exhaust velocity drop below half the increment of the vehicle velocity ($\min V\,(\Phi_u) \approx 0.63\,u_1$). *

3. **Displacement between points of rest.** The functional of the dynamic problem for an unthrottled engine is determined here by (6.43). Expressing the acceleration a_0 from (6.43), we write the payload (6.92) as a function of the working-fluid reserve $G_{\mu 0}/G_0 = 1 - \mu T_\mu$ and the time ratio T/T_μ in the form

$$\frac{G_\pi}{G_0} = 1 - \frac{G_{\mu 0}}{G_0} - \frac{\alpha}{2g}\,\frac{l^2}{T^3} \times \\ \times \frac{(G_{\mu 0}/G_0)^3\,(T/T_\mu)^3}{\{2\,(1 - \sqrt{1 - G_{\mu 0}/G_0}) - G_{\mu 0}/G_0 - {}^1\!/_2\,(G_{\mu 0}/G_0)\,[(T/T_\mu) - 1]\ln(1 - G_{\mu 0}/G_0)\}^2}. \tag{6.105}$$

Here, just as in § 5.2, the maneuver parameters appearing in the functional (6.100) for an ideal engine were grouped together.

* The solution obtained is also correct for the maneuver of rotating the plane of a circular orbit while simultaneously varying the radius when the engine is not turned off. This follows by comparing formulas (6.89) and (6.103). It is necessary to take $u_1 = \sqrt{r_0 g_0}\,[1 - 2\sqrt{r_0/r_1}\cos({}^1\!/_2\pi i) + r_0/r_1]^{1/2}$ as the velocity increment for such a maneuver.

267 We represent the weight $G_{\mu 0}$ in the form $G_{\mu 0} = G_0 (1 - e^{-\xi})$ (cf. (6.104)); the problem then reduces to finding

$$\max \frac{G_\pi}{G_0} = \max_{\xi,\, T/T_\mu} \left\{ e^{-\xi} - \frac{1}{12} \Phi_l \frac{(1 - e^{-\xi})(T/T_\mu)^3}{\left[\frac{1 - e^{-\xi/2}}{1 + e^{-\xi/2}} + \frac{1}{2} \xi \left(\frac{T}{T_\mu} - 1 \right) \right]^2} \right\}. \tag{6.106}$$

Since the partial derivatives with respect to (T/T_μ) and ξ must vanish, we obtain the solution of the weight part of the problem in the parametric form /6.1, 6.26/ (cf. (6.104))

$$\left.\begin{aligned} &\frac{G_\pi}{G_0} = \frac{\xi [2 - (e^{-\xi/2} + e^{-\xi})] - 3 + 6e^{-\xi/2} - 3e^{-\xi} - {}^1/_2 \xi^2}{\xi [(e^{\xi/2} + e^{\xi}) - 2] - 3 + 6e^{\xi/2} - 3e^{\xi} - {}^1/_2 \xi^2}, \\ &\frac{G_{\mu 0}}{G_0} = 1 - e^{-\xi}, \quad \frac{G_\varkappa}{G_0} = e^{-\xi} - \frac{G_\pi}{G_0}, \\ &\Phi_l = \frac{\alpha}{2g} 12 l^2 T^{-3} = \frac{{}^2/_9 \xi^4}{\xi [(e^{\xi/2} + e^{\xi}) - 2] - 3 + 6e^{\xi/2} - 3e^{\xi} - {}^1/_2 \xi^2}, \\ &\frac{T_\mu}{T} = \frac{2}{3} \frac{\xi}{{}^1/_2 \xi - \dfrac{1 - e^{-\xi/2}}{1 + e^{-\xi/2}}}. \end{aligned}\right\} \tag{6.107}$$

From these formulas we calculate the optimum weight ratios $G_{\mu 0}(G_\pi)$ and $G_\varkappa (G_\pi)$ (curves 2 in Figure 6.19), the dependence of the maximum payload G_π/G_0 on the functional Φ_l (curve 2 in Figure 6.20), and the optimum engine operating time T_μ/T as a function of Φ_l (Figure 6.22). The limit of the functional Φ for an unthrottled engine is smaller than for the case of velocity build-up ($G_\pi = 0$ at $\Phi_l \approx 0.56$; compare curves 1 and 2 in Figure 6.20). The optimum engine operating time depends weakly on Φ_l and contributes about two-thirds of the total time of motion.

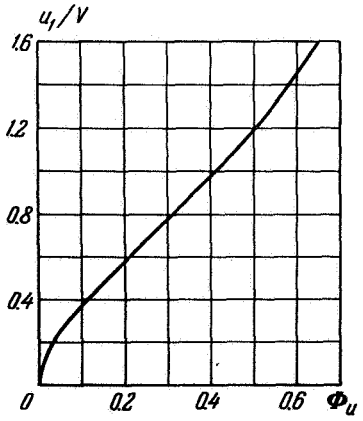

FIGURE 6.21. Optimum exhaust velocity V as function of $\Phi_u = (\alpha/2g) u_1^2 T^{-1}$ for build-up maneuver of given velocity magnitude u_1.

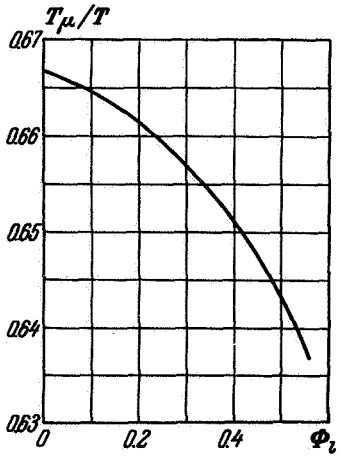

FIGURE 6.22. Optimum engine operating time T_μ/T as function of $\Phi_l = (\alpha/2g) 12 l^2 T^{-3}$ for maneuver of displacement between points of rest at distance l apart.

4. **Interplanetary Earth—Mars flight.** The resulting relationship $T_{\mu\sigma}(a_0, V)$ for the dynamic part of the problem is shown in Figure 6.11. The values of a_0 and V which maximize (6.92) are found numerically for each pair of values of T_σ and α using the data of Figure 6.11.

269 The optimum values of a_0 and V are shown in Figures 6.23 and 6.24 as a function of the flight time for fixed values of the unit engine weight. The corresponding values of the engine operating time are marked in Figure 6.25.

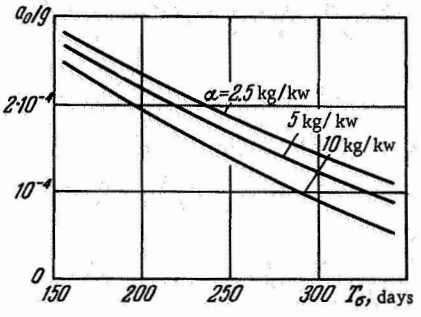

FIGURE 6.23. Optimum initial thrust acceleration a_0 for Earth—Mars flight as function of flight time T_σ and unit engine weight α.

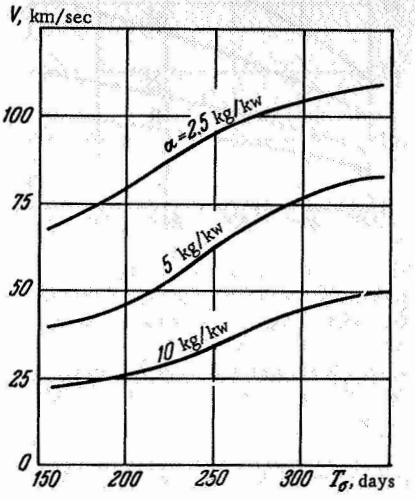

FIGURE 6.24. Optimum exhaust velocity V for Earth—Mars flight.

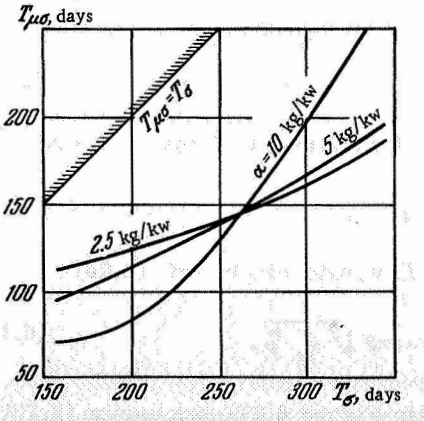

FIGURE 6.25. Optimum engine operating time $T_{\mu\sigma}$ for Earth—Mars flight.

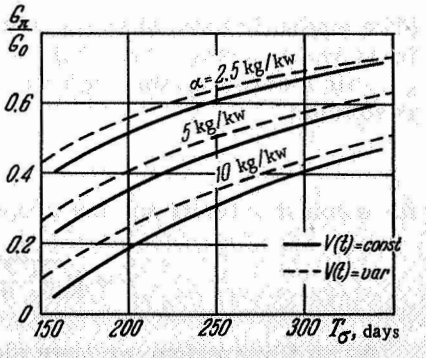

FIGURE 6.26. Comparison of payload of Earth—Mars vehicles with ideally throttled (dashed curves) and unthrottled (solid curves) power-limited engines.

The maximum payload G_π/G_0 is represented in Figure 6.26 as a function of T_σ and α. The dashed curves on the same figure correspond to an ideal power-limited engine.

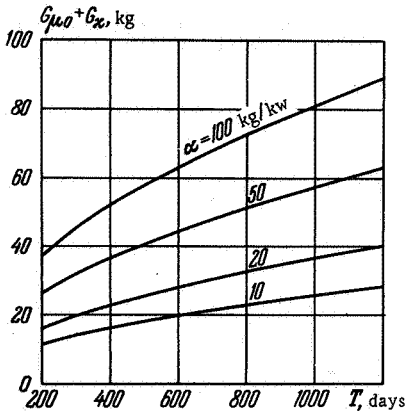

FIGURE 6.27. Example of dependence of minimum total weight $G_{\mu 0}+G_\varkappa$ of working-fluid reserve $G_{\mu 0}$ and engine $G_\varkappa$ on time during which satellite remains in a spherical layer. (α represents unit engine weight, $G_{\mu 0}=G_\varkappa$, $R=0.5$ g is the resistance, engine operates every 16-th revolution).

5. Holding the satellite in a specified spherical layer. The functional T_μ of the dynamic part of problem (6.73) for the maneuver considered is a function of the initial acceleration a_0 only, and is independent of the propellant flow rate μ or the exhaust velocity V. The optimum weight ratios (6.97) will therefore be correct here (cf. curve 3 in Figure 6.19). In (6.73) we pass from the parameter $\varkappa$ to the resistance* $F=\varkappa G_0/g$ and from the acceleration a_0 to the thrust $P=a_0G_0/g$. Since the resistance F is not directly related to the take-off weight, and is determined by the vehicle shape, the weight part of the problem can be solved independently of the take-off weight.

We shall look for the minimum sum of the weights of working fluid and engine, i.e., for the minimum of expression (6.96).

After substituting (6.73), the solution of the dynamic problem, into (6.96), we obtain

$$\min (G_{\mu 0}+G_\varkappa) = \min_P \sqrt{2g\alpha TFP}. \tag{6.108}$$

It is seen from here that the thrust must be minimized. According to (6.68), the acceleration a_0 has a lower bound, and therefore in the optimum case

$$P=mR, \quad G_{\mu 0}=G_\varkappa=F\sqrt{{}^1/_2 g\alpha mT}. \tag{6.109}$$

(The engine is fired at every m-th revolution, and the satellite is held in its layer during a time T.)

This means that the engine must function during the entire powered revolution

$$T_\mu = T/m; \tag{6.110}$$

270 the exhaust velocity and the propellant flow rate will be (cf. (6.94)):

$$V=\sqrt{\frac{2g}{\alpha}\frac{T}{m}}, \quad q=mF\sqrt{\frac{\alpha}{2g}\frac{m}{T}}. \tag{6.111}$$

As an illustration, we have plotted (in Figure 6.27) expression (6.109) for the minimum total weight $(G_{\mu 0}+G_\varkappa)$ as a function of the time T of sojourn of the satellite within the limits of the spherical layer for different values of the unit engine weight α (the resistance F is 0.5 g, $m=16$).

* It is assumed here that $\rho=$ const, $j_z=0$ (cf. (A.70)).

6. Rotating the plane of a circular orbit. The solution of the dynamic part of the problem is given by (6.88), for which we again have $\partial T_\mu/\partial\mu = 0$ (or $\partial T_\mu/\partial V = 0$). It follows that the optimum weight ratios are determined by (6.97) (curve 3 on Figure 6.19). Substituting a_0 from (6.88) in (6.95), we obtain the payload as a function of the relative engine operating time T_μ/T (in (6.88) $T = 2\pi s$, $s = 1, 2, \ldots$):

$$\frac{G_\pi}{G_0} = 1 - \frac{\pi\sqrt{T_\mu/T}}{\sqrt{2}\sin(\frac{1}{2}\pi T_\mu/T)}\sqrt{\Phi_i}$$

$$\left(\Phi_i = \frac{\alpha}{2g}\,2kr_0^{-1}i^2T^{-1}, \qquad T = 2\pi sk^{-3/2}r_0^{3/2}\right). \tag{6.112}$$

The optimum value of T_μ/T (obtained by maximizing (6.112)) is given by $T_\mu/T = 0.7420$; the payload G_π/G_0, the engine weight $G_\varkappa/G_0$, the working-fluid weight $G_{\mu 0}/G_0$, the exhaust velocity V, and the initial acceleration a_0 are then equal to

$$\left.\begin{aligned} G_\pi/G_0 &= 1 - 2.0822\sqrt{\Phi_i}, \quad G_{\mu 0}/G_0 = G_\varkappa/G_0 = 1.0411\sqrt{\Phi_i}, \\ V &= 1.219\sqrt{gT/\alpha}, \qquad\qquad a_0 = gP/G_0 = 0.544k^{1/2}r_0^{-3/2}iT^{-1}. \end{aligned}\right\} \tag{6.113}$$

Curve 3 of Figure 6.20 represents the payload in the form $\Phi_i = (\alpha/2g)\,J_i$. We recall that the solution of the dynamic problem (6.88) was obtained under the assumption that $G(t)$ is constant, and therefore relations (6.112) and (6.113) are correct for $\Phi_i \ll 1$ only (for $\Phi_i \sim 1$, (6.113) gives low values of the payload). In addition, the maneuvering time T was assumed to be a multiple of the period of revolution of the satellite ($T = 2\pi sk^{-3/2}r_0^{3/2}$, $s = 1, 2, \ldots$).

Chapter Seven

REAL POWER-LIMITED ENGINES

271 Real power-limited propulsion systems differ mainly in the following points from ideal propulsion systems.

1) In real engines some working fluid and power are lost due to phase transitions (ionization, neutralization), inhomogeneity of the jet in the nozzle, etc. These losses are characterized by the coefficients η_μ and η_ν describing the utilization of the working fluid and power respectively. With the aid of these coefficients the expression for the thrust of a real engine becomes (cf. (4.1))

$$P = \sqrt{2\eta_\gamma N_\gamma q}, \tag{7.1}$$

where $\eta_\gamma = \eta_\mu \eta_\nu$ is the over-all efficiency. The latter depends on the power N_γ, on the flow rate q of propellant supplied to the engine, as well as on the geometric parameters and on those of the electric circuit, so that

$$\eta_\gamma = \eta_\gamma (N_\gamma, q, w_1, \ldots, w_l).$$

2) The engine can be controlled by varying the power N_γ and flow rate q of propellant supplied to it, while the geometrical parameters and those of the electric circuit $w_1, \ldots, w_l$ remain constant.

We shall consider two possible ways of controlling the propulsion system. Their use will depend on the form of the function $\eta_\gamma (N_\gamma, q)$.

The extent to which an engine with constant parameters $w_1, \ldots, w_l$ can be controlled is determined by the values of N_γ, q inside which $\eta_\gamma (N_\gamma, q) > 0$. Two limiting cases are possible. In the first, the surface $\eta_\gamma (N_\gamma, q)$ represents the plane $\eta_\gamma (N_\gamma, q) = 0$ excluding the point N_γ^*, q^* for which $\eta_\gamma > 0$; this case corresponds to an unthrottled engine defined over the range N_γ^*, q^*. The other extreme case is that of an ideally-throttled engine for which $\eta_\gamma (N_\gamma, q) = \text{const}$; here the control range is unlimited. Actually, for real engines the range is either relatively narrow or relatively wide, but it is always limited. The
272 function $\eta_\gamma (N_\gamma, q)$ has either a sharp maximum or a broad one at the point N_γ^*, q^*, whose position is determined by the values of the parameters $w_1, \ldots, w_l$.

The thrust of a propulsion system with a wide control range can be varied not only by altering the power N_γ and the propellant flow rate q, but also by varying the number of operating elements (in the case of a composite engine).

If the control range of the engine is narrow, the thrust is varied by switching over from one rocket (or block of rockets) to another which uses different values of N_γ^*, q^* obtained by suitably selecting the parameters $w_1, \ldots, w_l$.

In the latter case, smooth control of the propulsion system is impossible because both the thrust and propellant flow rate are step functions of the time. *

3) In an ideal engine the weights of the power source and converter, and nozzle are functions of the maximum power only (cf. (4.1)); the weight G_v of the real power source and converter are likewise determined by the value of the maximum power

$$G_v = f(N_{\max}), \tag{7.2}$$

while the nozzle weight G_γ depends on the type of nozzle being used and the limiting values of the independent controls. Thus, the weight of the real propulsion system includes at least two components, where

$$G_\varkappa = G_v + G_\gamma. \tag{7.3}$$

4) While the operating time of an ideal power-limited engine is unlimited, that of a real engine has an upper bound determined by the working-fluid reserve of the engine.

These properties of real engines are general, so that the actual expressions for the weight G_γ and the thrust P depend on the type of nozzle used.

Note that for real propulsion systems, we may allow for the weight
273 of the working-fluid tanks in the weight formula. This weight is usually taken as a function of the initial working-fluid weight $G_\beta = f(G_{\mu 0})$; the linear relationship

$$G_\beta = \beta_\mu G_{\mu 0} \qquad (\beta_\mu = \text{const}) \tag{7.4}$$

is the one most widely used /7.4—7.6/.

§ 1. ADDITIONAL WEIGHT COMPONENTS

An ideal spacecraft with an ideal power-limited engine is considered as having three weight components: the payload G_π, the working-fluid weight G_μ, and the engine weight $G_\varkappa$, which is proportional to the maximum power. The variational problems are formulated in this section so that additional weights, the weight of the tanks G_β and the weight of the nozzle G_γ, may be allowed for. These weight components are studied separately, and their influence on the optimum controls is investigated.

1. Allowing for the weight of the tanks. We complete the expression for the weight in the original formulation of the variational problem (II. 2) by adding the component G_β, the weight of the tanks, in the form (7.4). The variational problem (II.5) then becomes

$$\left.\begin{aligned}
&\dot G_\pi = 0, && G_\pi(0) + G_\varkappa + G_\pi(T) = \max,\\
&\dot G_\mu = -gq, && +(1+\beta_\mu)G_\mu(0) = G_0, \quad G_\mu(T) = 0,\\
&\dot{\mathbf{r}} = \mathbf{v}, && \mathbf{r}(0) = \mathbf{r}_0, \quad \mathbf{r}(T) = \mathbf{r}_1,\\
&\dot{\mathbf{v}} = \frac{gP\mathbf{e}}{G_\pi + G_\mu + G_\beta + G_\varkappa} + \mathbf{R}, && \mathbf{v}(0) = \mathbf{v}_0, \quad \mathbf{v}(T) = \mathbf{v}_1.
\end{aligned}\right\} \tag{7.5}$$

* Restrictions can also be imposed on the control of the thrust-vector direction; thus, a tangential direction /7.1, 7.2/, and an invariable or stepwise-variable direction /7.3/ have been considered.

If the weight formula does not contain components of the type G_β, depending on the initial weight of the working fluid, this variational problem can be reduced to the form (II. 8), where the part of the functional is played by the final value of the sum of weights given by

$$G_\sigma = G_\pi + G_\mu.$$

The new problem has one boundary condition less than the original one, and is therefore simpler.

Let problem (7.5) be reduced to a boundary-value problem for ordinary differential equations; then, in spite of the presence of the term G_β, one can make several substitutions to simplify the boundary-value problem in the same way as if the term G_β was absent.

The Mayer problem (7.5) will be reduced to a boundary-value problem
274 by Pontryagin's method. The Hamiltonian and momentum equations are:

$$\left.\begin{aligned} &H = p_\pi \cdot 0 - p_\mu g q + \mathbf{p}_r \cdot \mathbf{v} + \mathbf{p}_v \cdot \left(\frac{gPe}{G_\pi + G_\mu + G_\beta + G_\varkappa} + \mathbf{R} \right), \\ &\dot{p}_\pi = \dot{p}_\mu = (\mathbf{p}_v \cdot \mathbf{e})\, gP\, (G_\pi + G_\mu + G_\beta + G_\varkappa)^{-2}, \\ &p_\pi(T) = -1, \dot{\mathbf{p}}_r = -\frac{\partial}{\partial \mathbf{r}} (\mathbf{p}_v \cdot \mathbf{R}), \dot{\mathbf{p}}_v = -\mathbf{p}_r. \end{aligned}\right\} \tag{7.6}$$

Note that the differential equations for p_π and p_μ are identical, and that initially their values satisfy the transversality condition

$$p_{\mu 0} = (1 + \beta_\mu)\, p_{\pi 0}. \tag{7.7}$$

The latter follows from the fact that the weights G_μ, G_π are not initially specified separately, but are linked through one of the equations (7.5).

In view of these facts we may find an expression for $p_\mu(t)$ in terms of $p_\pi(t)$ and β_μ where

$$p_\mu(t) = p_\pi(t) + \beta_\mu p_{\pi 0}, \tag{7.8}$$

which is then used to eliminate $p_\mu(t)$ from the equations and the Hamiltonian (7.6).

We introduce a new phase coordinate $G_\theta(t)$ defined by

$$G_\theta = G_\pi + G_\mu + \beta_\mu G_{\mu 0}, \tag{7.9}$$

and so replace G_μ in the differential equations (7.5) and (7.6) and in the Hamiltonian (7.6) by G_θ. The system of differential equations and boundary conditions, and the Hamiltonian thus obtained have the form

$$\left.\begin{aligned} &\dot{G}_\theta = -gq, && G_\theta(0) = G_0 - G_\varkappa, && \\ &\dot{\mathbf{r}} = \mathbf{v}, && \mathbf{r}(0) = \mathbf{r}_0, && \mathbf{r}(T) = \mathbf{r}_1, \\ &\dot{\mathbf{v}} = \frac{gPe}{G_\theta + G_\varkappa} + \mathbf{R}, && \mathbf{v}(0) = \mathbf{v}_0, && \mathbf{v}(T) = \mathbf{v}_1, \\ &\dot{p}_\pi = (\mathbf{p}_v \cdot \mathbf{e}) \frac{gP}{G_\theta + G_\varkappa}, && && p_\pi(T) = -1, \\ &\dot{\mathbf{p}}_r = -\frac{\partial}{\partial \mathbf{r}} (\mathbf{p}_v \cdot \mathbf{R}), && && \\ &\dot{\mathbf{p}}_v = -\mathbf{p}_r && && \\ &\left(H = -(p_\pi + \beta_\mu p_{\pi 0})\, gq + \mathbf{p}_r \cdot \mathbf{v} + \mathbf{p}_v \cdot \left[\frac{gPe}{G_\theta + G_\varkappa} + \mathbf{R} \right] \right). && && \end{aligned}\right\} \tag{7.10}$$

275 After problem (7.10) has been solved, the payload G_π is determined in terms of $G_\theta(0)$ and $G_\theta(T)$ (cf. (7.9)): $G_\pi = (1+\beta_\mu)G_\theta(T) - \beta_\mu G_\theta(0)$.

The control variables entering into (7.10) are found from the condition that the function H must attain an absolute minimum. To determine the engine control variables it is necessary to know its characteristics, i.e., expressions like (II.9) and (II.10).

Unlike the initial boundary-value problem, (7.10) does not contain a finite condition for the working-fluid weight G_μ, and neither does it contain a differential equation for p_μ; the new problem is therefore simpler than the original one.

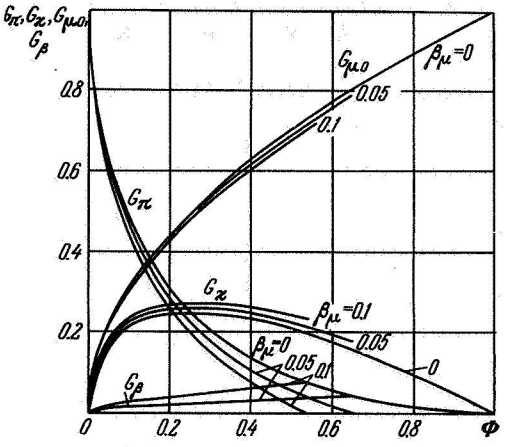

FIGURE 7.1. Influence of weight of tanks on the optimum weight ratios of a vehicle with ideal power-limited engine (β_μ is unit weight of tanks, Φ is functional of dynamic maneuver).

We shall illustrate how the weight of the tanks influences the optimum weight ratios of the vehicle for an ideal power-limited engine /7.6/. The engine weight will be considered as fixed. The problem is again split into a weight part and a dynamic part. By performing calculations similar to those of § 1 of Chapter Four we find that, compared with the previous optimum ratios (4.15) to (4.17), the optimum weight of the engine increases, $G_\varkappa = \sqrt{(1+\beta_\mu)\Phi} - \Phi$, and the weight of the working fluid decreases, $G_{\mu 0} = \sqrt{\Phi/(1+\beta_\mu)}$, so that the payload naturally drops to $G_\pi = 1 - 2\sqrt{(1+\beta_\mu)\Phi} + \Phi$ (Figure 7.1). The range of maneuvers performed ($G_\pi \geqslant 0$) is restricted to $0 \leqslant \Phi \leqslant 1 - 2\sqrt{\beta_\mu}\,(\sqrt{1+\beta_\mu} - \sqrt{\beta_\mu})$.

276 2. **Allowing for the nozzle weight.** We shall assume that the weight of the engine $G_\varkappa$ consists of two components, the weight of the power source and converter G_ν, and the weight of the nozzle G_γ /7.7/, so that

$$G_\varkappa = G_\nu + G_\gamma. \tag{7.11}$$

The first is a linear function of the maximum power $N_{\max}$,

$$G_\nu = \alpha N_{\max} \quad (\alpha = \text{const}), \tag{7.12}$$

while the second is a function of the maximum power N_{max} and the maximum thrust P_{max},

$$G_\gamma = f(N_{max}, P_{max}). \tag{7.13}$$

We shall consider the case in which f is a linear function of its arguments,

$$G_\gamma = \alpha' N_{max} + \gamma P_{max} \qquad (\alpha',\ \gamma = \text{const}). \tag{7.14}$$

Since the weights G_ν, G_γ enter additively into the weight formula (7.11), the term $\alpha' N_{max}$ in (7.14) can be added to G_ν, where

$$G_\nu + \alpha' N_{max} = (\alpha + \alpha')\, N_{max}, \tag{7.15}$$

so that the nozzle weight component in (7.14), which is proportional to N_{max}, is excluded from consideration. Bearing this in mind, we shall let

$$G_\gamma = \gamma P_{max}. \tag{7.16}$$

It is assumed that the control characteristic is ideal and given by (4.3); in accordance with (7.16), we shall impose an upper bound on the value of the thrust: $0 \leqslant P(t) \leqslant P_{max}$.

The variational problem for delivering a maximum payload using a power-limited engine containing two weight components G_ν, G_γ is written as follows (cf. (II.6) to (II.8) and (4.3)):

$$\left.\begin{aligned}
&\dot G_\sigma = -gP^2/2N, \quad G_\sigma(0) = G_0 - G_\nu(0) - G_\gamma(0),\ G_\sigma(T) = \max,\\
&\dot{\mathbf{r}} = \mathbf{v}, \qquad\qquad \mathbf{r}(0) = \mathbf{r}_0, \quad \mathbf{r}(T) = \mathbf{r}_1,\\
&\dot{\mathbf{v}} = \frac{gP\mathbf{e}}{G_\sigma + G_\nu + G_\gamma} + \mathbf{R}, \qquad \mathbf{v}(0) = \mathbf{v}_0, \quad \mathbf{v}(T) = \mathbf{v}_1\\
&(G_\nu = \alpha N_{max},\ G_\gamma = \gamma P_{max},\ 0 \leqslant N(t) \leqslant N_{max},\\
&\qquad\qquad 0 \leqslant P(t) \leqslant P_{max},\ |\mathbf{e}(t)| \equiv 1).
\end{aligned}\right\} \tag{7.17}$$

The control functions are $\mathbf{e}(t)$, $N(t)$, $P(t)$, $G_\nu(t)$, $G_\gamma(t)$; the last four of them
277 are not independent. In order to separate the independent control functions we shall make some substitutions (cf. § 2 of Chapter Four). We express the power N and the thrust P as fractions of their maximum value,

$$N_{max} = G_\nu/\alpha, \quad P_{max} = G_\gamma/\gamma,$$

and add two differential relations to (7.17) which express the decrease in the weights G_ν, G_γ: $\dot G_\nu = -gq_\nu$, $\dot G_\gamma = -gq_\gamma$ $(0 \leqslant q_\nu \leqslant \infty,\ 0 \leqslant q_\gamma \leqslant \infty)$. Now G_ν, G_γ are the new phase coordinates, and q_ν, q_γ the control functions. We shall likewise represent all the weight components as fractions of the initial weight G_0, but preserve the old designations for the dimensionless thrust, power, propellant flow rates q_ν, q_γ, and weights. The variational problem will then be

$$\begin{aligned}
&\dot G_\sigma = -\frac{\alpha g}{2\gamma^2}\frac{G_\gamma^2 P^2}{G_\nu N}, && G_\sigma(0) + && G_\sigma(T) = \max,\\
&\dot G_\nu = -gq_\nu, && + G_\nu(0) + && G_\nu(T) = \text{opt},\\
&\dot G_\gamma = -gq_\gamma, && + G_\gamma(0) = 1, && G_\gamma(T) = \text{opt},
\end{aligned} \tag{7.18}$$

$$\dot{\mathbf{r}} = \mathbf{v}, \qquad \mathbf{r}(0) = \mathbf{r}_0, \qquad \mathbf{r}(T) = \mathbf{r}_1,$$
$$\dot{\mathbf{v}} = \frac{g}{\gamma}\frac{PG_\gamma \mathbf{e}}{G_\sigma + G_v + G_\gamma} + \mathfrak{R}, \qquad \mathbf{v}(0) = \mathbf{v}_0, \qquad \mathbf{v}(T) = \mathbf{v}_1 \tag{7.18}$$
$$(0 \leqslant N(t) \leqslant 1,\ 0 \leqslant P(t) \leqslant 1,\ 0 \leqslant q_v(t) \leqslant \infty,$$
$$0 \leqslant q_\gamma(t) \leqslant \infty,\ |\mathbf{e}(t)| \equiv 1).$$

To solve the variational problem (7.18) by Pontryagin's method, we form the Hamiltonian and write the differential equations of the momenta:

$$\left.\begin{aligned}
H &= -p_\sigma \frac{\alpha g}{2\gamma^2}\frac{G_\gamma^2 P^2}{G_v N} - p_v g q_v - p_\gamma g q_\gamma + \mathbf{p}_r \cdot \mathbf{v} + \mathbf{p}_v \cdot \left(\frac{g}{\gamma}\frac{PG_\gamma \mathbf{e}}{G_\sigma + G_v + G_\gamma} + \mathfrak{R}\right),\\
\dot{p}_\sigma &= (\mathbf{p}_v \cdot \mathbf{e})\frac{g}{\gamma}\frac{PG_\gamma}{(G_\sigma + G_v + G_\gamma)^2},\\
\dot{p}_v &= \dot{p}_\sigma - p_\sigma \frac{\alpha g}{2\gamma^2}\frac{G_\gamma^2 P^2}{G_v^2 N},\\
\dot{p}_\gamma &= -(\mathbf{p}_v \cdot \mathbf{e})\frac{g}{\gamma}\frac{P(G_\sigma + G_v)}{(G_\sigma + G_v + G_\gamma)^2} + p_\sigma \frac{\alpha g}{\gamma^2}\frac{G_\gamma P^2}{G_v N},\\
\dot{\mathbf{p}}_r &= -\frac{\partial}{\partial \mathbf{r}}(\mathbf{p}_v \cdot \mathfrak{R}),\ \dot{\mathbf{p}}_v = -\mathbf{p}_r.
\end{aligned}\right\} \tag{7.19}$$

The boundary conditions for the momenta are:

$$p_\sigma(0) = p_v(0) = p_\gamma(0), \qquad p_v(T) = p_\gamma(T) = 0, \qquad p_\sigma(T) = -1. \tag{7.20}$$

The optimum control variables $\mathbf{e}(t)$, $N(t)$, $P(t)$, $q_v(t)$, $q_\gamma(t)$ must provide an absolute minimum of the function H.

We obtain the form of $\mathbf{e}(t)$ from this condition,

$$\mathbf{e} = -\mathbf{p}_v / p_v \qquad (p_v = |\mathbf{p}_v|). \tag{7.21}$$

The function $1/N$ enters linearly into the expression for H, and therefore the control variable $N(t)$ takes the boundary values 0 or 1 depending on the sign of $p_\sigma(t)$. We shall show that $p_\sigma(t) < 0$ in the entire interval $0 \leqslant t \leqslant T$. For $p_\sigma(t) > 0$, the optima of $N(t)$ and $P(t)$ would be $N(t) = 0$, $P(t) = 1$ (cf. (7.19)). This corresponds to an infinite flow rate of the working fluid at zero exhaust velocity. Such a region is clearly not optimal, and therefore the assumption $p_\sigma(t) > 0$ is inaccurate; it follows that $p_\sigma(t) < 0$ when $0 \leqslant t \leqslant T$. Then

$$N(t) \equiv 1. \tag{7.22}$$

The function $P(t)$ varies as follows within the limits of the closed interval $0 \leqslant P(t) \leqslant 1$:

inside the interval

$$P(t) = P_{\text{opt}} \qquad \left(P_{\text{opt}} = -\frac{p_v}{p_\sigma}\frac{\gamma}{\alpha}\frac{G_v}{G_\gamma(G_\sigma + G_v + G_\gamma)}\right), \tag{7.23}$$

at the upper limit

$$P(t) = 1 \quad \text{for} \quad P_{\text{opt}} \geqslant 1, \tag{7.24}$$

at the lower limit

$$P(t)=0 \text{ at } \Delta>0\left(\Delta=-p_\sigma\frac{\alpha g}{2\gamma^2}\frac{G_\gamma^2P_{\text{opt}}^2}{G_\nu}-p_\nu\frac{g}{\gamma}\frac{G_\gamma P_{\text{opt}}}{G_\sigma+G_\nu+G_\gamma}\right). \tag{7.25}$$

Using (7.23) we transform the expression Δ where

$$\Delta=-p_\sigma\frac{\alpha g}{2\gamma^2}\frac{G_\gamma^2P^2}{G_\nu}\left(1-2\frac{P_{\text{opt}}}{P}\right). \tag{7.26}$$

Since $P_{\text{opt}}/P\geqslant 1$ we have $\Delta<0$ everywhere, and the lower limit (7.25) does not enter into the optimum control function $P(t)$, i.e., the flight is powered along the entire trajectory.

We shall now consider the optimum control variables $q_\nu(t)$ and $q_\gamma(t)$. If there is no upper bound to limit the control variables q_ν and q_γ, the
279 momenta p_ν and p_γ are nonpositive everywhere in $[0, T]$. We shall prove this assertion for p_ν. Let us assume the converse. At some time $t=t_*$ let $p_\nu(t_*)>0$; then the control variable q_ν takes the optimum value $q_\nu(t_*)=\infty$ (cf. (7.19)), which corresponds to an instantaneous discharge of a finite part of the weight G_ν. The derivative $\dot{p}_\nu$ remains finite at $q_\nu=\infty$, and therefore the function $p_\nu(t)$ does not change sign inside a finite time interval in the neighborhood of $t=t_*$. Therefore, during a finite time interval, $q_\nu=\infty$; this indicates the discharge of an infinite weight G_ν, which is impossible. The initial assumption is therefore incorrect and

$$p_\nu(t)\leqslant 0,\ p_\gamma(t)\leqslant 0 \quad \text{at} \quad 0\leqslant t\leqslant T. \tag{7.27}$$

If the control functions q_ν and q_γ have upper bounds, and in particular if $q_\nu(t)\equiv q_\gamma(t)\equiv 0$, deductions (7.27) become inaccurate for the sign of $p_\nu(t)$ and $p_\gamma(t)$.

The analysis of the optimum control variables $q_\nu(t)$ and $q_\gamma(t)$ yields two types of regions: boundary controls $q_\nu=0$, $q_\gamma=0$ when $p_\nu<0$, $p_\gamma<0$, corresponding to $G_\nu=\text{const}$, $G_\gamma=\text{const}$, and singular controls $\dot{p}_\nu(t)=0$, $\dot{p}_\gamma(t)=0$ at $p_\nu(t)=0$, $p_\gamma(t)=0$, corresponding to the partial minimum of the function H with respect to G_ν and G_γ. It should be noted that the existence of these two regimes is a property common to problems with boundary conditions of the type (7.18) imposed on the original control functions (in the case considered $G_\nu(t)$ and $G_\gamma(t)$).

Using (7.23), the expressions for $\dot{p}_\nu$, $\dot{p}_\gamma$ can be represented in the forms

$$\left.\begin{aligned}\dot{p}_\nu&=p_\nu\frac{g}{\gamma}\frac{PG_\gamma}{2G_\nu(G_\sigma+G_\nu+G_\gamma)}\left(\frac{P}{P_{\text{opt}}}-\frac{2G_\nu}{G_\sigma+G_\nu+G_\gamma}\right),\\ \dot{p}_\gamma&=p_\nu\frac{g}{\gamma}\frac{P}{G_\sigma+G_\nu+G_\gamma}\left(-\frac{P}{P_{\text{opt}}}+\frac{G_\sigma+G_\nu}{G_\sigma+G_\nu+G_\gamma}\right).\end{aligned}\right\} \tag{7.28}$$

The singular regions are obtained

$$\left.\begin{aligned}&\text{for } q_\nu \text{ at } \frac{P}{P_{\text{opt}}}=\frac{2G_\nu}{G_\sigma+G_\nu+G_\gamma},\\ &\text{for } q_\gamma \text{ at } \frac{P}{P_{\text{opt}}}=\frac{G_\sigma+G_\nu}{G_\sigma+G_\nu+G_\gamma}.\end{aligned}\right\} \tag{7.29}$$

If $P = P_{opt}$, the second condition of (7.29) is clearly not realized, and $\dot{p}_\gamma < 0$. Therefore, in the trajectory sections where the weight G_γ decreases ($q_\gamma > 0$), the control function $P(t)$ reaches its limit ($P = 1$).

280 In order to fulfill the boundary condition $p_\gamma(T) = 0$ in the case when no upper bound restricts the control variable $q_\gamma(t)$, it is necessary that the trajectory be closed by the section $P(t) = 1$. In fact, $p_\gamma(t)$ is nonpositive everywhere in $[0, T]$ (cf. (7.27)); therefore, in order to attain the upper limit $p_\gamma = 0$, the derivative $\dot{p}_\gamma$ must be nonnegative when approaching it from the left. In accordance with (7.28), this is so only at $P(t) = 1$.

If $P(t) = P_{opt}(t)$ and $G_\gamma = 0$, (7.29) reduces to (4.19), which determines the optimum law of weight decrease for an ideal power-limited engine.

When $q_v(t) \equiv q_\gamma(t) \equiv 0$ the weights G_v and G_γ are fixed, and the solution of the boundary-value problem (7.18), (7.19), (7.20) yields optimum values of the control parameters G_v and G_γ. Examples of such a solution are given in Chapter Eight.

Note that making allowance for a weight component proportional to the maximum thrust alters the structure of the optimum thrust control with respect to the ideal case; an upper bound of the control function $P(t)$ appears.

The proportionality factor γ entering in the equations of the variational problem determines an important characteristic of the engine, namely, the maximum attainable thrust acceleration. In fact, the thrust acceleration a is given by (cf. (7.18))

$$a = (g/\gamma) PG_\gamma (G_0 + G_v + G_\gamma)^{-1}, \tag{7.30}$$

from which it follows that

$$a(t) \leqslant a_{max} = g/\gamma. \tag{7.31}$$

At high values of the parameter γ ($\gamma \sim 10^2 - 10^5$) which characterize power-limited engines, the maximum attainable acceleration is small ($a \sim 10^{-5} - 10^{-2}\,g$) (cf. /7.8/); this justifies the name given to engines of this class: low-acceleration or low-thrust engines.

§ 2. SPECIFIED OPERATING TIME OF THE ENGINE

According to the optimum program, an ideal power-limited engine functions during the entire flight time. If this time is incompatible with the engine resources (as can be expected in interplanetary flights), the condition of specified engine operating time must figure in the variational formulation. This problem was already discussed to a certain extent in Chapter Six; here we give a general method of solving variational problems with fixed time of action of the control function, which is then applied to the problem studied /7.9, 7.10/.

281 **1. General method.** Consider the Mayer problem as applied to a dynamic system:

$$\dot{x}_i = f_i(x_j, u_k) \qquad (i, j = 0, 1, \ldots, n;\ k = 1, \ldots, r). \tag{7.32}$$

The magnitudes x_i, u_k are respectively the phase coordinates and the control functions. The boundary conditions are specified at $t = 0$ and at $t = T$, and the values of the phase coordinate $x_0(T)$ represent the control functional. One of the control functions has a lower bound, given by $u_1 \geqslant 0$. The control function u_1 will be called "switched on" if $u_1 > 0$, and "switched off" if $u_1 = 0$. The total time during which the control function u_1 is switched on will be called the time of action of the control T_μ.

By solving the variational problem, we find the time $T_{\mu\,\mathrm{opt}} \leqslant T$ which is the optimum time of action of the control function u_1. Let us specify a time of action of the control function u_1 smaller than the optimum time, $T_\mu < T_{\mu\,\mathrm{opt}}$, in addition to the variational problem formulated above. This complicated variational formulation can be reduced to the standard Mayer form, by making use of the instantaneous time of action of the control t_μ and the delta function $\delta(t)$, introduced in Chapter Six; these are linked by the differential relation

$$\dot{t}_\mu = \delta. \tag{7.33}$$

The control function $\delta(t)$ is a step function, which takes the value 1 when the control is switched on, and the value 0 when it is switched off. Using this property of the function $\delta(t)$, we replace the control function u_1 by $u_1\delta$; this product coincides with u_1 when the control is switched on, and vanishes when it is switched off.

We write the system of differential equations for the variational problem as follows:

$$\begin{gathered}\dot{x}_i = f_i(x_j, u_1\delta, u_k), \quad \dot{t}_\mu = \delta \\ (i, j = 0, 1, \ldots, n; \quad k = 2, \ldots, r).\end{gathered} \tag{7.34}$$

If, together with the above-mentioned boundary conditions for the phase coordinates, the boundary conditions are satisfied for the auxiliary coordinate t_μ,

$$t_\mu(0) = 0, \quad t_\mu(T) = \int_0^T \delta(t)\,dt = T_\mu < T_{\mu\,\mathrm{opt}}, \tag{7.35}$$

and the function $\delta(t)$ together with $u_1(t), \ldots, u_r(t)$ is selected so as to be optimal in the sense of the control functional $x_0(T)$, the variational problem with the additional condition of specified time $T_\mu < T_{\mu\,\mathrm{opt}}$ will be solved.
282 In other words, we shall know the optimum number of times the engine is fired and the optimum operating time of the control variable u_1 for each powered section.

When using Pontryagin's method to solve the problem formulated, we form the Hamiltonian as usual and write the momentum equations

$$H = \sum_{i=0}^{n} p_i f_i(x_j, u_1\delta, u_k) + p_\mu\delta, \quad \dot{p}_i = -\partial H / \partial x_i, \quad \dot{p}_\mu = 0. \tag{7.36}$$

We represent H in the following form as a function of δ:

$$\left.\begin{aligned} H &= H_0 + (H_1 - H_0 + p_\mu)\,\delta, \\ H_0 &= H_{\delta=0} = \sum_{i=0}^{n} p_i f_i(x_j, 0, u_k), \\ H_1 &= H_{\delta=1} - p_\mu = \sum_{i=0}^{n} p_i f_i(x_j, u_1, u_k). \end{aligned}\right\} \tag{7.37}$$

To be specific we assume that we are looking for the maximum of the control functional $x_0(T)$, i.e., the function H must attain an absolute minimum for the optimum controls u_1, u_k, δ. For the control function δ the absolute minimum of H is attained when the following conditions are fulfilled:

$$\delta = 0 \text{ at } H_1 - H_0 + p_\mu > 0, \ \delta = 1 \text{ at } H_1 - H_0 + p_\mu < 0. \tag{7.38}$$

The difference $H_1 - H_0$ is nonpositive. In fact, it follows from definition (7.37) of the functions H_0 and H_1 that $H_1 = H_0$ at $u_1 = 0$; for other values of u_1 the difference $H_1 - H_0$ must be negative, since otherwise it would have been possible to decrease the Hamiltonian H by taking $u_1 = 0$, and then we would have $H_1 - H_0 = 0$. This determines the sign of p_μ to give

$$p_\mu > 0. \tag{7.39}$$

For $p_\mu < 0$, the expression $H_1 - H_0 + p_\mu$ would nowhere change sign, and we would have $\delta(t) \equiv 1$; in that case $t_\mu(T) = T$, which clearly contradicts boundary condition (7.35).

Note that for $u_1 = 0$ the optimum value of the step function δ is zero, since $p_\mu > 0$, $H_1 = H_0$. If $p_\mu = 0$, the time T_μ obtained coincides with the optimum time $T_\mu = T_{\mu\,\mathrm{opt}}$.

This method will also be applied to several control functions with a specified time of action shorter than the optimum time; instead of one auxiliary control function δ we substitute the required number.

283 2. **Application of the general method to the problem studied.** In the original equations (II.8) we multiply the propellant flow rate q and the thrust P by the function $\delta(t)$, and add to the system the differential equation for the instantaneous operating time of the engine t_μ. We obtain the following formulation of the variational problem:

$$\left.\begin{array}{lll} \dot{G}_\sigma = -gq\delta, & G_\sigma(0) = G_0 - G_\varkappa, & G_\sigma(T) = \max, \\ \dot{t}_\mu = \delta, & t_\mu(0) = 0, & t_\mu(T) = T_\mu, \\ \dot{\mathbf{r}} = \mathbf{v}, & \mathbf{r}(0) = \mathbf{r}_0, & \mathbf{r}(T) = \mathbf{r}_1, \\ \dot{\mathbf{v}} = \frac{gP\delta}{G_\sigma + G_\varkappa}\mathbf{e} + \mathbf{R}, & \mathbf{v}(0) = \mathbf{v}_0, & \mathbf{v}(T) = \mathbf{v}_1. \end{array}\right\} \tag{7.40}$$

In the case of a power-limited engine without losses, with which we deal in this section, the variational problem (7.40) reduces to (cf. (5.2)):

$$\left.\begin{array}{lll} \dot{J} = a^2\delta, & J(0) = 0, & J(T) = \min, \\ \dot{t}_\mu = \delta, & t_\mu(0) = 0, & t_\mu(T) = T_\mu, \\ \dot{\mathbf{r}} = \mathbf{v}, & \mathbf{r}(0) = \mathbf{r}_0, & \mathbf{r}(T) = \mathbf{r}_1, \\ \dot{\mathbf{v}} = a\delta\mathbf{e} + \mathbf{R}, & \mathbf{v}(0) = \mathbf{v}_0, & \mathbf{v}(T) = \mathbf{v}_1 \\ (a(t) \geqslant 0, \ \delta(t) = 1 \text{ or } 0, \ |\mathbf{e}(t)| = 1). & & \end{array}\right\} \tag{7.41}$$

In order to find the optimum functions $\mathbf{e}(t)$, $a(t)$, $\delta(t)$, we make use of Pontryagin's method and write the Hamiltonian and the momentum equations as

$$\left.\begin{array}{l} H = -a^2\delta + p_\mu\delta + \mathbf{p}_r \cdot \mathbf{v} + \mathbf{p}_v \cdot (a\delta\mathbf{e} + \mathbf{R}), \\ \dot{p}_\mu = 0, \quad \dot{\mathbf{p}}_r = -\frac{\partial}{\partial \mathbf{r}}(\mathbf{p}_v \cdot \mathbf{R}), \quad \dot{\mathbf{p}}_v = -\mathbf{p}_r \quad (p_\mu < 0). \end{array}\right\} \tag{7.42}$$

In the optimum region the control functions $\mathbf{e}(t)$ and $a(t)$ must satisfy the relations

$$\mathbf{e} = \mathbf{p}_v / p_v, \quad a = {}^1/_2 p_v \qquad (p_v = |\mathbf{p}_v|). \tag{7.43}$$

The optimum times of engine firing ($\delta = 1$) and cutoff ($\delta = 0$) are linked with a reversal of the sign of the expression Δ:

$$\delta = 1 \text{ at } \Delta > 0, \quad \delta = 0 \text{ at } \Delta < 0 \; (\Delta = {}^1/_4 p_v^2 + p_\mu). \tag{7.44}$$

If T_μ is not specified beforehand, $p_\mu = 0$ and $\Delta(t) > 0$ for $0 \leqslant t \leqslant T$; therefore, there are no coasting periods in the trajectory.

284 **3. Maneuvers in a gravity-free field.** In the case of motion in a gravity-free field* there can be no more than two powered-flight periods. In fact, for $\mathbf{R} = 0$ the differential equations of the momenta $\mathbf{p}_r$ and $\mathbf{p}_v$ in (7.42) can be integrated to yield

$$\mathbf{p}_r = 2\mathbf{b}_1, \quad \mathbf{p}_v = 2\mathbf{b}_1 t + 2\mathbf{b}_2, \tag{7.45}$$

and the magnitude ${}^1/_4 p_v^2$ entering in (7.44) is expressed as

$${}^1/_4 p_v^2 = b_1^2 t^2 + 2\mathbf{b}_1 \cdot \mathbf{b}_2 t + b_2^2. \tag{7.46}$$

The equation $\Delta(t) = 0$ is a quadratic equation in t and has at most two roots, $t_1(\mathbf{b}_1, \mathbf{b}_2)$ and $t_2(\mathbf{b}_1, \mathbf{b}_2)$, determining the beginning and end of the single coasting period, which separates the two periods of powered flight.

The optimum program of the thrust-acceleration vector $a\mathbf{e}$ in the sections of powered flight is a linear function of time. To find the constant vectors $\mathbf{b}_1$ and $\mathbf{b}_2$, which depend on the specified initial and final values of the coordinates $(\mathbf{r}_0, \mathbf{r}_1)$ and the velocities $(\mathbf{v}_0, \mathbf{v}_1)$, it is necessary to integrate the equation of motion in (7.41) along the powered-flight and coasting sections, with

$$\begin{gathered} a\mathbf{e} = \mathbf{b}_1 t + \mathbf{b}_2, \; \delta = 1 \text{ at } 0 \leqslant t < t_1, \quad t_2 < t \leqslant T; \\ \delta = 0 \text{ at } t_1 < t < t_2. \end{gathered} \tag{7.47}$$

We shall first consider the build-up maneuver of a specified velocity magnitude u_1 in a gravity-free field for specified maneuvering time T and engine operating time T_μ.

The final values of the coordinates $\mathbf{r}(T)$ in this maneuver are not fixed, and we therefore have the following transversality condition:

$$\mathbf{p}_r(T) = 2\mathbf{b}_1 = 0. \tag{7.48}$$

According to (7.44), (7.46) and (7.48), the expression Δ is independent of time, and neither its sign nor its magnitude are determined. This means that the location of the coasting section on the trajectory is not determined and does not influence the control functional $J(T)$; the latter is given by the expression (cf. (5.32))

$$J(T) = u_1^2 / T_\mu. \tag{7.49}$$

* Or in a plane-parallel field.

Note that the maneuvering time T does not enter into expression (7.49).

Next, we study the maneuver of transfer between two positions of rest in a gravity-free field situated at a distance l from each other, for a specified maneuvering time T and engine operating time T_μ. After integrating the equations of motion along the powered and coasting sections we can express the constants $\mathbf{b}_1$ and $\mathbf{b}_2$ by means of the maneuver parameters l, T and the time T_μ. Substituting these expressions in the formulas for t_1 and t_2, we obtain

$$t_1 = {}^1/_2 T_\mu, \quad t_2 = T - {}^1/_2 T_\mu. \tag{7.50}$$

The program for the thrust-acceleration vector ae has the form (cf. (5.33))

$$ae = \frac{6l}{T^2} \frac{1 - 2t/T}{1 - (1 - T_\mu/T)^3}, \tag{7.51}$$

and the expression for the functional $J(T)$ (cf. (5.33)) is

$$J(T) = \frac{12l^2}{T^3} \frac{1}{1 - (1 - T_\mu/T)^3}. \tag{7.52}$$

Thus, in the case considered the coasting section is located at the middle of the trajectory. For specified time of motion T and distance l the functional J increases monotonically with decreasing time T_μ (Figure 7.2). For specified time T_μ and distance l the functional J decreases monotonically with increasing time T (Figure 7.3).

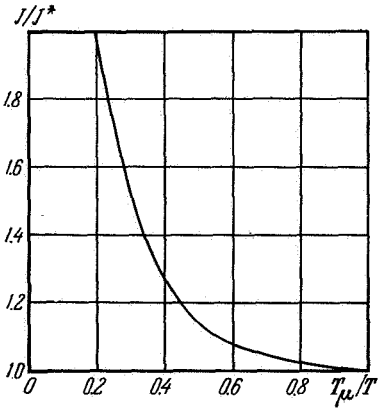

FIGURE 7.2. Functional J as function of operating time T_μ at specified maneuvering time T ($J^* = 12\, l^2/T^3$) for transfer between points of rest in gravity-free field.

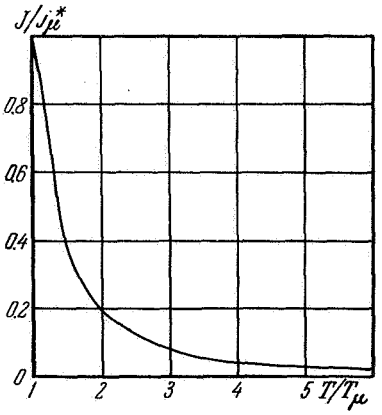

FIGURE 7.3. Functional J as function of maneuvering time T at specified operating time T_μ ($J_\mu = 12\, l^2/T_\mu^3$) for transfer between points of rest in gravity-free field.

4. Rotating the plane of a circular orbit. A similar study can be carried out for the maneuver of rotating the orbital plane. We shall give the final results. The following values of the parameters are selected (for a description of the maneuver cf. Appendix, § 3):

$$T = 2\pi, \quad \Omega_1 = {}^1/_2\pi, \tag{7.53}$$

where the inclination i is arbitrary within reasonable limits ($i \ll 1$), and the operating time of the engine T_μ is the parameter of the problem.

In the absence of restrictions on the operating time, the optimum functions $a(t)$, $e(t)$ and the value of the control functional $J(T)$ are (cf. (5.74), (5.75))

$$\left.\begin{aligned} ae &= (i/\pi)\sin t \quad \text{at} \quad 0 \leqslant t \leqslant 2\pi, \\ J(T) &= i^2/\pi \qquad\qquad (T = 2\pi). \end{aligned}\right\} \tag{7.54}$$

287 If the operating time T_μ is specified, expressions (7.54) are replaced by the following ones:

$$\left.\begin{aligned} a &= 0 && \text{for} \quad 0 \leqslant t < {}^1/_2\pi - {}^1/_4 T_\mu, \\ ae &= \frac{i \sin t}{{}^1/_2 T_\mu + \sin({}^1/_2 T_\mu)} && \text{for} \quad {}^1/_2\pi - {}^1/_4 T_\mu < t < {}^1/_2\pi + {}^1/_4 T_\mu, \\ a &= 0 && \text{for} \quad {}^1/_2\pi + {}^1/_4 T_\mu < t < {}^3/_2\pi - {}^1/_4 T_\mu, \\ ae &= \frac{i \sin t}{{}^1/_2 T_\mu + \sin({}^1/_2 T_\mu)} && \text{for} \quad {}^3/_2\pi - {}^1/_4 T_\mu < t < {}^3/_2\pi + {}^1/_4 T_\mu, \\ a &= 0 && \text{for} \quad {}^3/_2\pi + {}^1/_4 T_\mu < t \leqslant 2\pi. \end{aligned}\right\} \tag{7.55}$$

The functions $a(t)$ are given in Figure 7.4 for $T_\mu = 2\pi$, ${}^3/_2\pi$, π; the dependence of the control functional on the operating time T_μ ($0 < T_\mu \leqslant 2\pi$) is illustrated in Figure 7.5.

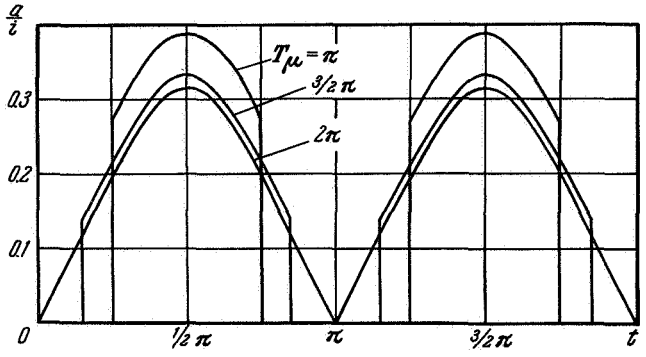

FIGURE 7.4. Variation of thrust-acceleration magnitude $a(t)$ for different values of operating time $T_\mu = \pi$, ${}^3/_2\pi$, 2π for rotation of orbital plane through angle i during time $T = 2\pi$.

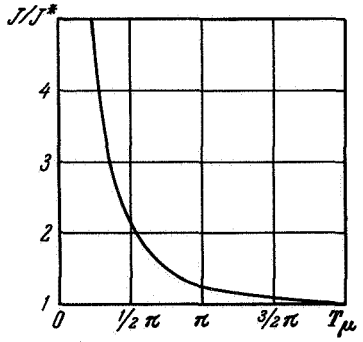

FIGURE 7.5. Functional J as function of operating time T_μ at fixed maneuvering time $T = 2\pi$ ($J^* = i^2/\pi$) for rotation of orbital plane through angle i.

5. Orbital transfer. We shall consider plane motion in a central field using cartesian coordinates (cf. Appendix, § 2).

The variational problem (7.41) for the maneuver of transfer between circular orbits is written as follows /7.10/:

$$\left.\begin{aligned}
&\dot J = a^2\delta, && J(0)=0, \quad J(T)=\min,\\
&\dot t_\mu = \delta, && t_\mu(0)=0, \quad t_\mu(T)=T_\mu,\\
&\dot x = u, && x(0)=1, \quad x(T)=r_1\cos\varphi_1,\\
&\dot y = v, && y(0)=0, \quad y(T)=r_1\sin\varphi_1,\\
&\dot u = a\delta e_x - \frac{x}{(x^2+y^2)^{3/2}}, && u(0)=0, \quad u(T)=-r_1^{-1/2}\sin\varphi_1,\\
&\dot v = a\delta e_y - \frac{y}{(x^2+y^2)^{3/2}}, && v(0)=1, \quad v(T)=r_1^{-1/2}\cos\varphi_1\\
&\qquad (a(t)\geqslant 0, \quad \delta(t)=1 \text{ or } 0, \quad e_x^2(t)+e_y^2(t)=1).
\end{aligned}\right\} \tag{7.56}$$

The Hamiltonian and the momentum equations (7.42) in this case have the form

$$\left.\begin{aligned}
&H = -a^2\delta + p_\mu\delta + p_x u + p_y v + p_u[a\delta e_x - x(x^2+y^2)^{-3/2}] +\\
&\qquad + p_v[a\delta e_y - y(x^2+y^2)^{-3/2}],\\
&\dot p_\mu = 0, \quad \dot p_u = -p_x, \quad \dot p_v = -p_y,\\
&\dot p_x = \frac{p_u}{(x^2+y^2)^{3/2}} - \frac{3x(p_u x + p_v y)}{(x^2+y^2)^{5/2}}, \quad \dot p_y = \frac{p_v}{(x^2+y^2)^{3/2}} - \frac{3y(p_u x + p_v y)}{(x^2+y^2)^{5/2}}.
\end{aligned}\right\} \tag{7.57}$$

288 Expressions for the optimum programs for a, e_x, e_y, δ are obtained from the condition that H has a maximum. These are

$$\left.\begin{aligned}
&e_x = p_u(p_u^2+p_v^2)^{-1/2}, \quad e_y = p_v(p_u^2+p_v^2)^{-1/2}, \quad a = {}^1/_2\sqrt{p_u^2+p_v^2},\\
&\delta = 1 \text{ at } \Delta>0, \quad \delta = 0 \text{ at } \Delta<0 \quad (\Delta = {}^1/_4(p_u^2+p_v^2)+p_\mu).
\end{aligned}\right\} \tag{7.58}$$

Thus, the variational problem has been reduced to the boundary-value problem

$$\left.\begin{aligned}
&\dot t_\mu = \delta, && t_\mu(0)=0, \quad t_\mu(T)=T_\mu,\\
&\dot x = u, && x(0)=1, \quad x(T)=r_1\cos\varphi_1,\\
&\dot y = v, && y(0)=0, \quad y(T)=r_1\sin\varphi_1,\\
&\dot u = {}^1/_2 p_u\delta - x(x^2+y^2)^{-3/2}, && u(0)=0, \quad u(T)=-r_1^{-1/2}\sin\varphi_1,\\
&\dot v = {}^1/_2 p_v\delta - y(x^2+y^2)^{-3/2}, && v(0)=1, \quad v(T)=r_1^{-1/2}\cos\varphi_1\\
&(\delta=1 \text{ at } \Delta>0, \quad \delta=0 \text{ at } \Delta<0, \quad \Delta = {}^1/_4(p_u^2+p_v^2)+p_\mu),\\
&\qquad \dot p_\mu = 0, \quad \dot p_u = -p_x, \quad \dot p_v = -p_y,\\
&\qquad \dot p_x = \frac{p_u}{(x^2+y^2)^{3/2}} - \frac{3x(p_u x + p_v y)}{(x^2+y^2)^{5/2}},\\
&\qquad \dot p_y = \frac{p_v}{(x^2+y^2)^{3/2}} - \frac{3y(p_u x + p_v y)}{(x^2+y^2)^{5/2}}.
\end{aligned}\right\} \tag{7.59}$$

The functions $x(t)$, $y(t)$, $u(t)$, $v(t)$, $p_\mu(t)$, . . ., $p_u(t)$, $p_v(t)$ are determined after solving the boundary-value problem, and it becomes possible to calculate the control functional

$$J(T) = \int_0^T a^2\delta\,dt = \frac{1}{4}\int_0^T (p_u^2+p_v^2)\,\delta\,dt. \tag{7.60}$$

Problem (7.59) contains the four parameters T, φ_1, r_1, T_μ. If the parameter T_μ takes a number of values, it is convenient to calculate p_μ and not T_μ. In this case the necessity of satisfying the condition $t_\mu(T) = T_\mu$ in the boundary-value problem (7.59) disappears; the equation for t_μ can be integrated after
289 determining the functions $x(t), \ldots, \delta(t)$ and the control functional (7.60), where

$$T_\mu = \int_0^T \delta(t)\, dt. \tag{7.61}$$

The boundary-value problem (7.59) was solved by successively selecting the missing initial values $p_x(0)$, $p_y(0)$, $p_u(0)$ and $p_v(0)$. The calculations were conducted for transfer from circular orbits of unit radius to circular orbits of radius $r_1 = 1.52$ (Earth—Mars). In most cases the average angular velocity during the transfer was taken as equal to the angular velocity of motion along the initial orbit, i.e., $\varphi_1/T = 1$. The results are shown in Figure 7.6 to 7.8.

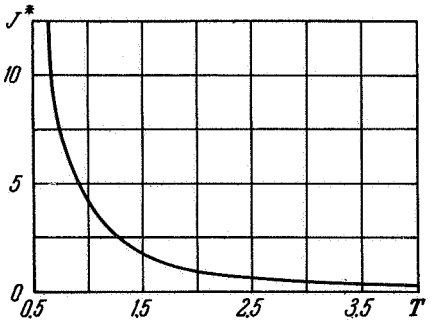

FIGURE 7.6. Functional J^* as function of time of motion for transfer between circular orbits ($r_0 = 1$, $r_1 = 1.52$, $T_\mu = T = \varphi_1$).

Figure 7.6 represents the functional $J^* = J(T_\mu = T)$ as a function of the time of motion T where there are no coasting periods in the trajectory ($T_\mu = T = \varphi_1$). Figure 7.7 shows a family of curves $J(T_\mu, T)/J^*(T)$ with different values of the parameter T ($\varphi_1 = T$ as before). For $0.5 \leqslant T \leqslant 4.5$, $0.8 \leqslant T_\mu/T \leqslant 1.0$ the relative variation of the functional, namely the magnitude $(J/J^*) - 1$, depends weakly on the time of flight T; for $T_\mu/T = 0.5$ the relative variation of the functional for different T is of the order of 12—13%, which agrees well with the results for a gravity-free field (cf. Figure 7.2). Within the range of parameters studied ($0.5 \leqslant T \leqslant 4.5$; $0.4 \leqslant T_\mu/T \leqslant 1$) there is one coasting section in the trajectory. Figure 7.8 shows the optimum programs of the thrust-acceleration magnitude $a(t)$ for $T = 4.5$ and different values of T_μ.

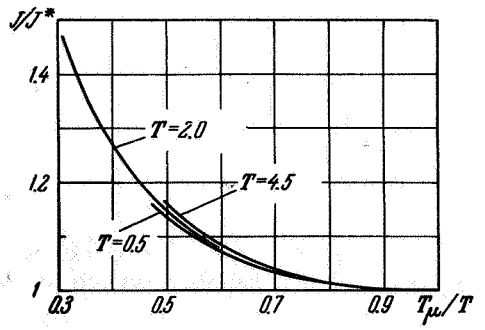

FIGURE 7.7. Functional J as function of operating time ratio T_μ/T for fixed time of motion T and transfer between circular orbits ($J^* = J(T_\mu = T)$, $r_0 = 1$, $r_1 = 1.52$, $\varphi_1 = T$).

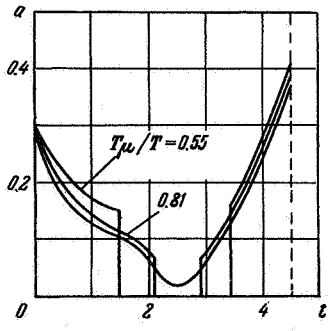

FIGURE 7.8. Form of thrust acceleration $a(t)$ for different values of T_μ/T for transfer between circular orbits ($T = \varphi_1 = 4.5$, $r_0 = 1$, $r_1 = 1.52$).

In concluding this paragraph we note the following two points.

1) The motion in a central field can be studied in either cartesian or polar coordinates. The latter have the advantage that integrals of the type ν and λ (see § 1 of Chapter Five) are fairly easily separated from systems of differential equations for the extremals, as in (7.59), thus reducing the
290 differential order of the system. During the coasting section of a trajectory the equations of motion and the momentum equations can be integrated, and their solution is obtained in closed form. By means of integration we obtain analytic relations between the parameters at the beginning and end of the coasting period. In this section, cartesian coordinates are preferred because the numerical method of solution developed is more easily applicable to equations written in these coordinates.

2) There exists also another method for obtaining the optimum relations between parameters at the beginning and end of a coasting period, which does not necessitate the introduction of the step function $\delta(t)$. This method is based on representing the variational problem as the Lagrange problem (5.1) or (5.3).

If there are two powered periods during the trajectory, the total functional is equal to the sum of the functionals corresponding to the first and second periods. The initial values of the coordinates and velocities for the first functional and the final values for the second functional are specified; the coordinates and velocities at the beginning and end of the coasting period are linked via integral relations which hold for coasting motion in a central field. The missing parameters are selected using the condition that the first variation of the sum of the functionals vanishes. As a result we obtain the optimum relations between the parameters at the beginning and end of the coasting period mentioned in the first note, including the optimum location of this section on the trajectory. Unlike the method which uses the function $\delta(t)$, this method is incapable of indicating the optimum number of coasting periods.

291§ 3. OPTIMUM STAGED THRUST PROGRAM

When using engines with a narrow control range, the thrust and propellant flow rate of the propulsion system are varied by switching the propellant discharge and the power from one nozzle to another. The resulting thrust and flow rate functions are staged, and are characterized by the number of levels (stages), their height, and the time of switching from one level to the next (the staging points). The number of levels is equal to the number of differently tuned engines; the addition of a new level leads to an increase in the weight of the system due to the extra engine required.

The solution of the variational problem for the delivery of maximum payload in a given case determines the optimum number of levels (differently-tuned engines), the optimum height of the levels, and the staging points.

In this section we start by describing the general method of solving the variational problem of a staged approximation for the optimum control with a given number of levels /7.11/. By this method, we determine the optimum thrust and thrust-acceleration staging programs for a number of maneuvers. It is assumed that the thrust acceleration is obtained without

losses; therefore the thrust, the propellant flow rate, and the power in the equations of the variational problem are linked by the ideal relation (4.1).

1. **General method.** Let the dynamic system be described by the following differential equations:

$$\dot{x}_i = f_i(x_j, u_k, t) \qquad (i, j = 0, 1, \ldots, n;\ k = 1, \ldots, r). \tag{7.62}$$

Here x_i are phase coordinates, u_k are control functions (position of the controls), and the problem functional is $x_0(T)$.

The solution of Mayer's variational problem (7.62) for the extremum of the functional $x_0(t)$ yields the optimum controls $u_{1\,\mathrm{opt}}(t), \ldots, u_{r\mathrm{opt}}(t)$. Consider the situation when the program for one of the control functions, for instance u_1, has to have s stages, unlike $u_{1\mathrm{opt}}(t)$, which is continuous together with its first derivative. The heights of the levels and the staging points of the step function $u_1(t)$ must be selected so that $u_1(t)$ is the best approximation (in the sense of the control functional $x_0(T)$) to the optimum control function $u_{1\mathrm{opt}}(t)$.

We introduce step functions $\delta_1(t), \ldots, \delta_{s-1}(t)$ taking the values 0 or 1, and parameters $\pi_1, \ldots, \pi_s$; these define respectively the staging points and the
292 height of the stages. The step function $u_1(t)$, which takes s values, can be represented in terms of $\delta_1, \ldots, \delta_{s-1}, \pi_1, \ldots, \pi_s$ in the following way:*

$$u_1(t) = ((\ldots(\pi_1\delta_1 + \pi_2)\,\delta_2 + \ldots + \pi_{s-2})\,\delta_{s-2} + \pi_{s-1})\,\delta_{s-1} + \pi_s = u_1(\pi, \delta), \tag{7.63}$$

where the s values of the control function $u_1(t)$ (the heights of the levels) are then given by

$$u_1^{(s)} = \pi_s, \quad u_1^{(s-1)} = \pi_{s-1} + \pi_s, \ldots, u_1^{(1)} = \pi_1 + \pi_2 + \ldots + \pi_{s-1} + \pi_s. \tag{7.64}$$

We shall determine the time of action of the parameters $\pi_1, \ldots, \pi_s$. The parameter π_s is switched on during the entire process ($0 \leqslant t \leqslant T$), the parameter π_{s-1} is switched on at $\delta_{s-1}(t) = 1, \ldots$, the parameter π_2 is switched on when $\delta_2(t)\,\delta_3(t) \ldots \delta_{s-1}(t) = 1$ and the parameter π_1 is switched on when $\delta_1(t) \ldots \delta_{s-1}(t) = 1$. The instantaneous operating times of the parameters $t_{\mu 1}, \ldots, t_{\mu s}$ are linked with the functions $\delta(t)$ by the following differential relations:

$$\dot{t}_{\mu s} = 1, \quad \dot{t}_{\mu s-1} = \delta_{s-1}, \ldots, \quad \dot{t}_{\mu 1} = \delta_1\delta_2 \ldots \delta_{s-1}. \tag{7.65}$$

* Equation (7.63) can also be written in the form

$$u_1(\pi, \delta) = \pi_1\delta_1\delta_2 \ldots \delta_{s-2}\delta_{s-1} + \pi_2\delta_2 \ldots \delta_{s-2}\delta_{s-1} + \ldots + \pi_{s-2}\delta_{s-2}\delta_{s-1} + \pi_{s-1}\delta_{s-1} + \pi_s.$$

Note that the notation

$$u_1(\pi, \delta) = \pi_1\delta_1 + \pi_2\delta_2 + \ldots + \pi_{s-1}\delta_{s-1} + \pi_s,$$

which at first seems the most natural one, is unsuitable, since the number of values that such a function can take exceeds s (except in the case $s = 2$); at $s > 3$ and $\pi_i \neq \pi_j$ it is equal to

$$C_{s-1}^{s-1} + C_{s-1}^{s-2} + \ldots + C_{s-1}^{1} + 1 = 1 + (s-1) + \ldots + (s-1) + 1 = 2s + \ldots;$$

at $s = 3$ it takes four values.

The total operating times are given by the integrals

$$T_{\mu s} = T, \quad T_{\mu s-1} = \int_0^T \delta_{s-1}\,dt, \ldots, \quad T_{\mu 1} = \int_0^T \delta_1\delta_2 \cdots \delta_{s-1}\,dt. \tag{7.66}$$

The selection of the parameters $\pi_1, \ldots, \pi_s$ and the staging points of the step functions $\delta_1, \ldots, \delta_{s-1}$ will be subjected to the condition that the functional $x_0(T)$ is an extremum. To that end Pontryagin's method is used; we form
293 the Hamiltonian H and write the differential equations of momentum as

$$H = \sum_{i=0}^{n} p_i f_i(x_j, u_1(\pi, \delta), u_k, t), \quad \dot{p}_i = -\frac{\partial H}{\partial x_i} \tag{7.67}$$
$$(i, j = 0, 1, \ldots, n;\ k = 2, \ldots, r).$$

The optimum controls $u_2, \ldots, u_r$ are determined by the standard method. To determine the programs $\delta_1(t), \ldots, \delta_{s-1}(t)$ it is necessary to calculate the function H for the following sets of values of these controls at each instant:

$$\left.\begin{array}{llll} H_1, & H_2, \quad \ldots, & H_{s-1}, & H_s, \\ \delta_{s-1} = 0, & \delta_{s-1} = 1, & \delta_{s-1} = 1, & \delta_{s-1} = 1, \\ & \delta_{s-2} = 0, & \delta_{s-2} = 1, & \delta_{s-2} = 1, \\ & & \vdots & \vdots \\ & & \delta_2 = 1. & \delta_2 = 1, \\ & & \delta_1 = 0, & \delta_1 = 1. \end{array}\right\} \tag{7.68}$$

The largest of the s values of H calculated (or the smallest one, depending on the character of the extremum of $x_0(T)$) indicates the optimum set of values of the step functions at time t.

The optimum values of the parameters $\pi_1, \ldots, \pi_s$ can be determined by the following method. If the parameters $\pi_1, \ldots, \pi_s$ are regarded as new phase coordinates, we add to system (7.62) the trivial differential equations

$$\dot{\pi}_1 = 0, \ldots, \dot{\pi}_s = 0. \tag{7.69}$$

This does not alter the Hamiltonian; however, we must also add s differential equations to the momentum equations (7.67) of the form

$$\dot{p}_1 = -\frac{\partial H}{\partial \pi_1} = -\frac{\partial H}{\partial u_1}\delta_1 \ldots \delta_{s-1}, \quad \dot{p}_2 = -\frac{\partial H}{\partial u_1}\delta_2 \ldots \delta_{s-1}, \ldots,$$
$$\dot{p}_{s-1} = -\frac{\partial H}{\partial u_1}\delta_{s-1}, \quad \dot{p}_s = -\frac{\partial H}{\partial u_1}. \tag{7.70}$$

The initial and final values of the phase coordinates $\pi_1, \ldots, \pi_s$ are not fixed, and therefore the momenta $p_1, \ldots, p_s$ vanish at $t = 0$ and $t = T$. This gives the following integral relations for the optimum values of the parameters
294 $\pi_1, \ldots, \pi_s$:

$$\int_0^T \frac{\partial H}{\partial u_1}\delta_1 \ldots \delta_{s-1}\,dt = 0, \quad \int_0^T \frac{\partial H}{\partial u_1}\delta_2 \ldots \delta_{s-1}\,dt = 0, \ldots,$$
$$\int_0^T \frac{\partial H}{\partial u_1}\delta_{-1}\,dt = 0, \quad \int_0^T \frac{\partial H}{\partial u_1}\,dt = 0. \tag{7.71}$$

With the aid of (7.65) and (7.66) these are reduced to the standard form

$$\int_0^T \frac{\partial H}{\partial u_1} dt_{\mu 1} = 0, \quad \int_0^T \frac{\partial H}{\partial u_1} dt_{\mu 2} = 0, \ldots,$$
$$\int_0^T \frac{\partial H}{\partial u_1} dt_{\mu s-1} = 0, \quad \int_0^T \frac{\partial H}{\partial u_1} dt_{\mu s} = 0. \tag{7.72}$$

To conclude this section, we note the following points.

1) It can happen that the representation of the control function $u_1(\pi, \delta)$ in terms of the parameters $\pi_1, \ldots, \pi_{s-1}$ and the step functions $\delta_1, \ldots, \delta_{s-1}$ is not unique. We shall establish this fact for $s = 2$.

Assume that the optimum two-step control function

$$u_1(t) = \pi_1 \delta_1(t) + \pi_2 \tag{7.73}$$

has been determined, i.e., that the function $\delta_1(t)$ and the parameters π_1 and π_2 have been selected. Now, replace the function δ_1 by $\delta_1' = 1 - \delta_1$ and find parameters π_1' and π_2' which, together with δ_1', form the control function $u_1(t)$ given by

$$u_1'(t) = \pi_1' \delta_1'(t) + \pi_2', \tag{7.74}$$

such that $u_1'(t) \equiv u_1(t)$. At $\delta_1 = 0$ we have $u_1 = \pi_2$, $\delta_1' = 1$ and $u_1' = \pi_1' + \pi_2'$; at $\delta_1 = 1$ we have $u_1 = \pi_1 + \pi_2$, $\delta_1' = 0$ and $u_1' = \pi_2'$. Therefore, in order that the identity $u_1'(t) = u_1(t)$ should hold, the following conditions must be fulfilled:

$$\pi_2 = \pi_1' + \pi_2', \ \pi_1 + \pi_2 = \pi_2' \ \text{ or } \ \pi_1' = -\pi_1, \ \pi_2' = \pi_1 + \pi_2. \tag{7.75}$$

In this way, we obtain a second representation of the control function $u_1(\pi, \delta)$, which does not coincide with the first one, but gives the same function $u_1(t)$, and therefore the same value of the control functional.

295 2) Let the control function be limited to the interval $0 \leqslant u_1(t) \leqslant 1$; we then obtain the following limits for the parameters $\pi_1, \ldots, \pi_s$:

$$\min_{\pi_i} u_1(\pi, \delta) \geqslant 0, \quad \max_{\pi_i} u_1(\pi, \delta) \leqslant 1. \tag{7.76}$$

These limits can be built into the optimum step control function $u_1(t)$. Thus, a three-step control function $u_1(\pi, \delta)$ including both the lower ($u_1 = 0$) and upper ($u_1 = 1$) limits can be written as

$$u_1 = ((1 - \pi_2)\, \delta_1 + \pi_2)\, \delta_2; \tag{7.77}$$

here $0 \leqslant \pi_2 \leqslant 1$ (it being assumed that the optimum control function $u_{1\text{opt}}(t)$ can also take intermediate values). If we are given the total time during which the lower limit u_1 vanishes, the variational problem contains an additional differential equation $\dot{t}_{\mu 3} = \delta_2$ and an additional boundary condition $t_{\mu 3}(T) = T_{\mu 3}$ (according to the method described in the preceding section).

3) One can indicate a numerical approach when solving the problem of a step approximation of the control, which avoids the use of delta functions such as (7.63).

Take the required s levels of the control functions u_1 as $u_1^{(1)}, u_1^{(2)}, \ldots, u_1^{(s)}$ and solve the problem by means of Pontryagin's method. The staging points are determined from the condition that the Hamiltonian be an extremum, and the optimum heights of the levels are found from the condition that the control functional be an extremum too. This procedure requires the use of numerical methods.

The delta function method yields analytical relations for selecting the optimum heights of the level.

4) An example of a step approximation to the optimum control function was considered in Chapter Four. An optimum step program was established there without making use of the proposed method, because the variational problem possesses the property that the control $G_x(G_o)$ is a non-decreasing function of its argument, so that each level of the step control function can be occupied only once. This property enables one to reduce the variational problem via a step control function $G_x(G_o)$ to a problem involving a maximum.

Another example of determining the optimum step program can be found in /7.12/. This is considered in the following subsection as an illustration of the general method. In the paper mentioned the solution was found using a special form of the optimum continuous control function.

296 **2. Examples of a step approximation to the thrust-acceleration program.** In this subsection we give a method of solving variational problem (4.11) under the condition that the control function $a(t)$ is selected from the class of step functions $a(\pi, \delta)$ with a specified number of levels. Two maneuvers are considered, namely, transfer in a gravity-free field between two positions of rest at a distance l apart during a time interval T, and rotating the plane of a circular orbit through an angle i during one revolution ($T = 2\pi$) for $\Omega_1 = -\pi/2$.

The variational problem (4.11) with $a = a(\pi, \delta)$ is written as follows for the first maneuver considered:

$$\left.\begin{aligned} &\dot{J} = a^2,\ J(0) = 0,\ J(T) = \min,\\ &\dot{x} = u,\quad x(0) = 0,\ x(T) = l,\\ &\dot{u} = ae,\ u(0) = 0,\ u(T) = 0\\ &\quad (a(t) = a(\pi, \delta),\ e(t) = \pm 1). \end{aligned}\right\} \tag{7.78}$$

If no restrictions are imposed on the control function $a(t)$, the optimum functions $a(t)$ and $e(t)$, and the minimum value of the control functional $J(T)$ are given by (5.33) (curve ∞ on Figure 7.9).

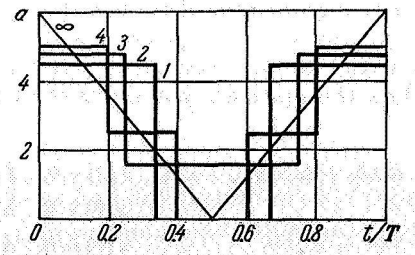

FIGURE 7.9. Step approximation to control function $a(t)$ for transfer between points of rest in gravity-free field.

We give below a number of optimum step programs $a(t)$ for problem (7.78); the procedure will be explained in detail in the last example.

1) For $a(\pi, \delta) = \pi_1$ the optimum functions governing $a(t)$ and $e(t)$ are (Figure 7.9, curve 1)

$$\left.\begin{aligned} &a(t) = 4l/T^2, \quad e(t) = 1 \quad \text{at} \quad 0 \leqslant t < {}^1/_2T, \\ &a(t) = 4l/T^2, \quad e(t) = -1 \quad \text{at} \quad {}^1/_2T < t \leqslant T, \\ &J(T) = 16l^2/T^3. \end{aligned}\right\} \tag{7.79}$$

2) For $a(\pi, \delta) = \pi_1\delta_1$ the optimum functions governing $a(t)$ and $e(t)$ are (Figure 7.9, curve 2)

$$\left.\begin{aligned} &a(t) = 4.5l/T^2, \quad e(t) = 1 \quad \text{at} \quad 0 \leqslant t < {}^1/_3T, \\ &a(t) = 0 \quad \text{at} \quad {}^1/_3T < t < {}^2/_3T, \\ &a(t) = 4.5l/T^2, \quad e(t) = -1 \quad \text{at} \quad {}^2/_3T < t \leqslant T, \\ &J(T) = 13.5l^2/T^3. \end{aligned}\right\} \tag{7.80}$$

297 3) For $a(\pi, \delta) = \pi_1\delta_1 + \pi_2$ the optimum functions governing $a(t)$ and $e(t)$ are (Figure 7.9, curve 3)

$$\left.\begin{aligned} &a(t) = 4.8l/T^2, \quad e(t) = 1 \quad \text{at} \quad 0 \leqslant t < {}^1/_4T, \\ &a(t) = 1.6l/T^2, \quad e(t) = 1 \quad \text{at} \quad {}^1/_4T < t < {}^1/_2T, \\ &a(t) = 1.6l/T^2, \quad e(t) = -1 \quad \text{at} \quad {}^1/_2T < t < {}^3/_4T, \\ &a(t) = 4.8l/T^2, \quad e(t) = -1 \quad \text{at} \quad {}^3/_4T < t \leqslant T, \\ &J(T) = 12.8l^2/T^3. \end{aligned}\right\} \tag{7.81}$$

4) For $a(\pi, \delta) = (\pi_1\delta_1 + \pi_2)\,\delta_2$ the optimum functions governing $a(t)$ and $e(t)$ are (Figure 7.9, curve 4)

$$\left.\begin{aligned} &a(t) = 5l/T^2, \quad e(t) = 1 \quad \text{at} \quad 0 \leqslant t < {}^1/_5T, \\ &a(t) = 2.5l/T^2, \quad e(t) = 1 \quad \text{at} \quad {}^1/_5T < t < {}^2/_5T, \\ &a(t) = 0 \quad \text{at} \quad {}^2/_5T < t < {}^3/_5T, \\ &a(t) = 2.5l/T^2, \quad e(t) = -1 \quad \text{at} \quad {}^3/_5T < t < {}^4/_5T, \\ &a(t) = 5l/T^2, \quad e(t) = -1 \quad \text{at} \quad {}^4/_5T < t \leqslant T, \\ &J(T) = 12.5l^2/T^3. \end{aligned}\right\} \tag{7.82}$$

In the second and fourth examples, levels with a given (zero) height are included in the control function; for regions in which the control functions have specified values only their optimum positions need to be determined.

We shall explain how to determine the optimum three-step control function $a(\pi, \delta)$ with zero lower level (the fourth example).

The differential equations for the phase coordinates, the boundary conditions, the Hamiltonian, the differential equations of momentum, and the equations for selecting the optimum parameters π_1 and π_2 are (cf. (7.78), (7.67), (7.71))

$$\begin{aligned} &\dot{J} = \pi_1^2\delta_1\delta_2 + 2\pi_1\pi_2\delta_1\delta_2 + \pi_2^2\delta_2, \quad J(0) = 0, \quad J(T) = \min, \\ &\dot{x} = u, \qquad\qquad x(0) = 0, \quad x(T) = l, \\ &\dot{u} = (\pi_1\delta_1 + \pi_2)\,\delta_2 e, \qquad u(0) = 0, \quad u(T) = 0, \\ &H = -(\pi_1^2\delta_1\delta_2 + 2\pi_1\pi_2\delta_1\delta_2 + \pi_2^2\delta_2) + p_x u + p_u(\pi_1\delta_1 + \pi_2)\,\delta_2 e, \\ &\dot{p}_x = 0, \quad \dot{p}_u = -p_x, \end{aligned} \tag{7.83}$$

$$\pi_1\int_0^T \delta_1\delta_2\,dt + \pi_2\int_0^T \delta_1\delta_2\,dt = \frac{1}{2}\int_0^T p_u e\delta_1\delta_2\,dt,$$
$$\pi_1\int_0^T \delta_2\,dt + \pi_2\int_0^T \delta_2\,dt = \frac{1}{2}\int_0^T p_u e\delta_2\,dt. \tag{7.83}$$

298 The solution of the differential equation for p_u can be written as (cf. (6.32))

$$p_u = b_1(t_* - t). \tag{7.84}$$

The optimum control functions $e(t)$, $\delta_1(t)$, $\delta_2(t)$ are subjected to the conditions

$$\left.\begin{array}{l} e(t) = \operatorname{sgn} p_u(t) \quad (ep_u = |p_u|), \\ \delta_1(t) = 1 \text{ at } \Delta_1 > 0, \quad \delta_1(t) = 0 \text{ at } \Delta_1 < 0 \\ (\Delta_1 = \pi_1(-\pi_1 - 2\pi_2 + |p_u|)), \\ \delta_2(t) = 1 \text{ at } \Delta_2 > 0, \quad \delta_2(t) = 0 \text{ at } \Delta_2 < 0 \\ (\Delta_2 = \pi_2(-\pi_2 + |p_u|) + \delta_1\Delta_1). \end{array}\right\} \tag{7.85}$$

The parameter π_2 can only be positive, since $a(t) \geqslant 0$. The parameter π_1 can be either positive or negative; in the latter case $|\pi_1| < \pi_2$, since $a(t) \geqslant 0$. Consider initially the case $\pi_1 > 0$. Let $|p_u| - \pi_1 - 2\pi_2 > 0$; then $\Delta_1 > 0$ when $\pi_1 > 0$ (cf. (7.85)) and $\delta_1 = 1$. The expression $|p_u| - \pi_2$ is then clearly positive; therefore $\Delta_2 > 0$ (cf. (7.85)) and $\delta_2 = 1$. Let $|p_u| - \pi_2 < 0$; then $\Delta_1 < 0$, and therefore $\delta_1 = 0$. Moreover, $\Delta_2 < 0$ and $\delta_2 = 0$.

These considerations lead to the following conclusions. If $\delta_1 = 1$, then $\delta_2 = 1$, and if $\delta_1 = 0$, then $\delta_2 = 0$; i.e., the region in which $\delta_2 = 0$ lies inside that in which $\delta_1 = 0$, and the region where $\delta_1 = 1$ is not larger than that where $\delta_2 = 1$. The layout of the regions is shown in Figure 7.10, where $t_1^-, t_2^-, t_2^+, t_1^+$ are the roots of equations

$$\left.\begin{array}{l} \Delta_1(t_1^-) = -\pi_1 - 2\pi_2 + |b_1|(t_* - t_1^-) = 0, \\ \Delta_2(t_2^-) = |b_1|(t_* - t_2^-) - \pi_2 = 0, \\ \Delta_1(t_1^+) = -\pi_1 - 2\pi_2 + |b_1|(t_1^+ - t_*) = 0, \\ \Delta_2(t_2^+) = |b_1|(t_2^+ - t_*) - \pi_2 = 0. \end{array}\right\} \tag{7.86}$$

From (7.86) it follows in particular that

$$t_1^+ + t_1^- = 2t_*, \quad t_2^+ + t_2^- = 2t_*. \tag{7.87}$$

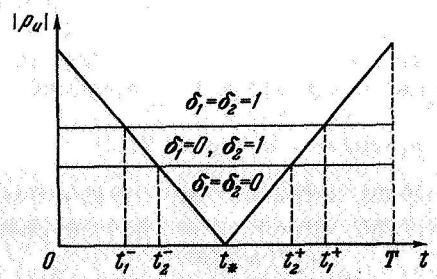

FIGURE 7.10. Layout of levels of control function $a(t)$ for transfer between points of rest in gravity-free field.

299 The optimum programs $e(t)$, $\delta_1(t)$, $\delta_2(t)$ can be written in the following form with the aid of the parameters t_1^-, t_2^-, t_*, t_2^+, t_1^+ (cf. (7.85)):

$$\left.\begin{array}{llll} \delta_1(t)=1, & \delta_2(t)=1, & e(t)=1 & \text{at } 0\leqslant t<t_1^-, \\ \delta_1(t)=0, & \delta_2(t)=1, & e(t)=1 & \text{at } t_1^-<t<t_2^-, \\ \delta_1(t)=0, & \delta_2(t)=0 & & \text{at } t_2^-<t<t_2^+, \\ \delta_1(t)=0, & \delta_2(t)=1, & e(t)=-1 & \text{at } t_2^+<t<t_1^+, \\ \delta_1(t)=1, & \delta_2(t)=1, & e(t)=-1 & \text{at } t_1^+<t\leqslant T. \end{array}\right\} \tag{7.88}$$

After integrating the equations of motion and satisfying the boundary conditions we obtain

$$2t_* = T, \quad \pi_1 t_1^- (T - t_1^-) + \pi_2 t_2^- (T - t_2^-) = l. \tag{7.89}$$

The parameters π_1 and π_2 are expressed as follows in terms of $|b_1|$, t_1^-, t_2^- (cf. the last two equalities of (7.83)):

$$\pi_1 = {}^1/_4 |b_1| t_2^-, \quad \pi_2 = {}^1/_4 |b_1| (T - t_2^- - t_1^-). \tag{7.90}$$

From (7.86) and (7.90) we obtain

$$t_1^- = {}^1/_5 T, \quad t_2^- = {}^2/_5 T, \tag{7.91}$$

and from the second relation of (7.89) we find

$$|b_1| = 25l/T^2, \tag{7.92}$$

so that (cf. (7.90))

$$\pi_1 = 2.5l/T^2, \quad \pi_2 = 2.5l/T^2. \tag{7.93}$$

The form of the optimum control functions is given in the fourth example.

If we consider the parameter π_1 as negative, the optimum law $\delta_1(t)$ and the parameters π_1 and π_2 are different when compared to the case considered ($\delta_1 = 0$ at $0 \leqslant t < {}^1/_5 T$ and ${}^4/_5 T < t \leqslant T$, $\delta_1 = 1$ at ${}^1/_5 T < t < {}^2/_5 T$ and ${}^3/_5 T < t < {}^4/_5 T$, δ_1 indeterminate at ${}^2/_5 T < t < {}^3/_5 T$; $\pi_1 = -2.5$; $\pi_2 = 5$); the optimum laws $a(t)$ and $e(t)$ and the magnitude $J(T)$ remain unchanged (cf. the first note in the preceding subsection).

We shall consider the maneuver of rotating the plane of a circular satellite orbit. If no restrictions are imposed on the control function $a(t)$, the optimum programs for $a(t)$, $e(t)$ and the minimum values of $J(T)$ will be given by (5.74) and (5.75) (curve ∞ in Figure 7.11).

If the control function $a(t)$ is selected from the class of step functions, the optimum programs for $a(t)$, $e(t)$ and the magnitude $J(T)$ will have the following forms.

300 1) When $a(\pi, \delta) = \pi_1$ (curve 1 in Figure 7.11)

$$\left.\begin{array}{lll} a(t)=0.25i, & e(t)=-1 & \text{at } 0\leqslant t<3.14, \\ a(t)=0.25i, & e(t)=1 & \text{at } 3.14<t\leqslant 6.28, \\ & J(T)=0.393\,i^2. & \end{array}\right\} \tag{7.94}$$

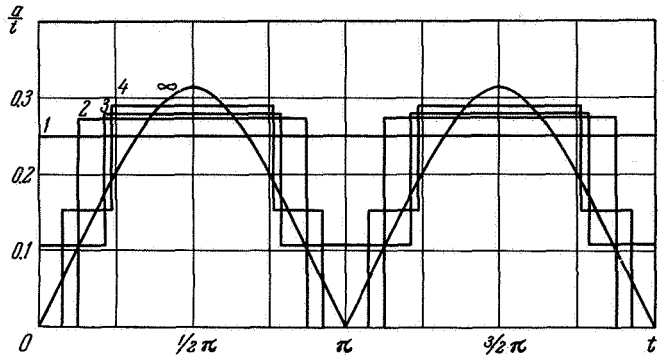

FIGURE 7.11. Step approximation of control function $a(t)$ for rotation of plane of circular orbit through angle i during time $T = 2\pi$.

2) When $a(\pi, \delta) = \pi_1\delta_1$ (curve 2 in Figure 7.11)

$$\left.\begin{array}{llll} a(t) = 0 & & \text{at} & 0 \leqslant t < 0.404, \\ a(t) = 0.273i, & e(t) = -1 & \text{at} & 0.404 < t < 2.74, \\ a(t) = 0 & & \text{at} & 2.74 < t < 3.54, \\ a(t) = 0.273i, & e(t) = 1 & \text{at} & 3.54 < t < 5.88, \\ a(t) = 0 & & \text{at} & 5.88 < t \leqslant 6.28, \\ & J(T) = 0.345i^2. & & \end{array}\right\} \quad (7.95)$$

3) When $a(\pi, \delta) = \pi_1\delta_1 + \pi_2$ (curve 3 in Figure 7.11)

$$\left.\begin{array}{llll} a(t) = 0.106i, & e(t) = -1 & \text{at} & 0 \leqslant t < 0.664, \\ a(t) = 0.280i, & e(t) = -1 & \text{at} & 0.664 < t < 2.48, \\ a(t) = 0.106i, & e(t) = -1 & \text{at} & 2.48 < t < 3.14, \\ a(t) = 0.106i, & e(t) = 1 & \text{at} & 3.14 < t < 3.80, \\ a(t) = 0.280i, & e(t) = 1 & \text{at} & 3.80 < t < 5.62, \\ a(t) = 0.106i, & e(t) = 1 & \text{at} & 5.62 < t \leqslant 6.28, \\ & J(T) = 0.333i^2 & & \end{array}\right\} \quad (7.96)$$

301 4) When $a(\pi, \delta) = (\pi_1\delta_1 + \pi_2)\,\delta_2$ (curve 4 in Figure 7.11)

$$\left.\begin{array}{llll} a(t) = 0 & & \text{at} & 0 \leqslant t < 0.238, \\ a(t) = 0.154i, & e(t) = -1 & \text{at} & 0.238 < t < 0.750, \\ a(t) = 0.291i, & e(t) = -1 & \text{at} & 0.750 < t < 2.39, \\ a(t) = 0.154i, & e(t) = -1 & \text{at} & 2.39 < t < 2.90, \\ a(t) = 0 & & \text{at} & 2.90 < t < 3.38, \\ a(t) = 0.154i, & e(t) = 1 & \text{at} & 3.38 < t < 3.89, \\ a(t) = 0.291i, & e(t) = 1 & \text{at} & 3.89 < t < 5.53, \\ a(t) = 0.154i, & e(t) = 1 & \text{at} & 5.53 < t < 6.04, \\ a(t) = 0 & & \text{at} & 6.04 < t \leqslant 6.28, \\ & J(T) = 0.326i^2. & & \end{array}\right\} \quad (7.97)$$

The examples show that the value of the control functional $J(T)$ decreases monotonically with an increasing number of levels s, approaching the ideal value as $s \to \infty$.

In conclusion we make a number of observations concerning the application of the results. It was indicated at the beginning of this section that an engine with a narrow control range is characterized by a staged variation of the thrust and propellant flow rate. The assumption is made here that we have a step thrust-acceleration program. Such a transition is possible when the working-fluid consumption during a maneuver is small and the program of the dimensionless thrust and thrust acceleration do not differ much from each other.

The problem as stated at the beginning of the section also differs in that when a new level of thrust acceleration or thrust is added, the additional weight necessary for achieving this level is not accounted for. This difference can be justified if the additional weight is independent of the variables appearing in the variational problem.

We shall formulate in the following subsections a variational problem which does not have these restrictions, and shall give examples of its solution for the maneuver of orbital transfer.

3. The problem of approximating the thrust program while allowing for the engine weight. We shall denote the increment in the engine weight resulting from the addition of a new i-th level of thrust and flow rate by $G_\lambda^{(i)}$. If it is independent of the characteristics of the engine in general and the level in particular, the procedure for determining the optimum step control function can be split into two stages. The problem is first solved for a fixed number of thrust levels and given flow rate (here the weight characteristics of the levels are unnecessary). Then the optimum number of levels

is selected for a given weight (cf. the preceding subsection).

In the general case $G_\lambda^{(i)}$ is a function of the characteristics of the engine and the level. If the variation of the thrust and flow rate is performed by switching over from one engine with a limited performance to another one (this method is considered here), the extra weight can be taken as equal to the weight of the engine creating the new level, so that

$$G_\lambda^{(i)} = G_\gamma^{(i)}. \tag{7.98}$$

It will be assumed that the weight of the engine depends only on the maximum thrust it can provide; then

$$G_\lambda^{(i)} = \gamma P_i, \quad G_\lambda = \sum_{i=1}^{s} G_\lambda^{(i)} = \gamma \sum_{i=1}^{s} P_i \tag{7.99}$$

(all engines are considered to be of the same type, so that the parameter γ is the same for any number i of them).

The variational problem of delivering a maximum payload for a staged variation of the thrust and flow rate is (cf. (7.17))

$$\left.\begin{aligned} &\dot G_\sigma = -g\alpha P^2/2G_v, && G_\sigma(0) = 1 - G_v - G_\lambda, && G_\sigma(T) = \max, \\ &\dot{\mathbf{r}} = \mathbf{v}, && \mathbf{r}(0) = \mathbf{r}_0, && \mathbf{r}(T) = \mathbf{r}_1, \\ &\dot{\mathbf{v}} = \frac{gP\mathbf{e}}{G_\sigma + G_v + G_\lambda} + \mathfrak{R}, && \mathbf{v}(0) = \mathbf{v}_0, && \mathbf{v}(T) = \mathbf{v}_1 \\ &(P(t) = P(\pi, \delta), && G_v = \text{const}, && G_\lambda = \text{const}, \quad |\mathbf{e}(t)| = 1). \end{aligned}\right\} \tag{7.100}$$

It has been assumed in (7.100) that the vehicle weight consists of the payload $G_\pi = G_\sigma(T)$, the working fluid $G_\mu = G_\sigma - G_\pi$, the weight of the power source G_v, and the engine weights G_λ (the weight of the s levels of thrust and flow rate $G_\lambda = \gamma \Sigma P_i$); the process of accelerating the engine is considered to be free of losses; the quantities G_π, G_σ, G_v, G_λ are dimensionless as is the thrust P (all these are expressed as fractions of the takeoff weight G_0); the weight of the power source G_v is the control parameter.

The step function $P(\pi, \delta)$, has s levels and can therefore be expressed as follows in terms of the delta functions $\delta_1(t), \ldots, \delta_{s-1}(t)$ and the parameters $\pi_1, \ldots, \pi_s$:

$$P(\pi, \delta) = ((\ldots(\pi_1\delta_1 + \pi_2)\,\delta_2 + \ldots + \pi_{s-2})\,\delta_{s-2} + \pi_{s-1})\,\delta_{s-1} + \pi_s. \qquad (7.101)$$

303 The parameters π_i determine the height of the thrust levels P_j, where

$$P_1 = \pi_1 + \pi_2 + \ldots + \pi_s, \quad P_2 = \pi_2 + \pi_3 + \ldots + \pi_s, \ldots, \quad P_s = \pi_s, \qquad (7.102)$$

and the functions $\delta_i(t)$ define the staging points.

The total weight of the engines creating the levels, G_λ, determined by (7.99), is, by (7.102),

$$G_\lambda = \gamma \sum_{i=1}^{s} i\pi_i. \qquad (7.103)$$

In the variational problem (7.100), it is necessary to find the optimum number of levels s, the optimum control functions $\mathbf{e}(t)$, $\delta_1(t), \ldots, \delta_{s-1}(t)$ and the optimum control parameters $G_v, \pi_1, \ldots, \pi_s$, in addition to the expressions already found for $P(\pi, \delta)$ and G_λ in the forms (7.101), (7.103).

We note the following points with regard to the variational problem as formulated.

1) The number of levels s is a natural number ($s = 1, 2, 3, \ldots$), and therefore the determination of the optimum value of s requires the examination of a number of values of s and their corresponding solutions of the problem. For $\gamma = 0$ (and hence $G_\lambda = 0$), the optimum number s is infinite.

2) If the lowest thrust level is the zero level (i.e., if engine cutoff is allowed), then $P_s = \pi_s = 0$ and the problem of optimizing a given level consists of determining the optimum time during which this level is used.

3) In (7.100) the weight of the power source G_v is the control parameter, i.e., it is determined from the condition that a given maneuver is carried out and a maximum payload delivered.

If the maneuver is elementary but is part of a complex maneuver, the optimum value G_v for the first maneuver is not the optimum for the whole maneuver. Therefore, when solving the variational problem for one elementary maneuver we must consider the parameter $\varkappa = \alpha/G_v = G_0/N$ as a structural parameter, and not a control parameter, since its optimum value is determined from the final result. In such a case we alter the variational formulation (7.100), introducing a new symbol for the sum of the weights

$$G_\psi = G_\sigma + G_v = G_\pi + G_\mu + G_v, \qquad (7.104)$$

304 and consider the final value of the weight as the control functional $G_\psi(T) = G_\pi + G_v$; the notation in (7.100) is then transformed into

$$\left.\begin{array}{lll} \dot{G}_\psi = -{}^1/_2 \varkappa g P^2, & G_\psi(0) = 1 - G_\lambda, & G_\psi(T) = \max, \\ \dot{\mathbf{r}} = \mathbf{v}, & \mathbf{r}(0) = \mathbf{r}_0, & \mathbf{r}(T) = \mathbf{r}_1, \\ \dot{\mathbf{v}} = \frac{gP\mathbf{e}}{G_\psi + G_\lambda} + \mathfrak{R}, & \mathbf{v}(0) = \mathbf{v}_1, & \mathbf{v}(T) = \mathbf{v}_1 \\ \left(P(t) = P(\pi, \delta), \quad G_\lambda = \gamma \sum_{i=1}^{s} i\pi_i, \quad |\mathbf{e}(t)| = 1\right). & & \end{array}\right\} \qquad (7.105)$$

4) In systems (7.100) and (7.105) we have allowed for the fact that the optimum power control is the limiting control. Therefore in what follows, instead of speaking about step programs of thrust and flow rate, we shall speak only about the step program of the thrust, bearing in mind that the flow rate program at $N(t) = 1$ is expressed in terms of $P(t)$ and the parameter $\varkappa$.

4. Staged thrust program with an optimum number of levels for an orbital transfer. The unthrottled engine has the simplest staged thrust program; it has two levels, one of which is the zero level. We ask the following question: for which maneuvers can the addition of new thrust levels to these two basic levels give a gain in payload, taking into account the increase in engine weight?

To answer this question, we shall compare the optimum thrust program of an ideal engine with the thrust program of the unthrottled engine.

It was mentioned in Chapter Five that when accelerating out of a circular orbit to acquire a parabolic velocity the ideal program for the thrust-acceleration magnitude represents an almost constant function of time. If the working-fluid consumption is small (this corresponds to large acceleration times), then the function governing the weight expended during constant acceleration is close to that during constant thrust. Therefore at a low acceleration the use of several thrust levels instead of only one will apparently not yield any extra payload. This is due to the extra weights required to achieve these levels.

A similar result follows from analyzing the build-up maneuver of a specified velocity magnitude in a gravity-free field; the latter is a model of a slow-acceleration maneuver in a central field. A staged thrust program is also inefficient for holding a satellite within a specified spherical layer.

305 For orbital transfer in a central field (e.g., transfer between two positions of rest in a gravity-free field), as well as for rotating the plane of a satellite orbit, the ideal thrust formulas differ substantially from the uncontrolled ones. The optimum staged programs can contain several levels (not just one), in addition to the zero level.

The last two maneuvers (flight in a gravity-free field and rotation of the orbital plane) have so far been studied under two simplifying assumptions. The variational problem (7.105) will now be solved for the maneuver of transfer between two circular orbits without using these assumptions.

The problem is expressed as follows (cf. (7.105), (7.56)):

$$\left.\begin{array}{llll}
\dot{G}_\psi = -l_2 \varkappa P^2, & G_\psi(0) = 1 - G_\lambda, & G_\psi(T) = \max, & \\
\dot{x} = u, & x(0) = 1, & x(T) = r_1 \cos\varphi_1, & \\
\dot{y} = v, & y(0) = 0, & y(T) = r_1 \sin\varphi_1, & \\
\dot{u} = \dfrac{l_1 P e_x}{G_\psi + G_\lambda} - \dfrac{x}{(x^2+y^2)^{3/2}}, & u(0) = 0, & u(T) = -r_1^{-1/2}\sin\varphi_1, & \\
\dot{v} = \dfrac{l_1 P e_y}{G_\psi + G_\lambda} - \dfrac{y}{(x^2+y^2)^{3/2}}, & v(0) = 1, & v(T) = r_1^{-1/2}\cos\varphi_1 & \\
\multicolumn{4}{c}{\left(P(t) = P(\pi, \delta),\ e_x^2(t) + e_y^2(t) = 1,\ G_\lambda = \gamma \sum_{i=1}^{s} i\pi_i\right).}
\end{array}\right\} \quad (7.106)$$

Here r_1, φ_1, T, $\varkappa$, s are the parameters of the problem; the coefficients l_1 and l_2 appear after transforming to the dimensionless magnitudes t, x, y, u, v. The first coefficient, l_1, is equal to the ratio of the acceleration of gravity on the Earth's surface (g) to the acceleration of gravity on the original orbit, and the second coefficient, l_2, is equal to the product of $\frac{1}{2}g$ by the period of revolution along the original orbit divided by 2π. If the average circular orbit of the Earth is taken as the original orbit, then

$$l_1 = 0.167 \cdot 10^4, \quad l_2 = 0.2448 \cdot 10^6 \text{ kw/kg}. \quad (7.107)$$

We shall reduce the variational problem (7.106) to a boundary-value problem for ordinary differential equations; the Hamiltonian and the momentum derivatives are given by

306

$$\left.\begin{array}{ll}
H = -p_\psi l_2 \varkappa P^2 + p_x u + p_y v + p_u\left(\dfrac{l_1 P e_x}{G_\psi + G_\lambda} - \dfrac{x}{(x^2+y^2)^{3/2}}\right) + & \\
\qquad + p_v\left(\dfrac{l_1 P e_y}{G_\psi + G_\lambda} - \dfrac{y}{(x^2+y^2)^{3/2}}\right), & \\
\dot{p}_\psi = l_1 P (G_\psi + G_\lambda)^{-2}(p_u e_x + p_v e_y), & p_\psi(T) = -1, \\
\dot{p}_x = p_u (x^2+y^2)^{-3/2} - 3x(p_u x + p_v y)(x^2+y^2)^{-5/2}, & \dot{p}_u = -p_x, \\
\dot{p}_y = p_v (x^2+y^2)^{-3/2} - 3y(p_u x + p_v y)(x^2+y^2)^{-5/2}, & \dot{p}_v = -p_y.
\end{array}\right\} \quad (7.108)$$

The formulas for the optimum control functions e_x and e_y coincide with (7.58). The optimum delta control functions $\delta_1, \ldots, \delta_{s-1}$ are found using the method in subsection 1 (cf. (7.68)).

In order to determine the optimum values of the parameters $\pi_1, \ldots, \pi_s$ in the boundary conditions of (7.106), we shall use the same method as in subsection 1, namely, we add to the original system (7.106) trivial equations similar to (7.69), and write differential equations for the new momenta $p_1, \ldots, p_s$; these have the form (cf. (7.70))

$$\dot{p}_1 = -\frac{\partial H}{\partial P}\delta_1 \ldots \delta_{s-1}, \quad \dot{p}_2 = -\frac{\partial H}{\partial P}\delta_2 \ldots \delta_{s-1}, \ldots$$

$$\dot{p}_{s-1} = -\frac{\partial H}{\partial P}\delta_{s-1}, \qquad \dot{p}_s = -\frac{\partial H}{\partial P} \quad (7.109)$$

$$\left(-\frac{\partial H}{\partial P} = l_1 \frac{\sqrt{p_u^2 + p_v^2}}{G_\psi + G_\lambda} + 2 l_2 \varkappa p_\psi P\right).$$

The final values of $p_1, \ldots, p_s$ vanish as in subsection 1; at the initial instant the momenta satisfy the transversality conditions

$$\left.\begin{aligned} &p_1(0) = \gamma p_\psi(0), \quad p_2(0) = 2\gamma p_\psi(0), \quad \ldots, \quad p_s(0) = s\gamma p_\psi(0), \\ &p_1(T) = 0, \qquad p_2(T) = 0, \qquad\qquad \ldots, \qquad p_s(T) = 0. \end{aligned}\right\} \tag{7.110}$$

Thus, the variational problem has been reduced to the boundary-value problem (7.109), (7.108), (7.110). The latter was solved numerically by
307 consecutively selecting the missing initial values $p_x(0)$, $p_y(0)$, $p_u(0)$, $p_v(0)$, $p_\psi(0)$ and the parameters $\pi_1, \ldots, \pi_s$.

The object of the calculations was to determine the optimum number of levels s in terms of the structural parameters γ and $\varkappa$. The following values were used for the final radius r_1, the angular range of flight φ_1, and the time T:

$$r_1 = 1.52, \quad \varphi_1 = 1.57, \quad T = 1.57. \tag{7.111}$$

The structural parameters γ and $\varkappa$ were selected from the values

$$\gamma = 0;\ 25;\ 50;\ 100;\ 200;\ 400\,\text{kg/kg}, \quad \varkappa = 5;\ 12.5;\ 25\,\text{kg/kw}. \tag{7.112}$$

The number of thrust stages s was selected from

$$s = 1, 2, 3, 4, \tag{7.113}$$

where the zero thrust level was always included. Figure 7.12 shows the characteristic form of the function $P(t)$ for $\gamma = 25$ kg/kg, $\varkappa = 25$ kg/kw, $s = 4$.

It is interesting to note that for certain values of $s, \varkappa, \gamma > 0$ the trajectory has no coasting section in the optimum case. This can be explained as follows. Coasting sections reduce the engine operating time and increase the average thrust level, thus decreasing the required working-fluid reserve $G_{\mu 0}$, and increasing the total weight G_λ needed for all the stages. It could happen that as a result the weight $G_\psi(T)$ decreases; the inclusion of a coasting section in the trajectory is then inefficient. Such a situation does not arise for $\gamma = 0$ (weightless engine).

Figure 7.13 shows four curves representing $G_\psi(T)$ as a function of the parameter γ for different values of s, the number of stages, with $\varkappa = 25$ kg/kw. The optimum value of s for each given value of γ is determined from the envelope (drawn as a thick line). The symbol $s + 0$ represents cases with engine cutoff; the dots on the lines of constant s separate those cases with and without cutoff.

The influence of the parameter $\varkappa$ on the maximum value of $G_\psi(T)$ is seen in Figure 7.14, which contains the envelopes of the three families $\varkappa = 5$, 12.5, 25 kg/kw. The dots on the curves represent those points at which the number of stages changes; thus the dot marked $s = 2$ corresponds to that point at which the optimum number of stages equals 2 (up to the right of the dot marked $s = 1$).

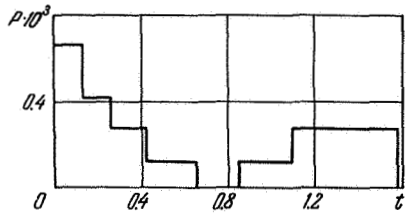

FIGURE 7.12. Stages in the variation of thrust $P(t)$ for transfer between circular orbits ($r_0 = 1$, $r_1 = 1.52$, $\varphi_1 = T = 1.57$, $G_0/N = \varkappa = 25$ kg/kw, $G_\gamma^{(i)}/P_i = \gamma = 25$ kg/kg).

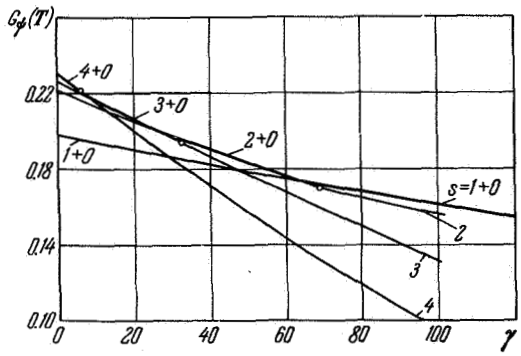

FIGURE 7.13. Weight $G_\psi(T) = G_\pi + G_\nu$ as function of unit weight of engines γ with different number s of thrust stages for transfer between circular orbits ($r_0 = 1$, $r_1 = 1.52$, $\varphi_1 = T = 1.57$, $\varkappa = 25$ kg/kw).

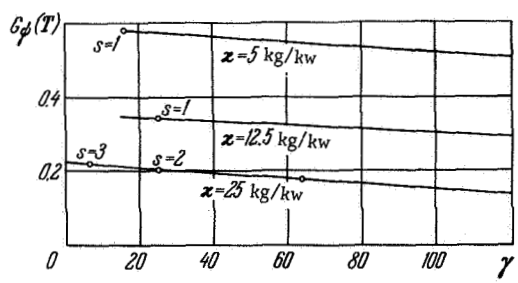

FIGURE 7.14. Weight $G_\psi(T) = G_\pi + G_\nu$ as function of unit weight of engines γ with different values of parameter $\varkappa = G_0/N$ and optimum number s of thrust stages for transfer between circular orbits ($r_0 = 1$, $r_1 = 1.52$, $\varphi_1 = T = 1.57$).

309 § 4. REAL CONTROL AND WEIGHT CHARACTERISTICS

The control and weight characteristics (II.9), (II.10) of power-limited propulsion systems depend on the type of engine used; each specific type determines the expressions for the weight G_Υ and thrust P. The thrust P can be represented either explicitly as a function of the power N_Υ, the rate of propellant flow q, and the parameters $w_1, \ldots, w_l$, i.e.,

$$P = P(N_\Upsilon, q, \mathbf{w}), \tag{7.114}$$

or in a parametric form with the aid of one general parameter u, where

$$P = P(N_\Upsilon, u, \mathbf{w}),\ q = q(N_\Upsilon, u, \mathbf{w}), \tag{7.115}$$

or finally with the aid of two general parameters u_1 and u_2, where

$$P = P(u_1, u_2, \mathbf{w}),\ q = q(u_1, u_2, \mathbf{w}),\ N_\Upsilon = N_\Upsilon(u_1, u_2, \mathbf{w}). \tag{7.116}$$

The situation is similar as regards the function G_Υ, which depends on the limiting values of N_Υ and q (or N_Υ and u, or u_1 and u_2).

This section gives the control and weight characteristics of a power-limited electrostatic engine, and describes the corresponding procedure of selecting the optimum control programs and the optimum parameters.

In /7.13—7.19, 7.25/, the question of allowing for the real control characteristics of power-limited engines in optimization problems is considered.

1. Characteristics of an electrostatic engine. The processes taking place in an electrostatic engine with surface ionization were described in § 4 of Chapter Two (/7.20—7.24/ etc.).

The parametric expressions for the thrust P and the flow rate q of this type of engine are written in accordance with Child—Langmuir's power law (the "3/2 law"), derived for a one-dimensional monochromatic beam under conditions of unlimited ion supply

$$P = \frac{2}{9\pi d^2}\mathcal{F}\mathcal{U}^2, \quad q = \frac{1}{9\pi d^2}\left(\frac{2m}{e}\right)^{1/2}\mathcal{F}\mathcal{U}^{3/2}; \tag{7.117}$$

the distance between the emitter and the accelerating electrode is d, $\mathcal{F}$ is the cross-sectional area of the beam, m and e are the mass and charge of the ion respectively, and $\mathcal{U}$ is the attracting potential.

The power N_Υ creating the thrust consists of the jet power together with that radiated from the incandescent surface of the emitter (main source of
310 losses), so that

$$N_\Upsilon = \frac{1}{9\pi d^2}\left(\frac{2e}{m}\right)^{1/2}\mathcal{F}\mathcal{U}^{3/2} + \mathcal{F}L, \tag{7.118}$$

where L represents constant radiational losses per unit area.

When selecting the potential $\mathcal{U}$ and the distance d one must take into account their limiting values

$$\mathcal{U}/d \leqslant \mathrm{E}_{\max}, \quad d \geqslant d_{\min}. \tag{7.119}$$

If the first inequality is not satisfied (the average electric field strength E in the accelerating gap exceeds $\mathbf{E}_{max}$), breakdown will occur; the second inequality represents a geometrical restriction.

Figures 7.15 and 7.16 represent the thrust P and the propellant flow rate q as functions of the area $\mathcal{F}$ for different values of the power N_γ (the geometric parameter d is constant at 0.3 cm, $\mathbf{E}_{max} = 30{,}000$ v/cm, $L = 11$ w/cm^2 /7.22/); the extreme left-hand points of the curves correspond to the situation $\mathcal{U}/d = \mathbf{E}_{max}$. The function $P(N_\gamma, q)$ is plotted in Figure 7.17, where, for comparison, curves representing the thrust of an ideal engine are represented by dotted lines. The double-valuedness of the thrust function in Figure 7.17 (upper branch is the broken line, lower branch is the dash-dot line) is discussed in the next subsection.

The weight of this type of engine can be assumed proportional to the maximum area of the beam cross-section, so that

$$G_\gamma = \gamma_f \mathcal{F}_{max}. \tag{7.120}$$

Equation (7.120), together with expression (7.2) for the weight of the power source and converter, determine the weight of an engine of the given type.

The thrust, flow rate, and power of an electrostatic engine with surface ionization vary when either the potential $\mathcal{U}$ or the area $\mathcal{F}$ are varied (the latter is altered by changing the number of elementary engines which are in operation). Conditions (7.119), as well as (cf. (7.2), (7.120))

$$N_\gamma(t) \leqslant N_{max} = G_\nu/\alpha, \quad \mathcal{F}(t) \leqslant \mathcal{F}_{max} = G_\gamma/\gamma_f \tag{7.121}$$

must be fulfilled during the control process.

2. **Optimum control programs of real engines.** The variational problem for the delivery of a maximum payload is described in a general form (without specifying the forms of P and G_γ) by the following system of
312 differential equations and boundary conditions (cf. (II.8)):

$$\left.\begin{aligned}
&\dot{G}_\sigma = -gq, && G_\sigma(0) = G_0 - G_\nu - G_\gamma, && G_\sigma(T) = \max,\\
&\dot{\mathbf{r}} = \mathbf{v}, && \mathbf{r}(0) = \mathbf{r}_0, && \mathbf{r}(T) = \mathbf{r}_1,\\
&\dot{\mathbf{v}} = \frac{gP\mathbf{e}}{G_\sigma + G_\nu + G_\gamma} + \mathfrak{R}, && \mathbf{v}(0) = \mathbf{v}_0, && \mathbf{v}(T) = \mathbf{v}_1\\
&(P(t) = P(N_\gamma, q, \mathbf{w}), \ |\mathbf{e}(t)| = 1, \ G_\nu = \alpha N_{max}, && && \\
&\qquad G_\gamma = G_\gamma(N_{max}, q_{max}, \mathbf{w})).
\end{aligned}\right\} \tag{7.122}$$

In order to find the condition for selecting the optimum controls, we write the Hamiltonian and the momentum differential equations for the problem as expressed in (7.122):

$$\left.\begin{aligned}
&H = -p_\sigma gq + \mathbf{p}_r \cdot \mathbf{v} + (\mathbf{p}_v \cdot \mathbf{e}) gP(G_\sigma + G_\nu + G_\gamma)^{-1} + \mathbf{p}_v \cdot \mathfrak{R},\\
&\dot{p}_\sigma = (\mathbf{p}_v \cdot \mathbf{e}) gP(G_\sigma + G_\nu + G_\gamma)^{-2}, \quad p_\sigma(T) = -1,\\
&\dot{\mathbf{p}}_r = -\frac{\partial}{\partial \mathbf{r}}(\mathbf{p}_v \cdot \mathfrak{R}), \qquad \dot{\mathbf{p}}_v = -\mathbf{p}_r.
\end{aligned}\right\} \tag{7.123}$$

The optimum program of the control vector $\mathbf{e}(t)$ is determined by (7.21); the controls through which the thrust P (cf. (7.114)), or the thrust P and the flow rate q (cf. (7.115)) are expressed, will be optima if they yield an

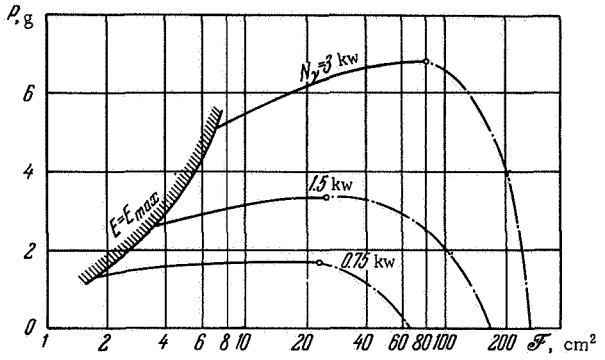

FIGURE 7.15. Thrust P of electrostatic engine as function of area $\mathcal{F}$ and power N_γ; extreme left-hand points of curve correspond to regime of maximum electric field E.

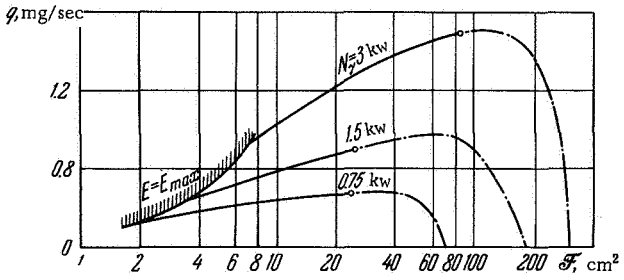

FIGURE 7.16. Flow rate q of electrostatic engine as function of area $\mathcal{F}$ and power N_γ; extreme left-hand points of curve correspond to regime of maximum electric field E.

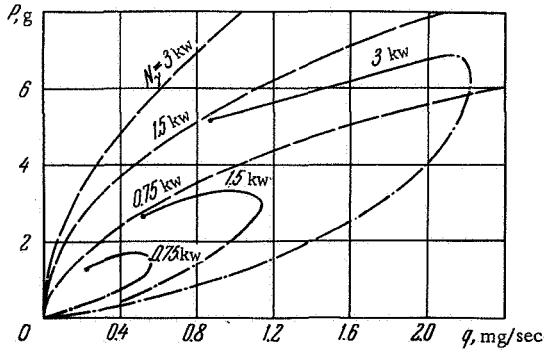

FIGURE 7.17. Thrust P of electrostatic engine as function of propellant flow rate q and power N_γ; extreme left-hand points of curve correspond to regime of maximum E. Broken curves represent results for an ideal engine.

solute minimum of the function H or that part of it depending on P and q, i.e.,

$$\min\,[-(p_\sigma q + p_v P/G)] \qquad (p_v = |\mathbf{p}_v|,\ G = G_\sigma + G_v + G_\gamma). \tag{7.124}$$

We shall use (7.124) to determine the optimum power-variation program for an electrostatic engine. Consider the thrust P as a function of the power N_γ and the flow rate q in the form (7.114). If the thrust P depends on the power N_γ for any q such that the thrust increases with increasing power, i.e., $\partial P/\partial N_\gamma > 0$, the optimum value of the control N_γ will be, according to (7.124),

$$N_\gamma(t) = N_{\max} = G_v/\alpha. \tag{7.125}$$

Figure 7.17 (the broken curves) indicates that this conclusion is correct for the type of engine considered. We recall that the same is true for ideal power-limited engines as well.

313 We shall now examine the optimum control programs of an electrostatic engine. The propellant flow rate q, the thrust P, and the power N_γ of the electrostatic engine with surface ionization are determined by the area $\mathcal{F}$ and the potential $\mathcal{U}$ (cf. (7.117) and (7.118)). The structure of the optimum control functions $q(t)$ and $P(t)$ will now be established with the aid of criterion (7.124).

In place of $\mathcal{F}$, $\mathcal{U}$ we introduce the dimensionless controls σ, ε defined by

$$\sigma(t) = \mathcal{F}(t)/\mathcal{F}_{\max} = \gamma_f \mathcal{F}(t)/G_\gamma, \qquad \varepsilon(t) = \mathcal{U}(t)/\mathrm{E}_{\max} d; \tag{7.126}$$

here

$$0 \leqslant \sigma(t) \leqslant 1, \qquad 0 \leqslant \varepsilon(t) \leqslant 1. \tag{7.127}$$

The flow rate and the thrust (7.117) are expressed in terms of σ and ε by

$$P = c_1 G_\gamma \sigma \varepsilon^2, \qquad q = c_2 G_\gamma \sigma \varepsilon^{3/2} \left(c_1 = \frac{2}{9\pi}\frac{\mathrm{E}_{\max}^2}{\gamma_f},\ c_2 = \frac{1}{9\pi\gamma_f}\left(\frac{2m}{ed}\right)^{1/2}\mathrm{E}_{\max}^{3/2}\right). \tag{7.128}$$

The optimum condition for the power (7.125) determines the relation between σ and ε. If (7.125) and (7.126) are substituted into (7.118), we obtain

$$G_v/G_\gamma = \sigma(c_3\varepsilon^{3/2} + c_4) \quad \left(c_3 = \frac{\alpha}{9\pi\gamma_f d^2}\left(\frac{2e}{m}\right)^{1/2}\mathrm{E}_{\max}^{3/2},\ c_4 = \frac{\alpha L}{\gamma_f}\right). \tag{7.129}$$

From (7.128) we express ε in terms of σ and substitute the expression thus obtained into (7.117) for the thrust and the flow rate. The bounds on ε are transferred to σ, where

$$P = c_1 G_\gamma \sigma\left(\frac{G_v}{c_3 G_\gamma \sigma} - \frac{c_4}{c_3}\right)^{4/3}, \qquad q = c_2 G_\gamma \sigma\left(\frac{G_v}{c_3 G_\gamma \sigma} - \frac{c_4}{c_3}\right)^{3/2},$$
$$\frac{G_v}{(c_3 + c_4) G_\gamma} \leqslant \sigma(t) \leqslant 1. \tag{7.130}$$

Outside this range $\sigma(t)$ can take the value $\sigma = 0$. This corresponds to engine cutoff for which $P = q = 0$.

The relationships (7.130) are plotted in Figure 7.15 with $(P, \mathcal{F})$ coordinates with a parameter N_γ, and in Figure (7.16) in $(q, \mathcal{F})$ coordinates with the same parameter; the functions $P(\mathcal{F})$ and $q(\mathcal{F})$ have maxima (as $\mathcal{F} \to 0$ the functions $P, q \to 0$, and as $\mathcal{F} \to N_\gamma/L$ the functions $P, q \to 0$). It follows that the function $P(q)$ and the inverse function $q(P)$ are double-valued (cf. Figure 7.17), so that the same value of the thrust is achieved for two values of the flow rate,
314 and correspondingly for two values of the area. The second situation (smaller flow rate and smaller area for a given value of the thrust) is always more expedient than the first one; therefore, the optimum regimes are not realized at those parts of the curves in Figure 7.17 lying to the right of the maxima. These parts (and those corresponding to them in Figures 7.15 and 7.16) are represented by the dash-dot lines.

When the expressions for the thrust and the flow rate (7.130) are substituted into the expression for H, we obtain the following condition for determining the optimum law $\sigma(t)$:

$$\min_{\sigma}\left\{-gG_\gamma\left[c_1p_a\sigma\left(\frac{G_v}{c_3G_\gamma\sigma}-\frac{c_4}{c_3}\right)^{4/5}+c_2p_v\frac{\sigma}{G}\left(\frac{G_v}{c_3G_\gamma\sigma}-\frac{c_4}{c_3}\right)^{3/5}\right]\right\}, \tag{7.131}$$

where $G_v/G_\gamma(c_3 + c_4) \leqslant \sigma(t) \leqslant 1$ or $\sigma(t) = 0$.

The optimum control function $\sigma(t)$ consists of separate variable sections, so that $\sigma = \sigma_{opt}(t)$ is determined from the condition for a minimum of expression (7.131) without restrictions on σ, the intervals of the limiting control function $\sigma = 1$ for $\sigma_{opt}(t) > 1$, the intervals of the limiting control function $\sigma = G_v/G_\gamma(c_3 + c_4)$ at $\sigma_{opt}(t) < G_v/G_\gamma(c_3 + c_4)$ and also the intervals of engine cut off $\sigma = 0$ in the case when expression (7.131) is positive at $\sigma = G_v/G_\gamma(c_3 + c_4)$.

3. Optimum parameters of unthrottlable real engines. In this paragraph we show how to determine the optimum parameters of unthrottled real electrostatic engines. Two dynamic maneuvers are considered, namely, rotating the orbital plane of a satellite, and holding the satellite in a specified spherical layer (drag compensation).

The solution of the dynamic part of the variational problem for both maneuvers is given in Chapter Six. The result, $T_\mu(gP/G_0,\ gq/G_0)$, has the following form for the first maneuver (cf. (6.88)):

$$T_\mu = r_0^{3/2}k^{-1/2}4s\arcsin\left(\frac{iG_0k}{4sPgr_0^2}\right). \tag{7.132}$$

The calculations were conducted for rotating the plane of the circular orbit of a 24-hour Earth satellite where the expression $iG_0k/4gr_0^2$ was taken equal to 1000 g, and the number of revolutions s is 10 to 100. For these values, (7.132) reduces to

$$T_\mu[\text{sec}] = 5.5\cdot10^4 s\arcsin(10^3/sP\ [\text{g}]). \tag{7.133}$$

The second maneuver (drag compensation) is characterized by the function $T_\mu(gP/G_0,\ gq/G_0)$ (cf. (6.73)) and has the form

$$T_\mu = {}^1/_2c_x\rho v^2ST/P. \tag{7.134}$$

315 It will be assumed that the engine operates at every sixteenth revolution. The drag $^1/_2 c_{x0} \rho v^2 S$ will be taken equal to 0.5 g; (7.134) then reduces to

$$T_\mu = 0.5\, T/P \text{ [g]} \qquad (T_\mu \leqslant T/16,\ P \geqslant 8 \text{ g}). \tag{7.135}$$

For the propulsion system under consideration, one must determine the optimum area $\mathcal{F}$ and the field strength E; as to the electrode gap d, it is possible to prove that for an optimum

$$d = d_{\min}. \tag{7.136}$$

316 The calculations were based on the values of the parameters $d_{\min}$, L, $E_{\max}$, e, m indicated in subsection 1. In the first problem (rotation of the orbital plane) the unit weight of the power source and converter, α, was taken as 20 kg/kw, and in the second problem (drag compensation) as 50 kg/kw; the calculations were performed for $\gamma_f = 0.1$ kg/cm^2.

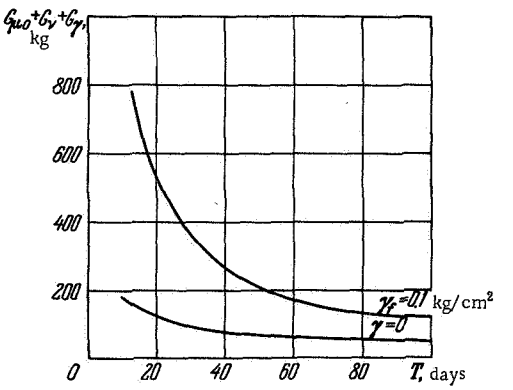

FIGURE 7.18. Weight $G_{\mu 0} + G_\nu + G_\gamma$ expended for rotating satellite orbit plane, as function of maneuvering time T; curve $\gamma = 0$ corresponds to weightless engine with ideal acceleration.

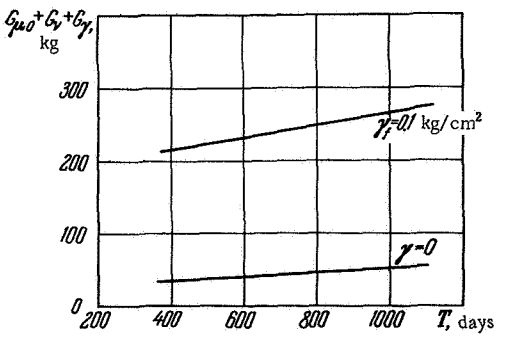

FIGURE 7.19. Weight $G_{\mu 0} + G_\nu + G_\gamma$ expended for holding satellite in specified spherical layer, as function of maneuvering time T; curve $\gamma = 0$ corresponds to weightless engine with ideal acceleration.

The numerical results for an electrostatic engine for these two maneuvers are presented in Figures 7.18 and 7.19. These figures show the total weight expended for performing the maneuver $G_{\mu_0} + G_\nu + G_\gamma$ as a function of the maneuvering time T. Figure 7.18 corresponds to the maneuver of rotating the orbital plane, and Figure 7.19 to the maneuver of holding the satellite within a given layer. Curves corresponding to a power-limited unthrottled engine without losses have been plotted for comparison and are designated by the symbol $\gamma = 0$.

Chapter Eight

ENGINES WITH LIMITED EXHAUST VELOCITY. OPTIMUM COMBINATION OF ENGINES WITH LIMITED EXHAUST VELOCITY AND LIMITED POWER

317 All thermal rocket engines belong to the category of engines with limited exhaust velocity. This velocity is limited due to the maximum temperature which the combustion chamber walls or the heat exchanger can withstand (cf. Part I). Engines in this category are characterized by a relatively low weight γ_* per unit thrust ($\gamma_* \sim 10^{-2}$). They are capable of delivering high thrusts and are, therefore, called high-thrust engines.

In view of the low unit weight γ_*, the engine weight G_* is usually neglected in optimization problems involving engines with limited exhaust velocities. Such an approximation is, however, inaccurate when a high thrust acceleration is required (i.e., when the condition $G_*/G_1 = \gamma_* (aG)_{max}/gG_1 \ll 1$ is not satisfied).

The low unit weight of engines with limited exhaust velocities is an advantage, but a drawback is that their exhaust velocities are substantially lower than those whose power is limited. The question arises as to which engines are to be preferred, the limited exhaust velocity type (high-thrust engines) or the power-limited type (low-thrust engines). An attempt at answering this question initiated the investigations into low-thrust engines (cf. for instance /8.1—8.6/ etc.). It is, however, more correct to formulate this question differently, namely, to determine the regions for which each type of propulsion system is best suited, and the efficiency when using different types of engines in the same vehicle.

We shall define the space of the maneuver parameters, the parameters of the engine with limited exhaust velocity, and the parameters of the power-limited engine for each maneuver. That region of space in which the use of a given type of engine is advantageous will be called the region
318 of application for the given engine. The space is divided into regions of application for the limited-exhaust velocity engine, the power-limited engine, and an intermediate region for the simultaneous use of both engines.

In this chapter we describe the characteristics and optimum work regimes of engines with limited exhaust velocities; the optimum conditions of combining engines with limited exhaust velocity and limited power are established; a criterion for finding the regions of application of power-limited engines is given. The boundaries of these regions are determined for a number of maneuvers.

§ 1. CHARACTERISTICS AND OPTIMUM OPERATING REGIMES FOR ENGINES WITH LIMITED EXHAUST VELOCITIES

1. Characteristics of engines with limited exhaust velocities. An ideal engine with limited exhaust velocity is represented by the following expressions for the thrust P, the propellant flow rate q, and the weight $G_\varkappa$ (cf. (II.9), (II.10), for $u_1 = P$, $u_2 = V$):

$$P = P, \quad q = P/V, G_\varkappa = 0 \,(0 \leqslant P\,(t) \leqslant \infty, 0 \leqslant V\,(t) \leqslant V_{\max}), \tag{8.1}$$

i.e., the ideal engine is weightless, the exhaust velocity has an upper bound, and the thrust has no upper bound. This implies the existence of impulses operating during infinitesimal time intervals over which the thrust and the flow rate are infinite, while the amount of working fluid discharged remains finite.

The weight of a real engine with limited exhaust velocity is either a function of the maximum thrust (liquid propellant engines), for which we have, in place of (8.1),

$$P = P, \; q = P/V, \; G_\varkappa = \gamma P_{\max} \,(0 \leqslant P\,(t) \leqslant P_{\max}, \; 0 \leqslant V\,(t) \leqslant V_{\max}), \tag{8.2}$$

or it is a function of the initial weight of the working fluid (solid propellant engines), for which

$$P = P, \; q = P/V, \; G_\varkappa = \gamma G_{\mu 0} \,(0 \leqslant P\,(t) \leqslant \infty, \, 0 \leqslant V\,(t) \leqslant V_{\max}) \tag{8.3}$$

(the values of the unit weights γ are given in Chapter Two and the subscript of γ is dropped). The thrust in real engines of the type (8.3) is not bounded and, as in the ideal case, the existence of impulses is allowed.

2. Characteristic features of the optimum operating regimes for an ideal engine with limited exhaust velocity. We write the variational problem
319 for ideal engines with limited exhaust velocities in the form (II.8)

$$\left.\begin{aligned} &\dot G_\sigma = -gP/V, && G_\sigma(0) = G_0, && G_\sigma(T) = \max, \\ &\dot{\mathbf{r}} = \mathbf{v}, && \mathbf{r}(0) = \mathbf{r}_0, && \mathbf{r}(T) = \mathbf{r}_1, \\ &\dot{\mathbf{v}} = gP\mathbf{e}/G_\sigma + \mathfrak{R}, && \mathbf{v}(0) = \mathbf{v}_0, && \mathbf{v}(T) = \mathbf{v}_1 \\ &(0 \leqslant P(t) \leqslant \infty, && 0 \leqslant V(t) \leqslant V_{\max}, && |\mathbf{e}(t)| = 1). \end{aligned}\right\} \tag{8.4}$$

The weight formula consists of only two components, the payload G_π and the working-fluid weight G_μ ($G_\pi + G_\mu = G_\sigma = G$), where the engine weight $G_\varkappa$ vanishes (according to the definition of an ideal engine with limited exhaust velocity).

Substituting the thrust acceleration $a = gP/G = gP/G_\sigma$ into equations (8.4) in place of the thrust P, and expressing the weight components G_π, G_σ as fractions of the takeoff weight G_0, we obtain (using the same symbols for the dimensionless weight components as for the dimensional ones)

$$\left.\begin{aligned} &\dot G_\sigma = -aG_\sigma/V, && G_\sigma(0) = 1, && G_\sigma(T) = \max, \\ &\dot{\mathbf{r}} = \mathbf{v}, && \mathbf{r}(0) = \mathbf{r}_0, && \mathbf{r}(T) = \mathbf{r}_1, \\ &\dot{\mathbf{v}} = a\mathbf{e} + \mathfrak{R}, && \mathbf{v}(0) = \mathbf{v}_0, && \mathbf{v}(T) = \mathbf{v}_1 \\ &(0 \leqslant a(t) \leqslant \infty, && 0 \leqslant V(t) \leqslant V_{\max}, && |\mathbf{e}(t)| = 1). \end{aligned}\right\} \tag{8.5}$$

The Hamiltonian H and the momentum equations are now given by

$$\left.\begin{aligned} &H = -p_\sigma a G_\sigma / V + \mathbf{p}_r \cdot \mathbf{v} + \mathbf{p}_v \cdot (a\mathbf{e} + \mathbf{R}), \\ &\dot{p}_\sigma = p_\sigma \frac{a}{V}, \quad \dot{\mathbf{p}}_r = -\frac{\partial}{\partial \mathbf{r}} (\mathbf{p}_v \cdot \mathbf{R}), \\ &\dot{\mathbf{p}}_v = -\mathbf{p}_r \quad (p_\sigma(T) = -1). \end{aligned}\right\} \tag{8.6}$$

The function $p_\sigma(t)$ is negative everywhere within the interval $0 \leqslant t \leqslant T$, since the equation for p_σ is linear homogeneous, and at $t = T$ the function p_σ is negative.

The factor multiplying $1/V$ in the expression for H can either be positive (allowing for the sign before the whole term) or vanish at $a(t) = 0$, and therefore along the powered sections of the trajectory ($a(t) \neq 0$) the optimum control function $V(t)$ (which minimizes the Hamiltonian H) is

$$V(t) = V_{\max}. \tag{8.7}$$

The optimum control vector $\mathbf{e}(t)$ is

$$\mathbf{e}(t) = -\mathbf{p}_v / p_v \qquad (p_v = |\mathbf{p}_v|). \tag{8.8}$$

320 The optimum control function $a(t)$ can consist of three components composed of the two boundary ones

$$\left.\begin{aligned} &a(t) = 0 \qquad\quad \text{at} \quad \Delta < 0 \\ &a(t) = a_{\max} \to \infty \quad \text{at} \quad \Delta > 0 \end{aligned}\right\} \quad \left(\Delta = p_v + p_\sigma \frac{G_\sigma}{V}\right) \tag{8.9}$$

and one singular

$$a(t) = a_{\text{opt}}(t) < \infty \quad \text{at} \quad \Delta(t) \equiv 0. \tag{8.10}$$

The duration τ_i of the powered sections with $a \to \infty$ must be zero, otherwise the integrals

$$\int_t^{t+\tau_i} a(t)\, dt \tag{8.11}$$

would not be finite (infinite fuel consumption); it follows that the expression Δ cannot be positive during a finite time interval.

The expression $p_\sigma G_\sigma / V$ in the Hamiltonian (8.6) is time-independent and negative; this first property is checked by differentiating and substituting for the derivatives $\dot{p}_\sigma$ and $\dot{G}_\sigma$ from (8.5) and (8.6), while the second is determined by the sign of p_σ.

By the methods used in Chapter Four, we conclude that the variational problem (8.5) for the maximum of $G_\sigma(T)$ is equivalent to that for the minimum of the characteristic velocity I, where

$$\left.\begin{aligned} &\dot{I} = a, \qquad I(0) = 0, \quad I(T) = \min, \\ &\dot{\mathbf{r}} = \mathbf{v}, \qquad \mathbf{r}(0) = \mathbf{r}_0, \quad \mathbf{r}(T) = \mathbf{r}_1, \\ &\dot{\mathbf{v}} = a\mathbf{e} + \mathbf{R}, \quad \mathbf{v}(0) = \mathbf{v}_0, \quad \mathbf{v}(T) = \mathbf{v}_1 \\ &\qquad (a(t) \geqslant 0 \quad |\mathbf{e}(t)| = 1). \end{aligned}\right\} \tag{8.12}$$

The control functional (8.5), for which the payload $G_\sigma(T) = G_\pi$, is linked with the characteristic velocity $I(T)$ by the relation

$$G_\pi = e^{-\Psi} \left(\Psi = I(T)/V_{\max}, \quad I(T) = \int_0^T a\,dt \right). \tag{8.13}$$

Thus, for an ideal engine with limited exhaust velocity the general variational problem (8.4) is reduced to the dynamic one (8.12). Comparing (8.13) and (4.16), it is possible to establish region 2 (see Figure 8.1) in the plane of the functionals Ψ, Φ throughout which the payload for a power-limited engine is larger than that for an engine with limited exhaust velocity. In region 1 the payload for an engine with limited exhaust velocity is larger than that for a power-limited engine.

321 Note that Mayer's problem (8.12) can be replaced by a Lagrange problem in the same way as was done for an ideal power-limited engine:

$$I = \int_0^T \sqrt{[\ddot{\mathbf{r}} - \mathbf{R}(\mathbf{r}, t)] \cdot [\ddot{\mathbf{r}} - \mathbf{R}(\mathbf{r}, t)]}\, dt \tag{8.14}$$

$$(\mathbf{r}(0) = \mathbf{r}_0, \ \dot{\mathbf{r}}(0) = \mathbf{v}_0, \ \mathbf{r}(T) = \mathbf{r}_1, \ \dot{\mathbf{r}}(T) = \mathbf{v}_1).$$

The application of the classical method of variational analysis (making the first variation vanish) does not give, however, in this case a full solution of the variational problem; the extrema of the integral functional (8.14) only correspond to the single component (8.10).

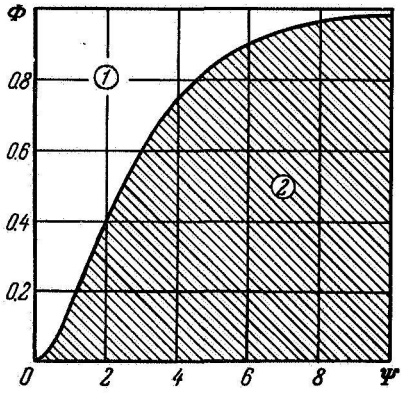

FIGURE 8.1. Boundary of regions in which ideal engines with limited exhaust velocity (1) and limited power (2) are used, in (Ψ,Φ) plane of functionals of dynamic problem (Ψ for engine 1, Φ for engine 2).

The variational problem (8.12) of minimizing the characteristic velocity I (corresponding to the problem of maximum payload for an ideal engine with limited exhaust velocity) was solved for a wide class of maneuvers in papers listed in the introduction, /1.1—1.49/. We investigate below how the real characteristics of an engine with limited exhaust velocity affect the parameters of optimum motion.

3. Allowing for the engine weight. Consider a real engine with limited exhaust velocity and characteristic (8.2) for which the thrust is bounded and the engine weight is proportional to the maximum thrust. We represent the thrust P as a fraction of the maximum thrust $P_{\max}$, and all weights as fractions of the takeoff weight of the vehicle, where the same symbols are used for these dimensionless variables as for the corresponding dimensional ones. The problem of delivering a maximum payload is written as follows

(cf. (8.4)):

$$\left.\begin{aligned}
&\dot G_\sigma = -a_0 P/V, && G_\sigma(0) + \gamma a_0/g = 1, \quad G_\sigma(T) = \max,\\
&\dot{\mathbf{r}} = \mathbf{v}, && \mathbf{r}(0) = \mathbf{r}_0, \quad \mathbf{r}(T) = \mathbf{r}_1,\\
&\dot{\mathbf{v}} = \frac{a_0 P \mathbf{e}}{G_\sigma + \gamma a_0/g} + \mathfrak{R}, && \mathbf{v}(0) = \mathbf{v}_0, \quad \mathbf{v}(T) = \mathbf{v}_1\\
&(0 \leqslant P(t) \leqslant 1,\ 0 \leqslant V(t) \leqslant V_{\max},\ |\mathbf{e}(t)| = 1, && a_0 = gP_{\max}/G_0 = \text{const}).
\end{aligned}\right\} \tag{8.15}$$

322 It is necessary here to determine the optimum programs $V(t)$, $P(t)$, $\mathbf{e}(t)$ and to select the optimum value of the parameter a_0 which maximizes the payload $G_\pi = G_\sigma(T)$ (the unit engine weight γ is specified). As for unthrottled engines (Chapter Six), one can here separate the dynamic part, which is independent of the structural parameter γ.

We proceed in (8.15) from the weight G_σ to the total weight $G(t) = G_\sigma(t) + \gamma a_0/g$; for the functional we take the terminal value

$$G(T) = G_\pi + \gamma a_0/g. \tag{8.16}$$

For fixed values of a_0 the maxima of the functional (8.16) and that in (8.15) coincide, and problem (8.15) reduces to the standard problem of rocket dynamics, namely, to maximize the terminal weight for bounded thrust and exhaust velocity:

$$\left.\begin{aligned}
&\dot G = a_0 P/V, && G(0) = 1, \quad G(T) = \max,\\
&\dot{\mathbf{r}} = \mathbf{v}, && \mathbf{r}(0) = \mathbf{r}_0, \quad \mathbf{r}(T) = \mathbf{r}_1,\\
&\dot{\mathbf{v}} = a_0 P\mathbf{e}/G + \mathfrak{R}, && \mathbf{v}(0) = \mathbf{v}_0, \quad \mathbf{v}(T) = \mathbf{v}_1\\
&(0 \leqslant P(t) \leqslant 1,\ 0 \leqslant V(t) \leqslant V_{\max},\ |\mathbf{e}(t)| = 1).
\end{aligned}\right\} \tag{8.17}$$

The solution of (8.17) determines the dependence of the functional on the parameter a_0, $G(T) = G_1(a_0)$. With such a relationship, the optimum value of the parameter a_0 can be determined from the condition of maximum payload G_π (cf. (8.16))

$$\max G_\pi = \max_{a_0} [G_1(a_0) - \gamma a_0/g]. \tag{8.18}$$

The dynamic problem (8.17) has been thoroughly studied by numerous authors /8.7—8.54/. Their results can therefore be used to solve the complete problem (8.15).

Consider now an engine with limited exhaust velocity and characteristic (8.3) for which the thrust is unbounded, and the engine weight is proportional to the initial working-fluid reserve. Since no restrictions are imposed on the thrust, the variational problem can be written in the form (II. 5), (7.5) using the thrust acceleration (cf. (8.5)):

$$\left.\begin{aligned}
&\dot G_\pi = 0, && G_\pi(0) + && G_\pi(T) = \max,\\
&\dot G_\mu = -\frac{G_\pi + G_\mu + \gamma G_\mu(0)}{V} a_0, && + (1+\gamma) G_\mu(0) = 1, && G_\mu(T) = 0,\\
&\dot{\mathbf{r}} = \mathbf{v}, && && \mathbf{r}(0) = \mathbf{r}_0,\ \mathbf{r}(T) = \mathbf{r}_1,\\
&\dot{\mathbf{v}} = a\mathbf{e} + \mathfrak{R}, && && \mathbf{v}(0) = \mathbf{v}_0,\ \mathbf{v}(T) = \mathbf{v}_1\\
&(0 \leqslant a(t) \leqslant \infty,\ 0 \leqslant V(t) \leqslant V_{\max},\ |\mathbf{e}(t)| = 1).
\end{aligned}\right\} \tag{8.19}$$

323 As in problem (8.5), it is possible to prove the optimality of the control $V(t) = V_{\max}$. Having integrated the second equation of (8.19) with $V(t) = V_{\max}$ and allowing for the boundary conditions, we can express the problem functional G_n in terms of the characteristic velocity I (cf. (8.13)) in the form

$$G_n = (1+\gamma)e^{-I/V_{\max}} - \gamma \qquad \left(I = \int_0^T a(t)\,dt\right). \tag{8.20}$$

The payload G_n is once more a decreasing function of the characteristic velocity I, and therefore problem (8.19) reduces to the dynamic problem (8.12) for an ideal engine with limited exhaust velocity.

If, in addition to the characteristic (8.3), we impose a limited thrust ($0 \leqslant P(t) \leqslant P_{\max}$, where $P_{\max}$ is the structural parameter), the problem of maximum payload reduces to (8.17). For $G_k = \gamma G_{\text{p0}}$ the payload is equal to

$$G_n = G_1 - G_k = (1+\gamma)\,G_1 - \gamma, \tag{8.21}$$

i.e., the optimum condition for G_n is equivalent to the condition of maximum terminal weight G_1.

In order to obtain a quantitative idea of the influence of the engine weight, we consider the analogous problem of the vertical climb of a rocket in a vacuum under constant gravitational acceleration ($g = \text{const}$) /8.45–8.54/. The initial altitude and initial velocity are zero ($y_0 = v_0 = 0$), and at the end a specified value of the total energy $E_1 = {}^1/_2 v_1^2 + g y_1$ is required for maximum payload. The engine characteristic is taken in the form (8.2).

We introduce the dimensionless variables

$$t = \frac{gt}{V_{\max}}, \quad \bar{G} = \frac{G}{G_0}, \quad \bar{E} = \frac{E}{V_{\max}^2}, \quad \bar{v} = \frac{v}{V_{\max}}, \quad \bar{P} = \frac{P}{P_{\max}}, \quad \bar{V} = \frac{V}{V_{\max}}, \quad \bar{a}_0 = \frac{P_{\max}}{G_0} \tag{8.22}$$

and replace the second equation of (8.15) by an equation describing the variation of the energy. The variational problem (8.15) is written as

$$\left.\begin{aligned} &\dot{G}_\sigma = -a_0 P/V, \quad G_\sigma(0) + \gamma a_0 = 1, \quad G_\sigma(T) = \max, \\ &\dot{E} = v\frac{a_0 P}{G_\sigma + \gamma a_0}, \qquad E(0) = 0, \quad E(T) = E_1, \\ &\dot{v} = \frac{a_0 P}{G_\sigma + \gamma a_0} - 1, \qquad v(0) = 0, \quad v(T) = \text{opt} \\ &(0 \leqslant P(t) \leqslant 1,\ 0 \leqslant V(t) \leqslant 1,\ a_0 = \text{const},\ T = \text{opt}). \end{aligned}\right\} \tag{8.23}$$

324 The thrust is here directed along the velocity; the bars above the dimensionless variables are omitted.

Note that the control parameter a_0 (the ratio of the maximum thrust to the takeoff weight) must be larger than unity at takeoff; its upper bound ($1 < a_0 < 1/\gamma$) is imposed by the limiting situation $G_k = \gamma P_{\max} = G_0$. The optimum value of this control parameter can be selected by the standard procedure of adding the formal equation $\dot{a}_0 = 0$ to system (8.23). The optimum control functions $V(t)$ and $P(t)$, which maximize the payload, are

determined from the condition for an absolute minimum of the Hamiltonian

$$\left.\begin{aligned} H &= -p_\sigma \frac{a_0 P}{V} + p_e v \frac{a_0 P}{G_\sigma + \gamma a_0} + p_v \left(\frac{a_0 P}{G_\sigma + \gamma a_0} - 1 \right), \\ \dot{p}_\sigma &= (p_e v + p_v) a_0 P (G_\sigma + \gamma a_0)^{-2}, \quad \dot{p}_e = 0, \\ \dot{p}_v &= -p_e a_0 P (G_\sigma + \gamma a_0)^{-1} \quad (p_\sigma (T) = -1). \end{aligned}\right\} \tag{8.24}$$

The function H vanishes identically on the optimum trajectory, since it does not explicitly contain the variable t, and since the final time T is not fixed. At $t = T$ we must have $V(T) = 1$ in order that H should be a minimum.

Since $v(T)$ is unspecified, we require $p_v(T) = 0$. In addition, $v(T) > 0$, $P(t) > 0$, since otherwise $E(T) = 0$ and the trajectory could be brought to an end at $t < T$. It therefore follows from the condition for $H(T) = a_0 P(T) \times$ $\times [p_e v(T) (G_\pi + \gamma a_0)^{-1} + 1] = 0$ and from the second equation of (8.24) that the momentum p_e has a constant negative value $p_e = \text{const} < 0$.

From (8.23) and (8.24) one may determine the momentum p_v

$$\dot{p}_v = -p_e (1 + \dot{v}), \quad p_v = p_{v0} - p_e t - p_e v, \tag{8.25}$$

where, from the conditions at $t = T$,

$$p_{v0} = p_e [T + v(T)] < 0. \tag{8.26}$$

Note that p_v is a non-decreasing function of t, and vanishes at the end of the interval.

At $t = 0$, $H(0) = p_{v0} (a_0 P(0) - 1) - a_0 P(0) \times p_\sigma (0)/V(0) = 0$; from the takeoff condition we have $a_0 P > 1$; it follows that

$$p_\sigma (0) < 0, \quad V(0) = 1. \tag{8.27}$$

From (8.25) and the last equation of (8.24) we obtain

$$\dot{p}_\sigma = (p_{v0} - p_e t)\, a_0 P (G_\sigma + \gamma a_0)^{-2}. \tag{8.28}$$

325 Relations (8.26) to (8.28) and the boundary condition $p_\sigma(T) = -1$ imply that p_σ varies monotonically with t, so that $p_\sigma(t) < 0$ everywhere. Hence, the optimum control function $V(t)$, which minimizes the Hamiltonian H, everywhere attains its limit

$$V(t) = 1 \qquad (0 \leqslant t \leqslant T). \tag{8.29}$$

The optimum control function $P(t)$ depends on the sign of Δ, i.e.,

$$\left.\begin{aligned} P(t) &= 1 \text{ at } \Delta(t) < 0 \\ P(t) &= 0 \text{ at } \Delta(t) > 0 \end{aligned}\right\} \quad \left(\Delta = \frac{p_{v0} - p_e t}{G_\sigma + \gamma a_0} - p_\sigma \right). \tag{8.30}$$

We cannot have a singular control (for $\Delta \equiv 0$), since the derivative of Δ is different from zero everywhere:

$$\dot{\Delta} = -p_e (G_\sigma + \gamma a_0)^{-1} \neq 0.$$

The region where $P(t) = 0$ (for $\Delta > 0$) is likewise not realized within the interval $0 \leqslant t < T$, since this leads, according to (8.24), to the condition $p_v(t) = 0$, which is fulfilled only at the end of the interval ($p_v(T) = 0$).

Therefore, the optimum control function $P(t)$ in the problem considered similarly attains its limit everywhere, so that

$$P(t) = 1 \quad (0 \leqslant t < T). \tag{8.31}$$

With these optimum control functions (8.29), (8.31), i.e., $V(t) = 1$, $P(t) = 1$, system (8.23) is integrated to yield

$$\left.\begin{aligned} &\ln(G_\pi + \gamma a_0) = (G_\pi^2 + \gamma a_0 G_\pi - G_\pi)(G_\pi + \gamma a_0 - \gamma a_0^2)^{-1}, \\ &E_1 = {}^1/_2 \ln^2(G_\pi + \gamma a_0) + \frac{1}{a_0}[1 - G_\pi - \gamma a_0 + \ln(G_\pi + \gamma a_0)]. \end{aligned}\right\} \tag{8.32}$$

These results are illustrated in Figures 8.2 to 8.4. Figure 8.2 shows a typical example of the maximum energy E_1 as a function of the initial acceleration a_0 for fixed values of G_π and γ (the formulation is the inverse of G_π = max for E_1, γ = const). When the engine weight is neglected ($\gamma = 0$) the maximum energy E_1 is attained with an engine exerting infinite thrust ($a_{0\,\mathrm{opt}} \to \infty$). When the engine weight is allowed for, however, even if its value is as low as $\gamma = 0.01 - 0.02$ (the values of γ are taken from Figure 2.11), the maximum is displaced into the region of finite initial accelerations ($a_{0\,\mathrm{opt}} = 2.5 - 4$), and its magnitude is reduced considerably. The dependence of the optimum value of the initial acceleration a_0 on the unit engine weight γ for different values of the payload G_π is shown in Figure 8.3. The values of G_π affect weakly the optimum value of a_0; all the curves $a_0(\gamma)$ for $0.1 \leqslant G_\pi \leqslant 0.5$ lie within a narrow band (the shaded region in Figure 8.3). Figure 8.4 represents the payload as a function of the energy E_1 for fixed values of the unit weight γ.

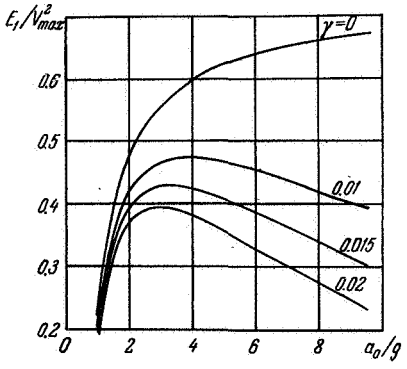

FIGURE 8.2. Maximum energy $E_1/V^2_{\max}$ as function of initial acceleration a_0/g for fixed values of unit engine weight γ; vertical climb of rocket (payload $G_\pi = 0.3$).

As a second example we consider the similar problem of the displacement between two points of rest at a distance l apart during time T. The solution of the dynamic part of the variational problem equivalent to (8.17) for this maneuver is described in § 2 of Chapter Six (cf. (6.43)). Recalling that $1 - \mu T_\mu = G_1$ and $\mu = a_0/V_{\max}$ we solve (6.43) for a_0/g:

$$\frac{a_0}{g} = \frac{(V_{\max}/gT)}{(l/TV_{\max}) + \ln\sqrt{G_1}}\,[(1 - \sqrt{G_1})^2 + (1 - G_1)\ln\sqrt{G_1}]. \tag{8.33}$$

This function $a_0(G_1)$ is the inverse function of $G_1(a_0)$, the dimensional expressions $(V_{\max}/gT)$ and $(l/TV_{\max})$ being the parameters of the problem.

Substituting (8.33) into (8.18), we obtain the payload G_π as a function of the terminal weight G_1, where

$$G_\pi = G_1 - \frac{(\gamma V_{\max}/gT)}{(l/TV_{\max}) + \ln \sqrt{G_1}} [(1 - \sqrt{G_1})^2 + (1 - G_1) \ln \sqrt{G_1}]. \qquad (8.34)$$

Here G_1 is the independent variable in terms of which the maximum of G_π is sought. The corresponding value of a_0 is determined by (8.33). The
327 results of this procedure are shown in Figures 8.5 and 8.6, and represent, respectively, the maximum payload G_π as a function of $(l/TV_{\max})$ for fixed values of $(\gamma V_{\max}/gT)$, and the optimum acceleration (a_0/g) as a function of $(l/TV_{\max})$ for $(V_{\max}/gT) = 0.5$ and $\gamma = 0.01,\ 0.02$.

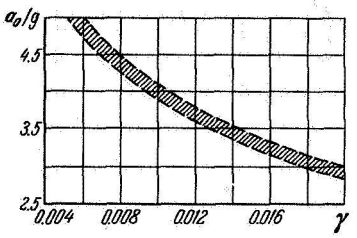

FIGURE 8.3. Region of optimum values of acceleration a_0/g for payload values in range $0.1 \leqslant G_\pi \leqslant 0.5$; vertical climb of rocket.

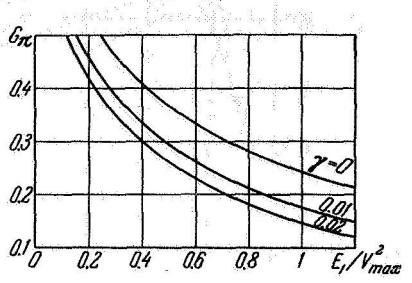

FIGURE 8.4. Influence of unit engine weight γ on maximum payload G_π (as function of terminal energy $E_1/V_{\max}^2$); vertical climb of rocket.

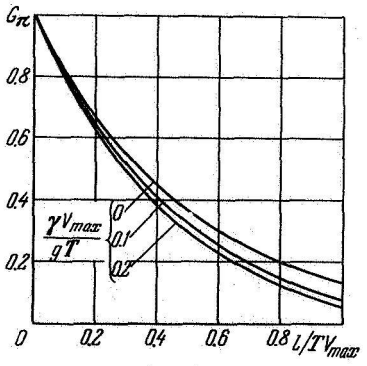

FIGURE 8.5. Payload G_π as function of parameter $(l/TV_{\max})$ for fixed values of $(\gamma V_{\max}/gT)$; displacement between points of rest.

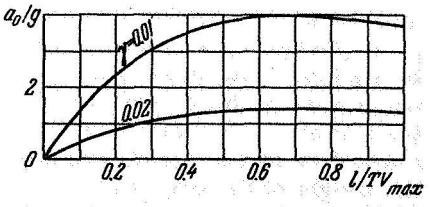

FIGURE 8.6. Optimum acceleration a_0/g as function of parameter $(l/TV_{\max})$ for $V_{\max}/gT = 0.5$ and two values of unit engine weight γ; displacement between points of rest.

The effects of the engine weight and drag will now be compared for the problem of the vertical climb of a rocket treated above. This comparison is performed for identical maneuver parameters. Figure 8.7 shows the terminal value of the energy E_1 as a function of the acceleration a_0 for a
328 payload $G_\pi = 0.5$. Curves a) represent motion in a vacuum allowing for the engine weight /8.45/, and curves b) represent motion in the atmosphere

with a weightless engine /8.49/. The quantity K_D is the dimensionless drag coefficient given by $K_D = c_x\rho_0 S\lambda g/2G_0$, ρ and λ are the parameters of the exponential law connecting the atmospheric density with the altitude, given by $\rho = \rho_0 \exp(-y/\lambda)$, and S is the midship area of the rocket.

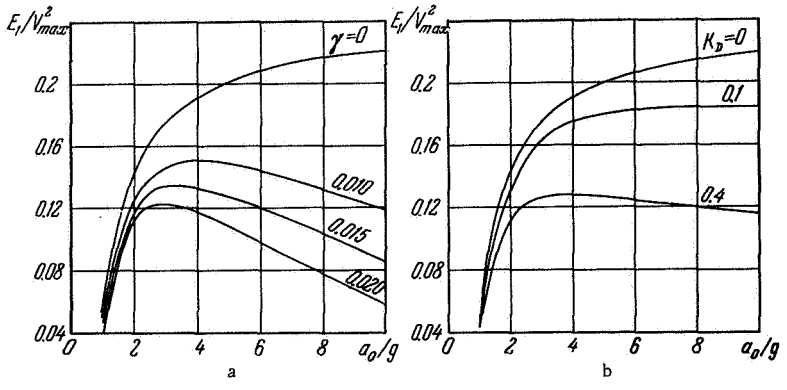

FIGURE 8.7. Influence of unit engine weight γ and drag coefficient K_D on terminal energy E_1/V^2_{max}; vertical climb of rocket ($G_\pi = 0.5$, a) $K_D = 0$, b) $\gamma = 0$).

Kur'yanov studied the variational problem of vertical climb with simultaneous allowance for the engine weight and aerodynamic drag.

§ 2. OPTIMUM CONDITIONS FOR COMBINING ENGINES OF LIMITED EXHAUST VELOCITIES AND LIMITED POWER.

The optimum conditions for combining unthrottled and ideal engines are derived in this section.

1. General conditions for optimum combination. Let the spacecraft be equipped with two engines, an engine with limited exhaust velocity 1, and a power-limited engine 2. We introduce the symbols P_1, P_2 to represent the thrusts, $\mathbf{e}_1$, $\mathbf{e}_2$ are the unit vectors of thrust orientation, q_1, q_2 are the mass flow rates, $G_{\mu 1}$, $G_{\mu 2}$ are the working-fluid weights, and $G_{\kappa 1}$, $G_{\kappa 2}$ represent the weight of the engines.

The operating regimes of engines 1 and 2 will be said to be in parallel if the engines can operate simultaneously, and in series if only one of the engines can operate at any given point of the trajectory.* To determine the optimum instant of switchover in the second case, we use the step function $\delta(t)$, which takes the value 1 over that part of the trajectory where engine 1 operates, and the value 0 over that part where engine 2 operates.

* The following cases are possible for a parallel regime (the plus sign corresponds to an operating engine, the minus sign to a cut-off engine): +1, −2; −1, +2; +1, +2; −1, −2. The series regime lacks the third possibility. The concept of a series regime was introduced to cover situations in which technical reasons prevent the simultaneous operation of both engines.

The total mass flow rate q and the resulting thrust vector $\mathbf{P}$ are as follows: for the parallel regime

$$q = q_1 + q_2, \quad \mathbf{P} = P_1\mathbf{e}_1 + P_2\mathbf{e}_2, \tag{8.35}$$

for the series regime

$$q = q_1\delta + q_2(1-\delta), \quad \mathbf{P} = P_1\mathbf{e}_1\delta + P_2\mathbf{e}_2(1-\delta). \tag{8.36}$$

329 A special symbol is introduced to represent the sum of the three weights:

$$G_\sigma = G_\pi + G_{\varkappa 1} + G_{\varkappa 2} \quad (G_\sigma(0) = G_0 - G_{\varkappa 1}(0) - G_{\varkappa 2}(0),\ G_\sigma(T) = G_\pi), \tag{8.37}$$

and we formulate the variational problem of delivering the maximum payload using two engines as follows:

in a parallel regime:

$$\left.\begin{array}{lll} \dot G_\sigma = -g(q_1+q_2), & G_\sigma(0) = G_0 - G_{\varkappa 1}(0) - G_{\varkappa 2}(0), & G_\sigma(T) = \max. \\ \dot{\mathbf{r}} = \mathbf{v}, & \mathbf{r}(0) = \mathbf{r}_0, & \mathbf{r}(T) = \mathbf{r}_1, \\ \dot{\mathbf{v}} = g\dfrac{P_1\mathbf{e}_1 + P_2\mathbf{e}_2}{G_\sigma + G_{\varkappa 1} + G_{\varkappa 2}} + \mathfrak{R}, & \mathbf{v}(0) = \mathbf{v}_0, & \mathbf{v}(T) = \mathbf{v}_1 \\ (0 \leqslant P_1(t),\ P_2(t),\ q_1(t),\ q_2(t) \leqslant \infty,\ \dot G_{\varkappa 1},\ \dot G_{\varkappa 2} \leqslant 0,\ |\mathbf{e}_1(t)| = |\mathbf{e}_2(t)| = 1). & & \end{array}\right\} \tag{8.38}$$

in a series regime:

$$\left.\begin{array}{lll} \dot G_\sigma = -g[q_1\delta + q_2(1-\delta)], & G_\sigma(0) = G_0 - G_{\varkappa 1}(0) - G_{\varkappa 2}(0), & G_\sigma(T) = \max, \\ \dot{\mathbf{r}} = \mathbf{v}, & \mathbf{r}(0) = \mathbf{r}_0, & \mathbf{r}(T) = \mathbf{r}_1, \\ \dot{\mathbf{v}} = g\dfrac{P_1\mathbf{e}_1\delta + P_2\mathbf{e}_2(1-\delta)}{G_\sigma + G_{\varkappa 1} + G_{\varkappa 2}} + \mathfrak{R}, & \mathbf{v}(0) = \mathbf{v}_0, & \mathbf{v}(T) = \mathbf{v}_1 \\ (0 \leqslant P_1(t),\ P_2(t),\ q_1(t),\ q_2(t) \leqslant \infty,\ \dot G_{\varkappa 1},\ \dot G_{\varkappa 2} \leqslant 0, \delta(t) = 1 \text{ or } 0, & & \\ |\mathbf{e}_1(t)| = |\mathbf{e}_2(t)| = 1). & & \end{array}\right\} \tag{8.39}$$

Note the following points:

1) In order to complete the variational formulations (8.38) and (8.39), we must express the thrusts P_1 and P_2, and the flow rates q_1 and q_2 as functions of the independent controls of the propulsion systems, and also determine the weight of the engines $G_{\varkappa 1}$, $G_{\varkappa 2}$ as functions of the limiting values of these controls (cf. the introduction to Part II).

2) The control functions $G_{\varkappa 1}(t)$, $G_{\varkappa 2}(t)$ can vary continuously along the trajectory, subject to the optimum requirements and limitations in (8.38) and (8.39). Alternatively, they can remain fixed during the motion (then $G_{\varkappa 1}$ and $G_{\varkappa 2}$ are the control parameters). If one of the engines is cut off before the end of the motion, it can either be left on the vehicle after it ceases to function or be discarded; in the latter case its weight component
330 is eliminated from the equations after it has been discarded (cf. the examples in /8.55/, and also the general optimum discarding conditions in /8.56/). It is assumed below that the weights $G_{\varkappa 1}$ and $G_{\varkappa 2}$ are fixed along the trajectory.

3) To determine the optimum control vectors $\mathbf{e}_1$ and $\mathbf{e}_2$ we write the Hamiltonians and the momentum differential equations in the forms:

for problem (8.38)

$$\left.\begin{aligned} &H = -p_\sigma g(q_1+q_2) + \mathbf{p}_v\cdot\left(g\,\frac{P_1\mathbf{e}_1+P_2\mathbf{e}_2}{G_\sigma+G_{\varkappa 1}+G_{\varkappa 2}}+\mathfrak{R}\right)+\mathbf{p}_r\cdot\mathbf{v},\\ &\dot p_\sigma = \mathbf{p}_v\cdot g\,\frac{P_1\mathbf{e}_1+P_2\mathbf{e}_2}{(G_\sigma+G_{\varkappa 1}+G_{\varkappa 2})^2},\quad \dot{\mathbf{p}}_v = -\mathbf{p}_r,\\ &\dot{\mathbf{p}}_r = -\frac{\partial}{\partial \mathbf{r}}(\mathbf{p}_v\cdot\mathfrak{R}),\quad p_\sigma(T) = -1, \end{aligned}\right\} \tag{8.40}$$

and for problem (8.39)

$$\left.\begin{aligned} &H = -p_\sigma g[q_1\delta + q_2(1-\delta)] + \mathbf{p}_v\cdot\left[g\,\frac{P_1\mathbf{e}_1\delta+P_2\mathbf{e}_2(1-\delta)}{G_\sigma+G_{\varkappa 1}+G_{\varkappa 2}}+\mathfrak{R}\right]+\\ &\qquad\qquad +\mathbf{p}_r\cdot\mathbf{v},\\ &\dot p_\sigma = \mathbf{p}_v\cdot g\,\frac{P_1\mathbf{e}_1\delta+P_2\mathbf{e}_2(1-\delta)}{(G_\sigma+G_{\varkappa 1}+G_{\varkappa 2})^2},\quad \dot{\mathbf{p}}_v = -\mathbf{p}_r,\\ &\dot{\mathbf{p}}_r = -\frac{\partial}{\partial \mathbf{r}}(\mathbf{p}_v\cdot\mathfrak{R}),\quad p_\sigma(T) = -1. \end{aligned}\right\} \tag{8.41}$$

The vector controls $\mathbf{e}_1(t)$ and $\mathbf{e}_2(t)$ minimize the functions H in (8.40) and (8.41) when

$$\mathbf{e}_1 = \mathbf{e}_2 = -\,\mathbf{p}_v/p_v \qquad (p_v = |\mathbf{p}_v|). \tag{8.42}$$

In problem (8.38), conditions (8.42) mean that the directions of the thrust vectors of engines 1 and 2 coincide in the parallel regime. In view of (8.42), it can be assumed that in problems (8.38) and (8.39),

$$\mathbf{e}_1 = \mathbf{e}_2 = \mathbf{e}. \tag{8.43}$$

2. Optimum conditions for combining unthrottled engines. We assume the following characteristics of the unthrottled engines with limited exhaust velocities and limited power:

$$\left.\begin{aligned} &P_1 = P_{10} \text{ or } 0,\quad q_1 = P_{10}/V_{10} \text{ or } 0,\quad G_{\varkappa 1} = \gamma_1 P_{10},\\ &P_2 = P_{20} \text{ or } 0,\quad q_2 = P_{20}^2/2N_{20} \text{ or } 0,\quad G_{\varkappa 2} = \alpha N_{20} + \gamma_2 P_{20}, \end{aligned}\right\} \tag{8.44}$$

where $\alpha N_{20} = G_{v2}$, $\gamma_2 P_{20} = G_{\gamma 2}$ are the weights of the power source and the
331 engine of 2; it is understood in what follows that $V_1 \equiv V_{10}$.

The variational problem of delivering a maximum payload employing engines with characteristics (8.44) is written as follows:

for the parallel regime (cf. (8.38))

$$\left.\begin{aligned} &\dot G_\sigma = -\,g\left(\frac{G_{\varkappa 1}\pi_1}{\gamma_1 V_1}+\frac{\alpha G_{\gamma 2}^2\pi_2}{2\gamma_2^2 G_{v2}}\right), && G_\sigma(0) = G_0 - G_{\varkappa 1} - G_{v2} - G_{\gamma 2}, && G_\sigma(T) = \max,\\ &\dot{\mathbf{r}} = \mathbf{v}, && \mathbf{r}(0) = \mathbf{r}_0, && \mathbf{r}(T) = \mathbf{r}_1,\\ &\dot{\mathbf{v}} = g\,\frac{G_{\varkappa 1}\pi_1/\gamma_1 + G_{\gamma 2}\pi_2/\gamma_2}{G_\sigma+G_{\varkappa 1}+G_{v2}+G_{\gamma 2}}\mathbf{e}+\mathfrak{R}, && \mathbf{v}(0) = \mathbf{v}_0, && \mathbf{v}(T) = \mathbf{v}_1\\ &(\pi_1(t),\ \pi_2(t) = 1 \text{ or } 0,\ |\mathbf{e}(t)| = 1,\ G_{\varkappa 1},\ G_{v2},\ G_{\gamma 2} = \text{const}); \end{aligned}\right\} \tag{8.45}$$

for the series regime (cf. (8.39))

$$\left.\begin{aligned}
&\dot G_\sigma = -g\left(\frac{G_{\varkappa 1}\pi_1\delta}{\gamma_1 V_1}+\frac{\alpha G_{\gamma 2}^2\pi_2(1-\delta)}{2\gamma_2^2 G_{v2}}\right), && G_\sigma(0)= && G_\sigma(T)=\max,\\
&&& = G_0 - G_{\varkappa 1} - && \\
&&& - G_{v2} - G_{\gamma 2}, && \\
&\dot{\mathbf r} = \mathbf v, && \mathbf r(0)=\mathbf r_0, && \mathbf r(T)=\mathbf r_1,\\
&\dot{\mathbf v} = g\frac{G_{\varkappa 1}\pi_1\delta/\gamma_1 + G_{\gamma 2}\pi_2(1-\delta)/\gamma_2}{G_\sigma + G_{\varkappa 1} + G_{v2} + G_{\gamma 2}}\,\mathbf e + \mathbf R, && \mathbf v(0)=\mathbf v_0, && \mathbf v(T)=\mathbf v_1\\
&(\pi_1(t),\ \pi_2(t),\ \delta(t)=1 \text{ or } 0,\ |\mathbf e(t)|=1,\ G_{\varkappa 1},\ G_{v2},\ G_{\gamma 2}=\text{const}). &&&&
\end{aligned}\right\} \qquad (8.46)$$

In equations (8.45) and (8.46) we have introduced the dimensionless thrust π_1 and π_2 where

$$\pi_1 = \gamma_1 P_1/G_{\varkappa 1},\quad \pi_2 = \gamma_2 P_2/G_{\gamma 2}. \qquad (8.47)$$

According to the definition of the unthrottled engines, $P_1 = 0$ or $P_1 = G_{\varkappa 1}/\gamma_1$, $P_2 = 0$ or $P_2 = G_{\gamma 2}/\gamma_2$; it follows that either $\pi_1 = \pi_2 = 0$ or $\pi_1 = \pi_2 = 1$. To solve the variational problem (8.45) the optimum control functions $\mathbf e(t)$, $\pi_1(t)$, $\pi_2(t)$, and the parameters $G_{\varkappa 1}$, G_{v2}, $G_{\gamma 2}$ must be determined; in problem (8.46) the control variable $\delta(t)$ is added to those listed.

We apply Pontryagin's method to problems (8.45) and (8.46); the necessary Hamiltonians and differential equations for the momentum have the form (8.40), (8.41), provided expressions (8.44) are introduced in place of the thrusts, flow rates, and engine weights. The optimum control functions
332 $\mathbf e(t)$, $\pi_1(t)$, $\pi_2(t)$, and $\delta(t)$ for the series regime are

$$\left.\begin{aligned}
&\mathbf e(t) = -\mathbf p_v/p_v && (p_v = |\mathbf p_v|),\\
&\pi_1(t) = \begin{cases} 1 & \text{at } \Delta_1<0\\ 0 & \text{at } \Delta_1>0\end{cases} && \left(\Delta_1 = -g\frac{G_{\varkappa 1}}{\gamma_1}\left[\frac{p_\sigma}{V_1}+\frac{p_v}{G}\right]\right),\\
&\pi_2(t) = \begin{cases} 1 & \text{at } \Delta_2<0\\ 0 & \text{at } \Delta_2>0\end{cases} && \left(\Delta_2 = -g\frac{G_{\gamma 2}}{\gamma_2}\left[\frac{\alpha p_\sigma G_{\gamma 2}}{2\gamma_2 G_{v2}}+\frac{p_v}{G}\right]\right),\\
&\delta(t) = \begin{cases} 1 & \text{at } D<0\\ 0 & \text{at } D>0\end{cases} && (D = \Delta_1\pi_1 - \Delta_2\pi_2).
\end{aligned}\right\} \qquad (8.48)$$

Note that the expression $2\gamma_2 G_{v2}/\alpha G_{\gamma 2}$ in (8.48) represents the exhaust velocity V_2 of engine 2. In accordance with the optimum conditions (8.48), for $V_2 > V_1$ in the parallel regime the operating interval of engine 2 overlaps that of engine 1. In fact, for $\Delta_1 < 0$ we must have $\Delta_2 < 0$, and for $\Delta_2 > 0$ we must have $\Delta_1 > 0$.

This means that if engine 1 is operating, engine 2 must also be operating, and if engine 2 is cut off, engine 1 must also be cut off. Thus, in the parallel regime, the engine whose exhaust velocity is higher operates for a longer time.

As an illustration, we shall solve problem (8.46) (unthrottled engines connected in series) for the maneuver of velocity build-up in a gravity-free field. The equations of the variational problem, the boundary conditions, the Hamiltonian, and the momentum differential equations have the form (cf. (8.46), (8.41))

$$\left.\begin{aligned}
&\dot G_\sigma = -g\left(\frac{G_{\varkappa 1}\pi_1\delta}{\gamma_1 V_1}+\frac{\alpha G_{\gamma 2}^2\pi_2(1-\delta)}{2\gamma_2^2 G_{v2}}\right),\\
&G_\sigma(0) = G_0 - G_{\varkappa 1} - G_{v2} - G_{\gamma 2},\quad \dot p_\sigma = p_u e g\frac{G_{\varkappa 1}\pi_1\delta/\gamma_1 + G_{\gamma 2}\pi_2(1-\delta)/\gamma_2}{(G_\sigma + G_{\varkappa 1} + G_{v2} + G_{\gamma 2})^2},\\
&p_\sigma(T) = -1,
\end{aligned}\right\} \qquad (8.49)$$

$$\dot{u} = g\frac{G_{\varkappa 1}\pi_1\delta/\gamma_1 + G_{\gamma 2}\pi_2(1-\delta)/\gamma_2}{G_\sigma + G_{\varkappa 1} + G_{\nu 2} + G_{\gamma 2}}e,\ u(0) = 0,\ u(T) = u_1,\ \dot{p}_u = 0,$$
$$H = -p_u g\left(\frac{G_{\varkappa 1}\pi_1\delta_1}{\gamma_1 V_1} + \frac{\alpha G_{\gamma 2}^2\pi_2(1-\delta)}{2\gamma_2^2 G_{\nu 2}}\right) + p_u g\frac{G_{\varkappa 1}\pi_1\delta/\gamma_1 + G_{\gamma 2}\pi_2(1-\delta)/\gamma_2}{G_\sigma + G_{\varkappa 1} + G_{\nu 2} + G_{\gamma 2}}. \quad (8.49)$$

333 The optimum laws $e(t) = \pm 1$, $\delta(t)$, $\pi_1(t)$, $\pi_2(t) = 1$ or 0 are expressed by (8.48). The case considered yields the following results: $e(t) \equiv +1$ for $0 \leqslant t \leqslant T$; on the trajectory there exists a single switchover point of the step function $\delta(t)$; if $V_2 > V_1$, then $\delta(0) = 1$; for $\delta = 1$ the control function π_1 equals 1 and for $\delta = 0$, π_2 equals 1.

The fact that the function $e(t)$ does not alter its sign follows from the condition $p_u = \text{const}$ (cf. (8.49)); obviously, for $u_1 > 0$ we must have $e(t) \equiv +1$ and $p_u < 0$ (cf. (8.48)).

The last fact ($\pi_1 = 1$ for $\delta = 1$, and $\pi_2 = 1$ for $\delta = 0$) follows by examining the Hamiltonian (it remains constant along the trajectory). Write H in the following form (for the meaning of the symbols cf. (8.48)):

$$H = (\Delta_1\pi_1 - \Delta_2\pi_2)\delta + \Delta_2\pi_2 = c = \text{const}. \quad (8.50)$$

If $\delta = 1$, then $\Delta_1\pi_1 = c$, and if $\delta = 0$, then $\Delta_2\pi_2 = c$, where the constant c is negative. For $c = 0$, we would have had the following: $\pi_1 = 0$ for $\delta = 1$, and $\pi_2 = 0$ for $\delta = 0$, i.e., the two engines would have been cut off along the whole trajectory. The case $c > 0$ is excluded, since $\Delta_1\pi_1 \leqslant 0$ and $\Delta_2\pi_2 \leqslant 0$. It follows that for $\delta = 1$ the control function $\pi_1 = 1$, and for $\delta = 0$, $\pi_2 = 1$. Since π_1 and π_2 and the control function δ enter into all the equations in the combinations $\pi_1\delta$, $\pi_2(1-\delta)$, we could have put $\pi_1(t) \equiv 1$, $\pi_2(t) \equiv 1$.

The optimum formula for the step control function $\delta(t)$ is given in (8.48). The derivative of the function $D(t)$ given there too is

$$\dot{D}(t) = \frac{p_u g^2 G_{\varkappa 1} G_{\gamma 2}}{\gamma_1\gamma_2 G^2 V_1}\left(\frac{V_1}{V_2} - 1\right); \quad (8.51)$$

for $V_1 < V_2$ the derivative $\dot{D}(t) > 0$ (since $p_u < 0$), and the function $D(t)$ can change its sign from negative to positive. Therefore, if the trajectory has a section over which $\delta(t) = 1$, it is located at the beginning, $\delta(0) = 1$.

This analysis proves the assertions made above about the optimum formulas for $e(t)$, $\delta(t)$, $\pi_1(t)$, $\pi_2(t)$.

Introduce the symbol t_* to represent the instant of switchover of the function $\delta(t)$, and integrate the equations of motion and flow rate along the two intervals

$$\delta = 1 \text{ at } 0 \leqslant t < t_*,\ \delta = 0 \text{ at } t_* < t \leqslant T. \quad (8.52)$$

As a result we obtain expressions for the payload G_π and the velocity u_1
334 in terms of control parameters ($t_*, G_{\varkappa 1}, G_{\nu 2}, G_{\gamma 2}$), the structural parameters ($V_1, \gamma_1, \gamma_2, \alpha$) and the time T in the forms

$$G_\pi = G_0 - G_{\varkappa 1} - G_{\nu 2} - G_{\gamma 2} - gt_* G_{\varkappa 1}/V_1\gamma_1 - g\alpha(T - t_*)G_{\gamma 2}^2/2\gamma_2^2 G_{\nu 2},$$
$$u_1 = -V_1\ln\left(1 - \frac{gt_* G_{\varkappa 1}}{\gamma_1 V_1 G_0}\right) - \frac{2\gamma_2 G_{\nu 2}}{\alpha G_{\gamma 2}}\left[\ln\left(1 - \frac{gt_* G_{\varkappa 1}}{\gamma_1 V_1 G_0} - \frac{g\alpha(T-t_*)G_{\gamma 2}^2}{2\gamma_2^2 G_{\nu 2} G_0}\right) - \ln\left(1 - \frac{gt_* G_{\varkappa 1}}{\gamma_1 V_1 G_0}\right)\right]. \quad (8.53)$$

Given the values of the structural parameters $V_1, \alpha, \gamma_1, \gamma_2$, and of the velocity u_1, we determine the optimum values t_*, $G_{\times 1}$, $G_{\gamma 2}$, G_{v2}, and the maximum payload as functions of the maneuvering time T. Figure 8.8 shows the function $G_\pi(T)$, where the symbol 1 indicates the curve corresponding to the maneuver performed by engine 1 alone ($t_* = T$), the symbol 2 corresponds to that of engine 2 alone, and the symbol 1+2 to that of both engines simultaneously. Figures 8.9 and 8.10 show the optimum control parameters of engine 2, V_2/V_1, G_{v2}/G_0, as functions of T. The values of the structural parameters and the velocity u_1 assumed in the calculations are

$$V_1 = 4\cdot 10^3 \text{ m/sec}, \quad \gamma_1 = 0.02 \text{ kg/kg}, \quad \gamma_2 = 10^3 \text{ kg/kg},$$
$$\alpha = 10 \text{ kg/kw}, \quad u_1 = 11.2\cdot 10^3 \text{ m/sec}. \qquad (8.54)$$

We note that the optimum value of the exhaust velocity V_2 for large values of the time T exceeds $2V_1$, while for small values it is smaller than $2V_1$.

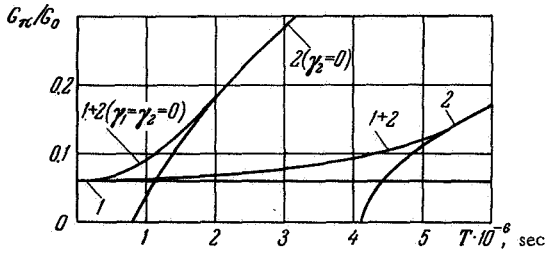

FIGURE 8.8. Relative payload G_π/G_0 as function of build-up time T of given velocity magnitude. The symbol 1 represents maneuver performed by single engine of limited exhaust velocity, symbol 2 is maneuver performed by single power-limited unthrottled engine, 1+2 is maneuver performed simultaneously by two unthrottled engines; 2 ($\gamma_2 = 0$) is maneuver performed by a single ideal power-limited engine, 1+2 ($\gamma_1 = \gamma_2 = 0$) is maneuver performed by two ideal engines simultaneously ($V_1 =$ 4000 m/sec, $\gamma_1 = 0.02$, $\gamma_2 = 1000$, $\alpha = 10$ kg/kw, $u_1 =$ = 1120 m/sec).

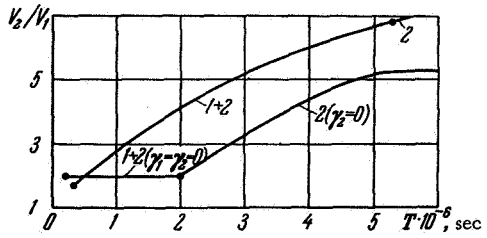

FIGURE 8.9. Optimum relative exhaust velocity V_2/V_1 as function of maneuvering time T (symbols and parameter values as in Figure 8.8).

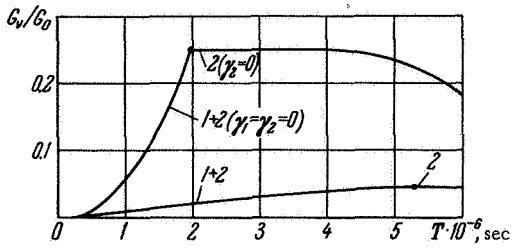

FIGURE 8.10. Optimum relative weight of power source G_v/G_0 as function of maneuvering time (symbols and parameter values as in Figure 8.8).

3. Optimum conditions for combining ideal engines. It is convenient to formulate the variational problem for the optimum combination of ideal engines with limited exhaust velocity 1 and limited power 2 in terms of the thrust accelerations

$$a_1 = gP_1/G, \quad a_2 = gP_2/G \qquad (a_1, a_2 \geqslant 0). \tag{8.55}$$

The flow-rate equations, written in terms of the accelerations a_1 and a_2, have the following form:

for the parallel regime (system (8.38))

$$\dot{G}_\sigma = -\frac{a_1 G}{V_1} - \frac{\alpha}{2g}\frac{a_2^2 G^2}{NG_v}, \tag{8.56}$$

and for the series regime (system (8.39))

$$\dot{G}_\sigma = -\frac{a_1 G}{V_1}\delta - \frac{\alpha}{2g}\frac{a_2^2 G^2}{NG_v}(1-\delta). \tag{8.57}$$

336 In equations (8.56) and (8.57) the quantity N represents the dimensionless power ($0 \leqslant N(t) \leqslant 1$); the weight G consists of four components, namely, the payload G_π, the working-fluid weights $G_{\mu 1}$, $G_{\mu 2}$ ($G_\pi + G_{\mu 1} + G_{\mu 2} = G_\sigma$), and the weight of the power-limited engine G_v. Thus, $G = G_\sigma + G_v$ where the weight of the engine G_v is considered as proportional to the maximum power, i.e., $G_v = \alpha N_{\max}$ (cf. Chapter Four).

Introduce the following symbols (cf. (8.13), (4.10)):

for (8.56)

$$K(t) = \exp\left(-\tfrac{1}{2}\int_0^t \frac{a_1}{V_1}dt\right), \qquad L(t) = -\left[\frac{\alpha}{2g}\int_0^t \frac{a_2^2}{N}\exp\left(-\int_0^t \frac{a_1}{V_1}dt\right)dt\right]^{1/2}, \tag{8.58}$$

and for (8.57)

$$K(t) = \exp\left(-\frac{1}{2}\int_0^t \frac{a_1\delta}{V_1}dt\right), L(t) = -\left[\frac{\alpha}{2g}\int_0^t \frac{a_2^2(1-\delta)}{N}\exp\left(-\int_0^t \frac{a_1\delta}{V_1}dt\right)dt\right]^{1/2}. \tag{8.59}$$

Using these symbols, we can write the solutions of equations (8.56) and (8.57) in the common form:

$$G(t) = G_\sigma(t) + G_v = G_0 K^2(t)/(1 + G_0 L^2(t)/G_v). \tag{8.60}$$

The value of the relative payload G_π/G_0 is expressed as follows in terms of $K_1 = K(T)$, $L_1 = L(T)$:

$$G_\pi/G_0 = K_1^2/(1 + L_1^2 G_0/G_\nu) - G_\nu/G_0. \tag{8.61}$$

The maximum of the relative payload G_π/G_0 for the control parameter G_ν/G_0 can be determined without solving the dynamic part of the variational problem (as in the case of a single ideal power-limited engine). The payload has a maximum if (cf. (4.15))

$$G_\nu/G_0 = -K_1 L_1 - L_1^2; \tag{8.62}$$

then (cf. (4.16), (8.13))

$$G_\pi/G_0 = (K_1 + L_1)^2. \tag{8.63}$$

Using (4.16), (8.13) and (8.63) one can represent these regions in which ideal engines are preferred in the functional space Φ, Ψ, $K + L$ (Figure 8.11).

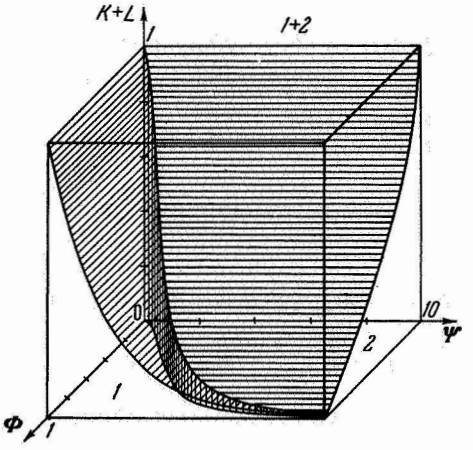

FIGURE 8.11. Surface dividing regions using ideal engines with limited exhaust velocity (1), limited power (2), and combination of engines (1+2) in functional space Ψ, Φ, $K + L$ of dynamic problems (Ψ for engine 1, Φ for engine 2, $K+L$ for combination of engines 1+2).

337 The variational problem of delivering the maximum payload has been reduced to the Lagrange problem with the following additional differential constraints:

for the parallel regime

$$\left.\begin{aligned} &\max(K_1 + L_1) = \\ &\quad = \max\left\{\exp\left(-\frac{1}{2}\int_0^T \frac{a_1}{V_1}\,dt\right) - \left[\frac{\alpha}{2g}\int_0^T \frac{a_2^2}{N}\exp\left(-\int_0^t \frac{a_1}{V_1}\,dt\right)dt\right]^{1/n}\right\}, \\ &\dot{\mathbf{r}} = \mathbf{v}, \qquad \mathbf{r}(0) = \mathbf{r}_0, \quad \mathbf{r}(T) = \mathbf{r}_1, \\ &\dot{\mathbf{v}} = (a_1 + a_2)\mathbf{e} + \mathfrak{R}, \quad \mathbf{v}(0) = \mathbf{v}_0, \quad \mathbf{v}(T) = \mathbf{v}_1; \end{aligned}\right\} \tag{8.64}$$

for the series regime

$$\left.\begin{aligned} &\max(K_1+L_1)= \\ &=\max\left\{\exp\left(-\frac{1}{2}\int_0^T\frac{a_1\delta}{V_1}dt\right)-\left[\frac{\alpha}{2g}\int_0^T\frac{a_2^2(1-\delta)}{N}\exp\left(-\int_0^t\frac{a_1\delta}{V_1}dt\right)dt\right]^{1/2}\right\}, \\ &\dot{\mathbf{r}}=\mathbf{v}, \qquad \mathbf{r}(0)=\mathbf{r}_0, \quad \mathbf{r}(T)=\mathbf{r}_1, \\ &\dot{\mathbf{v}}=[a_1\delta+a_2(1-\delta)]\,\mathbf{e}+\mathfrak{R}, \quad \mathbf{v}(0)=\mathbf{v}_0, \quad \mathbf{v}(T)=\mathbf{v}_1. \end{aligned}\right\} \tag{8.65}$$

338 Systems (8.64) and (8.65) can be expressed as Mayer's problem: system (8.64) becomes

$$\left.\begin{aligned} &\dot{K}=-{}^1/_2Ka_1/V_1, \qquad K(0)=1, \quad K(T)+ \\ &\dot{L}=(\alpha/4g)K^2a_2^2/LN, \quad L(0)=0, \quad +L(T)=\max, \\ &\dot{\mathbf{r}}=\mathbf{v}, \qquad \mathbf{r}(0)=\mathbf{r}_0, \qquad \mathbf{r}(T)=\mathbf{r}_1, \\ &\dot{\mathbf{v}}=(a_1+a_2)\,\mathbf{e}+\mathfrak{R}, \quad \mathbf{v}(0)=\mathbf{v}_0, \qquad \mathbf{v}(T)=\mathbf{v}_1 \\ &(a_1(t), \quad a_2(t)\geqslant 0, \quad 0\leqslant V_1(t)\leqslant V_{10}, \quad 0\leqslant N(t)\leqslant 1, \quad |\mathbf{e}(t)|=1); \end{aligned}\right\} \tag{8.66}$$

system (8.65) becomes

$$\left.\begin{aligned} &\dot{K}=-{}^1/_2Ka_1\delta/V_1, \qquad K(0)=1, \quad K(T)+ \\ &\dot{L}=(\alpha/4g)K^2a_2^2(1-\delta)/LN, \quad L(0)=0, \quad +L(T)=\max, \\ &\dot{\mathbf{r}}=\mathbf{v}, \qquad \mathbf{r}(0)=\mathbf{r}_0, \quad \mathbf{r}(T)=\mathbf{r}_1, \\ &\dot{\mathbf{v}}=[a_1\delta+a_2(1-\delta)]\,\mathbf{e}+\mathfrak{R}, \quad \mathbf{v}(0)=\mathbf{v}_0, \quad \mathbf{v}(T)=\mathbf{v}_1 \\ &(a_1(t), \ a_2(t)\geqslant 0, \ \delta(t)=1 \text{ or } 0, \ 0\leqslant V_1(t)\leqslant V_{10}, \ 0\leqslant N(t)\leqslant 1, \\ &\qquad\qquad |\mathbf{e}(t)|=1). \end{aligned}\right\} \tag{8.67}$$

The Hamiltonians and the momentum differential equations take the form: for problem (8.66)

$$\left.\begin{aligned} &H=-p_k\frac{Ka_1}{2V_1}+p_l\frac{\alpha}{4g}\frac{K^2a_2^2}{LN}+\mathbf{p}_r\cdot\mathbf{v}+\mathbf{p}_v\cdot[(a_1+a_2)\,\mathbf{e}+\mathfrak{R}], \\ &\dot{p}_k=p_k\frac{a_1}{2V_1}-p_l\frac{\alpha}{2g}\frac{Ka_2^2}{LN}, \quad \dot{p}_l=p_l\frac{\alpha}{4g}\frac{K^2a_2^2}{L^2N}, \\ &\dot{\mathbf{p}}_r=-\frac{\partial}{\partial\mathbf{r}}(\mathbf{p}_v\cdot\mathfrak{R}), \quad \dot{\mathbf{p}}_v=-\mathbf{p}_r, \quad p_k(T)=p_l(T)=-1; \end{aligned}\right\} \tag{8.68}$$

for problem (8.67)

$$\left.\begin{aligned} &H=-p_k\frac{Ka_1\delta}{2V_1}+p_l\frac{\alpha}{4g}\frac{K^2a_2^2(1-\delta)}{LN}+ \\ &\qquad +\mathbf{p}_r\cdot\mathbf{v}+\mathbf{p}_v\cdot\{[a_1\delta+a_2(1-\delta)]\,\mathbf{e}+\mathfrak{R}\}, \\ &\dot{p}_k=p_k\frac{a_1\delta}{2V_1}-p_l\frac{\alpha}{2g}\frac{Ka_2^2(1-\delta)}{LN}, \quad \dot{p}_l=p_l\frac{\alpha}{4g}\frac{K^2a_2^2(1-\delta)}{L^2N}, \\ &\dot{\mathbf{p}}_r=-\frac{\partial}{\partial\mathbf{r}}(\mathbf{p}_v\cdot\mathfrak{R}), \quad \dot{\mathbf{p}}_v=-\mathbf{p}_r, \quad p_k(T)=p_l(T)=-1. \end{aligned}\right\} \tag{8.69}$$

339 The differential equations for p_k and p_l, from systems (8.68) and (8.69), are integrated in closed form and the same expressions obtained in both cases, namely,

$$p_k=(L^2-K_1L_1-L_1^2)/KL_1, \quad p_l=-L/L_1. \tag{8.70}$$

The optimum formulas $\mathbf{e}(t)$, $a_2(t)$, $N(t)$, $V_1(t)$ for problems (8.66) and (8.67) are

$$\left.\begin{aligned} &\mathbf{e}(t)=-\mathbf{p}_v/p_v, \quad a_2(t)=-2gp_v\,L_1/\alpha K^2, \\ &N(t)=1, V_1(t)=V_{10}. \end{aligned}\right\} \tag{8.71}$$

The control function $a_1(t)$ enters linearly into the equations of the variational problems and the Hamiltonians; therefore the optimum function $a_1(t)$ consists, in general, of three parts, i.e., two limiting parts ($a_1 = 0$, $a_1 = a_{1\max} = \infty$), and the singular part ($a_1 = a_{1\text{opt}}$) (cf. (8.9), (8.10)).

Engine 1 is cut off ($a_1 = 0$) for (the subscript 0 of V_1 is omitted in what follows)

$$\Delta_1 = -p_k K/2V_1 - p_v > 0, \tag{8.72}$$

or (cf. (8.70))

$$\Delta_1 = (L_1^2 + K_1 L_1 - L^2)/2V_1 L_1 - p_v > 0. \tag{8.73}$$

With the expression for the exhaust velocity of a power-limited engine,

$$V_2(t) = 2gG_v/\alpha G a_2 = (L_1 K_1 + L_1^2 - L^2)/L_1 p_v \tag{8.74}$$

(obtained using (8.60), (8.62), (8.71)), we may express Δ_1 in the form

$$\Delta_1 = p_v (V_2/2V_1 - 1). \tag{8.75}$$

If the inequality

$$V_2(t) < 2V_1 \tag{8.76}$$

is satisfied along the whole trajectory, engine 1 will not operate at all and will therefore be superfluous when performing the given maneuver; this result was obtained in /8.56/. Condition (8.76) was obtained under the assumption that the weight of the power source G_v is optimum according to (8.62). This condition is, however, also true for a nonoptimum arbitrary weight G_v (from /8.56/).

The optimum form of the step function $\delta(t)$ figuring in problem (8.67) has the form

$$\delta = 0 \text{ at } D > 0, \delta = 1 \text{ at } D < 0 (D = \Delta_1 a_1 - g p_v^2 L_1/\alpha K^2). \tag{8.77}$$

340 If $a_1 = 0$, then $\delta = 0$. In fact, for vanishing a_1 the second term remaining in the expression for D is always positive; therefore for a series regime engine 1 will not be fired if inequality (8.76) is satisfied everywhere.

If $a_{1\max} = \infty$ (as in our example), conditions (8.76) and (8.77) coincide, and there is no difference between the parallel and series regions.

Inequality (8.76) helps to determine the boundary separating the region in which the single engine 2 is used from that region in which both engines are used, in the (α, V_1) plane of the ideal-engine parameters 1 and 2 for the given dynamic maneuver. For this, it is sufficient to know the solution of the variational problem of performing the given maneuver with the single engine 2. Examples of determining this boundary are given in the next section.

In conclusion we discuss the optimum combination of the ideal engines 1 and 2 to build up a specified velocity magnitude in a gravity-free field.

The equations of the variational problem, the boundary conditions, the Hamiltonian, and the expressions for the momenta have the form (cf. (8.66), (8.68), (8.70), (8.71))

$$\left.\begin{aligned} &\dot{K} = -Ka_1/2V_1, \qquad K(0)=1, \quad p_k(T)=-1, \\ &\qquad\qquad\qquad\qquad \dot{p}_k = (L^2 - K_1L_1 - L_1^2)/KL_1, \\ &\dot{L} = (\alpha/4g)K^2a_2^2/L, \quad L(0)=0, \quad p_l(T)=-1, \\ &\qquad\qquad\qquad\qquad \dot{p}_l = -L/L_1, \\ &\dot{u} = (a_1+a_2)e, \qquad u(0)=0, \quad u(T)=u_1, \\ &\qquad\qquad\qquad\qquad p_u = \text{const} < 0, \\ &H = -p_kKa_1/2V_1 + p_l(\alpha/4g)K^2a_2^2/L + p_u(a_1+a_2)e. \end{aligned}\right\} \tag{8.78}$$

The optimum control functions $e(t)$, $a_1(t)$, $a_2(t)$ must satisfy

$$e(t) = 1;\ a_1(0) = \infty,\ a_1(t) = 0\ (0 < t \leqslant T);\ a_2(t) = \text{const}. \tag{8.79}$$

We shall now discuss the optimum variables $a_1(t)$ and $a_2(t)$. The optimum expression for $e(t)$ coincides with that obtained in subsection 2 above. The expression Δ_1 (cf. (8.73)) can be positive everywhere throughout the interval $0 \leqslant t \leqslant T$, or, in the extreme case it can vanish at isolated points of the interval. When $p_u = \text{const}$ the derivative $\Delta \geqslant 0$, and therefore $t = 0$ is the only point at which $\Delta_1 = 0$ and condition (8.73) (cutoff of engine 1) is not fulfilled. Furthermore, since $K(T) = \text{const}$ for $0 < t \leqslant T$, we obtain $a_2 = \text{const}$ from (8.71).

341 The differential equations (8.78) are integrated, and yield

$$K_1 = \exp(-\Delta u/2V_1), \quad L_1 = -K_1\sqrt{(\alpha/2g)a_2^2T}, \quad u_1 = \Delta u + a_2T$$
$$\left(\Delta u = \lim_{\tau\to 0}\int_0^{\tau} a_1(t)\,dt,\ a_1 \to \infty \ \text{ at } \ t \to 0\right). \tag{8.80}$$

If a_2 is eliminated from the second and third equations of (8.80), we obtain the following expression for the control functional:

$$K_1 + L_1 = \exp(-\Delta u/2V_1)\left[1 - \sqrt{(\alpha/2g)(u_1-\Delta u)^2/T}\right]. \tag{8.81}$$

The quantity Δu represents the velocity increment produced by the acceleration a_1 $(0 \leqslant \Delta u \leqslant u_1)$. The value of Δu maximizing (8.81) is

$$\left.\begin{aligned} &\Delta u = u_1 + 2V_1 - \sqrt{2gT/\alpha} && \text{at} && -u_1 \leqslant 2V_1 - \sqrt{2gT/\alpha} \leqslant 0, \\ &\Delta u = 0 && \text{at} && 2V_1 - \sqrt{2gT/\alpha} \leqslant -u_1, \\ &\Delta u = u_1 && \text{at} && 2V_1 - \sqrt{2gT/\alpha} \geqslant 0. \end{aligned}\right\} \tag{8.82}$$

The first formula of (8.82) corresponds to the simultaneous use of both engines (1+2), the second one to using engine 2 alone, and the last represents using engine 1 alone.

Figure 8.8 shows curves of the relative payload G_π/G_0 corresponding to the three cases (8.82). The following values were taken for the parameters (cf. (8.54)):

$$V_1 = 4\cdot 10^3\ \text{m/sec}, \quad \alpha = 10\ \text{kg/kw}, \quad u_1 = 11.2\cdot 10^3\ \text{m/sec}. \tag{8.83}$$

These curves (unlike the corresponding curves for the unthrottled engines) are designated by the index $\gamma_1 = \gamma_2 = 0$.

The minimum exhaust velocity of engine 2 along the trajectory and the minimum weight of the power source were plotted in Figures 8.9, 8.10 as a function of the maneuvering time (curves $\gamma_1 = \gamma_2 = 0$). In view of (8.74), the minimum exhaust velocity V_2 is attained in this case at the initial point of the trajectory. During the interval of time T in which the two engines operate simultaneously the initial exhaust velocity is independent of the maneuvering time, $V_2(0) = 2V_1$, as follows from the condition of firing engine 1.

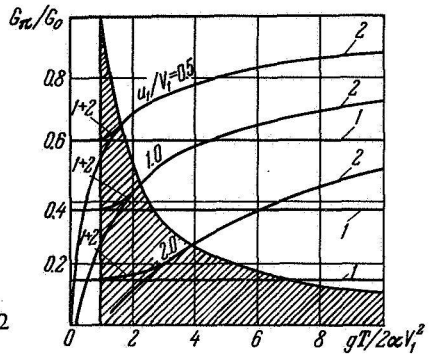

FIGURE 8.12. Relative payload G_π/G_0 as function of combinations of engines and maneuver parameters ($gT/2\alpha V_1^2$) and u_1/V_1 (for build-up of specified velocity magnitude in gravity-free field; ideal engines: curve 1 is for engine of limited exhaust velocity, curve 2 for engine of limited power, curve 1+2 for combination of engines 1 and 2; shading represents region of simultaneous use of both engines).

The results of this analysis for the problem of building up a specified velocity magnitude can also be represented in the following form /8.55/. It follows from (8.63), (8.81) and (8.82) that the relative payload G_π/G_0 is a function of two combinations of parameters, (u_1/V_1) and $(gT/2\alpha V_1^2)$. This functional relationship is shown in Figure 8.12. Curves 1 correspond to a single engine with limited exhaust velocity, curves 2 to a single power-limited engine, curves 1+2 to the combination of the two engines; the region in which both engines are simultaneously used has been shaded.

342

The following additional maneuvers are treated in /8.55/: displacement between two positions of rest in a gravity-free field, and build-up of parabolic and hyperbolic velocities in a central field. The analysis is based on a direct comparison between the payloads achieved by combining sections of motion in different ways using engines of the first and second types. Some results concerning the combination of engines with limited exhaust velocity and limited power are found in /8.57/.

The following conclusions can be drawn by analyzing the results obtained. Power-limited engines are most efficient for those maneuvers in which slow thrust accelerations are required. When the acceleration is increased (which corresponds, for instance, to a reduction in the time of motion) the payload delivered decreases (cf. Figure 8.8), tending to zero at the limit. Throughout this interval of time, an additional engine with limited exhaust velocity increases the payload. The part played by this engine increases with decreasing maneuvering time until a limit is attained. Below this limit, the power-limited engine becomes superfluous, and the maneuver is performed by the engine with limited exhaust velocity alone. When the two engines are used simultaneously, the greatest gain is obtained for those maneuvers in which the payloads delivered individually by each engine are close to one another.

This reasoning applies equally to ideal and unthrottled engines.

343 § 3. REGIONS OF APPLICATION OF POWER-LIMITED ENGINES

Assume that the variational problem corresponding to a single ideal power-limited engine has been solved for a given dynamic maneuver (Chapters Four and Five); this means that the optimum thrust acceleration $a_2(t)$ and the function $J(t)$ have been determined. The variation of the exhaust velocity $V_2(t)$ along the trajectory is calculated by the following formulas (cf. (5.102)):

$$V_2(t) = 2gN_0/G(t)\,a(t), \quad G(t) = G_0(1 + G_0 J(t)/2gN_0)^{-1}. \tag{8.84}$$

The parameter G_0/N_0 in (8.84) can either be specified beforehand,

$$G_0/N_0 = \varkappa, \tag{8.85}$$

or determined to be a minimum if the structural parameter α is specified:

$$G_0/N_0 = \alpha[\sqrt{(\alpha/2g)J(T)} - (\alpha/2g)J(T)]^{-1}. \tag{8.86}$$

Either the expression (cf. (8.76)

$$V_1 = \tfrac{1}{2}\min_t V_2(t, \varkappa) \tag{8.87}$$

or

$$V_1 = \tfrac{1}{2}\min_t V_2(t, \alpha) \tag{8.88}$$

for the minimum value of V_2 on the trajectory, determines the exhaust velocity of engine 1 below which it is advantageous to use engine 2 alone for performing a given maneuver. In this way we may calculate those curves in the (α, V_1) or $(\varkappa, V_1)$ planes which separate the region where engine 2 is applied from the region where engines 1+2 are applied. These indicate the ultimate possibilities of a single power-limited engine. The boundary between regions 1+2 and 1 is no less interesting as it determines the optimum use of the single engine with limited exhaust velocity. The absence in this second case of as simple a criterion as inequality (8.76) makes it impossible to find this boundary without completely solving the variational problem of engine combinations.

In the present section these boundaries are calculated for an ideal power-limited engine by (8.87) and (8.88) for three maneuvers: build-up of a parabolic velocity from a circular orbit, transfer between two circular orbits, and interplanetary flight. The optimum function $a_2(t)$ and functional $J(t)$, which are required for the calculations, are taken from Chapter Five.

344 **1. Build-up of parabolic velocity.** The spacecraft is trajected into a circular orbit and must then develop a parabolic velocity with the aid of two engines.

The traditional scheme of performing this maneuver assumes the use of a single power-limited engine. The optimum program of the thrust acceleration vector for the ideal engine is as follows (cf. Chapter Five):

its magnitude is almost constant, while its direction lies between the transversal and tangent to the trajectory; these almost coincide throughout the entire time of motion.

345 Since the thrust-acceleration magnitude is almost constant, the velocity V_2 has a minimum at the initial point of the trajectory. It follows that condition (8.76) can be violated at $t = 0$, and an additional engine with limited exhaust velocity can be fired at the beginning of the trajectory.

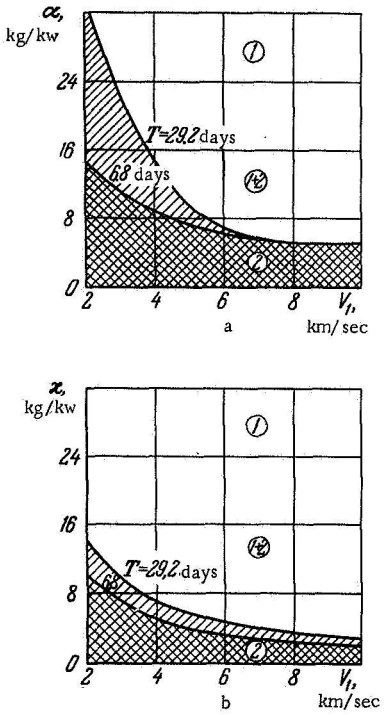

FIGURE 8.13. Regions for using ideal power-limited engine 2 for maneuver of building up parabolic velocity in Earth's field: a) (α, V_1) plane (unit weight of engine 2, exhaust velocity of engine 1); b) ($\varkappa$, V_1) plane ($\varkappa = G_0/N_{20}$ parameter of engine 2, maneuver parameter is time of motion T).

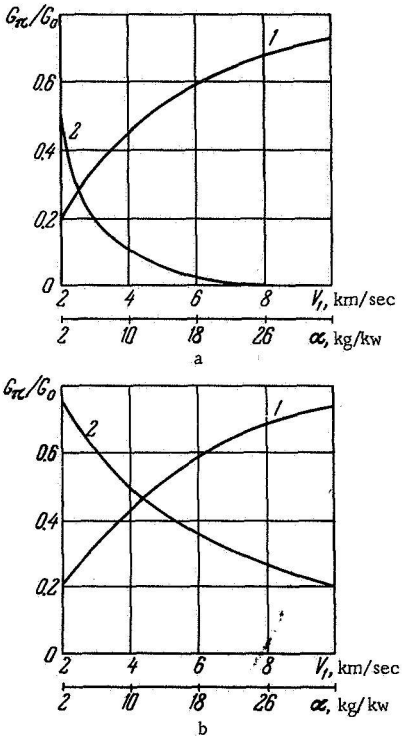

FIGURE 8.14. Payloads G_π/G_0 for ideal engines with limited exhaust velocity 1 and limited power 2 in build-up maneuver of parabolic velocity in Earth's field as function of corresponding structural parameters V_1 and α: a) $T = 6.8$ days, b) $T = 29.2$ days (cf. Figure 8.13).

The limiting relationships $\alpha(V_1)$ and $\varkappa(V_1)$ are represented in Figure 8.13. In those regions where parameters α and V_1 (or $\varkappa, V_1$) lie below the curves it is more efficient to use a single power-limited engine (shaded regions). The initial data are now given for an altitude of the initial circular orbit above the Earth's surface of 300 km. First example: $T = 6.8$ days, $J(T) = 80.8$ m^2/sec^3, $a_{20} = 0.895$ cm/sec^2; second example: $T = 29.2$ days, $J(T) = 17.95$ m^2/sec^3, $a_{20} = 0.269$ cm/sec^2. The corresponding relationships between the relative payloads and the structural parameters of the engines have been plotted on Figure 8.14 (characteristic velocity $I = 3.167 \cdot 10^3$ m/sec, and for the values of the functional J cf. above).

2. **Transfer between circular orbits.** This maneuver is characterized by the following optimum function $a_2(t)$ (cf. Chapter 5): the function $a_2(t)$ decreases at first, and then increases, so that the maximum values of a_2 are attained at the beginning and end of the trajectory. Correspondingly, the exhaust velocity V_2 increases at first, and then decreases either up to the terminal point, or till some point near the terminal one, where the function $V_2(t)$ has a local minimum. Thus, the firing of engine 1 can take place either at the beginning or towards the end of the trajectory, depending on where condition (8.76) is first violated.

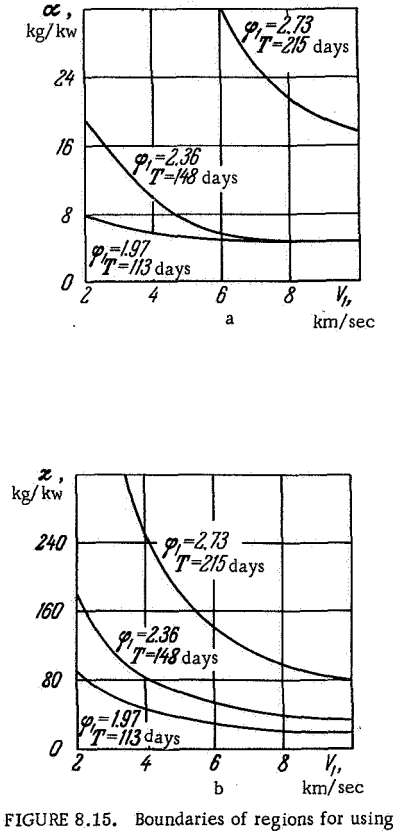

FIGURE 8.15. Boundaries of regions for using ideal power-limited engine for maneuver of transfer between circular coplanar orbits of Earth and Mars: a) (α, V_1) plane; b) $(\varkappa, V_1)$ plane; maneuver parameters are angular displacement φ_1 and time of motion T.

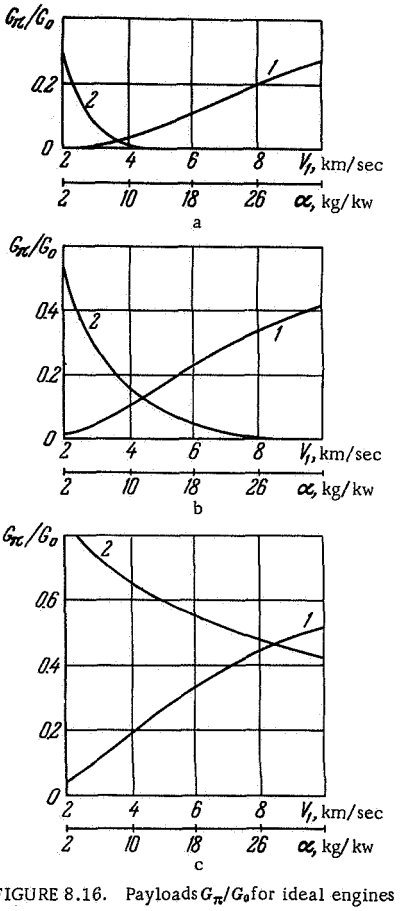

FIGURE 8.16. Payloads G_π/G_0 for ideal engines with limited exhaust velocity 1 and limited power 2 in transfer maneuver between orbits of Earth and Mars as functions of corresponding structural parameters V_1 and α: a) $\varphi_1 = 1.97$, $T = 113$ days; b) $\varphi_1 = 2.36$, $T = 148$ days; c) $\varphi_1 = 2.73$, $T = 215$ days (cf. Figure 8.15).

Figure 8.15 shows the boundaries of the regions in which the power-limited engine is used (the regions in which the engine is used lie below the curves) in the (α, V_1) and $(\varkappa, V_1)$ planes. The following values were

employed for the maneuver parameters (both dimensionless and dimensional values are given for the time T and the functional J, corresponding to the transfer from mean orbit of the Earth to mean orbit of Mars):

$$\left.\begin{aligned}
&\text{a) } r_0 = 1, \quad r_1 = 1.52, \quad \varphi_1 = 1.97, \\
&\quad T = 1.94 \to 113 \text{ days}, \; J(T) = 1.053 \to 187 \text{ m}^2/\text{sec}^3, \\
&\text{b) } r_0 = 1, \quad r_1 = 1.52, \quad \varphi_1 = 2.36, \\
&\quad T = 2.55 \to 148 \text{ days}, \; J(T) = 0.403 \to 71.4 \text{ m}^2/\text{sec}^3, \\
&\text{c) } r_0 = 1, \quad r_1 = 1.52. \quad \varphi_1 = 2.73, \\
&\quad T = 3.70 \to 215 \text{ days}, \; J(T) = 0.0416 \to 7.38 \text{ m}^2/\text{sec}^3.
\end{aligned}\right\} \qquad (8.89)$$

The relative payloads for engines with limited exhaust velocity and limited power are plotted in Figure 8.16 as a function of the structural
346 parameters of the engines for fixed maneuver parameters (8.89). The characteristic velocity values are: a) $I = 13 \cdot 10^3$ m/sec, b) $I = 9 \cdot 10^3$ m/sec, c) $I = 6.5 \cdot 10^3$ m/sec according to the data of /8.58/; for the functional J cf. (8.89).

347 3. **Round-trip interplanetary flight.** This maneuver is represented as a combination of the two elementary maneuvers considered above (cf. Chapter Five). Depending on the parameters of the elementary maneuvers, the minimum exhaust velocity V_2 is attained either at the beginning of one of the sections of motion in the neighborhood of the planets, or at the beginning or end of one of the heliocentric sections. According to the condition for an optimum combination of the elementary maneuvers forming the round-trip interplanetary flight (§ 3 of Chapter Five), the thrust accelerations in the accelerating and decelerating sections have the same magnitude. Therefore, the beginning of the acceleration near the destination planet and the beginning of the deceleration near the takeoff planet are excluded from the sections to be discussed.

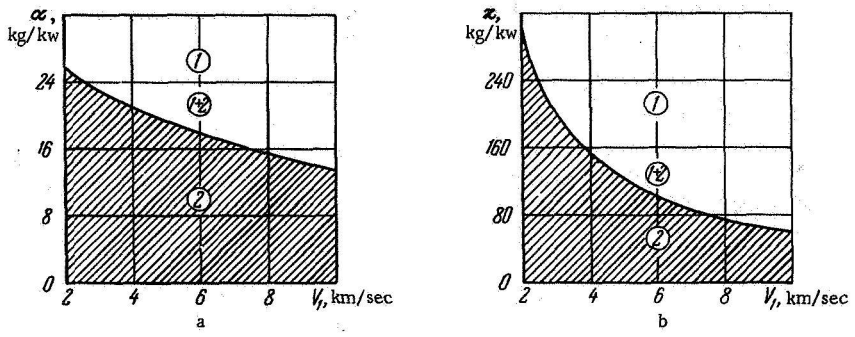

FIGURE 8.17. Region for using ideal power-limited engine 2 for maneuver of interplanetary flight Earth—Mars—Earth: a) (α, V_1) plane; b) $(\varkappa, V_1)$ plane; maneuver parameters are total time $T_0 =$ 644 days, time of sojourn in neighborhood of Mars $T_\omega = 48$ days.

For the Earth—Mars—Earth flight the optimum thrust acceleration in the neighborhood of Mars is usually lower than in the neighborhood of the Earth, and therefore only the following sections remain to be compared: the beginning of the acceleration in the Earth's field and the beginning and end of the Earth—Mars—Earth orbital transfers (here the early use of an additional impulse provided by an engine with a limited exhaust velocity can be advantageous).

348 As an example, consider the Earth—Mars—Earth flight with the following parameters: total time $T_\sigma = 644$ days, time of sojourn in the neighborhood of Mars $T_\omega = 48$ days. Relationships $a(t)$, $J(t)$, and $V(t)$ for $\alpha = 5$ and 10 kg/kw are shown for this flight in Figure 5.32. The minimum exhaust velocity is attained as follows: for $\alpha < 5$ kg/kw at the beginning of the Mars—Earth orbital transfer ($a_2 = 0.215$ cm/sec^2), and for $\alpha \geqslant 5$ kg/kw at the beginning of the acceleration in the Earth's field ($a_2 = 0.165$ cm/sec^2). The region in which a power-limited engine should be used is determined by criterion (8.76), and shown in Figure 8.17. The relative payloads for engines with limited exhaust velocities and limited power are plotted in Figure 8.18 as functions of the structural parameters of the engines (characteristic velocity $I_\sigma = 22.2 \cdot 10^3$ m/sec according to the data of /8.58/, and the functional $J_\sigma = 63.6$ m^2/sec^3 according to Table 5.7).

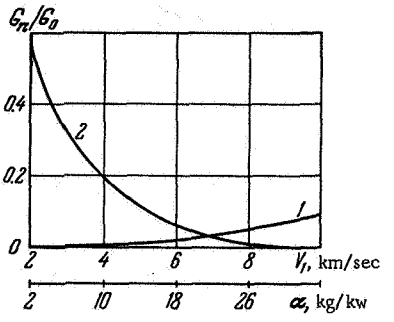

FIGURE 8.18. Payloads G_n/G_0 for ideal engines with limited exhaust velocity 1 and limited power 2 in maneuver of interplanetary flight Earth—Mars—Earth; $T_\sigma = 644$ days, $T_\omega = 48$ days (cf. Figure 8.17).

4. Notes. 1) Criterion (8.76) was obtained for an ideal power-limited engine. Applied to real engines, it gives an inaccurate answer; the example with unthrottled engines (cf. Figure 8.8 of § 2) corroborates this fact. Therefore, for real engines, (8.76) gives only a tentative determination of the boundary of the region in which the ideal power-limited engine should be used.

2) The analysis of the examples of maneuvers in a central field and for similar maneuvers in a gravity-free field leads to the conclusion that the necessity of an additional engine with limited exhaust velocity appears earlier when the dynamic maneuver is more "strained" (i.e., when the single power-limited engine delivers a smaller payload).

3) From the results presented in Figure 8.13 to 8.18 one can form an opinion concerning the advisability of using power-limited engines singly or in combination with an engine with limited exhaust velocity, at the different stages of interplanetary flight.

Chapter Nine

PROPULSION SYSTEMS WITH ENERGY AND MASS ACCUMULATION. ENGINES WHOSE THRUST AND POWER ARE FUNCTIONS OF THE COORDINATES AND TIME

349 This chapter treats optimization problems of the parameters and control functions for the following types of propulsion systems:

1) Power-limited engines with accumulation of thermal or electric energy (§§ 1 and 2).

2) Engines with limited power or limited exhaust velocity which accumulate atmospheric gas to be used as working fluid (§ 3).

3) Solar sail (the maximum thrust depends on the distance from the Sun and the sail orientation (§ 4)).

4) Isotopic sail (the maximum thrust depends on the time (§ 5)).

5) Engines with solar power source (the maximum power depends on the distance from the Sun (§ 6)).

6) Engines with isotopic power source (the maximum power depends on the time (§ 7)).

§ 1. POWER-LIMITED ENGINES WITH ENERGY ACCUMULATION: THE IDEAL CASE

If the solution of the dynamic part of the optimization problem (Chapters Five and Six) is analyzed, we may conclude that the application of a thrust is more advantageous in some sections of the trajectory than in others. For orbital transfers in a central field and displacements between points of rest in a gravity-free field these applications are best in the neighborhoods of the initial and terminal points of a trajectory. When rotating the plane of a circular orbit in a central field, a thrust should be applied over that section represented by the final position of the nodal line. In the case of an ideal power-limited engine the thrust acceleration level in these sections is, according to the optimum program, much higher than that over the rest of the trajectory; in the case of unthrottled engines the powered sections are located there, while for the remaining sections the thrust is cut off.

In the power-limited engines studied above, the energy produced by the generator is fed directly to the engine. Therefore throughout those sections during which the optimum thrust is small or vanishes, the power generator is not used. It has been shown that the efficiency of the power source can be increased by storing the energy produced along the

350 sections of zero (or almost zero) thrust, and using it for the powered sections /9.1—9.3/. To that end one can use thermal /9.1/ or electric /9.2/ accumulators (cf. § 2 of Chapter Two). The gain in payload achieved with such accumulators has been assessed tentatively in /9.1, 9.2/.

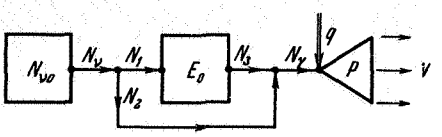

FIGURE 9.1. Block diagram of power-limited powerplant with energy accumulator; N_{v0} is the power source, E_0 is the energy accumulator, P is the engine.

Energy accumulators are also necessary in satellites with solar powerplants if their trajectory passes through shaded zones.

1. Control and weight characteristics. The power-limited powerplant with energy accumulation consists of the power source N_v, the energy accumulator E, and the engine P (Figure 9.1) /9.3/. The power produced by the power source ($0 \leqslant N_v \leqslant N_{v0}$) can be directed into the accumulator ($N_1 \geqslant 0$) or into the engine ($N_2 \geqslant 0$), so that $N_1 + N_2 = N_v$. The energy accumulator can transmit to the engine a power $N_3 = N_1 - \dot{E}$ ($N_3 \geqslant 0$, $0 \leqslant E \leqslant E_0$), so that the engine receives a total power $N_\gamma = N_2 + N_3$ which is used for creating the thrust, where

$$P = qV, \quad N_\gamma = {}^1/_2 qV^2 \qquad (0 \leqslant P \leqslant P_0). \tag{9.1}$$

Here q is the mass flow rate of the working fluid and V the exhaust velocity. The acceleration of the working fluid is considered to be ideal. The thrust has an upper bound in the general case, except for an ideal engine where P_0 (the maximum thrust) can be infinite. For an unthrottled engine $P = P_0$ or 0, assuming no losses in the engine.

Eliminating $N_2 = N_v - N_1$ and replacing $N_3 - N_1 = N_e$, we can represent the power balance equation for this system in the form

$$\begin{gathered} \dot{E} = -N_e, \quad N_v + N_e = {}^1/_2 qV^2 \\ (0 \leqslant E \leqslant E_0, \quad N_e \geqslant -N_v, \quad 0 \leqslant N_v \leqslant N_{v0}). \end{gathered} \tag{9.2}$$

The negative values of the power N_e correspond to the charging phase and are bounded by the value of the power N_v produced by the source. The
351 positive values of N_e correspond to the discharge phase.

The weight of the power-limited engine with energy accumulator

$$G_\varkappa = G_v + G_e + G_\gamma \tag{9.3}$$

consists of the following components: weight of the power source (taken proportional to the maximum power of the source N_{v0})

$$G_v = \alpha N_{v0}, \tag{9.4}$$

weight of the energy accumulator (taken proportional to the maximum accumulated energy E_0)

$$G_e = \beta E_0, \tag{9.5}$$

weight of the engine (taken proportional to the maximum thrust P_0)

$$G_\gamma = \gamma P_0 \tag{9.6}$$

(for an ideal engine $G_\gamma = 0$).

2. **Formulation of the variational problem; structure of the optimum control function.** The maximum payload problem for a power-limited propulsion system with an energy accumulator is formulated as follows. The payload G_0, the unit weights α, β, γ of the power source, the accumulator, and the engine are specified; the boundary conditions and the maneuvering time T are given too. The optimum operating regimes of the power source, the energy accumulator, the engine, as well as the optimum weight parameters (9.4) to (9.6) must be found so that the payload G_π is a maximum /9.3/.

The full system of differential equations, boundary conditions, bounds of the control functions, and phase coordinates of this variational problem are written as follows in Mayer's formulation (similarly to (II.8)):

$$\begin{aligned}
&\dot G_\sigma = -\frac{k_1 P^2}{N_\nu(1+N_e)}, && G_\sigma(0)+G_\varkappa = 1, && G_\sigma(T) = \max,\\
&\dot E = -k_2 N_\nu N_e, && E(0) = 1, && E(T) = 0,\\
&\dot{\mathbf{r}} = \mathbf{v}, && \mathbf{r}(0) = \mathbf{r}_0, && \mathbf{r}(T) = \mathbf{r}_1,\\
&\dot{\mathbf{v}} = k_3\frac{P\mathbf{e}}{G_\sigma+G_\varkappa} + \mathfrak{R}, && \mathbf{v}(0) = \mathbf{v}_0, && \mathbf{v}(T) = \mathbf{v}_1\\
&(0 \leqslant P(t) \leqslant 1,\ 0 \leqslant N_\nu(t) \leqslant 1,\ N_e(t) \geqslant -1, && && \\
&\qquad |\mathbf{e}(t)| \equiv 1,\ 0 \leqslant E(t) \leqslant 1, && && \\
&k_1 = \frac{gP_0^2}{2N_{\nu 0}G_0} = \frac{\alpha g G_\gamma^2}{2\gamma^2 G_\nu},\ k_2 = \frac{N_{\nu 0}}{E_0} = \frac{\beta G_\nu}{\alpha G_e},\ k_3 = \frac{gP_0}{G_0} = \frac{gG_\gamma}{\gamma}\Big). && &&
\end{aligned} \tag{9.7}$$

352 Here the first equation is the continuity equation for the working fluid, ($G_\sigma(t) = G_\pi + G_\mu(t)$ is the total weight of the payload G_π and the working-fluid reserve G_μ), the second one is the equation governing the accumulator energy, and the third and fourth equations are vectorial equations for the motion of the vehicle center of mass in an inertial reference frame.

The initial weights G_σ and $G_\varkappa$ correspond to the specified takeoff weight G_0 (all weights are represented as fractions of G_0). At the end of the motion the weight $G_\sigma(T)$ coincides by definition with G_π and must be a maximum. The boundary conditions for the energy E (as a fraction of E_0), the radius vector $\mathbf{r}$, and the velocity vector $\mathbf{v}$ change according to the type of maneuver.

The control functions P, N_ν, N_e, $\mathbf{e}$ are dimensionless. The thrust P and the power of the source N_ν are represented as fractions of their maximum values P_0 and N_0. The power N_e is given as a fraction of the instantaneous power of the source; $\mathbf{e}$ is a unit vector in the thrust direction.

The control parameters G_ν, G_e, G_γ are the weights of the power source, the energy accumulator, and the engine (fractions of G_0), and enter the right-hand sides of equations (9.7) and also the initial condition governing a specified takeoff weight. The selection of the optimum values of these parameters can be reduced to the standard procedure of adding the formal equations

$$\dot G_\nu = 0, \quad \dot G_e = 0, \quad \dot G_\gamma = 0 \tag{9.8}$$

and boundary conditions

$$\begin{gathered} G_\sigma(0) + G_v(0) + G_e(0) + G_\gamma(0) = 1, \\ G_v(T) = \text{opt},\ G_e(T) = \text{opt},\ G_\gamma(T) = \text{opt} \end{gathered} \tag{9.9}$$

to system (9.7) (the first condition replaces $G_\sigma(0) + G_\varkappa = 1$). As a result the control parameters G_v, G_e, G_γ are transformed into phase coordinates, whose initial values are linked by the transversality condition, and whose final values vary.

The optimum control functions $\mathbf{e}(t)$, $P(t)$, $N_e(t)$, $N_v(t)$ are determined by Pontryagin's method of requiring the Hamiltonian H to be an absolute minimum, where

$$\begin{gathered} H = -p_\sigma \frac{k_1 P^2}{N_v(1+N_e)} - p_e k_2 N_v N_e + (\mathbf{p}_v \cdot \mathbf{e}) \frac{k_3 P}{G_\sigma + G_\varkappa} + (\mathbf{p}_v \cdot \mathbf{R}) + (\mathbf{p}_r \cdot \mathbf{v}) \\ \left(\dot{p}_\sigma = -\frac{\partial H}{\partial G_\sigma},\quad \dot{p}_e = -\frac{\partial H}{\partial E},\quad \dot{\mathbf{p}}_v = -\frac{\partial H}{\partial \mathbf{v}},\quad \dot{\mathbf{p}}_r = -\frac{\partial H}{\partial \mathbf{r}} \right). \end{gathered} \tag{9.10}$$

One must distinguish between trajectory sections of two types, i.e., those lying within the region $0 \leqslant E \leqslant 1$, and those lying on the boundaries $E = 0$ or $E = 1$. Avoiding the details in determining the minimum of H, we give the solutions for the optimum controls.

353 The thrust direction $\mathbf{e}$ and the power of the source N_v have the same time-dependence on the inner and boundary sections of the trajectory:

$$\mathbf{e} = -\mathbf{p}_v / p_v,\quad N_v = 1 \qquad (p_v = |\mathbf{p}_v|), \tag{9.11}$$

i.e., the thrust vector is in the opposite direction to the vector $\mathbf{p}_v$, and the source power has a maximum (as for power-limited propulsion systems without accumulation — cf. Chapter Four above).

The power N_e (controlling the accumulator energy) and the magnitude of the thrust P obey the following:

within region $0 \leqslant E \leqslant 1$

$$\left.\begin{gathered} N_e = \left(\frac{k_1 p_\sigma}{k_2 p_e}\right)^{1/2},\quad P = 1 \text{ at } p_v^2 > \varphi_1, \\ N_e = -1,\qquad P = 0 \text{ at } p_v^2 < \varphi_1 \\ \left(\varphi_1 = 4 p_\sigma p_e (G_\sigma + G_\varkappa)^2 \frac{k_1 k_2}{k_3^2}\right); \end{gathered}\right\} \tag{9.12}$$

on the boundaries $E = 0$ and $E = 1$

$$\left.\begin{gathered} N_e = 0,\quad P = 1 \qquad\qquad \text{at } p_v^2 > \varphi_2, \\ N_e = 0,\quad P = \frac{-p_v k_3}{2 k_1 p_\sigma (G_\sigma + G_\varkappa)} \quad \text{at } p_v^2 < \varphi_2 \\ \left(\varphi_2 = 4 p_\sigma^2 (G_\sigma + G_\varkappa)^2 \frac{k_1^2}{k_3^2}\right), \end{gathered}\right\} \tag{9.13}$$

where p_σ and p_e are everywhere negative.

Thus, within the region $0 \leqslant E \leqslant 1$ the accumulator energy is either discharged at an optimally varying rate (discharge regime), for which the thrust is a maximum (cf. the first relation of (9.12)), or it is stored at a maximum rate (charging regime), for which the thrust is zero (cf. the second relation of (9.12)). On the boundaries $E = 0$ and $E = 1$ the energy

accumulator discharge naturally vanishes, and the thrust varies as if the accumulator is absent; it is either a maximum (first relation of (9.13)), or optimally controlled (second relation of (9.13)).

To establish how the optima (9.12), (9.13) alternate, we require the behavior of the momenta p_σ, p_e, $p_v = |\mathbf{p}_v|$ and the phase coordinate G_σ. The momenta p_σ, $\mathbf{p}_v$, $\mathbf{p}_r$ and the phase coordinates are everywhere continuous, while p_e has a first-order discontinuity when moving from the boundaries $E = 0$ and $E = 1$, in accordance with the jump condition /9.4/ (the form of the function H and the momentum differential equations (9.10) are preserved).

354 From equations (9.10) and (9.7), allowing for (9.11), we have

$$\dot{p}_\sigma = -\frac{k_3 p_v P}{(G_\sigma + G_\varkappa)^2} \leqslant 0, \quad \dot{p}_e = 0, \quad \dot{G}_\sigma = -\frac{k_1 P^2}{1 + N_e} \leqslant 0. \tag{9.14}$$

It can be shown that p_σ and p_e are everywhere negative, and that the functions φ_1 and φ_2 in conditions (9.12), (9.13) are positive. With the aid of (9.14) we conclude that these functions are nondecreasing:

$$\begin{aligned}
&\dot{\varphi}_1 > 0, \quad \dot{\varphi}_2 > 0 \text{ at } p_v^2 > \varphi_1;\\
&\dot{\varphi}_1 = 0, \quad \dot{\varphi}_2 = 0 \text{ at } p_v^2 < \varphi_1;\\
&\dot{\varphi}_1 > 0, \quad \dot{\varphi}_2 > 0 \text{ at } p_v^2 > \varphi_2;\\
&\dot{\varphi}_1 = 0, \quad \dot{\varphi}_2 > 0 \text{ at } p_v^2 < \varphi_2.
\end{aligned}$$

The behavior of $\mathbf{p}_v$ is determined mainly by the type of maneuver. The following examples are characterized by the nonmonotonic behavior of $p_v^2(t)$, with a minimum within the interval $[0,T]$.

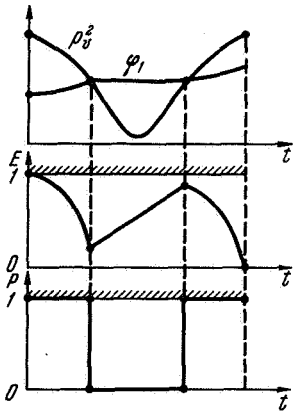

FIGURE 9.2. Optimum variation with time of relative energy stored in accumulator E and thrust P, when function E does not reach boundary.

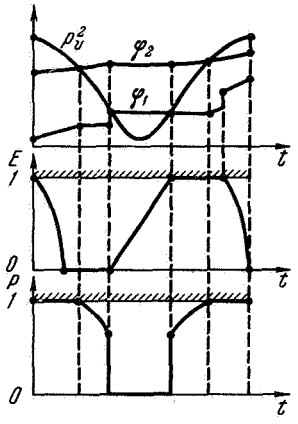

FIGURE 9.3. Optimum variation with time of relative energy of accumulator E and thrust P, when function E reaches boundaries $E = 1$, $E = 0$.

If the energy E remains within the boundaries $E = 0$ and $E = 1$ throughout the motion, $E(t)$ and $P(t)$ will have the form shown in Figure 9.2. In the general case, sections of motion along the boundaries $E = 0$ and $E = 1$

respectively can appear between the transition points from the discharge regime to the charging regime and vice versa (Figure 9.3). The instant at which the boundary is left is not determined by the maximum principle, and must be found either with the aid of one of the optimality principles,
355 or by varying the length of the boundary section (subsection 3).

Finally a propulsion system could exist with energy accumulation but no power source. Such a system will be efficient for sufficiently low values of β, the unit weight of the energy accumulator (9.5), where

$$\beta T/\alpha \leqslant 1. \tag{9.15}$$

In fact, a power source of weight G_v, which produces an energy $E^* = (G_v/\alpha)\,T$ at $\beta T/\alpha = 1$ during time T, can be replaced by an energy accumulator of capacity E^*, initially fully charged, with the same weight $G_e^* = \beta E^* = G_v\beta T/\alpha = G_v$. At $\beta T/\alpha < 1$ we have $G_e^* < G_v$, and therefore the use of a power source would be inefficient.

For a propulsion system with an energy accumulator but no power source, the equations (9.7) reduce to ($G_v = 0$)

$$\left.\begin{aligned}
&\dot G_\sigma = -k_1\frac{P^2}{N_e}, && G_\sigma(0)+G_\varkappa = 1, \quad G_\sigma(T) = \max.\\
&\dot E = -k_2 N_e, && E(0) = 1, \quad E(T) = 0,\\
&\dot{\mathbf{r}} = \mathbf{v}, && \mathbf{r}(0) = \mathbf{r}_0, \quad \mathbf{r}(T) = \mathbf{r}_1,\\
&\dot{\mathbf{v}} = k_3\frac{P\mathbf{e}}{G_\sigma+G_\varkappa} + \mathfrak{R}, && \mathbf{v}(0) = \mathbf{v}_0, \quad \mathbf{v}(T) = \mathbf{v}_1\\
&&& (0 \leqslant P(t) \leqslant 1,\ N_e(t) \geqslant 0,\ |\mathbf{e}(t)| \equiv 1,\\
&k_1 = \frac{gTP_0^2}{2E_0G_0} = \frac{g\beta TG_\gamma^2}{2\gamma^2G_e}, \quad k_2 = \frac{1}{T}, \quad k_3 = \frac{gP_0}{G_0} = \frac{gG_\gamma}{\gamma}\Big).
\end{aligned}\right\} \tag{9.16}$$

Here N_e is represented as a fraction of E_0/T, unlike (9.7); there is no limitation on the phase coordinate E (this limitation is fulfilled automatically if the boundary conditions for E when $N_e \geqslant 0$ are fulfilled).

The optimum variations of the control functions are (cf. (9.11), (9.12))

$$\left.\begin{aligned}
&\mathbf{e} = -\mathbf{p}_v/p_v,\\
&N_e = \sqrt{\frac{k_1p_\sigma}{k_2p_e}}, \quad P = 1 \ \text{ at } \ p_v^2 > \varphi_1,\\
&N_e = 0, \qquad\quad P = 0 \ \text{ at } \ p_v^2 < \varphi_1\\
&\Big(\varphi_1 = 4p_\sigma p_e(G_\sigma+G_\varkappa)^2\frac{k_1k_2}{k_3^2}\Big).
\end{aligned}\right\} \tag{9.17}$$

3. Ideally throttlable propulsion system is characterized by the absence of an upper bound for the thrust ($P \geqslant 0$) and by vanishing engine weight
356 ($G_\gamma = 0$). An investigation of this case enables us to establish an upper limit for the system, and to partially separate the general variational problem into weight and dynamic parts.

The absence of an upper bound for the thrust makes it possible to pass from the thrust P to the thrust acceleration a in equations (9.7)

$$a = k_3P\,(G_\sigma + G_\varkappa)^{-1}. \tag{9.18}$$

The first equation of (9.7) can then be integrated by quadratures and solved for the problem functional (as was carried out above for the power-limited propulsion system without an energy accumulator):

$$G_\pi = \left(1 + \frac{1}{G_v}\frac{\alpha}{2g}\int_0^T \frac{a^2 dt}{N_v(1+N_e)}\right)^{-1} - G_v\left(1 + \frac{G_e}{G_v}\right). \tag{9.19}$$

The relative weight of the power source G_v enters the other equations of the variational problem (9.7) only in terms of the ratio G_v/G_e. Therefore, even before we solve the full problem, we can find the optimum value G_e/G_v which maximizes G_v, by fixing the value of the integral and the ratio G_π in (9.19) as follows

$$G_{v\,\mathrm{opt}} = \frac{1}{1+\xi}(\sqrt{\Phi_e} - \Phi_e)$$
$$\left(\xi = \frac{G_e}{G_v},\quad \Phi_e = (1+\xi)\frac{\alpha}{2g}\int_0^T \frac{a^2 dt}{N_v(1+N_e)}\right); \tag{9.20}$$

here

$$G_{\pi\,\max} = (1 - \sqrt{\Phi_e})^2,\quad G_\varkappa = G_v + G_e = \sqrt{\Phi_e} - \Phi_e. \tag{9.21}$$

The last relations (Figure 9.4) for the maximum payload G_π and the optimum total weight of the propulsion system G coincide with solutions (4.15) in § 1 of Chapter Four, where Φ_e from (4.14) replaces Φ, and the weight of the propulsion system consists of the weight of the power source only so that $G_\varkappa = G_v$.

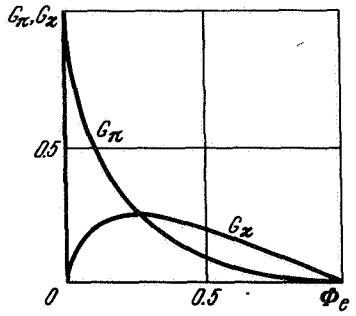

FIGURE 9.4. Maximum relative payload G_π and optimum weight of propulsion system with energy accumulator $G_\varkappa$ as function of problem functional Φ_e.

357 Note that in the problem with energy accumulation as well the optimum full weight of the propulsion system does not exceed 25% of the takeoff weight G_0.

The payload (9.21) decreases monotonically with increasing Φ_e, and therefore the second part of the problem reduces to finding the minimum of the

functional (the parameter α is specified) given by

$$J_e = (1+\xi)\int_0^T \frac{a^2 dt}{N_v(1+N_e)} \qquad \left(\Phi_e = \frac{\alpha}{2g} J_e\right). \tag{9.22}$$

The efficiency of an energy accumulator will be denoted by the ratio of the functional (9.22) to the usual functional

$$J = \int_0^T a^2 dt; \tag{9.23}$$

if $0 < J_e/J < 1$, it is efficient to use an accumulator.

The equations of the variational problem for the minimum of J_e are

$$\left.\begin{aligned} &\dot{J}_e = \frac{(1+\xi)a^2}{N_v(1+N_e)}, \quad J_e(0) = 0, \quad J_e(T) = \min, \\ &\dot{E} = -\frac{\beta}{\alpha\xi} N_v N_e, \quad E(0) = 1, \quad E(T) = 0, \\ &\dot{\mathbf{r}} = \mathbf{v}, \qquad\qquad \mathbf{r}(0) = \mathbf{r}_0, \quad \mathbf{r}(T) = \mathbf{r}_1, \\ &\dot{\mathbf{v}} = a\mathbf{e} + \mathfrak{R}, \qquad \mathbf{v}(0) = \mathbf{v}_0, \quad \mathbf{v}(T) = \mathbf{v}_1 \\ &(a(t) \geqslant 0,\ 0 \leqslant N_v(t) \leqslant 1,\ N_e(t) \geqslant -1,\ |\mathbf{e}(t)| \equiv 1,\ 0 \leqslant E(t) \leqslant 1). \end{aligned}\right\} \tag{9.24}$$

The optimum control functions are (cf. (9.11) to (9.13))

$$\left.\begin{aligned} &\mathbf{e} = \frac{\mathbf{p}_v}{p_v}, \qquad N_v = 1, \quad a = \frac{p_v(1+N_e)}{2(1+\xi)}, \\ &N_e = \infty \quad \text{at} \quad p_v^2 > 4\frac{\beta(1+\xi)}{\alpha\xi} p_e, \quad 0 < E < 1 \ (p_e > 0), \\ &N_e = -1 \quad \text{at} \quad p_v^2 < 4\frac{\beta(1+\xi)}{\alpha\xi} p_e, \quad 0 < E < 1, \\ &N_e = 0 \quad \text{at} \quad E = 0 \text{ and } E = 1, \end{aligned}\right\} \tag{9.25}$$

i.e., the discharge regime turns out to be impulsive.

The optimum time for the phase coordinate E to move away from the boundaries $E = 0$ (beginning to charge the energy accumulator) and $E = 1$ (beginning to discharge it), will be selected by the optimum conditions /9.5/, since the maximum principle /9.4/ does not determine the specific values
358 of the constant p_e for the different stages of motion (cf. (9.25)). The sufficient optimum condition /9.6/ necessitates maximizing the function R with respect to the coordinates and the control functions; the part R^* which depends on the coordinate E has the form

$$R^* = cp_v\dot{p}_v E \qquad (0 < c = \text{const}).$$

The optimum values of E turn out to be

$$\left.\begin{aligned} &E = 1 \quad \text{at} \quad p_v\dot{p}_v > 0, \\ &E = 0 \quad \text{at} \quad p_v\dot{p}_v < 0. \end{aligned}\right\} \tag{9.26}$$

The transition of E from the boundary value 1 to the boundary value 0 (discharge of the energy accumulator) can be carried out instantaneously ($\dot{E} \sim -N_e = -\infty$, cf. (9.25)). According to (9.26), this transition occurs as soon as the product $p_v\dot{p}_v$ changes its sign from plus to minus. Since $p_v = |\mathbf{p}_v| \geqslant 0$ such a change of sign is only possible at maximum $p_v(t)$.

The inverse transition of E from the boundary $E = 0$ to the boundary $E = 1$ (charging the accumulator) must be carried out (see (9.26)) near those values of t for which the product $p_v \dot{p}_v$ changes sign from minus to plus. These are the points which yield minimum $p_v(t)$. However, charging, unlike discharging, cannot be realized instantaneously, since in this case (cf. (9.25)) $\dot{E} = \beta/\alpha\xi \leqslant 1$. Therefore, relations (9.26) cannot be fulfilled exactly in some neighborhood of the point t_3 (Figure 9.5). The extent of this neighborhood depends on the ratio of the source power, which is fully applied to charging the accumulator ($N_e = -1$, $N_v = 1$) to its capacity. The value of the constant p_e, which, with relation (9.25), determines the time τ at which charging begins, must be as near as possible to the value p_e corresponding to instantaneous charging (p_{e3} in Figure 9.5), but such that relation (9.26) is fulfilled beyond the ends of the charging interval. The value of p_{e1} in Figure 9.5 satisfies the conditions indicated above, while p_{e2} is unapplicable even though it does not differ as much as p_{e1} from the ideal value p_{e3}. This is so because if we charged up to p_{e2} (the dashed lines on Figure 9.5) we would have a situation in which the limit $E = 1$ is not attained. Since the value of p_e can vary only when the coordinate E reaches the boundary or moves away from it, it remains constant immediately after the end of charging (at time Θ_2 there occurs an impulsive discharge of the accumulator according to (9.25)). Thus, charging up to p_{e2} leads to the breakdown of relations (9.26), since $p_v \dot{p}_v > 0$ for $t > \Theta_2$, and $E = 0$ for the same values of t. Instead of the optimum value p_{e1} we can directly calculate the values τ_1 and Θ_1, the optimum times of the charging interval, using the following relations:

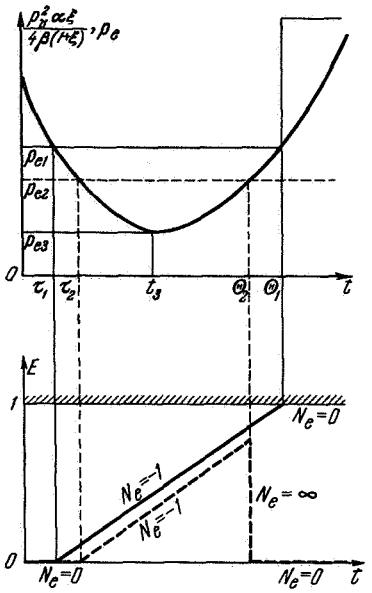

FIGURE 9.5. Determination of optimum time for displacing function E away from the boundaries.

$$\int_{\tau_1}^{\Theta_1} E\,dt = \frac{\beta}{\alpha\xi}(\Theta_1 - \tau_1) = 1, \quad p_v(\tau_1) = p_v(\Theta_1). \tag{9.27}$$

The first relation is the condition for the transition of E from the boundary value 0 to the boundary value 1; the second relation indicates the maximum possible difference between the selected value p_{e1} and the ideal value p_{e3}.

Relation (9.25), which determines the optimum value of the thrust acceleration, enables one to give a simple physical interpretation of the results obtained. The use of the energy stored in the accumulator is an optimum for values of the acceleration near the maximum value. This in turn leads to an increase in the acceleration. Thus, the accumulator energy is discharged when it can have a maximum effect in bringing about the kinematic conditions of the maneuver. The process of charging, which

359

causes the engine to be cut off ($a = 0$), occurs near the minimum values of $a(t)$. Here, this process has its least effect in retarding the development of the required kinematic conditions.

The following relation is obtained with which to determine the optimum value of the parameter ξ (cf. (9.25)):

$$\xi = \left(\frac{\beta}{\alpha}\int_0^T p_e N_e dt\right)^{1/2} \left(\int_0^T \frac{a^2 dt}{1+N_e}\right)^{-1/2}. \tag{9.28}$$

As long as the values of ξ in (9.28) satisfy the condition $\xi > 0$, the system with energy accumulation is superior to the system without it. The quantity $(\beta T/\alpha)^\circ$ represents the value of the dimensionless combination of the unit weights of the accumulator and power source corresponding to a zero value of the optimum ξ. The use of an energy accumulator of unit
360 weight β' combined with an ideally-throttlable propulsion system whose power source has unit weight α', is efficient when the following inequality holds:

$$\frac{\beta' T}{\alpha'} \leqslant \left(\frac{\beta T}{\alpha}\right)^\circ. \tag{9.29}$$

To determine the value of $(\beta T/\alpha)^\circ$, relation (9.28) is written for β/α:

$$\frac{\beta}{\alpha} = \xi^2 \left(\int_0^T \frac{a^2 dt}{1+N_e}\right)\left(\int_0^T p_e N_e dt\right)^{-1}. \tag{9.30}$$

The integrals on the right-hand side of (9.30) can be calculated using the function $p_v(t)$ /9.5/.

If we study the limiting case of a propulsion system without power source, relations (9.21) remain valid, and we need only write

$$G_v = 0, \quad \Phi_e = \frac{\beta T}{2g}\int_0^T \frac{a^2 dt}{N_e}$$

(the power N_e is represented as a fraction of E_0/T).

The equations of the variational problem (9.24) are the same as those at the end of the preceding subsection; the functional becomes

$$J_e = \int_0^T \frac{a^2 dt}{N_e}.$$

4. Maneuvers of displacement between points of rest and rotating the plane of a circular orbit. These two maneuvers are examples of the solution of the general problem, for which the equations of the variational problem can be integrated fully /9.3/.

For the displacement between points of rest ($v_0 = v_1 = 0$), at a distance l apart ($r_0 = 0$, $r_1 = l$) over a period of time T, the momentum p_v is a linear function of the time, i.e., $p_v^2 = (b_2 - b_1 t)^2$. Without an energy accumulator the function (9.23) is here equal to (5.33)

$$J_l = 12\frac{l^2}{T^3}, \quad \Phi_l = 6\frac{\alpha}{g}\frac{l^2}{T^3}. \tag{9.31}$$

[361] As in Subsection 2, the optimum programs $E(t)$, $N_e(t)$, and $a(t)$ are determined from (9.25) for known $p_v^2(t)$ and shown in Figure 9.6, where $t_{1,2} = {}^1/_2 (T \mp \xi\alpha/\beta T)$. Integrating equations (9.24) by parts, and satisfying the boundary conditions, we obtain the functional (9.22)

$$J_e = \frac{12l^2}{T^3} \frac{1+\xi}{1+6x-x^3} \qquad \left(x = \frac{\alpha}{\beta T}\,\xi\right).$$

The minimum of this expression at $T_* = \sqrt{r}$ is attained when

$$\frac{\beta T}{\alpha} = \frac{3(2-x^2)}{1+2x^3} \tag{9.32}$$

and equals

$$J_e/J_l = \Phi_e/\Phi_l = (1+2x^3)^{-1}. \tag{9.33}$$

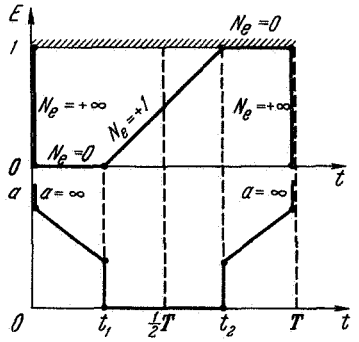

FIGURE 9.6. Optimum control of relative energy of accumulator E and thrust acceleration a in analogous problem of flight between two points of rest with ideally-throttlable power-limited propulsion system and energy storage.

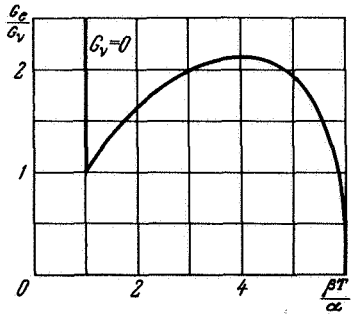

FIGURE 9.7. Optimum ratio of energy accumulator weight to power source weight, G_e/G_v, for flight between points of rest with ideally-throttlable power-limited engine.

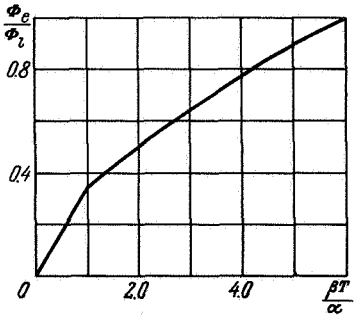

FIGURE 9.8. Relative decrease (due to use of accumulator) of functional Φ for flight between points of rest with ideally-throttlable power-limited engine.

Figure 9.7 shows the optimum ratio G_e/G_v (accumulator to source weight) as a function of the dimensionless parameter $\beta T/\alpha$ as given by (9.32). The decrease in the functional Φ when using an accumulator is shown in Figure 9.8. Employing the data of this figure the gain in payload is determined from either the first formula of (9.21) or Figure 9.4. It is seen that in the problem of flight between points of rest the power-limited propulsion system with an energy accumulator is better than the system without an accumulator over the range $1 \leqslant \beta T/\alpha \leqslant 6$. When $0 \leqslant \beta T/\alpha \leqslant 1$,
362 it is most efficient, as mentioned above, to use a system with an accumulator but without a power source ($G_v = 0$ in Figure 9.7), for which

$$\Phi_e/\Phi_l = {}^1/_3\,(\beta T/\alpha).$$

When rotating the plane of a circular orbit of radius r_0 through an angle i during s revolutions p_v varies according to

$$p_v^2 = b\cos^2 t$$

(the time t is represented as a fraction of $T_* = \sqrt{r_0/g_0}$, the period of revolution divided by 2π; g_0 is the gravitational acceleration when the radius is r_0). For an ideal power-limited propulsion system without an accumulator the functional (9.23) is given by (5.75)

$$J_i = \frac{r_0^2}{T_*^3}\frac{i^2}{s\pi}, \qquad \Phi_i = \frac{\alpha}{2g}J_i. \tag{9.34}$$

For the problem with accumulation it can be shown that the optimum control functions $E(t)$, $N_e(t)$, $a(t)$ are periodic functions of time over half a revolution. Their variation over one revolution is shown in Figure 9.9, where

$$t_{1,2} = {}^1/_2\,(\pi \mp \xi\alpha/\beta T_*),$$
$$t_{3,4} = t_{1,2} + \pi.$$

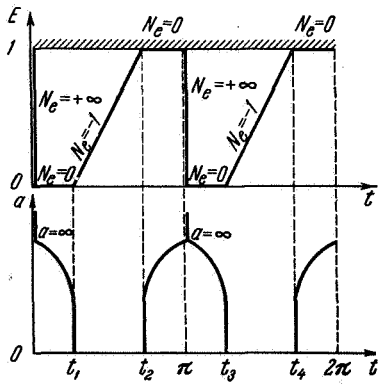

FIGURE 9.9. Optimum control of relative accumulator energy E and thrust acceleration a for rotation of plane of circular orbit with ideally-throttlable power-limited propulsion system and energy accumulator.

The formulas for the optimum value of ξ and the minimum ratio Φ_e/Φ are similar to (9.32) and (9.33), and are given by

$$\frac{\beta T_*}{\alpha} = \frac{1 + \cos x + 1/s}{\pi + \sin x - x\cos x}, \qquad \frac{\Phi_e}{\Phi_i} = \frac{\pi}{\pi + \sin x - x\cos x}. \tag{9.35}$$

The dependence of G_e/G_v and Φ_e/Φ_i on $\beta\pi T_*/\alpha$ (πT_* is the half-period of revolution, i.e., the maximum charging time) for different values of s is shown in Figures 9.10 and 9.11. It is seen that within the range $^1/_2 s \leqslant \beta\pi T_*/\alpha \leqslant 2 + 1/s$ a power-limited propulsion system with energy accumulation is most advantageous, and in the range $0 \leqslant \beta\pi T_*/\alpha \leqslant {}^1/_2 s$ a propulsion
363 system with energy accumulation and without power source is best; here $\Phi_e/\Phi_i = s\,(\beta\pi T_*/\alpha)$ (cf. the linear sections of Figure 9.11).

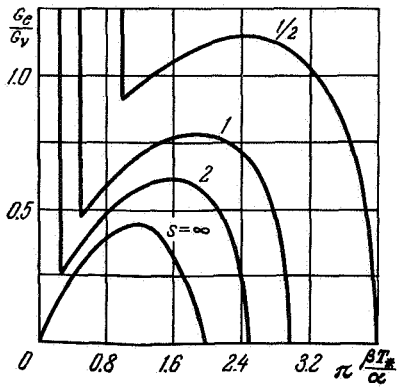

FIGURE 9.10. Optimum ratio of energy accumulator weight to power source weight, G_e/G_v, for rotation of plane of circular orbit with ideally-throttlable engine; s = number of revolutions along orbit during maneuver.

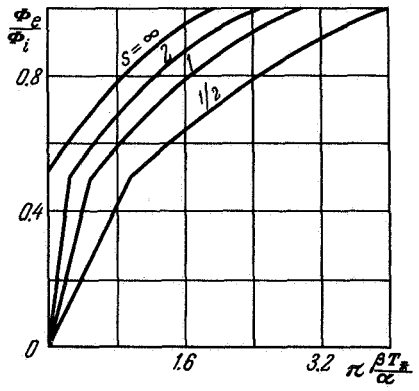

FIGURE 9.11. Relative decrease of functional Φ_e/Φ_i due to accumulator for rotation of plane of circular orbit with power-limited ideally-throttlable propulsion system.

As in the first example, the gain in payload is determined by the first formula of (9.21) or by Figure 9.4, using the data of Figure 9.11.

§ 2. POWER-LIMITED ENGINES WITH ENERGY ACCUMULATION: ADDITIONAL RESTRICTIONS ON THE CONTROL CHARACTERISTIC OF THE ENGINE

In the preceding section the engine was assumed ideally throttlable and weightless. The optimum operating regime of such an engine without an accumulator is the continuous regime (finite thrust, no specific restrictions); in fact, since the power fed to the engine is finite, the exhaust velocity drops with increasing thrust. With an accumulator we may have impulsive regimes (infinite thrust), since an infinite power can be fed to the engine.

In addition to these sections with impulsive applications of the thrust, the optimum control function contains, as before, sections of finite thrust.

The assumption of a weightless engine is hardly applicable in this case, since its unit weight is large, and the optimum thrust is infinite at some instants of time. In addition, heavy restrictions are imposed on the
364 engine operation since the thrust must be varied from finite values to infinity. We shall investigate how the actual properties of the engine influence the parameters of the optimum motion in the following cases.

1) The thrust and the power N_γ fed to the engine are either constant or zero; the engine weight is proportional to the power used (discussed in subsection 1 according to the treatment in /9.3/).

2) The thrust is unbounded but the engine power has an upper bound; the engine weight is proportional to the maximum power used (discussed in subsection 2 according to /9.7/).

3) The thrust is unbounded and the engine power is constant (or equal to zero); the engine weight is proportional to the power used (discussed in subsection 3 according to /9.7, 9.9/).

4) The thrust has upper and lower bounds (or is equal to zero) and the engine power is constant (or equal to zero); the engine weight is proportional to the power (discussed in subsection 4 according to /9.7/).

5) The thrust and power of the engine are unlimited and the exhaust velocity has an upper bound; the engine is weightless (discussed in subsection 5 according to /9.10/).

6) The operating time of the engine is limited, the thrust is unbounded, and the engine power is constant (or equal to zero); the engine weight is proportional to the power used (discussed in subsection 6 according to /9.7/).

If the vehicle weight varies little, the conditions imposed on the thrust in cases 1) and 4) are replaced by corresponding conditions for the thrust acceleration.

1. **Unthrottled engine.** An unthrottled propulsion system has constant thrust (for constant power of the jet). We allow variation of the thrust direction and engine cut off. This second limiting case yields the lower limits of the system.

The first two equations of (9.7) for this case are written somewhat differently in the form

$$\dot{G}_\sigma = -k_1 P/N_\gamma,\ \dot{E} = k_2\,[N_\nu\,(1-P) - (N_\gamma - 1)\,P] \qquad (P\,(t) = 1 \text{ or } 0,\ N_\gamma = \text{const},\ 0 \leqslant N_\nu\,(t) \leqslant 1). \tag{9.36}$$

The control function $P\,(t)$ can only take the two values zero and unity (the exponent of P in (9.7) can therefore be omitted). The power N_γ used by the engine is constant and represents the control parameter (as a fraction of N_{ν_0}). In the powered sections ($P = 1$) we have a discharge at constant power $N_\gamma - 1$, where $E = -k_2\,(N_\gamma - 1)$, and in the coasting sections ($P = 0$) we have charging at a power $0 \leqslant N_\nu\,(t) \leqslant 1$, where $\dot{E} = k_2 N_\nu$.

The equations of motion are written as before, and the control function $\mathbf{e}\,(t)$ (direction of the thrust vector) remains.

The condition for constant thrust is replaced for simplicity by the
365 condition for a constant thrust acceleration (9.18). This substitution is correct if the relative weight of the working fluid G_μ is considerably less

than unity. In addition, the weight of the engine, unlike (9.6), is taken proportional to the power used, i.e.,

$$G_\gamma = (\gamma/\alpha)\, G_v N_\gamma. \tag{9.37}$$

As in the preceding section, it is possible with such an approximation to find the optimum weight of the power source before solving the complete problem. The weight of the payload G_π and the weight of the propulsion system $G_\varkappa = G_v + G_e + G_\gamma$ will be expressed by (9.21), where

$$\Phi_e = \left(1 + \xi + \frac{\gamma}{\alpha} N_\gamma\right) \frac{\alpha}{2g} \int_0^T \frac{a^2 dt}{N_\gamma}. \tag{9.38}$$

For a system without accumulation the functional Φ (allowing for the engine weight (9.37)) will be equal to

$$\Phi^* = \left(1 + \frac{\gamma}{\alpha}\right) \frac{\alpha}{2g} \int_0^T a^2 dt \tag{9.39}$$

(in (9.38) and (9.39) $a^2(t) = a_0^2 P(t)$, $a_0 = \text{const}$, $P(t) = 1$ or 0). The variational problem is written in a form similar to (9.24):

$$\left.\begin{aligned}
&\dot J_e = \left(\frac{1+\xi}{N_\gamma} + \frac{\gamma}{\alpha}\right) a_0^2 P, && J_e(0) = 0, \quad J_e(T) = \min,\\
&\dot E = \frac{\beta}{\alpha\xi}\left[N_v(1-P) - (N_\gamma - 1)\, P\right], && E(0) = 1, \quad E(T) = 0,\\
&\dot{\mathbf{r}} = \mathbf{v}, && \mathbf{r}(0) = \mathbf{r}_0, \quad \mathbf{r}(T) = \mathbf{r}_1,\\
&\dot{\mathbf{v}} = a_0 P \mathbf{e} + \mathfrak{R}, && \mathbf{v}(0) = \mathbf{v}_0, \quad \mathbf{v}(T) = \mathbf{v}_1\\
&P(t) = 1 \text{ or } 0, \quad 0 \leqslant N_v(t) \leqslant 1, && |\mathbf{e}(t)| \equiv 1,\\
& && 0 \leqslant E(t) \leqslant 1;\ N_\gamma,\ \xi,\ a_0 = \text{const}).
\end{aligned}\right\} \tag{9.40}$$

In addition to the control functions $P(t)$, $N_v(t)$, $\mathbf{e}(t)$, the problem contains three constant control parameters a_0, N_γ and ξ. To select the optimum values of these parameters we can use the method described in subsection 2 of the preceding section.

Without explicitly writing the optimum control functions, we give the results for the analogous problems treated in § 1.

For the displacement between points of rest the ratio of functionals (9.38) and (9.39) is

$$\frac{\Phi_e}{\Phi_i^*} = \frac{4\left[\varepsilon(1 - 4t_* + 2t_*^2) - 2t_*^2\right]}{27 t_*^2 (1 - 4t_*)(1 - t_*)^2 (1 + \varepsilon)} \qquad \left(\varepsilon = \frac{\gamma}{\alpha}\right), \tag{9.41}$$

366 where the optimum parameters ξ and t_*, which replace $a_0 = t_*^{-1}(1 - t_*)^{-1}$, $N_\gamma = (1 - t_*)\, t_*^{-1}$, are found from the relations

$$\xi = \frac{\beta T}{\alpha}(1 - 2t_*), \qquad \frac{\beta T}{\alpha} = \frac{\varepsilon(1 - t_*)(1 - 3t_*) - 3t_*^2}{t_*^2(1 - 4t_*)}. \tag{9.42}$$

For $\beta T/\alpha \leqslant (\beta T/\alpha)^*$ it is more efficient not to use a power source; then

$$\frac{\Phi_e}{\Phi_i^*} = \frac{2\varepsilon}{27 t_*^2 (1 - t_*)(1 + \varepsilon)} \qquad \left(2t_*^2 - \frac{\beta T}{\alpha}(1 - 3t_*) = 0\right). \tag{9.43}$$

The dependence of the ratios G_e/G_v and functionals Φ_e/Φ_l^* on $\beta T/\alpha$ for different values of $\varepsilon = \gamma/\alpha$ (ratio of unit engine weight to unit power-source weight) is shown in Figures 9.12 and 9.13.

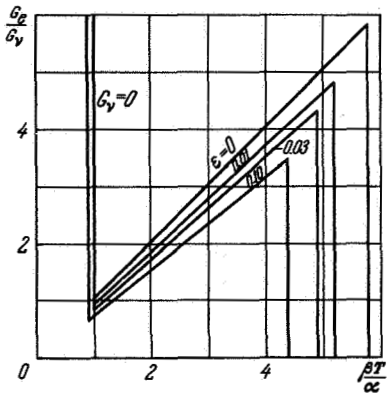

FIGURE 9.12. Optimum ratio of accumulator weight to power-source weight G_e/G_v for flight between points of rest with unthrottled power-limited propulsion system ($\alpha = 0$ or a_0); ε is ratio of unit weight of engine to unit weight of power source.

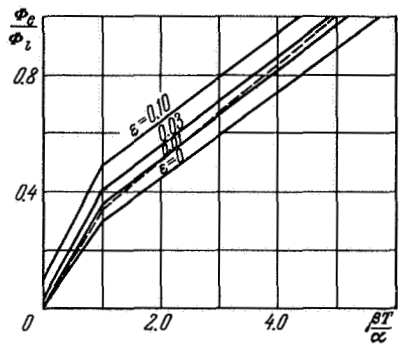

FIGURE 9.13. Decrease of functional Φ as result of using accumulator in flight between points of rest with unthrottled power-limited engine; dashed curve represents relative decrease of functional Φ_e / Φ_l compared with ideally-throttlable engine for $\varepsilon = 0$.

In this problem the value of J for a constant thrust acceleration with cutoff is (cf. (9.31))

$$J_l^* = 13.5\,\frac{l^2}{T^3}\left(1+\frac{\gamma}{\alpha}\right), \quad \Phi_l^* = 6.75\,\frac{\alpha}{g}\,\frac{l^2}{T^3}\left(1+\frac{\gamma}{\alpha}\right). \tag{9.44}$$

The ratio Φ_e/Φ_l for $\gamma/\alpha = 0$ (instead of Φ_e/Φ_l^*) has also been plotted in
367 Figure 9.13 for comparison (dashed line). Comparing this dashed line with Figure 9.8, we see that as in the case of a power-limited propulsion system without accumulation, the transition from the ideally-throttlable system requires a small increase in the functional Φ. By decreasing the parameter $\beta T/\alpha$ the difference vanishes, since both systems pass into an impulsive regime.

When rotating the orbital plane the ratio of the functionals is equal to

$$\left.\begin{aligned} \frac{\Phi_e}{\Phi_i^*} &= \frac{1.45\,[t_*^2 \operatorname{tg} t_* + \varepsilon\pi t_* \operatorname{tg} t_* (t_* - \pi/4)]}{\pi(1+\varepsilon)\sin^2 t_*\,[t_*(\pi - 2t_*) - (\pi - 3t_*)\operatorname{tg} t_*]} \\ \left(\xi = \frac{\beta T_*}{\alpha}(\pi - 2t_*),\ \frac{\beta T}{\alpha} &= \frac{(t_* + {}^1/_4\,\varepsilon\pi)\operatorname{tg} t_* - {}^1/_2\,\varepsilon\pi t_* - t_*^2}{t_*^2(\pi - 2t_*) - (\pi - 3t_*)\,t_*\operatorname{tg} t_*},\right. \\ a_0 &= \frac{i}{4s\sin t_*},\quad N_\gamma = \frac{\pi}{2t_*},\quad \left.J_i^* = \frac{r_0^2 i^2}{2.9 s T_*^2}\right). \end{aligned}\right\} \tag{9.45}$$

The system without a power source is more advantageous in the region $0 \leqslant \beta T_*/\alpha \leqslant (\beta T_*/\alpha)^*$ for which

$$\left.\begin{aligned} \frac{\Phi_e}{\Phi_i^*} &= \frac{0.3625 t_* \varepsilon}{(1+\varepsilon)(\sin t_* - t_* \cos t_*)\sin t_*} \\ \left(\frac{\beta T_*}{\alpha} &= \varepsilon\,\frac{2t_* \cos t_* - \sin t_*}{8 s t_* (\sin t_* - t_* \cos t_*)}\right). \end{aligned}\right\} \tag{9.46}$$

Figures 9.14 and 9.15 were plotted according to these relations. The gain in payload due to using an accumulator is determined as above, with
368 the aid of Figure 9.4 or the first formula of (9.21).

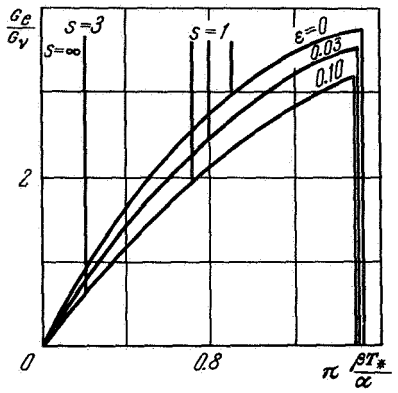

FIGURE 9.14. Optimum ratio of accumulator weight to power-source weight G_e/G_γ for rotating plane of circular orbit with unthrottled propulsion system; s is number of revolutions along orbit during maneuver.

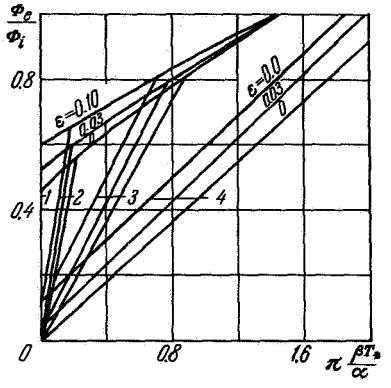

FIGURE 9.15. Relative decrease of functional Φ as result of using accumulator for rotating plane of circular orbit with unthrottled power-limited engine: 1) $s=\infty$, 2) $s=3$, 3) $s=1$, 4) $s={}^1/_2$.

2. **Power-limited engine.** In the above case of an unthrottled engine the impulsive regimes of thrust application were excluded both by directly restricting the thrust and by allowing for the engine weight. The effect of these two restrictions will now be examined separately.

Let the engine thrust be unbounded, while its power has an upper bound. As in case 1), the engine weight is assumed proportional to the maximum power it uses. The control characteristic and the weight formula of the propulsion system with energy accumulation and this type of engine are written as follows (cf. (9.1) to (9.6)):

$$\left.\begin{aligned} &P = qV, \quad N_\gamma = {}^1/_2\, qV^2 = N_v + N_e, \quad \dot{E} = -N_e \\ &(P \geqslant 0,\ 0 \leqslant N_\gamma \leqslant N_{\gamma 0}, \\ &0 \leqslant N_v \leqslant N_{v0},\ N_{\gamma 0} - N_{v0} \geqslant N_e \geqslant -N_v,\ 0 \leqslant E \leqslant E_0), \\ &G_\gamma = \gamma N_{\gamma 0},\ G_v = \alpha N_{v0},\ G_e = \beta E_0. \end{aligned}\right\} \tag{9.47}$$

This problem of the maximum payload is also reduced to the variational problem for the minimum of the functional

$$J_e = (1 + \xi + \varepsilon N_{\gamma 0}) \int_0^T \frac{a^2 dt}{N_v (1 + N_e)} \tag{9.48}$$

$(0 \leqslant N_v(t) \leqslant 1,\ -1 \leqslant N_e(t) \leqslant N_{\gamma 0} - 1,\ a(t) \geqslant 0,\ N_{\gamma 0}$ is represented as a fraction of $N_{v0})$.

The optimum values of the control functions, obtained by Pontryagin's method /9.4/, are

$$\mathbf{e} = \frac{p_v}{p_v},\quad N_v = 1,\quad a = \frac{p_v (1 + N_e)}{2 (1 + \xi + \varepsilon N_{\gamma 0})}, \tag{9.49}$$

$$N_e = \begin{cases} N_{\gamma 0} - 1 & \text{at } \Delta > 0 \text{ and } 0 < E < 1, \\ -1 & \text{at } \Delta < 0 \text{ and } 0 < E < 1, \\ 0 & \text{at } E = 0 \text{ and } E = 1 \end{cases} \tag{9.49}$$

$$\left(\Delta = \frac{p_v^2}{4(1+\xi+\varepsilon N_{\gamma 0})} - p_e \frac{\beta}{\alpha\xi},\ p_e > 0\right).$$

The determination of the optimum sequence of accumulator charge and discharge intervals has been described above. As an illustration we consider the problem of the displacement between two points of rest at a distance l apart in a gravity-free field ($\mathfrak{R} = 0$) where E has the symmetrical
369 boundary conditions $E(0) = E(T) = 1/2$. This excludes propulsion systems having energy accumulation but no power source.

If $x = N_{\gamma 0} - 1$, $z = \xi\alpha/\beta T$, we can write the functional J_e as

$$J_e = \frac{12x^2[1 + (\beta T/\alpha)z + (1+x)\varepsilon]}{(1+3x-z^3)x^2 - 3z^2x + z^3} l^2 T^{-3}. \tag{9.50}$$

The values of the parameters x and z for which J_e has a minimum can be determined from

$$\left.\begin{aligned} x^3(1+2z^3)\varepsilon - 3xz^2(1+\varepsilon) + 2z^3(1+\varepsilon) = 0, \\ (\beta T/\alpha)z^2(3x-2z) - 3\varepsilon x[(x-z)^2 - x^2z^2] = 0. \end{aligned}\right\} \tag{9.51}$$

The efficiency of an energy accumulator is given by the ratio of the functional J_e to the corresponding functional J_l for the system without accumulation (for the given problem $J_l = 12(1+\varepsilon)l^2T^{-3}$). This ratio can be written in terms of x and z (solutions of (9.51)) in the form

$$\frac{J_e}{J_l} = \frac{\varepsilon x^3}{(1+\varepsilon)(3x-2z)z^2}. \tag{9.52}$$

The quantity J_e/J_l has been plotted in Figure 9.16 as a function of $\beta T/\alpha$ for two ratios of the unit weights of the engine and the power source: $\varepsilon = 0.1$ and $\varepsilon = 0.001$. As in Figures 9.13 and 9.15, the increase in the relative weight of the engine ε is accompanied by a decrease in the functional J (and respectively in the payload) produced by using an energy

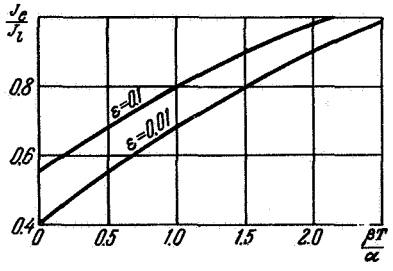

FIGURE 9.16. Influence of relative weight of engine ε on decrease of functional J for flight between two points of rest (with symmetrical boundary conditions) using energy accumulator.

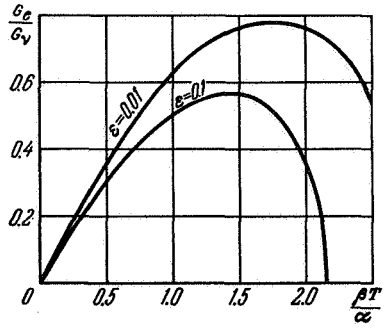

FIGURE 9.17. Influence of relative engine weight ε on optimum ratio of accumulator weight to power-source weight.

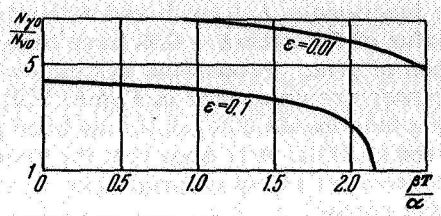

FIGURE 9.18. Values of maximum engine power (represented as fraction of power-source power) for flight between points of rest using energy accumulator.

370 accumulator. The dependence of the optimum value of the parameter $\xi = G_e/G_v$ on the quantity $\beta T/\alpha$ for this problem is shown in Figure 9.17, while Figure 9.18 shows how the maximum power of the engine $N_{\gamma 0}$ (as a fraction of the power-source power N_{v0}) varies with $\beta T/\alpha$.

3. **Constant-power engine.** If the only assumption is that the engine weight is proportional to the maximum power (as in case 2)), the power consumed by the engine in the optimum case during accumulator discharge can exceed by five to ten times the power at which it operates during the remaining part of the powered flight (Figure 9.18). As in case 1), we consider propulsion systems with a constant engine power N_γ (selected from optimum considerations), but without directly restricting the thrust. It will again be assumed that the engine weight is proportional to the power N_γ.

For such a system the differential equations (cf. (9.40)) become

$$\dot{J}_e = \left(\frac{1+\xi}{N_\gamma} + \varepsilon\right) a^2\delta, \quad \dot{E} = -\frac{\beta}{\alpha\xi}(N_\gamma\delta - N_v),$$
$$\dot{\mathbf{r}} = \mathbf{v}, \quad \dot{\mathbf{v}} = a\delta\mathbf{e} + \mathbf{R} \tag{9.53}$$

(N_γ = const is expressed as a fraction of N_{v0}, $\delta(t) = 1$ or 0, $0 \leqslant N_v(t) \leqslant 1$, $0 \leqslant E(t) \leqslant 1$, $a(t) \geqslant 0$). The boundary conditions given in (9.40) remain unchanged. The control function δ takes the value 1 along the powered sections and 0 along the coasting sections. It can be shown that the optimum forms of $a(t)$ and $\delta(t)$ are

$$\left.\begin{aligned} a &= \frac{1}{2} p_v \left(\frac{1+\xi}{N_\gamma} + \varepsilon\right)^{-1}, \\ \delta &= \begin{cases} 1 & \text{at } \Delta > 0, \\ 0 & \text{at } \Delta < 0 \end{cases} \\ \left(\Delta &= \frac{1}{4} p_v^2 \left(\frac{1+\xi}{N_\gamma} + \varepsilon\right)^{-1} - \frac{\beta}{\alpha\xi} p_e N_\gamma, \quad p_e > 0\right). \end{aligned}\right\} \tag{9.54}$$

371 The control functions $\mathbf{e}(t)$ and $N_v(t)$ are of the same forms as in the cases considered above. For flight in a gravity-free field between two points of rest with symmetrical boundary conditions $E(0) = E(T) = 1/2$ the functional J_e is equal to

$$J_e = 12 l^2 T^{-3} \frac{[1 + (\beta T/\alpha) z](1-z) + \varepsilon}{1 - z^3} \quad \left(z = \frac{\xi\alpha}{\beta T}\right) \tag{9.55}$$

and has a minimum when z satisfies the relation

$$\frac{\beta T}{\alpha} = \frac{(1+2z)(1-z^3) - 3z^3\varepsilon}{(1-z^2)(1-z)^2}. \tag{9.56}$$

The ratio of the functionals J_e/J_i (with and without an energy accumulator) and the optimum value of the ratio $\xi = G_e/G_v$ have been plotted in Figures 9.19 and 9.20 as functions of $\beta T/\alpha$. Propulsion systems with constant and unbounded engine power are compared in Figure 9.21, where the ratio of the corresponding functionals $(J_e)_{N=\text{const}}/J_e$ has been plotted as a function of $\beta T/\alpha$ (cf. (9.50) and (9.55)). It is seen that the requirement of constant engine power has a stronger effect on propulsion systems with a lower relative weight of the engine.

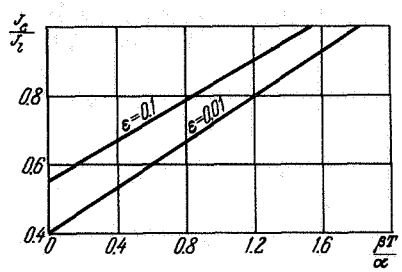

FIGURE 9.19. Decrease of functional J for flight between two points of rest (with symmetrical boundary conditions) using energy accumulator and constant-power engine.

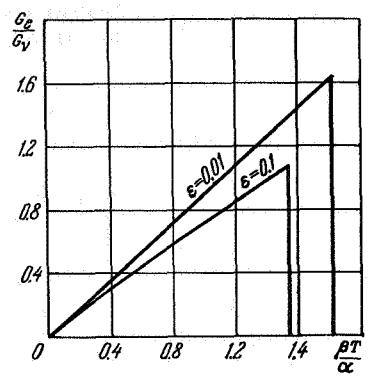

FIGURE 9.20. Optimum ratio of energy-accumulator weight to power-source weight for flight between two points of rest with constant-power engine.

Consider motion along nearly-circular orbits. The equations of plane motion in a central gravitational field can be written as follows (A.15):

$$\left.\begin{aligned} \dot{r} &= v\sin\vartheta, \quad \dot{v} = a\cos\gamma - r^{-2}\sin\vartheta, \\ r\dot{\varphi} &= v\cos\vartheta, \quad v\dot{\vartheta} = a\sin\gamma + (v^2/r - 1/r^2)\cos\vartheta. \end{aligned}\right\} \tag{9.57}$$

372 Equations (9.57) are dimensionless. The magnitude r gives the distance of the vehicle center of mass from the attracting center as a fraction of the initial radius, and v is the vehicle velocity as a fraction of the velocity of free motion along the orbit of the original radius. The thrust acceleration a is expressed as a fraction of the gravitational acceleration at a distance from the center equal to the original radius, and the time is represented as a fraction of the period of revolution along the circular orbit of the original radius, divided by 2π. The angles φ, ϑ, and γ are shown on the Figure in (A.2).

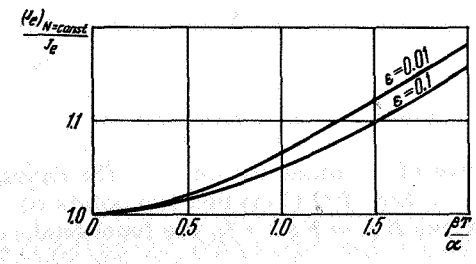

FIGURE 9.21. Restricting influence of constant-thrust engine on increase of functional J for flight between two points of rest using energy accumulator.

We now consider maneuvers for which the instantaneous values of the coordinates and velocities of the center of mass of the vehicle differ from the corresponding ones for free

motion along the circular orbit of the original radius by amounts much smaller than unity. Denote these new values by

$$r = 1 + \eta, \quad \varphi = t + \xi, \quad v = 1 + \zeta$$
$$(\eta, \dot{\eta}, \xi, \zeta, \dot{\xi}, \vartheta, \dot{\vartheta} \ll 1). \tag{9.58}$$

If relations (9.58) are substituted into (9.57) and we restrict ourselves to first-order terms, the linearized system of equations of motion

$$\left.\begin{aligned} \dot{\eta} &= \vartheta, & \dot{\zeta} &= a\delta\cos\gamma - \vartheta, \\ \dot{\xi} &= \zeta - \eta, & \dot{\vartheta} &= a\delta\sin\gamma + \eta + 2\zeta \end{aligned}\right\} \tag{9.59}$$

are obtained ($\delta(t)$ is the step control function equal to 1 along the powered sections of the flight and 0 along the coasting sections).

The boundary conditions for the system consisting of (9.59) and the first two equations of (9.53), together with the symmetrical conditions for E, are

$$\left.\begin{aligned} J_e(0) = 0, \quad E(0) = \tfrac{1}{2}, \quad \eta(0) = \eta_0, \quad \xi(0) = \xi_0, \\ \zeta(0) = \zeta_0, \quad \vartheta(0) = \vartheta_0, \\ J_e(T) = \min, \quad E(T) = \tfrac{1}{2}, \quad \eta(T) = \eta_1, \quad \xi(T) = \xi_1, \\ \zeta(T) = \zeta_1, \quad \vartheta(T) = \vartheta_1. \end{aligned}\right\} \tag{9.60}$$

373 Using the maximum principle, we obtain the following expressions for the optimum control functions:

$$\left.\begin{aligned} N_v = 1, \quad a = \tfrac{1}{2}\sqrt{p_\zeta^2 + p_\vartheta^2}\left(\frac{1+\xi}{N_\gamma} + \varepsilon\right)^{-1}, \\ \gamma = \arcsin\left[p_\vartheta (p_\zeta^2 + p_\vartheta^2)^{-1/2}\right] = \arccos\left[p_\zeta (p_\zeta^2 + p_\vartheta^2)^{-1/2}\right], \\ \delta = \begin{cases} 1 & \text{at } \Delta > 0 \\ 0 & \text{at } \Delta < 0 \end{cases} \\ \left(\Delta = \tfrac{1}{4}(p_\zeta^2 + p_\vartheta^2)\left(\frac{1+\xi}{N_\gamma} + \varepsilon\right)^{-1} - \frac{\beta}{\alpha\xi} p_e N_\gamma\right). \end{aligned}\right\} \tag{9.61}$$

The momentum equations

$$\dot{p}_\eta = p_\xi - p_\vartheta, \quad \dot{p}_\xi = 0, \quad \dot{p}_\zeta = -p_\xi - 2p_\vartheta,$$
$$\dot{p}_\vartheta = -p_\eta + p_\vartheta, \quad \dot{p}_e = 0 \tag{9.62}$$

are integrated independently of the main system to yield

$$\left.\begin{aligned} p_\xi &= b_1, \quad p_\vartheta = b_2\sin t + b_3\cos t - 2b_1, \\ p_\zeta &= 2b_2\cos t - 2b_3\sin t + 3b_1 t + b_4, \\ p_\eta &= b_2\cos t - b_3\sin t + 3b_1 t + b_4. \end{aligned}\right\} \tag{9.63}$$

The quantities b_1, b_2, b_3, b_4 are integration constants.

The optimum sequence of powered and coasting sections along the trajectory was investigated above. The integration constants of the equations of motion and the constants b_1, b_2, b_3, b_4 are determined from the boundary conditions (9.60) governing each specific maneuver.

As a first example we consider the problem of the optimum rendezvous of two vehicles trajected along the same circular orbit, revolving in the same direction, and situated at time $t = 0$ at an angular displacement φ_0. The rendezvous is to be realized after one of the vehicles (assumed unthrottled) has made half a revolution along the orbit ($T = \pi$). The boundary conditions (9.60) then have the form

$$\left.\begin{aligned} &J_e(0) = 0,\ E(0) = {}^1/_2,\ \eta(0) = 0,\quad \xi(0) = 0,\quad \zeta(0) = 0,\quad \vartheta(0) = 0,\\ &J_e(\pi) = \min,\ E(\pi) = {}^1/_2,\ \eta(\pi) = 0,\ \xi(\pi) = \varphi_0,\ \zeta(\pi) = 0,\ \vartheta(\pi) = 0. \end{aligned}\right\} \tag{9.64}$$

374 The optimum programs for the control functions are

$$\left.\begin{aligned} &a = \sqrt{a_1^2 (t - \pi/2)^2 + a_2^2},\\ &\delta = \begin{cases} 1 & \text{at } 0 \leqslant t < \tau \text{ и } \pi - \tau < t \leqslant \pi,\\ 0 & \text{at } \tau < t < \pi - \tau, \end{cases}\\ &\gamma = \arcsin \frac{a_2}{a} = \arccos \frac{a_1 (t - \pi/2)}{a}. \end{aligned}\right\} \tag{9.65}$$

The constants a_1 and a_2 can be expressed in terms of φ_0 and the duration time of the powered sections τ, so that

$$\left.\begin{aligned} a_1 &= \frac{-4\varphi_0 (1 - \cos\tau)}{16\tau [2(1 - \cos\tau) + (\pi - 2\tau)\sin\tau] - (1 - \cos\tau)[\pi^3 - (\pi - 2\tau)^3]},\\ a_2 &= \frac{4\varphi_0 [2(1 - \cos\tau) + (\pi - 2\tau)\sin\tau]}{16\tau [2(1 - \cos\tau) + (\pi - 2\tau)\sin\tau] - (1 - \cos\tau)[\pi^3 - (\pi - 2\tau)^3]}. \end{aligned}\right\} \tag{9.66}$$

The functional J_e for the problem stated is expressed as follows in terms of φ_0 and τ:

$$J_e = \frac{4\varphi_0^2 \{24\tau L^2(\tau) + (1 - \cos\tau)^2 [\pi^3 - (\pi - 2\tau)^3]\} M(\tau)}{3\pi 16\tau L^2(\tau) - (1 - \cos\tau)[\pi^3 - (\pi - 2\tau)^3]^2}, \tag{9.67}$$

where

$$L(\tau) = 2(1 - \cos\tau) + (\pi - 2\tau)\sin\tau,$$
$$M(\tau) = \left\{2\tau\left[1 + \frac{\beta T}{\alpha}(\pi - 2\tau) + \pi\varepsilon\right]\right\}.$$

The values of the parameters ξ and N_γ are linked with τ via the relations

$$\xi = \frac{\beta T}{\alpha}(\pi - 2\tau),\ N_\gamma = \frac{\pi}{2\tau}. \tag{9.68}$$

For a power-limited propulsion system without energy accumulation, the value of the functional J for the maneuver considered is

$$J = \frac{4\varphi_0^2 (48 + \pi^2)(1 + \varepsilon)}{3\pi (16 - \pi^2)^2}. \tag{9.69}$$

Figure 9.22 shows the ratio of the functionals as given by (9.67) and (9.69). This ratio is a function of the unit weights of the energy accumulator β and the power source α, and is plotted for two values of the relative
375 engine weight $\varepsilon = 0.1$ and 0.01. Energy accumulation is expedient as long as the ratio J_e/J does not exceed unity. The gain in the payload when using an energy accumulator is determined as above from the decrease in the

functional, and using either the data of Figure 9.4 or the first formula of (9.21). The curves on Figure 9.23 determine the optimum values of the parameters

$$\xi = G_e/G_v \text{ and } N_\gamma,$$

which minimize the functional J_e.

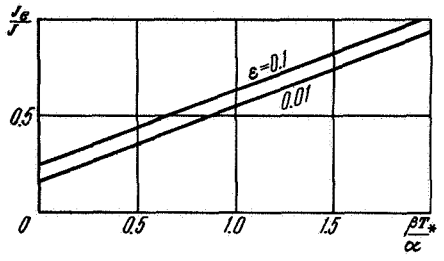

FIGURE 9.22. Decrease of functional J in rendezvous problem of vehicles on circular orbit using energy accumulation and constant-power engine.

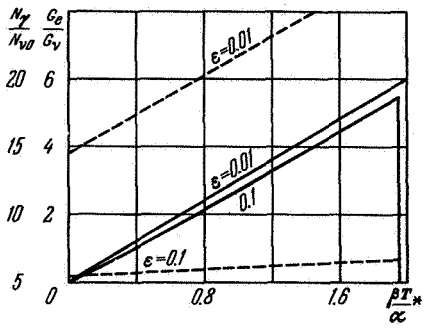

FIGURE 9.23. Ratio of energy-accumulator weight to power-source weight G_e/G_v (solid lines) and relative power of engine (dashed lines) in rendezvous problem of vehicles on circular orbit using energy accumulation.

As a second example we consider the transfer from the circular orbit of radius $r = 1 + \eta_0$ to a circular orbit of radius $r = 1$. The boundary conditions (9.60) here become

$$\begin{aligned} &J_e(0) = 0,\ E(0) = {}^1/_2, && \eta(0) = \eta_0, && J_e(\pi) = \min,\ E(\pi) = {}^1/_2, && \eta(\pi) = 0, \\ &\xi(0) = 0,\ \zeta(0) = -{}^1/_2\eta_0, && \vartheta(0) = 0, && \xi(\pi) = \text{opt},\ \zeta(\pi) = 0, && \vartheta(\pi) = 0. \end{aligned} \qquad (9.70)$$

The initial condition for ζ is obtained by linearizing the relation $r^3\omega^2 = \text{const}$ which links the radii r and the angular velocities ω of the bodies traveling along circular orbits and around the same central body. The value of the angular displacement coordinate $\xi(\pi)$ is not fixed beforehand.

It is assumed that the thrust-acceleration vector is directed along the tangent to the trajectory ($\gamma = 0$ or $\gamma = \pi$). Introduce the control function $e = \cos\gamma$, which takes the value 1 at $\gamma = 0$ and -1 at $\gamma = \pi$, instead of the angle γ, and write the equations of motion as

$$\dot\eta = \vartheta \quad \dot\xi = \zeta - \eta,\ \dot\zeta = ae\delta - \vartheta,\ \dot\vartheta = 2\zeta + \eta. \qquad (9.71)$$

The system of optimum control functions (9.61) becomes

$$\left.\begin{aligned} &N_v = 1, \quad a = \tfrac{1}{2}|p_\zeta|\left(\frac{1+\xi}{N_\gamma} + \varepsilon\right)^{-1}, \quad e = \operatorname{sgn} p_\zeta, \\ &\delta = \begin{cases} 1 \text{ at } \Delta > 0, \\ 0 \text{ at } \Delta < 0 \end{cases} \left(\Delta = \tfrac{1}{4}p_\zeta^2\left(\frac{1+\xi}{N_\gamma} + \varepsilon\right)^{-1} - \frac{\beta}{\alpha\xi}p_e N_\gamma\right). \end{aligned}\right\} \qquad (9.72)$$

376 As in the first example, the trajectory consists of two powered sections of duration periods τ, separated by one coasting section. The optimum program of thrust acceleration is written in the form

$$ae = a_1 - a_2 \sin t, \tag{9.73}$$

where

$$a_1 = \frac{-1/2\,\eta_0(\tau - \sin\tau\cos\tau)}{2\tau(\tau - \sin\tau\cos\tau) - 4(1-\cos\tau)^2},$$

$$a_2 = \frac{-\eta_0(1-\cos\tau)}{2\tau(\tau - \sin\tau\cos\tau) - 4(1-\cos\tau)^2}.$$

The value of the functional J_e is

$$J_e = \frac{\eta_0^2(2\tau - \sin 2\tau)\{2\tau[1 + (\beta T/\alpha)(\pi - 2\tau)] + \pi\varepsilon\}}{4\pi[2\tau(2\tau - \sin 2\tau) - 8(1-\cos\tau)^2]}. \tag{9.74}$$

Figure 9.24 compares the decrease in the functional J of the problem considered with the corresponding functional J_η for a propulsion system without an energy accumulator

$$J_\eta = \frac{\pi\eta_0^2(1+\varepsilon)}{4(\pi^2 - 8)}. \tag{9.75}$$

The optimum values $\xi = G_e/G_v$, N_γ are illustrated in Figure 9.25.

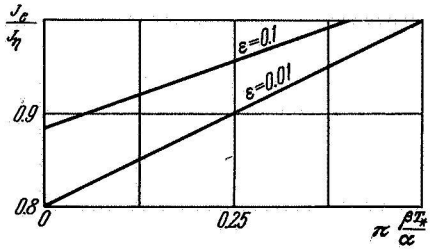

FIGURE 9.24. Decrease of functional J for transfer between nearly equal circular orbits using energy accumulator and constant-power engine.

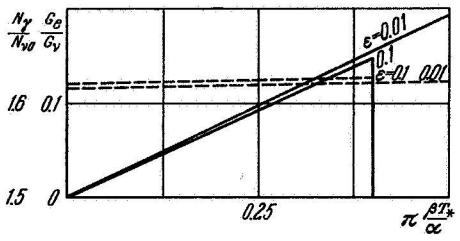

FIGURE 9.25. Ratio of energy-accumulator weight to power-source weight (solid lines) and relative power of engine (dashed lines) for transfer between nearly equal circular orbits.

As a third example we consider the problem of correcting the velocity-vector direction. Let the velocity vector of the vehicle make an angle ϑ_0 with the tangent to the reference orbit at time $t = 0$. The maneuver consists in stabilizing the vehicle motion on the reference orbit throughout a time equal to half its period of revolution ($T = \pi$). The angular displacement $\xi(\pi)$ is arbitrary (as in the preceding example). The boundary conditions are

$$\left.\begin{array}{lll} J_e(0) = 0, & E(0) = 1/2, & \eta(0) = 0, \\ \xi(0) = 0, & \zeta(0) = 0, & \vartheta(0) = \vartheta_0, \\ J_e(\pi) = \min, & E(\pi) = 1/2, & \eta(\pi) = 0, \\ \xi(\pi) = \text{opt}, & \zeta(\pi) = 0, & \vartheta(\pi) = 0. \end{array}\right\} \tag{9.76}$$

377 The thrust-acceleration vector is directed along the normal to the trajectory ($\gamma = {}^1/_2\pi$ or $\gamma = -{}^1/_2\pi$), and the equations of motion (9.59) are written in the form

$$\dot\eta = \vartheta, \quad \dot\xi = \zeta - \eta, \quad \dot\zeta = -\vartheta, \quad \dot\vartheta = ae\delta + \eta + 2\zeta \qquad (e = \sin\gamma = \pm 1). \tag{9.77}$$

The optimum control functions are determined by

$$\left.\begin{aligned} &N_\nu = 1, \quad ae = \tfrac{1}{2} p_\vartheta \left(\frac{1+\xi}{N_\gamma} + \varepsilon\right)^{-1}, \\ &\delta = \begin{cases} 1 & \text{at } \Delta > 0, \\ 0 & \text{at } \Delta < 0 \end{cases} \\ &\left(\Delta = \tfrac{1}{4} p_\vartheta^2 \left(\frac{1+\xi}{N_\gamma} + \varepsilon\right)^{-1} - \frac{\beta}{\alpha\xi} p_e N_\gamma\right), \end{aligned}\right\} \tag{9.78}$$

or

$$ae = a_1 \cos t \quad (a_1 = -2\vartheta_0 (2\tau + \sin 2\tau)^{-1}); \tag{9.79}$$

the sequence of powered and coasting sections along the trajectory coincides with the preceding examples.

The value of the functional J_e is

$$J_e = \frac{2\vartheta_0^2 \{2\tau [1 + (\beta T/\alpha)(\pi - 2\tau)] + \pi\varepsilon\}}{\pi (2\tau - \sin 2\tau)}, \tag{9.80}$$

and the corresponding value of the functional J_ϑ for a propulsion system without energy accumulation is

$$J_\vartheta = \frac{2}{\pi}\vartheta_0^2 (1 + \varepsilon). \tag{9.81}$$

The ratio of J_e to J_ϑ and the optimum values of the parameters $\xi = G_e/G_\nu$, $N_\gamma/N_{\nu 0}$ are shown in Figure 9.26.

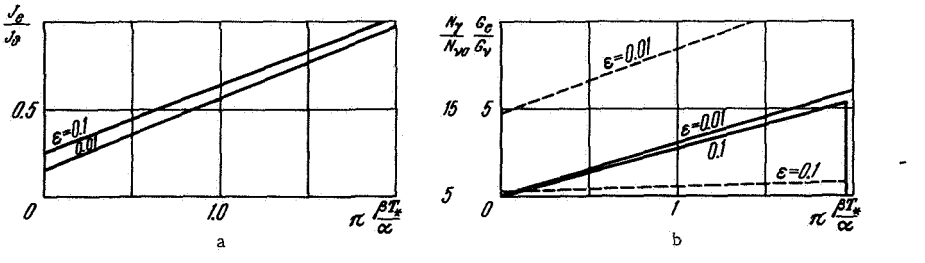

FIGURE 9.26. a) Decrease of functional J when correcting velocity-vector direction, using energy accumulator and constant-power engine; b) Optimum parameters of problem: solid lines represent G_e/G_ν and dashed lines represent $N_\gamma/N_{\nu 0}$.

One can similarly treat the problem of orbital plane rotation. The optimum programs for the magnitude and direction of the thrust acceleration and the values of the functionals J_e and J coincide with those obtained in the problem of correcting the velocity-vector direction, where the angle ϑ_0 is taken as the specified angle of orbital plane rotation, and the thrust vector is assumed perpendicular to the orbital plane /9.9/.

4. Engine with limited thrust. Consider the intermediate case between
378 the ideally throttled and unthrottled engines. The thrust can assume all values within a certain range or it may vanish. The engine power is constant or equal to zero, and the engine weight is proportional to the power consumed.

When the amount of working fluid consumed in a specified maneuver is small compared with the total weight of the vehicle, the thrust acceleration is assumed to be approximately proportional to the thrust developed by the engine. Let a_{max} be the upper limit of the thrust acceleration and a_{min} the lower limit, and consider a parameter governing the throttle of the engine, given by $\lambda = 1 - a_{max}/a_{min}$ where $0 \leqslant \lambda \leqslant 1$. The value $\lambda = 1$ corresponds to an ideally-throttlable system, while $\lambda = 0$ corresponds to an unthrottlable one. The value of λ will be fixed, while the value of a_{max} will be selected from optimum considerations. The initial relations of the variational problem for the minimum of the functional J_e do not differ from those given above in (9.48), with the exception of the inequality which limits $a(t)$. The relationship $a(t) \geqslant 0$ in (9.48) is replaced by $a_{max}(1-\lambda) \leqslant \leqslant a(t) \leqslant a_{max}$. The optimum values for the control functions $a(t)$ and $\delta(t)$ are

$$\left.\begin{aligned} a &= \begin{cases} a_{max} & \text{at } \frac{1}{2}\frac{p_v}{a_{max}} > \left(\frac{1+\xi}{N_\gamma}+\varepsilon\right), \\ \frac{1}{2}p_v\left(\frac{1+\xi}{N_\gamma}+\varepsilon\right)^{-1} & \text{at } \left(\frac{1+\xi}{N_\gamma}+\varepsilon\right)(1-\lambda) < \\ & \quad < \frac{1}{2}\frac{p_v}{a_{max}} < \left(\frac{1+\xi}{N_\gamma}+\varepsilon\right), \\ (1-\lambda)a_{max} & \text{at } \frac{1}{2}\frac{p_v}{a_{max}} < \left(\frac{1+\xi}{N_\gamma}+\varepsilon\right)(1-\lambda) \end{cases} \\ \delta &= \begin{cases} 1 & \text{at } \Delta > 0, \\ 0 & \text{at } \Delta < 0 \end{cases} \\ &\left(\Delta = a\left[p_v - \left(\frac{1+\xi}{N_\gamma}+\varepsilon\right)a\right] - \frac{\beta}{\alpha\xi}p_e N_\gamma,\ p_e > 0\right) \end{aligned}\right\} \tag{9.82}$$

379 The powered section can end over any one of the following three intervals in which the acceleration is controlled: at $a = a_{max}$, in $(1-\lambda)a_{max} < a < a_{max}$ and at $a = a_{max}(1-\lambda)$.

In the analogous problem of flight between two points of rest (with symmetrical boundary conditions) in which charging starts in the first interval, the value of the functional J_e is independent of λ and is

$$J_e = \frac{16\left[\left(1+\frac{\beta T}{\alpha}z\right)(1-z)+\varepsilon\right]}{(1-z^2)(1+z)} \qquad \left(z = \frac{\xi\alpha}{\beta T}\right). \tag{9.83}$$

The optimum value of z is determined from the relation

$$\frac{\beta T}{\alpha} = \frac{2(1-z)^2 - \varepsilon(3z-1)}{(1-z)^3}. \tag{9.84}$$

If the coasting section starts with a variable acceleration $(a_{max}(1-\lambda) < < a(t) < a_{max})$ the functional J_e is written differently in the form

$$J_e = \frac{12\left[\left(1+\frac{\beta T}{\alpha}z\right)(1-z)+\varepsilon\right](12\varphi^2 - 16\varphi^3 - z^3)}{(3\varphi - 4\varphi^3 - z^3)^2}. \tag{9.85}$$

Here $\varphi = {}^1/_2 - \tau$, where τ is determined by

$$p_v(\tau) = 2\left(\frac{1+\xi}{N_\gamma} + \varepsilon\right) a_{\max}. \tag{9.86}$$

From the condition of minimum J_e with respect to φ (which corresponds to the minimum of J_e with respect to $a_{\max}$) we obtain

$$\varphi = z/2.$$

If this result is substituted into (9.85), the relation for J_e, it is reduced to the form (9.83). Thus, the optimum value of $a_{\max}$ is such that the system functions in this case as an unthrottled one ($a(t) = a_{\max}$).

Finally, if the coasting section starts at a minimum value of the acceleration, the functional J_e can be written in the following form:

$$J_e = \frac{48\left[\left(1+\frac{\beta T}{\alpha} z\right)(1-z) + \varepsilon\right][3(1-\omega^2 z) - 4\varphi(1-\omega^3)]}{[3(1-\omega z^2) - 4\varphi^2(1-\omega^3)]^2}. \tag{9.87}$$

380 Here $\omega = 1 - \lambda$. The magnitude J_e attains its minimum value given by

$$J_e = \frac{12\left[\left(1+\frac{\beta T}{\alpha} z\right)(1-z) + \varepsilon\right](1+\omega^{3/2})^2}{(1+z\omega^{1/2})^2[1+2\omega^{3/2} - z\omega^{1/2}(2+\omega^{3/2})]}, \tag{9.88}$$

when $2\varphi = (1 + z\omega^{1/2})(1 + \omega^{3/2})^{-1}$. The absolute minimum of J_e, determined by (9.88), is attained when z satisfies

$$\frac{\beta T}{\alpha} = \frac{(1+z\omega^{1/2})Q(\omega) + 3(1-z+\varepsilon)\omega[\omega - z(2+\omega^{3/2})]}{(1-2z)(1+z\omega^{1/2})Q(\omega) - 3(1-z)\omega z[\omega - z(2+\omega^{3/2})]}, \tag{9.89}$$

where $Q(\omega) = 1 + 2\omega^{3/2} - z\omega^{1/2}(2 + \omega^{3/2})$. Figure 9.27 shows the dependence of the ratio of the functional J_e (for the system with limited variation of the acceleration and energy accumulation) to the corresponding value of functional J_l (for the system without accumulation), where

$$J_l = 12\frac{(2+\omega^{3/2})^2(1+\varepsilon)}{4+4\omega^{3/2}}. \tag{9.90}$$

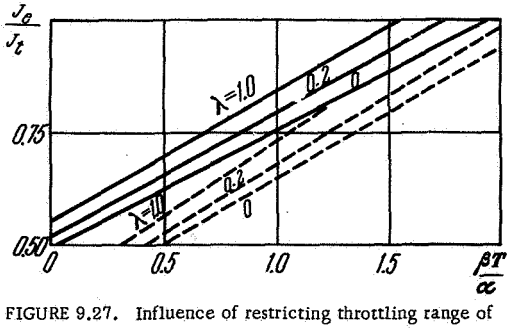

FIGURE 9.27. Influence of restricting throttling range of thrust acceleration λ on decrease of functional J, for flight between two points of rest with energy accumulation and constant-power engine; solid lines represent engine of relative weight $\varepsilon = 0.1$; dashed lines represent one with $\varepsilon = 0.01$.

Figure 9.27 illustrates the decrease of the functional J (and the corresponding increase of the payload — cf. Figure 9.4) produced by using an energy accumulator when restrictions are imposed on the control range of the thrust acceleration.

5. Engine with limited exhaust velocity. It was mentioned at the
381 beginning of § 1 that the energy accumulation can be attained using thermal accumulators. In such cases, thermal engines are used and require a restriction on the exhaust velocity of the jet $0 \leqslant V \leqslant V_{\max}$ (§ 1 of Chapter Two).

We now make the following additional assumptions: the thrust and power of the engine are unlimited, and it is weightless.

The full system of differential equations, boundary conditions, restrictions on the control functions, and phase coordinates of the variational problem for the payload maximum in this situation is

$$\left.\begin{aligned}
&\dot{G}_\sigma = -k_1 \frac{N_v(1+N_e)}{V^2}, && G_\sigma(0) + G_e + G_v = 1,\\
&&& G_\sigma(T) = \max,\\
&\dot{E} = -k_2 N_v N_e, && E(0) = 1,\\
&&& E(T) = 0,\\
&\dot{\mathbf{r}} = \mathbf{v}, && \mathbf{r}(0) = \mathbf{r}_0,\\
&&& \mathbf{r}(T) = \mathbf{r}_1,\\
&\dot{\mathbf{v}} = k_1 \frac{N_v(1+N_e)}{V(G_\sigma + G_e + G_v)}\mathbf{e} + \mathfrak{R}, && \mathbf{v}(0) = \mathbf{v}_0,\ \mathbf{v}(T) = \mathbf{v}_1\\
&(0 \leqslant V(t) \leqslant V_{\max},\ 0 \leqslant N_v(t) \leqslant 1,\ N_e(t) \geqslant -1, && \\
&&& |\mathbf{e}(t)| = 1,\ 0 \leqslant E(t) \leqslant 1;\\
&k_1 = 2gN_{v0}/G_0 = 2gG_v/\alpha,\ k_2 = N_{v0}/E_0 = \beta G_v/\alpha G_e).
\end{aligned}\right\} \qquad (9.91)$$

Here, as in § 1, all the weight components are represented as fractions of the takeoff weight G_0, the source power N_v as a fraction of its maximum value N_{v0}, and the power N_e as a fraction of the instantaneous power of the source.

The direction of the thrust $\mathbf{e}(t)$ is the same for $0 < E(t) < 1$ and $E = 0$, $E = 1$ and coincides with that obtained earlier

$$\mathbf{e} = \mathbf{p}_v/p_v. \qquad (9.92)$$

The exhaust velocity $V(t)$ of the jet is a function of the momenta p_v and p_σ, where

$$V = \begin{cases} V_{\text{opt}} & \text{at } V_{\text{opt}} < V_{\max}, \\ V_{\max} & \text{at } V_{\text{opt}} > V_{\max} \end{cases} \quad (V_{\text{opt}} = -2(G_\sigma + G_e + G_v)\, p_\sigma/p_v) \qquad (9.93)$$

(p_σ and p_e are everywhere negative).

The optimum variation of the source power is $N_v(t) = 1$. Note that for
382 an engine with limited power and limited exhaust velocity but no energy accumulation there were sections when the power supply was cut off. Here we have no such sections, since the power is directed into the accumulator when the engine is cut off.

The optimum value of the power N_e, which controls the accumulator energy, is

$$N_e = \begin{cases} \infty & \text{at} \quad -\frac{k_1}{V}\left(\frac{p_\sigma}{V} - \frac{p_v}{G}\right) - k_2 p_e < 0, \\ -1 & \text{at} \quad -\frac{k_1}{V}\left(\frac{p_\sigma}{V} - \frac{p_v}{G}\right) - k_2 p_e > 0. \end{cases} \tag{9.94}$$

On the boundaries $E = 0$ and $E = 1$ the power N_e vanishes.

An analysis of (9.93) and (9.94) shows that the optimum trajectory can contain sections of motion with optimally varying exhaust velocity, sections in which the exhaust velocity equals its boundary value, and also coasting sections. In the latter the engine is cut off (cf. the right-hand part of the fourth equation of (9.91) for $N_e = -1$) and the energy accumulator is charged.

If the value of V_{max} is so large that

$$V_{max} > [-2(G_\sigma + G_e + G_v)\, p_\sigma / p_v]_{max} \quad \text{at} \quad 0 \leqslant t \leqslant T, \tag{9.95}$$

the optimum trajectory will not have $V = V_{max}$ at all. The equations of motion (9.91) and the momentum differential equations then contain the integral (cf. the case considered above)

$$(G_\sigma + G_e + G_v)^2\, p_\sigma = \text{const}. \tag{9.96}$$

The absence of sections in which $V = V_{max}$ enables us to consider the thrust acceleration

$$a = \frac{k_1 N_v (1 + N_e)}{V (G_\sigma + G_e + G_v)} \tag{9.97}$$

and to reduce the variational problem for the delivery of a maximum payload to that of minimizing the functional

$$J_e = (1 + \xi) \int_0^T \frac{a^2 dt}{N_v (1 + N_e)}, \tag{9.98}$$

considered in § 1. If the quantity V_{max} satisfies the inequality

$$V_{max} < [-2(G_\sigma + G_e + G_v)\, p_\sigma / p_v]_{min} \quad \text{at} \quad 0 \leqslant t \leqslant T, \tag{9.99}$$

383 the propulsion system will function as an unthrottled system at the limits $E = 0$ and $E = 1$ for which $N_v = 1$, $V = V_{max}$.

6. Engine with limited operating time. Consider the case in which the resources of the engine are less than those of the power source and are not enough to continue throughout the total time of motion. We assume for simplicity that the resources of the power source are sufficient to last the total time.

In addition, the thrust will be considered as unbounded, the power consumed by the engine as constant, and the weight of the engine as proportional to the power used.

Indicate the maximum allowable period of the powered sections by $T_\mu \leqslant T$ and consider it as given. In this case we add relation /9.8/

$$\dot{t}_\mu = \delta,$$

and the expression for Δ in (9.54) is replaced by

$$\Delta = \frac{1}{4} p_v^2 \left(\frac{1+\xi}{N_\gamma} + \varepsilon \right)^{-1} - \frac{\beta}{\alpha\xi} p_e N_\gamma + p_\mu \qquad (9.100)$$

(the magnitude $p_\mu = \text{const} < 0$ is the momentum corresponding to t_μ).

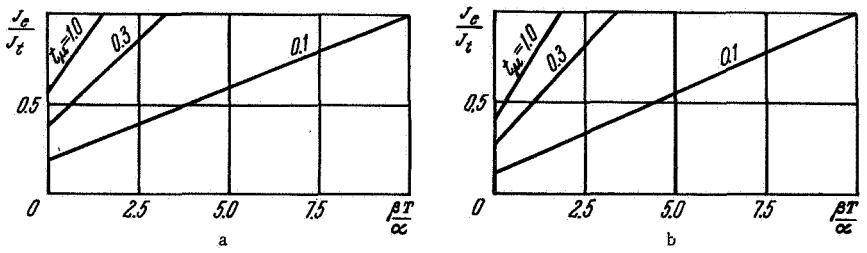

FIGURE 9.28. Influence of limiting the engine operating time $T_\mu < T$ in the model problem of flight between points of rest with engine of constant power; J_e/J_l is ratio of functionals in flights with and without energy accumulation, a) relative engine weight $\varepsilon = 0.1$; b) $\varepsilon = 0.01$.

In the analogous problem of flight between points of rest the expression for the functional J_e coincides with (9.55)

$$J_e = 12 l^2 T^{-3} \frac{[1 + (\beta T/\alpha) z](1 - z) + \varepsilon}{1 - z^3}. \qquad (9.101)$$

The value of z which minimizes J_e is determined by (9.56) as long as the values obtained for z satisfy the inequality $z > 1 - T_\mu/T$. If not, the value $z = 1 - T_\mu/T$ is selected. The dependence of the ratio $\beta T/\alpha$ of the functionals with and without energy accumulation, on J_e/J_l is given in Figure 9.28. The
384 value of the functional J_l for a system without energy accumulation is equal to (7.52)

$$J_l = \frac{12 l^2 T^{-3}}{1 - (1 - T_\mu/T)^3}. \qquad (9.102)$$

The results given in Figure 9.28 show that when the engine operating time is restricted the gain in using an energy accumulator increases.

§ 3. PROPULSION SYSTEMS WHICH ACCUMULATE AIR

A considerable part (often the main part) of the spacecraft weight in the optimum case consists of the working fluid (fuel). It was shown in /9.11—9.17/ that if the spacecraft is projected empty into orbit (or with just a fraction of its working-fluid reserve), and then filled with fuel whilst in orbit, the weight of the rocket carrier is considerably reduced.

The following fuelling method has been suggested /9.11—9.17/. The vehicle is provided with an air inlet duct. The initial orbit is selected so that it passes through the upper layers of the atmosphere. During its orbital motion the vehicle takes in air and compresses it. After accumulating the required quantity, the vehicle then performs the specified maneuver.

Another fuelling method has also been suggested /9.17/. This consists of placing an auxiliary vehicle in orbit which takes in the air. The space vehicle is launched with empty tanks and fuelled while in orbit by the auxiliary one; it then performs the required maneuver.

These two orbital fuelling methods are compared with the standard ground-fuelling method by investigating the relative payload of the spacecraft. In the first method the payload is represented as a fraction of the weight of the spacecraft without fuel. The latter is higher than in the ground-fuelling method, due to the additional equipment comprising air inlet duct, compression unit, etc. If this additional weight is less than that of the working fluid carried by a ground-fuelled vehicle to perform the maneuver, the first orbital-fuelling method will be better than the ground-fuelling one. In the second orbital method the spacecraft dry weight is the same as that in the case of ground fuelling; on the other hand, we have to place an additional vehicle into orbit. To allow for this in the analysis, we add to the dry weight of each vehicle a value equal to the
385 dry weight of the auxiliary vehicle divided by the number of vehicles it fuels. If the extra weight is less than that of the additional equipment necessary in the first method, and less than the necessary working-fluid reserve when fuelling on the ground, then the second method of orbital fuelling is better. Its advantages, naturally, increase with an increasing number of fuellings.

1. Characteristics of the propulsion system with working-fluid accumulation. The block diagram of a propulsion system designed for taking in working fluid during flight in the upper layers of the atmosphere is shown in Figure 9.29, reproduced from /9.17/. The system consists of an air inlet duct, a compression unit, a tank to contain the working fluid taken in, an engine for compensating the drag, and a power source to feed the engine and the compression unit /9.11—9.17/. If the vehicle powered by this propulsion system has to fly in outer space too, then another engine and a tank with an additional reserve of working fluid can be included in the propulsion system to operate this extra engine (e.g., a chemical propellant).

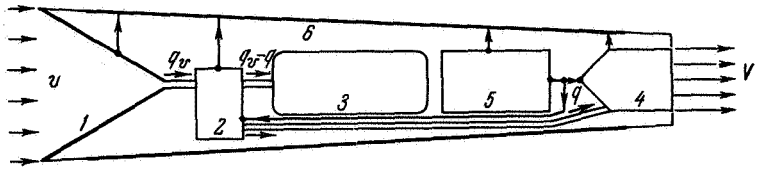

FIGURE 9.29. Block diagram of propulsion system taking in working fluid during orbital flight in upper atmospheric layers:

1) hypersonic air inlet duct; 2) compression unit; 3) tank for accumulating working fluid; 4) rocket engine; 5) energy source; 6) radiator.

The mass flow rate through the inlet duct equals

$$q_v = \rho v S, \tag{9.103}$$

where ρ is the atmospheric density, v is the vehicle velocity (taken equal to the relative velocity of the stationary atmosphere), and S is the area of the inlet duct.

The vehicle drag is

$$F = {}^1/_2 c_x \rho v^2 S = {}^1/_2 c_x v q_v, \tag{9.104}$$

where c_x is the drag coefficient (divided by the area S of the inlet duct).
386 Neglecting friction and assuming that the whole vehicle is no wider than the inlet duct (Figure 9.29), the drag equals the momentum vq_v of the air entering the inlet duct ($c_x = 2$). These assumptions are correct for a rarefied atmosphere and a vehicle configuration like a frustrum. A more detailed discussion is found in /9.17/.

The air mass that is taken in (less the amount flowing through the engine) is directed into the compression unit. This consumes a power N_v proportional to the mass flow rate. It is further assumed that the whole mass that enters the inlet duct is compressed, and therefore

$$N_v = k_v q_v \qquad (k_v = \text{const}). \tag{9.105}$$

Some of the compressed air mass is consumed by the engine (flow rate q), to compensate for the drag. In a stationary regime the thrust $P = qV$ must equal the drag (9.104). For accumulation ($q_v - q > 0$), the exhaust velocity V of the nozzle must be greater than the vehicle velocity v. For an Earth satellite in a circular orbit, $v \sim 8$ km/sec, and therefore electric engines are envisaged for this purpose. Thus, a part N_γ of the power N_s produced by the source must be spent on feeding the engine, so

$$N_\gamma = P^2/2\eta_\gamma q \qquad (N_\gamma + N_v = N_s), \tag{9.106}$$

where η_γ is the engine efficiency.

The weight G_μ of the accumulated working fluid (allowing for the discharge q through the engine) is given by

$$\dot{G}_\mu = g(q_v - q). \tag{9.107}$$

The total weight G_κ of the propulsion system consists of the following components /9.11—9.17/: the weight of the air inlet duct and compression unit G_v, which is proportional to the maximum flow rate $q_{v\max}$, where

$$G_v = \gamma_v q_{v\max} \qquad (\gamma_v = \text{const}), \tag{9.108}$$

the weight of the power source G_s, which is proportional to the maximum power N_{s0} produced, where

$$G_s = \alpha N_{s0} \qquad (\alpha = \text{const}), \tag{9.109}$$

the weight of the engine G_γ, which is proportional to the maximum thrust P_0 or to the maximum power $N_{\gamma 0}$ consumed, where

$$G_\gamma = \gamma P_0 \text{ at } G_\gamma = \gamma N_{\gamma 0} \; (\gamma = \text{const}), \tag{9.110}$$

387 and the weight G_β of the tank, which is proportional to the maximum working-fluid weight $G_{\mu 1}$, where

$$G_\beta = \beta_\mu G_{\mu 1} \quad (\beta_\mu = \text{const}). \tag{9.111}$$

2. Accumulation in a stationary regime. Consider the problem of selecting the optimum parameters and operating regime for the propulsion system of the auxiliary vehicle /9.11—9.18/. In Subsections 4 and 5 a similar procedure is used (with some additional restrictions) to discuss the accumulation phase of a vehicle designed for outer-space maneuvers.

The problem is formulated as follows: for a given takeoff weight G_0 and during a specified time T_v, we wish to accumulate the maximum quantity of working fluid G_μ. Equivalent formulations are: we wish to accumulate a specified quantity of working fluid during a given time for a minimum takeoff weight, or, we wish to accumulate a given quantity of working fluid for a fixed takeoff weight during a minimum time.

It will be assumed that air is taken in on a circular orbit, that the atmospheric density along the orbit is constant, and that the thrust equals the drag (stationary regime).

Since $P = qV$ and $F = {}^1/_2 c_x v q_v$, we express the weight of working fluid accumulated during time T_v, $G_{\mu 1} = g\,(q_v - q)\,T_v$ and the takeoff weight* $G_0 = G_v + G_\nu + G_\gamma + G_\beta$ in the forms

$$\left.\begin{aligned} G_{\mu 1} &= g q_v (1 - {}^1/_2 c_x v/V)\, T_v, \\ G_0 &= g q_v \left[\frac{\gamma_v}{g} + \frac{\alpha}{g}\left(k_v + \frac{c_x v V}{4\eta}\right) + \frac{\gamma c_x v}{2g} + \beta_\mu \left(1 - \frac{c_x v}{2V}\right) T_v\right]. \end{aligned}\right\} \tag{9.112}$$

The takeoff weight G_0 and the time T_v are fixed. With the expression for q_v in the second relation of (9.112), we obtain the relative rate of accumulation as a function of the exhaust velocity V as

$$\left.\begin{aligned} &\frac{\dot G_\mu}{G_0} = \frac{G_{\mu 1}}{G_0 T_v} = \frac{1 - b_1/V}{b_2 V + b_3 - b_4/V} \\ &\left(b_1 = \frac{1}{2} c_x v, \quad b_2 = \frac{\alpha c_x v}{4 g \eta_\gamma}, \quad b_3 = \frac{2\gamma_v + 2\alpha k_v + \gamma c_x v}{2g} + \beta_\mu T_v, \right. \\ &\left. b_4 = \frac{1}{2} c_x \beta_\mu v T_v\right). \end{aligned}\right\} \tag{9.113}$$

388 It is assumed that the engine efficiency η_γ is independent of the exhaust velocity V and the power N_γ consumed by the engine. If the air-intake orbit is fixed (v, c_x = const), the coefficients b_1, b_2, b_3, b_4 will be constant, and the problem reduces to finding the maximum of (9.113) with respect to V. This yields

$$\left.\begin{aligned} V_{\text{opt}} &= b_1\left(1 + \sqrt{1 + \frac{b_1 b_3 - b_4}{b_1^2 b_2}}\right), \\ \left(\frac{\dot G_\mu}{G_0}\right)_{\max} &= \frac{\sqrt{1 + (b_1 b_3 - b_4)/b_1^2 b_2}}{2 b_1 b_2 + b_3 + (b_1 b_2 - 2 b_4)/b_1 + (2 b_1 b_2 + b_3)\sqrt{1 + (b_1 b_3 - b_4)/b_1^2 b_2}}, \end{aligned}\right\} \tag{9.114}$$

* This only takes account of the weight components directly linked with the air intake.

the other parameters of the propulsion system being calculated from the formulas

$$q_v = \frac{G_0}{g}(b_2 V + b_3 - b_4/V)^{-1}, \quad q = {}^1/_2 q_v c_x v/V, \quad S = q_v/\rho v. \tag{9.115}$$

If only the weight of the power source is taken into account in the weight formula ($G_0 = G_v$, $\gamma_v = \gamma = \beta_\mu = 0$) and if the power consumption of the compression unit is neglected ($k_v = 0$) and we assume that $c_x = 2$, relations (9.114) and (9.115) are considerably simplified ($b_1 = v$, $b_2 = \alpha v/2g\eta_\gamma$, $b_3 = b_4 = 0$):

$$V_{opt} = 2v, \quad \left(\frac{\dot G_\mu}{G_0}\right)_{max} = \frac{g\eta_\gamma}{2\alpha v^2}, \quad q_v = 2q = G_0 \frac{\eta_\gamma}{\alpha v^2},$$
$$S = G_0 \frac{\eta_\gamma}{\alpha \rho v^3}. \tag{9.116}$$

Comparing expressions (9.114) and (9.116) for the optimum exhaust velocity, we see that allowing for the additional weight components and the power consumption of the compressing unit yields an increase in the velocity.

Within this formulation the parameters of the air-intake orbit only enter via the flight velocity v and the drag c_x (if the relations for the area of the inlet duct S are ignored and the latter is determined after solving the problem). The magnitudes v and c_x are practically constant for the range of altitudes considered (100—120 km above the Earth). Therefore, in order to determine the optimum orbital height additional considerations are required linked with the thermal regions, the ratios of the inlet duct area and the midship section of the vehicle, etc.

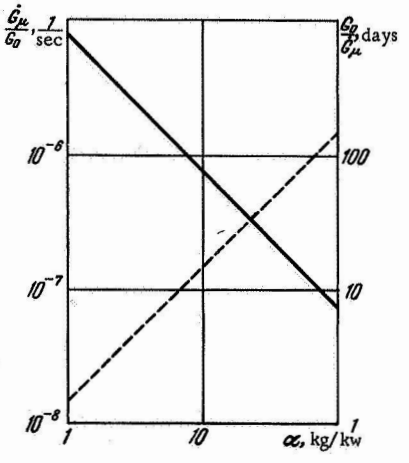

FIGURE 9.30. Weight of working fluid $\dot G_\mu$ accumulated per unit time (as fraction of power-plant weight) as function of unit weight of power plant per unit jet power α/η_γ, represented by solid line; dashed line $1/\dot G_\mu$ represents time of accumulating working fluid equal to power-source weight.

We now give a numerical example of air intake in the Earth's atmosphere ($v \approx 8$ km/sec, $c_x = 2$). Figure 9.30 shows the relative rate of accumulation ($\dot G_\mu/G_0$) in (9.116) (where $G_0 = G_v$) as a function of the unit weight α of the power source divided by the engine efficiency η_γ. Note that the reciprocal quantity $G_0/\dot G_\mu$ equals the time during which a quantity of air equal in weight to the power source is accumulated. The optimum exhaust velocity in the case considered is equal to 16 km/sec. For an orbit at a height of 100 km and an inlet duct area of 1 m^2 the quantity of air taken in is roughly 200 kg daily.

389

3. Air intake in a nonstationary regime. Let the initial and final points of the trajectory (or the initial point only) lie outside the atmosphere (i.e., in the region where the density is too low for air to be taken in). Such a situation arises for instance during refuelling, which must either be carried out outside the atmosphere, or on the stationary intake orbit (if the auxiliary

vehicle is incorrectly situated). We wish to establish a program for controlling the thrust vector so that at the end of this motion, the vehicle is on the specified orbit with a maximum quantity of accumulated air mass during a fixed time /9.19/.

As at the end of the preceding subsection, only the weight of the power source is allowed for ($G_0 = G_v$, $\gamma_v = \gamma = \beta_\mu = 0$), the power consumed by the compression process is neglected ($k_v = 0$), and the drag coefficient is $c_x = 2$ (i.e., only the momentum of the air mass passing through the inlet duct is taken into consideration). We consider the two extreme regions of thrust control (from the point of view of throttling the engine). In the first case the exhaust velocity and the thrust are constant along the trajectory, and the control is achieved by firing and cutting off the engine (unthrottled engine). In the second case there are no restrictions on the exhaust velocity and thrust apart from the condition of constant power (ideally-throttlable engine). In both cases there are no losses when operating the engine ($\eta_\gamma = 1$). Regarding the thrust direction, it is assumed that the vehicle
390 possesses weathercock stability during its flight in the atmosphere. It is further assumed that it is impossible to vary the thrust direction relative to the vehicle axes. As a result of these two assumptions the thrust vector will be collinear with the velocity vector (and therefore also with the drag force). In the case of an ideally-throttlable engine, we allow the thrust direction to be reversed, while for an unthrottled engine the thrust is only directed along the velocity.

We now investigate plane motion in the neighborhood of a circular orbit (the base orbit), and assume that only small deviations take place from it. To describe the resulting motion we use the second, third, fifth, and sixth linearized equations in (5.88):

$$\ddot{\xi} = a_\xi + 2\dot{\eta}, \quad \ddot{\eta} = a_\eta + 3\eta - 2\dot{\xi} \qquad (\varphi = t - \xi, \ r = 1 + \eta). \tag{9.117}$$

Here all the variables are dimensionless. The radius of the base orbit is taken as the characteristic distance, and the period of revolution along this orbit divided by 2π as the characteristic time. The coordinate $\xi = t - \varphi$ corresponds to a phase shift, and the coordinate $\eta = r - 1$ to a radial deviation relative to a point moving uniformly along the base orbit.

The acceleration components a_ξ and a_η on the right-hand side of (9.117), represent the projections of the difference between the thrust and drag vectors, divided by the instantaneous vehicle mass. The projection a_η onto the radial direction is neglected. The motion is considered over several revolutions, and therefore the variation of the vehicle weight is small. Hence,

$$a_\xi = -(g/g_0)(P - F)/G_0, \ a_\eta = 0 \tag{9.118}$$

(the direction of the ξ-axis is opposed to that of increasing angle φ, g_0 is the gravitational acceleration on the base orbit).

No boundary conditions are imposed on the angle φ. In this case equations (9.117) reduce to a third-order equation for the radial component η (allowing for (9.118))

$$\dddot{\eta} + \dot{\eta} = 2g\,(P - F)/g_0 G_0. \tag{9.119}$$

The variation of density with altitude is approximated to by the linear relationship

$$\rho = \rho_0 (1 - \lambda\eta), \tag{9.120}$$

where ρ_0 is the density of the atmosphere on the base orbit, and the coefficient λ is of order $\sim 2 \cdot 10^3$ at altitudes 100—150 km in the Earth's atmosphere.

391 With the value of the coefficient λ, we can write approximate expressions for the drag and the mass flow rate ($c_x = 2$),

$$F = F_0 (1 - \lambda\eta), \; q_v = q_{v0} (1 - \lambda\eta) \tag{9.121}$$

(F_0 and q_{v0} are the drag and mass flow rate on the base orbit), i.e., we can neglect the variation of drag and mass flow (caused by changing velocity) when compared with the influence of the flight altitude.

For constant power $N_{v0} = G_0/\alpha$, we express the thrust and flow rate of the engine in terms of the exhaust velocity (recall that $G_v = G_0$, $k_v = 0$, the engine efficiency $\eta_T = 1$):

$$P = \frac{2G_0}{\alpha V}, \quad q = \frac{2G_0}{\alpha V^2} \tag{9.122}$$

and introduce the step function $\delta(t) = 1$ or 0 to represent engine firing and cutoff. With these variables the variational problem becomes

$$\left.\begin{aligned}
&\dot{G}_\mu = f_0 (1 - \lambda\eta) - a_0 \delta / V^2, && G_\mu (0) = 0, \\
&&& G_\mu (T_v) = \max, \\
&\dot{\eta} = v_r, && \eta (0) = \Delta r_0, \\
&&& \eta (T_v) = \Delta r_1, \\
&\dot{v}_r = f_r, && v_r (0) = v_{r0}, \\
&&& v_r (T_v) = v_{r1}, \\
&\dot{f}_r = 2a_0 \delta / V - v_r - 2f_0 (1 - \lambda\eta), && f_r (0) = \Delta r_0 - 2\Delta v_{\varphi 0}, \\
&&& f_r (T_v) = \Delta r_1 - 2\Delta v_{\varphi 1} \\
&(a_0 = (2g/\alpha) g_0^{-3/2} r_0^{-1/2}, \quad f_0 = g F_0 / g_0 G_0).
\end{aligned}\right\} \tag{9.123}$$

The weight of the accumulated working fluid G_μ is given as a fraction of the takeoff weight of the vehicle G_0, and the exhaust velocity V as a fraction of the circular velocity along the base orbit $v_0 = \sqrt{g_0 r_0}$. The parameter a_0 represents the dimensionless thrust acceleration at an exhaust velocity equal to v_0, and the parameter f_0 is the dimensionless drag along the original orbit. To represent the equations of the maximum principle in a more convenient form we have introduced additional symbols for the derivatives, so that $\dot{\eta} = v_r$ is the radial velocity, and $\ddot{\eta} = f_r$ is the radial acceleration. The boundary conditions for η, v_r, f_r are written in terms of the increments of the radius Δr, and the radial and transversal velocity components v_r and Δv_φ respectively from their corresponding values on the base circular orbit.

392 This procedure is illustrated by numerical results for the values of the problem parameters given by

$$a_0 = 1.33 \cdot 10^{-3}, \; f_0 = 1.67 \cdot 10^{-4}, \; \lambda = 1.94 \cdot 10^3, \; T_v = 2\pi, \tag{9.124}$$

where the following boundary conditions are assumed:

$$\eta(0) = \eta(2\pi) = \Delta r, \quad v_r(0) = v_r(2\pi) = 0, \quad f_r(0) = f_r(2\pi) = 0. \tag{9.125}$$

We firstly investigate an unthrottled engine. The exhaust velocity is constant $V = V_0$, and the problem reduces to finding the optimum value of the parameter V_0 and establishing the optimum program $\delta(t)$ of firing and cutting off the engine while ensuring a maximum accumulation of $G_\mu(T_v)$.

The Hamiltonian is

$$H = -\left[(1-\lambda\eta) f_0 - \frac{a_0\delta}{V^2}\right] + p_\eta v_r + p_v f_r + \\ + p_f\left[2\frac{a_0\delta}{V} - v_r - 2(1-\lambda\eta) f_0\right] \tag{9.126}$$

and the momentum differential equations are

$$\dot{p}_\eta = -\lambda(1+2p_f) f_0, \quad \dot{p}_v = -p_\eta + p_f, \quad \dot{p}_f = -p_v. \tag{9.127}$$

The Hamiltonian H is represented as a function of the control variable δ, where

$$H = H_0 + \frac{a_0}{V^2}\Delta\delta, \quad \Delta = 1 + 2p_f V. \tag{9.128}$$

From the condition of minimum H with respect to δ we obtain

$$\delta = 0 \text{ at } \Delta > 0, \ \delta = 1 \text{ at } \Delta < 0. \tag{9.129}$$

The roots of the equation $\Delta(t) = 0$ determine the instants of switchover and their total number within the interval $[0, T_v]$.

The momentum differential equations (9.127) are integrated independently of the basic system; in particular, the expression for p_f, which determines the behavior of the function Δ, has the following form:

$$\left.\begin{aligned} p_f &= c_1 e^{-b_1 t} + e^{1/2 b_1 t}(c_2 \cos b_2 t + c_3 \sin b_2 t) - 1/2, \\ b_1 &= (\lambda f_0 + \sqrt{(\lambda f_0)^2 + 1/27})^{1/3} + (\lambda f_0 - \sqrt{(\lambda f_0)^2 + 1/27})^{1/3}, \\ b_2 &= (\lambda f_0 + \sqrt{(\lambda f_0)^2 + 1/27})^{1/3} - (\lambda f_0 - \sqrt{(\lambda f_0)^2 + 1/27})^{1/3}. \end{aligned}\right\} \tag{9.130}$$

Substituting $p_f(t)$ from (9.130) into (9.128), we obtain an expression for the function $\Delta(t)$ which contains three unknown constants c_1, c_2, c_3. These constants must be determined from the boundary conditions of (9.123) after integrating the equations of motion in (9.123) along the powered ($\delta^{(i)} = 1$)
393 and coasting ($\delta^{(i)} = 0$) sections:

$$\eta^{(i)}(t) = c_4^{(i)} e^{b_1 t} + e^{-1/2 b_1 t}(c_5^{(i)} \cos b_2 t + c_6^{(i)} \sin b_2 t) - \frac{1}{\lambda}\left(\frac{a_0\delta^{(i)}}{V_0 f_0} - 1\right) \\ (t_{i-1} < t < t_i, \quad i = 1, 2, \ldots, n+1, \quad t_{n+1} = T_v), \tag{9.131}$$

where $t_i = t_i(c_1, c_2, c_3)$ are the roots of the equation $\Delta(t) = 0$; $c_4^{(i)}$, $c_5^{(i)}$, $c_6^{(i)}$ are integration constants along these sections. Adjacent sections are joined so that $\eta, \dot{\eta}, \ddot{\eta}$ are given by

$$\eta^{(i)}(t_i) = \eta^{(i+1)}(t_i), \quad \dot{\eta}^{(i)}(t_i) = \dot{\eta}^{(i+1)}(t_i), \quad \ddot{\eta}^{(i)}(t_i) = \ddot{\eta}^{(i+1)}(t_i). \tag{9.132}$$

With (9.131) and (9.132) the constants of the $(i+1)$-th section can be expressed in terms of those of the i-th section and the switchover time t_i (obtained by solving the corresponding system of linear algebraic equations) in the forms

$$\left.\begin{aligned} c_4^{(i+1)} &= c_4^{(i)} + \frac{{}^1/_4 b_1^2 + b_2^2}{{}^9/_4 b_1^2 + b_2^2} \frac{a_0}{\lambda V_0 f_0} (\delta^{(i)} - \delta^{(i+1)})\, e^{-b_1 t_i}, \\ c_5^{(i+1)} &= c_5^{(i)} + \frac{b_1 / b_2}{1 + 3b_1^2} \frac{a_0}{\lambda V_0 f_0} (\delta^{(i)} - \delta^{(i+1)}) \times \\ &\qquad \times (2b_1 b_2 \cos b_2 t_i + \sin b_2 t_i), \\ c_6^{(i+1)} &= c_6^{(i)} + \frac{b_1}{1 + 3b_1^2} \frac{a_0}{\lambda V_0 f_0} (\delta^{(i)} - \delta^{(i+1)}) \times \\ &\qquad \times (2b_1 b_2 \sin b_2 t_i - \cos b_2 t_i). \end{aligned}\right\} \tag{9.133}$$

The constants for the first section ($i = 1$) are determined from the initial values, where

$$\left.\begin{aligned} c_4^{(1)} &= \frac{1}{1 + 3b_1^2} \left\{ \left[\eta(0) + \frac{1}{\lambda} \left(\frac{a_0 \delta^{(1)}}{V_0 f_0} - 1 \right) \right] (1 + b_1^2) + \dot{\eta}(0)\, b_1 + \ddot{\eta}(0) \right\}, \\ c_5^{(1)} &= \frac{1}{1 + 3b_1^2} \left\{ \left[\eta(0) + \frac{1}{\lambda} \left(\frac{a_0 \delta^{(1)}}{V_0 f_0} - 1 \right) \right] 2b_1^2 - \dot{\eta}(0)\, b_1 - \ddot{\eta}(0) \right\}, \\ c_6^{(1)} &= \frac{1}{1 + 3b_1^2} \left\{ - \left[\eta(0) + \frac{1}{\lambda} \left(\frac{a_0 \delta^{(1)}}{V_0 f_0} - 1 \right) \right] \frac{b_1}{b_2} + \right. \\ &\qquad \left. + \dot{\eta}(0) \frac{1 + {}^3/_2 b_1^2}{b_2} - \ddot{\eta}(0) \frac{3b_1}{2b_2} \right\}. \end{aligned}\right\} \tag{9.134}$$

By successively substituting into (9.133) for the constants of each section in terms of those of the preceding one, we obtain expressions for $c_4^{(i+1)}$, $c_5^{(i+1)}$, $c_6^{(i+1)}$ in terms of $c_4^{(1)}$, $c_5^{(1)}$, $c_6^{(1)}$ and the switchover instants $t_1, t_2, \ldots, t_i$, so that

$$\left.\begin{aligned} c_4^{(i+1)} &= c_4^{(1)} + [\operatorname{sgn} \Delta(0)]\, b_3 [(-1)^2 e^{-b_1 t_1} + (-1)^3 e^{-b_1 t_2} + \cdots \\ &\qquad \cdots + (-1)^{i+1} e^{-b_1 t_i}], \\ c_5^{(i+1)} &= c_5^{(1)} + [\operatorname{sgn} \Delta(0)]\, b_4 [(-1)^2 (b_5 \cos b_2 t_1 + \sin b_2 t_1)\, e^{{}^1/_2 b_1 t_1} + \cdots \\ &\qquad \cdots + (-1)^{i+1} (b_5 \cos b_2 t_i + \sin b_2 t_i)\, e^{{}^1/_2 b_1 t_i}], \\ c_6^{(i+1)} &= c_6^{(1)} - [\operatorname{sgn} \Delta(0)]\, b_4 [(-1)^2 (\cos b_2 t_1 - b_5 \sin b_2 t_1)\, e^{{}^1/_2 b_1 t_1} + \cdots \\ &\qquad \cdots + (-1)^{i+1} (\cos b_2 t_i - b_5 \sin b_2 t_i)\, e^{{}^1/_2 b_1 t_i}], \\ &\left(b_3 = \frac{a_0}{\lambda V_0 f_0} \frac{1 + b_1^2}{1 + 3b_1^2},\ b_4 = \frac{a_0}{\lambda V_0 f_0} \frac{b_1 / b_2}{1 + 3b_1^2},\ b_5 = 2b_1 b_2 \right). \end{aligned}\right\} \tag{9.135}$$

The constants c_1, c_2, c_3, which determine the switchover times $t_1, t_2, \ldots, t_n$, are selected so that the constants $c_4^{(n+1)}$, $c_5^{(n+1)}$, $c_6^{(n+1)}$ calculated by (9.135) correspond to the specified final conditions in (9.123) for $\eta, \dot{\eta}, \ddot{\eta}$.

The results obtained by this method for the boundary conditions (9.125) with $\Delta r = 0$ and the parameter values (9.124) are presented in Figures 9.31 to 9.33 for different exhaust velocities V_0. Figure 9.31 shows the function $\Delta(t)$, which determines the switchover instants defined by (9.128) and (9.129). The equation $\Delta(t) = 0$ has three roots t_1, t_2, t_3. They are shown in Figure 9.32 as a function of the exhaust velocity. The motion starts with a coasting section ($\delta(t) = 0$ for $0 < t < t_1$) followed by a powered section ($\delta(t) = 1$ for $t_1 < t < t_2$), followed by another coasting section ($\delta(t) = 0$ for $t_2 < t < t_3$) and ending with a powered section ($\delta(t) =$ for $t_3 < t < 2\pi$). The optimum trajectory $\eta(t)$ (Figure 9.33) at first enters the dense layers of the atmosphere, but then regains the original orbit.

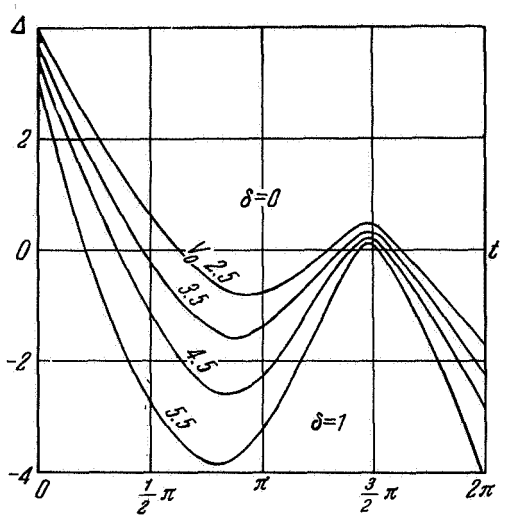

FIGURE 9.31. Function $\Delta(t)$, determining times of firing and cutting off unthrottled engine on accumulation trajectory, for different values of exhaust velocity V_0 (represented as fraction of circular velocity).

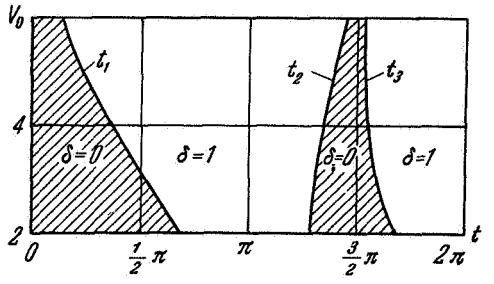

FIGURE 9.32. Distribution of coasting ($\delta = 0$) and powered ($\delta = 1$) sections on air-intake trajectory with unthrottled engine.

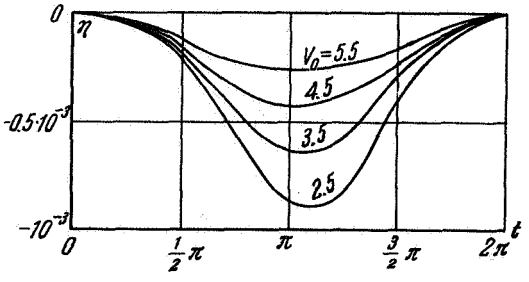

FIGURE 9.33. Examples of optimum air-intake trajectories (η is radial component) at different exhaust velocities for unthrottled engine.

The known trajectory $\eta(t)$ and function $\delta(t)$ enable us to calculate the accumulated mass

$$G_\mu(T_v) = T_v f_0 - \sum_{i=0}^{n} \left[\lambda f_0 \int_{t_i}^{t_{i+1}} \eta(t)\, dt + a_0 (t_{i+1} - t_i)\, \delta^{(i)} \right]. \tag{9.136}$$

Figure 9.34 shows the relative accumulated mass $G_\mu(2\pi)$ as a function of the exhaust velocity V_0 for different values of the initial radius Δr. It is seen that for each Δr there is a corresponding optimum exhaust velocity.
396 The dashed line represents the limiting curve corresponding to the exhaust velocities for which the motion is along the initial circular orbit (the thrust $P = F_0$, the minimum possible thrust).

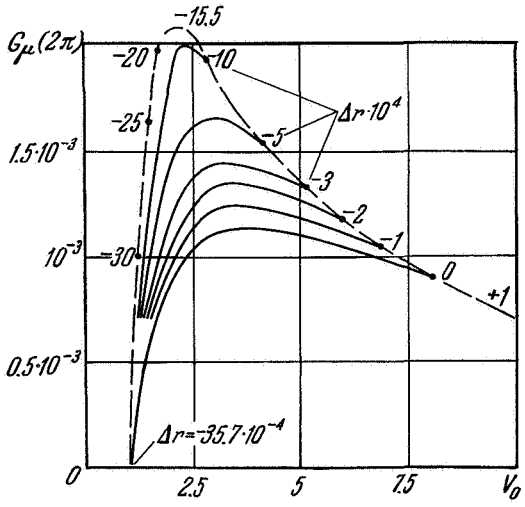

FIGURE 9.34. Mass taken in during one revolution (as fraction of vehicle takeoff mass) as function of exhaust velocity for different initial radii; unthrottled engine.

We now consider an ideally-throttlable engine. Here there are no restrictions on the exhaust velocity V, and in addition thrust reversal is allowed. If the quantity V in (9.123) lies in the interval $-\infty \leqslant V(t) \leqslant +\infty$, we may omit the function δ from the equations. The values $V = \pm\infty$ correspond to engine cutoff (zero thrust and flow rate). Negative values of the exhaust velocity $-\infty < V(t) < 0$ correspond to a thrust reversal.

From the condition for the Hamiltonian (9.126) to be a minimum, where $\delta \equiv 1$, the optimum program of the exhaust velocity is

$$V(t) = -1/p_f. \tag{9.137}$$

The momentum equations (9.127) and (9.130) are unaltered. Thus, the explicit expression for the optimum formula $V(t)$ is

$$V(t) = -\left[c_1 e^{-b_1 t} + e^{1/2 b_1 t}\left(c_2 \cos b_2 t + c_3 \sin b_2 t\right) - 1/2\right]^{-1}, \tag{9.138}$$

where the constants b_1 and b_2 are determined by formulas (9.130).

397 The zeros of $p_f(t)$ give the times when the thrust is cut off, $V = \infty$; if the function $p_f(t)$ changes sign as it passes through zero, we have a reversal of the thrust. Since the function $p_f(t)$ is continuous, a thrust reversal only occurs when the thrust vanishes.

Substituting (9.138) into the equation of motion (9.123) and integrating, we obtain the variation of the radius

$$\eta(t) = c_1 \frac{a_0}{2\lambda f_0} e^{-b_1 t} + \frac{16 a_0}{b_1 + 30\lambda f_0}(c_2 \cos b_2 t + c_3 \sin b_2 t)\, e^{1/2 b_1 t} + \\ + c_4 e^{b_1 t} + (c_5 \cos b_2 t + c_6 \sin b_2 t)\, e^{-1/2 b_1 t} + \frac{1}{\lambda}\left(1 - \frac{a_0}{2f_0}\right). \qquad (9.139)$$

The constants $c_1, \ldots, c_6$ are determined from the boundary conditions of the equations of motion by solving a linear system of algebraic equations.

If the parameters of the problem are selected so that $2f_0 - a_0 = 0$, and, in addition $\eta(0) = \dot\eta(0) = \eta(0) = \eta(T_v) = \dot\eta(T_t) = \ddot\eta(T_v) = 0$, we derive $c_1 = c_2 = \ldots = c_6 = 0$. This implies that $V(t) \equiv 2$ and $\eta(t) \equiv 0$.

The numerical results corresponding to an ideally-throttlable engine are given in Figures 9.35 to 9.37. An example of the optimum program $V(t)$ of the exhaust velocity and the corresponding trajectory $\eta(t)$ for $\Delta r = 0$ is shown in Figures 9.35 and 9.36. For comparison, we have plotted $\eta(t)$ in Figure 9.36 (the dashed curve) corresponding to an unthrottled engine for the optimum value of the velocity $V_0 = 3.5$. Due to thrust reversal (negative values of V in Figure 9.35), the vehicle with an ideal engine enters the dense layers of the atmosphere more rapidly, and the possibility of controlling (increasing) the thrust allows it to descend lower than the vehicle with an unthrottled engine.

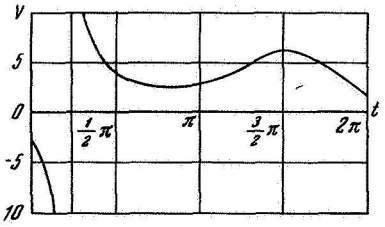

FIGURE 9.35. Optimum exhaust velocity program of ideal engine on air-intake trajectory (negative values of V correspond to thrust reversal).

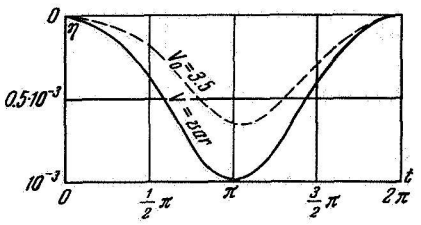

FIGURE 9.36. Examples of optimum air-intake trajectories with ideal engine (solid curve) and with unthrottled engine (dashed curve).

398 The value of the air mass taken in by a vehicle with an ideal engine is calculated from the known trajectory $\eta(t)$ and the exhaust velocity $V(t)$, using

$$G_\mu(T_v) = T_v f_0 - \lambda f_0 \int_0^{T_v} \eta(t)\, dt - a_0 \int_0^{T_v} V^{-2}(t)\, dt. \qquad (9.140)$$

Figure 9.37 shows the dependence of the air mass taken in, (9.140), on the radius Δr of the initial orbit for different values of f_0 (the drag on the

base orbit). The envelope of this family of curves is a horizontal line. The exhaust velocity at the tangential points is constant along the trajectory and equal to 2.

A comparison of the air mass taken in by the ideal $(G_\mu)_{V=var}$ and unthrottled $(G_\mu)_{V\equiv V_0}$ engines is presented in Figure 9.38 in the form of the ratio $(G_\mu)_{V\equiv V_0}/(G_\mu)_{V=var}$. The curves are plotted for different radii Δr as functions of the exhaust velocity V_0 of an unthrottled engine. The extreme right-hand ends of the curves (linked by the hatched line) correspond to the maximum possible velocity V_0 (the minimum thrust). If this is the initial velocity, flight along the orbit with the corresponding radius becomes impossible. It is seen from the figure that within the velocity range $2.5 < V_0 < 5$ the loss in air mass taken in over the given values of the radii Δr is a minimum and does not exceed 15%.

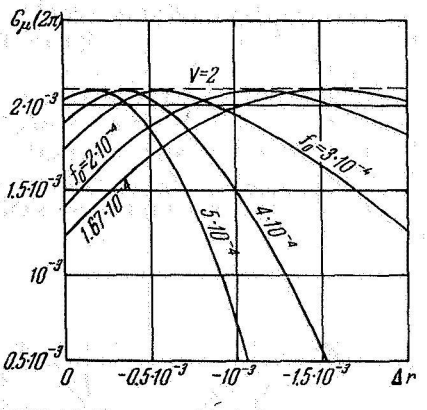

FIGURE 9.37. Mass taken in during one revolution as function of initial radius with different values of f_0 (drag on base orbit) for ideal engine.

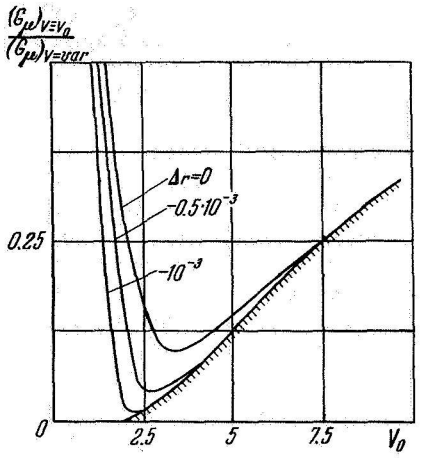

FIGURE 9.38. Ratio of air masses taken in by unthrottled engine, $(G_\mu)_{V\equiv V_0}$, and ideal engine, $(G_\mu)_{V=var}$, as function of exhaust velocity of unthrottled engine for fixed values of initial radius.

4. Outer-space maneuver of an air-breathing vehicle with a power-limited engine. Consider a vehicle which, after performing an air-intake orbit must undertake an outer-space maneuver. A power-limited engine is used both during the air-intake phase and for performing the basic maneuver. Its parameters can no longer be determined by just considering the optimum condition for one of the phases; they must ensure the optimum realization of the maneuver as a whole /9.18/. We determine below the optimum parameters of the propulsion system and the optimum air-intake time as a function of the maneuver and unit-weight characteristics of the system. The region in which the utilization of a power-limited engine with working-fluid intake is advantageous is determined by comparing its payload with that of a system without intake.

399

The problem is formulated as follows. The total time T for carrying out the two phases of the maneuver is established, and the time during which the basic maneuver is undertaken is the difference between this time and the air-intake time T_v. For a given takeoff weight G_0 we require a maximum payload G_π. The air-intake orbit is assumed to be circular with a fixed air density throughout. The transition from the intake orbit to the required trajectory is ignored.

The power-limited propulsion system is considered as ideally throttlable, so

$$P = qV, \quad N_\Upsilon = \frac{1}{2} qV^2 \qquad (0 \leqslant V \leqslant \infty, \quad 0 \leqslant N_\Upsilon \leqslant N_{v0}). \tag{9.141}$$

During the outer-space maneuver the flow rate and thrust acceleration will be taken as

$$\dot{G} = -gq, \quad a = -\frac{\dot{G}}{G} V, \tag{9.142}$$

where G is the instantaneous weight of the engine.

The weight of an ideally-throttlable power-limited propulsion system is determined by the weight of the power source

$$G_\varkappa = G_v = \alpha N_{v0}. \tag{9.143}$$

Eliminating q and V from (9.142) using the optimum condition $N_\Upsilon(t) = N_{v0} = G_v/\alpha$, we obtain, as in § 1 of Chapter Four, the differential equation governing the vehicle weight

$$-\frac{dG}{G^2} = \frac{1}{G_v} \frac{\alpha}{2g} a^2 dt. \tag{9.144}$$

400 The integral of this equation from the beginning to the end of the outer-space maneuver is written as

$$\frac{1}{G}\Big|_{G_0+G_\mu}^{G_0} = \frac{1}{G_v} \frac{\alpha}{2g} \int_{T_v}^{T} a^2 dt. \tag{9.145}$$

The takeoff weight G_0 consists of the weights of the payload G_π and the power source G_v; $G_0 = G_\pi + G_v$.

The working fluid consumed during the basic maneuver throughout time $T - T_v$ must first be accumulated during time T_v. For a stationary accumulation regime

$$G_\mu = g(q_v - q) T_v. \tag{9.146}$$

With an inlet duct cross section S and an atmospheric mass density ρ, the intake rate of the inlet duct equals

$$q_v = S\rho v. \tag{9.147}$$

The corresponding condition for the thrust during intake is written in the form

$$P = qV = \frac{1}{2} c_x S\rho v^2. \tag{9.148}$$

Using (9.147) and (9.148), we can rewrite equation (9.146) as

$$G_\mu = gq\left(\frac{2}{c_x}V - 1\right)T_v. \tag{9.149}$$

Here the exhaust velocity V is represented as a fraction of the orbital flight velocity v. We represent the weight components G_μ and G_v as fractions of the takeoff weight G_0, preserving the previous symbols for the dimensionless quantities. Equation (9.145) then becomes

$$\frac{G_\mu}{1+G_\mu} = \frac{1}{G_v}\Phi, \quad \Phi = \frac{\alpha}{2g}\int_{T_v}^{T} a^2\,dt. \tag{9.150}$$

If the flow rate through the nozzle is $q = 2G_v/\alpha v^2V^2$, we can determine its magnitude from (9.149) and (9.150) in the form

$$q = \frac{\Phi}{\alpha v^2 V^2}\left(1 + \sqrt{1 + \frac{2\alpha v}{g\Phi}\frac{V^2}{T_v\left(\frac{2}{c_x}V - 1\right)}}\right). \tag{9.151}$$

Equation (9.151) is obtained under the assumption that the weight of the compression unit is zero and the power plant uses up no power when compressing (allowance for these factors is made later). It is then possible
401 to determine the payload

$$G_n = 1 - G_v = 1 - \frac{\Phi}{2}\left(1 + \sqrt{1 + \frac{2\alpha v}{g\Phi}\frac{V^2}{T_v\left(\frac{2}{c_x} - 1\right)}}\right) \tag{9.152}$$

as a function of the exhaust velocity, the air-intake time, and the quantity Φ which characterizes the given maneuver.

We shall now find the optimum values of T_v and V which maximize the payload. The exhaust velocity of the working fluid, which maximizes G_n, is equal (as in subsection 2) to

$$V_{\text{opt}} = c_x. \tag{9.153}$$

The optimum intake time is determined when establishing the form of the functional Φ with respect to the maneuvering time. As an example, following the treatment in /9.18/, we consider the reciprocal relationship corresponding to the problem of escape from a central gravitational field*

$$\Phi = \frac{\Phi_0}{1 - T_v} \qquad \left(\Phi_0 = \frac{\alpha}{2g}\frac{\Delta v^2}{T}\right), \tag{9.154}$$

where Δv is the specified velocity increment, and the time T_v is represented as a fraction of T.

An increase in T_v leads to an increase in Φ, and it therefore becomes necessary to increase the initial working-fluid reserve G_μ; simultaneously,

* This dependence of the functional on the maneuvering time exists in the problem of transition between two coplanar circular orbits, and in the problem of rotating the plane of a circular orbit, when the thrust acceleration is much smaller than the gravitational acceleration on the original orbit (§§ 2, 3 of Chapter Five).

the mass taken in on the orbit increases, and therefore an optimum intake time must exist. In the case considered (9.154) it is given by

$$(T_v)_{opt} = \frac{\varkappa}{2(\varkappa + \sqrt{\Phi_0})}, \quad \varkappa = \sqrt{2\alpha v^2 c_x^2 / gT}. \tag{9.155}$$

Note that for the case considered in subsection 2, when the drag is equal to the momentum of the jet taken in by the inlet duct, the drag coefficient is equal to $c_x = 2$. The corresponding link between the parameter $\varkappa$ and G_μ/G_0 from (9.116) is then written as $\varkappa = \sqrt{4G_0/G_\mu T}$.

Substituting the values of V_{opt} and $(T_v)_{opt}$ from (9.153) and (9.155) respectively into (9.152), we obtain

$$G_\pi = 1 - \varkappa\sqrt{\Phi_0} - \Phi_0. \tag{9.156}$$

402 The range throughout which the mass intake is expedient can be determined by comparing the payload (9.156) with the payload for a power-limited propulsion system without accumulation (4.16):

$$G_\pi^* = 1 - 2\sqrt{\Phi_0} + \Phi_0. \tag{9.157}$$

A gain ($\Delta G_\pi = G_\pi - G_\pi^* > 0$) is realized for the following range of the parameters Φ_0 and $\varkappa$:

$$0 < \Phi_0 < (1 - {}^1/_2\varkappa)^2. \tag{9.158}$$

This gain ΔG_π will be maximum for a given value of $\varkappa$ when $\Phi_0 = (2 - \varkappa)^2/16$, so that

$$\Delta G_{\pi\,max} = \frac{1}{8}(2 - \varkappa)^2. \tag{9.159}$$

The relative gain in payload is equal to

$$\bar{G}_\pi = \frac{G_\pi}{G_\pi^*} = \frac{1 - \varkappa\sqrt{\Phi_0} - \Phi_0}{1 - 2\sqrt{\Phi_0} + \Phi_0} \tag{9.160}$$

and is a maximum when

$$\bar{G}_{\pi\,max} = \frac{4 + \varkappa^2}{4\varkappa} \quad \text{and} \quad \Phi_0 = \left(\frac{2 - \varkappa}{2 + \varkappa}\right)^2. \tag{9.161}$$

Figure 9.39 represents the payload as a function of the functional Φ_0 for different values of the parameter $\varkappa$. The dashed curve represents $G_\pi^*(\Phi_0)$ for the case without air intake. The optimum intake time has been plotted in Figure 9.40. The limiting curve corresponds to the values of $\varkappa$ and Φ_0 for which the basic maneuver can no longer be fulfilled (point of intersection with the line $G_\pi = 0$ in Figure 9.39).

Since the weight of the compression unit was taken equal to zero, the weight of the power source is $G_v = 1 - G_\pi(\varkappa, \Phi_0)$. Thus, for an ideal propulsion system with air intake, the optimum weight of the power source G_v depends not only on the maneuver characteristic Φ_0 (as assumed in /9.17/), but also on the parameter $\varkappa$.

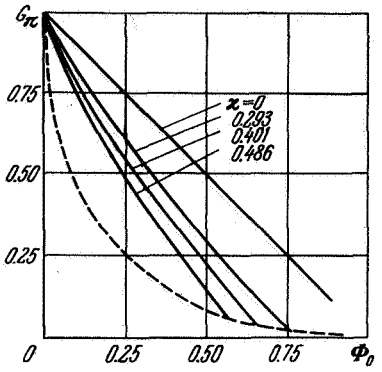

FIGURE 9.39. Maximum relative payload as function of problem functional Φ_0 when using working-fluid intake in upper atmospheric layers with power-limited engine. Dashed curve represents payload values for flight without mass intake.

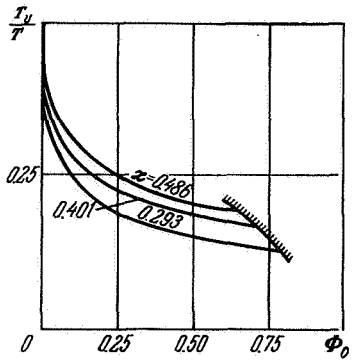

FIGURE 9.40. Optimum relative intake time T_v/T for flights with power-limited propulsion system.

The additional power expended in executing the intake process and in transporting the additional weight of the compression unit /9.18/ has not yet been accounted for. The takeoff weight G_0 will then comprise the sum of the three terms

$$G_0 = G_п + G_v + G_v, \tag{9.162}$$

403 where $G_v = \gamma_v q_v$ in what follows and the coefficient γ_v is taken as constant (9.108). In the mass-intake regime, power will be used for thrust production and compression. The latter will be assumed proportional to the gas flow rate, q_v (9.105). Then

$$N_{v0} = \frac{qV^2}{2} + k_v q_v, \quad G_v = \alpha\left(\frac{qV^2}{2} + k_v q_v\right), \tag{9.163}$$

where the proportionality factor k_v is taken as constant. Using equation (9.143) and making transformations similar to those performed above, we obtain an expression for the flow rate q of working fluid through the nozzle necessary for compensating the drag

$$q = \frac{g}{\alpha v^2}\frac{\Phi}{V^2\left(1+\frac{4k_v}{c_x v^2 V}\right)}\left(1+\sqrt{1+\frac{2\alpha v^2}{g\Phi T_v}\frac{V^2\left(1+\frac{4k_v}{c_x v^2 V}\right)}{\left(\frac{2}{c_x}V-1\right)}}\right). \tag{9.164}$$

The expression for the flow rate of working fluid through the nozzle was obtained assuming that all the gas mass taken in by the inlet duct is compressed, and a corresponding amount of power is consumed in the compression process The relative payload will now be written as a

404 function of the exhaust velocity, the intake time, and the maneuver characteristic Φ in the form

$$G_\pi = 1 - \frac{\Phi}{2}\frac{1+\frac{4k_v}{c_x v^2}\left(1+\frac{\gamma_v}{\alpha k_v}\right)\frac{1}{V}}{1+\frac{4k_v}{c_x v^2}\frac{1}{V}} \times \times\left(1+\sqrt{1+\frac{2\alpha v^2}{g\Phi T_v}\frac{V^2\left(1+\frac{4k_v}{c_x v^2 V}\right)}{\left(\frac{2}{c_x}V-1\right)}}\right). \tag{9.165}$$

For $\gamma_v = 0$ and $k_v = 0$, equations (9.164) and (9.165) naturally reduce to (9.151) and (9.152). As in the preceding case, we may prove the existence of an optimum intake time and exhaust velocity. Once again, the maneuver of escape from a central field, for which the magnitude Φ is determined by (9.154), is considered. The optimum relative intake time, which gives a maximum payload, equals

$$(T_v)_{\text{opt}} = \frac{1}{2}\left[1+\sqrt{\frac{g\Phi_0 T}{2\alpha v^2}\frac{\frac{2}{c_x}V-1}{V^2\left(1+\frac{4k_v}{c_x v^2 V}\right)}}\right]^{-1}. \tag{9.166}$$

The optimum exhaust velocity is not expressed explicitly in this case. The link between the optimum exhaust velocity and Φ_0 is given by the expression

$$\sqrt{\Phi_0} = \frac{c_1}{2c_2(c_3-1)}\sqrt{\frac{V+c_2}{V\left(V-\frac{c_x}{2}\right)^3}}\left[V^3-(c_x+c_2c_3-2c_2)V^2- - \frac{3}{2}c_x c_2 V - \frac{c_x}{2}c_2^2 c_3\right], \tag{9.167}$$

where

$$c_1 = v\sqrt{\frac{c_x\alpha}{gT}}, \quad c_2 = \frac{4k_v}{c_x v^2}, \quad c_3 = 1+\frac{\gamma_v}{\alpha k_v} \tag{9.168}$$

are dimensionless quantities.

Thus, the optimum parameters of the propulsion system (the exhaust velocity of the working fluid during intake and the relative weight of the power source) are established for this case.

Figure 9.41 illustrates the results of calculating the relative weights of the payload G_π and the power source G_v for the two sets of parameters
405 1) $\alpha = 2.5$ kg/kw, $c_1 = 0.15$, $c_2 = 0.16$, $c_3 = 9$; 2) $\alpha = 5.0$ kg/kw, $c_1 = 0.21$, $c_2 = 0.16$, $c_3 = 5$.

Figure 9.42 shows, for the same values of the parameters, the optimum relative exhaust velocity of the jet. The dependence of the optimum intake time on the functional Φ_0 is shown in Figure 9.43. Figure 9.44 shows the
406 relative increase of the payload $\bar{G}_\pi$ achieved by using mass intake with power-limited powerplants. The same figure shows for comparison (dash-dot curve) the relative gain in the ideal case for $\varkappa = 0.401$ (cf. (9.160)), which corresponds to the values of the parameters of curve 2.

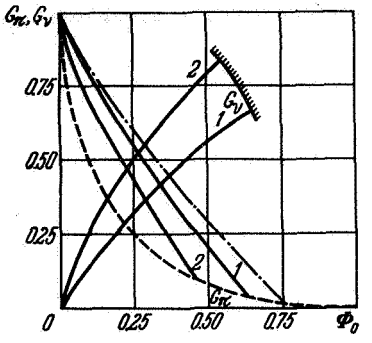

FIGURE 9.41. Variation of weight and power expended in taking in working fluid during orbital flight, with relative payload G_π and power-source weight G_v: 1) $\alpha = 2.5$ kg/kw, 2) $\alpha = 5$ kg/kw. Dash-dot curve corresponds to case 2 without these processes.

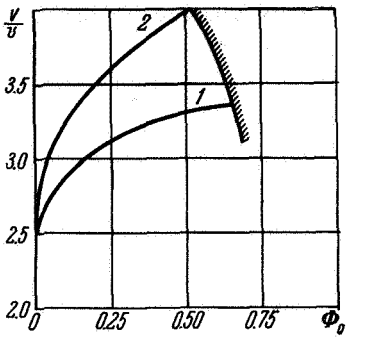

FIGURE 9.42. Optimum values of relative exhaust velocity V/v during intake phase allowing for weight and power used by intake system. Cases 1 and 2 correspond to data of Figure 9.41.

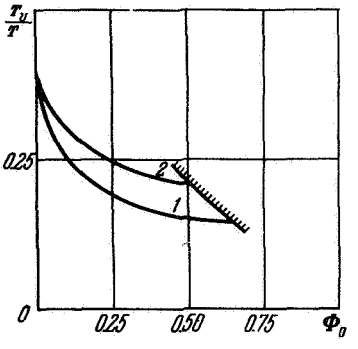

FIGURE 9.43. Optimum relative time of working-fluid intake T_v/T for power-limited engines allowing for weight and power used by intake system. Cases 1 and 2 correspond to data of Figure 9.41.

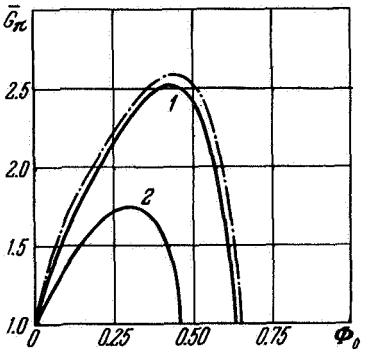

FIGURE 9.44. Gain in payload by using mass intake with power-limited propulsion systems. Cases 1 and 2 correspond to data of Figure 9.41. Dash-dot curve corresponds to case 2 without allowing for weight and energy expended when taking in air.

5. Outer-space maneuver of a vehicle with an engine of limited exhaust velocity when taking in air. Consider the combination of a propulsion system with air intake and a power-limited engine /9.20/. The unit, which takes in working fluid on a stationary circular orbit, will be considered as ideal (cf. the conditions in formula (9.116)), and the engine with limited exhaust velocity $V \leqslant V_{max}$, which carries out the basic maneuver, as weightless and ideally throttlable.

For this formulation the takeoff weight of the vehicle G_0 on the intake orbit will consist of the payload, the weight of the power source G_v, the

weight of the fuel $G_{\mu m}$, and the weight of the oxidizer $G_{\mu 01}$ (for a chemical engine), i.e.,

$$G_0 = G_\pi + G_v + G_{\mu m} + G_{\mu 01}. \tag{9.169}$$

We require the optimum relation between the weight components in (9.169), while ensuring a maximum of the relative payload, for performing a maneuver with a specified value of the characteristic velocity Δv; the intake time T_v is fixed (parameter of the problem).

It will be assumed that the substance of weight $G_{\mu 02}$ taken in during the orbital flight is the oxidizer (the necessary separation of the oxygen can be allowed for by a suitable correction factor). Its value for an intake time T_v equals (in accordance with (9.116) for $\eta_\gamma = 1$)

$$G_{\mu 02} = \frac{gG_v}{2\alpha v^2} T_v \quad \text{or} \quad G_{\mu 02} = \tau_* G_v \left(\tau_* = \frac{gT_v}{2\alpha v^2}\right). \tag{9.170}$$

Since the magnitude $2\alpha v^2/g$ (Figure 9.30) characterizes the time during which a quantity of working fluid equal to the weight of the power source G_v is taken in, τ_* represents the ratio of the intake time T_v to the time necessary for taking in working fluid of weight G_v.

The ratio of the fuel weight to the total weight of the oxidizer is given by the conditions of the chemical reaction

$$G_{\mu m} = k(G_{\mu 01} + G_{\mu 02}). \tag{9.171}$$

Taking relations (9.170) and (9.171) into account, expression (9.169) can be written as

$$G_0 = G_\pi + (1 + k\tau_*) G_v + (1 + k) G_{\mu 01}. \tag{9.172}$$

407 At the end of the accumulation phase the vehicle weight will be

$$G(T_v) = G_\pi + G_v + G_{\mu m} + G_{\mu 02} + G_{\mu 01} = G_0 + \tau_* G_v, \tag{9.173}$$

and after completing the maneuver (Δv) whilst consuming fuel and oxidizer in an engine with limited exhaust velocity, the terminal weight of the vehicle will be

$$G_1 = G_\pi + G_v, \tag{9.174}$$

where $\Delta v/V_{\max} = \ln [G(T_v)/G_1]$.

For given values of G_π, α, v, $V_{\max}$, and T_v the maximum of the characteristic velocity Δv corresponds to the minimum value of the ratio $G_1/G(T_v)$, namely,

$$\frac{G_1}{G(T_v)} = \frac{G_\pi + G_v}{1 + \tau_* G_v} \tag{9.175}$$

(here all the weight components are represented as fractions of the takeoff weight G_0).

Figure 9.45 shows the variation of $G_1/G(T_v)$ with G_v for two characteristic regions. For $G_\pi \leqslant 1/\tau_*$ the minimum value of $G_1/G(T_v)$ is attained at $G_v = 0$; in this case the use of an intake unit is inefficient. For $G_\pi > 1/\tau_*$ the minimum

value of $G_1/G(T_v)$ corresponds to the maximum value of G_v, which, according to (9.172), is attained at $G_{\mu 01} = 0$. In this situation

$$G_{v\,\mathrm{opt}} = \frac{1 - G_\pi}{1 + k\tau_*}. \tag{9.176}$$

Under these circumstances, the combination of an intake unit and an engine with limited exhaust velocity ensures a larger characteristic velocity for given takeoff weight and payload than that obtained with an engine of limited exhaust velocity only. According to (9.174) to (9.176) the maximum value of the characteristic velocity attained for this optimum combination of systems is given by

$$\frac{\Delta v}{V_{\max}} = \ln \frac{1 + \tau_* + k\tau_* - \tau_* G_\pi}{1 + k\tau_* G_\pi}. \tag{9.177}$$

408 As an example, we have plotted in Figure 9.46 the dependence of the relative payload G_π on the maneuver parameter $\Delta v/V_{\max}$ for $k = 0.2$, and different values of τ_* from (9.170). Tsiolkovskii's solution for an engine with limited exhaust velocity without mass intake is shown for comparison (dashed curve).

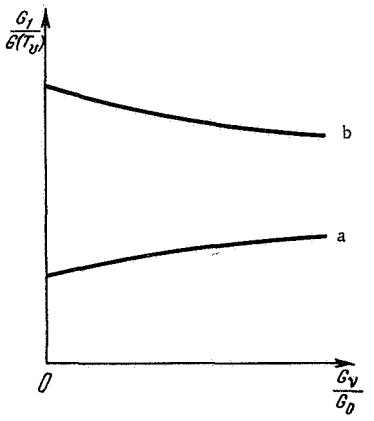

FIGURE 9.45. Ratio of terminal weight of vehicle with limited-velocity engine, G_1, to weight at end of intake phase, $G(T_v)$, as function of relative weight of power source G_v/G_0: a) regime $G_\pi < 1/\tau_*$; b) regime $G_\pi > 1/\tau_*$.

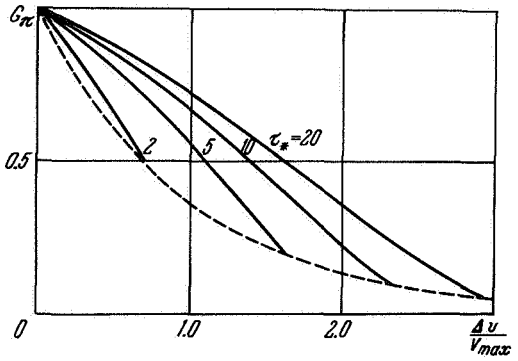

FIGURE 9.46. Maximum values of relative payload G_π for flight with propulsion system of limited exhaust velocity and working-fluid intake. Dashed curve represents Tsiolkovskii's solution for limited-velocity engine without mass intake.

To compare the characteristics of intake systems combined with ideal engines of limited exhaust velocity (treated in this subsection) and those of limited power (subsection 4) for the maneuver of a velocity build-up, we require the same values of $\tau_* = 4/\varkappa^2$ (cf. (9.170) and (9.155) for $c_x = 2$). This is because the build-up of a velocity using an ideal engine with limited exhaust velocity is instantaneous, and therefore the intake time T_v coincides with the total time T required to carry out both phases of the maneuver. The payload of the vehicle with an ideal power-limited engine (calculated

by (9.156) for the same values of $4/\varkappa^2 = \tau_*$ as were used in Figure 9.46) is shown in Figure 9.47.

409 Unlike the system with a power-limited engine, the intake system with an engine of limited velocity can be considered to be without a power source during the space maneuver. Here the increment in the characteristic velocity is larger than (9.177), and is determined by the minimum of the ratio

$$\frac{G_1'}{G'(T_v)} = \frac{G_\pi}{1 + (\tau_* - 1) G_v}. \qquad (9.178)$$

For $\tau_* \leqslant 1$ the minimum of (9.178) is attained at $G_v = 0$; in this case the use of an intake unit is inefficient. For $\tau_* > 1$ the optimum value of the relative weight of the power source in the intake phase is determined by (9.176).

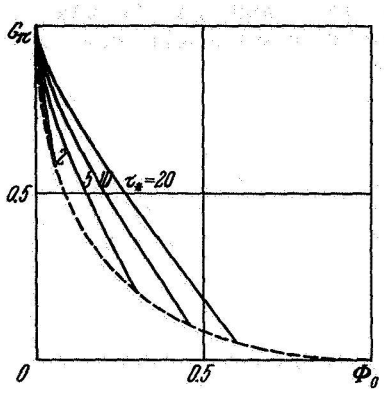

FIGURE 9.47. Maximum values of relative payload G_π for flight with ideally-throttlable power-limited propulsion system and working-fluid intake.

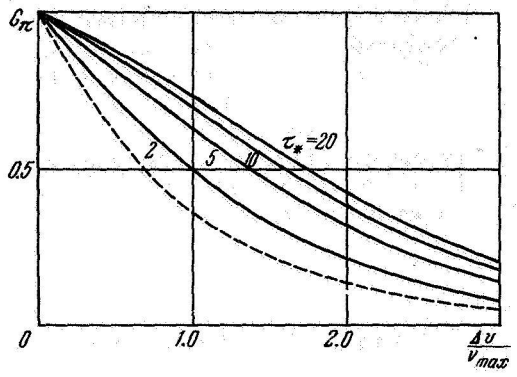

FIGURE 9.48. Maximum values of relative payload G_π for combination of intake system with engine of limited exhaust velocity, when accelerating payload alone during space maneuver. Dashed curve represents Tsiolkovskii's solution.

The maximum value of the characteristic velocity for the combination of an intake system with an engine of limited exhaust velocity, for accelerating the payload alone during the space-maneuver phase (without the power source) is given by

$$\frac{\Delta v}{V_{max}} = \ln \frac{(1+k)\tau_* - (\tau_* - 1) G_\pi}{G_\pi (1 + k\tau_*)}. \qquad (9.179)$$

An example of the dependence of G_π on $\Delta v/V_{max}$ for $k = 0.2$ and different values of τ_* is given in Figure 9.48.

410 § 4. SOLAR SAIL

1. Statement of the optimization problem for flight with solar sail. We consider a plane sail with an ideally-reflecting mirror surface (§ 2 of Chapter Two). If only the gravitational forces and the solar pressure

are considered, the motion of the center of mass of a spacecraft with solar sail is described by equation (1.1) with $\mathbf{F} = 0$. The thrust direction vector in this equation coincides with the normal to the shaded side of the sail $\mathbf{n}$, while the magnitude of the thrust is determined from (2.53).

The weight of a spacecraft with solar sail (the sail surface area is assumed constant, $S(t) = S_0$, and we neglect the phenomenon of "wear" of the sail) remains invariant with time, $G(t) = G_0$, and consists of two components: the payload G_π and the weight of the sail $G_s = gS_0\rho\delta$ (2.54). Substituting these relations into the equation of motion, we obtain

$$\ddot{\mathbf{r}} = \frac{p_{\odot}^{\wedge} S_0}{S_0\rho\delta + G_\pi/g}\left(\frac{R_\odot}{R}\right)^2 (\mathbf{n}\cdot\mathbf{i})^2\,\mathbf{n} + \mathfrak{R}, \tag{9.180}$$

where $\mathbf{n}$ is a unit normal to the shaded side of the sail, $\mathbf{i}$ is a unit vector in the direction of the solar rays, $(\mathbf{n}\cdot\mathbf{i})$ is the cosine of the angle $\widehat{\mathbf{ni}}$ between the normal to the sail and the incident solar rays, and $p_{\odot}^{\wedge}$ is the solar pressure per unit area of a sail set perpendicular to the solar rays, all measured on the Earth orbit $R_\odot$; $R = R(\mathbf{r})$ is the distance from the vehicle to the Sun (in the heliocentric system of coordinates $R = r$), and ρ and δ are the density and thickness of the sail material.

The sail parameters S_0, ρ, δ and the payload G_π are thus introduced into the equation of motion. We may replace the acceleration communicated by the sail to the spacecraft at a distance $R_\odot$ from the Sun when the sail is set perpendicular to the solar rays ($\mathbf{n} = \mathbf{i}$) by combining the parameters in (9.180):

$$a_0 = \frac{p_{\odot}^{\wedge} S_0}{G_\pi/g + S_0\rho\delta} \leqslant \frac{p_{\odot}^{\wedge}}{\rho\delta}. \tag{9.181}$$

The payload and the sail area are expressed in terms of this parameter

$$\frac{G_\pi}{G_0} = 1 - \frac{a_0\rho\delta}{p_{\odot}^{\wedge}}, \quad S_0 = G_\pi \frac{a_0}{g p_{\odot}^{\wedge}(1 - a_0\rho\delta/p_{\odot}^{\wedge})}, \tag{9.182}$$

while the equation of motion (9.180) becomes

$$\ddot{\mathbf{r}} = a_0\left(\frac{R_\odot}{R}\right)^2 (\mathbf{n}\cdot\mathbf{i})^2\,\mathbf{n} + \mathfrak{R}. \tag{9.183}$$

411 The link between the equation of motion (9.183) and the weight characteristics G_π, S_0, ρ, δ is expressed in terms of the single parameter a_0, whose maximum value is determined by the mass per unit sail area $\rho\delta$ (9.181). The acceleration a_0 plays the part of a constant control parameter for the equation of motion (9.183). The only control function in this equation is the sail orientation (the direction of the normal to the shaded side of the sail), which can be varied over the range $(-\pi/2, \pi/2)$ relative to the solar rays:

$$|\mathbf{n}(t)| \equiv 1 \quad (-\pi/2 \leqslant \widehat{\mathbf{n}(t)\mathbf{i}} \leqslant \pi/2).$$

Two equivalent formulations of the general optimization problem can be considered: 1. The total weight of the vehicle G_0 and the maneuvering time T are specified, and we require the maximum payload G_π. 2. The total weight of the vehicle G_0 and the payload G_π are specified, and we require the minimum maneuvering time T.

For a vehicle with a solar sail we need not consider G_π and G_0 separately. We can either use the ratio G_π/G_0 in (9.182), regarding it as specified, and determine the minimum of T, or we can consider T as specified and determine the maximum of G_π/G_0. According to the first relation of (9.182), the relative payload G_π/G_0 determines the value of the product $a_0\rho\delta$. The mass per unit sail area $\rho\delta$ depends on the structural quality and must be a minimum. Thus, the relative payload can be considered as uniquely linked to the acceleration a_0.

On the other hand, the quantity a_0 determines the maneuvering time T via the equation of motion (9.183); so the optimization problem reduces to determining the control function for the sail orientation $n(t)$ which either ensures minimum T for given a_0, or minimum a_0 for given T. The second formulation is less convenient, since the value found for the acceleration a_0 may be larger than $a_{0\max} = p_A^2/\rho\delta$ in (9.181).

2. Interorbital transfer of a spacecraft with solar sail. The transfer between the circular and coplanar orbits of two planets takes place in the central gravitational field of the Sun alone under the action of the solar pressure. Therefore, if we put $R = r$, $\mathbf{R} = -g_0 r_0^2 r^{-3}\mathbf{r}$ in equations (9.183) and designate the sail orientation angle by ϑ (the angle between the normal to the shaded side of the sail and the radius vector $\mathbf{r}$, the latter coinciding here with the direction of the solar rays $\mathbf{i} = \mathbf{r}/r$ i.e., $(\mathbf{n}\cdot\mathbf{i}) = \cos\vartheta$)
412 (cf. Figure 9.49), we obtain the following equations for plane motion:

$$\left.\begin{aligned} \dot r &= v_r, \qquad \dot v_r = \frac{v_\varphi^2}{r} + (a_0\cos^3\vartheta - g_0)\left(\frac{r_0}{r}\right)^2, \\ \dot\varphi &= \frac{v_\varphi}{r}, \qquad \dot v_\varphi = -\frac{v_r v_\varphi}{r} + a_0\cos^2\vartheta\sin\vartheta\left(\frac{r_0}{r}\right)^2, \end{aligned}\right\} \tag{9.184}$$

where g_0 is the gravitational acceleration of the Sun at a radius r_0.

The motion between the orbits of planets of a spacecraft with solar sail and sail-orientation angle ϑ = const have been discussed in /9.21—9.27/. A number of approximate and exact solutions were obtained (§§ 1 and 2 of Chapter Thirteen), and the optimum value of the constant orientation angle was established. With the aid of this group of analytic solutions we obtained an idea of the possible uses of solar sails for interplanetary travel. These solutions, however, have a grave shortcoming in that the boundary conditions for the coordinates and the velocity components at both ends of the trajectory cannot be satisfied.

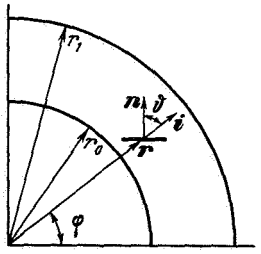

FIGURE 9.49. Scheme of interplanetary flight with solar sail.

Solutions of the variational problem of the orbital transfer of a spacecraft with solar sail (minimum transfer time T for given a_0) were obtained in /9.28, 9.29/. Following the treatment of /9.29/, we write equations (9.184) in dimensionless variables, where linear dimensions are expressed as fractions of r_0, the velocities as fractions of $\sqrt{g_0 r_0}$, the accelerations as fractions of g_0, and the time as a fraction of $\sqrt{r_0/g_0}$:

$$\left.\begin{aligned} \dot r &= v_r, \qquad \dot v_r = \frac{v_\varphi^2}{r} + \frac{a_0\cos^3\vartheta - 1}{r^2}, \\ \dot\varphi &= \frac{v_\varphi}{r}, \qquad \dot v_\varphi = -\frac{v_\varphi v_r}{r} + \frac{a_0\sin\vartheta\cos^2\vartheta}{r^2}. \end{aligned}\right\} \tag{9.185}$$

The optimum control function $\vartheta(t)$ must ensure the transfer from the point ($r = 1$, $v_r = 0$, $v_\varphi = 1$) to the point ($r = r_1$, $v_r = 0$, $v_\varphi = r_1^{-1/2}$) during a minimum time (the angular displacement is not fixed). To that end (in accordance with the maximum principle /9.4/), the control function $\vartheta(t)$ must yield an absolute maximum of the function

$$H = p_{v_r}\left(\frac{v_\varphi^2}{r} + \frac{a_0\cos^3\vartheta - 1}{r^2}\right) + p_{v_\varphi}\left(-\frac{v_\varphi v_r}{r} + \frac{a_0\sin\vartheta\cos^2\vartheta}{r^2}\right) + \\ + p_r v_r + p_\varphi\frac{v_\varphi}{r}, \tag{9.186}$$

413 where the system of control functions for the momenta $p_{v_r}, p_{v_\varphi}, p_r, p_\varphi$ has the form

$$\left.\begin{aligned} \dot{p}_{v_r} &= \frac{p_{v_\varphi}v_\varphi}{r} - p_r,\quad \dot{p}_{v_\varphi} = -\frac{2p_{v_r}v_\varphi}{r} + \frac{p_{v_\varphi}v_r}{r}, \\ \dot{p}_r &= \frac{p_{v_r}v_\varphi^2}{r^2} - \frac{2p_{v_r}}{r^3} + \frac{2a_0p_{v_r}\cos^3\vartheta}{r^3} - \frac{p_{v_\varphi}v_\varphi v_r}{r^2} + \frac{2a_0p_{v_\varphi}\sin\vartheta\cos^2\vartheta}{r^3}, \\ \dot{p}_\varphi &= 0,\quad p_\varphi(T) = 0. \end{aligned}\right\} \tag{9.187}$$

The optimum program for the sail-orientation angle $\vartheta(t)$ is determined from

$$\operatorname{tg}\vartheta = \frac{\sqrt{9p_{v_r}^2 + 8p_{v_\varphi}^2} - 3p_{v_r}}{4p_{v_\varphi}}. \tag{9.188}$$

If this expression for ϑ is substituted into equations (9.185) and (9.187), a system of seven differential equations results. It can be shown that at the initial time $p_{v_\varphi} = +1$ for $r_1 > r_0$, $p_{v_\varphi} = -1$ for $r_1 < r_0$ (the value 1 is obtained as a result of normalization). With these boundary conditions the solution was found numerically by Newton's method. Figures 9.50
414 and 9.51 give examples of the solution in /9.29/ for the transfer from an Earth orbit to a Mars orbit, and from an Earth orbit to a Venus orbit, for $a_0 = 2\cdot10^{-3}$ m/sec^2.

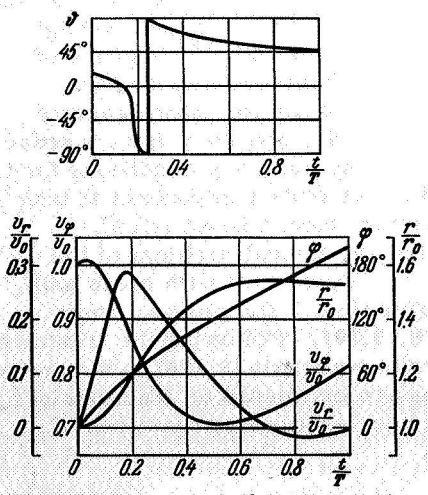

FIGURE 9.50. Parameters of optimum transfer with solar sail between Earth and Mars orbits with $a_0 = 2\cdot10^{-3}$ m/sec^2, time of flight $T =$ = 322 days.

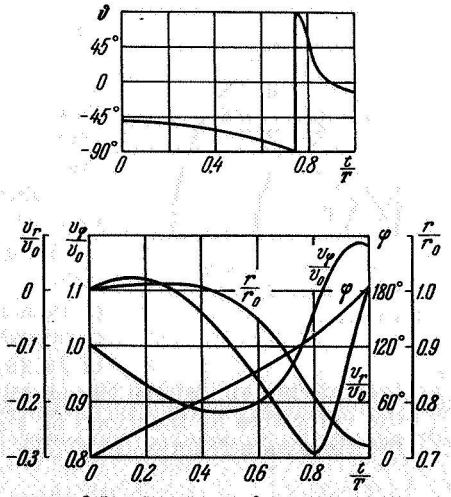

FIGURE 9.51. Parameters of optimum transfer with solar sail between Earth and Venus orbits with $a_0 = 2\cdot10^{-3}$ m/sec^2, time of flight $T =$ = 164 days.

Figure 9.52 gives a solution for the problem of transfer to Mars /9.28/ for $a_0 = 10^{-3}$ m/sec^2. In addition to the sail control function $\vartheta_{opt}(t)$ corresponding to the boundary condition $v_{r1} = 0$, $v_{\varphi 1} = 1/\sqrt{r_1}$, the figure also shows the function $\vartheta(t)$ on a Mars orbit for an unspecified value of the vehicle velocity which is determined from optimum considerations. Naturally, the transfer time for such an orbit around Mars is reduced from $T = 420$ days to $T = 170$ days.

For comparison Figure 9.52 also contains the solution /9.22/ with constant optimum sail orientation $\vartheta = \vartheta_*$ (the initial and final conditions for the velocity are not fulfilled in this solution).

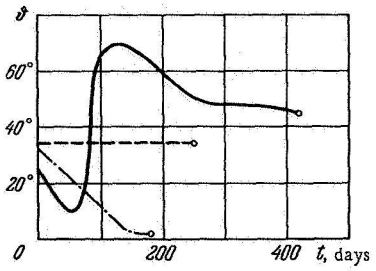

FIGURE 9.52. Optimum control programs of the sail orientation for transfer between Earth and Mars orbits with $a_0 = 10^{-3}$ m/sec^2. Solid curve represents optimum transfer with escape on orbital velocity of Mars; dash-dot curve represents transfer with optimum terminal velocity; dashed curve represents transfer with constant sail orientation.

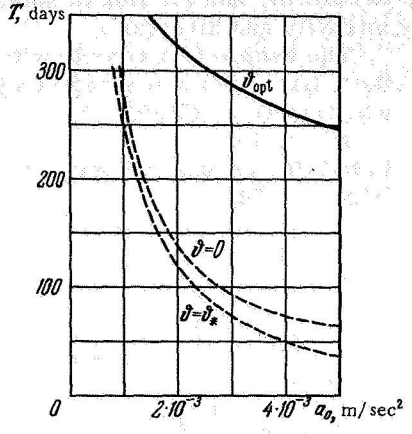

FIGURE 9.53. Time of transfer with solar sail from Earth orbit to Mars orbit as function of a_0. Solid curve represents exact optimum solution; dashed curves represent transfers with constant sail orientation (velocity boundary conditions not fulfilled).

Figure 9.53 shows the dependence of the minimum transfer time with solar sail between Earth and Mars orbits as a function of the acceleration a_0 (the solid curve) /9.29/. A comparison with the solutions for $\vartheta = \text{const}$ (the dashed curves) /9.23, 9.24/ indicates the strong influence of the velocity boundary conditions on the time of flight. Therefore, since the
415 solutions with constant sail orientation cannot satisfy all the velocity boundary conditions, their applications are very limited.

The results of the numerical calculations for the optimum transfers with solar sail from the Earth orbit to the orbits of all the planets in the Solar system are given in Table 9.1 for an initial acceleration $a_0 = 2 \cdot 10^{-3}$ m/sec^2 /9.29/.

We conclude this subsection with an example. Suppose we want to transfer a payload weighing 1 ton from the Earth orbit to the Mars orbit in 420 days using a minimum area of plastic solar sail ($\rho\delta = 5 \cdot 10^{-4}$ g/cm^2). Then, according to the data in Figures 9.52 and 9.53, $a_0 = 10^{-3}$ m/sec^2, and by (9.182) $S_0 = 0.26 \cdot 10^4$ m^2, which is equivalent to a circle of diameter 575 m. The total weight of the vehicle is then equal to 2.3 tons.

TABLE 9.1. Minimum transfer time from Earth orbit to orbit of solar-system planets with solar sail, $a_0 = 2 \cdot 10^{-3}$ m/sec^2

Planet	Mercury	Venus	Mars	Jupiter	Saturn	Uranus	Neptune	Pluto
T, years	0.53	0.45	1.12	6.6	17	49	96	145

416 **3. Escape of a spacecraft with solar sail from the field of planetary attraction.** The escape of a spacecraft with solar sail from the field of planetary attraction is treated in /9.30, 9.31/ with the following assumptions: the vehicle is projected into an initial circular orbit, the gravitational field is central, and the flux of solar light is plane-parallel with constant intensity and direction.

The escape of a vehicle with solar sail from the planetary field, where the initial orbit and escape trajectory lie in the plane of the ecliptic, was treated in /9.30/. The sail, whose two surfaces are considered as ideally reflecting, rotates about its axis at an angular velocity equal to half the angular velocity of revolution of the vehicle about the planet (Figure 9.54).

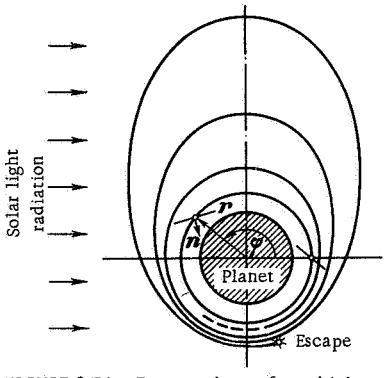

FIGURE 9.54. Escape scheme for vehicle with solar sail from field of planetary attraction along trajectory lying in plane of ecliptic.

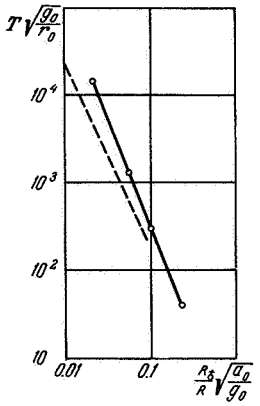

FIGURE 9.55. Escape time T of vehicle with solar sail from field of planetary attraction as function of initial acceleration a_0. Solid curve represents escape in plane of ecliptic, and dashed line represents escape with orbit perpendicular to ecliptic plane.

The equations of motion are written as follows (the planetary umbra is neglected):

$$\left.\begin{aligned} \ddot{r} - r\dot{\varphi}^2 + g_0\left(\frac{r_0}{r}\right)^2 &= -a_0\left(\frac{R_\delta}{R}\right)^2 \left|\sin\left(\frac{\varphi}{2}\right)\right| \sin\varphi, \\ r\ddot{\varphi} + 2\dot{r}\dot{\varphi} &= a_0\left(\frac{R_\delta}{R}\right)^2 \left|\sin\left(\frac{\varphi}{2}\right)\right|^3, \end{aligned}\right\} \qquad (9.189)$$

where R is the radius of the planetary orbit and g_0 is the acceleration of gravity on the initial orbit of the satellite.

After transforming to dimensionless variables and replacing the independent variable t by the polar angle φ, the system of equations (9.189) is

integrated numerically from the commencement of the initial circular orbit to the time when the total energy of the spacecraft relative to the planet vanishes.

The trajectory is shown in Figure 9.54. During acceleration the orbit gradually becomes elliptic, the perihelial distance varying only slightly. The build-up of zero energy (the escape) occurs in the neighborhood of the perihelion.

The dependence of the escape time T on the value of the initial acceleration a_0 is shown in Figure 9.55 (the solid line) in dimensionless variables. In these variables and on a logarithmic scale, the results obtained for the different values of a_0 and r_0 roughly lie on the same straight line. The scatter along the dimensionless time is indicated on the figure. The number of revolutions up to the instant of escape approximately equals $0.1\, g_0R^2/a_0R_\odot^2$. Table 9.2 gives the dimensional parameters for escape from the gravitational field of the Earth /9.30/. Note that the effect of the Earth's umbra on the escape characteristics for solar-sail propulsion was not taken into account in /9.30/. Obviously, when this effect is allowed for, a trajectory
417 considerably different from the one studied here is obtained, in particular at the initial stage of the motion.

TABLE 9.2. Parameters of spacecraft with solar sail on escape trajectory from Earth's field of attraction

Payload $G_п$, tons	Mass per unit sail area ρ_s, g/cm^2	Sail dimensions: area S_s, m^2	Sail dimensions: diameter of equivalent circular area, m	Total vehicle weight G_0, tons	Initial acceleration produced by solar pressure a_0, m/sec^2	Duration of maneuver T, days	Radius of initial circular orbit r_0, km	Maximum distance of trajectory up to instant of escape, km
0.1	10^{-4}	10^6	$1.12\cdot10^3$	1.1	$0.85\cdot10^{-2}$	54	$7.25\cdot10^3$	$4.2\cdot10^5$
0.1	$2\cdot10^{-4}$	10^6	$1.12\cdot10^3$	2.1	$0.44\cdot10^{-2}$	112	$7.25\cdot10^3$	$6.1\cdot10^5$
0.1	$3\cdot10^{-4}$	10^6	$1.12\cdot10^3$	3.1	$0.3\cdot10^{-2}$	119	$7.25\cdot10^3$	$7.62\cdot10^5$
0.1	10^{-4}	$2.45\cdot10^5$	$0.56\cdot10^3$	0.35	$0.67\cdot10^{-2}$	73	$7.25\cdot10^3$	$4.78\cdot10^5$
0.1	10^{-4}	10^5	$0.36\cdot10^3$	0.2	$0.46\cdot10^{-2}$	105	$7.25\cdot10^3$	$5.87\cdot10^5$

To ensure that the escape trajectory will not traverse the Earth's umbra and will not contain sections of motion toward the solar rays, the motion must take place outside the plane of the ecliptic. The following scheme for a vehicle with solar sail to escape from the planetary gravitational field is considered in /9.31/.

418 The plane $(x^{(2)}, x^{(3)})$ of the initial orbit is perpendicular to the plane $(x^{(1)}, x^{(2)})$ of the ecliptic (Figure 9.56). The equations of motion are written in a cartesian reference frame based on the Earth $(x^{(1)}, x^{(2)}, x^{(3)})$, which is considered immobile:

$$\ddot{x}^{(i)} - a_0\left(\frac{R_\odot}{R}\right)^2 \cos\alpha^{(i)}\cos^2\alpha^{(1)} + \frac{g_0 r_0^2 x^{(i)}}{\left[\sum_{i=1}^{3}(x^{(i)})^2\right]^{3/2}} = 0 \qquad (i = 1, 2, 3). \qquad (9.190)$$

Here cos $\alpha^{(i)}$ are the direction cosines of the normals to the shaded side of the sail, which are selected from the local optimum condition for a maximum rate of increase of the energy for max $(\mathbf{n}\cdot\mathbf{v})$:

$$\cos\alpha^{(1)} = (3\cos\beta^{(1)} + \sqrt{\cos^2\beta^{(1)} + 8})/k, \qquad \cos\alpha^{(i)} = 2\cos\beta^{(i)}/k$$

$$(k^2 = 6\cos^2\beta^{(1)} + 6\cos\beta^{(1)}\sqrt{\cos^2\beta^{(1)} + 8} + 12,\ \beta^{(i)} = \arccos(\dot{x}^{(i)}/|\mathbf{v}|),\ i = 1,2,3). \quad (9.191)$$

At the beginning of the motion the displacement along the $x^{(1)}$ axis is compensated by the gravitational force, and the trajectory is almost plane and quasicircular. In this section we use the approximate solution of /9.32/, which is based on a numerical solution of system (9.190), (9.191), written in dimensionless variables.

The dashed line in Figure 9.55 gives the time required to reach the escape point according to this solution. It is seen that the escape time obtained by the method of /9.31/is shorter than that obtained for a plane trajectory in /9.30/. This should not be considered however, as conclusive proof that it is better to accelerate in the plane perpendicular to the ecliptic, since in both cases use is made of nonoptimum sail-orientation programs. A comparison with the time of interorbital transfers shows that for a vehicle with solar sail the escape time from the planetary gravitational field forms a considerable part of the total time of interplanetary flight.

419 We conclude by mentioning that the local optimum control of the sail orientation for the problem of escape from the gravitational field of the Sun was studied in /9.33/. Figure 9.57 represents the optimum sail orientation yielding the largest increment in the eccentricity of the initial orbit $\varepsilon_0 = 0.5$ during one revolution. The same paper analyzes the question of flight stability for vehicles with solar sail.

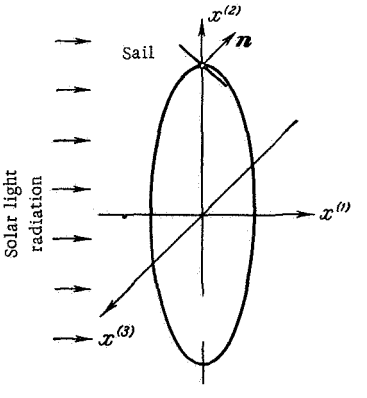

FIGURE 9.56. Escape scheme for vehicle with solar sail from field of planetary attraction with orbit perpendicular to ecliptic plane.

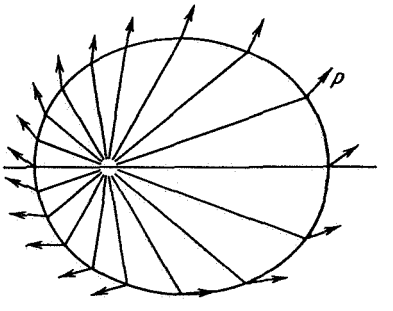

FIGURE 9.57. Optimum direction of thrust of solar sail ensuring maximum increment in eccentricity of initial heliocentric orbit $\varepsilon_0 = 0.5$ during one revolution about Sun.

§ 5. ISOTOPIC SAIL

1. Basic characteristics of the isotopic sail and formulation of the variational problem. It was shown in Chapters Two and Three that the maximum thrust of the isotopic sail decreases exponentially with time, while the sail weight is almost constant and proportional to the maximum sail area (i.e., to the maximum thrust)

$$0 \leqslant P(t) \leqslant P_{\max} e^{-\lambda t}, \quad G_{\varkappa} = \gamma P_{\max}. \tag{9.192}$$

The thrust can be controlled by varying the sail area ("hoisting down" the sail). It will be shown below that the area (thrust) of the sail in the optimum regime must be a maximum. No restrictions are imposed on the thrust orientation.

The variational problem will be formulated as one of maximum operating speed. The minimum maneuvering time is required for a fixed value of the relative payload /9.20/.

The full weight of a vehicle with isotopic sail remains practically constant throughout the flight; it consists of two components given by

$$G(t) \equiv G_0 = G_{\pi} + G_{\varkappa} = \text{const}. \tag{9.193}$$

It follows from (9.192) and (9.193) that, as for the solar sail, the dynamic part of the problem contains a single constant parameter, namely, the maximum thrust acceleration a_0, whose value is determined by the unit weight γ of the propulsion system and the specified value of G_{π}/G_0, where

$$a_0 = \frac{g}{\gamma}\left(1 - \frac{G_{\pi}}{G_0}\right). \tag{9.194}$$

420 The instantaneous value of the thrust acceleration is given by the expression

$$a = \tilde{a} a_0 e^{-\lambda t} \quad (0 \leqslant \tilde{a} \leqslant 1). \tag{9.195}$$

Here the control function $\tilde{a}(t)$ determines which part of the thrust is utilized.

The full system of differential equations, boundary conditions, and restrictions on the control functions of this variational problem is written in the form

$$\left.\begin{array}{llll} \dot{t} = 1, & t(0) = 0, & T = \min, \\ \dot{\mathbf{r}} = \mathbf{v}, & \mathbf{r}(0) = \mathbf{r}_0, & \mathbf{r}(T) = \mathbf{r}_1, \\ \dot{\mathbf{v}} = \tilde{a} a_0 e^{-\lambda t}\mathbf{e} + \mathbf{R}, & \mathbf{v}(0) = \mathbf{v}_0, & \mathbf{v}(T) = \mathbf{v}_1 \\ (0 \leqslant \tilde{a}(t) \leqslant 1, & |\mathbf{e}(t)| \equiv 1). & \end{array}\right\} \tag{9.196}$$

The problem reduces to determining the optimum control functions of the thrust magnitude $\tilde{a}(t)$ and direction $\mathbf{e}(t)$, which ensure a minimum maneuvering time T for a fixed value of the maximum acceleration a_0.

2. **Determination of the optimum control.** The control programs $\tilde{a}(t)$ and $\mathbf{e}(t)$ are determined from the condition of absolute maximum of the Hamiltonian, where

$$\left.\begin{aligned} H &= \tilde{a}a_0 e^{-\lambda t}(\mathbf{p}_v\cdot\mathbf{e}) + (\mathbf{p}_v\cdot\mathfrak{R}) + (\mathbf{p}_r\cdot\mathbf{v}) + p_t, \\ \dot{\mathbf{p}}_v &= -\mathbf{p}_r, \quad \dot{\mathbf{p}}_r = -\frac{\partial}{\partial \mathbf{r}}(\mathbf{p}_v\cdot\mathfrak{R}), \\ \dot{p}_t &= \lambda(\mathbf{p}_v\cdot\mathbf{e})\tilde{a}a_0 e^{-\lambda t}, \quad p_t(T) = -1. \end{aligned}\right\} \tag{9.197}$$

The unit vector $\mathbf{e}(t)$ entering the first term of H must be selected so as to maximize the scalar product $(\mathbf{p}_v\cdot\mathbf{e})$, which has a nonnegative coefficient. Hence,

$$(\mathbf{p}_v\cdot\mathbf{e}) = p_v \text{ or } \mathbf{e} = \mathbf{p}_v/p_v, \tag{9.198}$$

i.e., the thrust vector must be in the same direction as the vector $\mathbf{p}_v$. By analyzing this same term of the function H and allowing for condition (9.198) it follows that the control function $\tilde{a}(t)$ must be everywhere a maximum, i.e.,

$$\tilde{a}(t) \equiv 1. \tag{9.199}$$

3. **Model problem.** An an example, we now consider the model problem of flight during a minimum time using an isotopic sail between two points of rest situated at a distance l apart in a gravity-free field $(\mathfrak{R}=0, \mathbf{v}_0=0, \mathbf{v}_1=0, |\mathbf{r}_1-\mathbf{r}_0| = l)$.

421 For a homogeneous gravitational field the momentum $\mathbf{p}_v$ is a linear function of time (cf. (9.197) for $\mathfrak{R}\equiv 0$); and so the thrust vector $\mathbf{e}$ is directed either along the velocity or opposed to it, and can change its direction only once at some intermediate point t_* in the interval $[0, T]$ (Figure 9.58).

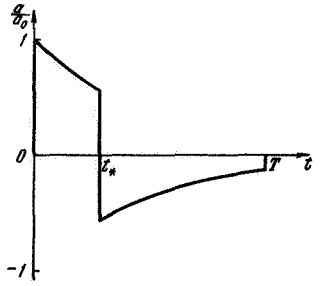

FIGURE 9.58. Optimum thrust control of isotopic sail for flight between two points of rest in gravity-free field.

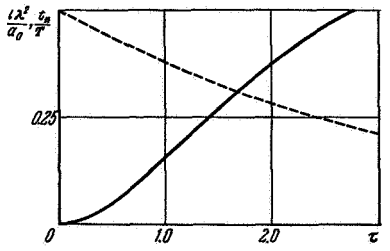

FIGURE 9.59. Instant changing thrust direction t_*/T (dashed curve) and relative distance $l\lambda^2/a_0$ (solid curve) as functions of characteristic time $\tau = \lambda T$ for flight between two points of rest using isotopic sail.

The integration of equations (9.196), taking this fact into consideration and allowing for (9.198) and (9.199), determines the connection between both the ratio t_*/T and the relative distance $l\lambda^2/a_0$, and the characteristic time of the problem $\tau = \lambda T$ (Figure (9.59):

$$\left.\begin{aligned} \frac{t_*}{T} &= \frac{1}{\tau^*}\ln\frac{2}{1+e^{-\tau}}, \\ \frac{l\lambda^2}{a_0} &= \ln\frac{2}{1+e^{-\tau}} - \frac{1}{e^{-\tau}}\left(\tau - \ln\frac{2}{1+e^{-\tau}}\right). \end{aligned}\right\} \tag{9.200}$$

Note that the characteristic time τ represents the ratio of the maneuvering time T to the half-life of the isotope $1/\lambda$. The second relation in (9.200) and formula (9.194) determine the minimum time T as a function of the payload $G_п/G_0$, the sail parameters λ, γ and the maneuver parameter l.

§ 6. ENGINE WITH SOLAR POWER SOURCE

We consider the problem of delivering a maximum payload by means of an ideal power-limited engine using solar energy /9.34/. The distinctive feature of this propulsion system is the dependence of its maximum power on the vehicle distance from the Sun. The approach is the same as that used in the case of constant maximum power. The optimum weight ratios are determined and the variational problem is set up for the optimum program of thrust acceleration and the selection of the design distance to the Sun. Approximate solutions are given for gravity-free and central fields.

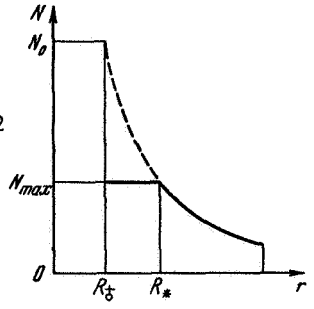

FIGURE 9.60. Maximum net power propulsion system with solar power source as function of distance from Sun.

1. Formulation of the optimization problem. The weight of a power-limited propulsion system utilizing solar energy can be represented as the sum of two components (neglecting the engine weight): the weight of either the solar energy concentrator (mirrors, Fresnel lenses) or of the plane converter (photoelectric cells, thermoelectric generators), and the weight of the converter of thermal energy into electric energy. The first component is proportional to the area S of the captured solar radiation flux, and the second to the maximum power N_{max} which can be processed by the converter. Thus, the weight of an engine with solar energy source is written as

$$G_к = \alpha N_{max} + \beta S \quad (\alpha, \beta = \text{const}). \tag{9.201}$$

The density of the solar energy flux decreases as the square of the distance from the Sun according to the law $\mathfrak{N}_A(R) = 1{,}4\,(R_☉/R)^2$ kw/m^2. The maximum power N_{max} is attained at a distance R_* from the Sun which will be called the design distance. This power is $N_{max} = \mathfrak{N}_A(R_*)\,S\eta$ where η is the conversion factor of solar energy into electrical energy. If the power generated by the powerplant on an Earth orbit is N_0, then, neglecting the variation of the efficiency, we can write $N_{max} = (R_☉/R_*)^2 N_0$. When approaching closer to the Sun the power must remain constant, since the converter of thermal energy into electric energy cannot function at a power exceeding the maximum design power, i.e., at a distance R_* from the Sun we must introduce a restriction on the powerplant (Figure 9.60):

$$N_v \leqslant N(R) = \begin{cases} (R_☉/R_*)^2 N_0 = N_{max} & \text{at } R \leqslant R_*, \\ (R_☉/R)^2 N_0 & \text{at } R \geqslant R_*. \end{cases} \tag{9.202}$$

Expression (9.201) can be represented in the form

$$G_\varkappa = \alpha_s[1 + (R_\delta/R_*)^2 \chi] N_0, \tag{9.203}$$

423 where $\alpha_s = \beta/\eta\mathfrak{N}_{\mathring{A}}(R_\delta)$ is the weight of the concentrator or plane converter per unit power, and $\chi = \alpha/\alpha_s$. It should be noted that in systems with plane converters $\chi \ll 1$, and therefore we can assume $G_\varkappa = \alpha_s N_0$ and $R_* = R_\delta$.

Consider the problem of determining the maximum payload for a given maneuver; the maneuvering time T, the takeoff weight of the vehicle G_0, and the unit weights α_s and χ are fixed. It is assumed that the engine is ideal, i.e., that the whole power supplied to the engine is transformed into jet power, and that the engine parameters, namely, the mass flow rate of working fluid and the exhaust velocity, can attain any value. In this problem we must indicate the optimum values of the weights $G_\varkappa$, $G_{\mu 0}$ and the design distance R_*, and also establish optimum programs for the thrust-acceleration vector $\mathbf{a}(t)$ and the power $N_v(t)$.

2. Optimum weight ratios and design distance to the Sun. We start by assessing the magnitude of the forces acting on the vehicle. The solar pressure is shown to be small compared with the thrust and gravitational forces. A flux of solar energy radiation $\mathfrak{N}_{\mathring{A}} S$ falls on the converter surface per unit time; as a result, the vehicle acquires momentum not exceeding $2\mathfrak{N}_{\mathring{A}} S/c$ (here $c = 3 \cdot 10^8$ m/sec is the velocity of light). The momentum imparted to the vehicle by an engine using solar energy is not less than $2\mathfrak{N}_{\mathring{A}} S\eta/V_{\max}$ (here $V_{\max} \sim 10^5$ m/sec is the maximum exhaust velocity). A comparison shows that the latter exceeds the former by at least two orders of magnitude.

The following estimate is valid for an acceleration under solar pressure: $f_{\mathring{A}} = 2\mathfrak{N}_{\mathring{A}} S/cG < 2\mathfrak{N}_{\mathring{A}} S/cG_\varkappa$. Using expression (9.201), this inequality can be written as $f_{\mathring{A}} < 2[\mathfrak{N}_{\mathring{A}}(R_\delta)/c\beta](R_\delta/R)^2$. For $\beta = 0.3$ kg/m^2 the acceleration produced by the solar pressure $f_{\mathring{A}} < 3 \cdot 10^{-5} (R_\delta/R)^2$ m/sec^2, which is at least two orders of magnitude smaller than the gravitational acceleration of the Sun, i.e., $5.92 \cdot 10^{-3} (R_\delta/R)^2$.

On the basis of these estimates, the solar pressure will be neglected in the following calculation.

As for motion with constant maximum power, one can here too integrate the equation governing the vehicle weight independently of the equations of motion and so obtain an expression for the payload (§ 1 of Chapter Four) in the form

$$\frac{G_\pi}{G_0} = \left(1 + \frac{G_0}{2g}\int_0^T \frac{a^2}{N_v}\,dt\right)^{-1} - \frac{G_\varkappa}{G_0}. \tag{9.204}$$

424 It follows that the power N_v must be a maximum as before:

$$N_v \equiv N(R). \tag{9.205}$$

With the aid of (9.202) and (9.203) we find that for a fixed value of the functional

$$J = \left[1 + \left(\frac{R_\delta}{R}\right)^2 \chi\right] \int_0^T \frac{a^2}{N}\,dt \tag{9.206}$$

$$(N = (R_\delta/R_*)^2 \text{ at } R \leqslant R_*,\ N = (R_\delta/R)^2 \text{ at } R \geqslant R_*)$$

G_π ($G_\varkappa$) has a maximum for $G_\varkappa/G_0 = \sqrt{\Phi - \Phi}$ at which its value is

$$G_\pi/G_0 = (1 - \sqrt{\Phi})^2, \qquad \Phi = (a_0/2g)J. \tag{9.207}$$

Thus, the problem of determining the optimum weight ratios can be solved if the value of the functional J is known. This latter is independent of the weight ratios and can be found as soon as the trajectory and the parameter R_* are known. For motion with constant power the factor multiplying the integral in (9.206) and the denominator of the integrand are equal to unity (4.10).

The problem thus reduces to finding a value of the parameter R_* and a thrust-acceleration program $\mathbf{a}(t)$ which minimize the functional J. This corresponds to the displacement between points $(\mathbf{r}_0, \dot{\mathbf{r}}_0)$ and $(\mathbf{r}_1, \dot{\mathbf{r}}_1)$ during a time T. The problem is then examined in a heliocentric system of coordinates, where $R = r$, $R_* = r_*$, $R_\odot = r_0$.

We shall show that the optimum value of the parameter r_* lies within the segment $[r_0, r_1]$. Let $J(r_*)$ be the minimum value of the functional J, which depends on the parameter r_* both explicitly and through the functions $a(t, r_*)$ and $N(r, r_*)$ which enter the integrand. Suppose $r_0 < r_1$; then, when the parameter r_* lies outside the segment $[r_0, r_1]$, the function $J(r_*)$ has the form

$$J(r_*) = \begin{cases} [1 + (r_0/r_*)^2 \chi] J_0 \quad \text{at} \quad r_* \leqslant r_0 \left(J_0 = \min\limits_{a(t)} \int\limits_0^T (r/r_0)^2 a^2 dt\right), \\ [(r_*/r_0)^2 + \chi] J_1 \quad \text{at} \quad r_* \geqslant r_1 \left(J_1 = \min\limits_{a(t)} \int\limits_0^T a^2 dt\right) \end{cases} \tag{9.208}$$

425 (it is assumed that the entire trajectory $r(t)$ lies within the interval $[r_0, r_1]$). Obviously, expressions J_0 and J_1 must remain constant; therefore with increasing r_*, $J(r_*)$ decreases when $r_* \leqslant r_0$ and increases when $r_* \geqslant r_1$.

At points r_0 and r_1 the function $J(r_*)$ is continuous and has the left-hand and right-hand derivatives given by

$$\left(\frac{dJ}{dr_*}\right)_{r_0-0} = -\frac{2\chi}{r_0} J_0, \qquad \left(\frac{dJ}{dr_*}\right)_{r_1+0} = \frac{2}{r_1} J_1. \tag{9.209}$$

It can be shown that the derivative of $J(r_*)$ is continuous at these points. If $r_* = r_1 - \Delta r_*$ the following inequality will then hold:

$$\int\limits_0^T \left(\frac{r_1 - \Delta r_*}{r_0}\right)^2 a^2 dt \leqslant \int\limits_0^T \frac{a^2 dt}{N(r, r_1 - \Delta r_*)}. \tag{9.210}$$

Let the functions $a(t)$ which minimize the right-hand and left-hand sides of the inequality be $a_1(t)$ and $a_2(t)$ respectively; then

$$\int\limits_0^T \left(\frac{r_1 - \Delta r_*}{r_0}\right)^2 a_2^2 dt \leqslant \int\limits_0^T \frac{a_1^2 dt}{N(r, r_1 - \Delta r_*)} \leqslant \int\limits_0^T \frac{a_2^2 dt}{N(r, r_1 - \Delta r_*)}. \tag{9.211}$$

It is easily shown that

$$\int\limits_0^T \frac{a_2^2 dt}{N(r, r_1 - \Delta r_*)} = \int\limits_0^T \left(\frac{r_1 - \Delta r_*}{r_0}\right)^2 a_2^2 dt + o(\Delta r_*); \tag{9.212}$$

we thus obtain from (9.211)

$$\min_{a(t)} \int_0^T \frac{a^2 dt}{N(r, r_1 - \Delta r_*)} = \min_{a(t)} \int_0^T \left(\frac{r_1 - \Delta r_*}{r_0}\right)^2 a^2 dt + o(\Delta r_*). \tag{9.213}$$

With the aid of (9.213) we can directly calculate the derivative dJ/dr_* at the point $r_1 - 0$. Consider an increment Δr_* in the value of r_* at r_1 and consider the limit as $\Delta r_* \to 0$. The corresponding expression is obtained from (9.209). The continuity of the derivative at the point $r_* = r_0 + 0$ can be demonstrated in the same way.

Thus, the function $J(r_*)$ remains positive on the segment $[r_0, r_1]$, but its derivative changes sign from minus to plus. It follows that the minimum value of $J(r_*)$ occurs at some point such that $r_0 < r_{*\text{opt}} < r_1$. In addition, knowing the derivatives dJ/dr_* at the points r_0 and r_1, we can find an optimum value near $r_{*\text{opt}}$, e.g., the abscissa of the point of intersection of the
426 tangents to the curve of $J(r_*)$ at r_0 and r_1.

3. Equations of the optimum trajectory. Consider a plane motion in the central field of the Sun. The equations of motion of the vehicle, written in polar coordinates, have the form (A.8)

$$\dot{r} = v_r, \quad r\dot{\varphi} = v_\varphi, \quad \dot{v}_r = a_r + v_\varphi^2/r - k/r^2, \quad \dot{v}_\varphi = a_\varphi - v_r v_\varphi / r. \tag{9.214}$$

We require the trajectory on which the minimum of the functional defined by

$$J = \int_0^T \frac{a^2 dt}{N(r, r_*)} \left(N(r, r_*) = \left(\frac{r_0}{r_*}\right)^2 \text{ at } r \leqslant r_*, N(r, r_*) = \left(\frac{r_0}{r}\right)^2 \text{ at } r \geqslant r_*\right) \tag{9.215}$$

(here r_* is fixed) is attained. The Euler equations for problem (9.214), (9.215) are (cf. (5.13)):

$$\left.\begin{aligned}
&\text{at } r_0 \leqslant r < r_* \\
&\dot{a}_r = \frac{1}{v_r}\left[\frac{1}{2}(a_r^2 + a_\varphi^2) + a_r\left(\frac{v_\varphi^2}{r} - \frac{k}{r^2}\right) - \lambda\left(\frac{r_0}{r_*}\right)^2 - \nu\frac{v_\varphi}{r}\left(\frac{r_0}{r_*}\right)^2\right], \\
&\dot{a}_\varphi = \frac{1}{r}\left[a_\varphi v_r - 2a_r v_\varphi + \nu\left(\frac{r_0}{r_*}\right)^2\right]; \\
&\text{at } r_* < r \leqslant r_1 \\
&\dot{a}_r = \frac{1}{v_r}\left[\frac{1}{2}(a_r^2 + a_\varphi^2) + a_r\left(\frac{v_\varphi^2}{r} - \frac{k}{r^2}\right) - \right. \\
&\qquad\qquad \left. - \lambda\left(\frac{r_0}{r}\right)^2 - \nu\frac{v_\varphi}{r}\left(\frac{r_0}{r}\right)^2\right] - 2\frac{a_r v_r}{r}, \\
&\dot{a}_\varphi = \frac{1}{r}\left[a_\varphi v_r - 2a_r v_\varphi + \nu\left(\frac{r_0}{r}\right)^2\right] - 2\frac{a_\varphi v_r}{r},
\end{aligned}\right\} \tag{9.216}$$

where λ and ν are integrals of the system (constants of isoperimetricity, corresponding to the specified time of motion and the specified angular displacement). At $r = r_*$ the partial derivative with respect to r of the integrand of functional (9.215) has a discontinuity. The Weierstrass — Erdmann conditions are fulfilled for the optimum trajectory, i.e.,

$$\left.\begin{aligned}
a_r(r_* - 0) = a_r(r_* + 0), \quad \dot{a}_r(r_* + 0) - \dot{a}_r(r_* - 0) = -(2a_r v_r/r)_{r_*}, \\
a_\varphi(r_* - 0) = a_\varphi(r_* + 0), \quad \dot{a}_\varphi(r_* + 0) - \dot{a}_\varphi(r_* - 0) = -(2a_\varphi v_r/r)_{r_*}.
\end{aligned}\right\} \tag{9.217}$$

427 Equations (9.214) and (9.216) together with the two first integrals λ and ν have in all 14 orders. The boundary conditions and the Weierstrass—Erdmann conditions give fourteen conditions for determining the trajectory.

The point at which $v_r = 0$ is a singular point of the node type (cf. (5.13)). The property of invariance of the optimum trajectory equations relative to the sign-reversal (5.16) and linear (5.15) transformations remains likewise in force.

4. Approximate method for determining the optimum trajectory. The problem of finding the minimum of functional (9.215) can be solved by iterations. We shall describe this method using the analogous one of the displacements between points of rest in a gravity-free field:

$$\dot{x} = u, \quad \dot{u} = a, \qquad x(0) = x_0, \; u(0) = 0, \; x(T) = l + x_0, \; u(T) = 0. \tag{9.218}$$

Let us determine the optimum trajectory in the sense of minimizing the functional

$$J = \int_0^T \left(\frac{x}{x_0}\right)^3 a^2 dt \tag{9.219}$$

(it is assumed for simplicity that $x_* = x_0$). The Euler equation for this problem has the form

$$\frac{d^2}{dt^2}(ax^2) + a^2 x = 0. \tag{9.220}$$

The function $N = (x_0/x)^3$ is replaced by some known function of time $\xi^{(0)}(t)$, which takes the same values as $N(x, x_0)$ at the ends of the interval, so that $\xi^{(0)}(0) = 1$, $\xi^{(0)}(T) = [x_0/(x_0 + l)]^3$.

The Euler equation for the new functional is

$$\frac{d^2}{dt^2}\left(\frac{a}{\xi^{(0)}(t)}\right) = 0. \tag{9.221}$$

This equation easily integrates to yield

$$x^{(0)}(t) = c_1 + c_2 t + \int_0^t \xi^{(0)}(\tau)(x - \tau)(c_3 + c_4\tau)\, d\tau, \tag{9.222}$$

where $c_1, \ldots, c_4$ are integration constants. From this trajectory we determine the new function $N[x^{(0)}(t), x_0] = \xi^{(1)}(t)$. By repeating this procedure, we find a new approximation $x^{(1)}(t)$, etc.

428 As a zero approximation, we used the linear function $\xi^{(0)}(t) = 1 - bt$, where $b = l(2x_0 + l)/(x_0 + l)^3 T$. In the following steps the function $\xi^{(i)}(t)$ is replaced by its approximate expressions with the aid of Newton's interpolation polynomial, the number of interpolation nodes being increased at each step of the process. This enables us to end the interpolation each time.

Figure 9.61 shows the functions $a^{(i)}(t)$ corresponding to the successive approximations; for comparison, the law of variation $a(t)$ for motion with constant power is shown by the dashed line (the boundary conditions x_0 and $x_0 + l$ correspond roughly to the mean radii of Earth and Mars orbits). The value of the functional (9.219) was found, by this method, to be $\sim 19 l^3 T^{-3}$.

Note that for motion at constant power given by $N \equiv 1$ and $N \equiv [x_0 / (x_0+l)]^2$ the minimum values of the functional are equal to $12l^2T^{-3}$ and $27l^2T^{-3}$ respectively.

The result is assessed as follows. The required magnitude obviously does not exceed the value of the functional (9.219) on the trajectory corresponding to the optimum motion with constant power $\sim 19.8\, l^2T^{-3}$. On the other hand, since we know the derivatives of the minimum value of the functional (9.215) with respect to the parameter x_* at the points x_0 and $x_0 + l$ (cf. subsection 2) and that its value at $x_* = x_0 + l$ equals $27l^2T^{-3}$, we find that $\min J \approx 18l^2T^{-3}$. Thus, the approximate method described provides a method of determining a trajectory which is very close to the optimum one.

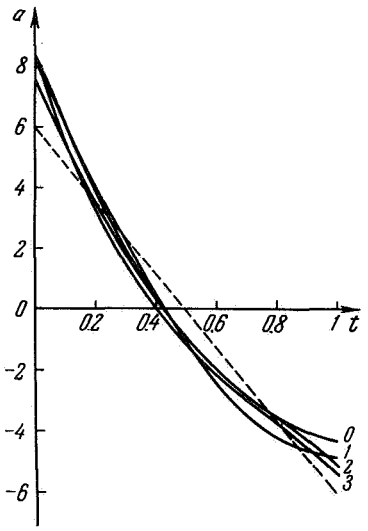

FIGURE 9.61. Successive approximations to optimum thrust-acceleration control function $a(t)$ for flight between points of rest with propulsion system using solar energy. Dashed line represents optimum control function $a(t)$ for constant power.

429

The elementary analogous problem considered has revealed the peculiar features of the thrust-acceleration program for flight along a trajectory which is an optimum as regards the functional (9.219). The variation pattern of the acceleration differs in this case considerably from the linear law (Figure 9.61) corresponding to optimum motion with constant power. The law of variation $a(t)$ which was obtained has a simple physical interpretation, namely, that it is efficient to maintain a high acceleration level in those places where the powerplant power is higher, i.e., at the beginning of the flight. Deceleration takes place at a lower power, and therefore the acceleration level at the end of the flight must be lower so that the consumption of working fluid should not be high.

5. Calculation of the orbital transfer by means of the transport trajectory. To determine approximately the optimum trajectory in a central field we use the transport trajectory method (§ 2 of Chapter Five) combined with the iterative process described in the preceding subsection.

The system describing the motion of the center of mass of the vehicle is written in the form

$$\ddot{\mathbf{r}} = \mathbf{a} + \operatorname{grad} U, \tag{9.223}$$

where U is the potential of the gravitational field. In the zero approximation the functional (9.215) has the form

$$J = \int_0^T \frac{a_x^2 + a_y^2 + a_z^2}{\xi^{(0)}(t)}\, dt, \tag{9.224}$$

where a_x, a_y, a_z are the components of the thrust-acceleration vector in a cartesian system of coordinates.

The Euler equations for problem (9.223), (9.224) are

$$\ddot{\eta} - A\eta = 0, \quad \eta = \mathbf{a}/\xi^{(0)}(t),$$

$$A = \begin{pmatrix} U_{xx} & U_{xy} & U_{xz} \\ U_{yx} & U_{yy} & U_{yz} \\ U_{zx} & U_{zy} & U_{zz} \end{pmatrix}. \tag{9.225}$$

Let us represent the trajectory of the motion in the form $\mathbf{r}(t) = \mathbf{r}^*(t) + \rho(t)$, where $\mathbf{r}^*(t)$ is a known trajectory, satisfying part of the boundary conditions, for instance the conditions governing $\mathbf{r}$ (the transport trajectory), and $\rho \ll r^*$. The transport trajectory $\mathbf{r}^*(t)$ is described by the equation

$$\ddot{\mathbf{r}}^* - \operatorname{grad} U^* = 0. \tag{9.226}$$

Now substitute $\mathbf{r} = \mathbf{r}^* + \rho$ into (9.225) and, if second-order magnitudes are ignored, the system becomes

$$\ddot{\rho} - A^*\rho = \mathbf{a}, \quad \ddot{\eta} - A^*\eta = 0 \qquad (\mathbf{a} = \xi^{(0)}(t)\eta), \tag{9.227}$$

where U^* and A^* are values of the potential U and the matrix A along the transport trajectory.

430 If we write, in equations (9.227), $A^* = 0$ (which corresponds to small deviations of the trajectory from the transport trajectory for which one can neglect the disturbances of the gravitational forces compared with the thrust), the equations of optimum motion in a system of coordinates moving along the transport trajectory will be

$$\ddot{\rho} = 0, \quad \ddot{\eta} = 0. \tag{9.228}$$

In this approximation the optimum thrust control function will have the form (at the i-th step of the process)

$$\mathbf{a}^{(i)}(t) = \xi^{(i)}(t)\,(\mathbf{c}_1^{(i)}t + \mathbf{c}_2^{(i)}) \tag{9.229}$$

($\mathbf{c}_1^{(i)}$ and $\mathbf{c}_2^{(i)}$ are integration constants). If $\xi^{(i)}(t)$ has a form convenient for integration, then $\rho^{(i)}(t)$ is now found either by quadratures or analytically.

As an example consider the trajectory of the flight to Mars which is optimum in the sense of minimizing the functional

$$J = \int_0^T \left(\frac{r}{r_0}\right)^* a^2 dt \qquad (r_* = r_0). \tag{9.230}$$

Assume for simplicity that the trajectory is plane. The boundary conditions can be taken to be those given in § 2.5 of Chapter Five for a
431 flight to Mars of duration $T = 212$ days in the plane of the ecliptic.

The approximate expression $N[r(t), r_*]$, which corresponds to the flight trajectory to Mars with a constant-power engine (given in Figure 5.8), can be taken as the function $\xi^{(0)}(t)$. Figure 9.62 shows the flight trajectory in the transport system of coordinates; the dashed curve represents the flight trajectory with an engine of constant power. The control function $\mathbf{a}(t)$

is shown in Figure 9.63. The value of the functional is $J = 16.4\ m^2/sec^3$. For motions with constant power $N \equiv 1$ and $N \equiv (r_0/r_1)^2$ the minimum values of the functional are respectively equal to $9.25\ m^2/sec^3$ and $25.1\ m^2/sec^3$.

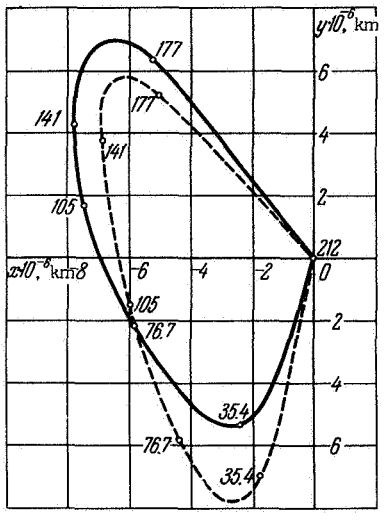

FIGURE 9.62. Optimum trajectory of Earth—Mars orbital transfer in 212 days with power-limited propulsion system and solar energy source. Dashed curve corresponds to constant-power propulsion system (transport system of coordinates).

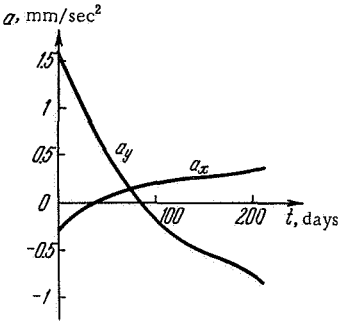

FIGURE 9.63. Optimum control program of thrust acceleration during Earth—Mars orbital transfer with power-limited propulsion system and solar energy source ($T = 212$ days).

When the minimum values of the functional at $r_* = r_0$ and $r_* = r_1$ are known, we can determine approximately the optimum value of the parameter r_* and the functional $J(r_*)$ (subsection 2). For $\alpha = 1$ kg/kw, $\beta = 1.5$ kg/m², $\eta = 0.1$ the optimum design distance to the Sun is $r_{*opt} \approx 175 \cdot 10^6$ km, ($r_0 = 150 \cdot 10^6$ km, $r_1 = 250 \cdot 10^6$ km), and the minimum value of the functional $J(r_{*opt}) = 17\ m^2/sec^3$ ($J(r_0) = 18\ m^2/sec^3$).

§ 7. ENGINE WITH ISOTOPIC ENERGY SOURCE

1. Engine characteristics and formulation of the variational problem. The maximum power of an engine with isotopic energy source, similar to the maximum thrust of an isotopic sail (§ 5), decreases exponentially with time:

$$0 \leqslant N \leqslant N_0 e^{-\lambda t}, \tag{9.231}$$

where N_0 is the maximum jet power at the initial time $t = 0$, and λ is a parameter characterizing the decrease of power with time ($1/\lambda$ is the half-life of the isotope). As above, maximum power utilization is always preferred during a powered flight with power-limited propulsion systems. In this case the basic parameters of the propulsion system are linked via

the relations (where the working fluid is accelerated without losses)

$$N = N_0 e^{-\lambda t}, \quad P = qV, \quad N = {}^1/_2 qV^2. \tag{9.232}$$

Consider an engine with a limited control range of the exhaust velocity:

$$0 \leqslant V(t) \leqslant V_{\max}, \tag{9.233}$$

in the limiting case $V_{\max} \to \infty$. This corresponds to ideal throttling.

The weight of the propulsion system is determined by the initial value of the power given by

$$G_\varkappa = \alpha N_0. \tag{9.234}$$

The problem of delivering a maximum payload is written in the form

$$\left.\begin{array}{lll} \dot{G}_\sigma = -k_1 G_\varkappa e^{-\lambda t} V^{-2}\delta, & G_\sigma(0) + & G_\sigma(1) = \max, \\ \dot{G}_\varkappa = 0, & + G_\varkappa(0) = 1, & G_\varkappa(1) = \text{opt}, \\ \dot{\mathbf{r}} = \mathbf{v}, & \mathbf{r}(0) = \mathbf{r}_0, & \mathbf{r}(1) = \mathbf{r}_1, \\ \dot{\mathbf{v}} = \sqrt{\frac{k_1}{\Phi}} \frac{G_\varkappa e^{-\lambda t}}{(G_\sigma + G_\varkappa) V} \mathbf{e}\delta + \mathbf{R}, & \mathbf{v}(0) = \mathbf{v}_0, & \mathbf{v}(1) = \mathbf{v}_1 \\ \left(k_1 = \frac{2gT}{\alpha V_{\max}^2}, \Phi = \frac{\alpha l^2}{2gT^3}, 0 \leqslant V(t) \leqslant 1, \delta(t) = 1 \text{ or } 0, |\mathbf{e}(t)| = 1\right). & & \end{array}\right\} \tag{9.235}$$

Here all the variables are dimensionless. The weights G_σ, $G_\varkappa$ are written as fractions of the takeoff weight, and the time t and the half-life $1/\lambda$ as fractions of the total time of flight. The radius vector $\mathbf{r}$ is expressed as a fraction of the characteristic distance l, the velocity of motion $\mathbf{v}$ as a fraction of l/T, and the exhaust velocity as a fraction of $V_{\max}$.

The above variational problem corresponds to the standard formulation of the Mayer problem. We must determine the control functions $\mathbf{e}(t)$, $\delta(t)$, $V(t)$, and the parameter $G_\varkappa$ such that the final value of the phase coordinate $G_\sigma(1) = G_\pi$ is a maximum. The solution of this problem for two similar maneuvers in a gravity-free field is considered below.

2. **Build-up of a velocity.** Let $u_1 T$ be the characteristic distance, where u_1 is the specified increment in the velocity magnitude. The expression Φ is written in the form $\Phi = (\alpha/2g)u_1^2 T^{-1}$ and the boundary conditions are $x(0) = 0$, $\dot{x}(0) = 0$, $x(1) = \text{opt}$, $\dot{x}(1) = 1$.

According to the maximum principle the optimum control functions $e(t) = \pm 1$, $\delta(t)$, $V(t)$ must yield an absolute minimum of the Hamiltonian

$$H = G_\varkappa e^{-\lambda t} \frac{\delta}{V}\left(\sqrt{\frac{k_1}{\Phi}} \frac{p_u e(t)}{G_\sigma + G_\varkappa} - \frac{k_1 p_\sigma}{V}\right) + p_x u, \tag{9.236}$$

where the momenta p are determined by the system of differential equations

$$\left.\begin{array}{l} \dot{p}_x = 0, \quad \dot{p}_u = -p_x, \\ \dot{p}_\sigma = \frac{k_1}{\Phi} \frac{p_u e(t) G_\varkappa e^{-\lambda t}}{V(G_\sigma + G_\varkappa)^2}\delta, \\ \dot{p}_\varkappa = \dot{p}_\sigma - \frac{k_1}{\Phi} \frac{p_u e(t) e^{-\lambda t}}{V(G_\sigma + G_\varkappa)} + \frac{k_1 p_\sigma e^{-\lambda t}}{V^2}\delta, \end{array}\right\} \tag{9.237}$$

433 with boundary conditions

$$p_\sigma(0) = p_\varkappa(0), \quad p_\varkappa(1) = 0, \quad p_x(1) = 0, \quad p_\sigma(1) = -1. \tag{9.238}$$

The optimum control functions in the problem considered are determined by the following relations:

$$\left.\begin{aligned} &e(t) \equiv 1, \quad \delta(t) \equiv 1, \\ &V(t) = \begin{cases} V_{\text{opt}} & \text{at} \quad V_{\text{opt}} < 1 \\ 1 & \text{at} \quad V_{\text{opt}} \geqslant 1 \end{cases} \left(V_{\text{opt}} = -\frac{2\sqrt{k_1\Phi}\,(G_\sigma + G_\varkappa)}{p_u} \right). \end{aligned}\right\} \tag{9.239}$$

It follows from analyzing the Hamiltonian H and the boundary conditions that the control functions $e(t)$ and $\delta(t)$ found in the problem of build-up of a specified velocity magnitude remain the same for any engine control regime.

At time t_1 the exhaust velocity reaches its limit $V_{\text{opt}}(t_1) = 1$, where

$$t_1 = -\frac{1}{\lambda}\ln\left\{1 - (1 - e^{-\lambda}) \times \right.$$
$$\left. \times \frac{\sqrt{k_1\Phi} - \ln\left(\frac{1}{2} + k_1\frac{1 - e^{-\lambda}}{2\lambda}\right)}{\sqrt{k_1\Phi} - \ln\left(\frac{1}{2} + \frac{k_1}{2}\frac{1 - e^{-\lambda}}{\lambda}\right) + 1 - 2\left(1 + k_1\frac{1 - e^{-\lambda}}{\lambda}\right)^{-1}} \right\}. \tag{9.240}$$

Since t_1 can take different values, depending on the parameters, three different expressions for the functional G_π are obtained when solving equations (9.235) and (9.237). These are

$$\text{at} \quad t_1 \leqslant 0: \quad G_\pi = e^{-\sqrt{k_1\Phi}} - \frac{\lambda}{1 - e^{-\lambda}}\frac{1 - e^{-\sqrt{k_1\Phi}}}{k_1}, \tag{9.241}$$

$$\text{at} \quad t_1 \geqslant 1: \quad G_\pi = \left(1 - \sqrt{\frac{\lambda}{1 - e^{-\lambda}}\Phi}\right)^2, \tag{9.242}$$

$$\text{at} \quad 0 < t_1 < 1: \quad G_\pi = \frac{1}{k_1}\frac{\lambda}{1 - e^{-\lambda}}\left[1 + \right.$$
$$\left. + \sqrt{k_1\Phi} - \ln\left(\frac{1}{2} + k_1\frac{1 - e^{-\lambda}}{2\lambda}\right)\right]^2. \tag{9.243}$$

In case (9.241) the control function $V(t)$ reaches its limit $V(t) \equiv 1$; (9.242) corresponds to the ideal control $V(t) \equiv V_{\text{opt}}(t)$; in case (9.243), $V(t) = V_{\text{opt}}(t)$ at $0 < t < t_1$, $V(t) = 1$ at $t_1 < t < 1$.

434 The optimum value of the engine weight $G_\varkappa$ is

$$G_\varkappa = \frac{2\lambda}{k_1(1 - e^{-\lambda})}\left[\sqrt{k_1\Phi} - 1 - \ln\left(\frac{1}{2} + \frac{k_1}{2}\frac{1 - e^{-\lambda}}{\lambda}\right)\right] \times$$
$$\times \left\{-1 - \frac{1}{2}\left[\sqrt{k_1\Phi} - 1 - \ln\left(\frac{1}{2} + \frac{k_1}{2}\frac{1 - e^{-\lambda}}{\lambda}\right)\right] + \right.$$
$$\left. + \left(1 + k_1\frac{1 - e^{-\lambda}}{\lambda}\right)^{-1}\right\}. \tag{9.244}$$

The results of this solution are illustrated in Figure 9.64. This shows the relative payload as a function of λT during the velocity build-up using an ideally-throttlable engine ($0 \leqslant V \equiv V_{\text{opt}} < \infty$).

3. Displacement between points of rest. For the second analogous problem, that of the flight between two points of rest situated at a distance

l apart, an analytic solution is obtained for an ideally-throttlable engine only.

The full system of differential equations governing the motion, weight variation, and conjugated momenta has the following form in dimensionless coordinates:

$$\left.\begin{aligned}
&\dot{x} = u,\\
&\dot{u} = \frac{12}{\Phi}\frac{G_\varkappa e^{-\lambda t}}{V(G_\sigma + G_\varkappa)}\, e(t)\,\delta,\\
&\dot{G}_\sigma = -\frac{12}{\Phi}\frac{G_\varkappa}{V^2}\, e^{-\lambda t}\delta,\\
&\dot{G}_\varkappa = 0,\\
&\dot{p}_x = 0, \quad \dot{p}_u = -p_x, \quad \dot{p}_\sigma = \frac{12 p_u e(t)\, G_\varkappa e^{-\lambda t}}{\Phi V (G_\sigma + G_\varkappa)^2}\,\delta,\\
&\dot{p}_\varkappa = \dot{p}_\sigma - \frac{12 p_u e(t)\, e^{-\lambda t}}{\Phi V (G_\sigma + G_\varkappa)}\,\delta + \frac{p_\sigma e^{-\lambda t}}{\Phi V^2}\,\delta.
\end{aligned}\right\} \qquad (9.245)$$

435 The Hamiltonian is given by

$$H = \frac{12 G_\varkappa e^{-\lambda t}}{\Phi V}\left(\frac{p_u e(t)}{G_\sigma + G_\varkappa} - \frac{p_\sigma}{V}\right)\delta + p_x u, \qquad (9.246)$$

where $\Phi = (\alpha/2g)\ 12 l^2 T^{-3}$.

The boundary conditions for the momenta and the coordinates

$$\left.\begin{aligned}
&p_\sigma(0) = p_\varkappa(0), \quad p_\sigma(1) = -1, \quad p_\varkappa(1) = 0,\\
&G_\sigma(0) + G_\varkappa(0) = 1, \quad x(0) = 0, \quad u(0) = 0, \quad x(1) = 1, \quad u(1) = 0
\end{aligned}\right\} \qquad (9.247)$$

completely define the problem.

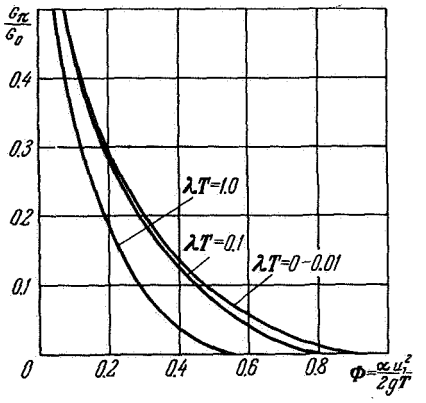

FIGURE 9.64. Influence of decrease in jet power with time on relative payload G_π/G_0 for specified velocity build-up u_1 during time T (λT is ratio of maneuvering time to isotope half-life).

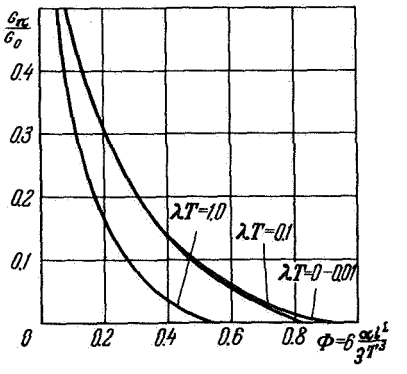

FIGURE 9.65. Influence of the decrease in jet power with time on relative payload G_π/G_0 for flight during time T between two points of rest situated distance l apart.

The minimum of the Hamiltonian is achieved for the following optimum control functions:

$$\left.\begin{aligned} e(t) &= -\operatorname{sgn} p_u, \quad \delta(t) \equiv 1, \\ V &= -\frac{2p_\sigma (G_\sigma + G_\varkappa)}{p_u}. \end{aligned}\right\} \tag{9.248}$$

The maximum payload is found from the following expression in terms of the functional Φ:

$$G_n = \left(1 - \sqrt{\frac{\lambda^3 (1 - e^{-\lambda}) \Phi}{12 [(1 - e^{-\lambda})^2 - \lambda^2 e^{-\lambda}]}}\right)^2. \tag{9.249}$$

Figure 9.65 shows the relative payload as a function of λT for flight between two points of rest with an ideally-throttlable engine. The data in Figures 9.64 and 9.65 show that the decrease in jet power with time has a noticeable effect on the payload for ratios of the maneuvering time to the half-life which are of order $\lambda T \geqslant 0.1$.

Chapter Ten

MODIFICATIONS OF THE OPTIMUM CRITERION

436 So far, the weight criterion for an optimum has been used when formulating the variational problems, namely, maximum payload for given takeoff weight. The dynamic maneuver was fixed. Each set of maneuver parameters had its corresponding suitable values of the dynamic system parameters to ensure delivery of a maximum payload.

In this chapter the formulation of the optimization problems is changed in two senses. First, the weight criterion is replaced by the cost criterion (§ 1, /10.1/) and second, the propulsion system parameters are selected not for a single maneuver but for a range of maneuvers (§§ 2 and 3). The distribution of the required number and types of maneuvers is either fixed (§ 2, /10.2/), or considered as unknown; in the latter case use is made of the theory of games (§ 3, /10.3/). For each specific maneuver, the optimum working-fluid reserve is determined for selected universal parameters of the propulsion system (§ 4, /10.4/).

§ 1. MINIMIZING THE COST OF A MANEUVER

If the same maneuver is to be performed several times, it is preferable to replace the weight criterion by the cost criterion. The cost of a maneuver consists of the costs of the main vehicle components; the latter are considered proportional to the corresponding weights.

1. Cost formula. The cost C of a maneuver is given by

$$C = C_0 + C_\varkappa + C_\mu + C_e. \tag{10.1}$$

Here C_0 is the cost of injection into the initial orbit (taken proportional to the initial weight $G_0 = G_\varkappa + G_{\mu 0} + G_\pi$) where

$$C_0 = c_0 G_0; \tag{10.2}$$

$C_\varkappa$ is the cost of the propulsion system (taken proportional to the engine weight $G_\varkappa$) given by

$$C_\varkappa = c_\varkappa G_\varkappa; \tag{10.3}$$

437 C_μ is the cost of the working-fluid reserve with the tanks (taken proportional to the initial weight of working fluid $G_{\mu 0}$) written as

$$C_\mu = c_\mu G_{\mu 0}; \tag{10.4}$$

C_e are other expenses, independent of the weight parameters of the vehicle. The coefficients c_0, $c_\varkappa$, c_μ, and the cost C_e are considered constant and specified.

2. **Optimum criterion.** The cost of the delivery per unit payload (cf. (10.1)) is chosen as the optimum criterion

$$c = C/G_\pi \tag{10.5}$$

which, when using the relations (10.2) to (10.4) connecting the costs and weights, may be expressed as

$$c = \frac{1}{G_\pi}(c_0 G_0 + c_\varkappa G_\varkappa + c_\mu G_{\mu 0} + C_e). \tag{10.6}$$

The takeoff weight G_0 is specified, and therefore instead of (10.6) we introduce the following functional to characterize the maneuvering cost:

$$S = \frac{1 + s_\varkappa G_\varkappa + s_\mu G_{\mu 0}}{1 - G_\varkappa - G_{\mu 0}}, \tag{10.7}$$

where the weights $G_\varkappa$ and $G_{\mu 0}$ are represented as fractions of the takeoff weight G_0, and the coefficients $s_\varkappa$ and s_μ are fixed by

$$s_\varkappa = \frac{c_\varkappa}{c_0 + C_e/G_0} > 0, \quad s_\mu = \frac{c_\mu}{c_0 + C_e/G_0} > 0. \tag{10.8}$$

The functional (10.7) differs from (10.6) by a constant factor where

$$c = (c_0 + C_e/G_0)S, \tag{10.9}$$

so that the problem of minimizing S is equivalent to that of minimizing c.

3. **Formulation of the variational problem.** With the above assumptions the formulation of the optimization problem is analogous to that given in the introduction to Part II; only the functional is different.

We introduce a differential equation describing the variation of the functional (10.7) with time, and write the variational problem in Mayer's
438 form (cf. (II. 5))

$$\left.\begin{aligned}
\dot S &= q\,\frac{1 + s_\mu + (s_\varkappa - s_\mu)G_\varkappa}{(1 - G_\varkappa - \Delta G_\mu)^2}, & S(0) &= \frac{1 + s_\varkappa G_\varkappa}{1 - G_\varkappa}, & S(T) &= \min,\\
\Delta\dot G_\mu &= q, & \Delta G_\mu(0) &= 0, & \Delta G_\mu(T) &= \text{opt},\\
\dot{\mathbf{r}} &= \mathbf{v}, & \mathbf{r}(0) &= \mathbf{r}_0, & \mathbf{r}(T) &= \mathbf{r}_1,\\
\dot{\mathbf{v}} &= P\mathbf{e}(1 - G_\varkappa - \Delta G_\mu)^{-1} + \mathbf{R}, & \mathbf{v}(0) &= \mathbf{v}_0, & \mathbf{v}(T) &= \mathbf{v}_1.
\end{aligned}\right\} \tag{10.10}$$

Here, a new phase coordinate $\Delta G_\mu = G_{\mu 0} - G_\mu(t)$, which is the weight of working fluid consumed up to time t, replaces G_μ (the instantaneous working-fluid reserve). The object of this transformation is to minimize the terminal value $S(T)$ (and not the initial one) of the phase coordinate S. All weights in (10.10) are given as fractions of the takeoff weight G_0, and the thrust and flow rate as fractions of G_0/g. In order to close formulation (10.10) the characteristics of the propulsion system (II.9), (II.10) must be specified.

For fixed engine weight $G_\varkappa$ the problem of minimum cost S reduces to that of minimum working-fluid weight $G_{\mu 0}$. This is clear from physical considerations. It follows formally from the fact that the partial derivative of S is positive:

$$\frac{\partial S}{\partial G_{\mu 0}} = \frac{s_\mu}{1 - G_\varkappa - G_{\mu 0}} + \frac{1 + s_\varkappa G_\varkappa + s_\mu G_{\mu 0}}{(1 - G_\varkappa - G_{\mu 0})^2} > 0, \tag{10.11}$$

since s_μ and $s_\varkappa$ are positive (cf. (10.8)), and $G_\varkappa + G_{\mu 0} < 1$.

This observation enables one to use the optimum programs of engine control found earlier. Now, only new optimum values of the constant control parameters remain to be found.

4. **Ideal power-limited engine.** The characteristics of such an engine are given by formulas (4.1) to (4.4). After integrating the flow-rate equation we have (allowing for the fact that $N(t) = N_{\max}$, cf. (4.9))

$$G_{\mu 0} = \frac{\Phi}{\Phi + G_\varkappa} \qquad \left(\Phi = \frac{\alpha}{2g}\int_0^T a^2\,dt, \quad \alpha = \text{const}\right). \tag{10.12}$$

The optimum engine weight $G_\varkappa$ can be found as before without solving the dynamic part of the problem to minimize the functional J. Substituting (10.12) in (10.7), $G_\varkappa$ is found from the condition $\partial S/\partial G_\varkappa = 0$:

$$G_\varkappa = \sqrt{\zeta\Phi + \zeta(\zeta - 1)\Phi^2} - \zeta\Phi \qquad \left(\zeta = \frac{1 + s_\mu}{1 + s_\varkappa}\right). \tag{10.13}$$

440 The parameter ζ represents the ratio of the cost per working-fluid weight to the cost per unit engine weight (cf. (10.8)). For $\zeta = 1$ (equal costs) (10.13) yields expression (4.15) for the engine weight which ensures a maximum payload. The optimum ratio between the weight of the working fluid and the engine indicates that the working-fluid reserve should be increased for $\zeta < 1$, or that the engine weight be increased for $\zeta > 1$ (Figure 10.1). It is seen from the figure that the difference between the optimum weight relations when substituting the cost criterion for the weight criterion can be quite considerable, depending on the difference in cost between the working fluid and engine.

Consider the loss in the functionals if, when calculating one functional we use the optimum weight ratios of the other one. To decrease the number of parameters we separate from the cost functional (10.7) that part which only depends on ζ and Φ, i.e.,

$$\sigma(\zeta, \Phi) = \frac{\zeta G_{\mu 0} + G_\varkappa}{1 - G_{\mu 0} - G_\varkappa} \qquad (S = (1 + s_\varkappa)\sigma + 1). \tag{10.14}$$

As for S, the variable σ represents the maneuvering cost. The solid curves in Figure 10.2 represent $\sigma(\zeta, \Phi)$ for the optimum values of $G_{\mu 0}$ and $G_\varkappa$ obtained using the cost criterion (10.12) and (10.13). The dashed curves correspond to the optimum values of $G_{\mu 0}$ and $G_\varkappa$ obtained using the weight criterion $G_{\mu 0} = \sqrt{\Phi}$, $G_\varkappa = \sqrt{\Phi} - \Phi$ (cf. (10.12), (10.13) for $\zeta = 1$, and (4.17), (4.15)). The same figure shows the dependence of the payload $G_\pi = 1 - G_\varkappa - G_{\mu 0}$ on Φ for different values of the parameter ζ. It is seen that the loss in payload when using one optimum weight ratio in place of the other is greater than the loss in cost.

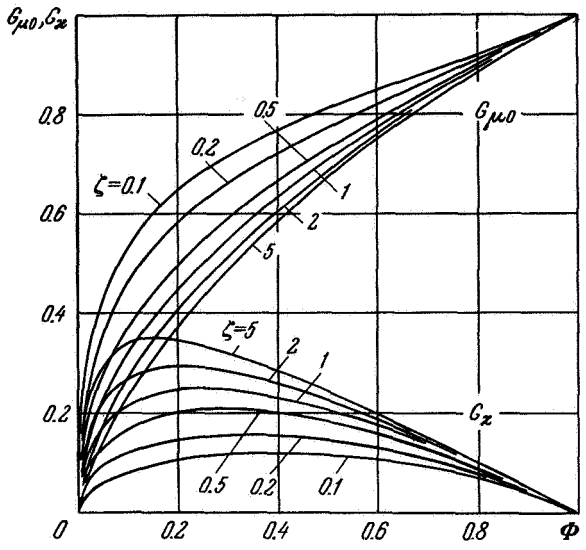

FIGURE 10.1. Optimum cost relations between engine weight $G_{\varkappa}$ (ideal, power-limited) and working-fluid reserve $G_{\mu 0}$ (ζ is ratio of unit cost of working fluid and engine, Φ is functional of dynamic problem).

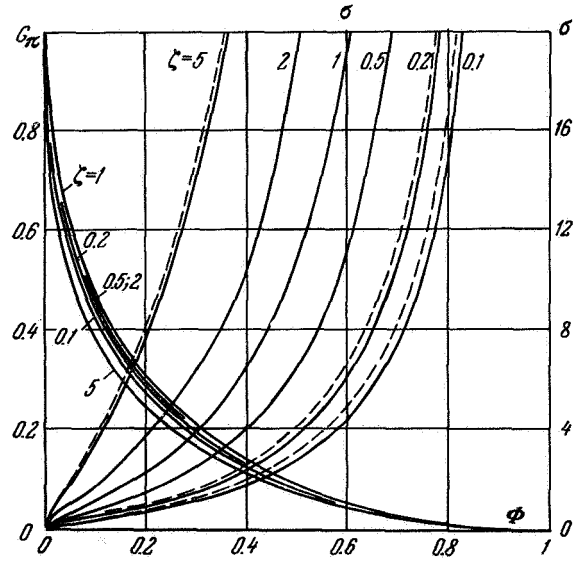

FIGURE 10.2. Cost σ and payload G_{π} for ideal power-limited engine (weight relations taken from Figure 10.1; dashed curves represent cost for maximum payload).

§ 2. UNIVERSAL PROPULSION SYSTEM FOR A GIVEN CLASS OF MANEUVERS

We consider here the problem of selecting the parameters of the propulsion system which executes a specific range of maneuvers (and not just one maneuver as until now). Such a universal system yields a reduction in the number of nonidentical systems, and therefore also their development expenses. Optimization is realized using the weight criterion.

1. General formulation of the problem. Consider a controllable object (dynamic system), whose state is described by a system of ordinary
441 differential equations of the form

$$\dot{x}_i = f_j(x_j, u_k, w_l, t),\ x_i(0) = x_{i0},\quad x_i(T) = x_{i1}$$
$$(u_{k\min} \leqslant u_k(t) \leqslant u_{k\max},\ w_l = \text{const};$$
$$i, j = 0, 1, \ldots, n;\ k = 1, \ldots, r;\ l = 1, \ldots, q), \tag{10.15}$$

where x_i are the phase coordinates, $u_k(t)$ are the control functions and w_l are the control parameters.

The maneuver is here represented by a set of boundary values for the phase coordinates x_i $(i = 1, \ldots, m \leqslant n)$ and the time T; the set of these values is designated by the vector

$$\mathbf{b} = (x_{10}, \ldots, x_{m0}, x_{11}, \ldots, x_{m1}, T). \tag{10.16}$$

The dynamic system is characterized by the set of control-parameter values w_l and by the vector

$$\mathbf{w} = (w_1, \ldots, w_q) \tag{10.17}$$

(the limiting values of the control functions $u_{k\min}$, $u_{k\max}$ can also belong to the parameters w_l).

The criterion of maneuver "quality" is the extreme value of the phase coordinate x_0:

$$x_0(T) = \text{extr} \quad (x_0(0) = 0). \tag{10.18}$$

When usually formulating optimum control problems, functions $u_k(t)$ must be established and values of the parameters w_l selected from the class of allowable ones to ensure that the boundary conditions (10.15) are satisfied and yield an extremum of the functional (10.18).

The optimum control functions $u_k(t)$ and the optimum values of the parameters w_l, which form the solution of the problem, generally depend on the maneuver parameters $\mathbf{b}$. The dynamic systems (10.15) will be considered as different if the values of the corresponding parameters $\mathbf{w}$ do not coincide. It is assumed that different control functions $u_k(t)$ can be realized in the same system.

The optimum realization (in the sense of the functional (10.18)) of a large number of maneuvers with different sets of parameters

$$\mathbf{b}^{(s)} = (x_{i0}^{(s)}, x_{i1}^{(s)}, T^{(s)}),\quad s = 1, \ldots, S \tag{10.19}$$

necessitates the creation of a large number of nonidentical systems. The latter may be inefficient from an economic point of view.

Consider the problem of performing S different maneuvers with a given number Ω of types of systems (10.15), smaller than S, i.e.,
442 $1 \leqslant \Omega < S$. The value of the functional (10.18) averaged over all maneuvers is taken as the optimum criterion.

The optimum number Ω of types of systems must be determined from the criterion of minimum cost. To that end one must know the cost of developing system (10.15) with parameters which are different from the former ones and to know how the cost and functional (10.18) are related. Here the latter problem is not considered and the number Ω of types of systems is taken as known.

The problem of universalizing the optimum system parameters can also be formulated in another way. If system (10.15) is assembled from elementary sections, its parameters $\mathbf{w}$ can be represented in the form

$$\mathbf{w} = \mathbf{w}(\sigma, \Delta\mathbf{w}), \quad \sigma = 1, 2, \ldots, \tag{10.20}$$

where $\Delta\mathbf{w}$ are the parameters of the elementary sections (in particular, relationship (10.20) can be linear so that $\mathbf{w} = \sigma\Delta\mathbf{w}$). The problem is to select universal optimum parameters $\Delta\mathbf{w}$ for all the S types of maneuvers, and to determine the optimum number σ of sections for each maneuver.

2. **Optimum criterion.** The statistical approach is used to set up the optimum criterion for the two problems stated above. The distribution of the required number of maneuvers is specified according to their parameters (10.19). If the required number of each type of maneuver is expressed as a fraction of the total number of all the types of maneuvers, we can treat this distribution as the distribution representing the probability p_s of the maneuvers occurring according to the types

$$p_s = p_s(\mathbf{b}^{(s)}), \quad \sum_{s=1}^{S} p_s = 1. \tag{10.21}$$

The optimum criterion will then be the mathematical expectation of the functional (10.18)

$$\langle x_{01} \rangle = \sum_{s=1}^{S} p_s x_{01}(\mathbf{b}^{(s)}), \tag{10.22}$$

i.e., the value of the functional (10.18) averaged over all the types of maneuvers (10.19).

Instead of being specified discretely, as in (10.19), the maneuver parameters can also be specified continuously, for instance as a function of one variable

$$\mathbf{b} = \mathbf{b}(s), \quad 0 \leqslant s \leqslant S, \tag{10.23}$$

where s can take all values within the interval $[0, S]$ (not only integral values). In this case the distribution of probabilities (10.21) is replaced by the density
443 of the probability distribution

$$\rho = \rho(s), \quad \int_0^S \rho(s)\, ds = 1, \tag{10.24}$$

and the functional (10.22) is replaced by

$$\langle x_{01}\rangle = \int_0^S \rho(s)\, x_{01}(\mathbf{b}(s))\, ds. \tag{10.25}$$

3. Formulation of the problem for a given number of types of systems. Consider the case when the parameters of system (10.15) can take Ω values $\mathbf{w}^{(\omega)}$, $\omega = 1, \ldots, \Omega$. We must realize S types of maneuvers (10.19) with a probability distribution (10.21), and ensure the maximum (minimum) of the functional (10.22).

Introduce for each s-th type of maneuver a new independent variable

$$\tau = t/T^{(s)} \tag{10.26}$$

to replace the time t so that one can relate the final conditions (10.15) and the functional (10.22) to the same point $\tau = 1$ for all maneuvers. The problem can then be reduced to the standard one (10.15) to (10.18), for an expanded system of differential equations

$$\begin{gathered}\frac{dx_i^{(s)}}{d\tau} = T^{(s)} f_i(x_j^{(s)}, u_k^{(s)}, w_l^{(\omega)}, T^{(s)}\tau) \\ (0 \leqslant \tau \leqslant 1;\ s = 1, \ldots, S;\ \omega = 1, \ldots, \Omega < S; \\ i, j = 0, 1, \ldots, n;\ k = 1, \ldots, r;\ l = 1, \ldots, q)\end{gathered} \tag{10.27}$$

with boundary conditions

$$\begin{gathered}x_0^{(s)}(0) = 0, \quad x_i^{(s)}(0) = x_{i0}^{(s)}, \quad x_i^{(s)}(1) = x_{i1}^{(s)} \\ (s = 1, \ldots, S;\ i = 1, \ldots, n)\end{gathered} \tag{10.28}$$

and functional

$$\langle x_{01}\rangle = \sum_{s=1}^{S} p_s x_0^{(s)}(1) = \text{extr}. \tag{10.29}$$

Here, as before, $x_i^{(s)}$ are the phase coordinates ($S(n+1)$ in number), $u_k^{(s)}$ are the control functions (Sr in number) and $w_l^{(\omega)}$ are the constant control parameters (Ωq in number).

444 For the continuous distribution (10.23)–(10.25) we obtain the two-dimensional variational problem for the system

$$\begin{gathered}\frac{\partial x_i}{\partial \tau} = T(s) f_i(x_j, u_k, w_l, T(s)\tau) \\ (0 \leqslant \tau \leqslant 1;\ 0 \leqslant s \leqslant S;\ i, j = 0, 1, \ldots, n; \quad k = 1, \ldots, r;\ l = 1, \ldots, q)\end{gathered} \tag{10.30}$$

with boundary conditions

$$\begin{gathered}x_0(0, s) = 0, \quad x_i(0, s) = x_{i0}(s), \quad x_i(1, s) = x_{i1}(s) \\ (0 \leqslant s \leqslant S,\ i = 1, \ldots, n)\end{gathered} \tag{10.31}$$

and functional

$$\langle x_{01}\rangle = \int_0^S \rho(s)\, x_0(1, s)\, ds = \text{extr}. \tag{10.32}$$

Here $x_i = x_i(\tau, s)$, $u_k = u_k(\tau, s)$ are the phase coordinates and control functions, depending on two variables, and $w_l = w_l(s)$ are the step control functions with a specified number of levels w_l^{ω}, $\omega = 1, \ldots, \Omega$, depending only on s ($\partial w_l/\partial\tau = 0$).

4. Formulating the problem for the universal section. The formulations of the variational problems (10.27) to (10.29) and (10.30) to (10.32) are transformed to the case considered with several alterations. The boundary conditions (10.28), (10.31) and the functionals (10.29), (10.32) are preserved. The notation of the differential equations is somewhat altered as follows (relationship (10.20) is considered as linear to simplify the notation):

for a discrete distribution (cf. (10.27))

$$\frac{dx_i^{(s)}}{d\tau} = T^{(s)} f_i\left(x_j^{(s)}, u_k^{(s)}, \sigma^{(s)}\Delta w_l, T^{(s)}\tau\right) \quad (0 \leqslant \tau \leqslant 1;\ s = 1, \ldots, S;\ i, j = 0, 1, \ldots, n;\ k = 1, \ldots, r;\ l = 1, \ldots, q), \tag{10.33}$$

for a continuous distribution (cf. (10.30))

$$\frac{\partial x_i}{\partial\tau} = T(s) f_i(x_j, u_k, \sigma\Delta w_l, T(s)\tau) \quad (0 \leqslant \tau \leqslant 1;\ 0 \leqslant s \leqslant S;\ i, j = 0, 1, \ldots, n;\ k = 1, \ldots, r;\ l = 1, \ldots, q). \tag{10.34}$$

In equations (10.33) the constant control parameters Δw_l are identical for all s; $\sigma^{(s)} = 1, 2, \ldots$ are integers, which can be different for each s (unlike (10.27), where the number Ω of parameters $w_l^{(\omega)}$ is smaller than the number S of groups of equations).

445 In equations (10.34) Δw_l are the constant control parameters ($\partial\Delta w_l/\partial\tau = \partial\Delta w_l/\partial s = 0$); $\sigma = \sigma(s)$ is the step control function of the single variable s, which takes any integer values (unlike (10.30), where the number Ω of levels $w_l^{(\omega)}$ of the step control function $w_l(s)$ is specified).

5. Ideal power-limited engine. The only parameter w in this case is the engine weight $G_{\varkappa}$ or the maximum power $N_{\max} = G_{\varkappa}/\alpha$ where, in the general case, $\alpha = \alpha(N_{\max})$ or $\alpha = \alpha(G_{\varkappa})$ (cf. § 1 of Chapter Four). The functional (10.18) of the initial problem (10.15) to (10.17) is the payload (4.5).

After solving the dynamic problem (5.2) for each set of maneuver parameters (10.19) $\mathbf{b} = (\mathbf{r}_0, \mathbf{v}_0, \mathbf{r}_1, \mathbf{v}_1, T)$ we have a value for the integral J which is here considered as a parameter of the maneuver b. The payload is expressed in terms of $G_{\varkappa}$ and J (cf. (4.10)) where

$$G_{\pi} = G_{\varkappa}\left(\frac{1}{G_{\varkappa} + (\alpha/2g)J} - 1\right). \tag{10.35}$$

It is assumed that the distributions of maneuvers according to types are specified in the following form:

discrete distribution (10.21)

$$p_s = p_s(J^{(s)}), \quad \sum_{s=1}^{S} p_s = 1, \tag{10.36}$$

continuous distribution (10.24)

$$\rho = \rho(J), \quad \int_{J_0}^{J_1} \rho(J)\, dJ = 1. \tag{10.37}$$

The problem functional is written correspondingly in the following forms:

for the discrete distribution (cf. (10.22))

$$\langle G_\pi \rangle = \sum_{s=1}^{S} p_s G_\varkappa \left(\frac{1}{G_\varkappa + (\alpha/2g) J^{(s)}} - 1 \right), \tag{10.38}$$

for the continuous distribution (cf. (10.25))

$$\langle G_\pi \rangle = \int_{J_0}^{J_1} \rho(J) G_\varkappa \left(\frac{1}{G_\varkappa + (\alpha/2g) J} - 1 \right) dJ \tag{10.39}$$

(the magnitude $\langle G_\pi \rangle$ represents the average payload per maneuver over the range $[J_0, J_1]$).

Thus, the problem of performing a given class of maneuvers (10.36), (10.37) with the aid of a specified number $\Omega < S$ of propulsion system types
446 (cf. Subsection 3) reduces to finding the maximum of the sum (10.38) for $G_\varkappa = G_\varkappa^{(\omega)}, \omega = 1, \ldots, \Omega$ or the maximum of the integral (10.39) for $G_\varkappa(J) = G_\varkappa^{(\omega)}, \omega = 1, \ldots, \Omega$, where Ω is specified, and the levels $G_\varkappa^{(\omega)}$ must be selected so that they are optima.

If we consider the problem of selecting the optimum parameters of the universal section (cf. Subsection 4), we must substitute $\sigma \Delta G_\varkappa$ for $G_\varkappa$ in (10.38) and (10.39), and consider the unit weight α as dependent on $\Delta G_\varkappa$ instead of $G_\varkappa$. The functional (10.38) is then rewritten in the form

$$\langle G_\pi \rangle = \Delta G_\varkappa \sum_{s=1}^{S} p_s \sigma^{(s)} \left(\frac{1}{\sigma^{(s)} \Delta G_\varkappa + [\alpha(\Delta G_\varkappa)/2g] J} - 1 \right), \tag{10.40}$$

and the functional (10.39) in the form

$$\langle G_\pi \rangle = \Delta G_\varkappa \int_{J_0}^{J_1} \rho(J) \sigma \left(\frac{1}{\sigma \Delta G_\varkappa + [\alpha(\Delta G_\varkappa)/2g] J} - 1 \right) dJ. \tag{10.41}$$

In (10.40) $\sigma^{(s)}$, $s = 1, \ldots, S$, are arbitrary positive integers, and in (10.41) σ is a step function of J with an arbitrary number of integer levels.

We introduce the symbols

$$\Phi = \frac{\alpha_*}{2g} J, \quad \chi = \frac{\alpha}{\alpha_*} \qquad (0 \leqslant \Phi < 1, \ \chi > 1), \tag{10.42}$$

where α_* is the limiting value of the unit section weight for infinitely large power, and consider the case when the maneuvers are continuously distributed over the range $[\Phi_0, \Phi_1]$ with the same probability, i.e.,

$$\rho(\Phi) = \frac{1}{\Phi_1 - \Phi_0} \ \text{ at } \ \Phi_0 < \Phi < \Phi_1, \qquad \rho(\Phi) = 0 \ \text{ at } \ \Phi < \Phi_0, \ \Phi > \Phi_1. \tag{10.43}$$

The dependence of the unit engine weight α on its absolute parameters N_{max} or $G_\varkappa$ ($\partial\alpha/\partial N_{max}$, $\partial\alpha/\partial G_\varkappa < 0$, cf. Figure 2.96) is unnecessary for the method of solution. For the problem with a fixed number of levels $G_\varkappa^{(\omega)}$ the introduction of this dependence does not even lead to qualitative peculiarities. When treating the universal section, however, the dependence

$\alpha(\Delta G_\varkappa)$ or $\chi(\Delta G_\varkappa)$ is important from the qualitative point of view. For $\chi \equiv 1$ the optimum size of the section tends to zero ($\Delta G_\varkappa \to 0$) while if $\partial\chi/\partial G_\varkappa < 0$ the optimum size of the section is finite. Therefore the functional (10.39) of the first problem is written in the form ($\chi \equiv 1$)

$$\langle G_\pi \rangle = \frac{1}{\Phi_1 - \Phi_0} \int_{\Phi_0}^{\Phi_1} G_\varkappa \left(\frac{1}{G_\varkappa + \Phi} - 1 \right) d\Phi, \tag{10.44}$$

[447] and the functional (10.41) of the second problem in the form ($\chi = \chi(\Delta G_\varkappa)$)

$$\langle G_\pi \rangle = \frac{\Delta G_\varkappa}{\Phi_1 - \Phi_0} \int_{\Phi_0}^{\Phi_1} \sigma \left(\frac{1}{\sigma \Delta G_\varkappa + \Phi \chi(\Delta G_\varkappa)} - 1 \right) d\Phi. \tag{10.45}$$

The integral (10.44) is taken along the segments $\Phi_0^{(\omega)} < \Phi < \Phi_1^{(\omega)}$, where the level $G_\varkappa^{(\omega)}$ is optimum, and

$$\langle G_\pi \rangle = \frac{1}{\Phi_1 - \Phi_0} \sum_{\omega=1}^{\Omega} G_\varkappa^{(\omega)} \left[\ln \frac{\Phi_1^{(\omega)} + G_\varkappa^{(\omega)}}{\Phi_0^{(\omega)} + G_\varkappa^{(\omega)}} - (\Phi_1^{(\omega)} - \Phi_0^{(\omega)}) \right]. \tag{10.46}$$

The time of switchover from one level to another is determined from the condition of maximum integrand (10.44). The problem then reduces to finding the maximum of the function with Ω variables $\langle G_\pi \rangle = f(G_\varkappa^{(1)}, \ldots, G_\varkappa^{(\Omega)})$ under the condition that the integrand of (10.44) is nonnegative. This is equivalent to the condition

$$0 \leqslant \min_{\omega} \{G_\varkappa^{(\omega)}\} \leqslant 1 - \Phi_1. \tag{10.47}$$

This procedure can be carried out numerically by the method of steepest descent (cf. Chapter Fourteen). For $\Omega = 1$ the optimum value of the single level $G_\varkappa^{(1)}$ is determined by solving the equation

$$\frac{\partial \langle G_\pi \rangle}{\partial G_\varkappa^{(1)}} = \frac{1}{\Phi_1 - \Phi_0} \ln \frac{\Phi_1 + G_\varkappa^{(1)}}{\Phi_0 + G_\varkappa^{(1)}} - \frac{G_\varkappa^{(1)}}{(\Phi_0 + G_\varkappa^{(1)})(\Phi_1 + G_\varkappa^{(1)})} - 1 = 0 \tag{10.48}$$

when the root of this equation is smaller than $(1 - \Phi_1)$; otherwise $G_\varkappa^{(1)} = 1 - \Phi_1$.

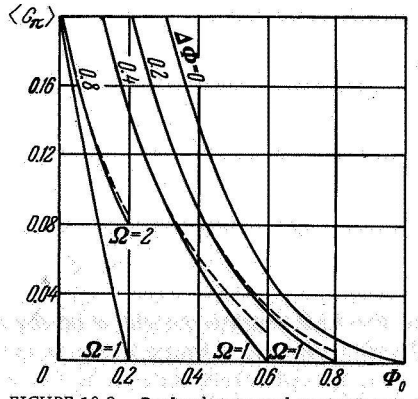

FIGURE 10.3. Payload averaged over maneuver $\langle G_\pi \rangle$, when performance of maneuvers over range $[\Phi_0, \Phi_0 + \Delta\Phi]$ is ensured by fixed number of propulsion systems $\Omega = 1, 2$. Dashed curves correspond to $\Omega \to \infty$.

Figure 10.3 shows the averaged payload $\langle G_\pi \rangle$ for intervals of different length $\Delta\Phi = \Phi_1 - \Phi_0 = 0;\ 0.2;\ 0.4;\ 0.8$ plotted as a function of the initial point of the interval Φ_0. The dashed curves correspond to the continuous optimum law of variation $G_x(\Phi) = \sqrt{\Phi} - \Phi$ (an infinite number of types of
448 propulsion systems, cf. the dashed curve in Figure 10.4). It is seen that with the aid of a single type of propulsion system (the curves $\Omega = 1$) one can approach close to the maximum possible value of the payload. The transition to two types of propulsion systems reduces the loss in payload to practically zero (the dashed curves and the curves $\Omega = 2$ are practically indistinguishable in the scale of the figure, except for the case $\Delta\Phi = 0.8$).

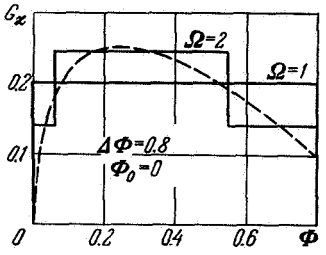

FIGURE 10.4. Example of step approximation ($\Omega = 1, 2$) to optimum distribution of engine weight G_x for maneuvers over range $[\Phi_0,\ \Phi_0 + \Delta\Phi]$.

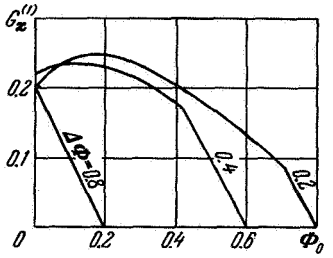

FIGURE 10.5. Universal curve of optimum engine weight $G_x^{(1)}$ for maneuvers over range $[\Phi_0,\ \Phi_0 + \Delta\Phi]$.

Figure 10.4 represents the optimum distribution of the propulsion system weight G_x according to the maneuver parameter Φ for $\Omega = 1, 2, \infty$. The relationship $G_x^{(1)}(\Phi_0, \Delta\Phi)$ for $\Omega = 1$ is shown in Figure 10.5. The straight line segments correspond to the limits in (10.47).

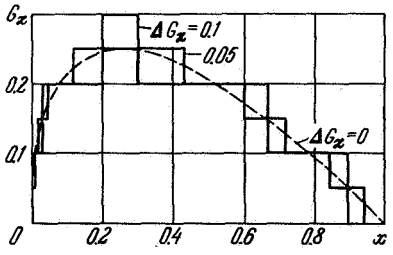

FIGURE 10.6. Approximation to optimum distribution of engine weight G_x over range of maneuvers by a step curve with equidistant levels $\Delta G_x = 0.1,\ 0.05$ (problem of universal section).

In the second problem a step function $\sigma(\Phi)$ with integer levels must be built, and the value of the parameter ΔG_x which maximizes the integral (10.45) must be selected when the integrand is nonnegative.

Consider the transformation $x = \chi\Phi$ and introduce the symbol

$$K(x, \Delta G_x) = \int_0^x \sigma \Delta G_x \left(\frac{1}{\sigma \Delta G_x + x} - 1 \right) dx. \tag{10.49}$$

Expression (10.45) is then rewritten

$$\langle G_\pi \rangle = \frac{1}{(\Phi_1 - \Phi_0)\chi} [K(\chi\Phi_1, \Delta G_x) - K(\chi\Phi_0, \Delta G_x)]. \tag{10.50}$$

449 The integral (10.49), similarly to (10.44), is taken over the segments between the level switchovers σ_j, while the switchover time is determined from the condition of maximum integrand in (10.49) with respect to the integer values $\sigma_j = 1, 2, \ldots, \sigma_{max}$; $\sigma_{max} = [1/4\Delta G_x] + 1$ (where $[\ldots]$ designates the whole part of the number); cf. $G_x = \sigma(\Phi)\,\Delta G_x$ in Figure 10.6. The curve $K(x)$ has been plotted in Figure 10.7 for different values of ΔG_x. It is seen that for $\Delta G_x < 0.1$ the curves practically coincide with the limiting curve

$$K(x, 0) = x(1 - {}^4/_3\sqrt{x} + {}^1/_2 x) \quad (\Delta G_x \to 0). \tag{10.51}$$

As an approximation replace $K(x, \Delta G_x)$ in (10.50) by $K(x, 0)$ to obtain

$$\langle G_\pi \rangle = 1 - \frac{4}{3}\sqrt{\chi}\,\frac{\Phi_1^{3/2} - \Phi_0^{3/2}}{\Phi_1 - \Phi_0} + \frac{1}{2}\chi(\Phi_1 + \Phi_0) \text{ at } \Delta G_x < 0.1, \tag{10.52}$$

where $1 < \chi = \chi(\Delta G_x) \leqslant (1 - \Delta G_x)/\Phi_1$ (the upper bound was obtained from the condition that the integrand in (10.49) is nonnegative). In order to find the optimum value of ΔG_x the relationship $\chi(\Delta G_x)$ must be given, for instance

$$\chi(\Delta G_x) = \alpha(\Delta G_x)/\alpha_* = \Delta G_x/(\Delta G_x - \Delta G_x^*), \tag{10.53}$$

450 where ΔG_x^* is the limiting weight of the section for a power tending to zero. The form of this relationship coincides with those described in the literature (cf. Figure 10.8 and Figure 2.96).

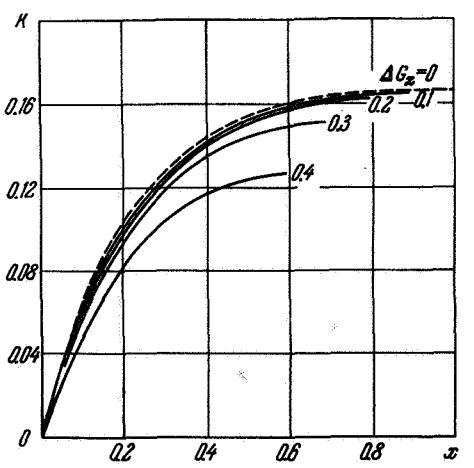

FIGURE 10.7. Function $K(x, \Delta G_x)$ (cf. (10.49), (10.50)).

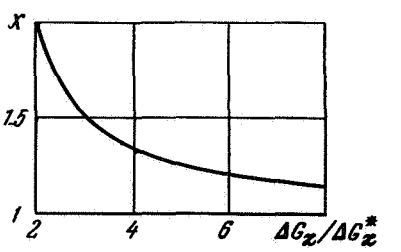

FIGURE 10.8. Unit engine weight $\chi = \alpha/\alpha^*$ as function of section size $\Delta G_x/\Delta G_x^*$ (α^*, $\Delta G_x^* = \text{const}$).

From the condition for nonnegative payload for each maneuver over the range $[\Phi_0, \Phi_1]$, the allowable range over which χ varies is

$$\chi_1 \leqslant \chi \leqslant \chi_2, \quad \chi_{1,2} =$$

$$= \frac{1}{2}\left(1 + \frac{1 - \Delta G_\varkappa^*}{\Phi_1}\right) \mp \sqrt{\frac{1}{4}\left(1 + \frac{1 - \Delta G_\varkappa^*}{\Phi_1}\right)^2 - \frac{1}{\Phi_1}}. \qquad (10.54)$$

Within this interval, (10.52) indicates that $\langle G_\pi \rangle$ is a monotonic decreasing function of χ. Hence, the optimum values of χ and $\Delta G_\varkappa$ are

$$\chi = \chi_1, \quad \Delta G_\varkappa = \Delta G_\varkappa^* \chi_1/(\chi_1 - 1). \qquad (10.55)$$

For $\Delta G_\varkappa > 0.1$ the problem is solved numerically with the known relationship $K(x, \Delta G_\varkappa)$ (shown in Figure 10.7) and by formula (10.50). The results are given in Figures 10.9 and 10.10 ($\Delta G_\varkappa^* = 0.001$), which are similar to Figures 10.3 and 10.5.

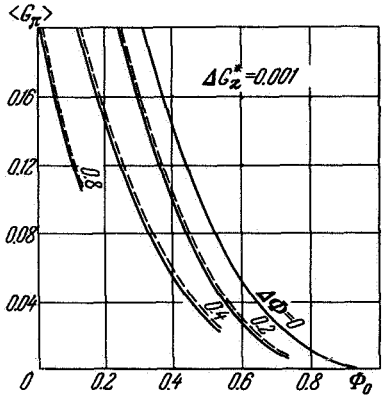

FIGURE 10.9. Payload $\langle G_\pi \rangle$ averaged over range of maneuvers, when performance of maneuvers from range $[\Phi_0, \Phi_0 + \Delta\Phi]$ is obtained by propulsion systems assembled from universal sections (cf. Figure 10.3).

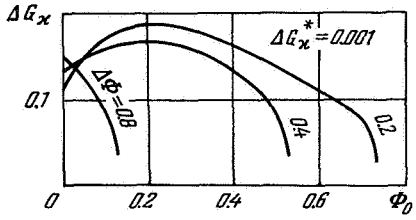

FIGURE 10.10. Optimum size of universal section $\Delta G_\varkappa$ as function of the parameters of the maneuver range $[\Phi_0, \Phi_0 + \Delta\Phi]$ (cf. Figure 10.5).

When the maneuvers over the given range are performed by a single propulsion system (first problem), the loss in payload is increased considerably by expanding the range and transferring it to the region of energetically-strained maneuvers (Figure 10.3). The use of universal sections from which to assemble the engine for each specific maneuver (the second problem) improves the situation. The loss in payload is approximately just as small over any range of maneuvers.

451

§ 3. THE GAME APPROACH TO THE PROBLEM OF SELECTING THE OPTIMUM PARAMETERS OF THE PROPULSION SYSTEM

The parameters of a universal engine for some given class of maneuvers were written above assuming that the frequency of each maneuver is known. This assumption is discarded here, and only the limits of the range of possible maneuvers are considered as known. The parameters of the optimum engine must be determined over this range of maneuvers.

The problem is formulated in terms of the theory of antagonistic games. The game approach guarantees that, when the propulsion system parameters are correctly selected, the loss resulting from the universal requirement of the engine and the lack of complete information about the maneuvers will be no higher than some fixed value [the value of the game], independently of the specified frequency distribution of the maneuvers.

1. **Statement of the problem.** Consider first, as in the preceding section, the general case consisting of a dynamic system (10.15) with parameters $\mathbf{w}$ and control functions $u_k(t)$. The maneuver is specified by the vector $\mathbf{b}$ (10.16), and the maneuver quality is characterized by the functional $x_0(T)$ (10.18).

The control functions $u_k(t)$ are selected from the class of allowable functions such that the boundary conditions (10.15) are satisfied and such that an extremum of the functional (10.18) is attained, where

$$\operatorname*{extr}_{u_k(t)} x_0(T) = x_{01}(\mathbf{b}, \mathbf{w}). \tag{10.56}$$

For a fixed vector $\mathbf{w}$ different system control parameters $u_k(t)$ can be selected, depending on the vector $\mathbf{b}$ of the maneuver parameters. It is assumed that the variational problem of establishing the optimum control functions $u_k(t)$ has been solved and that the function (10.56) is known.

The parameters of maneuver $\mathbf{b}$ can take any values within a fixed region B or a fixed discrete set B with a frequency ν. The frequency $\nu(\mathbf{b})$ with which the maneuver $\mathbf{b}$ must be performed is unknown. This quantity $\nu(\mathbf{b})$ is written in terms of the distribution function $F_\nu(\mathbf{b})$ with the aid of a
452 Stiltjes integral (step functions are allowed as distribution functions). The frequency $\nu(\mathbf{b} \in B')$ with which maneuvers belonging to region $B' \subset B$ appear is equal to

$$\nu(\mathbf{b} \in B') = \int\limits_{\mathbf{b} \in B'} dF_\nu(\mathbf{b}) \quad \left(\int\limits_{\mathbf{b} \in B} dF_\nu(\mathbf{b}) = 1 \right), \tag{10.57}$$

where the distribution function $F_\nu(\mathbf{b})$ is unknown (according to the assumption about $\nu(\mathbf{b})$).

The vector $\mathbf{w}$, representing the parameters (10.17) of the dynamic system, can take only one value for all values $\mathbf{b} \in B$ (requirement of universality of the dynamic system for the given class of maneuvers). If, for each maneuver $\mathbf{b}$ we could select its system $\mathbf{w}(\mathbf{b})$, it would be possible to ensure the maximum (minimum) value of the functional (10.56) given by

$$\operatorname*{extr}_{u_k(t),\, \mathbf{w}} x_0(T) = x_{01}(\mathbf{b}), \tag{10.58}$$

which is the ideal solution. The universal system ensures a value of the functional (10.56) which is lower (higher) than (10.58), except for the maneuver **b** for which the parameters of the universal system **w** are optimum in the sense of condition (10.18).

The loss $\mathcal{M}$ when compared with the ideal solution will be given for each maneuver by the relative deviation

$$\mathcal{M}(\mathbf{b}, \mathbf{w}) = \left| \frac{x_{01}(\mathbf{b}) - x_{01}(\mathbf{b}, \mathbf{w})}{x_{01}(\mathbf{b})} \right|. \tag{10.59}$$

The total loss of the system with parameters **w** for the series of maneuvers **b** from the set B with a frequency distribution $F_\nu(\mathbf{b})$ is

$$M(F_\nu(\mathbf{b}), \mathbf{w}) = \int_{\mathbf{b}\in B} \mathcal{M}(\mathbf{b}, \mathbf{w})\, dF_\nu(\mathbf{b}). \tag{10.60}$$

A typical game situation arises in which two players, "Nature" and the "Designer", participate. Nature specifies the maneuver frequency distribution (10.57) according to the maneuver parameters (Nature's "move") such that the Designer's loss increases. The Designer selects the parameters of the dynamic system (10.17) (the Designer's "move") so as to decrease this loss. The Designer makes the first move; he only knows the boundaries of the range over which Nature can select the maneuver parameters. Nature moves next, without knowing the Designer's move.

Had the Designer been permitted to select a value of **w** for each maneuver **b** instead of just one universal value, and were complete information on the maneuvers available to him, his loss would have been equal to zero. In the
453 situation described above the loss always differs from zero.* We consider the problem of calculating the loss when Nature plays so as to maximize the loss for any move of the Designer, and when the Designer wants to minimize the loss for any move of Nature. The solution of this problem determines the parameters of the dynamic system which are optimum in the following sense: for every maneuver frequency distribution specified by Nature, the loss of the Designer will not exceed the minimum value of the loss found (value of the game /10.5—10.8/).

In this formulation Nature and the Designer do not have equal rights. Nature can specify any number of different maneuvers from the allowable set B (Nature's move specifies the distribution function $F_\nu(\mathbf{b})$ of the frequency within set B), while the Designer can only select one dynamic system (the Designer's move fixes one value of the vector **w**). We shall confer equal rights on both sides, as is usual in the theory of antagonistic games. The Designer is allowed to select any number of different dynamic systems from an allowable set W, i.e., the move of the Designer will consist in specifying the distribution function $F_\lambda(\mathbf{w})$ of the frequency λ with which the different systems are to be used. In the terms of the distribution function, the frequency of utilization of systems with parameters lying within the region $W \subset W$ is given by (cf. (10.57))

$$\lambda(\mathbf{w}\in W') = \int_{\mathbf{w}\in W'} dF_\lambda(\mathbf{w}) \quad \left(\int_{\mathbf{w}\in W} dF_\lambda(\mathbf{w}) = 1 \right). \tag{10.61}$$

* This excludes the improbable case when only those maneuvers need be fulfilled for which the selected system **w** is optimum in the sense of (10.18).

The assumption that each player is ignorant of the moves of his opponent remains in force, i.e., the Designer must decide which of the dynamic systems to use for performing the next maneuver before having the maneuver parameters.

The loss for Nature's move $F_\nu(\mathbf{b})$ and the Designer's move $F_\lambda(\mathbf{w})$ will in this case equal

$$M(F_\nu(\mathbf{b}), F_\lambda(\mathbf{w})) = \iint\limits_{\substack{\mathbf{b}\in B \\ \mathbf{w}\in W}} \mathcal{M}(\mathbf{b}, \mathbf{w})\, dF_\nu(\mathbf{b})\, dF_\lambda(\mathbf{w}). \tag{10.62}$$

Suppose that the payoff function $\mathcal{M}(\mathbf{b}, \mathbf{w})$ has positive second derivatives in the entire region over which it is defined $\partial^2\mathcal{M}/\partial w_1^2 > 0, \ldots, \partial^2\mathcal{M}/\partial w_q^2 > 0$ and that the game is continuous (the allowable sets B and W represent
454 regions). Then, as proved in the theory of games /10.5—10.8/, the optimum strategy of the Designer will be the "pure" strategy

$$\lambda(\mathbf{w}) = \begin{cases} 1 & \text{at } \mathbf{w} = \mathbf{w}^*, \\ 0 & \text{at } \mathbf{w} \neq \mathbf{w}^*, \end{cases} \tag{10.63}$$

i.e., it is advantageous for the Designer to select only one dynamic system $\mathbf{w}^*$. This means that in the given case the solution of (10.62) coincides with that of the earlier-stated problem (10.60).

An analysis is now carried out for an ideal power-limited engine (cf. Chapter Four). The maneuver can here be characterized by a single parameter, namely, the functional of the dynamic problem J or the combination $\Phi = (\alpha/2g)J$, and the engine is represented by its maximum power $N_{\max}$ or its weight $G_\varkappa = \alpha N_{\max}$ (the unit engine weight α = const is specified). The loss $\mathcal{M}$ is measured in units of the payload G_π. The parameters of the engine and the maneuver can be continuously varied within certain limits (continuous game).

2. **Payoff function.** The payload (the functional (10.56)) for an ideal power-limited engine of weight $G_\varkappa$ for the maneuver with functional Φ is equal to (4.14)

$$G_\pi(\Phi, G_\varkappa) = G_\varkappa\left(\frac{1}{\Phi + G_\varkappa} - 1\right) \qquad \left(\Phi = \frac{\alpha}{2g}\int_0^T a^2\, dt\right) \tag{10.64}$$

(the weights G_π and $G_\varkappa$ are represented as fractions of the takeoff weight G_0).

For each value of Φ there exists an optimum engine weight (4.15) which maximizes the payload (10.64). This maximum value (the ideal solution (10.58)) is equal to (4.16)

$$G_{\pi\max}(\Phi) = (1 - \sqrt{\Phi})^2. \tag{10.65}$$

The payoff function (10.59) is formed from the relative loss in payload (10.64) and its maximum possible value (10.65), and takes the form

$$\mathcal{M}(\Phi, G_\varkappa) = \frac{G_{\pi\max}(\Phi) - G_\pi(\Phi, G_\varkappa)}{G_{\pi\max}(\Phi)} = 1 - \frac{G_\varkappa(1 - \Phi - G_\varkappa)}{(\Phi + G_\varkappa)(1 - \sqrt{\Phi})^2}. \tag{10.66}$$

The region over which the function $\mathcal{M}(\Phi, G_\varkappa)$ is defined is (Figure 10.11)

$$0 \leqslant \Phi \leqslant 1, \quad 0 \leqslant G_\varkappa \leqslant \min\{1/4, (1 - \Phi)\}. \tag{10.67}$$

The upper bound of Φ corresponds to the condition of nonnegativeness of the maximum payload (10.65). The alternative bound imposed on G_x is
455 due to the fact that, in the first place, there is no sense in making the engine weight larger than 1/4 (cf. (4.15) and Figure 4.2), and in the second place, the engine weight should not be made larger than the limit corresponding to zero payload (10.64). The second restriction on G_x operates within the range $3/4 \leqslant \Phi \leqslant 1$.

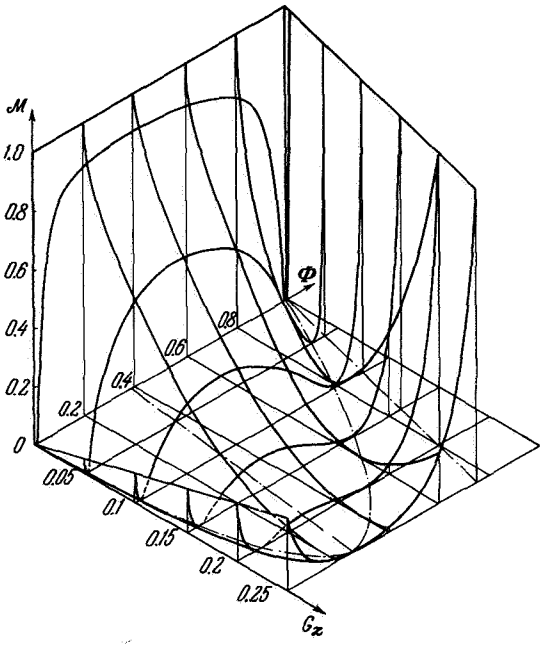

FIGURE 10.11. Payoff function $\mathcal{M}(\Phi, G_x)$ of "Nature-Designer" game for ideal power-limited engine (relative loss in payload as function of maneuver parameter Φ and engine parameter G_x. Dash-dot curves represent minima and maxima in (Φ, G_x) plane).

The function $\mathcal{M}(\Phi, G_x)$ is bounded everywhere within region (10.67), $0 \leqslant \mathcal{M}(\Phi, G_x) \leqslant 1$, and continuous and differentiable with respect to both variables within the open region. At the boundary points (0, 0) and (1, 0) it suffers discontinuities (cf. Figure 10.11), where

$$\left.\begin{aligned} \lim_{G_x \to 0} \mathcal{M}(0, G_x) = 0 \neq \lim_{\Phi \to 0} \mathcal{M}(\Phi, 0) = 1, \\ \lim_{\Phi \to 1} \mathcal{M}(\Phi, \sqrt{\Phi} - \Phi) = 0 \neq \lim_{\Phi \to 1} \mathcal{M}(\Phi, 1 - \Phi) = 1. \end{aligned}\right\} \qquad (10.68)$$

In the sections of the planes Φ = const the function $\mathcal{M}$ decreases at first and then increases with increasing G_x, while the second derivative with

456 respect to G_x is everywhere positive (Figure 10.12):

$$\left.\begin{aligned}
&\frac{\partial \mathcal{M}}{\partial G_x} = \frac{1}{(1-\sqrt{\Phi})^2}\left[1-\frac{\Phi}{(\Phi+G_x)^2}\right],\\
&\frac{\partial \mathcal{M}}{\partial G_x} < 0 \text{ at } G_x < \sqrt{\Phi}-\Phi,\\
&\frac{\partial \mathcal{M}}{\partial G_x} > 0 \text{ at } G_x > \sqrt{\Phi}-\Phi,\\
&\frac{\partial^2 \mathcal{M}}{\partial G_x^2} = \frac{1}{(1-\sqrt{\Phi})^2}\frac{2\Phi}{(\Phi+G_x)^3} > 0.
\end{aligned}\right\} \tag{10.69}$$

On the planes $G_x = \text{const}$ the function $\mathcal{M}$ has two minima and three maxima (two on the boundary and one inside) (Figure 10.13). This is established by studying the partial derivatives of $\mathcal{M}$ with respect to Φ, namely

$$\left.\begin{aligned}
&\frac{\partial \mathcal{M}}{\partial \Phi} = \frac{1}{G_{\pi\max}^2}\left(G_\pi \frac{\partial G_{\pi\max}}{\partial \Phi} - G_{\pi\max}\frac{\partial G_\pi}{\partial \Phi}\right),\\
&\frac{\partial^2 \mathcal{M}}{\partial \Phi^2} = -\frac{2}{G_{\pi\max}}\frac{\partial \mathcal{M}}{\partial \Phi}\frac{\partial G_{\pi\max}}{\partial \Phi} +\\
&\quad + \frac{1}{G_{\pi\max}^2}\left(G_\pi \frac{\partial^2 G_{\pi\max}}{\partial \Phi^2} - G_{\pi\max}\frac{\partial^2 G_\pi}{\partial \Phi^2}\right).
\end{aligned}\right\} \tag{10.70}$$

457 Solving the equation $\partial \mathcal{M}/\partial \Phi = 0$ for G_x, we obtain

$$G_{x\,1,2} = (1/2 - \Phi) \pm (1/2 - \sqrt{\Phi}). \tag{10.71}$$

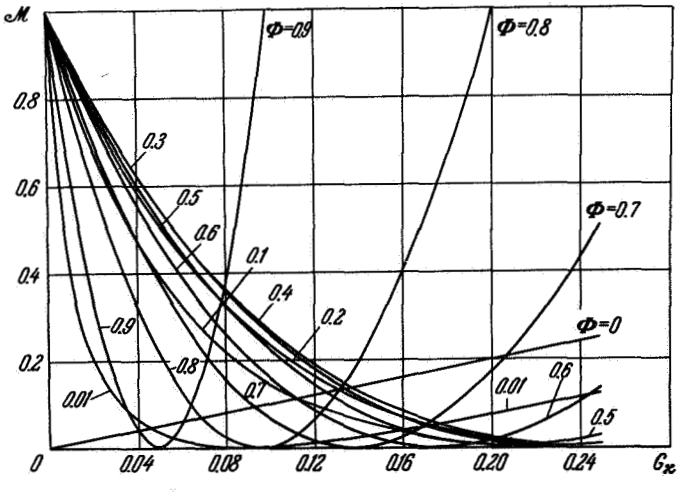

FIGURE 10.12. Intersections of payoff function $\mathcal{M}(\Phi, G_x)$ with planes $\Phi = \text{const}$ (curve $\Phi = 0.3$ almost coincides with curve (10.72) of maxima of $\mathcal{M}$ with respect to G_x).

The first solution of (10.71) yields the maximum point of $\mathcal{M}$ with respect to Φ (Figure 10.13):

$$\left.\begin{aligned} &G_x = 1 - \sqrt{\Phi} - \Phi \quad \text{or} \quad \Phi = (\sqrt{5/4 - G_x} - 1/2)^2, \\ &\mathcal{M} = 1 - \frac{G_x(\sqrt{5/4 - G_x} - 1/2)}{(3/2 - \sqrt{5/4 - G_x})^3} = \max \\ &\left(\frac{\partial \mathcal{M}}{\partial \Phi} = 0, \ \frac{\partial^2 \mathcal{M}}{\partial \Phi^2} < 0, \ 0 < \Phi < \frac{1}{4}\right). \end{aligned}\right\} \tag{10.72}$$

The maxima in the (Φ, G_x) plane are shown in Figure 10.11 by the dash-dot curve. The curve $\mathcal{M}(G_x)$ of the maxima (10.72) practically coincides with the curve $\mathcal{M}(0.3, G_x)$, where the latter is plotted in Figure 10.12.

The second solution of (10.71) corresponds to the points of minimum $\mathcal{M}$ (the zeros of the function $\mathcal{M}$; cf. the dash-dot line in Figure 10.11):

$$\left.\begin{aligned} &G_x = \sqrt{\Phi} - \Phi \quad \text{or} \quad \Phi = (1/2 \pm \sqrt{1/2 - G_x})^2, \\ &\mathcal{M} = 0 = \min \ \left(\frac{\partial \mathcal{M}}{\partial \Phi} = 0, \ \frac{\partial^2 \mathcal{M}}{\partial \Phi^2} > 0, \ 0 \leqslant \Phi \leqslant 1\right). \end{aligned}\right\} \tag{10.73}$$

This solution yields the engine weight (4.15) which is an optimum in the ordinary sense, and is a function of the maneuver parameter Φ. The loss in payload given by solution (10.73) is zero (in order to attain this solution, one must have full information about the maneuver parameter Φ and select for each value of Φ the corresponding engine parameter G_x).

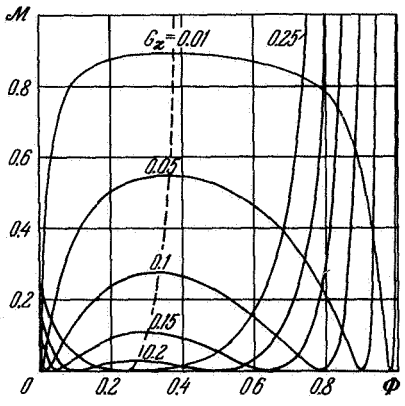

FIGURE 10.13. Intersections of payoff function $\mathcal{M}(\Phi, G_x)$ with planes G_x = const (dashed curve connects maximum points of function $\mathcal{M}$ with respect to Φ).

3. Value of the game. Optimum strategies of the Designer and Nature. Let the parameters of the maneuvers specified by Nature lie within the range $\Phi_0 \leqslant \Phi \leqslant \Phi_1$ (the boundaries $0 < \Phi_0 < \Phi_1 < 1$ are known to the Designer). The boundaries of the range from which the Designer can select the engine parameter G_x will then be (cf. (10.67)) $0 \leqslant G_x \leqslant \min\{1/4, (1 - \Phi_1)\}$. In this region $[\Phi_0, 0; \Phi_1, \min\{1/4, (1 - \Phi_1)\}]$ the payoff function $\mathcal{M}$ is continuous (cf. (10.68)) and differentiable a sufficient number of times. The second derivative $\partial^2 \mathcal{M}/\partial G_x^2$ is here strictly positive (10.69), and therefore the minimum of the loss (10.62)

$$M(F_\nu(\Phi), F_\lambda(G_x)) = \iint_{\Phi, G_x} \mathcal{M}(\Phi, G_x)\, dF_\nu(\Phi)\, dF_\lambda(G_x) \tag{10.74}$$

is attained for any strategy $F_\nu(\Phi)$ of Nature in the class of pure strategies $F_\lambda(G_x)$ of the Designer (10.63):

$$\min_{F_\lambda(G_x)} M(F_\nu(\Phi), F_\lambda(G_x)) = \min_{G_x} \int_\Phi \mathcal{M}(\Phi, G_x)\, dF_\nu(\Phi). \tag{10.75}$$

In this case the value of the game M^* is /10.5—10.8/

$$M^* = \min_{G_\varkappa} \max_{F_\nu(\Phi)} \int_\Phi \mathcal{M}(\Phi, G_\varkappa)\, dF_\nu(\Phi) =$$

$$= \max_{F_\nu(\Phi)} \int_\Phi [\min_{G_\varkappa} \mathcal{M}(\Phi, G_\varkappa)]\, dF_\nu(\Phi) = \min_{G_\varkappa} \max_{\Phi} \mathcal{M}(\Phi, G_\varkappa). \qquad (10.76)$$

The maximum of $\mathcal{M}$ with respect to Φ is attained for fixed values of $G_\varkappa$ (depending on Φ_0, Φ_1, $G_\varkappa$) at one of the three values (cf. (10.70), (10.72), and Figure 10.13): $\Phi=\Phi_0, \Phi=\Phi_1, \Phi=\Phi_2=(\sqrt{5/4-G_\varkappa}-1/2)^2$; the value $\Phi = \Phi_2$ occurs if $\Phi_0 \leqslant \Phi_2 \leqslant \Phi_1$. If we introduce the symbols $\mathcal{M}(\Phi_0, G_\varkappa) = f_0(G_\varkappa)$, $\mathcal{M}(\Phi_1, G_\varkappa) = f_1(G_\varkappa)$, $\mathcal{M}(\Phi_2, G_\varkappa) = f_2(G_\varkappa)$ we can express the results of determining the maximum of $\mathcal{M}(\Phi, G_\varkappa)$ with respect to Φ as follows:

$$f(G_\varkappa) = \max_{\Phi_0 \leqslant \Phi \leqslant \Phi_1} \mathcal{M}(\Phi, G_\varkappa) = \max_{i=0,1,2} \{f_i(G_\varkappa)\}. \qquad (10.77)$$

We now find the minimum of function (10.77) with respect to $G_\varkappa$. It is easily shown that the minimum of $f(G_\varkappa)$ is only attained at the points where the functions intersect, $f_i(G_\varkappa) = f_j(G_\varkappa)$, $i \neq j$. Assume that the contrary happens, i.e., that $f(G_\varkappa)$ has a minimum at the point $G_{\varkappa i}^{(0)}$, in the neighborhood of which $f(G_\varkappa)$ identically equals one of the functions $f_i(G_\varkappa)$. Then $\min f(G_\varkappa) = \min f_i(G_\varkappa) = 0$, since the minimum of the function $f_i(G_\varkappa)$ is only attained at one point and equals zero (cf. (10.69) and Figure 10.12). All the functions $f_j(G_\varkappa)$ are nonnegative, and their zeros $G_{\varkappa j}^{(0)}$ do not coincide, i.e., $G_{\varkappa j}^{(0)} \neq G_{\varkappa i}^{(0)}$ for $i \neq j$. This implies that at the point $G_{\varkappa i}^{(0)}$ a function $f_j(G_\varkappa)$ exists such that $f_j(G_{\varkappa i}^{(0)}) > f_i(G_{\varkappa i}^{(0)})$ i.e., the function $f(G_\varkappa)$ cannot be identically equal to $f_i(G_\varkappa)$ in the neighborhood of the point $G_{\varkappa i}^{(0)}$; and so our initial assumption was incorrect.

Once this fact has been established, the minimum of $f_i(G_\varkappa)$ is found by just comparing the values of $f_i(G_\varkappa)$ at the points of intersection, namely, when
459 $f_0(G_\varkappa) = f_1(G_\varkappa)$, $f_0(G_\varkappa) = f_2(G_\varkappa)$, $f_1(G_\varkappa) = f_2(G_\varkappa)$. Only those points of intersection at which $f_i(G_\varkappa) = f_j(G_\varkappa) > f_l(G_\varkappa)$, $i \neq j \neq l$ is fulfilled need be compared. From these, we require the point $G_\varkappa^*$ at which the function has a minimum value. This is

$$\min_{G_\varkappa} f(G_\varkappa) = \min_{i \neq j} \{f_i(G_\varkappa) = f_j(G_\varkappa) > f_l(G_\varkappa)\} = f(G_\varkappa^*) \qquad (10.78)$$

(the pair Φ_i, Φ_j corresponding to the functions $f_i(G_\varkappa) = \mathcal{M}(\Phi_i, G_\varkappa)$, $f_j(G_\varkappa) = \mathcal{M}(\Phi_j, G_\varkappa)$ and satisfying condition (10.78) will be written Φ^*, Φ^{**}).

The equation $f_0(G_\varkappa) = f_1(G_\varkappa)$ reduces to a quadratic equation for $G_\varkappa$, and the equations $f_0(G_\varkappa) = f_2(G_\varkappa)$ and $f_1(G_\varkappa) = f_2(G_\varkappa)$ reduce to fifth-order equations for $\sqrt{G_\varkappa}$. These latter can be replaced by quadratic equations in $G_\varkappa$, if the function $f_2(G_\varkappa)$ is approximated by the function $\mathcal{M}(0.3, G_\varkappa)$. This is correct to three-figure accuracy. In this approximation the points of intersection $G_{\varkappa i,j}$ of the functions $f_i(G_\varkappa) = f_j(G_\varkappa)$ for any pair i, j are determined from the same type of equations

$$G_{\varkappa i,j}^2 - (1 - \Phi_i - \Phi_j) G_{\varkappa i,j} - \frac{(1-\Phi_j)\Phi_i G_{\pi i} - (1-\Phi_i)\Phi_j G_{\pi j}}{G_{\pi i} - G_{\pi j}} = 0 \qquad (10.79)$$

$$(G_{\pi i} = (1 - \sqrt{\Phi_i})^2,\ G_{\pi j} = (1 - \sqrt{\Phi_j})^2,\ i \neq j,\ i, j = 0, 1, 2;\ \Phi_2 = 0.3).$$

The selection of the roots $G_{\varkappa i,j}$ of equations (10.79) using (10.78) determines a single value $G_\varkappa^*$ for the engine parameter and the two values Φ^*, Φ^{**}

for the maneuver parameter at which the min-max value of the payoff function is attained (coincides with the max-min)

$$\min_{G_x}\max_{\Phi} \mathcal{M}(\Phi, G_x) = \mathcal{M}(\Phi^*, G_x^*) = \mathcal{M}(\Phi^{**}, G_x^*) =$$
$$= 1 - \frac{G_x^*(1-\Phi^*-G_x^*)}{(\Phi^*+G_x^*)(1-\sqrt{\Phi^*})^2} = 1 - \frac{G_x^*(1-\Phi^{**}-G_x^*)}{(\Phi^{**}+G_x^*)(1-\sqrt{\Phi^{**}})^2} = M^*. \tag{10.80}$$

The value of G_x^* found by this method represents the only optimum strategy of the Designer; the quantities Φ^*, Φ^{**} are the maneuver parameters which Nature should select, and M^* is the value of the game. If the Designer selects the engine G_x^*, his loss will be no larger than M^* for any frequency distributions of the maneuvers. In its turn, if Nature selects the maneuvers Φ^* and Φ^{**}, the Designer's loss will be no less than M^*, independently of the engine he selects.

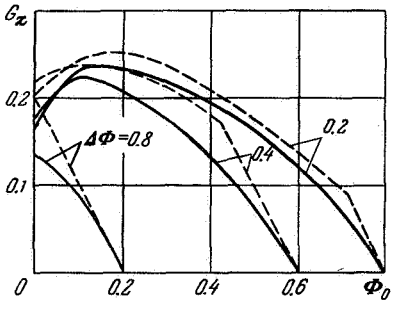

FIGURE 10.14. Optimum weight $G_x^*(\Phi_0, \Delta\Phi)$ of universal engine for maneuvers $\Phi_0 \leqslant \Phi \leqslant \Phi_0 + \Delta\Phi$. Solid curves represent no information relative to maneuver distribution, dashed curves represent known uniform distribution.

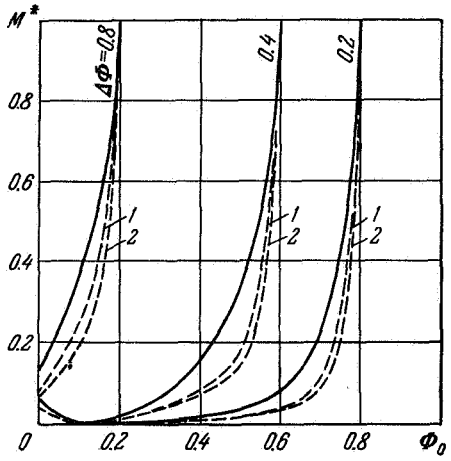

FIGURE 10.15. Relative loss $\mathcal{M}^*(\Phi_0, \Delta\Phi)$ in payload when undertaking maneuvers $\Phi_0 \leqslant \Phi \leqslant \Phi_0 + \Delta\Phi$ with single universal engine. Solid curves correspond to Nature and Designer optimum strategies with no information, and dashed curves to uniform maneuver and engine-parameter distribution, optimum in absence (1) and in presence (2) of information about maneuver distribution.

460 The solid curves in Figures 10.14 and 10.15 present the optimum engine weight G_x^* and the value of the game M^* as functions of the parameters Φ_0 and $\Delta\Phi = \Phi_1 - \Phi_0$ of the maneuver range. It is seen that the value of the game increases with the expansion of the maneuver range (increasing $\Delta\Phi$) and with the displacement of the range into the region of energetically-strained maneuvers (increasing Φ_0). The dashed curves in Figure 10.14 show for comparison the optimum weights of the universal engine G_x found in § 2 under the assumption that the frequency distribution of the maneuvers

$\nu(\Phi)$ is known: $\nu(\Phi) = 1/\Delta\Phi$ at $\Phi_0 \leqslant \Phi \leqslant \Phi_1$ is the uniform maneuver distribution within the allowed range. The loss $M_{\nu=\text{const}}$ for such a distribution is equal to

$$M_{\nu=\text{const}}(\Phi_0, \Phi_1, G_\varkappa) = \frac{1}{\Phi_1 - \Phi_0}\int_{\Phi_1}^{\Phi} \mathcal{M}(\Phi, G_\varkappa)\, d\Phi = 2A \ln \frac{1-\sqrt{\Phi_0}}{1-\sqrt{\Phi_1}} +$$

$$+ B\frac{\sqrt{\Phi_1}-\sqrt{\Phi_0}}{(1-\sqrt{\Phi_1})(1-\sqrt{\Phi_0})} + C\ln\frac{G_\varkappa+\Phi_1}{G_\varkappa+\Phi_0} + \frac{D}{\sqrt{G_\varkappa}}\operatorname{arctg}\frac{(\sqrt{\Phi_1}-\sqrt{\Phi_0})\sqrt{G_\varkappa}}{G_\varkappa+\sqrt{\Phi_1\Phi_0}} \qquad (10.81)$$

$$\left(A = 1 + \frac{1-G_\varkappa}{(1+G_\varkappa)^2}, \qquad B = \frac{1-G_\varkappa}{1+G_\varkappa} - 1,\right.$$

$$\left. C = \frac{1-G_\varkappa}{(1+G_\varkappa)^2}, \quad D = \frac{(1-G_\varkappa)^2}{(1+G_\varkappa)^2} - 1\right).$$

461 This loss is represented by the dashed curves 1 in Figure 10.15 for $G_\varkappa = G_\varkappa^*$, and the curves 2 for $G_\varkappa$ from § 2. The transition of Nature from its optimum frequency distribution $\nu(\Phi)$ to the uniform distribution at $G_\varkappa = G_\varkappa^*$ decreases the loss (cf. the solid curves and the dashed curves 1 in Figure 10.15). If the Designer knows beforehand that Nature will select the uniform distribution $\nu(\Phi) = 1/\Delta\Phi$ the optimum weight for him will be $G_\varkappa$ as given in § 2 (cf. the dashed curves in Figure 10.14). It can be seen in Figure 10.15 that the loss will only slightly decrease as compared with the case $G_\varkappa = G_\varkappa^*$ (cf. the difference between the dashed curves 1 and 2, and the difference between the solid curves and the dashed curves 1).

The optimum strategy of Nature is a mixed one. It is advantageous for it to select the maneuvers Φ^*, Φ^{**} with frequencies ν^*, ν^{**} determined from the equations $\partial M^*/\partial G_\varkappa^* = 0$, $M^* = \nu^*\mathcal{M}(\Phi^*, G_\varkappa^*) + \nu^{**}\mathcal{M}(\Phi^{**}, G_\varkappa^*)$ /10.5—10.8/:

$$\nu^*\left(\frac{\partial\mathcal{M}}{\partial G_\varkappa}\right)_{\Phi^*, G_\varkappa^*} + (1-\nu^*)\left(\frac{\partial\mathcal{M}}{\partial G_\varkappa}\right)_{\Phi^{**}, G_\varkappa^*} = 0, \quad \nu^{**} = 1-\nu^* \qquad (10.82)$$

$$\left(\frac{\partial\mathcal{M}}{\partial G_\varkappa} = \frac{1}{(1-\sqrt{\Phi})^2}\left[1 - \frac{\Phi}{(\Phi+G_\varkappa)^2}\right]\right).$$

Depending on the parameters Φ_0, Φ_1 of the maneuver range, we can represent Φ^*, Φ^{**} by either the boundary points of the range $\Phi^* = \Phi_0$, $\Phi^{**} = \Phi_1$, or one of the boundary points Φ_0, Φ_1 and the maximum point $\Phi_2 = (\sqrt{5/4 - G_\varkappa^*} - 1/2)^2$: $\Phi^* = \Phi_0$, $\Phi^{**} = \Phi_2$ or $\Phi^* = \Phi_2$, $\Phi^{**} = \Phi_1$. This is illustrated in Table 10.1, which represents the optimum values Φ_0 and Φ_1, and their corresponding frequencies Φ^* and Φ^{**}, for a number of values of ν^* and ν^{**}.

TABLE 10.1. Optimum values Φ^*, Φ^{**} of maneuver parameter and frequencies with which Nature must specify maneuvers ν^*, ν^{**} within different allowable ranges $\Phi_0 \leqslant \Phi \leqslant \Phi_1$ $(\Delta\Phi = \Phi_1 - \Phi_0)$

$\Delta\Phi$	0.8			0.4						0.2						
Φ_0	0.01	0.1	0.19	0.01	0.1	0.2	0.4	0.5	0.59	0.01	0.1	0.2	0.4	0.6	0.7	0.79
Φ_1	0.81	0.9	0.99	0.41	0.5	0.6	0.8	0.9	0.99	0.21	0.3	0.4	0.6	0.8	0.9	0.99
Φ^*	0.31	0.34	0.38	0.01	0.26	0.28	0.4	0.5	0.59	0.01	0.1	0.2	0.4	0.6	0.7	0.79
Φ^{**}	0.81	0.9	0.99	0.29	0.5	0.6	0.8	0.9	0.99	0.21	0.26	0.26	0.6	0.8	0.9	0.99
ν^*	0.84	0.82	0.98	0.63	0.55	0.6	0.7	0.8	0.97	0.62	0.65	0.6	0.59	0.64	0.78	0.99
ν^{**}	0.16	0.18	0.02	0.37	0.45	0.4	0.3	0.2	0.03	0.38	0.35	0.4	0.41	0.36	0.22	0.01

462 § 4. OPTIMUM WORKING-FLUID RESERVE FOR A GIVEN MANEUVER WITH FIXED ENGINE PARAMETERS

Assume the engine parameters have been selected by one of the optimum criteria. This procedure, as we have already seen, can be carried out relative to either a single maneuver or a whole series of maneuvers. We now require to carry out with a given engine a maneuver which is either different from the design maneuver (if the engine is designed for a specific maneuver), or different from all the maneuvers within an allowable range (if the engine was designed for a range of maneuvers).

The vehicle payload G_π is specified, the engine weight $G_\varkappa$ is known, and the working-fluid reserve $G_{\mu 0}$ is limited by the tanks' capacity; this limitation is written in the form $0 \leqslant G_{\mu 0} \leqslant G_0 - (G_\pi + G_\varkappa)$ where the maximum takeoff weight of the engine is fixed. The working-fluid reserve $G_{\mu 0}$ can be varied within the limits determined by the last inequality, and the engine control within the bounds set by the specified control characteristic. It is necessary to ensure that the specified maneuver is performed in a minimum time.

When the initial working-fluid reserve is decreased the takeoff weight of the vehicle decreases too. This leads to a higher initial thrust acceleration and a shorter maneuvering time for a fixed thrust P. On the other hand, a low working-fluid reserve can turn out to be insufficient for completing a specified maneuver. Using qualitative considerations it is expected that in many cases the optimum working-fluid reserve will be less than the maximum allowable, i.e., $G_{\mu 0} < G_0 - (G_\pi + G_\varkappa)$. Let us thus choose an engine with a limited flow rate $0 \leqslant q \leqslant q_{\max}$, designed for an energetically-strained maneuver. If an unstrained maneuver is to be carried out with this engine, it may happen that the maximum-allowable quantity of working fluid will not be entirely consumed in the course of the maneuver. Such reasoning becomes incorrect for ideal engines, in which no restrictions are imposed on the flow rate of the working fluid.

1. Formulation of the variational problem. The problem formulated above belongs to the class of variational problems for the maximum operating speed and can be written as follows:

$$\left.\begin{array}{llll} \dot{G} = -gq, & G(0) \leqslant G_0, & G(T) = G_\pi + G_\varkappa, & \\ \dot{\mathbf{r}} = \mathbf{v}, & \mathbf{r}(0) = \mathbf{r}_0, & \mathbf{r}(T) = \mathbf{r}_1, & T = \min, \\ \dot{\mathbf{v}} = gP\mathbf{e}/G + \mathfrak{R}, & \mathbf{v}(0) = \mathbf{v}_0, & \mathbf{v}(T) = \mathbf{v}_1 & \\ (q = q(\mathbf{u}),\ P = P(\mathbf{u}),\ \mathbf{u}_{\min} \leqslant \mathbf{u}(t) \leqslant \mathbf{u}_{\max},\ |\mathbf{e}(t)| = 1, & & & \\ G_0,\ G_\pi,\ G_\varkappa = \text{const}). & & & \end{array}\right\} \qquad (10.83)$$

463 Here G_0, G_π, $G_\varkappa$ are (specified) design parameters; $q = q(\mathbf{u})$, $P = P(\mathbf{u})$, $\mathbf{u}_{\min} \leqslant \mathbf{u}(t) \leqslant \mathbf{u}_{\max}$ is the control characteristic of the engine (likewise specified), and $\mathbf{u}(t)$ are the independent engine control functions (II. 9). The takeoff weight $G(0)$ must be selected, and the program $\mathbf{u}(t)$ established to yield a flow rate q, a thrust P, and a thrust-direction program $\mathbf{e}(t)$, which would ensure a minimum time T during which the specified maneuver must be carried out (the kinematic parameters at the beginning of the trajectory $\mathbf{r}_0$, $\mathbf{v}_0$ and at its end $\mathbf{r}_1$, $\mathbf{v}_1$ are fixed).

The initial condition (10.83) imposed on the vehicle weight is split in two: either

$$G(0) = \text{opt} \quad (\text{at } G(0) < G_0), \qquad (10.84)$$

and then the initial value of the momentum p corresponding to the phase coordinate G vanishes, i.e., $p(0) = 0$, or

$$G(0) = G_0, \tag{10.85}$$

for which the initial value of p is unknown.

Replacing the condition $G(0) \leqslant G_0$ in (10.83) by (10.84) or (10.85), we obtain standard problems for the maximum operating speed. If we fix the weight $G(0)$ in (10.83), it is equivalent to the problem already studied of maximizing the terminal weight for fixed maneuvering time or to the corresponding dynamic problem (cf. Chapters Four to Eight). There is, therefore, no need to once again consider here the problem of the optimum control programs, and it only remains to find the optimum value of the weight $G(0)$, i.e., the optimum working-fluid reserve. This procedure is carried out below for ideal, unthrottled engines.

2. **Ideal engines with limited power and limited exhaust velocity.** The dynamic maneuver for an ideal power-limited engine is characterized by the functional J, the integral of the square of the thrust acceleration (Chapter Four). The shorter the maneuvering time T, the larger the magnitude J (Chapter Five). The terminal weight of the engine $G(T)$ is expressed in terms of the functional J or Φ by formula (4.6)

$$G(T) = G_\pi + G_\varkappa = \frac{G(0)}{G_\varkappa + \Phi G(0)} \qquad \left(\Phi = \frac{\alpha}{2g} J\right) \tag{10.86}$$

(the unit weight of the engine α is fixed). If this relationship is solved in terms of Φ, then problem (10.83) reduces to finding the maximum of $\Phi(G(0), G_\varkappa, G_\pi)$ with respect to $G(0)$, namely,

$$\max \Phi = \frac{G_\varkappa}{G_\pi + G_\varkappa} \max_{G(0) \leqslant G_0} \left(1 - \frac{G_\pi + G_\varkappa}{G(0)}\right) \tag{10.87}$$

464 for fixed values of G_0, G_π, $G_\varkappa$. This maximum (10.87) is attained when $G(0) = G_0$ (maximum possible working-fluid reserve) and equals

$$\Phi_{\max} = \frac{G_\varkappa}{G_\pi + G_\varkappa}\left(1 - \frac{G_\pi + G_\varkappa}{G_0}\right), \quad G(0)_{\text{opt}} = G_0. \tag{10.88}$$

With the value of $\Phi_{\max}$ and the unit engine weight α, we may calculate the maximum value of the functional $J_{\max} = (2g/\alpha)\Phi_{\max}$ and from it the minimum time $T_{\min}$ corresponding to each specific maneuver.

The results of such a calculation for the maneuvers of interplanetary flight Earth—Mars—Earth, of rotating the orbital plane, and of varying the radius of the orbit of a 24-hour Earth satellite are given in Table 10.2.

The table gives the minimum maneuvering time for different values of the relative payload G_π/G_0, the relative engine weight $G_\varkappa/G_0$, and the unit engine weight α (per unit power). The relationships for $J(T)$ are taken from Chapter Five, those for the Earth—Mars—Earth flight from Figure 5.2, and for the maneuvers of the 24-hour Earth satellite from Figure 5.33. In the first case it was assumed that the time of sojourn on Mars was T_ω = 48 days, and so the necessary adjustments were made to the value of J, from Figure 5.27, due to the deceleration and acceleration on Mars:

$$J_{-2} + J_{+2} = 8 \text{ m}^2/\text{sec}^3$$

(cf. Table 5.7). Two values are given in each box for the magnitudes G_π/G_0 and α; the first corresponds to the interplanetary flight and the second to the maneuvers of the guided satellites.

TABLE 10.2. Minimum possible maneuvering time T_{min} for fixed values of payload G_π/G_0 and parameters $G_\varkappa/G_0$, α of ideal power-limited engine (top row with values of G_π and α correspond to interplanetary flight, bottom row to satellite maneuvers)

	G_π/G_0	0.3								0.2								0.1							
		0.8								0.7								0.6							
	$G_\varkappa/G_0$	0.1		0.15		0.2		0.25		0.1		0.15		0.2		0.25		0.1		0.15		0.2		0.25	
	α, kg/kw	5	10	5	10	5	10	5	10	5	10	5	10	5	10	5	10	5	10	5	10	5	10	5	10
		10	20	10	20	10	20	10	20	10	20	10	20	10	20	10	20	10	20	10	20	10	20	10	20
T_{min}, days	Earth—Mars—Earth ($T_\omega = 48$ days)	680	970	600	850	585	820	580	820	575	705	510	675	500	665	495	665	450	585	435	550	420	545	415	545
	24-hour Earth satellite, $\frac{\Delta r}{r_0} = 0.24$, $i = 0$	1	2	1	2	∞	∞	—	—	1	1	1	1	1	1	1	1	1	1	1	1	1	1	1	1
	24-hour Earth satellite, $\frac{\Delta r}{r_0} = 0$, $i = 10°$	4	7	5	10	∞	∞	—	—	2	3	1	3	2	3	2	6	1	2	1	2	1	2	1	1
	24-hour Earth satellite, $\frac{\Delta r}{r_0} = 0.24$, $i = 10°$	4	8	6	12	∞	∞	—	—	2	4	2	3	2	4	2	6	1	2	1	2	1	2	1	2

A similar procedure is also carried out for ideal engines with limited exhaust velocities. In this case the energy expended performing the maneuver is determined by the characteristic velocity 1, which is the integral of the thrust acceleration (Chapter Eight). When the maneuvering time T is shortened, the value of I increases. Expressing I from Tsiolkovskii's formula (8.13) in the form

$$I = -V_{max} \ln [G_\pi/G(0)] \tag{10.89}$$

(the exhaust velocity V_{max} is fixed and the engine weight vanishes, so that $G(T) = G_\pi$), we see that the maximum of I is attained for $G(0) = G_0$, at which

$$I_{max} = -V_{max} \ln (G_\pi/G_0), \qquad G(0)_{opt} = G_0. \tag{10.90}$$

466 It thus follows that for both types of ideal engines studied here the minimum maneuvering time for fixed values of the payload and the engine parameters is attained when the maximum possible value is taken for the working-fluid reserve.

3. **Unthrottled engines.** If the thrust, flow rate, and exhaust velocity of the engine throughout the powered sections of the flight are constant ($P(t) = P_0$ or 0, $q(t) = q_0$ or 0, $V(t) = V_0$ or 0) then we have to solve the dynamic problem independently of the type of engine used. Either the

minimum maneuvering time T must be found for fixed values of both the engine operating time T_μ and the parameters $a_0 = gP_0/G_0$, $\mu = gq_0/G(0)$, or the minimum T_μ for specified T (Chapter Six).

The engine operating time T_μ is expressed in terms of the specified weights G_π, $G_\varkappa$, the flow rate q_0, and the unknown weight $G(0)$, where $gq_0 T_\mu = G(0) - G_\pi - G_\varkappa$. The solution of the dynamic problem can be represented as

$$T = T\left(\frac{gP_0}{G(0)},\ \frac{gq_0}{G(0)},\ \frac{G(0)-G_\pi-G_\varkappa}{gq_0}\right). \tag{10.91}$$

We shall consider relationship (10.91) as known. The problem then reduces to finding the minimum of (10.91) for $G(0) \leqslant G_0$. We give below a solution of this problem for three maneuvers: (a) a velocity build-up u_1 in a gravity-free field, (b) displacement between points of rest situated a distance l apart in a gravity-free field, (c) rotating the plane of a circular orbit in a central field.

(a) Velocity build-up. The solution of the dynamic problem for this maneuver is (6.30)

$$T = T_\mu = \frac{V_0 G(0)}{gP_0}\left(1 - e^{-u_1/V_0}\right). \tag{10.92}$$

Recalling the relationship $T_\mu = (G(0) - G_\pi - G_\varkappa) V_0/gP_0$ we see that the takeoff weight $G(0)$ or the working-fluid reserve $G_{\mu 0} = G(0) - G_\pi - G_\varkappa$ are uniquely determined by (10.92) in the form

$$G(0) = (G_\pi + G_\varkappa)\, e^{u_1/V_0} \quad \left(0 \leqslant u_1 \leqslant V_0 \ln \frac{G_0}{G_\pi + G_\varkappa}\right). \tag{10.93}$$

467 The required working-fluid reserve varies from zero for

$$u_1/V_0 = 0$$

to its maximum possible value for

$$u_1/V_0 = \ln\left[G_0 / (G_\pi + G_\varkappa)\right],$$

depending on the combination u_1/V_0 of the maneuver parameter u_1 and the engine parameter V_0. With larger values of u_1/V_0 for given G_0, G_π, $G_\varkappa$ the maneuver cannot be performed. The takeoff weight $G(0)$, represented as a fraction of the maximum weight G_0, has been plotted in Figure 10.16 as a function of the ratio u_1/V_0 for fixed values of $(G_\pi + G_\varkappa)/G_0$. The deviation of $G(0)/G_0$ from unity gives the difference between the maximum possible and the necessary working-fluid reserves.

(b) Displacement between points of rest. The solution of the dynamic problem (6.43) can be presented here in the form

$$T = c_1\left\{(\xi - 1) + 2\left[c_2 - (\sqrt{\xi} - 1)^2\right] \ln^{-1} \xi\right\}$$
$$\left(c_1 = \frac{(G_\pi + G_\varkappa) V_0}{gP_0},\quad c_2 = \frac{gP_0 l}{(G_\pi + G_\varkappa) V_0^2},\quad \xi = \frac{G(0)}{G_\pi + G_\varkappa}\right). \tag{10.94}$$

From the condition of minimum T for ξ ($\partial T/\partial \xi = 0$) we derive an implicit expression for the optimum value of ξ in terms of c_2, which is composed of the maneuver parameter and the vehicle parameter (Figure 10.17), where

$$c_2 = {}^1/_2 \xi \ln^2 \xi - \sqrt{\xi}\,(\sqrt{\xi} - 1) \ln \xi + (\sqrt{\xi} - 1)^2. \qquad (10.95)$$

468 If ξ is now taken as a parameter, we may substitute (10.95) into (10.94) and obtain an expression for the minimum time

$$T_{\min} = c_1 [\xi \ln \xi - (\sqrt{\xi} - 1)^2]; \qquad (10.96)$$

(10.95) enables this to be represented as a function of c_2 (Figure 10.17).

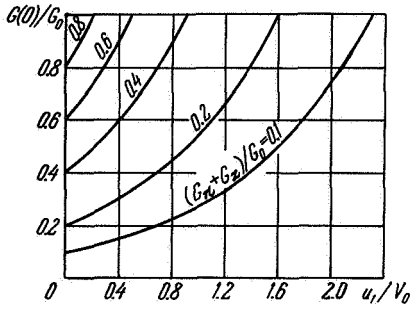

FIGURE 10.16. Relative takeoff weight $G(0)/G_0$ as function of parameter u_1/V_0 for fixed values of total weight $(G_п + G_н)/G_0$ of the engine and payload, for velocity build-up u_1 with unthrottled engine.

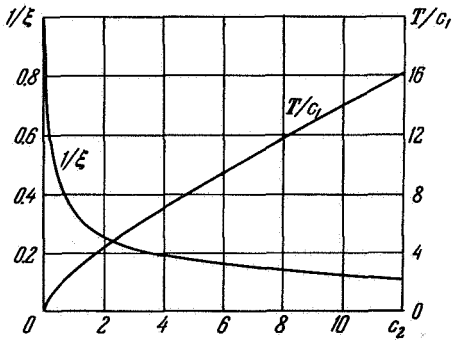

FIGURE 10.17. Optimum weight $1/\xi = (G_п + G_н)/G(0)$ and minimum maneuvering time T/c_1 as function of c_2 composed of maneuver parameter l and engine parameter, for displacement between points of rest with unthrottled engine ($c_1 = (G_п + G_н) \times V_0/gP_0$, $c_2 = gP_0 l\ (G_п + G_н)^{-1} V_0^{-2}$).

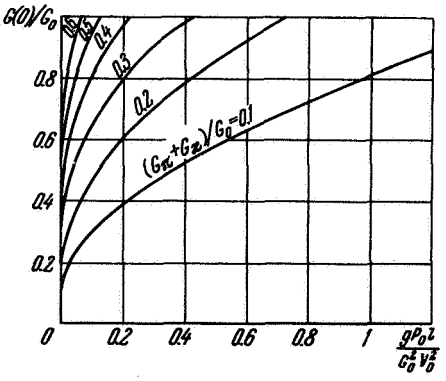

FIGURE 10.18. Optimum takeoff weight $G(0)/G_0$ as function of parameter $gP_0 l/G_0^2 V_0^2$ for fixed values of total weight $(G_п + G_н)/G_0$ of engine and payload; displacement between points of rest with unthrottled engine.

Relationships (10.95) and (10.96) give the complete solution of the problem. The dependence of the optimum takeoff weight $G(0) = \xi(G_\pi + G_\varkappa)$ on the quantity $gP_0 l/G_0^2 V_0^2$ as calculated from (10.95) and (10.96) for fixed values of $(G_\pi + G_\varkappa)/G_0$ is shown in Figure 10.18.

(c) Rotating the plane of a circular orbit. For the maneuver of rotating the plane of a circular orbit of radius r_0 through an angle i the functional of the dynamic problem (10.91) is written in the implicit form (6.88)

$$\xi - 1 = (T/c_1)\arcsin[(c_1/T)c_2\xi] \qquad \left(c_1 = \frac{\pi(G_\pi + G_\varkappa)V_0}{2gP_0},\quad c_2 = \frac{i\sqrt{k/r_0}}{V_0},\quad \xi = \frac{G(0)}{G_\pi + G_\varkappa}\right) \tag{10.97}$$

(here the time T is considered as a multiple of the period of orbital revolution, equal to $2\pi k^{-1/2} r_0^{3/2}$).

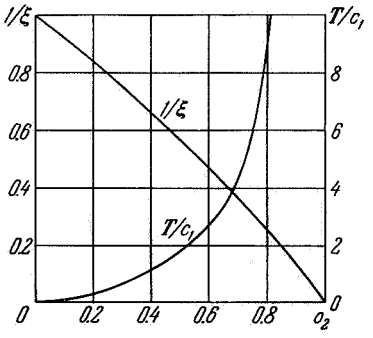

FIGURE 10.19. Optimum weight $1/\xi = (G_\pi + G_\varkappa)/G(0)$ and minimum maneuvering time T/c_1 as function of c_2 composed of maneuver parameter i, r_0, k, and engine parameters for rotating orbital plane of unthrottled engine ($c_1 = \pi(G_\pi + G_\varkappa)V_0/2gP_0$, $c_2 = i\sqrt{k/r_0}V_0^{-1}$).

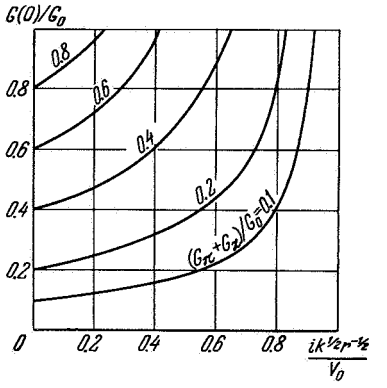

FIGURE 10.20. Optimum takeoff weight $G(0)/G_0$ as function of parameter $i\sqrt{k/r_0}V_0^{-1}$ for fixed values of total weight $(G_\pi + G_\varkappa)/G_0$ of engine and payload; rotation of orbital plane of unthrottled engine.

469 The optimum value of the parameter ξ (the relative takeoff weight) and the minimum value of the maneuvering time T are equal to (Figure 10.19)

$$\left.\begin{aligned} \xi_{\text{opt}} &= \left(\frac{G(0)}{G_\pi + G_\varkappa}\right)_{\text{opt}} = \frac{\sqrt{1-c_2^2}}{\sqrt{1-c_2^2} - c_2\arcsin\sqrt{1-c_2^2}}, \\ T_{\min} &= \frac{c_1 c_2}{\sqrt{1-c_2^2} - c_2\arcsin\sqrt{1-c_2^2}}. \end{aligned}\right\} \tag{10.98}$$

The ratio of the takeoff weight $G(0)$ to the maximum possible weight G_0 has been plotted in Figure 10.20 as a function of the quantity $c_2 = i\sqrt{k/r_0}V_0^{-1}$ for different values, where $(G_\pi + G_\varkappa)/G_0 = \text{const}$.

The results of this section show that for unthrottled engines, as opposed to ideal engines, there exists, for definite values of the maneuver and engine parameters, an optimum working-fluid reserve which differs from the maximum possible. We recall that these results apply to all types of unthrottled engines.

Chapter Eleven

RELIABILITY CONSIDERATIONS IN OPTIMIZATION PROBLEMS

470 During flight the propulsion system is subjected to random factors which may cause failures. We distinguish between external and internal factors; meteoric punctures belong to the first category, while processes such as wear exemplify the second. The probability of failure could depend on the time, the coordinates, the parameters of the engine and vehicle, or the engine operating regime. Allowance for a reliability factor will therefore lead to an adjustment in the usual programs for the optimum controls and parameters /11.1—11.4/.

Reliability is defined as the probability of uninterrupted engine operation during a specified maneuver. The maneuver is considered as unfulfilled if (and only if) the engine fails; therefore, the phrases "probability of engine operation without failure" and "probability of successfully executing the maneuver" coincide here and are interchangeable. In this chapter, the probability of executing a maneuver is either specified (§§ 1 to 3) or is selected so as to be an optimum in some sense (§ 4). Single-section (§ 1) and multi-sectional (§§ 2 and 3) engines are considered; the variational problems are solved for models of the basic maneuvers. The case of a fixed engine operating time, treated in § 2 of Chapter Seven can be considered a particular case of the problem of fixed reliability (assuming the probability of engine failure to be a function of the operating time only).

§ 1. OPTIMUM CONTROL FOR A SPECIFIED PROBABILITY OF SUCCESSFULLY EXECUTING THE MANEUVER

1. Formulation of the variational problem. Consider the general problem of optimum control, and suppose we have a dynamic system whose behavior is described by equations of the form

$$\dot{x}_i = f_i(x_j, u_k, w_l, t), \quad i, j = 0, 1, \ldots, n; \quad k = 1, \ldots, r; \quad l = 1, \ldots, q, \tag{11.1}$$

471 where x_i are the phase coordinates of the system, $u_k(t)$ are the control functions and w_l are the constant control parameters.

The boundary conditions for x_i at given initial and final times, $t = 0$ and $t = T$, are specified. The maximum (minimum) value of the control functional of the problem $x_0(T)$ is required. This variational problem will be termed the basic problem.

We turn now to the formulation of the variational problem with a specified reliability.

The dynamic system is considered as a single entity with regard to failures since the failure of a single element leads to the breakdown of the whole system. The maneuver is considered as unfulfilled if the system breaks down at any instant (the system is not afterwards repaired).

A control program must be set up and values of the parameters chosen such that a specified probability of the system operating (specified reliability) is obtained, and also that all the conditions listed above are satisfied.

The average number of failures per unit time λ is assumed to be specified in the form

$$\lambda = \lambda(t,\ x_j,\ u_k,\ w_l) \tag{11.2}$$

as a function of the time, the phase coordinates, the control functions, and the control parameters; it is, however, independent of the previous history /11.5—11.8/.

The probability R of there being no failures in the interval $[0,\ T]$ will then be equal to /11.5—11.8/

$$R = \exp\left(-\int_0^T \lambda\, dt\right), \tag{11.3}$$

where λ is calculated along the trajectory $\lambda = \lambda(t,\ x_j(t),\ u_k(t),\ w_l)$.

In (11.3) the probability R is fixed and represents the condition of specified reliability $0 < R < 1$. It must be added to the equations of the basic variational problem. If we use Lagrange's formulation, it is convenient to add it in the form of an isoperimetricity condition

$$\int_0^T \lambda(t, x_j(t), u_k(t), w_l)\, dt = -\ln R. \tag{11.4}$$

In Mayer's formulation, we must express (11.3) as a differential equation with boundary conditions

$$\dot{\Lambda} = \lambda(t,\ x_j,\ u_k,\ w_l), \quad \Lambda(0) = 0,\ \Lambda(T) = -\ln R. \tag{11.5}$$

472 The variable Λ will appear as an additional phase coordinate of system (11.1). The value $\Lambda_1 = \Lambda(T)$ will be conventionally called the allowable average number of failures throughout the whole time of motion. If we specify a reliability $R = 1$, then $\Lambda_1 = 0$; this cannot be realized. As the reliability decreases, the allowable number of failures increases (thus, for R in the range $[1;\ 0.5]$ Λ_1 varies over the range $[0;\ 0.7]$).

Let $x_j^*(t)$, $u_k^*(t)$, w_l^* be a solution of the basic variational problem (disregarding the reliability factor). If for this solution

$$\Lambda_1^* = \int_0^T \lambda(t, x_j^*(t), u_k^*(t), w_l^*)\, dt \leqslant -\ln R, \tag{11.6}$$

the reliability R will be ensured. Note that when $\lambda_{\max} T \leqslant -\ln R$ the condition of specified reliability is necessarily fulfilled.

If (11.6) is not satisfied, the system of equations governing the problem of optimum control with a specified reliability, (11.1) to (11.5), is written in the form

$$\left.\begin{aligned} &\dot{x}_i = f_i(t, x_j, u_k, w_l),\ x_i(0) = x_{i0},\ x_i(T) = x_{i1}, \\ &\dot{\Lambda} = \lambda(t, x_j, u_k, w_l),\ \Lambda(0) = 0,\quad \Lambda(T) = -\ln R, \end{aligned} \right\} \quad x_0(T) = \text{extr.} \qquad (11.7)$$

This notation is the ordinary Mayer variational problem. We make two comments about generalizing (11.7).

1) Let λ also depend on the instantaneous engine operating time $t_\mu \leqslant t$. Then, as in § 2 of Chapter Seven, we must add to (11.7) another differential equation with corresponding boundary conditions

$$\dot{t}_\mu = \delta,\quad t_\mu(0) = 0,\quad t_\mu(T) = \text{opt}, \qquad (11.8)$$

where $\delta(t)$ is the Dirac delta function which equals one when the system operates and zero when it is not operating. The control functions δ in (11.7) must be multiplied by u so that they vanish when the system is not operating.*

2. Suppose the control function u takes values within the range $[u_{\min}, u_{\max}]$ and vanishes when the engine is cut off. The value of λ equals $\lambda(u)$ when the system operates and $\lambda(0)$ when it is nonoperating (Figure 11.1, a).

473 In order to represent the last equation of (11.7) as a function whose form does not change, use is once more made of the control function δ so that

$$\dot{\Lambda} = \lambda(0) + [\lambda(u) - \lambda(0)]\,\delta; \qquad (11.9)$$

in the other equations, u is replaced by $u\delta$.

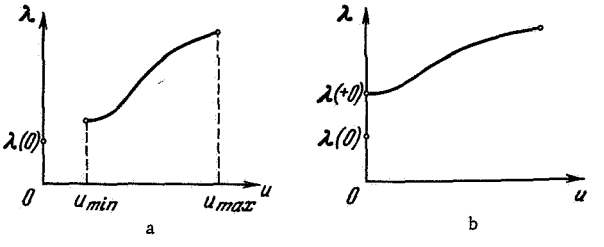

FIGURE 11.1. Two examples of coasting ($u = 0$) with discontinuity points where λ depends on control function u.

The same method can be used during coasting when $\lambda(0)$ (cold reserve) is not equal to the limit $\lambda(+0)$ as $u \to 0$ (hot reserve) (Figure 11.1, b).

This formulation described above is now applied to the problem of delivering a maximum payload. The two cases of engines with limited power and limited exhaust velocity are considered.

2. Power-limited engines. When reliability considerations are neglected, the operation of power-limited propulsion systems is optimum when the power is fully utilized in the powered flight periods. If the propulsion system is ideal, the optimum trajectory does not contain coasting periods.

* The terminal value $t_\mu(T)$ is not given, unlike the basic problem in § 2 of Chapter Seven, and has to be selected from trajectory optimum considerations.

Now introduce the probability (11.3) of successfully carrying out the maneuver. The parameter λ (11.2) is written as a function of the power N, (a fraction of the maximum power $N_{\max}$) and of the structural parameter w in the form

$$\lambda = \lambda(t,\ N,\ w)$$
$$(0 \leqslant N(t) \leqslant 1,\ \ w = \text{const},\ \ \partial\lambda/\partial N \geqslant 0,\ \ \partial\lambda/\partial w < 0). \tag{11.10}$$

The effect of maximum power is not accounted for here; the nonnegativeness of the derivative $\partial\lambda/\partial N$ corresponds to the intuitive concept that the probability of failure increases as the work increases. The parameter w represents the structural measures taken to increase the reliability, so that an increase in w implies a corresponding decrease in the failures λ ($\partial\lambda/\partial w < 0$); on the other hand, this is accompanied by an increase in the unit engine weight α ($\partial\alpha/\partial w > 0$).

We restrict ourselves to the case of an ideal engine (cf. Chapter Four); the problem of delivering a maximum payload for a specified reliability R is written, according to the general formulation (11.7) and similarly to (4.42), as

$$\left.\begin{aligned}
&\dot{G}_\sigma = -\frac{(G_\sigma + G_\varkappa)^2}{G_\varkappa}\frac{\alpha(w)}{2g}\frac{a^2}{N},\ \ G_\sigma(0)+G_\varkappa=1,\ \ G_\sigma(T)=\max,\\
&\dot{\mathbf{r}} = \mathbf{v}, && \mathbf{r}(0)=\mathbf{r}_0, && \mathbf{r}(T)=\mathbf{r}_1,\\
&\dot{\mathbf{v}} = a\mathbf{e} + \mathfrak{R}, && \mathbf{v}(0)=\mathbf{v}_0, && \mathbf{v}(T)=\mathbf{v}_1,\\
&\dot{\Lambda} = \lambda(t, N, w), && \Lambda(0)=0, && \Lambda(T)=\\
& && && = -\ln R\\
&(a(t)\geqslant 0,\ 0\leqslant N(t)\leqslant 1,\ |\mathbf{e}(t)|=1;\ G_\varkappa, w=\text{const}).
\end{aligned}\right\} \tag{11.11}$$

Optimum values of the parameters $G_\varkappa$, w must be selected here and optimum programs $a(t)$, $N(t)$, $\mathbf{e}(t)$ established. As in § 1 of Chapter Four, one can find the optimum relation for the weight $G_\varkappa$ before the whole problem has been solved (since this weight G_σ only enters the first equation and the initial condition of (11.11)). In the usual way (cf. Chapter Four, §§ 1.1 and 1.2), expressions are obtained for the functional $G_\sigma(T) = G_\pi$ and for the optimum engine weight $G_\varkappa$. These coincide in form with (4.15) and (4.16),

$$G_\pi = (1 - \sqrt{\Phi})^2,\ \ G_\varkappa = \sqrt{\Phi} - \Phi, \tag{11.12}$$

where Φ is taken as (cf. (4.14))

$$\Phi = \frac{\alpha(w)}{2g}J,\ \ \ J = \int_0^T \frac{a^2}{N}\,dt. \tag{11.13}$$

The problem then reduces to minimizing the functional Φ, as well as J for fixed w; the latter problem (J = min) will be called the dynamic problem.

If the reliability is not taken into account, we can establish that the control function $N(t) = 1$ is optimum without solving the dynamic problem. When the reliability is accounted for, however, this becomes impossible. In addition, qualitative considerations indicate that a regime different from the ideal one $N(t) = 1$ exists. In fact, the increase of power N for a fixed program $a(t)$ leads to a decrease in the functional J (i.e., to an increase in the payload G_π (11.12)). This implies an increase in the average number of failures per unit time (11.10) (i.e., decreasing reliability).

475 The variational problem under consideration (minimizing the functional J) is written as follows in terms of Mayer's problem (cf. (5.2)):

$$\left.\begin{array}{llll} \dot{J} = a^2/N, & J(0) = 0, & J(T) = \min, & \\ \dot{\mathbf{r}} = \mathbf{v}, & \mathbf{r}(0) = \mathbf{r}_0, & \mathbf{r}(T) = \mathbf{r}_1, & \\ \dot{\mathbf{v}} = a\mathbf{e} + \mathfrak{R}, & \mathbf{v}(0) = \mathbf{v}_0, & \mathbf{v}(T) = \mathbf{v}_1, & \\ \dot{\Lambda} = \lambda(t, N, w), & \Lambda(0) = 0, & \Lambda(T) = -\ln R & \\ (a(t) \geqslant 0, & 0 \leqslant N(t) \leqslant 1, & |\mathbf{e}(t)| = 1). & \end{array}\right\} \tag{11.14}$$

The parameter w in (11.14) is considered as fixed, and the optimum value of w is determined after solving (11.14), i.e., after the relationship $J_{\min}(w)$ has been obtained from the condition for a minimum of $\Phi(w) = [\alpha(w)/2g]\, J_{\min}(w)$.

In accordance with the maximum principle, the optimum functions for the thrust acceleration $a(t)$, the power $N(t)$, and the direction of the thrust vector $\mathbf{e}(t)$ must ensure an absolute maximum of the Hamiltonian H (the object is to minimize J). The latter has the form

$$H = -a^2/N + a(\mathbf{p}_v \cdot \mathbf{e}) + \lambda p_\lambda + (\mathbf{p}_r \cdot \mathbf{v}) + (\mathbf{p}_v \cdot \mathfrak{R}), \tag{11.15}$$

where the momenta $\mathbf{p}_r$, $\mathbf{p}_v$, p_λ, p_j satisfy the equations

$$\left.\begin{array}{ll} \dot{\mathbf{p}}_r = -\dfrac{\partial H}{\partial \mathbf{r}} = -\dfrac{\partial}{\partial \mathbf{r}}(\mathbf{p}_v \cdot \mathfrak{R}), & \dot{\mathbf{p}}_v = -\dfrac{\partial H}{\partial \mathbf{v}} = -\mathbf{p}_r, \\ \dot{p}_\lambda = -\dfrac{\partial H}{\partial \Lambda} = 0, & p_j = -1. \end{array}\right\} \tag{11.16}$$

The maximum of H with respect to $\mathbf{e}$ and a is attained when

$$\mathbf{e} = \mathbf{p}_v/p_v, \quad a = {}^1/_2 p_v N \qquad (p_v = |\mathbf{p}_v|). \tag{11.17}$$

The part of the function H depending on N, with the control variable a taken from (11.17), is written as

$$H_N = {}^1/_4 p_v^2 N + \lambda(t, N)\, p_\lambda. \tag{11.18}$$

By examining (11.18) one may establish the sign of the momentum p_λ. Let $p_\lambda \geqslant 0$; then H will have a maximum when $N \equiv 1$ (since, according to (11.10), $\partial\lambda/\partial N \geqslant 0$). We therefore obtain the same optimum trajectory if the reliability is not accounted for. When formulating the general problem (11.7) it is assumed that condition (11.6) is not fulfilled, so the specified reliability R cannot be ensured for such a trajectory. Therefore,

$$p_\lambda = \text{const} < 0. \tag{11.19}$$

476 Note two properties of the optimum trajectories (when reliability is taken into account) which follow from the condition for a maximum of (11.18) with respect to N.

1) Consider a family of reliability characteristics $\lambda(t, N)$ having two common points $\lambda(t, 0) = \lambda_0(t)$ and $\lambda(t, 1) = \lambda_1(t)$. For all $\lambda(t, N)$ in (11.10) satisfying the condition

$$\lambda(t, N) \geqslant \lambda_0(t) + [\lambda_1(t) - \lambda_0(t)]N \tag{11.20}$$

(cf. the shaded region in Figure 11.2), the control variable $N(t)$ reaches its limiting value, and the optimum trajectories and values of the functional J are the same.

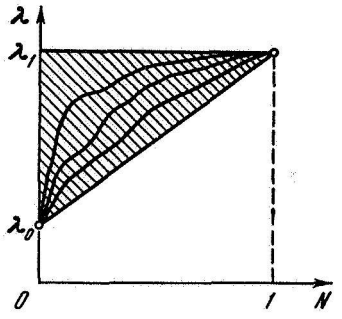

FIGURE 11.2. Region in (λ, N) plane (shaded), indistinguishable in sense of problem functional J.

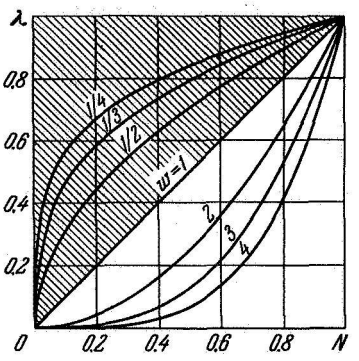

FIGURE 11.3. Power-law relationship between λ and N for different values of structural parameter w (shaded region indicates where functional is independent of form of $\lambda(N)$).

In fact, by substituting the linear function of N from inequality (11.20) into (11.18), we obtain the function

$$H_{N\,\mathrm{maj}} = p_\lambda \lambda_0 + [{}^1/_4 p_v^2 + p_\lambda (\lambda_1 - \lambda_0)]\, N \tag{11.21}$$

which, in view of (11.19), will maximize all H_N composed of functions $\lambda(t, N)$ satisfying (11.20). Therefore,

$$H_N(N) \leqslant H_{N\,\mathrm{maj}}(N),\ H_N(0) = H_{N\,\mathrm{maj}}(0),\ H_N(1) = H_{N\,\mathrm{maj}}(1). \tag{11.22}$$

Hence, $\max H_N \leqslant \max H_{N\,\mathrm{maj}}$; since $H_{N\,\mathrm{maj}}$ is a linear function of N and its maximum is attained at the limiting points given by

$$N = 1 \text{ at } p_v^2 > -4p_\lambda(\lambda_1 - \lambda_0),\ N = 0 \text{ at } p_v^2 < -4p_\lambda(\lambda_1 - \lambda_0). \tag{11.23}$$

For these values the functions $H_{N\,\mathrm{maj}}$ and H_N coincide, and therefore the maximum of H_N for all λ in (11.20) is attained at the same points. Thus, the optimum value of the control variable $N(t)$ turns out to be the limiting values (11.23), and the intermediate values of λ do not figure at all in the problem. At the points $N = 1$ and $N = 0$ all $\lambda(t, N)$ from (11.20) take the same values $\lambda_1(t)$ and $\lambda_0(t)$. This means that the optimum trajectories and values of the functional J are identical (i.e., the shaded part of the region $\lambda(t, N)$ in Figure 11.2 turns out to be indistinguishable in the sense of the problem functional).

2) If $\partial\lambda/\partial N \neq 0$ for $N = 0$, the optimum trajectory does not contain coasting periods. In this case the partial derivative of (11.18) with respect to N

$$\partial H_N/\partial N = {}^1/_4 p_v^2 + p_\lambda \partial\lambda/\partial N \tag{11.24}$$

477 at $N = 0$ is always positive (except at isolated instants of time when $p_v = 0$). Therefore, the optimum value of N to ensure that (11.18) is a maximum, is always greater than zero, i.e., there are no coasting periods.

Consider now a particular form of (11.10)

$$\lambda = \lambda(N, w) = \lambda_{\max} N^w \qquad (\lambda_{\max},\ w = \text{const} > 0) \tag{11.25}$$

(see Figure 11.3). For all $0 \leqslant w \leqslant 1$ (the shaded region in Figure 11.3) the optimum value of the control variable $N(t)$ is determined by relation (11.23), into which we must substitute $\lambda_0 = 0$, $\lambda_1 = \lambda_{\max}$ according to the first property. For $w > 1$ we derive the second property, namely, that the optimum value of the control variable $N(t)$ is

$$\begin{aligned} &N = 1 \quad \text{at} \quad p_v^2 \geqslant -4w\lambda_{\max} p_\lambda, \\ &N = \left(\frac{-p_v^2}{4w\lambda_{\max} p_\lambda}\right)^{\frac{1}{w-1}} \quad \text{at} \quad p_v^2 \leqslant -4w\lambda_{\max} p_\lambda, \end{aligned} \tag{11.26}$$

i.e., there appear to be sections with variable power, lower than the maximum.

All the results obtained above are independent of the type of dynamic maneuver (i.e., of $\mathbf{r}_0$, $\mathbf{r}_1$, $\mathbf{v}_0$, $\mathbf{v}_1$, $\mathfrak{R}(\mathbf{r}, t)$). In order to complete the solution of the variational problem (11.14), we specify elementary maneuvers to be the displacement between two points of rest, and the build-up of a specific velocity in a gravity-free field.

If the reliability is not specified ($\Lambda(T) = \text{opt}$ or $p_\lambda = 0$), the solution of the problem for a displacement between points of rest is (5.33)

$$\begin{aligned} N^*(t) &= 1, \\ a^*(t)\, e^*(t) &= 6\,(l/T^2)\,(1 - 2t/T), \\ J^*(T) &= 12\,(l^2/T^3). \end{aligned} \tag{11.27}$$

For a given reliability R the solution depends on the parameter

$$\varkappa = -\ln R/\lambda_{\max} T \qquad (0 < \varkappa \leqslant 1), \tag{11.28}$$

which represents the ratio of the allowable number of failures $\Lambda(T) = -\ln R$ to the maximum possible number of them $\Lambda_{\max} = \lambda_{\max} T$.

478 The solution is written finally as follows:*

$$\left.\begin{aligned} &\text{if } 0 \leqslant w \leqslant 1,\ 0 < \varkappa \leqslant 1 \text{ (Figure 11.4, a), then} \\ &N(t) = 1, \quad a(t) = a_0(1 - 2t/T) \quad \text{at} \quad 0 \leqslant t < t_1, \\ &N(t) = 0, \qquad a(t) = 0 \qquad\quad \text{at} \quad t_1 < t < {}^1/_2 T \\ &\left(a_0 = \frac{6l}{T^2}\,[1 - (1 - 2t_1/T)^3]^{-1},\ t_1 = {}^1/_2 \varkappa T\right), \\ &J(T) = 12\,(l^2/T^3)\,[1 - (1 - \varkappa)^3]^{-1}; \end{aligned}\right\} \tag{11.29}$$

* The functions $N(t)$ and $a(t)$ are even relative to the middle of the interval $t = {}^1/_2 T$; the function $e(t) = \pm 1$ is odd since $e(t) = +1$ at $0 \leqslant t < {}^1/_2 T$, $e(t) = -1$ at ${}^1/_2 T < t \leqslant T$.

$$
\left.\begin{aligned}
&\text{if}\quad w>1,\ (w-1)/(3w-1)\leqslant \varkappa\leqslant 1\\
&\qquad\qquad\qquad\qquad\text{(Figure 11.4, b), then}\\
&N(t)=1, \qquad a(t)=a_0\,(1-2t/T)\\
&\qquad\qquad\qquad\qquad\text{at}\quad 0\leqslant t<t_1,\\
&N(t)=\left(\frac{1-2t/T}{1-2t_1/T}\right)^{\frac{2}{w-1}},\quad a(t)=a_0\frac{(1-2t/T)^{\frac{w+1}{w-1}}}{(1-2t_1/T)^{\frac{2}{w-1}}}\\
&\qquad\qquad\qquad\qquad\text{at}\quad t_1<t<{}^1/_2T\\
&\left(a_0=\frac{6l}{T^2}\left[1-\frac{1}{3w-1}(1-2t_1/T)^3\right]^{-1},\right.\\
&\qquad\qquad\qquad\left.t_1=\frac{3w-1}{4w}\left[\varkappa-\frac{w-1}{3w-1}\right]T\right),\\
&J(T)=12\,(l^2/T^3)\left[1-\frac{(3w-1)^2}{4w^3}(1-\varkappa)^3\right]^{-1};\\
&\text{if}\quad w>1,\ 0<\varkappa\leqslant (w-1)/(3w-1)\\
&\qquad\qquad\qquad\qquad\text{(Figure 11.4, c), then}\\
&N(t)=\varkappa\left(\frac{3w-1}{w-1}\right)^{\frac{1}{w}}(1-2t/T),\\
&a(t)=\frac{6l}{T^2}\frac{3w-1}{3(w-1)}(1-2t/T)^{\frac{w+1}{w-1}}\quad\text{at}\quad 0\leqslant t<{}^1/_2T,\\
&J(T)=12\,(l^2/T^3)\,\frac{1}{3}\left(\frac{3w-1}{w-1}\right)^{\frac{w-1}{w}}\varkappa^{-\frac{1}{w}}.
\end{aligned}\right\}\qquad (11.29)
$$

Note that for values of the structural parameter $0\leqslant w\leqslant 1$, $\varkappa$ has the same value as the ratio T_μ/T of the total engine operating time to the maneuvering time, and the corresponding solution is equivalent to (7.50) — (7.52). The optimum functions (11.27) (in the absence of failures) and (11.29) (in the general case) for the power $N(t)$ and the thrust acceleration $a(t)$ have been plotted side by side in Figure 11.4, a to c; functions (11.29) are represented by the solid curves, and (11.27) by the dashed lines.

479

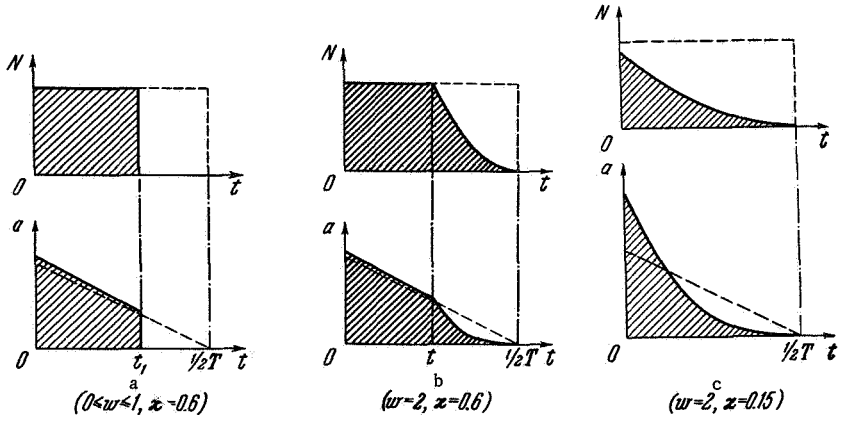

FIGURE 11.4. Three possible types of optimum programs of power $N(t)$ and thrust acceleration $a(t)$ for displacement between points of rest:
a) $0\leqslant w\leqslant 1$, $\varkappa=0.6$; b) $w=2$, $\varkappa=0.6$; c) $w=2$, $\varkappa=0.15$ (w is parameter of family of curves $\lambda(N)$, cf. Figure 11.3; $\varkappa$ is ratio of allowable number of failures to the maximum possible number; dashed lines represent optimum programs when failures are neglected).

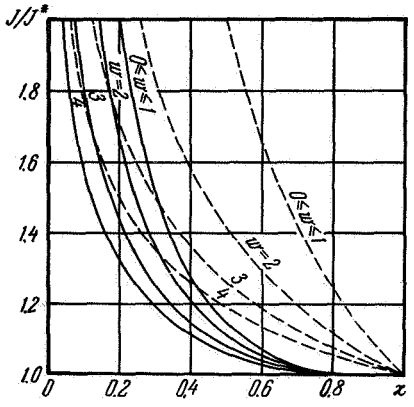

FIGURE 11.5. Functional J as function of parameter w (of family of curves $\lambda(N)$ in Figure 11.3) and ratio $\varkappa$ of allowable number of failures to the maximum number. Solid curves represent displacement between points of rest for which $J^* = 12l^2/T^3$; dashed curves represent velocity build-up for which $J^* = u_1^2/T$.

480

The solid curves in Figure 11.5 represent the value of the functional J divided by J^* (given in (11.27)) as a function of the reliability parameter $\varkappa$ for different values of the structural parameter w (the exponent in (11.25)). An increase in the reliability R (a decrease in the parameter $\varkappa$), all other conditions being equal, leads to an increase of the functional J. The difference between the curves corresponding to $0 \leqslant w \leqslant 1$ and $w = 2, 3, 4$ gives an idea of the gain when using intermediate values of the power. If the condition of specified reliability were only satisfied for $w > 1$ as a result of cutting off the engine (11.23), the functional would have been identical for all $\lambda(N, w)$ (the curve $0 \leqslant w \leqslant 1$). The transition to (11.26) enables a substantial reduction to be made in the value of the functional.

In the problem of velocity build-up, when the reliability is ignored ($p_\lambda = 0$) no coasting periods are obtained, and the solution is (5.32)

$$N^*(t) = 1,\ a^*(t)\, e^*(t) = u_1/T,\ J^*(T) = u_1^2/T. \tag{11.30}$$

If the exponent in formula (11.25) is chosen within the range $0 \leqslant w \leqslant 1$, coasting periods appear. Their number and location do not affect the problem functional, while the total duration is obtained from the condition of specified reliability $\Lambda(T) = -\ln R$. For $w > 1$, according to property 2 above, there are no coasting periods, and the condition $\Lambda(T) = -\ln R$ is satisfied because N decreases. Performing all the operations, we obtain (for $e(t) = 1$):

$$\left.\begin{aligned}
&\text{if } 0 \leqslant w \leqslant 1,\ 0 < \varkappa \leqslant 1 \text{ (Figure 11.6, a), then}\\
&\quad N(t) = 1,\ a(t) = u_1/t_1 \quad \text{at } 0 \leqslant t < t_1,\ (t_1 = \varkappa T),\\
&\quad N(t) = 0,\ a(t) = 0 \quad \text{at } t_1 < t < T\\
&\qquad J(T) = (u_1^2/T)\,\varkappa^{-1};\\
&\text{if } w > 1,\ 0 < \varkappa \leqslant 1 \text{ (Figure 11.6, b), then}\\
&\qquad N(t) = \varkappa^{\frac{1}{w}},\ a(t) = u_1/T \quad \text{at } 0 \leqslant t \leqslant T,\\
&\qquad\qquad J(T) = (u_1^2/T)\,\varkappa^{-\frac{1}{w}}
\end{aligned}\right\} \tag{11.31}$$

(here, as in (11.29), $\varkappa = T_\mu/T$ at $0 \leqslant w \leqslant 1$).

The ratio of the functionals (11.31) and (11.30) has been plotted in Figure 11.5 as a function of $\varkappa$ for different values of w (the dashed curves). It is seen that for the problem of displacement between points of rest (the solid curves) the requirement of specified reliability yields a considerably smaller increase in functional than for the problem of velocity build-up (for the same values of $\varkappa$ and w).

Consider now the selection of the optimum value of the structural parameter w. The values of $\varkappa$ and w (the unit engine weight) depend on this parameter; λ decreases with increasing w (cf. (11.25)), while a increases with w (cf. the explanations about (11.10)). Assume the elementary relationship

$$a(w) = a^*(1+w) \qquad (a^* = \text{const}, w \geqslant 0); \tag{11.32}$$

481 the solutions (11.29) and (11.31) of the dynamic problem (11.14) yield the parameter w from the condition for a minimum of (cf. (11.12), (11.13)) $\Phi(w, \varkappa) = [a(w)/2g]\, J(w, \varkappa)$:

for the maneuver of displacement between points of rest

$$\min_w \frac{\Phi(w,\varkappa)}{\Phi^*} = \min_w \begin{cases} (1+w)[1-(1-\varkappa)^3]^{-1} \\ \text{at } 0 \leqslant w \leqslant 1,\ 0 < \varkappa \leqslant 1, \\ (1+w)\left[1-\frac{(3w-1)^3}{4w^3}(1-\varkappa)^3\right]^{-1} \\ \text{at } w \geqslant 1,\ (w-1)/(3w-1) \leqslant \varkappa \leqslant 1, \\ (1+w)\frac{1}{3}\left(\frac{3w-1}{w-1}\right)^{\frac{w-1}{w}} \varkappa^{-\frac{1}{w}} \\ \text{at } w \geqslant 1,\ 0 < \varkappa \leqslant (w-1)/(3w-1) \end{cases} \tag{11.33}$$

$$(\Phi^* = (a^*/2g)\, 12 l^3 T^{-3}),$$

for the maneuver of velocity build-up

$$\min_w \frac{\Phi(w,\varkappa)}{\Phi^*} = \min_w \begin{cases} (1+w)\varkappa^{-1} & \text{at } 0 \leqslant w \leqslant 1,\ 0 < \varkappa \leqslant 1, \\ (1+w)\varkappa^{-\frac{1}{w}} & \text{at } w \geqslant 1,\ 0 < \varkappa \leqslant 1 \end{cases} \tag{11.34}$$

$$(\Phi^* = (a^*/2g)\, u_1^2 T^{-1}).$$

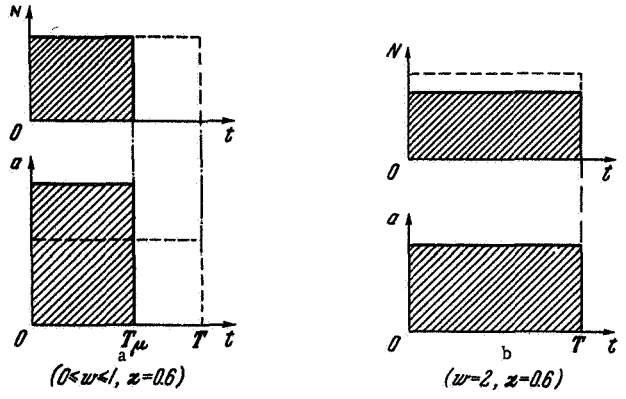

FIGURE 11.6. Two possible types of optimum programs for power $N(t)$ and thrust acceleration $a(t)$ for velocity build-up: a) $0 \leqslant w \leqslant 1$, $\varkappa = 0.6$; b) $w = 2$, $\varkappa = 0.6$ (same symbols as in Figure 11.4).

482 The curves representing these two solutions are shown in Figures 11.7 and 11.8. Figure 11.7 indicates the optimum values of the parameter w as a function of $\varkappa$, the ratio of the allowable number of failures to their

maximum possible number; Figure 11.8 shows the corresponding minimum values of the functional Φ as a function of $\varkappa$ too. The solid curves correspond to a displacement between points of rest, and the dashed curves to a velocity build-up.

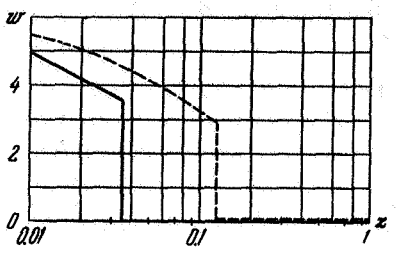

FIGURE 11.7. Optimum values of structural parameter w determining reliability curve (Figure 11.3) as function of $\varkappa$ (ratio of allowable number of failures Λ_i to their maximum number Λ_{max}). Solid curves represent displacement between points of rest; dashed curves represent velocity build-up.

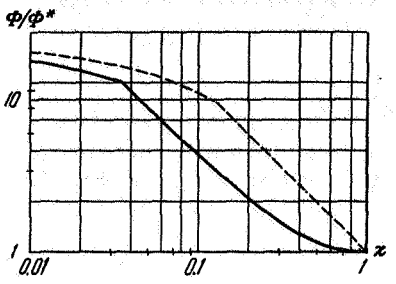

FIGURE 11.8. Values of functional $\Phi(\varkappa) = \min[\alpha(w)/2g]\, J(\varkappa, w)$ minimized with respect to w, corresponding to relationship $\alpha(w) = (1 + w)\alpha^*$ and $J(\varkappa, w)$ in Figure 11.5 (same symbols as in Figures 11.5, 11.7; $\Phi^* = (\alpha^*/2g)J^*$).

After completing this final stage of the problem one can calculate the optimum weight relations using formulas (11.12) and (11.13). Figure 11.9 gives an example of how the payload depends on the probability R of successfully executing a maneuver, where $R = \exp(-\varkappa\Lambda_{max})$. The horizontal portions of the curves correspond to values of R ensured on the optimum trajectory when the reliability is not allowed for (i.e., when inequality (11.6) is fulfilled).

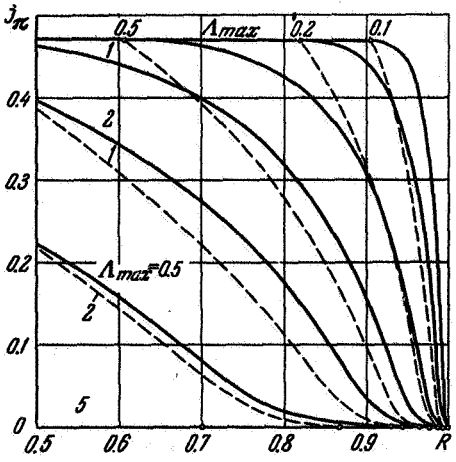

FIGURE 11.9. Example of how maximum payload G_π depends on probability R of successfully executing a maneuver, for different values of Λ_{max}, maximum number of failures ($\Phi^* = (\alpha^*/2g)\, J^* = 0.1$; optimum values of w; other symbols given in Figures 11.7, 11.8).

483 **3. Engine with limited exhaust velocity.** It was established in Chapter Eight that the optimum operating regime for an engine with limited exhaust velocity is attained for $V(t) = V_{\max}$. Suppose λ (11.2) increases with increasing exhaust velocity (i.e., with increasing temperature) (cf. (11.10))

$$\lambda = \lambda(t, V, w) \qquad (\partial\lambda/\partial V \geqslant 0,\ 0 \leqslant V \leqslant V_{\max},\ \partial\lambda/\partial w < 0,\ w = \text{const}). \tag{11.35}$$

As in (11.10), the structural parameter w is present; it is assumed that w decreases with increasing w ($\partial\lambda/\partial w < 0$), and this implies an increase in unit engine weight ($\partial\gamma/\partial w > 0$, $\gamma = G_{\varkappa}/P_{\max}$ — cf. (8.1), relationship $\gamma(w)$ is considered as known).

According to the general formulation (11.7), the problem of delivering a maximum payload with an engine of limited exhaust velocity is written in the following form (cf. (8.15), (11.11); the thrust, the exhaust velocity, and the weight are represented as fractions of the corresponding maximum values):

$$\left.\begin{aligned}
&\dot{G}_{\sigma} = -\mu P\delta/V, && G_{\sigma}(0) + \gamma(w)\, a_0/g = 1,\\
&&& G_{\sigma}(T) = \max,\\
&\dot{\mathbf{r}} = \mathbf{v}, && \mathbf{r}(0) = \mathbf{r}_0,\\
&&& \mathbf{r}(T) = \mathbf{r}_1,\\
&\dot{\mathbf{v}} = \frac{a_0 P\delta}{G_{\sigma} + \gamma(w)\, a_0/g}\mathbf{e} + \mathbf{R}, && \mathbf{v}(0) = \mathbf{v}_0,\\
&&& \mathbf{v}(T) = \mathbf{v}_1,\\
&\dot{\Lambda} = \lambda_0(t, w) + [\lambda(t, V, w) - \lambda_0(t, w)]\,\delta, && \Lambda(0) = 0,\\
&&& \Lambda(T) = -\ln R\\
&(0 \leqslant P(t) \leqslant 1,\ 0 \leqslant V(t) \leqslant 1,\ \delta(t) = 1 \text{ or } 0, |\mathbf{e}(t)| = 1;\\
&\mu = gP_{\max}/G_0 V_{\max},\ a_0 = gP_{\max}/G_0,\ w = \text{const}).
\end{aligned}\right\} \tag{11.36}$$

It is assumed here that when the engine is cut off, the value of λ is λ_0 ($\lambda_0 = \lambda_0(t, w) < \lambda(t, V, w)$, a particular case of which is $\lambda_0 = 0$). In order to express this fact in the equations, we make use of the method outlined in note 2 of subsection 1. If we know that the thrust does not take intermediate values within the interval (0, 1), the singular regime for any optimum trajectory, we need not introduce the function $\delta(t)$. In the last equation it would have then been necessary to write P in place of δ. The absence of periods with singular control from the optimum trajectory, is, however, not obvious a priori.

484 For problem (11.36), in addition to the optimum control variables $P(t)$, $V(t)$, $\delta(t)$, $\mathbf{e}(t)$, optimum values of the parameters a_0, μ, w (or $P_{\max}$, $V_{\max}$, w) must also be selected. If a_0, μ and w are specified, problem (11.36) reduces to the following (cf. § 1 of Chapter Eight):

$$\left.\begin{aligned}
&\dot{G} = -\mu P\delta/V, && G(0) = 1, \quad G(T) = \max,\\
&\dot{\mathbf{r}} = \mathbf{v}, && \mathbf{r}(0) = \mathbf{r}_0, \quad \mathbf{r}(T) = \mathbf{r}_1,\\
&\dot{\mathbf{v}} = (a_0 P\delta/G)\mathbf{e} + \mathbf{R}, && \mathbf{v}(0) = \mathbf{v}_0, \quad \mathbf{v}(T) = \mathbf{v}_1,\\
&\dot{\Lambda} = \lambda_0 + [\lambda(V) - \lambda_0]\,\delta, && \Lambda(0) = 0, \quad \Lambda(T) = -\ln R\\
&(0 \leqslant P(t) \leqslant 1,\ 0 \leqslant V(t) \leqslant 1,\ \delta(t) = 1 \text{ or } 0,\\
&&& |\mathbf{e}(t)| = 1).
\end{aligned}\right\} \tag{11.37}$$

Once (11.37) is solved, the functional $G(T) = G_1$ will be a function of the parameters a_0, μ and w whose optimum values are determined from the condition of maximum payload $G_\pi = G_\sigma(T) = G_1(a_0, \mu, w) - \gamma(w)a_0/g$. Problem (11.37) will be considered later.

To analyze the structure of the optimum control, we require the absolute minimum of H (the maximum of G_1 is required) with respect to $\mathbf{e}$, P, δ and V (cf. (11.15)):

$$H = \left\{\left[-p_\mu \frac{\mu}{V} + \frac{a_0}{G}(\mathbf{p}_v \cdot \mathbf{e})\right] P + p_\lambda [\lambda(V) - \lambda_0]\right\}\delta + \\ + \lambda_0 p_\lambda + (\mathbf{p}_r \cdot \mathbf{v}) + (\mathbf{p}_v \cdot \mathbf{R}). \tag{11.38}$$

The momenta $\mathbf{p}_r$, $\mathbf{p}_v$ and p_λ are determined as before by equations (11.16), and p_μ is given by

$$\dot{p}_\mu = -\partial H/\partial G = (\mathbf{p}_v \cdot \mathbf{e})\, a_0 G^{-2} P\delta, \quad p_\mu(T) = -1. \tag{11.39}$$

From the minimum of (11.38) with respect to $\mathbf{e}$ it follows that (cf. (11.17))

$$\mathbf{e} = -\mathbf{p}_v/p_v. \tag{11.40}$$

As in subsection 2 (cf. (11.19)), it can be shown that

$$p_\mu(t) \leqslant 0, \quad p_\lambda = \text{const} > 0. \tag{11.41}$$

Suppose at some instant $p_\mu(t) > 0$; it follows that if H is a minimum then $V = 0$ (independently of the sign of p_λ) and $P = \delta = 1$. The regime $P\delta = 1$ for $V = 0$ is physically absurd, and therefore we must have $p_\mu(t) \leqslant 0$ everywhere. If we now assume $p_\lambda < 0$, we obtain that $V = 1$ everywhere; this indicates a later cutoff of the engine ($\delta = 0$) than in the case $p_\lambda = 0$. As a result, the condition of specified reliability will not be fulfilled, it being assumed that inequality (11.6) is not satisfied.

485 We shall now show that on the optimum trajectory the control variable $P(t)$ cannot take intermediate values $0 < P < 1$. Since P enters (11.38) linearly, intermediate values of P can only be optima when the coefficient multiplying P vanishes during some time interval (singular regime). But then $\delta = 0$, since $p_\lambda > 0$ (cf. (11.41)), i.e., the thrust $P\delta$ must be cut off. This is true for any maneuver in an arbitrary gravitational field.

Having established the absence of a singular regime in the composition of the optimum control function, we eliminate $\delta(t)$ in (11.37)—(11.39); when the product $P\delta$ appears we simply write P, and when the function δ appears without P we replace it by P. Taking (11.40) into account, that part of the function H which depends on the control variables V and P will be written as

$$H_{V,P} = \left(H_V - p_v \frac{a_0}{G} - \lambda_0 p_\lambda\right) P, \quad H_V = -\mu p_\mu \frac{1}{V} + \lambda(t, V)\, p_\lambda. \tag{11.42}$$

From the condition for a minimum of H_V with respect to V it follows that

$$V(t) = 1 \quad \text{for } \lambda(t, V) \geqslant \lambda(t, 1) + \frac{\mu p_\mu}{p_\lambda}\left(\frac{1}{V} - 1\right). \tag{11.43}$$

If condition (11.43) is not satisfied, there will exist at each time t an optimum intermediate value $0 < V(t) < 1$, determined from the equation

$$V^2 \partial\lambda/\partial V = -\mu p_\mu / p_\lambda \qquad (0 < V < 1). \tag{11.44}$$

Equation (11.44) can have several roots; in this situation we must select that value which gives an absolute minimum of H_V in (11.42). Zero values of V do not appear in the composition of the optimum control function. If

$$\lambda(t, V) \geqslant \lambda(t, 1) + (\mu p_{\mu_0}/p_\lambda)(V^{-1} - 1), \tag{11.45}$$

condition (11.43) will be fulfilled along the entire trajectory, since $\dot{p}_\mu \leqslant 0$, $p_\mu \leqslant 0$ (cf. (11.39)—(11.41)). In this case the exhaust velocity nowhere takes intermediate values.

The optimum thrust control function can only be a limiting control function (as proved above). The alternation of powered and coasting periods on the trajectory is determined by the relation

$$P(t) = \begin{cases} 1 & \text{at} \quad H_V - p_v a_0 G^{-1} - \lambda_0 p_\lambda < 0, \\ 0 & \text{at} \quad H_V - p_v a_0 G^{-1} - \lambda_0 p_\lambda > 0, \end{cases} \tag{11.46}$$

obtained from the condition of absolute minimum of the function (11.42) with respect to P.

486 In order to fully solve the problem one must integrate the system of equations (11.37), (11.39) with the finite relations (11.40), (11.43)—(11.46) governing the control functions.

Now consider the case of a limited acceleration $a = a_0 P/G$ (instead of a limited thrust $0 \leqslant P \leqslant 1$). Here, problem (11.37) for the maximum of the terminal weight G_1 reduces to finding the minimum of the functional

$$I = \int_0^T \frac{a}{V}\, dt \quad (G_1 = G_0 e^{-I/V_{\max}}, \quad 0 \leqslant V \leqslant 1, \quad 0 \leqslant a \leqslant a_0) \tag{11.47}$$

(the functional (11.47) is obtained by integrating the first equation of (11.37) by quadratures, and represents a generalization of the characteristic velocity (8.13)).

Similarly, we can prove the absence of intermediate values of the thrust acceleration $0 < a < a_0$ in the composition of the optimum control function. Bearing this in mind, (11.37) can be used to represent the equations of the variational problem, where the first and third equations are replaced by

$$\dot{I} = a_0 \delta / V \quad (I(0) = 0, \ I(T) = \min), \quad \dot{\mathbf{v}} = a_0 \delta \mathbf{e} + \mathfrak{N}. \tag{11.48}$$

The optimum thrust direction will be determined by the first relation in (11.17). The control variables $V(t)$ and $\delta(t)$ are found from the condition for a maximum of the functions (cf. (11.42))

$$\begin{aligned} H_{V,\delta} &= (H_V + p_v a_0 - \lambda_0 p_\lambda)\, \delta, \\ H_V &= -a_0 V^{-1} + \lambda(t, V)\, p_\lambda \quad (p_\lambda < 0). \end{aligned} \tag{11.49}$$

The optimum exhaust-velocity program is determined by relations (11.43) and (11.44) with $\mu p_\mu = -a_0$ substituted in them; if $\partial\lambda/\partial t = 0$, the optimum exhaust velocity will be constant along the trajectory.

The firing and cutoff times of the engine at which $\delta = 1$ and $\delta = 0$ are found from a relation similar to (11.46):

$$\delta(t) = \begin{cases} 1 & \text{at } H_V + p_v a_0 - \lambda_0 p_\lambda > 0, \\ 0 & \text{at } H_V + p_v a_0 - \lambda_0 p_\lambda < 0. \end{cases} \tag{11.50}$$

§ 2. FORMULATION AND EQUATIONS OF THE VARIATIONAL PROBLEM FOR A COMPOSITE POWER-LIMITED ENGINE

When the average number of failures per unit time λ and the total time of motion T are large (so that the maximum number of failures $\Lambda_{max} = \lambda_{max} T > 1$), a single-section propulsion system will be unable to ensure an acceptable payload level at a sufficiently high probability of successfully executing a maneuver (cf. Figure 11.9). In this case the propulsion system (or its least reliable elements) must consist of autonomous sections. The sections are identical, and the breakdown of any one of them leads to a deterioration of the engine characteristics (for instance, to a drop in the power of power-limited engines), but does not cause an interruption of engine operation, since all sections are connected in parallel.

487

1. Expected failure times. To forecast the weight characteristics of the vehicle one must know how the number of operating sections $n(t)$ vary with time. As in the first paragraph of this chapter, it is assumed that the failures of the different sections are random and form an ordinary Poisson distribution with no aftereffect.

The average number of failures in one section per unit time, λ, is

$$\lambda = \lambda(t, \mathbf{r}, \mathbf{w}). \tag{11.51}$$

This quantity is taken as a function of the time t and the position $\mathbf{r}$ of the vehicle in space. This assumption reflects the fact that failures can be caused by phenomena such as unsteady inhomogeneous meteoric streams. In addition, λ is also a function of the structural parameters of the engine $\mathbf{w}$. Thus, the structural parameters of the (cooling) radiator which determine the probability of its being punctured by meteors, are the vulnerable area of the radiator cross section and the wall thickness. The case of an ideal power-limited engine is dealt with, and w determines the maximum power N_0/n_0 per unit section at the beginning of the motion (λ is a nondecreasing function of N_0/n_0).

If section j is put out of order at time t_j, the probability $R_k(t - t_j)$ that no more than k sections will break down in the interval (t_j, t) is determined for a Poisson distribution by the following relation /11.5—11.8/:

$$R_k(t - t_j) = \sum_{i=0}^{k} \frac{(n_0 - j)!}{i!\,(n_0 - j - i)!} \times \\ \times \left[1 - \exp\left(-\int_{t_j}^{t} \lambda\, dt\right)\right]^i \exp\left[-(n_0 - j - i)\int_{t_j}^{t} \lambda\, dt\right] \tag{11.52}$$

(n_0 is the total number of sections; if repeated failures are allowed in the sections, they are neglected in the calculation).

The time at which the next failure occurs, t_{j+1}, will be determined from the condition that the probability of no failures ($k = 0$) in the interval (t_j, t_{j+1})
488 is equal to a specified value R. Substituting $k = 0$ and $t = t_{j+1}$ in (11.52), we obtain (cf. (11.3))

$$R = \exp\left[-(n_0 - j)\int_{t_j}^{t_{j+1}} \lambda\, dt\right]. \tag{11.53}$$

It will be assumed that the next failure takes place at time t_{j+1} determined by relation (11.53). Actually this is the least favorable case, since, with the same probability and according to formula (11.52), it can be claimed that no more than one failure occurs in the interval (t_j, t), which is larger than (t_j, t_{j+1}). A strict assessment of the probability of failures occuring will be given in the next subsection.

The following expression is finally adopted for the expected failure time:

$$\left.\begin{aligned} &\int_{t_j}^{t_{j+1}} \lambda\,(\mathbf{r}\,(t),\ t)\,dt = \frac{\Lambda_1}{n_0 - j} \qquad (j = 0, 1, \ldots, m-1), \\ &\int_{t_m}^{T} \lambda\,(\mathbf{r}\,(t), t)\,dt = \frac{\Lambda_1}{n_0 - m} \quad (\Lambda_1 = -\ln R) \end{aligned}\right\} \tag{11.54}$$

($m < n_0$ is the total number of failures during the flight).

2. Probability of the failures occurring. Relations (11.54) define some law to decrease the number of undamaged sections with time

$$n^*(t) = n_0 - j \text{ for } t_j < t < t_{j+1}\ (j = 0, 1, \ldots, n,\ t_{m+1} = T). \tag{11.55}$$

A specific law, $n(t)$, governing the number of section failures, corresponds to the execution of each maneuver. This law differs from the expected law $n^*(t)$ ((11.54), (11.55)). Consider the problem of determining the probability with which inequality $n(t) \geqslant n^*(t)$, $0 \leqslant t \leqslant T$, will be fulfilled for any execution of a maneuver. The fulfillment of this inequality guarantees that the actual working-fluid consumption for the entire maneuver will not exceed the value calculated according to the law $n^*(t)$; it therefore ensures the delivery of a payload no smaller than the design payload. It follows that the probability of satisfying the inequality $n(t) \geqslant n^*(t)$ for $0 \leqslant t \leqslant T$ can be considered as the probability of the problem.

Let A represent the event

$$A:\ n(t) \geqslant n^*(t) \quad \text{at} \quad 0 \leqslant t \leqslant T \tag{11.56}$$

489 where $P(A)$ is the probability of its realization (the probability to be determined). Take the following system of $(m + 1)$ events into consideration:

$$\left.\begin{aligned} &A_0:\ n(t) = n_0 && \text{at}\ \ 0 \leqslant t < t_1, \\ &A_1:\ n(t) \geqslant n_0 - 1 && \text{at}\ \ t_1 < t < t_2, \\ &\ldots\ldots\ldots\ldots\ldots\ldots \\ &A_j:\ n(t) \geqslant n_0 - j && \text{at}\ \ t_j < t < t_{j+1}, \\ &\ldots\ldots\ldots\ldots\ldots\ldots \\ &A_m:\ n(t) \geqslant n_0 - m && \text{at}\ \ t_m < t \leqslant T. \end{aligned}\right\} \tag{11.57}$$

Event A is the intersection (product) of these events:

$$A = A_0 A_1 \ldots A_j \ldots A_m. \tag{11.58}$$

This is illustrated in Figure 11.10, where the occurrence of each event $A_j (j = 0, 1, 2)$ corresponds to a point representing it in a region which is shaded in a distinctive manner. The intersection of events A_0, A_1, A_2 is represented by the region possessing all types of shading (the common part of regions A_0, A_1, A_2); this region lies above the step function $n^* (t)$.

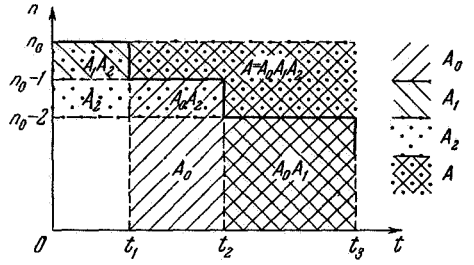

FIGURE 11.10. Step function $n^* (t)$ representing decrease in number of operating sections with time, and regions corresponding to events A_0, A_1, A_2, and A in (11.57), (11.58).

According to the multiplication theorem (cf. for instance /11.6/), the probability of realizing an intersection of events (11.58) is

$$\begin{aligned} P(A) = P(A_0 \ldots A_m) = P(A_m/A_0 \ldots A_{m-1})\, P(A_0 \ldots A_{m-1}) = \ldots \\ \ldots = P(A_0)\, P(A_1/A_0) \ldots P(A_j/A_0 \ldots A_{j-1}) \ldots \\ \ldots P(A_m/A_0 \ldots A_{m-1}), \end{aligned} \tag{11.59}$$

where $P(A_j/A_0 \ldots A_{j-1})$ is the probability of event A_j occurring when event $A_0 \ldots A_{j-1}$ has taken place (conditional probability).

490 We now calculate the conditional probability $P(A_j/A_0 \ldots A_{j-1})$. If event $A_0 \ldots A_{j-1}$ has occurred, the number of undamaged sections $n(t_j)$ at time t_j is equal to one of the j values

$$n(t_j) = n_0 \text{ or } n_0 - 1, \text{ or } n_0 - 2, \ldots, \text{ or } n_0 - (j-1). \tag{11.60}$$

The event $A_j/A_0 \ldots A_{j-1}$ can accordingly occur by one of the following transitions:

	(0)	(α)	(j−1)
(0)	$n_0 \to n_0$	$n_0 - \alpha \to n_0 - \alpha$	$n_0 - j + 1 \to n_0 - j + 1$
(1)	$n_0 \to n_0 - 1$	$n_0 - \alpha \to n_0 - \alpha - 1$	$n_0 - j + 1 \to n_0 - j$
. . .	. . . . .	. . . . .	
(i)	$n_0 \to n_0 - i$	$n_0 - \alpha \to n_0 - \alpha - i$	
. . .	. . . . .		
(j − α)	$n_0 \to n_0 - j + \alpha$	$n_0 - \alpha \to n_0 - j$	
. . .	. . . . .		
(j)	$n_0 \to n_0 - j$		

(11.61)

(the column index $\alpha = 0, 1, \ldots, j-1$ corresponds to the initial state $n(t_j) = n_0 - \alpha$, and the row index $i = 0, 1, \ldots, j-\alpha$ to the final state $n(t_{j+1}) = n_0 - \alpha - i$).

The transition

$$n(t_j) = n_0 - \alpha \to n(t_{j+1}) = n_0 - \alpha - i$$

means that during the time interval $t_j < t < t_{j+1}$ exactly i sections will break down from among the $(n_0 - \alpha)$ undamaged ones at the beginning of the interval (it does not matter which ones).

The number of different ways of distributing i breakdowns among $(n_0 - \alpha)$ sections is equal to $C^i_{n_0-\alpha}$, the number of combinations of i elements out of $(n_0 - \alpha)$ since the manner in which the sections are put out of order is immaterial. All these combinations are equally probable, and the probability of each of them occurring is

$$\exp\Big[-(n_0 - \alpha - i)\int_{t_j}^{t_{j+1}} \lambda\, dt\Big]\Big[1 - \exp\int_{t_j}^{t_{j+1}} \lambda\, dt\Big]^i. \tag{11.62}$$

491 If (11.62) is multiplied by the number of combinations, we obtain the probability of the transition $n(t_j) = n_0 - \alpha \to n(t_{j+1}) = n_0 - \alpha - i$:

$$P(n_0 - \alpha \to n_0 - \alpha - i) = \\ = C^i_{n_0-\alpha} \exp\Big[-(n_0 - \alpha - i)\int_{t_j}^{t_{j+1}} \lambda\, dt\Big]\Big[1 - \exp\int_{t_j}^{t_{j+1}} \lambda\, dt\Big]^i. \tag{11.63}$$

In order to determine the probability of the event $A_j/A_0 \ldots A_{j-1}$, we must sum (11.63) over i and α (by the rows and columns of (11.61)) so that

$$P(A_j/A_0 \ldots A_{j-1}) = \sum_{\alpha=0}^{j-1}\sum_{i=0}^{j-\alpha} P(n_0 - \alpha \to n_0 - \alpha - i). \tag{11.64}$$

The required probability $P(A)$ is found by substituting (11.63), (11.64) into (11.59) to obtain

$$P(A) = \prod_{j=0}^{m}\Big\{\sum_{\alpha=0}^{j-1}\sum_{i=0}^{j-\alpha} C^i_{n_0-\alpha} \exp \times \Big[-(n_0 - \alpha - i)\int_{t_j}^{t_{j+1}} \lambda\, dt\Big]\Big[1 - \exp\int_{t_j}^{t_{j+1}} \lambda\, dt\Big]^i\Big\} \\ (C^0_{n_0-\alpha} = 1, \quad t_0 = 0, \quad t_{m+1} = T). \tag{11.65}$$

With this formula one may calculate the probability of any law $n^*(t)$ governing section failures occurring (i.e., the probability of the inequality $n(t) \geqslant n^*(t)$ for $0 \leqslant t \leqslant T$). We apply it to (11.53)—(11.55). Substituting the integrals (11.54) into (11.65), we obtain

$$P(A) = \prod_{j=0}^{m}\Big\{\sum_{\alpha=0}^{j-1}\sum_{i=0}^{j-\alpha} C^i_{n_0-\alpha} R^{\frac{n_0-\alpha-i}{n_0-j}}\Big(1 - R^{\frac{1}{n_0-j}}\Big)^i\Big\}. \tag{11.66}$$

To third-order accuracy relative to $(1 - R)$ we may write (11.66) in the form (after summing and multiplying)

$$P(A) = R - \frac{n_0}{2(n_0 - 1)}(1 - R)^2 + o[(1 - R)^2]. \tag{11.67}$$

If we require a high probability $P(A)$ of achieving a solution near to unity (this is the case of practical interest), we must take $(1-R) \ll 1$, according to (11.67). Then, with second-order accuracy relative to $(1-R)$, the probability $P(A)$ of obtaining the solution as a whole for the law $n^*(t)$ from
492 (11.53)—(11.55) will coincide with the probability R of no failures in the $(n_0 - j)$ sections during the interval (t_j, t_{j+1}):

$$P(A) = P(n(t) \geqslant n^*(t), \quad 0 \leqslant t \leqslant T) = R + o[(1-R)],$$
$$R = \exp\left[-(n_0 - j)\int_{t_j}^{t_{j+1}} \lambda\, dt\right]. \tag{11.68}$$

3. Weight relations. The engine section which breaks down at time t_j is cut off. This will generally lead to a change in the operating regime of the remaining sections and to a drop in the maximum power, where

$$0 \leqslant N(t) \leqslant N_{\max}[n(t)] \text{ or } 0 \leqslant \bar{N}(t) \leqslant \bar{N}_j$$
$$\text{at } t_j < t < t_{j+1}, \; j = 0, 1, \ldots, m. \tag{11.69}$$

Here $N_{\max}[n(t)]$ represents the dependence of the maximum power on the number of operating sections, and $\bar{N}_j$ is the power represented as a fraction of the initial power N_0 $(\bar{N}_j < \bar{N}_{j-1} < \ldots < \bar{N}_0 = 1)$. For completely autonomous sections, the relationship $N_{\max}[n(t)]$ is linear and given by

$$N_{\max}[n(t)] = [n(t)/n_0]\, N_0 \text{ or } \bar{N}_j = 1 - j/n_0. \tag{11.70}$$

If the broken down sections are not discarded, we obtain the equation governing the variation of the vehicle weight by integrating over segments (t_j, t_{j+1}),

$$\frac{G_1}{G_0} = \left(1 + \frac{G_0}{2gN_0}\sum_{j=0}^{m}\int_{t_j}^{t_{j+1}} \frac{a^2}{\bar{N}}\, dt\right)^{-1}. \tag{11.71}$$

The t_j are interpreted here as the expected failure points (11.54). Formula (11.71) then yields the quantity $(G_1/G_0)^*$ which sets a lower limit to events with a probability not lower than R, so that $(G_1/G_0) \geqslant (G_1/G_0)^*$; in what follows we shall use the ratio $(G_1/G_0)^*$.

The engine weight $G_\varkappa$ does not vary in the course of the flight and is linked with the initial value of the maximum power N_0 by the relation

$$G_\varkappa = \alpha N_0. \tag{11.72}$$

The unit weight α is considered a function of the power per section N_0/n_0 (nonincreasing function of N_0/n_0, Figure 2.96).

As in the situation for which failures were not considered, one can use
493 (11.71) to express the total relative weight of the engine and the required averaged working-fluid reserve to perform the maneuver in the form

$$G_\varkappa + G_{\mu 0} = \frac{1}{1 + G_\varkappa/\Phi} + G_\varkappa \quad \left(\Phi = \frac{\alpha}{2g}\sum_{j=0}^{m}\int_{t_j}^{t_{j+1}} \frac{a^2}{N}\, dt\right) \tag{11.73}$$

(the bars above the dimensionless variables are omitted here and below).

4. **Formulation of the problem.** The minimum sum of the weights of the engine and the averaged working-fluid reserve, (11.73), is used as an optimum criterion. This corresponds to a maximum payload, whose probability of delivery is not smaller than R.

The total weight $(G_\varkappa + G_{\mu 0})$ is monotonic decreasing with increasing Φ, as seen from (11.73). The problem of finding the minimum of $(G_\varkappa + G_{\mu 0})$ can therefore be split into two parts comprising (a) the dynamic problem, and (b) the weight problem. These problems are stated as follows.

(a) For given quantities Λ_1, N_0, n_0 and for a known relationship $\lambda(\mathbf{r}, t, N_0/n_0)$, the power $N(t)$ and the thrust acceleration $\mathbf{a}(t)$ must be found such that the sum of the integrals (cf. (4.11))

$$\left.\begin{aligned} J = \sum_{j=0}^{m} \int_{t_j}^{t_{j+1}} \frac{a^2}{N}\, dt = \min, \\ \ddot{\mathbf{r}} = \mathbf{a} + \mathbf{R}, \quad \mathbf{r}(0) = \mathbf{r}_0, \quad \dot{\mathbf{r}}(0) = \mathbf{v}_0, \\ \mathbf{r}(T) = \mathbf{r}_1, \quad \dot{\mathbf{r}}(T) = \mathbf{v}_1 \\ (0 \leqslant N(t) \leqslant N_j \quad \text{at} \quad t_j < t < t_{j+1}, \quad j = 0, 1, \ldots, m) \end{aligned}\right\} \tag{11.74}$$

is a maximum for a specified dynamic maneuver (with a fixed probability). The quantities t_j are determined from the isoperimetricity conditions (11.54).

(b) For given values of G_0 and $(N_0/n_0)_{\min}$ (minimum possible section size) and given relationships

$$\alpha = \alpha(N_0/n_0), \quad J = J_{\min}(N_0, n_0, \Lambda_1), \tag{11.75}$$

we require the optimum power N_0 and number of sections n_0 which minimize the function (11.73).

In dynamic problem (a) (the variational problem), the engine parameters (the number of sections n_0 and the power N_0) enter via conditions (11.54), which define the failure points t_j. This problem is thus distinguished from problem (4.11) in which failures were ignored. The weight problem is one
494 of a function extremum. Its solution depends on the specific form of relationships (11.75); an example will be given in subsection 1 of § 3.

5. **Equations of the variational problem (11.74).** We assume for simplicity that λ is independent of the operating regime of the sections, i.e., of the intermediate values of the power. The effect of this has already been discussed in § 1 with respect to a single-section engine.

The relative power N only enters the numerator of the integrand of the functional which is being minimized (11.74). The expected failure points (11.54) and the equations of motion (11.74) are independent of N. Therefore, in order to minimize the functional (11.74) the power N must be maximum at each instant, so that

$$N(t) = N_j \quad \text{at} \quad t_j < t < t_{j+1}, \quad j = 0, 1, \ldots, m, \tag{11.76}$$

i.e., the power is constant between failures, and drops at the failure points as the number of operating sections decreases.

The problem then reduces to minimizing the functional

$$J = \sum_{j=0}^{m} \frac{1}{N_j} \int_{t_j}^{t_{j+1}} a^2\, dt \tag{11.77}$$

(where $N(t) = N_j$ is removed from the integral sign) relative to the differential relations (11.74) and the isoperimetricity conditions (11.54).

If, in (11.77) $\mathbf{a} = \ddot{\mathbf{r}} - \mathfrak{R}$, we free ourselves from the differential constraints. The isoperimetricity conditions (11.54) with the constant multipliers ν_j/N_j are added according to Lagrange's rule to the basic functional (11.77). We require the minimum of the expanded functional

$$\tilde{J} = \sum_{j=0}^{m} \frac{1}{N_j} \int_{t_j}^{t_{j+1}} [(\ddot{\mathbf{r}} - \mathfrak{R})^2 + \nu_j \lambda(\mathbf{r}, t)]\, dt \qquad (11.78)$$

$$(\mathbf{r}(0) = \mathbf{r}_0, \quad \dot{\mathbf{r}}(0) = \mathbf{v}_0, \quad \mathbf{r}(T) = \mathbf{r}_1, \quad \dot{\mathbf{r}}(T) = \mathbf{v}_1).$$

To solve the problem, we must find the extrema of this functional and obtain the conjugational conditions for them (the fact that the extrema $\mathbf{r}(t)$ have discontinuities of the second derivatives at $t = t_j$ follows from the presence of the weight coefficients ν_j in the integrands).

495 Euler's equations must be fulfilled along the extrema (cf. (5.6)). These equations are

$$\ddot{\mathbf{a}} - \frac{\partial}{\partial \mathbf{r}}(\mathbf{a} \cdot \mathfrak{R}) + \nu_j \frac{\partial \lambda}{\partial \mathbf{r}} = 0 \qquad (11.79)$$

$$(\mathbf{a} = \ddot{\mathbf{r}} - \mathfrak{R}, \; t_j < t < t_{j+1}, \; j = 0, 1, \ldots, m, \; \nu_m = 0).$$

If the sum of the coefficients of the increments $\delta\mathbf{r}$ and $\delta\dot{\mathbf{r}}$ in the expressions for the first variation of the functional $\tilde{J}$ is equated to zero at the points $t = t_j$, we obtain the following conjugational conditions for the extrema:

$$\frac{1}{N_j}\mathbf{a}_j^+ = \frac{1}{N_{j-1}}\mathbf{a}_j^-, \quad \frac{1}{N_j}\dot{\mathbf{a}}_j^+ = \frac{1}{N_{j-1}}\dot{\mathbf{a}}_j^- \qquad (j = 1, \ldots, m). \qquad (11.80)$$

The subscript j here indicates the time t_j, and the superscript plus or minus indicates whether the value of the function is taken to the right or to the left of the discontinuity. Thus, the thrust acceleration and its derivative at the failure points decrease proportionally to the power, i.e., the exhaust velocity $V = 2gN/aG$ suffers no discontinuity.

If the average number of failures λ depends on $\mathbf{r}$, the points t_j must be varied when forming the first variation of $\tilde{J}$. This yields the additional set of conditions

$$\lambda_j \left(\frac{\nu_j}{N_j} - \frac{\nu_{j-1}}{N_{j-1}}\right) + \frac{N_{j-1} - N_j}{N_j^2}(a_j^+)^2 = 0 \qquad (j = 1, \ldots, m-1). \qquad (11.81)$$

The problem has been reduced to solving the system of differential equations (11.79) with the boundary conditions of (11.78) and the restraints in (11.54), (11.80), and (11.81). The inequality in (11.54) helps to determine the total number m of sections which fail during the whole flight.

6. Continuous approximation to the step function governing failures. For a large number n_0 of engine sections, the solution of the variational problem using the step function $n^*(t)$ (which governs the decrease in the number of undamaged sections) is complicated by conditions (11.54), (11.80), (11.81). However, if the number of sections is sufficiently large, so that $n_0 - m \gg 1$, the step function in (11.54), (11.55) can be replaced by a continuous function, which is naturally free of these restrictions. We

therefore introduce the differential equation

$$\dot{n} = -\frac{\lambda(\mathbf{r},t)}{\Lambda_1} n, \quad n(0) = n_0 \qquad (\Lambda_1 = -\ln R = \text{const}). \tag{11.82}$$

The solution $n(t)$ of this equation approximates the step function $n^*(t)$ from below ($n(t) \leqslant n^*(t)$), and resembles it at the approximation nodes $t = t_j$.
496 To prove this, we integrate equation (11.82) from t_j to t_{j+1} so that

$$\ln \frac{n(t_j)}{n(t_{j+1})} = \frac{1}{\Lambda_1} \int_{t_j}^{t_{j+1}} \lambda \, dt. \tag{11.83}$$

Replace $n(t)$ by the step function $n^*(t)$ in (11.55), and the right-hand side by the corresponding expressions (11.54).

Equality is satisfied with an accuracy of order $1/n_0^2$. It can be deduced from here that the decrease in the number of undamaged sections between any two failure points for the continuous (11.82) and the step (11.55) failure functions coincide for $n_0 \to \infty$. The solutions given in the next section show that the integral characteristics corresponding to both laws become similar from the value $n_0 \sim 10$.

For the continuous failure function (11.82) the problem reduces to one of finding the extrema of the following functional:

$$\begin{gathered} \tilde{J} = \int_0^T \left[\frac{(\ddot{\mathbf{r}} - \mathfrak{R})^2}{N(n)} + \nu \left(\dot{n} + \frac{n\lambda(\mathbf{r},t)}{\Lambda_1} \right) \right] dt \\ (\mathbf{r}(0) = \mathbf{r}_0, \quad \dot{\mathbf{r}}(0) = \mathbf{v}_0, \quad \mathbf{r}(T) = \mathbf{r}_1, \quad \dot{\mathbf{r}}(T) = \mathbf{v}_1), \end{gathered} \tag{11.84}$$

where $\nu = \nu(t)$ is the variable Lagrange multiplier of the differential constraint (11.82), and $N(n)$ represents the dependence of the maximum power $N_{\max}/N_0$ on the number of undamaged sections.

The equations for the extrema of the functional (11.84) are (cf. (11.79))

$$\left.\begin{aligned} &\ddot{\mathbf{r}} = \mathbf{a} + \mathfrak{R}, \ \mathbf{r}(0) = \mathbf{r}_0, \ \dot{\mathbf{r}}(0) = \mathbf{v}_0, \ \mathbf{r}(T) = \mathbf{r}_1, \ \dot{\mathbf{r}}(T) = \mathbf{v}_1, \\ &\frac{d^2}{dt^2}\left(\frac{\mathbf{a}}{N(n)}\right) - \frac{1}{N(n)} \frac{\partial}{\partial \mathbf{r}} (\mathbf{a} \cdot \mathfrak{R}) + \frac{\nu n}{2\Lambda_1} \frac{\partial \lambda}{\partial \mathbf{r}} = 0, \\ &\dot{\nu} - \nu \frac{\lambda}{\Lambda_1} + \frac{a^2}{N^2(n)} \frac{\partial N}{\partial n} = 0, \quad \nu(T) = 0, \\ &\dot{n} = -\lambda n/\Lambda_1, \quad n(0) = n_0. \end{aligned}\right\} \tag{11.85}$$

Thus, conditions (11.54), (11.80), (11.81) are replaced by two first-order differential equations (cf. the last two equations of (11.85)).

497 § 3. SOME SOLUTIONS FOR MANEUVERS WITH A COMPOSITE POWER-LIMITED ENGINE

In this section we give some analytic solutions of the equations of the variational problem obtained in the preceding section.

The equations are simplified by means of two assumptions: 1) the gravitational forces are neglected ($\mathfrak{R} = 0$), so that the problem considered is that of a one-dimensional motion (along the Ox axis) between two points

of rest in a gravity-free field; 2) the value of λ for one section is considered independent of $\mathbf{r}$ and t, i.e., $\lambda(\mathbf{r}, t) \equiv \lambda_0$.

It is further assumed (except in the last subsection) that the sections are fully autonomous:

$$N(n) = n/n_0.$$

1. Step function governing failures. With these assumptions, (11.54) gives an explicit expression for the expected failure points

$$t_{j+1} - t_j = \frac{\varkappa T}{n_0 - j}, \quad T - t_m \leqslant \frac{\varkappa T}{n_0 - m} \qquad (j = 0, 1, \ldots, m-1, \ \varkappa = \Lambda_1/\lambda_0 T). \tag{11.86}$$

Integrating the equations of the extrema (11.79) over the segments $t_j < t < t_{j+1}$ and taking (11.80) and (11.86) into consideration, we obtain

$$\left.\begin{aligned}
&\dot{a}_j^+ = \left(1 - \frac{j}{n_0}\right)\dot{a}_0, \quad a_j^+ = \left(1 - \frac{j}{n_0}\right)(a_0 + \dot{a}_0 t_j),\\
&t_j = \frac{\varkappa T}{n_0}\sum_{i=0}^{j-1}\frac{1}{1 - i/n_0},\\
&\dot{x}_j = \frac{\varkappa T}{n_0}\left[j a_0 + \dot{a}_0\left(\sum_{i=1}^{j-1} t_i + \frac{1}{2} t_j\right)\right],\\
&x_j = \left(\frac{\varkappa T}{n_0}\right)^2\left[a_0\sum_{i=0}^{j-1}\frac{i + 1/2}{1 - i/n_0} + \right.\\
&\qquad \left. + \dot{a}_0\left(\sum_{i=1}^{j-1}\frac{1}{1 - i/n_0}\sum_{l=1}^{i} t_l + \frac{1}{6}\frac{\varkappa T}{n_0}\sum_{i=0}^{j-1}\frac{1}{(1 - i/n_0)^2}\right)\right].
\end{aligned}\right\} \tag{11.87}$$

498 The quantities a_0 and $\dot{a}_0$ are determined by solving the system of linear algebraic equations derived from the boundary conditions $x(0) = \dot{x}(0) = \dot{x}(T) = 0$, $x(T) = l$:

$$\left.\begin{aligned}
&a_0\left[m\frac{\varkappa T}{n_0} + \left(1 - \frac{m}{n_0}\right)(T - t_m)\right] + \\
&\quad + \dot{a}_0\left[\frac{\varkappa T}{n_0}\left(\sum_{j=1}^{m-1} t_j + \frac{1}{2} t_m\right) + \frac{1}{2}\left(1 - \frac{m}{n_0}\right)(T^2 - t_m^2)\right] = 0,\\
&a_0\left\{\left(\frac{\varkappa T}{n_0}\right)^2\sum_{j=0}^{m-1}\frac{j + 1/2}{1 - j/n_0} + \right.\\
&\qquad \left. + (T - t_m)\left[m\frac{\varkappa T}{n_0} + \frac{1}{2}\left(1 - \frac{m}{n_0}\right)(T - t_m)\right]\right\} + \\
&+ \dot{a}_0\left\{\left(\frac{\varkappa T}{n_0}\right)^2\left[\sum_{j=1}^{m-1}\frac{1}{1 - j/n_0}\sum_{i=1}^{j} t_i + \frac{1}{6}\frac{\varkappa T}{n_0}\sum_{j=0}^{m-1}\frac{1}{(1 - j/n_0)^2}\right] + \right.\\
&\qquad + (T - t_m)\left[\frac{\varkappa T}{n_0}\left(\sum_{j=1}^{m-1} t_j + \frac{1}{2} t_m\right) + \right.\\
&\qquad \left.\left. + \frac{1}{6}\left(1 - \frac{m}{n_0}\right)(T - t_m)(T + 2t_m)\right]\right\} = l.
\end{aligned}\right\} \tag{11.88}$$

Using the second condition of (11.86), the total number of failures m during the whole time of motion is found from

$$\frac{\varkappa T}{n_0}\sum_{j=0}^{m-1}\frac{1}{1 - j/n_0} = t_m \leqslant T \leqslant t_{m+1} = \frac{\varkappa T}{n_0}\sum_{j=0}^{m}\frac{1}{1 - j/n_0}. \tag{11.89}$$

The minimum value of the functional J is expressed in terms of $(\varkappa T/n_0)$, n_0, m, a_0, $\dot{a}_0$:

$$J = \frac{\varkappa T}{n_0}\sum_{j=0}^{m-1}\left[(a_0 + \dot{a}_0 t_j)^2 + (a_0 + \dot{a}_0 t_j)\frac{\dot{a}_0}{1 - j/n_0}\frac{\varkappa T}{n_0} + \right.$$
$$\left. + \frac{\dot{a}_0^2}{3(1 - j/n_0)^2}\left(\frac{\varkappa T}{n_0}\right)^2\right] + \left(1 - \frac{m}{n_0}\right)(T - t_m)\times \tag{11.90}$$
$$\times[(a_0 + \dot{a}_0 t_m)^2 + (a_0 + \dot{a}_0 t_m)\,\dot{a}_0\,(T - t_m) + {}^1/_3\dot{a}_0^2(T - t_m)^2].$$

This value of the functional J, divided by the value of the functional J^* for the maneuver without failures, is

$$J/J^* = J\Big/\left(\frac{12l^2}{T^3}\right) \geqslant 1, \tag{11.91}$$

and is shown in Figure 11.11 as a function of the parameter $1/\varkappa = (\lambda_0 T)/(-\ln R)$ for different values of n_0 (the solid curves).

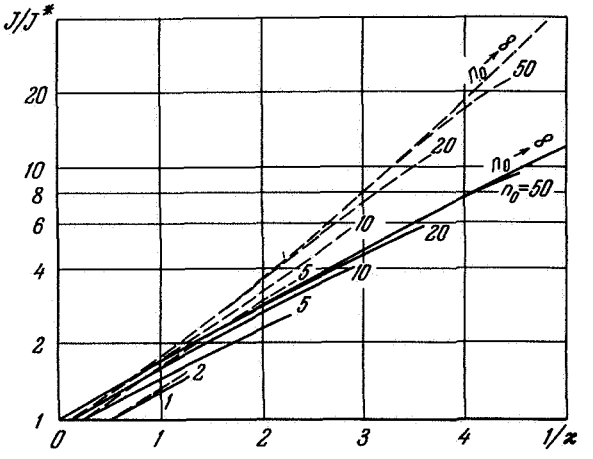

FIGURE 11.11. Functional J/J^* of dynamic problem (11.74) as function of parameter $1/\varkappa$ (ratio of maximum number of failures in one section $\Lambda_{max}=\lambda_0 T$, to their allowable number $\Lambda_1 = -\ln R$) for fixed number of sections n_0; maneuver is displacement between points of rest ($J^* = 12\,l^2/T^3$). Solid curves correspond to optimum thrust-acceleration program allowing for failures and dashed curves to optimum program when failures are ignored.

499 Figure 11.12 represents an optimum thrust-acceleration program

$$a(t)/a_0^* = a(t)\Big/\left(\frac{6l}{T^2}\right), \tag{11.92}$$

which takes failures into account (the solid curve). The function $a^*(t)$ (cf. (5.33)), namely the optimum one when failures are ignored (the dashed line), is also shown in this figure. The dashed curves in Figure 11.11 represent the functional which corresponds to this linear function $a^*(t)$ when failures are allowed for. It is seen that modifying the thrust-acceleration program enables one to substantially reduce the functional.

We shall now investigate how the number of sections n_0 influences the functional J. Two cases must be distinguished: a) λ_0 for one section is independent of the power of the section N_0/n_0; b) λ_0 decreases with decreasing N_0/n_0. Case a) occurs when the processes which cause the failures are independent of the engine scale; case b) corresponds, for instance, to meteoric punctures, where the number of punctures is directly proportional to the radiator cross-sectional area ($\lambda_0 \sim \lambda^* N_0/n_0$, $\lambda^* =$ = const). The total initial power N_0 is considered fixed and the number of sections n_0 is varied. Furthermore, we assume that the maneuver parameters are specified and that λ is independent of n_0. In case a) this corresponds to $\varkappa = -\ln R/(\lambda_0 T) = \text{const}$ (Figure 11.13, a); in case b) it corresponds to $\varkappa^* = -\ln R/(\lambda^* T) = \text{const}$ or $\varkappa/n_0 = \text{const}$ (Figure 11.13, b). In the first case (Figure 11.13, a) the functional J slightly increases with an increasing number of sections n_0, but on the other hand if n_0 is increased we can perform maneuvers which are more strained from the point of view of reliability (i.e., maneuvers with a lower value of $\varkappa$; of the limiting curve $m = n_0$ in Figure 11.13, a, where m is the total number of nonoperating sections during the whole flight). In the second case (Figure 11.13, b) an increase of n_0 has a positive effect with regard to these two aspects in that both the functional J and the limiting value $\varkappa/n_0$ decrease.

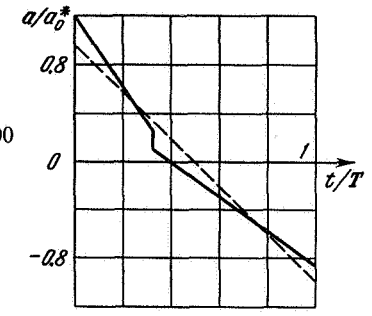

FIGURE 11.12. Example of optimum thrust-acceleration program $a(t)/a^*$ allowing for failures (solid curve) for maneuver of displacement between points of rest ($n_0 =$ 2, $\varkappa = 2/3$, $a^* = 6l/T^2$); dashed line represents optimum program when failures are ignored.

When considering the influence of n_0 on the functional of the dynamic part of the problem, one should not forget that a decrease of power N_0/n_0 in one section leads also to an increase in the unit weight α. This has a negative effect on the functional (11.73) of the full problem. A final decision on the optimum number of sections can only be made after the weight part of the problem has been solved (subsection 4 of § 2).

We shall give an example of its solution. In place of (11.75) we take

$$\alpha = \alpha^* (1 + n_0 \Delta N^*/N_0), \ \alpha^*, \ \Delta N^* = \text{const}, \text{ and (11.90)}.$$

The following numerical values are specified:

$$\Phi^* = (\alpha^*/2g) J^* = 0.1 \quad \text{and} \quad \Delta G_\varkappa^* = \alpha^* \Delta N^* = 0.001.$$

Consider once more the two cases indicated above, namely, a) $\lambda_0 = \text{const}$ or $\varkappa = -\ln R/(\lambda_0 T) = \text{const}$, b) $\lambda_0 = \lambda^* \alpha^* N_0/(G_\varkappa^* n_0)$; λ^*, α^*, $G_\varkappa^* = \text{const}$ or $\varkappa^* =$ $= -\ln R/(\lambda^* T) = \text{const}$, $G_\varkappa^* = \sqrt{\Phi^*} - \Phi^* = 0.216$.

The results for the minimum total weight (11.73) of the engine and working-fluid reserve with respect to $G_\varkappa = \alpha N_0$ and n_0 are given in Figures 11.14, a and 11.14, b. The relationships between the payload G_π and
501 the parameter $\varkappa$ have been replotted in Figures 11.15, a and Figure 11.15, b, where G_π is represented as a function of the probability R of successfully

performing the maneuver when $\Lambda_{max} = \text{const}$ ($R = \exp[-\varkappa\Lambda_{max}]$). These figures indicate that the division of the engine into autonomous sections operating in parallel is not too efficient in case a) (when λ_0 in one section is independent of the section size), but gives satisfactory results in case b) (when λ decreases linearly with decreasing section power).

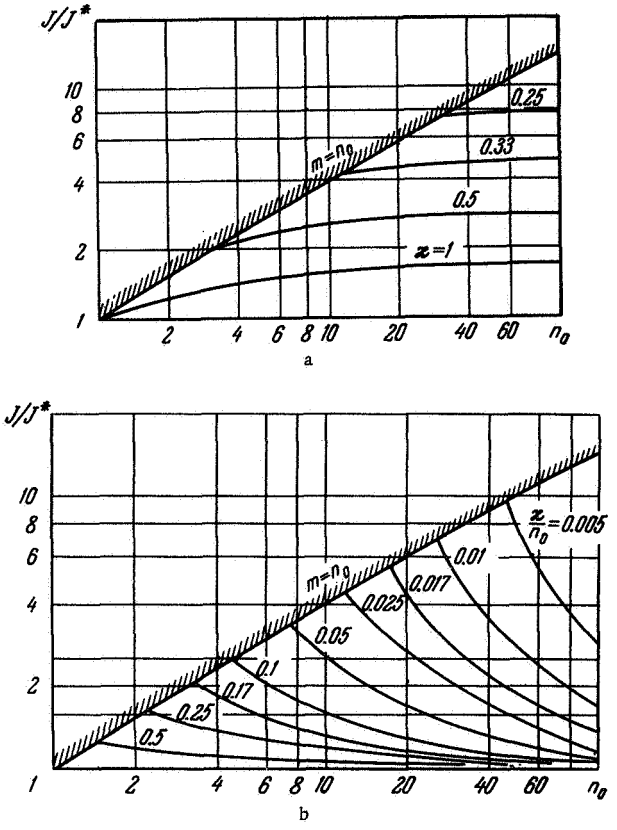

FIGURE 11.13. Functional J as function of number n_0 of autonomous sections, plotted according to Figure 11.11 (total power N_0 fixed). a) λ_0 independent of N_0/n; b) $\lambda_0 \sim \lambda^* N_0/n$; further explanations given in caption of Figure 11.11.

503 **2. Continuous function governing failures.** For constant $\lambda(\mathbf{r}, t) \equiv \lambda_0$ equation (11.82), which determines the number of undamaged sections $n(t)$, can be integrated to give

$$n(t)/n_0 = e^{-t/\varkappa T} \qquad (\varkappa = -\Lambda_1/\lambda_0 T). \tag{11.93}$$

For the maneuver considered the functional J can then be written in the form (with fully-autonomous sections)

$$J = \int_0^T \ddot{x}^2 e^{t/\varkappa T}\, dt \qquad (x(0) = \dot{x}(0) = \dot{x}(T) = 0,\ x(T) = l). \tag{11.94}$$

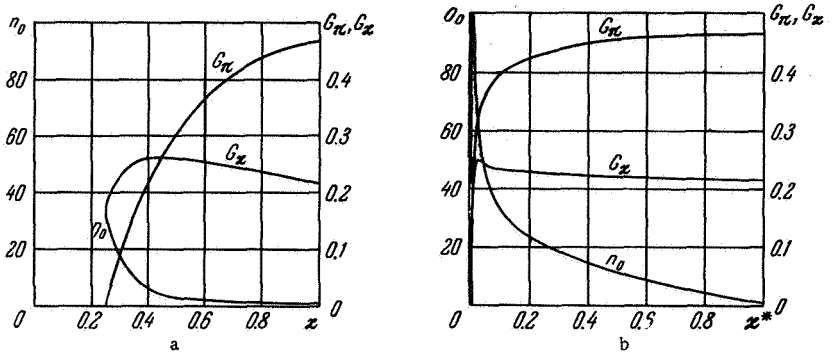

FIGURE 11.14. Maximum payload G_π, optimum engine weight G_x, and optimum number of sections n_0 for displacement between points of rest ($\Phi^* = (\alpha^*/2g)\, 12l^2T^{-3} = 0.1$ is combination of maneuver parameters l, T, and unit weight α^* for section of unit size; $\Delta G_x^* = 0.001$ is minimum section size).

a) λ_0 independent of section power N_0/n where $\varkappa = -\ln R/\lambda_0 T$; b) λ_0 decreases linearly with decreasing power N_0/n, where $\varkappa = -\ln R/\lambda^* T$ and λ^* corresponds to section of unit size.

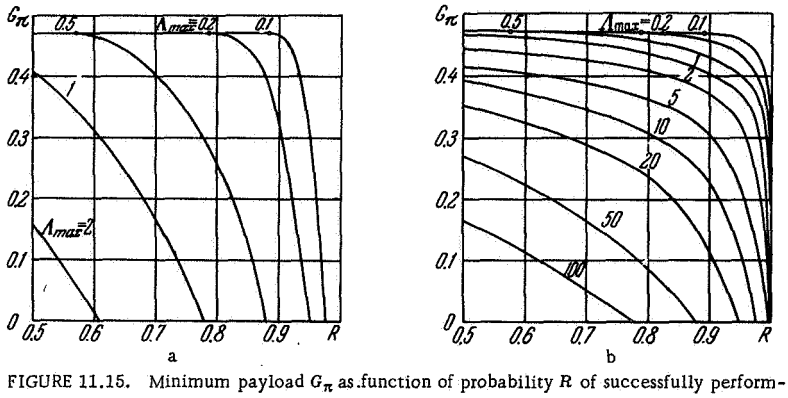

FIGURE 11.15. Minimum payload G_π as function of probability R of successfully performing a maneuver.

a) $\Lambda_{max} = \lambda_0 T$; b) $\Lambda_{max} = \lambda^* T$ (cf. caption of Figure 11.14).

The optimum program $a(t)$ is

$$a(t) = \frac{l}{T^2} \frac{\varkappa - (e^{1/\varkappa} - 1)^{-1} - t/T}{\varkappa^3 (1 - e^{-1/\varkappa}) - \varkappa^{-2}/(e^{1/\varkappa} - 1)^{-1}} e^{-t/\varkappa T}. \tag{11.95}$$

The minimum value of the problem functional is equal to

$$J = \frac{l^2}{T^3} \varkappa^{-2} \left(1 - e^{-1/\varkappa} - \frac{\varkappa^{-2}}{e^{1/\varkappa} - 1}\right)^{-1}. \tag{11.96}$$

The relationship $J(1/\varkappa)$ is shown in Figure 11.11 (the curve $n \to \infty$). It is seen from this figure that, beginning with $n = 10$, the exact value of the functional and its limiting value are quite close to each other.

3. **Round-trip flight.** Let the total time T of the trip (from one point of rest to a second one, and back) be given in the form

$$x(0) = \dot{x}(0) = 0, \quad x(t_1) = l, \quad \dot{x}(t_1) = 0, \quad x(T) = \dot{x}(T) = 0 \quad (0 < t_1 < T). \tag{11.97}$$

This maneuver represents a rapid round-trip interorbital transfer. The problem functional for a continuous failure function (11.93) consists of the sum of the two integrals,

$$J = \int_0^{t_1} \ddot{x}^2 e^{t/\varkappa T}\, dt + e^{t_1/\varkappa T} \int_{t_1}^{T} \ddot{x}^2 e^{(t-t_1)/\varkappa T}\, dt, \tag{11.98}$$

whose extrema are described by relations similar to (11.95). By varying the time t_1 we obtain the condition for equality of the squares of the accelerations on the left and right of t_1. From this condition the optimum value of t_1 is found when

$$\frac{e^{t_1/\varkappa T} - 1 - \varkappa^{-1} - (t_1/\varkappa T)(e^{t_1/\varkappa T} - 1)}{(1 - e^{-t_1/\varkappa T})(e^{t_1/\varkappa T} - 1) - \varkappa^{-2}} = \frac{e^{t_1/\varkappa T} - e^{1/\varkappa} + \varkappa^{-1} e^{t_1/\varkappa T}}{(e^{-t_1/\varkappa T} - e^{-1/\varkappa})(e^{1/\varkappa} - e^{t_1/\varkappa T}) - \varkappa^{-2}}. \tag{11.99}$$

504 The solution of this equation $t_1(1/\varkappa)$ is represented in Figure 11.16 by a dashed curve. It is seen that the outbound flight ($0 \leqslant t < t_1$) is faster than the return one ($t_1 < t \leqslant T$). This lack of symmetry increases with increasing $1/\varkappa$, and is due to the following reason.

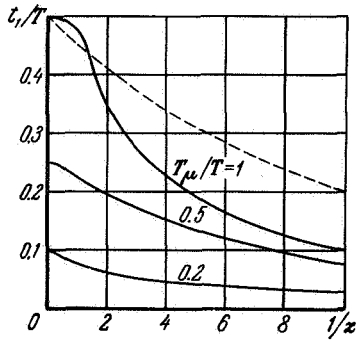

FIGURE 11.16. Optimum time distribution between outbound t_1 and return flights (dashed curve), and between first t_1 and second powered periods (solid curves, where T_μ is total engine operating time) as function of $1/\varkappa$ (ratio of maximum number of failures for one section $\Lambda_{max} = \lambda_0 T$ to the allowable number $\Lambda_1 = -\ln R$).

On the outbound flight, the decrease in power is negligible, so that the optimum acceleration is higher than during the return journey.

Such a thrust-acceleration program ensures a sufficiently-high exhaust velocity everywhere, i.e., a low discharge of working fluid.

4. Motion with a specified time of powered flight. We introduce the condition of a specified engine operating time $T_\mu < T$ (§ 2 of Chapter Seven). We show that, as in the case when failures are ignored, there is just one coasting period during the middle part of the trajectory, i.e.,

$$a(t) = 0 \text{ at } 0 < t_1 < t < t_2 < T. \tag{11.100}$$

It was shown in § 2 of Chapter Seven that the inclusion of a coasting period during a trajectory with an ideal power-limited engine worsens the characteristic. This is also true when failures are taken into account, and the failure probability for a cut-off engine is the same as for an operating one. We shall now examine the case when the failure probability is zero during the coasting period, and is constant and nonzero during the powered periods; thus

$$\lambda = \begin{cases} \lambda_0 = \text{const} \neq 0 & \text{at} \quad a \neq 0, \\ 0 & \text{at} \quad a = 0. \end{cases} \tag{11.101}$$

The expression for the functional when using the continuous failure function (11.93) has the same form as (11.98):

$$J = \int_0^{t_1} \ddot{x}^2 e^{t/\varkappa T}\, dt + e^{t_1/\varkappa T} \int_{t_2}^{T} \ddot{x}^2 e^{(t-t_2)/\varkappa T}\, dt. \tag{11.102}$$

505 The terms not under an integral sign in the first variation of (11.102) are

$$\begin{aligned} \delta J = e^{t_1/\varkappa T} \Big\{ & \Big[2\dot{x}_1 \Big(\dot{a}_1^{(1)} + \frac{1}{\varkappa T}\, a_1^{(1)} \Big) - (a_1^{(1)})^2 \Big] \delta t_1 + 2a_1^{(1)} \delta \dot{x}_1 - \\ & - 2 \Big(\dot{a}_1^{(1)} + \frac{1}{\varkappa T}\, a_1^{(1)} \Big) \delta x_1 - \Big[2\dot{x}_2 \Big(\dot{a}_2^{(2)} + \frac{1}{\varkappa T}\, a_2^{(2)} \Big) - (a_2^{(2)})^2 \Big] \delta t_2 - \\ & - 2a_2^{(2)} \delta \dot{x}_2 + 2 \Big(\dot{a}_2^{(2)} + \frac{1}{\varkappa T}\, a_2^{(2)} \Big) \delta x_2 \Big\}. \end{aligned} \tag{11.103}$$

Here $a^{(1)}$ and $a^{(2)}$ are the optimum programs of thrust acceleration during the first and second periods respectively, and are

$$a^{(1)}(t) = (b_2^{(1)} + b_1^{(1)} t)\, e^{-t/\varkappa T}, \qquad a^{(2)}(t) = (b_2^{(2)} + b_1^{(2)} t)\, e^{-(t-T-T_\mu)/\varkappa T}. \tag{11.104}$$

The velocities $\dot{x}_1$, $\dot{x}_2$ and the coordinates x_1, x_2 at the limits of the coasting period are linked by the simple relations

$$\dot{x}_2 = \dot{x}_1, \quad x_2 = x_1 + (t_2 - t_1)\, \dot{x}_1. \tag{11.105}$$

If t_1 and t_2 are varied independently in order to find the optimum duration of the coasting period, it follows from the equality $\delta J = 0$ that

$$\left.\begin{aligned} & 2\dot{x}_1 \Big[\Big(\dot{a}_1^{(1)} + \frac{1}{\varkappa T}\, a_1^{(1)} \Big) - \Big(\dot{a}_2^{(2)} + \frac{1}{\varkappa T}\, a_2^{(2)} \Big) \Big] - (a_1^{(1)})^2 = 0, \\ & a_2^{(2)} = 0, \quad a_1^{(1)} - a_2^{(2)} + (t_2 - t_1) \Big(\dot{a}_2^{(2)} + \frac{1}{\varkappa T}\, a_2^{(2)} \Big) = 0, \\ & \Big(\dot{a}_1^{(1)} + \frac{1}{\varkappa T}\, a_1^{(1)} \Big) - \Big(\dot{a}_2^{(2)} + \frac{1}{\varkappa T}\, a_2^{(2)} \Big) = 0. \end{aligned}\right\} \tag{11.106}$$

These equations give

$$a_1^{(1)} = a_2^{(2)} = 0, \quad (t_2 - t_1)\, \dot{a}_2^{(2)} = 0. \tag{11.107}$$

From the last condition of (11.106) we obtain $b_1^{(1)} = b_1^{(2)} = b_1$, and equations (11.107) then yield

$$b_1 t_1 + b_2^{(1)} = 0, \quad b_1 t_2 + b_2^{(2)} = 0, \quad (t_2 - t_1)\, b_1 = 0. \tag{11.108}$$

We cannot assume $b_1 = 0$, since it would then follow that $b_2^{(1)} = b_2^{(2)} = 0$, i.e., $a(t) \equiv 0$. Therefore $t_2 = t_1$. This means that the optimum trajectory will contain no coasting periods if the engine operating time is unspecified (we recall that the probability of failures during the coasting period was assumed to be zero in (11.101)). If the duration of the coasting period is fixed $t_2 - t_1 = T - T_\mu$, then $\delta t_2 = \delta t_1$, and three relations similar to (11.106) yield

$$b_2^{(1)} = b_2^{(2)} = b_2, \quad b_1^{(1)} = b_1^{(2)} = b_1, \quad 2b_2 + 2b_1 t_1 + b_1 (T - T_\mu) = 0. \tag{11.109}$$

506 Integrating the equation of motion by parts, where $a(t)$ is determined by (11.104) and (11.109), we find the constants b_1 and b_2 from the boundary conditions of the maneuver:

$$\left.\begin{aligned} &b_2 \frac{1}{\varkappa T}(1 - e^{-T_\mu/\varkappa T}) + b_1 \left[1 - \left(1 + \frac{1}{\varkappa}\right) e^{-T_\mu/\varkappa T} + \right. \\ &\qquad \left. + \frac{1}{\varkappa}\left(1 - \frac{T_\mu}{T}\right) e^{-t_1/\varkappa T}\right] = 0, \\ &b_2 \frac{1}{\varkappa T}\left[\left(\frac{1}{\varkappa} - 1\right) - e^{-T_\mu/\varkappa T} + \frac{1}{\varkappa}\left(1 - \frac{T_\mu}{T}\right) e^{-T_\mu/\varkappa T}\right] + \\ &\qquad + b_1\left[\left(\frac{1}{\varkappa} - 2\right) + \left(\frac{1}{\varkappa} + 2\right) e^{-T_\mu/\varkappa T} + \right. \\ &\qquad \left. + \frac{1}{\varkappa}\left(1 - \frac{T_\mu}{T}\right)\left(\frac{1}{\varkappa} - 2\right) e^{-t_1/\varkappa T}\right] = \varkappa^3 l T^{-2}. \end{aligned}\right\} \tag{11.110}$$

The optimum position of the coasting period is determined by the third relation of (11.109), where b_2/b_1 is substituted for from the first formula of (11.110). This results in

$$t_1 - \frac{(T - T_\mu) e^{-T_\mu/\varkappa T}}{1 - e^{-t_1/\varkappa T}} = \varkappa + \frac{1}{2}\frac{T_\mu}{T} - \frac{1 + e^{-T_\mu/\varkappa T}}{2(1 - e^{-T_\mu/\varkappa T})}. \tag{11.111}$$

The solution of this equation $t_1/T = f(1/\varkappa, T_\mu/T)$ is shown by the solid curves in Figure 11.16. It is seen that the distribution of engine operating time between the first and second powered periods is not symmetrical (as for the roundtrip flight). The duration of the first powered period is shorter, while for $1/\varkappa = 0$ it was $t_1 = {}^1/_2\, T_\mu$.

5. Nonlinear dependence of the power on the number of operating sections. Consider a power source which works like a Carnot cycle. The thermal energy source (the heater) at a temperature T_n (maximum temperature of the cycle) provides the power N_n. The unused thermal energy is radiated by the radiator at an average temperature T (minimum temperature of the cycle). If the work capacity of the radiator is impaired by meteoric punctures, the radiator is split into autonomous sections. A failure in each section leads to a decrease in the radiating area.

The efficiency of the Carnot cycle (the coefficient of conversion of thermal energy into electric energy) is equal to

$$\eta_c = 1 - T/T_n. \tag{11.112}$$

According to the condition of thermal equilibrium, the radiator must radiate a power $(1 - \eta_c) N_n$, i.e.,

$$\varepsilon\sigma S T^3 T_n = N_n, \tag{11.113}$$

507 where S is the radiating area of the radiator and $\varepsilon\sigma$ is the product of the emissivity and the Stephan-Boltzmann constant.

From (11.112) and (11.113) we obtain an expression for the electric power (which provides the thrust in the ideal case)

$$N = \eta_c N_n = \varepsilon\sigma S T^3 (T_n - T). \tag{11.114}$$

Let the maximum thermal power of the heater N_n^*, its maximum temperature T_n^*, and the initial radiator area S_0 be specified. The optimum values of the temperatures T_n and T at each instant must be selected from the condition of maximum power (11.114), so that

$$\left.\begin{aligned} T_n(t) &\equiv T_n^* && \text{at } 0 \leqslant t \leqslant T, \\ T(t) &= \begin{cases} \sqrt[3]{N_n^* / \varepsilon\sigma S(t)\, T_n^*} & \text{at } \frac{27}{64}\varepsilon\sigma S(t)\, T_n^{*4} > N_n^*, \\ {}^3/_4 T_n^* & \text{at } \frac{27}{64}\varepsilon\sigma S(t)\, T_n^{*4} < N_n^*; \end{cases} \end{aligned}\right\} \tag{11.115}$$

the temperature $T = {}^3/_4 T_n^*$ is considered to be allowable for the radiator.

The control program of the thermal power is determined by relations (11.113) and (11.115)

$$N_n(t) = \begin{cases} N_n^* & \text{at } \frac{27}{64}\varepsilon\sigma S(t)\, T_n^{*4} > N_n^*, \\ N_n^* S(t)/S_0 & \text{at } \frac{27}{64}\varepsilon\sigma S(t)\, T_n^{*4} < N_n^*. \end{cases} \tag{11.116}$$

It can be shown that for given T_n^* and N_n^* the initial radiator area S_0 must satisfy the inequality

$$\frac{27}{64}\varepsilon\sigma S_0 T_n^{*4} > N_n^*. \tag{11.117}$$

If this is not satisfied, (11.116) indicates that the thermal power of the heater will never be fully used so that a radiator of lower power, and therefore of smaller weight, could be used instead.

Thus, the optimum control of the thermodynamic cycle of the power source must satisfy the following scheme (cf. (11.115)—(11.117)). The heater temperature T_n is continually maintained at its maximum level T_n^*. The thermal power at the beginning of the motion is likewise a maximum. Punctures of different sections of the radiator are accompanied by a decrease in its radiating area and an increase in the temperature T, until
508 finally it attains the value $T = {}^3/_4 T_n^*$. From this moment on, the radiator temperature remains constant, while the thermal power decreases proportionally to the radiating area.

The decrease of the radiating area of a radiator consisting of a large number of sections is described by equation (11.82), where n/n_0 must be replaced by S/S_0. For a constant probability of punctures we obtain

$$S(t)/S_0 = e^{-t/\varkappa T}. \tag{11.118}$$

A minimum functional J for the maneuver of a displacement between points of rest determines the following optimum program of thrust acceleration:

$$a(t) = \begin{cases} \left(1 - \frac{3}{4}\sqrt[3]{\nu} e^{t/3\varkappa T}\right)(b_2 + b_1 t) & \text{at} \quad 0 \leqslant t < t_*, \\ \frac{1}{4\nu} e^{-t/\varkappa T}(b_2 + b_1 t) & \text{at} \quad t_* < t \leqslant T. \end{cases} \tag{11.119}$$

Here

$$\left.\begin{aligned} \nu &= N_n^* \left(\frac{27}{64} \varepsilon\sigma S_0 T_n^{*4}\right)^{-1} < 1, \\ t_* &= -\varkappa T \ln \nu, \quad \varkappa = -\Omega_0 \lambda^*(\delta)\, T/n_0 \ln R \end{aligned}\right\} \tag{11.120}$$

($\lambda^*(\delta)$ gives the dependence of the average number of punctures of a unit section per unit time on the wall thickness δ; $\Omega_0 = kS_0$ $(0 < k \leqslant 1)$ is the initial vulnerable area of the radiator).

As soon as the constants b_1 and b_2 are found from the boundary conditions (11.94), we can plot the relationship $J(\nu, \varkappa)$. From the condition of minimum total weight (11.73) we must then determine the optimum values of the initial radiator area S_0, the wall thickness δ, the number of sections n_0, the maximum thermal power N_n^*, and the maximum temperature T_n^*. In order to conclude this solution we must know how the average number of punctures per unit section depends on the wall thickness $\lambda^*(\delta)$ and the dependence of the propulsion system weight on all the parameters listed above, i.e., $G_\varkappa = G_\varkappa(N_n^*, T_n^*, S_0, \delta, n_0)$.

§ 4. OPTIMUM PROBABILITY OF EXECUTING A MANEUVER

We have so far treated the optimization problem for a fixed probability of performing a maneuver. The formulation guaranteed that each maneuver would be successful with a probability R. Consider now the transportation problem. We wish to deliver a very large payload at the terminal point of the trajectory, so that the maneuver has to be performed repeatedly; alternatively, we can consider the problem of regularly supplying a station.

509 It was seen from the solutions given in §§ 1 to 3 that the probability of successfully executing the maneuver each time is increased by reducing the payload which is delivered at the end of every flight, i.e., we must increase the number of successful trips to carry out the transportation problem. If the probability of successfully executing the maneuver is decreased after each flight, the number of successful journeys must therefore be increased. On the other hand the number of unsuccessful trips will increase, and the total number of journeys from some instant on will once more increase. Therefore there must exist some optimum probability R of executing the maneuver at each stage; this optimum value always lies inside the interval (0, 1), since for $R = 0$ the percentage of successful trips is zero, while for some value $0 < R < 1$ the payload vanishes.

1. **Formulation of the transportation problem.** The treatment is based on a scheme of independent experiments. The parameters of the vehicles for each maneuver are considered identical, and the outcome of a journey is considered independent of the preceding outcomes.* Each i-th trip can have two outcomes: either the payload is delivered at the terminal point of the trajectory, or it is not. These are two incompatible elementary events, and they form a full system of possible events. If the probability of the first event is R, the probability of the second event is $1 - R$.

The outcome of the i-th journey will be characterized by the random variable $G^{(i)}$, which is the weight delivered at the terminal point for this trip. If we are successful, the weight $G^{(i)}$ will equal the payload G_π to be delivered after each journey; if we are unsuccessful, the weight $G^{(i)}$ equals zero. In this notation the first elementary event will be $G^{(i)} = G_\pi$, and the second one $G^{(i)} = 0$; the probability of these events is written in the form

$$P(G^{(i)} = G_\pi) = R, \quad P(G^{(i)} = 0) = 1 - R. \tag{11.121}$$

We recall that according to §§ 1 to 3 the probability R and the payload G_π are linked in that G_π decreases with increasing R (cf. for instance Figures 11.19 and 11.15).

Two different formulations of the transportation problem are considered (in both cases the takeoff weight of the vehicle and the maneuver parameters are considered as fixed).

510 a) We require to maximize the mathematical expectation of delivering a total load G_Σ at the terminal point over a fixed number of trips $n \gg 1$.

b) We require to deliver a maximum total load G_Σ over a fixed number of trips n with a specified probability R_0.

The mathematical expectation of delivering a load G_Σ enters formulation a) and therefore the problem can only be solved on the average taken over a very large number of journeys ($n \gg 1$ or $G_\Sigma \gg G_\pi$). In formulation b), on the other hand, we have a specified probability R_0 for any number of journeys. Formulations reciprocal to a) and b) may also be used; we shall deal with them in subsections 2 and 3.

In treating these two problems it will be assumed that we know the solution $G_\pi(R)$ of the problem for maximum payload at a fixed probability of executing the maneuver each time. Otherwise the variational problem must be written according to the given optimum criterion (cf. subsection 2).

The transportation problem can also be examined in terms of the cost criterion, as in § 1 of Chapter Ten. The cost of a successful trip equals the cost of the vehicle without the payload (assuming that the vehicle is used only once). For an unsuccessful trip we must add the cost of the damage, here taken equal to the value of the payload (proportional to G_π). The vehicle cost is linked with the weights of its main components via formulas (10.1) to (10.4).

Formulations a) and b) given above are easily rephrased in cost terms.

a) To minimize the mathematical expectation of the transportation cost of a specified load G_Σ.

b) To minimize the transportation cost of a given load G_Σ with a specified probability R_0.

* This implies, in particular, that the vehicles are not used repeatedly.

2. **Maximum mathematical expectation of the total load (Problem a).** The mathematical expectation* of the value of the total load G_Σ delivered over n trips is

$$\langle G_\Sigma \rangle = \left\langle \sum_{i=1}^{n} G^{(i)} \right\rangle = \sum_{i=1}^{n} \langle G^{(i)} \rangle = \sum_{i=1}^{n} [RG_\pi + (1-R)\cdot 0] = nRG_\pi \qquad (11.122)$$

(the mathematical expectation of a sum of random variables is equal to the sum of their mathematical expectations).

511 It is seen from (11.122) that problem a) is independent of n and reduces to finding the minimum mathematical expectation with respect to the probability R for the weight $G^{(i)}$ to be successfully delivered in one trip:

$$\langle G^{(i)} \rangle = \frac{1}{n} \langle G_\Sigma \rangle = \max_R RG_\pi(R). \qquad (11.123)$$

For a known relationship $G_\pi(R)$ this is a problem of maximizing a function of one variable. If the relationship $G_\pi(R)$ is unknown, we must write out the full variational formulation. To that end we introduce the instantaneous value of (11.123) for a single-section engine (§ 1)

$$\langle G^{(i)} \rangle_t = e^{-\Lambda(t)} G_\sigma(t), \qquad (11.124)$$

where $G_\sigma(t) = G_\pi + G_\mu(t)$, $\Lambda(t) = \int_0^t \lambda\, dt$, $\Lambda(T) = -\ln R$. At the end of the journey $\langle G^{(i)} \rangle_t$ coincides with (11.123), and the problem reduces to maximizing the final value of (11.124). To obtain Mayer's formulation, we express (11.124) as the differential equation

$$\frac{d}{dt}\langle G^{(i)} \rangle = -\dot{\Lambda}(G_\sigma + \dot{G}_\sigma) e^{-\Lambda}, \quad \langle G^{(i)} \rangle_{t=0} = G_\sigma(0), \ \langle G^{(i)} \rangle_{t=T} = \max, \qquad (11.125)$$

and add this to the system of equations governing the variational problem to maximize the payload $G_\pi = G_\sigma(T)$ for a fixed probability R. The boundary conditions $G_\sigma(T) = \max$ and $\Lambda(T) = -\ln R$ must then be replaced by $G_\sigma(T) = \text{opt}$ and $\Lambda(T) = \text{opt}$. For an ideal power-limited engine (11.11) the new variational problem has the following form:

$$\left.\begin{aligned}
&\frac{d}{dt}\langle G^{(i)} \rangle = e^{-\Lambda}\left[\lambda G_\sigma - \frac{(G_\sigma + G_\varkappa)^2}{G_\varkappa}\frac{\alpha(w)}{2g}\frac{a^2}{N}\right], \\
&\qquad\qquad \langle G^{(i)} \rangle_{t=0} = G_\sigma(0), \ \langle G^{(i)} \rangle_{t=T} = \max, \\
&\dot{G}_\sigma = -\frac{(G_\sigma + G_\varkappa)^2}{G_\varkappa}\frac{\alpha(w)}{2g}\frac{a^2}{N}, \\
&\qquad\qquad G_\sigma(0) + G_\varkappa = 1, \qquad G_\sigma(T) = \text{opt}, \\
&\dot{\mathbf{r}} = \mathbf{v}, \qquad \mathbf{r}(0) = \mathbf{r}_0, \qquad \mathbf{r}(T) = \mathbf{r}_1, \\
&\dot{\mathbf{v}} = a\mathbf{e} + \mathfrak{R}, \qquad \mathbf{v}(0) = \mathbf{v}_0, \qquad \mathbf{v}(T) = \mathbf{v}_1, \\
&\dot{\Lambda} = \lambda(t, N, w), \qquad \Lambda(0) = 0, \qquad \Lambda(T) = \text{opt} \\
&(a(t) \geqslant 0, \ 0 \leqslant N(t) \leqslant 1, \ |\mathbf{e}(t)| = 1, \ G_\varkappa, w = \text{const}).
\end{aligned}\right\} \qquad (11.126)$$

512 The procedure used to determine the optimum control variables and their properties in (11.11) applies to (11.126) as well. We shall therefore restrict

* Designated by the symbol $\langle\ \rangle$.

ourselves to the example of finding the maximum of (11.123), where $G_\pi(R)$ is taken from subsection 2 of § 1. Figure 11.17 shows the mathematical expectation of the weight $\langle G_\Sigma \rangle$ per trip (as a fraction of G_0), as a function of the probability R of successfully executing the maneuver. The data given correspond to Figure 11.9. The curves are distinguished by the values of the parameter $\Lambda_{max} = \lambda_{max} T$ which is the maximum possible number of failures during one flight. The solid curves correspond to the problem of a displacement between points of rest, and the dashed curves to the problem of a velocity build-up. The optimum values of the probability R and the maximum values of the weight $\langle G_\Sigma \rangle$, which correspond to the maximum points in Figure 11.17, are given in Figures 11.18 and 11.19 as a function of Λ_{max} for different values of the maneuver parameter Φ^* (cf. (11.33), (11.34)). For the same values of Λ_{max} and Φ^*, the optimum probability R and the maximum weight $\langle G_\Sigma \rangle$ for the problem of flights between points of rest (the solid curves) are substantially higher than for the problem of a velocity build-up (the dashed curves).

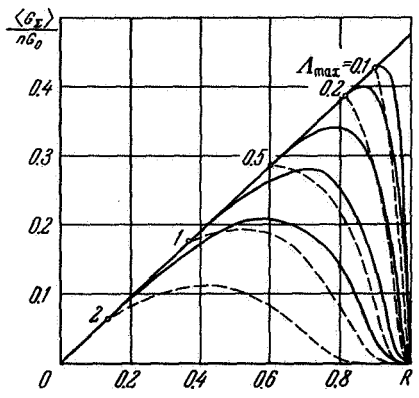

FIGURE 11.17. Average value of payload delivered in one trip at terminal point of trajectory, as function of probability R of a successful trip for fixed maximum number of failures Λ_{max} Solid curves represent displacement between points of rest; dashed curves represent velocity build-up.

Consider now another formulation of Problem a), namely, to find the minimum mathematical expectation of the number of flights which are necessary to deliver a specific load G_Σ; we shall show that the two formulations are equivalent.

The number of successful trips necessary to deliver a load G_Σ is*

$$n_* = [G_\Sigma/G_\pi] + 1; \tag{11.127}$$

the mathematical expectation of the total number of trips is (by definition)

$$\langle n \rangle = \sum_{n=n_*}^{\infty} nP_n, \quad P_n = P\left(\sum_{i=1}^{n} G^{(i)} \geqslant G_\Sigma, \sum_{i=1}^{n-1} G^{(i)} < G_\Sigma\right), \tag{11.128}$$

513 where P_n is the probability that the necessary number n_* of successful trips is attained at exactly the n-th trip (not earlier and not later). This means that $(n-1)$ of the first $(n-n_*)$ journeys are unsuccessful, and that the n-th one is a success. Such a situation can be achieved by $C_{n-1}^{n-n_*}$ equally-probable combinations, and the probability of each of them is $(1-R)^{n-n_*}R^{n_*}$.

Introducing the notation $i = n - n_*$, we can write formula (11.128) as

$$\langle n \rangle = R^{n_*} \sum_{i=0}^{\infty} \frac{(n_* + i - 1)!}{i!\,(n_* - 1)!} (n_* + i)(1-R)^i. \tag{11.129}$$

* The symbol $[G_\Sigma/G_\pi]$ represents the integral part of the number G_Σ/G_π, i.e., the nearest whole number smaller than G_Σ/G_π.

Note that the series on the right-hand side of (11.129) represents the expansion of $[1 - (1 - R)]^{-(n_*+1)}$ and so the mathematical expectation of the total number of trips will equal*

$$\langle n \rangle = n_*/R. \tag{11.130}$$

Substituting the expression for n_* from (11.127) into (11.130), and discarding the symbol for the integral part, we obtain $\langle n \rangle = G_\Sigma R G_\pi$. For a fixed
514 value of G_Σ the minimum of $\langle n \rangle$ with respect to R is attained when the product RG_π is a maximum. This means that the solutions of the problems to minimize $\langle n \rangle$ and maximize $\langle G_\Sigma \rangle$ coincide with an accuracy of up to the difference between the fraction G_Σ/G_π and its integral number (when $G_\Sigma \gg G_\pi$ this difference is immaterial).

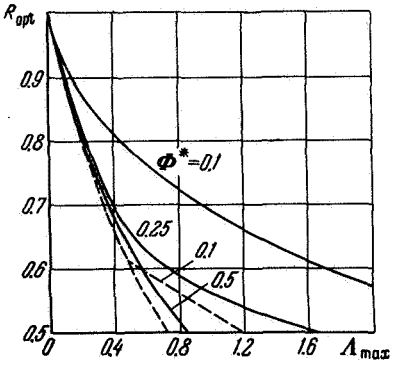

FIGURE 11.18. Optimum probability of successfully executing maneuver at each trip (Problem a)) as function of maximum number of failures Λ_{max} for fixed values of maneuver functional Φ^*. Solid curves represent displacement between points of rest; dashed curves represent velocity build-up.

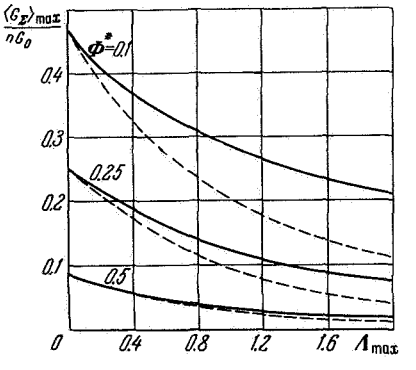

FIGURE 11.19. Maximum mathematical expectation of delivering load in one trip, as function of maximum number of failures Λ_{max} for fixed values of maneuver functional Φ^*. Solid curves represent displacement between points of rest; dashed curves represent velocity build-up.

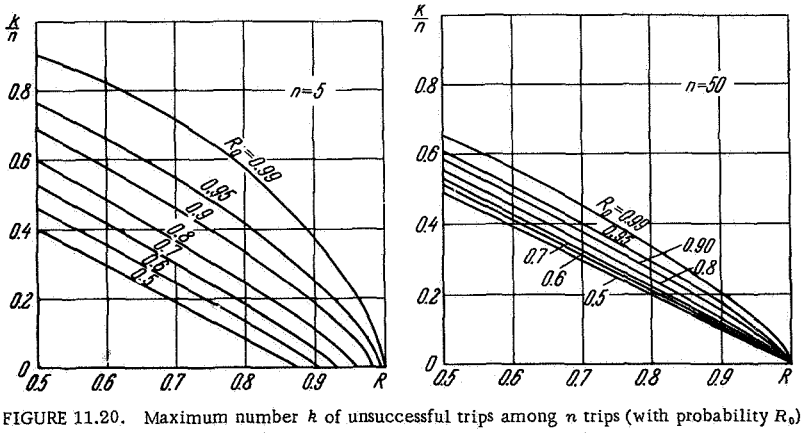

FIGURE 11.20. Maximum number k of unsuccessful trips among n trips (with probability R_0) as function of probability R of successfully executing maneuver in one trip.

* Relationship (11.130) can be written directly if one proceeds from the statistic definition of the probability.

3. **Maximum total load for specified probability of achieving the solution** (Problem b)). We guarantee with a probability R_0 that among n trips there will be no more than $k < n$ unsuccessul ones. The probability R_0 consists of the probabilities of the events forming the given one:

$$R_0 = \sum_{i=0}^{k} P_n^{(i)}, \quad P_n^{(i)} = P\left(\sum_{j=1}^{n} G^{(j)} = (n-i)\,G_\pi\right), \tag{11.131}$$

where $P_n^{(i)}$ is the probability that i trips will be unsuccessful among n. The latter can be achieved in C_n^i ways. The probability of requiring all of them is the same: $(1-R)^i R^{n-i}$, therefore $P_n^{(i)} = C_n^i (1-R)^i R^{n-i}$. Substituting this expression into (11.131), we derive

$$R_0 = P\left(\sum_{j=1}^{n} G^{(j)} \geqslant (n-k)\,G_\pi\right) = \sum_{i=0}^{k} \frac{n!}{i!\,(n-i)!}(1-R)^i R^{n-i} \tag{11.132}$$

(the binomial distribution for the scheme of independent tests /11.6/).

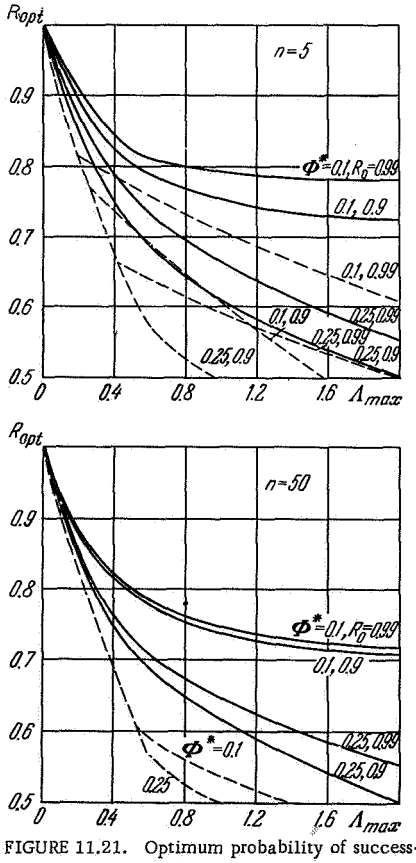

FIGURE 11.21. Optimum probability of successfully executing maneuver in each trip (Problem b)), as function of maximum number of failures Λ_{max} for fixed values of maneuver functional Φ^*, probability R_0, and number of trips n. Solid curves represent displacement between points of rest; dashed curves represent velocity build-up.

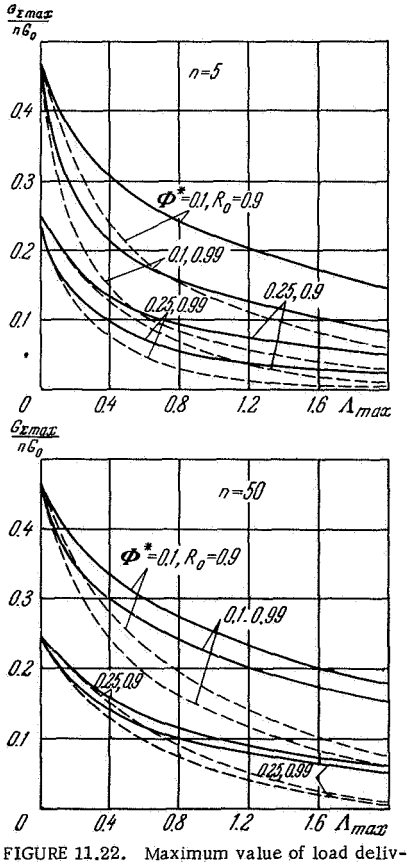

FIGURE 11.22. Maximum value of load delivered in one trip, as function of Λ_{max} for fixed values of Φ^*, R_0, and n. Solid curves represent displacement between points of rest; dashed curves represent velocity build-up.

515 For given R_0 and n (11.132) determines the relationship between the probability R of one successful execution of the maneuver and the number of unsuccessful trips k: $k=k(R, R_0, n)$ (Figure 11.20).

516 According to (11.132), the total load G_Σ delivered over n trips will not be less than

$$\sum_{i=1}^{n} G^{(i)} \geqslant (n-k)\, G_n, \tag{11.133}$$

with a probability R_0. Therefore, Problem b) reduces to finding the maximum value of the right-hand side of inequality (11.133) with respect to the probability R of a single successful maneuver:

$$G_\Sigma = \max_R [n-k(R)]\, G_n(R). \tag{11.134}$$

A solution of (11.134) for the relationship $G_n(R)$ from Figure 11.9 is given in Figures 11.21 and 11.22. These show the optimum probability R and the maximum value of the total load G_Σ for one trip out of the n made, as a function of Λ_{max} — the maximum possible number of failures during a single flight.

The magnitude of the load G_Σ/n decreases as we increase the probability R_0 of attaining the solution. The probability decreases when increasing the total number of trips n. For large n the solution of Problem b) (Figures 11.21 and 11.22 for $n = 50$) approaches that of Problem a) (Figures 11.18 and 11.19).

When studying Problem b) equivalent formulations may be used in addition to the one studied here; e.g., to deliver a given load with a specified probability R_0 over a minimum number of trips n, or, to ensure a maximum probability R_0 of transporting a specified load G_Σ over a fixed number of trips n.

Additional information on reliability questions as applied to flight mechanics can be found in /11.9—11.11/.

Chapter Twelve

EXTRA WEIGHT REQUIRED FOR TRAJECTORY CORRECTION

517 The subject of trajectory correction embraces a very wide circle of problems. These include:

1) Study of the perturbing factors which affect the vehicle during flight; estimating the deviations from the required trajectory.

2) Investigating the accuracy required to carry out the required trajectory; decision on the necessity of a correction.

3) Measuring the parameters of the actual trajectory and processing the results.

4) Determining the control function which ensures a given accuracy when executing the required trajectory with minimum weight.

The full treatment of these problems lies beyond the scope of this book. We have accordingly given a very extensive (but by no means complete) bibliography of the papers dealing with them /12.1—12.103/.

In this chapter we shall consider the question of assessing the fuel requirements for a trajectory correction, as applied to an ideal power-limited engine. For this the problem reduces to determining the minimum mathematical expectation of the increment in the integral of the square of the thrust acceleration. Errors in the execution of the optimum thrust-acceleration program, errors in the measurements of the coordinates and velocities, and deviations from the initial conditions are taken into account. The probability characteristics of these random variables (the mathematical expectation, the correlation function, the dispersion) are considered as known. Restrictions are imposed on the dispersion of the final deviations of the coordinates and velocities.

The vehicle trajectory is corrected by successive discrete corrections of the thrust program of the continuously-operating main engine; these are
518 based on measurements taken at specific instances of time (the correction points). The optimum distribution and optimum number of correction points are selected from the condition of minimum mathematical expectation of the increment in the problem functional /12.62, 12.69/.

§ 1. ERRORS WHEN IMPLEMENTING THE THRUST-ACCELERATION PROGRAM, AND DEVIATIONS FROM THE REQUIRED TRAJECTORY

1. Errors in the thrust acceleration. The extremal $\mathbf{a}^{(0)}(t)$ which was found by solving the variational problem to minimize the functional J

(Chapters Four and Five), will probably be achieved with some errors

$$\delta\mathbf{a} = \mathbf{a}(t) - \mathbf{a}_*^{(0)}(t). \tag{12.1}$$

This leads to a deviation in the actual trajectory $\mathbf{r}(t)$ from the required one $\mathbf{r}_*^{(0)}(t)$:

$$\delta_a\dot{\mathbf{r}}(t) = \dot{\mathbf{r}}(t) - \dot{\mathbf{r}}_*^{(0)}(t), \quad \delta_a\mathbf{r}(t) = \mathbf{r}(t) - \mathbf{r}_*^{(0)}(t). \tag{12.2}$$

Assuming these quantities are small, we can express them by the linearized system of equations

$$\delta_a\ddot{\mathbf{r}} = \delta\mathbf{a} + (\partial\mathfrak{R}/\partial\mathbf{r})^{(0)}\cdot\delta_a\mathbf{r}. \tag{12.3}$$

To obtain analytic results, we neglect the second term on the right-hand side of (12.3), i.e., we assume

$$\delta_a\ddot{\mathbf{r}} = \delta\mathbf{a}. \tag{12.4}$$

For the same reason we take as the initial undisturbed motion the displacement in a gravity-free field between two points of rest located at a distance l apart during time T (5.33):

$$a_*^{(0)}(t) = \frac{6l}{T^2}\left(1 - 2\frac{t}{T}\right), \quad x_*^{(0)}(t) = l\frac{t^2}{T^2}\left(3 - 2\frac{t}{T}\right). \tag{12.5}$$

When finding the average deviations $\delta_a\mathbf{r}$, $\delta_a\dot{\mathbf{r}}$ caused by the errors $\delta\mathbf{a}$, the probability characteristics of the latter must be known, i.e., their mathematical expectation and their correlation function. Suppose these characteristics are specified, for instance

$$\begin{gathered} M[\delta a(t)] \equiv 0, \\ K[\delta a(t),\ \delta a(t')] = \sigma_a^2 A(t) A(t') e^{-|t-t'|/\delta t}. \end{gathered} \tag{12.6}$$

519 Here M and K represent the mathematical expectation and the correlation function; σ_a and δt can be interpreted as constants, characterizing the accuracy and response of the control system which implements the thrust-acceleration program; $A(t)$ is a nonrandom known function, determined by the type of control, where $A(t) = a(t)$ when the control is based on the relative deviation, and $A(t) \equiv \text{const}$ when it is based on the absolute deviation (in what follows $A(t) \equiv l/T^2$).

2. Mean square deviations from the required trajectory. We calculate the mathematical expectation and the dispersion of the deviations $\delta_a\dot{x}$ and $\delta_a x$. The operators of mathematical expectation and integration are commutative /12.4/, and therefore

$$\left.\begin{aligned} M[\delta_a\dot{x}(t)] &= M\int_0^t \delta a\,dt = \int_0^t M(\delta a)\,dt = 0, \\ M[\delta_a x(t)] &= M\int_0^t dt\int_0^t \delta a\,dt = \int_0^t dt\int_0^t M(\delta a)\,dt = 0. \end{aligned}\right\} \tag{12.7}$$

The dispersions of $\delta_a x$ and $\delta_a \dot{x}$ will differ from zero; using once more the commutativity of the operators, we obtain

$$D[\delta_a \dot{x}(t)] = M[\delta_a \dot{x}(t)\,\delta_a \dot{x}(t)] = M\left[\left(\int_0^t \delta a(\xi)\,d\xi\right)\left(\int_0^t \delta a(\zeta)\,d\zeta\right)\right] =$$

$$= M\int_0^t d\xi \int_0^t \delta a(\xi)\,\delta a(\zeta)\,d\zeta = \int_0^t d\xi \int_0^t M[\delta a(\xi)\,\delta a(\zeta)]\,d\zeta. \qquad (12.8)$$

The last integrand represents by definition the correlation function (12.6), and therefore

$$D[\delta_a \dot{x}(t)] = \frac{l}{T^2}\sigma_a^2 \int_0^t d\xi \int_0^t e^{-|\xi-\zeta|/\delta t} d\zeta. \qquad (12.9)$$

If this integral is calculated and a similar procedure is carried out for $\delta_a x$, we obtain the final expression for the dispersions of the random deviations (12.2), caused by errors δa of the type (12.6)':

$$\left.\begin{aligned} D[\delta_a v(\tau)] &= 2\sigma_a^2\theta[\tau - \theta(1-e^{-\tau/\theta})] \quad \left(v = \frac{\dot{x}T}{l},\ \tau = \frac{t}{T},\ \theta = \frac{\delta t}{T}\right), \\ D[\delta_a s(\tau)] &= \frac{2}{3}\sigma_a^2\theta\{\tau^3 - 3\theta[{}^1\!/_2\,\tau^2 + \theta\tau e^{-\tau/\theta} + \theta^2(1-e^{-\tau/\theta})]\} \\ &\left(s = \frac{x}{l}\right). \end{aligned}\right\} \qquad (12.10)$$

520 Deviations from the required trajectory are caused not only by the errors δa, but also by the inexact fulfillment of the initial conditions:

$$\delta_0 \dot{\mathbf{r}} = \dot{\mathbf{r}}(0) - \dot{\mathbf{r}}_0, \quad \delta_0 \mathbf{r} = \mathbf{r}(0) - \mathbf{r}_0. \qquad (12.11)$$

The errors $\delta_0 \dot{\mathbf{r}}$ and $\delta_0 \mathbf{r}$ are considered as independent random vectors, whose components are not correlated and are distributed about zero with known mean square deviations; for one-dimensional motion it is assumed that

$$M(\delta_0 v) = M(\delta_0 s) = 0,\ D(\delta_0 v) = \sigma_{0v}^2,\ D(\delta_0 s) = \sigma_{0s}^2. \qquad (12.12)$$

If at the end of the motion the expected deviations of the actual trajectory from the required one exceed the given allowable deviations $\delta \dot{r}_{\max}$ and $\delta r_{\max}$, the trajectory must be corrected during the motion. In the example considered, this correction becomes necessary when the inequalities

$$2\sigma_a^2\theta + \sigma_{0v}^2 \leqslant \delta v_{\max}^2,\ \frac{2}{3}\sigma_a^2\theta + \sigma_{0v}^2 + \sigma_{0s}^2 \leqslant \delta s_{\max}^2 \qquad (12.13)$$

are not fulfilled. These two inequalities result from adding the dispersions $D(\delta_a v)$ and $D(\delta_0 v)$, $D(\delta_a s)$ and $D(\delta_0 s)$, where the deviations δ_a and δ_0 are independent and $D(\delta_a + \delta_0) = D(\delta_a) + D(\delta_0)$. The terms of order θ^2 and higher are neglected here, since it is physically obvious that $\delta t \ll T$, or $\theta = \delta t/T \ll 1$.

§ 2. OPTIMUM CORRECTION PROGRAM

1. Measurement of the coordinates and velocities. We shall assume that inequalities (12.13) are unsatisfied, i.e., that the trajectory must be

corrected during the motion. To do this, we must know the true values of the coordinates and the velocities. Single measurements are not accurate enough for this purpose; it is, therefore, assumed that measurements are taken regularly and often; the results of the measurements taken during the time interval t_{i-1} to t_i ($i = 1, 2, \ldots, m$) are taken as the readings at time t_i and averaged. A certain error nevertheless remains,

$$\delta_n \dot{\mathbf{r}}_i = \dot{\rho}(t_i) - \dot{\mathbf{r}}(t_i), \quad \delta_n \mathbf{r}_i = \rho(t_i) - \mathbf{r}(t_i), \tag{12.14}$$

where $\rho(t_i)$ and $\dot{\rho}(t_i)$ are the radius vector and the velocity vector obtained as a result of the method used to obtain the readings corresponding to time t_i and the averaging of the measurements. In the example considered it is assumed that

$$M(\delta_n v_i) = M(\delta_n s_i) = 0, \quad D(\delta_n v_i) = (\sigma_{nv}^{(i)})^2, \quad D(\delta_n s_i) = (\sigma_n^{(i)})^2 \tag{12.15}$$

521 and that the errors $\delta_n v_i$, $\delta_n s_i$ ($i = 1, \ldots, m$) are not correlated.

The mean square errors in the measurements $\sigma_{nv}^{(i)}$, $\sigma_{ns}^{(i)}$ depend on the length of the averaging interval $(t_i - t_{i-1})$. As this interval increases they will decrease at first, due to the elimination of random errors, and then increase, due to the effect of the errors δa introduced by the engine (which become significant as the time interval increases). By averaging the measurements at the times t_i ($i = 1, \ldots, m$) we know, to a certain degree of accuracy, the deviations of the actual trajectory from the $(i-1)$-th required trajectory,

$$\Delta \dot{\mathbf{r}}_i = \dot{\rho}(t_i) - \dot{\mathbf{r}}_*^{(i-1)}(t_i), \quad \Delta \mathbf{r}_i = \rho(t_i) - \mathbf{r}_*^{(i-1)}(t_i). \tag{12.16}$$

2. Optimum corrections of the thrust-acceleration program. The corrections of the thrust-acceleration program $a_*^{(i-1)}(t)$ are selected from the general optimum condition. The optimum correction

$$\Delta \mathbf{a}_*^{(i)} = \mathbf{a}_*^{(i)}(t) - \mathbf{a}_*^{(i-1)}(t), \tag{12.17}$$

calculated for time t_i (the i-th correction) must ensure a minimum of the functional

$$J_i = \int_{t_i}^{T} a^2 dt, \tag{12.18}$$

which corresponds to a displacement between the points in the phase space $\{\rho(t_i), \dot{\rho}(t_i)\}$ and $\{\mathbf{r}_1, \dot{\mathbf{r}}_1\}$ during a time interval $\Delta t_i = T - t_i$.

It is thus required that the correction $\Delta \mathbf{a}_*^{(i)}(t)$ of the thrust acceleration makes the deviations $\Delta \dot{\mathbf{r}}_i$ and $\Delta \mathbf{r}_i$ vanish at the end of the trajectory using a minimum of energy. The vehicle does not need to be placed on the required trajectory before the end of the flight.

When calculating the corrections $\Delta \mathbf{a}_*^{(i)}(t)$ it is assumed that no errors are introduced. For one-dimensional motion in a gravity-free field the correction of the acceleration program is

$$\Delta a_*^{(i)}(\tau) = \frac{6l}{T^3} \frac{1}{1-\tau_i} \left[\left(2 \frac{\Delta s_i}{1-\tau_i} + \Delta v_i \right) \frac{\tau - \tau_i}{1-\tau_i} - \left(\frac{\Delta s_i}{1-\tau_i} + \frac{2}{3} \Delta v_i \right) \right]. \tag{12.19}$$

The program executed in the interval of time between t_i and t_{i+1} is $\mathbf{a}_*^{(i)}(t)$; at time t_{i+1} it is replaced by a new optimum program $\mathbf{a}_*^{(i+1)}(t)$, etc.

522 **3. Increment of the functional.** The expression for the functional J for a motion with errors and corrections can be written as

$$J=\sum_{i=0}^{m}\int_{t_i}^{t_{i+1}}(\mathbf{a}_*^{(i)}+\delta\mathbf{a})^2dt \qquad (t_0=0,\ t_{m+1}=T). \tag{12.20}$$

In a gravity-free field the equations for the optimum corrections $\Delta a_*^{(i)}$ are linear. Therefore

$$a_*^{(i)}(t)=a_*^{(0)}(t)+\Delta a_*^{(1)}(t)+\ldots+\Delta a_*^{(i)}(t), \tag{12.21}$$

which enables us to transform the functional (12.20) into the form

$$\begin{aligned}\Delta J=J-J_0=T\Big\{&2\Big[\sum_{i=1}^{m}\int_{\tau_i}^{1}a_*^{(0)}\Delta a_*^{(i)}d\tau+\int_0^1 a_*^{(0)}\delta a\,d\tau\Big]+\\&+2\Big[\sum_{i=3}^{m}\int_{\tau_i}^{1}\Delta a_*^{(i)}\Big(\sum_{j=1}^{i-2}\Delta a_*^{(j)}\Big)d\tau+\sum_{i=1}^{m}\int_{\tau_i}^{1}\Delta a_*^{(i)}\delta a\,d\tau\Big]+\\&+\Big[2\sum_{i=2}^{m}\int_{\tau_i}^{1}\Delta a_*^{(i)}\Delta a_*^{(i-1)}d\tau+\sum_{i=1}^{m}\int_{\tau_i}^{1}(\Delta a_*^{(i)})^2d\tau+\int_0^1(\delta a)^2d\tau\Big]\Big\},\end{aligned} \tag{12.22}$$

where

$$J_0=T\int_0^1(a_*^{(0)})^2d\tau=\frac{12l^2}{T^3}. \tag{12.23}$$

If $\Delta J/J_0\ll 1$, and we restrict ourselves to the linear terms in $\Delta J/J_0$, we obtain approximate expressions for the weight components in the case of a motion with corrections (cf. (4.15) to (4.17))

$$\left.\begin{aligned}&G_\pi\approx(1-\sqrt{\Phi_0})^2-\Delta\Phi\left(\frac{1}{\sqrt{\Phi_0}}-1\right),\\&G_\varkappa\approx(\sqrt{\Phi_0}-\Phi_0)+\Delta\Phi\left(\frac{1}{2\sqrt{\Phi_0}}-1\right),\\&G_{\mu 0}\approx\sqrt{\Phi_0}+\frac{\Delta\Phi}{2\sqrt{\Phi_0}}\quad\left(\Delta\Phi=\frac{\alpha}{2g}\Delta J,\ \Phi_0=\frac{\alpha}{2g}J_0\right).\end{aligned}\right\} \tag{12.24}$$

When maximizing the averaged quantity G_π a distribution of the correction points $\tau_i\,(i=1,\ldots,\ m)$ must be determined and a number m of such points chosen so that the mathematical expectation ΔJ is minimized when satisfying (on the average) the specified accuracy at the end of the motion.

523 In order to calculate $M(\Delta J)$, we require the mathematical expectation of the integrands in (12.22). These expressions represent the corrections $\Delta a_*^{(i)}$, the errors δa, and their products. According to (12.19), the corrections $\Delta a_*^{(i)}$ depend on the total deviations Δv_i, Δs_i. These consist of the deviations caused by the errors δa, and the deviations of the $(i-1)$-th and i-th measurements.

With relations (12.2), (12.4), (12.14), and (12.16) it can be shown that

$$\left.\begin{aligned}\Delta v_i &= \frac{T^2}{l}\int_{\tau_{i-1}}^{\tau_i}\delta a\,d\tau + \delta_n v_i + \delta_n v_{i-1},\\ \Delta s_i &= \frac{T}{l}\int_{\tau_{i-1}}^{\tau_i} d\tau \int_{\tau_{i-1}}^{\tau_i}\delta a\,d\tau + \delta_n s_i - \delta_n s_{i-1} - \delta_n v_i\,(\tau_i - \tau_{i-1}).\end{aligned}\right\} \tag{12.25}$$

The mathematical expectation of the terms contained in the first brackets of (12.22) is zero, since the integrands of these terms are linear relative to the random variables Δv_i, Δs_i, and δa, whose mathematical expectations vanish (12.6), (12.7).

Since the random deviations $\delta a\,(\tau)$ on each side of the points τ_i are not correlated when passing to the new program $a_*^{(i+1)}$,

$$\begin{gathered}K\,[\delta a\,(\tau),\ \delta a\,(\tau')] = 0\\ \text{at}\quad \tau_{i-1} < \tau < \tau_i,\ \ \tau_{j-1} < \tau' < \tau_j,\ \ i \neq j,\end{gathered} \tag{12.26}$$

and so we obtain the same result for the second bracket of (12.22) as well because the superscripts of the factors in these terms differ by more than unity. On the basis of (12.25), this means that the factors are not correlated, and that the mathematical expectation for each of them vanishes.

The first two terms in the last bracket of (12.22) are expressed in terms of the deviations Δv_{i-1}, Δv_i, Δs_{i-1}, and Δs_i in the forms

$$\begin{aligned}\int_{\tau_i}^{1}\Delta a_*^{(i)}\Delta a_*^{(i-1)}\,d\tau &= \frac{12l^2}{T^3}\frac{1}{1-\tau_{i-1}}\left[\frac{\Delta s_i\Delta s_{i-1}}{(1-\tau_{i-1})^2} + \frac{\Delta s_i\Delta v_{i-1}}{2(1-\tau_{i-1})} + \right.\\ &\left. + \left(1 - 2\,\frac{\tau_i-\tau_{i-1}}{1-\tau_{i-1}}\right)\frac{\Delta v_i\Delta s_{i-1}}{2(1-\tau_{i-1})} + \left(\frac{1}{3} - \frac{1}{2}\,\frac{\tau_i-\tau_{i-1}}{1-\tau_{i-1}}\right)\Delta v_i\Delta v_{i-1}\right],\\ \int_{\tau_i}^{1}(\Delta a_*^{(i)})^2\,d\tau &= \frac{12l^2}{T^3}\frac{1}{1-\tau_i}\left[\frac{\Delta s_i^2}{(1-\tau_i)^2} + \frac{\Delta s_i\Delta v_i}{1-\tau_i} + \frac{1}{3}\,\Delta v_i^2\right].\end{aligned} \tag{12.27}$$

524 The mathematical expectation for the increment of the functional is therefore equal, with an accuracy of order θ, to

$$\begin{aligned}M(\Delta J) = \frac{12l^2}{T^3}\left\{\sum_{i=1}^{m}\left[\frac{1}{3}\,\sigma_a^2\theta\,(2\xi_i^3 - 3\xi_i^2 + 2\xi_i - 1) + \right.\right.\\ + \frac{(\sigma_{nv}^{(i-1)})^2}{1-\tau_i}\,\xi_i\,(\xi_i - 1) + \frac{(\sigma_{nv}^{(i-1)})^2 - (\sigma_{nv}^{(i)})^2}{3\,(1-\tau_i)} + \frac{(\sigma_{ns}^{(i-1)})^2 - (\sigma_{ns}^{(i)})^2}{(1-\tau_i)^3}\Big] +\\ \left. + \frac{\sigma_a^2}{12} + \frac{2}{3}\,\frac{(\sigma_{nv}^{(m)})^2}{1-\tau_m} + 2\,\frac{(\sigma_{ns}^{(m)})^2}{(1-\tau_m)^2}\right\};\\ \sigma_{nv}^{(0)} = \sigma_{0v},\ \ \sigma_{ns}^{(0)} = \sigma_{0s},\ \ \xi_i = \frac{1-\tau_{i-1}}{1-\tau_i}.\end{aligned} \tag{12.28}$$

At the end of the motion ($\tau = 1$) the trajectory must enter the specified region of terminal values of the coordinates and velocities, i.e., the expected deviations from the required trajectory at the end of the motion must have an upper bound. This condition is expressed, similarly to (12.13), in the forms

$$\left.\begin{aligned}&2\sigma_a^2\theta\,(1-\tau_m) + (\sigma_{nv}^{(m)})^2 \leqslant \delta v_{\max}^2,\\ &\frac{2}{3}\,\sigma_a^2\theta\,(1-\tau_m)^3 + (\sigma_{nv}^{(m)})^2\,(1-\tau_m)^2 + (\sigma_{ns}^{(m)})^2 \leqslant \delta s_{\max}^2.\end{aligned}\right\} \tag{12.29}$$

4. Optimum distribution of the correction points. The inequalities impose restrictions on τ_m when investigating the minimum of $M(\Delta J)$ with respect to $\tau_i\,(i = 1, \ldots, m)$.

If measurement errors are neglected ($\sigma_{nv}^{(i)} = \sigma_{ns}^{(i)} = 0$) and if the initial conditions are considered to be exactly satisfied ($\sigma_{0v} = \sigma_{0s} = 0$) we obtain the geometric progression formula for the optimum distribution of the correction points:

$$\xi_{i\,\mathrm{opt}} = \left(\frac{1-\tau_{i-1}}{1-\tau_i}\right)_{\mathrm{opt}} = (1-\tau_m)^{-1/m} \qquad (i = 1, \ldots, m). \tag{12.30}$$

The minimum value for the mathematical expectation of the functional increment of J for the specified number of correction points

$$\left.\begin{aligned} M(\Delta J)_{\min} &= \frac{12l^2}{T^3}\sigma_a^2\left(\frac{1}{3}\theta\varphi_1 + \frac{1}{12}\right), \\ \varphi_1 &= m\left[2(1-\tau_m)^{-3/m} - 3(1-\tau_m)^{-2/m} + 2(1-\tau_m)^{-1/m} - 1\right] \end{aligned}\right\} \tag{12.31}$$

is monotonic decreasing with increasing m, and

$$\lim_{m\to\infty}\varphi_1 = -\ln(1-\tau_m) \tag{12.32}$$

525 (cf. $\log(1+\varphi_1)$ in Figure 12.1, a as a function of m and $(1-\tau_m)$). It is also seen that φ_1 decreases with an increase in $(1-\tau_m)$; therefore the optimum point for the last correction must be located when the vehicle is at the maximum possible distance from the end of the trajectory and must be compatible with the above inequalities, where

$$(1-\tau_m)_{\mathrm{opt}} = \min\left\{\frac{1}{2}\frac{\delta v_{\max}^2}{\sigma_a^2\theta},\ \sqrt[3]{\frac{3}{2}\frac{\delta s_{\max}^2}{\sigma_a^2\theta}}\right\}. \tag{12.33}$$

For a constant finite dispersion of the measurement errors ($\sigma_{nv}^{(i)} = \sigma_v$, $\sigma_{ns}^{(i)} = \sigma_s$, $i = 0, 1, \ldots, m$) the optimum distribution of the correction points

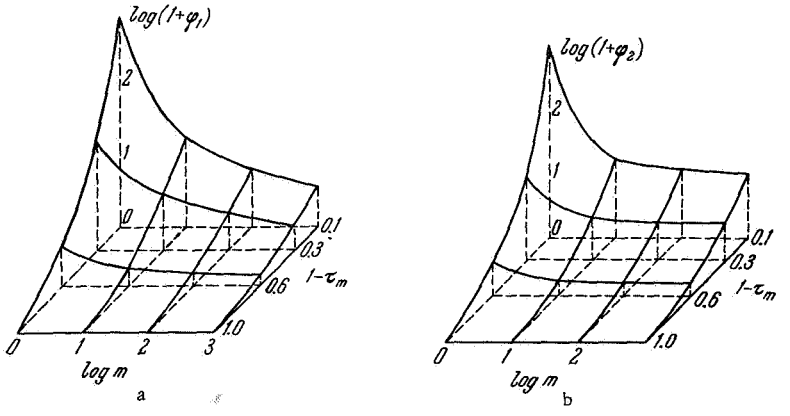

FIGURE 12.1. Mathematical expectation of increment of functional J necessary for correcting trajectory of ideal power-limited engine, as function of number of correction points m and of interval $(1-\tau_m)$ between last correction and trajectory end. Maneuver is that of displacement between positions of rest, where φ_1 is dispersion factor of errors in executing thrust-acceleration program, φ_2 is dispersion factor of errors when measuring velocity (cf. (12.31), (12.34)).

will not be expressed by a formula as simple as (12.30), and must be determined linearly. If we use (12.30), the manner in which $M(\Delta J)$ depends on m and $(1-\tau_m)$ is preserved (Figure 12.1, b), so that

$$\left.\begin{aligned} M(\Delta J) &= \frac{12l^2}{T^3}\left\{\sigma_a^2\left(\frac{1}{3}\theta\varphi_1+\frac{1}{12}\right)+\sigma_v^2\varphi_2+2\sigma_s^2(1-\tau_m)^{-3}\right\}, \\ \varphi_1 &= m\left[2(1-\tau_m)^{-3/m}-3(1-\tau_m)^{-2/m}+2(1-\tau_m)^{-1/m}-1\right], \\ \varphi_2 &= (1-\tau_m)^{-2/m}\left[(1-\tau_m)^{-1}-1\right]+\frac{2}{3}(1-\tau_m)^{-1}. \end{aligned}\right\} \qquad (12.34)$$

526 We shall discuss the results obtained. Optimum correction in the formulation given here involved an a priori selection of the weight relations (which are optimum on the average) and the optimum thrust-acceleration programs (which ensure the maximum payload).

For exact measurements the optimum distribution for the correction points is given by the geometric-progression formula (12.30). The correction points are more closely spaced towards the end of the trajectory. The point at which the last correction must be carried out should be as far from the trajectory end as is compatible with the condition that the trajectory end lies within the specified region of terminal values of the coordinates and velocities.

The concentration of correction points near the end of the trajectory is wholly natural. At the beginning of the motion we have ample time to correct deviations from the required trajectory, and can tolerate large deviations without using the corrections $\Delta a_*^{(i)}$ (12.19) very much. This means we may fly a longer time during the intermediate stages without correcting the path than we can toward the end of the motion. Such spacing of the correction points was also obtained in /12.14/, which treats the impulsive correction of ballistic trajectories. In the case of an impulsive correction an error is only introduced at the times of applying the impulses, while in our case the error is continuously accumulated, independently of whether or not a correction is made. Therefore, in the case of exact measurements no optimum number m of correction points exists.

If, however, the dispersion of the errors differs from zero and depends on the intervals between the correction points, it follows from (12.28) that an optimum number of correction points exists for which $M(\Delta J)$ has a minimum.

Part III

ESTABLISHING OPTIMUM SOLUTIONS

Chapter Thirteen

ANALYTIC SOLUTIONS OF THE EQUATIONS OF DYNAMICS

529 The variational problems formulated in the first two parts generally lead to complex systems of differential equations. It is almost always impossible to establish optimum control functions and optimum trajectories of motion in analytic forms for true gravitational fields. Analytic solutions are however of particular interest in view of their greater clarity and the possibilities they offer of parametric analysis.

These undoubted advantages led to the development of different methods for obtaining explicit solutions. Naturally, these solutions are obtained at the price of replacing the true gravitational field by a simpler one, and of deviations from the optimum criterion of the control functions.

The first of these simplifications affects the result relatively little. In fact, the motion of the spacecraft in the complex field of several gravitational centers can be split, with sufficient accuracy, into stages in each of which only one of the centers is considered as acting. Thus, the transfer of a low-thrust vehicle from the artificial-satellite orbit of one planet to that of another one in the true gravitational field can be split into two zones: a zone of motion in the field of a planet under the perturbing action of the Sun and the other planets, and a zone of flight in the field of the Sun under the perturbing action of the planets. In each of these zones perturbations may be neglected and the gravitational fields considered as central (cf. the Appendix for more details).

The latter assumption is adopted in this chapter. The equations of dynamics are written for two-dimensional or three-dimensional motion in a central field. The differential equations are hence simplified, but not sufficiently so to yield explicit expressions for the optimum control functions and trajectories.

To achieve this aim we shall consider control functions which are, generally speaking, nonoptimum but enable us to obtain exact or approxi-
530 mate formulas which govern the motion. Each such solution represents an elementary space maneuver, where the specified maneuver is split into elementary ones. The control functions and the trajectory of the motion thus obtained will be nonoptimum, but will nevertheless supply information about the main features of the maneuver.

The following space maneuvers are usually considered for vehicles with low-thrust engines: interplanetary transfer from the artificial-satellite orbit of one planet to that of another one (Earth—Mars, Earth—Venus); variation of the satellite orbit in space; holding a specified orbit under the action of perturbing influences caused by the noncentral effects of the gravitational field of the planet, the atmosphere, etc.

These maneuvers will be called complex maneuvers. They are split into elementary ones: escape in a central gravitational field from a circular initial orbit, the inverse maneuver, i.e., capture of the vehicle by the gravitational field into a circular orbit, transfer between circular coplanar orbits, rotation of the orbital plane, altering the satellite position on the orbit and changing the orbit elements (major semiaxis, eccentricity, inclination, apogee and perigee radii, focal parameter), etc. Some of these maneuvers are described in the Appendix.

Attention is paid mainly to elementary maneuvers with a specified orientation of the thrust-acceleration vector of constant magnitude α; the acceleration vector, as a rule, has some specified direction: radial, transverse, tangential or normal to the trajectory, perpendicular to the instantaneous orbital plane, constant in space, etc.

This chapter aims at describing the solutions of the equations of dynamics for the cases listed; preliminary data on the form of the equations of motion are given in § 1 of the Appendix.

§ 1. RADIAL ACCELERATION ($a_\varphi = 0$ in (A.9))

1. Equations and integrals of motion. For $a_\varphi = 0$ the system (A.9) has the form*

$$\left.\begin{aligned} v_r v_r' &= a_r + v_\varphi^2/r - 1/r^2, \\ v_r v_\varphi' &= -v_r v_\varphi / r. \end{aligned}\right\} \tag{13.1}$$

The second equation expresses the law of conservation of angular momentum (A.12); its solution is

$$v_\varphi = M/r. \tag{13.2}$$

531 With the aid of this expression for v_φ the first equation of system (13.1) may be represented in the form

$$\frac{d}{dr}\left(\frac{1}{2}v_r^2\right) = \frac{M^2}{r^3} - \frac{1}{r^2} + a_r. \tag{13.3}$$

If the thrust acceleration is constant ($a_r \equiv \text{const}$), this equation is integrable and yields

$$\frac{1}{2}v_r^2 - \frac{1}{2}v_{r0}^2 = -\frac{M^2}{2r^2} + \frac{1}{r} + a_r r + \frac{M^2}{2r_0^2} - \frac{1}{r_0} - a_r r_0. \tag{13.4}$$

Here v_{r0}, r_0, $M = v_{\varphi 0} r_0$ are the initial motion parameters. If the initial orbit is circular, i.e., $r_0 = 1$, $v_{r0} = 0$, $v_{\varphi 0} = 1$, equation (13.4) simplifies and gives the radial velocity in the form

$$v_r = \pm\sqrt{-\frac{1}{r^2} + \frac{2}{r} + 2a_r(r-1) - 1} = \pm\sqrt{\frac{2a_r}{r_2}(r-1)(r-r_1)(r-r_2)}, \tag{13.5}$$

* In this chapter the equations are presented in dimensionless form; the transformation to dimensionless variables is described in § 1 of the Appendix.

where

$$r_1 = \frac{1+\sqrt{1-8a_r}}{4a_r}, \quad r_2 = \frac{1-\sqrt{1-8a_r}}{4a_r}. \tag{13.6}$$

These expressions show that different regimes of motion exist depending on the magnitude and sign of the acceleration a_r. For $a_r < 0$ the motion is bounded ($1 \geqslant r \geqslant r_2 > 0$); for $1/8 > a_r > 0$ it is likewise bounded ($1 \leqslant r \leqslant r_1 \leqslant 2$); for $a_r > 1/8$ it is unbounded ($r \geqslant 1$).

The last regime was studied in /13.1/ for the problem of escape from a central gravitational field. The motion with low values of the radial acceleration ($a_r \ll 1/8$) was studied in /13.2/. A general study of the regimes was undertaken in /13.3/, where formulas were derived for the angle φ and the time t as functions of the radius r (cf. also /13.4, 13.5/). These formulas have the form:

for $a_r < 0$,

$$\left.\begin{aligned} t &= \int_1^r \frac{dr}{v_r} = \frac{\sqrt{2}}{\sqrt{-a_r(1-r_1)}}\left[r_1 F(\beta, k) + (1-r_1)E(\beta, k) + \right. \\ &\qquad \left. + \frac{(1-r_2)\sin 2\beta}{2\sqrt{1-k^2\sin^2\beta}}\right], \\ \varphi &= \int_1^r \frac{dr}{v_r r^2} = -\frac{\sqrt{2}}{r_1\sqrt{-a_r(1-r_1)}}\left[\frac{r_2-r_1}{r_2}\pi\left(\beta, -\frac{r_1}{r_2}, k\right) - F(\beta, k)\right], \end{aligned}\right\} \tag{13.7}$$

where

$$k^2 = \frac{1-r_2}{1-r_1}, \quad r = \frac{-r_1 k^2 \sin^2\beta + r_2}{-k^2\sin^2\beta + 1}; \tag{13.8}$$

for $0 < a_r < 1/8$,

$$\left.\begin{aligned} t &= \frac{\sqrt{2}}{\sqrt{a_r(r_1-1)}}[r_1 F(\beta, k) - (r_1-1)E(\beta, k)], \\ \varphi &= \frac{\sqrt{2}}{\sqrt{a_r(r_1-1)}}\pi(\beta, r_2-1, k), \end{aligned}\right\} \tag{13.9}$$

where

$$k^2 = \frac{r_2-1}{r_1-1}, \quad r = (r_2-1)\sin^2\beta + 1; \tag{13.10}$$

for $a_r = 1/8$,

$$\left.\begin{aligned} t &= 4[2\ln \operatorname{tg}(\pi/4 + \xi/2) - \sin\xi], \\ \varphi &= 2[\omega + 1/2 \ln \operatorname{tg}(\pi/4 + \omega)], \end{aligned}\right\} \tag{13.11}$$

where

$$\sin^2\xi = r - 1, \quad \operatorname{tg}^2\omega = r - 1; \tag{13.12}$$

for $a_r > 1/8$,

$$\left.\begin{aligned} t &= \sqrt{\frac{2}{a_r}}\left[\frac{1+\cos\beta}{\sin\beta}\sqrt{1-k^2\sin^2\beta} - F(\beta, k) + E(\beta, k)\right], \\ \varphi &= \arcsin(k\sin\beta) - \frac{1}{\sqrt{8a_r}}F(\beta, k), \end{aligned}\right\} \tag{13.13}$$

where

$$r = \frac{2}{1 - \cos\beta}, \quad k^2 = \frac{1}{8a_r}. \tag{13.14}$$

In formulas (13.7) to (13.14) we employ standard symbols for the elliptic integrals of the first $F(\beta, k)$, second $E(\beta, k)$, and third $\pi(\beta, \alpha, k)$ kinds. The integration constants are selected with the aid of the initial condition $t = \varphi = 0$; r_1 and r_2 are the roots of the equation for the radial velocity (cf. (13.6)).

2. **Build-up of a parabolic velocity.** For $a_r > 1/8$ the motion is unbounded, and therefore the corresponding regime can be used to analyze the maneuver of parabolic velocity build-up from an initial circular orbit /13.1/.

If we substitute the expressions for the velocity vector components v_r and v_φ from (13.2) and (13.5) into (A.11) for the energy E, we obtain the energy as a function of the radius r:

$$E = a_r(r - 1) - 1/2 \tag{13.15}$$

533 (the initial value of the energy in dimensionless units is $E_0 = -1/2$ for $r_0 = 1$).

The following relation between the radius at the terminal point r_1, and the value of the radial acceleration is derived from the condition of a parabolic velocity build-up ($E_1 = 0$):

$$r_1 = 1 + \frac{1}{2a_r}. \tag{13.16}$$

The maximum value of the terminal radius is $r_1 = 5$ ($a_r = 1/8$) and its minimum value is $r_1 = 1$ ($a_r = \infty$). The time t_1 and the angle φ_1 at the end of the maneuver are found from formulas (13.13) and (13.14), if we replace r by r_1. The radial and transverse velocity components at the terminal point are determined by the expressions

$$v_{r1} = \frac{2\sqrt{a_r + a_r^2}}{1 + 2a_r}, \quad v_{\varphi_1} = \frac{2a_r}{1 + 2a_r}. \tag{13.17}$$

The values in (13.16) and (13.17) for a parabolic velocity build-up with constant radial acceleration are correct for $a_r \geqslant 1/8$; smaller values of a_r correspond to bounded motions. Unbounded motion can also be obtained at low values of the acceleration ($a_r < 1/8$), if its direction is reversed at appropriate points of the trajectory.

The solution of the problem to build up a parabolic velocity with low alternately positive and negative radial accelerations is given in /13.6/ and /13.7/. Following the treatment in /13.7/, we consider a geometric curve of the square of the eccentricity vs. radius. When deriving the formulas we do not assume an initial circular orbit.

In the Appendix (cf. (A.21), (A.22)) the eccentricity ε is expressed as a function of the perihelion radius r_π

$$\varepsilon = \frac{M^2}{r_\pi} - 1. \tag{13.18}$$

With the energy equation one may link the perihelion radius with the instantaneous radius r and the radial velocity v_r so that

$$E = \frac{v_r^2}{2} + \frac{M^4}{2r^2} - \frac{1}{r} = \frac{M^4}{2r_\pi^2} - \frac{1}{r_\pi}, \tag{13.19}$$

whence

$$\varepsilon^2 = M^4 v_r^2 + \left(1 - \frac{M^4}{r}\right)^2. \tag{13.20}$$

534 This is a basic relation in the following discussion. Figure 13.1 shows the curve of zero velocity in $(r/M^4, \varepsilon^2)$ coordinates (the solid curve). As $r \to \infty$ the curve approaches $\varepsilon^2 = 1$ asymptotically, and intersects the horizontal line $\varepsilon^2 = 1$ at $r = {}^1/_2 M^4$. In the absence of a perturbing acceleration the motion shown on the curve corresponds to a finite (for $\varepsilon^2 < 1$) or infinite (for $\varepsilon^2 > 1$) displacement along the horizontal line.

The derivative $d\varepsilon^2/dr$ is (using equation (13.3))

$$\frac{d\varepsilon^2}{dr} = 2M^4 a_r, \tag{13.21}$$

from which, for a constant value of a_r, we obtain

$$\varepsilon^2 = \varepsilon_0^2 + 2M^4 a_r (r - r_0). \tag{13.22}$$

The motion under a perturbing acceleration of constant direction corresponds to a finite or infinite displacement along a straight line of $2M^4 a_r$. In Figure 13.1 a trajectory with constant radial acceleration and direction is represented by the line 1—2, where point 1 is the perihelion, and point 2 is the aphelion of the perturbed orbit. Here the motion oscillates along the line 1—2, and the maximum value of the eccentricity is attained at point 2 when

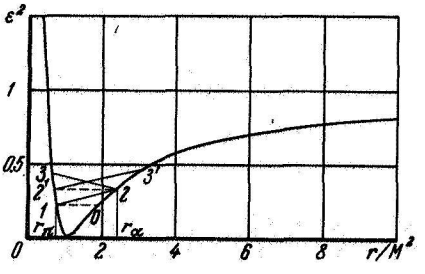

FIGURE 13.1. Square of eccentricity ε^2 vs. relative radius r/M^4.

$$\varepsilon_2^2 = \varepsilon_1^2 + 2M^4 a_r (r_2 - r_1).$$

If the perturbing force changes sign at point 2 ($a_r < 0$), the value of the eccentricity on such an orbit (point 3) exceeds the previous maximum (point 2). Repeated execution of such a maneuver 1—2, 2—3 ensures the build-up of a specified eccentricity for an arbitrarily low perturbing acceleration. In this manner one may control a parabolic velocity build-up ($\varepsilon^2 = 1$) using a radial acceleration lower than the limiting value ($a_r < {}^1/_8$).

The same effect can be achieved if instead of reversing the acceleration we introduce coasting segments, as shown in Figure 13.1 (the segments 1—2—2'—3').

It has already been established that the limiting value of the constant
535 acceleration for building up a zero energy from a circular orbit is $^1/_8$ in dimensionless units (the radius and time on this circular orbit are taken as measurement units). At take-off from an elliptic orbit the limiting value may be higher. Figure 13.1 shows that the worst conditions in this sense occur on the right-hand branch of the curve of zero radial velocity (at the apogee) when the slope is maximum $r_0/M^2 = 1.5$, $\varepsilon_0^2 = {}^1/_9$ at which $a_r = 4/(27M^4)$.

3. Orbital transfer. Examples of transfer to the orbits of Mars and Venus with a constant radial acceleration are given in /13.3—13.5/. So that the transfer orbit might have a zero radial velocity at the orbit of Mars or Venus, we must have an acceleration lower than $^1/_8$ (bounded motion). In view of condition (13.2), the transverse component of the velocity cannot be made equal to the circular velocity on the destination orbit by selecting any magnitude or sign for the thrust acceleration. Therefore, the velocity of the vehicle relative to the destination planet always differs from zero.

The orbital transfer to the orbits of Mars and Venus with a radial acceleration was also studied in /13.8/; in that paper the magnitude of the acceleration is not constant, however, but is proportional to the radial distance, i.e., $a_r = br$.

The case of a variable radial acceleration, ensuring a constant radial velocity,

$$v_r = \text{const}, \qquad a_r = \frac{M^2}{r^3} - \frac{1}{r^2} \tag{13.23}$$

is examined in /13.7/ in addition to the case of constant acceleration.

The motion with a radial acceleration given by

$$a_r = \frac{a_0}{r^2} \tag{13.24}$$

was studied in /13.9—13.10/.

This thrust acceleration holds for vehicles with solar sail set perpendicular to the solar rays (cf. § 4 of Chapter Nine).

The equations of motion (13.1) with the acceleration in the form (13.24) describe a Keplerian trajectory with a different gravitational constant (replaced by a_0).

Let the vehicle be placed initially on a circular orbit of unit radius. The eccentricity ε and the semimajor axis A are (cf. (A.21) to (A.23))

$$\varepsilon = \frac{a_0}{1 - a_0}, \qquad A = \frac{1}{|2 - 1/(1 - a_0)|}. \tag{13.25}$$

It follows that when $a_0 < 0.5$ the flight trajectory is an ellipse, when $a_0 = 0.5$ it is a parabola, and when $a_0 > 0.5$ it is a hyperbola.

536 For transfer between the circular orbits $r_0 = 1$ and $r_1 > 1$ along an ellipse which is tangential to the circular destination orbit at the apogee, we require

$$a_0 = (r_1 - 1)/2r_1. \tag{13.26}$$

The flight time is then $\sqrt{2r_1/(r_1 + 1)}$ times larger than the flight time along the corresponding Hohmann ellipse, and the final velocity is $\sqrt{r_1}$ times larger

than the circular velocity at radius r_1. The dependence of the time of flight from the Earth orbit to the Mars orbit on the quantity a_0 is shown in Figure 13.2.

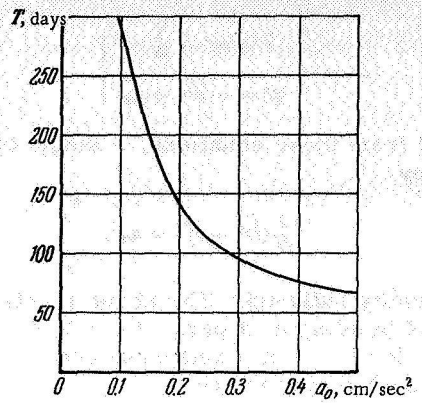

FIGURE 13.2. Dependence of flight time from Earth orbit to Mars orbit on a_0 ($a_r = a_0/r^2$).

4. Variation of the orbital elements. The angular momentum M and the radii of the points situated at maximum and minimum distances from the center, r_α and r_π respectively, remain fixed for trajectories with a constant radial acceleration. These properties follow from Subsections 1 and 2 of this section.

If the unperturbed orbit is circular or quasicircular ($\varepsilon_0 \ll 1$), and the perturbing acceleration is low ($a_r \ll 1/8$), the greatest difference between the maximum and minimum radii is

$$r_\alpha - 1 \approx 2a_r, \tag{13.27}$$

and the maximum value of the eccentricity, determined by expression (13.20), is then given by

$$\varepsilon_{\max} = 2a_r \tag{13.28}$$

(in (13.27) and (13.28) the minimum distance, equal to the radius of the unperturbed orbit, is taken as unit length).

The line of apsides, defined as the line connecting the points situated at maximum and minimum distances from the center, shifts by $2\pi a_r$ radians per revolution under the action of a low radial acceleration.

The results described here have been obtained by many authors. Reference /13.2/ uses the expansion in terms of the small parameter a_r in the expressions for the variation of the orbital elements. In /13.11/ the
537 Krylov—Bogolyubov method was applied to equations (A.26). The results obtained in /13.11/ coincide with those of /13.2/, except for one conclusion regarding the regression of the line of apsides. Another method, that of varying the parameters (as applied to the analysis of altering the orbital parameters) is described in /13.12, 13.13/. The results obtained in these papers also agree with those presented above.

§ 2. TRANSVERSE ACCELERATION ($a_r = 0$ in (A.7))

1. Equations of motion. When only the transverse component of the thrust acceleration is preserved, equations (A.7) reduce to

$$\left.\begin{aligned} \ddot{r} &= r\dot{\varphi}^2 - \frac{1}{r^2}, \\ \dot{\varphi}r &= -2\dot{r}\dot{\varphi} + a_\varphi. \end{aligned}\right\} \tag{13.29}$$

If $\dot{\varphi}$ is eliminated from these equations, a single cubic equation results for r given by

$$\frac{d}{dt}(\ddot{r}r^3 + r)^{1/3} = a_\varphi r. \tag{13.30}$$

2. Parabolic velocity build-up. The above-mentioned paper /13.1/ treats the problem of building up a parabolic velocity from a circular orbit under the action of a low constant transverse acceleration ($a_\varphi \ll 1$). The initial conditions of such a motion are

$$r_0 = 1, \quad \dot{r}(0) = 0, \quad \dot{\varphi}_0 = 1. \tag{13.31}$$

The initial value of the second derivative $\ddot{r}_0$, which is required when solving equation (13.30) instead of system (13.29), is found from the first equation of (13.29)

$$\ddot{r}_0 = 0. \tag{13.32}$$

It is assumed in /13.1/ that for small a_φ the term $\ddot{r}r^3$ in (13.30) is considerably smaller than r, and so can be neglected. A simple differential equation is then obtained whose solution is

$$r = (1 - a_\varphi t)^{-2}. \tag{13.33}$$

The remaining parameters of motion $\dot{r}(t)$, $\ddot{r}(t)$, $\varphi(t)$, $\dot{\varphi}(t)$ are now expressed using this result in the forms

$$\left.\begin{aligned} \dot{r}(t) &= 2a_\varphi(1 - a_\varphi t)^{-3}, & \ddot{r}(t) &= 6a_\varphi^2(1 - a_\varphi t)^{-4}, \\ \varphi(t) &= (4a_\varphi)^{-1}[1 - (1 - a_\varphi t)^4], & \dot{\varphi}(t) &= (1 - a_\varphi t)^3. \end{aligned}\right\} \tag{13.34}$$

In polar coordinates $r(\varphi)$ the orbit equation takes the form

$$r = (1 - 4a_\varphi\varphi)^{-1/2}; \tag{13.35}$$

for low a_φ the orbit is a shallow spiral.

According to (13.34), the initial values $\dot{r}_0$, $\ddot{r}_0$ differ from zero:

$$\dot{r}_0 = 2a_\varphi, \quad \ddot{r}_0 = 6a_\varphi^2, \tag{13.36}$$

which contradicts the initial conditions (13.31) and (13.32).

At the point of parabolic velocity build-up ($E_1 = 0$) the parameters of the motion are

$$\left.\begin{aligned} &T = a_\varphi^{-1}[1 - (2a_\varphi)^{1/4}], \quad \varphi_1 = (4a_\varphi)^{-1} - 1/2, \quad \dot{\varphi}_1 = (2a_\varphi)^{3/4}, \\ &r_1 = (2a_\varphi)^{-1/2}, \qquad\qquad \dot{r}_1 = (2a_\varphi)^{1/4}, \qquad\qquad \ddot{r}_1 = 3a_\varphi. \end{aligned}\right\} \tag{13.37}$$

The term $\ddot{r}r^3$, which is neglected in equation (13.30), is larger than r at the final point, at which

$$\ddot{r}_1 r_1^3 = 3/2\,(2a_\varphi)^{-1/4}, \quad r_1 = (2a_\varphi)^{1/2}. \tag{13.38}$$

This implies that it is incorrect to simplify differential equation (13.30) for the final part of the trajectory.

The motion described by (13.34) is characterized by the equality of the centrifugal and gravitational accelerations ($r\dot{\varphi}^2 = 1/r^2$) at each point. The fact that the second derivative $\ddot{r}$ does not vanish along the whole trajectory indicates that the first equation of (13.29) is not quite satisfied. If, in addition to the transverse acceleration component, we introduce a radial component $a_r = \ddot{r} = 6a_\varphi^2(1 - a_\varphi t)^{-4}$, the solution obtained above is the exact solution of equations (13.29) with components a_r, a_φ. During the initial stage of the motion the component a_r, taken in this form, is of second-order magnitude as compared with a_φ. On that part of the trajectory where the velocity approaches the local parabolic velocity, the radial component a_r becomes commensurate with the transverse component a_φ (cf. /13.14—13.16/).

3. **Representing the solution in series form.** A different approach is suggested in /13.17/ with regard to determining the characteristics of the motion with transverse acceleration. Using the method of variation of the parameters, one may express the functions $r(t)$, $\dot{r}(t)$, $M(t) = r^2(t)\dot{\varphi}(t)$ as a power series in the small variable a_φ:

$$\left.\begin{aligned} r(t) &= 1 + a_\varphi(2t - 2\sin t) + a_\varphi^2(3t^2 + 3t^2\cos t - \\ &\qquad - t\sin t - 4\sin^2 t + 2\cos t - 2) + \ldots, \\ \dot{r}(t) &= a_\varphi(2 - 2\cos t) + a_\varphi^2(6t + 5t\cos t - 3t^2\sin t - \\ &\qquad - 3\sin t - 8\sin t\cos t) + \ldots, \\ M(t) &= 1 + a_\varphi t + a_\varphi^2(t^2 + 2\cos t - 2) + \ldots \end{aligned}\right\} \tag{13.39}$$

539 These functions exactly satisfy the initial conditions (13.31), and approximately satisfy equations (13.29) (with an accuracy of order a_φ^3).

A similar approach is used in /13.12, 13.13/; a correction to solution (13.34) was obtained in /13.18/.

4. **Variation of the orbital elements.** The eccentricity of the osculating ellipse for motion along the spiral (13.34) is a monotonic function of time given by

$$\varepsilon = 2a_\varphi(1 - a_\varphi t)^{-4}; \tag{13.40}$$

for motion along the trajectory described by expressions (13.39), it is a periodic function of time

$$\varepsilon = 4a_\varphi\left|\sin\frac{t}{2}\right|. \tag{13.41}$$

The maximum increment in the radial distance Δr per revolution at take-off from a circular orbit of unit radius is equal to /13.11/

$$\Delta r = 4\pi a_\varphi. \tag{13.42}$$

§ 3. TANGENTIAL ACCELERATION ($\nu = 0$ in (A.16))

The tangential direction of the thrust-acceleration vector is the direction nearest to the optimum in the problem of parabolic velocity build-up from a circular orbit. It was shown in /13.19—13.20/ that the acceleration vector of constant magnitude in the optimum build-up program lies at any instant between two directions: the tangential and the transverse; it coincides with the latter at the final point of the maneuver. If the acceleration is constant and directed tangentially throughout the motion, the difference between the escape time and the optimum escape time does not exceed 0.5% for values of a in the range $0 < a \leqslant 0.1$. Over the same range of values of the acceleration magnitude the difference between the optimum and the transverse program is less than 8.5%. These results were obtained in analytic form; the calculations /13.31/ corroborated the values given (cf. § 3 of Chapter Six).

Similar results were obtained in /13.22/; these dealt with transverse and tangential programs for a thrust of constant magnitude.

540 **1. Equations and integral of motion.** For a tangential direction of the acceleration vector system (A.16) has the form

$$\left.\begin{aligned} v\frac{dv}{ds} &= a - \frac{dr}{ds}\frac{1}{r^2}, \\ v^2\left[\frac{d^2r}{ds^2}r - 1 - \left(\frac{dr}{ds}\right)^2\right] &= \frac{1}{r}\left[\left(\frac{dr}{ds}\right)^2 - 1\right]. \end{aligned}\right\} \tag{13.43}$$

Here the derivative dr/ds replaces the functions of the angle ϑ.

The initial conditions for the problem of parabolic velocity build-up from a circular orbit are

$$r = 1,\ dr/ds = 0,\ v = 1 \quad \text{at} \quad s = 0. \tag{13.44}$$

The first equation of (13.43) can be integrated in an explicit form for the case of an acceleration of constant magnitude; allowing for the initial conditions (13.44), we obtain

$$^1/_2 v^2 = 1/r + as - {}^1/_2. \tag{13.45}$$

This equation shows how the energy E varies along the trajectory,

$$E = as - {}^1/_2; \tag{13.46}$$

the length of the transfer trajectory is

$$s_1 = 1/(2a). \tag{13.47}$$

Note that the tangential direction of the acceleration corresponds to the maximum rate of energy increase, where $\dot{E} = av$ (cf. (A.14)).

When the expression for v^2 is substituted into the second equation of (13.43), we obtain a second-order differential equation for $r(s)$ with initial conditions (13.44),

$$\left[\frac{d^2r}{ds^2}r - 1 + \left(\frac{dr}{ds}\right)^2\right](2 + 2ras - r) = \left(\frac{dr}{ds}\right)^2 - 1. \tag{13.48}$$

System (13.43) was reduced to this form in /13.23/.

2. **Approximate solutions of (13.48).** For small values of the argument s ($s \ll 1$) the solution of equation (13.48) can be represented as a power series in a. The first three terms of the series have the form /13.23/

$$r = 1 + 2a(s - \sin s) + \\ + 4a^2(s^2 + {}^1/_2 s^2 \cos s - {}^1/_2 s \sin s + 2\cos s - 2) + \ldots \tag{13.49}$$

The first two terms of expansions (13.39) and (13.49) are alike; it follows that the transverse and tangential acceleration programs yield the same functional expressions for r at low values of the argument t or s (at the beginning of the motion $s \approx t$, since $ds/dt = v \approx 1$).

541 Similar expressions were obtained in /13.24, 13.25/, where the parameters of motion were expressed in terms of φ, the angular displacement.

With the aid of (13.49) one may find the first two terms of the expansion for the velocity magnitude v, so that

$$v = 1 - a(s - 2\sin s). \tag{13.50}$$

It is seen from (13.49) and (13.50) that the motion is oscillatory. Oscillations with a period of revolution 2π on the initial orbit, are superposed on the average motion ($\bar{r} = 1 + 2as$, $\bar{v} = 1 - as$). These oscillations originate from the mutual transitions of kinetic and potential energies.

An interesting fact is that the centrifugal and gravitational accelerations on the average trajectory are equal with an accuracy of order a^2: $v^2/r \approx 1/r^2$.

A simple analytic expression for r was suggested in /13.23/, where

$$r = (1 - 2as)^{-1}. \tag{13.51}$$

This formula is obtained by eliminating the term $(d^2r/ds^2)\,r$ in (13.48) (considering it as small compared with unity). A similar method was studied in the preceding section in connection with expression (13.33), and the comments made there apply to this case too with no basic modifications.

3. **Asymptotic solutions of the acceleration problem.** The problem of accelerating from a circular orbit under the action of a tangential acceleration was solved in /13.26/. The final position of the motion is characterized by a specified energy, which is not necessarily equal to zero (acceleration to hyperbolic velocities).

The analysis starts with a system which describes plane motion in osculating variables:

$$\dot{p} = \frac{2p}{v}a, \qquad \dot{\varphi}_n = \frac{2\sin\nu}{v\varepsilon}a, \\ \dot{\varepsilon} = 2\frac{\varepsilon + \cos\nu}{v}a, \qquad \dot{\nu} = \frac{\sqrt{p}}{r^2} - \frac{2\sin\nu}{v\varepsilon}a, \tag{13.52}$$

where p is the focal parameter, ε is the eccentricity, φ_π is the angular
542 displacement of the perihelion, and ν is the true anomaly. The velocity v and the radius r are determined by the formulas of the unperturbed motion

$$r = \frac{p}{1 + \varepsilon \cos \nu}, \quad v = \sqrt{\frac{1}{p}(1 + \varepsilon^2 + 2\varepsilon \cos \nu)} \tag{13.53}$$

(all parameters in (13.52) and (13.53) are dimensionless). Equations (13.52) and (13.53) represent a particular case of system (A.37) in osculating variables for a tangentially-directed thrust-acceleration vector.

As in /13.25/, we made the substitutions

$$v = (2a)^{1/4}V, \; r = (2a)^{-1/2}R, \; p = (2a)^{-1/2}\pi, \; t = (2a)^{-3/4}\tau. \tag{13.54}$$

System (13.52), (13.53) is then transformed into

$$\left.\begin{aligned} &\frac{d\pi}{d\tau} = \frac{\pi}{V}, \quad \frac{d\varepsilon}{d\tau} = \frac{\varepsilon + \cos \nu}{V}, \\ &\frac{d\varphi_\pi}{d\tau} = \frac{\sin \nu}{V\varepsilon}, \quad \frac{d\nu}{d\tau} = \frac{\sqrt{\pi}}{R^2} - \frac{\sin \nu}{V\varepsilon} \\ &\left(R = \frac{\pi}{1 + \varepsilon \cos \nu}, \quad V = \sqrt{\frac{1}{\pi}(1 + \varepsilon^2 + 2\varepsilon \cos \nu)}\right). \end{aligned}\right\} \tag{13.55}$$

The time τ and the angle φ_π do not appear on the right-hand sides of (13.55), and the system can therefore be split in two parts. The first part is

$$\left.\begin{aligned} &\frac{d\varepsilon}{d\pi} = \frac{\varepsilon + \cos \nu}{\pi}, \\ &\frac{d \cos \nu}{d\pi} = -\frac{1}{\pi^3}\sqrt{1 + \varepsilon^2 + 2\varepsilon \cos \nu}\,(1 + \varepsilon \cos \nu)^2 \sqrt{1 - \cos^2 \nu} + \\ &\qquad + \frac{1 - \cos^2 \nu}{\pi\varepsilon}; \end{aligned}\right\} \tag{13.56}$$

the second is

$$\left.\begin{aligned} &\frac{d\tau}{d\pi} = \sqrt{\frac{1}{\pi^3}(1 + \varepsilon^2 + 2\varepsilon \cos \nu)}, \\ &\frac{d\varphi_\pi}{d\pi} = \frac{\sin \nu}{\pi\varepsilon}. \end{aligned}\right\} \tag{13.57}$$

The solution of the second part is obtained by quadratures after solving the first one, which is a closed system of equations and determines ε and $\cos \nu$ as functions of π.

As a result of transformation (13.54) the acceleration a is eliminated from the right-hand sides of the equations of motion; on the other hand, it is easily seen that the initial conditions represent the problem of accelerating from a circular orbit. As a result, two motions starting from the
543 same circular orbit with different values of a can be described by the same equations, but with different initial conditions.

The solution of the problem of accelerating with a low tangential acceleration possesses one important feature: the trajectories corresponding to different values of a differ little from one another and from the universal trajectory starting from the gravitational center. This universal trajectory may be divided into parts corresponding to different initial conditions in accordance with a specific rule. However, the boundary conditions

are then only approximately fulfilled in that the initial orbit is not a circle, but an ellipse of small eccentricity (which decreases as the acceleration grows smaller).

The existence of a universal trajectory was established by Perkins /13.25/ by numerical analysis. The universal trajectory was plotted in /13.26/; we shall follow the treatment given in that paper, and give the results obtained in it.

It is convenient to split the required trajectory into three characteristic portions. The first portion, the beginning of the trajectory, is described by an asymptotic solution for small π ($\pi \ll 1$, and also $\varepsilon \ll 1$, $\cos \nu \ll 1$); the second portion, the middle of the trajectory, is determined by numerical analysis; the third portion, the end of the trajectory, is described by an asymptotic solution for large π ($\pi \gg 1$, and also $\varepsilon \gg 1$).

For small π the asymptotic formulas for the quantities ε, $\cos \nu$, τ, φ_π have the form

$$\left.\begin{aligned} \varepsilon &= \pi^2 \sum_{k=0} e_k \pi^{4k}, \\ \cos \nu &= \pi^2 \sum_{k=0} \nu_k \pi^{4k}, \\ \varphi_\pi &= -3.40942 + \pi^{-2} \sum_{k=0} \varphi_k \pi^{4k}, \\ \tau &= 1.34571 + \pi^{-1/2} \sum_{k=0} \tau_k \pi^{4k}. \end{aligned}\right\} \qquad (13.58)$$

The values of the expansion coefficients e_k, ν_k, φ_k, τ_k are given in Table 13.1.

TABLE 13.1. Expansion coefficients for formulas (13.58)

k	e_k	ν_k	φ_k	τ_k
0	$1.0 \cdot 10^0$	$1.0 \cdot 10^0$	$-0.5 \cdot 10^0$	$-2.0 \cdot 10^0$
1	$-6.0 \cdot 10^0$	$-3.0 \cdot 10^1$	$2.75 \cdot 10^0$	$-4.285714 \cdot 10^1$
2	$3.53 \cdot 10^2$	$3.177 \cdot 10^3$	$-4.835417 \cdot 10^1$	$-5.75 \cdot 10^0$
3	$-5.0216 \cdot 10^4$	$-6.58080 \cdot 10^5$	$4.292169 \cdot 10^3$	$3.604946 \cdot 10^2$
4	$1.271935 \cdot 10^7$	$2.162289 \cdot 10^8$	$-8.098106 \cdot 10^5$	$-5.110699 \cdot 10^4$
5	$-5.007378 \cdot 10^9$	$-1.051549 \cdot 10^{11}$	$2.555165 \cdot 10^8$	$1.281759 \cdot 10^7$
6	$2.829338 \cdot 10^{12}$	$7.073346 \cdot 10^{13}$	$-1.204903 \cdot 10^{11}$	$-5.010652 \cdot 10^9$
7	$-2.173519 \cdot 10^{15}$	$-6.303206 \cdot 10^{16}$	$7.935154 \cdot 10^{13}$	$2.819974 \cdot 10^{12}$

For large π the expansions of ε, $\cos \nu$, τ, φ_π are

$$\left.\begin{aligned} \varepsilon &= 0.76649\pi + \sum_{k=1} \varepsilon'_k \pi^{-k}, \\ \cos \nu &= \sum_{k=1} \nu'_k \pi^{-k}, \\ \varphi_\pi &= -1.5708 + \pi^{-1} \sum_{k=0} \varphi'_k \pi^{-k}, \\ \tau &= -1.611 + \sum_{k=0} \tau'_k \pi^{-k}. \end{aligned}\right\} \qquad (13.59)$$

544 The coefficients of the series are given in Table 13.2.

The functions $\varepsilon(\pi)$, $\cos \nu(\pi)$, $\varphi_\pi(\pi)$, $\tau(\pi)$ for intermediate values of π are given in Table 13.3, together with the corresponding values of twice the total energy given by

$$\eta = \frac{\varepsilon^2 - 1}{\pi}. \qquad (13.60)$$

TABLE 13.2. Expansion coefficients for formulas (13.59)

k	ε'_k	ν'_k	φ'_k	τ'_k
0	—	—	$-1.30465\cdot10^{0}$	$1.53298\cdot10^{0}$
1	$-4.58000\cdot10^{-1}$	$9.16000\cdot10^{-1}$	0	0
2	$6.80189\cdot10^{-1}$	$-2.04057\cdot10^{0}$	$-7.74093\cdot10^{-2}$	$-7.40216\cdot10^{-1}$
3	$-8.45172\cdot10^{-1}$	$3.38069\cdot10^{0}$	$-3.20210\cdot10^{-1}$	$5.44150\cdot10^{-1}$
4	$8.85247\cdot10^{-1}$	$-4.42624\cdot10^{0}$	$1.05876\cdot10^{0}$	$-3.77374\cdot10^{-1}$
5	$-4.86283\cdot10^{-1}$	$2.91770\cdot10^{0}$	$-2.39421\cdot10^{0}$	$-1.23027\cdot10^{-2}$
6	$-9.64784\cdot10^{-1}$	$6.75349\cdot10^{0}$	$4.44336\cdot10^{0}$	$8.58759\cdot10^{-1}$
7	$4.43942\cdot10^{0}$	$-3.55154\cdot10^{1}$	$-6.81926\cdot10^{0}$	$-2.41946\cdot10^{0}$
8	$-1.10624\cdot10^{1}$	$9.95619\cdot10^{1}$	$7.74454\cdot10^{0}$	$4.80913\cdot10^{0}$
9	$2.11182\cdot10^{1}$	$-2.11182\cdot10^{2}$	$-2.45367\cdot10^{0}$	$-7.51642\cdot10^{0}$
10	$-3.13216\cdot10^{1}$	$3.44538\cdot10^{2}$	$-1.89947\cdot10^{1}$	$8.38035\cdot10^{0}$
11	$2.90194\cdot10^{1}$	$-3.48233\cdot10^{2}$	$7.31602\cdot10^{1}$	$-1.84542\cdot10^{0}$
12	$1.76253\cdot10^{1}$	$-2.29129\cdot10^{2}$	$-1.79535\cdot10^{2}$	$-2.32322\cdot10^{1}$
13	$-1.71363\cdot10^{2}$	$2.39908\cdot10^{3}$	$3.41319\cdot10^{2}$	$8.44939\cdot10^{1}$
14	$5.27883\cdot10^{2}$	$-7.91825\cdot10^{3}$	$-4.90991\cdot10^{2}$	$-2.00619\cdot10^{2}$

TABLE 13.3. Parameters of motion in intermediate region

π	ε	$\cos\nu$	φ_π	τ	η
0.10	0.009994	0.009970	—53.3820	—4.97871	—9.99900
0.12	0.014382	0.014313	—38.0922	—4.42754	—8.33161
0.14	0.019556	0.019382	—28.8661	—3.99908	—7.14013
0.16	0.025503	0.025128	—22.8710	—3.65360	—6.24594
0.18	0.032207	0.031475	—18.7539	—3.36729	—5.54979
0.20	0.039646	0.038332	—15.8022	—3.12493	—4.99214
0.22	0.047793	0.045597	—13.6115	—2.91623	—4.53507
0.24	0.056615	0.053158	—11.9390	—2.73398	—4.15331
0.26	0.066076	0.060904	—10.6313	—2.57297	—3.82936
0.28	0.076137	0.068730	—9.58789	—2.42927	—3.55073
0.30	0.086757	0.076539	—8.74073	—2.29994	—3.30824
0.32	0.097896	0.084250	—8.04234	—2.18264	—3.09505
0.34	0.109512	0.091795	—7.45886	—2.07556	—2.90590
0.36	0.121566	0.099118	—6.96556	—1.97723	—2.73673
0.38	0.134020	0.106179	—6.54409	—1.88645	—2.58431
0.40	0.146838	0.112949	—6.18056	—1.80226	—2.44610
0.45	0.180027	0.110190	—5.39184	—1.61006	—2.15020
0.50	0.215315	0.142001	—4.93070	—1.45562	—1.90728
0.55	0.251470	0.153636	—4.50292	—1.31363	—1.70321
0.60	0.288902	0.163344	—4.20657	—1.19254	—1.52756
0.70	0.365541	0.178381	—3.73868	—0.98117	—1.23769
0.80	0.443994	0.188657	—3.41258	—0.80437	—1.00359
0.90	0.523513	0.195430	—3.17267	—0.65205	—0.80659
1.0	0.603641	0.199643	—2.98886	—0.51783	—0.63562
1.2	0.764699	0.202929	—2.72567	—0.28806	—0.34603
1.4	0.925942	0.202030	—2.54612	—0.09406	—0.10188
1.6	1.08688	0.198833	—2.41563	0.07546	0.11332
1.8	1.24734	0.194388	—2.31640	0.22720	0.30881
2.0	1.40726	0.189299	—2.23832	0.36543	0.49019
2.2	1.56666	0.183923	—2.17524	0.49306	0.61110
2.4	1.72556	0.178472	—2.12318	0.61211	0.82398
2.6	1.88401	0.173075	—2.07947	0.72406	0.98058
2.8	2.04205	0.167807	—2.04223	0.83004	1.13213
3.0	2.19972	0.162713	—2.01012	0.93090	1.27959
3.5	2.59250	0.150857	—1.94631	1.16480	1.63459
4.0	2.98367	0.140292	—1.89878	1.37817	1.97558
4.5	3.37360	0.130929	—1.86198	1.57570	2.30692
5.0	3.76253	0.122627	—1.83263	1.76056	2.63133
6.0	4.53820	0.108656	—1.78875	2.10061	3.26588
8.0	6.08385	0.088240	—1.73408	2.69644	4.50165
10.0	7.62514	0.074166	—1.70136	3.21638	5.71428
12.0	9.16399	0.063919	—1.67957	3.68410	6.91490
14.0	10.7014	0.056140	—1.66402	4.11294	8.10847
16.0	12.2377	0.050040	—1.65236	4.51134	9.29756
18.0	13.7733	0.045130	—1.64329	4.88505	10.4836
20.0	15.3085	0.041095	—1.63604	5.23819	11.6675

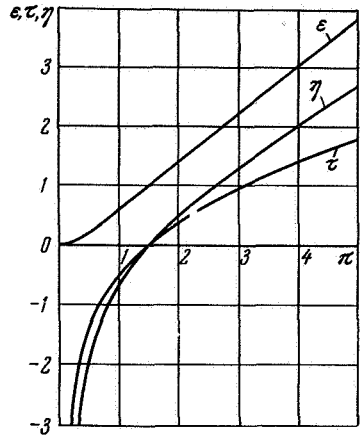

FIGURE 13.3. Functions $\varepsilon(\pi)$, $\tau(\pi)$, $\eta(\pi)$.

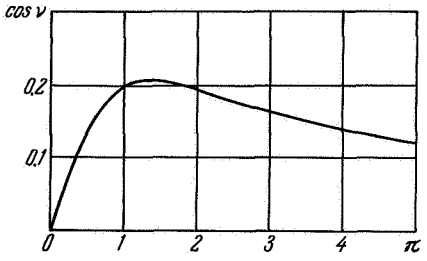

FIGURE 13.4. Function $\cos \nu(\pi)$.

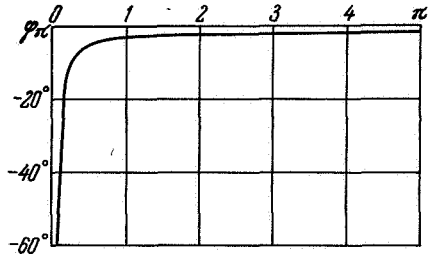

FIGURE 13.5. Function $\varphi_\pi(\pi)$.

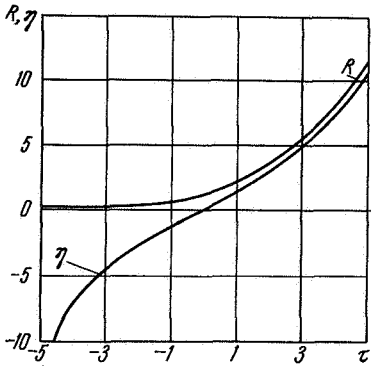

FIGURE 13.6. Radius R and energy η as function of time τ.

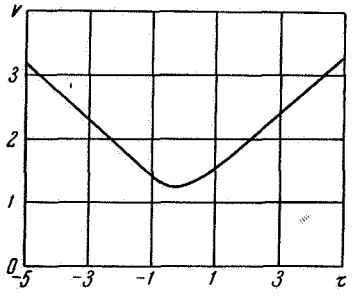

FIGURE 13.7. Velocity V as function of time τ.

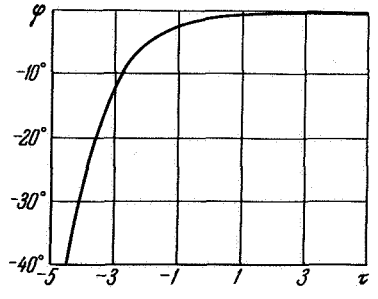

FIGURE 13.8. Polar angle as function of time τ.

Figure 13.3 shows the functions $\varepsilon(\pi)$, $\tau(\pi)$, $\eta(\pi)$ and Figure 13.4 illustrates $\cos\nu(\pi)$. The function $\varphi_\pi(\pi)$ is shown in Figure 13.5, and Figures 13.6 to
547 13.8 present the dependence of the dimensionless radius R, the energy η, the velocity V, and the polar angle φ on the dimensionless time τ. The polar angle φ ($\varphi = \varphi_\pi + \nu$) is measured from the direction corresponding to an infinitely large value of π; the value $\tau = 0$ corresponds to the point at which the parabolic velocity is attained ($\eta = 0$).

Note that the velocity V decreases at first, and then starts to increase in the vicinity of the parabolic velocity.

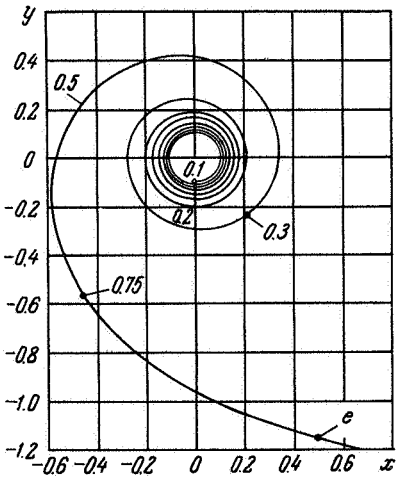

FIGURE 13.9. Trajectory when accelerating with tangential acceleration; values of parameter π marked on trajectory; e is the point where parabolic velocity is attained.

Figure 13.9 presents the trajectory of the motion in (x,y) coordinates ($x=R\cos\varphi$, $y=R\sin\varphi$); the values of π are marked on the trajectory. The point at which the parabolic velocity is attained is characterized by the following values of the radius R and the velocity V:

$$R = 1.24259,\ V = 1.26846. \tag{13.61}$$

We shall now consider how to plot the trajectory whilst accelerating. This corresponds to a specified initial radius $\bar{r}_0$, an acceleration $\bar{a}$, and a terminal energy $\bar{E}$ ($\bar{r}_0$, $\bar{a}$, $\bar{E}$ are dimensionless quantities) where the universal trajectory is used.

The radius of the initial circular orbit r_0 is equated to the initial value of the semimajor axis $\bar{A}_0$ for the osculating motion; the dimensionless quantity A_0 is

$$A_0 = \bar{A}_0\sqrt{2\bar{a}/k} = \bar{r}_0\sqrt{2\bar{a}/k} \tag{13.62}$$

(k is the gravitational constant of the central body; $k = f\mathfrak{M}$). From A_0 we find the dimensionless energy η_0, where

$$\eta_0 = -1/A_0. \tag{13.63}$$

The final value of this energy η_1 is given by the formula

$$\eta_1 = 2\bar{E}_1/\sqrt{2k\bar{a}}. \tag{13.64}$$

The given trajectory whilst accelerating is represented by either the dimensional parameters $\bar{r}_0$, $\bar{a}$, $\bar{E}_1$, or the dimensionless parameters η_0, η_1, and represents the part of the universal trajectory (cf. (13.58), (13.59), Tables 13.1, 13.2, 13.3) from $\eta = \eta_0$ to $\eta = \eta_1$.

548

The dimensional time of motion T and the increment in the angle φ_π are determined by the relations

$$\left.\begin{aligned} T &= (\tau_1 - \tau_0)\, k^{1/4} (2a)^{-3/4}, \\ \Delta\varphi_\pi &= \varphi_{\pi 1} - \varphi_{\pi 0}, \end{aligned}\right\} \tag{13.65}$$

where τ_0, τ_1, $\varphi_{\pi 0}$, $\varphi_{\pi 1}$ are the values of the dimensionless time and the angular position of the perihelion. These may either be calculated from the asymptotic formulas (13.58) and (13.59), or taken from the values η_0, η_1 in Table 13.3.

As an illustration, some results in /13.26/ are given. Table 13.4 gives the time of accelerating to the parabolic point T_1 and its distance from the center r_1 for trajectories which start from a circular orbit. This orbit is situated at a distance of 500 km above the Earth surface; the dimensional acceleration $\bar{a}$ is the parameter of the table.

TABLE 13.4. Trajectory parameters of parabolic-velocity build-up with tangential acceleration

$\bar{a}$[mm/sec^2]	r_1 [10^3·km]	T [days]	$\bar{a}$[mm/sec^2]	r_1 [10^3·km]	T [days]
0.3	1012.8	275.7	30	101.3	2.365
1	554.7	80.80	100	55.47	0.649
3	320.3	26.16	300	32.03	0.192
10	175.4	7.508	1000	17.54	0.048

4. Motion along a logarithmic spiral. Consider the equations of motion (A.17); a particular solution of these equations is

$$\left.\begin{aligned} &\gamma = 0, \\ &a = \tfrac{1}{2}\sin\vartheta_0 \exp(-2\varphi \operatorname{tg}\vartheta_0), \\ &v = v_0 \exp\left(-\tfrac{1}{2}\varphi \operatorname{tg}\vartheta_0\right), \\ &\vartheta = \vartheta_0 = \text{const}, \\ &r = \exp(\varphi \operatorname{tg}\vartheta_0), \\ &t = \frac{2}{3\sin\vartheta_0}\left[\exp\left(\tfrac{3}{2}\varphi \operatorname{tg}\vartheta_0\right) - 1\right]; \end{aligned}\right\} \tag{13.66}$$

the initial conditions are

$$t = 0,\ \varphi(0) = 0,\ r(0) = 1,\ v(0) = v_0. \tag{13.67}$$

549 In this case the thrust-acceleration magnitude varies as the inverse square of the radius (cf. (13.66)),

$$a = \frac{\sin \vartheta_0}{2r^2}, \tag{13.68}$$

and the initial acceleration is

$$a_0 = \frac{1}{2} \sin \vartheta_0, \tag{13.69}$$

where the direction of the thrust acceleration is tangential. The velocity magnitude v is given by

$$v = v_0 r^{-1/2}. \tag{13.70}$$

If $\vartheta_0 \neq 0$, then the radial velocity component is never zero throughout the motion, while the transverse component differs from the circular one; if $\vartheta_0 = 0$, the motion takes place along a circular orbit of unit radius, and there is no perturbing force. As $\vartheta_0 \to \frac{1}{2}\pi$ the trajectory degenerates into a straight line and coincides with the radius vector. The results described are in /13.14, 13.27, 13.28/.

Examples of the solution of the problem of orbital transfer from an Earth-satellite orbit to a Mars-satellite orbit are presented in /13.28/; the angle ϑ_0 varies when passing from one stage of the motion to another. In /13.29/ the logarithmic spiral is used as the base trajectory when applying the method of varying the parameters. An analytic solution of the equations of motion, near to the logarithmic spiral, is given in /13.30/; unlike the latter solution, this one has the same number of constants as the order of the system of differential equations. Here the acceleration is directed tangentially and varies roughly as the inverse square of the distance from the center.

§ 4. NORMAL ACCELERATION ($\gamma = \pi/2$ in (A.14)). BINORMAL ACCELERATION ($a_R = 0$, $a_\Phi = 0$ in (A.37)).

1. Equations and integrals of motion with normal acceleration. System (A.14) is much simplified when $\gamma = \frac{1}{2}\pi$ (the thrust acceleration is perpendicular to the velocity in the orbital plane):

$$\left.\begin{aligned} E &= \text{const} = E_0, \\ M' &= -\frac{ar}{v}. \end{aligned}\right\} \tag{13.71}$$

550 Since $v = \sqrt{2E_0 + 2/r}$ (cf. (A.11)), the integral of the last equation is

$$M(r) = M_0 - \frac{1}{\sqrt{2}} \int_{r_0}^{r} \frac{ar^{3/2}}{\sqrt{E_0 r + 1}}\, dr. \tag{13.72}$$

For a = const this yields elementary functions /13.31/.

2. **Properties of the trajectories of motion with normal acceleration.** Since the total energy is constant, $E = E_0$, escape from the gravitational field is impossible since the motion is bounded. The distance from the center r lies within the limits $r_{\min} \leqslant r \leqslant r_{\max}$, where $r_{\min}$ and $r_{\max}$ are the roots of the equation

$$M^2(r)/2r^2 - 1/r = E_0. \tag{13.73}$$

If the initial orbit is circular ($r_0 = 1, E_0 = -1/2, M_0 = 1$) the following approximate formulas for $r_{\max}$. $M_{\min}$, and $\varepsilon_{\max}$ are obtained for small values of a /13.32/:

$$\left.\begin{aligned} r_{\max} &\approx \frac{1}{1-2a}, \\ M_{\min} &\approx \sqrt{1-4a^2}, \\ \varepsilon_{\max} &\approx 2a. \end{aligned}\right\} \tag{13.74}$$

At the point of the trajectory where $r = r_{\min} = 1$, the quantities M and ε return to their initial values

$$r_{\min} = 1, \quad M_{\max} = 1, \quad \varepsilon_{\min} = 0. \tag{13.75}$$

The length A of the semimajor axis of the osculating ellipse (cf. (A.23)) remains unchanged throughout the motion, since the energy E is constant:

$$A = -1/(2E_0) = \text{const}. \tag{13.76}$$

If the acceleration direction is reversed at those points of the trajectory situated at maximum and minimum distances from the center ($\gamma = 1/2\pi \rightleftarrows \gamma = 3/2\pi$), the eccentricity corresponding to such a motion has a maximum increase /13.31/. In the limit the orbit can be transformed into a segment of a straight line of length A with the perihelion at the gravitational center.

3. **Equations and integrals of motion with binormal acceleration.** For $a_R \equiv 0$, $a_\Phi \equiv 0$ the thrust-acceleration vector is perpendicular to the plane of the instantaneous orbit. It follows from system (A.37) that the parameters determining the orbit geometry in the plane are invariant. These are the length A of the major semiaxis, the eccentricity ε, and the time T_π of passage of the perihelion in the absence of forces corresponding to a_R and
551 a_Φ. The remaining equations for the inclination i, the longitude of the ascending node Ω, the argument of the perihelion φ_π, together with equation (A.38), describe the rotation of the orbital plane.

The problem of rotating the orbital plane under the action of a binormal acceleration has been studied in numerous papers /13.17, 13.32—13.36/. The authors of /13.17, 13.32, 13.34/ used a system of equations like (A.37) with osculating variables in their analyses. In /13.33/ a system of equations with mixed variables (A.44), (A.45) was selected. Circular and elliptic take-off orbits were considered there, and the Krylov—Bogolyubov averaging method was used in the latter case. In /13.35/ the equations of motion were represented in spherical coordinates (cf. (A.5)); we shall follow this paper in our treatment.

The orbital plane is defined by the radius vector and the velocity vector. It is therefore possible to immediately establish two facts arising from the given acceleration. First, the acceleration has no radial component (in spherical coordinates $a_r = 0$, since the binormal acceleration is perpendicular to the radius vector). Second, the equations of motion (A. 5) possess an energy integral (the work done by the binormal acceleration is zero, since the acceleration vector is perpendicular to the velocity vector). From these conditions we obtain

$$E = {}^1/_2 (\dot{r}^2 + r^2\dot{\varphi}^2 \cos^2\theta + r^2\dot{\theta}^2) - 1/r = \text{const}, \tag{13.77}$$

and

$$a_\varphi r\dot{\varphi} \cos\theta + a_\theta r\dot{\theta} = 0. \tag{13.78}$$

From the second relation the components a_φ, a_θ may be expressed in terms of the binormal acceleration vector ae ($e = \pm 1$ is the orientation of the acceleration vector relative to the instantaneous orbit):

$$a_\varphi = -\frac{ae\dot{\theta}}{\sqrt{\dot{\theta}^2 + \dot{\varphi}^2 \cos^2\theta}}, \quad a_\theta = \frac{ae\dot{\varphi}\cos\theta}{\sqrt{\dot{\theta}^2 + \dot{\varphi}^2\cos^2\theta}}. \tag{13.79}$$

The equations of motion (A. 5) then reduce to

$$\left.\begin{aligned} \ddot{r} - r\dot{\varphi}^2\cos^2\theta - r\dot{\theta}^2 &= -\frac{1}{r^2}, \\ 2\dot{r}\dot{\varphi} + r\ddot{\varphi}\cos\theta - 2r\dot{\varphi}\dot{\theta}\sin\theta &= -\frac{ae\dot{\theta}}{\sqrt{\dot{\theta}^2 + \dot{\varphi}^2\cos^2\theta}}, \\ 2\dot{r}\dot{\theta} + r\dot{\varphi}^2\sin\theta\cos\theta + r\ddot{\theta} &= \frac{ae\dot{\varphi}\cos\theta}{\sqrt{\dot{\theta}^2 + \dot{\varphi}^2\cos^2\theta}}. \end{aligned}\right\} \tag{13.80}$$

552

Suppose the motion starts from a circular orbit located on the equator:

$$r(0) = \dot{\varphi}(0) = 1, \ \dot{r}(0) = \varphi(0) = \theta(0) = \dot{\theta}(0) = 0; \tag{13.81}$$

system (13.80) is then transformed to

$$\left.\begin{aligned} r &\equiv 1, \\ \dot{\varphi}^2\cos^2\theta + \dot{\theta}^2 &= 1, \\ \ddot{\theta} + (1 - \dot{\theta}^2)\operatorname{tg}\theta &= ae\sqrt{1 - \dot{\theta}^2}. \end{aligned}\right\} \tag{13.82}$$

If $ae = \text{const}$, the last two equations can be integrated to give the explicit relations /13.35/

$$\left.\begin{aligned} \theta &= \arcsin\left[\frac{ae}{1 + a^2}(1 - \cos\sqrt{1 + a^2}t)\right], \\ \varphi &= \operatorname{arctg}\frac{\sqrt{1 + a^2}\sin\sqrt{1 + a^2}t}{a^2 + \cos\sqrt{1 + a^2}t}. \end{aligned}\right\} \tag{13.83}$$

For $a \ll 1$ we obtain the form given by L. A. Simonov, namely,

$$\sin\theta = ae(1 - \cos t). \tag{13.84}$$

4. Properties of the trajectories of motion with binormal acceleration. It follows from (13.83) that the angle θ is a periodic function of time with a period T_a and an amplitude θ_{max}, where

$$T_a = \frac{2\pi}{\sqrt{1+a^2}}, \quad \theta_{max} = \arcsin\frac{2a}{1+a^2}. \tag{13.85}$$

The trajectory of the motion is a small circle of radius r_a given by

$$r_a = \frac{1}{\sqrt{1+a^2}}, \tag{13.86}$$

whose plane is inclined to the initial plane at an angle i_a, so that

$$\left.\begin{aligned} i_a &= {}^1/_2\theta_{max} \quad \text{at} \quad a \leqslant 1, \\ i_a &= {}^1/_2\pi - {}^1/_2\theta_{max} \quad \text{at} \quad a \geqslant 1; \end{aligned}\right\} \tag{13.87}$$

at the end of the period T_a the trajectory of the perturbed motion returns to its starting point.

If the action of the perturbing acceleration is interrupted at the point $\theta = \theta_{max}$, the orbit will be rotated through an angle i_a relative to the initial orbit.

553 § 5. CONSTANT ACCELERATION VECTOR ($a_y = a_z = 0$, $a_x = a = \text{const}$ in (A.3))

1. Equations and integrals of motion. If the thrust acceleration has a constant magnitude and is directed along one of the coordinate axes, the equations of motion are integrated by quadratures /13.37/.

Let the acceleration vector be directed along the x-axis; equations (A.3) are then written as follows:

$$\left.\begin{gathered} \ddot{x} = -\frac{x}{r^3} + a, \quad \ddot{y} = -\frac{y}{r^3}, \quad \ddot{z} = -\frac{z}{r^3} \\ (r = \sqrt{x^2+y^2+z^2}, \ a = \text{const}). \end{gathered}\right\} \tag{13.88}$$

System (13.88) has three first integrals: the energy integral

$$\frac{1}{2}(\dot{x}^2 + \dot{y}^2 + \dot{z}^2) - \frac{1}{r} - ax = E, \tag{13.89}$$

the angular-momentum integral (projection on the x-axis)

$$z\dot{y} - y\dot{z} = -M_x \tag{13.90}$$

and a third integral

$$\dot{x}r\dot{r} - \frac{x}{r} - \frac{3}{2}ax^2 - \frac{1}{2}ar^2 - 2Ex = B. \tag{13.91}$$

We introduce the new variables

$$\left.\begin{gathered} u = r - x, \quad v = r + x, \\ \cos w = y/\sqrt{y^2+z^2}, \quad \sin w = z/\sqrt{y^2+z^2} \end{gathered}\right\} \tag{13.92}$$

and replace differentiation with respect to the time t by differentiation with respect to the variable τ, where

$$d\tau = dt/r. \tag{13.93}$$

The initial system can then be reduced to quadratures, in which new variables u, v, w, τ appear in the forms

$$\left.\begin{aligned} \int \frac{dv}{\sqrt{V(v)}} &= \tau + c_1, \\ \int \frac{du}{\sqrt{U(u)}} &= \tau + c_2, \\ M_x \int_0^\tau \frac{u+v}{2uv}\, d\tau &= w - w_0, \end{aligned}\right\} \tag{13.94}$$

554 where

$$\left.\begin{aligned} V(v) &= av^3 + 2Ev^2 + 2(1+B)v - M_x^2, \\ U(u) &= -au^3 + 2Eu^2 + 2(1-B)u - M_x^2. \end{aligned}\right\} \tag{13.95}$$

Relations (13.94) define the functions $v(\tau), u(\tau), w(\tau)$. The relation between τ and t is derived from (13.93), and is

$$t = {}^1/_2 \int_0^\tau (u+v)\, d\tau. \tag{13.96}$$

Using this relation, we may transform to the functions $v(t)$, $u(t), w(t)$. Inverting formulas (13.92), we obtain expressions for x, y, z in terms of $v(t), u(t), w(t)$. These are

$$\left.\begin{aligned} x &= {}^1/_2 [u(t) - v(t)], \\ y &= u(t)\, v(t) \cos w(t), \\ z &= u(t)\, v(t) \sin w(t). \end{aligned}\right\} \tag{13.97}$$

The problem has thus been reduced to quadratures. Note that the integrals in (13.94) are elliptical.

2. **Classification of plane trajectories.** If the motion takes place in the (x, y) plane (i.e., $z \equiv 0$), then $M_x = 0$, $w = w_0 = 0$, and the polynomials $V(v)$ and $U(u)$ can be represented in the forms

$$\left.\begin{aligned} V &= av(v - v_2)(v - v_3), \\ U &= -au(u - u_2)(u - u_3), \end{aligned}\right\} \tag{13.98}$$

where

$$\left.\begin{aligned} v_2 &= \frac{1}{a}[-E + \sqrt{E^2 - 2a(1+B)}], \\ v_3 &= \frac{1}{a}[-E - \sqrt{E^2 - 2a(1+B)}], \\ u_2 &= \frac{1}{a}[E + \sqrt{E^2 + 2a(1-B)}], \\ u_3 &= \frac{1}{a}[E - \sqrt{E^2 - 2a(1-B)}]. \end{aligned}\right\} \tag{13.99}$$

Figure 13.10 presents four classes of trajectories of plane motion: a) unbounded self-intersecting trajectories, which do not enclose the

gravitational center; b) unbounded self-intersecting trajectories which enclose the gravitational center; c) unbounded nonintersecting trajectories; d) bounded trajectories.

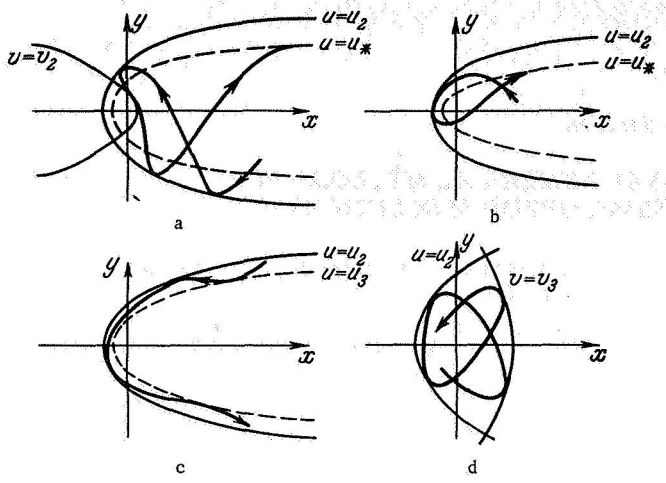

FIGURE 13.10. Classification of trajectories of plane motion with constant acceleration vector.

555 The regions which can be attained are limited by parabolas in the (x, y) plane given by

$$\left.\begin{aligned}\sqrt{x^2+y^2}-x&=u=\text{const},\\ \sqrt{x^2+y^2}+x&=v=\text{const}.\end{aligned}\right\} \tag{13.100}$$

The constants which define these parabolas take the values u_2, v_2, u_3, v_3, u^*. The first four values are given by (13.99); the last one corresponds to the case $v=\infty$.

Consider the case of an initial circular orbit. Let φ be the angle made by the initial radius vector with the acceleration vector. When the following conditions are fulfilled simultaneously,

$$a<{}^1/_2,\ a^2-a\,(2-\cos\varphi)+{}^1/_4>0, \tag{13.101}$$

the motion is bounded. For $a>{}^1/_2$ the motion is unbounded for all values of φ.

If $\varphi=0$, the motion is bounded for $0<a<{}^1/_2$; the maximum value of the radius for $a=0.5$ is $r_{\max}\approx 1.4$.

If $\varphi=\pi$, the motion is bounded for $0<a<{}^3/_2-\sqrt{2}\approx 0.086$; the maximum radius for $a=0.086$ is $r_{\max}\approx 3.4$.

A possible application of this solution is to calculate the trajectory of an Earth satellite subject to the action of radiation pressure.

Chapter Fourteen

FUNCTIONAL NUMERICAL METHODS FOR ESTABLISHING OPTIMUM SOLUTIONS

556 The variational problems described so far can be represented in the following general form.

Consider a dynamic system described by n differential equations in terms of the phase coordinates $x_i(t)$:

$$\dot{x}_i = f_i(x_j, u_k, t), \quad (i, j = 0, 1, \ldots, n;\ k = 1, \ldots, m;\ 0 \leqslant t \leqslant T). \tag{14.1}$$

We require the control functions $u_k(t)$, which ensure an extremum of the functional — the terminal value of the coordinate $x_0(T)$ — and transform the system from a given initial state

$$x_i(0) = x_{i0} \quad (i \in I_0) \tag{14.2}$$

to a given final state

$$x_j(T) = x_{j1} \quad (j \in J_1). \tag{14.3}$$

This is the formulation of Mayer's classic variational problem. Another classic problem of variational analysis (already met with above) is the Lagrange problem, which is formulated as follows. Consider a dynamic system described by n differential equations in terms of the phase coordinates

$$\dot{x}_i = f_i(x_j, u_k, t) \quad (i, j = 1, \ldots, n;\ k = 1, \ldots, m). \tag{14.4}$$

Control functions u_k must be established which ensure the extremum of the integral functional

$$J = \int_0^T \Phi(x_i, u_k, t)\, dt \tag{14.5}$$

and which transform the system from a given initial state

$$x_i(0) = x_{i0} \quad (i \in I_0) \tag{14.6}$$

to a given final state

$$x_j(T) = x_{j1} \quad (j \in J_1). \tag{14.7}$$

557 The Lagrange problem (14.4)—(14.7) can often be reduced to a form which is free of the differential constraints (14.4). The extrema of the integral functional

$$J = \int_0^T \Phi(x_i, \dot{x}_i, \ddot{x}_i, \ldots, x_i^{(q_i)})\, dt \qquad (i = 1, \ldots, n) \tag{14.8}$$

must be found which satisfy the boundary conditions

$$\left.\begin{aligned} x_i(0) = x_{i0},\ \dot{x}_i(0) = \dot{x}_{i0}, \ldots,\ x_i^{(q_i-1)}(0) = x_{i0}^{(q_i-1)}, \\ x_i(T) = x_{i1},\ \dot{x}_i(T) = \dot{x}_{i1}, \ldots,\ x_i^{(q_i-1)}(T) = x_{i1}^{(q_i-1)} \\ (i = 1, \ldots, n) \end{aligned}\right\} \tag{14.9}$$

(we have written here the full system of separated and symmetrical boundary conditions).

These variational formulations can be reduced by means of the formalism of Lagrange—Euler or Pontryagin to solving boundary-value problems of ordinary differential equations. Such problems have the general form

$$\left.\begin{aligned} \dot{x}_i = f_i(x_j, t) \quad (i, j = 1, \ldots, n), \\ x_i(0) = x_{i0} \quad (i = 1, 2, \ldots, l), \\ x_j(T) = x_{j1} \quad (j \in J_1). \end{aligned}\right\} \tag{14.10}$$

Numerical methods of solving the variational problems (14.1)—(14.3), (14.4)—(14.7), (14.8)—(14.9) are classified into direct and indirect ones. Those belonging to the first class are based on various iterative processes of successively decreasing (or increasing) the functional; indirect methods, on the other hand, start by reducing the variational problem to a boundary-value problem like (14.10).

The methods of solving the above-formulated problems are described in this chapter and in the following one. Chapter Fourteen deals with functional analysis, and Chapter Fifteen with analyses which use just a finite number of dimensions. The general ideas are illustrated by examples from spaceflight mechanics.

The list of methods is by no means exhaustive. Analyses based on dynamic programming /14.1—14.5/ are not considered, neither are those based on the optimum principle /14.6/, etc. The ways of solving linear problems are also not looked at since these are rarely encountered in spaceflight mechanics.

558 § 1. STEEPEST DESCENT IN PHASE SPACE

The main feature of those methods is the direct study of the first variation of the functional in order to determine the conditions of steepest descent (or ascent) to the required value of the functional at each step of the iterative process. These methods are divided in two groups: descent in the space of the control variables, and descent in the phase space. The method of steepest descent in the space of control variables is applicable to the problems of Mayer (14.1)—(14.3) or Lagrange (14.4)—(14.7); the first variation of the functional $\delta x_0(T)$ or δJ is expressed in terms of the variation

of the control functions $\delta u_k(t)$. The method of steepest descent in the phase space is applicable to the Lagrange problem in the form (14.8)—(14.9) with no differential constraints and control functions; the first variation of the functional δJ is expressed in terms of the variation of the phase coordinates $\delta x_i(t)$. It is this difference which led to separate treatments of these two essentially similar methods. The steepest descent in phase space is treated in this section, and the steepest descent in the space of the control variables in the next one.

The method of steepest descent was suggested in 1908 by Hadamard for solving the problem of a clamped plate. Later, Courant /14.7/ pointed out the possibility of wide applications of the idea of steepest descent in a functional space. During the years 1945—1948, Kantorovich /14.8—14.10/ formulated the method of steepest descent as a functional analysis of quadratic functionals. He proved the convergence of the method and established its rate of convergence. The generalized method, proposed by Kantorovich for quadratic functionals, was examined in later papers /14.11, 14.12/. Finally, it was suggested in /14.13/ (cf. also /14.14/) that the method of steepest descent in phase space be applied to arbitrary functionals, and not only to quadratic ones. The same paper gave some estimates of the convergence of the method, which were then generalized in /14.15/ to the case of multidimensional functionals.

The results of applying the method to numerical analyses of variational problems in spaceflight mechanics are described in /14.16, 14.17/.

1. Algorithm of the method. We shall describe the functional analysis of steepest descent in phase space for the following simplest case of the Lagrange problem (14.8), (14.9).

The extrema of the functional

$$J = \int_0^T \Phi(x, \dot{x}, t)\, dt \tag{14.11}$$

559 must be found, where the function $x(t)$ takes the following values at the ends of the interval:

$$x(0) = x_0,\ x(T) = x_1. \tag{14.12}$$

Boundary conditions of this type are called separated and symmetrical; the general form of separated and symmetrical boundary conditions is given in (14.9).

Assume that a zero approximation $x^{(0)}(t)$ for the extrema of functional (14.11) is known and satisfies the boundary conditions (14.12). We represent the next approximation in the form

$$x^{(1)}(t) = x^{(0)}(t) + \delta x(t). \tag{14.13}$$

The boundary values of the functional $\delta x(t)$ are then equal to zero, i.e.,

$$\delta x(0) = \delta x(T) = 0. \tag{14.14}$$

The variation of the functional, caused by the small variation $\delta x(t)$ satisfying conditions (14.14), has the form

$$\delta J = \int_0^T E^{(0)}(t)\,\delta x(t)\,dt, \tag{14.15}$$

where $E^{(0)}(t)$ is the deviation of the Euler equation on the trajectory $x^{(0)}(t)$, such that

$$E^{(0)}(t) = \frac{\partial \Phi}{\partial x}[x^{(0)}(t), \dot{x}^{(0)}(t), t] - \frac{d}{dt}\frac{\partial \Phi}{\partial \dot{x}}[x^{(0)}(t), \dot{x}^{(0)}(t), t]. \tag{14.16}$$

Integrating (14.15) by parts and using (14.14), we obtain the following expression for the variation of the integral:

$$\delta J = -\int_0^T \left[\int_0^t E^{(0)}(\tau)\,d\tau + c\right]\delta\dot{x}(t)\,dt. \tag{14.17}$$

The constant c in the integrand of the outer integral is arbitrary in the sense that the variation δJ is independent of it. This can be established by calculating the derivative

$$\frac{\partial \delta J}{\partial c} = -\int_0^T \delta\dot{x}(t)\,dt = -\delta x(T) + \delta x(0) = 0 \tag{14.18}$$

(the last equality in (14.18) follows from boundary conditions (14.14)).

We select the following expression for the variational derivative $\delta\dot{x}(t)$:

$$\delta\dot{x}(t) = \lambda\left[\int_0^t E^{(0)}(\tau)\,d\tau + c\right]. \tag{14.19}$$

Integration of this expression yields

$$\delta x(t) = c_1 + \lambda\left\{\int_0^t \left[\int_0^t E^{(0)}(\tau)\,d\tau\right]dt + ct\right\}. \tag{14.20}$$

We determine the constants c and c_1 so as to fulfill the specified boundary conditions (14.14); this gives

$$c_1 = 0,\quad c = -\frac{1}{T}\int_0^T \left[\int_0^t E^{(0)}(\tau)\,d\tau\right]dt \tag{14.21}$$

and

$$\delta x(t) = \lambda\left\{\int_0^t \left[\int_0^t E^{(0)}(\tau)\,d\tau\right]dt - \frac{t}{T}\int_0^T \left[\int_0^t E^{(0)}(\tau)\,d\tau\right]dt\right\}. \tag{14.22}$$

For a given value of $\delta x(t)$ the variation of the functional δJ will either have a sign opposite to that of the parameter λ, or vanish independently of the value of λ. In fact

$$\delta J = -\lambda\int_0^T \left[\int_0^t E^{(0)}(\tau)\,d\tau + c\right]^2 dt, \tag{14.23}$$

so that

$$\left.\begin{array}{l}\delta J<0 \text{ at } \lambda>0,\\ \delta J>0 \text{ at } \lambda<0,\\ \delta J=0 \text{ at } E^{(0)}(\tau)\equiv 0.\end{array}\right\} \tag{14.24}$$

If we want to decrease the functional J, it can be achieved by taking $\delta x(t)$ in the form (14.22) and selecting a small positive value for the parameter λ (small so that we do not overstep the limits of applicability of the formula for the first variation).

The expression in curly brackets in (14.22) is the functional gradient; the parameter λ defines the length along the gradient.

Writing (14.22) in the form

$$\delta x(t) = \lambda\eta(t), \tag{14.25}$$

where

$$\eta(t)=\int_0^t\left[\int_0^t E^{(0)}(\tau)\,d\tau\right]dt - \frac{t}{T}\int_0^T\left[\int_0^t E^{(0)}(\tau)\,d\tau\right]dt, \tag{14.26}$$

we obtain the following expression for the first approximation $x^{(1)}(t)$:

$$x^{(1)}(t) = x^{(0)}(t) + \lambda\eta(t). \tag{14.27}$$

561 The function $\eta(t)$ is fully determined by the zero approximation $x^{(0)}(t)$ (cf. (14.26)), and the parameter λ remains arbitrary. The latter can be taken at each step as equal to a small magnitude so selected as to remain within the limits of applicability of the linear representation of the functional. There exists another possibility as well — to select the parameter λ at each step of the process from the condition for a minimum functional J.

The functional (14.11) corresponding to the family of functions $x^{(1)}(t)$, where $\eta(t)$ is taken in the form (14.26), depends on the parameter λ alone. The condition that the functional has a minimum with respect to λ $J^{(1)} = J[x^{(0)}(t) + \lambda\eta(t)]$ has the form

$$\frac{dJ^{(1)}}{d\lambda}=\int_0^T E^{(1)}(t,\lambda)\,\eta(t)\,dt = \int_0^T\left[\int_0^t E^{(1)}(\tau,\lambda)\,d\tau + c\right]\left[\int_0^t E^{(0)}(\tau)\,d\tau + c\right]dt = 0. \tag{14.28}$$

Here

$$E^{(1)}(t,\lambda) = \frac{\partial\Phi}{\partial x}(x^{(0)}+\lambda\eta, \dot{x}^{(0)}+\lambda\dot{\eta}, t) - \\ - \frac{d}{dt}\frac{\partial\Phi}{\partial\dot{x}}(x^{(0)}+\lambda\eta, \dot{x}^{(0)}+\lambda\dot{\eta}, t). \tag{14.29}$$

If $\lambda = 0$, then $E^{(1)} = E^{(0)}$ and the derivative $(dJ^{(1)}/d\lambda) \leqslant 0$. When the deviation of the Euler equation $E^{(0)}$ vanishes identically, the derivative $dJ^{(1)}/d\lambda$ is zero for any value of the parameter λ.

The algorithm of the method of steepest descent in phase space can therefore be formulated as follows:

At each step of the iterative process (14.27), the function $\eta(t)$ must be calculated from the deviation of the Euler equation (14.26) and the parameter λ from the condition that the derivative (14.28) vanishes.

2. **Computational procedure.** Expression (14.26) for the function $\eta(t)$ can be transformed into

$$\eta(t) = t\int_0^t \frac{\partial\Phi^{(0)}}{\partial x}\,dt - \int_0^t t\frac{\partial\Phi^{(0)}}{\partial x} - \int_0^t \frac{\partial\Phi^{(0)}}{\partial \dot{x}}\,dt - \\ - \frac{t}{T}\Big[T\int_0^T \frac{\partial\Phi^{(0)}}{\partial x}\,dt - \int_0^T t\frac{\partial\Phi^{(0)}}{\partial x}\,dt - \int_0^T \frac{\partial\Phi^{(0)}}{\partial \dot{x}}\,dt\Big]. \tag{14.30}$$

We obtain (14.30) by integrating (14.26) by parts; the partial derivatives $\partial\Phi^{(0)}/\partial x$, $\partial\Phi^{(0)}/\partial\dot{x}$ enter the Euler operator as in (14.16).

562 The calculation of $\eta(t)$ reduces to finding the integrals from tables of the functions $x^{(0)}(t)$, $\dot{x}^{(0)}(t)$. Instead of storing the values of $\dot{x}^{(0)}(t)$ in the computer memory, we may use numerical differentiation to find $\dot{x}^{(0)}(t)$ from the existing values of $x^{(0)}(t)$.

According to the definition of the algorithm, at each step of the process we must determine the minimizing value of the parameter λ once the function $\eta(t)$ is known. To calculate the minimum of $J^{(0)}$ with respect to λ to a given accuracy, we need a special iterative process, such as Newton's method, or the method of secants as applicable to equation (14.28). It is frequently expedient to ignore such a labor-consuming procedure and to determine the minimizing value of the parameter λ by some simpler method. We suggest here one such method. The value of the functional J for $\lambda = 0$ is known from the preceding step of the iterative process. Calculate J for $\lambda = \lambda'$ and $\lambda = \lambda''$, where λ', λ'' are some trial values of the parameter. Through the three points in the (λ, J) plane, $\lambda = 0$, $J = J_0$; $\lambda = \lambda'$, $J = J'$; $\lambda = \lambda''$, $J = J''$, draw a second-order parabola, and hence find the minimizing value of λ.

The process can be considered as completed if the increment of the functional ΔJ at the last step does not exceed the specified accuracy, i.e., when

$$|\Delta J| \leqslant \varepsilon. \tag{14.31}$$

3. **Generalization of the algorithm.** Consider the case when the value of the function $x(t)$ at the end of the interval $t = T$ is not specified, and has to be optimized in the sense of the functional J. The algorithm must then be altered as follows.

The variation of the function $\delta x(t)$ must vanish as before at the beginning of the interval, while at its end it must differ from zero, so that

$$\delta x(0) = 0,\ \delta x(T) \neq 0. \tag{14.32}$$

We add a new term to the variation of the functional δJ. This was absent in (14.15). The new form is

$$\delta J = \int_0^T E^{(0)}(t)\,\delta x(t)\,dt + \frac{\partial\Phi^{(0)}}{\partial \dot{x}_1}\,\delta x_1\Big(\frac{\partial\Phi^{(0)}}{\partial \dot{x}_1} = \frac{\partial\Phi^{(0)}}{\partial \dot{x}}(T), \delta x_1 = \delta x(T)\Big). \tag{14.33}$$

Integrating (14.33) by parts, we obtain the variation δJ similar to (14.17):

$$\delta J = -\int_0^T \Big[\int_0^t E^{(0)}(\tau)\,d\tau + c\Big]\delta\dot{x}(t)\,dt + \Big[\int_0^T E^{(0)}(t)\,dt + \frac{\partial\Phi^{(0)}}{\partial \dot{x}_1} + c\Big]\delta x_1. \tag{14.34}$$

563 The variation δJ is independent of the constant c in (14.34); this can be proved by calculating the derivative $\partial \delta J/\partial c$ (cf. (14.18)).

We select the variational derivative $\delta \dot{x}$ in the form (14.19) as before, and the final value of the variation δx_1 in the form

$$\delta x_1 = -\lambda T\left[\int_0^T E^{(0)}(t)\,dt + \frac{\partial \Phi^{(0)}}{\partial \dot{x}_1} + c\right]. \tag{14.35}$$

The expression for the variation $\delta x(t)$ is given, as above, by (14.20); we determine the constants c and c_1 in this formula so that the boundary conditions (14.32), (14.35) are satisfied; we obtain

$$c_1 = 0,\ c = -\frac{1}{2}\left\{\frac{\partial \Phi^{(0)}}{\partial \dot{x}_1} + \int_0^T E^{(0)}(t)\,dt + \frac{1}{T}\int_0^T\left[\int_0^t E^{(0)}(\tau)\,d\tau\right]dt\right\} \tag{14.36}$$

and

$$\begin{aligned}\delta x(t) = \lambda\Big\{\int_0^t\left[\int_0^t E^{(0)}(\tau)\,d\tau\right]dt - \frac{t}{2T}\int_0^T\left[\int_0^t E^{(0)}(\tau)\,d\tau\right]dt - \\ - \frac{1}{2}t\int_0^T E^{(0)}(t)\,dt - \frac{1}{2}t\frac{\partial \Phi^{(0)}}{\partial \dot{x}_1}\Big\}.\end{aligned} \tag{14.37}$$

For such a choice of $\delta x(t)$ the variation of the functional δJ will either have a sign opposite to that of the parameter λ or vanish, whatever the value of λ; in fact

$$\delta J = -\lambda\left\{\int_0^T\left[\int_0^t E^{(0)}(\tau)\,d\tau + c\right]^2 dt - \left[\int_0^T E^{(0)}(t)\,dt + \frac{\partial \Phi^{(0)}}{\partial \dot{x}_1} + c\right]^2\right\}, \tag{14.38}$$

so that

$$\left.\begin{aligned}&\delta J < 0 \text{ for } \lambda > 0,\\ &\delta J > 0 \text{ for } \lambda < 0,\\ &\delta J = 0 \text{ for } E^{(0)}(\tau) \equiv 0 \text{ and } \partial \Phi^{(0)}/\partial \dot{x}_1 = 0.\end{aligned}\right\} \tag{14.39}$$

The last equality in (14.39) is the known condition for determining the optimum value of $x(T)$.

The parameter λ in (14.37) is found using the same considerations as in Subsection 1.

The method of steepest descent described in the first subsection can be generalized when the integrand depends on derivatives of order higher than
564 the first, provided appropriate boundary conditions for these higher derivatives are added. The method can be extended for functionals depending on several unknown functions.

4. Example. Consider the problem of determining the minimum of the integral functional

$$J = \int_0^T \{[\ddot{x} + x/(x^2+y^2)^{3/2}]^2 + [\ddot{y} + y\,(x^2+y^2)^{-3/2}]^2\}\,dt \tag{14.40}$$

with boundary conditions

$$\left.\begin{aligned} &x(0)=1,\ y(0)=0,\ \dot{x}(0)=0,\ \dot{y}(0)=1,\\ &x(T)=r_1\cos\varphi_1,\ y(T)=r_1\sin\varphi_1,\\ &\dot{x}(T)=-r_1^{-1/2}\sin\varphi_1,\ \dot{y}(T)=-r_1^{-1/2}\cos\varphi_1. \end{aligned}\right\} \tag{14.41}$$

This variational problem deals with finding the optimum trajectories and optimum operating regimes of an ideal power-limited engine (cf. Chapter Five). The calculations are carried out for $r_1 = 1.52$; the values φ_1 and T are the parameters of the problem.

The variational problem (14.40)—(14.41) belongs to the Lagrange type without differential constraints, where the boundary conditions are separated and symmetrical. We shall describe the procedure of the method of steepest descent in phase space for this problem.

From the known zero approximation $x^{(0)}(t)$, $y^{(0)}(t)$, satisfying the boundary conditions (14.41), we determine the functions $\eta_x(t)$, $\eta_y(t)$, which vanish at the ends of the interval together with their first derivatives. Thus, the expression for η_x has the form

$$\begin{aligned}\eta_x(t)=\int_0^t\int_0^t\int_0^t\int_0^t E_x^{(0)}dt^4-\frac{t^3}{T^3}\Big(T\int_0^T\int_0^t\int_0^t\int_0^t E_x^{(0)}dt^3-2\int_0^T\int_0^t\int_0^t\int_0^t E_x^{(0)}dt^4\Big)-\\ -\frac{t^2}{T^3}\Big(3\int_0^T\int_0^t\int_0^t\int_0^t E_x^{(0)}dt^4-T\int_0^T\int_0^t\int_0^t E_x^{(0)}dt^3\Big),\end{aligned} \tag{14.42}$$

where

$$\left.\begin{aligned} &E_x^{(0)}=\Big(\frac{d^2}{dt^2}\frac{\partial}{\partial\ddot{x}}+\frac{\partial}{\partial x}\Big)\Phi\left[x^{(0)}(t),y^{(0)}(t),\ddot{x}^{(0)}(t),\ddot{y}^{(0)}(t)\right],\\ &\Phi=[\ddot{x}+x(x^2+y^2)^{-3/2}]^2+[\ddot{y}+y(x^2+y^2)^{-3/2}]^2. \end{aligned}\right\} \tag{14.43}$$

565 The expression for η_y is obtained if x is replaced by y.

At the next step of the iterative process we have

$$x^{(1)}(t)=x^{(0)}(t)+\lambda_x\eta_x(t),\ y^{(1)}(t)=y^{(0)}(t)+\lambda_y\eta_y(t). \tag{14.44}$$

The descent parameters λ_x, λ_y are found from the condition for a minimum of the function $J^{(1)}(\lambda_x,\lambda_y)$ at the given step, i.e., when

$$\partial J^{(1)}/\partial\lambda_x=0,\ \partial J^{(1)}/\partial\lambda_y=0. \tag{14.45}$$

We represent the double integrals in (14.42) as follows:

$$\int_0^t\int_0^t E_x^{(0)}dt^2=\frac{\partial\Phi^{(0)}}{\partial\ddot{x}}(t)-\frac{\partial\Phi^{(0)}}{\partial\ddot{x}}(0)+\int_0^t\int_0^t\frac{\partial\Phi}{\partial x}dt^2-t\frac{d^2}{dt^2}\frac{\partial\Phi^{(0)}}{\partial\ddot{x}}(0) \tag{14.46}$$

(and a similar expression in the variable y). The functions $x^{(0)}(t)$, $y^{(0)}(t)$ and their second derivatives $\ddot{x}^{(0)}(t)$, $\ddot{y}^{(0)}(t)$ appear here, while the third derivatives $\dddot{x}^{(0)}(t)$, $\dddot{y}^{(0)}(t)$ and the fourth ones $\ddddot{x}^{(0)}(t)$, $\ddddot{y}^{(0)}(t)$ are absent from the right-hand side of (14.46).

When determining the functions $\eta_x(t)$, $\eta_y(t)$ by (14.41) and (14.46) numerical differentiation may be avoided if at each step we store the second derivatives

$\ddot{x}(t)$, $\ddot{y}(t)$ together with the functions $x(t)$, $y(t)$. Similarly, we must store the second derivatives $\ddot{\eta}_x(t)$, $\ddot{\eta}_y(t)$ together with the functions $\eta_x(t)$, $\eta_y(t)$ (cf. the discussion in Subsection 2). The expressions for η_x, $\ddot{\eta}_x$, given by (14.42) and (14.46), are written as (the expressions for η_y, $\ddot{\eta}_y$ are obtained by replacing x by y)

$$\eta_x = t\int_0^t M_x dt - \int_0^t t M_x dt - \frac{1}{6} c_{0x} t^3 - \frac{1}{2} c_{1x} t^2, \tag{14.47}$$

where

$$\left.\begin{aligned} M_x(t) &= t\int_0^t \frac{\partial \Phi^{(0)}}{\partial x}\, dt - \int_0^t t \frac{\partial \Phi^{(0)}}{\partial x}\, dt + \frac{\partial \Phi^{(0)}}{\partial \ddot{x}}, \\ c_{1x} &= \frac{6}{T^2}\int_0^T \left(\frac{2}{3}T - t\right) M_x dt. \\ c_{0x} &= \frac{6}{T^3}\int_0^T (2t - T) M_x dt. \end{aligned}\right\} \tag{14.48}$$

The functions taken for the zero approximation are

$$\left.\begin{aligned} x^{(0)}(t) &= 1 + \left[\frac{3(r_1\cos\varphi_1 - 1)}{T^2} + \frac{\sin\varphi_1}{\sqrt{r_1}T}\right] t^2 - \\ &\quad - \left[\frac{2(r_1\cos\varphi_1 - 1)}{T^3} + \frac{\sin\varphi_1}{\sqrt{r_1}T^2}\right] t^3, \\ y^{(0)}(t) &= t + \left(\frac{3r_1\sin\varphi_1 - 2T}{T^2} - \frac{\cos\varphi_1}{\sqrt{r_1}T}\right) t^2 + \\ &\quad + \left(-\frac{2r_1\sin\varphi_1 - T}{T^3} + \frac{\cos\varphi_1}{\sqrt{r_1}T^2}\right) t^3. \end{aligned}\right\} \tag{14.49}$$

These functions are the solution of the variational problem (14.40)—(14.41) for the case of a gravity-free field (cf. Chapter Five).

This iterative process turns out to be very efficient when applied to problem (14.40)—(14.41). One case (i.e., one pair of values φ_1, T) can be calculated in 1 to 2 minutes on the M-20 electronic computer to 4—5 places.

The convergence of this method is illustrated in Figure 14.1, where the abscissa represents the iteration number, and the ordinate gives the corresponding value of the functional; the discrete points are linked by a continuous curve. On curve 1, $\varphi_1 = 1.047$, $T = 3.456$; on curve 2, $\varphi_1 = 3.141$, $T = 3.456$.

In both examples, the optimum trajectory in a gravity-free field (14.49) was selected as the zero approximation. The comparison of the number of iterations in both cases enables us to estimate the rationality of the given zero approximation: the shorter the trajectory and the shorter the time of motion along it, the better the approximation to a central field by means of a gravity-free field.

The variations of the parameters φ_1, T used in the calculations were

$$0 \leqslant \varphi_1 \leqslant \pi, \quad 0 \leqslant T \leqslant \pi. \tag{14.50}$$

The attempt to use (14.49) as the zero approximation for angles $\varphi_1 > \pi$ encounters the following difficulty. It appears that the functional studied possesses more than one minimum at these angles of flight, and the use of

567 the solution in a gravity-free field as the zero element yields values of the minimum exceeding the expected ones. This means that it is impossible to use a single zero element over the whole range of variation of the parameters.

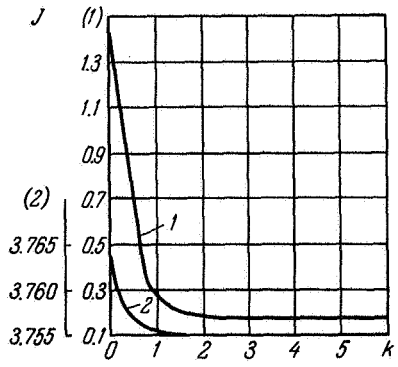

FIGURE 14.1. Decrease of functional J as iterative process progresses, by method of steepest descent in phase space. Curve 1: $\varphi_1 = 1.047$, $T = 3.456$; curve 2: $\varphi_1 = 3.141$, $T = 3.456$.

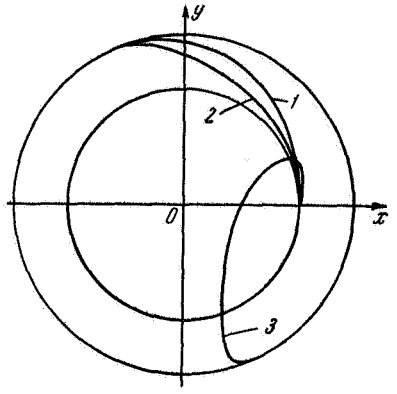

FIGURE 14.2. Optimum trajectories in gravity-free (1) and central (2) fields for $\varphi_1 = 2$, $T = 2$, and optimum trajectory in gravity-free field (3) for $\varphi_1 = 5.23$, $T = 4.92$.

This is illustrated in Figure 14.2, which represents the optimum trajectories in gravity-free and central fields for the case $\varphi_1 = 2$, $T = 2$, and the optimum trajectory in a gravity-free field for the case $\varphi_1 = 5.23$, $T = 4.92$. The latter does not envelop the origin of coordinates; this can serve as an external indicator of the unsuitability of the given trajectory as a zero element for an iterative process.

The following method is recommended when finding the initial element in parametric calculations. Let the optimum trajectory be known for some values of the parameters, and suppose we want to establish a new optimum trajectory for values of the parameters near to the first ones; the boundary conditions on the new trajectory differ from the old boundary conditions. We transform the old trajectory, for instance by multiplying it by an arbitrary function differing slightly from unity, so that the given boundary conditions are satisfied on the new trajectory. This trajectory can then be used as a zero element.

§ 2. STEEPEST DESCENT IN THE SPACE OF CONTROL VARIABLES

The method of steepest descent in the space of control variables /14.18—14.30/ is based on the variational approach suggested in a paper by D.E. Okhotsimskii /14.31/. The first application of this method to numerical analysis concerned selecting the optimum control program for the inclination of a solar sail /14.20/. The control function (the

orientation of the sail) was not constrained in this case. The same applies to problems of selecting the optimum thrust direction for transfer between orbits in a central field /14.28/, and also to the problem of a parabolic-velocity build-up /14.29/.

568 A generalization of the method for constrained control functions is given in /14.19, 14.21, 14.30/, while /14.25, 14.26, 14.32/ contain a development of the method for problems with phase constraints.

1. **Algorithm of the method for problems with a free trajectory terminal point.** We shall describe the algorithm of the method for the Mayer problem (14.1) to (14.3). In this section the trajectory terminal point is considered as free, and only one control function is considered for simplicity.

Consider the dynamic system described by the differential equations and the initial conditions

$$\dot{x}_i = f_i(x_j, u, t),\ x_i(0) = x_{i0}\ (i, j = 0, 1, \ldots, n;\ 0 \leqslant t \leqslant T). \tag{14.51}$$

We require the control function $u(t)$ which minimizes the functional $x_0(T)$; the end of the time interval $t = T$ is specified.

Suppose the zero approximation for the control function $u^{(0)}(t)$ is known, and that the trajectory $x_i^{(0)}(t)$ which satisfies the initial conditions (14.51) has been plotted for this function, where

$$x_i^{(0)}(0) = x_{i0}. \tag{14.52}$$

We represent the first approximation to the control function in the form

$$u^{(1)}(t) = u^{(0)}(t) + \delta u(t), \tag{14.53}$$

where $\delta u(t)$ is the variation of the control function.

The functions $x_i^{(1)}(t)$ corresponding to $u^{(1)}(t)$ can be represented in a form similar to (14.53),

$$x_i^{(1)}(t) = x_i^{(0)}(t) + \delta x_i(t), \tag{14.54}$$

where $\delta x_i(t)$ are the variations of the phase coordinates.

The initial system (14.51), linearized with respect to $\delta u(t)$, $\delta x_i(t)$, yields the equations

$$\left.\begin{aligned} \delta\dot{x}_i &= \sum_{j=0}^{n} \frac{\partial f_i^{(0)}}{\partial x_j}\,\delta x_j + \frac{\partial f_i^{(0)}}{\partial u}\,\delta u \quad (i = 0, 1, \ldots, n); \\ \left(\frac{\partial f_i^{(0)}}{\partial x_j} = \frac{\partial f_i}{\partial x_j}\,[x_j^{(0)}(t), u^{(0)}(t), t];\right. & \\ \left.\frac{\partial f_i^{(0)}}{\partial u} = \frac{\partial f_i}{\partial u}\,[x_j^{(0)}(t), u^{(0)}(t), t]\right). & \end{aligned}\right\} \tag{14.55}$$

569 The initial conditions for $\delta x_i(t)$ are (cf. (14.52))

$$\delta x_i(0) = 0 \qquad (i = 0, 1, \ldots, n). \tag{14.56}$$

Introduce the linear system of differential equations

$$\dot{p}_i = -\sum_{j=0}^{n} \frac{\partial f_j^{(0)}}{\partial x_i}\,p_j \qquad (i = 0, 1, \ldots, n), \tag{14.57}$$

conjugate to the linear system (14.55). The main property of (14.55) and (14.57) is that

$$\frac{d}{dt}\sum_{i=0}^{n} p_i \delta x_i = \sum_{i=0}^{n} p_i \frac{\partial f_i^{(0)}}{\partial u}\delta u. \tag{14.58}$$

With the aid of the initial conditions (14.56), we can write this equality in the integral form

$$\sum_{i=0}^{n} p_{i1}\delta x_{i1} = \int_0^T \sum_{i=0}^{n} p_i \frac{\partial f_j^{(0)}}{\partial u}\delta u\, dt. \tag{14.59}$$

If the boundary values of the functions p_i of the conjugate equations are specified at the end of the interval (at $t = T$) in the forms

$$p_0(T) = 1,\ p_i(T) = 0 \qquad (i = 1, \ldots, n), \tag{14.60}$$

the formula (14.59) yields a value for the increment in the functional $\delta x_0(T)$, corresponding to the increment of the control function $\delta u(t)$, given by

$$\delta x_0(T) = \int_0^T \sum_{i=0}^{n} p_i \frac{\partial f_i^{(0)}}{\partial u}\delta u\, dt. \tag{14.61}$$

Now select the variation of the control function δu in the form

$$\delta u(t) = -\lambda \sum_{i=0}^{n} p_i \frac{\partial f_i^{(0)}}{\partial u}. \tag{14.62}$$

The variation of the functional will either have a sign opposite to that of the parameter λ or vanish, whatever the value of λ; in fact,

$$\delta x_0(T) = -\lambda \int_0^T \Big(\sum_{i=0}^{n} p_i \frac{\partial f_i^{(0)}}{\partial u}\Big)^2 dt, \tag{14.63}$$

570 so that

$$\left.\begin{aligned} &\delta x_0(T) < 0 \ \text{ at } \ \lambda > 0, \\ &\delta x_0(T) > 0 \ \text{ at } \ \lambda < 0, \\ &\delta x_0(T) = 0 \ \text{ at } \ \sum_{i=0}^{n} p_i \frac{\partial f_i^{(0)}}{\partial u} = 0. \end{aligned}\right\} \tag{14.64}$$

The structure of (14.62) chosen for the variation of the control function δu is the same as for the variation $\delta \dot{x}$ in the method of steepest descent in phase space (cf. (14.19)): one factor indicates the direction of the ascendent in the space of control variables, and the other factor determines the length of the step along the ascendent.

The particular value of the parameter λ will depend upon the condition for a minimum functional $x_0^{(1)}(T)$ at the given step of the iterative process. The functional $x_0^{(1)}(T)$ corresponding to the family of control functions (14.53) with variations δu taken in the form (14.62), is a function of the single parameter λ:

$$\dot{x}_i = f_i\Big(x_j, u^{(0)} - \lambda \sum_{i=0}^{n} p_i \frac{\partial f_i^{(0)}}{\partial u}, t\Big), \quad x_i(0) = x_{i0}\ (i, j = 0, 1, \ldots, n). \tag{14.65}$$

The latter is determined from the condition for minimum $x_0^{(1)}(T)$ using any numerical method (cf. § 1, Subsection 2).

We shall now formulate the algorithm of the steepest descent in the space of control variables for problems with free trajectory terminal points.

The Cauchy problem for the initial system (14.51) is solved with the aid of the known function $u^{(0)}(t)$. The result of this solution, i.e., the functions $x_i^{(0)}(t)$, is used to determine the partial derivatives $\partial f_i^{(0)}/\partial x_j$ so that the functions $p_i(t)$ of the conjugate system may be calculated; the Cauchy problem for system (14.57) with boundary conditions (14.60) is solved here by the inverse process. The variation $\delta u(t)$ is then expressed in the form (14.62); the parameter λ is determined from the condition for a minimum functional $x_0^{(1)}(T)$ at the given step of the process.

2. **Control function with constraints.** If the control function is constrained by

$$u_{\min}(t) \leqslant u(t) \leqslant u_{\max}(t), \tag{14.66}$$

the algorithm described above is altered as follows.

We establish $u^{(1)}(t)$ by the rule given in the preceding subsection, and then assume $u^{(1)}(t) = u_{\min}(t)$ in those segments where $u^{(1)}(t) < u_{\min}(t)$, and $u^{(1)}(t) = u_{\max}(t)$ in those segments where $u^{(1)}(t) > u_{\max}(t)$. In other words, the segments of the curve $u^{(1)}(t)$ which overstep the boundaries are cut off.

571 3. **Algorithm of the method for problems with fixed initial and terminal points of the trajectory.** We shall now describe the method of steepest descent in the space of control variables for the general problem (14.1) to (14.3); here $x_0(T)$, as before, is the function which is being minimized; the values of the phase coordinates at the end of the motion are specified by

$$\left.\begin{aligned} \dot{x}_i &= f_i(x_j, u, t) && (i, j = 0, 1, \ldots, n),\\ x_i(0) &= x_{i0} && (i = 0, 1, \ldots, n),\\ x_i(T) &= x_{i1},\ x_0(T) = \min && (i = 1, \ldots, n). \end{aligned}\right\} \tag{14.67}$$

We start by describing the method of penalty terms, as suggested by Courant /14.32/.

We form the following function composed of the final coordinate values /14.32, 14.18, 14.21, 14.27/:

$$P[x_0(T), x_1(T), \ldots, x_n(T)] = x_0(T) + \sum_{m=1}^{n} q_m [x_i(T) - x_{i1}]^2, \qquad q_m > 0. \tag{14.68}$$

When the final conditions $x_i(T) = x_{i1}$ are satisfied and the required minimum $x_0(T)$ is attained, the expression $P(T)$ also has a minimum which coincides with that of $x_0(T)$.

We now look for the minimum of $P(T)$ by simultaneously selecting values for the free parameters q_m which make the differences $x_i(T) - x_{i1}$ vanish. To that end we adjust the method to include a process which successively increases the parameters q_m. Suppose the initial approximation for the control function $u^{(0)}(t)$ is known. For small positive values $q_i^{(0)}$, we determine the control function $u^{(1)}(t)$ for the problem with a free terminal point by using an iterative process such that (14.68) is minimized (cf. Subsection 1).

If we take the control function $u^{(I)}(t)$ as the next approximation and choose parameters $q_m^{(I)}$ which exceed the corresponding values at the first step, e.g., $q_m^{(0)}$ ($q_1^{(I)} > q_1^{(0)}, \ldots, q_n^{(I)} > q_n^{(0)}$), the procedure may be repeated. Minimum $P(T)$ is given by the solution in the limit $q_m^{(K)} \to \infty$ /14.33/.

The sequence $q_m^{(0)}, q_m^{(I)}, \ldots, q_m^{(K)}$ is determined by the specific conditions of the problem. As a result, the trajectory terminal point can be considered as free at each progressive step of the process ($0 \to I \to \ldots \to K$). In the algorithm of the method, given in Subsection 1, we must alter the boundary conditions for the conjugate system to read

$$p_i(T) = \partial P^{(0)}/\partial x_i(T). \tag{14.69}$$

572 Note that if some of the final values of the phase coordinates are free according to the conditions of the problem, the corresponding terms will not figure in the expression for P.

Another way of satisfying the specified boundary conditions is now described /14.19, 14.22—14.24/.

Let the zero approximation for the control function $u^{(0)}(t)$ be known, and assume that the trajectory $x_i^{(0)}(t)$ has been calculated from this function. The initial conditions on the trajectory are satisfied exactly, and the final values differ from the specified values by the small magnitudes $\Delta_i^{(0)}$, so that

$$\left.\begin{aligned} x_i^{(0)}(0) &= x_{i0} \qquad (i = 0, 1, \ldots, n), \\ x_i^{(0)}(T) &= x_{i1} + \Delta_i^{(0)} \ (i = 1, \ldots, n). \end{aligned}\right\} \tag{14.70}$$

The order of smallness of these quantities must be such as to ensure that the variation in the control program $\delta u(t)$, necessary for correcting the final conditions, is situated within the limits of accuracy for the linear representation.

Consider $n+1$ conjugate systems of type (14.57) and final conditions

$$p_i^m(T) = \begin{cases} 0 & \text{at } i \neq m, \\ 1 & \text{at } i = m \end{cases} \quad (i, m = 0, 1, \ldots, n) \tag{14.71}$$

(the superscript without parentheses, m, gives the number of the system). With these systems, $n+1$ integral relations similar to (14.61) may be derived:

$$\left.\begin{aligned} \delta x_0(T) &= \int_0^T \sum_{i=0}^n p_i^0 \frac{\partial f_i^{(0)}}{\partial u}\,\delta u\,dt, \\ \delta x_m(T) &= \int_0^T \sum_{i=0}^n p_i^m \frac{\partial f_i^{(0)}}{\partial u}\,\delta u\,dt \quad (m = 1, \ldots, n). \end{aligned}\right\} \tag{14.72}$$

We determine the function $\delta u(t)$ which makes $\delta x_0(T)$ negative and ensures that the final conditions for the phase-coordinate variations are satisfied:

$$\delta x_0(T) < 0, \quad \delta x_m(T) = -\Delta_m^{(0)} \qquad (m = 1, \ldots, n). \tag{14.73}$$

Consider the Lagrange function

$$X = \int_0^T \Big(\sum_{i=0}^n p_i^0 \frac{\partial f_i^{(0)}}{\partial u}\,\delta u + \sum_{m=1}^n \lambda_m \sum_{i=0}^n p_i^m \frac{\partial f_i^{(0)}}{\partial u}\,\delta u \Big) dt + \sum_{m=1}^n \lambda_m \Delta_m^{(0)}. \tag{14.74}$$

573 If the variation of the control function $\delta u\,(t)$ is selected so that the n final conditions in (14.73) are satisfied, the Lagrange function X coincides with the variation of the control functional $\delta x_0\,(T)$. Choose the following expression for $\delta u\,(t)$:

$$\delta u = -\lambda\Big(\sum_{i=0}^{n} p_i^0 \frac{\partial f_i^{(0)}}{\partial u} + \sum_{m=1}^{n} \lambda_m \sum_{i=0}^{n} p_i^m \frac{\partial f_i^{(0)}}{\partial u}\Big) - \nu \sum_{m=1}^{n} \lambda_m \Delta_m^{(0)}. \tag{14.75}$$

If the parameters λ and ν are fixed, the Lagrange multipliers $\lambda_1, \ldots, \lambda_n$ in (14.75) may be selected so that the final conditions in (14.73) are satisfied. In fact, the multipliers $\lambda_1, \ldots, \lambda_n$ are determined from the system of linear equations

$$\sum_{m=1}^{n} \lambda_m \Big[\nu\Delta_m^{(0)} + \lambda \int_0^T \Big(\sum_{i=0}^{n} p_i^k \frac{\partial f_i^{(0)}}{\partial u}\Big)\Big(\sum_{j=0}^{n} p_j^m \frac{\partial f_j^{(0)}}{\partial u}\Big) dt\Big] =$$
$$= \Delta_k^{(0)} - \lambda \int_0^T \Big(\sum_{i=0}^{n} p_i^k \frac{\partial f_i^{(0)}}{\partial u}\Big)\Big(\sum_{j=0}^{n} p_j^0 \frac{\partial f_j^{(0)}}{\partial u}\Big) dt \quad (k = 1, \ldots, n). \tag{14.76}$$

This system is obtained from (14.73), if δu is replaced by (14.75) under the integral sign.

We now determine the parameters λ and ν which make the Lagrange function X negative for any value of the deviations $\Delta_m^{(0)}$; according to the previous note this means that the variation of the control functional $\delta x_0\,(T)$ is negative. For selected δu, (14.74) takes the form

$$X = -\lambda \int_0^T \Big(\sum_{i=0}^{n} p_i^0 \frac{\partial f_i^{(0)}}{\partial u} + \sum_{m=1}^{n} \lambda_m \sum_{i=0}^{n} p_i^m \frac{\partial f_i^{(0)}}{\partial u}\Big)^2 dt +$$
$$+ \sum_{m=1}^{n} \lambda_m \Delta_m^{(0)} \Big[1 - \nu \int_0^T \Big(\sum_{i=0}^{n} p_i^0 \frac{\partial f_i^{(0)}}{\partial u} + \sum_{m=1}^{n} \lambda_m \sum_{i=0}^{n} p_i^m \frac{\partial f_i^{(0)}}{\partial u}\Big) dt\Big]. \tag{14.77}$$

A value of $\lambda > 0$ and the parameter ν are required so that the second term in (14.77) becomes negative. The determination of ν is linked with the difficulties of multiple choice, since the multipliers λ_m depend on ν according to (14.76).

If $\Delta_1^{(0)} = 0, \ldots, \Delta_n^{(0)} = 0$ then $X < 0$ independently of the value of ν. The solution of the problem is attained when the following set of conditions is realized:

$$p_i^m \frac{\partial f_i}{\partial u} \equiv 0 \quad (m = 1, \ldots, n), \quad p_i^0 \frac{\partial f_i}{\partial u} \equiv 0. \tag{14.78}$$

574 Unlike the preceding case, the parameter λ is not selected from the condition of minimizing the control functional $x_0^{(1)}\,(T)$ at the given step of the process, but from the following considerations. The smaller the value of λ, the smaller the length of the step and the smaller the increment in the functional. On the other hand, if the parameter λ is too large, the length of the step is large and the accuracy to which the linear equations (14.55) describe the motion oversteps the specified limits; moreover, the fulfillment of the final conditions (14.73) in a linear formulation does not guarantee that the final conditions are properly satisfied to the given accuracy; this imposes an upper bound on the parameter λ. It is therefore best to take the parameter λ as equal to its upper limit, which generally depends on the properties of the specific problem.

4. Generalization of the procedure for arbitrary boundary conditions. The analysis described in the preceding subsection can be generalized to the case when some relations between the coordinates at the end of an interval are specified rather than the coordinates themselves:

$$\psi_i [x_1 (T), \ldots, x_n (T)] = 0 \qquad (i = 1, \ldots, l \leqslant n). \tag{14.79}$$

The formulas which have to be altered are (14.68), (14.71)—(14.73). Expression (14.68) is replaced by

$$P [x_0 (T), x_1 (T), \ldots, x_n (T)] = x_0 (T) + \sum_{m=1}^{l} q_m \psi_m^2. \tag{14.80}$$

Instead of (14.71), we must write the boundary conditions for the system of conjugate functions as

$$p_i^0 (T) = \begin{cases} 1 & \text{at } i = 0, \\ 0 & \text{at } i \neq 0, \end{cases} \qquad p_i^m = \frac{\partial \psi_m^{(0)}}{\partial x_i} \begin{matrix} (i = 1, \ldots, n, \\ m = 1, \ldots, l); \end{matrix} \tag{14.81}$$

expressions (14.72) for the terminal values of the coordinates are then replaced by

$$\left.\begin{aligned} \delta x_0 (T) &= \int_0^T \sum_{i=0}^{n} p_i^0 \frac{\partial f_i^{(0)}}{\partial u} \delta u \, dt, \\ \delta \psi_m &= \int_0^T \sum_{i=0}^{n} p_i^m \frac{\partial f_i^{(0)}}{\partial u} \delta u \, dt \quad (m = 1, \ldots, n), \end{aligned}\right\} \tag{14.82}$$

and in (14.73) we will have $\Delta_m^{(0)} = \psi_m^{(0)}$.

5. Algorithm of the method for problems with free terminal point and free time of motion. So far, the beginning and end of the time interval have been assumed given. There are however many problems in which the time T at the end of the motion is unspecified. The class of problems of maximum rapid action belongs to these.

Suppose the results obtained above are generalized to the case of a free trajectory terminal point and unspecified duration time T of the motion. If the functional being minimized has the form (cf. (14.68))

$$P [x_0 (T), x_1 (T), \ldots, x_n (T), T], \tag{14.83}$$

the values $x_0 (T)$, $x_1 (T), \ldots, x_n (T), T$ are free. The value T at each step of the iterative process is determined as that point $t = T$ at which the function $P (t)$, calculated along the trajectory, has a minimum. Suppose there is only one such point on the trajectory; then

$$\frac{d}{dt} P [x_0 (t), x_1 (t), \ldots, x_n (t), t] = \frac{\partial P}{\partial t} + \sum_{i=0}^{n} \frac{\partial P}{\partial x_i} f_i = 0. \tag{14.84}$$

The increment in the functional $\delta P (T)$, which is caused by an increment in the control function $\delta u (t)$, is written as

$$\delta P (T) = \sum_{i=0}^{n} \frac{\partial P^{(0)}}{\partial x_i (T)} \delta x_i (T) + \left[\sum_{i=0}^{n} \frac{\partial P^{(0)}}{\partial x_i (T)} f_i^{(0)} (T) + \frac{\partial P^{(0)}}{\partial T} \right] \delta T \tag{14.85}$$

(the superscript 0 indicates as usual that the functions were calculated from the zero approximation for the control function $u^{(0)}(t)$). Since in a zero approximation the time $T^{(0)}$ is likewise determined from condition (14.84), the variation of the functional becomes

$$\delta P(T) = \sum_{i=0}^{n} \frac{\partial P^{(0)}}{\partial x_i(T)} \delta x_i(T). \tag{14.86}$$

The boundary conditions for the conjugate system of equations are (cf. (14.69))

$$p_i(T) = \frac{\partial P^{(0)}}{\partial x_i(T)}. \tag{14.87}$$

The distinguishing feature of the method for problems with a free trajectory terminal point and free duration time is that the latter is determined by (14.84) after the control function has been found at the given step of the iterative process.

It may happen that (14.84) is not satisfied in the region over which the control function is defined, i.e., that the length of the time interval over
576 this step exceeds that over the preceding step. This does not occur when the region over which the control function is defined is not smaller than the maximum value of the interval at all steps of the iterative process. Consequently, we must refine the process of finding the variation of the control function at each k-th step. Thus, the control function itself alters over the interval $T_{\max}$ to $T^{(k-1)}$. This can be carried out if the conjugate system is integrated not only inversely from $t = T^{(k-1)}$ to $t = 0$, but also directly from $t = T^{(k-1)}$ to $t = T_{\max}$. It is true that the value $T_{\max}$ cannot be exactly established beforehand.

6. Examples. The method of steepest descent in the space of control variables can be illustrated by two examples given in /14.20, 14.26/ (cf. also /14.27/).

The first of them /14.20/ deals with the transfer between the circular orbits of the Earth and Mars using a solar sail. The variational problem consists in determining the optimum program of the sail orientation $\psi(t)$ to ensure a minimum displacement time T between the two circular orbits. The equations of motion and the boundary conditions are, in dimensionless variables (cf. Chapter Nine),

$$\left.\begin{aligned} &\dot{r} = v_r, && r(0) = 1, \quad r(T) = r_1, \\ &\dot{v}_r = \frac{a_0}{r^2}|\cos^3\psi| + \frac{v_\varphi^2}{r} - \frac{1}{r^2}, && v_r(0) = 0, \ v_r(T) = 0, \\ &\dot{v}_\varphi = \frac{a_0}{r^2}\sin\psi\cos^2\psi - \frac{v_r v_\varphi}{r}, && v_\varphi(0) = 1, \ v_\varphi(T) = r_1^{-1/2}, \\ & && T = \min. \end{aligned}\right\} \tag{14.88}$$

The angular displacement of the vehicle is not specified; examples are given for $r_1 = 1.52$, $a_0 = 0.17$ ($= 0.1\ \text{cm/sec}^2$).

The second example /14.28/ involves interorbital Earth—Mars transfer with a constantly-operating thrust of fixed magnitude (cf. Chapter Six). In the variational problem we must determine the optimum direction of the thrust vector $\theta(t)$ which minimizes the time of displacement between

two specified points on circular orbits. The equations of motion and the boundary conditions are

$$\left.\begin{aligned}
&\dot r = v_r, && r(0)=1,\quad r(T)=r_1,\\
&\dot\varphi = v_\varphi/r, && \varphi(0)=0,\quad \varphi(T)=\varphi_1,\\
&\dot v_r = \frac{a_0\sin\theta}{1-\mu_0 t}+\frac{v_\varphi^2}{r}-\frac{1}{r^2}, && v_r(0)=0,\quad v_r(T)=0,\\
&\dot v_\varphi = \frac{a_0\cos\theta}{1-\mu_0 t}-\frac{v_r v_\varphi}{r}, && v_\varphi(0)=1,\quad v_\varphi(T)=r_1^{-1/2},\\
&&& T=\min;
\end{aligned}\right\} \qquad (14.89)$$

577 the quantity a_0 is the initial thrust acceleration ($a_0 = gP/G_0$) and μ_0 is the reduced mass discharge ($\mu_0 = gq'/G_0$). The values used in the example were $a_0 = 0.846 \cdot 10^{-4}$ g, $\mu_0 = 1.29 \cdot 10^{-3}$ days^{-1}.

Both (14.88) and (14.89) belong to the class of problems of maximum rapid action; the procedure for solving such problems was described in Subsection 5 of this section. Both methods described in Subsection 3 are used so that the given boundary conditions are satisfied.

In (14.88) the boundary conditions are satisfied by a similar method to the conventional one of steepest descent (formulas (14.71), (14.75), (14.76)); in (14.89) they were satisfied by the method of penalty terms (formulas (14.68), (14.69)). A way of selecting the coefficients q_m is suggested in /14.28/. Towards the beginning of the process the values of q_m are small, and after the 25-th step q_m increases proportionally to $|x_i^{(25)}(T) - x_{i1}|$.

Figures 14.3, 14.4 represent the programs $\psi(t)$ of the sail orientation and the trajectories which correspond to the zero approximation (0), the first (1) and second (2) steps of the iterative process, and the final (∞) solution of problem (14.88).

Figures 14.5, 14.6 give $\theta(t)$, the thrust-vector direction, and the trajectory corresponding to the zero approximation (0), the second (2) and seventh (7) steps of the process, and also the final (∞) solution of problem (14.89) with a free angular displacement φ_1.

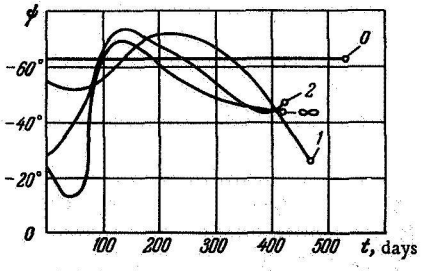

FIGURE 14.3. Programs $\psi(t)$ of sail orientation corresponding to zero approximation (0), first (1) and second (2) steps of iterative process, and final solution (∞), by method of steepest descent in space of control variables.

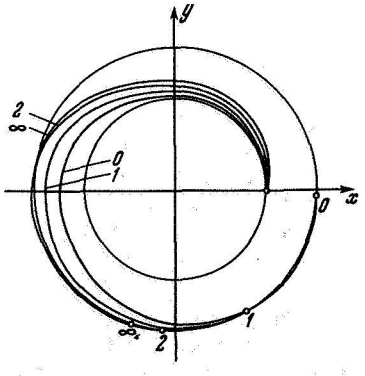

FIGURE 14.4. Flightpath corresponding to zero approximation (0), first (1) and second (2) steps of iterative process, and final solution (∞), by method of steepest descent in space of control variables.

578 The functionals of the problems, i.e., the times of motion T are given on the horizontal axes of Figures 14.3, 14.5.

Although problem (14.89) requires a much larger number of iterative steps to achieve the required accuracy, the total calculation time for the method of penalty terms is smaller than for the conventional steepest-descent method. This is because the latter method requires time-consuming operations to determine the Lagrange multipliers $\lambda_1, \ldots, \lambda_n$.

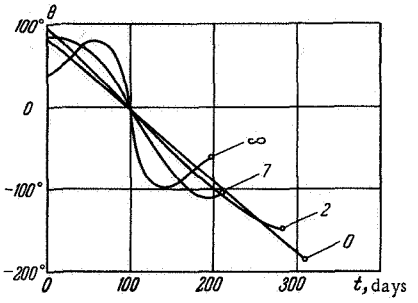

FIGURE 14.5. Programs $\theta(t)$ of thrust-vector direction corresponding to zero approximation (0), second (2) and seventh (7) steps of iterative process, and final solution (∞), by method of steepest descent in space of control variables.

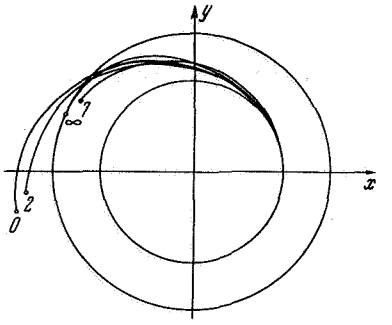

FIGURE 14.6. Flightpath corresponding to zero approximation (0), second (2) and seventh (7) steps of iterative process, and final solution (∞), by method of steepest descent in space of control variables.

7. Constraints on the phase coordinates. In addition to a free terminal point (14.51), the Mayer problem also has a condition that the combination of phase coordinates and control variables be limited in value.

In this new formulation we require a control function $u(t)$ which makes the control functional $x_0(T)$ a minimum, while satisfying the following inequalities along the trajectory:

$$\varphi_{\min} \leqslant \varphi(x_j, u, t) \leqslant \varphi_{\max}. \tag{14.90}$$

Analytic solutions of variational problems with phase constraints are given in /14.33/ and /14.25/; numerical solutions are described in /14.18, 14.26, 14.32/.

Following the treatment in /14.26/, we now classify these constraints.

Let inequality (14.90) be a phase constraint of zero order when the control variable φ figures explicitly in the function u, i.e., $(\partial\varphi/\partial u) \not\equiv 0$. A phase constraint of the second order is when the control variable u appears explicitly in the first full derivative with respect to time of the function φ, i.e., $(\partial\dot{\varphi}/\partial u) \not\equiv 0$, etc.

579 The phase constraint of zero order is the only one which can be treated as a constraint of the control function. If the substitution

$$v = \varphi(x_j, u, t) \tag{14.91}$$

is introduced, we may express the control variable u in terms of v, x_j, t (assume that this can be done analytically) so that $u = \psi(x_j, v, t)$; the control

variable v, which is constrained according to (14.90), will now appear in (14.51) instead of u.

If u is not constrained, such a substitution leads to the Mayer problem with a constrained control function v; the method of solving this problem is given in Subsection 2.

Suppose u is constrained together with v. We split the interval $[0, T]$ into three types of segments. In the first type of segments the control variable u takes a boundary value, and v lies within the permissible range of values; in the second type of segments v lies on the boundary and u lies within the permissible range of values, while in the third type, u and v are both located within their range of values. The first and second types of segments do not overlap. The idea underlying this method of solving the Mayer problem (14.51) with a constraint on u and a zero-order phase constraint on v is described below.

In the first type of segments the variation of the control functional is expressed in terms of the variation $u(t)$ and is determined by the optimum variation of this control variable. For the second type of segments the control functional is written in terms of the variation of $v(t)$ and is determined by the optimum variation of $v(t)$. In the third type of segments both control variables $u(t)$ and $v(t)$ can appear in the expression for the variation of the control functional. The method of solving the Mayer problem with a constraint on the control variable is known (cf. Subsection 2), and therefore we may establish the optimum control for each segment, allowance being made for the corresponding constraint. Unlike (14.57), the following conjugate system is introduced:

$$\left.\begin{aligned} \dot{p}_i &= \sum_{j=0}^{n} p_j \left[-\frac{\partial f_j^{(0)}}{\partial x_i} + \frac{\partial f_j^{(0)}}{\partial u} \left(\frac{\partial \varphi^{(0)}}{\partial x_i} \Big/ \frac{\partial \varphi^{(0)}}{\partial u} \right) \delta \right], \\ p_0(T) &= 1, \quad p_i(T) = 0 \quad (i = 1, \ldots, n). \end{aligned}\right\} \tag{14.92}$$

Here $\delta(t)$ is the Dirac function, taking the value 1 over segments in which the solution is governed by the constraints $v = \varphi_{\min}$, $v = \varphi_{\max}$, and the value 0 over segments in which the solution is governed by the constraints $u = u_{\min}$, $u = u_{\max}$. Over segments in which neither u nor v are constrained, the function may be taken as equal to either 0 or 1.

580 The variation of the control functional $\delta x_0(T)$ is expressed as

$$\delta x_0(T) = \int_0^T \sum_{i=0}^{n} p_i \frac{\partial f_i^{(0)}}{\partial u} \left[\sum_{j=0}^{n} \left(\frac{\partial \varphi^{(0)}}{\partial x_j} \Big/ \frac{\partial \varphi^{(0)}}{\partial u} \right) \delta x_i \delta + \delta u \right] dt. \tag{14.93}$$

Taking into account that

$$\delta v = \sum_{j=0}^{n} \frac{\partial \varphi^{(0)}}{\partial x_j} \delta x_j + \frac{\partial \varphi^{(0)}}{\partial u} \delta u, \tag{14.94}$$

the variation $\delta x_0(T)$ can be written in the form

$$\delta x_0(T) = \int_0^T \sum_{i=0}^{n} p_i \frac{\partial f_i^{(0)}}{\partial u} \left[\delta v \delta / (\partial \varphi^{(0)} / \partial u) + \delta u (1 - \delta) \right] dt. \tag{14.95}$$

Suppose there are no constraints on the control variables u and v; we then select the following expressions for the variations of the control functions δu, δv:

$$\left.\begin{aligned} &\text{at } \delta(t)=0 \\ &\qquad \delta u = -\lambda_u \sum_{i=0}^{n} p_i \frac{\partial f_i^{(0)}}{\partial u}, \\ &\text{at } \delta(t)=1 \\ &\qquad \delta v = -\lambda_v \frac{\partial \varphi^{(0)}}{\partial u} \sum_{i=0}^{n} p_i \frac{\partial f_i^{(0)}}{\partial u}. \end{aligned}\right\} \tag{14.96}$$

The descent parameters λ_u, λ_v are linked by the continuity condition of the variation δu at the points where the function $\delta(t)$ changes value; at $t = t'$, where $\delta(t)$ jumps from 0 to 1, this relation is written as

$$\begin{gathered} \delta u(t'-0) = \delta u(t'+0), \\ \delta u(t'+0) = \delta v(t'+0)/(\partial \varphi^{(0)}/\partial u)' - \sum_{i=0}^{n} \left(\frac{\partial \varphi^{(0)}}{\partial x_i}\right)' \delta x_i' \end{gathered} \tag{14.97}$$

and

$$\lambda_v = \lambda_u + \frac{\sum_{i=0}^{n} \left(\frac{\partial \varphi^{(0)}}{\partial x_i}\right) \delta x_i'}{\sum_{i=0}^{n} p_i' \left(\frac{\partial f_i^{(0)}}{\partial u}\right)'} \tag{14.98}$$

(the primes indicate values corresponding to $t = t'$).

581 For $v(t)$ unconstrained and $u(t)$ constrained, we must write $\delta(t) \equiv 0$; this case corresponds to a constraint on the control function $u(t)$, considered in Subsection 2.

For $u(t)$ unconstrained and $v(t)$ constrained, we must put $\delta(t) \equiv 1$. Any further step depends on whether we are able to find an analytic solution of the equation $v = \varphi(x_i, u, t)$ for u. If this is possible, the problem reduces to the preceding case; if not, the following procedure has to be followed (cf. Subsection 2).

The variation δv is taken as (cf. (14.96))

$$\delta v(t) = \begin{cases} -\lambda \frac{\partial \varphi^{(0)}}{\partial u} \sum_{i=0}^{n} p_i \frac{\partial f_i^{(0)}}{\partial u}, & \text{if } \varphi_{\min} \leqslant v^{(0)} - \lambda \frac{\partial \varphi^{(0)}}{\partial u} \sum_{i=0}^{n} p_i \frac{\partial f_i^{(0)}}{\partial u} \leqslant \varphi_{\max}, \\ \varphi_{\max} - v^{(0)}, & \text{if } v^{(0)} - \lambda \frac{\partial \varphi^{(0)}}{\partial u} \sum_{i=0}^{n} p_i \frac{\partial f_i^{(0)}}{\partial u} \geqslant \varphi_{\max}, \\ \varphi_{\min} - v^{(0)}, & \text{if } \varphi_{\min} \geqslant v^{(0)} - \lambda \frac{\partial \varphi^{(0)}}{\partial u} \sum_{i=0}^{n} p_i \frac{\partial f_i^{(0)}}{\partial u}, \end{cases} \tag{14.99}$$

where the parameter λ is kept small so that the problem has a linear representation. For a known function $\delta v(t)$ (cf. (14.69)), (14.94) determines the variation of the control function δu in terms of the variation of the coordinates δx_i. This expression is substituted into (14.55) and the Cauchy problem (14.55)—(14.56) is then solved. The solution for the functions $\delta x_i(t)$ is used to determine the variation of the control functions $\delta u(t)$.

Note that the control function $u^{(1)}(t)$ which was found satisfies constraint (14.90) only to a linear approximation.

Consider again the problem in which $u(t)$ and $v(t)$ are both constrained. If $v(t)$ is unconstrained at the beginning of the trajectory ($0 \leqslant t \leqslant t'$), we may put $\delta(t) = 0$ in the first segment and calculate the variation $\delta u(t)$ at each time t using formulas similar to (14.99). At the same time we may integrate the Cauchy problem (14.51) with the known control function $u^{(1)}(t)$ and test inequalities (14.90). Suppose $t = t'$ is the first instant at which one of the inequalities (14.90) is not satisfied. We then put $\delta(t) = 1$ and determine the variation $\delta v(t)$ by formulas (14.99). At $t = t'$ the variation $\delta u(t)$ must be
582 continuous (cf. (14.98)). At each instant we may calculate $\delta u(t)$ from the known function $\delta v(t)$, according to the rule given above. We then test whether $u^{(1)}(t)$, the function obtained, satisfies inequalities (14.66). In this way the required solution is obtained by alternating steepest descents in the $u(t)$ space and the $v(t)$ space.

This algorithm for the solution is suitable for variational problems with zero-order phase constraints.

For arbitrary phase constraints, we may obtain optimum solutions using a penalty function /14.18, 14.26, 14.32/.

An equation for the penalty function x_{n+1} is added to the initial system of differential equations (14.51),

$$\dot{x}_{n+1} = K(\varphi)(\varphi - \varphi_{\min})(\varphi_{\max} - \varphi), \tag{14.100}$$

where K is defined as follows:

$$\left.\begin{array}{lll} K(\varphi) = K_1 = \text{const} & \text{at} & \varphi < \varphi_{\min}, \\ K(\varphi) = K_1 = \text{const} & \text{at} & \varphi > \varphi_{\max}, \\ K(\varphi) = 0 & \text{at} & \varphi_{\min} \leqslant \varphi \leqslant \varphi_{\max}. \end{array}\right\} \tag{14.101}$$

Let

$$x_{n+1}(0) = 0; \tag{14.102}$$

the value $x_{n+1}(T) \leqslant 0$ will then characterize the extent to which inequalities (14.90) are violated. If $x_{n+1}(T) = 0$, then according to the definition of $K(\varphi)$ inequalities (14.90) will be satisfied everywhere in the interval $[0, T]$.

We determine the control function $u(t)$, which minimizes the control functional $x_0(T)$ and ensures a zero terminal value of the penalty function $x_{n+1}(T)$, i.e.,

$$x_{n+1}(T) = 0. \tag{14.103}$$

When condition (14.103) is satisfied inequalities (14.90) will also be satisfied.

8. Numerical methods based on Pontryagin's maximum principle. In this subsection a method is described which is similar to that of steepest descent in the space of the control variables and based on the maximum principle /14.21, 14.35/.

Consider the Mayer problem with a free terminal point (14.51). In order to solve it by Pontryagin's method we form the Hamiltonian H and write the equations for the momenta p_i as

$$\left.\begin{aligned} H &= \sum_{i=0}^{n} p_i f_i(x_j, u, t), \\ \dot{p}_i &= -\frac{\partial H}{\partial x_i} = -\sum_{j=0}^{n} p_j \frac{\partial f_j}{\partial x_i}. \end{aligned}\right\} \tag{14.104}$$

583 The terminal values of the momenta $p_i(T)$ are

$$p_0(T) = -1, \; p_i(T) = 0 \qquad (i = 1, \ldots, n) \tag{14.105}$$

(compare the terminal values of the functions of the conjugate system (14.60); in Pontryagin's method the momenta are normalized so that the momentum corresponding to the control functional is negative at the terminal point).

So that the functional $x_0(T)$ attains a minimum, the optimum control function $u(t)$ must maximize the function H, where

$$u_{\text{opt}}(t) \to \max_{u(t)} H(x_i, p_i, u, t). \tag{14.106}$$

The following algorithm for solving this problem was suggested in /14.21, 14.35/.

With the specified zero approximation for the control function $u^{(0)}(t)$, the Cauchy problem may be solved directly for the system of phase variables (14.51). Hence, the values of the phase coordinates $x_i^{(0)}(t)$ are obtained at each point. With the known $x^{(0)}(t)$, $u^{(0)}(t)$, we now solve the Cauchy problem inversely for the equations governing the momenta (14.104), (14.105); as a result we obtain the functions $p_i^{(0)}(t)$. The control function at the next step, $u^{(1)}(t)$, is found from the condition of maximizing the Hamiltonian H,

$$\max_{u^{(1)}(t)} H[x_i^{(0)}(t), p_i^{(0)}(t), u^{(1)}, t]. \tag{14.107}$$

A modification of this algorithm is suggested in /14.21/. If the control function $u^{(1)}(t)$ which maximizes the Hamiltonian (cf. (14.107)) is represented by $\bar{u}$, the next approximation can be expressed in the form

$$u^{(1)}(t) = u^{(0)}(t) + \lambda\,[\bar{u}(t) - u^{(0)}(t)]. \tag{14.108}$$

The parameter λ is found from the condition for a minimum control functional at each step of convergence of the process.

We now discuss the rate of convenience of the method (cf. /14.35/).

The increment in the functional $\Delta x_0(T)$ caused by the variation of the control function $\delta u(t)$ is given by

$$\Delta x_0(T) = -\int_0^T [H(x_i^{(0)}, p_i^{(0)}, u^{(1)}, t) - H(x_i^{(0)}, p_i^{(0)}, u^{(0)}, t)]\,dt - L, \tag{14.109}$$

584 where L is the residual term, assessed as follows:

$$|L| \leqslant A\left(\int_0^T |u^{(1)}(t) - u^{(0)}(t)|\,dt\right)^2 \tag{14.110}$$

(A is a fixed constant related to the constants in the Lipshitz conditions for the functions f_i and $\partial H/\partial x_i$). At each step of the iterative process the control function $u^{(1)}(t)$ (or $\bar{u}(t)$ in the modified method (14.108)) is selected from the condition for a maximum H with respect to u. This method, with an accuracy of up to high-order infinitesimals relative to $|u^{(1)}(t) - u^{(0)}(t)|$, thus ensures a more rapid variation of the functional as compared with the other methods, which only allow for the first variation. The smallness of $|u^{(1)}(t) - u^{(0)}(t)|$ is understood here in the sense of the integral norm figuring in the estimate of the residual term (14.110), i.e., the magnitude $|u^{(1)}(t) - u^{(0)}(t)|$ can be finite, but only during a short time interval.

The method can be applied with no modifications whatsoever to problems with constrained control functions.

Note that for right-hand sides of (14.104) of the form

$$f_i = \sum_{j=0}^{n} a_{ij}(t)x_j + b_i(u, t) \tag{14.111}$$

the above iterative process is expressed in one step. In fact, the phase coordinates x_j and the control functions u do not appear in the differential equations for the momenta (cf. (14.104))

$$\dot{p}_i = -\sum_{j=0}^{n} a_{ji}p_j; \tag{14.112}$$

therefore the functions $p_i(t)$ are found by solving the Cauchy problem for (14.112) with boundary conditions (14.105) once only by the inverse process. The optimum control function $u(t)$ is determined from the condition for a maximum of

$$\sum_{i=0}^{n} p_i(t)b_i(u, t). \tag{14.113}$$

This method can be applied to Mayer's problem (14.67) with fixed initial and terminal points of the trajectory by using the method of penalty terms (14.68). The terminal conditions for the momenta (14.105) are then replaced by

$$p_0(T) = -1, \quad p_i(T) = \frac{\partial P^{(0)}}{\partial x_i} \qquad (i = 1, \ldots, n) \tag{14.114}$$

(the expression for the function P is given by (14.68)).

585 An application of this method is described in /14.35/; the same paper gives suggestions about programming the method with a view to saving memory space.

§ 3. NEWTON'S FUNCTIONAL METHOD

The solutions $x_i(t)$ of the boundary-value problem (14.10) to which the variational problems are reduced must satisfy differential equations as well as initial and final conditions. Two types of iterative processes can be used to solve the problems. The first type consists in exactly satisfying

the initial and final conditions, but only approximately satisfying the differential equations at each step; the exact solution is approached during the iterative process, and the accuracy is evaluated in terms of the norm in the functional space. The second type consists in exactly satisfying the differential equations and the initial conditions at each step of the process; with each step the final values $x_j(T)$ approach the required values x_{j1}, and the degree of approximation is assessed in terms of the norm of the finite-dimensional space.

In this subsection Newton's functional method described and its generalization with respect to iterative processes of the first type. The algorithm is derived for the generalized functional method of Newton; the traditional method of Newton is obtained as a particular case.

Newton's functional method was studied in /14.10, 14.13, 14.36/.

1. Algorithm of the method. We describe the algorithm of Newton's generalized functional method applied to a boundary-value problem of the first kind for a second-order differential equation:

$$\ddot{x} = f(x, \dot{x}, t);\ x(0) = x_0,\ x(T) = x_1. \tag{14.115}$$

The functional, the distance in the functional space $x(t)$, is defined by

$$J = \int_0^T [\ddot{x} - f(x, \dot{x}, t)]^2\, dt. \tag{14.116}$$

The functional tends to zero when the boundary conditions (14.115) are satisfied; this will indicate that we are approaching the required element $x^*(t)$.

Suppose we know a zero approximation to the required solution, $x^{(0)}(t)$ say, which satisfies the boundary conditions. The next approximation is represented in the form

$$x^{(1)}(t) = x^{(0)}(t) + \delta x(t). \tag{14.117}$$

586 The function $\delta x(t)$ has a norm which is small compared with the norm of $x^{(0)}(t)$. We select the following boundary values for $\delta x(t)$:

$$\delta x(0) = \delta x(T) = 0. \tag{14.118}$$

The variation of the functional J caused by $\delta x(t)$ is

$$\delta J = 2\int_0^T (\ddot{x}^{(0)} - f^{(0)})\left(\delta\ddot{x} - \frac{\partial f^{(0)}}{\partial \dot{x}}\delta\dot{x} - \frac{\partial f^{(0)}}{\partial x}\delta x\right) dt; \tag{14.119}$$

here $\ddot{x}^{(0)}$, $f^{(0)}$, $\partial f^{(0)}/\partial \dot{x}$, $\partial f^{(0)}/\partial x$ are functions of t calculated at $x = x^{(0)}(t)$.

From all the variations $\delta x(t)$ which satisfy the boundary conditions (14.118) we select a variation which decreases the value of the functional $x^{(0)}(t)$ calculated according to the zero approximation $\delta x(t)$, i.e., we choose one which makes the first variation δJ negative.

Such a variation is given by the function $\delta x(t)$ subject to the conditions

$$\delta\ddot{x} - \frac{\partial f^{(0)}}{\partial \dot{x}}\delta\dot{x} - \frac{\partial f^{(0)}}{\partial x}\delta x = -\lambda(\ddot{x}^{(0)} - f^{(0)}),\quad \delta x(0) = \delta x(T) = 0, \tag{14.120}$$

where λ is a positive parameter.

Introduce a function $\eta(t)$ defined by (cf. (14.25))

$$\eta(t) = \delta x(t)/\lambda; \tag{14.121}$$

relation (14.117) is then rewritten as

$$x^{(1)}(t) = x^{(0)}(t) + \lambda\eta(t), \tag{14.122}$$

and the differential equation and boundary conditions (14.120) become

$$\ddot{\eta} - \frac{\partial f^{(0)}}{\partial \dot{x}}\dot{\eta} - \frac{\partial f^{(0)}}{\partial x}\eta = -\ddot{x}^{(0)} + f^{(0)}, \quad \eta(0) = \eta(T) = 0. \tag{14.123}$$

Thus, the procedure for determining the function $\delta x(t)$ is split into two parts: the determination of $\eta(t)$ satisfying conditions (14.123), and finding the parameter λ. When solving the boundary-value problem (14.123) for linear differential equations one can use the P-process ("progonka" process) or any other suitable method (cf. for instance /14.37—14.39/). The determination of the parameter λ is linked with the solution of the following problem for a minimum.

Assume that the function $\eta(t)$ has been found from (14.123); the dependence
587 of $x^{(1)}$ on t and λ is then known, and the functional J is a known function of the parameter λ. We look for a value of λ which minimizes the integral (14.116) at the given step of the process:

$$J_{\min} = \min_{\lambda} \int_0^T [\ddot{x}^{(0)} + \lambda\ddot{\eta} - f(x^{(0)} + \lambda\eta, \dot{x}^{(0)} + \lambda\dot{\eta}, t)]^2 dt. \tag{14.124}$$

This method for determining the parameter λ is similar to the one used in the method of steepest descent to find the descent parameter (cf. (14.28), (14.65)).

The iterative process considered can be formulated as follows:

At each step of the process, described by an expression like (14.122), the boundary-value problem must be solved for the linear equation (14.123) where the coefficients and the right-hand side are determined by the results of the preceding step; the value of the parameter λ must also be found using a numerical method and condition (14.124).

If the initial differential equation (14.115) is linear, the iterative process degenerates into a single step, and the minimizing value of the parameter λ is unity. In fact, when the function f is linear with respect to the arguments x and $\dot{x}$, $J(\lambda)$ takes the form

$$J(\lambda) = J^{(0)}(1 - \lambda)^2, \tag{14.125}$$

where $J^{(0)}$ is the value of the integral (14.116) calculated by the zero approximation ($\lambda = 0$). The minimum of $J(\lambda)$ is attained for $\lambda = 1$ and is equal to zero; this corroborates the opinion advanced above.

For an arbitrary non-linear equation (14.115) the relationship $J(\lambda)$ contains other terms, in addition to the first term $J^{(0)}(1 - \lambda)^2$, depending

on powers of λ higher than the first; the coefficients multiplying the powers of λ decrease as the expansion of f in terms of the linear terms $x - x^*$, $\dot{x} - \dot{x}^*$ improves. In the course of the iterative process $J(\lambda)$ approaches the form (14.125), and therefore the minimizing value of λ approaches unity.

If the parameter λ is taken as unity in all iterations for an arbitrary non-linear equation, the proposed method reduces to the traditional functional analysis of Newton.

The method can be generalized to cover non-linear differential equations of arbitrary order, and also a system of equations. The functional being minimized can be represented respectively by the integral of the square of the deviation of the differential equation, or by the integral of the sum of squares of the deviations of the different equations comprising the system.

2. Example. To illustrate the rate of convergence of the proposed method, and to compare it with other methods, we consider motion in a central field.

588 The transfer between given coordinates in a central field is described by the system of two second-order differential equations

$$\left.\begin{aligned} \ddot{x} &= -kx\,(x^2+y^2)^{-3/2}, \quad x(0)=x_0, \quad x(T)=x_1, \\ \ddot{y} &= -ky\,(x^2+y^2)^{-3/2}, \quad y(0)=y_0, \quad y(T)=y_1. \end{aligned}\right\} \tag{14.126}$$

Unlike the scale which is usually adopted (cf. the Appendix), the time unit is here taken as 100 average solar days, while, as before, the astronomic unit is taken as the unit of linear distance; the coefficient k is then $k = 2.9591$.

Following the treatment in /14.17/, the initial and final coordinates and the times are defined by

$$\left.\begin{aligned} x(0) &= 0.99850, \quad x(2) = -1.3558, \\ y(0) &= 0.07107, \quad y(2) = 0.96570, \end{aligned}\right\} \tag{14.27}$$

and the zero approximations $x^{(0)}(t)$, $y^{(0)}(t)$ are

$$\left.\begin{aligned} x^{(0)}(t) &= \frac{\sin n(2-t)}{\sin 2n}\,x_0 + \frac{\sin nt}{\sin 2n}\,x_1, \\ y^{(0)}(t) &= \frac{\sin n(2-t)}{\sin 2n}\,y_0 + \frac{\sin nt}{\sin 2n}\,y_1 \\ (n &= 1.0462). \end{aligned}\right\} \tag{14.128}$$

The iterative process of Newton's generalized functional method is given by

$$x^{(1)}(t) = x^{(0)}(t) + \lambda\eta_x(t), \quad y^{(1)}(t) = y^{(0)}(t) + \lambda\eta_y(t). \tag{14.129}$$

The functions $\eta_x(t)$, $\eta_y(t)$ are found from the solution of the boundary-value problem

$$\left.\begin{aligned} &\ddot{\eta}_x + \frac{\partial X^{(0)}}{\partial x}\,\eta_x + \frac{\partial X^{(0)}}{\partial y}\,\eta_y = -\ddot{x}^{(0)} - X^{(0)}, \quad \eta_x(0) = \eta_x(2) = 0, \\ &\ddot{\eta}_y + \frac{\partial Y^{(0)}}{\partial x}\,\eta_x + \frac{\partial Y^{(0)}}{\partial y}\,\eta_y = -\ddot{y}^{(0)} - Y^{(0)}, \quad \eta_y(0) = \eta_y(2) = 0, \\ &\qquad (X = kx\,(x^2+x^2)^{-3/2}, \quad Y = ky\,(x^2+y^2)^{-3/2}), \end{aligned}\right\} \tag{14.130}$$

and the parameter λ from the condition for a minimum of the expression

$$\min_{\lambda} \int_0^2 \{[\ddot{x} + \lambda\ddot{\eta}_x + X(x^{(0)} + \lambda\eta_x, y^{(0)} + \lambda\eta_y)]^2 + \\ + [\ddot{y}^{(0)} + \lambda\ddot{\eta}_y + Y(x^{(0)} + \lambda\eta_x, y^{(0)} + \lambda\eta_y)]^2\} dt. \qquad (14.131)$$

The linear boundary-value problem (14.130) was solved by the method of conjugate equations /14.39/; the minimizing values of the parameters λ are simultaneously obtained while plotting $J(\lambda)$.

590 The following results were obtained by this method.

TABLE 14.1. Decrease of functional for progressively higher iterations in Newton's generalized $J^{(k)}_{\lambda=\text{opt}}$ and traditional $J^{(k)}_{\lambda=1}$ functional methods

Iteration k	0	1	2	3
$J^{(k)}_{\lambda=\text{opt}}$	12.346	7.0862	0.25858	$0.46302 \cdot 10^{-4}$
$J^{(k)}_{\lambda=1}$	12.346	460.12	29.233	4.0145
Iteration k	4	5	6	7
$J^{(k)}_{\lambda=\text{opt}}$	$0.565 \cdot 10^{-8}$	0	0	0
$J^{(k)}_{\lambda=1}$	3.3005	0.030773	$0.46178 \cdot 10^{-4}$	$0.52063 \cdot 10^{-6}$

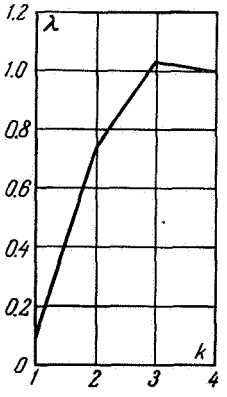

FIGURE 14.7. Variation of the minimizing parameter λ as a function of iteration number k according to Newton's generalized functional method.

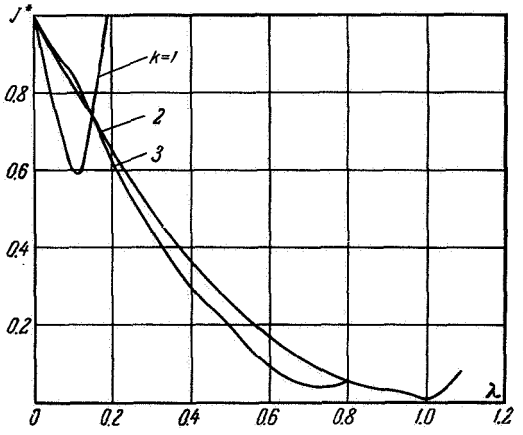

FIGURE 14.8. Example of how relative value of functional J^* depends on parameter λ for first, second, third iterations, using Newton's generalized functional method.

The rate of convergence of the process is described by Table 14.1, which gives the values of the integral J at each step k (the second row $J_{\lambda=\text{opt}}$). For comparison, the third row of the table gives the values of the functional J which are obtained by the traditional Newton's method ($J_{\lambda=1}$). It follows from the data of the table that if the parameter λ is chosen according to (14.131) we reduce the number of iterations by three.

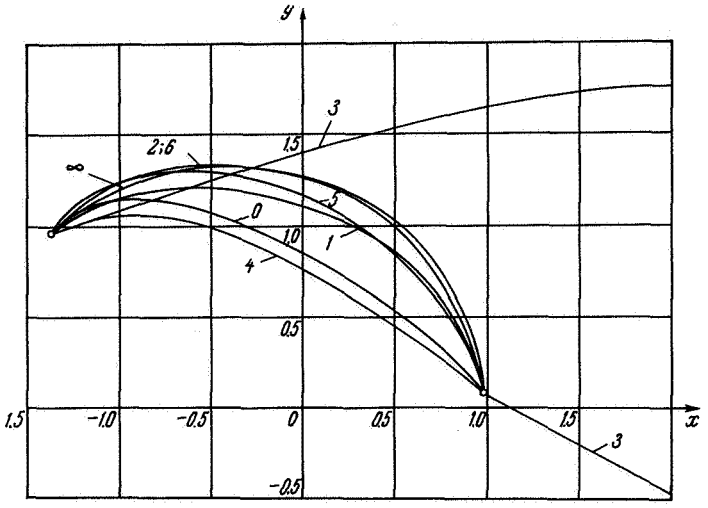

FIGURE 14.9. Trajectories corresponding to first and second steps of Newton's generalized method (1, 2), Newton's traditional analysis (3, 4), steepest-descent method in phase space (5, 6); symbol 0 indicates initial trajectory, and symbol ∞ indicates solution.

Figure 14.7 shows how the minimizing parameter λ varies at each step of the iterative process (the discrete points are connected by solid lines). At the beginning of the process $\lambda \ll 1$, and at the end $\lambda \sim 1$; this corroborates the opinion advanced above.

The dependence of the integral (14.127) on the parameter λ is shown in Figure 14.8 for three steps of the process. The vertical axis represents the integral as a fraction of its value at the given step for $\lambda = 0$ (this value is designated by J^*).

Figure 14.9 gives the trajectories corresponding to the first and second steps of Newton's generalized method (curves 1, 2), Newton's traditional method (curves 3, 4), and the steepest-descent method in phase space (curves 5, 6). The initial trajectory, common to all three methods, is designated by the symbol 0, and the solution by ∞. The data concerning the method of steepest descent are taken from /14.17/, where it was used when minimizing the action integral (cf. § 1 of this chapter).

Chapter Fifteen

FINITE-DIMENSIONAL NUMERICAL METHODS OF ESTABLISHING OPTIMUM SOLUTIONS

591 In this chapter we discuss finite-dimensional methods of establishing optimum solutions. Two approaches are available to reduce the variational problems (14.1)—(14.9) into a suitable form so that these methods may be applied. The first replaces the functionals by functions of a finite number of variables, e.g., the Ritz method, the method of polygonal lines, etc; the second consists in reducing the variational problem to a boundary-value one and finding the finite number of missing initial conditions (cf. the beginning of Chapter Fourteen).

The chapter is divided into two sections: in the first the most common finite-dimensional methods are described, and in the second, methods of reducing the variational problems to the required form are outlined.

§ 1. MINIMIZING A FUNCTION SUBJECT TO ADDITIONAL CONSTRAINTS

The function of n variables,

$$J = J(x_1, \ldots, x_n) \tag{15.1}$$

must be minimized subject to the additional constraints

$$\psi_j(x_1, \ldots, x_n) = 0 \quad (j = 1, \ldots, l < n); \tag{15.2}$$

the variables $x_1, \ldots, x_n$ vary within an unbounded region.

It is assumed a priori that (15.1), (15.2) has a solution, and that it is unique.

The required point x_i^* is found by an analytic method using Lagrange multipliers λ_j. A new function,

$$I(x_1, \ldots, x_n; \lambda_1, \ldots, \lambda_l) = J(x_i) + \sum_{j=1}^{l} \lambda_j \psi(x_i), \tag{15.3}$$

is formed and the conditions for it to be a minimum with respect to the x_i are written:

$$\frac{\partial I}{\partial x_i} = \frac{\partial J}{\partial x_i} + \sum_{j=1}^{l} \lambda_j \frac{\partial \psi_j}{\partial x_i} = 0 \quad (i = 1, \ldots, n). \tag{15.4}$$

592 The system of n equations (15.4), together with the l equations (15.2), determine the unknowns $x_1^*, \ldots, x_n^*$; $\lambda_1, \ldots, \lambda_l$. We write these two groups of equations as the one system

$$f_i(\bar{x}_j) = 0, \qquad (i,j = 1,2,\ldots, m), \tag{15.5}$$

where

$$\bar{x}_1 = x_1, \ldots, \bar{x}_n = x_n, \ \bar{x}_{n+1} = \lambda_1, \ldots, \bar{x}_{n+l} = \lambda_l,$$
$$f_1 = \frac{\partial I}{\partial x_1}, \ldots, f_n = \frac{\partial I}{\partial x_n}, \ f_{n+1} = \psi_1, \ldots, f_{n+l} = \psi_l$$
$$(m = n + l).$$

If $J(x_1, \ldots, x_n)$ is a quadratic function of its arguments, and $\psi_j(x_1, \ldots, x_n)$ are linear functions, system (15.5) is linear in the variables $\bar{x}_1, \ldots, \bar{x}_n, \ldots, \bar{x}_{n+l}$. To determine the minimum subject to additional constraints, in this case reduces to solving a system of linear algebraic equations.

1. **The gradient method.** In the absence of additional constraints (15.2), the gradient method, as applied to minimizing the function $J(x_1, \ldots, x_n)$, consists of the following.

From a known zero approximation for the arguments $x_i^{(0)}$ we calculate the derivatives of the function being minimized:

$$\frac{\partial J^{(0)}}{\partial x_i} = \frac{\partial J}{\partial x_i}(x_1^{(0)}, \ldots, x_n^{(0)}); \tag{15.6}$$

the first approximation is represented in the form

$$x_i^{(1)} = x_i^{(0)} - \lambda \frac{\partial J^{(0)}}{\partial x_i}. \tag{15.7}$$

The parameter λ is determined from the condition that the function

$$J\left(x_i^{(0)} - \lambda \frac{\partial J^{(0)}}{\partial x_i}\right) \tag{15.8}$$

be a minimum at the given step of the iterative process.

Two modifications of this procedure are suggested when solving the original problem (15.1)—(15.2).

The first modification consists in replacing the constrained minimum problem (15.1)—(15.2) by an unconstrained minimum problem by means of introducing penalty terms (cf. § 2 of Chapter Fourteen). We form the auxiliary function $Y(x_1, \ldots, x_n)$ with coefficients $q_j > 0$ $(j = 1, \ldots, l)$,

$$Y(x_1, \ldots, x_n) = J(x_1, \ldots, x_n) + \sum_{j=1}^{l} q_j \psi_j^2(x_1, \ldots, x_n) \tag{15.9}$$

593 and minimize the new function $Y(x_1, \ldots, x_n)$ by the gradient method described above (15.7)—(15.8). The coefficients q_j are also successively increased.

The second modification resembles a method described in § 2 of Chapter Fourteen. We shall consider the simplified case, when the zero approximation $x_i^{(0)}$ exactly satisfies the additional constraints

$$\psi_j(x_i^{(0)}) = \psi_j^{(0)} = 0 \qquad (j = 1, \ldots, l). \tag{15.10}$$

Represent the unknown x_i at the initial step of the process in the form

$$x_i^{(1)} = x_i^{(0)} + \delta x_i \quad (i = 1, \ldots, n). \tag{15.11}$$

The variations of the functions J and ψ_j caused by the small increments δx_i can then be written as (restricting ourselves to the linear terms of the expansions)

$$\left.\begin{aligned} J^{(1)} - J^{(0)} \approx \delta J &= \sum_{i=1}^{n} \frac{\partial J^{(0)}}{\partial x_i} \delta x_i, \\ \psi_j^{(1)} - \psi_j^{(0)} \approx \delta \psi_j &= \sum_{i=1}^{n} \frac{\partial \psi_j^{(0)}}{\partial x_i} \delta x_i \quad (j = 1, \ldots, l). \end{aligned}\right\} \tag{15.12}$$

The variations δx_i are determined from the condition that the variation δJ is not positive when the following additional relations are satisfied:

$$\delta \psi_j = \psi_j^{(1)} = \sum_{i=1}^{n} \frac{\partial \psi_j^{(0)}}{\partial x_i} \delta x_i = 0 \qquad (j = 1, \ldots, l). \tag{15.13}$$

As in § 2 of Chapter Fourteen, we form an auxiliary function with Lagrange multipliers λ_j given by

$$\Gamma = \delta J + \sum_{j=1}^{l} \lambda_j \delta \psi_j = \sum_{i=1}^{n} \left(\frac{\partial J^{(0)}}{\partial x_i} + \sum_{j=1}^{l} \lambda_j \frac{\partial \psi_j^{(0)}}{\partial x_i} \right) \delta x_i. \tag{15.14}$$

We select δx_i in the form

$$\delta x_i = -\lambda \left(\frac{\partial J^{(0)}}{\partial x_i} + \sum_{j=1}^{l} \lambda_j \frac{\partial \psi_j^{(0)}}{\partial x_i} \right) \qquad (i = 1, \ldots, n). \tag{15.15}$$

If $\lambda > 0$, the auxiliary function Γ is not positive for any λ_j, i.e.,

$$\Gamma = -\lambda \sum_{i=1}^{n} \left(\frac{\partial J^{(0)}}{\partial x_i} + \sum_{j=1}^{l} \lambda_j \frac{\partial \psi_j^{(0)}}{\partial x_i} \right)^2 \leqslant 0. \tag{15.16}$$

594 The Lagrange multipliers λ_j are determined from equations (15.13), which are linear in them (the δx_i in (15.13) are taken from (15.16)):

$$\sum_{i=1}^{n} \frac{\partial \psi_k^{(0)}}{\partial x_i} \left(\frac{\partial J^{(0)}}{\partial x_i} + \sum_{j=1}^{l} \lambda_j \frac{\partial \psi_j^{(0)}}{\partial x_i} \right) = 0 \qquad (k = 1, \ldots, l). \tag{15.17}$$

In view of this property of the parameters λ_j the sum over j in the expression for Γ vanishes:

$$\sum_{j=0}^{l} \lambda_j \delta \psi_j = 0. \tag{15.18}$$

It follows from here that Γ coincides with δJ, and therefore the given selection of the variations δx_i ensures that δJ is not negative.

The parameter λ in formulas (15.15) determines the length of the step along the conditional gradient, which is bounded from above by the

requirement that the error in the linear representation of the functions J and ψ_j be small (compare § 2 of Chapter Fourteen).

Note that the original formulation (15.1)—(15.2) does not contain restrictions on the region over which the parameters x_i vary. To a considerable extent the computational procedure is simplified. A more general case is described in Zoutendijk's treatise /15.1/ (which also contains an extensive bibliography). The gradient method in a finite-dimensional space and its modification of problem (15.1)—(15.2) is treated in /15.2—15.4/.

2. **Newton's method.** The system of algebraic equations (15.5) (to which (15.1) and (15.2) reduce) is solved as follows by the traditional Newton's method. The derivatives $\partial f_i^{(0)}/\partial x_j$ are calculated from the zero approximation $x_j^{(0)}$, and the $x_j^{(1)}$ at the first step of Newton's method are determined by the linear equations

$$\sum_{j=1}^{n} \frac{\partial f_i^{(0)}}{\partial x_j}(x_j^{(1)} - x_j^{(0)}) = -f_i^{(0)} \qquad (i = 1, \ldots, n) \tag{15.19}$$

(in order to use a familiar notation we have replaced x_i by x_i, and the order of the system $n + l$ by n in (15.5)).

We describe a generalization of Newton's method /15.5—15.9/, which differs from its traditional form by introducing a parameter resembling the descent parameter λ in the steepest descent method. This method represents a finite-dimensional analog of Newton's generalized functional analysis.

595 Consider the system of n algebraic equations with n unknowns

$$f_i(x_j) = 0 \qquad (i, j = 1, \ldots, n); \tag{15.20}$$

we require the solution of the system, x_i^*. Form the function

$$\Phi = \frac{1}{2}\sum_{i=1}^{n} f_i^2(x_j), \tag{15.21}$$

such, that it and its first derivatives vanish at the required point $x_i = x_i^*$,

$$\Phi^* = \frac{1}{2}\sum_{i=1}^{n} f_i^* f_i^* = 0, \quad \frac{\partial \Phi^*}{\partial x_j} = \sum_{i=1}^{n} f_i^* \frac{\partial f_i^*}{\partial x_j} = 0. \tag{15.22}$$

The value of the function Φ indicates how close we are to the solution in the n-dimensional space $(x_1, \ldots, x_n)$. Suppose the point $x_1^{(0)}, \ldots, x_n^{(0)}$, which is not a solution, is given in the n-dimensional space, and suppose we calculate the functions $f_i^{(0)}$, $\Phi^{(0)}$ and their derivatives $\partial f_i^{(0)}/\partial x_j$, $\partial \Phi^{(0)}/\partial x_j$. Now represent the coordinates x_j at the next step of the iterative process in the form

$$x_j^{(1)} = x_j^{(0)} + \delta x_j \qquad (j = 1, \ldots, n), \tag{15.23}$$

where δx_j is a small increment. The corresponding increment in the function Φ is written as

$$\delta\Phi = \sum_{j=1}^{n} \frac{\partial \Phi^{(0)}}{\partial x_j}\delta x_j = \sum_{i,j=1}^{n} f_i^{(0)} \frac{\partial f_i^{(0)}}{\partial x_j}\delta x_j. \tag{15.24}$$

A necessary condition for the convergence of the iterative process is $\Phi^{(1)} < \Phi^{(0)}$, i.e., $\delta\Phi < 0$. The increments δx_j can be selected in two ways so as to satisfy this condition, namely,

$$\delta x_j = -\lambda \sum_{i=1}^{n} f_i^{(0)} \frac{\partial f_i^{(0)}}{\partial x_j}, \qquad \lambda > 0 \qquad (j = 1, \ldots, n) \tag{15.25}$$

and

$$\sum_{j=1}^{n} \delta x_j \frac{\partial f_i^{(0)}}{\partial x_j} = -\lambda f_i^{(0)}, \quad \lambda > 0 \qquad (i = 1, \ldots, n). \tag{15.26}$$

Expression (15.25) defines the algorithm of the steepest descent method (cf. (15.7)); for $\lambda = 1$ in (15.26), it defines the algorithm of Newton's method.

596 By means of the substitution

$$\delta x_j = \lambda \eta_j \qquad (j = 1, \ldots, n), \tag{15.27}$$

(15.26) may be transformed into

$$\sum_{j=1}^{n} \frac{\partial f_i^{(0)}}{\partial x_j} \eta_j = -f_i^{(0)} \qquad (i = 1, \ldots, n), \tag{15.28}$$

and the coordinates $x_j^{(1)}$ at the first step of the iterative process become

$$x_j^{(1)} = x_j^{(0)} + \lambda \eta_j \qquad (j = 1, \ldots, n). \tag{15.29}$$

After determining η_j from the linear system (15.28) and substituting them into (15.29), we find that Φ has become a function of the parameter λ alone:

$$\Phi(x_j^{(0)} + \lambda \eta_j) = \Psi(\lambda). \tag{15.30}$$

This parameter is selected from the condition that the function $\Psi(\lambda)$ is a minimum at each step of the iterative process (as for the gradient method):

$$\min_{\lambda} \Psi(\lambda). \tag{15.31}$$

Expand the function $\Psi(\lambda)$ as a power series in λ given by

$$\Psi(\lambda) = \Psi(0)(1-\lambda)^2 + a\lambda^2(1-\lambda) + b\lambda^3(1-\lambda) + c\lambda^4 + \ldots \tag{15.32}$$

The coefficients a, b, c are expressed here in terms of the products of η_j, $f_j^{(0)}$, $\partial^2 f_i^{(0)}/\partial x_i \partial x_k$, $\partial^3 f_j^{(0)}/\partial x_i \partial x_k \partial x_l$, $\partial^4 f_j^{(0)}/\partial x_i \partial x_k \partial x_i \partial x_m$, ... If the f_j are linear functions of their arguments, then

$$a = b = c = \ldots = 0. \tag{15.33}$$

In this case the parameter λ, which minimizes the function $\Psi(\lambda)$, equals unity and the iterative process degenerates into one step. In the neighborhood nearest the solution x_i^* the functions f_j are described by the linear terms of the expansion; therefore, the parameter λ tends to unity as the solution is approached.

Hence, the algorithm for solving system (15.20) consists of the following: At each step of the iterative process, η_j are found from the linear system (15.28), after which the parameter λ is determined by condition (15.31); the values of the coordinates x_j at the next step are expressed in the form (15.29).

As noted above, the proposed method coincides with Newton's method if
597 $\lambda = 1$ for all iterations. In the neighborhood of the solution the minimizing value of λ approaches unity, and the method is no better than Newton's traditional method. The application of this method is efficient in that region of space x_j over which Newton's method is either inefficient or divergent; in this case the minimizing value of λ is much smaller than unity. The selection of λ at each step of the process guarantees, in a certain sense, the convergence of the method, as for the gradient method.

Let us compare some aspects of the gradient method and Newton's method. It is well known that minimizing quadratic functionals and solving linear equations are mutually-equivalent problems. By Newton's method linear equations are solved in one step, while the gradient method uses an iterative process to determine the minimum of the quadratic functional. The gradient method is thus inferior to Newton's method regarding the number of steps (and, frequently, the computation time) required to attain a given accuracy; this is true in the neighborhood of the solution of a nonlinear equation (and respectively of a nonquadratic functional).

On the other hand, Newton's process may diverge in those situations in which the gradient method converges. This is partly due to the descent parameter, which can be determined at each step of the process so that the functional being minimized does not increase.

In view of these considerations, the introduction of a parameter λ into Newton's method guarantees convergence to a certain extent; a rational selection of the parameter may ensure a saving in the time required to attain the result.

It has been suggested in /15.8, 15.9/ that the parameter λ is chosen from the interval (0, 1) so that only the condition that the method converges is satisfied: $\Phi^{(1)} < \Phi^{(0)}$. This choice consists in successively increasing λ from unity to the value at which the convergence condition is satisfied.

§ 2. REDUCTION OF VARIATIONAL PROBLEMS TO FINITE-DIMENSIONAL PROBLEMS

We describe here methods for replacing functionals by functions of a finite number of variables, e.g., the Ritz method, for which the coefficients are determined by the steepest descent method, and the method of polygonal lines for the problems of Lagrange and Mayer; in addition, the correct way of selecting the missing initial conditions for the boundary-value problem is also described.

1. The Ritz method with the coefficients determined by the steepest descent method. The classic Ritz method is described in many textbooks
598 (cf. for instance /15.2, 15.10—15.52/); in this section we discuss its application /15.13/ to determine the minimum value of the integral functional (14.40)—(14.41).

The algorithm of the method is as follows.

A complete system of n linearly independent functions $\{\psi_i(t)\}$, which satisfy the conditions

$$\psi_i(0) = \dot{\psi}_i(0) = \psi_i(T) = \dot{\psi}_i(T) = 0, \tag{15.34}$$

is selected, as well as functions $x^{(0)}(t)$, $y^{(0)}(t)$ satisfying the boundary conditions (14.41). A solution is sought in the form of the linear combination

$$x_n(t) = x^{(0)}(t) + \sum_{i=0}^{n} a_i\psi_i(t), \quad y_n(t) = y^{(0)}(t) + \sum_{i=0}^{n} b_i\psi_i(t). \tag{15.35}$$

After replacing $x(t)$, $y(t)$ by $x_n(t)$, $y_n(t)$ in the integral (14.40), the latter becomes a function of the coefficients a_i, b_i, so that

$$J_1 = J_1(a_i, b_i). \tag{15.36}$$

The problem to determine the minimum value of the functional (14.40) is reduced to minimizing the function $J_1(a_i, b_i)$ with respect to a finite number of variables.

The function $J_1(a_i, b_i)$ can be minimized by the steepest descent method, whose algorithm was described in § 1 of this chapter. We shall describe the formulas required for this.

Let the zero approximation for the coefficients a_i, b_i be known; we represent the next approximation in the form

$$\begin{aligned} a_i^{(1)} &= a_i^{(0)} - \lambda\,(\partial J_1^{(0)}/\partial a_i), \\ b_i^{(1)} &= b_i^{(0)} - \lambda(\partial J_1^{(0)}/\partial b_i). \end{aligned} \tag{15.37}$$

The descent parameter λ is determined from the condition for a minimum of

$$J_1(\lambda) = J_1[a_i^{(0)} - \lambda\,(\partial J_1^{(0)}/\partial a_i),\ b_i^{(0)} - \lambda\,(\partial J_1^{(0)}/\partial b_i)]. \tag{15.38}$$

Thus, the minimization procedure proposed here consists of two nested iterative processes:

1) The Ritz iterative process, which consists of increasing the number n of coefficients a_i, b_i in expansion (15.35) from step to step.

2) The iterative process of steepest descent method, which consists in determining the minimum of (15.36) at each step of the Ritz iterative process.

599 Power functions are selected to represent the basic functions $\psi_i(t)$ /15.13/,

$$\psi_i(t) = (t/T)^{i+2}(1 - t/T)^2 \qquad (i = 0, 1, \ldots, n), \tag{15.39}$$

while the functions (14.49) are taken as the zero approximation $x^{(0)}(t)$, $y^{(0)}(t)$.

An application of the Ritz method in conjunction with the method of steepest descent to this problem turned out to be much less efficient than applying the method of steepest descent in phase space (cf. § 1 of Chapter Fourteen); the time to calculate one functional to 4—5 places was 100 minutes (instead of 1 to 2 minutes by the steepest descent method).

The convergence of the functional J_1 as a function of the iteration number k in the Ritz process (for the parameters $r_1 = 1.52$, $\varphi_1 = T = 2$) is shown in Figure 15.1, where the discrete points $J_1^{(0)}, J_1^{(1)}, \ldots, J_1^{(8)}$ have been joined by a continuous curve. At the first iteration there are five coefficients a_i and five coefficients b_i ($n = 5$); with the transition to each successive iteration the number of coefficients increases by 10 ($\Delta n = 5$). The initial values (for the method of steepest descent) of the ten new coefficients vanish, while the initial values of the old coefficients are taken from the preceding iteration.

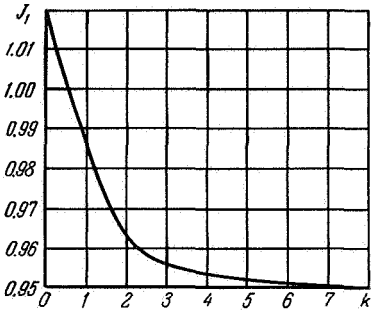

FIGURE 15.1. Convergence of functional J_1 as function of number k of iterations in Ritz process, for transfer in a central field: $r_1 = 1.52$, $\varphi_1 = T = 2$.

The dependence of the quantities a_i, b_i on the number i for $k = 8$ is represented tentatively by the continuous curves in Figure 15.2.

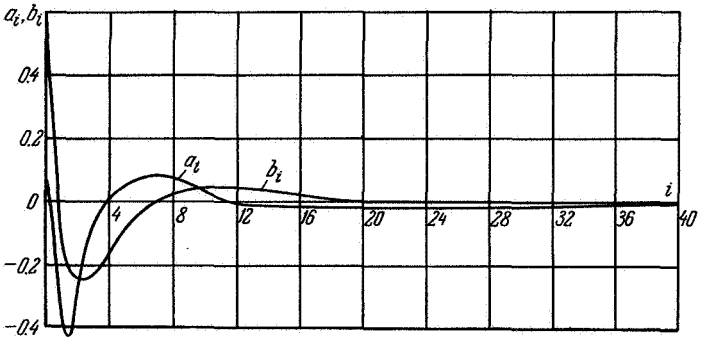

FIGURE 15.2. Variation of coefficients a_i, b_i of expansions $x(t)$, $y(t)$ in terms of basic functions $\psi_i(t)$ as function of i for $k = 8$ (Ritz method for same example as in Figure 15.1).

2. Method of polygonal lines for the Lagrange problem. This method is based on replacing integration by summation, and the function by a polynomial.

600 To illustrate the method, consider the simple problem (14.11), (14.12). Introducing the symbol

$$\dot{x} = u, \tag{15.40}$$

we write

$$J = \int_0^T \Phi(x, u, t)\, dt. \tag{15.41}$$

Split the interval over which the argument varies into m equal parts $\tau = T/m$; then $t_k = k\tau$. Represent the function $u(t)$ over the interval (t_k, t_{k+1}) as the linear function

$$u(t) = u_k + (u_{k+1} - u_k)(t - t_k)/\tau \quad (t_k \leqslant t \leqslant t_{k+1}, \quad u_k = u(t_k)). \tag{15.42}$$

In view of (15.40), the required function $x(t)$ will then be a quadratic function of t over the interval (t_k, t_{k+1}), i.e.,

$$x(t) = x_k + u_k (t - t_k) + (u_{k+1} - u_k)(t - t_k)^2/2\tau \quad (k = 1, \ldots, m), \tag{15.43}$$

and the values of x_k, x_{k+1} at the interpolation points will be linked by

$$x_{k+1} = x_k + {}^1/_2\tau (u_{k+1} + u_k) \qquad (k = 1, \ldots, m). \tag{15.44}$$

If we express the integral (15.41) as the sum of m integrals over segments of length τ, then represent the integrand Φ in each segment in a form similar to (15.42), and afterwards calculate all these integrals, we obtain J in the form

$$J = \frac{1}{2}\tau\left[\Phi(x_0, u_0, 0) + \Phi(x_m, u_m, T) + 2\sum_{k=1}^{m-1} \Phi(x_k, u_k, t_k)\right] \tag{15.45}$$

(here $x_0 = x(0)$, $x_m = x(T)$ are specified values of the function at the ends of the interval).

The recurrence equation (15.44) makes it possible to express the value of the function at any interpolation point x_l $(l = 1, \ldots, m)$ in terms of the values $u_l, u_{l-1}, \ldots, u_0$. In fact, adding up the right- and left-hand sides of (15.44), we obtain

$$x_l = x_0 + \frac{1}{2}\tau\left(u_0 + u_l + 2\sum_{k=1}^{l-1} u_k\right) \qquad (l = 1, \ldots, m), \tag{15.46}$$

601 and, in particular, for $l = m$

$$x(T) = x_0 + \frac{1}{2}\tau\left(u_0 + u_m + \sum_{k=1}^{m-1} u_k\right). \tag{15.47}$$

With the aid of (15.46), the expression for the functional (15.45) can be made to depend only on the values of $u(t)$ at the interpolation points, so that

$$J = \frac{1}{2}\tau\left[\Phi(x(0), u_0, 0) + \Phi(x(T), u_m, T) + 2\sum_{k=1}^{m-1} \Phi(x(0), u_0, \ldots, u_k)\right]. \tag{15.48}$$

Thus, the original variational problem (14.11), (14.12) has been reduced to that of finding $m+1$ values u_k to give the extremum of (15.48) when the additional condition (15.47) is satisfied.

This method was applied in /15.14/ to calculate the extrema of the functional (14.40) written in polar coordinates. If the constraint of a given angular displacement is not imposed on the orbital transfer in a central field, the transition to polar coordinates in (14.40) lowers by one the order of the derivative of one of the functions (cf. Chapter Five); in the integrand, one function enters with its first and second time derivatives, while the other only involves a first derivative.

The original problem was reduced in /15.14/ to one of determining the minimum of a function of two groups of variables with three additional constraints, which correspond to the three specified final values. In the authors' opinion, satisfactory results were obtained for a number m of interpolation nodes as low as 10 to 20 for times of flight not exceeding the period of one revolution on the initial orbit.

3. Method of polygonal lines for the Mayer problem. This method is based on replacing the differential equations by finite difference equations; its application to optimization problems was described in /15.15/, where it was called the critical direction method.

We shall describe the algorithm of the method for the Mayer problem with a free right-hand endpoint.

Consider a system of differential equations and initial conditions

$$\left.\begin{aligned} \dot{x}_i &= f_i(x_j, u, t), \\ x_i(0) &= x_{i0} \quad (i, j = 1, \ldots, n), \end{aligned}\right\} \tag{15.49}$$

602 where the functional to be minimized depends on the terminal values of the phase coordinates

$$P(x_1(T), \ldots, x_n(T)). \tag{15.50}$$

The optimum control function $u(t)$ must be established. The interval over which the argument varies is again split into m equal parts of length $\tau = T/m$. The differential equations (15.49) establish a connection between the values of the coordinates at any two adjacent points t_k, t_{k+1}:

$$\begin{gathered} x_{i,\,k+1} = x_{i,\,k} + \tau f_i(x_{j,\,k}, u_k, t_k) \\ (x_{i,k} = x_i(t_k), \quad u_k = u(t_k), \quad t_k = k\tau; \quad i, j = 1, \ldots, n; \\ k = 0, \ldots, m-1). \end{gathered} \tag{15.51}$$

The functional (15.50), which depends on the terminal values of the coordinates, is here considered as a function of the control function $u(t)$ at discrete points of the interval $u_0, u_1, \ldots, u_{m-1}$. The determination of the minimum value of the function P with respect to $u_0, u_1, \ldots, u_{m-1}$ is linked with the calculation of the partial derivatives $\partial P/\partial u_k$ by

$$\frac{\partial P}{\partial u_k} = \tau \sum_{i,j=1}^{n} \frac{\partial P}{\partial x_i(T)} \frac{\partial x_i(T)}{\partial x_{j,\,k+1}} \frac{\partial f_j(x_{s,\,k}, u_k, t_k)}{\partial u_k} \quad (k = 0, 1, \ldots, m-1). \tag{15.52}$$

The quantity $\tau\sum_{i=1}^{n}[\partial P/\partial x_i(T)]\,[\partial x_i(T)/\partial x_{j,\,k+1}]$ coincides with the solution of the following system of differential equations at the interpolation points (cf. /15.15/):

$$\dot{p}_i = -\sum_{j=1}^{m}\frac{\partial f_j}{\partial x_i}p_j \qquad (i=1,\ldots,n) \tag{15.53}$$

with boundary conditions

$$p_i(T) = \frac{\partial P}{\partial x_i(T)} \qquad (i=1,\ldots,n), \tag{15.54}$$

so that

$$\sum_{i=1}^{n}\frac{\partial P}{\partial x_i(T)}\frac{\partial x_i(T)}{\partial x_{j,\,k+1}} = p_i(t_k). \tag{15.55}$$

This last fact is easily seen to be due to the link between the method described here and the functional method of steepest descent in the space of control variables. Using the results of § 2 of Chapter Fourteen, we write the
603 variation of the functional P caused by varying the control function δu as

$$\delta P = \int_0^T \sum_{i=1}^{n} p_i\frac{\partial f_i}{\partial u}\delta u\,dt; \tag{15.56}$$

here $p_i(t)$ is the solution of the system of equations (15.53) governed by the boundary conditions (15.54). The integral in the last formula is replaced by

$$\delta P = \tau\sum_{k=0}^{n}\sum_{i=1}^{m} p_i(t_k)\frac{\partial f_{i,\,k}}{\partial u}\delta u(t_k), \tag{15.57}$$

and the partial derivative is written as

$$\frac{\partial P}{\partial u(t_k)} = \tau\sum_{i=1}^{m} p_i(t_k)\frac{\partial f_{i,\,k}}{\partial u(t_k)}. \tag{15.58}$$

A comparison of (15.52) and (15.58) substantiates (15.55).

4. Selecting the missing initial values in the boundary-value problem. The variational problem is reduced by means of the formalism of either Euler-Langrange or Pontryagin to a two-point boundary-value problem for a system of ordinary differential equations (cf. the beginning of Chapter Fourteen and system (14.10)). The solutions $x_i(t)$ of the boundary-value problem (14.10) must satisfy the differential equations, as well as the initial and terminal conditions. The following iterative process can be used to solve the problem: the differential equations and the initial conditions are exactly satisfied at each step of the process, while the terminal values $x_i(T)$ approach the required values x_{i1} as each step is taken.

These processes are based on reducing the boundary-value problem to a Cauchy problem, and subsequently selecting the missing initial conditions according to some algorithm. Finally the problem is reduced to that of solving a system of algebraic equations.

To each set of missing initial values $x_{l+1}(0),\ldots,x_n(0)$ (cf. (14.10)) there correspond definite terminal values $x_j(T)$ $(\Sigma j = n-l)$. We select the missing

initial values so that the terminal conditions are satisfied. The deviations are now formed, i.e., the differences between the values of the functions $x_j(T)$ at the end of the interval and the required values x_{j1}. These are denoted by

$$\Psi_j(x_{i0}) = x_j(T) - x_{j1} \qquad (i = l+1, \ldots, n;\ \Sigma j = n-l). \tag{15.59}$$

The solution of the problem is obtained by selecting values $x_{l+1}(0), \ldots$
604 $\ldots, x_n(0)$ such that all deviations Ψ_j vanish, i.e., by solving the system of implicit algebraic equations

$$\Psi_j(x_{i0}) = 0 \qquad (i = l+1, \ldots, n;\ \Sigma j = n-l). \tag{15.60}$$

In order to apply some numerical method of solution to this system of algebraic equations we must calculate the derivatives $\partial\Psi_j/\partial x_{i0} = \partial x_j(T)/\partial x_{i0}$. This can be done by either applying the formulas of numerical differentiation, or integrating the system of equations (cf. (14.10))

$$\frac{d}{dt}\frac{\partial x_k}{\partial x_i(0)} = \sum_{s=1}^{n}\frac{\partial f_k}{\partial x_s}\frac{\partial x_s}{\partial x_i(0)} \qquad (i = l+1, \ldots, n;\ k = 1, \ldots, n) \tag{15.61}$$

with the initial conditions

$$\frac{\partial x_k}{\partial x_i(0)}(0) = \begin{cases} 0 \text{ for } i \neq k, \\ 1 \text{ for } i = k \end{cases} \tag{15.62}$$

together with system (14.10).

The boundary conditions of the original problem (14.10), which were given in their simplest form, may be replaced by the general conditions

$$\psi_k(x_{i0}, x_{j1}) = 0 \qquad (i, j, k = 1, \ldots, n). \tag{15.63}$$

This representation does not violate the method of replacing the boundary-value problem by a system of algebraic equations, since n more relations can be obtained by integrating the differential equations (for each set of initial values x_{i0} there is a set of terminal values x_{j1}). If these are added to the n relations (15.63), we obtain a closed algebraic system of $2n$ equations with $2n$ unknowns. If the end of the interval $t = T$, over which the argument varies, is unknown, we may add the condition which determines it to relations (15.63).

This system of algebraic equations can be solved by either the gradient method or Newton's method (cf. § 1 of this chapter). If the problem contains control parameters which must be determined from the condition that the function involving the terminal coordinates and these parameters be extrema, then it is best to use one of the modifications of the gradient method, as presented in § 1 of this chapter.

The methods of solving boundary-value problems described in this section have found applications in many papers on rocket dynamics /15.4, 15.8, 15.9, 15.16—15.23, etc./. In these papers the variational problems were reduced to boundary-value ones governed by systems of equations for the phase coordinates and the momenta (the Lagrange multipliers); the optimum

605 controls were expressed in terms of the momenta and the phase coordinates. The initial and terminal values of the phase coordinates (the physical coordinates and the velocities in problems of rocket dynamics) are usually specified, and we must determine the missing initial values of the momenta so that we ensure that the trajectory attains a specified point in phase space.

In /15.8, 15.16, 15.19, 15.22, 15.23/ the selection of the missing initial values is carried out by Newton's method; a comparative analysis of this and the steepest descent method is made in /15.8/. The steepest descent method for finding the optimum control parameters, while satisfying the boundary conditions, is described in /15.4/.

Appendix

DESCRIPTION OF THE DYNAMIC MANEUVERS

606 This appendix summarizes the system of differential equations and their boundary conditions, which describe the following basic dynamic maneuvers characterizing low-thrust engines: interplanetary flight (§ 2), holding the satellite within a specified spherical layer, rotating the orbital plane of a satellite (§ 3). The corresponding elementary models of the maneuvers are also given here. The maneuvers are described in a section which gives various forms of the equations of motion and transformations between different types of variables.

§ 1. FORMS OF THE EQUATIONS OF MOTION

1. **Equations of motion in a central field.** In a cartesian inertial reference frame (x, y, z) with origin at the gravitational center, the equations of motion are

$$\left.\begin{aligned} &\ddot{x} = a_x - kx/r^3, \\ &\ddot{y} = a_y - ky/r^3, \\ &\ddot{z} = a_z - kz/r^3 \\ &(r = \sqrt{x^2 + y^2 + z^2}), \end{aligned}\right\} \qquad (A.1)$$

where a_x, a_y, a_z are the projections of the thrust-acceleration vector onto the axes, and $k = f\mathfrak{M}$ is the gravitational constant (product of the universal gravitational constant f and the mass of the central body $\mathfrak{M}$). The characteristic distance r_* is selected; the characteristic time t_*, velocity v_*, and acceleration g_* are then given by the expression

$$t_* = k^{-1/2} r_*^{3/2}, \quad v_* = k^{1/2} r_*^{-1/2}, \quad g_* = k r_*^{-2}. \qquad (A.2)$$

These quantities have the following physical meaning: $2\pi t_*$ is the period of revolution along a circular orbit of radius r_*, v_* is the magnitude of the orbital velocity, and g_* is the acceleration produced by the gravitational center at a distance r_* from it. If we take r_*, t_*, v_*, g_* as units of linear
607 distance, time, velocity, and acceleration, equations (A.1), written in the corresponding dimensionless variables, will not contain the parameter k:

$$\ddot{x} = a_x - x/r^3, \quad \ddot{y} = a_y - y/r^3, \quad \ddot{z} = a_z - z/r^3. \qquad (A.3)$$

We preserve the previous symbols for the dimensionless variables on which the treatment in this section will be based.

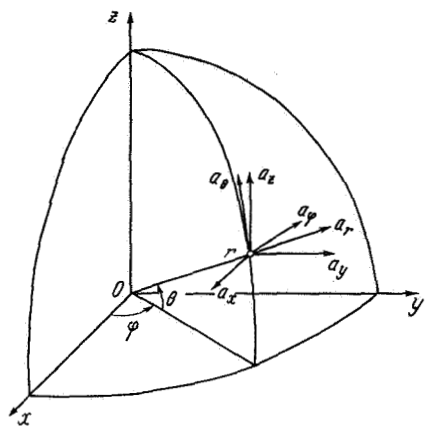

FIGURE A.1. Rectangular and spherical coordinate systems.

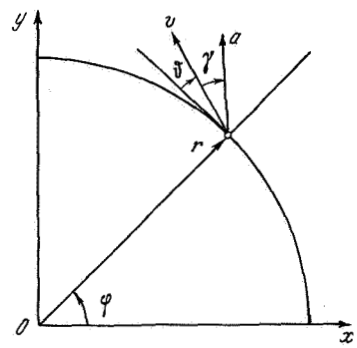

FIGURE A.2. Polar coordinate system.

Consider the spherical coordinates r, φ, θ ; the cartesian coordinates are expressed in terms of the spherical coordinates by (cf. Figure A.1)

$$x = r\cos\theta\cos\varphi,\ y = r\cos\theta\sin\varphi,\ z = r\sin\theta. \tag{A.4}$$

The equations of motion in spherical coordinates take the form

$$\left.\begin{aligned} &\ddot{r} - r\dot{\varphi}^2\cos^2\theta - r\dot{\theta}^2 + 1/r^2 = a_r,\\ &r\cos\theta\ddot{\varphi} + 2\dot{r}\dot{\varphi}\cos\theta - 2r\dot{\varphi}\dot{\theta}\sin\theta = a_\varphi,\\ &r\ddot{\theta} + 2\dot{r}\dot{\theta} + r\dot{\varphi}^2\sin\theta\cos\theta = a_\theta. \end{aligned}\right\} \tag{A.5}$$

The thrust-acceleration projections a_r, a_φ, a_θ are expressed as follows in terms of a_x, a_y, a_z:

$$\left.\begin{aligned} a_r &= a_x\cos\theta\cos\varphi + a_y\cos\theta\sin\varphi + a_z\sin\theta,\\ a_\varphi &= -a_x\sin\varphi + a_y\cos\varphi,\\ a_\theta &= a_x\sin\theta\cos\varphi + a_y\sin\theta\sin\varphi - a_z\cos\theta. \end{aligned}\right\} \tag{A.6}$$

A special case of (A.5) is that of plane motion ($\theta = 0$, $a_\theta = 0$):

$$\left.\begin{aligned} \ddot{r} &= a_r + r\dot{\varphi}^2 - 1/r^2,\\ r\ddot{\varphi} &= a_\varphi - 2\dot{r}\dot{\varphi}. \end{aligned}\right\} \tag{A.7}$$

We now introduce the velocity components in polar coordinates (r, φ) (Figure A.2), where $v_r = \dot{r}$ is the radial velocity, and $v_\varphi = r\dot{\varphi}$ is the transverse velocity. System (A.7) can then be written as

$$\left.\begin{aligned} \dot{r} &= v_r,\\ r\dot{\varphi} &= v_\varphi,\\ \dot{v}_r &= a_r + v_\varphi^2/r - 1/r^2,\\ \dot{v}_\varphi &= a_\varphi - v_r v_\varphi/r. \end{aligned}\right\} \tag{A.8}$$

If the accelerations a_r and a_φ are independent of t and φ, the order of this system is reduced by two and it reads

$$v_r v_r' = a_r + v_\varphi^2/r - 1/r^2, \quad v_r v_\varphi' = a_\varphi - v_r v_\varphi/r; \tag{A.9}$$

the primes here represent differentiation with respect to r.

After integrating system (A.9), the functions $t(r)$ and $\varphi(r)$ are found from the differential equations

$$t' = \frac{1}{v_r(r)}, \quad \varphi' = \frac{v_\varphi(r)}{r v_r(r)}. \tag{A.10}$$

In the absence of thrust accelerations, system (A.9), similar to (A.8), has two well-known integrals; these are the energy integral

$$E = \frac{1}{2}(v_r^2 + v_\varphi^2) - \frac{1}{r} \tag{A.11}$$

and the angular-momentum integral

$$M = v_\varphi r. \tag{A.12}$$

These can be used as the unknown functions in equations (A.9) to replace v_r and v_φ, so that

$$E' = \frac{1}{v_r}(a_r v_r + a_\varphi v_\varphi), \quad M' = \frac{a_\varphi r}{v_r}. \tag{A.13}$$

The functions v_r and v_φ entering the right-hand sides of (A.13) must be expressed in terms of r, E and M from (A.11) and (A.12).

The projections of the velocities v_r, v_φ and accelerations a_r, a_φ can be written in terms of the magnitude of the velocity v, the acceleration a,
609 and the angles defining the directions of the vectors $\mathbf{v}$ and $\mathbf{a}$ (Figure A.2). The quantity ϑ at a point is the angle between the velocity vector and the perpendicular to the radius vector in the direction of positive rotation of the latter; γ is the angle between the vector of the perturbing acceleration and the velocity vector. The right-hand sides of equations (A.13) are replaced by

$$E' = \frac{a\cos\gamma}{\sin\vartheta}, \quad M' = \frac{ar}{v}\frac{\cos(\vartheta+\gamma)}{\sin\vartheta}. \tag{A.14}$$

In these variables, system (A.8) is transformed into

$$\left.\begin{aligned} \dot r &= v\sin\vartheta, \\ r\dot\varphi &= v\cos\vartheta, \\ \dot v &= a\cos\gamma - \sin\vartheta/r^2, \\ v\dot\vartheta &= a\sin\gamma + (v^2/r - 1/r^2)\cos\vartheta. \end{aligned}\right\} \tag{A.15}$$

If in the last equations we introduce the variable s, which is the length of the trajectory arc, to replace the independent variable t ($ds^2 = dr^2 + r^2 d\varphi^2 = v^2 dt^2$);

we then obtain the equations

$$\left.\begin{aligned} \frac{dr}{ds} &= \sin\vartheta, \\ r\frac{d\varphi}{ds} &= \cos\vartheta, \\ v\frac{dv}{ds} &= a\cos\gamma - \frac{1}{r^2}\sin\vartheta, \\ v^2\frac{d\vartheta}{ds} &= a\sin\gamma + \left(\frac{v^2}{r} - \frac{1}{r^2}\right)\cos\vartheta. \end{aligned}\right\} \tag{A.16}$$

In terms of the independent variable φ, (A.15) becomes

$$\left.\begin{aligned} \frac{dr}{d\varphi} &= r\,\mathrm{tg}\,\vartheta, \\ \frac{dt}{d\varphi} &= \frac{r}{v\cos\vartheta}, \\ \frac{v\cos\vartheta}{r}\frac{dv}{d\varphi} &= a\cos\gamma - \frac{1}{r^2}\sin\varphi, \\ \frac{v^2\cos\vartheta}{r}\frac{d\vartheta}{d\varphi} &= a\sin\gamma + \left(\frac{v^2}{r} - \frac{1}{r^2}\right)\cos\vartheta. \end{aligned}\right\} \tag{A.17}$$

We now turn to the original system (A.7), which describes plane motion in polar coordinates, and write the differential equation for the orbit $r(\varphi)$. Introduce the following substitutions:

$$r = \frac{1}{u}, \quad r^2\dot{\varphi} = M, \quad \frac{d}{dt} = \dot{\varphi}\frac{d}{d\varphi} \tag{A.18}$$

610 (as before, it is assumed that when replacing the argument t by φ, the projections of the perturbing acceleration are independent of t). System (A.7) is then transformed into

$$\frac{d^2u}{d\varphi^2} + u = \frac{1}{M^2}\left(1 - \frac{a_r}{u^2} - \frac{a_\varphi}{u^3}\frac{du}{d\varphi}\right), \quad \frac{dM}{d\varphi} = \frac{a_\varphi}{Mu^3}. \tag{A.19}$$

The time t can be found in terms of the known functions $u(\varphi)$, $M(\varphi)$ from the differential equation

$$\frac{dt}{d\varphi} = \frac{1}{M(\varphi)\,u^2(\varphi)}. \tag{A.20}$$

If there are no perturbing accelerations ($a_r \equiv 0$, $a_\varphi \equiv 0$) the solution of (A.19) is easily found to be

$$M = \text{const}, \quad u = \frac{1}{M^2} + \left(u_\pi - \frac{1}{M^2}\right)\cos(\varphi - \varphi_\pi), \tag{A.21}$$

or, for the variable r,

$$r = \frac{p}{1 + \varepsilon\cos\nu}, \tag{A.22}$$

where the orbit $r(\nu)$ is a conic section with parameter p and eccentricity ε.

The following symbols have been used in formulas (A.21) and (A.22): $p = M^2$ is the focal parameter of the conic section, $\varepsilon = M^2u_\pi - 1 = M^2/r_\pi - 1 = \sqrt{1 + 2M^2E}$ is the eccentricity of the conic section ($\varepsilon = 0$ for a circle,

$1 > \varepsilon > 0$ for an ellipse, $\varepsilon = 1$ for a parabola, $\varepsilon > 1$ for a hyperbola), r_π and φ_π are the radial and angular displacements of the perihelion, $\nu = \varphi - \varphi_\pi$ is the true anomaly, and the angular displacement is measured from the direction $F_1\pi$ (the line of apsides).

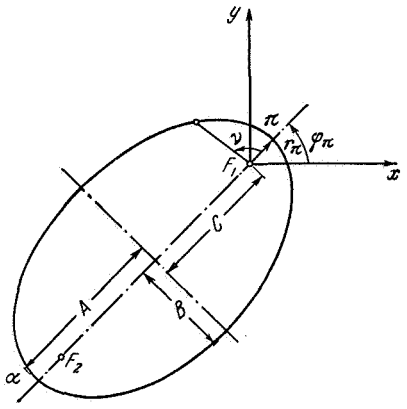

FIGURE A.3. Elements defining elliptic orbit in plane.

Figure A.3 shows an elliptic orbit; the gravitational center is located at one of the foci F_1, which is chosen as the origin of the coordinates. The major axis of the ellipse $\alpha\pi$ is the line of apsides, where α is the aphelion and π the perihelion. The length of the semimajor axis is A, the length of the semimajor axis is B, and the distance from the focus to
611 the ellipse center C, are linked by the following relations in terms of the parameter p and the eccentricity ε:

$$A = \frac{p}{1-\varepsilon^2}, \quad B = \frac{p}{\sqrt{1-\varepsilon^2}}, \quad C = \frac{p\varepsilon}{1-\varepsilon^2}. \tag{A.23}$$

Thus, in the absence of perturbing accelerations, (A.19) has integration constants involving the quantities r_π, φ_π, M or some arbitrary combination of them. For $a_r \not\equiv 0$, $a_\varphi \not\equiv 0$ these quantities are not constant. The differential equations which determine $\varphi_\pi(\varphi), M(\varphi), S(\varphi) = u_\pi - M^{-2}$ can be expressed as a function of a_r and a_φ.

Introduce the new functions $w = du/d\varphi$, $p = M^2$; with these, (A.19) may be transformed into

$$\frac{du}{d\varphi} = w, \quad \frac{dw}{d\varphi} = -u + \frac{1}{p} - \frac{a_r}{pu^2} - \frac{a_\varphi w}{pu^3}, \quad \frac{dp}{d\varphi} = \frac{2a_\varphi}{u^3}. \tag{A.24}$$

The functions u and w are written in the forms (cf. (A.21))

$$u = \frac{1}{p} + s\cos(\varphi - \varphi_\pi), \quad w = -s\sin(\varphi - \varphi_\pi) \tag{A.25}$$

(regarding the representations of u and w cf. /A.1, A.2/); we then obtain a system of differential equations for S, φ_π and p, namely

$$\left.\begin{aligned}
&\frac{ds}{d\varphi} = \frac{a_r \sin\nu}{pN^2} + \frac{2a_\varphi \cos\nu}{p^2N^2} - \frac{a_\varphi s \sin^2\nu}{pN^2},\\
&\frac{d\varphi_\pi}{d\varphi} = -\frac{a_r \cos\nu}{spN^2} + \frac{2a_\varphi \sin\nu}{sp^2N^3} + \frac{a_\varphi \sin\nu\cos\nu}{pN^3},\\
&\frac{dp}{d\varphi} = \frac{2a_\varphi}{N^3}\\
&\left(\nu = \varphi - \varphi_\pi,\ N = \frac{1}{p} + s\cos(\varphi - \varphi_\pi)\right).
\end{aligned}\right\} \qquad (A.26)$$

If we replace (A.25) by /A.3, A.4/

$$u = \frac{1}{p} + \frac{Q}{p}, \qquad w = -\frac{L}{p}, \qquad (A.27)$$

this system of equations becomes

$$\left.\begin{aligned}
&\frac{dQ}{d\varphi} = -L + \frac{2a_\varphi p^2}{(Q+1)^2},\\
&\frac{dL}{d\varphi} = Q + \frac{a_r p^2}{(Q+1)^2} + \frac{a_\varphi p^2}{(Q+1)^2}L,\\
&\frac{dp}{d\varphi} = \frac{2a_\varphi p^3}{(Q+1)^2}.
\end{aligned}\right\} \qquad (A.28)$$

612 For $a_r \equiv 0$, $a_\varphi \equiv 0$ this system reduces to the equations of an unperturbed Keplerian motion in a Hamilton form.

Systems (A.26), (A.28) are written in osculating variables, i.e., variables which, in the absence of perturbations ($a_r \equiv 0$, $a_\varphi \equiv 0$), become constant. Any combination of the parameters S, φ_π, p, or Q, L, p likewise possesses this property. The selection of a particular system of osculating variables depends on the character of the perturbing accelerations.

The reduction of the equations of motion in a central field in the presence of perturbing accelerations to equations in osculating variables represents a standard operation, which has long been used in celestial mechanics. To describe space maneuvers we require osculating variables, which define the spatial motion of a point. To avoid cumbersome computations, we shall describe this operation along general lines, and shall conclude with the final formulas (cf. for instance /A.5/). The derivation of these formulas can be found in textbooks and treatises /A.6—A.13/.

Take the differential equations of motion in rectangular coordinates (A.3) as the initial system. The three second-order equations (A.3) can be transformed into the six first-order differential equations

$$\dot{x}_i = X_i(x_j) + a_i \qquad (i, j = 1, \ldots, 6), \qquad (A.29)$$

where

$$\left.\begin{aligned}
&x_1 = x,\ x_2 = \dot{x},\ x_3 = y,\ x_4 = \dot{y},\ x_5 = z,\ x_6 = \dot{z},\\
&X_1 = x_2,\ X_2 = -\frac{x_1}{r^3},\ X_3 = x_4,\ X_4 = -\frac{x_3}{r^3},\ X_5 = x_6,\ X_6 = -\frac{x_5}{r^3},\\
&a_1 = 0,\ a_2 = a_x,\ a_3 = 0,\ a_4 = a_y,\ a_5 = 0,\ a_6 = a_z\\
&\qquad\qquad (r = \sqrt{x_1^2 + x_3^2 + x_5^2}).
\end{aligned}\right\} \qquad (A.30)$$

If $a_i = 0$ $(i = 2, 4, 6)$, equations (A.30) define a motion in a central field, and can be integrated in finite form, as is well known. Suppose the initial conditions for (A.30) are

$$x_i(0) = f_i(p_1, \ldots, p_6) \qquad (i = 1, \ldots, 6), \tag{A.31}$$

where p_i are the complete set of orbital parameters in a two-body problem. The solution of equations (A.30) with no perturbing accelerations is found in the form

$$x_i = F_i(p_1, \ldots, p_6, t) \quad (F_i(p_1, \ldots, p_6, 0) = f_i(p_1, \ldots, p_6). \tag{A.32}$$

In the presence of perturbing forces the orbital parameters $p_1, \ldots, p_6$
613 can be considered as a new set of variables, which replace the old variables x_i by (A.32). We shall write the differential equations in terms of the osculating variables $p_1, \ldots, p_6$. First, take the total derivatives of x_i (given in A.32) which are

$$\frac{dx_i}{dt} = \frac{\partial F_i}{\partial t} + \sum_{j=1}^{6} \frac{\partial F_i}{\partial p_j} \frac{dp_j}{dt} = X_i + a_i \qquad (i = 1, \ldots, 6). \tag{A.33}$$

The definition of the osculating variables gives

$$\frac{\partial F_i}{\partial t} = X_i; \tag{A.34}$$

therefore

$$\sum_{j=1}^{6} \frac{\partial F_i}{\partial p_j} \frac{dp_j}{dt} = a_i. \tag{A.35}$$

This is a system in osculating variables and defines the variation of the orbital elements in the presence of perturbing accelerations. Note that equations (A.35) are linear in the derivatives dp_j/dt, and that we may therefore express dp_j/dt in terms of the perturbing accelerations a_i as

$$\frac{dp_j}{dt} = \sum_{i=1}^{6} A_{ji}(p_1, \ldots, p_6, t)\, a_i \qquad (j = 1, \ldots, 6). \tag{A.36}$$

614 Take the following set as orbital parameters (Figure A.4): the length of the semimajor axis A and the eccentricity ε, which define the geometry of the elliptic orbit; the inclination i and the longitude of the ascending node Ω, which define the orientation of the orbital plane; the argument φ_π, measured from the line of nodes, the time of passage T_π of the perihelion, which define the orbit in its plane. The perturbing acceleration vector can be resolved along three orthogonal directions: a_N perpendicular to the instantaneous orbital plane, a_R radial and lying in the plane of the instantaneous orbit, and a_Φ perpendicular to the radius vector. The differential

equations for the osculating variables $A, \varepsilon, i, \Omega, \varphi_\pi, \tau = -nT_\pi$ have the form

$$\left.\begin{aligned}
\frac{dA}{dt} &= \frac{2\varepsilon \sin \nu}{n\sqrt{1-\varepsilon^2}}\, a_R + \frac{2A\sqrt{1-\varepsilon^2}}{nr}\, a_\Phi,\\
\frac{d\varepsilon}{dt} &= \frac{\sqrt{1-\varepsilon^2}\sin \nu}{nA}\, a_R + \frac{\sqrt{1-\varepsilon^2}}{nA^2\varepsilon}\left(\frac{Ap}{r} - r\right) a_\Phi,\\
\frac{di}{dt} &= \frac{r\cos(\nu+\varphi_\pi)}{nA^2\sqrt{1-\varepsilon^2}}\, a_N,\\
\frac{d\Omega}{dt} &= \frac{r\sin(\nu+\varphi_\pi)}{nA^2\sqrt{1-\varepsilon^2}\sin i}\, a_N,\\
\frac{d\varphi_\pi}{dt} &= -\frac{\sqrt{1-\varepsilon^2}\cos \nu}{nA\varepsilon}\, a_R + \frac{\sqrt{1-\varepsilon^2}}{nA\varepsilon}\sin \nu\left(1+\frac{r}{p}\right) a_\Phi - \\
&\qquad - \sqrt{A(1-\varepsilon^2)}\sin(\nu+\varphi_\pi)\operatorname{ctg} i\, a_N,\\
\frac{d\tau}{dt} &= -\frac{1}{nA}\left(\frac{2r}{A} - \frac{1-\varepsilon^2}{\varepsilon}\cos \nu\right) a_R - \frac{1-\varepsilon^2}{nA\varepsilon}\sin \nu\left(1+\frac{r}{p}\right) a_\Phi.
\end{aligned}\right\} \qquad (A.37)$$

Here $n = A^{-3/2}$ is the average (dimensionless) angular velocity of motion, $p = A(1-\varepsilon^2)$ is the focal parameter, $r = p(1+\varepsilon\cos\nu)^{-1}$ is the equation of the osculating ellipse, and ν is the true anomaly. The system (A.37) must be completed by the relation defining the rate of variation of the true anomaly,

$$\frac{d\nu}{dt} = \frac{\sqrt{A(1-\varepsilon^2)}}{r^2} - \frac{d\varphi_\pi}{dt} - \cos i\,\frac{d\Omega}{dt}. \qquad (A.38)$$

As seen from equations (A.37), (A.38), the system of orbital parameters becomes meaningless when the eccentricity and inclination vanish, or when the eccentricity equals unity. At these points the right-hand sides of some

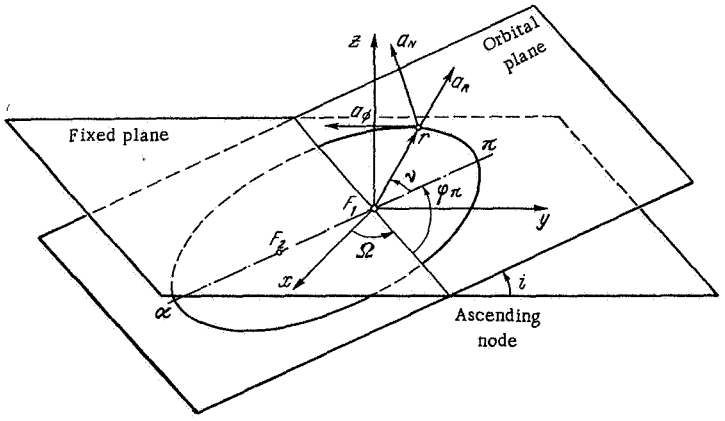

FIGURE A.4. Elements defining elliptic orbit in space.

of the equations are either indeterminate or infinite. In fact, the position
615 of the perihelion on the circular orbit ($\varepsilon = 0$), or the position of the nodal line when the fixed and orbital planes coincide ($i = 0$), are indeterminate. This fact restricts the region over which this system of orbital parameters can be numerically integrated, and is the reason why other better-suited systems must be found. In particular, in order to avoid problems connected with the degeneration of an orbit into a circular one ($\varepsilon = 0$), we replace the

parameters ε, φ_π by their combinations $\varepsilon \sin \varphi_\pi$, $\varepsilon \cos \varphi_\pi$, the components of the Laplace vector. The differential equations for these combinations do not contain ε in the denominator (cf. (A.26), (A.28)).

The system of orbital parameters proposed in /A.14/ is likewise free of these features. The system consists of two vectors: the angular-momentum vector, and the Laplace vector ε which is directed from the center to the perihelion and equal in magnitude to the eccentricity ε.

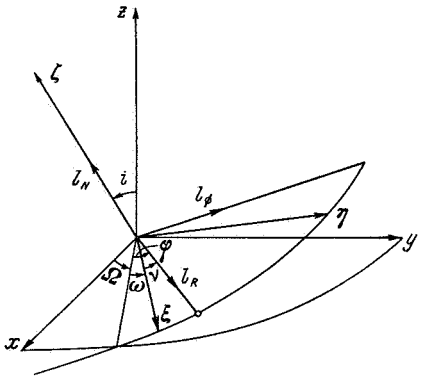

FIGURE A.5. Mixed system of coordinates.

The author of /A.13/ used the initial values of the coordinates and velocities as osculating variables for quasi-circular orbits with small inclination. These variables were used in /A.16/ for arbitrary orbits.

For many three-dimensional problems it is best to use a system of mixed variables containing both polar coordinates and osculating variables. The system of space variables given in /A.17, A.18/ is convenient for analyzing perturbed motions. As before, three orthogonal directions with origin at the gravitational center are defined here (Figure A.5) where $\mathbf{l}_R$ is the unit radius vector of the moving point, $\mathbf{l}_\Phi$ is the unit vector perpendicular to the radius vector in the instantaneous orbital plane, and $\mathbf{l}_N$ is the unit vector perpendicular to the instantaneous orbital plane.

Let ω_R, ω_Φ, ω_N be the projections of the angular velocity in the (R, Φ, N) coordinate system relative to the inertial (x, y, z) frame. If the coordinates (R, Φ, N) at each instant of time are defined by the angles Ω (longitude of the ascending node), i (inclination), φ (angular distance of the moving point in the orbital plane, measured from the line of nodes (cf. Figure A.5), then the angular velocities ω_R, ω_Φ, ω_N will be expressed as

616

$$\left.\begin{aligned} \omega_R &= \dot{\Omega} \sin\varphi \sin i + \dot{i} \cos\varphi, \\ \omega_\Phi &= \dot{\Omega} \cos\varphi \sin\varphi - \dot{i} \sin\varphi, \\ \omega_N &= \dot{\varphi} + \dot{\Omega} \cos i. \end{aligned}\right\} \tag{A.39}$$

According to the definition of the instantaneous orbit, the velocity vector must not contain components perpendicular to the instantaneous orbit, i.e.,

$$\mathbf{r} \cdot \mathbf{l}_N = -r\omega_\Phi = 0. \tag{A.40}$$

Allowing for this condition, the vectorial equation of motion

$$\ddot{\mathbf{r}} = \mathbf{a} - \mathbf{r}/r^3 \tag{A.41}$$

has the following form when projected onto the axes $\mathbf{l}_R$, $\mathbf{l}_\Phi$, $\mathbf{l}_N$:

$$\left.\begin{aligned} \ddot{r} - r\omega_N^2 - 1/r^2 &= a_R, \\ 2\dot{r}\omega_N + r\dot{\omega}_N &= a_\Phi, \\ r\omega_N\omega_R &= a_N. \end{aligned}\right\} \tag{A.42}$$

In the last equations we may make a change of variables as in the two-dimensional case. We introduce $u = r^{-1}$, $M = \omega_N r^2$, and define the angle ν by the differential equation

$$\dot{\nu} = \omega_N = M/r^2. \tag{A.43}$$

System (A.42) is then transformed into

$$\frac{d^2u}{d\nu^2} + u = \frac{1}{M^2}\left(1 - \frac{a_R}{u^2} - \frac{a_\Phi}{u^3}\frac{du}{d\nu}\right), \quad \frac{dM}{d\nu} = \frac{a_\Phi}{Mu^3}, \quad \omega_R = \frac{a_N}{Mu}. \tag{A.44}$$

Allowing for the symbols used, the first two equations coincide with the equations for plane motion (A.19). If the acceleration components a_R and a_Φ depend only on the two variables u and ν, the system can be split so that the first two equations can be integrated independently of the others.

If the differential equations governing the unit vectors $\mathbf{l}_R$, $\mathbf{l}_\Phi$, $\mathbf{l}_N$,

$$\frac{d\mathbf{l}_R}{d\nu} = \mathbf{l}_\Phi, \quad \frac{d\mathbf{l}_\Phi}{d\nu} = -\mathbf{l}_R\frac{a_N}{M^2u^3}, \quad \frac{d\mathbf{l}_N}{d\nu} = -\mathbf{l}_\Phi\frac{a_N}{M^2u^3} \tag{A.45}$$

are added to (A.44), a closed system of equations results.

Instead of determining the unit vectors $\mathbf{l}_R$, $\mathbf{l}_\Phi$, $\mathbf{l}_N$ from the differential equations (A.45) and then finding the functions $\Omega(\nu)$, $i(\nu)$, $\varphi(\nu)$, we can use directly
617 the differential equations for the angles (A.39). Following the treatment in /A.17/, we introduce coordinates (ζ, η) in the orbital plane (cf. Figure A.5); these revolve relative to the unit vectors $\mathbf{l}_R$, $\mathbf{l}_\Phi$ at an angular velocity $\dot{\omega} = \dot{\varphi} - \dot{\nu}$. If in expressions (A.39) we everywhere replace the angle φ by $\nu + \omega$, the differential equations for the angles Ω, i, ω become

$$\left.\begin{aligned} \frac{d\Omega}{d\nu} &= \frac{a_N}{M^2u^3}\frac{\sin(\omega+\nu)}{\sin i}, \\ \frac{di}{d\nu} &= \frac{a_N}{M^2u^3}\cos(\omega+\nu), \\ \frac{d\omega}{d\nu} &= -\frac{a_N}{M^2u^3}\sin(\omega+\nu)\operatorname{ctg} i. \end{aligned}\right\} \tag{A.46}$$

These equations together with (A.42) also yield a closed system.

2. Equations of motion in a field with two gravitational centers. The vectorial equation of motion in an arbitrary gravitational field is written as follows:

$$\ddot{\mathbf{r}} = \mathbf{a} + \mathfrak{R}(\mathbf{r}, t), \tag{A.47}$$

where $\mathfrak{R}(\mathbf{r}, t)$ is the gravitational acceleration. We considered in the preceding subsection the equations of motion in a field with one gravitational center given by

$$\mathfrak{R}(\mathbf{r}, t) = -k\mathbf{r}/r^3. \tag{A.48}$$

We now give the equations of plane motion in a field with two centers, 1 and 2 say. It is assumed that gravitational center 1 is fixed, and therefore the coordinate system linked with it is inertial. Center 2 revolves about center 1 with constant angular velocity ω and at a fixed distance R_0 from it, so that the coordinate system linked with it is therefore noninertial.

The motion can be studied using either inertial (1) or noninertial (2) reference systems. Both systems of equations, written in the same form (the symbols and the relationship between the two coordinate systems are shown in Figure A.6), are

$$\left.\begin{aligned} \ddot{r}_i &= a_{ri} + r_i\dot{\varphi}_i^2 - k_i/r_i^2 - \mathfrak{R}_i, \\ r_i\ddot{\varphi}_i &= a_{\varphi i} - 2\dot{r}_i\dot{\varphi}_i - \Psi_i \end{aligned}\right\} \quad (i = 1, 2) \tag{A.49}$$

618 (where k_1 and k_2 are the gravitational constants of centers 1 and 2) and

$$\left.\begin{aligned} &\varphi_1 = \psi_1 + \omega t, \quad \varphi_2 = \psi_2 + \omega t, \\ &\mathfrak{R}_1 = \frac{k_2}{r_2^2}\cos(\psi_2 - \psi_1), \\ &\Psi_1 = \frac{k_2}{r_2^2}\sin(\psi_2 - \psi_1), \\ &\mathfrak{R}_2 = \frac{k_1}{R_0^2}\cos\psi_2 - \frac{k_1}{r_1^2}\cos(\psi_2 - \psi_1), \\ &\Psi_2 = \frac{k_1}{R_0^2}\sin\psi_2 - \frac{k_1}{r_1^2}\sin(\psi_2 - \psi_1). \end{aligned}\right\} \tag{A.50}$$

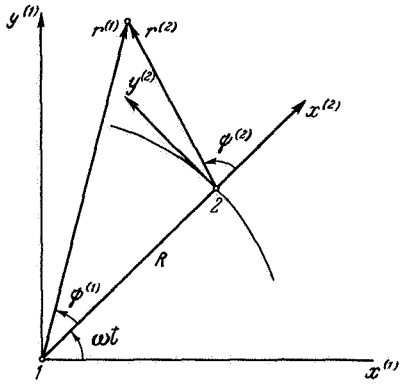

FIGURE A. 6. System of coordinates for describing motion in field with two gravitational centers.

3. Equations of motion for model fields. Take the linearized and homogeneous central field, the plane-parallel field, and the gravity-free field as the models.

Let the trajectory be bounded by small angular and radial displacements; the projections of the gravitational acceleration can then be expanded as a Taylor series in the neighborhood of some characteristic point of the trajectory, such as the initial point (x_0, y_0, z_0) /A.19, A.20/. If the system of coordinates is oriented so that the initial point lies on the x-axis ($x_0 = r_0$, $y_0 = 0$, $z_0 = 0$), the equations of three-dimensional motion have the following form, when just the leading terms of the expansion of the projections of the gravitational acceleration are preserved:

$$\left.\begin{aligned} \ddot{x} &= a_x - g_0 + 2g_0(x - r_0)/r_0, \\ \ddot{y} &= a_y - g_0 y/r_0, \\ \ddot{z} &= a_z - g_0 z/r_0 \quad (g_0 = k/r_0^2). \end{aligned}\right\} \tag{A.51}$$

When the displacements $x(t) - r_0$, $y(t)$, $z(t)$ are small compared with the initial distance from the center r_0, so that

$$|a_x - g_0| \gg 2g_0|1 - x/r_0|, \quad |a_y| \gg g_0|y/r_0|, \quad a_z \gg g_0|z/r_0|,$$

it is convenient to choose a plane-parallel field as the model. The equations of motion reduce to

$$\ddot{x} = a_x - g_0, \quad \ddot{y} = a_y, \quad \ddot{z} = a_z. \tag{A.52}$$

Finally, if the thrust acceleration is much greater than the gravitational acceleration, the latter can be ignored in the equations of motion (model of gravity-free field), which now become

$$\ddot{\mathbf{r}} = \mathbf{a}. \tag{A.53}$$

If the magnitude of the radius vector hardly varies throughout the motion in a central field (the trajectory lies within a thin spherical layer), the
619 model of a homogeneous central field will be a good choice /A.21, A.22/; the vectorial equation of motion in this case has the form

$$\ddot{\mathbf{r}} = \mathbf{a} - \omega^2\mathbf{r}, \tag{A.54}$$

where $\omega^2 = g_*/r_* = k/r_*^3$.

§ 2. INTERPLANETARY FLIGHT

1. Dividing the interplanetary flight into elementary maneuvers. The trajectory of the interplanetary flight with a low-thrust engine consists of the following stages (Figure A.7): acceleration from the initial orbit in the neighborhood of the take-off planet (represented by the index +1), inter-orbital transfer in the field of the Sun (index 1), deceleration in the neighborhood of the destination planet (index −2); the same stages are repeated in the reverse order for the return flight (represented by indices +2, 2, and −1 respectively).

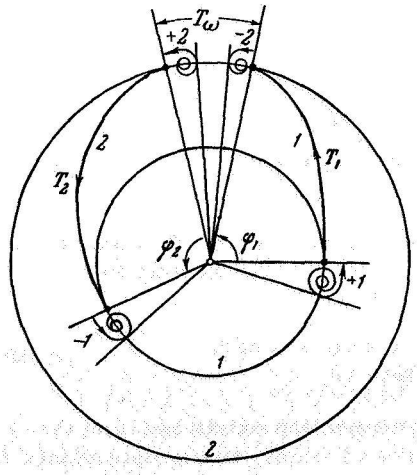

FIGURE A.7. Scheme of interplanetary roundtrip flight.

The trajectory of the interplanetary flight contains two characteristic stages, namely, motion in the neighborhood of the planets and motion in the field of the Sun. For a two-body problem, we assume that the gravitational field for each of these stages is respectively created by one center, i.e., the planet or the Sun.

In this formulation it is usually assumed that the stage of the motion

in the neighborhood of the planet extends from the initial orbit to that point at which full zero energy is attained (parabolic velocity), and that the stage of orbital transfer starts at a given point of one heliocentric orbit and ends at a given point of the second one. The velocity components at the initial point of the first maneuver and at the initial and final points of the second maneuver coincide with the corresponding projections of the orbital velocity vector.

620 This subsection only deals with plane motion, and ignores the third component. The question of joining the stages of the interplanetary flight is likewise not considered, in view of the weak dependence of the position of the junction point on the expended energy.

According to these two simplifications, two elementary maneuvers form the interplanetary flight, i.e., the build-up of zero energy (or the acceleration to a parabolic velocity) and the orbital transfer. These are described by the system of equations with a central field (A.8) or (A.3) (the latter without the third equation since $z \equiv 0$, $a_z \equiv 0$).

The boundary conditions for (A.8) are:

for the first elementary maneuver

$$\left.\begin{aligned} &r(0) = 1,\ \varphi(0) = 0,\ v_r(0) = v_{r0}, \quad v_\varphi(0) = v_{\varphi 0}, \\ &E(T) = {}^1/_2\,[v_r^2(T) + v_\varphi^2(T)] - 1/r(T) = 0; \end{aligned}\right\} \tag{A.55}$$

for the second elementary maneuver

$$\left.\begin{aligned} &r(0) = 1, \quad \varphi(0) = 0, \quad v_r(0) = v_{r0}, \quad v_\varphi(0) = v_{\varphi 0}, \\ &r(T) = r_1, \quad \varphi(T) = \varphi_1, \quad v_r(T) = v_{r1}, \quad v_\varphi(T) = v_{\varphi 1}. \end{aligned}\right\} \tag{A.56}$$

In both cases we use the initial radius r_* as the characteristic linear dimension (cf. (A.2)); therefore $r(0) = 1$. The origin of the system of coordinates is defined by locating the take-off point on the abscissa, i.e., where $\varphi(0) = 0$.

If the initial orbit of the first maneuver, and the initial and final orbits of the second maneuver are all circular, conditions (A.55), (A.56) are written as follows:

for the build-up of zero energy

$$\left.\begin{aligned} &r(0) = 1, \quad \varphi(0) = 0, \quad v_r(0) = 0, \quad v_\varphi(0) = 1, \\ &E(T) = {}^1/_2\,[v_r^2(T) + v_\varphi^2(T)] - 1/r(T) = 0; \end{aligned}\right\} \tag{A.57}$$

for the orbital transfer

$$\left.\begin{aligned} &r(0) = 1, \quad \varphi(0) = 0, \quad v_r(0) = 0, \quad v_\varphi(0) = 1, \\ &r(T) = r_1, \quad \varphi(T) = \varphi_1, \quad v_r(T) = 0, \quad v_\varphi(T) = r_1^{-1/2}. \end{aligned}\right\} \tag{A.58}$$

The boundary conditions for the equations in cartesian coordinates (A.3) are obtained by transforming the formulas from a polar system to a cartesian one (cf. (A.4)) using

$$\begin{aligned} x = r\cos\varphi,\ y = r\sin\varphi;\ \ u = v_r\cos\varphi - v_\varphi\sin\varphi, \\ v = v_r\sin\varphi + v_\varphi\cos\varphi. \end{aligned} \tag{A.59}$$

621 **2. Round-trip interplanetary flight.** A connection exists between the kinematic parameters at the different stages of flight, and is determined by the condition that the spacecraft returns to the take-off planet.

For simplicity, we replace the force fields of the planets by point forces along their orbits; in the heliocentric reference frame the trajectory of the spacecraft in the neighborhood of the planets will then be indistinguishable from the orbits of the planets.

Consider that part of the round-trip trajectory which lies outside the take-off orbit. This consists of the transfer from orbit 1 to orbit 2, the motion along orbit 2 together with the planet, and the reverse transfer from orbit 2 to orbit 1. The quantities $T_1, \varphi_1, T_2, \varphi_2$ represent the durations and angular displacements of the orbital transfers (index 1 implies "from orbit 1 to orbit 2", index 2 implies "from orbit 2 to orbit 1" (Figure A.7)), and T_ω is the time of sojourn on orbit 2 (consisting of the times during which deceleration, acceleration, and coasting occur near the destination planet).

A relation between the parameters $T_1, \varphi_1, T_2, \varphi_2, T_\omega$ follows from the equality of the angular displacements of the take-off planet and spacecraft. If orbits 1 and 2 are circular, we obtain

$$T_\omega = [\varphi_1 + \varphi_2 - (T_1 + T_2) \pm 2n\pi]/(1 - \omega_2), \tag{A.60}$$

where ω_2 is the angular velocity of planet 2 along a circular orbit about the Sun ($\omega_1 = 1$), n is the integral number of revolutions of planet 1 ($n = 0, 1, 2, \ldots$), the plus sign corresponds to $\omega_2 < \omega_1$ and the minus sign to $\omega_2 > \omega_1$.

If orbits 1 and 2 are not circular, integrals appear in formula (A.60); in order to allow for the size of the force fields produced by the planets, we must add the angular displacements between points of entry into, and exit from the force fields when equating angular displacements (cf. /A.23/).

In the boundary-value problem formulated for the stage of interplanetary flight considered here, we usually assume that the time T_ω of sojourn on orbit 2 and the time T_σ of sojourn outside orbit 1 are specified, so that $T_\sigma = T_1 + T_\omega + T_2$. The angular displacements φ_1, φ_2 and times T_1, T_2 are defined by

$$\varphi_1 + \varphi_2 = T_\sigma - \omega_2 T_\omega \mp 2n\pi; \quad T_1 + T_2 = T_\sigma - T_\omega,$$

and not separately as in boundary conditions (A.56).

If orbits 1 and 2 are circular, the boundary conditions for the orbital transfers (outward and return) are as follows:

transfer from orbit 1 to orbit 2

$$\left.\begin{aligned} &r(0) = 1,\ \varphi(0) = 0,\ v_r(0) = 0,\ v_\varphi(0) = 1, \\ &r(T_1) = r_1,\ \varphi(T_1) = \varphi_1,\ v_r(T_1) = 0,\ v_\varphi(T_1) = r_1^{-1/2}; \end{aligned}\right\} \tag{A.61}$$

622 transfer from orbit 2 to orbit 1

$$\left.\begin{aligned} &r(T_1 + T_\omega) = r_1,\ \varphi(T_1 + T_\omega) = \varphi_1 + T_\omega\omega_2, \\ &v_r(T_1 + T_\omega) = 0,\ v_\varphi(T_1 + T_\omega) = r_1^{-1/2}, \\ &r(T_\sigma) = 1,\ \varphi(T_\sigma) = T_\sigma \mp 2n\pi,\ v_r(T_\sigma) = 0,\ v_\varphi(T_\sigma) = 1 \end{aligned}\right\} \tag{A.62}$$

(in these formulas the quantities φ_1, T_1 are not determined).

The parameters φ_1, T_1 (the angular displacement and the duration of the transfer), which appear here in the boundary conditions for the orbital transfer, may be replaced by parameters t_0 and T_1 (the take-off date, the flight duration). The relation between these two pairs is obtained from

the condition for equal angular displacements of the spacecraft and destination planet at the instant of encounter.

If orbits 1 and 2 are circular, and the take-off date t_0 is reckoned from the time of opposition of planets 1 and 2, the transformation is

$$\varphi_1 = t_0 + T_1 - \omega_2 t_0 \pm 2\pi n \quad (n = 0, 1, 2, \ldots). \tag{A.63}$$

The parameters t_0 and T_1 are more amenable to calculation when the actual positions of the planets along their orbits are employed.

3. Models of maneuvers. In this subsection two examples of one-dimensional motions in a gravity-free field are given: build-up of a specified velocity magnitude u_1 throughout a specified time T, and displacement during time T between two points of rest situated a distance l apart.

These reflect the characteristic features of maneuvers in a central field. The first models the maneuver of slow build-up of zero energy from a circular take-off orbit (cf. (A.8), (A.57)), and the second a rapid orbital transfer (cf. (A.8), (A.58)).

The equations of motion and boundary conditions for the problem of building up a given velocity magnitude are

$$\dot{u} = ae;\ u(0) = 0,\ u(T) = u_1. \tag{A.64}$$

For transfer between two positions of rest, the system is

$$\dot{x} = u,\ \dot{u} = ae;\ x(0) = 0,\ u(0) = 0,\ x(T) = l,\ u(T) = 0. \tag{A.65}$$

Here, a is the thrust-acceleration magnitude and $e = \pm 1$ is the thrust-vector direction.

623 § 3. SATELLITE MANEUVERS

1. Holding a satellite within a given spherical layer. The satellite is placed in a circular orbit located in the upper layers of the atmosphere. The gravitational forces of an attracting body give the motion a periodic component, while the aerodynamic drag leads to a secular motion away from the initial orbit. The problem is to compensate the drag forces so that the satellite remains within the bounds of the spherical layer of given maximum and minimum radii during a specified time (cf. /A.13, A.24, A.25/).

The motion in a gravitational field in the presence of drag is described by the following system of first-order differential equations:

$$\dot{\mathbf{r}} = \mathbf{v},\ \dot{\mathbf{v}} = a\mathbf{e} + \mathbf{R} - g\mathbf{F}/G; \tag{A.66}$$

this system contains the new term $g\mathbf{F}/G$, which allows for the aerodynamic deceleration, a is the thrust-acceleration magnitude, and $\mathbf{e}$ is the unit vector of thrust orientation.

We select an inertial cartesian reference frame $Oxyz$. The plane xOy coincides with the equatorial plane, the x-axis is directed towards the vernal equinox, the z-axis to the north pole, and the y-axis is so chosen as to complete a right-handed system.

The components of the gravitational acceleration $\mathfrak{R}$ are determined by the potential U of the attracting body, in this case the Earth, so that $\mathfrak{R} = \partial U/\partial \mathbf{r}$. Taking into account the first two harmonics of the potential of an oblate spheroid, we have

$$U(x, y, z) = \frac{k}{r}\left[1 + \frac{\beta}{r^2}\left(1 - 3\frac{z^2}{r^2}\right)\right] \qquad (r = \sqrt{x^2 + y^2 + z^2}); \tag{A.67}$$

the quantities $k, \beta = \frac{j}{3} R_s^2$ are given in Chapter One (1.9).

The aerodynamic drag force $\mathbf{F}$ acting on a vehicle in an impinging flow with relative velocity $\mathfrak{B}$ is

$$\mathbf{F} = {}^1/_2 c_x \mathcal{F} \rho \mathfrak{B} \mathfrak{B}, \tag{A.68}$$

where c_x is the drag coefficient, $\mathcal{F}$ is the characteristic cross-sectional area of the vehicle, and ρ is the density of the atmosphere.

If the atmosphere is stationary, the velocity $\mathfrak{B}$ in the inertial frame $Oxyz$ coincides with the velocity $\mathbf{v}$ of the vehicle; when we allow the atmosphere to rotate with an angular velocity $\mathbf{j}(0, 0, j_z)$, equal to the velocity of revolution of the Earth, we add the vector product $\mathbf{r} \times \mathbf{j}$ to $\mathbf{v}$ so that

$$\mathfrak{B} = \mathbf{v} + \mathbf{r} \times \mathbf{j}. \tag{A.69}$$

624 The projections of the drag force onto the axes of the inertial frame are

$$\left.\begin{aligned} F_x &= {}^1/_2 c_x \mathcal{F} \rho \mathfrak{B} (\dot{x} + j_z y), \\ F_y &= {}^1/_2 c_x \mathcal{F} \rho \mathfrak{B} (\dot{y} - j_z x), \\ F_z &= {}^1/_2 c_x \mathcal{F} \rho \mathfrak{B} \dot{z} \\ (\mathfrak{B} &= [(\dot{x} + j_z y)^2 + (\dot{y} - j_z x)^2 + \dot{z}^2]^{1/2}). \end{aligned}\right\} \tag{A.70}$$

The value j_z in (A.70) is considered positive when the angle between the vehicle velocity $\mathbf{v}$ and the stream velocity $\mathbf{r} \times \mathbf{j}$ is less than $\pi/2$ (the satellite is initially projected in the direction of the Earth's rotation).

The density ρ in expressions (A.68), (A.70) is a function not only of the altitude above the Earth's surface, but also of the latitude and the time of year. The density as a function of these arguments is given in /A.26/.

We pass now to a spherical noninertial reference frame (r, φ, θ) (Figure A.8), whose equatorial plane makes a constant angle i with the plane of the equator and revolves at an angular velocity Ω about the polar axis z /A.24/; at the initial instant of time this equatorial plane coincides with the orbital plane of the satellite, and the angle $\Omega(t)$ is an arbitrary function which must be determined later on. The coordinates (x, y, z) are expressed as follows in terms of $r, \varphi, \theta, \Omega, i$:

$$\left.\begin{aligned} x &= r(\cos\varphi\cos\theta\cos\Omega - \sin\varphi\cos\theta\sin\Omega\cos i + \sin\theta\sin\Omega\sin i), \\ y &= r(\cos\varphi\cos\theta\sin\Omega + \sin\varphi\cos\theta\cos\Omega\cos i - \sin\theta\cos\Omega\sin i), \\ z &= r(\sin\varphi\cos\theta\sin i + \sin\theta\cos i). \end{aligned}\right\} \tag{A.71}$$

625 By-passing the process of transforming to the new variables, the final result is

$$\left.\begin{aligned}
&\ddot{r} - r(\theta + \dot{\Omega}\cos\varphi\sin i)^2 - r[\dot{\varphi}\cos\theta + \dot{\Omega}(\cos\theta\cos i - \\
&- \sin\theta\sin\varphi\sin i)]^2 = -\frac{1}{r^2} - \frac{3\beta}{r^4}[1 - 3(\sin\theta\cos i + \\
&+ \cos\theta\sin i\sin\varphi)^2] - \varkappa\frac{\rho\mathfrak{B}\dot{r}}{G} + ae_r, \\
&\frac{d}{dt}\{r^2\cos\theta[\dot{\varphi}\cos\theta + \dot{\Omega}(\cos i\cos\theta - \sin\theta\sin i\sin\varphi)]\} - \\
&- r^2\dot{\Omega}\sin i[\dot{\theta}\sin\varphi - \dot{\varphi}\sin\theta\cos\theta\cos\varphi - \\
&- \dot{\Omega}\cos\varphi\cos\theta(\sin\theta\cos i + \cos\theta\sin\varphi\sin i)] = \\
&= -\frac{6\beta}{r^3}(\sin\theta\cos i + \cos\theta\sin i\sin\varphi)\cos\theta\sin i\cos\varphi - \\
&- \varkappa\frac{\rho\mathfrak{B}r^2}{G}\cos\theta[\dot{\varphi}\cos\theta + (\dot{\Omega} - j_z)(\cos\theta\,\mathrm{ccs}\,i - \sin\theta\sin\varphi\sin i)] + \\
&+ ae_\varphi\cos\theta r, \\
&\frac{d}{dt}[r^2(\dot{\theta} - \dot{\Omega}\cos\varphi\sin i)] + r^2[\dot{\varphi}^2\sin\theta\cos\theta + \dot{\Omega}^2(\sin\theta\cos i + \\
&+ \cos\theta\sin\varphi\sin i)(\cos\theta\cos i - \sin\theta\sin\varphi\sin i)] + \\
&+ \dot{\varphi}\dot{\Omega}[\cos\theta(\sin\theta\cos i + \cos\theta\sin\varphi\sin i) + \sin\theta(\cos\theta\cos i - \\
&- \sin\theta\sin\varphi\sin i)] = -\frac{6\beta}{r^3}(\sin\theta\cos i + \cos\theta\sin\varphi\sin i)\times \\
&\times(\cos\theta\cos i - \sin\theta\sin\varphi\sin i) - \\
&- \varkappa\frac{\rho\mathfrak{B}r^2}{G}[\dot{\theta} - (\dot{\Omega} - j_z)\cos\varphi\sin i] + ae_\theta r.
\end{aligned}\right\} \qquad (A.72)$$

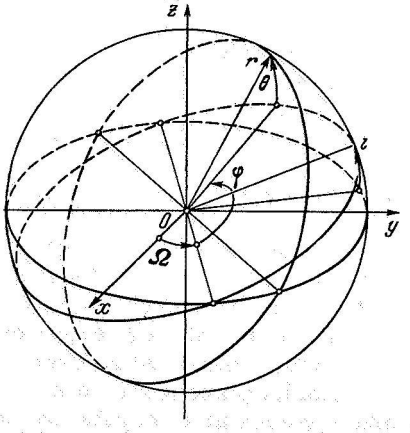

FIGURE A.8. System of coordinates for problem of holding satellite within given spherical layer.

These are three projections of Newton's equation in dimensionless form. The linear distances are represented as fractions of the initial radius r_0, the time as a fraction of $r_0^{3/2}k^{-1/2}$, the angular velocities (including j_z) as a fraction of $k^{1/2}r_0^{-3/2}$, the accelerations as fractions of the gravitational acceleration kr_0^{-2}, the density as a fraction of the maximum density ρ_0 at radius r_0, the coefficient β in the expansion for the potential as a fraction of r_0^2, the square of the initial radius, and the engine weight as a fraction of its take-off

weight G_0; the old symbols have been preserved for the dimensionless variables (compare the transformation from (A.1) to (A.3)). The drag parameter $\varkappa$ is expressed as follows:

$$\varkappa = gc_x\mathcal{F}\rho_0 r_0/2G_0. \tag{A.73}$$

The quantities e_r, e_φ and e_θ represent the projections of the unit thrust-direction vector $\mathbf{e}$ ($e_r^2 + e_\varphi^2 + e_\theta^2 = 1$) on the axes of the spherical system of coordinates.

626

The initial conditions on the circular orbit in the adopted coordinate system are

$$r(0) = 1,\ \dot{r}(0) = 0,\ \varphi(0) = \varphi_0,\ \dot{\varphi}(0) = 1,\ \theta(0) = \dot{\theta}(0) = 0. \tag{A.74}$$

The final values of these quantities are undefined, except for the radius r, which remains bounded at the final instant (just as throughout the motion), so that

$$r_{\min} \leqslant r(t) \leqslant r_{\max} \quad (0 \leqslant t \leqslant T). \tag{A.75}$$

We restrict ourselves in what follows to high altitudes, where the parameter $\varkappa$ is small; the other dimensionless parameters of the problem j_z, β have the following numerical values:

$$j_z \approx 0.6 \cdot 10^{-1},\ \beta \approx 0.5 \cdot 10^{-3}. \tag{A.76}$$

If the oblateness of the attracting body, the atmospheric drag, and the thrust all vanish ($\beta = \varkappa = 0$, $a(t) \equiv 0$) and the arbitrary function $\Omega(t)$ vanishes too, i.e., $\Omega(t) \equiv 0$, equations (A.72) describe a Keplerian orbit, which lies in the equatorial plane $\theta = 0$ of the (r, φ, θ) system of coordinates. Throughout the actual motion the Keplerian orbit is perturbed by the small oblateness and the small drag force.

According to the conditions of the problem, the trajectory of the motion must lie within a thin spherical layer Δr ($\Delta r = r_{\max} - r_{\min} \ll 1$). Therefore, throughout the motion the functions $r(t)$, $\dot{r}(t)$, $\dot{\varphi}(t)$ must have values which hardly differ from the corresponding values on the unperturbed spherical orbit. Consequently $|r(t) - 1| \ll 1$, $|\dot{r}(t)| \ll 1$, $|\dot{\varphi}(t) - 1| \ll 1$. It follows that the trajectory parameters $r(t)$ and $\varphi(t)$ can be represented by

$$r(t) = 1 + \xi(t),\quad \varphi(t) = \varphi_0 + t + \eta(t), \tag{A.77}$$

where $|\xi(t)| \ll 1$, $|\dot{\xi}(t)| \ll 1$, $|\dot{\eta}(t)| \ll 1$. The problem can now be linearized with respect to the variables ξ, $\dot{\xi}$, η.

The condition of sojourn of the satellite within a thin spherical layer ($r_{\max}$, $r_{\min}$) imposes no physical restrictions on the region over which the angle $\theta(t)$ varies. Since however in the unperturbed motion $\theta(t) \equiv 0$, and since the perturbing forces of the actual motion are small, it can be assumed that at the initial stage of motion the functions $\theta(t)$ and $\dot{\theta}(t)$ are small:

$$|\dot{\theta}(t)| \ll 1,\ |\theta(t)| \ll 1 \text{ for } 0 \leqslant t \leqslant t_1.$$

Assuming that the derivative of the arbitrary function $\dot{\Omega}(t)$ is small too, $|\dot{\Omega}(t)| \ll 1$, we linearize system (A.72) with respect to the variables ξ, $\dot{\xi}$, $\dot{\eta}$, θ, $\dot{\theta}$, $\dot{\Omega}$; this yields

627

$$\left.\begin{aligned}
&\ddot{\xi} - 3\xi - 2\dot{\eta} = 2\dot{\Omega}\cos i - 3\beta\,[1 - 3\sin^2 i \sin^2(\varphi_0 + t)] + ae_r,\\
&\ddot{\eta} + 2\dot{\xi} = -\ddot{\Omega}\cos i - 6\beta \sin^2 i \sin(\varphi_0 + t)\cos(\varphi_0 + t) - \\
&\qquad\qquad - \varkappa \frac{\rho}{G}(1 - j_z \cos i) + ae_\varphi,\\
&\ddot{\theta} + \theta = \ddot{\Omega}\sin i \cos(\varphi_0 + t) - 2\dot{\Omega}\sin i \sin(\varphi_0 + t) - \\
&\qquad - 6\beta \sin i \cos i \sin(\varphi_0 + t) - \varkappa j_z \frac{\rho}{G}\sin i \cos(\varphi_0 + t) + ae_\theta.
\end{aligned}\right\} \qquad (A.78)$$

In these variables the boundary conditions (A.74), (A.75) are

$$\xi(0) = \dot{\xi}(0) = \eta(0) = \dot{\eta}(0) = \theta(0) = \dot{\theta}(0) = 0,$$
$$\xi_{\min} \leqslant \xi(t) \leqslant \xi_{\max} \quad (0 \leqslant t \leqslant T). \qquad (A.79)$$

On the right-hand sides of (A.78) we only preserve first-order terms with respect to j_z; terms of second and higher orders are discarded, since the small quantity $\varkappa$ appears as a factor multiplying them. For the same reason only the zero term must be retained when expanding the density in terms of ξ, η, θ; the density ρ in (A.78) is a known function of the time, and is determined by the initial circular orbit ($\xi(t) = \eta(t) = \theta(t) = 0$).

We select the following expression for the arbitrary function $\Omega(t)$ /A.25/:

$$\dot{\Omega} = -3\beta \cos i = \text{const} \qquad (A.80)$$

(this expression satisfies the above-mentioned condition that the derivative $\dot{\Omega}$ is small).

The third equation of (A.78) is transformed into

$$\ddot{\theta} + \theta = -\varkappa \frac{\rho}{G} j_z \sin i \cos(\varphi_0 + t) + ae_\theta \quad (\theta(0) = \dot{\theta}(0) = 0). \qquad (A.81)$$

It is assumed that there is no thrust component in the direction of θ ($e_\theta = 0$); with this assumption we estimate the maximum value of the angle θ attained up to $t = t_1$. For this, we put $\rho(t) \equiv 1$, $G(t) = G_1$; hence

$$\theta(t_1) = \varkappa j_z \frac{\sin i}{2G_1}[\sin\varphi_0 \sin t_1 - t_1 \sin(\varphi_0 + t_1)]. \qquad (A.82)$$

The presence of a mixed term in solution (A.82) points to the presence of increasing-amplitude oscillations of the radius vector relative to the equatorial plane. For $t_1 \ll 1/j_z\varkappa$ the angle θ_1 is small, and we may only allow for the linear term when expanding in terms of θ.

628 Finally, the differential equations and boundary conditions, which describe the maneuver of holding a satellite within a given spherical layer, are

$$\left.\begin{aligned}
&\ddot{\xi} - 3\xi - 2\dot{\eta} = -3\beta\,[1 + 2\cos^2 i - 3\sin^2 i \sin^2(\varphi_0 + t)] + ae_r,\\
&\ddot{\eta} + 2\dot{\xi} = -6\beta \sin^2 i \sin(\varphi_0 + t)\cos(\varphi_0 + t) - \\
&\qquad\qquad - \varkappa \frac{\rho}{G}(1 - j_z \cos i) + ae_\varphi,\\
&\ddot{\theta} + \theta = -\varkappa j_z \frac{\rho}{G}\sin i \cos(\varphi_0 + t) + ae_\theta,\\
&\xi(0) = \dot{\xi}(0) = \eta(0) = \dot{\eta}(0) = 0\,(0) = \dot{\theta}(0) = 0,\\
&\qquad\qquad \xi_{\min} \leqslant \xi(t) \leqslant \xi_{\max} \quad (0 \leqslant t \leqslant T).
\end{aligned}\right\} \qquad (A.83)$$

If the satellite motion is investigated over a sufficiently large time duration, it is best to study the variation of the parameters $\xi, \dot{\xi}, \eta, \dot{\eta}, \theta, \dot{\theta}$ over an integral number of revolutions s. After a time $2s\pi$ the parameters $\xi, \dot{\xi}, \dot{\eta}$ take the values

$$\left.\begin{aligned}
\xi_s &= 2\varkappa(1-2j_z\cos i)\Big(-\int_0^{2s\pi}\frac{\rho\,dt}{G}+\int_0^{2s\pi}\frac{\rho\cos t}{G}\,dt\Big)+2\int_0^{2s\pi}ae_\varphi dt- \\
&\qquad -2\int_0^{2s\pi}ae_\varphi\cos t\,dt-\int_0^{2s\pi}ae_r\sin t\,dt, \\
\dot{\xi}_s &= 2\varkappa(1-2j_z\cos i)\int_0^{2s\pi}\frac{\rho\sin t}{G}\,dt-2\int_0^{2s\pi}ae_\varphi\sin t\,dt+ \\
&\qquad +\int_0^{2s\pi}ae_r\cos t\,dt, \\
\dot{\eta}_s &= \varkappa(1-2j_z\cos i)\Big(3\int_0^{2s\pi}\frac{\rho\,dt}{G}-4\int_0^{2s\pi}\frac{\rho\cos t}{G}\,dt\Big)- \\
&\quad -3\int_0^{2s\pi}ae_\varphi dt+4\int_0^{2s\pi}ae_\varphi dt+4\int_0^{2s\pi}ae_\varphi\cos t\,dt+2\int_0^{2s\pi}ae_r\sin t\,dt
\end{aligned}\right\} \qquad (A.84)$$

(the expressions for the other parameters are written similarly; they are not given here, since we do not require them in what follows).

The terms in the solution $\xi(t)$, $\dot{\xi}(t)$, $\dot{\eta}(t)$ which are proportional to the coefficient β, have an oscillating character and are absent in the averaged solution (A.84). They affect the trajectory over the interval $0 \leqslant t \leqslant 2\pi$. If $\beta \gg \varkappa$, the quantities max ξ, min ξ depend mainly on β during the revolu-
529 tion, i.e., the thickness of the layer within which the trajectory lies in the course of one revolution is determined by the forces produced by the oblateness of the attracting body. It is assumed that the amplitude of the oscillations of the radius during one revolution ($r_{\max} - r_{\min}$) lies within the given thickness of the spherical layer.

2. **Rotating the plane of the circular orbit of a satellite by a lateral thrust.** We derive the differential equations and boundary conditions describing this maneuver, where the initial equations are expressed in osculating variables.

Lateral thrust is a thrust perpendicular to the instantaneous orbital plane (it is sometimes called binormal thrust). In terms of the symbols used in (A.37) it is represented by the projection a_N. If, in (A.37), $a_\Phi = a_R = 0$, then the length of the semimajor axis A, the eccentricity ε, and the time T_π of passage of the perihelion remain fixed during the motion, so that the geometry of the initial orbit is preserved. If the initial orbit is circular, then the dimensionless radius r, the dimensionless semimajor axis A, and the eccentricity ε are

$$r(t) \equiv 1,\ A(t) \equiv 1,\ \varepsilon(t) \equiv \qquad (A.85)$$

Three equations remain to describe the motion, namely

$$\frac{di}{dt} = ae\cos\varphi, \quad \frac{d\Omega}{dt} = ae\frac{\sin\varphi}{\sin i}, \quad \frac{d\varphi}{dt} = 1 - ae\operatorname{ctg} i\sin\varphi. \qquad (A.86)$$

The symbols used in (A.86) have the following meaning: $a_N = ae$, a is the thrust-acceleration magnitude, $e = \pm 1$ is the orientation of the thrust vector relative to the instantaneous orbit ($e = +1$ along the normal, $e = -1$ opposite to the normal); $\varphi = \nu + \varphi_\pi$ is the argument of the latitude, measured from the nodal line in the instantaneous plane.

If the initial orbit lies within the plane of the equator, then

$$i(0) = 0, \tag{A.87}$$

and the longitude of the ascending node ($\Omega(0)$) and the argument of the latitude ($\varphi(0)$) at the initial time instant are not defined separately; their sum, the latitude of the take-off point in the inertial reference frame, is given by the position of this system.

Suppose

$$\varphi(0) + \Omega(0) = 0. \tag{A.88}$$

At the final instant the inclination and longitude of the ascending node are both specified by

$$i(T) = i_1, \ \Omega(T) = \Omega_1. \tag{A.89}$$

630 Let $i_1 \ll 1$; the trigonometric functions of the angle i can then be replaced in equations (A.86), where

$$di/dt = ae\cos\varphi, \ \dot{\Omega} = ae\sin\varphi/i, \ \dot{\varphi} = 1 - ae\sin\varphi/i. \tag{A.90}$$

It follows from (A.88), (A.90) that

$$\varphi = t - \Omega. \tag{A.91}$$

Substituting this last expression in the first two equations of (A.90), we obtain

$$di/dt = ae\cos(t - \Omega), \ \dot{\Omega} = ae\sin(t - \Omega)/i. \tag{A.92}$$

Now introduce new variables defined by

$$\chi = i\sin(\Omega - \Omega_1), \ \omega = i\cos(\Omega - \Omega_1). \tag{A.93}$$

In terms of these variables the equations and boundary conditions, which describe the maneuver of rotating the plane of the circular orbit, are

$$\left.\begin{array}{ll} \dot{\chi} = ae\sin(t - \Omega_1), & \dot{\omega} = ae\cos(t - \Omega_1), \\ \chi(0) = 0, & \omega(0) = 0, \\ \chi(T) = 0, & \omega(T) = i_1. \end{array}\right\} \tag{A.94}$$

NOMENCLATURE

$\mathbf{a}$ thrust acceleration.
$\Delta\mathbf{a}$ correction to thrust-acceleration program.
$\delta\mathbf{a}$ errors in executing thrust-acceleration program.
a magnitude of thrust acceleration.
a_x, a_y, a_z components of thrust-acceleration vector in cartesian system of coordinates (x, y, z).
a_r, a_φ components of thrust–acceleration vector in polar system of coordinates (r, φ).
a_ξ, a_η, a_ζ components of thrust–acceleration vector in (ξ, η, ζ) system of coordinates.
a_0 initial thrust acceleration.
C, c cost and unit cost of executing maneuver (per unit payload G_π).
C_e cost of maneuver without accounting for vehicle's weight.
components.
$C_\varkappa, c_\varkappa$ engine cost and unit cost (per unit engine weight $G_\varkappa$).
C_μ, c_μ cost and unit cost of working–fluid reserve (per unit take–off weight of working fluid $G_{\mu 0}$).
c_F friction coefficient per unit wetted surface.
c_x aerodynamic drag coefficient.
c_{xp} wave drag coefficient.
c^*_{xp} wave drag coefficient for cone.
$c_{x\tau}$ friction coefficient.
c_* molar specific heat.
D diameter.
D° intensity of meteoric stream.
d distance between source and accelerating electrode in ion–propulsion engine.
E energy.
$\mathscr{E}$ total energy of motion in gravitational field.
$\mathbf{e}$ unit vector in thrust direction.
e electric charge of particle.
e_x, e_y components of unit vector in thrust direction for plane cartesian system of coordinates $(e_x^2 + e_y^2 = 1)$.
e_r, e_φ, e_θ components of unit vector in thrust direction for spherical system of coordinates $(e_r^2 + e_\varphi^2 + e_\theta^2 = 1)$.
$\mathbf{F}$ external forces acting on vehicle.
$F_{x, y, z}$ components of external forces acting on vehicle.

$\mathcal{F}$ cross-sectional area.

f universal gravitational constant.

G instantaneous vehicle weight.

G_e weight of energy accumulator.

G_i^-, G_i^+ vehicle weight before and after discarding i-th engine section.

G_n weight of energy generator.

G_p weight of propulsion system.

G_q weight of working-fluid feed system.

G_v weight of working-fluid storage system with inlet duct.

G_β weight of working-fluid tanks.

G_γ weight of nozzle.

G_ζ weight of power-removal system.

G_θ total weight of payload, working fluid, and tanks. ($G_\theta = G_\pi + G_\mu(t) + G_\beta$).

$G_\varkappa$ engine weight.

$G_\varkappa^{(i)}$ engine weight during i-th flight stage $t_{i-1} < t < t_i$.

$\Delta G_\varkappa$ weight of engine section.

G_λ total weight of s differently-tuned unthrottled engines.

$G_\lambda^{(i)}$ weight increment of unthrottled engine produced by adding i-th stage of thrust and consumption.

G_μ instantaneous weight of working-fluid reserve.

$G_{\mu 0}$ take-off weight of working fluid.

$\Delta G_\mu^{(i)}$ weight of working fluid remaining at instant of discarding i-th section of engine.

$\Delta G_\mu(t)$ weight of working fluid discharged up to time t ($\Delta G_\mu(t) = G_{\mu 0} - G_\mu(t)$).

G_ν weight of power source.

G_π payload.

$G_\pi^{(i)}$ payload at i-th stage (sum of true payload G_π and weight of working fluid $\Delta G_\mu^{(i)}$ remaining at instant of discarding i-th section of engine).

G_Σ total load delivered at end of trajectory after n maneuvers.

G_σ total weight of payload and working fluid.

G_τ weight of energy converter.

G_ψ total weight of payload, working-fluid reserve, and power source ($G_\psi = G_\pi + G_\mu(t) + G_\nu$).

G_0 vehicle take-off weight.

G_1 vehicle terminal weight.

g coefficient of proportionality between weight and mass (gravitational acceleration on Earth surface).

g_0 gravitational acceleration at radius r_0.

H Hamiltonian in Pontryagins's maximum-principle procedure.

h height.

I functional of dynamic part of problem for ideal engine with limited exhaust velocity (time integral of thrust acceleration, characteristic velocity).

I° specific impulse.

$\mathbf{i}$ unit vector in direction of solar light radiation.

i electric-current density; angle between initial and terminal positions of orbital plane.

$\mathcal{J}$ current intensity.

J functional of dynamic part of problem for ideal power-limited engine (time integral of square of thrust acceleration)

ΔJ increment of functional J, characterizing cost of trajectory correction.

J_σ total functional of dynamic problem for interplanetary round-trip flight ($J_\sigma = J_1 + J_2 + J_{+1} + J_{-1} + J_{+2} + J_{-2}$).

J_1, J_2 values of functional of dynamic problem for outbound (1) and return (2) flights between orbits of planets.

J_{+1}, J_{-1}, J_{+2}, J_{-2} values of dynamic-problem functional for maneuvers of acceleration (+) and deceleration (−) at take-off (1) and destination (2) planets.

$K(\ldots)$ correlation function.

$K + L$ functional of maneuver for combined engine: ideal engine with limited exhaust velocity + ideal power-limited engine.

k gravitational constant for central field (universal gravitational constant multiplied by body mass).

L length.

$\mathcal{L}$ inductance.

l distance between points of rest in gravity-free field.

M angular momentum.

$M(\ldots)$ mathematical expectation (also represented by $\langle \ldots \rangle$).

M_0 Mach number corresponding to flight velocity.

m mass.

N jet power.

$N_{\max}$ maximum jet power.

N_e power consumed by energy accumulator.

N_i power corresponding to losses in ion-propulsion engine.

N_n total power released by energy generator.

N_q power of working-fluid feed system.

N_{qv} power transmitted to vehicle by working fluid taken in by accumulator.

N_v power consumed by working-fluid accumulator.

N_γ power consumed by engine.

N_ζ power released by energy-removal system.

N_λ total jet power

N_ν net power of energy generator.

N_τ net power of energy converter.

$\mathbf{n}$ unit vector in direction of normal to surface.

$\mathbf{P}$ thrust vector.

P thrust magnitude.

$P(\ldots)$ probability of event $(\ldots)$.

p parameter of conic section.

p_i auxiliary function (momentum) in Pontryagin's maximum-principle procedure, corresponding to phase coordinate x_i.

Q heat flux.

q mass flow rate of working fluid through nozzle.

q_v rate of flow into accumulator (rate of mass influx through inlet duct).

q_β mass flow rate from tanks.

q_γ mass flow rate from engine.

q_ε mass consumption during energy production.

$q_\times$ mass consumption of engine.

q_ν mass consumption of power source.

q_σ total mass consumption of vehicle.

R distance to Sun; reliability (probability of successfully executing the maneuver).

$\mathbf{R}_i$ vector distance to gravitational center.

R_i distance to gravitational center.

R_s radius of celesital body.

R_δ average radius of Earth orbit.

Re Reynolds number.

$\mathcal{R}$ gas constant.

$\mathbf{r}$ radius vector of vehicle center of mass.

r radius in polar system of coordinates.

$\Delta\mathbf{r}$ measured deviations of trajectory from calculated trajectory.

$\delta_a\mathbf{r}$ deviations from calculated trajectory caused by errors δa.

$\delta_n\mathbf{r}$ errors in measurement of trajectory.

r_λ intensity of solar light radiation on Earth orbit.

S cross-sectional surface area.

S_ζ radiator surface area.

s number of revolutions in orbit.

$s_\times$, s_μ dimensionless cost coefficients of engine and working-fluid reserve.

T total time of executing space maneuver.

T_μ total engine operating time.

$T_{\mu 1}, \ldots, T_{\mu s}$ total firing intervals of stages $\pi_1, \ldots, \pi_s$ of step control.

$T_{\mu\sigma}$ total engine operating time in round-trip interplanetary flight ($T_{\mu\sigma} = T_{\mu 1} + T_{\mu 2} + T_{\mu,+1} + T_{\mu,-1} + T_{\mu,+2} + T_{\mu,-2}$).

$T_{\mu 1}$, $T_{\mu 2}$ engine operating times for outbound and return segments of round-trip flight.

$T_{\mu,+1}$, $T_{\mu,-1}$, $T_{\mu,+2}$, $T_{\mu,-2}$ engine operating times during acceleration (+) and deceleration (—) segments at take-off (1) and destination (2) planets.

T_σ total duration of round-trip interplanetary flight ($T_\sigma = T_\omega + T_1 + T_2 + T_{+1} + T_{-1}$).

T_ω time of sojourn in neighborhood of destination planet.

T_1, T_2 outbound (1) and return (2) transfer times between orbits of planets.

T_{+1}, T_{-1}, T_{+2}, T_{-2} acceleration (+) and deceleration (–) times at take-off (1) and destination (2) planets.

t time.

t_μ instantaneous engine operating time.

$t_{\mu 1}, \ldots, t_{\mu s}$ instantaneous times of firing levels $\pi_1, \ldots, \pi_s$ of stepped control.

t_0 take-off date, reckoned from opposition of take-off and destination planets.

U potential of gravitational field.

$\mathcal{U}$ voltage.

u, v, w components of velocity vector $\mathbf{v}$ in rectangular systems of coordinates (x, y, z) and (ξ, η, ζ).

u_1 increment of velocity magnitude in gravity-free field.

V jet exhaust velocity.

$\mathbf{v}$ velocity vector of vehicle center of mass.

v_r, v_φ velocity vector components in polar system of coordinates (r, φ).

X, Y, Z components of gravitational acceleration vector in cartesian coordinates (x, y, z).

x, y, z cartesian coordinates.

α unit weight of power source.

α^* ratio of fuel mixture composition.

β unit weight of energy accumulators.

β_μ unit weight of working-fluid containers (tanks).

γ unit weight of nozzle.

γ_f unit weight of electrostatic engine (per unit area of ionic beam).

γ_v unit weight of working-fluid accumulation system (per unit rate of mass influx).

$\gamma_\varkappa$ unit weight of engine.

γ_Σ unit weight of propulsion system.

δ engine delta functions; symbol representing the first variation; wall thickness.

$\delta_1, \ldots, \delta_{s-1}$ Dirac functions corresponding to firing and cutoff of the corresponding stage $\pi_1, \ldots, \pi_{s-1}$ of step control.

E electric field strength.

ε ratio of unit weights of engine and energy generator; eccentricity; reflection coefficient.

ε_* coefficient of light radiation reflected by body.

H magnetic field strength.

η propulsion efficiency.

η_c efficiency of power source operating according to Carnot cycle.

η_γ over-all efficiency of engine $(\eta_\gamma = \eta_\mu \eta_\nu)$.

η_γ^* energy efficiency of ion-propulsion-engine.

η_θ energy efficiency.

η_μ coefficient of utilization of working fluid in engine.

η_ν coefficient of utilization of power in engine.

η_τ efficiency of energy converter.

ϑ orientation of solar sail; true anomaly.

$\varkappa$ coefficient of converting material of discarded engine sections into working fluid; ratio of allowable number of failures to their maximum-possible number Λ_{max}; specific heat ratio.

Λ_{max} maximum possible number of failures.

Λ_1 allowable number of failures.

λ relative velocity of gas stream.

λ_A wavelength of light radiation.

λ_τ decay constant of radioisotopes.

λ_* heat conductivity.

μ mass of elementary particle.

ν kinematic viscosity.

ξ ratio of energy-accumulator weight to energy-generator weight; ratio of unit cost of working-fluid reserve and engine.

$\left.\begin{matrix}\xi\\ \eta\\ \zeta\end{matrix}\right\}$ coordinates in transported system.

$\left.\begin{matrix}\pi_1\\ \ldots\\ \pi_s\end{matrix}\right\}$ levels of step control.

ϱ radius vector in transported system of coordinates.

ρ atmospheric density.

$\rho_\Im$ density of photon distribution in outer space.

σ Stephan — Boltzmann constant.

σ_* electric conductivity.

T temperature.

T_n temperature of heater.

T_s surface temperature of celestial body.

T_v air temperature at inlet to compression unit.

T_τ effective temperature.

T_0 stagnation temperature of gas stream.

T_* radiator temperature.

$T_\odot$ surface temperature of Sun.

τ dimensionless time (as fraction of period of revolution along initial orbit, divided by 2π: $\tau = k^{1/2} r_0^{-3/2}$ (in Chapter Five), or by total time).

τ° friction stress.

Φ functional of maneuver for ideal power-limited engine ($\Phi = (\alpha/2g)\, J$).

Φ_e functional of maneuver for ideal power-limited engine with energy accumulator.

φ polar angle.

$\left.\begin{matrix}\varphi_1\\ \varphi_2\end{matrix}\right\}$ angular displacements of outbound (1) and return (2) orbital transfers.

Υ total impulse of gas stream.

Ψ functional of maneuver for ideal engine with limited exhaust velocity ($\Psi = I/V_{max}$).

Ω position of the line of nodes.

Ω_0 initial vulnerable (to meteoric punctures) radiator area ($\Omega_0 = kS_0$, $0 < k \leqslant 1$).

ω surface emissivity; longitude of perigee.

ω_s angle at which celestial body is seen.

ω_1, ω_2 average angular velocities of revolution for take-off (1) and destination (2) planets about Sun.

$\omega_\odot$ angle at which Sun is seen.

a velocity of sound.

a_* critical sound velocity.

b unit potential energy.

$\mathfrak{J}$ intensity of corpuscular radiation of Sun.

$\mathfrak{M}_i$ mass of gravitational center.

m mass of meteoric particle.

$\mathfrak{N}_A$ unit power of solar light radiation.

$\mathfrak{N}_k$ unit power of cosmic heat radiation.

$\mathfrak{N}_\mathfrak{J}$ unit power of corpuscular flux from Sun.

$\mathfrak{P}$ probability of wall puncture by meteoric particles.

p pressure.

p_A light pressure.

$p_{A\odot}$ maximum pressure of solar light in Earth orbit.

p_E electrostatic pressure.

p_H magnetic pressure.

p_h atmospheric pressure.

$p_\mathfrak{J}$ pressure of corpuscular flux from Sun.

p_0 total pressure in gas stream.

$\mathfrak{R}$ acceleration vector produced by gravitational forces.

v volume.

w velocity of solar wind.

BIBLIOGRAPHY

Introduction and Chapter One

1.1. Meshcherskii, I.V. Raboty po mekhanike tel peremennoi massy (The Mechanics of Bodies of Varying Mass).— Moskva, Gostekhizdat. 1949.

1.2. Tsiolkovskii, K.E. Issledovanie mirovykh prostranstv reaktivnymi priborami (Study of Outer Space by Jet-Propelled Vehicles).— Nauchnoe Obozrenie, No. 5, Moskva. 1903.

1.3. Tsiolkovskii, K.E. Sobranie sochinenii (Collected Works).— Moskva, Izdatel'stvo AN SSSR. 1954.

1.4. Goddard, R.H. A Method of Reaching Extreme Altitudes.— Smithsonian Inst., Washington. 1919.

1.5. Tsander, F.A. Problema poleta pri pomoshchi reaktivnykh apparatov. Mezhplanetnye puteshestviya (The Problem of Flight With Rocket-Propelled Vehicles. Interplanetary Flights).— Moskva, Oborongiz. 1961.

1.6. Oberth, H. Die Rakete zu den Planetenraumen.— R. Oldenbourg, München. 1923.

1.7. Hohmann, W. Die Erreichbarkeit der Himmelskörper.— R. Oldenbourg, München. 1925.

1.8. Esnault-Pelterie, R. L'Astronautique. Paris. 1930.

1.9. Korolev, S.P. Raketnyi polet v stratosfere (Rocket Flight in the Stratosphere).— Moskva, Voenizdat. 1934.

1.10. Kosmodem'yanskii, A.A. Ekstremal'nye zadachi dlya tochki peremennoi massy (Extremum Problems for a Varying Point Mass).— Doklady AN SSSR, Vol. 53, No. 1. 1946.

1.11. Okhotsimskii, D.E. K teorii dvizheniya raket (The Theory of Motion of Rockets).— Prikladnaya Matematika i Mekhanika, Vol. 10, No. 2. 1946.

1.12. Ishlinskii, A.Yu. Dva zamechaniya k teorii dvizheniya raket (Two Notes on the Theory of Rocket Motions).— Doklady AN SSSR, Vol. 53, No. 7. 1946.

1.13. Kosmodem'yanskii, A.A. Kurs teoreticheskoi mekhaniki (A Course in Theoretical Mechanics).— Moskva, Uchpedgiz. 1955.

1.14. Kosmodem'yanskii, A.A. Osnovnye teoremy mekhaniki tela peremennoi massy. Lektsii po mekhanike tel peremennoi massy (Basic Theorems on the Mechanics of a Body of Varying Mass. Lectures on the Mechanics of Bodies of Varying Mass).— Uchenye Zapiski MGU, Mekhanika, Nos. 152, 154. 1951.

1.15. Tsien, H. and R. Evans. Optimum Thrust Programming for a Sounding Rocket.— J. Amer. Rock. Soc., Vol. 21, No. 5. 1951.
1.16. Lawden, D.F. Minimal Rocket Trajectories.— J. Amer. Rock. Soc., Vol. 23, Nos. 11—12. 1953.
1.17. Krotov, V.F. Raschet optimal'noi traektorii dlya perekhoda rakety na zadannuyu krugovuyu traektoriyu okolo Zemli (Calculation of the Optimum Transfer Trajectory of a Rocket to a Specified Circular Trajectory about the Earth).— In: Sbornik "Mekhanika" MVTU, Moskva, Oborongiz. 1955.
1.18. Okhotsimskii, D.E. and T.M. Eneev. Nekotorye variatsionnye zadachi, svyazannye s zapuskom iskusstvennogo sputnika Zemli (Some Variational Problems of Launching an Artificial Earth Satellite).— UFN, Vol. 63, No. 1a. 1957.
1.19. Egorov, V.A. Nekotorye problemy dinamiki poleta k Lune (Some Problems of the Dynamics of Flight to the Moon).— Doklady AN SSSR, Vol. 113, No. 1. 1957.
1.20. Egorov, V.A. Nekotorye zadachi dinamiki poleta k Lune (Some Problems of the Dynamics of Flight to the Moon).— UFN, Vol. 63, No. 1a. 1957.
1.21. Barrère, M., A. Jaumotte, B.F. Veubeke, and J. Vandenkerckove. La propulsion par fusées, Paris. 1957.
1.22. Miele, A. An Extension of the Theory of the Optimum Burning Program for the Level Flight of a Rocket-Powered Aircraft.— J. Aeronaut. Sci., Vol. 24, No. 12. 1957.
1.23. Veubeke, B.F. Le problème du maximum de rayon d'action dans un champ de gravitation uniforme.— Astronaut. Acta, Vol. 4, No. 1. 1958.
1.24. Egorov, V.A. O reshenii odnoi vyrozhdennoi variatsionnoi zadachi i optimal'nom pod"eme kosmicheskoi rakety (The Solution of a Degenerate Variational Problem of the Optimum Lift of a Space Rocket).— Prikladnaya Matematika i Mekhanika, Vol. 22, No. 1. 1958.
1.25. Sadovskii, I.N., editor. Issledovanie optimal'nykh rezhimov dvizheniya raket (The Optimum Regimes of Rocket Motions), Collection of translations.— Moskva, Oborongiz. 1959.
1.26. Miele, A. General Variational Theory of the Flight Paths of Rocket-Powered Aircraft, Missiles and Satellite Carriers.— Astranaut. Acta, Vol. 4, No. 4. 1958.
1.27. Breakwell, J.V. The Optimization of Trajectories.— J. Soc. Industrial and Appl. Math., Vol. 7, No. 2. 1959.
1.28. Gantmakher, F.R. and L.M. Levin. The Flight of Uncontrolled Rockets.— Pergamon Press. 1964.
1.29. Herrick, S. Astrodynamics.— Princeton, N.J., Elsevier Publ. Co. 1959.
1.30. Lawden, D.F. Interplanetary Rocket Trajectories.— Advances in Space Sci., Academic Press. N.Y. —London. 1959.
1.31. Lur'e, A.I. Uravneniya vozmushchennogo dvizheniya v zadache Keplera (Equations of Perturbed Motion in a Keplerian Problem).— Prikladnaya Matematika i Mekhanika, Vol. 23, No. 3. 1959, cf. also Iskusstvennye sputniki Zemli, No. 4. 1960.

1.32. Gorelov, Yu.A. O dvukh klassakh ploskikh ekstremal'nykh dvizhenii rakety v pustote (On Two Classes of Plane Extremum Rocket Motions in Vacuum).— Prikladnaya Matematika i Mekhanika, Vol. 24, No. 2. 1960.

1.33. Isaev, V.K. Printsip maksimuma L. S. Pontryagina i optimal'noe programmirovanie tyagi raket (Pontryagin's Maximum Principle and Optimum Programing of the Rocket Thrust).— Avtomatika i Telemekhanika, Vol. 22, No. 8. 1961; Vol. 23, No. 1. 1962.

1.34. Leitmann, G. The Optimization of Rocket Trajectories — a survey.— Progr. in Astronaut. Sci., Vol. 1, Amsterdam. 1962.

1.35. Illarionov, V.F. and L.M. Shkadov. Povorot ploskosti krugovoi orbity sputnika (Rotating the Plane of the Circular Orbit of a Satellite).— Prikladnaya Matematika i Mekhanika, Vol. 26, No. 1. 1962.

1.36. Lur'e, A.I. Ob odnoi forme uravnenii dvizheniya material'noi tochki. Primenenie k zadache o povorote ploskosti orbity iskusstvennogo sputnika Zemli (One Form of the Equations of Motion of a Point Mass. Application to the Problem of Rotating the Plane of the Orbit of an Artificial Earth Satellite).— Trudy Mezhvuz konferentsii po prikladnoi teorii ustoichivosti dvizheniya, Kazan. 1962.

1.37. Leitmann, G., editor. Optimization Techniques.—N. Y., Acad. Press. 1962.

1.38. Ehricke, K.A. Spaceflight.— N. Y., Princeton, Van Nostrand, Vol. 1. 1960; Vol. 2. 1962.

1.39. Lawden, D.F. Optimal Trajectories for Space Navigation.— London, Butterworths. 1963.

1.40. Kuzmak, G.E., V.K. Isaev, and B. Kh. Davidson. Optimalnye rezhimy dvizheniya tochki peremennoi massy v odnorodnom tsentral'nom pole (Optimum Regimes of Motion of a Varying Point Mass in a Homogeneous Central Field).— Doklady AN SSSR, Vol. 149, No. 1. 1963.

1.41. Il'in, V.A. Optimal'nyi perekhod kosmicheskogo apparata, tormozyashchegosya v atmosfere planety, na orbitu iskusstvennogo sputnika Zemli (Optimum Transfer of a Spacecraft Decelerated in the Atmosphere of a Planet, to the Orbit of an Artificial Earth Satellite).— Inzhenernyi Zhurnal, Vol. 3, No. 2. 1963.

1.42. Tarasov, E.V. Optimal'nye rezhimy poleta letatel'nykh apparatov (Optimum Flight Regimes of Flying Vehicles).— Moskva, Oborongiz. 1963.

1.43. Breakwell, J.V. The Optimum Spacing of Corrective Thrusts in Interplanetary Navigation.— Math. Optimiz. Techn., California Press. 1963.

1.44. Miele, A. Flight Mechanics, Vol. 1. Massachusetts-London. 1963.

1.45. Il'in, V.A. K raschetu traektorii pereleta kosmicheskikh apparatov mezhdu komplanarnymi krugovymi orbitami v n'yutonianskom gravitatsionnom pole (Calculating Transfer Trajectories of Space Vehicles Between Coplanar Circular Orbits in a Newtonian Gravitational Field).— Kosmicheskie Issledovaniya, Vol. 2, No. 5. 1964.

1.46. Kuzmak, G.E. and Yu.M. Kopnin. Novaya forma uravneniya dvizheniya sputnika i prilozhenie ee k issledovaniyu dvizhenii, blizkikh k keplerovym (A New Form of the Equations of Motion of a Satellite, and Its Application to Near-Keplerian Motions).— Zhurnal Vychislitel'noi Matematiki i Matematicheskaya Fizika, Vol. 3, No. 4. 1963.

1.47. Isaev, V.K., A.I. Kur'yanov, and V.V. Sonin. Primenenie printsipa maksimuma v raketodinamiki (Application of the Maximum Principle in Rocket Dynamics).— Proc. 14 Internat. Astronaut. Congr. 1963, Warsaw. 1964.

1.48. Alekseev, K.B. and G.G. Bebenin. Upravlenie Kosmicheskim letatel'nym apparatom (Spacecraft Guidance).— Mashinostroenie, Moskva, 1964.

1.49. Korenev, G.V. Vvedenie v mekhaniku upravlyaemogo tela (Introduction to the Mechanics of a Guided Body).— Nauka, Moskva. 1964.

1.50. Andreescu, D. St. and M.M. Nita. Zborul rachetei.— Editura Militara, Bucuresti. 1964.

1.51. Lidov, M.L., D.E. Okhotsimskii, and N.M. Teslenko. Issledovanie odnogo klassa traektorii ogranichennoi zadachi trekh tel (A Class of Trajectories of the Limited Three-Body Problem).— Kosmicheskie Issledovaniya, Vol. 2, No. 6. 1964.

1.52. Ross, S. Optimal Ascent into Orbit — A New Look at an Old Problem.— Proc. 15 Internat. Astronaut. Congr., 1964, Warsaw. 1965.

1.53. Ostoslavskii, I.V. editor. Issledovaniya po dinamike poleta (Flight Mechanics).— In: Sbornik "Mashinostroenie," Moskva. 1965.

1.54. Ponomarev, V.M. Teoriya upravleniya dvizheniem kosmicheskikh apparatov (Theory of Spacecraft Guidance).— Nauka, Moskva. 1965.

1.55. Veubeke, B.F. and J. Geerts. Application du principe de maximum à la syntèse des transferts optimaux dans un champ de gravitation planétaire.—Proc. XV Internat. Astronaut. Congr., 1964, Warsaw. 1965.

1.56. Kuzmak, G.E. Linearizirovannaya teoriya optimalnykh pereletov (Linearized Theory of Optimum Transfers).— Kosmicheskie Issledovaniya, Vol. 3, No. 1. 1965.

1.57. Egorov, V.A. Prostranstvennaya zadacha dostizheniya Luny (The Three-dimensional Problem of Reaching the Moon).— Nauka, Moskva. 1965.

1.58. Chebotarev, G.A. Analiticheskie i chislennye metody nebesnoi mekhaniki (Analytical and Numerical Methods of Celestial Mechanics).— Nauka, Moskva-Leningrad. 1965.

1.59. Appazov, R.F., S.S. Lavrov, and V.P. Mishin. Ballistika upravlyaemykh raket dal'nego deistviya (Ballistics of Long-Range Guided Rockets).— Nauka, Moskva. 1966.

1.60. Grodzovskii, G.L., Yu.N. Ivanov, and V.V. Tokarev. Mekhanika kosmicheskogo poleta s maloi tyagoi (Mechanics of Low-Thrust Spaceflight).— Inzhenernyi Zhurnal AN SSSR, Vol. 3, Nos. 3 and 4, 1963; Vol. 43, Nos. 1 and 2. 1964. Cf. also Trudy 2 Vsesoyuznogo s"ezda po teoreticheskoi i prikladnoi mekhanike, No. 1, Nauka, Moskva. 1965; and Proc. 15 Internat. Astronaut. Congr., 1964, Warsaw. 1965.

1.61. Stechkin, B.S., P.K. Kazandzhan, A.P. Alekseev, A.N. Govorov, N.E. Konovalov, Yu.N. Nechaev, and R.M. Fedorov. Teoriya reaktivnykh dvigatelei (Theory of Rocket Engines).— Moskva, Oborongiz. 1958.

1.62. Corliss, W.R. Propulsion Systems for Spaceflight.— McGraw-Hill. 1960.
1.63. Au, G.F. Entwicklungsstand zukünftiger Raumfahrtantriebe.— Luftfahrtechnik, Vol.7, No.1. 1961.
1.64. Sutton, G. Rocket Propulsion Elements.— New York-London, Wiley. 1949.
1.65. Bussard, R.W. and R.D. DeLaver. Nuclear Rocket Propulsion.— McGraw-Hill. 1958.
1.66. Kvasnikov, A.V. Teoriya zhidkostnykh raketnykh dvigatelei (Theory of Liquid Rocket Engines).— Leningrad, Sudpromgiz. 1959.
1.67. Snyder, N.W. editor. Space Power Systems.—New York-London, Acad. Press 1961.
1.68. Beletskii, V.V. Dvizhenie iskusstvennogo sputnika otnositel'no tsentra mass (Motion of an Artificial Satellite About the Center of Mass).— Nauka, Moskva. 1965.
1.69. Duboshin, G.N. Teoriya prityazheniya (Theory of Attraction).— Moskva, Fizmatgiz. 1961.
1.70. Allen, C.W. Astrophysical Quantities.— London, Athlone Press. 1963.
1.71. Duboshin, G.N. Nebesnaya mekhanika (Celestial Mechanics).— Moskva, Fizmatgiz. 1963.
1.72. Subbotin, M.F. Kurs nebesnoi mekhaniki (A Course in Celestial Mechanics).— Vol.1, Gostekhizdat. 1963; ONTI, Vol.2, and 3. 1949.
1.73. Cameron, A.G.W., editor. Physics of the Planets.— Space Physics, New York-London. 1964.
1.74. Reiffel, L. Structural Damage and Other Effects of Solar Plasmas.— J. Amer. Rock. Soc., Vol.30, No.3. 1960.
1.75. Landsberg, G.S.. Optika (Optics).— Moskva-Leningrad, Gostekhizdat. 1947.
1.76. Aleksandrov, S.G. and R.E. Fedorov. Sovetskie sputniki i kosmicheskie korabli (Soviet Satellites and Spaceships). 2nd edition.— Moskva, Izdatel'stvo AN SSSR. 1961.
1.77. Whipple, F.L. The Meteoritic Risk to Space Vehicles.— Vistas in Astronautics, Vol.2, New York. 1958.
1.78. Gehring, J.W., D.R. Cristman, and A.R. McMillan. Experimental Studies Concerning the Meteoroid Hazard to Aerospace Materials and Structures.— J. Spacecraft and Rock., Vol.2, No.5. 1965.
1.79. Bjork, R.L. Meteoroids vs Space Vehicles.— J. Amer. Rock. Soc., Vol.31, No.6. 1961.
1.80. Stanyukovich, K.P. and V.V. Fedynskii. O razrushitel'nom deistvii meteoritnykh udarov (The Destructive Effects of Meteoric Impacts).— Doklady AN SSSR, Vol.57, No.2. 1947.
1.81. Bjork, R.L. Effects of a Meteoroid Impact on Steel and Aluminum in Space.— Proc.10 Internat. Astronaut Congr., 1959; Vien. 1960.
1.82. Lavrent'ev, M.A. Problema probivaniya pri kosmicheskikh skorostyakh (The Problem of Punctures at Cosmic Velocities).— Iskusstvennye Sputniki Zemli, No.3. 1959.

1.83. Kornhauser, M. Satellite Pressure Losses Caused by Meteoroid Impacts.— J. Amer. Rock. Soc., Vol. 30, No. 5. 1960.
1.84. Zel'dovich, Ya. B. and Yu. P. Raizer. Fizika udarnykh voln i vysokotemperaturnykh gidrodinamicheskikh yavlenii (Physics of Shock Waves and High-Temperature Hydrodynamic Phenomena).— Moskva, Fizmatgiz. 1963.
1.85. Andriankin, E. I. O probivanii pregrad meteoritami (The Puncturing of Barriers by Meteorites).— Kosmicheskie Issledovaniya, Vol. 4, No. 2. 1966.
1.86. Mukhamedzhanov, A. K. O proboe tonkogo ekrana meteoritom (On the Puncture of a Thin Screen by a Meteorite).— Kosmicheskie Issledovaniya, Vol. 4, No. 2. 1966.

Chapter Two

2.1. Prandtl, L. Führer durch die Stromungslehre. Göttingen. 1944.
2.2. Stechkin, B. S., P. K. Kazandzhan, A. P. Alekseev, A. N. Govorov, N. E. Konovalov, Yu. N. Nechaev, and R. M. Fedorov. Teoriya reaktivnykh dvigatelei (Theory of Rocket Engines).— Moskva, Oborongiz. 1958.
2.3. Zel'dovich, Ya. B. Teoriya udarnykh voln i vvedenie v gazodinamiku (Theory of Shock Waves and Introduction to Gas Dynamics).— Moskva, Izdatel'stvo AN SSSR. 1946.
2.4. Khristianovich, S. A., V. G. Gal'perin, M. D. Millionshchikov, and L. A. Simonov. Prikladnaya gazovaya dinamika (Applied Gas Dynamics).— TsAGI. 1948.
2.5. Sedov, L. I. Ploskie zadachi gidrodinamiki (Two-Dimensional Problems of Hydrodynamics and Aerodynamics).— Moskva, Gostekhizdat. 1950.
2.6. Abramovich, G. N. Prikladnaya gazovaya dinamika (Applied Gas Dynamics).— Moskva, Gostekhizdat. 1951.
2.7. Bolgarskii, A. V. and V. K. Shchukin. Rabochie protsessy v zhidkostnoreaktivnykh dvigatelyakh (Work Processes in Liquid Propellant Engines).— Moskva, Oborongiz. 1953.
2.8. Mel'kumov, T. M., E. V. Kuznetsov, and N. I. Melik-Pashaev. Teoriya zhidkostnykh reaktivnykh dvigatelei (Theory of Liquid Propellant Engines).— Moskva, Izd. VVIA im. N. E. Zhukovskogo. 1956.
2.9. Barrère, M., A. Jaumotte, B. F. Veubeke, and J. Vandenkerckove. La propulsion par fusées. Paris. 1957.
2.10. Kvasnikov, A. V. Teoriya zhidkostnykh raketnykh dvigatelei (Theory of Liquid Rocket Engines).— Moskva, Sudpromgiz. 1959.
2.11. Alemasov, V. E. Teoriya raketnykh dvigatelei (Theory of Rocket Engines).— Moskva, Oborongiz. 1962.
2.12. Landau, L. D. and E. M. Lifshits. Mekhanika sploshnykh sred (Mechanics of Continuous Media).— Moskva, Fizmatgiz. 1962.

2.13. Guderley, G. and E. Hantsch. Baste formen für achsensymmetrische überschallschubdüsen.— Zeitschrift für Flugwissenschaften, Braunschweig, No. 9. 1955.

2.14. Dorodnitsyn, A.A. Raschet raspredeleniya davlenii po telam vrashchenii v sverkhzvukovom potoke gaza (Calculating the Pressure Distributions Over Bodies of Revolution in a Supersonic Gas Stream).— In: Sbornik teoretecheskikh rabot po aerodinamike, Moskva, Oborongiz. 1957.

2.15. Shmyglevskii, Yu.D. Nekotorye variatsionnye zadachi gazovoi dinamiki osesimmetrichnykh sverkhzvukovykh techenii (Some Variational Problems of the Gas Dynamics of Axially-Symmetric Supersonic Flows).— Prikladnaya Matematika i Mekhanika, Vol. 21, No. 2. 1957.

2.16. Rao, G.V. Exhaust Nozzle Control for Optimum Thrust.— Jet. Prop., Vol. 28, No. 6. 1958.

2.17. Sternin, L.E. K raschetu osesimmetrichnogo reaktivnogo sopla naimen'shego vesa (Calculating the Minimum-Weight Axially-Symmetric Jet Nozzle).— Izvestiya AN SSSR, Mekhanika i Mashinostroenie, No. 1. 1959.

2.18. Guderley, G. On Rao's Method for the Computation of Exhaust Nozzles.— Zeitschrift für Flugwissenschaften, Vol. 12, No. 7. 1959.

2.19. Shmyglevskii, Yu.D. Variatsionnye zadachi sverkhzvukovykh tel vrashcheniya i sopel (Variational Problems for Supersonic Bodies of Revolution and Nozzles).— V.Ts AN SSSR, Moskva. 1961.

2.20. Grodzovskii, G.L., Yu.E. Kuznetsov, and M.V. Tokarev. Priblizhennyi metod rascheta osesimmetrichnykh sverkhzvukovykh techenii v usloviyakh vnutrennei zadachi (An Approximate Method of Calculating Axially-Symmetric Supersonic Flows under the Conditions of the Internal Problem).— Promyshlennaya Aerodinamika, No. 24, Moskva, Oborongiz. 1962.

2.21. Sergienko, A.A. and I.D. Sandomirskaya. O profilirovanii sverkhzvukovoi chasti osesimmetrichnogo sopla naibol'shei tyagi (Shaping the Supersonic Part of a Maximum-Thrust Axially-Symmetric Nozzle).— In: Sbornik rabot Vychislitel'nogo tsentra Moskovskogo Universiteta, No. 4. 1955.

2.22. Grodzovskii, G.L. Osobennosti odnostoronnikh opticheskikh ustanovok dlya issledovaniya gazovogo potoka i deformatsii ploskikh poverkhnostei (Special Features of Unidirection Optical Installations for Studying a Gas Stream and the Deformations of Plane Surfaces).— Izvestiya AN SSSR, OTN, No. 7. 1955.

2.23. Grodzovskii, G.L. Eksperimental'noe issledovanie vzaimodeistviya skachkov uplotneniya i pogranichnogo sloya v diapazone chisel $1.0 \leq M \leq 1.8$ (Experimental Study of the Interaction of Compression Shocks and the Boundary Layer for $1.0 \leq M \leq 1.8$).— Izvestiya AN SSSR, OTN. Energetika i Avtomatika, No. 4. 1960.

2.24. Petrov, G.I. Soobshchenie o doklade na sessii AN SSSR (A Communication on a Report to a Session of AN SSSR).— Izvestiya AN SSSR, OTN, No. 9. 1958.
2.25. Migdal, D., J.J. Horgan, and A. Chamay. An Experimental evaluation of Plug Cluster Nozzles.— AIAAJ. Vol. 2, No. 7. 1964.
2.26. Bono, P., J.L. Woodworth, and G.A. Ursini. The Reusable Booster for Lunar Logistics and Planetary Exploration.— Proc. 15 Internat. Astronaut. Congr. 1964, Warsaw. 1965.
2.27. Stöckel, K. Chemische Raumfahrttriebwerke.— Jahrb. Wiss. Ges. Luft-und Kaumfahrt. 1962.
2.28. Shepherd, L.R. and A.V. Cleaver. The Atomic Rocket.— J. Brit. Interpl. Soc., Vol. 7, No. 5. 1948; Vol. 8, No. 2. 1949; Realities of Space Travel, London. 1957.
2.29. Bussard, R.W. and R.D. DeLauer. Nuclear Rocket Propulsion.— New York, McGraw-Hill. 1958.
2.30. Seifert, H., editor. Space Technology.— New York, Wiley. 1959.
2.31. Sutton, G.P. Rocket Propulsion Systems for Interplanetary Flight.— JASS, Vol. 26, No. 10. 1959.
2.32. Corliss, W.R. Propulsion Systems for Spaceflight.— McGraw-Hill. 1960.
2.33. Camac, M. Plasma Propulsion Devices.— Advances in Space Science, Vol. 2, N.Y. 1960.
2.34. Stenning, A.H. Rapid Approximate Method for Analyzing Nuclear Rocket Performance.— J. Amer. Rock. Soc., Vol. 30, No. 2. 1960.
2.35. Cohen, A.D. and L.S. Beers. Mars Capabilities for Electrical, Nuclear and Chemical Propulsion Systems.— IAS Paper, No. 120. 1962.
2.36. Willinski, M.J., E.C. Orr, S.L. Ailenberd, A.L. Huebner, A. Kantrowitz, G.S. Janes, M. Camac, E. Kunen, W. McIllroy, et al. Ionic, Plasma, and Arc Propulsion Devices, Collection of Articles. 1958—1959.
2.37. Meghreblian, R.V. Gaseous Propulsion Reactors.— Nucleonics, Vol. 19, No. 4. 1961.
2.38. Au, G.F. Entwicklungsstand zukünftiger Raumfahrtantriebe.— Luftfahrttechnik, Vol. 7, No. 1. 1961.
2.39. Linhardt, H.D. Comparison of Solar-Thermal and Solar-Electric-thermal Propulsion Methods.— IAS Paper, No. 63—20. 1968.
2.40. Wilks, W.E. "Poodle" Interests Saturn Officials.— Missiles and Rockets, Vol. 14, No. 23. 1964; cf. also New York Times, 1 June 1964.
2.41. Beckewith, W.C. and H.L. Johnson. Advanced Space Mission Capabilities of Nuclear Rockets.— J. Spacecraft and Rock., Vol. 1, No. 4. 1964.
2.42. Praining, O. Produktion von hohen Temperaturen (bis zu 55,000°K) in Laboratoriumbedingungen.— Osterreichische Chem Ker — Zeitung, Vol. 55, Nos. 5/6. 1954.

2.43. Dautov, G.Yu., M.F. Zhukov, and B.Ya. Smolyakov. Issledovanie raboty plazmatrona s vozdushnoi stabilizatsiei dugi (Operation of a Plasmatron with Air Stabilization of the Arc).— Prikladnaya Matematika i Tekhnicheskaya Fizika, No. 6. 1961.
2.44. German, V.O. and M.G. Morozov. Plazmatron postoyannogo toka i nekotorye rezul'taty issledovaniya ego raboty (A Direct-Current Plasmatron and Some Results of Studying Its Operation).— Teplofizika Vysokikh Temperatur, Vol.3, No.5, AN SSSR. 1965.
2.45. Kantrowitz, A. Horizons in Plasma Dynamics.— Astronaut. and Aeronaut., Vol.3, No.1. 1965.
2.46. Brogan, T.R. Electric Arcs Gas Heater for Re-Entry Simulation and Space Propulsion.— Presented at the 13th Ann. Meeting, Amer. Rock. Soc., N.Y. 1958.
2.47. Preston-Thomas, H. International Transport Technique.— J. Brit. Interpl. Soc., Vol.11, No.4. 1952.
2.48. Stuhlinger, E. Possibilities of Electrical Space Ship Propulsion.— Proc. 5 Internat. Astronaut. Congr., 1954, Vienna. 1955.
2.49. Stuhlinger, E. Advanced Propulsion Systems for Space Vehicles.— Proc.9. Internat. Astronaut. Congr., 1958, Vienna. 1959.
2.50. Stavisskii, Yu.A., I.I. Bondarenko, V.I. Krotov, S.Ya. Lebedev, V.Ya. Pupko, and E.A. Stumbur. Opyt polucheniya reaktivnoi tyagi v laboratornoi modeli ionnogo dvizhitelya (Creating Jet Thrust in a Laboratory Model of an Ion Thruster).— Zhurnal Tekhnicheskoi Fiziki, Vol.29, No.8. 1959.
2.51. Boden, R.H. Ion Propulsion.— Adv. Prop. Techn. 1960, Oxford. 1961.
2.52. Kaufman, H.R. and P.D. Reader. Experimental Performance of Ion Rockets Employing Electron-Bombardment Ion Sources.— Electrostatic Prop. Conf., Monterey, Calif. 1960.
2.53. Stuhlinger, E. and R.N. Seitz. Electrostatic Propulsion Systems for Space Vehicles.— Advances in Space Science, Vol.2, N.Y. 1960.
2.54. Mickelsen, W.R. Comparative Performance of Electrostatic Rocket Engines.— IAS Paper, No.62—74. 1962.
2.55. Brown, H. and H.E. Nicoll. Electrical Propulsion Capabilities for Lunar Exploration.— AIAAJ. Vol.1, No.2. 1963.
2.56. Kaufman, H.R. The Electron-Bombardment Ion Rocket.— Proc.3rd Sympos. Advanced Propuls. Concepts. Vol.1, N.Y.— London. 1963.
2.57. Winicur, D.H. Electric Propulsion Characteristics of a Pulsed Plasma Rail Accelerator.— AIAAJ., Vol.2, No.9. 1964.
2.58. Kuskevics, G. and B.L. Thompson. Comparison of Commercial, Spherical Powder, and Wire Bundle Tungsten Ionizers.— AIAA J., Vol.2, No.2. 1964.
2.59. Stuhlinger, E. Ion Propulsion.— New York, McGraw-Hill. 1964.
2.60. Davis, J. A Step Towards Nuclear Electric Propulsion.— Astronaut. and Aeronaut., Vol.3, No.1. 1965.

2.61. Mickelsen, W.R. and P.D. Reader. Ion Propulsion Systems for Spacecraft.— J. of Spacecraft and Rock., Vol.2, No.4. 1965.
2.62. Brewer, G.R. Physical Electronic Phenomena in Ion Propulsion Engines.— IEEE Spectrum, Vol.2, No.8. 1965.
2.63. Tamm, I.E. Osnovy teorii elektrichestva (Fundamentals of the Theory of Electricity).— Moskva, Gostekhizdat. 1957.
2.64. Artsimovich, L.A. Upravlyaemye termoyadernye reaktsii (Controlled Thermonuclear Reactions).— Moskva, Fizmatgiz. 1961.
2.65. Artsimovich, L.A., S.Yu. Luk'yanov, I.M. Podgornyi, and S.A. Chuvatin. Elektrodinamicheskoe uskorenie sgustkov plazmy (Electrodynamic Acceleration of Plasma Blobs).— ZhETF, Vol.33, No.7. 1957.
2.66. Podgornyi, I.M., S.A. Chuvatin, G.A. Bykov, and V.D. Pis'mennyi. Issledovanie protsessa elektrodinamicheskogo uskoreniya sgustkov plazmy. II. Fizika plazmy i problema upravlyaemykh termoyadernykh reaktsii (The Process of Electrodynamic Acceleration of Plasma Blobs. II. Plasma Physics and the Problem of Controlled Thermonuclear Reactions). Vol.4, Izd. AN SSSR. 1958.
2.67. Kaptsov, N.A. Elektronika (Electronics).— Moskva, Gostekhizdat. 1956.
2.68. Dobretsov, L.N. Eledktronnaya i Ionnaya Emissiya (Electronic and Ionic Emission).— Moskva, Gostekhizdat. 1950.
2.69. Braun, S. Elementarnye protsessy v plazme gazovogo razryada (Elementary Processes in a Gas Discharge Plasma).— Moskva, Gosatomizdat. 1961.
2.70. Lewis Tests Large Ion Engine.— Aviation Week and Space Technology, Vol.81, No.4. 1964.
2.71. Tsander, F.A. Problema poleta pri pomoshchi reaktivnykh apparatov. Mezhplanetnye puteshestviya (The Problem of Rocket Flight. Interplanetary Trips).— Moskva, Oborongiz. 1961.
2.72. Karymov, A.A. Opredelenie sil i momentov sil svetovogo davleniya, deistvuyushchikh na telo pri dvizhenii v kosmicheskom prostranstve (Determination of the Forces and Moments Acting on a Body Moving in Outer Space).— Prikladnaya Matematika i Mekhanika, Vol.26, No.5. 1962.
2.73. Jahsman, W.E. Mass Consideration in Ring Supported Solar Sails.— J.Amer. Rock. Soc., Vol.30, No.3. 1960.
2.74. Glushko, V.P. Zhidkoe toplivo dlya reaktivnykh dvigatelei (Liquid Fuel for Rocket Engines).— Moskva, Izd. Voenno-Vozolushnoi Inzhenernoi Akademii. 1936.
2.75. Mel'nikov, M.V. Vliyanie formy kamery i sopla na tyagu ZhRD (Influence of the Chamber Profile and Nozzle on the Thrust of Liquid-Propellant Rockets) Moskva, Izd. BNT. 1946.
2.76. Vanichev, A.P. Termodinamicheskii raschet goreniya i istecheniya v oblasti vysokikh temperatur (Thermodynamics of the Combustion and Exhaust for High Temperatures).— Moskva, Izd. BNT. 1947.
2.77. Zel'dovich, Ya.B. and A.I. Polyarnyi. Raschety teplovykh protsessov pri vysokoi temperature (High-Temperature Thermal Processes).— Moskva, Izd. BNT. 1947.

2.78. Varshavskii, G.A. K voprosu o povedenii bystrodvizhushchegosya potoka szhimaemogo gaza v pryamoi tsilindricheskoi trube pri nalichii okhlazhdeniya (The Behavior of a Rapidly-Moving Stream of Compressible Gas in a Straight Cylindrical Tube with Cooling).— Zhurnal Tekhnicheskoi Fiziki, No.4. 1946.

2.79. Romanenko, S.V. Techenie vyazkogo gaza v tsilindricheskoi trube pri nalichii konvektivnogo teploobmena (Flow of a Viscous Gas in a Cylindrical Tube with Convective Heat Exchange).— Doklady AN SSSR, Vol.91, No.6. 1953.

2.80. Grodzovskii, G.L. Nekotorye tochnye resheniya zadachi o techenii gaza v trube s uchetom treniya i konvektivnogo teploobmena (Some Exact Solutions of the Problem of Gas Flow in a Tube Allowing for Friction and Convective Heat Exchange).— Izvestiya AN SSSR, OTN, No.8. 1958.

2.81. Mezhirov, I.I. O techenii gaza v tsilindricheskoi trube pri nalichii treniya i teploobmena (Gas Flow in a Cylindrical Tube with Friction and Heat Exchange).— Izvestiya AN SSSR, OTN, No.8. 1958.

2.82. Goldsmith, W. and R.A. Seban. Pressure Drop and Heat Transfer for Subsonic Air Flow in a Smooth Pipe.— Trans. of ASME, No. 50-F-18. 1950.

2.83. Avduevskii, V.S., Yu.I. Danilov, V.K. Koshkin, I.N. Kutyrin, M.M. Mikhailova, Yu.S. Mikheev, and O.S. Sergel. Osnovy teploperedachi v aviatsionnoi i raketnoi tekhnike (Fundamentals of Heat Transfer in Aircraft and Rocket Engineering).— Moskva, Oborongiz. 1960.

2.84. Grodzovskii, G.L., Yu.E. Kuznetsov, and G.E. Khudyakov. Gazodinamicheskaya teoriya techeniya dvukhfaznoi zhidkosti s izmeneniem agregatnogo sostoyaniya (Gas Dynamics of the Flow of a Two-Phase Liquid with a Variation in the State of Aggregation).— Trudy TsKTI, Kotloturbostroenie, No.59, Leningrad. 1965.

2.85. Kimel', L.R. Opredelenie optimal'noi formy zashchitnogo bar'era (Determination of the Optimum Shape of the Shielding Barrier).— Atommaya Energiya, Vol.7, No.3. 1959.

2.86. Tokarev, V.V. and V.I. Tsvetkov. Optimal'naya forma zashchity ot gamma-izlucheniya (Optimum Form of Gamma-Radiation Shielding).— Zhurnal Prikladnoi Mekhaniki i Tekhnicheskoi Fiziki, No.1. 1964.

2.87. Snyder, N.W. editor. Energy Conversion for Space Power. Space Power Systems.— New York-London, Acad. Press. 1961.

2.88. Vernet-Lozet, M. Les véhicules spatiaux à source d'énergie solaire. Le projet Phaëtan.— Ann. geofis., Vol.17, No.1. 1964.

2.89. Stafford, G.B. Capabilities of Power Subsystems for Space.—Mechanical Engineering, Vol.87, No.9. 1965.

2.90. Osmun, W.G. Space Nuclear Power: SNAP-50/SPUR.— Space Aeronaut. Vol.42, No.7. 1964.

2.91. Au, G.F. "Snapshot" ein electrostatisches Ionentriebwerk mit nuclearer Energieversorgung.— Luftfahrttechnik Raumfahrttechnik, No.7. 1965.

2.92. Glassman, A.J. and W.L. Stewart. Thermodynamic Characteristics of Brayton Cycles for Space Power.— J. Spacecraft and Rock, Vol.1, No.1. 1964.

2.93. Cochran, D. L. Working Fluids for Dynamic APN Systems.—Space Aeronaut., R and D. Techn. Handbook, Vol. 38, No. 2. 1962—1963.
2.94. Beale, R.J., E.W. Speiser, and J.R. Womack. Electric Space Cruiser for High-Energy Missions.— J. Spacecraft and Rock., Vol. 1, No. 1. 1964.
2.95. Deich, M.E. Tekhnicheskaya gazodinamika (Technical Gas Dynamics).— Moskva, Gosenergoizdat. 1953.
2.96. Loitsyanskii, L.G. Mekhanika zhidkosti i gaza (Fluid Mechanics).— Moskva, Gostekhizdat. 1957.
2.97. Stepanov, G.Yu. Gidrodinamika reshetok turbomashin (Hydrodynamics of the Gratings of Turbines).— Moskva, Fizmatgiz. 1962.
2.98. Abiants, V.Kh. Teoriya gazovykh turbin reaktivnykh dvigatelei (Theory of the Gas Turbines of Rocket Engines).— Mashinostroenie, Moskva. 1965.
2.99. Dorogov, B.S. Eroziya lopatok v parovykh turbinakh (Erosion of the Blades in Steam Turbines).— Energiya, Moskva. 1965.
2.100. Elliott, D.G. Two-fluid Magnetohydrodynamic Cycle for Nuclear Electric Power Conversion.— J. Amer. Rock. Soc., Vol. 32, No. 10. 1962.
2.101. MHD Power Converters for Space.— Nucleonics, Vol. 21, No. 7. 1963.
2.102. Ioffe, A.I. Poluprovodnikovye termoelementy (Semi-Conducting Thermo-elements).— Moskva-Leningrad, Izd. AN SSSR. 1956.
2.103. Dieckamp, H.M., R. Balent, and J.R. Wetch. Reactor Direct-Conversion Units.— Proc. 3rd Unit. Nat. Internat. Conf. on the Peaceful Uses of Atomic Energy, Geneva. 1964.
2.104. Stamm, H. Radionuklid-Batterien fur die Raumfahrt.— Weltraumfahrt, No. 4. 1963.
2.105. Mariner to Mars.— Flight, Vol. 86, No. 2906, 19 XI. 1964.
2.106. Hamilton, R.C. Solar Power System.— Proc. 15 Internat. Astronaut. Congr. 1964. Warsaw. 1965.
2.107. Tonkin, S. Solar Cell Arrays for Rigid Earth-Pointing Satellites.— Proc. 15 Internat. Astronaut. Congr. 1964, Warsaw. 1965.
2.108. Grover, G.M. Los-Alamos Plasma Thermocouple.— Nucleonics, Vol. 17, No. 2. 1959.
2.109. Dobretsov, L.N. Termoelektronnye preobrazovateli teplovoi energii v elektricheskuyu (Thermionic Converters of Thermal into Electrical Energy).— Zhurnal Tekhnicheskoi Fiziki, Vol. 30, No. 4. 1960.
2.110. Harvey, R.J. Propulsion and Auxiliary Power Systems.— Ballistic Missile and Space Technology, Vol. 2, N.Y. 1960.
2.111. Cobb, J.E., W.E. Cutler, A.F. Dugan, R.H. Olds, and G.B. Shook. A Nuclear-Thermionic-Ionic Propulsion System.— Proc. XI Internat. Astronaut. Congr. 1960, Vienna. 1961.
2.112. Morgulis, N.D. Termo-elektronnyi (plazmennyi) preobrazovatel' energii (Thermionic (Plasma) Energy Converter).— Moskva, Gosatomizdat. 1961.
2.113. Miller, H. Thermionic-Nuclear Space Power Systems.— Proc. 3rd Sympos. Advanced Propuls. Concepts, Cincinnati, 1962, Vol. 1, N.Y.— London, Acad. Press. 1963.

2.114. Gronich, A., R.W. Hallet, and P.W. Miller. A Nuclear Electric Propulsion System for Manned Interplanetary Missions.— Proc. 14 Internat. Astronaut. Congr. 1963, Vol. 1, Warsaw. 1965.
2.115. Psarouthakis, J. Thermionic Conversion for Electric Propulsion Power.— Proc. 16 Internat. Astronaut. Congr. 1965, Warsaw. 1966.
2.116. Kratkii fiziko-tekhnicheskii spravochnik (A Handbook of Physics and Engineering), Vol. 1.— Moskva, Fizmatgiz. 1960.
2.117. Inzhenerno-tekhnicheskii spravochnik po elektrosvyazi, elektroustanovki (Engineering Handbook of Electrical Plants and Communications).— Moskva, Izdatel'stvo literatury po svyazi i radio. 1962.
2.118. Sinyarev, G.B. and M.V. Dobrovol'skii. Zhidkostnye raketnye dvigateli (Liquid Rocket Engines).— Moskva, Oborongiz. 1957.
2.119. Burlage, H. Liquid Engines for Advanced Launch Vehicles.— Astronautics and Aeronautics, Vol. 2, No. 7. 1964.
2.120. S-1B Tanks, Missile and Space.— Daily, Vol. 10, No. 26, 9 XII. 1964.
2.121. Stechkin, B.S. Teoriya vozdushnogo reaktivnogo dvigatelya (Theory of the Ramjet Engine).— Tekhnika Vozdushnogo Flota, No. 2. 1929.
2.122. Roy, M. Recherches théoriques sur le rendement et les conditions de réalisation des systèmes motopropulseurs a réaction. Paris. 1930.
2.123. Abramovich, G.N. Gazovaya dinamika vozdushno-reaktivnykh dvigatelei (Gas Dynamics of Ramjet Engines).— Moskva, Izd. BNT. 1947.
2.124. Inozemtsev, N.V. and V.S. Zuev. Aviatsionnye gazoturbinnye dvigateli (Aircraft Gas-Turbine Engines).— Moskva, Oborongiz. 1949.
2.125. Cherkez, A.Ya. Primenenie metoda malykh otklonenii v teorii i raschete aviatsionnykh TRD (Application of the Perturbation Method to the Theory of Aircraft Solid-Propellant Engines).— Moskva, Oborongiz. 1955.
2.126. Bondaryuk, M.M. and O.M. Il'yashenko. Pryamotochnye vozdushnoreaktivnye dvigateli (Ramjet Engines).— Moskva, Oborongiz. 1958.
2.127. Lane, R.J. Recoverable Air-Breathing Boosters for Space Vehicles.— J. Roy. Aeronaut. Soc., Vol. 66, No. 618. 1962.
2.128. Ferri, A. Review of Problems in Application of Supersonic Combustion.— J. Roy. Aeronaut. Soc., Vol. 68, No. 645. 1964.
2.129. Gossick, L.V. and H.M. Cook. Trends in Aerospace Propulsion Development Testing, Their Influence on Future Flight Simulation Facility Requirements.— Proc. 16 Internat. Astronaut. Congr. 1965, Warsaw. 1966.
2.130. Skubachevskii, G.S. Aviatsionnye gazoturbinnye dvigateli (Aircraft Gas-Turbine Engines).— Mashinostroenie, Moskva. 1965.
2.131. Kholshchevnikov, K.V. Soglasovanie parametrov kompressora i turbiny v aviatsionnykh gazoturbinnykh dvigatelyakh (Aligning the Parameters of the Compressor and the Turbine in Aircraft Gas-Turbine Engines).— Mashinostroenie, Moskva. 1965.
2.132. Grodzovskii, G.L. Sverkhzvukovye osesimmetrichnye konicheskie techeniya s konicheskimi skachkami, granichashchimi s parallel'nym potokom (Supersonic Axially-Symmetric Flows with Conic Shocks Adjoining

a Parallel Uniform Stream).— Prikladnaya Matematika i Mekhanika, Vol. 23, No. 2. 1959.

2.133. Grodzovskii, G.L. Avtomodel'noe dvizhenie gaza pri sil'nom periferiinom vzryve (Simulation of the Gas Motion for a Strong Peripheral Explosion).— Doklady AN SSSR, Vol. 111, No. 5. 1956.

2.134. Demetriades, S.T. A Novel System for Space Flight Using a Propulsive Fluid Accumulator.— J. Brit. Interpl. Soc., Vol. 17, No. 5. 1959.

2.135. Camac, M. and F. Berner. An Orbital Air-Scooping Vehicle.— Astronautics, Vol. 6, No. 8. 1961.

2.136. Reichel, R.H., T.L. Smith, and D.R. Hanford. Potentialities of Air-scooping Electrical Space Propulsion Systems.— Progr. in Astronaut. and Aeronaut. Vol. 9, Electrical Prop. Devel., N.Y. 1963.

2.137. Tokarev, V.V. and Yu. M. Fatkin. Nakopitel' rabochego veshchestva v zadachakh optimizatsii dvizheniya s ogranichennoi moshchnost'yu (Working Fluid Accumulator in Optimization Problems of Limited-Power Motion).— Inzhenernyi Zhurnal AN SSSR, Vol. 5, No. 3. 1965.

2.138. Kapitsa, P.L. Turbodetander dlya polucheniya nizkikh temperatur i ego primenenie dlya szhizheniya vozdukha (Turboexpander for Producing Low Temperatures and Its Application to Air Compression).— Tekhnicheskaya Fizika, No. 2. 1939.

2.139. Tekhnika nizkikh temperatur (Low-Temperature Technology).— Energiya, Moskva-Leningrad. 1964.

2.140. Sedov, L.I. Metody podobiya i razmernosti v mekhanike (Methods of Similitude and Dimensionality in Mechanics).— Nauka, Moskva. 1965.

2.141. Alder, R. and J. Lecompte. Études sur la propulsion nucléothermique. Estimation de performances d'un étage nucléaire pour lanceur lourd européen.— Proc. 16 Internat. Astronaut. Congr., 1963, Warsaw. 1965.

2.142. Goldstein, S. editor. Modern Development in Fluid Dynamics, Vol. 2, London, O.U.P. 1943.

2.143. Grodzovskii, G.L. Turbulentnyi pogranichnyi sloi ploskoi plastiny (Turbulent Boundary Layer of a Flat Plate).— Zhurnal Prikladnoi Mekhaniki i Tekhnicheskoi Fiziki, No. 4. 1962.

2.144. Liepmann, H.W. and A. Roshko. Elements of Gasdynamics.— Wiley. 1957.

2.145. Hayes, W.D. and R.F. Probstein. Hypersonic Flow Theory.— New York-London, Acad. Press. 1959.

2.146. Karman, T. Supersonic Aerodynamics.— J. Aeronaut. Sci., Vol. 14, No. 7. 1947.

2.147. Kochin, N.E., I.A. Kibel', and N.V. Roze. Teoreticheskaya gidromekhanika (Theoretical Hydromechanics).— Fizmatgiz. 1963.

2.148. Martynov, A.K. Eksperimental'naya aerodinamika (Experimental Aerodynamics).— Oborongiz. 1958.

2.149. Tsien, H.S. Supersonic Flow Over an Inclined Body of Revolution.— J. Aeronaut. Sci., Vol. 5, No. 12. 1938.

2.150. Frankl', F.I. and E.A. Karpovich. Gazodinamika tonkikh tel (Gas Dynamics of Thin Bodies).— Moskva-Leningrad, Gostekhizdat. 1948.
2.151. Ferri, A. Elements of Aerodynamics of Supersonic Flows.— Macmillan. 1949.
2.152. Nikol'skii, A.A. O telakh vrashcheniya s protokom, obladayushchikh naimen'shim vneshnim volnovym soprotivleniem v sverkhzvukovom potoke (Bodies of Revolution Possessing Minimum Wave Drag in a Supersonic Flow).— In: Sbornik teoreticheskikh rabot po aerodinamike.— Moskva, Oborongiz. 1957.
2.153. Krasnov, N.F. Aerodinamika tel vrashcheniya (Aerodynamics of Bodies of Revolution).— Moskva, Oborongiz. 1958.
2.154. Sedov, L.I. O nekotorykh neustanovivshikhsya dvizheniyakh szhimaemoi zhidkosti (Unsteady Compressible Flows).— Prikladnaya Matematika i Mekhanika, Vol. 9, No. 4. 1945.
2.155. Taylor, G.J. The Air Wave Surrounding an Expanding Sphere.— Proc. Roy. Soc., Ser. A., Vol. 186. 1946.
2.156. Sakurai, A. On the Propagation and Structure of the Blast Wave.— J. Phys. Soc. Japan, Vol. 8, No. 5. 1953; Vol. 9, No. 2. 1954.
2.157. Krasheninnikova, N.L. O neustanovivshemsya dvizhenii gaza, vytesnyaemogo porshnem (Unsteady Flow of a Gas Ejected by a Piston).— Izvestiya AN SSSR, OTN, No. 8. 1955.
2.158. Stanyukovich, K.P. Neustanovivshiesya dvizheniya sploshnoi sredy (Unsteady Flow of a Continuous Medium).— Moskva, Gostekhizdat. 1955.
2.159. Chernyi, G.G. Odnomernye neustanovivshiesya dvizheniya sovershennogo toka s sil'nymi udarnymi volnami (One-Dimensional Unsteady Flow of an Ideal Current with Strong Shock Waves).— Doklady AN SSSR, Vol. 107, No. 5. 1956.
2.160. Grigoryan, S.S. Zadacha Koshi i zadacha o porshne dlya uravnenii odnomernykh neustanovivshikhsya dvizhenii gaza (avtomodel'nye dvizheniya) (The Cauchy Problem and the Piston Problem for the Equations of One-Dimensional Unsteady Gas Flow (Model Flows)).— Prikladnaya Matematika i Mekhanika, Vol. 22, No. 2. 1958.
2.161. Kochina, N.N. and N.S. Mel'nikova. O neustanovivshemsya dvizhenii gaza, vytesnyaemogo porshnem (Unsteady Flow of a Gas Ejected by a Piston).— Prikladnaya Matematika i Mekhanika, Vol. 22, No. 4. 1958.
2.162. Chernyi, G.G. Techeniya gaza s bol'shoi sverkhzvukovoi skorost'yu (Gas Flows at Hypersonic Velocities).— Moskva, Fizmatgiz. 1959.
2.163. Hayes, W.D. On Supersonic Similitude.— Quart. Appl. Math., Vol. 5, No. 1. 1947.
2.164. Bam-Zelikovich, G.M., A.I. Bunimovich, and M.P. Mikhailova. Dvizhenie tonkikh tel s bol'shimi sverkhzvukovymi skorostyami. Teoreticheskaya gidrodinamika (Motion of Slender Bodies at Hypersonic Velocities. Theoretical Hydromechanics).— Sbornik No. 4, Moskva, Oborongiz. 1949.
2.165. Grodzovskii, G.L. Nekotorye osobennosti obtekaniya tel pri bol'shikh sverkhzvukovykh skorostyakh (Some Features of the Hypersonic Flow Past Bodies).— Izvestiya AN SSSR, OTN, No. 6. 1957.

2.166. Lees, L. and T. Kubota. Inviscid Hypersonic Flow Over Blunt-Nosed Slender Bodies.— J. Aeronaut. Sci., Vol. 24, No. 3. 1957.

2.167. Grodzovskii, G.L. and N.L. Krasheninnikova. Avtomodel'nye dvizheniya gaza s udarnymi volnami, rasprostranyayushehimisya po stepennomu zakonu po pokoyashchemusya gazu (Model Gas Flows with Shock Waves Propagating According to the Power Law in a Gas at Rest).— Prikladnaya Matematika i Mekhanika, Vol. 23, No. 5. 1959.

2.168. Sychev, V.V. On the Theory of Hypersonic Flow Over Blunt-Nosed Slender Bodies.— Adv. Aeronaut. Sci., Vol. 3, New York, 1960. 1961.

2.169. Grodzovskii, G.L. Optimal'naya forma teplootvodyashchikh reber, okhlazhdaemykh izlucheniem (Optimum Shape of the Radiating Fins).— Izvestiya An SSSR, OTN, Energetika i Avtomatika, No. 6. 1962; cf. also Proc. XII Internat. Astronaut. Congr. 1961, Vien., 1962; Acta Astronautika No. 8. 1962.

2.170. Pontryagin, L.S., V.G. Boltyanskii, E.F. Mishchenko, and R.V. Gamkrelidze. Matematicheskaya teoriya optimal'nykh protsessov (Mathematical Theory of Optimum Processes).— Moskva, Fizmatgiz. 1961.

2.171. Wilkins, J.E. Minimizing the Mass of Thin Radiating Fins.— JASS, Vol. 27, No. 2. 1960.

2.172. Wilkins, J.E. Minimum Mass Thin Fins Which Transfer Heat Only by Radiation to Surroundings at Absolute Zero.— J. Soc. Ind. Appl. Math., Vol. 8, No. 4, XII. 1960.

2.173. Wilkins, J.E. Minimum Mass Thin Fins for Space Radiators.— Proc. of 1960, Heat-Transfer and Mechanics Inst., Stanford University. 1960.

2.174. Wilkins, J.E. Minimum Mass Fins and Constant Temperature Gradient.— J. Soc. Ind. Appl. Math., Vol. 10, No. 1. 1962.

2.175. Bartas, J.G. and W.H. Sellers. Radiation Fin Effectiveness.— Trans. ASME. J. Heat Transfer, Vol. 82, No. 1. 1960.

2.176. Chen, Y.L. On Minimum-Weight Rectangular Fins.— JASS, Vol. 27, No. 11. 1960.

2.177. Nilson, E.N. and R. Curry. The Minimum-Weight Straight Fin of Triangular Profile Radiating to Space.— JASS, Vol. 27, No. 2. 1960.

2.178. Grodzovskii, G.L. and V.V. Frolov. Optimal'nye kontury teplootvodyashchikh reber, okhlazhdaemykh izlucheniem (Optimum Contours of Radiating Fins).— Part 2, Proc. XIII Internat. Astronaut. Congr. 1962. Vien. 1963.

2.179. Frolov, V.V. Optimal'naya forma teplootvodnashchikh reber s uchetom vzaimnogo oblucheniya (Optimum Shape of Radiating Fins, Allowing for Mutual Irradiation).— Izvestiya AN SSSR, OTN, Energetika i Avtomatika, No. 6. 1962.

2.180. Eckert, E.R.G., T.F. Irvine Jr., and M. Sparrow. Analytical Formulation for Radiating Fins with Mutual Irradiation.— J. Amer. Rock Soc., Vol. 30, No. 7. 1960.

2.181. Sparrow, M., E.R.G. Eckert, and T.F. Irvine Jr. The Effectiveness of Radiating Fins with Mutual Irradiation.— JASS, Vol. 28, No. 10. 1961.

2.182. Kreith, F. Radiation Heat Transfer for Spacecraft and Solar Power Plant Design.— Scranton, Pa., Internat. Textbook Co. 1962.

2.183. Sparrow, E.M. and E.R.G. Eckert. Radiant Interaction Between Fin and Base Surfaces.— J. Heat Transfer, Vol.84, Ser.C, No.1. 1962.

2.184. Plamondon, J.A. Thermal Efficiency of Coated Fins.— J. Heat Transfer, Ser.C, Vol.84, No.4. 1962.

2.185. Karlekar, B.V. and B.T. Chao. Mass Minimization of Radiating Trapezoidal Fins with Negligible Base Cylinder Interaction.— Int. J. Heat and Mass Transfer, Vol.6, No.1. 1963.

2.186. Haller, H.C. and N.O. Stockman. A Note on Fin-Tube View Factors.— J. Heat Transfer, Ser.C, Vol.85, No.4. 1963.

2.187. Johnson, V.K. and E.M. Sparrow. Angle Factors Radiant Interchange Between Parallel-Oriented Tubes.— J. Heat Transfer, Ser.C, Vol.85, No.4. 1963.

2.188. Vasanov, Yu.A. and Yu.G. Zhulev. Optimal'naya forma treugol'nykh teplootvodyashchikh reber s uchetom vzaimnogo oblucheniya reber i oklazhdaemoi poverkhnosti (Optimum Shape of Triangular Radiating Fins Allowing for Mutual Irradiation of the Fins and the Cooled Surface).— Izvestiya AN SSSR, Energetika i Transport, No.3. 1964; cf. also Proc. XV Internat. Astronaut. Congr. 1964, Warsaw. 1965.

2.189. Solov'ev, B.A. Grafoanaliticheskii metod opredeleniya parametrov teplovnositelya v kholodil'nike-izluchatele na neraschetnykh rezhimakh ego raboty (Graphic-Analytical Method of Determining the Coolant Parameters in the Radiator for Work Conditions Differing from the Design Conditions).— Izvestiya AN SSSR, Energetika i Transport, No.4. 1965.

2.190. Vasanov, Yu.A. Kharakteristiki teplovogo izlucheniya sistemy zvezdoobraznykh izluchatelei (Characteristics of the Thermal Radiation ofa System of Star-Shaped Radiators).— Izvestiya AN SSSR, Energetika i Transport, No.5. 1964.

2.191. Vasanov, Yu.A. Vliyanie termicheskogo soprotivleniya pokrytii na kharakteristiki teplovogo izlucheniya zvezhdoobraznykh izluchatelei (Influence of the Thermal Resistance of Coatings on the Characteristics of the Thermal Radiation of Star-Shaped Radiators).— Izvestiya AN SSSR, Energetika i Transport, No.6. 1964.

2.192. Frolov, V.V. Optimal'naya sistema izluchayushchikh reber (Optimum System of Radiating Fins).— Izvestiya AN SSSR, Energetika i Transport, No.6. 1964.

2.193. Novoseletskii, O.Yu. and V.L. Ukolov. Opredelenie optimal'nykh razmerov izluchayushchikh reber (Determination of the Optimum Size of Radiating Rins).— Inzhenerno-Fizicheskii Zhurnal, No.12. 1964.

2.194. Vasanov, Yu.A. and Yu.G. Zhulev. Issledovanie teplovogo izlucheniya sistemy zvezdoobraznykh izluchatelei (Radiation of a System of Star-Shaped Radiators).— Teplofizika Vysokikh Temperatur, No.6. 1965. Cf. also Proc. XVI Internat. Astronaut. Congr. 1965. Warsaw. 1966.

2.195. Zhulev, Yu.G. and V.A. Kosarenkov. Izluchatel'naya sposobnost' trubchatogo radiatora (Radiating Capacity of a Tube Radiator).— Teplofizika Vysokikh Temperatur, No.3. 1966.

2.196. Weatherston, R.C. and W.E. Smith. A Method of Heat Rejection from Space Powerplants.— J. Amer. Soc., Vol.30, No.3. 1960.
2.197. Stasenko, A.L. Forma gibkoi niti v pole tsentrobezhnykh sil (Shape of a Flexible Thread in a Field of Centrifugal Forces).— Izvestiya AN SSSR, OTN, Mekhanika i Mashinostroenie, No.6. 1962.
2.198. Grodzovskii, G.L. and A.L. Stasenko. O forme teplootvodyashchikh elementov, okhlazhdaemykh izlucheniem (Shape of Heat Radiating Elements), Part 3.— Proc. XIV Internat. Astronaut. Congr. 1963. Warsaw. 1964.
2.199. Weatherston, R.S. and W.E. Smith. A New Type of Thermal Radiator for Space Vehicles.— Aeronaut. Eng., Vol.20, No.1. 1961.
2.200. Burge, H.L. Revolving Belt Space Radiator.— J. Amer. Rock. Soc., Vol.32, No.8. 1962.
2.201. Shipper, L., R.C. Siegler, and E.B. Zwick. Advanced 1-Megawatt Space Power Plant Study.— AIAA Paper, Nos.63—270. 1963.
2.202. Grodzovskii, G.L., A.L. Stasenko, and V.V. Frolov. O forme teplootvodyashchikh elementov, okhlashdaemykh izlucheniem (Shape of Heat-Radiating Elements), Part 4.— Proc. XV Internat. Astronaut. Congr. 1964. Warsaw. 1965.
2.203. Stasenko, A.L. Ravnovesnye formy i malye kolebaniya gibkoi niti, vrashchayushcheisya v bessilovom pole (Equilibrium Shapes and Small Oscillations of a Flexible Thread Revolving in a Gravity-Free Field).— Izvestiya AN SSSR, Mekhanika i Mashinostroenie, No.1. 1964.
2.204. Stasenko, A.L. Predel'nye kharakteristiki lentochnogo radiatora s uchetom samooblucheniya (Limiting Characteristics of a Belt Radiator Allowing for Self-Irradiation).— Izvestiya AN SSSR, Energetika i Transport, No.2. 1965.
2.205. Stasenko, A.L. Vliyanie vneshnego izlucheniya na predel'nye kharakteristiki lentochnogo radiatora (Influence of the External Radiation on the Limiting Characteristics of a Belt Radiator).— Izvestiya AN SSSR, Energetika i Transport, No.5. 1965.
2.206. Shlykov, Yu.P. and E.A. Ganin. Kontaktnyi teploobmen (Contact Heat Exchange).— Moskva-Leningrad, Energoizdat. 1963.
2.207. Fenech, H. and W.H. Rohsenow. Prediction of Thermal Conductance of Metallic Surfaces in Contact.— J. Heat Transfer, Vol.85, No.1. 1963.
2.208. Stasenko, A.L. Dvumernyi periodicheskii kontakt. Kontaktnoe soprotivlenie s uchetom vtorichnykh potokov v obshchem sluchae (Two-Dimensional Alternating Contact. Contact Resistance Allowing for Secondary Fluxes in the General Case).— Zhurnal Prikladnoi Mekhaniki i Tekhnicheskoi Fiziki, No.4. 1964.
2.209. English, R.E., H.O. Slone, D.T. Bernatowicz, E.H. Davison, and S. Lieblein. A 20,000-Kilowatt Nuclear Turboelectric Power Supply for Manned Space Vehicles.— NASA Memo 2-20-59E. March 1959.
2.210. Gonor, A.L. Opredelenie formy prostranstvennogo optimal'nogo tela s uchetom sily treniya (Determining the Shape of a Three-Dimensional Optimum Body Allowing for Friction Forces).— Izvestiya AN SSSR, Mekhanika, No.4. 1965.

Chapter Three

3.1. Stechkin, B.S., P.K. Kazandzhan, A.P. Alekseev, A.N. Govorov, N.E. Konovalov, Yu.N. Nechaev, and R.M. Fedorov. Teoriya reaktivnykh dvigatelei (Theory of Rocket Engines).— Oborongiz. 1958.
3.2. Corliss, W.R. Propulsion Systems for Spaceflight.— McGraw-Hill. 1960.
3.3. Grodzovskii, G.L., Yu.N. Ivanov, and V.V. Tokarev. Mekhanika kosmicheskogo poleta s maloi tyagoi (Mechanics of Low-Thrust Spaceflight).— Inzhenernyi Zhurnal AN SSSR, Vol.3, Nos.3 and 4. 1963; Vol.4, Nos.1 and 2. 1964.

Chapter Four

4.1. Preston-Thomas, H. Interorbital Transport Techniques.— J. Brit. Interpl. Soc., Vol.11, No.4. 1952.
4.2. Preston-Thomas, H. Two Aspects of the Time Element in Interplanetary Flight.— Proc. V Internat. Astronaut. Congr. 1954, Vien. 1955.
4.3. Stuhlinger, E. Possibilities of Electrical Spaceship Propulsion.— Proc. V Internat. Astronaut. Congr. 1954, Vien. 1955.
4.4. Bussard, R.W. A Nuclear-Electric Propulsion System.— J. Brit. Interpl. Soc., Vol.15, No.6. 1956.
4.5. Preston-Thomas, H. Interorbital Transport Techniques. Realities of Space Travel. London. 1957.
4.6. Stuhlinger, E. Design and Performance Data of Spaceships with Ionic Propulsion Systems.— Proc. VIII Internat. Astronaut. Congr. 1957, Vien. 1958.
4.7. Preston-Thomas, H. A Note on a Nuclear Electrical Propulsion System.— J. Brit. Interpl. Soc., Vol.16, No.9. 1958.
4.8. Preston-Thomas, H. Some Design Parameters of a Simplified Ion Rocket.— J. Brit. Interpl. Soc., Vol.16, No.10. 1958.
4.9. Leitmann, G. The Nuclear-Powered Ion Rocket.— J. Brit. Interpl. Soc., Vol.16, No.10. 1958.
4.10. Cornog, R. The Optimum Velocity of Propellant Ejection.— Vistas in Astronaut., Vol.1. New York. 1958.
4.11. Stuhlinger, E. Advanced Propulsion Systems for Space Vehicles.— Proc. IX Internat. Astronaut. Congr. Madrid, 1958. Vien. 1959.
4.12. Moeckel, W.E. Propulsion Method in Astronautics.— Proc. IX Internat. Astronaut. Congr., Madrid, 1958. Vien. 1959.
4.13. Preston-Thomas, H. The Nuclear-Powered Ion Rocket.— J. Brit. Interpl. Soc., Vol.17, Nos.3/4. 1959.
4.14. Langmuir, D.B. Optimization of Rockets in Which Fuel is not Used as Propellant.— Space Technol., p.9. New York. 1959.
4.15. Irving, J.H. Low-Thrust Flight: Variable Exhaust Velocity in Gravitational Fields.— Space Technol., p.10. New York. 1959.

4.16. Stuhlinger, E. and R.N. Seitz. Electrostatic Propulsion Systems for Space Vehicles.— Adv. Space Sci., Vol.2. 1960.

4.17. Camac, M. Use of Energy Storage in Low-Thrust Spaceflight.— J. Amer. Rock. Soc., Vol.30, No.1. 1960.

4.18. Crocco, L. Meccanica della propulsione spaziale.— Proc. Seminar Adv. on Astronaut. Prop. 1960. Milan. 1962.

4.19. Grodzovskii, G.L. O dvizhenii tela peremennoi massy s uchetom relyativistskikh effektov (Motion of a Body of Varying Mass Allowing for Relativistic Effects).— Izvestiya AN SSSR, OTN, Mekhanika i Mashinostroenie, No.5. 1962.

4.20. Grodzovskii, G.L., Yu.N. Ivanov, and V.V. Tokarev. Mekhanika kosmicheskogo poleta s maloi tyagoi (Mechanics of Low-Thrust Spaceflight).— Inzhenernyi Zhurnal AN SSSR, Vol.3, No.3. 1963.

4.21. Irving, J.H. and E.K. Blum. Comparative Performance of Ballistic and Low-Thrust Vehicles for Flight to Mars.— Vistas in Astronaut., Vol.2. New York. 1959.

4.22. Grodzovskii, G.L., Yu.N. Ivanov, and V.V. Tokarev. O dvizhenii tela peremennoi massy s postoyannoi i ubyvayushchei zatratoi moshchnosti v gravitatsionnom pole, ch.3 (Motion of a Body of Varying Mass with Constant, Decreasing Power Expenditure in a Gravitational Field. Part 3).— Proc. XIV Internat. Astronaut. Congr. 1963.

4.23. Grodzovskii, G.L., Yu.N. Ivanov, and V.V. Tokarev. O dvizhenii tela peremennoi massy s postoyannoi zatratoi moshchnosti v gravitatsionnom pole (Motion of a Body of Varying Mass with Constant Power Consumption in a Gravitational Field).— Doklady AN SSSR, Vol.137, No.5. 1961; Proc. XII Internat. Astronaut. Congr. Washington. 1961. New York. 1963.

4.24. Ivanov, Yu.M. Optimal'noe izmenenie moshchnosti pri dvizhenii tela peremennoi massy v gravitatsionnom pole (Optimum Variation of the Power During the Motion of a Body of Varying Mass in a Gravitational Field).— Prikladnaya Matematika i Mekhanika, Vol.26, No.4. 1962.

4.25. Grodzovskii, G.L., Yu.N. Ivanov, and V.V. Tokarev. O dvizhenii tela peremennoi massy s postoyannoi i ubyvayushchei zatratoi moshchnosti v gravitatsionnom pole, ch.2 (Motion of a Body of Varying Mass with Constant, Decreasing Power Expenditure in a Gravitational Field, Part 2).— Proc. XIII Internat. Astronaut. Congr., Varna, 1962. Vien-New York. 1964.

4.26. Martelly, J. Optimization of Interplanetary Propulsion Systems.— IRE Trans. on Nuclear Sci., Vol.NS-9, No.1. 1962.

4.27. Tsander, F.A. Primenenie metallicheskogo topliva v raketnykh dvigatelyakh (Utilization of Metallic Fuel in Rocket Engines).— In: Sbornik "Raketnaya tekhnika," No.1. 1936; cf. Tsander, F.A. Problemi poleta pri pomoshchi reaktivnykh apparatov. Mezhplanetnye puteshestviya (The Problem of Jet-Propelled Flight. Interplanetary Trips).— Moskva, Oborongiz. 1961.

4.28. Tokarev, V.V. Optimal'noe upravlenie istochnikom moshchnosti pri dvizhenii tela peremennoi massy v gravitatsionnom pole s aktivnym sbrosom moshchnosti (Optimum Control of the Power Source During Motion of a Body of Varying Mass in a Gravitational Field with Active Power Discharge).— Prikladnaya Matematika i Mekhanika, Vol.27, No.4. 1963.

Chapter Five

5.1. Beletskii, V.V. and V.A. Egorov. Mezhplanetnye polety s dvigatelyami postoyannoi moshchnosti (Interplanetary Flights with Constant-Power Engines).— Kosmicheskie Issledovaniya, Vol.2, No.3. 1964.

5.2. Isaev, V.K. and V.V. Sonin. Ob odnoi nelineinoi zadache optimal'nogo upravleniya (A Nonlinear Optimum Control Problem).— Avtomatika i Telemekhanika, Vol.23, No.9. 1962.

5.3. Grodzovskii, G.L., Yu.N. Ivanov, and V.V. Tokarev. O dvizenii tela peremennoi massy s postyannoi zatratoi moshchnosti v gravitatsionnom pole (Motion of a Body of Varying Mass with Constant-Power Consumption in a Gravitational Field).— Doklady AN SSSR, Vol.137, No.5. 1961; Proc. XII Internat. Astronaut. Congr. Washington, 1961. New York. 1963.

5.4. Ivanov, Yu.N., V.V. Tokarev, and Yu.V. Shalaev. Optimal'nye traektorii i optimal'nye parametry kosmicheskikh apparatov s dvigatelyami ogranichennoi moshchnosti (Optimum Trajectories and Optimum Parameters of Space Vehicles with Power-Limited Engines).— Kosmicheskie Issledovaniya, Vol.2, No.3. 1964.

5.5. Irving, J.H. Low-Thrust Flight: Variable Exhaust Velocity in Gravitational Fields.— Space Technol., Ch.10. New York. 1959.

5.6. Lebedev, L.A. and S.A. Sakovskii. O neobkhodimykh i dostatochnykh usloviyakh ekstremuma funktsionala v zadache optimal'nogo pereleta apparata s dvigatelem maloi tyagi (Necessary and Sufficient Conditions for Functional Extrema in the Problem of Optimum Transfer of a Vehicle with Low-Thrust Engine).— Izv. vuzov. ser. Aviats. tekhn., No.4. 1964.

5.7. Leitmann, G. Minimum Transfer Time for a Power-Limited Rocket.— J. Appl. Mekhan., Vol.28, No.2. 1961.

5.8. Preston-Thomas, H. Interorbital Transport Techniques. Realities of Space Travel. London. 1957.

5.9. Preston-Thomas, H. Some Design Parameters of a Simplified Ion Rocket.— J. Brit. Interpl. Soc., Vol.16, No.10. 1958.

5.10. Isaev, V.K., V.V. Sonin, and B.Kh. Davidson. Optimal'nye rezhimy dvizheniya tochki peremennoi massy s ogranichennoi moshchnost'yu v odnorodnom tsentral'nom pole (Optimum Regimes of Motion of a Limited-Power Varying Point Mass in a Homogeneous Central Field).— Kosmicheskie Issledovaniya, Vol.2, No.4. 1964.

5.11. Beletskii, V.V. and V.A. Egorov. Razgon kosmicheskogo apparata v sfere deistviya planety (Acceleration of a Spacecraft in the Sphere of Action of a Planet).— Kosmicheskie Issledovaniya, Vol.2, No.3. 1964.

5.12. Irving, J.H. and E.K. Blum. Comparative Performance of Ballistic and Low-Thrust Vehicles for Flight to Mars.— Vistas in Astronaut., Vol.2. New York. 1959.

5.13. Melbourne, W.G., C.G. Sauer, and D.E. Richardson. Interplanetary Trajectory Optimization with Power-Limited Systems.— Proc. IAS Symp. on Vehicle Syst. Optim. New York. 1961.

5.14. Melbourne, W.G. Three-Dimensional Optimum Thrust Trajectories for Power-Limited Propulsion Systems.— J. Amer. Rock. Soc., Vol. 31, No. 12. 1961.

5.15. Melbourne, W.G. and C.G. Sauer. Optimum Thrust Programs for Power-Limited Propulsion Systems.— Astronaut. Acta, Vol. 8, No. 4. 1962.

5.16. Melbourne, W.G. and C.G. Sauer. Optimum Interplanetary Rendezvous with Power-Limited Vehicles.— AIAA, Vol. 1, No. 1. 1963.

5.17. Melbourne, W.G. and C.G. Sauer. Optimum Earth-Mars Roundtrip Trajectories Utilizing a Low-Thrust Power-Limited Propulsion System.— Adv. in the Astronaut. Sci., Vol. 13. 1963.

5.18. Saltzer, C. and C.W. Fetheroff. A Direct Variational Method for the Calculation of Optimum Thrust Program for Power-Limited Interplanetary Flight.— Astronaut. Acta, Vol. 7, No. 1. 1961.

5.19. Sherman, B. Low-Thrust Escape Trajectories.— Proc. IAS Symp. on Vehicle Syst. Optim. New York. 1961.

5.20. Ivanov, Yu.N. and Yu.V. Shalaev. Metod skoreishego spuska v primenenii k raschetu mezhorbital'nykh traektorii s dvigatelyami orgranichennoi moshchnosti (Steepest-Descent Method as Applied to Calculating Interorbital Trajectories with Power-Limited Engines).— Kosmicheskie Issledovaniya, Vol. 2, No. 3. 1964.

5.21. Pokrovskaya, S.A. O reshenii prostranstvennoi zadachi geliotsentricheskikh pereletov s dvigatelem postoyannoi moshchnosti metodom skoreishego spuska (Solution of the Three-Dimensional Problem of Heliocentric Transfers with a Constant-Power Engine by the Steepest-Descent Method).— Kosmicheskie Issledovaniya, Vol. 2, No. 6. 1964.

5.22. Faulders, C.R. Optimum Thrust Programming of Electrically Powered Rocket Vehicles in Gravitational Field.— J. Amer. Rock. Soc., Vol. 30, No. 10. 1960.

5.23. Faulders, C.R. Optimum Thrust Programming of Electrically Powered Rocket Vehicles for Earth Escape.— AIAA J., Vol. 1, No. 1. 1963.

5.24. Edelbaum, T.N. The Use of High and Low-Thrust Propulsion in Combination for Space Mission.— Prepr. Amer. Astronaut. Soc., No. 61—104. 1961.

5.25. Beletskii, V.V., V.A. Egorov, and V.G. Ershov. Analiz traektorii mezhplanetnykh poletov s dvigatelem postoyannoi moshchnosti (Analysis of the Trajectories of Interplanetary Flights with a Constant-Power Engine).— Kosmicheskie Issledovaniya, Vol. 3, No. 4. 1965.

5.26. Lebedev, V.N. Variatsionnaya zadacha o vzlete kosmicheskogo apparata s krugovoi orbity (Variational Problem of the Takeoff of a Spacecraft from a Circular Orbit).— Zhurnal Vychislitel'noi Matematiki i Matematicheskoi Fiziki, Vol. 3, No. 6. 1963.

5.27. Ivanov, Yu.N. and Yu.V. Shalaev. Optimal'nyi povorot ploskosti krugovoi orbity poperechnoi siloi (Optimum Rotation of the Plane of a Circular Orbit by a Lateral Force).— Kosmicheskie Issledovaniya, Vol. 3, No. 5. 1965.

5.28. Gobetz, F.W. Optimal Variable-Thrust Transfer of a Power-Limited Rocket Between Neighboring Circular Orbits.— AIAA J., Vol. 2, No. 2. 1964.

5.29. Gobetz, F.W. Errata: Optimal Variable-Thrust Transfer of a Power-Limited Rocket Between Neighboring Circular Orbits.— AIAA, Vol.2, No.12. 1964.
5.30. Leitmann, G. and S. Ross. Low Acceleration Trajectory Optimization in a Strong Central Force Field.— Proc. IAS Symp. on Vehicle Syst. Optim. New York. 1961.
5.31. Edelbaum, T.N. Theory of Maxima and Minima.— Optimiz. Techn. Ch.1, G. Leitmann, editor, Acad. Press. 1961.
5.32. Edelbaum, T.N. Propulsion Requirements for Controllable Satellites.— J. Amer. Rock. Soc., Vol.31, No.8. 1961.
5.33. Edelbaum, T.N. Optimum Low-Thrust Transfer Between Circular and Elliptic Orbits.— Proc. 4th U.S. Nat. Congr. Appl. Mech., Berkeley, Calif. Vol.1. 1962; Pergamon Press. 1962.
5.34. Billik, B.H. Some Optimal Low-Acceleration Rendezvous Maneuvers.— AIAA J., Vol.2, No.3. 1964.
5.35. Gobetz, F.W. A Linear Theory of Optimum Low-Thrust Rendezvous Trajectories.— J. Astronaut. Sci., Vol.12, No.13. 1965.
5.36. Isaev, V.K., A.I. Kuriyanov, and V.V. Sonin. Primenenie printsipa maksimuma v raketodinamike (Application of the Maximum Principle in Rocket Dynamics).— Proc. XIV Internat. Astronaut. Congr. 1963. Warsaw. 1964.
5.37. Efimov, G.B. and D.E. Okhotsimskii. Ob optimal'nom razgone kosmicheskogo apparata v tsentral'nom pole (Optimum Boosting of a Spacecraft in a Central Field).— Kosmicheskie Issledovaniya, Vol.3, No.6. 1965.

Chapter Six

6.1. Ivanov, Yu.N. O dvizhenii tela peremennoi massy s ogranichennoi moshchnost'yu i zadannym aktivnym vremenem (Motion of a Body of Varying Mass with Limited Power and Specified Operating Time).— Prikladnaya Matematika i Mekhanika, Vol.27, No.5. 1963.
6.2. Ivanov, Yu.N. and Yu.V. Shalaev. Optimal'nyi povorot ploskosti krugovoi orbity poperechnoi siloi (Optimum Rotation of the Plane of a Circular Orbit by a Lateral Force).— Kosmicheskie Issledovaniya, Vol.3, No.5. 1965.
6.3. Isaev, V.K. Printsip maksimuma L.S. Pontryagina i optimal'noe programmirovanie tyagi raket (L.S. Pontryagin's Maximum Principle and the Optimum Programming of the Thrust of Rockets).— Avtomatika i Telemekhanika, Vol.22, No.8. 1961; Vol.23, No.1. 1962.
6.4. Lebedev, V.N. Variatsionnaya zadacha o vzlete kosmicheskogo apparata s krygovoi orbity (The Variational Problem of the Takeoff of a Spacecraft from a Circular Orbit).— Zhurnal Vychislitel'noi Matematiki i Matematicheskoi Fiziki, Vol.3, No.6. 1963.
6.5. Lebedev, V.N. and N.N. Moiseev. Zadachi teorii optimal'nykh upravlenii kosmicheskimi apparatami (Problems of the Theory of Optimum Controls of Space Vehicles.).— Proc. XVI Internat. Astronaut. Congr. 1965. Warsaw. 1966.

6.6. Lawden, D.F. Optimal Escape from a Circular Orbit.— Astronaut. Acta, Vol.4, No.3. 1958.
6.7. Moeckel, W.E. Trajectories with Constant Tangential Thrust in Central Gravitational Fields.— NASA Techn. Rep. R-53. Washington. 1959.
6.8. Moeckel, W.E. Fast Interplanetary Mission with Low-Thrust Propulsion Systems.— NASA Techn. Rep. R-79. Washington. 1961.
6.9. Moeckel, W.E. Interplanetary Trajectories for Electrically Propelled Space Vehicles.— Astronaut. Acta, Vol.7, Nos.5,6. 1961.
6.10. Beletskii, V.V. and V.A. Egorov. Razgon kosmicheskogo apparata v sfere deistviya planety (Acceleration of a Spacecraft in the Sphere of Action of a Planet).— Kosmicheskie Issledovaniya, Vol.2, No.3. 1964.
6.11. Avramchenko, R.F., V.M. Bezmenov, V.A. Vinokurov, and V.V. Tokarev. Optimal'nyi perelet Zemlya-Mars-Zemlya s nereguliruemym dvigatelem maloi tyagi (Optimum Earth-Mars-Earth Transfer with Low-Thrust Unthrottled Engine).— Kosmicheskie Issledovaniya, Vol.5, No.2. 1967.
6.12. MacKay, J.S., L.G. Rossa, and A.V. Zimmerman. Optimum Low-Acceleration Trajectories for Earth-Mars Transfer.— Proc. IAS Symp. on Vehicle Syst. Optim., New York. 1961.
6.13. Zehle, H. Zur Optimalisierung interplanetarer Ubergangsbahnen mit kleiner Schubbeschleunigung. Teil 2 und 3.— Raumfahrtforschung, Vol.8, No.3. 1964.
6.14. Lindorfer, W. and H.G. Moyer. Application of a Low-Thrust Trajectory Optimization Scheme to Planar Earth-Mars Transfer.— J. Amer. Rock. Soc., Vol.32, No.2. 1962.
6.15. Beletskii, V.V. and V.A. Egorov. Mezhplanetnye polety s dvigatelem postoyannoi moshchnosti (Interplanetary Journeys with Constant-Power Engines).— Kosmicheskie Issledovaniya, Vol.2, No.3. 1964.
6.16. Lebedev, V.N. and B.N. Rumyantsev. Variatsionnaya zadacha o perelete mezhdu dvumya tochkami v tsentral'nom pole (Variational Problem of Transfer Between Two Points in a Central Field).— In: Sbornik "Iskusstvennye sputniki Zemli," No.16. 1963.
6.17. Faulders, C.R. Minimum Time Steering Programs for Orbital Transfer with Low-Thrust Rocket.— Astronaut. Acta, Vol.7, No.1. 1961.
6.18. Melbourne, W.G., C.G. Sauer, and D.E. Richardson. Interplanetary Trajectory Optimization with Power-Limited Systems.— Proc. IAS Symp. on Vehicle Syst. Optim. New York. 1961.
6.19. Melbourne, W.G. and C.G. Sauer. Optimum Thrust Programs for Power-Limited Propulsion Systems.— Astronaut. Acta, Vol.8, No.4. 1962.
6.20. Melbourne, W.G. and C.G. Sauer. Payload Optimization for Power-Limited Vehicles.— Prog. in Astronaut. and Aeronaut., Vol.9, Electric Prop. Devel. New York. 1963.
6.21. Kopnin, Yu.M. K zadache o povorote ploskosti orbity sputnika (Problem of Rotating the Satellite Plane).— Kosmicheskie Issledovaniya, Vol.3, No.4. 1965.
6.22. Stuhlinger, E. Design and Performance Data of Spaceships with Ionic Propulsion Systems.— Proc. VIII Internat. Astronaut. Congr. 1957. Vien. 1958.

6.23. Moeckel, W.E. Propulsion Method in Astronautics.— IX Internat. Astronaut. Congr. 1958. Vien. 1959.
6.24. Preston-Thomas, H. A Note on a Nuclear Electrical Propulsion System.— J. Brit. Interpl. Soc., Vol.16, No.9. 1958.
6.25. Grodzovskii, G.L. O dvizhenii tela peremennoi massy s postoyannoi zatratoi moshchnosti v gravitatsionnom pole s uchetom relyativistskikh effektov (Motion of a Body of Varying Mass with Constant Power Consumption in a Gravitational Field Allowing for Relativistic Effects).— Izvestiya AN SSSR, OTN, Mekhanika i Mashinostroenie, No.5. 1962.
6.26. Preston-Thomas, H. Interorbital Transport Techniques.— J. Brit. Interpl. Soc., Vol.11, No.4. 1952.
6.27. Preston-Thomas, H. Two Aspects of the Time Element in Interplanetary Flight.— Proc. V Internat. Astronaut. Congr. 1954. Vien. 1955.

Chapter Seven

7.1. Faulders, C.R. Optimum Thrust Programming of Electrically Powered Rocket Vehicles in a Gravitational Field.— J. Amer. Rock. Soc., Vol.30, No.10. 1960.
7.2. Faulders, C.R. Optimum Thrust Programming of Electrically Powered Rocket Vehicles for Earth Escape.— AIAA J., Vol.1, No.1. 1963.
7.3. Melbourne, W.G. and C.G. Sauer. Constant-Attitude Thrust Program Optimization.—AIAA J., Vol.3, No.8. 1965.
7.4. Bussard, R.W. A Nuclear-Electric Propulsion System.— J. Brit. Interpl. Soc., Vol.15, No.6. 1956.
7.5. Preston-Thomas, H. A Note on a Nuclear Electrical Propulsion System.— J. Brit. Interpl. Soc., Vol.16, No.9. 1958.
7.6. Irving, J.H. and E.K. Blum. Comparative Performance of Ballistic and Low-Thrust Vehicles for Flight to Mars.— Vistas in Astronaut., Vol.2. New York. 1959.
7.7. Ivanov, Yu.N. Dopolnitel'nye vesovye komponenty v zadachakh optimizatsii dvizheniya s organichennoi moshchnost'yu (Additional Weight Components in Optimization Problems of Power-Limited Motion).— Prikladnaya Matematika i Mekhanika, Vol.28, No.1. 1964.
7.8. Au, G.F. Entwicklungsstand zukunftiger Raumfahrtantriebe.— Luftfahrttechnik, Vol.7, No.1. 1961.
7.9. Ivanov, Yu.N. O dvizhenii tela peremennoi massy s ogranichennoi moshchnost'yu i zadannym aktivnym vremenem (Motion of a Limited-Power Body of Varying Mass with Specified Operating Time).— Prikladnaya Matematika i Mekhanika, Vol.27, No.5. 1963.
7.10. Vinokurov, V.A. and Yu.N. Ivanov. Optimal'noe dvizhenie v tsentral'nom pole pri zadannom vremeni raboty istochnika moshchnosti (Optimum Motion in a Central Field in a Specified Operating Time of the Power Source).— Izvestiya AN SSSR, Mekhanika, No.5. 1965.

7.11. Ivanov, Yu. N. Stupenchataya approksimatsiya optimal'nykh upravlenii (Step Approximation of Optimum Controls).— Prikladnaya Matematika i Mekhanika, Vol. 28, No. 3. 1964.

7.12. Beletskii, V.V. and V.A. Egorov. Mezhplanetarnye polety s dvigatelem postoyannoi moshchnosti (Interplanetary Journeys with Constant-Power Engines).— Kosmicheskie Issledovaniya, Vol. 2, No. 3. 1964.

7.13. Isaev, V.K. and V.V. Sonin. Ob odnoi nelineinoi zadache optimal'nogo upravleniya (A Nonlinear Problem of Optimum Control).— Avtomatika i Telemekhanika, Vol. 23, No. 9. 1962.

7.14. Isaev, V.K., V.V. Sonin, and B.Kh. Davidson. Optimal'nye rezhimy dvizheniya tochki peremennoi massy s ogranichennoi moshchnost'yu v tsentral'nom odnorodnom pole (Optimum Regimes of Motion of a Limited-Power Varying Point Mass in a Central Homogeneous Field).— Kosmicheskie Issledovaniya, Vol. 2, No. 4. 1964.

7.15. Melbourne, W.G., C.G. Sauer, and D.E. Richardson. Interplanetary Trajectory Optimization with Power-Limited Systems.— Proc. IAS Symp. on Vehicle Syst. Optim. New York. 1961.

7.16. Melbourne, W.G. and C.G. Sauer. Optimum Thrust Programs for Power-Limited Propulsion Systems.— Astronaut. Acta, Vol. 8, No. 4. 1962.

7.17. Melbourne, W.G. and C.G. Sauer. Payload Optimization for Power-Limited Vehicles.— Progr. in Astronaut. and Aeronaut., Vol. 9, Electric Prop. Devel. New York. 1963.

7.18. Shelton, R.D., R.A. Potter, L. Lacy, and E. Stuhlinger. Evaluation and Analysis of Thrust Units for Power-Limited Propulsion Systems.— AIAA J., Vol. 2, No. 4. 1964.

7.19. Lawden, J.H. Trajectory Optimization for a Rocket with Generalized Thrust Characteristic.— Astronaut. Acta, Vol. 10, Nos. 5, 6. 1964.

7.20. Dulgeroff, C.R., R.S. Speiser, and A.T. Forrester. Experimental Studies with Small-Scale Ion Motors.— ARS 14th Annual Meeting, Washington. 16—20 November 1959.

7.21. Fox, R. Physics of the Ion-Thrust System.— ARS 14th Annual Meeting, Washington. 16—20 November 1959.

7.22. Kash, S.W. and W.L. Starr. Experimental Results with a Collinear Electrode Plasma Accelerator and a Comparison with Ion Accelerators.— ARS 14th Annual Meeting, Washington. 16—20 November 1959.

7.23. Moser, W.A. Ion Engine Operation Analysis.— ARS Electrical Propulsion Conference, Berkeley. 14—16 March 1961.

7.24. Brown, H. and H.E. Nicoll. Electrical Propulsion Capabilities for Lunar Exploration.— ARS Electrical Propulsion Conference, Berkeley. 14—16 March 1961.

7.25. Isaev, V.K., A.I. Kur'yanov, and V.V. Sonin. Primenenie printsipa maksimuma v raketodinamike (Application of the Maximum Principle in Rocket Dynamics).— Proc. 14th Internat. Astronaut. Congr. 1963. Warsaw. 1964.

Chapter Eight

8.1. Hunter, M.W. and I.M. Tschirgi. The Advantages of High-Thrust Space Vehicles.— Prepr. Amer. Rock. Soc., No. 991. 1959.

8.2. Craig, R., C.W. Fetheroff, and C. Saltzer. Comparison of Chemical and Electric Propulsion Systems for Interplanetary Travel.— Proc. IRE, Vol. 48 No. 4. 1960.

8.3. Stearns, I.W. Electropropulsion System Applications.— Astronautics, Vol. 7, No. 3. 1962.

8.4. Beers, L.S. and A.D. Cohen. Mars Capabilities for Electrical, Nuclear, and Chemical Propulsion Systems.— IAS Paper, No. 120. 1962.

8.5. Stuhlinger, E. The Rocket with Electrical Propulsion System.— Electrical Engineering, Vol. 82, No. 7. 1963.

8.6. Boucher, R.A. Electrical Propulsion for Control of Stationary Satellites.— J. cf. Spacecraft and Rock., Vol. 1, No. 2. 1964.

8.7. Okhotsimskii, D.E. K teorii dvizheniya raket (Theory of Motion of Rockets).— Prikladnaya Matematika i Mekhanika, Vol. 10, No. 2. 1946.

8.8. Okhotsimskii, D.E. and T.M. Eneev. Nekotorye variatsionnye zadachi, svyazannye s zapuskom iskusstvennogo sputnika Zemli (Some Variational Problems Linked with the Launching of an Artificial Earth Satellite).— UFN, Vol. 63, No. 1a. 1957.

8.9. Lawden, D.F. Optimal Rocket Trajectories.— Jet. Prop., Vol. 27, No. 12. 1957.

8.10. Miele, A. General Variational Theory of the Flight Paths of Rocket-Powered Aircraft, Missiles and Satellite Carriers.— Astronaut. Acta, Vol. 4, No. 4. 1958.

8.11. Miele, A. and J.O. Cappellari. Topics in Dynamic Programming for Rockets.— Z. Flugwiss, Vol. 7, No. 1. 1959.

8.12. Breakwell, J.V. The Optimization of Trajectories.— J. Soc. Indust. Appl. Math., No. 7. 1959.

8.13. Leitmann, G. On a Class of Variation Problems in Rocket Flight.— JASS, Vol. 26, No. 8. 1959.

8.14. Leitmann, G. Extremal Rocket Trajectories in Position and Time Dependent Force Fields.— VII Ann. Meet. Amer. Astronaut. Soc., No. 30. 1961.

8.15. Leitmann, G. On a Class of Variational Problems in Rocket Flight.— J. Aerospace Sci., Vol. 26, pp. 586—591. 1959.

8.16. Isaev, V.K. Printsip maksimuma L.S. Pontryagina i optimal'noe programmirovanie tyagi raket (L.S. Pontryagin's Maximum Principle and the Optimum Programming of the Thrust of Rockets).— Avtomatika i Telemekhanika, Vol. 22, No. 8. 1961; Vol. 23, No. 1. 1962.

8.17. Isaev, V.K. Dopolnenie k rabote "Printsip maksimuma L.S. Pontryagina i optimal'noe programmirovanie tyagi raket" (Supplement to the Paper "L.S. Pontryagin's Maximum Principle and Optimum Programming of the Rocket Thrust").— Avtomatika i Telemekhanika, Vol. 23, No. 1. 1962.

8.18. Leitmann, G. The Optimization of Rocket Trajectories. A Survey.— Progr. in Astronaut. Sci., Vol. 1. Amsterdam. 1962.
8.19. Lawden, D.F. Optimal Intermediate-Thrust Arcs in a Gravitational Field.— Astronaut. Acta, No. 8. 1962.
8.20. Contensou, P. Étude théoretique des trajectories optimales dans un champ de gravitation.— Astronaut. Acta, No. 8. 1962.
8.21. Miele, A. The Calculus of Variations in Applied Aerodynamics and Flight Mechanics. Optimization Techniques with Applications to Aerospace Systems, ed. by Leitman, G.— New York-London, Acad. Press. 1962.
8.22. Kuzmak, G.E., V.K. Isaev, and B.Kh. Davidson. Optimal'nye rezhimy dvizheniya tochki peremennoi massy v odnorodnom tsentralnom pole (Optimum Regimes of Motion of a Varying Point Mass in a Homogeneous Central Field).— Doklady AN SSSR, Vol. 149, No. 1. 1963.
8.23. Lur'e, A.I. Upravlenie tyagoi v tsentral'nom pole tyagoteniya (Thrust Control in a Central Gravitational Field).— Vtoroi Vsesoyuznyi s"ezd po teoreticheskoi i prikladnoi mekhanike, 1964. Annotatsii i doklady. Moskva. 1964.
8.24. Diamandiev, V. and K. Todorov. Optimalni traektorii pri reaktivnogo dvizhenie (Optimum Trajectories in Jet-Propelled Motion).— Godishnik Sofiiskogo Universiteta, Matem. Fak., 57. 1962—1963 (1964).
8.25. Keller, J.L. On Minimum Propellant Paths for Thrust-Limited Rockets.— Astronaut. Acta, Vol. 10, Nos. 3—4. 1964.
8.26. Pines, S. Constants of the Motion for Optimum Thrust Trajectories in a Central Force Field.— AIAA J., Vol. 2, No. 11. 1964.
8.27. Veubeke, B.F. and J. Geerts. Application du principe de maximum à la syntèse des transferts optimaux dans un champ de gravitation planétaire.— Proc. XV Internat. Astronaut. Congr. 1964. Warsaw. 1965.
8.28. Novoselov, V.S. Teoriya priblizhennogo resheniya variatsionnykh zadach i ee prilozhenie k issledovaniyu dvizheniya tochki peremennoi massy (Theory of the Approximate Solution of Variational Problems and Its Application to the Motion of a Varying Point Mass).— Vestnik Leningradskogo Universiteta, No. 1. 1965.
8.29. Novoselov, V.S. Analiticheskaya dinamika i optimal'nye perelety (Analytical Dynamics and Optimum Transfers).— Trudy 2 Vsesoyuznogo s"ezda po teoreticheskoi i prikladnoi mekhanike. 1964; Obzor nauchnykh dokladov, No. 1, Nauka. Moskva. 1965.
8.30. Cavoti, C.R. Optimization of Multistage Processes.— J. Spacecraft and Rock., Vol. 2, No. 1. 1965.
8.31. Lubowe, A.G. Application of Dynamic Programming to the Optimum Staging of Rockets.— J. Spacecraft and Rock., Vol. 2, No. 1. 1965.
8.32. Gurley, I.G. Optimal-Thrust Trajectories in an Arbitrary Gravitational Field.— J. Soc. Industr. and Appl. Math., Ser. A, Vol. 2, No. 3. 1965.
8.33. Robbins, H.M. Optimality of Intermediate Thrust Arcs of Rocket Trajectories.— AIAA J., Vol. 3, No. 6. 1965.
8.34. Cavoti, C.R. Method of Characteristic Constants and Retrothrust Optimality in a Gravitational Field. Necessary and Sufficient Conditions.— J. Franklin Inst., Vol. 279, No. 3. 1965.

8.35. Bell, D.I. Optimal Trajectories and the Accessory Minimum Problem.— Aeronaut. Quart., Vol.16, No.3. 1965.
8.36. Gurman, V.I. Ob optimal'nykh traekotriyakh reaktivnogo apparata v tsentral'nom pole (Optimum Trajectories of a Rocket Vehicle in a Central Field).— Kosmicheskie Issledovaniya, Vol.3, No.3. 1965.
8.37. Gorelov, Yu.A. K teorii ekstremal'nykh dvizhenii tochki peremennoi massy v tsentral'nom gravitatsionnom pole (Theory of Extremal Motions of a Varying Point Mass in a Central Gravitational Field).— Inzhenernyi Zhurnal, Vol.5, No.3. 1965.
8.38. Troitskii, V.A. Optimizatsiya dvizheniya dvukhstupenchatoi rakety (Optimization of the Motion of a Two-Stage Rocket).— Prikladnaya Matematika i Mekhanika, Vol.29, No.4. 1965.
8.39. Mil'shtein, G.N. Ob optimal'nom osushchestvlenii traektorii (Optimum Execution of Trajectories).— Avtomatika i Telemekhanika, Vol.26, No.4. 1965.
8.40. Isaev, V.K. O nekotorykh osobennostyakh variatsionnoi zadachi Maiera v raketodinamike (Some Features of Mayer's Variational Problem in Rocket Dynamics).— Avtomatika i Telemekhanika, Vol.26, No.7. 1965.
8.41. Litovchenko, I.A. Optimizatsiya sistem pri stupenchatykh ogranicheniyakh na upravlenie (System Optimization Under Step Constraints on the Control Variables).— Avtomatika i Telemekhanika, Vol.26, No.8. 1965.
8.42. Bolonkin, A.A. Optimizatsiya traektorii mnogostupenchatykh letatel'nykh apparatov (Trajectory Optimization of Multistaged Flying Vehicles).— In: Sbornik "Issledovaniya po dinamike poleta," No.1, Mashinostroenie, Moskva. 1965.
8.43. Kopp, R.E. and H.G. Moyer. Necessary Conditions for Singular Extremals).— AIAA J., Vol.3, No.8. 1965.
8.44. Marec, J.P. Transferts orbitaux economiques (orbites élliptiques, coplanaires coaxiales).— Rech. Aérospatiale, No.105. 1965.
8.45. Grodzovskii, G.L. Nekotorye variatsionnye zadachi mekhaniki kosmicheskogo poleta (Some Variational Problems of Spaceflight Mechanics).— Mekhanika Tverdogo Tela (Inzhenernyi Zhurnal), AN SSSR, No.6. 1968.
8.46. Malina, F.I. and A.M. Smith. Flight Analysis of the Sounding Rocket.— IAS, Vol.5, No.5. 1938.
8.47. Okhotsimskii, D.E. O pod'eme rakety v vozdukhe na maksimal'nuyu vysotu (The Climb of a Rocket in Air to a Maximum Altitude).— Prikladnaya Matematika i Mekhanika, Vol.10, No.6. 1946.
8.48. Beletskii, V.V. O vertikal'nom pod'eme tochki peremennoi massy v srede postoyannoi plotnosti (Vertical Climb of a Varying Point Mass in a Medium of Uniform Density).— Prikladnaya Matematika i Mekhanika, Vol.20, No.6. 1956.
8.49. Miele, A. Generalized Variational Approach to the Optimum Thrust Programming for the Vertical Flight of a Rocket.— Z. Flugwiss., Vol.6, No.3. 1958.
8.50. Leitmann, G. An Elementary Derivation of the Optimum Control Conditions.— Proc. XII Internat. Astronaut. Congr. 1961. Vien. 1962.

8.51. Barrère, M., A. Jaumotte, B.F. Veubeke, J. Vandenkerckove. Rocket Propulsion.— Amsterdam-London-New York, Elsevier Publ. Co. 1960.

8.52. Isaev, V.K., A.I. Kur'yanov, and V.V. Sonin. Primenenie printsipa maksimuma v raketodinamike (Application of the Maximum Principle in Rocket Dynamics).— Proc. XIV Internat. Astronaut. Congr. 1963. Warsaw. 1964.

8.53. Miele, A. Flight Mechanics, Vol. 1. Massachusetts-London. 1963.

8.54. Munick, H. Goddard Problem with Bounded Thrust.— AIAA J., Vol. 3, No. 7. 1965.

8.55. Edelbaum, T.N. The Use of High- and Low-Thrust Propulsion in Combination for Space Missions.— Amer. Astron. Soc., prep. 61—104. 1961.

8.56. Ivanov, Yu.N. Optimal'noe sochetanie dvigatel'nykh sistem (Optimum Combination of Propulsion Systems).— Izvestiya AN SSSR, Mekhanika i Mashinostroenie, No. 2. 1964.

8.57. Fimple, W.R. An Improved Theory of the Use of High- and Low-Thrust Propulsion in Combination.— J. Astronaut. Sci., Vol. 10, No. 10. 1963.

8.58. Il'in, V.A. K raschetu traektorii pereleta kosmicheskikh apparatov mezhdu komplanarnymi krugovymi orbitami v n'yutonianskom gravitatsionnom pole (Calculating the Transfer Trajectories of Space Vehicles Between Coplanar Circular Orbits in a Newtonian Gravitational Field).— Kosmicheskie Issledovaniya, Vol. 2, No. 5. 1964.

Chapter Nine

9.1. Linhardt, H.D. Comparison of Solar-Thermal and Solar-Electric-Thermal Propulsion Methods.— IAS Paper, No. 63—20. 1963.

9.2. Camac, M. Use of Energy Storage in Low-Thrust Spaceflight.— J. Amer. Rock. Soc., Vol. 30, No. 1. 1960.

9.3. Grodzovskii, G.L., B.N. Kiforenko, and V.V. Tokarev. Nakopitel' energii v zadachakh optimizatsii dvizheniya s ogranichennoi moshchnost'yu (Energy Accumulator in Optimization Problems of Power-Limited Motion).— Izvestiya AN SSSR, Mekhanika, No. 3. 1965; cf. also Proc. XVI Internat. Astronaut. Congr. 1965. Warsaw. 1966.

9.4. Pontryagin, L.S., V.G. Boltyanskii, R.V. Gamkrelidze, and E.F. Mishchenko. Matematicheskaya teoriya optimal'nykh protsessov (Mathematical Theory of Optimum Processes).— Moskva, Fizmatgiz. 1961.

9.5. Kiforenko, B.N. K vyboru optimal'nykh parametrov dvigatel'noi ustanovki v zadachakh optimizatsii dvizheniya s ogranichennoi moshchnost'yu i nakopitelem energii (Selection of the Optimum Parameters of the Propulsion System in Optimization Problems of Power-Limited Motion with Energy Accumulation).— Izvestiya AN SSSR, Mekhanika, No. 3. 1966.

9.6. Krotov, V.F. Metody resheniya variatsionnykh zadach (Methods of Solving Variational Problems), Part 2.— Avtomatika i Telemekhanika, Vol. 24, No. 5. 1963.

9.7. Kiforenko, B.N. Nekotorye zadachi optimizatsii dvizheniya s ogranichennoi moshchnost'yu i nakopitelem energii (Some Problems of Optimizing a Power-Limited Motion with Energy Accumulation).— Mekhanika Tverdogo Tela (Inzhenernyi Zhurnal), No. 5. 1966.

9.8. Ivanov, Yu.N. O dvizhenii tela peremennoi massy s ogranichennoi moshchnost'yu izadannym aktivnym vremenem (Motion of a Limited-Power Body of Varying Mass with Specified Operating Time).— Prikladnaya Matematika i Mekhanika, Vol. 27, No. 5. 1963.

9.9. Kiforenko, B.N. O dvizhenii po orbitam, blizkim k krugovym, pri ispol'zovanii dvigatel'noi sistemy s nakopleniem energii i dvizhitelem postoyannoi moshchnosti (Motion Along Quasi-Circular Orbits Using a Propulsion System With Energy Accumulation and Constant-Power Engine).— Mekhanika Tverdogo Tela (Inzhenernyi Zhurnal), No. 2. 1967.

9.10. Grodzovskii, G.L. and B.N. Kiforenko. O dvizhenii tela peremennoi massy s nakopleniem energii i dvizhitelem s organichennoi skorost'yu istecheniya reaktivnoi strui (Motion of a Body of Varying Mass with Energy Accumulation and Engines of Limited Exhaust Velocities), Part 2.— Proc. XVII Internat. Astronaut. Congr. 1966. Warsaw. 1967.

9.11. Demetriades, S.T. A Novel System for Spaceflight Using a Propulsive Fluid Accumulator.— J. Brit. Interpl. Soc., Vol. 17, No. 5. 1959.

9.12. Berner, F. and M. Camac. Air Scooping Vehicle.—Air Force Ballistic Missile Div., TR 59-17. 1959.

9.13. Demetriades, S.T. Orbital Propulsion System for Space Maneuvering (PROFAC).— Astronaut. Sci. Rev., Vol. 1, No. 4. 1959.

9.14. Demetriades, S.T. Preliminary Study of Propulsive Fluid Accumulator Systems.— Proc. XI Internat. Astronaut. Congr. 1960. Vien. 1961.

9.15. French, E.P. Operation of an Electric Ramjet in a Planetary Atmosphere.— Prepr. Techn. Ses. Amer. Astronaut. Soc., No. 90. 1960.

9.16. Camac, M. and F. Berner. An Orbital Air-Scooping Vehicle.— Astronautics, Vol. 6, No. 8. 1961.

9.17. Reichel, R.H., T.L. Smith, and D.R. Handord. Potentialities of Air-Scooping Electrical Space Propulsion Systems.— Progr. in Astronaut. and Aeronaut., Vol. 9, Electric. Prop. Devel. New York. 1963.

9.18. Tokarev, V.V. and Yu.M. Fatkin. Nakopitel' rabochego veshchestva v zadachakh optimizatsii dvizheniya s ogranichennoi moshchnost'yu (Working Fluid Accumulator in Optimization Problems of Power-Limited Motion).— Inzhenernyi Zhurnal AN SSSR, Vol. 5, No. 3. 1965.

9.19. Fatkin, Yu.M. Vybor optimal'nogo zakona upravleniya tyagoi v zadache dvizheniya v rezhime nakopleniya massy (Selecting the Optimum Thrust Control Law in the Problem of Motion in the Mass-Accumulation Regime).— Mekhanika Tverdogo Tela (Inzhenernyi Zhurnal), No. 1. 1967.

9.20. Grodzovskii, G.L. Nekotorye variatsionnye zadachi mekhaniki kosmicheskogo poleta (Some Variational Problems of Spaceflight Mechanics).— Mekhanika Tverdogo Tela (Inzhenernyi Zhurnal), AN SSSR, No. 6. 1968.

9.21. Tsander, F.A. Ob ispol'zovanii sily davleniya sveta dlya poletov v mezhplanetnom prostranstve (Using Light Pressure Force in Interplanetary Spaceflight). 1924—1925. Cf. Tsander, F.A. Problema poleta pri pomoshchi reaktivnykh apparatov (The Problem of Jet-Propelled Flight).— Mezhplanetnye puteshestviya, Moskva, Oborongiz. 1961.

9.22. Tsu, T.C. Interplanetary Travel by Solar Sail.— J. Amer. Rock. Soc., Vol.29, No.6. 1959.

9.23. Tsu, T.C. Straight-Line Flight to Mars.— Proc. VI Ann. Meet. Amer. Astronaut. Soc., 1960, Adv. Astronaut Sci., Vol.6. New York. 1961.

9.24. London, H.S. Some Exact Solution of the Equation of Motion of Solar Sail with Constant Sail Setting.— J. Amer. Rock. Soc., Vol.30, No.2. 1960.

9.25. Pozzi, A. Su un metodo di soluzionne del problema della vela solare.— Missile, Vol.3, No.6. 1961.

9.26. Pozzi, A. and L. Socio. Some Remarks on Solar Sail.— J. Amer. Rock. Soc., Vol.31, No.8. 1961.

9.27. Socio, L. La navigazione con vela solare.— Missili, Vol.3, No.3. 1961.

9.28. Kelley, H.J. Gradient Theory of Optimum Flight Paths.— J. Amer. Rock. Soc., Vol.30, No.10. 1960.

9.29. Zhukov, A.N. and V.N. Lebedev. Variatsionnaya zadacha o perelete mezhdu geliotsentricheskimi krugovymi orbitami s pomoshch'yu solnechnogo parusa (The Variational Problem of Transfer Between Heliocentric Circular Orbits by Means of a Solar Sail).— Kosmicheskie Issledovaniya, Vol.2, No.1. 1964.

9.30. Sands, N. Escape from Planetary Gravitational Fields by Use of Solar Sails.— J. Amer. Rock. Soc., Vol.31, No.4. 1961.

9.31. Fimple, W.R. A Generalized Three-Dimensional Trajectory Analysis of Planetary Escape by Solar Sail.— J. Amer. Rock. Soc., Vol.32, No.6. 1962.

9.32. Perkins, F.M. Flight Mechanics of Low-Thrust Spacecraft.— JASS, Vol.26, No.5. 1959; Vistas in Astronaut., Vol.2. New York. 1959.

9.33. Valeev, K.G. Kachestvennoe issledovanie differentsial'nykh uravnenii poleta pri pomoshchi solnechnogo parusa (Qualitative Study of the Differential Equations of Solar-Sail Flight).— Prikladnaya Matematika i Tekhnicheskaya Fizika, No.2. 1964.

9.34. Ilyutovich, A.E. Optimal'nyi perelet s dvigatelem, ispol'zuyushchim solnechnuyu energiyu (Optimum Transfer with an Engine Using Solar Energy).— Kosmicheskie Issledovaniya, Vol.4, No.6. 1966.

9.35. Ovsyannikov, R.N. and L.N. Semenova. O dvizhenii tela peremennoi massy s eksponentsial'no ubyvayushchei moshchnost'yu reaktivnoi strui (Motion of a Body of Varying Mass with Exponentially Decreasing Jet Power).— Mekhanika Tverdogo Tela (Inzhenernyi Zhurnal), No.4. 1966.

Chapter Ten

10.1. Tokarev, V.V. Nekotorye voprosy nadezhnosti v zadachakh optimal'nogo upravleniya (Some Reliability Questions in Optimum Control Problems).— Prikladnaya Matematika i Mekhanika, Vol.30, No.2. 1967.

10.2. Tokarev, V.V. K vyboru parametrov dinamicheskoi sistemy, universal'noi dlya zadannogo klassa manevrov (Selecting the Parameters of a Universal Dynamic System for a Given Class of Maneuvers).— Izvestiya AN SSSR, Mekhanika i Mashinostroenie, No.5. 1964; Proc. XVI Internat. Astronaut. Congr. 1965. Warsaw. 1966.

10.3. Tokarev, V.V. and Yu.M. Fatkin. Igrovoi pedkhod k zadache vybora optimal'nykh parametrov dinamicheskoi sistemy (The Game Approach to the Problem of Selecting the Optimum Parameters of a Dynamic System).— Mekhanika Tverdogo Tela (Inzhenernyi Zhurnal), No.6. 1966.

10.4. Avramchenko, R.F. and V.V. Tokarev. Zapas rabochego veshchestva, optimal'nyi dlya vypolneniya zadannogo manevra pri fiksirovannykh parametrakh dvigatel'noi sistemy (Optimum Working-Fluid Stock for Executing a Specified Maneuver with Fixed Propulsion System Parameters).— Kosmicheskie Issledovaniya, Vol.5, No.1. 1967.

10.5. Venttsel', E.S. Elementy teorii igr (Elements of the Theory of Games).— Moskva, Fizmatgiz. 1959.

10.6. McKinsey, J.C.C. Introduction to the Theory of Games.— McGraw-Hill. 1952.

10.7. Teoriya igr. Beskonechnye antagonisticheskie igry (Theory of Games: Infinite Antagonistic Games).— Col. edited by Vorob'ev, N.N.— Moskva, Fizmatgiz. 1963.

10.8. Dresher, M. Games of Strategy; Theory and Applications.— Prentice-Hall. 1961.

Chapter Eleven

11.1. Tokarev, V.V. Vliyanie sluchainykh protsessov umen'sheniya moshchnosti na dvizhenie tela peremennoi massy v gravitatsionnom pole (Influence of Random Power-Drop Processes on the Motion of a Body of Varying Mass in a Gravitational Field).— Prikladnaya Matematika i Mekhanika, Vol.26, No.4. 1962.

11.2. Grodzovskii, G.L., Yu.N. Ivanov, and V.V. Tokarev. O dvizhenii tela peremennoi massy s postoyannoi i ubyvayushchei zatratoi moshchnosti v gravitatsionnom pole, ch.2 (Motion of a Body of Varying Mass with Constant, Decreasing Power Expenditure in a Gravitational Field, Part 2).—Proc. XIII Internat. Astronaut. Congr. 1962, Vien-New York. 1964.

11.3. Grodzovskii, G.L., Yu.N. Ivanov, and V.V. Tokarev. Mekhanika kosmicheskogo poleta s maloi tyagoi (Mechanics of Low-Thrust Spaceflight), III.—Inzhenernyi Zhurnal AN SSSR, Vol.4, No.1. 1964.

11.4. Tokarev, V.V. Nekotorye voprosy nadezhnosti v zadachakh optimal'nogo upravleniya (Some Reliability Questions in Optimum Control Problems).— Prikladnaya Matematika i Mekhanika, Vol.30, No.1. 1967.

11.5. Khinchin, A.Ya. Matematicheskie metody teorii massovogo obsluzhivaniya (Mathematical Methods of the Theory of Mass Conservation).— Moskva, Fizmatgiz. 1963.
11.6. Gnedenko, B.V. Kurs teorii veroyatnostei (A Course on the Theory of Probability).— Nauka, Moskva. 1965.
11.7. Polovko, A.M. Osnovy teorii nadezhnosti (Fundamentals of the Theory of Reliability).— Nauka, Moskva. 1964.
11.8. Gnedenko, B.V., Yu.K. Belyaev, and A.D. Solov'ev. Matematicheskie metody v teorii nadezhnosti (Mathematical Methods in the Theory of Reliability).— Nauka, Moskva. 1965.
11.9. Edelbaum, T.N. Multi-Engine Reliability for Electric Propulsion Systems.— ARS Prepr. 2388—62. 1962.
11.10. Pinkel, B. Electrical Propulsion for Space: Mission Comparison, Development Cost, Reliability, and Their Implications for Planning.— The Rand Corp. Rep. RM-4056-NASA. 1963.
11.11. Ragsac, R.V. Study of Low-Acceleration Space Transportation Systems.— United Aircraft Corp. Research Labor. Rep. D-910262-3. 1965.

Chapter Twelve

12.1. Lur'e, A.I. Nekotorye nelineinye zadachi teorii avtomaticheskogo regulirovaniya (Some Nonlinear Problems of the Theory of Automatic Control).— Moskva, Gostekhizdat. 1951.
12.2. Kamenkov, G.V. Ob ustoichivosti dvizheniya na konechnom intervale vremeni (Motion Stability During a Finite Time Interval).— Prikladnaya Matematika i Mekhanika, Vol.17, No.5. 1953.
12.3. Galiullin, A.S. Ob odnoi zadache ustoichivosti dvizheniya tyazheloi tochki peremennoi massy na konechnom intervale vremeni (A Problem of Motion Stability of a Heavy Varying Point Mass During a Finite Time Interval).— Trudy Kazanskogo Aviatsionnogo Instituta, No.28. 1953.
12.4. Pugachev, V.S. Teoriya sluchainykh funktsii i ee primenenie k zadacham avtomaticheskogo upravleniya (Theory of Random Functions and Its Application to Problems of Automatic Control).— Moskva, Gostekhizdat. 1957.
12.5. Laning, J.H. and R.H. Battin. Random Processes in Automatic Control.— McGraw-Hill. 1956.
12.6. Krasovskii, N.N. Nekotorye zadachi teorii ustoichivosti dvizheniya (Some Problems of the Theory of Motion Stability).— Moskva, Fizmatgiz. 1959.
12.7. Galiullin, A.S. Ob ustoichivosti dvizheniya tyazheloi tochki peremennoi massy (Motion Stability of a Heavy Varying Point Mass).— Trudy Kazanskogo Aviatsionnogo Instituta, No.35. 1959.
12.8. Barbashin, E.A. Ob otsenke srednekvadratichnogo znacheniya otkloneniya ot zadannoi traektorii (The Assessment of the Mean-Square Deviation from the Nominal Trajectory).— Avtomatika i Telemekhanika, Vol.21, No.7. 1960.

12.9. Barbashin, E.A. Ob otsenke maksimuma otkloneniya ot zadannoi traektorii (The Assessment of the Maximum Deviation from the Nominal Trajectory).— Avtomatika i Telemekhanika, Vol. 21, No. 10. 1960.

12.10. Kats, I.Ya. and N.N. Krasovskii. Ob ustoichivosti sistem so sluchainymi parametrami (The Stability of Systems with Random Parameters).— Prikladnaya Matematika i Mekhanika, Vol. 24, No. 5. 1960.

12.11. Solodovnikov, V.V. Statisticheskaya dinamika lineinykh sistem avtomaticheskogo upravleniya (Statistical Dynamics of Automatic-Control Linear Systems).— Moskva, Fizmatgiz. 1960.

12.12. Breakwell, J.V. Fuel Requirements for Crude Interplanetary Guidance.— Adv. in Astronaut. Sci., Vol. 5. New York, Plenum Press. 1960.

12.13. Kalman, R.E. A New Approach to Linear Filtering and Prediction Problems.— J. of Basic Eng., Vol. 82, pp. 35—45. 1960.

12.14. Lawden, D.F. Optimal Program for Correctional Maneuvers.— Astronaut. Acta, Vol. 6, Nos. 1, 4. 1960.

12.15. Minneman, M.J. Application of Inertial Techniques to Interplanetary Navigation.— Conf. Proc. IV Nat. Convention on Military Electronics, Washington. 1960.

12.16. Renaudin, D. Principes du guidance.— Journées d'Information Astronaut., Vol. 1. 1960.

12.17. Stearns, E.V. Guidance for Interplanetary Landings.— Techn. Session prepr. AAS, No. 11. 1960.

12.18. Zaborszky, J. and J.M. Diesel. Investigation of the Feasibility of Designing Homing Aircraft Flight Control Systems for Minimum Probabilistic Error.— Applications and Industry, No. 48. 1960.

12.19. Al'brekht, E.G. Ob optimal'noi stabilizatsii nelineinykh sistem (Optimum Stabilization of Nonlinear Systems).— Prikladnaya Matematika i Mekhanika, Vol. 25, No. 5. 1961.

12.20. Barbashin, E.A. O priblizhennom osushchestvlenii dvizheniya po zadannoi traektorii (The Approximate Execution of Motion Along a Specified Trajectory).— Avtomatika i Telemekhanika, Vol. 22, No. 6. 1961.

12.21. Bodner, V.A. Teoriya avtomaticheskogo upravleniya poletom (Theory of Automatic Flight Guidance).— Izdatel'stvo, Nauka. 1964.

12.22. Kirillova, F.M. K zadache ob analiticheskom konstruirovanii regulyatorov (The Problem of the Analytic Design of Control Systems).— Prikladnaya Matematika i Mekhanika, Vol. 25, No. 3. 1961.

12.23. Krasovskii, N.N. and E.A. Lidskii. Analiticheskoe konstruirovanie regulyatorov v stokhasticheskikh sistemakh pri ogranicheniyakh na skorost' izmeneniya upravlyayushchego vozdeistviya (Analytic Design of Controls in Stochastic Systems in the Case of Constrained Rate of Variation of the Control Parameter).— Prikladnaya Matematika i Mekhanika, Vol. 25, No. 3. 1961.

12.24. Krasovskii, N.N. O srednekvadratichnoi optimal'noi stabilizatsii pri sluchainykh zatukhayushchikh vozmushcheniyakh (Optimum Mean-Square

Stabilization for Random-Damped Perturbations).— Prikladnaya Matematika i Mekhanika, Vol. 25, No. 5. 1961.

12.25. Krasovskii, N.N. and E.A. Lidskii. Analiticheskoe konstruirovanie regulyatorov v sistemakh so sluchainymi svoistvami (Analytic Design of Control Systems with Random Properties).— Avtomatika i Telemekhanika, Vol. 22, Nos. 9—11. 1961.

12.26. Kurzweil, J. Analytic Design of Control Systems.— Automat. Remote Control, Vol. 22, pp. 593—599. 1961.

12.27. Letov, A.N. Analiticheskoe konstruirovanie regulyatorov (Analytic Design of Controls).— Avtomatika i Telemekhanika, Vol. 21, Nos. 4/6. 1960; Vol. 22, No. 4. 1961; Vol. 23, No. 11. 1962.

12.28. Lidskii, E.A. O stabilizatsii stokhasticheskikh sistem (Stabilization of Stochastic Systems).— Prikladnaya Matematika i Mekhanika, Vol. 25, No. 5. 1961.

12.29. Litovchenko, I.A. K isoperometricheskoi zadache analiticheskogo konstruirovaniya optimal'nogo regulyatora (The Isoperimetric Problem of Analytic Design of an Optimum Control).— Avtomatika i Telemekhanika, Vol. 22, No. 12. 1964.

12.30. Popov, V.M. Ob absolyutnoi ustoichivosti nelineinykh sistem avtomaticheskogo regulirovaniya (The Absolute Stability of Nonlinear Automatic Control Systems).— Avtomatika i Telemekhanika, Vol. 22, No. 8. 1961.

12.31. Salukvadze, M.E. Analiticheskoe konstruirovanie regulyatorov. Postoyanno desitvuyushchie vozmushcheniya (Analytic Design of Controls. Continuously Acting Perturbations).— Avtomatika i Telemekhanika, Vol. 22, No. 10. 1961.

12.32. Battin, R.H. and J.H. Laning. A Navigation Theory for Roundtrip Reconnaissance to Venus and Mars.— Proc. 4th AFMD/STL Symp. Adv. in Ballistic Missile and Space Technol., Vol. 3. 1961.

12.33. Breakwell, J.V. The Spacing of Corrective Thrusts in Interplanetary Navigation.— Techn. Session Prepr. Amer. Astronaut. Soc., No. 76. 1960; Adv. in Astronaut. Sci., Vol. 7. New York, Plenum Press. 1961.

12.34. Bryson, A.E. and W. Denham. Multivariable Terminal Control for Minimum Mean-Square Deviation from a Nominal Path.— Rept. BR-133, Missile and Space Div., Raytheon Co., Bedford, Mass. 1961.

12.35. Wiener, N. Nonlinear Problems in Random Theory.— Mass. Inst. of Techn.; Wiley. 1958; Chapman. 1959.

12.36. Friedlander, A.L. and D.P. Harry. A Study of Statistical Data-Adjustment and Logic Techniques as Applied to the Interplanetary Midcourse Guidance Problem.— NASA TRR-113, Washington. 1961.

12.37. Kalman, R.E. New Methods and Results in Linear Prediction and Filtering Theory.— RIAS, Techn. Rep., No. 1. 1961.

12.38. Kalman, R.E. and R.S. Bucy. New Results in Linear Filtering and Prediction Theory.— J. of Basic Eng., Vol. 83, pp. 95—108. 1961.

12.39. Kalman, R.E. Physical and Mathematical Mechanisms of Instability in Nonlinear Automatic Control Systems.— Trans. ASME, Vol. 79, pp. 553—563. 1957.

12.40. Pfeiffer, C.G. Guidance for Space Missions.— Current Research in Astronaut. Sci., Oxford. 1961.
12.41. Scull, J.R. Guidance of Space Vehicles.— Navigation, Vol.8, No.1. 1961.
12.42. Kostychev, G.I. Ob optimal'nom programmirovanii v sluchae razlichnykh uslovii realizatsii protsessa (Optimum Programming Under Different Conditions of Executing a Maneuver).— Izvestiya Vysshikh Uchebnykh Zavedenii, Seriya Aviatsionnaya Tekhnika, No.2. 1962.
12.43. Krasovskii, N.N. Ob analiticheskom konstruirovanii optimal'nogo regulyatora v sisteme s zapazdyvaniem vremeni (The Analytic Design of an Optimum Control System with Time Lag).— Prikladnaya Matematika i Mekhanika, Vol.26, No.1. 1962.
12.44. Krasovskii, N.N. Ob odnoi zadache presledovaniya (Interception Problem).— Prikladnaya Matematika i Mekhanika, Vol.26, No.2. 1962.
12.45. Krasovskii, N.N. and A.M. Letov. K teorii analiticheskogo konstruirovaniya regulyatorov (The Theory of the Analytic Design of Control Systems).— Avtomatika i Telemekhanika, Vol.23, No.6. 1962.
12.46. Letov, A.M. Ustoichivost' nelineinykh reguliruemykh sistem (Stability of Nonlinear Controlled Systems).— Moskva, Fizmatgiz. 1962.
12.47. Lidskii, E.A. Ob analiticheskom konstruirovanii regulyatorov v sistemakh so sluchainymi svoistvami (Analytic Design of Control Systems with Random Properties).— Prikladnaya Matematika i Mekhanika, Vol.26, No.2. 1962.
12.48. Salukvadze, M.E. K zadache sinteza optimal'nogo regulyatora v lineinykh sistemakh s zapazdyvaniem, podverzhennykh postoyanno deistvuyushchim vozmushcheniyam (The Problem of Synthesizing an Optimum Linear Control System with Lag, Subjected to Continuously Acting Perturbations).— Avtomatika i Telemekhanika, Vol.23, No.12. 1962.
12.49. Salukvadze, M.E. Ob analiticheskom konstruirovanii regulyatora pri postoyanno deistvuyushchikh vozmushcheniyakh (Analytic Design of a Control System Under Continuously Acting Perturbations).— Avtomatika i Telemekhanika, Vol.23, No.6. 1962.
12.50. Chang Jên-Wei. K zadache sinteza optimal'nogo regulyatora v sistemakh s zapazdyvaniem (The Problem of Synthesizing Optimum Control Systems with Lag).— Avtomatika i Telemekhanika, Vol.22, No.10. 1962.
12.51. A Study of Interplanetary Transportation Systems by S.E. Ross.— Lockheed Missiles and Space Comp. Rept., 3-17-62-1. 1962.
12.52. Bellman, R., I. Glicksberg, and O. Gross. Some Aspects of the Mathematical Theory of Control Processes.— Rand Corporation. California. 1958.
12.53. Breakwell, J.V. The Optimum Spacing of Corrective Thrusts in Interplanetary Navigation. Optimization Techniques with Application to Aerospace Systems. New York, Acad. Press. 1962.
12.54. Bryson, A. and W. Denham. A Guidance Scheme for Supercircular Reentry of a Lifting Vehicle.— ARS J., Vol.32, No.6. 1962.

12.55. Kalman, R.E. Control of Randomly Varying Linear Dynamical Systems.— Proc. of Symp. in Appl. Math., Vol. 13. 1962.
12.56. Kelley, H.J. Guidance Theory and Extremal Fields.— Inst. Radio Engrs. Natl. Aerospace Electronics Conf., Dayton, Ohio. 1962; Inst. Radio Engrs. Trans., Auto Control, AC-7, pp. 75—81. 1962.
12.57. Leach, R. and G.E. Townsend. Guidance and Control Requirements.— Design Guide to Orbital Flight. New York, Acad. Press. 1962.
12.58. Peske, A. and M. Ward. Techniques for Error Analysis of Trajectories.— Guidance and Control. New York-London, Acad. Press. 1962.
12.59. Rosenbloom, A. Orbital Rendezvous Systems.— Navigation, Vol. 9, No. 4. 1962—1963.
12.60. Akim, E.L. and T.M. Eneev. Opredelenie parametrov dvizheniya kosmicheskogo letatel'nogo apparata po dannym traektornykh izmerenii (Determining Motion Parameters of a Spacecraft Using Trajectory Measurements).— Kosmicheskie Issledovaniya, Vol. 1, Nos. 1, 3. 1963.
12.61. Gal'perin, E.A. and N.N. Krasovskii. O stabilizatsii ustanovivshikhsya dvizhenii nelineinykh upravlyaemykh sistem (The Stabilization of Steady-State Motions of Nonlinear Guided Systems).— Prikladnaya Matematika i Mekhanika, Vol. 27, No. 6. 1963.
12.62. Grodzovskii, G.L., Yu.N. Ivanov, and V.V. Tokarev. O dvizhenii tela peremennoi massy s postoyannoi i ubyvayushchei zatratoi moshchnosti v gravitatsionnom pole, ch. 3 (Motion of a Body of Varying Mass with Constant, Decreasing Power Expenditure in a Gravitational Field, Part 3).— Proc. XIV Internat. Astronaut. Congr. 1963. Warsaw. 1964.
12.63. Zaitsev, A.G. Analiticheskoe konstruirovanie optimal'nykh regulyatorov pri sluchainykh vozmushcheniyakh (Analytic Design of Optimum Regulators Under Random Perturbations).— Avtomatika i Telemekhanika, Vol. 24, No. 4. 1963.
12.64. Kirillova, L.S. Zadacha ob optimizatsii konechnogo sostoyaniya reguliruemoi sistemy (The Problem of Optimizing the Terminal State of a Guided System).— Avtomatika i Telemekhanika, Vol. 23, No. 12. 1962; Vol. 24, Nos. 8, 9. 1963.
12.65. Krasovskii, N.N. O stabilizatsii neustoichivykh dvizhenii dopolnitel'nymi silami pri nepolnoi obratnoi svyazi (Stabilizing Unstable Motions by Additional Forces, in the Case of Incomplete Feedback).— Prikladnaya Matematika i Mekhanika, Vol. 27, No. 4. 1963.
12.66. Lidskii, E.A. Optimal'noe regulirovanie sistem so sluchainymi svoistvami (Optimum Control of Systems with Random Properties).— Prikladnaya Matematika i Mekhanika, Vol. 27, No. 1. 1963.
12.67. Lur'e, A.I. Minimal'nyi kvadratichnyi kriterii kachestva reguliruemoi sistemy (Minimum-Square Criterion of the Performance of a Controlled System).— Tekhnicheskaya Kibernetika, No. 4. 1963.
12.68. Roitenberg, Ya.N. Nekotorye zadachi upravleniya dvizheniem (Some Problems of Motion Guidance).— Moskva, Fizmatgiz. 1963.
12.69. Tokarev, V.V. Vliyanie sluchainykh otklonenii ot optimal'noi programmy po tyage na dvizhenie tela peremennoi s postoyannoi zatratoi moshchnosti v gravitatsionnom pole (Influence of Random Deviations from the Optimum

Thrust Program on the Motion of a Body with Constant Power Consumption in a Gravitational Field).— Prikladnaya Matematika i Mekhanika, Vol. 27, No. 1. 1963.

12.70. Fel'dbaum, A.A. Osnovy teorii optimal'nykh avtomaticheskikh sistem (Fundamentals of the Theory of Optimum Automatic Systems).— Moskva, Fizmatgiz. 1963.

12.71. Anderson, T. Introduction to Multivariate Statistical Analysis.—Wiley. 1958.

12.72. Berman, L.J., G.E. Steinker, and R. Krupp. Optimization of Stochastic Trajectories.— AIAA J., Vol. 1, No. 4. 1963.

12.73. Breakwell, J.V. and C.T. Striebel. Minimum Effort Control in Interplanetary Guidance.— IAS Prepr., pp. 63—80. 1963.

12.74. Breakwell, J.V. The Optimum Spacing of Corrective Thrusts in Interplanetary Navigation.— Math. optim. techn., Berkeley-Los Angeles, Univ. of Calif. Press. 1963.

12.75. Curkendall, D.W. and C.G. Pfeiffer. A Discussion of Guidance Policies for Multiple-Impulse Correction of the Trajectory of a Spacecraft.— AIAA Paper, Nos. 63—334. New York. 1963.

12.76. Kraft, J.D.— Guidance and Control. Space Flight Handbook, Vol. 1. Washington. 1963.

12.77. Kraft, J.D.— Orbit Computation. Space Flight Handbook, Vol. 1. Washington. 1963.

12.78. Lawden, D.F. Necessary Conditions for Optimal Roket Trajectories.— Quart. J. Mech. Appl. Math., Vol. 7, pp. 488—504. 1954.

12.79. Pfeiffer, C.G. A Technique for Optimum Final Value Control of Powered Flight Trajectories. New York. 1963.

12.80. Stearns, E.V. Navigation and Guidance in Space.— Prentice Hall. 1963.

12.81. Steinker, G.E. Solutions for Optimal Stochastic Trajectories, S.M. Thesis.— Mass. Inst. Techn. 1963.

12.82. Townsend, G.E. Maneuvers.— Space Flight Handbook, Vol. 1. Washington. 1963.

12.83. Kozhevnikov, Yu.V. K optimizatsii upravlyaemykh sistem so sluchainymi parametrami (Optimization of Guided Systems with Random Parameters).— Prikladnaya Matematika i Mekhanika, Vol. 28, No. 3. 1964.

12.84. Lidov, M.L. K apriornym otsenkam tochnosti opredeleniya parametrov po metodu naimen'shikh kvradratov (A Priori Assessment of the Accuracy of Determining Parameters by the Least-Square Method).— Kosmicheskie Issledovaniya, Vol. 2, No. 5. 1964.

12.85. Breakwell, J.V., F. Tung, and R.R. Smith. Application of the Continuous and Discrete Strategies of Minimum Effort Theory to Interplanetary Guidance.— AIAA J., Vol. 2, No. 5. 1964.

12.86. Duncan, R.C. and A.A. Gunnersen. Inertial Guidance Navigation and Control Systems.— J. Spacecraft and Rock., Vol. 1, No. 6. 1964.

12.87. Fusca, J.A. Advanced Guidance Concepts.— Space Aeronautics, Vol. 42, No. 7. 1964.

12.88. Jazwinski, A.H. Optimal Trajectories and Linear Control of Nonlinear Systems.— AIAA J., Vol. 2, No. 8. 1964.
12.89. Traenkle, C.A. Mittkurs Navigation für interplanetare Raumtrajektorien.— Ztschr. für Flugwissenschaften, Vol. 12, No. 9. 1964.
12.90. Andreevskii, V.V. Ob optimal'nom utochnenii programmy upravleniya (The Optimum Improvement of Guidance Programs).— In: Sbornik "Issledovaniya po dinamike poleta," No. 1; Mashinostroenie. Moskva. 1965.
12.91. Issledovaniya po dinamike poleta (Studies of Flight Dynamics), No. 1.— Mashinostroenie. 1965.
12.92. Krasovskii, N.N. Problemy upravlyaemosti, nablyudaemosti i stabiliziruemosti dinamicheskikh sistem (Problems of the Guidance, Observation and Stabilization of Dynamic Systems).— Trudy 2 Vsesoyuznogo S"ezda po Teoreticheskoi i Prikladnoi Mekhanike, No. 1, Nauka, Moskva. 1965.
12.93. Letov, A.M. Optimal'noe upravlenie i ustoichivost' (Optimum Guidance and Stability).— Trudy 2 Vsesoyuznogo S"ezda po Teoreticheskoi i Prikladnoi Mekhanike, No. 1, Nauka. Moskva. 1965.
12.94. Letov, A.M. Teoriya optimal'nogo upravleniya (Optimum Guidance Theory).— Proceedings 2nd International Congress IFAC, Vol. 2, Nauka 1965.
12.95. Mil'shtein, G.N. Ob optimal'nom osushchestvlenii traektorii (The Optimum Realization of Trajectories).— Avtomatika i Telemekhanika, Vol. 26, No. 4. 1965.
12.96. Optimal'nye sistemy. Statisticheskie metody (Optimum Systems. Statistical Methods).— Proceedings of the 2nd International Congress of the International Federation on Automatic Control, Vol. 2, Nauka. Moskva. 1965.
12.97. Platonov, A.K., A.A. Dashkov, and V.N. Kubasov. Optimal'noe upravlenie poletom kosmicheskogo apparata (Optimum Guidance of a Space flight).— Proceedings of the 1st Symposium "Automatic Guidance in the Peaceful Utilization of Outer Space." 1965.
12.98. Ponomarev, V.M. Teoriya upravleniya dvizheniem kosmicheskikh apparatov (Theory of Spacecraft Guidance).— Nauka. Moskva. 1965.
12.99. Kozhevnikov, Yu.V. Vybor programmy dvizheniya i parametrov sostavnykh letatel'nykh apparatov iz usloviya naibolee veroyatnoi dostavki poleznogo gruza v zadannuyu oblast' (Selecting the Motion Program and the Parameters of Composite Flying Vehicles from the Condition of Most-Probable Delivery of the Payload in a Specified Region).— Prikladnaya Matematika i Mekhanika, Vol. 30, No. 6. 1966.
12.100. Boguslavskii, I.A., O.I. Ivashchenko, and Yu.G. Shepelev. Ob upravlenii kosmicheskim apparatom s dvigatelyami maloi tyagi na uchastke razgona pri otsutstvii informatsii o tekushchem vektore skorosti (The Guidance of a Spacecraft with Low-Thrust Engines in the Acceleration Segment with no Information on the Instantaneous Velocity Vector).— Kosmicheskie Issledovaniya, Vol. 4, No. 2. 1966.
12.101. Stratonovich, R.L. Uslovnye markovskie protsessy i ikh primenenie k teorii optimal'nogo upravleniya (Markov Processes and Their Application to to the Optimum Guidance Theory).— Izdatel'stvo MGU. 1966.

12.102. Yaroshevskii, V.A. and G.V. Parysheva. Optimal'noe raspredelenie korrektiruyushchikh impul'sov pri odnoparametricheskoi korrektsii (Optimum Distribution of Correcting Impulses for a One-Parameter Correction).— Kosmicheskie Issledovaniya, Vol.3, No.6. 1965; Vol.4, No.1. 1966.
12.103. Breakwell, J.V. and H.E. Rauch. Optimum Guidance for a Low-Thrust Interplanetary Vehicle.— AIAA J., Vol.4, No.4. 1966.

Chapter Thirteen

13.1. Tsien, H.S. Takeoff from Satellite Orbit.— J. Amer. Rock. Soc., Vol.23, No.4. 1953.
13.2. Dobrowolski, A. Satellite Orbit Perturbation Under a Continuous Radial Thrust of Small Magnitude.— J. Amer. Rock. Soc., Vol.28, No.7. 1958.
13.3. Copeland, J. Interplanetary Trajectories Under Low-Thrust Radial Acceleration.— J. Amer. Rock. Soc., Vol.29, No.4. 1959.
13.4. Karrenberg, H.K. Note on Interplanetary Trajectories Under Low-Thrust Radial Acceleration.— J. Amer. Rock. Soc., Vol.30, No.1. 1960.
13.5. Au, G. Corrections for Interplanetary Trajectories Under Low-Thrust Radial Acceleration.— J. Amer. Rock. Soc., Vol.30, No.7. 1960.
13.6. Paiewonsky, B. The Motion of an Orbiting Vehicle Subjected to Continuous Radial Thrust, Including a Study of Planetary Encounters.— Proc. X Internat. Astronaut. Congr., London, 1959. Vien. 1960.
13.7. Petty, C.M. Interplanetary Maneuvers, Using Radial Thrust.— J. Amer. Rock. Soc., Vol.33, No.9. 1961.
13.8. Au, G. Interplanetare Bahnen für Raumfahrtzeuge mit kleiner Schubbeschleunigung.— Raketentechnik und Raumfahrtforschung, Vol.5, No.2.
13.9. Tsander, F.A. Ob ispol'zovanii sily davleniya sveta dlya poletov v mezhplanetnom prostranstve (Using Light Pressure Force in Interplanetary Spaceflight). 1924—1925. Cf. Tsander, F.A. Problema poleta pri pomoshchi reaktivnykh apparatov (The Problem of Jet-Propelled Flight).— Mezhplanetnye puteshestviya. Moskva, Oborongiz. 1961.
13.10. London, H.S. Some Exact Solution of the Equation of Motion of Solar Sail with Constant Sail Setting.— J. Amer. Rock. Soc., Vol.30, No.2. 1961.
13.11. Lass, H. and J. Lorrel. Low Acceleration Takeoff from a Satellite Orbit.— J. Amer. Rock. Soc., Vol.31, No.1. 1961.
13.12. Citron, S.J. Solution for Satellite Motion Under Low Acceleration Using Method of Variation of Parameters.— J. Amer. Rock. Soc., Vol.31, No.12. 1961.
13.13. Arthur, P.D., H.K. Karrenberg, and H.M. Stark. Simple Method for Approximation of the Characteristics of Low-Thrust Trajectories.— J. Amer. Rock. Soc., Vol.30, No.7. 1960.
13.14. Forbes, G.F. The Trajectory of a Powered Rocket in Space.— J. Brit. Interpl. Soc., Vol.9, No.2. 1950.

13.15. Grodzovskii, G.L., Yu.N. Ivanov, and V.V. Tokarev. O dvizhenii tela peremennoi massy s postoyannoi zatratoi moshchnosti v gravitatsionnom pole (Motion of a Body of Varying Mass with Constant Power Consumption in a Gravitational Field).— Doklady AN SSSR, Vol. 137, No. 5. 1961; Proc. XII Internat. Astronaut. Congr. 1963. Warsaw. 1964.

13.16. Beletskii, V.V. and V.A. Egorov. Mezhplanetnye polety s dvigatelem postoyannoi moshchnosti (Interplanetary Journeys with Constant-Power Engines).— Kosmicheskie Issledovaniya, Vol. 2, No. 3. 1964.

13.17. Levin, E. Low-Thrust Transfer Between Circular Orbits.— ASME prepr., 59-AV-2. March 1959.

13.18. Lur'e, A.I. and M.K. Cheremsin. Dvizhenie material'noi tochki v pole tsentral'noi sily tyagoteniya pri nalichii maloi transversal'noi tyagi (Motion of a Point Mass in the Field of a Central Gravitational Force Given a Small Transverse Thrust).— In: Sbornik "Iskusstvennye sputniki Zemli," No. 16, Izdatel'stvo AN SSSR. 1963.

13.19. Lawden, D.F. Optimal Programming of Thrust Direction.— Astronaut. Acta, Vol. 1, No. 1. 1955.

13.20. Lawden, D.F. Optimal Escape from a Circular Orbit.— Astronaut. Acta, Vol. 4, No. 3. 1958.

13.21. Lebedev, V.N. Variatsionnaya zadacha o vzlete kosmicheskogo apparata s krugovoi orbity (Variational Problem of the Takeoff of a Spacecraft from a Circular Orbit).— Zhurnal Vychislitel'noi Matematiki i Matematicheskoi Fiziki, Vol. 3, No. 6. 1963.

13.22. Moeckel, W.E. Trajectories with Constant Tangential Thrust in Central Gravitational Fields.— NASA TRR-53. 1959.

13.23. Benney, D.J. Escape from a Circular Orbit Using Tangential Thrust.— J. Amer. Rock. Soc., Vol. 28, No. 3. 1958.

13.24. Anthony, M.L. and C.J. Maday. Motion of Orbiting Vehicles Under Application of Tangential Microthrust.— Prepr. Amer. Astronaut. Soc., No. 102, p. 21. 1961.

13.25. Perkins, F.M. Flight Mechanics of Low-Thrust Spacecraft.— JASS, Vol. 26, No. 5. 1959.

13.26. Okhotsimskii, D.E. Issledovanie dvizheniya v tsentral'nom pole pod deistviem postoyannogo kasatel'nogo uskoreniya (Motion in a Central Field Under the Action of a Constant Tangential Acceleration).— Kosmicheskie Issledovaniya, Vol. 2, No. 6. 1964.

13.27. Bacon, R.H. Logarithmic Spiral: an Ideal Trajectory for the Interplanetary Vehicle with Engines of Low Sustained Thrust.— Amer. J. Phys., Vol. 27, pp. 164—165. 1959.

13.28. Hughes, J.V. and G.N. Nomicas. Trajectories for Continuously Applied Propulsive Thrust.— Planet Space Sci., No. 7, pp. 145—153. 1961.

13.29. Stark, H.M. and P.D. Arthur. Simple Approximate Solutions for Tangential Low-Thrust Trajectories.— JASS, Vol. 28, No. 7. 1961.

13.30. Pinkham, G. Reference Solution for Low-Thrust Trajectories.— J. Amer. Rock. Soc., Vol. 32, No. 5. 1962.

13.31. Rodriguez, G. Method for Determining Steering Programs for Low-Thrust Interplanetary Vehicles.— J. Amer. Rock. Soc., Vol. 29, No. 10. 1959.
13.32. Levin, E. Low-Acceleration Transfer Orbits.— Handbook of Astronaut. Eng. New York, McGraw-Hill. 1961.
13.33. Lass, H. and G.B. Solloway. Motion of a Satellite Under the Influence of a Constant Normal Thrust.— J. Amer. Rock. Soc., Vol. 32, No. 1. 1962.
13.34. Rider, L. Low-Thrust Correction of Orbital Orientation.— J. Amer. Rock. Soc., Vol. 30, No. 7. 1960.
13.35. Illarionov, V.F. and L.M. Shkadov. Povorot ploskosti krugovoi orbity sputnika (Rotating the Plane of the Circular Orbit of a Satellite).— Prikladnaya Matematika i Mekhanika, Vol. 26, No. 1. 1962.
13.36. Gus'kov, Yu.P. Metod upravleniya povorotom ploskosti krugovoi orbity sputnika (Method of Controlling the Rotation of the Plane of the Circular Orbit of a Satellite).— Prikladnaya Matematika i Mekhanika, Vol. 27, No. 3. 1963.
13.37. Beletskii, V.V. O traektoriyakh kosmicheskikh poletov s postoyannym vektorom reaktivnogo uskoreniya (Trajectories of Spaceflights with Constant-Thrust Acceleration Vector).— Kosmicheskie Issledovaniya, Vol. 2, No. 3. 1964.

Chapter Fourteen

14.1. Bellman, R.E. Dynamic Programming.— Princeton Univ. Press. 1957.
14.2. Bellman, R., I. Glicksberg, and O. Gross. Some Aspects of the Mathematical Theory of Control Processes.— Rand Corporation. Calif. 1958.
14.3. Bellman, R.E. Adaptive Control Processes; a Guided Tour.— Princeton Univ. Press. 1961.
14.4. Bellman, R.E. and S. Dreyfus. Applied Dynamic Programming.— Princeton Univ. Press. 1962.
14.5. Moiseev, N.N. Metody dinamicheskogo programmirovaniya v teorii optimal'nykh upravlenii (Dynamic Programming Methods in the Theory of Optimum Controls).— Zhurnal Vychislitel'noi Matematiki i Matematicheskoi Fiziki, Vol. 4, No. 3. 1964; Vol. 5, No. 1. 1965.
14.6. Krotov, V.F. Metody resheniya variatsionnykh zadach na osnove dostatochnykh uslovii absolyutnogo minimuma (Methods of Solving Variational Problems with Sufficient Absolute-Minimum Conditions).— Avtomatika i Telemekhanika, Vol. 23, No. 12. 1962; Vol. 24, No. 5. 1963.
14.7. Courant, R. Dirichlet's Principle, Conformal Mapping, and Minimal Surfaces.— Interscience. 1950.
14.8. Kantorovich, L.V. Ob odnom effektivnom metode resheniya ekstremal'nykh zadach dlya kvadratichnogo funktsionala (An Efficient Method of Solving Extremal Problems for a Quadratic Functional).— Doklady AN SSSR, Vol. 48, No. 7. 1945.
14.9. Kantorovich, L.V. O metode naiskoreishego spuska (The Steepest-Descent Method).— Doklady AN SSSR, Vol. 56, No. 3. 1947.

14.10. Kantorovich, L. V. Funktsional'nyi analiz i prikladnaya matematika (Functional Analysis and Applied Mathematics). — Uspekhi Matematicheskikh Nauk, Vol. 3, No. 6. 1948.

14.11. Birman, M. Sh. Nekotorye otsenki dlya metoda naiskoreishego spuska (Some Estimates for the Steepest-Descent Method). — Uspekhi Matematicheskikh Nauk, Vol. 5, Nos. 3 (37). 1950.

14.12. Samokish, B. A. Issledovanie bystroty skhodimosti metoda naiskoreishego spuska (Convergence Rate of the Steepest-Descent Method). — Uspekhi Matematicheskikh Nauk, Vol. 12, No. 1 (3). 1957.

14.13. Stein, M. L. On Methods for Obtaining Solutions of Fixed Endpoint Problems in the Calculus of Variations. — Nat. Bur. Standards, J. Res., Vol. 50, No. 5. 1953.

14.14. Tompkins, C. B. Steepest-Descent Methods. — In: "Modern Mathematics for the Engineer," ed. E. F. Beckenbach, McGraw-Hill. 1956.

14.15. Rosenblum, P. C. The Method of Steepest Descent. — Proc. of the Sixth Symp. in Appl. Math. of the Amer. Math. Soc., McGraw-Hill. 1956.

14.16. Ivanov, Yu. N. and Yu. V. Shalaev. Metod skoreishego spuska v primenenii k raschetu mezhorbital'nykh traektorii s dvigatelyami ogranichennoi moshchnosti (The Steepest-Descent Method as Applied to Calculating Interorbital Trajectories with Power-Limited Engines). — Kosmicheskie Issledovaniya, Vol. 2, No. 3. 1964.

14.17. Brumberg, V. A. Chislennoe reshenie kraevykh zadach nebesnoi mekhaniki metodom naiskoreishego spuska (Numerical Solution of the Boundary-Value Problems of Celestial Mechanics by the Steepest-Descent Method). — Byulleten' Instituta Teoreticheskoi Astronomii, Vol. 8, No. 4. 1962.

14.18. Shatrovskii, L. I. Ob odnom chislennom metode resheniya zadach optimal'nogo programmirovaniya (A Numerical Method of Solving Optimum Programing Problems). — Zhurnal Vychislitel'noi Matematiki i Matematicheskoi Fiziki, Vol. 2, No. 3. 1962.

14.19. Eneev, T. M. O primenenii gradientnogo metoda v zadachakh teorii optimal'nogo regulirovaniya (Application of the Gradient Method to Problems of Optimum Control). — Doklad na Vsesoyuznom simpoziume po mnogoekstremal'nym zadacham, Vilnius. 13 — 15 June 1963.

14.20. Kelley, H. J. Gradient Theory of Optimal Flightpaths. — J. Amer. Rock. Soc., Vol. 30, No. 10. 1960.

14.21. Kelley, H. J., R. E. Kopp, and H. G. Moyer. Successive Approximation Techniques for Trajectory Optimization. — Proc. of the Symp. on Vehicle System Optimization. New York. 1961.

14.22. Bryson, A. E. and W. F. Denham. Multivariable Terminal Control for Minimum Mean-Square Deviation from a Nominal Path. — Proc. of the Symp. on Vehicle System Optimization. New York. 1961.

14.23. Bryson, A. E. and W. F. Denham. A Steepest-Ascent Method for Solving Optimum Programing Problem. — Trans. ASME, No. 2. 1962.

14.24. Bryson, A. E., W. F. Denham, F. J. Carroll, and K. Mikami. Determination of Lift or Drag Programs that Minimize Re-entry Heating. — JASS Vol. 29, No. 4. 1962.

14.25. Bryson, A.E., W.F. Denham, and S.E. Dreyfus. Optimal Programing Problems with Inequality Constraints: Necessary Conditions for Extremal Solutions. – AIAA J., Vol. 1, No. 11. 1963.

14.26. Denham, W.F. and A.E. Bryson. Optimal Programing Problems with Inequality Constraints II: Solution by Steepest Ascent. – AIAA J., Vol. 2, No. 1. 1964.

14.27. Kelley, H.J. Method of Gradients. Optimization Techniques, Ch. 6, ed. by G. Leitman. New York, Acad. Press. 1962.

14.28. Lindorfer, W. and H.G. Moyer. Application of a Low-Thrust Trajectory Optimization Scheme to Planar Earth-Mars Transfer. – J. Amer. Rock. Soc., Vol. 32, No. 2. 1962.

14.29. Sherman, B. Low-Thrust Escape Trajectories. – Proc. of the Symp. on Vehicle System, Optimization. New York. 1961.

14.30. Lukes, D.L. Steepest-Descent and Maximum Principle Techniques of System Optimization. – Proc. of the Symp. on Vehicle System Optimization. – New York. 1961.

14.31. Okhotsimskii, D.E. K teorii dvizheniya raket (Theory of the Motion of Rockets). – Prikladnaya Matematika i Mekhanika, Vol. 10, No. 2. 1946.

14.32. Jazwinski, A.N. Inequality Constraints in Steepest-Descent Trajectory Optimization. – J. of Aerospace Sci., Vol. 29, No. 10. 1962.

14.33. Courant, R. Calculus of Variations and Supplementary Notes and Exercises. – New York University, Institute of Mathematical Sciences, 1945 – 1946. (Revised and amended by J. Moser. 1956 – 1957).

14.34. Pontryagin, L.S., V.G. Boltyanskii, R.V. Gamkrelidze, and E.F. Mishchenko. Matematicheskaya teoriya optimal'nykh protsessov (Mathematical Theory of Optimum Processes). – Moskva, Fizmatgiz. 1961.

14.35. Krylov, I.A. and F.L. Chernous'ko. O metode posledovatel'nykh priblizhenii dlya resheniya zadach optimal'nogo upravleniya (The Method of Successive Approximations for Solving Optimum Control Problems). – Zhurnal Vychislitel'noi Matematiki i Matematicheskaya Fizika, Vol. 2, No. 6. 1962.

14.36. Akilov, G.P. O primenenii odnogo metoda resheniya nelineinykh funktsional'nykh uravnenii k issledovaniyu sistem differentsial'nykh uravnenii (A Method of Solving Nonlinear Functional Equations Applied to Systems of Differential Equations). – Doklady AN SSSR, Vol. 48, No. 4. 1949.

14.37. Abramov, A.A. Variant metoda progonki (A Variant of the P Method). – Zhurnal Vychislitel'noi Matematiki i Matematicheskoi Fiziki, Vol. 1, No. 2. 1961.

14.38. Abramov, A.A. O perenose granichnykh uslovii dlya sistem lineinykh obyknovennykh differentsial'nykh uravnenii (Transferring the Boundary Conditions for Systems of Linear Ordinary Differential Equations). – Zhurnal Vychislitel'noi Matematiki i Matematicheskoi Fiziki, Vol. 1, No. 3. 1961.

14.39. Goodman, T.R. and G.N. Lance. The Numerical Integration of Two-Point Boundary-Value Problems. – Mathem. Tables and Other Aids to Comput., Vol. 10, No. 4. 1956.

Chapter Fifteen

15.1. Zoutendijk, G. Methods of Feasible Directions.— Elsevier Publishing Co. 1960.

15.2. Berezin, I.S. and N.P. Zhidkov. Metody vychislenii (Computing Methods), Vol. 2. — Moskva, Fizmatgiz. 1961.

15.3. Bryson, A.E. and W.F. Denham. A Steepest-Ascent Method for Solving Optimum Programing Problems. — Trans ASME, No. 2. 1962.

15.4. Lindorfer, W. and A. Nathan. Optimization of Missile Intercept Range. — Proc. of the Symp. on Vehicle System Optimization. New York. 1961.

15.5. Eneev, T.M., A.K. Platonov, and R.K. Kazakova. Opredelenie parametrov orbity iskusstvennogo sputnika po dannym nazemnykh izmerenii (Evaluating the Orbital Parameters of an Artificial Satellite by Measurements Recorded on the Earth). — In: Sbornik "Iskusstvennye sputniki Zemli," No. 4, Izdatel'stvo AN SSSR. 1960.

15.6. Akim, E.L. and T.M. Eneev. Opredelenie parametrov dvizheniya kosmicheskogo letatel'nogo apparata po dannym traektornykh izmerenii (Evaluating the Motion Parameters of a Spacecraft by Using Trajectory Measurements). — Kosmicheskie Issledovaniya, Vol. 1, No. 1. 1963.

15.7. Gavurin, M.K. Nelineinye funktsional'nye uravneniya i nepreryvnye analogii iterativnykh metodov (Nonlinear Functional Equations and Continuous Analogies of the Iterative Methods). — Izvestiya Vysshikh Uchebnykh Zavedenii, No. 5. 1958.

15.8. Jurovics, St.A. and J.E. McIntyre. The Adjoint Method and Its Application to Trajectory Optimization. — J. Amer. Rock. Soc., Vol. 32, No. 9. 1962.

15.9. Isaev, V.K. and V.V. Sonin. Ob odnoi modifikatsii metoda N'yutona chislennogo resheniya kraevykh zadach (A Modification of Newton's Method of Solving Numerically Boundary-Value Problems). — Zhurnal Vychislitel'noi Matematiki i Matematicheskoi Fiziki, Vol. 3, No. 6. 1963.

15.10. Gel'fand, I.M. and S.V. Fomin. Variatsionnoe ischislenie (Variational Calculus). — Moskva, Fizmatgiz. 1961.

15.11. Kantorovich, L.V. and V.I. Krylov. Priblizhennye metody vysshego analiza (Approximate Methods of Higher Analysis). — Moskva, Gostekhizdat. 1941.

15.12. Mikhlin, S.R. Pryamye metody matematicheskoi fiziki (Direct Methods of Mathematical Physics). — Moskva, Gostekhizdat. 1950.

15.13. Ivanov, Yu.N. and Yu.V. Shalaev. Metod skoreishego spuska v primenenii k raschetu mezhorbital'nykh traektorii s dvigatelyami ogranichennoi moshchnosti (The Steepest-Descent Method Applied to Calculating Interorbital Trajectories with Power-Limited Engines). — Kosmicheskie Issledovaniya, Vol. 2, No. 3. 1964.

15.14. Saltzer, C. and C.W. Fetheroff. A Direct Variational Method for the Calculation of Optimum Thrust Programs for Power-Limited Interplanetary Flight. — Astronaut. Acta, Vol. 7, No. 1. 1961.

15.15. Pfeiffer, C.G. Theory and Application of the Critical Direction Method of Trajectory Optimization.—Proc. of the Symposium on Vehicle System Optimization, N.Y. 1961.
15.17. Breakwell, I.V. The Optimization of Trajectories.—J. Soc. Industrial and Appl. Math., Vol. 7, pp. 215—247. 1959.
15.18. Kulakowski, L.I. and R.T. Stancil. Rocket Boost Trajectories for Maximum Burnout Velocity.—J. Amer. Rock. Soc., Vol. 30, No. 7. 1960.
15.19. Stancil, R.T. and L.I. Kulakowski. Rocket Boost Vehicle Mission Optimizations.—J. Amer. Rock. Soc., Vol. 31, No. 7. 1961.
15.20. Jurovics, St. A. Optimum Steering Program for Entry of Multistage Vehicle Into a Circular Orbit.—J. Amer. Rock. Soc., Vol. 31, No. 4. 1961.
15.21. Breakwell, I.V. Optimum Ascent Into a Circular Orbit.—Proc. of the Symposium on Vehicle System Optimization, N.Y. 1961.
15.22. McIntyre, I.E., St. A. Jurovics, W.P. Gardill, and B. Johnson. The Application of Optimum Trajectory Analysis to Boost Vehicle Design.—Proc. of the Symposium on Vehicle System Optimization. New York. 1961.
15.23. Lebedev, V.N. and B.N. Rumyantsev. Variatsionnaya zadacha o perelete mezhdu dvumya tochkami v tsentral'nom pole (Variational Problem of Transfer Between Two Points in a Central Field).— In: Sbornik "Iskusstvennye sputniki Zemli," No. 16. 1963.

Appendix

A.1. Lass, H. and J. Lorrel. Low Acceleration Take-off from a Satellite Orbit.—J. Amer. Rock. Soc., Vol. 31, No. 1. 1961.
A.2. Moiseev, N.N. Metody nelineinoi mekhaniki v zadachakh dinamiki sputnikov (Methods of Nonlinear Mechanics in Satellite Dynamics Problems).—Proc. XIII Internat. Astronaut. Congr. 1962, Vien. 1964.
A.3. Laricheva, V.V. and M.V. Rein. Zamechanie ob osrednenii uravnenii vozmushchennogo dvizheniya v oskuliruyushchikh elementakh pri izmenenii ekstsentrisiteta v shirokikh predelakh (Note on Averaging the Equations of Perturbed Motion in Osculating Variables when the Eccentricity Varies Widely).—Kosmicheskie Issledovaniya, Vol. 3, No. 3. 1965.
A.4. Laricheva, V.V. and M.V. Rein. Asimptotika uravnenii nebesnoi mekhaniki, prigodnaya pri bol'shom diapazone izmeneniya ekstsentrisiteta (Asymptotes of the Equations of Celestial Mechanics When the Eccentricity Varies Widely).—Kosmicheskie Issledovaniya, Vol. 3, No. 1. 1965.
A.5. Smith, F.T. Optimization of Multistage Orbit Transfer Processes by Dynamic Programming.—J. Amer. Rock. Soc., Vol. 31, No. 11. 1961.
A.6. Moulton, F.R. An Introduction to Celestial Mechanics. McMillan, N.Y. 1914.
A.7. Duboshin, G.N. Nebesnaya mekhanika (Celestial Mechanics).—Fizmatgiz. 1963.

A.8. Subbotin, M.F. Kurs nebesnoi mekhaniki (A Course in Celestial Mechanics).— Vol. 1, GTTI. 1933; Vol. 2, ONTI. 1937; Vol. 3, ONTI. 1949.

A.9. Herrick, S. Earth Satellites and Related Orbit and Perturbation Theory.— Space Technol., Ch. 5, ed. Seifert. New York. 1959.

A.10. Herrick, S. — Astrodynamics. — New Jersey, Princeton University Press. 1959.

A.11. Ehricke, K.A. — Spaceflight, Vol. 1, Environment and Celestial Mechanics, Ch. 6, Perturbation. Princeton, Van Nostrand. 1960.

A.12. Herrick, S. Trajectory Fundamentals. — Handbook of Astronaut. Eng., p. 4. McGraw-Hill, New York. 1961.

A.13. Okhotsimskii, D.E., T.M. Eneev, and T.P. Taratynova. Opredelenie vremeni sushchestvovaniya iskusstvennogo sputnika Zemli i issledovanie vekovykh vozmushchenii ego orbity (The Life of an Artificial Earth Satellite and the Secular Perturbations of Its Orbit).— UFN, Vol. 63, No. 1a. 1957.

A.14. Newton, R.R. Variables that Are Determined for Any Orbit.— J. Amer. Rock. Soc., Vol. 31, No. 3. 1961.

A.15. Pines, S. Variation of Parameters for Near Circular and Low Inclination Orbits.— IAS Paper, No. 61—7; 29th Ann. Meet. IAS. New York. 1961.

A.16. Wong, P. Nonsingular Variation of Parameter Equation for Computation of Space Trajectories.— J. Amer. Rock. Soc., Vol. 32, No. 2. 1962.

A.17. Kuzmak, G.E. and Yu. M. Kopnin. Novaya forma uravneniya dvizheniya sputnika i prilozhenie ee k issledovaniyu dvizhenii, blizkikh k keplerovym (A New Form of the Equations of Motion of a Satellite, and Its Application to Near-Keplerian Motions).— Zhurnal Vychislitel'noi Matematiki i Matematicheskaya Fizika, Vol. 3, No. 4. 1963.

A.18. Lass, H. and G.B. Solloway. Motion of a Satellite under the Influence of a Constant Normal Thrust.— J. Amer. Rock. Soc., Vol. 32, No. 1. 1962.

A.19. Okhotsimskii, D.E. and T.M. Eneev. Nekotorye variatsionnye zadachi, svyazannye s zapuskom iskusstvennogo sputnika Zemli (Some Variational Problems of Launching an Artificial Earth Satellite).— UFN, Vol. 63, No. 1a. 1957.

A.20. Okhotsimskii, D.E. and T.M. Eneev. O vyvedenii iskusstvennogo sputnika Zemli na orbitu (Injecting an Artificial Earth Satellite into Orbit).— Proc. VIII Internat. Astronaut. Congr. 1957. Vien. 1958.

A.21. Kuzmak, G.E., V.K. Isaev, and B.Kh. Davidson. Optimalnye rezhimy dvizheniya tochki peremennoi massy v admorodnom tsentralnom pole (Optimum Regimes of Motion of a Varying Point Mass in a Homogeneous Central Field).— Doklady AN SSSR, Vol. 149, No. 1. 1963.

A.22. Isaev, V.K., V.V. Sonin, and B.Kh. Davidson. Optimal'nye rezhimy dvizheniya tochki peremennoi massy s ogranichennoi moshchnost'yu v odnorodnom tsentral'nom pole (Optimum Regimes of Power-Limited Motion of a Varying Point Mass in a Homogeneous Central Field).— Kosmicheskie Issledovaniya, Vol. 2, No. 4. 1964.

A.23. Ivanov, Yu.N., V.V. Tokarev, and Yu.V. Shalaev. Optimal'nye traektroii i optimal'nye parametry kosmicheskikh apparatov s dvigatelyami ogranichennoi moshchnosti (Optimum Trajectories and Optimum Parameters of Space Vehicles with Power-Limited Engines).— Kosmicheskie Issledovaniya, Vol.2, No.3. 1964.

A.24. Roberson, R.E. Orbital Behavior of Earth Satellites, I, II.— J. Franklin Inst., Vol.264. 1957.

A.25. Citron, S.J. Satellite Lifetimes under the Influence of Continuous Thrust, Atmospheric Drag, and Planet Oblateness.— AIAA J., Vol.1, No.6. 1963.

A.26. Cospar International Reference Atmosphere (CIRA-64).

AUTHOR INDEX*

Russian Authors

Abiants, V.Kh. 84, 87; 2.98
Abramov, A.A. 586; 14.37, 14.38
Abramovich, G.N. 37, 38, 93, 95; 2.6, 2.123
Akilov, G.P. 586; 14.36
Akim, E.L. 517, 594; 12.60, 15.6
Al'brekht, E.G. 517; 12.19
Aleksandrov, S.G. 32; 1.76
Alekseev, K.B. 14, 21, 36, 37, 76—78, 92—95, 122; 1.48, 1.61, 3.1
Alemasov, V.E. 37, 39, 46, 76, 93; 2.11
Andreevskii, V.V. 517; 12.90
Andriankin, E.I. 34; 1.85
Appazov, R.F. 13; 1.59
Artsimovich, L.A. 54—57, 67; 2.65
Avduevskii, V.S. 79; 2.83
Avramchenko, R.F. 244, 247, 436; 6.11, 10.4

Bam-Zelikovich, G.M. 101; 2.164
Barbashin, E.A. 517; 12.8, 12.9, 12.20
Bebenin, G.G. 13; 1.48
Beletskii, V.V. 17, 170, 176, 178—180, 183, 186, 188, 190, 192, 197, 200, 201, 243, 247, 295, 322, 538, 553; 1.68, 5.1, 5.11, 5.25, 6.10, 6.15, 7.12, 8.48, 13.16, 13.37
Belyaev, Yu.K. 471, 487; 11.8
Berezin, I.S. 594, 597; 15.2
Bezmenov, V.M. 244; 6.11
Birman, M.Sh. 558; 14.11
Bodner, V.A. 517; 12.21
Boguslavskii, I.A. 517; 12.100
Bolgarskii, A.V. 37, 39, 76; 2.7
Bolonkin, A.A. 322; 8.42
Boltyanskii, V.G. 109, 353, 582; 2.170, 9.4, 14.34
Bondarenko, I I. 54, 59, 63; 2.50
Bondaryuk, M.M. 93, 95; 2.126
Braun, S. 63, 66; 2.69
Brumberg, V.A. 558; 14.17
Bunimovich, A.I. 101; 2.164
Bykov, G.A. 55, 56; 2.66

Chang Jên-Wei. 517; 12.50
Chebotarev, G.A. 13; 1.58
Cheremsin, M.K. 539; 13.18
Cherkez, A.Ya. 93, 95; 2.125
Chernous'ko, F.L. 582, 583; 14.35
Chernyi, G.G. 101; 2.159, 2.162
Chuvatin, S.A. 55, 56; 2.65, 2.66

Danilov, Yu.I. 79; 283
Dashkov, A.A. 517; 12.97
Dautov, G.Yu. 52; 2.43
Davidson, B.Kh. 13, 177, 309, 619; 1.40, 5.10, 7.14, 8.22, A.21, A.22

* [Page numbers refer to those of the Russian original, which appear in the left-hand margin of the text. The other references, e.g., 2.15, indicate bibliography items.]

Deich, M.E. 84, 87; 2.95
Diamandiev, V. 322; 8.24
Dobretsov, L.N. 63, 66, 84, 89; 2.68, 2.109
Dobrovol'skii, M.V. 92; 2.118
Dorodnitsyn, A.A. 39, 101; 2.14
Dorogov, B.S. 84, 87; 2.99
Duboshin, G.N. 25, 612; 1.69, 1.71 A.7

Efimov, G.B. 186; 5.37
Egorov, V.A. 13, 170, 178–180, 183, 186, 188, 190, 197, 201, 243, 247, 295, 538; 1.19, 1.20, 1.24, 1.57, 5.1, 5.11, 5.25, 6.10, 6.15, 7.12, 13.16
Eneev, T.M. 321, 322, 567, 568, 572, 594; 8.8, 12.60, 14.19, 15.5, 15.6, A.13, A.19, A.20
Ershov, V.G. 201; 5.25

Fatkin, Yu.M. 93, 96, 389; 2.137, 9.18, 9.19, 10.3
Fedorov, R.E. 32; 1.76
Fedorov, R.M. 14, 21, 36, 37, 76–78, 92–95, 122; 1.61, 3.1
Fedynskii, V.V. 34; 1.80
Fel'dbaum, A.A. 517; 12.70
Fomin, S.V. 597; 15.10
Frankl', F.I. 101; 2.150
Frolov, V.V. 115, 116; 2.178, 2.179, 2.192, 2.202

Galiullin, A.S. 517; 12.3, 12.7
Gal'perin, E.A. 517; 12.61
Gal'perin, V.G. 37, 38, 79, 95; 2.4
Gamkrelidze, R.V. 109, 353, 582; 2.170, 9.4, 14.34
Ganin, E.A. 118; 2.206
Gantmakher, F.R. 13, 321; 1.28
Gavurin, M.K. 594; 15.7
Gel'fand, I.M. 597; 15.10
German, V.O. 52; 2.44
Glushko, V.P. 76; 2.74
Gnedenko, B.V. 471, 487, 489; 11.6, 11.8
Gonor, A.L. 102; 2.210
Gorelov, Yu.A. 13, 321, 322; 1.32, 8.37
Govorov, A.N. 14, 21, 36, 37, 76–78, 92–95, 122; 1.61, 3.1
Grigoryan, S.S. 101; 2.160
Grodzovskii, G.L. 14, 21, 39, 41–43, 79, 80, 94, 100, 102, 104, 108, 110–112, 115, 116, 122, 135, 138, 139, 143, 151, 170–172, 175, 176, 179, 263, 322, 328, 360, 364, 406, 419, 470, 517, 518, 538; 1.60, 2.20, 2.22, 2.23, 2.80, 2.84, 2.132, 2,133, 2.143, 2.165, 2.167, 2.169, 2.178, 2.198, 2.202, 3.3, 4.19, 4.20, 4.22, 4.23, 4.25, 5.3, 6.25, 8.45, 9.3, 9.10, 9.20, 11.2, 11.3 12.62, 13.15
Gurman, V.I. 322; 8.36
Gus'kov, Yu.P. 551, 585; 13.36

Il'in, V.A. 13, 321; 1.41, 1.45, 8.58
Illarionov, V.F. 13, 321, 551, 552, 585; 1.35, 13.35
Il'yashenko, O.M. 93, 95; 2.126
Ilyutovich, A.E. 421; 9.34
Inozemtsev, N.V. 93, 95; 2.124
Ioffe, A.I. 84, 88; 2.102
Isaev, V.K. 13, 170, 177, 203, 215, 234, 236, 239, 309, 321, 322, 594, 597, 604, 619; 1.33, 1.40, 1.47, 5.2, 5.10, 5.36, 6.3; 7.13, 7.14, 7.25, 8.16, 8.17, 8.22, 8.40, 8.52, 15.9, A.21, A.22
Ishlinskii, A.Yu. 13, 321; 1.12
Ivanov, Yu.N. 14, 21, 122, 143, 170, 172, 179, 180, 183, 184, 187, 188,

192, 197, 198, 202, 203, 209, 231, 236, 239, 258, 267, 276, 280, 291, 328, 339, 383, 558, 598, 621; 1.60, 3.3, 4.20, 4.22, 4.23, 4.24, 4.25, 5.3, 5.4, 5.20, 5.27, 6.1, 6.2, 7.7, 7.9, 7.10, 7.11, 8.56, 9.8, 11.2, 11.3, 12.62, 13.15, 14.16, 15.13, A.23
Ivashchenko, O.I. 517; 12.100

Kamenkov, G.V. 517; 12.2
Kantorovich, L.V. 558, 585, 597; 14.8, 14.9, 14.10, 15.11
Kapitsa, P.L. 96; 2.138
Kaptsov, N.A. 60, 61, 63, 66, 68; 2.67
Karpovich, E.A. 101; 2.150
Karymov, A.A. 70; 2.72
Kats, I.Ya. 517; 12.10
Kazakova, R.K. 594; 15.5
Kazandzhan, P.K. 14, 21, 36, 37, 76—78, 92—95, 122; 1.61, 2.2, 3.1
Khinchin, A.Ya. 471, 487; 11.5
Kholshchevnikov, K.V. 93, 95; 2.131
Khristianovich, S.A. 37, 28, 79, 95; 2.4
Khudyakov, G.E. 80; 2.84
Kibel', I.A. 101; 2.147
Kiforenko, B.N. 357, 360, 364, 377; 9.3, 9.5, 9.7, 9.9, 9.10
Kimel', L.R. 81; 2.85
Kirillova, F.M. 517. 12.22
Kirillova, L.S. 517, 518. 12.64
Kochin, N.E. 101; 2.147
Kochina, N.N. 101; 2.161
Korovalov, N.E. 14, 21, 36, 37, 76—78, 92—95, 122; 1.61, 2.2, 3.1
Kopnin, Yu.M. 13, 261; 6.21, A.17
Korolev, S.P. 13, 321; 1.9
Korenev, G.V. 13, 321; 1.49
Kosarenkov, V.A. 116; 2.195
Koshkin, V.K. 79; 2.83
Kosmodem'yanskii, A.A. 13, 321; 1.10, 1.13, 1.14
Kostychev, G.N. 517; 12.42
Kozhevnikov, Yu.V. 517; 12.83, 12.99
Krasheninnikova, N.L. 101, 102; 2.157, 2.167
Krasnov, N.F. 101; 2.153
Krasovskii, N.N. 517, 518; 12.6, 12.10, 12.23, 12.24, 12.25, 12.43, 12.44, 12.45, 12.61, 12.65, 12.92
Krotov, V.F. 13, 321, 358, 557; 1.17, 9.6, 14.6
Krotov, V.I. 54, 63; 2.50
Krylov, I.A. 582, 583; 14.35
Krylov, V.I. 597; 15.11
Kubasov, V.N. 517; 12.97
Kur'yanov, A.I. 13, 203, 309, 322, 328; 1.47, 5.36, 7.25, 8.52
Kutyrin, I.N. 79; 2.83
Kuzmak, G.E. 13, 321, 322, 615, 617, 619; 1.40, 1.46, 1.56, 8.22, A.17, A.21
Kuznetsov, E.V. 37, 39, 76; 2.8, 2.84
Kuznetsov, Yu.E. 39, 41, 43, 80; 2.20
Kvasnikov, A.V. 14, 21, 37, 39, 76, 77; 1.66, 2.10

Landau, L.D. 37, 101; 2.12
Landsberg, G.S. 31; 1.75
Laricheva, V.V. 611; A.3, A.4
Lavrent'ev, M.A. 34; 1.82
Lavrov, S.S. 13; 1.59
Lebedev, L.A. 175; 5.6
Lebedev, S.Ya. 54, 63; 2.50
Lebedev, V.N. 183, 242, 243, 247, 261, 604, 605; 5.26, 6.4, 6.5, 6.16, 9.29, 13.21, 15.73
Letov, A.M. 517; 12.27, 12.45, 12.46, 12.83, 12.94
Levin, L.M. 13; 1.28
Lidov, M.L. 13; 1.51, 12.84
Lidskii, E.A. 517; 12.23, 12.25, 12.38, 12.47, 12.66
Lifshits, E.M. 37, 101; 2.12
Litovchenko, I.A. 322, 517; 8.41, 12.29

Loitsyanskii, L. S. 84, 87; 2.96
Luk'yanov, S. Yu. 55, 56; 2.65
Lur'e, A. I. 13, 322, 517, 539; 1.31, 1.36, 8.23, 12.1, 12.67, 13.18

Martynov, A. K. 101; 2.148
Melik-Pashaev, N. I. 37, 39, 76; 2.8
Mel'kumov, T. M. 37, 39, 76; 2.8
Mel'nikov, M. V. 77; 2.75
Mel'nikova, N. S. 101; 2.161
Meshcherskii, I. V. 13, 321; 1.1
Mezhirov, I. I. 79; 2.81
Mikhailova, M. M. 79; 2.83
Mikhailova, M. P. 101; 2.164
Mikheev, Yu. S. 79; 2.83
Mikhlin, S. R. 597; 15.12
Millionshchikov, M. D. 37, 38, 79, 95; 2.4
Mil'shtein, G. N. 322, 517; 8.39, 12.95
Mishchenko, E. F. 109, 353, 582; 2.170, 9.4, 14.34.
Mishin, V. P. 13; 1.59
Moiseev, N. N. 557, 611; 6.5, 14.5, A.2
Morgulis, N. D. 84, 88, 89; 2.112
Morozov, M. G. 52; 2.44
Mukhamedzhanov, A. K. 34; 1.86

Nechaev, Yu. N. 14, 21, 36, 37, 76–78, 92–95, 122; 1.61, 2.2, 3.1
Nikol'skii, A. A. 101; 2.152
Novoseletskii, O. Yu. 116; 2.293
Novoselov, V. S. 322; 8.28, 8.29

Okhotsimskii, D. E. 13, 186, 321, 322, 541, 543, 548, 567, 612, 615, 618, 623; 1.11, 1.18, 1.51, 5.37, 8.7, 8.8, 8.47, 13.26, 14.31, A.13, A.19, A.20
Ostoslavskii, I. V. 13; 1.53
Ovsyannikov, R. N. 435; 9.35

Parysheva, G. V. 517; 12.102
Petrov, G. I. 42; 2.24
Pisimennyi, V. D., 55, 56; 2.66
Platonov, A. K. 517; 12.97, 15.5
Podgornyi, I. M. 55, 56; 2.65, 2.66
Pokrovskaya, S. A. 179, 187, 203; 5.21
Polovko, A. M. 471, 487; 11.7
Polyarnyi, A. I. 77; 2.77
Ponomarev, V. M. 13, 517; 1.54, 12.98
Pontryagin, L. S. 109, 353, 357, 368, 412; 2.170, 9.4, 14.34
Popov, V. M. 517; 12.30
Pugachev, V. S. 517, 519; 12.4
Pupko, V. Ya. 54, 63; 2.50

Raizer, Yu. P. 34; 1.84
Rein, M. V. 606; A.3, A.4
Roitenberg, Ya. N. 517, 518; 12.68
Romanenko, S. V. 79; 2.79
Roze, N. V. 101; 2.147
Rumyantsev, B. N. 247, 605; 6.16, 15.23

Sadovskii, I. N. 13; 1.25
Sakovskii, S. A. 175; 5.6
Salukvadze, M. E. 517; 12.31, 12.48, 12.49
Samokish, B. A. 558; 14.12
Sandomirskaya, I. D. 39; 2.21
Sedov, L. I. 37, 99, 101; 2.5, 2.140, 2.154
Semenova, L. N. 435; 9.35
Sergel', O. S. 79; 2.83
Sergienko, A. A. 39; 2.21
Shalaev, Yu. V. 170, 192, 203, 209, 558, 598, 621; 5.4, 5.20, 5.27, 6.2; 14.16, 15.13, A.23
Shatrovskii, L. I. 567, 578, 582; 14.18

Shchukin, V.K. 37, 39, 76; 2.7
Shepelev, Yu.G. 517; 12.100
Shkadov, L.M. 13, 321, 551, 552, 585; 1.35, 13.35
Shlykov, Yu.P. 118; 2.206
Shmyglevskii, Yu.D. 39; 2.15, 2.19
Simonov, L.A. 37, 38, 79, 95; 2.4
Sinyarev, G.B. 92; 2.118
Skubachevskii, G.S. 93, 95; 2.130
Smolyakov, B.Ya. 52; 2.43
Solodovnikov, V.V. 517; 12.11
Solov'ev, A.D. 471, 487; 11.8
Solov'ev, B.A. 116; 2.189
Sonin, V.V. 13, 170, 177, 203, 309, 594, 619; 1.47, 5.2, 5.10, 5.36, 7.13, 7.14, 7.25, 8.52, 15.9
Stanyukovich, K.P. 34, 101; 1.80, 2.158
Stasenko, A.L. 116, 118; 2.197, 2.198, 2.202, 2.203, 2.204, 2.205, 2.208
Stavisskii, Yu.A. 54, 63; 2.50
Stechkin, B.S. 14, 21, 36, 76—78, 92—95, 122; 1.61, 2.121, 3.1
Stapanov, G.Yu. 84, 87; 2.97
Sternin, L.E. 39; 2.17
Stratonovich, R.L. 517; 12.101
Stumbur, E.A. 54, 63; 2.50
Subbotin, M.F. 25, 612; 1.72, A.8
Sychev, V.V. 102; 2.168

Tamm, I.E. 54; 2.63
Tarasov, E.V. 13, 321; 1.42
Taratynova, T.P. 623; A.13
Teslenko, N.M. 13; 1.51
Todorov, K. 322; 8.24
Tokarev, M.V. 39, 41, 43; 2.20
Tokarev, V.V. 14, 21, 81, 93, 96, 122, 151, 387, 398, 401, 402, 436, 470, 517, 518; 1.60, 2.20, 2.86, 2.137, 3.3, 4.20, 4.22, 4.23, 4.25, 4.28, 5.3, 5.4, 6.11, 9.3, 9.18, 10.1, 10.2, 10.3, 10.4, 11.1, 11.2, 11.3, 11.4, 12.62, 12.69, 13.15, A.23
Troitskii, V.A. 322; 8.38
Tsander, F.A. 13, 70, 71, 104, 151, 321, 410, 412, 535; 1.5, 2.71, 4.27, 9.21, 13.9
Tsiolkovskii, K.E. 13, 321; 1.2, 1.3
Tsvetkov, V.I. 81; 2.86

Ukolov, V.L. 116; 2.193

Valeev, K.G. 410, 419; 9.33
Vanichev, A.P. 77; 2.76
Varshavskii, G.A. 79; 2.78
Vasanov, Yu.A. 116; 2.188, 2.190, 2.191, 2.194
Venttsel', E.S. 453, 458, 461; 10.5
Vinokurov, V.A. 287; 6.11, 7.10
Vorob'ev, N.N. 453, 458, 461; 10.7

Yaroshevskii, V.A. 517; 12.102

Zaitsev, A.G. 517, 518; 12.63
Zel'dovich, Ya.B. 34, 37, 77; 2.3, 2.77
Zhidkov, N.P. 594; 15.2
Zhukov, A.N. 410, 412, 413, 415; 9.29
Zhukov, M.F. 52; 2.43
Zhulev, Yu.G. 116; 2.188, 2.194, 2.195
Zuev, V.S. 93, 95; 2.124

Non-Russian Authors

Ailenberg, S.L. 48; 2.36
Alder, K. 99; 2.141
Allen, K.U. 25; 1.70
Anderson, T. 517; 12.71

Andreescu D. St. 13; 1.50
Anthony, M. L. 541; 13.24
Arthur, P. D. 537, 539; 13.13, 13.29
Au, G. F. 14, 21, 48, 52, 54, 58, 74, 76, 78, 81, 82, 84, 120, 280, 531, 535; 1.63, 2.38, 2.91, 7.8, 13.5, 13.8

Bacon, R. H. 549; 13.27
Balent, R. 84, 88; 2.103
Barrere, M. 13, 37, 39, 76, 321, 322; 1.21, 2.9, 8.51
Bartas, J. G. 111, 112; 2.175
Battin, R. H. 517; 12.5, 12.32
Beale, R. J. 84, 87, 93; 2.94
Beckewith, W. C. 48, 50; 2.41
Beers, L. S. 48, 87, 317; 2.35, 8.4
Bell, D. J. 322; 8.35
Bellman, R. 517, 557; 12.52, 14.1, 14.2, 14.3, 14.4
Benney, D. J. 540, 541; 13.23
Berman, L. J. 517; 12.72
Bernatowicz, D. T. 118; 2.209
Berner, F. 93, 96, 98, 384, 385, 386, 387; 2.135, 9.12, 9.16
Billik, B. H. 221; 5.34
Bjork, R. L. 34, 35; 1.79, 1.81
Blum, E. K. 135, 179, 180, 183, 188, 197, 272, 275; 4.21, 5.12, 7.6
Boden, R. H. 54; 2.51
Bono, P. 43; 2.26
Boucher, R. A. 317; 8.6
Breakwell, J. V. 13, 321, 322, 517, 604, 605; 1.25, 1.43, 8.12, 12.12, 12.33, 12.53, 12.73, 12.74, 12.85, 12.103, 15.17, 15.21
Brewer, G. R. 54, 66; 2.62
Brogan, T. R. 53; 2.46
Brown, H. 54, 309; 2.55, 7.24
Bryson, A. F. 517, 567, 568, 572, 578, 594; 12.34, 12.54, 14.22, 14.23, 14.24, 14.25, 15.3
Bucy, R. S. 517; 12.38
Burge, H. L. 116; 2.200
Burlage, H. 92; 2.119
Bussard, R. W. 14, 21, 48, 51, 76, 77, 135, 272; 1.65, 2.29, 4.4, 7.4

Camac, M. 48, 52, 58, 76, 93, 96, 98, 135, 350, 384, 385, 386, 387; 2.33, 2.36, 2.135, 4.17, 9.2, 9.12, 9.16
Cameron, A. G. W. 30; 1.73
Cappellari, J. O. 3.22; 8.11
Carroll, F. J. 567; 14.24
Cavoti, C. R. 322; 8.30, 8.34
Chamay, A. 43; 2.25
Chao, B. T. 116; 2.185
Chen, Y. L. 111; 2.176
Citron, S. J. 537, 539, 623, 627; 13.12, A.25
Cleaver, A. V. 48, 76, 77, 80; 2.28
Cobb, J. E. 84, 88, 89; 2.111
Cochran, D. L. 84, 87; 2.93
Cohen, A. D. 48, 87; 2.35, 8.4
Contensou, P. 322; 8.20
Cook, H. M. 93, 95; 2.129
Copeland, T. 531, 535; 13.3
Corliss, W. R. 14, 21, 33, 48, 51, 54, 59, 78, 80, 81, 82, 84, 87–90, 92, 106, 107, 113, 122; 1.62, 2.32, 3.2
Cornog, R. 135; 4.10
Courant, R. 558, 571, 578; 14.7, 14.33
Craig, R. 317; 8.2
Cristman, D. R. 34; 1.78
Crocco, L. 135; 4.18
Curkendall, D. W. 517; 12.75
Curry, R. 111; 2.177
Cutler, W. E. 84, 88, 89; 2.111

Davis, J. 54; 2.60
Davison, E. H. 118; 2.209
De Lauer, R. D. 14, 21, 48, 51, 76, 77; 1.65, 2.29
Demetriades, S. T. 93, 96, 98, 384, 402; 2.134, 9.11, 9.13, 9.14

Denham, W.F. 567, 568, 576, 578, 582; 12.34, 12.54, 14.22, 14.23, 14.24, 14.25, 14.26, 15.3
Dieckamp, H.M. 84, 88; 2.103
Diesel, J.M. 517; 12.18
Dobrowolski, A. 531, 537; 13.2
Dreyfus, S.E. 557, 567; 14.4, 14.25
Drescher, M. 453, 458, 461; 10.8
Dugan, A.F. 84, 88, 89; 2.111
Dulgeroff, C.R. 309; 7.20
Duncan, R.C. 517; 12.86

Eckert, E.R.G. 115, 116; 2.180, 2.181, 2.183
Edelbaum, T.N. 179, 186, 221, 328, 341, 342, 516; 5.24, 5.31, 5.32, 5.33, 8.55, 11.9
Ehricke, K.A. 13, 321, 612; 1.38, A.11
Elliott, D.G. 84, 88; 2.100
English, R.E. 118; 2.209
Esnault-Pelterie, R. 13, 321; 1.8
Evans, R. 13, 321; 1.15

Faulders, C.R. 179, 186, 247, 272; 5.22, 5.23, 6.17, 7.1, 7.2
Fenech, H. 118; 2.207
Ferri, A. 93, 95, 101; 2.128, 2.151
Fetheroff, C.W. 201, 317, 601; 5.18, 8.2, 15.14
Fimple, W.R. 342, 410, 415, 418; 8.57, 9.31
Forbes, G.F. 538, 549; 13.14
Forrester, A.T. 309; 7.20
Fox, R. 309; 7.21
French, E.P. 384, 387; 9.15
Friedlander, A.L. 517; 12.36
Fusca, J.A. 517; 12.87

Gardill, W.P. 605; 15.22
Geerts, J. 13, 322; 1.55, 8.27
Gehring, J.W. 34; 1.78
Glassman, A.J. 84; 2.92
Glicksberg, J. 517; 12.52
Gobetz, F.W. 219, 221; 5.28, 5.29, 5.35
Goddard, R.H. 13, 30, 321; 1.4
Goldsmith, W. 79; 2.82
Goldstein, S. 100; 2.142
Goodman, T.R. 586; 14.39
Gossick, L.V. 93, 95; 2.129
Gronich, A. 84, 88, 89; 2.114
Gross, O. 517, 557; 12.52, 14.2
Grover, G.M. 84, 88, 89; 2.108
Guderley, G. 39; 2.13, 2.18
Gunnersen, A.S. 517; 12.86
Gurley, J.G. 322; 8.32

Haller, H.C. 116; 2.186
Hallet, R.W. 84, 88, 89; 2.14
Hamilton, R.C. 84, 88; 2.106
Hanford, D.R. 93, 96, 98, 384—387; 2.136, 9.17
Hantsch, E. 39; 2.13
Harry, D.P. 517; 12.36
Harvey, R.J. 84, 88, 89; 2.110
Hayes, W.D. 100, 101; 2.145, 2.163
Herrick, S. 13, 321, 612; 1.29, A.9, A.10, A.12
Hohmann, W. 13, 321; 1.7
Horgan, J.J. 43; 2.25
Huebner, A.L. 48; 2.36
Hughes, J.V. 549; 13.28
Hunter, M.W. 317; 8.1

Irvine, T.F. 115, 116; 2.180, 2.181
Irving, J.H. 135, 171, 176, 179, 180, 183, 188, 197, 272, 275; 4.15, 4.21, 5.5, 5.12, 7.6

Jahsman, W.E. 72; 2.73
Janes, G.S. 48; 2.36
Jaumotte, A. 13, 37, 39, 76, 322, 323; 1.21, 2.9, 8.51

Jazwinski, A.H. 517, 568, 578, 582; 12.88, 14.31
Johnson, B. 605; 15.22
Johnson, H.L. 48, 50; 2.41
Johnson, V.K. 116; 2.187
Jurovics, St.A. 594, 597, 604, 605; 15.8, 15.20, 15.22

Kalman, R.E. 517; 12.13, 12.37, 12.38, 12.39, 12.55
Kantrowitz, A. 48, 52; 2.36, 2.45
Karlekar, B.V. 116; 2.185
Karman, T. 101; 2.146
Karrenberg, H.K. 531, 535; 13.4, 13.13
Kash, S.W. 309, 310; 7.22
Kaufman, H.R. 54, 66, 68; 2.52, 2.56
Keller, Jack, L. 322; 8.25
Kelley, H.J. 410, 412, 413, 517, 567, 568, 576, 582, 583; 9.28, 12.56, 14.20, 14.21, 14.27
Kopp, R.E. 322, 567; 8.43, 14.21
Kornhauser, M. 34; 1.83
Kraft, J.D. 517, 12.76, 12.77
Kreith, F. 116; 2.182
Krupp, R. 517; 12.72
Kubota, T. 102; 2.166
Kulakowski, L.J. 604, 605; 15.18, 15.19
Kunen, E. 48; 2.36
Kurzweil, J. 517; 12.26
Kuskevics, G. 54; 2.58

Lacy, L. 309; 7.18
Lance, G.N. 586; 14.39
Lane, R.J. 93, 95, 96; 2.127
Langmuir, D.B. 135; 4.14
Laning, D. 517, 662; 12.5, 12.32
Lass, H. 536, 537, 539, 551, 611, 615; 13.11, 13.33, A.1, A. 18
Lawden, D.F. 13, 242, 321, 322, 517, 526, 539; 1.16, 1.30, 1.39, 6.6, 8.9, 12.14, 12.78, 13.19, 13.20
Lawden, J.H. 309; 7.19
Leach, R. 517; 12.57
Lecompte, J. 99; 2.141
Lees, L. 102; 2.166
Leitmann, G. 13, 135, 176, 221, 321, 322; 1.34, 1.37; 4.9, 5.7; 5.30, 8.13, 8.14, 8.15, 8.18, 8.50
Levin, E. 538, 551; 13.17, 13.32
Lieblein, S. 118; 2.209
Liepmann, H.W. 100; 2.144
Lindorfer, W. 247, 567, 576, 577, 594, 604, 605; 6.14, 14.28, 15.4
Linhardt, H.D. 48, 50, 51, 83, 350; 2.39, 9.1
London, H.S. 410, 412, 415, 535; 9.24, 13.10
Lorrel, J. 536, 537, 611; 13.11, A.1
Lubowe, A.G. 322; 8.31
Lukes, D.L. 567, 568; 14.30

Mackay, J.S. 245; 6.12
Maday, C.J. 541; 13.24
Malina, F.J. 322; 8.46
Marec, J.P. 322; 8.44
Martelly, J. 148; 4.26
McIllroy, W. 48; 2.36
McIntyre, I.E. 604, 605; 15.8, 15.22
McKinsey, J.C.C. 453, 458, 461; 10.6
McMillan, A.R. 34; 1.78
Meghreblian, R.V. 48, 78; 2.37
Melbourne, W.G. 179, 188, 197, 198, 200, 201, 203, 204, 222, 224, 247, 272, 309; 5.13, 5.14, 5.15, 5.16, 5.17, 6.18, 6.19, 6.20, 7.3, 7.15, 7.17
Mickelsen, W.R. 54, 66, 69; 2.54, 2.61
Miele, A. 13, 321, 322, 328; 1.22, 1.26, 1.44, 8.10, 8.11, 8.21, 8.49, 8.53
Migdal, D. 43; 2.25
Mikami, K. 567; 14.24
Miller, H. 84, 88, 89; 2.113
Miller, P.W. 84, 88, 89; 2.114

Minneman, M. J. 517; 12.15
Moeckel, W. E. 135, 243, 263, 539; 4.12, 6.7, 6.8, 6.9, 6.23, 13.22
Moser, W. A. 309; 7.23
Moulton, F. R. 612; A. 6
Moyer, H. G. 247, 322, 567; 6.14, 8.43, 14.21, 14.28
Munick, H. 322; 8.54

Nathan, A. 594; 15.4
Newton, R. R. 615; A. 14
Nicoll, H. E. 54, 309; 2.55, 7.24
Nilson, E. N. 111; 2.177
Nita, M. M. 13; 1.50
Nomicas, G. N. 549; 13.28

Oberth, H. 13, 321; 1.6
Olds, R. H. 84, 88, 89; 2.111
Orr, E. C. 48, 84; 2.36
Osmun, W. G. 84, 120; 2.90

Paiewonsky, B. 533; 13.6
Perkins, F. M. 410, 418, 541, 542, 543; 9.32, 13.25
Peske, A. 517; 12.58
Petty, C. M. 533, 535; 13.7
Pfeiffer, C. G. 517, 601, 602; 12.40, 12.75, 15.15
Pines, S. 322; 8.26, A. 15
Pinkel, B. 516; 11.10
Pinkham, G. 549; 13.30
Plamondon, J. A. 116; 2.184
Potter, R. A. 309; 7.18
Pozzi, A. 410, 412; 9.25, 9.26
Prandt, L. 36, 37, 100, 101; 2.1
Preston-Thomas, H. 54, 84, 135, 177, 263, 267, 272; 2.47, 4.1, 4.2, 4.5, 4.7, 4.8, 4.13, 5.8, 5.9, 6.24, 6.26, 6.27, 7.5
Preining, O. 52; 2.42
Probstein, R. F. 100, 101; 2.145
Psarouthakis, J. 84, 88, 90; 2.115

Ragsac, R. V. 516; 11.11
Rao, G. V. 39; 2.16
Rauch, H. E. 517; 12.103
Reader, P. D. 54, 66, 68; 2.52, 2.61
Reichel, R. H. 93, 96, 98, 384 – 387; 2.136, 9.17
Reiffel, L. 30, 31; 1.74
Renaudin, D. 517; 12.16
Richardson, D. E. 179, 197, 201, 203, 247; 5.13, 7.15
Rider, L. 551; 13.34
Robbins, H. M. 322; 8.33
Roberson, R. E. 623, 624; A. 24
Rodriguez, G. 539, 550; 13.31
Rohsenow, W. H. 118; 2.207
Rosenbloom, A. 517; 12.59
Rosenblum, P. C. 517, 558; 14.15
Roshko, A. 100; 2.144
Ross, S. E. 13, 221; 1.52, 5.30, 12.51
Rossa, L. G. 245; 6.12
Roy, M. 93, 95; 2.122

Sakurai, A. 101; 2.156
Saltzer, C. 179, 187, 201, 601; 5.18, 8.2, 15.14
Sands, N. 410, 415, 416, 418; 9.30
Sauer, C. G. 179, 188, 197, 198, 200, 201, 203, 204, 222, 224, 247, 272, 309; 5.13, 5.15, 5.16, 5.17, 6.18, 6.19, 6.20, 7.3, 7.15, 7.16, 7.17
Scull, J. R. 517; 12.41
Seban, R. A. 79; 2.82
Seifert, H. 48, 76, 92, 93; 2.30
Seitz, R. N. 54, 61, 63, 65; 2.53, 4.16
Sellers, W. H. 111, 112; 2.175
Shelton, R. D. 309; 7.18
Shepherd, L. R. 48, 76, 77, 80; 2.28
Sherman, B. 179, 180, 182, 567; 5.19, 14.29
Shipper, L. 116; 2.201
Shook, G. B. 84, 88, 89; 2.111
Siegler, R. C. 116; 2.201
Slone, H. O. 118; 2.209
Smith, A. M. 322; 8.46

Smith, F.T. 612; 4.5
Smith, R.R. 517; 12.85
Smith, T.L. 93, 96, 98, 384—387; 2.136, 9.17
Smith W.E. 116—119; 2.196, 2.199
Snyder, N.W. 14, 21, 82, 83, 84, 87—90, 92, 106, 107; 1.67, 2.87, 2.92
Socio, L. 410, 412; 9.26, 9.27
Solloway, G.B. 551, 615; 13.33, A.18
Sparrow, E.M. 115, 116; 2.180, 2.181, 2.183, 2.187
Speiser, E.W. 84, 87, 93; 2.94
Speiser, R.S. 309; 7.20
Stafford, G.B. 84, 119; 2.89
Stamm, H. 84, 88, 120; 2.104
Stancil, R.T. 604, 605; 15.18, 15.19
Stark, H.M. 549; 13.13, 13.29
Starr, W.L. 309; 7.22
Stearns, E.V. 517; 8.3, 12.17, 12.80.
Stearns, Y.W. 317; 8.3
Stein, M.L. 558, 585; 14.13
Steinker, G.E. 517; 12.22, 12.81
Stenning, A.H. 48; 2.34
Stewart, W.L. 84; 2.92
Stöckel, K. 43, 46, 47, 76; 2.27
Stockman, N.O. 116; 2.186
Striebel, C.T. 517; 12.73
Stuhlinger, E. 54, 59, 61, 63, 65, 121, 135, 263, 317; 2.48, 2.49, 2.53, 2.59, 4.3, 4.6, 4.11, 4.16, 6.22, 7.18, 8.5
Sutton, G.P. 14, 21, 48, 76, 87, 88; 1.64, 2.31

Taylor, G.J. 101; 2.155
Thompson, B.L. 54; 2.58
Tompkins, C.B. 558; 14.14
Tonkin, S.W. 84, 88, 89; 2.107
Townsend, G.E. 517; 12.57, 12.82
Traenkle, C.A. 517; 12.89
Tschirgi, J.M. 317; 8.1
Tsien, H.S. 13, 101, 321, 531, 532, 537; 1.15, 2.149, 13.1
Tsu, T.C. 410, 412, 413, 415; 9.22, 9,23
Tung, F. 517; 12.85

Ursini, G.A. 43; 2.26

Vandenkerckove, J. 13, 37, 39, 76, 321, 322; 1.21, 2.9, 8.51
Vernet-Lozet, M. 83, 84; 2.88
Veubeke, B.F. 13, 37, 39, 76, 321, 322; 1.21, 1.23, 1.55, 2.9, 8.27, 8.51

Ward, M. 517; 12.58
Weatherston, R.C. 116—119; 2.196, 2.199
Wetch, J.R. 84; 2.103
Whipple, F.L. 34; 1.77
Wiener, N. 517; 12.35
Wilkins, J.E. 110; 2.171, 2.172, 2.173, 2.174
Wilks, W.E. 48, 50, 51; 2.40
Willinski, M.J. 48, 84; 2.36
Winicur, D.H. 54; 2.57
Womack, J.R. 84, 87, 93; 2.94
Wong, P. 615; A.16
Woodworth, J.L. 43; 2.26

Zaborszky, J. 517; 12.18
Zehle, H. 246; 6.13
Zimmerman, A.V. 245; 6.12
Zoutendijk, G. 594; 15.1
Zwick, E.B. 116; 2.201

[5140] Printed in Jerusalem, Israel NASA TT F-507
TT 68-50301